TECHNICAL UNIVERSITY – SOFIA
PLOVDIV BRANCH

# FIFTH INTERNATIONAL SCIENTIFIC CONFERENCE "ENGINEERING, TECHNOLOGIES AND SYSTEMS"

## *TECHSYS 2016*

26 - 28 May, Plovdiv

**PROCEEDINGS**

**СБОРНИК ДОКЛАДИ**

**ISSN Online: 2535-0048**



ТЕХНИЧЕСКИ УНИВЕРСИТЕТ – СОФИЯ
ФИЛИАЛ ПЛОВДИВ

# ПЕТА МЕЖДУНАРОДНА НАУЧНА КОНФЕРЕНЦИЯ "ТЕХНИКА, ТЕХНОЛОГИИ И СИСТЕМИ"

## *ТЕХСИС 2016*

26 - 28 май, Пловдив

The conference will be held within the framework of the ***Science Days of Technical University of Sofia and 30th anniversary of the Technical University of Sofia, Branch Plovdiv*** and under the patronage of Prof DSc Georgi Mihov - Rector of the Technical University of Sofia.

Конференцията ще се проведе в рамките на ***Дни на науката на Технически университет - София и 30 годишнината на Технически Университет – София, филиал Пловдив*** и под патронажа на проф. дтн. Георги Михов - Ректор на Технически Унивеверситет - София.

TECHNICAL UNIVERSITY – SOFIA, PLOVDIV BRANCH

# FIFTH INTERNATIONAL SCIENTIFIC CONFERENCE "ENGINEERING, TECHNOLOGIES AND SYSTEMS"

*TECHSYS 2016*
26 - 28 May, Plovdiv

• • •

*ТЕХСИС 2016*
26 - 28 май, Пловдив

ТЕХНИЧЕСКИ УНИВЕРСИТЕТ – СОФИЯ, ФИЛИАЛ ПЛОВДИВ

# ПЕТА МЕЖДУНАРОДНА НАУЧНА КОНФЕРЕНЦИЯ "ТЕХНИКА, ТЕХНОЛОГИИ И СИСТЕМИ"

This conference is technically co-sponsored by:
***IEEE Bulgaria Section***
***IEEE Young Professionals Affinity Group of Bulgaria***

Тази конференция е технически подпомогната от:
***Българска секция на IEEE***
***група IEEE Млади Професионалисти, България***

# TECHNICAL UNIVERSITY - SOFIA, PLOVDIV BRANCH

## Organizing Committee:

**Honorary Chairman:** Prof. DSc Georgi Mihov
**Chairman:** Prof. Dr. Valyo Nikolov
**Vice Chairman:** Prof. Dr. Michail Petrov

**Members:**

Prof. Dr. Grisha Spasov
Assoc. Prof. Dr. Krum Kutryansky
Assoc. Prof. Dr. Nikolay Kakanakov
Assoc. Prof. Dr. Ivan Kostov
Assoc. Prof. Dr. Stanislav Alexiev
Assoc. Prof. Dr. Borislav Penev
Assoc. Prof. Dr. Nikola Georgiev
Prof. Dr. Sonya Tabakova
Assoc. Prof. Dr. Pepo Yordanov
Assoc. Prof. Dr. Angel Lengerov
Assoc. Prof. Dr. Toni Mihova
Assoc. Prof. Dr. Anton Lechkov
Prof. Dr. Dobrin Seizinski
Assoc. Prof. Dr. Valentina Proycheva
Assoc. Prof. Dr. Nikolaj Petrishki
Assoc. Prof. Dr. Valentin Vladimirov

## International Programme Committee:

**Chairmen:** Prof. Dr. Veselka Boeva, Prof. Dr. Teofil Iamboliev

**Members:**

Acad. Prof. DSc Yuri Kuznetsov, Ukraine
Acad. Prof. DSc Nikolaj Mishkin, Belarus
Prof. Dr., Dr.h.c. Nikolai Ganev, Czech Republic
Prof. Dr. Marsel Popa, Romania
Prof. Dr. Ernst Wintner, Austria
Prof. DSc Mark Himbert, France
Prof. DSc Okyay Kaynak, Turkey
Prof. DSc Andre Barraco, France
Prof. DSc Edmunds Teirumnieks, Latvia
Prof. Dr. Frantisek Zezulka, Czech Republic
Prof. Dr. Petr Louda, Czech Republic
Prof. Dr. Nikola Kasabov, New Zealand
Prof. DSc Ivan Jachev, Bulgaria
Prof. DSc Emil Nikolov, Bulgaria
Prof. DSc Radi Romanski, Bulgaria
Prof. DSc Marin Nenchev, Bulgaria
Prof. DSc. Vesko Panov, Bulgaria
Prof. Dr. Ognyan Nakov, Bulgaria
Prof. Dr. Vladimir Pulkov, Bulgaraia
Prof. Dr. Petar Gecov, Bulgaria
Prof. Dr. Georgi Todorov, Bulgaria
Prof. Dr. Lubomir Dimitrov, Bulgaria
Prof. Dr. Mladen Velev, Bulgaria
Prof. Dr. Boncho Bonev, Bulgaria
Prof. Dr. Ilia Iliev, Bulgaria
Prof. Dr. Daniela Goceva, Bulgaria
Prof. Dr. Ivan Kralov, Bulgaria
Prof. Dr. Valeri Mladenov, Bulgaria
Prof. Dr. Andon Topalov, Bulgaria
Prof. DSc Todor Stoilov, Bulgaria

**Scientific Secretary:** Dr. Sevil Ahmed
**Technical Secretary:** Eng. Tsvetan Petrov, Eng. Christo Christev, Eng. Lalka Boteva

**ISSN Online: 2535-0048**

# ТЕХНИЧЕСКИ УНИВЕРСИТЕТ – СОФИЯ, ФИЛИАЛ ПЛОВДИВ

## Организационен комитет:

Почетен председател: проф. дтн. Георги Михов
Председател: проф. д-р Вълью Николов
Зам. Председател: проф. д-р Михаил Петров

### Членове:

проф. д-р Гриша Спасов
доц. д-р Крум Кутрянски
доц. д-р Никола Георгиев
доц. д-р Иван Костов
доц. д-р Станислав Алексиев
доц. д-р Борислав Пенев
доц. д-р Тони Михова
проф. д-р Соня Табакова
доц. д-р Пепо Йорданов
доц. д-р Ангел Ленгеров
доц. д-р Николай Каканаков
доц. д-р Антон Лечков
проф. д-р Добрин Сеизински
доц. д-р Валентина Пройчева
доц. д-р Николай Петришки
доц. д-р Валентин Владимиров

## Програмен комитет:

**Председатели:** проф. д-р Веселка Боева, проф. д-р Теофил Ямболиев

### Членове:

акад. проф. дтн. Юрий Кузнецов, Украйна
акад. проф. дтн. Николай Мишкин, Беларус
проф. д-р, д-р х.к. Николай Ганев, Чехия
проф. д-р Марсел Попа, Румъния
проф. дтн. Ернст Винтнер, Австрия
проф. дтн. Марк Химберт, Франция
проф. д-р Окияй Кайнак, Турция
проф. дтн. Андре Барако, Франция
проф. дтн. Едмундс Теирумниекс, Латвия
проф. д-р Франтишек Зезулка, Чехия
проф. д-р Петр Лоуда, Чехия
проф. д-р Никола Касабов, Нова Зеландия
проф. дтн. Иван Ячев, ФНТС, ТУ – София
проф. дтн. Емил Николов, ТУ – София
проф. дтн. Ради Романски, ТУ – София
проф. дтн. Тодор Стоилов, БАН
проф. дтн. Марин Ненчев, ТУ – София, филиал Пловдив
проф. дтн. Веско Панов, ТУ – София
проф. д-р Бончо Бонев, ТУ – София
проф. д-р Илия Илиев, ТУ – София
проф. д-р Даниела Гоцева, ТУ – София
проф. д-р Владимир Пулков, ТУ – София
проф. д-р Огнян Наков, ТУ – София
проф. д-р Петър Гецов, ИКИ, БАН
проф. д-р Георги Тодоров, ТУ – София
проф. д-р Любомир Димитров, ТУ – София
проф. д-р Младен Велев, ТУ – София
проф. д-р Иван Кралов, ТУ – София
проф. д-р Валери Младенов, ТУ – София
проф. д-р Андон Топалов, ТУ – София, ф-л Пловдив

**Научен секретар:** Д-р инж. Севил Ахмед
**Технически секретариат:** инж. Цветан Петров, инж. Христо Христев, инж. Лалка Ботева

# CONTENTS

PLENARY AND INVITED PAPERS • ПЛЕНАРНИ И ПОКАНЕНИ ДОКЛАДИ..... **I-11**

1. **Witold Pawlowski, Jakub Sikorski and Lukasz Kaczmarek -** ..... **I-12**
   Lodz University of Technology, Poland
   Space Applications of the Lightweight Gradient Materials Based on nc-Al alloys
2. **Rosen Kosturkov**
   Best practices in training people in field of automation ..... **I-16**

SECTION 1 • СЕКЦИЯ 1
**AUTOMATION AND CONTROL SYSTEMS**
**Автоматика и системи за управление**..... **II-1**

1. **Beladel Abdelkader, Kouzou Abdellah, Ahmed Hafaifa, Djilali Mahi** ..... **II- 2**
   Dual Matrix Converter Feeding an Open-End Load Based on Modified Direct Transfer Function Approach
2. **Nadji Hadroug, Ahmed Hafaifa, Abdellah Kouzou, Mouloud Guemana, Ahmed Chaibet**..... **II-9**
   Control of Gas Turbine Output Parameters Based on Multidisciplinary Optimization of Their Operating Variables
3. **Bachir Nail, Abdellah Kouzou, Ahmed Hafaifa, Belkacem Bekhiti**..... **II-18**
   Stabilizing Linear Multivariable Gas Turbine Model via Sliding Mode Control
4. **Ahmed Hafaifa, Kouzou Abdellah, Guemana Mouloud, Nadji Hadroug**..... **II-24**
   Reliability Analysis using Weibull Distribution Applied to a Booster Pump Used in Oil Drilling Installations
5. **Nina Dobrinkova** ..... **II-31**
   ICT Technologies in Wildland Fire Modelling
6. **Mircea Weingart, Dan Popescu, Orest Vascan**..... **II-37**
   Image Segmentation Techniques for Medical Image Processing Purposes
7. **Georgi Ruzhekov, Teofana Puleva, Tsonio Slavov** ..... **II-43**
   Experimental System for Wind Modelling
8. **Krasimir Donchev, Stefan Biliderov**..... **II-49**
   Development of Controller for Pellet Burner
9. **Dragomir Chantov, Hristina Stoycheva** ..... **II-55**
   Synchronization and Antisynchronization of a New Chaotic System with Specific Nonlinearity
10. **Dragomir Chantov, Hristina Stoycheva** ..... **II-61**
    Design of Chaotic Synchronization Systems with Different Types of Identical and Non-Identical Synchronization on The Basis of a Linear-Nonlinear Decomposition Approach
11. **Dimitar Spirov, Georgi Terziyski** ..... **II-67**
    Closed-Loop Phase Controlled DC Motor Drive
12. **Dimitar Spirov, Nikolay Komitov**..... **II-73**
    DSP Based Induction Motor Drive with Quasi-Resonant Converter

**13. Lyudmila Baltova, Vasilka Stancheva** ..... **II-79**
Learning of Students Of Faculty of Automatics and Faculty of Electrical Engineering in Subject „Fundamentals Of Engineering Design"– Part I

SECTION 2 • СЕКЦИЯ 2
**ELECTRICAL ENGINEERING AND ENERGETICS ELECTRONICS; ELECTRONIC TECHNOLOGIES AND OPTOELECTRONICS**
**Електротехника и електроенергетика; Електроника и оптоелектроника**..... **II-83**

**1. Kaddouri Ameur Miloud, Kouzou Abdellah, Hafaifa Ahmed** ..... **II-84**
Optimization of Multi-Layer Linear Gradient Index Antireflective Based on Oxynitride Silicon

**2. Dimitar Dimitrov, Atanas Iliev, Nevenka Kiteva - Rogleva** ..... **II-88**
Validation of a Model For Generation of Hourly Ambient Temperature Time Series

**3. Nikola Georgiev** ..... **II-94**
A Model of a Single-Phase Two-Rotor Axial Generator With Rare Earth Magnets

**4. Nikola Georgiev** ..... **II-100**
Calculating Magnetic Induction in The Air Gap of a Three-Phase Two-Rotor Axial Generator with Rare Earth Magnets

**5. Srefan Bobev** ..... **II-106**
Algorithms and Principles For Monitoring Selected Automatic System or Parameters

**6. Srefan Bobev** ..... **II-112**
Specialized Electronic System for Tracking Other Process, Electronic or Automatic System

**7. Vanya Plachkova**..... **II-118**
Fluorescent Spectroscopy Applications in Veterinary Medicine and Healthcare

**8. Svetoslav Ivanov, Yanka Ivanova** ..... **II-124**
Electronic Converter for Fiber Optic Thermometer

**9. Margarita Deneva** ..... **II-128**
Nd:YAG Laser in Two-Wavelength Coaxial Architecture

**10. Margarita Deneva, Marin Nenchev, Nadejda Kaymakanova, Ernst Wintner, Mark Himbert** ..... **II-134**
Light Based Techniques as Possibility to Solve the Pollution Problems in Laser Ignition Combustion of Gaseous Mater. A Pilot Study

**11. Margarita Deneva, Marin Nenchev, Valko Kazakov, Nadejda Kaymakanova** ..... **II-140**
Development of the Thermo-Sensitive Paper Application as Method for Laser Beam Spot Study

**12. Petar Mitsev, Angel Tanev, Tsvetelina Lazarova**..... **II-144**
Performance Sensing Solutions for a Green Environment Designed in Bulgaria

**13. Sevdalina Manolova, Stanimir Stojnov, Ivanka Mitova, Angelina Mikova, Petra Alexandrova, Georgi Stoimenov** ..... **II-149**
Energy Characteristics of Cabbage with Added Biochar

**14. Alexander Angelov** ..... **II-155**
Special Features Design of Facade/Roof PV Plant

SECTION 3 • СЕКЦИЯ 3
**INFORMATICS AND COMPUTER SYSTEMS AND TECHNOLOGIES**
**Информатика и компютърни системи и технологии** ..... **II-161**

**1. Veneta Aleksieva, Ivaylo Zhelyazkov** ..... **II-162**
Generator of Network DoS Attacks

**2. Simeon Tsvetanov** ..... **II-168**
Developing of a Libcloud Driver for OwnCloud

**3. Ivan Kanev, Petya Pavlova, Dimitre Kromichev, Jordan Genoff** ..... **II-172**
Generating 2D Gaussian Kernels for the Purpose of Studying FPGA-Based Linear Spatial Filters

**4. Lubomir Bogdanov** ..... **II-180**
Look-Up Table-Based Microprocessor Energy Model

**5. Dobrinka Petrova** ..... **II-186**
Big Data in Bioinformatics

**6. Tarik Yerlikaya, Şenol Şen** ..... **II-192**
DDoS Attacks as the Cyber-Warfare Tools

**7. Yasin Akman** ..... **II-196**
Implementation and Encryption Time Measurement of Skipjack

**8. Hristo Valchanov** ..... **II-199**
Communication System for LAN Searching

**9. Dimitre Kromichev** ..... **II-203**
Canny Edge Detection: A Survey

**10. Dimitre Kromichev** ..... **II-211**
Technology of Computations in Canny Edge Detection for FPGA Implementation

**11. Dimitar Garnevski** ..... **II-217**
Estimating Impact of Image Parameters on Method for Tracking And Mapping a Motion in Solar Corona

**12. Dimitar Garnevski** ..... **II-223**
Parallel Implementation of Anisotropic Diffusion

**13. Marin Marinov, Lora Marinova** ..... **II-227**
Hamming Code and Excel Application for Generation and Encode

**14. Dilyana Budakova, Rumen Trifonov, Nikola Tsaikin** ..... **II-233**
Generalized Net Model for Cooperative Behavior Investigation Between Intelligent Virtual Agents

**15. Nikola Tsaikin, Dilyana Budakova** ..... **II-239**
Modelling And Analysis of Social Behavior with Intelligent Virtual Agents with Cognitive Architectures

**16. Svetlana Vasileva, Delyan Vasilev** ..... **II-245**
Some Approaches to integration Simulation Modeling in Education

SECTION 4 • СЕКЦИЯ 4
**MECHANICAL ENGINEERING; MECHANICAL AND INSTRUMENT ENGINEERING**
**Машиностроителна техника и технологии;**
**Машиностроене и уредостроене** ..... **II-251**

**1. Nikolay Petkov, Totka Bakalova, Tetiana Cholakova, Lukáš Voleský, Petr Louda** ..... **II-252**
Mechanical and Tribological Properties of AlN Hard Films Deposited by Reactive Magnetron Sputtering

**2. Nikolay Petkov, Totka Bakalova** ..... **II-256**
Deposition of AlCN Thin Films by Reactive DC Magnetron Sputtering and Tribology

**3. Viktor Kopanov, Stanislava Rabadzhiyska** ..... **II-260**
Development of Specialized Holders for Bearing Balls and Rollers Coating by PVD Methods

**4. Dimitar Petrov, Petko Dobrev, Stanislav Alexiev** ..... **II-264**
Experimental Comparison of Wear Resistance and Cyclic Loading to Bending Between Cycloid and Involute Gears

**5. Cenk Misirli, Mehmet Ceviz** ..... **II-270**
Investigation of the Effects of Cutting Tool, Cutting Speed and Material Type on Surface Roughness

**6. Cem Misirli, Cenk Misirli** ..... **II-274**
5083 Aluminum Heat Treatment

**7. Lyubomir Lazov, Hristina Deneva** ..... **II-279**
Influence Pressure of Assisted Gas on Laser Cutting Process by Melting

**8. Ilia Popov, Pepo Yordanov, Sabi Sabev** ..... **II-285**
Experimental Determining of The Elasticity Module of Polymer Concrete Composites

**9. Trayan Stamov** ..... **II-291**
Combining of Basic Shapes in Design

**10. Zhivko Iliev, Georgi Dinev** ..... **II-297**
Improving the Maintenance of Drive Sheave of Hanging Ropeway

**11. Victor Rizov** ..... **II-303**
Longitudinal Fracture Analysis of Multilayered Beams Loaded in Torion

**12. Victor Rizov** ..... **II-307**
Longitudinal Fracture Analysis of a Multilayered Beam with Non-Linear Material Behavior

**13. Asen Vergov, Georgi Uchkunov** ..... **II- 311**
Kinematic Analysis of Lever-Gear Movement Convertor

**14. Yordan Kirov, Georgi Uchkunov** ..... **II-315**
Experimental Study of Pieces of Paper Used in Production of Corrugated Cardboard (Corrugated Layer)

**15. Zdravko Vitlarov** ..... **II-319**
Methods of Synthesis of Mechanisms of Electro Mechanical Press For Expanded Metal

**16. Angel Lengerov, Dechko Ruschev, Stiliyana Taneva, Georgy Levicharov** ..... **II-323**
Mathematical Model of Optical Glass Cutting by Applying Vibrating Impact

**17. Georgy Levicharov** ..... **II-326**
Study the Influence of Spherical Motion Burnishing Process on the Energy Balance of the System „Tool - Work-Piece"

**18. Teofil Iamboliev** ..... **II-331**
Study of Pulsed Tig Welding with Constant Frequency and Mean Current

SECTION 5 • СЕКЦИЯ 5
**TRANSPORT AND AVIATION ENGINEERING**
**Транспортна и авиационна техника** ..... **II-337**

**1. Konstantin Metodiev** ..... **II-338**
Accident Modelling of a Quadcopter

**2. Krasimir Ambarev** ..... **II-344**
An Experimental Study of The Influence of Advance Processor on Some Operating Performance Indicators of Spark Ignition Engine Working with LPG

**3. Radoslav Kostov** ..... **II-350**
Gas Exchange Process in Petrol Engine Turbocharged

**4. Nikolay Gueorguiev, Aleksandar Kolarov** ..... **II-356**
Trends in the Development of Naval Mine Countermeasures Systems

**5. Nikolay Gueorguiev, Aleksandar Kolarov** ..... **II-362**
Method of Enhancing Anti-Mining Resistance to Bottom Mines

SECTION 6 • СЕКЦИЯ 6
**NATURAL SCIENCES • Природни науки** ..... **II-368**

**1. Atanaska Georgieva, Albena Pavlova** ..... **II-369**
Lp (K) - Solution of Nonlinear Volterra-Hammerstein Integral Equations

**2. Ivan Badev, Georgi Zlatanov** ..... **II-375**
Odd-Dimensional Spaces with Symmetric Affine Connection

**3. Ivan Badev, Marta Teofilova, Georgi Zlatanov** ..... **II-379**
Cartesian Generalized Compositions in Spaces with a Symmetric Affine Connection

**4. Delyana Dimova** ..... **II-385**
An Algorithm for Determining and Comparing the Levels of Economic Development in the Districts in Bulgaria

**5. Iliycho Iliev** ..... **II-391**
Parametric Regression Models for CuBr Laser

**6. Liliya Petrova** ..... **II-395**
Rectangular Platesin Single Trigonometric Series with Symmetry

7. **Kiril Kolikov** ..... **II-401**
Magnetic Moment and Velocities of Self-Rotation in Toroidal Model of the Neutron

8. **Ivan Stoyanov Valkov** ..... **II-405**
Physics and Production

SECTION 7 • СЕКЦИЯ 7
**INDUSTRIAL MANAGEMENT • Индустриален мениджмънт** ..... **II-409**

1. **Toni Mihova, Valentina Nikolova - Alexieva** ..... **II-410**
Principles and instruments of LEAN Methodology

2. **Mina Angelova** ..... **II-415**
Management of the Motivation Process in Enterprises

3. **Thomas Moser** ..... **II-419**
Causes, Prevention and Correction of Project Failures and Budget Overruns

4. **Thomas Moser** ..... **II-425**
Will Agile Methods Resolve the Complexity Crisis in Software Engineering?

5. **Antonia Lazarova** ..... **II-431**
Integrated Use of Statistical Approaches for Evaluation the Business Environment Based Data Questionnaire Survey

6. **Nikolay Patonov, Ardian Durmishi** ..... **II-437**
Formation of a Modern Tax System in the Republic of Albania

7. **Ivanka Bankova** ..... **II-441**
Potentials for the Development of Transport infrastructure of Bulgaria in the Context of Sustainable Development

8. **Svetoslav Dimkow, Otman Ahmed** ..... **II-447**
Assessing the Effectiveness of Collaboration in Business Networks

9. **Svetoslav Dimkow** ..... **II-453**
Development of Business Organizations Through Collaborative innovations

10. **Svetlana Borisova** ..... **II-459**
Opportunities and Problems in the Assessment of Labour Achievements

© International Scientific Conference on Engineering, Technologies and Systems
TECHSYS 2016, Technical University – Sofia, Plovdiv branch
26 – 28 May 2016, Plovdiv, Bulgaria

# PLENARY AND INVITED PAPERS

# ПЛЕНАРНИ И ПОКАНЕНИ ДОКЛАДИ

© International Scientific Conference on Engineering, Technologies and Systems
TECHSYS 2016, Technical University – Sofia, Plovdiv branch
26 – 28 May 2016, Plovdiv, Bulgaria

# SPACE APPLICATIONS OF THE LIGHTWEIGHT GRADIENT MATERIALS BASED ON NC-AL ALLOYS

WITOLD PAWLOWSKI, JAKUB SIKORSKI, LUKASZ KACZMAREK

**Abstract:** *In the paper the latest achievements of the lightweight gradient materials based on nc-Al alloys were utilized in order to create manipulators applied in cryogenic conditions of the outer space. The properties of the modern material based on nc-Al alloys are discussed. The planetary, compact, 3-stage gearboxes made of modern structural materials are presented. The 5 degree-of-freedom (DOF) space manipulator arm with rotary joints in which the gearboxes are applied is also proposed. The advantages of the new lightweight materials in the construction of the space mechanisms are outlined.*

**Key words:** *light-weight materials, cryogenic conditions, space manipulators*

## 1. Introduction

Extremely high cost of launching unit weight into space (around 10k$/kg) is a driving force for the development of new lightweight structural materials (LwSM) for space vehicles which can sustain harsh cryogenic conditions. The aim of the research project being investigated is to develop LwSM based on nc-Al with deposited gradient C-coating with high wear and contact fatigue resistance under cryogenic conditions for space applications (e.g. gear boxes in extra-terrestrial vehicles).

This is highly motivated by the economic and technological requirements including cost effectiveness. According to the Russian Federal Space Agency, the cost of sending 1kg into Earth orbit is around 10k$ and it dramatically increases when the load has to be delivered to another planet within the solar system. The reduction of spacecraft weight is among the most cost effective ways and it requires using of more Lightweight Materials (LwM) which exhibit appropriate properties even in the cryogenic conditions of deep space. Obviously, the use of steel as a structural material for the Unmanned Space Vehicles (USV) is highly uneconomical. Large number of extensive studies on the existing and new LwM is carried out to replace steel and to meet requirements for their mechanical and tribological properties under those conditions while having low specific weight.

## 2. Properties of the nc-Al alloys

For a number of years, a trend to lighten the weight of products has dominated global industry. This applies to electronic components used in the production of mobile phones, tablets but also to devices such as tanks and aircraft [1 – 5]. The drive to lighten the weight of vehicles is the sum of a number of different needs. Decreasing fuel consumption (improving fuel economy) and enhancing the maximum range of vehicles are of major importance. It would be also extremely profitable for the military industry where increased range and maneuverability could be critical. Alloys of lightweight metals such as aluminum, titanium, magnesium or composites based on them are used in order to make products lighter [6 – 7], and of those, aluminum and its alloys have become an especially popular choice in many industries [8 – 11]. Their strength-to-density ratio is their major advantage and therefore they are more and more frequently used in structural components where component weight is very significant. Nevertheless, their mechanical properties in most cases are insufficient to render them a reliable substitute for functional steel components e.g. gearwheels.

To improve mechanical properties of aluminum based alloys, heat treatment parameters are optimized and combinations of thermal and mechanical treatments are used [12 – 16]. The combination of shot peening and two-stage age hardening appears to be very promising as not only

Copyright © 2016 by Technical University of Sofia, Plovdiv branch, Bulgaria ISSN Online: 2535-0048

does it lead to the hardening of the material and increased strength of the surface layer (due to the presence of core-shell type of phases in the continuous phase of some aluminum alloys) but it also introduces advantageous compressive stresses. Aluminum alloys subject to the combined treatments exhibit mechanical properties similar to those of steel, which significantly expands the range of their applications to include critical structural components as well as subcomponents working under friction conditions e.g. gears in unmanned vehicles. The synergistic effect of shot peening and two-stage age hardening has caused a surge in the number of studies on commercial applications of heat treated aluminum alloys. That is also the reason why the main objective of the foregoing study was to investigate the applicability of 7075 aluminum alloy treated with two-stage thermo-mechanical treatment to lightweight transmission gears. Such transmissions could be used in drones or military robots.

The novel core/shell precipitation hardened nc-Al alloys are among the most promising candidates with a number of advantages compared to the current Ti- and Mg-based alloys. The paper investigates the application possibility of these alloys in combination with carbon based coatings, which can potentially solve the main drawback of these materials insufficient wear and contact fatigue resistance under cryogenic conditions in space.

Unique properties of this material (low friction coefficient, higher yield strength and elongation with additional increase in fatigue resistance under cryogenic conditions) will allow its application for e.g., drive transmissions system with the reduce weight in space vehicles for planets exploration. Weight reduction subsequently contributes to the cost reduction of space transportation. This fully complies with the objectives of Russian Federal Space Agency and with NASA expedition program initiatives for the period 2014-2022 which are focused on the construction and transport of light mechanical assemblies for manipulators.

Besides space applications, the newly developed Al-based materials can be widely applied in general and even special aviation, e.g. for the construction of the advanced ultra-light drones, thus having wider societal impact.

## 3. Space construction requirements

The cost of launching unit weight of space vehicles into Earth orbit or even to the other planet is prohibitively high and there is a strong economic and societal pressure to reduce that cost. The reduction of spacecraft weight is among the most effective approaches and it is limited by the availability of more lightweight structural materials which exhibit sufficient properties even in the harsh cryogenic conditions in the space. Rapidly growing aerospace industry permanently looks for lightweight functional and structural materials. The properties of that material should comprise good resistance to stress in cryogenic conditions as well as high fatigue strength in order to sustain hostile outer space conditions without being prone to defects. Thermal expansion coefficient of that material should also be as low as possible not to induce any tensions or strains between cooperating mechanical elements. What is also important, the material should be free of internal defects such as air bubbles or pores, which should be avoided or eliminated during technological process of molding or casting. Those defects can be of high negative influence in high vacuum and low temperature in outer space conditions.

## 4. Planetary gear transmission system

The first attempt has been undertaken to construct the planetary transmission system which could be successfully applied in the robotic space arm. The requirements for low mass and good cryogenic behavior properties induced the need of introducing the optimization procedures into the design process. The planetary gearbox design prerequisites comprised the following requirements:

- compact construction,
- minimum input power: 800 W,
- maximum output rotational speed: 16 rpm,
- minimum output torque: 400 Nm.

Having selected the appropriate electrical motor which could withstand the outer space conditions as well as could drive the construction of the manipulator, the following parameters could be additionally specified and assumed to be the prerequisites in the planetary gearbox design process:

- input power: 900W,
- nominal rotational speed: 4600 rpm,
- torque: 1.87 Nm

The resultant overall gear ratio which had to be achieved was minimum 287.5 (reduction). The assumed ratio was 280. Value of the ratio is high enough to plan the planetary transmission as the three-stage gearbox with the ratios of the subsequent stages respectively: 8x6x6.

The planetary gearbox which meets all these requirements has been constructed and it is presented in Fig. 1.



***Fig. 1.*** *The planetary transmission system*

The exploded view of the planetary gearbox construction is presented in Fig. 2.



***Fig. 2.*** *The exploded view of the planetary gearbox*

In the first version of the construction the structural material which was applied was steel. The total mass of the gearbox made of steel was 11.847 kg.

In order to make these construction more lightweight the optimization process was performed. It comprised the strain and stress analysis by means of finite element method (FEM) of the whole construction (assembly). Therefore the contact definition among every cooperating elements had to be created according to the character of their mutual interaction. Having performed the analysis the total mass was minimized down to 9.754 kg.

The next attempt was to apply structural lightweight materials which could withstand the conditions both the strain and stress as well as those of the severe outer space environment. Therefore the following materials were applied:

- the casing – nc-Al alloy (2.7 g/cm$^3$),
- the gears, shafts, pins – Ti alloy (4.43 g/cm$^3$),
- bolts, nuts – stainless steel (8 g/cm$^3$),
- fully ceramic bearings (3.18 g/cm$^3$).

Additionally the ceramic lightweight bearings were applied which makes the gearbox possible to operate without any lubrication. After introducing the appropriate changes in the whole construction the overall mass of the planetary gearbox was minimized down to 4.250 kg.

The resultant properties of the newly designed planetary gearbox are listed below:

- input power: 900W,
- nominal rotational speed: 4600 rpm,
- total gear ratio: 8x6x6 = 288,
- output torque: 484 Nm,
- output rotational speed: 16.0 rpm,
- overall mass: 4.250 kg.

The result of mass optimization resulted in over 2 fold mass reduction of the mechanism, the number of which in the whole robotic arm construction is 3.

According to the assumptions and optimized design procedures, the smaller size planetary gearbox has been constructed. The parameters of the box are as follows:

- input power: 300W,
- nominal rotational speed: 8500 rpm,
- total gear ratio: 8x8x8 = 512,
- output torque: 155 Nm,
- output rotational speed: 16.6 rpm,
- overall mass: 2.095 kg.

The number of the smaller size gearboxes in the robotic arm construction is also three.

In the figure 2 the number of the elements is clearly visible. The casing and the plates constitute the main part of the mechanism that influences the total mass of the gearbox. That is why application the nc-Al alloy of low density resulted in that significant mass reduction.

## 5. Space manipulator arm

The planetary transmission systems have been applied in the space manipulator arm. The arm is designed to operate outside the satellite or spaceship in order to perform occasional amendments of the outer coating of the ship or any mechanisms which need repairing or servicing (antennas, solar panels, telescopes etc.).

The kinematics of the robotic arm comprises serial kinematics with rotary joints. The mechanical part of the arm is based on five rotary joints. Each joint is equipped with the planetary gearbox described above: three bigger size planetary gearboxes and the following two – smaller size gearboxes . The manipulation activities is performed by the gripper of parallel jaw motion. In the construction of the gripper the parallel lever mechanism is applied. In jaw clamping mechanism the planetary gearbox of small size was applied in order to save as much mass as it is possible. That results in lowering the mass placed on the long overhang in relation to the manipulator mounting plate. The arm construction is based on the typical

profiles made of lightweight nc-Al alloy. The 3D view of the manipulator is presented in Fig. 3. Zoomed view of the gripper construction, in which the small size planetary transmission system is applied is presented in Fig. 4.



***Fig. 3.*** *The outer space robot arm manipulator*

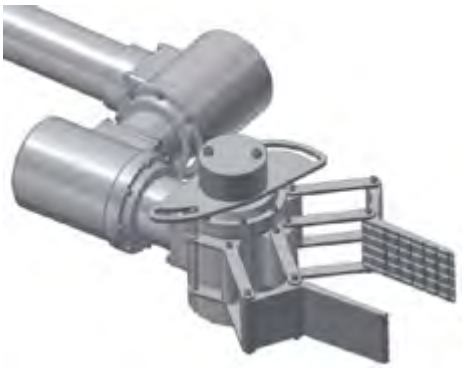


***Fig. 4.*** *The gripper construction*

## 6. Conclusions

In the paper the space application of the construction of robot manipulator arm equipped with specially designed planetary transmission systems is presented. The high performance of the mechanism accompanies with lightweight construction made of modern structural materials e.g. nc-Al alloy. Total mass of the initial robotic arm made of steel is 55.2 kg whereas the optimized construction mass made of lightweight structural material is 23.25 kg. The optimization and appropriate material selection made the whole construction robust, efficient and lightweight. These properties are of great importance as far as the space application are being concerned. The analysis showed that reaching comparative properties the constructions made of modern structural materials can be more than twice as lightweight as the traditional design. It highly influences the level of funds that have to be found to prepare the successful space mission.

This work was supported by European Commission from ERA.Net RUS Plus programme under project: LIGHTMAT4SPACE – Lightweight nanocrystalline aluminium based material for space applications (modelling and technology verification).

## REFERENCES

1. Bloch, K., Nabialek M., Pietrusiewicz P., Gondro J., Dospial M., Szota M., Gruszka K. (2012). *Acta Phys Pol A.* 126, 108.
2. Nabialek M., Szota M., Dospial M. (2012). *J Alloy Compd*. 526, 68.
3. Dospial M. J., Nabialek M. G., Szota M., Mydlarz T., Oźga K., Lesz S. (2012). *J Alloy Compd.* 536, 324,
4. Trško L., Guagliano M., Bokůvka O., Nový F. (2014). *Procedia Engineering*, 74, 246.
5. http://www.european-aluminium.eu/
6. Jiang F., Zhang H., Meng X., Li L. (2014). *Mater Design,* 55, 280.
7. Geng L., Huang L. (2014). *Acta Metall Sin. (Engl. Lett.)*, 27(5), 787.
8. Babalola P.O., Inegbenebor A.O., Bolu C.A., Inegbenebor A.I. (2015). *JOM,* 67(4).
9. Reilly C., Duan J., Yao L., Maijer D.M., Cockcroft S.L. (2013). *JOM*, 65(9).
10. Choi Y., Kim D. U., Kang B. Y., Park D. K., Lee D. J., Lee S.,. Shin H. T. (2013). *J Mech Sci Technol.* 27 (11), 3445.
11. Sakhrieh A., Al-Ghandoor A. (2013). *Energ Convers Manage.* 65, 715.
12. Kaczmarek Ł., Steglinski M., Sawicki J., Swiniarski J., Batory D., Kyzioł K., Kołodziejczyk Ł., Szymanski W. (2013). *Archives of Metallurgy and Materials*, 58 (2), 535.
13. Kreethi R., Verma P., Dutta K. (2015). *Trans Indian Inst Met.* 68(2), 229.
14. Emani S. V., Benedyk J., Nash P., Chen D. (2009). *J Mater Sci.* 44, 6384.
15. Byczkowska P., Sawicki J., Stegliński M. (2014). *Inż Mat.* 6(202), 459.
16. Farshidi M.H., Kazeminezhad M., Miyamoto H. (2013). *Mater Sci Eng A.* 580, 202.

Witold Pawlowski, PhD, DSc, TUL prof.
Jakub Sikorski, MSc.
Lukasz Kaczmarek, PhD, DSc, TUL prof.
Lodz University of Technology (TUL)
Address: 1/15 Stefanowskiego,
90-924 Lodz, Poland
E-mail: witold.pawlowski@p.lodz.pl
E-mail: jakub--sikorski@wp.pl
E-mail : lukasz.kaczmarek@p.lodz.pl

© International Scientific Conference on Engineering, Technologies and Systems
TECHSYS 2016, Technical University – Sofia, Plovdiv branch
26 – 28 May 2016, Plovdiv, Bulgaria

# SMC Industrial Automation Bulgaria
# "Best practices in training students in field of automation"

**Rosen Kosturkov**

SMC International Training is the educational division of SMC Corporation, the world leader in innovation and the sales of pneumatic and electro-pneumatic components for industrial automation.

SMC International Training has a clear commitment to offer Training adapted to the needs of industry; training orientated to the development of the professional expertise required for the most diverse sectors (automotive, pharmaceutical, semi-conductors, foodstuffs, etc.)

## What is happening in the Industry?

Let's take a short look in the past 50-60 years of the industry. What is happening in the Industry?
The **EVOLUTION** is the first word that came in mind.
The EVOLUTION of the classic technologies, like mechanics and electricity, bring in our life new branches like Electronics, Computer science, and Digital communication.
This was possible because of constant **INNOVATION** processes in the Industry.

And it is happened in very short period of time: Just think about - the first CNC model was built in MIT in 1952. What about the appearance of the PET bottles? Less than 50 years since that.

Now we see that the constant INNOVATION process is the driving force of the modern world.
The constant EVOLUTION and INNOVATION bring to the industry new feature – the **FLEXIBILITY**

**EVOLUTION, INNOVATION, FLEXIBILITY –** key terminology which defines the situation faced by industry in recent years.

New market demands are required greater level of automation in production process. Because of the increased competitions, the constant search for cost production effectiveness, increased product quality, diversity of product lines and families is a must for every World-Class producer.

Producing more different models on the one and the same production line – you can see this everywhere.

Today the **AUTOMATION of the processes** is available even for small companies.
Something more – it is not possible to be competitive on the market without **implementation of the state of the art technologies**.

**Efficiency, Productivity and Quality** is the key concepts unreachable without AUTOMATION

## It is moving!

Integration of technologies is the core of the AUTOMATION. The modern Industry **IS MOVING**.
The automated companies follow common concept – **INTEGRATION of Technologies**

Classic technologies involved, start one by one to merge into each other, creating multi-technical environment in which they all are interrelated.

Copyright © 2016 by Technical University of Sofia, Plovdiv branch, Bulgaria ISSN Online: 2535-0048

## Integration and Interaction of Technologies

This integration of technologies is represented well by using a "**Pyramid of Automation"**, which includes the five technological levels which can be considered in an industrial environment.




- The first level or "field level" comprises the physical devices existing in industry such as actuators and sensors.
- The second level or "control level" includes logical devices such as PCs, PLCs, PIDs, etc.
- The "supervisory level" (third level) corresponds to control and data acquisition systems (SCADA).
- The manufacturing execution systems or MES are at a higher level or "planning level".
- The top of the pyramid ("management level") is comprised of the company's integrated management system (ERP).

All technologies interrelate, both within each level and between the different levels by using **Industrial Communications.**

The multi –technological environment means that specialization (mechanics, electronics, etc.) are no longer sufficient and technician must develop a series of professional abilities to interact with technologies and to be able to undertake his/her work properly.

Analyze, Design, Teamwork, Installation & assembly, Diagnosis and repair of the equipment, Interpretation of documentation, Programming of controllers, Decision-taking, Coordination of processes for preventive maintenance, Monitoring of communication networks, Interaction with graphic interfaces and etc. are only basic example of professional skills which are must for professionals.

The main questions, which we are facing in our fast growing and evolving industry are:

**Are our graduated well qualified?**
**Are they prepared to face the real industry environment?**
**And how we educate and train the students?**
**How do we face these changes demanded from industry in the educational system?**

According to the **Learning Pyramid** developed by Edgar Dale (National Training Laboratory), the different percentage of knowledge is adopted by students with different methods:

5% of what students learn they've learned from lectures

10% of what students learn they've learned from readings

20% of what students learn they've learned from audio-video presentations

30% of what students learn they've learned when they see demonstrations

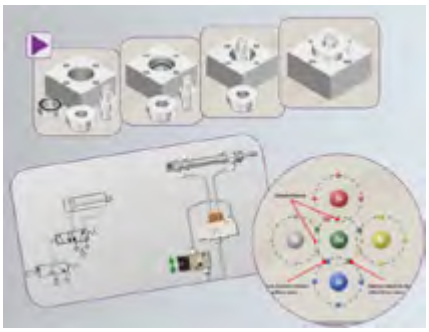
50% of what students learn they've learned in discussion groups with professionals



**75% of what students learn they've learned using training equipment**

Based on both pyramids – Automation and Learning, SMC developed series of designed for Technical High Schools and Technical Universities

## Training solutions, adapted to the modern industry demands



**eLEARNING-200 - The perfect theory companion**
eLEARNING-200 is a flexible learning system where knowledge can be acquired dependant on the user's available time and requirements. Students have the option to take actual classes and additional Internet courses when this suits them best.

To be able to develop different technology skills, theoretical knowledge must be acquired first. SMC International Training presents the eLEARNING-200 course programme: the perfect complement to our didactic equipment.

eLEARNING-200 offers a total of 13 courses based on the automation pyramid, covering technologies in automated systems.

- SMC-100 – Introduction to industrial automation
- SMC-101 – Principles of pneumatics
- SMC-102 – Introduction to electricity
- SMC-103 – DC electricity
- SMC-104 – AC electricity
- SMC-105 – Solid state
- SMC-106 – Introduction to wiring
- SMC-107 – Introduction to electric motors
- SMC-108 – Sensors technology
- SMC-109 – Programmable controllers
- SMC-110 – Process controls
- SMC-111 – Hydraulics / electrohydraulics
- SMC-113 – Robotics



**PNEUMATE-200**
Small-sized, light and portable training equipment that includes extensive features which provide an enjoyable and rapid way of acquiring the fundamental concepts of pneumatics and electro-pneumatics.



**PNEUTRAINER-200, VAC 200, HIDROTARINER – 200**

Fully modular systems designed for the development of professional skills related to **pneumatics and electro-pneumatics**, **vacuum** and **hydraulics**.



**AUTOMATE-200, MAP-200**

The series of automated Training stands, which allow students to will be able to study the basic **principles of automation easily and intuitively**.

It includes a multimedia DVD with guided lessons and activities. It can be controlled manually or automatically using a PLC



**IPC-200, MAS-200, FMS-200,CPS-200, FAS-200,ITS-200**

These series of systems is the ideal answer to integral training in industrial automation.

They are fully modular and flexible equipment and in keeping with industrial reality.

The technologies included in its different variations, as well as the assembly process with several variants, allow the students to develop the professional skills required by today's automated industry.



**HAS-200 Highly Automated System**

The HAS-200 system has been devised based on the training requirements in industries with a high level of automation. Its versatility and attractive design allow the reproduction (emulation) of the operation of a real factory, thus allowing the study of different scenarios.

The modular features of all training equipments enable the introduction of variations in its stations so that they adapt to the different requirements of companies and training centres.

From a simple configuration of one station only (working fully autonomously) to a complex configuration with eight or ten stations, the possibilities are endless.

In addition, it facilitates a staggered investment, i.e. starting with an initial simple configuration which can be easily enhanced by adding workstations.

All the components in the systems **are used in industry**, so that the students can work with real elements at all times making the learning process more meaningful.

The system includes a whole series of feeding, handling, verification and loading operations etc. carried out using components from different technologies (**pneumatics, hydraulics, sensors, robotics, communications, control and HMI**).They includes the breakdown simulation system which generates up to 16 different breakdowns to be diagnosed by the students.

The different process stations assemble a turning mechanism. To provide the system with greater flexibility, stations adapt to a wide variety of assemblies, introducing variations in the materials, colours and part sizes.

The combination of all these possibilities means that a lot of different assemblies can be obtained enabling the use of production management strategies.
The control panels are completely modular and can be rapidly disassembled so the students can design and integrate a new control.

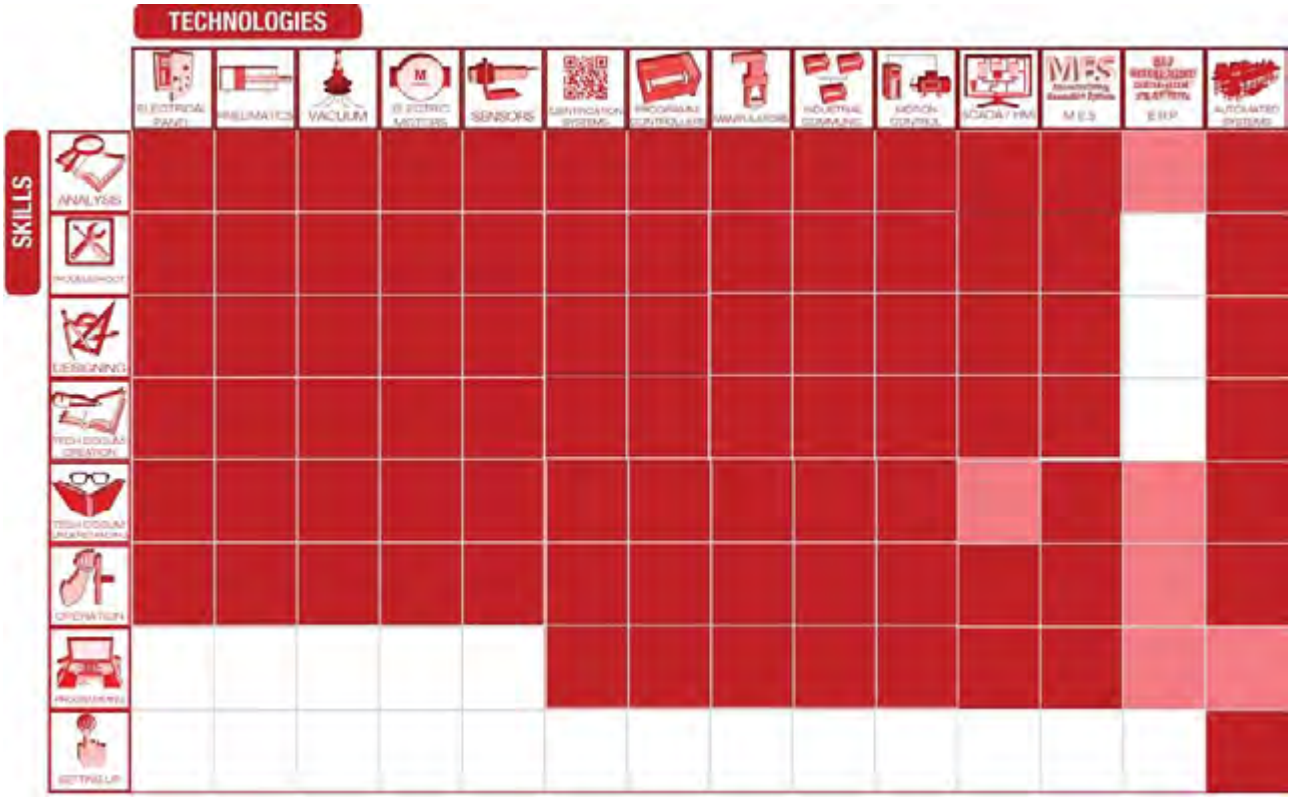
Aspects such as aesthetics, user motivation and the development of transversal skills (such as teamwork etc.) have also been taken into account in the conception and design process.

**At university level, these systems represent a powerful development platform for research projects**.

Every Training System includes complete documentation, oriented to the development of the professional skills. The documentation includes:

USER's MANUAL, THEORY MANUAL, EXERCISES MANUAL (STUDENT and PROFESSOR)

The acquired skills in different technologies when students use the SMC training equipments are represented in SKILLS/TECHNOLOGIES table.




SMC Industrial Automation Bulgaria EOOD
Business Park Sofia, Building 8C - 6th floor
1766 Sofia
www.smc.bg
www.smctraining.com

14.05.2016
Sofia, Bulgaria.

© International Scientific Conference on Engineering, Technologies and Systems
TECHSYS 2016, Technical University – Sofia, Plovdiv branch
26 – 28 May 2016, Plovdiv, Bulgaria

# SECTION 1 • СЕКЦИЯ 1

## AUTOMATION AND CONTROL SYSTEMS

## АВТОМАТИКА И СИСТЕМИ ЗА УПРАВЛЕНИЕ

© International Scientific Conference on Engineering, Technologies and Systems
TECHSYS 2016, Technical University – Sofia, Plovdiv branch
26 – 28 May 2016, Plovdiv, Bulgaria

# DUAL MATRIX CONVERTER FEEDING AN OPEN-END LOAD BASED ON MODIFIED DIRECT TRANSFER FUNCTION APPROACH

BELADEL ABDELKADER[1], KOUZOU ABDELLAH[1], AHMED HAFAIFA[1] , DJILALI MAHI[2]

**Abstract:** *The present paper deals with the control of the three-phase-to-three-phase dual matrix converter feeding an open-end three-phase load. The main objective is the use of the Direct transfer function approach of Venturini to achieve the required control of the presented dual matrix converter. The both matrix converters are supplied from the same three phase power source. Whereas; the two output voltage systems of the dual matrix converter are shifted with 180 degrees. The performance and the advantages of the proposed control approach applied to the presented topology are finally discussed through simulation results. Furthermore, a short comparison between the single matrix converter close-end load topology and the dual structure applied to open-end load are also discussed.*

**Key words:** *Matrix Converter, Direct Transfer Function Approach (DFTA), Simulation Model, Open-end load, Dual matrix converter.*

## 1. Basics

Matrix converter (MC) and cyclo-converter are direct AC-AC power electronics converter, whereas a matrix converter is a forced commutated converter which can achieve variable amplitude and frequency at the output side. Indeed, the matrix converter presents many advantages in comparison with the classical indirect power electronics conversion that are based on two stages power conversion DC-AC and AC-AC. The main outstanding advantage of the matrix converter can be summarized as follows[1-2].

- ✓ The absence of the bulky DC-link and energy storage elements;
- ✓ sinusoidal input and output currents can be achieved;
- ✓ the easiness of the input power factor control for any load,
- ✓ Four-quadrant operation
- ✓ Simple and compact design

On the other side, due to the high integration capability of the semiconductor structures, the matrix converter topology is being recommended for several extreme and critical applications. However, the topology of the matrix converter itself has pushed the researchers to run after more favorable control strategies. In this context several modulation techniques have been developed to fulfil the requirement of the matrix converter control. Among these techniques two main control approaches are being used, the scalar approach such as; the direct transfer function approach (DTF) proposed by Venturini [3-4], and the space vector approach such as; direct and indirect space vector modulation (DSVM and ISVM) [5-6].

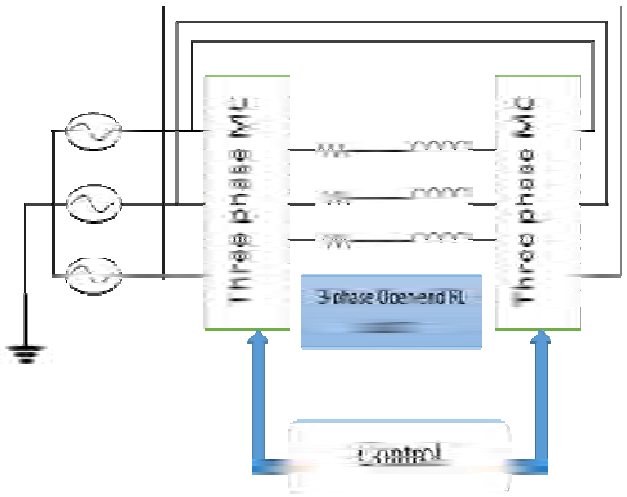



***Fig. 1.*** *Three phase Open-end Load drive system*

In the present paper, the direct transfer function control approach is applied to the matrix converter for feeding an open-end three-phase load topology to overcome the main problem of the common mode voltage and to achieve the more control flexibility and the operation reliability [7-8]. The

Copyright © 2016 by Technical University of Sofia, Plovdiv branch, Bulgaria ISSN Online: 2535-0048

principle of the mentioned topology is presented in Fig. 1. The both sides of the three-phase load are supplied via two three-phase to three-phase matrix converters. The two matrix converter have the same topology as it is shown in Fig. 2. The load is an open-end three-phase resistive-inductive load supplied by a dual matrix converter.

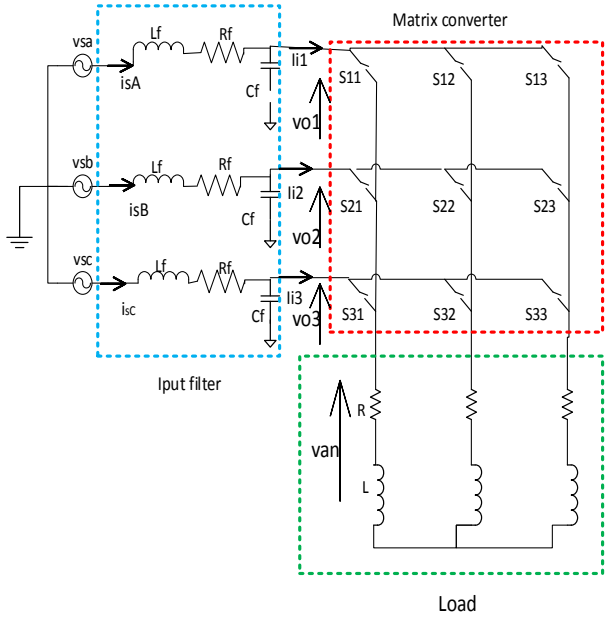



***Fig. 2.*** *Basics power circuit of Matrix converter with input filter*

A comparison between the application of one matrix converter for star load topology and the application of a dual matrix converter for open-end of the same load is presented in this paper. Simulation tests were performed for the single and dual matrix converter feeding the same load, the main aim is to demonstrate the effectiveness of the dual matrix converter topology and the used control approach is such application.

## 2. Formatting

The topology of a single three-phase input to three-phase output matrix converter is presented in Fig.2. Where $V_{i1}$, $V_{i2}$ and $V_{i3}$ are the input voltages and $V_{o1}$, $V_{o2}$ and $V_{o3}$ are the output voltages. Each leg has three bidirectional power switches to ensure the connection between one phase of the input and one phase of the output [9]. These switches are operating under the two main constraints, that the input should not be short-circuited and that the output side should not present an open-circuit at any instant. These are the two main important constraints imposed by the normal operation of the matrix converter to ensure its protection [10-16].

The vector of the input voltages are presenting the three phase power system network voltage that are expressed as follows:

$$\begin{bmatrix} V_{i1} \\ V_{i2} \\ V_{i3} \end{bmatrix} = V_{im} \begin{bmatrix} \cos(\omega_i t) \\ \cos(\omega_i t - 2\pi/3) \\ \cos(\omega_i t + 2\pi/3) \end{bmatrix} \quad (1)$$

The vector of the output voltages are given as follows:

$$\begin{bmatrix} V_{o1} \\ V_{o2} \\ V_{o3} \end{bmatrix} = V_{om} \begin{bmatrix} \cos(\omega_o t) \\ \cos(\omega_o t - 2\pi/3) \\ \cos(\omega_o t + 2\pi/3) \end{bmatrix} \quad (2)$$

$S_{ij}$ represents the ideal bidirectional states of the switches, where $i$ (=1, 2, 3) represents the index of the output side and $j$ (=1, 2, 3) represents the index of the input side. The relation between the output voltages and the input voltages can be achieved via an intermediate matrix M, which is known as the modulation matrix, hence the relation between the input and output voltages can be expressed as follows:

$$[V_o] = [M] \cdot [V_i] \quad (3)$$

the relation between the input current $[I_i]$ and the output current $[I_0]$ can be deduced as follows :

$$[I_i] = [M]^T \cdot [I_o] \quad (4)$$

Where $[M]^T$ represents the transposed matrix of $[M]$. Equation (3) can be represented in a developed manner as follows:

$$\begin{bmatrix} V_{o1} \\ V_{o2} \\ V_{o3} \end{bmatrix} = \begin{bmatrix} m_{11} & m_{12} & m_{13} \\ m_{21} & m_{22} & m_{23} \\ m_{31} & m_{32} & m_{33} \end{bmatrix} \begin{bmatrix} V_{i1} \\ V_{i2} \\ V_{i3} \end{bmatrix} \quad (5)$$

where the elements of the modulation matrix presenting the modulation coefficients are expressed as follows:

$$m_{ij} = \frac{t_{ij}^k}{T_s} \quad (6)$$

During the switching process, the bidirectional switches can connect or disconnect the phase $i$ of the input connected to the power source to/from the phase $j$ of the output connected to the load. In general the modulation coefficient must respect the following rules [7]:

- At every instant t, only one switch $S_{ij}$(i $= 1,2,3$)is conducting in order to avoid the short-circuit between the phases.

$$\sum_{i=1,2,3} S_{ij}(t) = 1; j = \{1,2,3\} \quad \forall t \quad (7)$$

- At every instant t, at least two switches $S_{ij}$ (j $= 1,2,3$) are conducting to ensure a closed loop load current.

- The switching frequency $f_s = {\omega_s}/{2\pi}$ must have a higher value than the maximum of $f_i, f_o (f_s \gg max\ (f_i, f_o))$.

- During the period $T_s$, the sum of the conducting time which is being used to synthesize the same output phase must be equal to $T_s$ this can be expressed by the following equation:

$$T_s = t_{1j} + t_{1j} + t_{1j} \quad \forall j \text{ with } j = 1,2,3 \quad (8)$$

## 3. Modified direct transfer function approach

The modified direct transfer function Approach was proposed in [1-3] and used in several previous research papers [11-14] to generate the appropriate firing pulses to the used bidirectional switches $S_{ij}$ of the 3x3 matrix converter. Whereas, The main aim is to ensure the ability of producing a three-phase output voltages $V_{o1}$,$V_{o2}$ and $V_{o3}$ with variable frequency and variable amplitude following the reference voltages, in the same time the power factor of the matrix converter input side which is supplied by a fixed amplitude-frequency three-phase voltages should be kept nearly equal to the unity and the harmonics content of the input currents $i_{i1}$, $i_{i2}$ and $i_{i3}$ should be decreased. It is obvious that the output voltages are rich in harmonics, however their fundamental components have to follow the behaviour of the desired or the reference voltages. Taking into account $t_{ij}$ as the conduction time of the $S_{ij}$ (when $S_{ij}$ is on) and Ts as the sampling time. The mean values of the output voltages over the $K^{th}$ sequence can be expressed as follows:

$$v_{o1}^{(k)} = v_{i1}^{(k)} \frac{t_{11}}{T_s} + v_{i2}^{(k)} \frac{t_{12}}{T_s} + v_{i3}^{(k)} \frac{t_{13}}{T_s}$$

$$v_{o2}^{(k)} = v_{i1}^{(k)} \frac{t_{21}}{T_s} + v_{i2}^{(k)} \frac{t_{22}}{T_s} + v_{i3}^{(k)} \frac{t_{23}}{T_s} \quad (9)$$

$$v_{o3}^{(k)} = v_{i1}^{(k)} \frac{t_{31}}{T_s} + v_{i2}^{(k)} \frac{t_{32}}{T_s} + v_{i3}^{(k)} \frac{t_{33}}{T_s}$$

The conduction time can be calculated function of each corresponding output, which means that for each phase there are three conduction times corresponding to the switches connected to the concerned phase. the details can be presented for each output phase as follows:

### 3.1. First phase

For the first phase, the conduction times of each switch is calculated as follows:

$$t_{11} = \frac{T_s}{3}(1 + 2qcos(\omega_m t + \theta_0))$$

$$t_{12} = \frac{T_s}{3}\left(1 + 2qcos(\omega_m t + \theta_0 - \frac{2\pi}{3})\right) \quad (10)$$

$$t_{13} = \frac{T_s}{3}\left(1 + 2qcos(\omega_m t + \theta_0 - \frac{4\pi}{3})\right)$$

### 3.2. Second phase

For the second phase, the conduction times of each switch are given by:

$$t_{21} = \frac{T_s}{3}\left(1 + 2qcos(\omega_m t + \theta_0 - \frac{4\pi}{3})\right)$$

$$t_{22} = \frac{T_s}{3}(1 + 2qcos(\omega_m t + \theta_0)) \quad (11)$$

$$t_{23} = \frac{T_s}{3}\left(1 + 2qcos(\omega_m t + \theta_0 - \frac{2\pi}{3})\right)$$

### 3.1. Third phase

Finally, for the third phase, the conduction times of each switch are presented as:

$$t_{31} = \frac{T_s}{3}\left(1 + 2qcos(\omega_m t + \theta_0 - \frac{2\pi}{3})\right)$$

$$t_{32} = \frac{T_s}{3}\left(1 + 2qcos(\omega_m t + \theta_0 - \frac{4\pi}{3})\right) \quad (12)$$

$$t_{33} = \frac{T_s}{3}(1 + 2qcos(\omega_m t + \theta_0))$$

Where $\theta_0$ is the initial phase angle.
The output voltage of the matrix converter at $K^{th}$ sequence can be obtained using the modulation matrix at $K^{th}$ sequence:

$$\left[V_o^{(k)}\right] = \left[M^{(k)}\right] \cdot \left[V_i^{(k)}\right] \quad (13)$$

where, the elements of the matrix $[M^{(k)}]$ are presenting the conduction times of each switch during one sampling time $T_s$, hence it is presented as follows:

$$[M^{(k)}] = \frac{1}{3}[\delta] + \frac{2q}{3}\begin{bmatrix} cos(A) & cos\left(A-\frac{2\pi}{3}\right) & cos\left(A-\frac{4\pi}{3}\right) \\ cos\left(A-\frac{4\pi}{3}\right) & cos(A) & cos\left(A-\frac{2\pi}{3}\right) \\ cos\left(A-\frac{2\pi}{3}\right) & cos\left(A-\frac{4\pi}{3}\right) & cos(A) \end{bmatrix} \quad (14)$$

Where:

$$\begin{cases} \delta_{ij} = 1 \\ A = \omega_m t + \theta \end{cases} \quad (15)$$

## 4. Equations and symbols

In this paper, two simulation tests were performed to prove the advantage of the use of the open-end load fed by a dual matrix converter having the same topology and characteristics. The first simulation is presenting a star three-phase load fed by a single matrix converter, where the output voltage is characterized by a fundamental frequency $f_0 = 25\,Hz$ and an amplitude of $V_0 = 150\,V$. The parameters of the input voltage and the balanced three-phase load are presented in Table. 1. On the other side, due to the distortion which may occur in the input current and to avoid the propagation of this kind of harmonics pollution toward the source an input LC filter is inserted as it is clearly shown in Fig. 2 and Table. 1.

***Table 1.*** *Simulation parameters*

| | | |
|---|---|---|
| $V_S$ | Input voltage | 220 V |
| $f_S$ | Input frequency | 50 Hz |
| $R_f$ | Input filter Resistance | $0.5\,\Omega$ |
| $L_f$ | Input filter inductance | $0.003\,H$ |
| $C_f$ | Input filter Capacitance | 2e-5 $\mu F$ |
| $R_L$ | Load Resistance | $10\,\Omega$ |
| $L_l$ | Load Inductance | $0.0112\,H$ |

### 4.1. Single Matrix Converter feeding to star three-phase load

In this case, a single matrix converter is feeding a three-phase load under star connection. The output voltages, the output currents and the output phase to phase voltages of the matrix converter are presented in Fig. 3. 4, and 5. respectively. The fundamental of the single phase output voltage is 153.9 V with a relatively high THD of 85.68% Fig. 6, in the same time a clear harmonics rays or a group of harmonics can be remarked clearly near the switching frequency $f_s = 2\,kHz$, however and due to the inductive nature of the load the output current is characterized by a low THD of 4.17%, where the high order harmonics are eliminated Fig. 7.

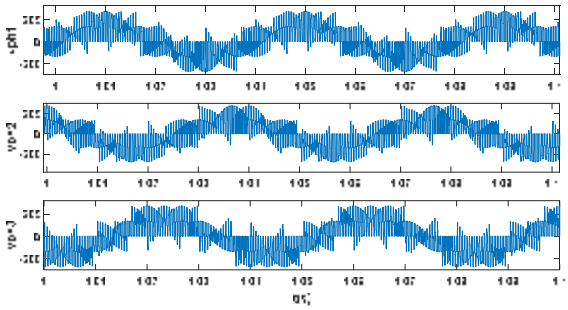


***Fig.3*** *The output voltage of the single matrix converter.*

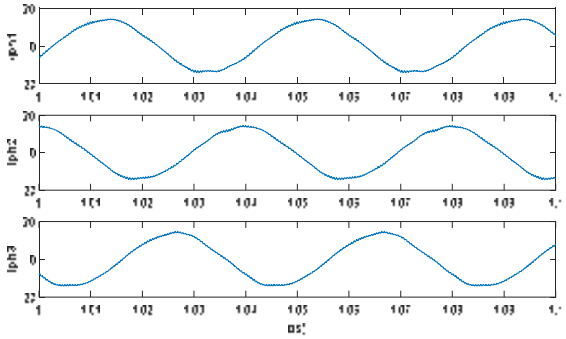


***Fig. 4.*** *The output currents of the matrix converter.*

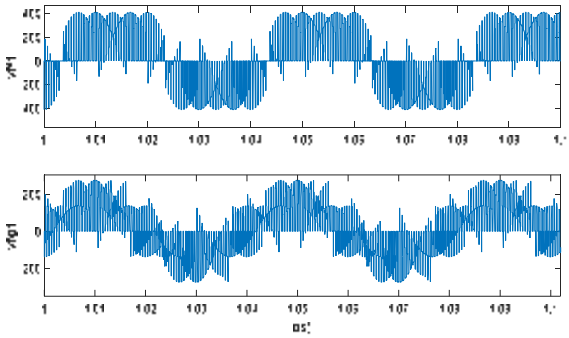


***Fig. 5.*** *The output phase to phase voltage and one phase voltage of the matrix converter.*

On the other side, the effect of the insertion of the input filter can be shown clearly in Fig. 8, where the input current from the source side is nearly sinusoidal with neglected ripples with THD = 11.37%, contrary the current from the matrix converter side has a THD = 84.95%. Unfortunately, an important value of the common mode voltage at the star point of the load is generated. It is due

mainly to the components of voltage harmonics possessing a frequency multiply of three times of the fundamental frequency Fig. 9. It can present a serious risk for the equipment, the insulation, the operator its self, and the quality of power.

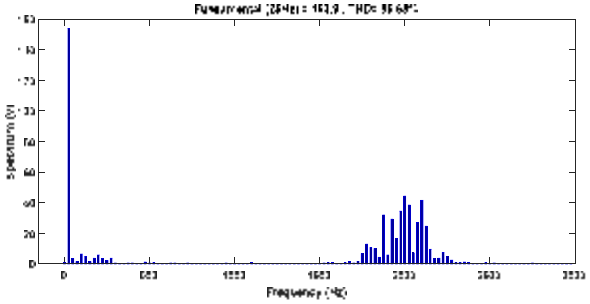


***Fig. 6.*** *The spectrum of the matrix converter output voltage.*

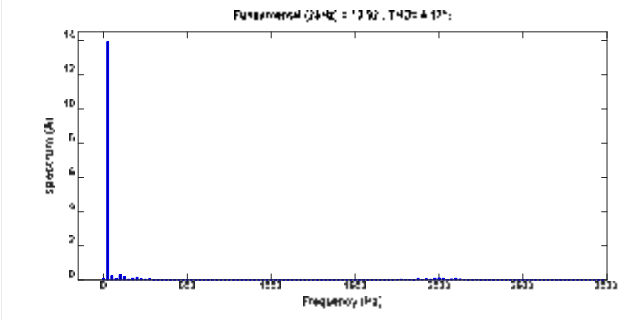


***Fig. 7.*** *The spectrum of the matrix converter output current.*

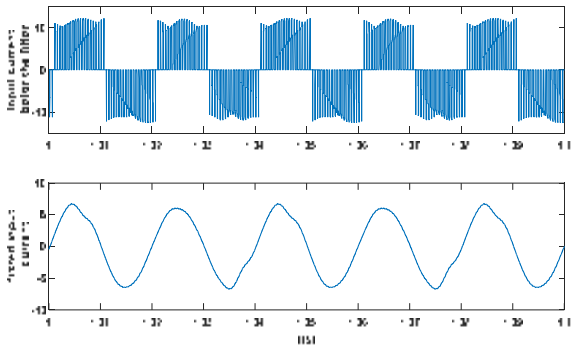


***Fig. 8***. *The input current of the Matrix converter.*

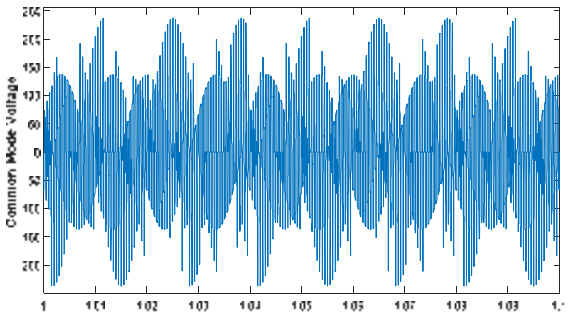



***Fig. 9.*** *The common-mode voltage waveforms*

### 4.2. Dual Matrix Converter applied to open-end three-phase load

In this case, the both sides of the three-phase load are connected to two similar matrix converter (dual matrix converter) with the same characteristics as the single matrix converter aforementioned. The idea concerning this topology is that the voltage applied at the load will have a three-level voltage and the dual matrix converter will be seen from the load as a three-level converter. Under this topology the common mode voltage (CMV) will be totally removed and the three-phase load can be controlled independently, however due to the balanced nature of the load, the voltage applied at each load phase is the same, taking into account the eventual required shift phase. Figures 10. and 11. present the voltages between the two terminals of the three-phase load and the currents in the load respectively.

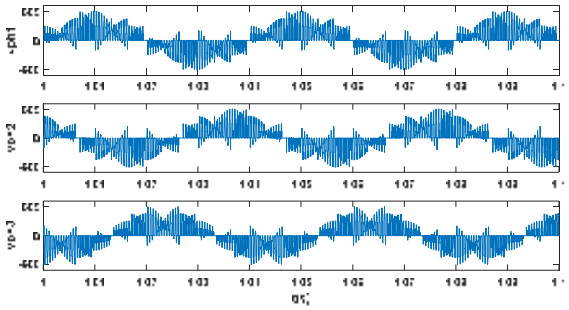


***Fig.10***. *The voltage between the two terminals of the three-phase load.*

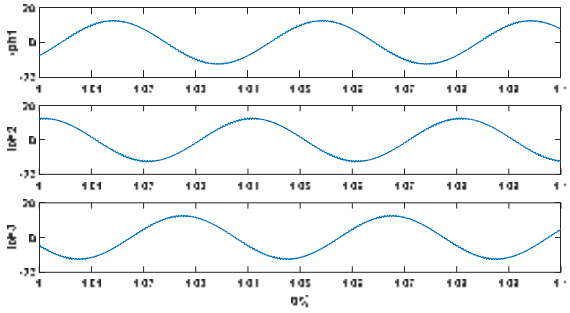


***Fig.11*** *Current of the open-end three-phase load.*

It is obvious that the fundamental magnitude of the voltage is 156.5 V with a THD of 91.59%,, whereas, the fundamental current is 12.46 with a THD of 2.01 % which means that there is an improved current quality in comparison with a single matrix converter Fig. 12 and Fig. 13. On the other side, the first matrix converter and the second matrix converter have a fundamental magnitude voltages 78.38 V and 78.16 V respectively.

Whereas the output voltage to ground and the phase to phase voltage of the both matrix converter are presented in Fig. 14. and 15. respectively. The two level nature voltage is clearly observed and the three-level voltage nature at the load terminals is also obviously observed. the effect of the input filter can be seen clearly in Fig. 16, where the input current from the matrix converter side is rich in harmonics with THD = 89.86%, however the source current is nearly sinusoidal with THD = 13.57 % which is little bit great than the one of the single matrix converter, it may due to the level of the fundamental of the output currents and voltages.

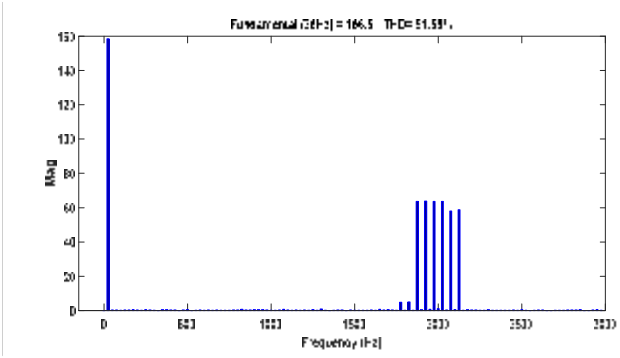


***Fig.12.*** *The spectrum of the matrix converter output voltage.*

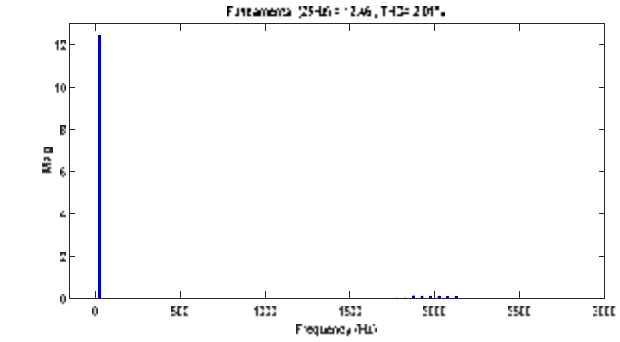


***Fig.13.*** *The spectrum of the matrix converter output current.*

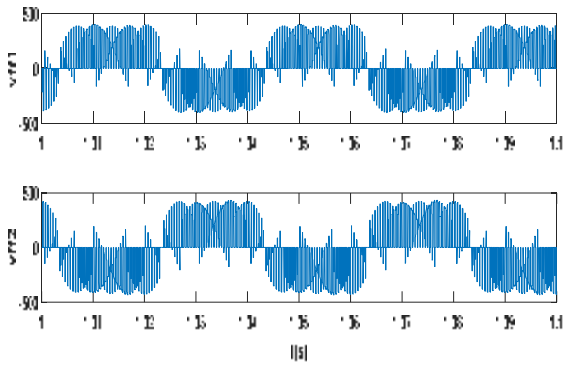


***Fig.14.*** *The output phase to phase voltage of MC1and MC2.*

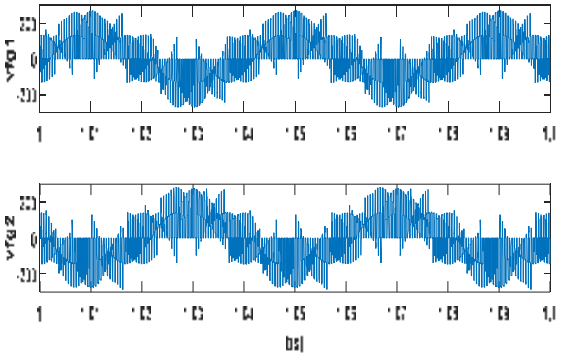


***Fig. 15.*** *The output voltage to ground of MC1and MC2.*

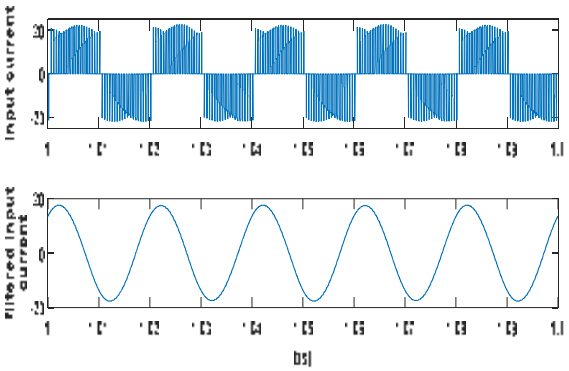


***Fig. 16****. The input currents before and after the input filter.*

## 5. Conclusion

In the present paper the great advantage of the use of the dual matrix converter under the topology of open-end is proved clearly. The obtained results show the net improvement of the quality of the voltages applied to the load and the net elimination of the common mode voltage which is presenting a great problem in all three-phases load applications, especially in three-phases electrical machines. On the other side, and due to the multilevel nature of the voltage applied at the terminal of the open-end load, the current quality is also improved, where the THD is decreased at nearly 48% compared to the classical topology based on one matrix converter. An important issue, is that the use of a dual matrix converter is more reliable in case of fault on one or more switches, this problem can be solved by just adjusting the control of the switches. finally, it can be said the to presented topology can have a large use in electric machines application in industrial plats based on the aforementioned advantages.

## REFERENCES


1. P.W. Wheeler, P.W., Rodriguez, J., Clare, J,C., Empringham, L., and Weinstein, A: "Matrix Converters: A Technology Review", IEEE Trans. On Ind. Elect. vol. 49, no. 2, April, 2002, pp. 276-288.
2. René Vargas, José Rodríguez, Ulrich Ammann, and Patrick W. Wheeler, "Predictive Current Control of an Induction Machine Fed by a Matrix Converter With Reactive Power Control", IEEE Tran. On Ind. Electronics, vol. 55, no. 12, pp. 4362-4371, Dec. 2008.
3. M. Venturini, "A new sine wave in sine wave out, conversion technique which eliminates reactive elements," in POWERCON 7, 1980, pp. E3_1-E3_15.
4. A. Alesina, and M. Venturini, "Analysis and design of optimum amplitude nine-switch direct ac-ac converters", IEEE Trans. Power Elect. vol. PE-4, no. 1, pp. 101-112, 1989.
5. Sk. Moin Ahmed1, Haitham Abu-Rub2, Abdellah Kouzou3, "Predictive Simultaneous Power and Current Control in a Three-phase Direct Matrix Converter " .
6. MM. REZAOUI, L. NEZLI, MO.MAHMOUDI," Study of Output Voltages of a Matrix Converter Feeding a Five AC – Induction Motor Using the Strategy PWM Modulation to Five Intervals", Sixth International Conference on Electrical Engineering CEE 2010, Batna, Algeria (Oct 2010).
7. Sk. Moin Ahmed,Haitham Abu-Rub,Zainal Salam, "Common-Mode Voltage Elimination in aThree-to-Five-Phase Dual Matrix Converter Feeding a Five-Phase Open-End Drive Using Space-Vector Modulation Technique" ,IEEE TRANSACTIONS ON INDUSTRIAL ELECTRONICS, VOL. 62, NO. 10, OCTOBER 2015
8. Sk. Moin Ahmed, Haitham Abu-Rub, Zainal Salam, "Investigation of Space Vector Modulated Dual Matrix Converters Feeding a Seven Phase Open-end Winding Drive ", Industrial Electronics Society, IECON 2014 - 40th Annual Conference of the IEEE, Oct. 29 2014-Nov. 1 2014
9. Ghalem BACHIR, Azeddine BENDIABDELLAH," A Comparative Study between Two Control Strategies for Matrix Converter", Advances in Electrical and Computer Engineering, Volume 9, Number 2, 2009.
10. H. Altun, S. Sunter,"matrix converter induction motor drives modeling simulation and control", Electrical Engineering, December 2003, Volume 86, Issue 1, pp 25-33.
11. J.RODRIGUEZ, E.SILVA, and P.WHELLER "matrix converter controlled with the direct transfer function approach: analysis, modelling and simulation "in International journal of electronics Vol.92, No.2 2, February 2005, 63-85.
12. Abdelkader Djahar, Benyounes Mazari "High Performance Motor Drive Using Matrix Converter" acta electrotechnica et informatica No.2, Vol.7, 2007.
13. J.Rodriguez, E.Silva, F.Blaabjerg, P.Wheeler, J.Clare ,and J.Pontt, "Matrix converter controlled with the direct transfer function approach: Analysis, modelling and simulation," Int. J. Electron.,vol.92, no.2, pp.63–85, Feb.2005.
14. L.Zhang, C.Watthanasarn, and W.Shepherd, "Control of AC–AC matrix converters for unbalanced and/or distorted supply voltage," in Proc. 32nd Annu. IEEE Power Electron. Spec. Conf., 2001,vol.2, pp.1108–1113.
15. J.Rzasa, "Capacitor clamped multilevel matrix converter controlled with Venturini method," in Proc.13th EPEPEMC, Sep.2008, pp.357–364.
16. Y. MeiandL. Huang, "Improved switching function modulation strategy for three-phase to single-phase matrix converter," in Proc. IEEE IPEMC, May2009,pp.1734–1737.



Authors' contacts:
Address:
[1]Applied Automation and Industrial Diagnostics Laboratory (LAADI), Djelfa Universitydepartments of science and technology, Algeria
[2] University Amar Telidji of Laghouat

E-mail: Beladel_abdelkader@yahoo.fr
E-mail: kouzouabdellah@ieee.org

© International Scientific Conference on Engineering, Technologies and Systems
TECHSYS 2016, Technical University – Sofia, Plovdiv branch
26 – 28 May 2016, Plovdiv, Bulgaria

# CONTROL OF GAS TURBINE OUTPUT PARAMETERS BASED ON MULTIDISCIPLINARY OPTIMIZATION OF THEIR OPERATING VARIABLES

NADJI HADROUG [(1)], AHMED HAFAIFA [(1)],ABDELLAH KOUZOU [(1)], MOULOUD GUEMANA [(2)] AND AHMED CHAIBET [(3)]

**Abstract:** *The use of gas turbines is widespread in the hydrocarbon industry and production of electrical energy; Despite their many advantages, their high sensitivity to accentual defects, is very important because the influence of these defects can be critical to the proper functioning of these rotating machines. This study propose the analysis of the output parameter control strategy of an examinee gas turbine, based on the multidisciplinary optimization of their operating variables, to meet operating constraints and maximize the life of this machine to avoid aerodynamic limitations caused by the dropout problem and ensure proper operation. The obtained results are satisfactory and reliable for performing economic contributions in the inspected facility.*

**Keywords:** *Multidisciplinary optimization, configuration control, gas turbine power turbine.*

## 1. Introduction

Currently, the study of the life of complex industrial systems has become a modern industrial challenge for the sustainability analysis of operation of industrial systems, ensured the extension of operating life and minimize repair time maintenance operations which are strongly related to regulation mode and system control. This certainly reduces intervention costs and allow better meet the objectives a priori for optimal system operation. For this purpose, this work proposes the study of output parameters control strategy discussed a gas turbine, based on optimizing their output variables to meet the operating constraints and maximize the duration life of this machine, to prevent the aerodynamic limitations caused by the dropout problem and ensure correct conduct of this system.

Indeed, the gas turbine system is made by sensitive organs to accidental faults can be critical and costly both humanly and financially on the correct operation of the gas pipeline. In order to achieve a predictive system capable of estimating the state of degradation of operation of gas turbines in operation even degrade mode to make predictions of operation of the gas turbine system. However, the complexity of the design optimization depends on the complexity of the relevant disciplines, the problem size and nature of objectives and constraints. In the case of the considered gas turbine, multidisciplinary optimization is proposed to the multivariable control of the discussed gas turbine output variable.

## 2. Multidisciplinary Optimization

Several multidisciplinary optimization strategies have been made in industrial literature [1, 7, 9, 15, 17]. This optimization can facilitate the control of variables in interaction between system elements and can be used as decision support in regulation. In the case of the examined gas turbine, the choice of parameters and modeling and implementation of a control strategy and decision making are obviously important inducers regarding supervisory system configurations eligible for the gas turbine. The optimization problem can be given

Copyright © 2016 by Technical University of Sofia, Plovdiv branch, Bulgaria ISSN Online: 2535-0048

as to minimize $f(x,y,z)$ with respect to a constraint functions, given by:

$$\begin{aligned} & f(x,y,z) \\ & x,y,z \\ & g(x,y,z) \le 0 \\ & h(x,y,z) = 0 \\ & \forall i, R_i(x_i,y_i,z_i) = 0 \\ & \forall j \ne i, y_{ij} = c_{ij}(x_j,y_j,z_j) \end{aligned} \quad (1)$$

where $x$ is the state variables, $y$ are the coupling variables, $z$ are the design variables, $c$ is a function of coupling, $f$ is an objective function, $g$ is the inequality constraints, $h$ are the equality constraints and $R$ is residues.

In this work, a more particular interest will be also transmitted to the defect detection phase, affect the system output variables examined gas turbine. Indeed, fault detection through the generation of a fault indicator called residue, this indicator is defined by a consistency relationship. It is designed to be zero on average in a case of operation. In contrast, in a case with default, the residue away from its mean value zero and is used to indicate the presence of a defect. The generation of residues characteristic of how the system is the fundamental problem of diagnosis model based. This technique relies on the use of a correct assumed system model and generate residues that are the differences between the measured output signals and estimate, as shown in Figure 1.

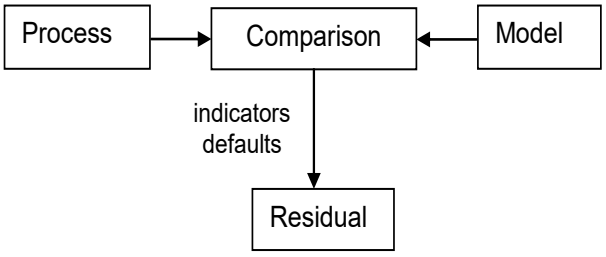



***Fig. 1.*** *Residual generation*

For minimizing the equation error, the process model is written as:

$$y(k) = \Psi^T \theta \quad (2)$$

With $\theta$ and $\Psi$ designating the parameters and regression vectors given by:

$$\theta^T = [a_1 .... a_n, b_1 .... b_n], \quad \Psi^T = [y(k-1) .... y(k-n) \;\; u(k-1) ..... u(k-n)]$$

The equation error $\varepsilon(.)$ is introduced to the parameter estimation defining discrete transfer function of the system using the flowing formula:

$$\frac{y(z)}{u(z)} = \frac{B(z)}{A(z)} = \frac{\sum_{i=1}^{n_b} b_i z^{-i}}{1 - \sum_{i=1}^{n_a} a_i z^{-i}} \quad (3)$$

The error is defined by equation:

$$e(z) = \hat{B}(z)u(z) - \hat{A}(z)y(z) \quad (4)$$

Where $\hat{A}(z)$ and $\hat{B}(z)$ are the estimates of $A(z)$ and $B(z)$.

May provide a recursive form of estimated $\hat{\theta}$ using the recursive least squares algorithm [12]:

$$\hat{\theta}(k+1) = \hat{\theta}(k) + \gamma(k)e(k+1) \quad (5)$$

with :

$$\begin{cases} \gamma(k) = \dfrac{1}{\Psi^T(k+1)P(k)\Psi(k+1)+1} P(k)\Psi(k+1) \\ P(k+1) = \left[I - \gamma(k)\Psi^T(k+1)\right]P(k) \\ \mathrm{e(k)} = \mathrm{y(k)} - \Psi^{\mathrm{T}}(k)\hat{\theta}(k-1) \end{cases}.$$

For the minimization of the output error, instead of as previously calculate the error equation, rather evaluates the output error, given by:

$$e(k) = y(k) - \hat{y}(\theta,k) \quad (6)$$

Where: $\hat{y}(\theta,z) = \dfrac{\hat{B}(z)}{\hat{A}(z)}u(z)$ and $\hat{y}(\theta,z)$ is the model output.

The output of error $e(.)$ in this case being a nonlinear function of the parameters to be estimated, then uses numerical optimization methods to minimize the error $e(k)$ with respect to $\theta$ parameters. Based on the modeling of these residues, a strategy of control output of a gas turbine parameters examined, based on the optimization of their operating variables will be introduced in the implementation section, which are typically zero mean and a variance determined in the absence of malfunctions.

## 3. Industrial Application

As part of this work, a gas turbine type two shafts TITAN 130 was examined, this gas turbine is installed at the gas compression station of Sonatrach SC3 in Djelfa, central Algeria. This gas compressor station is located on the pipeline of the GG1 line at a distance of 182 KM from the starting point to Hassi R'Mel southern Algeria, this station will enhance the transport capacity of the pipeline 07 to 13 billion m3 per year. It also has three turbochargers and a turbine generator, a control building equipped with DCS (Digital Control System).

The entire turbomachinery is a turbocharger or all mechanical transmission together by SOLAR TURBINES INCORPORTED factory a Caterpillar company. The turbomachinery comprises a turbine engine and a compressor mounted on a steel frame, with the support systems and ancillary anti-slip material, this turbomachinery is means; (Compressor Set / Mechanical Drive: All Compressor / Drive Mechanical), as shown on Figures 2.A and 2.B.

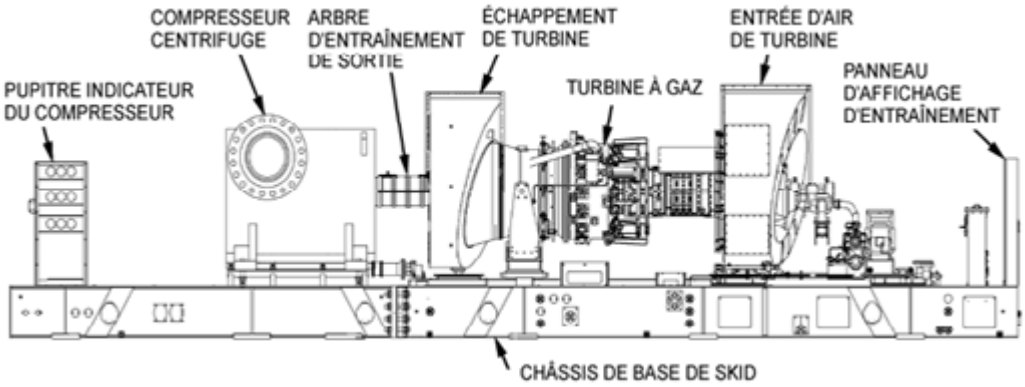



***Fig. 2.*** *A: Main components of the ensemble compressor Titan 130*

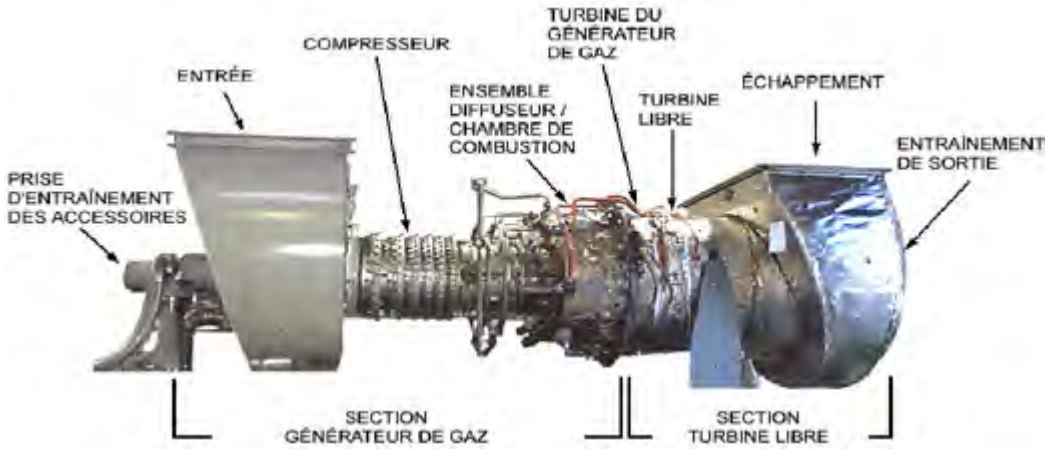



***Fig.2.*** *B: Key components of turbomachinery Titan 130*

The gas turbine provides the power to drive the compressor, is in two main parts: the gas generator (GP) and the power turbine (PT). The gas generator (GP) converts the energy of the fuel gas at high temperature that takes the power turbine and converts rotational energy. The fundamental principle of a gas turbine is converted fuel energy to mechanical energy by the application of a thermodynamic process known by the Brayton cycle, as shown in Figures 3.A and 3. B.

### 3.1. A gas turbine control

The model of the turbine discussed in this work has two entries: room temperature ($T_1$) and mass flow rate of fuel flow ($\dot{m}_2$), sensors supplied from the turbine outputs include: the speed of HP high pressure shaft (NGP), the low pressure shaft speed (NPT) and the temperature of the blades ($T_3$). These measurements can be used to provide

different pairs of input / output for the closed loop control. There are other important variables such as; The air mass flow ($\dot{m}_a$), the pressure ratio at the outlet of the axial compressor (PCD) and the fuel / air ratio ( $f$ ).

The proposed control configuration is shown in Figure 4, with the nonlinear model used for PI control configuration (proportional / integral). This closed loop control strategy is chosen for parameter optimization of a PI controller structure is designed for a nominal operating point of the discussed gas turbine.

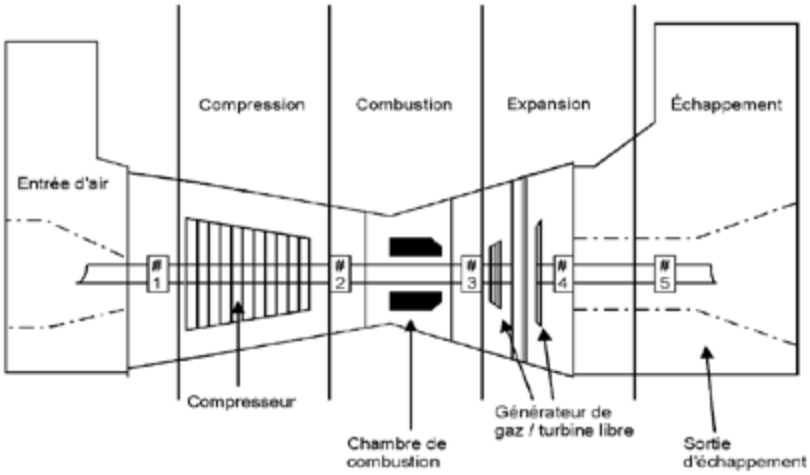



***Fig. 3.*** *A: States air flow of Brayton cycle*

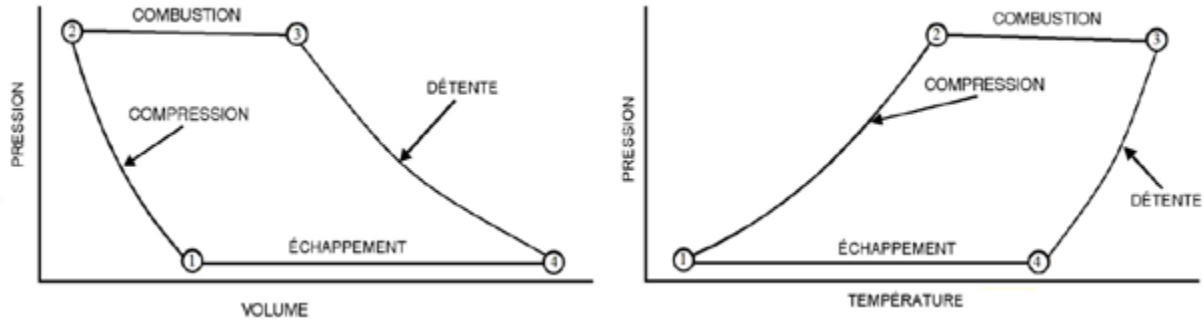



***Fig.3.*** *B Curves of Brayton cycle*

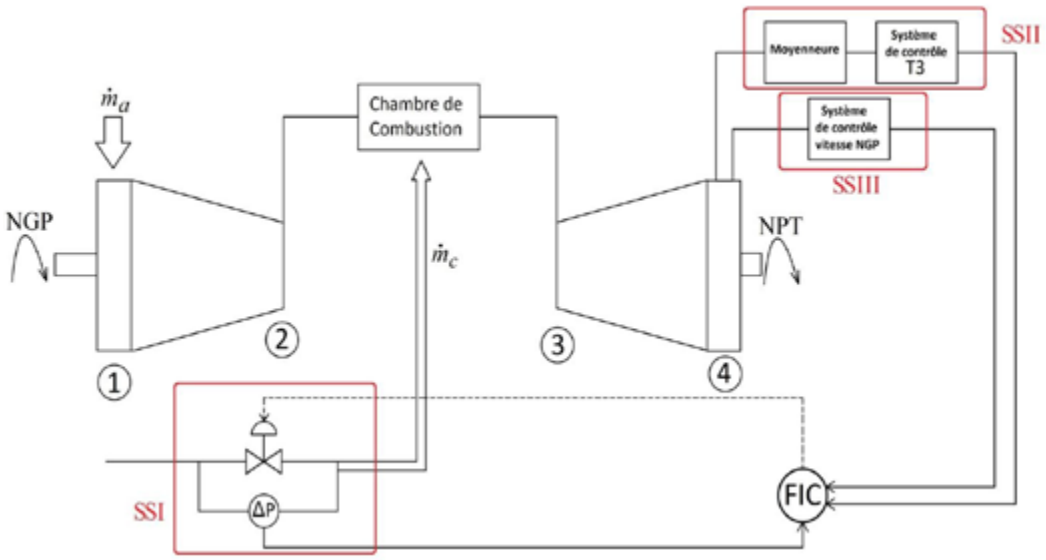



***Fig. 4.*** *Control setting of different subsystem of the TITAN 130 turbine*

The mass flow rate of fuel flow ($\dot{m}_c$) is given by:

$$\dot{m}_c = \sqrt{\Delta P}.\frac{1}{2}\rho\mu^2 = \frac{\sqrt{\Delta P}}{k} \quad (8)$$

The air mass flow ($\dot{m}_a$) is given by:

$$\begin{aligned} \dot{m}_a &= k'(P_2 - P_1) \\ \dot{m}_a &= k'(PVD - P_{atm}) \end{aligned} \quad (9)$$

The fuel / air ratio is calculated to control combustion to control the ratio $f$ which is given by:

$$f = \frac{(T_3 - T_2)}{\eta_b.CV + T_3} \quad (10)$$

### 3.2. Application results

The multidisciplinary optimization results developed in this work allows for control of gas turbine output variables. Figure 5.A shows the discharge pressure variation of the fuel gas valve in the combustion chamber, and the variation of its residue is shown in Figure 5.B. Figure 6.A shows the discharge pressure change axial compressor and the variation of its residue is given in Figure 6.B, the control of the position of the fuel valve to the gas inlet of the combustion chamber is shown in Figure 7.

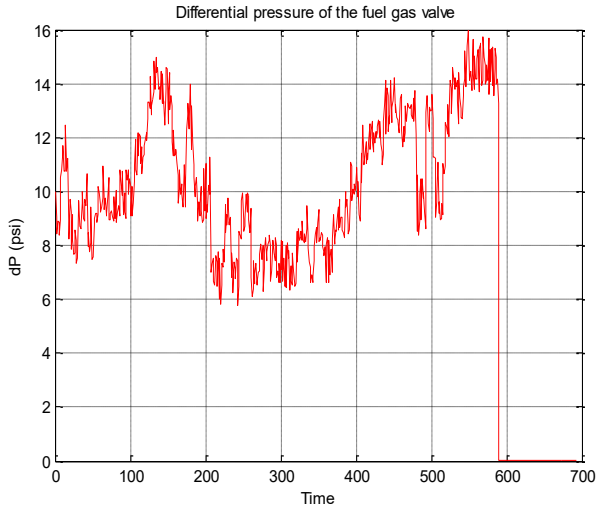



***Fig. 5.*** *A: Differential pressure of the fuel gas valve*

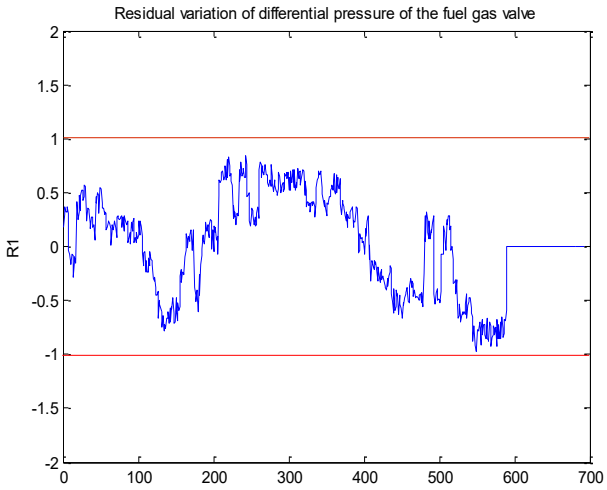



***Fig 5.B:*** *Residual variation of differential pressure of the fuel gas valve*

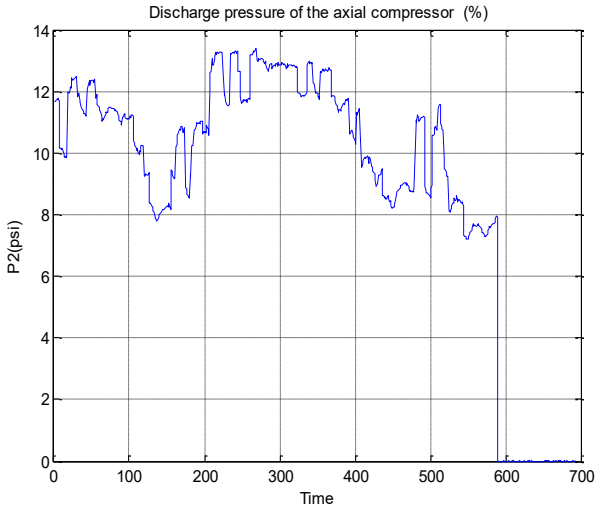
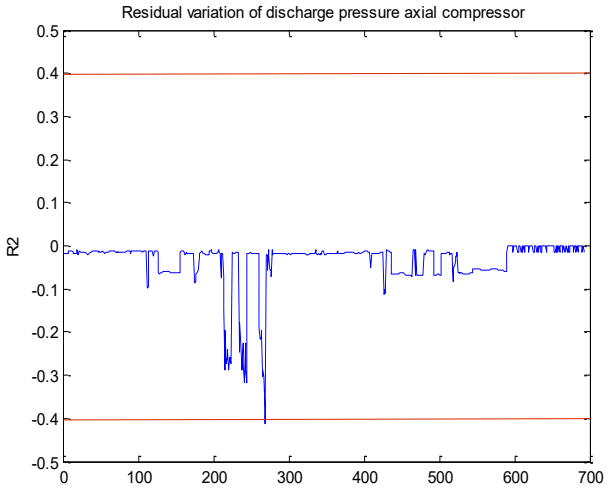



***Fig. 6****.A: Discharge pressure axial compressor*




***Fig/ 6.****B: Residual variation of discharge pressure axial compressor*

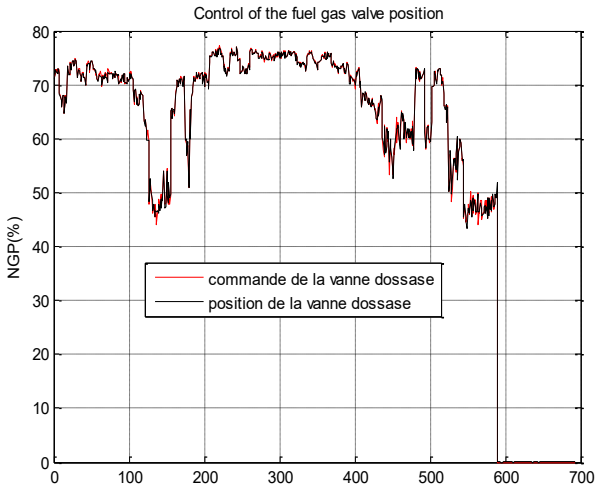



***Fig. 7.*** *Control of the fuel gas valve position*

The turbine rotational speed variation NGP are controlled, after optimizing the manipulated variables pressure and mass flow rate suction and gas turbine system of delivery is given in Figure 8, the speed sensor in order to measure the speed of rotation of the HP shaft of the axial compressor, with the target value recommended by the manufacturer is 100%.

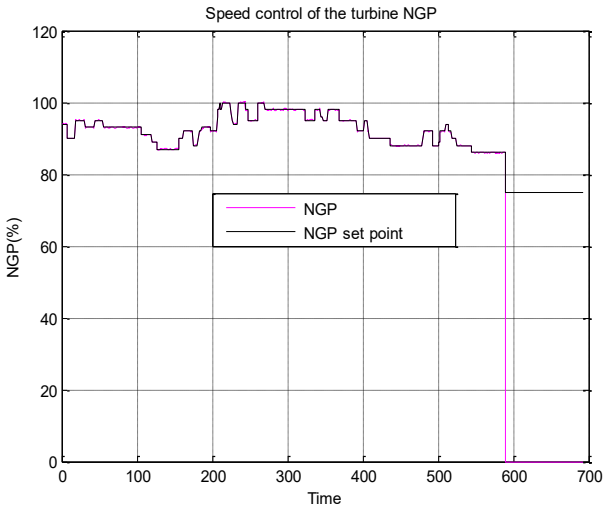



***Fig. 8.*** *Speed control of the turbine NGP*

To confirm the control performance in more detail, validation tests were performed on the considered gas turbine, Figure 9 shows the variation of exhaust temperature of the examined turbine.

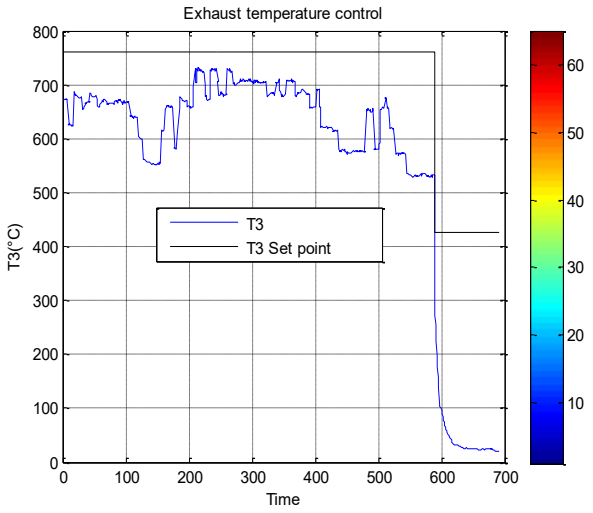



***Fig. 9.*** *Exhaust temperature control*

This method leads to an improvement of the efficiency of a gas turbine, Figure 10 shows the variation of combustion efficiency and Figures 11, 12 and 13 show the increase in efficiency and power output of the turbine examined. For normal operation of the examined gas turbine, when the ambient temperature rises above the reference machine performance decreases. The reduction becomes large when the room temperature is maximum, as shown in Figure 10.

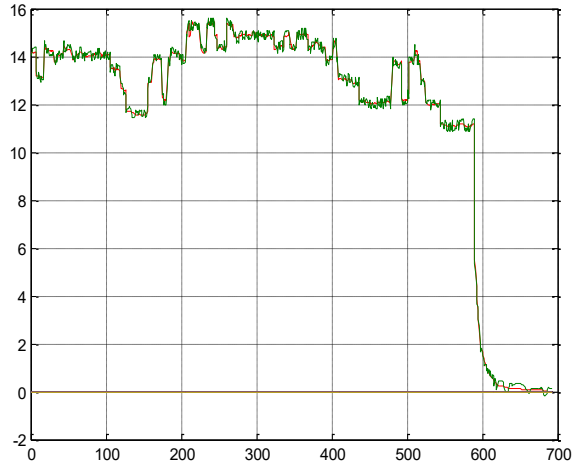


***Fig. 10.*** *Combustion efficiency*

It is seen in Figure 11 that the power absorbed by the compressor is proportional to the pressure ratio for an ambient temperature range (0 ° C <Tamb <50 ° C).

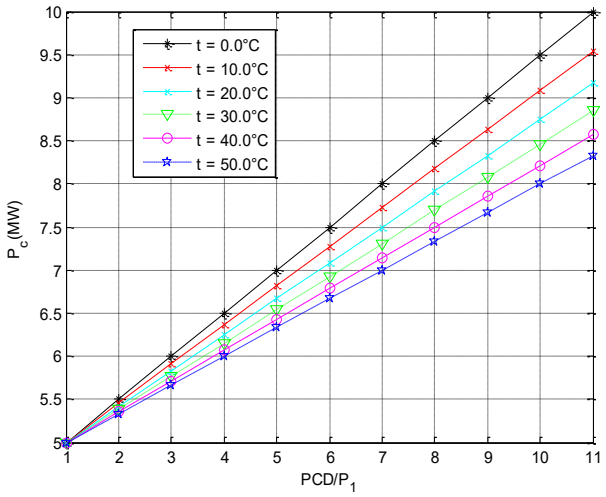



***Fig. 11.*** *Gas turbine power at different operating temperature*

In Figure 12, when the ambient temperature is high (> 30 ° C), we note that the performance of the profile tends to a maximum value of 7 <<9. Every time, it is not possible to exceed the value ( ε ≈ 8.7091) given by the manufacturer, because of the limitations imposed by the resistance of materials.

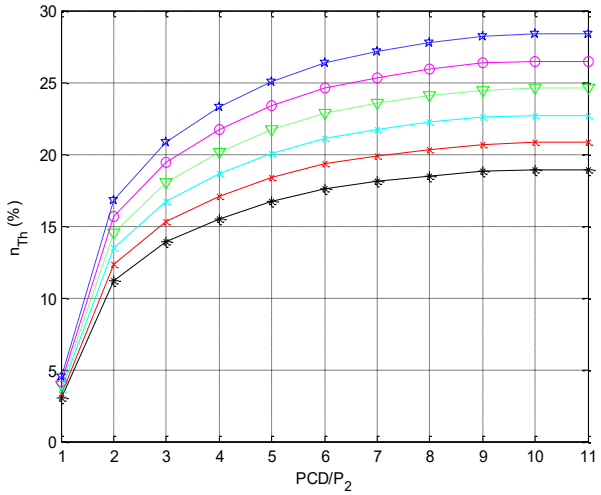



***Fig. 12.*** *Gas turbine efficiency at different operating temperature*

On Figure 13 and 14, the power absorbed by the compressor and that supplied by the turbine will vary proportionally with the ambient temperature and PT remains almost constant because the combustion temperature limit (given by the manufacturer).

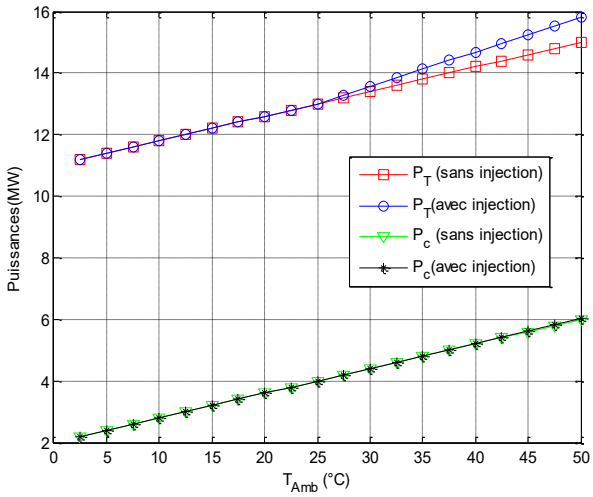



***Fig. 13.*** *Gas turbine power at different operating pressure*

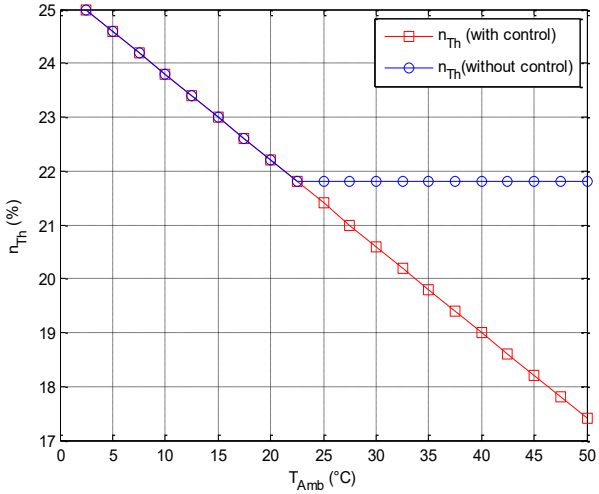



***Fig. 14.*** *Yield control of the examined gas turbine*

The results of multidisciplinary optimization, applied to the control of the gas turbine output variable are satisfactory, are used to solve some problems of supervision of this type of rotating machine. This allows for improvements in terms of cost oversight examined gas turbine, the control configuration proposed to also led to improvements in the operation of the studied gas turbine.

## 4. Conclusion

A multidisciplinary optimization of the output variables of a gas turbine were applied in this work to control the output parameters of an examined gas turbine, this system is composed by sensitive organs to accidental defects, can be critical and costly both humanly and financially on the

operation of the gas pipeline. Indeed, the complexity of the supervision in gas turbine plants is due to the strong interaction of control loops in these industrial system. For this purpose, in this work a multidisciplinary optimization was developed for efficient representation data of the examined gas turbine variables by integrating a control configuration for these variables, using the simplest to implement in this system. Improvements have been obtained by using the optimizing the examined gas turbine output variables to simplify there control. These improvements are reflected in the performance of the power quality and yield of the examined gas turbine.

## REFERENCES


1. Abdelhafid Benyounes, Ahmed Hafaifa and Mouloud Guemana, (2016). Gas turbine modelling based on fuzzy clustering algorithm using experimental data. *Journal of Applied Artificial Intelligence, Taylor & Francis*, vol. 30, no. 1, pp. 29-51.
2. Abdelhafid Benyounes, Ahmed Hafaifa and Mouloud Guemana, (2016). Fuzzy logic addresses turbine vibration on Algerian gas line. *Oil & Gas Journal* | Jan. 4, pp. 22-28
3. Ahmed Hafaifa, Guemana Mouloud and Saadat Boulanouar, (2016). Monitoring system based on real data acquisition for vibrations control in gas turbine system. *Revue de Nature & Technologie: A- Sciences fondamentales et Engineering*, vol. Jan. n° 14, pp. 13 – 18.
4. Boulanouar Saadat, Ahmed Hafaifa and Mouloud Guemana, (2016). Vibration analysis and measurement based on defect signal evaluation: Gas turbine investigation. *Journal of Advanced Research in Science and Technology*, vol. 3, no 1, pp.271-280
5. Benrabeh Djaidir, Ahmed Hafaifa and Kouzou Abdallaha, Vibration detection in gas turbine rotor usingartificial neural network. Proceedings of the International Conference on Acoustics and Vibration ATAVI'16, March 21-23, 2016, Hammamet -Tunisia
6. Mohamed Ben Rahmoune, Ahmed Hafaifa, Mouloud Guemana, Fault diagnosis in gas turbine based on neural networks: Vibrations speed application. Proceedings of the International Conference on Acoustics and Vibration ATAVI'16, March 21-23, 2016, Hammamet -Tunisia
7. Djamel Halimi, Ahmed Hafaifa and Elahmoune Bouali (2014). Maintenance actions planning in industrial centrifugal compressor based on failure analysis. *The quarterly Journal of Maintenance and Reliability*. Maintenance and Reliability, Vol. 16, no. 1, pp. 17–21
8. Bindi Chen, Peter C. Matthews, Peter J. Tavner, (2013). Wind turbine pitch faults prognosis using a-priori knowledge-based ANFIS. *Expert Systems with Applications*, vol. 40, no. 17, pp. 6863-6876.
9. Forbes G.L. and R.B. Randall, Simulated gas turbine casing response to rotor blade pressure excitation. Proceeding of the 5th Australasian Congress on Applied Mechanics, ACAM 2007, 2007, Brisbane, Australia.
10. Grondahl C.M., M.E. Guiler, G.E. Jurczynski and R. Zell (1990), Performance and reliability improvements for MS3002 and MS5001 turbines in pipeline applications. Proceeding of the Petroleum and Chemical Industry Conference: Industry Applications Society 37th Annual, Houston, TX , USA, pp. 135 – 144.
11. Gwo-Chung Tsai (2004), Rotating vibration behavior of the turbine blades with different groups of blades. Journal of Sound and Vibration, vol. 271, no. 3-5, 6, pp. 547-575.
12. Hector Sanchez, Teresa Escobet, Vicenç Puig, Peter Fogh Odgaard, (2015). Health-aware Model Predictive Control of Wind Turbines using Fatigue Prognosis. *IFAC-PapersOnLine*, vol. 48, no. 21, pp. 1363-1368.
13. Martha A. Zaidan, Andrew R. Mills, Robert F. Harrison, Peter J. Fleming, (2016). Gas turbine engine prognostics using Bayesian hierarchical models: A variational approach. *Mechanical Systems and Signal Processing,* vol. 70–71, pp. 120-140.
14. Qinming Liu, Ming Dong, Wenyuan Lv, Xiuli Geng, Yupeng Li, (2015). A novel method using adaptive hidden semi-Markov model for multi-sensor monitoring equipment health prognosis. *Mechanical Systems and Signal Processing*, vol. 64–65, pp. 217-232.
15. Ren-Jieh Kuo, Man-Hsin Huang, Wei-Che Cheng, Chih-Chieh Lin, Yung-Hung Wu, (2015). Application of a two-stage fuzzy neural network to a prostate cancer prognosis system.

*Artificial Intelligence in Medicine*, vol. 63, no. 2, pp. 119-133.

16. Yang Chen, Guobiao Cai, Zhenpeng Zhang, Yulong Huang, (2014). Multi-field coupling dynamic modeling and simulation of turbine test rig gas system. *Simulation Modelling Practice and Theory*, vol. 44, pp. 95-118.

**Authors' contacts**

**Nadji Hadroug [(1)], Ahmed Hafaifa [(1)], Kouzou Abdellah [(1)], Mouloud Guemana [(2)] and Ahmed Chaibet [(3)]**

[(1)] Applied Automation and Industrial Diagnostics Laboratory, Faculty of Science and Technology, University of Djelfa 17000 DZ, Algeria

[(2)] Faculty of Science and Technology, University of Medea, Algeria

[(3)] Aeronautical Aerospace Automotive Railway Engineering school, ESTACA Paris, France

**Nadji Hadroug [(1)]**
E-mail: N_Hadroug@univ-djelfa.dz
**Ahmed Hafaifa [(1)]**
E-mail: hafaifa.ahmed.dz@ieee.org
**Kouzou Abdellah [(1)]**
E-mail: kouzouabdellah@ieee.org
**Mouloud Guemana [(2)]**
E-mail: guemana_m@yahoo.fr
**Ahmed Chaibet [(3)]**
E-mail: **ahmed.chaibet@estaca.fr**

© International Scientific Conference on Engineering, Technologies and Systems
TECHSYS 2016, Technical University – Sofia, Plovdiv branch
26 – 28 May 2016, Plovdiv, Bulgaria

# STABILIZING LINEAR MULTIVARIABLE GAS TURBINE MODEL VIA SLIDING MODE CONTROL

BACHIR NAIL[1], ABDELLAH KOUZOU[1], AHMED HAFAIFA[1],BELKACEM BEKHITI[2]

**Abstract:***In this paper, linear sliding mode control(LSMC) theory is used to stabilize the dynamic behavior of a linear multiple input multiple output(MIMO)system (Power Gas turbine). The main pros in this kind ofcontrol is the discontinuity behavior which can be applied to the uncertainties systems. Where, the first step must define the hyper-planes inthe state space and calculate the equivalent control inputthe second step calculates the hyper-plane matrix G. The checking test of the robustness and thesensitivity under the variation of the dynamic and against therejection of the external perturbation gives a clear proof of the presented control robustness in such application.*

**Key words:** *LSMC, linear MIMOSystem, Hyper-planes,MRLS,Power Gas Turbine, Robustness.*

## 1. Introduction

The research on stability concept is attracting more attention and it occupies a large space in modern and classical control theory. Indeed, there are many theoriesin this area that have been introduced and used in several industrial control applications, such as; the Lyapunov stability theory based on energy [1], the bounded input bounded output (BIBO) stabilitytheory [2], the input output stability, the hyper-stability [Doré Landau], the state feedback static gain stability based on pole placement, the linear quadratic regulator ..etc.[3],[4], All of these theories and othersclarify that the stability study of systems is wide domain of research,. On the other side, the importance of this domain has its great impact in industrial systems applications, where the loss of stability in these systems can create dangerous and drastically problems, such as; the nuclear reactors, the jet engines, and the gas turbine which is the subject of the application presented in this paper.

Several papers has been written in recent years about the stability theories and their applications, particularly in linear MIMO systems such as; the optimal control [5], the multivariable feedback design [6], the Eigen structure assignment and controller optimization for mechanical systems [7], the optimal sliding mode control of a flexible spacecraft under stochastic disturbances[8],The left and right block pole placement comparison study applied to flight [9].

The main contribution of the present paper focuses mainly on the application of the linear sliding mode control, which is one of the control methods within the family of variable structure controls. This control strategy is applied on a gas turbine system, where thesignum function(sign) is used instead of the hyperbolic tangent function (tanh) [10].

## 2. SLIDING MODE CONTROL OF A LINEAR SYSTEM

Consider the following uncertain linear system:

$$\dot{x} = Ax + Bu \tag{1}$$

For m inputs, *m* hyper-planes in the state space are defined as:

$$s_i(t) = g_i^T x(t); \quad i = 1,2,...,m \tag{2}$$

These hyperplanes pass through the origin of the state space for $s_i = 0$ From (1) and (2), the followinf expression is obtained:

$$\dot{s}_i(t) = g_i^T \dot{x}(t) = g_i^T Ax + g_i^T Bu; i = 1,2,...,m \tag{3}$$

furthermore equation (3) can be rewritten in the matrix formas follows:

$$\dot{s}(t) = GAx + GBu \tag{4}$$

Where

$$s = \begin{bmatrix} s_1 & s_2 & . & . & . & s_m \end{bmatrix}^T \tag{5}$$

And

Copyright © 2016 by Technical University of Sofia, Plovdiv branch, Bulgaria ISSN Online: 2535-0048

$$G = \begin{bmatrix} g_1 & g_2 & \cdots & g_m \end{bmatrix}^T \quad (6)$$

it is noted that:

$$s(t) = Gx(t) \quad (7)$$

and the vector $s(t) = 0$ represents the intersection of all the m sliding hyper-planes passing through the origin of the state space.The corresponding equivalent control input $u_{eq}(t)$ based on (4) itis expressed as followsom (4)

$$u_{eq}(t) = -(GB)^{-1} GAx \quad (8)$$

Note that the matrix *GB* has been assumed to be nonsingular. The reaching condition for each hyper-plane is [8],[11],[12],[19]:

$$s_i \dot{s} < 0 \quad (9)$$

Conditions (9) are satisfied by the following control law:

$$u(t) = u_{eq}(t) - (GB)^{-1} diag(\eta)\,\mathrm{sgn}(s(t)) \quad (10)$$

Where $diag(\eta)$ is a diagonal matrix with the $i^{th}$diagonal element equal to a positive number $\eta_i$

### 2.1. Computation ofSliding mode control (SMC) Hyper-plane Matrix G

Define a similarity transformation

$$q(t) = Hx(t) \quad (11)$$

Where

$$H = \begin{bmatrix} N & B \end{bmatrix}^T \quad (12)$$

and the columns of the *nx*(*n*−*m*) matrix *N* arecomposed ofbasis vectors of the null space [16] of $B^T$ . From (1) and (11)

$$\dot{q} = \bar{A}q(t) + \bar{B}u(t) \quad (13)$$

Where

$$\bar{A} = HAH^{-1} \quad (14)$$

And

$$\bar{B} = HB \quad (15)$$

Because of thespecial structure of the matrix H, the first *(n*−*m)*rows of $\bar{B}$ turn out to be zeros. Hence, the vector q is decomposed as follows:

$$q = \begin{bmatrix} q_1 \\ q_2 \end{bmatrix} \quad (16)$$

Where $q_1$ and $q_2$ are *(n*−*m)* and m dimensional vectors, respectively. Partitioning (13),

$$\begin{bmatrix} \dot{q}_1 \\ \dot{q}_2 \end{bmatrix} = \begin{bmatrix} \bar{A}_{11} & \bar{A}_{12} \\ \bar{A}_{21} & \bar{A}_{22} \end{bmatrix} \begin{bmatrix} q_1 \\ q_2 \end{bmatrix} + \begin{bmatrix} 0 \\ \bar{B}_r \end{bmatrix} u \quad (17)$$

and the sliding hyper-planes can be described as

$$s(t) = q_2(t) + Kq_1(t) \quad (18)$$

From (7) and (18),

$$G = \begin{bmatrix} K & I_m \end{bmatrix} H \quad (19)$$

Equation (19) indicates that the matrix *G* can be determined via the matrix *K*. The first objective behind the choice of the matrix *G* or the matrix *K* is to ensure the system stability on the intersection of all hyper-planes. When, $s(t) = 0$

$$q_2(t) = -Kq_1(t) \quad (20)$$

Equation (17) yields,

$$\dot{q}_1 = \bar{A}_{11} q_1 + \bar{A}_{12} q_2 \quad (21)$$

And

$$\dot{q}_2 = \bar{A}_{21} q_1 + \bar{A}_{22} q_2 + \bar{B}_r u \quad (22)$$

For the system (21), $q_2(t)$ can be viewed as the input and equation (20) as the state feedback law. Authors in [3] have shown that $(\bar{A}_{11}, \bar{A}_{12})$ is controllable if $(A, B)$ is controllable. Therefore, the matrix *K* can be selected by using optimal control LQR [10]. From (21) and (8), the system dynamics on the intersection of sliding hyper-planes is given by

$$\dot{x} = \left[ A - B(GB)^{-1} GA \right] x \quad (23)$$

When *G* is chosen according to Equation (19*), (n-m)* eigenvalues of $\left[ A - B(GB)^{-1} GA \right]$ are those of $(\bar{A}_{11} - K\bar{A}_{12})$ and remaining *m* eigenvalues are 0, which is a reflection of the fact that m degrees of freedom of the system is lost when $s(t) = 0$

### 2.2. Computation of *K* Matrix

Linear quadratic regulator (LQR) [4], is one of the optimal linear control methods that are used to stabilize the system by state feedback control

$$q_2(t) = -kq_1(t)$$

where*k* is obtained by minimizing the cost function:

$$J = \int \left( q_1^T Q q_1 + q_2^T R q_2 \right) dt \quad (24)$$

where, *Q* and *R* are positive semi-definite and positive definite symmetric constant matrices respectively. The LQR gain vector *K* is given by :

$$K = R^{-1} \bar{A}_{12}^T P \quad (25)$$

Where, *P* is a positivedefinite symmetric constant matrixobtained from the solution of algebraic matrix RICCATIequation (ARE):

$$\bar{A}_{11}^T P + P\bar{A}_{11} - P\bar{A}_{12} R^{-1} \bar{A}_{12}^T P + Q = 0 \quad (26)$$

Finally,

$$A_c = A - B(GB)^{-1}(GA + \eta G) \quad (27)$$

$$C_c = C - D(GB)^{-1}(GA + \eta G) \quad (28)$$

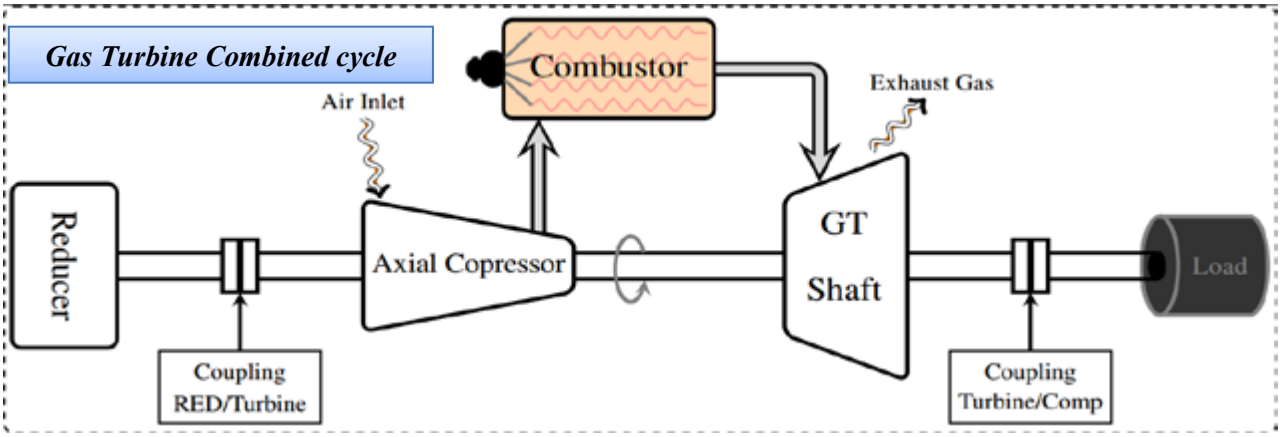



*Fig. 1. The Gas turbine combined cycle system*

## 1. System model

The GE MS9001E Gas turbine model Fig. 1 is obtained viathe parametric identification of the real data, using MIMO Recursive least square (MRLS) estimator [24-26], for the validation of this model, the order of estimated model has to be changed every time from theorder n=6 until the order n=15, this orders gives the best models that present all frequencies of the gas turbine dynamic behavior, with almost negligible norm error between data outputs and estimated model outputs.
In this paper, it is mandatory to present the gas turbine model, by the important characteristics and key, " Pole-Zero map" Fig. 2, because the system is with alarge scale, with 3 inputs and 3 outputs, which requires a big space.

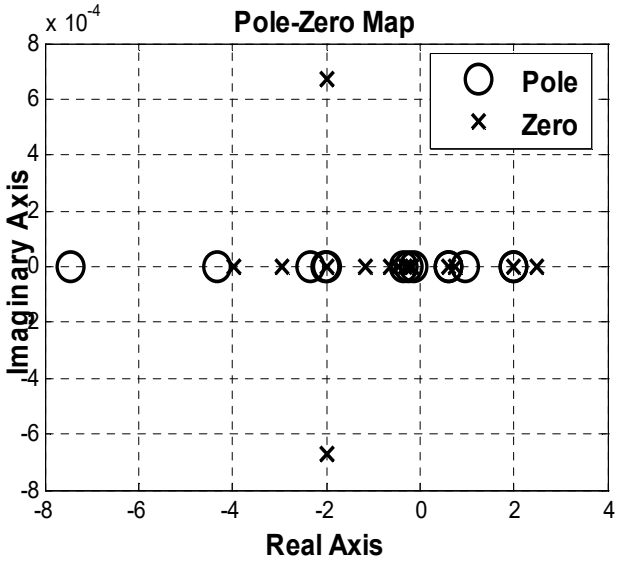



*Fig. 2. System representation via pole-zero map*

The values are chosen as follows:

$$\eta = \begin{bmatrix} 3 & 0 & 0 \\ 0 & 5 & 0 \\ 0 & 0 & 7 \end{bmatrix}, \; H = \begin{bmatrix} h_1 & h_2 & h_3 \end{bmatrix}$$

Whereas, the elements of the matrices $H,G,K$ are calculated based on equation (12), (19) and (25) respectively as follows:

$$h_1 = \begin{bmatrix} 0.0257 & -0.0965 & -0.1834 & 0.9549 & 0.0225 \\ -0.0129 & 0.0483 & 0.0917 & 0.0225 & 0.9887 \\ 0.8470 & 0.0577 & -0.0100 & 0.0021 & -0.0010 \\ -0.2253 & -0.1997 & 0.0122 & -0.0118 & 0.0059 \\ -0.1339 & -0.6529 & 0.0794 & -0.0303 & 0.0151 \\ 0.0590 & -0.2499 & 0.0818 & -0.0009 & 0.0004 \\ -0.0341 & 0.0614 & 0.2998 & 0.0668 & -0.0334 \\ 0.1075 & -0.4089 & -0.7441 & -0.1842 & 0.0921 \\ 0.0190 & -0.0714 & -0.1417 & -0.0346 & 0.0173 \\ 0.0048 & -0.0167 & -0.0300 & -0.0074 & 0.0037 \\ 0 & 0.0001 & 0 & 0 & 0 \\ 0 & 0 & -0.0001 & 0 & 0 \\ -2.3209 & 0 & 0 & 0 & 0 \\ 0 & 0.7071 & -0.7071 & 0 & 0 \\ 0 & 0 & 0 & 0.1118 & -0.0559 \end{bmatrix}$$

$$h_2 = \begin{bmatrix} -0.0105 & -0.0180 & -0.0630 & -0.0170 & 0.0618 \\ 0.0053 & 0.0090 & 0.0315 & 0.0085 & -0.0309 \\ 0.4718 & 0.1656 & 0.1701 & -0.0040 & 0.0050 \\ 0.1475 & 0.9319 & -0.1238 & -0.0291 & 0.0054 \\ 0.1074 & -0.1076 & 0.7049 & -0.1046 & 0.0092 \\ -0.0279 & -0.0178 & -0.0867 & 0.9584 & -0.0117 \\ 0.0160 & 0.0181 & 0.0626 & 0.0118 & 0.9041 \\ -0.0440 & -0.0747 & -0.2628 & -0.0718 & 0.2517 \\ -0.0077 & -0.0137 & -0.0475 & -0.0126 & 0.0476 \\ -0.0021 & -0.0030 & -0.0106 & -0.0029 & 0.0102 \\ -0.0000 & 0.0000 & 0.0000 & 0.0000 & 0.0000 \\ 0.0000 & -0.0000 & 0.0000 & 0.0000 & 0.0000 \\ 5.2502 & -1.5817 & -1.4614 & 0.1335 & -0.0498 \\ -0.5707 & 0.3850 & 0.9300 & 0.3209 & 0.1145 \\ -0.0685 & 0.0546 & 0.1156 & 0.0105 & -0.1618 \end{bmatrix}$$

$$h_3 = \begin{bmatrix} -0.1851 & -0.0344 & -0.0075 & 0.0000 & 0 \\ 0.0926 & 0.0172 & 0.0038 & -0.0000 & 0 \\ 0.0088 & 0.0017 & 0.0001 & 0 & 0 \\ -0.0500 & -0.0087 & -0.0020 & 0 & 0 \\ -0.1300 & -0.0221 & -0.0053 & 0.0001 & 0 \\ -0.0060 & -0.0002 & -0.0003 & 0 & 0 \\ 0.2736 & 0.0512 & 0.0111 & 0 & 0 \\ 0.2434 & -0.1407 & -0.0307 & 0 & 0 \\ -0.1421 & 0.9736 & -0.0058 & 0 & 0 \\ -0.0306 & -0.0057 & 0.9988 & 0 & 0 \\ 0 & 0 & 0 & 1 & 0 \\ 0 & 0 & 0 & 0 & 1 \\ 0.0016 & -0.0023 & 0.0027 & 0.0001 & -0.0001 \\ 0.0194 & -0.0034 & 0.0008 & -0.0002 & -0.0001 \\ 0.4574 & 0.0857 & 0.0185 & -0.0000 & 0 \end{bmatrix}$$

$$K = [k_1 \quad k_2]$$

$$k_1 = \begin{bmatrix} -0.1157 & 0.9110 & -1.7772 & 0.5903 & 0.2541 & -0.5139 \\ 0.0442 & 0.0409 & 0.0927 & -0.2920 & -1.3021 & -0.4220 \\ 2.1423 & 0.4090 & 0.1058 & 0.1186 & -0.2134 & -0.0962 \end{bmatrix}$$

$$k_2 = \begin{bmatrix} 0.4946 & -0.8322 & -0.1561 & -0.0352 & -0.0001 & 0.0000 \\ 0.0589 & -0.6737 & -0.1258 & -0.0328 & 0.0003 & 0.0000 \\ 0.1228 & -0.3037 & -0.0480 & 0.0099 & -0.0000 & 0.0001 \end{bmatrix}$$

$$G = [g_1 \quad g_2 \quad g_3]$$

$$g_1 = \begin{bmatrix} -4.1479 & 0.1796 & 0.8985 & 0.0842 & 0.8111 \\ 0.2174 & 2.0127 & -0.3161 & 0.2192 & -0.0466 \\ 0.0979 & 0.0937 & -0.1104 & 2.2378 & 0.3612 \end{bmatrix}$$

$$g_2 = \begin{bmatrix} 4.5922 & -1.2605 & -1.3196 & -0.3184 & 0.1475 \\ -0.6667 & 0.3287 & 0.2862 & 0.1112 & -0.0148 \\ -0.0261 & 0.1980 & -0.0557 & -0.0723 & -0.0094 \end{bmatrix}$$

$$g_3 = \begin{bmatrix} -0.0117 & -0.0058 & 0.0012 & 0.0000 & -0.0001 \\ 0.0733 & 0.0030 & -0.0026 & 0.0000 & -0.0000 \\ 0.0881 & 0.0251 & 0.0257 & -0.0001 & 0.0002 \end{bmatrix}$$

### 3. Simulation results

Two kind of tested have been performed for the validation of the proposed control to achieve the stability of the concerned gas turbine system and at the same time to check its robustness via the incertitude and the presence of noises and disturbances, that may occur in the real systems, especially those due to the perturbations in the measurements and the variation of the systems parameters. the first test was performed with the application of an incertitude Δ = 10-4 ×magic (15) in the system dynamic matrix Ac presented in (15). the second test was performed furthermore with the injection of some noise and disturbance in states xi. From the obtained results, in Fig 3. all eigenvalues are located in left half plane (negative real part ), so the dynamic behavior of gas turbine system is stabilized. Fig 4. and 5. clarify clearly the effect of the stability on all the states and the outputs that are ensuring the convergence to the origin in small time. Under noise and disturbance Fig. 6. and from the results obtained in Fig. 7, 8 and 9, it can be seen clearly that there is no much change in the place of Eigenvalues after adding the incertitude to the origin system, the states and the outputs have been conserve their convergence towards the origin. For the sensitivities of the eigenvalues, taking into account the distance between the origin and incertitude eigenvalues respectively, in real axis almost there is no shifting in real of eigenvalues, and from the imaginary axis there are some displacement of two eigenvalues but they do not have any effect on the stability and robustness of the system.

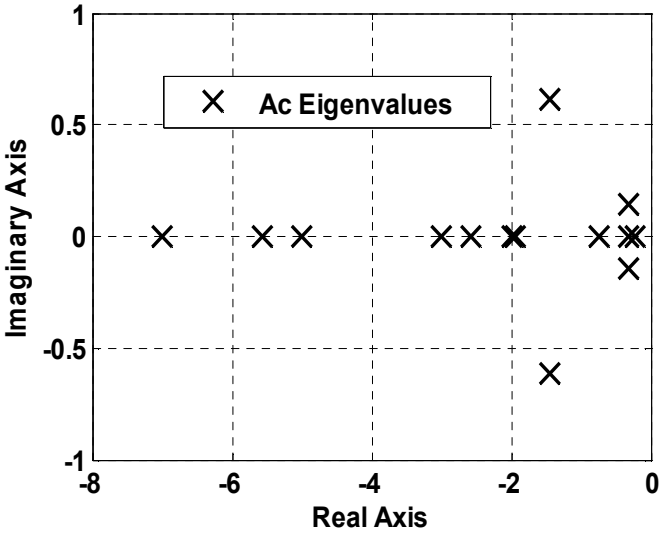



***Fig. 3.*** *Eigen-values of system Under control*

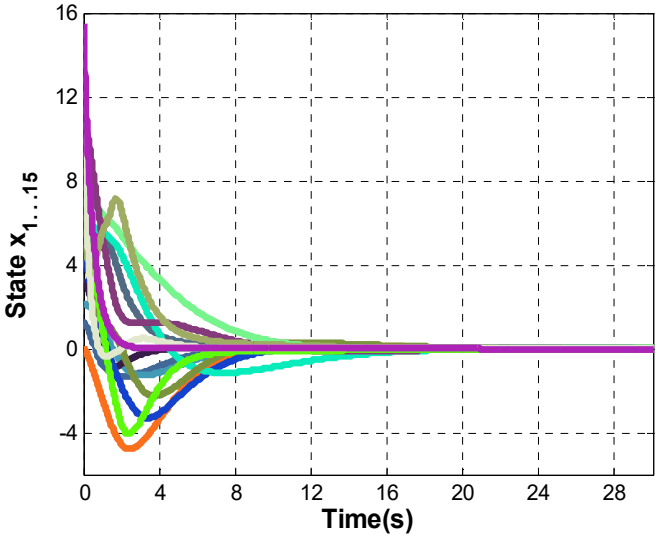



***Fig. 4.*** *The States After Stabilization*

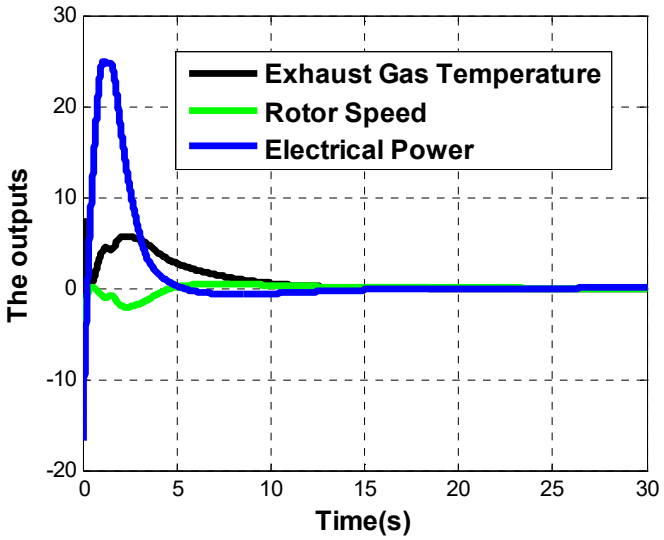



*Fig. 5. The Outputs After Stabilization*

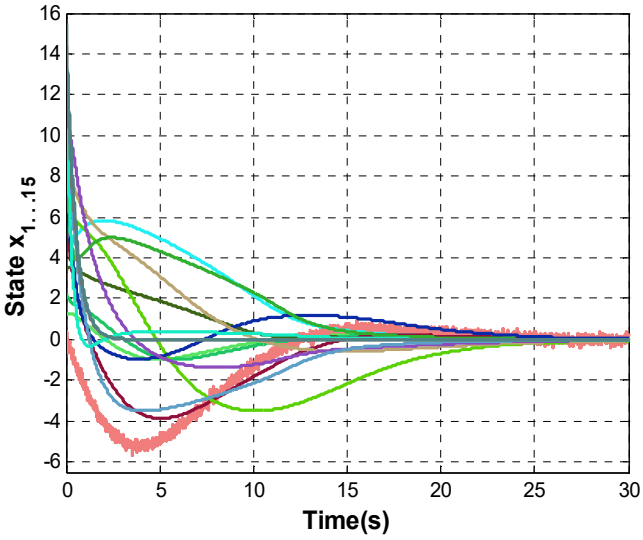



*Fig. 8. The States under noise and disturbance*

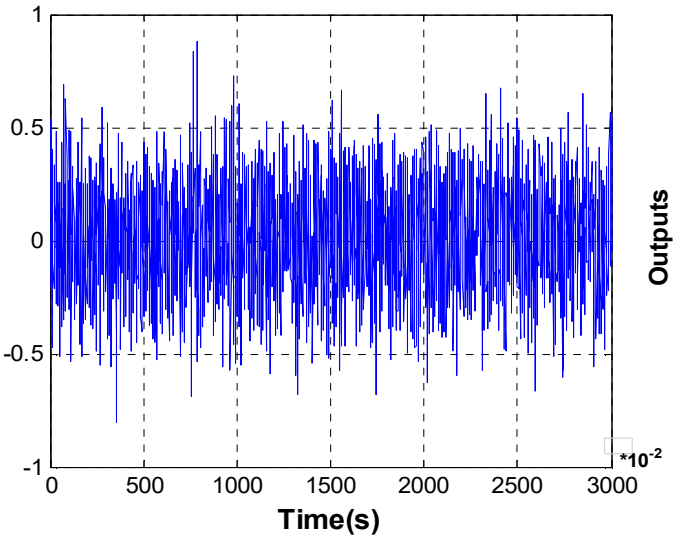



*Fig. 6. Noise and Disturbance*

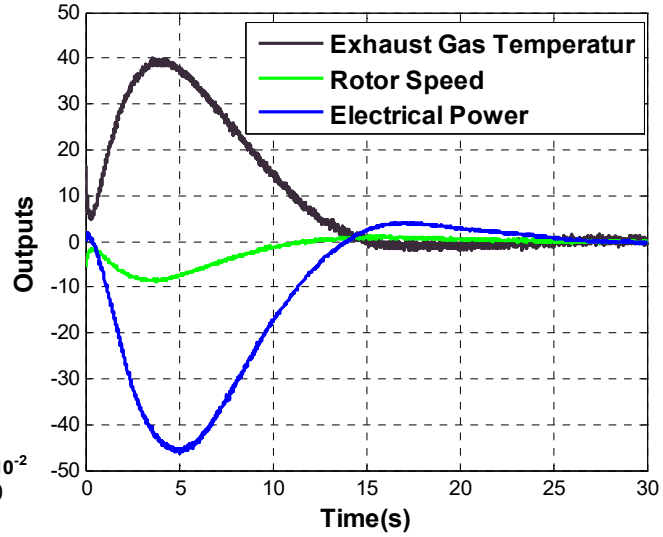



*Fig. 9. The Outputs under noise and disturbance*

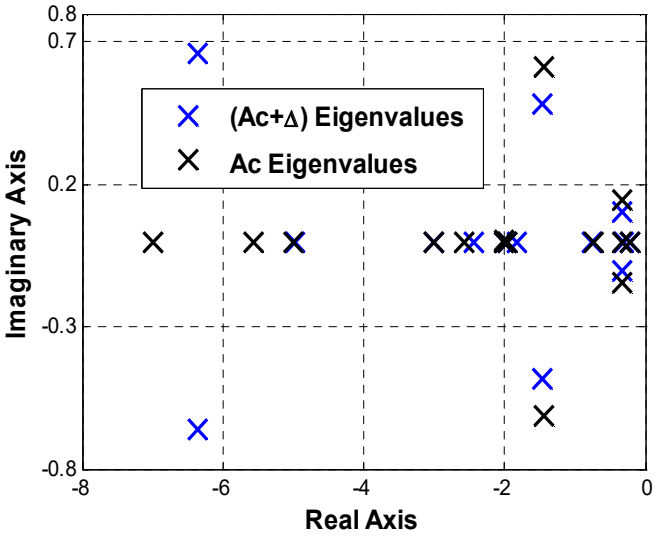



*Fig. 7. Robustness test of Eigen-values*

## 4. Conclusion

Based on the obtained results, it can be concluded that the application of the sliding mode control onalinear system gives best result. Whereas, a very interestingadvantagecan be ensured by this control which is the elimination of chattering problem due to the use of tanh function, on the same time the stability is guaranteed because the SMC is based on theory of lyapunov. On the other side, the robustness of this kind of control is observed, there is no big effect of the external noise and the uncertainties of system, this is due to the structure of this control which is independent on the system behavior.

However, it is important to clarify that there is a negative issue in this controller, which is common in allmost the controllers that are linked to the feedback static matrix gain. this problem is due

mainly to the large calculus and the dimension of the gain matrices*K*and*G*that are always depending on the size of the system order.

As a perspective to present work, future contributions will be oriented to the main aim of reducingthe size of the matrices K and G to overcome the above mentioned drawback.

## REFERENCES


1. H. K. Khalil, Nonlinear Systems, 3rd ed. Upper Saddle River, NJ: Prentice-Hall, 2002.
2. Gordon E. Carlson Signal and Linear Systems Analysis with Matlab second edition, Wiley, 1998, ISBN 0-471-12465-6.
3. M.H.Tu, C.M. Lin, Robust Stabilisation of Multivariable Feedback Systems with Desired Performance Requirement, IEE Proc. Vol. 139,N3, 1992.
4. K. Ogata, Modern Control Engineering, 5th ed, Pearson Education (New Jersey) Pvt. Ltd., USA, 2009, chapter 10-8.
5. Anderson, B.D.O. and Moore, J.B., Optimal Control: Linear Quadratic Methods, Prentice-Hall, Englewood Cliffs, NJ, 1990.
6. Doyle, J.C. and Stein, G., Multivariable feedback design: concepts for a classical/modern synthesis, IEEE Transactions on Automatic Control, Vol. AC-26, No. 1, February 1981.
7. Schultz, M.J. and Inman, D.J., Eigen-structure assignment and controller optimization for mechanica systems, IEEE Transactions on Control Systems Technology, Vol. 2, No.2, 88–100, 1994.
8. Sinha, A. and Miller, D.W., Optimal sliding mode control of a flexible spacecraft under Stochastic disturbances, AIAA Journal of Guidance, Dynamics and Control, Vol. 118, No. 3, 486-492, 1995.
9. BekhitiBelkacem, dahimeneAbdelhakim, Nail Bachir, and HARICHE Kamel, The Left And Right Block Pole Placement Comparison Study : Application To Flight, Dynamics, Informatics Engineering, an International Journal (IEIJ), Vol.4, No.1, March 2016.
10. B.Nail, B.Bekhiti, K.Bdirina, A.Kouzou, and A.Hafaifa, Sliding Mode Control And Optimal GPC Algorithm for Coupled Tanks, 3rd International Conference on Control, Engineering & Information Technology CEIT'2015 Tlemcen, Algeria, 25-27 May, 2015.
11. Alok K. Sinha-Linear systems_ optimal and robust control-CRC Press (2007).
12. Utkin, V. I., Variable Structure Systems with Sliding Modes, IEEE-Trans.Automat, Contr. AC-22 No. 2 (Apr 1977), 212-222.
13. Stein, G., Formal Control System Synthesis with $H_2/H_\infty$ Criteria, Lecture Notes for Multivariable Control Systems Course, MIT, Cambridge, MA, 1988.
14. BekhitiBelkacem, DahimeneAbdelhakim, Nail Bachir, and HARICHE Kamel, 2-DOF Block Pole Placement Control Application To : Have-Dash-Ii Missile , The International Journal of Information Technology, Modeling and Computing.
15. Panos J. Antsaklis, Anthony N. Michel, Linear system New York :McGraw-Hill, © 1997.
16. T. Kailath, Linear System, Englewood Cliffs, Prentice-Hall, NJ, 1980.
17. Chi-Tsong Chen, Linear Systems Theory and Design, Holt, Rinehart and Winston, NY,1984.
18. P.Lancaster, Lambda-Matrices and Vibrating Systems, New York, Pergamon Press, 1966.
19. Slotine J. J. E., J. K. Hedrick and E. A. Misawa, On sliding observers for nonlinear systems, Trans. of the ASME Journal of Dynamic Systems, Measurement and Control, Vol. 109, pp. 245-252, 1987b.
20. Utkin, V. I., Variable Structure Systems with Sliding Modes, IEEE-Trans.Automat, Contr. AC-22 No. 2 (Apr 1977), 212-222.
21. J.A.Mohamed, Y.P. Kakad, Improvement of Robustness and Sensitivity Reduction for Multivariable Nonminimum Phase Systems, IEEE, 1995.
22. Magdi S. Mahmoud and Yuanqing Xia, Applied Control Systems Design,Springer-Verlag London Limited 2012.
23. Alok K. Sinha-Linear systems optimal and robust control-CRC Press (2007).
24. Ljung, L., System Identification : Theory for the user (Prentice Hall ), 1999.
25. Katayama, T., Subspace methods for System Identification, Springer-Verlag, 2005.
26. Akroum, M., and Hariche K., A matrix fraction description-based identification algorithm for MIMO ARMAX models, submitted to Asian journal of control, 2008.



[1] The Applied Automation and Industrial Diagnostics Laboratory LAADI, University of DJELFA, Algeria.

[2]IGEE(Ex INELEC), Boumerdes University.

E-mail: b.nail@univ-djelfa.dz

E-mail: kouzouabdellah@yahoo.fr

Email:hafaifa@hotmail.com

Email:belkacem1988@hotmail.co.u

© International Scientific Conference on Engineering, Technologies and Systems
TECHSYS 2016, Technical University – Sofia, Plovdiv branch
26 – 28 May 2016, Plovdiv, Bulgaria

# RELIABILITY ANALYSIS USING WEIBULL DISTRIBUTION APPLIED TO A BOOSTER PUMP USED IN OIL DRILLING INSTALLATIONS

AHMED HAFAIFA [(1)], KOUZOU ABDELLAH [(1)],
GUEMANA MOULOUD [(2)], NADJI HADROUG [(1)]

**Abstract:** *The safety exploitation in various industrial projects has become an important issue of ergonomics and economics fields. This work proposes the study of the dependability based on reliability analysis of a booster pump used in oil drilling installations. The achieved tests results, presented in this paper, improved the performance of the examined oil drilling sites and determine maintenance of this installation strategy.*

**Keyword:** *Reliability analyses, dependability system, reliability modelling, oil drilling installations, safety system, industrial process, booster pump.*

## 1. Introduction

The safe operation in various industrial installations has become an important issue in ergonomics and economics fields. This dependability is based on the lifetime of a material, which is characterized by three concepts; reliability, maintainability and availability, which can be added that security [5, 9, 14 and 17]. With the technology advancement, in these last years, industrial installations become too complex, it leads the stain dependability become more complex. Several studies have focused on reliability analysis in industrials fields based on the evolution of the failure rate, this tool is very important to characterize the behavior of equipment in different phases of their lifetime exploitation [2, 3, 19 and 24]. In this work, a booster pump used in oil drilling installation into southern Algeria project are examined, the dependability system are studied based on the proposed reliability analysis approach. This study is based on reliability modelling of the global system availability of water pumping in oil drilling, using the feeder pumps. In this investigation Weibull distribution are applied to the examined pump.

The achieved tests results, based on real lifetime data of the examined pump, allows to model many situations of wear and fatigue in the examined system. Also, this approach allows to characterize the pump system behavior, in order to improve the performance of oil drilling sites and to determine the maintenance strategy of this installation.

## 2. Dependability based on reliability function

The safe operation of industrial equipment is based on the lifetime of this equipment, which is characterized mainly on the reliability study, based on failure rate evaluation to characterize the behavior of equipment in different phases of their lifetime in exploitation.

The reliability of a device after $t$ time in exploitation corresponds to the probability is that this device does not have a failure between $0$ and $t$ time in exploitation, expressed by the function $R(t)$, shown in figure 1.

$$R(t) = P(T \geq t) = 1 - F(t) \qquad (1)$$

Where $F(t)$ is the distribution function of the variable $t$.

Copyright © 2016 by Technical University of Sofia, Plovdiv branch, Bulgaria ISSN Online: 2535-0048

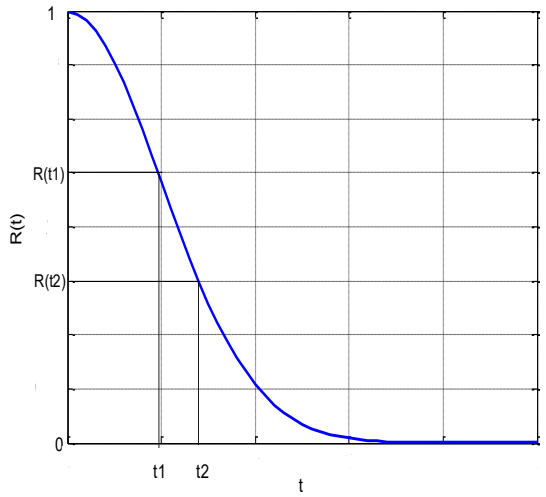



***Fig. 1.*** *Reliability function*

In the reliability study the main indicator is the failure rate $\lambda(t)$ which is the number of failures per cell and per time unit [4, 6], this failure rate is high at the beginning of the lifetime of the device. Then it decreases quite rapidly with time (decreasing failure rate), this phase of life is called period of youth. After it stabilizes at a value we want as low as possible during a period called life period (constant failure rate). In the end, it goes back when the wear and aging effects are felt, it is the aging period (increasing failure rate). The failure rate $\lambda(t)$ is given as follows:

$$\lambda(t) = \lim_{\Delta t \to 0}\left(\frac{1}{\Delta t}.\frac{R(t)-R(t-\Delta t)}{R(t)}\right) \tag{2}$$

$$\lambda(t) = -\frac{dR}{dt}.\frac{1}{R(t)} = \frac{dF(t)}{dt} = \frac{f(t)}{R(t)} \tag{3}$$

The failure rate $\lambda(t)$ knowledge is sufficient to determine the reliability using the following equation:

$$R(t) = \exp\left(-\int_0^t \lambda(t)dt\right) \tag{4}$$

In the most parts of industrial applications in reliability field, using the mean time between failure (MTBF), which is defined as the expected by $T$ value, given as follows:

$$MTBF = E(t) = \int R(t)dt \tag{5}$$

This work examine an industrial pump used in oil drilling installations into southern Algeria site, the study is based on reliability and availability calculations of the global pump system using Weibull distribution with three parameters [1, 16, 20 and 24]. The probability density is given by the flowing expression [3, 15 and 22]:

$$f(t) = \frac{\beta}{\eta}\left(\frac{t-\gamma}{\eta}\right)^{\beta-1} e^{-\left(\frac{t-\gamma}{\eta}\right)}; \quad t \geq \gamma \tag{6}$$

where $\beta \succ 0$ is the shape parameter, $\eta \succ 0$ is the scale parameter and $\gamma \succ 0$ is the position parameter.

The reliability function is given by the equation (7) and the failure rate is given by equation (8).

$$R(t) = -\left(\frac{t-\gamma}{\eta}\right)^{\beta} \tag{7}$$

$$\lambda(t) = \frac{\beta}{\eta}\left(\frac{t-\gamma}{\eta}\right)^{\beta-1}$$
$$f(t) = \frac{\beta}{\eta}\left(\frac{t-\gamma}{\eta}\right)^{\beta-1} e^{-\left(\frac{t-\gamma}{\eta}\right)} \; ; \quad t \geq \gamma \tag{8}$$

In the equations (7, 8) $\eta$ is the real scale parameter, when $\eta$ is not equal to unity, a simple change of scale necessary. The reliability law is given by the relation (9), by derivative of this distribution the probability density function is given by the equation (10).

$$R(t) = e^{-\left(\frac{t}{\eta}\right)^{\beta}} \tag{9}$$

$$f(t) = F'(t) = -R'(t)$$
$$f(t) = \left(1 - e^{-\left(\frac{t}{\eta}\right)^{\beta}}\right)' = -\left(e^{-\left(\frac{t}{\eta}\right)^{\beta}}\right) \tag{10}$$

The derivative of the formula (10) gives us the following:

$$f(t) = -\left(-\left(\left(\frac{t}{\eta}\right)^{\beta}\right)' e^{-\left(\frac{t}{\eta}\right)^{\beta}}\right)$$
$$= \left(\left(\frac{t}{\eta}\right)^{\beta}\right)' e^{-\left(\frac{t}{\eta}\right)^{\beta}}$$
$$f(t) = \beta\left(\frac{t}{\eta}\right)'\left(\frac{t}{\eta}\right)^{\beta-1} e^{-\left(\frac{t}{\eta}\right)^{\beta}} \tag{11}$$
$$= \beta\frac{1}{\eta}\left(\frac{t}{\eta}\right)^{\beta-1} e^{-\left(\frac{t}{\eta}\right)^{\beta}}$$

Finally, the probability density function is given by the relation:

$$f(t)=\frac{\beta}{\eta}\left(\frac{t}{\eta}\right)^{\beta-1} e^{-\left(\frac{t}{\eta}\right)^{\beta}} \quad (12)$$

In take accounts the equations (10, 11, and 12), the failure rate is given by the equation (13), is the same to the instantaneous failure rate.

$$\lambda(t)=\frac{f(t)}{R(t)}=\frac{f(t)}{1-F(t)}$$

$$\lambda(t)=\frac{f(t)}{1-F(t)}=\frac{\beta}{\eta}\left(\frac{t}{\eta}\right)^{\beta-1} .e^{-\left(\frac{t}{\eta}\right)^{\beta}} .\frac{1}{e^{-\left(\frac{t}{\eta}\right)^{\beta}}} \quad (13)$$

$$\lambda(t)=\frac{\beta}{\eta}\left(\frac{t}{\eta}\right)^{\beta-1}$$

### 2.1. Reliability Data Processing

The data reliability studies usually come from historical failure records of exploited system or from test results of the investigated system. In all cases, the time between failures TBF is calculated and classified in ascending order of the number recorded $N$ of the time between failures in sample size. The time between failures is grouped peer class, if $N \succ 50$ with the cumulative frequency given by [13, 21 and 22]:

$$F(i)=\frac{\sum n_i}{N} \quad (14)$$

where $F(i)$ is very similar to Weibull distribution $f(t)$.

The approximation formula of the average ranks given by equation (15) will be used in these work, where $20 \prec N \prec 50$.

$$F(i)=\frac{\sum n_i}{N+1} \quad (15)$$

In the case of $N \prec 20$, the approximation formula of median ranks given by the following equation in (16) will be applied for the examined pump [7, 8, 18 and 23].

$$F(i)=\frac{\sum n_i-0{,}3}{N+0{,}4} \quad (16)$$

In order to improve the maintainability of the examined system by minimization of the time average techniques to repair (MTTR), given by $MTTR=\frac{\sum TTR}{N}=\frac{\sum \text{Intervention Time}}{\text{Number of failures}}$. There is an analogy between the statistical study of the reliability and maintainability of the examined system, explained by the relationship between the variables reliability expressed by the probability density $g(t)$ and the duration of the reparation action $m(t)$ expressed by the probability of repairing in duration $TTR \prec t$ in the equation (17), with the repair rate $\mu(t)$ is given by the equation (18), [10, 11 and 12].

$$M(t)=\int_0^t g(t)dt \quad (17)$$

$$\mu(t)=\frac{g(t)}{1-M(t)} \quad (18)$$

In this examined case, to obtained a good availability, it must have the least possible downtime and quickly be repaired if it breaks down. The availability rate is steady as follows:

$$D=\frac{\mu(t)}{\mu(t)+\lambda(t)} \quad (19)$$

### 3. Application results

In this part of the present work, booster pumps used in oil drilling installations are examined. The real data of the uptime and duration breakdowns are grouped and sorted in ascending order, from historical records of the studied pump, during the operating period of 2000-2010, in the following table.

***Table 1.*** *Reliability data of the studied pump*

| Rang | TBF (h) | TTR (h) | F(t) (%) | R (t) (%) | $\lambda$ (t) $10^{-4}$ |
|---|---|---|---|---|---|
| 1 | 720 | 96 | 8,33 | 91,67 | 0,95 |
| 2 | 2160 | 108 | 20,23 | 79,77 | 1,12 |
| 3 | 2880 | 114 | 32,14 | 67,86 | 1,17 |
| 4 | 5760 | 48 | 44,04 | 55,96 | 1,30 |
| 5 | 6480 | 87 | 55,95 | 44,05 | 1,32 |
| 6 | 7200 | 56 | 67,85 | 32,15 | 1,35 |
| 7 | 16700 | 24 | 79,76 | 20,24 | 1,53 |
| 8 | 21600 | 67 | 91,66 | 8,34 | 1,59 |

The mean time between failures using Weibull distribution applied to the studied booster pump is 7925,7576 hours. The cumulative failure and the hazard function of the examined system, using Weibull distribution with tow parameters is shown respectively in the figures 2, 3 and the reliability function and Weibull probability paper in the figure 4 and 5.

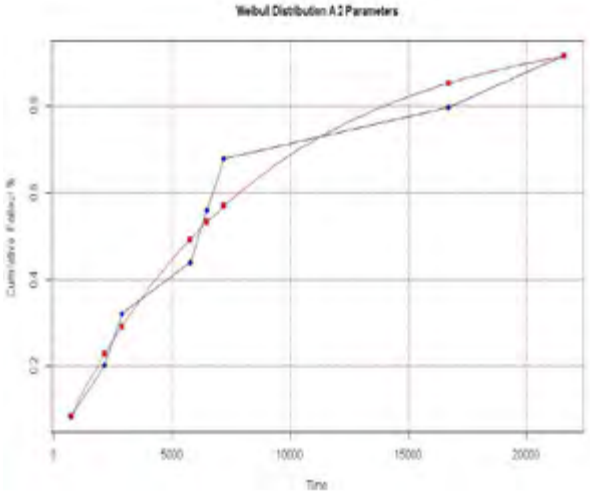



***Fig. 2.*** *Cumulative failure using Weibull distribution with tow parameters*

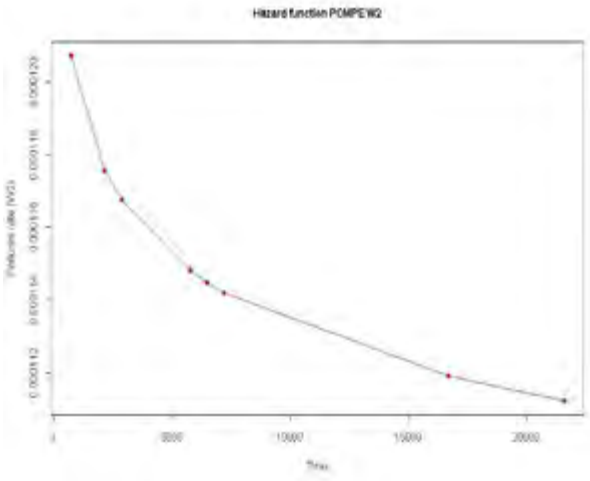



***Fig. 3.*** *Hazard function using Weibull distribution with tow parameters*

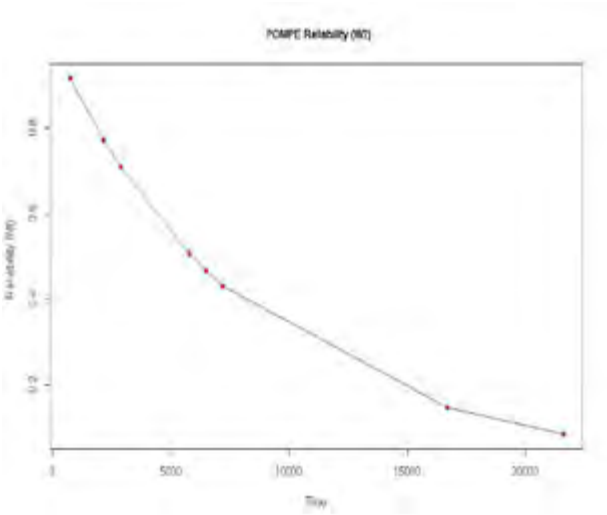



***Fig. 4.*** *Reliability function using Weibull distribution with tow parameters*

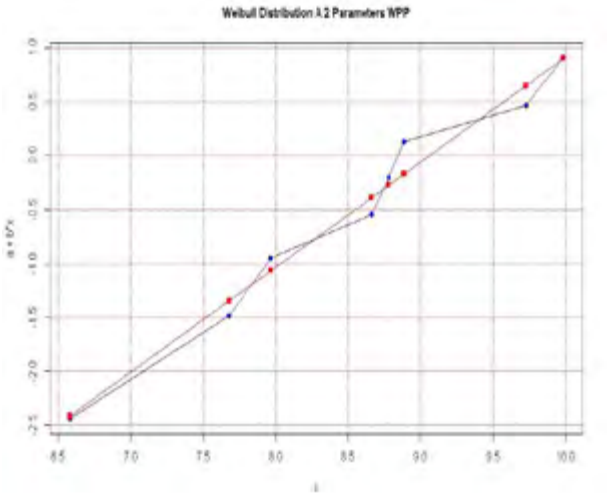



***Fig. 5.*** *Weibull probability paper using Weibull distribution with tow parameters*

The reliability curve decreases with time, which is normal and this is due to wear and failures are random. According to the graph the failure rate is strongly increasing at the beginning and then more slowly. Other validation tests on the examined pump were achieved using Weibull distribution with three parameters; this confirms the effectiveness of the proposed approach in this work.

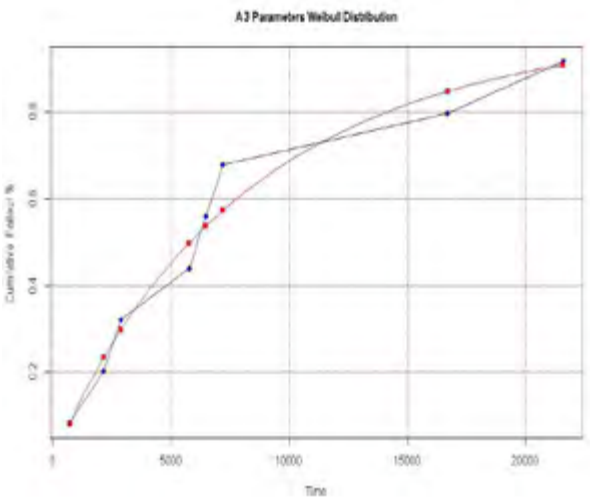



***Fig. 6.*** *Cumulative failure using Weibull distribution with tow parameters*

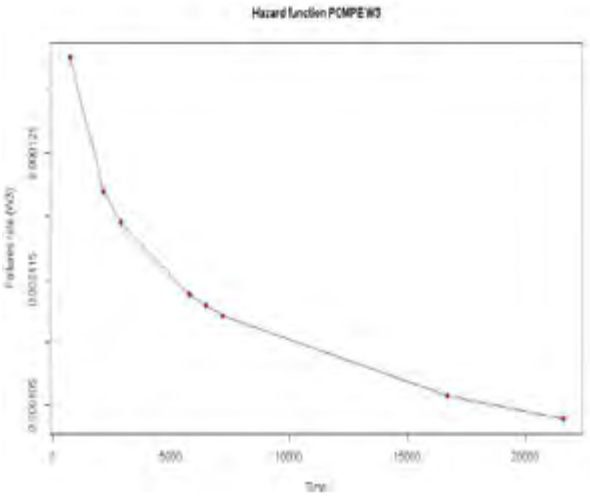



***Fig. 7.*** *Hazard function using Weibull distribution with tow parameters*

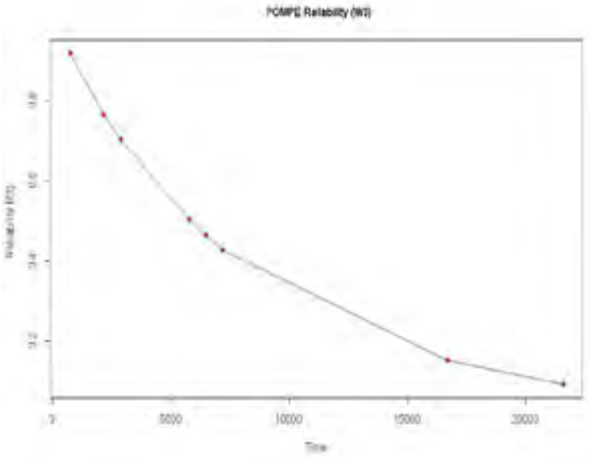



***Fig. 8.*** *Reliability function using Weibull distribution with tow parameters*

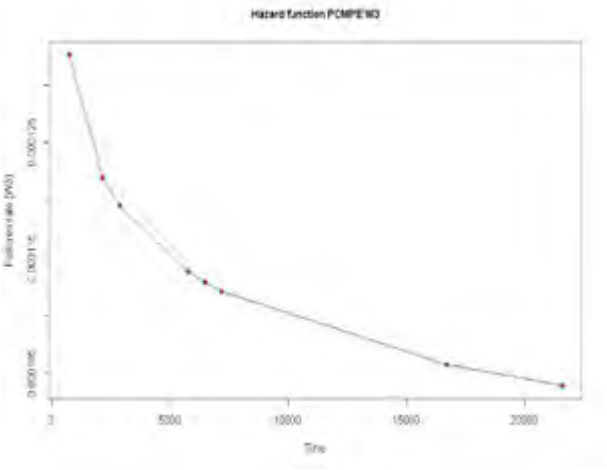



***Fig. 9.*** *Weibull probability paper using Weibull distribution with tow parameters*

On this basis, a reliability study was conducted; the average uptime was calculated on the basis of historical records. We note that the availability is high, as the booster pump. The calculating the reliability parameter using Weibull distribution with tow and three parameters, figure 10 shows that the booster pump out of the period of the useful life and enters the period of old age.

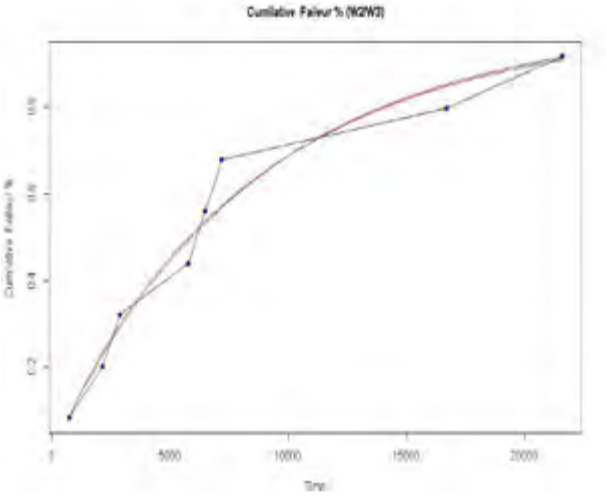



***Fig. 10.*** *Cumulative failure with Weibull distribution with tow and three parameters*

## 4. Conclusion

The reliability analysis is a very important tool to characterize the behavior of industrial systems in different phases of time life. In this paper, a booster pump used in oil drilling installations are examined, using Weibull distribution with tow and three parameters to there reliability analysis. The achieved tests results, improve the performance of the examined oil

drilling sites and determine maintenance of this installation strategy.

The obtained results in this work, has allowed us to analyze the reliability of the examined pump. That allows us to take technical decisions to determine their intervention program and assess maintenance and consequently the degree of confidence in exploitation of this system. Indeed, the studied operational reliability in this work is based on the experience feedback, given the time guarantee measure and decrypts the lifetime of the examined booster pump. This allowed us a better exploitation of the pump in order to optimize their operations and meet production.

## References


1. Asghar Moeini, Kouroush Jenab, Mohsen Mohammadi, Mehdi Foumani, (2013). Fitting the three-parameter Weibull distribution with Cross Entropy. *Applied Mathematical Modelling*, vol. 37, no. 9, pp. 6354-6363.
2. Chiacchio F., Cacioppo M., D'Urso D., Manno G., Trapani N., Compagno L., (2013). A Weibull-based compositional approach for hierarchical dynamic fault trees. *Reliability Engineering & System Safety*, vol. 109, pp. 45-52.
3. Djamel Halimi, Ahmed Hafaifa and Elahmoune Bouali, (2014). Maintenance actions planning in industrial centrifugal compressor based on failure analysis. *The quarterly Journal of Maintenance and Reliability*, vol. 16, no. 1, pp. 17–21.
4. Emad E. Elmahdy, Abdallah W. Aboutahoun, (2013). A new approach for parameter estimation of finite Weibull mixture distributions for reliability modeling. *Applied Mathematical Modelling*, vol. 37, no. 4, pp. 1800-1810.
5. Emilio Sarno, Vipin Kumar, Wei Li, (2005). A hybrid methodology for enhancing reliability of large systems in conceptual design and its application to the design of a multiphase flow station. *Research in Engineering Design*, vol. 16, no. 1-2, pp. 27-41.
6. Govind S. Mudholkar, Kobby O. Asubonteng, Alan D. Hutson, (2009). Transformation of the bathtub failure rate data in reliability for using Weibull-model analysis. *Statistical Methodology*, vol. 6, no. 6, pp. 622-633.
7. Hafaifa Ahmed, Belhadef Rachid, Guemana Mouloud, Reliability model exploitation in industrial system maintainability using expert system evaluation. Proceeding of the 4th International Conference on Integrity, Reliability and Failure IRF2013, 23-27 June 2013 in Funchal, Madeira, Portugal.
8. Hafaifa Ahmed, Mouloud Guemana and Attia Daoudi, Spectral analysis approach applied to the vibrations detection and isolation in centrifugal pump used in petroleum industry. Proceeding of the 5th International Congress on Technical Diagnostics, September 2012, Univeristy of Science and Technology, Kraków, Poland.
9. Hafaifa Ahmed, Ferhat Laaouad and Moulod Guemana, (2009). A New engineering method for fuzzy reliability analysis of surge control in centrifugal compressor. *American Journal of Engineering and Applied Sciences*, vol. 02 no. 04, pp. 676-682.
10. Hafaifa Ahmed, Ferhat Laaouad and Kouider Laroussi, A new engineering method for fuzzy reliability analysis of surge control in centrifugal compressor. Proceeding of the 2nd International Conference on Control, Instrumentation and Mechatronic Engineering (CIM2009), Melaka, Malaysia. 2-3 June 2009.
11. Isabel Sartori, Edilson M. de Assis, Adilton L. da Silva, Rosana L.F. Vieira de Melo, Ernesto P. Borges, e Silvio A.B. Vieira de Melo, (2009). Reliability Modeling of a Natural Gas Recovery Plant Using q-Weibull Distribution. *Computer Aided Chemical Engineering*, vol. 27, pp. 1797-1802.
12. Kucheryavyi V. I., Mil'kov S. N., (2009). Statistical modeling of the lifetime of face seals in an oil-transfer pump. *Journal of Machinery Manufacture and Reliability*, vol. 38, no. 1, pp 94-99.
13. Li Zhengmei, Zhou Qiong, An Qi, Tang Jianping, (2011). Influences of eccentric unbalances on loads and life of auto water pump bearing. *Mechanism and Machine Theory*, vol. 46, no. 3, pp. 253-263.
14. Mansour Aghababaei Jazi, Chin-Diew Lai, Mohammad Hossein Alamatsaz, (2010). A discrete inverse Weibull distribution and estimation of its parameters. *Statistical Methodology*, vol. 7, no. 2, pp. 121-132.
15. Mokronosov E. D., Bogdanov V. V. and Eltyshev M. N., (2007). Increase in the operating reliability of a well sucker-rod pump. *Chemical and Petroleum Engineering*, vol. 43, no. 11-12, pp. 756-758.
16. Mouloud Guemana, Slimane Aissani and Ahmed Hafaifa, (2011). Use a new calibration method for gas pipelines: An advanced method improves calibrating orifice flowmeters while reducing maintenance costs. *Hydrocarbon Processing Journal*, vol. 90, no. 8, pp. 63-68.

17. Qing Zhang, Cheng Hua, Guanghua Xu, (2014). A mixture Weibull proportional hazard model for mechanical system failure prediction utilising lifetime and monitoring data. *Mechanical Systems and Signal Processing*, vol. 43, no. 1–2, 3, pp. 103-112.
18. Raif Sakin, İrfan Ay, (2008). Statistical analysis of bending fatigue life data using Weibull distribution in glass-fiber reinforced polyester composites. *Materials & Design*, vol. 29, no. 6, pp. 1170-1181.
19. Saad J. Almalki, Saralees Nadarajah, (2014). Modifications of the Weibull distribution: A review. *Reliability Engineering & System Safety*, vol. 124, pp. 32-55.
20. Saad J. Almalki, Jingsong Yuan, (2013). A new modified Weibull distribution. *Reliability Engineering & System Safety*, vol. 111, pp. 164-170.
21. Schijve J., (2005). Statistical distribution functions and fatigue of structures. *International Journal of Fatigue*, vol. 27, no. 9, pp. 1031-1039.
22. Tieling Zhang, Min Xie, (2011). On the upper truncated Weibull distribution and its reliability implications. *Reliability Engineering & System Safety*, vol. 96, no. 1, pp. 194-200.
23. Vitkovskii V., Kirillov I. R., Chaika P. Yu., Kryuchkov E. A., Poplavskii V. M., Nosov Yu. V., Oshkanov N. N., (2007). Performance-based reliability assessment of electromagnetic pumps. *Atomic Energy*, vol. 102, no. 2, pp. 122-128.
24. Zhejun Gong, (2006). Estimation of mixed Weibull distribution parameters using the SCEM-UA algorithm: Application and comparison with MLE in automotive reliability analysis. *Reliability Engineering & System Safety*, vol. 91, no. 8, pp. 915-922.

**Authors' contacts**

**Ahmed Hafaifa [(1)], Kouzou Abdellah [(1)] , Mouloud Guemana [(2)] and Nadji Hadroug [(1)]**

[(1)] Applied Automation and Industrial Diagnostics Laboratory, Faculty of Science and Technology, University of Djelfa 17000 DZ, Algeria

[(2)] Faculty of Science and Technology, University of Medea, Algeria

**Ahmed Hafaifa [(1)]**
E-mail: hafaifa.ahmed.dz@ieee.org
**Kouzou Abdellah [(1)]**
E-mail: kouzouabdellah@ieee.org
**Mouloud Guemana [(2)]**
E-mail: guemana_m@yahoo.fr
**Nadji Hadroug [(1)]**
E-mail: N_Hadroug@univ-djelfa.dz

© International Scientific Conference on Engineering, Technologies and Systems
TECHSYS 2016, Technical University – Sofia, Plovdiv branch
26 – 28 May 2016, Plovdiv, Bulgaria

# ICT TECHNOLOGIES IN WILDLAND FIRES MODELLING FOR TEST CASES (BULGARIA)

NINA DOBRINKOVA

**Abstract:** *In this paper we will provide an overview of the used ICT tools for wildland fire propagation on the Bulgarian territory from a team working in IICT-BAS. Most of the data is received by the forest departments in Zlatograd and Harmanly where the main simulated wildland fires are located. The summary of the results is giving the conclusion that the fires in Bulgaria need more detailed burning materials classification, but with the ICT tools used the achieved results are quite promising.*

**Key words:** *wildland fires, simulations with ICT tools for wildland fires, Harmanly test case, Zlatograd test case*

## 1. Introduction

Due to climate change and very fast developing of the modern society forest fires are growing problem for the southern countries of Europe. Statistics concerning the development of forest fires in the last years are published in reports by the centres in the EU which monitor the forest conditions [1]. Observations in the member states of EU in the period 1980–2005 showed an increasing number of areas affected by the fires. Bulgaria was not included in the study because it was not a member of EU until 2007, but independent research done on the topic describes an increase of wildland fires since 1995 on the Bulgarian territory until now [2, 3]. The problem is not only in Bulgaria, but it is well known worldwide and research teams in the US have begun their research in the field in the beginning of last century to investigate the tools and methods to simulate wildland fire propagation. The Missoula Fire Laboratory in Rocky Mountains is the pioneer in the research with its scientist Richard Rothermel [4]. In fact, Rothermel and his team in Missoula are considered as founders of fire modelling research. The first working wildland fire behaviour model was created by them in 1972 and since then it has been improved several times. Every subsequent model's modifications included consideration of further parameters that could make the simulations obtained by scientists more realistic and accurate.

In the early 80s of the last century, M. Grishin, professor at the University of Tomsk, Russia, has worked and developed a model [5] which uses data on the types of burning materials in the taiga (mostly conifers) and takes into account that the main combustion intensity happens in the crowns of trees.

Approximately at the same time attempts at wildland simulations were made in laboratories in Sydney, Australia. These models did not become as popular as the US ones, because of some computational issues at that time, concerning PC power, data coverage, etc. Nowadays many laboratories are involved in modelling of wildland fire behavior propagation. It is easier to find such teams in the affected zones, simply because this knowledge saves time and efforts to the incident commanders on the field.

The development of modern information and communication tools allows application of cutting-edge technologies to solve problems related to the forest and field fires. The use of these tools not only allows early detection of fires but also enables the prediction of the dynamics related to fire spread of the fire line and the extent of the possible damages of the environment and citizens' property.

The main types of wildland fires described in the specialized literature are classified as follows: type 1—surface fires [4,6]; type 2—crown fires [5,7]; type 3—spotting fires as modified crown fires and type 4—fire acceleration, when the terrain has steep slopes.

In our paper we will present how through different ICT tools the knowledge about local Digital Elevation Model (DEM), land cover (burning materials) and meteorological conditions can give good enough predictions for fire spread according to the different scenarios elaborated by the fire analysts working with the data.

Copyright © 2016 by Technical University of Sofia, Plovdiv branch, Bulgaria ISSN Online: 2535-0048

## 2. First simulations with Harmanli test site

The first elaborated data was for a test case of a fire near by a village next to Harmanli town. The data collected there was processed by Geographical Information Systems (GIS) in order to have visual representation for the final burning scars of the simulated fires. That was needed for calibration purposes. The used technology was based on the parallel computations where semi-empirical approach for fire spread implies that the fire spreads toward the normal to the front line, which is expressed by a modified Rothermel's formula. The burning area for time $t$ has been presented as area Ω, which is a set of points in the (x, y) plane. Let:

$$\tilde{S} = \min\{B_0, R_0 + \phi_w + \phi_s\}, \quad (1)$$

where $B_0$ is the fire spread against the wind direction, $R_0$ is the fire spread in absence of wind, $\phi_w = a\,(\upsilon \cdot \dot{n})^b$ is the wind correction and $\phi_s = d\nabla z \cdot \vec{n}$ is the terrain correction, $\vec{\upsilon}$ is the wind, $\nabla z$ is a terrain component of the normal $\vec{n}$ of the fire line, $a$, $b$ and $d$ are certain constants. In this case the WRF-Fire model (renamed in 2011 SFire) describes the maximal fire spread with the formula:

$$S = \begin{cases} 0, \text{ако } \bar{S} < 0 \\ S_{\max}, \text{ако } \bar{S} > S_{\max} \\ \bar{S}, \text{ако } 0 \le \bar{S} \le S_{\max} \end{cases}, \quad (2)$$

where $S_{\max}$ is the maximal spread of the fire.
After the ignition of the combustible materials its amount of combustible material in point ($x$, $y$) decreases exponentially and is given by the formula:

$$F(x, y, t) = F_0(x, y)e^{-(t-t_i(x,y))/W(x,y)}, \quad (3)$$

where $t$ is the time, $t_i$ is the ignition time, $F_0$ is the initial quantity of the burning materials (before their ignition) and $W(x,y)$ does not depend on the time, but on the burning materials.

Heat flow released from the fire is presented in the atmospheric model as a layer above the ground deployed in height [8]. The flow depends on the amount of material burned and can be presented by the formula:

$$\Phi = -A(x, y)\frac{\partial}{\partial t}F(x, y, t). \quad (4)$$

This representation is needed because the atmospheric model from WRF does not support limits on heat flow. The coefficients and functions B0, R0, Smax, a, b, d, W and A are determined by laboratory experiments.
For each point in the plane the coefficients of combustible materials are given as representatives of one of Anderson's 13 categories [9], valid for US burning materials and applied to Bulgarian conditions. Different altitude values for the wind are also used. WRF-Fire has internal representation for each of the cathegories, which gives options for determining when the simulated area is outside US.
WRF-Fire uses a different modelling of the spread of fire through so called level-set functions [10]. In this approach a function $\psi = \psi(x, y, t)$ is set, which defines subareas of Ω by the rule:

$$\Omega(t) = \{(x, y) \in \Omega : \psi(x, y, t) < 0\}. \quad (5)$$

These areas are considered to be burned, and the line of fire is set by the curve:

$$\Gamma(t) = \{(x, y) \in \Omega : \psi(x, y, t) = 0\}. \quad (6)$$

The function $\psi(x, y, t)$ satisfies the equation:

$$\frac{\partial \psi}{\partial t} + S(x, y)\,|\nabla \psi| = 0, \quad (7)$$

which can be solved numerically.
The formulas (1–7) are sufficient for the general description of the simulation of the development of fire. At the beginning the atmospheric model interpolates the wind to match the size of the smaller area of the fire. Then a numerical method is applied for evaluating the level set function. The next step applies quadrature formulas for evaluation of the amount of the burning material. Simultaneously the heat flow released to the atmosphere is estimated. The last usually forces changes in the weather and therefore the steps need to be repeated again.
WRF-Fire is tested for first time with real wildland fire in Bulgaria. The fire happened near Leshnikovo village (Harmanli) in August 14–17, 2009. Unfortunately, unlike in the US, not all of the necessary data is available for free in Bulgaria. Thus we develop and present procedures for manual production of some data needed for the land cover and land use by applying GIS tools on available ortophoto pictures for the area of interest. The method

uses information about the terrain and the meteorological data (for the corresponding period) as an input file. The most successful simulation was done on the supercomputer at the University of Denver by distant connection. In Table 1 the simulation results are presented according to the number of the cores used.

***Table 1:*** *The time required for the simulation presented in seconds depending on the number of processors running the parallel execution of processes showing that in 120 cores the simulations run as real time. Everything above is faster than real fire propagation.*

| Cores | 6 | 12 | 24 | 36 | 60 | 120 | 240 | 360 | 480 | 720 | 960 | 1200 |
|---|---|---|---|---|---|---|---|---|---|---|---|---|
| Fire line propagation in km. | 1.91 | 1.08 | 0.50 | 0.34 | 0.22 | 0.13 | 0.08 | 0.06 | 0.06 | 0.04 | 0.10 | 0.04 |
| Region 1 | 6.76 | 7.05 | 2.90 | 2.06 | 1.20 | 0.73 | 0.45 | 0.32 | 0.26 | 0.23 | 0.24 | 0.17 |
| Region 2 | 0.00 | 0.00 | 0.00 | 0.02 | 0.02 | 0.04 | 0.04 | 0.06 | 0.06 | 0.08 | 0.07 | 0.15 |
| Total sec. which is the coeff. for real time | 10.59 | 9.21 | 3.91 | 2.75 | 1.64 | 0.99 | 0.61 | 0.44 | 0.37 | 0.31 | 0.44 | 0.26 |

With this first simulations of our team in the test site nearby Harmanli town has been elaborated a methodology for collection, procession and implementation of real data for test sites on Bulgarian territory. The selected model was having as input meteorological data, DEM and only 13 burning classes which led to the idea that we can experiment also with different models like BEHAVE Plus and FARSITE for our next tests.

## 3. BEHAVE Plus and FARSITE simulations for the test sites in Zlatograd forestry department

In the framework of bilateral cooperation program between Greece and Bulgaria 2007-2013 our team was having the opportunity to work in the Zlatograd forestry department. The study area was the territorial state-owned forestry department in Zlatograd, which covers an area of 33,532 ha, where 31,856 ha are state forests. Most forests are in early to mid-seral successional stages, with only small amounts of mature to old forest. Stand age is highly variable, ranging from 20 to 80 yrs; most stands range between 35 to 50 yrs with the average being 46 yrs. Average stem stock is 140 $m^3$ ha-1. The average forest canopy cover is 81%.

In terms of climate, the region is part of the continental-Mediterranean climatic region, south-Bulgarian climatic sub-region and East Rodopi mountain low climate region. The average annual temperature is 10.8ºC, with a maximum temperature in July of 20.6ºC and minimum temperature in January of -0.8ºC, indicating moderate summers and relatively mild winters. Extreme values of annual average maximum and minimum temperature are respectively 17.1ºC and 4.9ºC, the monthly maximum is in August (28.9ºC) and the average monthly minimum occurs in January (-3.9ºC). Average annual rainfall reaches 1000 mm. Maximum precipitation amounts for the period from April to October range from 10.0 mm for 5 min to 46.3 mm for 60 min and 59.7 mm for more than 60 min. The average annual relative humidity is 75% which is an indication of good growing conditions; maximum relative humidity values of 85% occur in November. However, approximately 13-15 days per year have relative humidity less than or equal to 30%, during which time wildfires may be of higher concern.

The data we were working on was about fifteen wildfires that occurred in 2011 to 2012 within the Zlatograd municipal territory were provided by the Zlatograd forestry department; this data included vegetation type, area burned (in decares where 10 decares = 1 hectare), date, and start and end hours of the fire event (Table 2). These wildfires burned in a variety of vegetation types and were more than likely started by humans to clear agricultural debris or prepare fields, based on the proximity to villages. Paper maps from the forestry department identified the ignition location and final fire shape; this data was digitized in a GIS which allowed each ignition point to be viewed with background orthophotos and the spatial Zlatograd vegetation classification showing pre-fire vegetation (Table 2)

**Table 2:** *Fire information provided by the Zlatograd Forestry Department for the period 2011-2012*

| Fire No. | Vegetation type | Burned area in decares | Date of occurrence | Hour of start | Hour of end |
|---|---|---|---|---|---|
| 1 | Dumasit | 3.0 | 25 March 2012 | 1330 | 1530 |
| 2 | Beechwood | 5.0 | 29 March 2012 | 1400 | 1800 |
| 3 | Scotch pine | 1.0 | 16 June 2012 | 1500 | 1700 |
| 4 | Scotch pine | 7.0 | 6Aug. 2012 | 1640 | 1950 |
| 5 | Scotch pine | 5.0 | 6 Aug. 2012 | 1710 | 2130 |
| 6 | European black pine | 4.0 | 27Aug. 2012 | 1200 | 1600 |
| 7 | Scotch pine | 3.0 | 5 Sept. 2012 | 1400 | 2030 |
| 8 | Scotch pine | 6.0 | 6 Sept. 2012 | 1400 | 1930 |
| 9 | Scotch pine | 2.0 | 6 Oct. 2012 | 1600 | 2320 |
| 10 | Scotch pine | 1.0 | 16 March 2011 | 1310 | 1400 |
| 11 | Scotch pine | 1.0 | 5 April 2011 | 1715 | 1900 |
| 12 | Scotch pine | 1.0 | 10 April 2011 | 1130 | 1530 |
| 13 | Grassland | 3.0 | 30 Aug. 2011 | 1400 | 1800 |
| 14 | Scotch pine | 4.0 | 12 Sept. 2011 | 1230 | 1900 |
| 15 | Scotch pine | 1.0 | 15 Sept. 2011 | 1600 | 1830 |

After we collected and located the forest fires we did runs with BehavePlus point based prediction system in order to analyze fire growth and behavior for homogeneous vegetation with static weather data. We used standard fuel models developed for US and we evaluated which fuel models were best able to produce estimates of fire behavior and growth in BehavePlus similar to those observed on each of the fifteen fires. In addition to fuel model, BehavePlus requires inputs for weather, fuel moisture, slope, and duration of the burning period. We obtained weather data for each fire from TV Met, a private company in Bulgaria, which provided the ability to calculate fine dead fuel moisture values. Due to the paucity of available weather data in Bulgaria, we had to assume that weather recorded for the weather station closest to each particular fire is consistent with weather experienced on the wildfire. We estimated live herbaceous and live woody fuel moisture values based on the expected phenological stage for the time of year that the fire occurred. To estimate slope, we first acquired a 30 m resolution digital elevation model (DEM) from the National Institute of Geophysics, Geodesy, and Geography in Bulgaria, then subsequently calculated the average slope for each fire using standard geospatial processing in ArcGIS (ESRI 2010). Burn period length for each fire was obtained from the Zlatograd forestry department data (Table 2).

Based on initial BehavePlus results using standard fuel models, custom fuel models were developed for some vegetation types not well represented by the US fuel models. Custom fuel models were developed for native durmast oak and grass as well as one of the Scotch pine sites by modifying fuel loading parameters to better match local vegetation and reflect the lack of woody debris in the understory.

Following evaluation of fuel models with BehavePlus, we then performed analyses in FARSITE, a spatial fire growth system that integrates fire spread models with a suite of spatial data and tabular weather, wind and fuel moisture data to project fire growth and behavior across a landscape. We defined our test landscapes using a 500 m buffer zone around each of the fifteen Zlatograd fires.

Input for FARSITE consists of spatial topographic, vegetation, and fuels parameters compiled into a multi-layered "landscape file" format. Topographic data required to run FARSITE include elevation, slope, and aspect. Using the aforementioned 30 m DEM, we calculated an aspect layer, and then clipped elevation, aspect, and slope rasters to the extent of our fifteen test landscapes. Required vegetation data include fuel model and canopy cover. Fuel models within the 500 m buffered analysis area for each individual fire were assigned based on our BehavePlus analyses; fuel model assignments were tied to the dominant vegetation for each polygon based on the Zlatograd forestry department's vegetation data. Canopy cover values were visually estimated from orthophoto images and verified with stand data from the Zlatograd forestry department. Additional canopy variables (canopy base height, canopy bulk density, and canopy height) that may be included in the landscape file were omitted, as these variables are most important for calculating crown fire spread or the potential for a surface fire to transition to a crown fire. None of the fifteen fires analyzed experienced crown fire.

Tabular weather and wind files for FARSITE were compiled using the weather and wind data from TV Met, Bulgarian meteorological company that included hourly records. Tabular fuel moisture files were created using the fine dead fuel moisture values calculated for the BehavePlus analyses for 1-hr timelag fuels. The 10-hr fuel moisture value was estimated by adding 1% to the 1-hr fuel moisture and the 100-hr fuel moisture was generally calculated by adding 3% to the 1-hr fuel moisture. The live fuel moisture values previously estimated for BehavePlus analyses were used to populate live herbaceous and live woody moisture values.

All simulations performed in FARSITE used metric data for inputs and outputs. An adjustment value was not used to alter rate of spread for standard fuel models, rather custom fuel models were created. Crown fire, embers from torching trees, and growth from spot fires were not enabled.

As an example of one of our successful FARSITE runs, we present the results from a single wildfire that burned in grassland vegetation, for which we developed custom fuel models. This fire occurred on August 30, 2011, starting at 1400 and ending around 1800, and burned a total area of 0.3 ha. We used the following input parameters to model this small grassland fire in FARSITE:

Fuel moisture values: 6% (1-hr), 7% (10-hr), 9% (100-hr), 45% (live herbaceous), and 75% (live woody);

Daily maximum temperatures: 17-21°C;

Daily minimum relative humidity: 24-50%;

Winds: generally from the west-southwest at 1-2 k h-1

The fire size as calculated using FARSITE was 0.5 ha, which seems reasonable considering the modeled size would not have included the suppression actions that most likely occurred given the close proximity of a village to this fire figure 1.

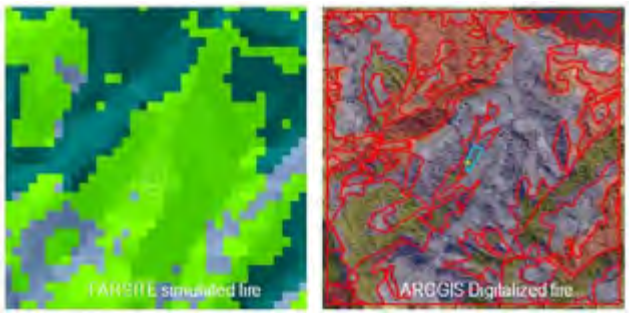



**Figure 1:** *FARSITE run for a grassland fire, where size of the fire is very close to the real one, but the shape is different, because of wind information discrepancies*

An example of another fire we modeled in FARSITE using standard fuel models was a fire that occurred on March 29, 2012 in a beechwood forest. This fire burned for a total of four hours, starting at 1400 and ending around 1800, and burned a total area of 0.5 ha. Wind speeds were variable throughout the burning period as they were quite high during the early afternoon but tapered off throughout the day. In this case we used the following input parameters in FARSITE:

Fuel moisture values: 3% (1-hr), 4% (10-hr), 5% (100-hr), 40% (live herbaceous) and 70% (live woody);

Daily maximum temperatures: 7-10°C;

Daily minimum relative humidity: 36-40%;

Winds: generally from the north-northeast at 10-2 k h-1

The projected fire size from FARSITE was 0.9 ha. Based on the close proximity of a village to the fire location (figure 2) it is quite reasonable to assume that local residents responded to the fire in a volunteer capacity; these suppression actions are not accounted for in the FARSITE analysis. Decreasing winds through the afternoon may have significantly helped suppression activities.

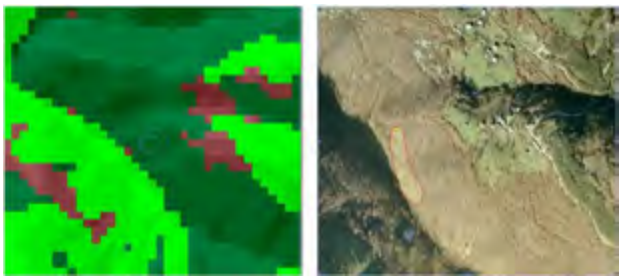


**Figure 2:** *FARSITE run for wildfire that burned in a beechwood forest, where size of the fire is very close to the real one, but the shape is different, because of wind information discrepancies*

From this two modeled fires we were able to estimate that the standard fuel models established for US can be run also for Bulgarian cases, but only after a good calibration with real case studies where vegetation and past events are well observed. However FARSITE and BehavePlus provided reasonable outputs for future work in the field of fire behavior fuel modeling on the Bulgarian territory. The work done in more details is described in [11,12,13,14].

## 4. Conclusion

This paper was an overview paper presenting the test case studies referring to wildland fire propagation and all related simulations. Our main goal was to show the used tools so far on Bulgarian territory and open the ground for a discussion in the field is similar or better tools can be used by having different ICT application than the ones described.

## 5. Acknowledgement

This work has been supported by the Bulgarian Academy of Sciences Program for support of young researchers No: ДФНП-95-А1 and by the National Science Fund of the Bulgarian Ministry of Education, Youth and Science under Grant FNI I02/20.

## REFERENCES

1. Report 6, Forest Fires in Europe 2005, Joint Research Centre—European Commision, EUR 22312 EN, European Communities 2006.
2. Internet resources of the National Fire Safety and Civil Protection Service of Bulgaria.
3. Ecopolis, bulletin 48 (2001), Forest fires reach catastrophic scales (In Bulgarian) http://www.bluelink.net/bg/bulletins/ecopolis12/1_os_1.htm.
4. ROTHERMEL R. C. A mathematical model for predicting fire spread in wildland fuels. Research Paper INT-115. Ogden, UT, US Department of Agriculture, Forest Service, Intermountain Forest and Range Experiment Station, 1972, 1–40.
5. GRISHIN A., A. GRUZIN, V. ZVEREV. Mathematical modelling of the spreading of high-level forest fires. *Soviet Physics Doklady*, 28 1983, No 4, 328-330.
6. ALBINI FRANK A. Estimating wildfire behavior and effects. Gen. Tech. Rep. INT-30, Ogden, UT, US Department of Agriculture, Forest Service, Intermountain Forest and Range Experiment Station, 1976.
7. PERMINOV V. Mathematical Modeling of Crown Forest Fires Initiation. Lecture Notes in Computer Science (including subseries Lecture Notes in Artificial Intelligence and Lecture

Notes in Bioinformatics), Vol. **2667**, 2003, 549-557.
8. Patton, E.G., Coen, J.L.: WRF-Fire: A coupled atmosphere-fire module for WRF. In: Preprints of Joint MM5/Weather Research and Forecasting Model UsersWorkshop, Boulder, CO, June 2225.NCAR(2004)221223.
9. Anderson, H.E.: Aids to determining fuel models for estimating fire behavior.USDA Forest Service, Intermountain Forest and Range Experiment Station, Research Report INT-122 (1982)http : //www.fs.fed.us/rm/pubsint/intgtr122.html.
10. http://ccm.ucdenver.edu/wiki/Jan_Mandel/Blog/2010_Dec_2011_Jan
11. Dobrinkov G., **Dobrinkova N.**, "Input Data Preparation for Fire Behavior Fuel Modeling of Bulgarian Test Cases (Main Focus on Zlatograd Test Case).", 10th International Conference on "Large-Scale Scientific Computations" LSSC'15, Sozopol 8-12 June 2015, Lecture Notes in Computer Science 9374, ISSN 0302-9743, ISSN 1611-3349 (electronic), ISBN: 978-3-319-26519-3, DOI 10.1007/978-3-319-26520-9, Springer Germany, pp. 335–342, **2015**.
12. **Dobrinkova N.**, Hollingsworth L., Heinsch F.A., Dillon G., Dobrinkov G., "Bulgarian fuel models developed for implementation in FARSITE simulations for test cases in Zlatograd area". (E-proceeding: http://www.treesearch.fs.fed.us/pubs/46778) Wade DD & Fox RL (Eds), Robinson ML (Comp) (**2014**) 'Proceedings of 4th Fire Behavior and Fuels Conference', 18-22 February 2013, Raleigh, NC and 1-4 July 2013, St. Petersburg, Russia. (International Association of Wildland Fire: Missoula, MT), p.513 - p.521.
13. Dobrinkov G., **Dobrinkova N.**, "Wildfire behavior modeling data preparation for FARSITE simulations in Bulgarian test cases", 5th International Conference on Cartography & GIS & Seminar with EU cooperation on Early Warning and Dissaster/Crisis Management 15-21 June **2014**, Proceedings Vol.2, ISSN:1314-0604, **2014**, Riviera, Bulgaria, p.763- p. 770.
14. **N.Dobrinkova**, G. Dobrinkov, "Farsite and WRF-Fire models, Pros and Cons For Bulgarian Cases", 9th International Conference on "Large-Scale Scientific Computations" LSSC'13, Sozopol 3-7 June 2013, Lecture Notes in Computer Science 8353, ISBN: 978-3-662-43879-4, Springer Germany, pp. 382–389, **2014**.

Authors' contacts: Institute of Information and Communication Technologies – Bulgarian Academy of Sciences (IICT-BAS)
Address: Acad. Georgi Bonchev str. Bl. 2 1113, Sofia, Bulgaria
E-mail: ninabox2002@gmail.com
E-mail: nido@math.bas.bg

© International Scientific Conference on Engineering, Technologies and Systems
TECHSYS 2016, Technical University – Sofia, Plovdiv branch
26 – 28 May 2016, Plovdiv, Bulgaria

# IMAGE SEGMENTATION TECHNIQUES FOR MEDICAL IMAGE PROCESSING PURPOSES

MIRCEA WEINGART*, DAN POPESCU**, OREST VASCAN

**Abstract:** *Image segmentation plays a key role in image preprocessing stage. The main purpose of image segmentation techniques is to split the input image into regions of interest such that a more detailed analysis can be conducted. The work reported in this paper aims a comparative analysis of some of the most commonly used segmentation techniques.*

**Key words:** *image segmentation techniques , image de-noising , image processing*

## 1. Introduction

Image segmentation partitions the image into regions or components.These regions are non-overlapping. Their union is the entire image [1]. These regions should be: homogenous and uniform in terms of grey levels(or colours) and texture ; the interior of these regions should be without holes; neighboring regions must have different values for the characteristic that is uniform for each such region. The boundaries of the segmentation regions must be simple The aim of segmentation is a better analysis of the selected image regions or for further image processing phases.

## 2. Short description of the techniques used in the experiments for image segmentation

### A. The objectives of experimenting the segmentation techniques in this article:

The first objective is to describe visually some efficient image segmentation techniques that are used at present. The second objective is to determine the influence of noise added to the images for the selected segmentation methods.For these two objectives are used segmentation techniques with a good topology preservation property of the objects from the image to be segmented based on the active contour methods.Below are presented in short the segmentation techniques used in the experiments.

Classical image segmentation subdivides the image into regions based on their homogeneity or other uniform characteristic.Yet, the practical usage of image segmentation focuses on specific objects called targeted segmentation. where certain information is supplied to select the object, called target specification [2] where is needed a regularization algorithm that uses data from the target specification to deliver a good segmentation of the target object(s). In this article examples of classical and targeted techniques are presented.

### B. Segmentation based on active contours without edges

The segmentation based on minimizing a piecewise-smooth Mumford-Shah functional on a graph is a technique that segments automatically the whole image and preserves well the edges. It is an energy based technique. The Mumford-Shah functional is defined on a graph as in [3] and represents a combinatorial approach of the piecewise smooth (continuous) case.

The technique of Chan and Vese (see [4] and [5]) is used frequently in segmentation of images. It derives from the Mumford-Shah functional minimization , curve evolution and level sets techniques. Here we present first the scalar case , namely for gray-scale images. In active contour models the aim is to evolve a curve, subject to constraints from the given image , in order to detect objects in that image. A generalization of the scalar case is the vector-valued images case as described in [5] and is used for example for color images segmentation.The vector-valued model does a minimization of the Mumford–Shah functional over the entire length of the contour, in addition to the fitting error over each component of the vector-valued image. As shown by the Chan–Vese model, the vector-valued model can detect edges in two ways , namely both with or without image gradient. For more than two segmentation regions a multiphase level set framework may be used also based on Mumford-Shah functional minimization and the solution consists of more than one contour and it is useful for more complex cases like triple-junctions, as shown in [6]. Matlab code for [4] , [5] and [6] application cases can be found in [7].

Copyright © 2016 by Technical University of Sofia, Plovdiv branch, Bulgaria ISSN Online: 2535-0048

### C. Random walks algorithm based segmentation

Random walk is an algorithm that describes a path followed by one or more pixels chosen from the image, and the path consists of a sequence of random steps.The random walk allows an interactive image segmentation. Two pixels called seeds are chosen to represent a reference to the background and to the foreground of the image [8].

These seeds are labeled by the user. It can be computed the probability of a random walker starting from an un-labeled pixel to reach one of the seeds and then assign to it the label of this seed. In this article is used a graph-based algorithm [8].

### D. Segmentation of non-homogenous regions of an image based on an energy fitting minimization

In some cases non-homogenous images need a proper segmentation.An initial contour may contain a non-homogenous region.A region based active contour technique allows solving this by minimizing a data fitting energy (defined on a contour) and get two fitting functions f1 and f2 that approximate locally the image intensity on both sides of the contour as presented in [9].In order to minimize the energy functional , the gradient flow is used as the level set evolution equation.

A curve evolution described by an equation also results from the minimization of the data fitting energy.

$$E(\phi, f_1(x), f_2(x)) = \sum_{i=1}^{2} \lambda_i \int K(x-y)\,|I(y) - f_i(x)|^2 M_i(\phi(y))\,dy \quad (1)$$

where K is a Gaussian kernel and C is a closed contour.

$$M_1(\phi) = H(\phi);$$
$$M_2(\phi) = 1 - H(\phi)$$

H is the Heaviside function

$H(\phi) = 0$ for $\phi < 0$ and $H(\phi) = 1$ for $\phi \geq 0$.

A regularization term is necessary for the level set function ϕ.The level set regularization term is:

$$P(\phi) = \int \frac{1}{2}(|\,grad(x)\,| - 1)^2\,dx \quad (2)$$

This term characterizes the deviation of the function from a

signed distance function.It means that we need to minimize:

$$E(\phi, f_1(x), f_2(x)) + \mu P(\phi) \quad (3)$$

μ is a positive parameter.In order to minimize the energy functional, the gradient flow is used as the level set evolution equation.

### E. Segmentation of non-homogenous regions of an image based on the level sets method

This technique is based on a local clustering criterion function for the intensities in a neighborhood of each point as presented in [10].

Using the level set approach it is defined an energy based on level set functions that represent the segmentation and a bias field that models the non-homogeneities in the image. The local clustering criterion is integrated over the neighborhood center to define an energy functional, which is then defined in a level set formulation.

#### The Two-Phase Level Set Formulation

For ϕ a level set function whose zero level contour is $C=\{x|\ \phi(x)=0\}$ , consider two disjoint regions of the image domain $\Omega_1 = \{x|\phi(x)>0\}$ , $\Omega_2 = \{x|\ \phi(x)<0\}$.An energy is defined in the level set formulation , $E(\phi, c, b)$ ,where the constants ci (average image intensities in each homogenous region) are represented by a vector $c = (c_1, c_2).$ The level set function $\phi$ , the c vector and the bias field are the variables of this energy. Two regularization terms will be used. $L(\Omega)$ that computes the arc length of the zero level contour of and is smoothing the contour by penalizing the arc length and the term $R_P(\phi)$ ,where p is a potential function (energy density).The energy $E(\phi, c, b)$ is used as the data term in the energy of this variational level set formulation, which is defined by

$$F(\phi, c, b) = E(\phi, c, b) + \nu L(\Omega) + \mu R_p(\phi) \quad (4)$$

Minimizing this energy, we obtain the result of image segmentation given by the level set function $\phi$ and the estimation of the bias field b. A multi-phase approach is used for multiple contours images.

### F. Localization of region-based active contours method

This procedure considers local image statistics and evolve a contour based on localization [11].

The foreground and background of the image are represented by using local-smaller regions.There are defined local energies for each point of the curve, that are optimized for each such point that moves along the curve. In order to calculate the energies the neighborhoods are divided by the evolving curve in local interior and local exterior parts and the optimization is done for each local region.

### 3. Experimental results , contributions interpretation of results

For each of the above mentioned segmentation techniques were performed experiments , and the results and their interpretation are presented in this article. Our specific contributions consist mainly in the following: There is presented a comparative approach of the segmentation techniques including the visual aspect;

It is proposed the usage for an efficient segmentation of de-noising techniques used after the segmentation for improving the quality of image ;the study of the effect of salt-and-pepper noise on image segmentation. A proposal for a better segmentation using post-processing for image de-noising is subject of further development we have in view.

For the experiments was used the scenario presented in the following figure.

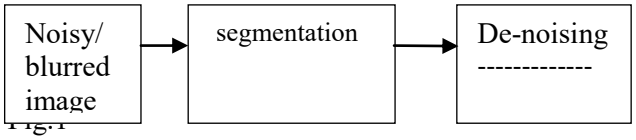



Fig.1

***Fig. 1.*** *The experimental setting for image segmentation*

Segmentation experiments were performed on noisy images as schematically is shown in in Fig.1 with results shown in TABLE 1. The noise that was added artificially consists of: 22% and 52% noise level of salt-and-pepper type.

### A.Visual results of the processed images explained

As mentioned in II.A. one of the article's objectives (the first one) is a visual display of the images resulted from the presented segmentation processing methods , having as aim a comparative presentation of some visual functionalities of the segmentation methods used , and in some cases to see the effect of noise upon segmentation.

There are three cases (Fig. 2,3,4) for Segmentation based on active contours without edges all three cases for gray-scale images one case for 400 iterations with an ellipse initial contour , one case for a rectangle initial contour with 220 iterations of the algorithm and the third case for 500 iterations and a rectangle initial contour.

The theoretical model presented in II.B. is used for the gray-scale images segmentation. contour, all three cases referring to a computer tomography of the brain.

More details can be seen for the first and third cases – they correspond to more iterations of the algorithm..

In Fig. 2, Fig.3 and Fig.4 there were 400, 220 and 500 iterations and it can be seen that both initialization contours –ellipse and rectangle-give good segmentation results.

Another segmentation technique is presented in Fig.5,6,7 –namely the random walker method, described in section II.C. applied for clean images resulted from an axial computer tomography(CT) slice. The blue and green seeds are manually selected through their coordinates , and the algorithm produces a segmentation based on these seeds , one placed in the foreground and one in the background and it can be seen the good segmentation for the foreground region where the green seed is placed , and the corresponding probabilities for pixels to do a random walk to the seeds.The outlined mask is the segmentation contour.

Fig.7,8 show the segmentation using II.E. method –the two phase case-for un-homogenous regions applied to the clean Heart image.It is seen that this segmentation improves the visualization of the Heart image regions.Fig. 9, 10 show the same method applied to the noisy(22% salt-and-pepper noise) Heart image with the segmentation that resulted.Fig.11 shows the histograms of the clean Heart image for both the original and bias-corrected image with the method. From II.E. indicating a better segmentation of the image regions after the bias-correction was applied.

Fig. 12, 13 show the multi-phase case of the level sets method from II.E. applied to the clean and noisy Heart image segmentation. The result is better –especially for the noisy image –compared with the two-phase case- from Fig. 7 and 8.

The contributions to this article consist in the comparative experimental study of different segmentation techniques presented.

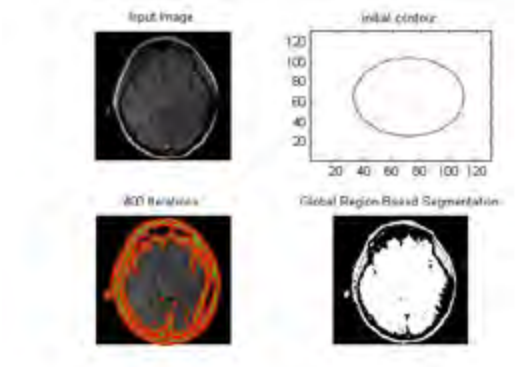



***Fig. 2.*** *Brain CT(computer tomography) image segmentation 400 iterations –initial ellipse contour*

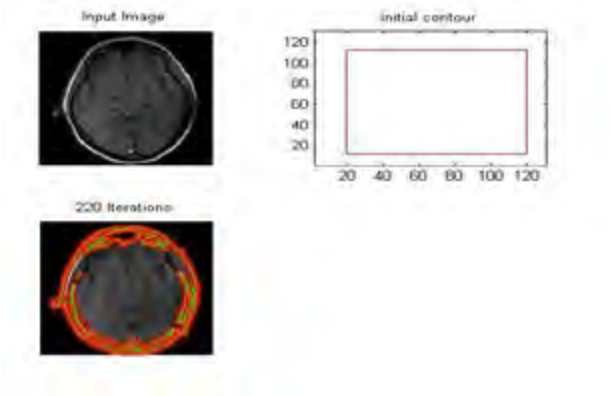



***Fig. 3.*** *Brain CT image segmentation after 220 iterations –initial rectangle contour*

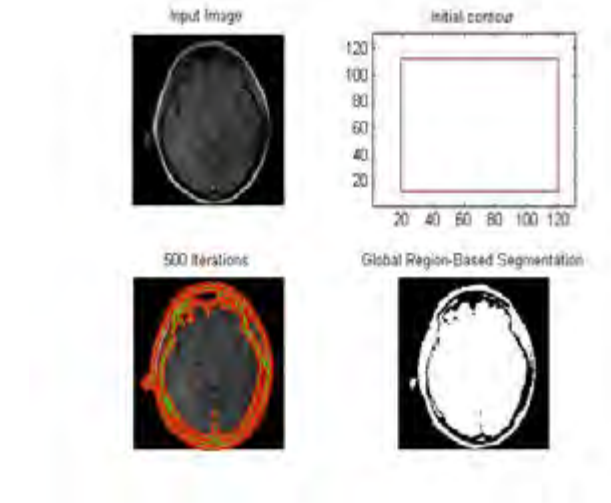



***Fig. 4.*** *Brain CT segmentation( 500 iterations )- Initial rectangle contour*



***Fig. 5.*** *Blue seed for the background and green seed for the foreground of this CT axial-scan*

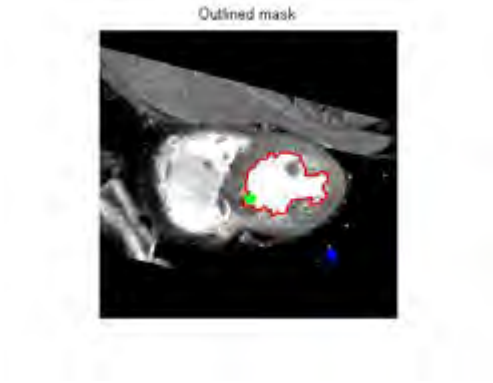



***Fig. 6.*** *CT axial-scan. The outlined mask.segmentation is present*

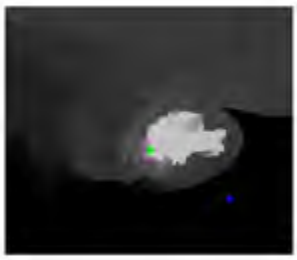


***Fig. 7.*** *CT axial-scan.*

The probability of unlabeled pixels to get to the seeds through random-walk algorithm is visualized.

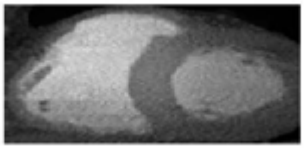


***Fig. 8.*** *Heart image – clean original image*

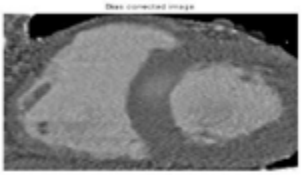


***Fig. 9.*** *Heart image –bias corrected image of the clean image*



***Fig. 10.*** *Heart image –blurred and noisy (22% salt- and- pepper noise)*



***Fig. 11.*** *Heart image –blurred and noisy (22% salt- and- pepper noise)*

Segmentation after 50 iterations

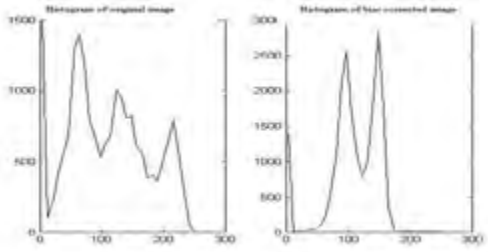


***Fig. 12.*** *Heart 1)original image histogram;2)bias corrected clean image histogram multiphase level set method with bias correction*

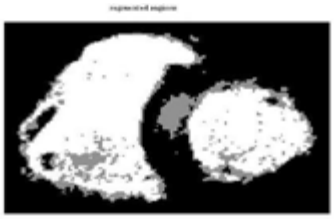


***Fig. 13.*** *Heart clean image segmentation - non-homogenous regions of an image based on the multi-phase level sets method*

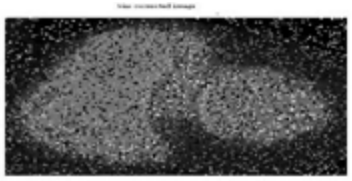


***Fig. 14.*** *Heart noisy image segmentation – (22% salt- and- pepper noise) non-homogenous regions of an image based on the multi-phase level set method*

***Table 1.*** *Computation time in seconds*

| **Segmentation of non-homogenous regions of an image** based on the level sets method | Heart clean image | Heart noisy image 22% salt-and-pepper noise |
|---|---|---|
| two-phase case | 49.535 | 176.797 |
| Multi-phase case | 92.413 | 415.127 |

## 4. Conclusions

In this article experiments with segmentation techniques are presented for certain categories of medical images (Heart and Brain). Different segmentation methods are applied on the clean (original) images , and on the noisy and blurred images. It is proposed in this article a multi-phase approach for image segmentation.

Gray-scale images were analyzed. Real-time remote visualization of medical imagery for example may be an application for our proposed solution , considering that noise can be added through the data acquisition and communication media and also that a high data volume must be processed. This solution allows to elaborate a correct diagnostic given by the remote specialist. Also can be concluded that noise and blur have an effect on image segmentation but for the cases mentioned in the text (for example for the multi-phase level sets method) image segmentation continues to work reasonably even in these conditions.

ACKNOWLEDGMENT

Many thanks to Orest Vascan, PhD in electronics engineering for critical observations and kind support.

## REFERENCES

1. R. Haralick , "*Segmentation," Enciclopedia of artificial intelligence*", second edition , copyright©1992 by John Willey and Sons.

2. L. Grady ," Targeted image segmentation using graph Methods" in "Image *Processing and Analysis with Graphs*", ed. O. Lezoray and L. Grady, CRC Press 2012
3. L. Grady , C. Alvino "The piecewise smooth Mumford-Shah functional on an arbitrary Graph," *IEEE TRANSACTION ON IMAGE PROCESSING*, VOL. 18, NO. 11, NOVEMBER 2009
4. T. Chan, L. Vese, "Active contours without edges," *IEEE TRANSACTIONS ON IMAGE PROCESSING*, VOL. 10, NO. 2, FEBRUARY 2001
5. T. Chan, Sandberg, L. Vese, "Active contours without edges for vector-valued images," Journal of Visual Communication and Image Representation **11**, 130–141 (2000)
6. T. Chan, L. Vese, "A multiphase level set framework for image segmentation using the Mumford-Shah model," *International Journal of Computer Vision* 50(3), 271–293, 2002
7. Y. Wu, "A simple introduction of active contour without edges" https://sites.google.com/site/rexstribeofimageprocessig/chan-vese-active-contours/wubiaotitiezi
8. L. Grady "Random walks for image segmentation,", *IEEE TRANSACTIONS ON PATTERN ANALYSIS AND MACHINE INTELLIGENCE*, VOL. 28, NO. 11, NOV. 2006
9. C. Li,Chiu-Yen Kao, J. Gore , Z. Ding, "Minimization of region-scalable fitting energy for image segmentation " *IEEE Trans Image Process*. 2008 October; 17(10): 1940–1949.
10. C. Li, R. Huang, Z. Ding, C. Gatenby, D. N. Metaxas,J. Gore, "A level set method for image segmentation in the presence of Intensity Inhomogeneities with Application to MRI" *IEEE Trans. Image Processing*, vol. 20 (7), pp. 2007- 2016, 2011.
11. S. Lankton , A. Tannenbaum, "Localizing Region-Based Active Contours", *IEEE TRANSACTIONS ON IMAGE PROCESSING*, VOL. 17 NO. 11, NOVEMBER 2008
12. B. Wohlberg , P. Rodriguez , AN L -1-TV ALGORITHM FOR DECONVOLUTION WITH SALT AND PEPPER NOISE –ICASSP 2009
13. P. Getreuer , http://www.mathworks.com/matlabcentral/fileexchange/29743-tvreg-variational-image-restoration-and-segmentation/content/tvreg/tvdenoise.m
14. R. C. Gonzalez, R. E. Woods, & S. L. Eddins, *Digital Image Processing Using MATLAB*, Prentice- Hall,2004

Authors' contacts :

* E-mail: mirceaw201@yahoo.com , PhD student at the Faculty of Automatics and Computer Science , , University Politehnica , Bucharest , Romania

** E-mail: decanat@acs.pub.ro Professor.Dr. at at the Faculty of Automatics and Computer Science , University Politehnica , Bucharest , Romania

*** E-mail: ovascan@crescendo.ro Engineer at Crescendo International SA , Bucharest, Romania

© International Scientific Conference on Engineering, Technologies and Systems
TECHSYS 2016, Technical University – Sofia, Plovdiv branch
26 – 28 May 2016, Plovdiv, Bulgaria

# EXPERIMENTAL SYSTEM FOR WIND MODELLING

GEORGI RUZHEKOV, TEOFANA PULEVA, TS. SLAVOV

**Abstract:** *The paper describes the developed airflow generation system which characteristics are closed to the real wind. It is a part of wind turbine laboratory test bench "Wind generator" and it will be used in research work to explore advanced control algorithms of wind turbine generator operation in different regimes and control strategies.*

**Key words:** *Wind Power Spectral Density, Wind Generator, Laboratory test bench, Programmable Logical Controller*

# ЕКСПЕРИМЕНТАЛНА СИСТЕМА ЗА МОДЕЛИРАНЕ НА ВЯТЪР

ГЕОРГИ РУЖЕКОВ, ТЕОФАНА ПУЛЕВА, ЦОНЬО СЛАВОВ

**Резюме:** *Статията описва разработената система за генериране на въздушен поток с характеристики, близки до тези на реален вятър. Тя е част от лабораторен стенд „Вятърен генератор" и ще се използва за провеждане на изследвания на съвременни алгоритми за управлението му в различни режими на работа и стратегии на управление.*

**Ключови думи:** *Спектрална плътност на вятър, Ветрогенератор, Лабораторен стенд, Програмируем логически контролер*

## 1. Introduction

The utilization of wind energy to perform mechanical work dates back thousands of years. Due to the oil crisis in the early 70s, the technology for the production of wind energy is undergoing strong development, from experimental technology for charging batteries became one of the main methods of generating electricity.

Wind energy is free, clean and infinite. Nowadays, the production of electricity from wind energy is the fastest growing method for obtaining electricity from a renewable energy source.

At the end of 2014 the worldwide installed capacity of wind turbine generators (WTG) is 369,6 GW, thereby only in 2014 is prevented the release of more than 600 tons of carbon emissions.

The main problem in using WTG is the unpredictable and continuously changing behavior of the primary energy source - the wind (a non-stationary stochastic process, with turbulence and extreme variations of the wind speed) and the high quality requirements of supplied electricity.

The conversion of wind energy in electric power and the technical quality standards make the utilization of wind turbines and their connection to the electric power system (EPS) impossible without application of advanced automatic control.

The presented system for experimental modeling of the wind is part of the control system of laboratory test bench for exploring control strategies and algorithms for wind turbine generator control [1, 2, 3 and 4]. It is designed to create an air flow with characteristics similar to those of real wind. This modeling approach allows research work to be carried out of wind turbine control system with air flow characteristics similar to those of the wind.

## 2. Laboratory test bench description

The laboratory test bench "Wind generator" (Fig.1) consists of the following components:

- Subsystem for air flow generation – (2): axis ventilator with diameter 1$m$, which is driven by an induction motor 4 kW (2). The ventilator is

Copyright © 2016 by Technical University of Sofia, Plovdiv branch, Bulgaria ISSN Online: 2535-0048

mounted in the wind tunnel (3). The induction motor is controlled by the frequency inverter ELDI/ B-4.0 kW (4) and a braking resistor FR-ABR-H5.5K – 110 Ω (4a).

- Sub-system for measuring the air flow speed - anemometer (5) (the output signal is an impulse sequence), speed measuring tube and differential pressure transmitter (6) (output signal 4-20 mA). These devices are mounted on guide rods, which allow measuring the wind speed at any point. The profile of the generated airflow has been explored which allows the position of the sensor to be determined, where it measures the airflow rate close to the average one.
- Subsystem „*Wind generator*“, which consists of the wind wheel (7), induction sensor for rotational speed measurement (8), sensor for torque measurement (9), three-phase alternator (10), three-phase rectifier (11). The generated power is supplied in the module for the load control of the generator (12). This module allows voltage and current measurement of the generator. Using the output signal from the controller the generator load can be controlled.
- Sub-system for technological process control (13) based on PLC produced by Siemens, CPU 1215 and input/output signal modules. The input signal are: the anemometer signal (impulse sequence), pressure differential transmitter signal – analog signal 0-10 V, turbine rotational speed (impulse sequence), signal from the torque sensor, generator voltage and the load current. The output signals are: control signal of the ventilator motor speed – frequency invertor reference signal 0-10 V and reference signal of the module for generator load control.
- SCADA system (14) – it provides a graphical interface which visualizes the plant operation, the measured signals, as well as setting the air flow rate and the load of the generator.

## 3. Wind dynamics

The dynamic characteristics of wind are a combination of weather conditions and characteristics of geographical location. In literature, the wind is modeled as a non-stationary stochastic process. It is a result of superposition of two components

$$v(t) = v_s(t) + v_t(t), \tag{1}$$

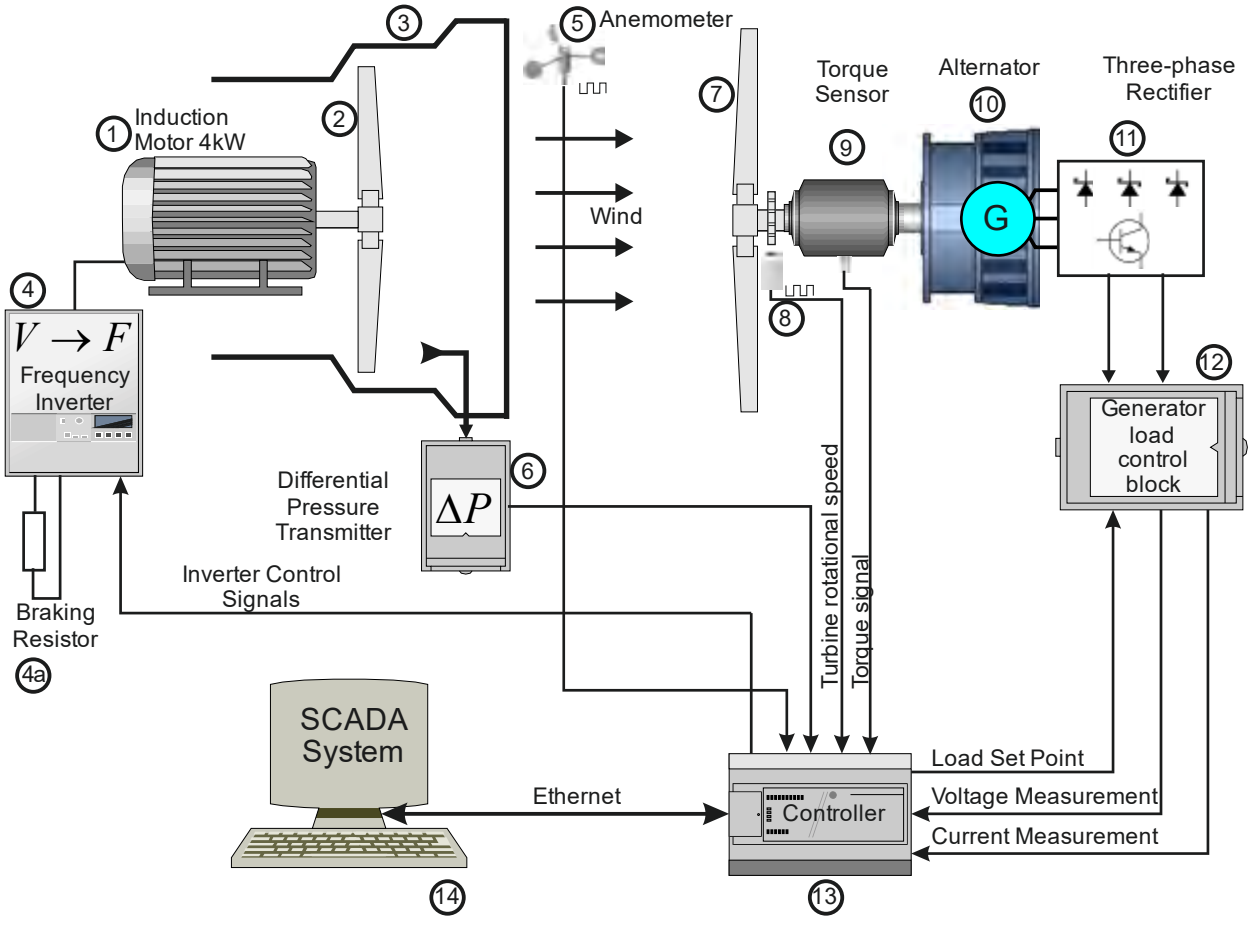



***Fig. 1*** *General structure of the laboratory bench*

where $v_s(t)$ is a low frequency component describing the slow fluctuations of the wind speed, $v_t(t)$ is a high frequency component which is a model of the turbulence (high rate wind speed variations). In Fig. 2 a wind model described by the Van der Hoven spectrum is shown [5].

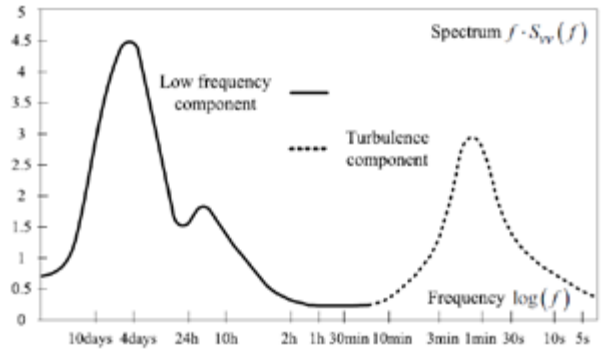



*Fig. 2 Van der Hoven spectrum of the wind speed*

The low frequency component is a model of the low rate variations of the wind speed. It depends on the characteristics of the geographical location. It can be represented by the Weibul distribution [5]:

$$v_s = ave^{-1/2a\bar{v}^{-2}}, \qquad (2)$$

where $\bar{v}$ is the mean value of the wind speed for a period of one hour, and $a$ is a parameter that depends on the mean value of the wind speed for a long time interval.

By definition the turbulence includes all wind speed variations with frequencies above the spectral gap. It is described by the power spectrum. Widespread models are the spectra of Karman and Kaimal [5, 6]:

$$\frac{f * S_{vv}(f)}{\sigma^2} = \frac{4f\frac{L_t}{v_s}}{\left(1+70.8\left(f\frac{L_t}{v_s}\right)^2\right)^{5/6}}, \qquad (3)$$

$$\frac{f * S_{vv}(f)}{\sigma^2} = \frac{4f\frac{L_t}{v_s}}{\left(1+6f\frac{L_t}{v_s}\right)^{5/3}}, \qquad (4)$$

where $S_w(f)$ a spectral density, $L_t$ is the range of the turbulence, which depends on the topology of the terrain, and $f$ is the frequency. Details on the calculation of these coefficients can be found in [5]. The normalized spectra of Karman (line) and Kailmal (dash line) are given in Fig.3.

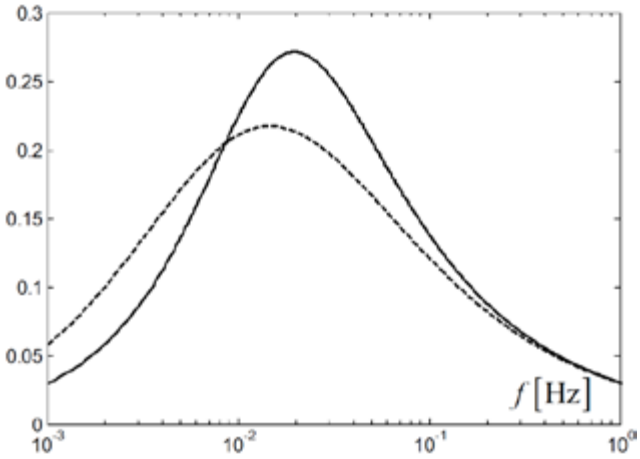



*Fig.3. Normalized spectra of Karman and Kaimal*

## 4. Air flow generation

The generation of the airflow is accomplished based on the spectrum density model (*Karman or Kaimal*) $S_{vv}(f)$ Eq. (3) and Eq. (4). We need a discrete representation of the spectrum with respect to the frequency and the magnitude. Let $f(i)$, $i = 1, N$ are discrete values with respect to the frequency. The maximum frequency value in the signal spectrum is chosen to be $f(N) = 0.35\ Hz$, and the minimal one - $10^{-4}$ Hz, number of discrete points - $N/2 = 20$, $N = 40$ [4]. A logarithmically spaced frequency is used which corresponds to the frequency range (0.1 mHz - 0.35Hz). In accordance with the Kotelnikov - Shennon sampling theorem the sample frequency is determined $F_S = 1\ Hz$, which corresponds to the sample time $T_S = 1\ s$. The spectral density magnitude quantization is performed using the trapezium rule – the energy between two neighbor points of frequency is calculated in accordance with the expression:

$$S_{vv}(f_i) = \frac{1}{2}\left(S_{vv}(i) + S_{vv}(i+1)\right).\left(f(i+1) - f(i)\right). \qquad (5)$$

The signal generation is performed by Discrete Fourier Transform (DFT). The signal has the following form

$$s(k) = \sum_{i=1}^{N/2} A_i.\cos\left(2\pi.f(i).k + \varphi(i)\right),\ k = 1\ldots N, \qquad (6)$$

where:

$A_i$ is the magnitude of the $i^{th}$ harmonic,
$f(i), i = 1, N/2$ are the frequency discrete points;
$\varphi(i)$ - initial phase value of each harmonic.

The values $A_i$ и $\varphi(i)$ have to be calculated. The harmonics magnitude calculation is performed by using the Parseval's theorem.

$$\sum_{k=0}^{N-1}|s(k)|^2 = \frac{1}{N}\sum_{n=0}^{N-1}|S_w(n)|^2, \quad (7)$$

where the left-hand side of the equation describes the signal energy, and the right-hand side – the sum of the energy of all harmonics in this signal realization with a length $N$.
The energy of each harmonic signal (sin, cos) is

$$E_i = \frac{A_i^2}{2}N. \quad (8)$$

In accordance with the Parseval's theorem for each of the harmonics is held

$$\frac{A_i^2}{2}N = \frac{2}{N}|S_w(f_i)|^2, \quad (9)$$

therefore

$$A_i = \frac{2}{N}|S_w(f_i)|. \quad (10)$$

The spectral density (Karman or Kaimal) $S_{vv}(f)$ represents the signal energy distribution in a frequency range, but it doesn't contain information about the initial phase of each of the harmonics. In the signal modelling the initial phase of the harmonics is given as a random number in the interval

$$\varphi(i) = [0 \div 2\pi] \text{ or } \varphi(i) = \text{rand}.2\pi,$$

where *rand* is a function, that generates an uniform distributed number in the interval $[0 \div 1]$.
Based on the above described theoretical procedure the signal that models the wind speed is described by the expression:

$$V(k) = V_S + \sum_{i=1}^{N-1} A_i \sin(2\pi f(i)kT_S + \phi_i), \quad (11)$$

where $k$ is the index of the current value of the wind speed.

The high frequency component can be obtained as an output signal of a shaping filter assuming a white noise as an input signal. The transfer function of the shaping filter is [5]

$$H_t(j\omega) = \frac{K_F}{(1+j\omega T_F)^{5/6}}, \quad (12)$$

where the parameters $K_F$ and $T_F$ depend on the low frequency component $v_s$ of the wind model. One of the approaches to obtain the values of these parameters is [5]

$$T_F = \frac{L_t}{v_s} \quad (13)$$

$$K_F = \sqrt{\frac{2\pi}{B(1/2,1/3)}.\frac{T_F}{T_s}}, \quad (14)$$

where the notation ***B*** is a beta-function.
The block-scheme of the algorithm for wind modeling is given in Fig. 4.

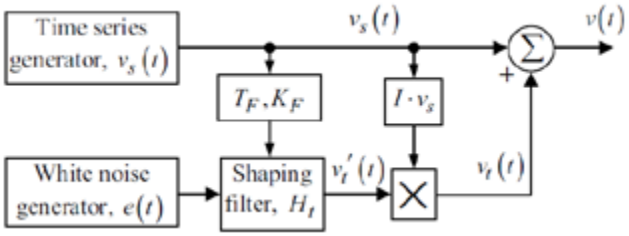



***Fig. 4*** *Block-scheme of the algorithm for wind modeling*

The implementation of the shaping filter described by non-rational transfer function Eq. (12) leads to computational problems. In this case an approximation of Eq. (12) by the transfer function Eq. (15) is applied [5]

$$H_t(s) = K_F.\frac{m_1T_Fs+1}{(T_Fs+1)(m_2T_Fs+1)}, \quad (15)$$
$$m_1 = 0.4, \quad m_2 = 0.25.$$

In the shaping filter implementation by PLC it is necessary to obtain a discrete representation of Eq. (15). For example the Euler approximation can be applied

$$s = \frac{z-1}{T_s},$$

where the sample time $T_s = 0.1\,s$.
As a result the discrete transfer function of the shaping filter is obtained

$$H_t(z) = \frac{4K_FT_Fz^{-1} - K_F(4T_F-1)z^{-2}}{25T_F^2 - (50T_F^2 - 12{,}5T_F).z^{-1} + (25T_F^2 - 12{,}5T_F+1)z^{-2}}. \quad (16)$$

The computational procedure is implemented in the PLC environment as a difference equation.

## 5. Implementation of the algorithm for modeling of the wind speed

A real time computation of the current value of wind speed using a sample time $T_s = 0.1\,s$ is performed in the PLC environment. The block scheme shown in Fig. 4 is applied. The algorithm is performed in following steps:

1. Computation of the current value of the low-frequency component in accordance of Eq. (11).
2. Computation of the shaping filter parameters $K_F$ and $T_F$.
3. Generation of uniform distributed random number in each sample time. A program for random number generator is developed in the PLC environment. It is based on a linear congruential algorithm [4].
4. Computation of the difference equation which represents the shaping filter implementation Eq. (16).
5. Computation of the turbulence component $v_t(k)$.
6. Computation of the resulting component as it is shown in Fig. 4.

On the base of the presented above algorithm the wind speed is performed. It has to be implemented by the system shown in Fig. 1. As can be seen the airflow is created by the ventilator, the induction motor of which is controlled by a frequency inverter. The airflow speed is determined by the motor rotational speed which depends on the frequency of the motor supply voltage.

$$V_{wind} = f(InvFreq), \tag{15}$$

where $V_{wind}$ is the airflow speed which is measured by the pressure differential transmitter and tube for airflow speed measurement, *InvFreq* - is the frequency of the inverter output voltage that supplies the ventilator. Hence the setting of the airflow speed is accomplished by the inverter frequency reference

$$InvF = f^{-1}(V_{wind}). \tag{16}$$

The implementation of Eq. (16) requires experiments to obtain the relationship described by Eq. (15) in look-up table format. The wind speed is measured for ten values of the inverter frequency. For this purpose an HMI application is developed which allows to set the inverter frequency and to record the values of the airflow velocity. Then Eq. (16) is implemented as an approximation of the collected data in the look-up table format.

Software for PLC implementation is developed. It comprises the following components:

- Setting the shape of the wind speed variation (constant or sinusoidal). A noise with a normal distribution can be added to these reference signals. The noise variance can be set by the user;
- Transforming the airflow speed into the frequency (inverter reference).
- Computation the inverter control signal;
- Measuring and data storage of the airflow, rotational speed of the wind turbine and the voltage of the generator terminals.

Experiments are carried out using an airflow modelled by:

- constant component and additive noise;
- sinusoidal component with or without additive noise;
- signal which characteristics are similar to the wind model.

The processes visualization and the data records are accomplished by SCADA system, the main window of which is shown in Fig. 5. The data records are in CSV format. This file format is compatible with other software systems. For this purpose a MATLAB function is developed which allows reading the file, visualization the data, selection of a certain interval and data storage for next processing.




***Fig. 5*** *The main window of the SCADA system*

The visualization of real experimental results obtained by the laboratory test bench is shown in Fig. 5. They are

- Inverter frequency (Inv Frequency, Hz);
- Airflow speed (Wind speed, m/s);
- Wind turbine rotational speed (Turbine *speed*, rpm).

The correlation of these three signals can be noticed as well as the stochastic nature of the airflow speed. The generated airflow can be used in investigation of the wind turbine generator control system performance. In Fig. 6 the main control window is

shown. It is possible to control the system from this screen in manual mode of operation. For example, it is possible to switch on or off the fan motor, to increase or to decrease the fan speed using a slider, to control the generator load or to visualize the main measured signals.

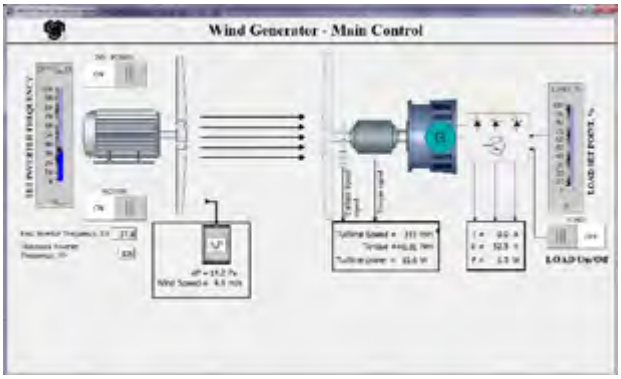



***Fig. 6*** *The main control window of the SCADA system*

## 6. Experimental results

Based on the above described approach for physical modeling of the airflow a software subsystem is implemented. It allows entering the main parameters of the simulated airflow:

- the magnitude of the spectrum harmonics $A_i$ and the corresponding frequencies $f_i$;
- the initial phase $\phi(i) = [0 \div 2\pi]$ generated by a developed program generator of normally distributed random number;
- Setting of the wind speed mean value, as well as the minimum and the maximum value of the wind speed;
- Setting the height of the point $z$ where the airflow model is calculated. Setting the coefficient $z_0$, that takes into account the roughness of the ground.

In Fig. 7 experimental data obtained by the physical model of the airflow is shown. It represents the random nature of the airflow with or without turbulence.

## 7. Conclusion

A multifunctional laboratory test bench is developed. It allows being explored different control strategies of wind generators. The presented subsystem for airflow generator offers convenient way different experiments to be carried out in laboratory conditions which are similar to the real applications. This system can be applied to study the effect of mechanical efforts to the system and to investigate different strategies and control algorithms in the field of renewable energy sources operation in power engineering.

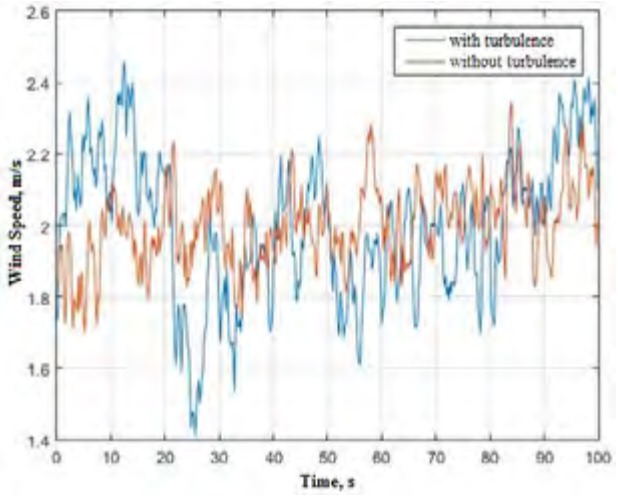



***Fig.7*** *Airflow with and without turbulence*

## References

1. Ruzhekov G., I. Tiyanov, Laboratory Bench "Wind Generator" – control system, Symposium with International participation "Control of Energy, Industrial and Ecological Systems' 2013, 7-8 Nov. 2013, Bankya, Proceedings, pp. 73-76 (in Bulgarian)
2. Ruzhekov G., I. Tiyanov, Laboratory Bench "Wind Generator" – control system, Stage 1, „*Automatics and Informatics*", №3, 2013, pp. 46-50. (in Bulgarian)
3. Tiyanov I., G. Ruzhekov, Multidisciplinary Wind Stand Control System "Wind Power Generator, NSSTC 2013, Sozopol, pp. 15-19.
4. Ruzhekov, G., T. Puleva, Experimental Test Bench for Wind Modelling, International Conference „Automatics and Informatics'15" 4-7 Nov., 2015, Sofia. (in Bulgarian)
5. Munteanu I., A. Bractu, N. Cutululis, *Optimal Control of Wind Energy Systems, Towards a Global Approach*, Springer, 2008.
6. Vihiala, H. Control of Variable Speed Wind Turbines, PhD Thesis, Tampere University of Technology, 2002.
7. Lubosny, Z. Wind Turbine Operation in Electric Power Systems, Springer 2003.

**Technical University of Sofia**
**Department of Systems and Control**
E-mail: g_ruzhekov@tu-sofia.bg
tpuleva@tu-sofia.bg
ts_slavov@tu-sofia.bg

© International Scientific Conference on Engineering, Technologies and Systems
TECHSYS 2016, Technical University – Sofia, Plovdiv branch
26 – 28 May 2016, Plovdiv, Bulgaria

# РАЗРАБОТВАНЕ НА АЛГОРИТЪМ ЗА УПРАВЛЕНИЕ НА ПЕЛЕТНА ГОРЕЛКА

КРАСИМИР ДОНЧЕВ, СТЕФАН БИЛИДЕРОВ

**Резюме:** *В този доклад се изследват възможностите за подобряване на работата на пелетните горелки. Извършено е разширение в информационното осигуряване на системата им за управление. Подбран е подходящ микроконтролер за тази система и е разработено неговото алгоритмично осигуряване.*

**Ключови думи:** *пелетна горелка, информациаонно осигуряване, алгоритъм за управление, микроконтролер*

# DEVELOPMENT OF AN ALGORITHM CONTROLLED PELLET BURNER

KRASIMIR DONCHEV, STEFAN BILIDEROV

**Abstract:** *In this report are explored opportunities to improve the performance of pellet burners. There has been expansion in the information which supplies controllers. It is selected suitable microcontroller for its automation system and developed its algorithmic insurance.*

**Key words:** *pellet burner, information supply, control algorithm, microcontroller*

## 1. Основни положения

Проблема с разхода на енергия в световен мащаб набира все по-голяма сила. Енергоспестяването е основен приоритет на повечето институции в цивилизованите държави.

С навлизането на компютърните технологии в управлението на всякакви обекти, стана възможно да се пести енергия на база на по-точно управление. Освен това, появиха се редица екологично технологии. Една такава технология е изгарянето на пелети, с което се постига минимално замърсяване на околната среда при високо к.п.д. на топлинната инсталация.

Проблемът в случая е, че при почти еднакви настройки на две горелки, разхода на пелети между двете е различен. При преглед на част от пелетните горелки, предлагани на пазара ([1], [2], [3], [4]), първото впечатление е, че контролът на горивния процес е с понижена информативност. При едни и същи условия, това води до разлика в количеството изгорени пелети, както между две различни горелки, така и при една и съща горелка в различни моменти от време.

Затова, целта на настоящия материал е да се определят нужните допълнителни сензори, които да следят параметрите на горивния процес. На тази база, да се предложи алгоритъм за неговото подобряване. Този алгоритъм да се реализира на конвенционални контролери от типа на “Ардуино”. Разглежданията са ограничени за една горелка, осигуряваща работата на битови котели в диапазон от мощности $15 \div 50$ kW.

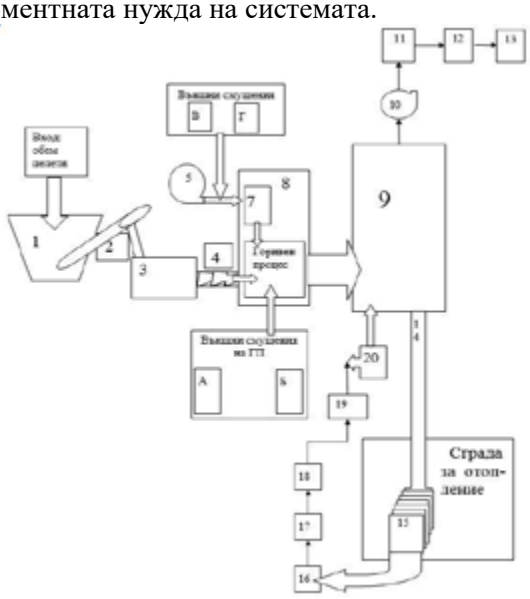
## 2. Теоретично изследване на проблема

Работният процес в пелетната горелка се основава на изгарянето на определено количество пелети, подавани върху горивната скара. Запалването на пелетите се осигурява от електрически нагревател, а процеса на горене се поддържа принудително, чрез изкуствено създадена струя въздух от вентилатор на входа на въздуховода. На Фиг.1 е показана функционалната блок-схема на системата.

След преглед на предлаганите на пазара системи за управление на пелетни горелки се установи, че се контролира единствено интервала, през което се подават и интервала, през който не се подават пелети за изгаряне,

Copyright © 2016 by Technical University of Sofia, Plovdiv branch, Bulgaria ISSN Online: 2535-0048

като струята въздух не се регулира спрямо моментната нужда на системата.




***Фиг. 1.*** *Функционална блок-схема на системата*

*1-бункер; 2-горивоподаващ шнек; 3-резервоар; 4-горивоподаващ шнек; 5-вентилатор за създаване на струя въздух с клапа; 6-горивен процес; 7-електрически нагревател; 8-горелка; 9-котел; 10-вентилатор за изкарване на дима към комина с клапа; 11-саждоуловител; 12-газ-анализатор; 13-комин; 14-изход на загрятата вода от котела; 15- консуматори на топлина (отоплителни радиатори); 16-уред за аериране на водата; 17-помпа; 18-пречистване на водата; 19-термостат; 20-филтър за постъпващата в котела вода.*
*А- промяна на температура в отопляемите помещения; Б-смущения при включване и изключване на консуматор; В-температура на входния въздух; Г- влажност на входния въздух.*

Ако, конструктивно системата горелка-котел е подбрана правилно, то в информационно отношение, контролерите продавани на пазара са снабдени само със сензори, които служат предимно за аварийното осигуряване на по-горе описаната система. Сензори, които да проследяват работата на процеса на горене липсват. Това от своя страна води до недооценяване на условията, в които работи горелката, а от там и до непълноценното изгаряне на пелетите и съответно до енергийни загуби. Освен това, при предлаганите контролери на пазара, липсва пряка обратна връзка между процеса на горене и необходимата моментна топлинна мощност, което води до преразход на пелети.

### 2.1. Определяне на основните параметри на горивният процес

Топлинната енергия се получава при изгарянето на три вида горива – твърдо, течно и газообразно. Горивата се състоят от следните основни елементи: въглерод -C; водород – H; азот – N; кислород – O; сяра – S; влага – W и пепел – A. Общата сума на изброените елементи в единица гориво е дадана с израз (1).

$$C+H+O+N+S+A+W=100\% \quad (1)$$

Основните горивни елементи, които отделят топлина при изгарянето са: C; H; N; O и S, докато W и A са баластни вещества.

При производството на пелети по изискванията на евростандартите е необходимо да се осигури следното съотношение на изброените елементи от израз (1) [5]:

$$C{=}43,75\%;H{=}6\%;O{=}41\%;\ N{=}0,4\%;S{=}0,05\%;A{=}0,8\%;W{=}8\% \quad (2)$$

Топлината на изгаряне на горивото (тяхната калоричност) се определя по два метода: калориметричен и аналитичен. Аналитичният метод се основава на формулата на Менделеев за топлината на изгаряне на течно и твърдо гориво (3):

$$Q{=}339C{+}1030H{+}109(O-S)-25W\,[\mathrm{KJ/kg}] \quad (3)$$

Замествайки процентните съдържания на елементите от (2) в (3) за топлината на изгаряне на 1[kg] пелети се получава 16347,7 [kJ/kg], което преобразувано в [kW/kg] е 4,5410 [kW/kg]. По каталожни данни, калоричността на горивото е 5 [kW/kg], което прави разлика между аналитичната формула и каталожните данни 9,18%. В тази грешка се включва закръгляването на каталожните данни от производителя, отклонението в елементния състав на пелетите при тяхното производство и други случайни грешки. Много често в разчетите за калоричност на горивото се взема стойността 4,77 [kW/kg], а това дава разлика с теоретично изчислената калоричност от 4,80%. За разработване на алгоритъм за работа на контролера, управляващ работата на горелката и задаване на входни първоначални настройки, описаното ниво на грешката е в технологичните граници.

При намирането на необходимия разход на въздух и получените продукти на горене е необходимо да се проведат изчисления по следният алгоритъм за 1 kg пелети [6]:

1. изчислява се необходимото количество кислород за пълното изгаряне на горивото:

$$V_{O_2} = 0,01(C+H+S-O) = 0,8662[m^3/kg] \quad (4)$$

2. след което се изчислява теоретичният раход на въздух:

$$L_0 = (1+k)V_{O_2} = 4,1229[m^3/kg] \quad (5)$$

където: k е отношението на обемното садържание на азот към кислород във въздуха.

3. действителният разход на въздух се получава по формулата:

$$L_\alpha = \alpha L_O = 4{,}9475 [m^3/kg] \quad (6)$$

където: α е коефициент на разхода на въздух и при този разчет се приема равен на 1,2.

4. изчисляват се обемите на отделните продукти на горене в [$m^3$/kg]:

за въглеродния диоксид:

$$Vco_2 = 0{,}01.1{,}867C = 0{,}8168 \quad (7)$$

за водните пари:

$$V_{H_2O} = 0{,}01\left(11{,}2H + 1{,}24\left(W + W_ф\right)\right) = 0{,}682 \quad (8)$$

където: $W_ф$ са загубите на пара.

за азота:

$$V_{N_2} = 0{,}01.\left(\frac{22{,}4}{28}\right).N + \alpha k V_{O_2} = 3.9113 \quad (9)$$

за серният диоксид се получава:

$$V_{SO_2} = 0{,}07S = 0{,}0035 \quad (10)$$

за излишъка на кислород:

$$V_{O_2}(изл) = (\alpha - 1).V_{O_2} = 0{,}1732 \quad (11)$$

Сумарния обем на продуктите на горене е:

$$V\alpha = Vco_2 + V_{H_2O} + V_{N_2} + V_{O_2}(изл) + V_{SO_2} \quad (12)$$

5. изчислява се процентното съдържание на отделните продукти на горене, към общият обем по формулата:

$$Z = \frac{V_г.100}{V\alpha} \quad (13)$$

6. плътността на дима се дава със съотношението:

$$p_0 = \frac{0.01(44CO_2 + 18H_2O + 28N_2 + 32O_2 + 64SO_2)}{22{,}4} \quad (14)$$

Резултата е $p_0 = 1{,}3065$ [kg/$m^3$ ].

7. изчисляването на топлината на изгаряне на пелетите (тяхната калоричност) се осъществява чрез израз (3).

8. намиране на енталпиите на продуктите на горене:

Теоретична температура на горене на пелетите се получава по формулата:

$$t = (Q + q_т + q_в)/(c_0.V_\alpha)\,[C^o] \quad (15)$$

където: $q_т$ е физическата топлина на единица гориво в [KJ/$m^3$ или KJ/kg]; $q_в$ е физическата топлина на въздуха изразходван за изгаряне на единица гориво в [KJ/$m^3$ или KJ/kg]; $c_o$- средна топлоемкост на продуктите на горене в интервала от 0 $C^o$ до t в [KJ/$m^3$ $C^o$].

В случая на (15), уравнението съдържа две неизвестни – температурата и топлоемкостта на продуктите на горене. За да се реши това уравнение е необходимо (15) да се преобразува, като за целта е удобно да се работи с енталпиите на продуктите на горене. Преработвайки (15) се получава [7]:

$$t.c_0 = i = i_x + i_т + i_в \quad (16)$$

където: $i$ е енталпия на продуктите на изгаряне; $i_x$ $i_в$ $i_T$ са съответно енталпиите на единица обем на продуктите на горене от химическата топлина на горивото и подгрева на въздуха и газа.

Химическата енталпия при изгарянето на пелетите е:

$$i_{xx} = \frac{Q}{V_\alpha} = 2926{,}0927 [kJ/m^3] \quad (17)$$

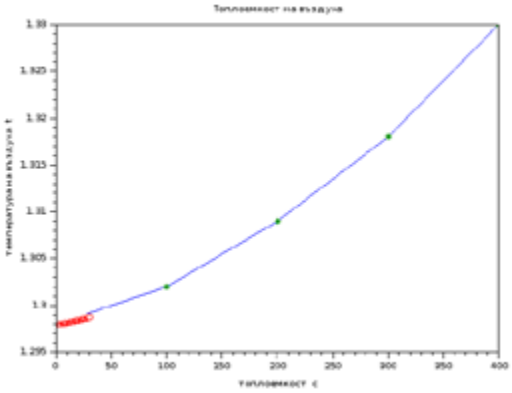
Енталпията на въздуха, участващ в горенето е:

$$i_B = \frac{L_\alpha}{V_\alpha}.\text{Interp}(f) \quad (18)$$

където: *interp(f)* е интерполираната стойност от Табл.1 за средната топлоемкост на въздуха в зависимост от неговото подгряване.

***Таблица 1.*** *Топлоемкост на въздуха*

| t [$C^o$] | 0 | 100 | 200 | 300 | 400 |
|---|---|---|---|---|---|
| c [KJ/$m^3$ $C^o$] | 1,298 | 1,302 | 1,309 | 1,318 | 1,330 |



***Фиг. 2.*** *Интерполационни стойности на топлоемкостта на въздуха при подгряване 0-30 $C^o$*

На Фиг.2 са показани получените стойности за топлоемкостта на въздуха при интерполиране в диапазона 0-30 $C^o$. При подаване на въздух със стайна температура 20 $C^o$ за топлоемкостта на въздуха се получава стойност c = 1,2985 [KJ/$m^3$ $C^o$] (Табл.1).

За енталпията на въздуха при негова температура от 20 $C^o$ се получава $i_в$ = 1,1499. Анализ на последата формула показва, че подгряването на въздуха води до подобряване на процеса на горене. Поради факта, че пелетите не се подгрява преди употреба то тогава $i_T$ = 0.

9. при изчисляване на общата енталпия на продуктите при горене на пелети се получава $i$ = 2927,2426[kJ/$m^3$];

10. определяне на теоретичната температура на изгаряне на пелетите:

Намирането на температурата на горене на пелетите в зависимост от топлосъдържанието на димните газове се осъществява по двата масива показани по-долу:

i_ent = [2405, 2585, 2785, 2955, 3170, 3385, 3625, 3890, 4190, 4520, 5015];

t_gor = [1500, 1600, 1700, 1800, 1900, 2000, 2100, 2200, 2300, 2400, 2500];

Използвайки методите на интерполацията за теоретична температура на горене на пелетите се получава t=1784,4226 [C°]. Практическата температура в горивната камера винаги е по-ниска от теоретичната с пирометричен коефициент, заради загубите на топлина в околната среда.

Важен параметър на горивния процес е коефициентът на разход на въздух. Когато има недостатък на въздух или горелката не е настроена правилно, тогава е налице химически непълно горене или недоизгаряне на пелетите. За това се съди и от наличието в дима на съставки, като окиси на въглерода, водород или въглерод на сажди. Увеличаването на коефициента на разхода на въздух води до по-пълното изгаряне на пелетите но повишава разход на въздух, а от там и значителни загуби на топлина през комина. Това води до влошаване на топлоотдаването в работното пространство и засилване на окислителните процеси.

Има два метода за определяне на α - аналитичен и опитен. От практична гледна точка, вторият метод е по-удобен защото за коефициента се съди по продуктите на изгаряне, регистрирани с газ-анализатор. Отчитайки съдържанието на $RO_2$, CO, $H_2$, $CH_4$ и $O_2$ в дима по формулата на Торйб се определя α:

$$\alpha = \frac{1 + U.O_2^{(изл.}}{\sum RO_2} \qquad (19)$$

където: $O_2^{(изл)}$ е съдържанието на излишъка на кислород; $\sum RO_2$ е сумата от процентните съдържания продуктите на изгаряне; U е коефициент зависещ от вида на горивото.

Видно е, че коефициентите α и k влияят пряко върху температурата на горене. В Табл.2 и Табл.3 е направено сравнение при различни коефициенти α и k.

***Таблица 2.*** *Сравнителна таблица за α*

| α (k=3,76) | 1,2 | 1,3 | 1,4 | 1,5 |
|---|---|---|---|---|
| *i* [KJ/m³] | 2927,2 | 2726,2 | 2550,9 | 2396,9 |
| t [C°] | 1784,4 | 1668,6 | 1583,2 | 1500 |

***Таблица 3.*** *Сравнителна таблица за k*

| k (α=1,2) | 3,70 | 3,75 | 3,76 | 3,80 | 3,82 |
|---|---|---|---|---|---|
| *i* [KJ/m³] | 2960,3 | 2932,7 | 2927,2 | 2905,6 | 2894,9 |
| t [C°] | 1802,9 | 1787,6 | 1784,4 | 1771,8 | 1765,4 |

Налагащите се изводи са, че повишаване на енталпията се постига чрез намаляване стойноста на коефициентите α и k. Изменение на k зависи от околната среда, затова измерването му и правилното отчитане подобрява алгоритъма за изчисляване на енталпията, докато α се настройва от потребителя.

### 2.2. Проектиране на система за управление на пелетна горелка

Настройката на топлинната мощност се реализира, като се определи разхода на гориво при отчитане на неговата калоричност и коефициента на полезно действие на системата: автоматизирана горелка - водогреен котел.

В стационарни режими, контролера, управляващ горивните процеси е необходимо да изчислява:

1. Количеството гориво за подържане на желания режим;
2. Потребната топлинна мощност на горелката;
3. Необходимата топлина във водната инсталация.

На Фиг. 3 е показана блок-схема на сигналите в системата.

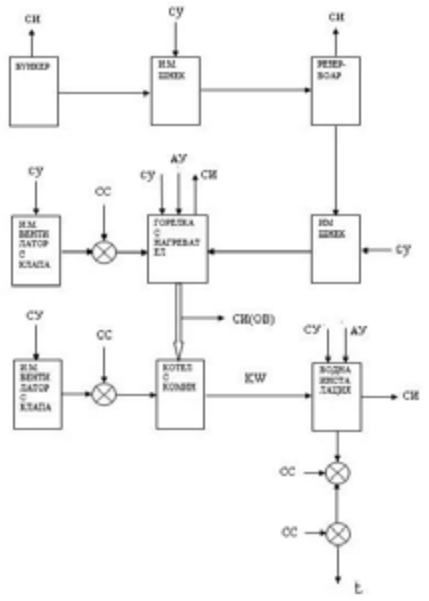
Така представената система на Фиг.3, условно се разделя на три части. Първата част е свързана с подаването на пелети към горелката, като задачата е да се преобразува: вход ->обем, изход->-тегло на подаваните пелети. Втората част определя горивните процеси: вход ->тегло, изход-> температура на горене. Третата част е свързана с работата на отоплителната система: вход ->мощност, изход-> желано отопление.

За работа в стационарни режими контролера решава две задачи. Правата задача е изчисляване на топлинната мощност на котела на база на подаденото гориво и обратната здача – при зададена топлинна мощност, да се изчисли необходимото за подаване гориво.

#### 2.2.1. Подсистема бункер-резервоар за пелети

В тази част, ситемата се състои от бункер за гориво, горивоподаващ шнек,

резервоар за гориво преди горелката и подаващ шнек към горелката Фиг.1 и Фиг.3. Вход на системата е обема на горивото (пелети)[m3], а изхода е маса на горивото (пелети)[kg] към горелката.



***Фиг. 3.*** *Блок-схема на сигналите в системата*

За да се автоматизират процесите е необходимо да се поставят сензори, съответно: за нивото на пелетите в основния бункер - три сензора (малко, нормално и високо ниво); за местоположение на пелетите в горивоподаващия шнек - три сензора (в началото, по средата, на изхода). Изпълнителният двигател на шнека се управлява чрез промяна на скоростта му с помощта на широчинно – импулсно модулиране.

Осигуряването на непрекъсната работа на горелката зависи от количеството гориво в резервоара преди горелката, затова са необходими три сензора за ниво (малко, нормално и високо), за да се пълни обема на резервоара навреме. От този резервоар, горивото с горивоподаващ шнек постъпва в горелката, тук отново се управляват оборотите на изпълнителния механизъм с широчинно-импулсна модулация. Така предложената система осигурява необходимата информация на контролера, която е свързана с количеството гориво осигуряващо процеса на горене.

### 2.2.2. Подситема горелка-котел с комин

За да се автоматизират процесите на горене, контролерът извършва изчисления за необходимата топлинна мощност, отдадена от горелката в котела. Вход е горивото (пелети и въздух), изход е енергията получена при горивния процес. Това е и главният тракт за регулиране на процеса на горене.

Смущения тук се явяват „В“ и „Г“ от Фиг.1, както и сигнала за смущение при липса на тяга на комина от Фиг.3. Смущения са и промяна на температурата в консуматорите и включване и/или изключване на топлинен консуматор.

Разглеждайки алгоритъма от т.2.1, от формула (3) се намира топлината на изгаряне на 1 [kg] пелети. Подавайки нужното количество пелети от подсистемата на т.2.2.1 във всеки един момент от време се намира топлината, необходима за тяхното изгаряне.

Действителният разход на въздух се базира на (6) при настройване на коефициента на излишък на въздух α. При изгарянето на 1 [kg] пелети в дима се отделят отпадъчни продукти, чието процентно съдържания е показано в пункт 5 на т.2.1.

По теоретичната плътност на дима (14) се определя необходимата големина на коминното тяло, а с помощта на енталпията (16) се намира температурата на горене на пелетите в зависимост от топлосъдържанието на димните газове. Сигналът за температурата на горене дава обратната връзка на системата по количеството топлина, което в момента се преобразува в топлинна мощност.

От казаното до тук, структурата на тази подсистема се изгражда от: силов елемент за управление на запалването (запалка); вентилатор с управляема клапа за подаване на свеж въздух; вентилатор с управляема клапа в коминното тяло (за тяга); дебитомер на входа на свежия въздух; газ-анализатор и инфрачервен сензор за продуктите на дима; саждоуловител; инфрачервени сензори за отчитане на огън в горивната камера и наличие на пламък в тръбата, идваща от шнека; сензор за налягане (сигнализиране за обратна тяга); сензор за дим в горивоподаващия шнек; сензор за температура и влажност на входа на свежия въздух; сензор отчитащ температурата на димните газове.

### 2.2.3. Подсистема на сградната отоплителна инсталация

Вход на системата е внесената в котела енергия, получена при протичането на горивния процес, а изходът е зададената температура на водата в сградната инсталация. При правилно подбиране на отоплителния котел се осигурява необходимата топлинна мощност за всички консуматори. Процесите се автоматизират чрез сигнал подаван от термостата, монтиран в ситемата на водната инсталация. Чрез него се управлява горивоподаващия шнек.

Подсистемата се състои от: сензори за измерване на постигнатата във водната система температура (на топлия и студения край на водната система); човекомашинен интерфейс (дисплей, клавиатура и др.). Към тази част спадат още уред за аериране на водата и филтър (Фиг.3).

### 3. Алгоритъм за работа на контролера

Алгоритъмът за работа на контролера се разглежда в стационарни режими, при което не се отчитат процесите на запалване (Режим „Старт“) и разгарянето (Режим „Разгаряне“) на пелетното гориво, изгасянето на горелката (Режим „Загасяне“), както и почистването и (Режим „Почистване“).

В известните ни литературни източници, разчетите на горивните процеси във водогрейните котли и инсталации се извършват в стационарни режими. Това ни дава правото да разработим първоначално алгоритъма за работа на пелетната горелка именно в този установен режим (Режим „Горене“). В настоящия алгоритъм не са залегнали и процесите на управление, под влиянието на различните видове смущения в работата на системата.

На Фиг.4 е показана блок-схемата на алгоритъма на работа на горелката в Режим „Горене“. В този режим първо се отчита необходимата топлинна мощност, след това контролера изчислява неоходимото гориво за достигане на тази мощност и започва подаването му към горивната камера чрез двигателя на горивоподаващия шнек.

Проверява се за достигане на изчислената температура на горене. Ако не е достигната се продължава с подаването на горивото, но ако температурата е достигната, тогава се проверява процентното съдържание на газовете в продуктите на горене – дима. Ако те не са в норма се настройва коефициента α и количеството на подавано гориво.

Последната проверка е за достигане на желаната мощност. Ако е достигната се продължава с така подаваното гориво, в противен случай се преизчислява необходимата температура и количеството на подавано гориво.

### 4. Заключение

Изследвана е възможността за подобряване работата на пелетни горелки, чрез повишаване на информативността при горивните процеси. Изчислени са теоретичните стойности на величините, участващи в процеса на горене на пелети. Предложен е алгоритъм за работа на пелетна горелка в стационарен режим.




***Фиг. 4.*** *Блок-схема на алгоритъма на работа на контролера*

### ЛИТЕРАТУРА


1. *ИНСТРУКЦИЯ за монтаж, настройка и сервизиране на автоматизирана горелка за пелети “ERATO GP20” и “ERATO GP20+” на стоманен водогреен котел “Junkers Supraclass S”*, <http://erato.bg/files/file_757_823.pdf>09.02.2016г.
2. *ИНСТРУКЦИЯ за монтаж и експлоатация на автоматизиран водогреен котел работещ с пелети ERATO PELLETHERM 25 автоматичен,* <http://www.erato.bg/files/file_515_204.pdf>09.02.2016г.
3. *Инструкция за монтаж, експлоатация и поддръжка на горелка за пелети със самопочистване серия „gp xx sc”,* <http://greenecotherm.bg/uploads/docs/213_bg_User Manual 20GP 20xx 20sc_BG.pdf> 09.02.2016г.
4. *Инструкция за монтаж и експлоатация на пелетна горелка GREYKO RB*, <http://www.greyko.com/1.pdf>09.02.2016г.
5. Брезин В., Антов П., Ковачева А., (2013). *Растителната биомаса -източник за получаване на биогенни горива*, 50стр. Издателска къща при ЛТУ, София.
6. Фокин В. М. (2006) *Теплогенерирующие установки систем теплоснабжения,* 210стр. Издательство машиностроение-1, Москва.
7. Амерханов Р. А., Драганов Б.Х. (2006). *Теплотехника*, 443стр. Энергоатомиздат, Москва.


Адрес:
E-mail: goldkeeper@abv.bg
E-mail: biliderow_ss@yahoo.com

© International Scientific Conference on Engineering, Technologies and Systems
TECHSYS 2016, Technical University – Sofia, Plovdiv branch
26 – 28 May 2016, Plovdiv, Bulgaria

# СИНХРОНИЗАЦИЯ И АНТИСИНХРОНИЗАЦИЯ НА НОВА ХАОТИЧНА СИСТЕМА СЪС СПЕЦИФИЧНА НЕЛИНЕЙНОСТ

ДРАГОМИР ЧАНТОВ, ХРИСТИНА СТОЙЧЕВА

**Резюме:** *В доклада се предлага синтез на хаотични синхронизационни системи с цел постигане на идентична синхронизация и антисинхронизация между две идентични хаотични системи. Управляващите функции се реализират с помощта на втория метод за устойчивост на Ляпунов. За основа на синхронизационните схеми е избран модел на открита през 2013 г. хаотична система със специфична нелинейност.*

**Ключови думи:** *хаотични системи, синхронизация на хаотични системи, анти-синхронизация*

# SYNCHRONIZATION AND ANTI-SYNCHRONIZATION OF A NEW CHAOTIC SYSTEM WITH SPECIFIC NONLINEARITY

DRAGOMIR CHANTOV, HRISTINA STOYCHEVA

**Abstract:** *In this paper synthesis of chaotic synchronization systems with the aim to achieve identical synchronization and anti-synchronization between two identical chaotic systems is proposed. The control functions are designed by means of the second Lyapunov stability method. A new chaotic model, reported first in 2013, which has a specific type of nonlinearity, is used as a basis for the synchronization schemes.*

**Key words:** *chaotic systems, chaotic synchronization, anti-synchronization*

## 1. Въведение

През последните години в научната общност се наблюдава повишен интерес към хаотичните системи – нелинейни системи със сложна динамика и поведение, близко до това на стохастичните системи [1]. В преобладаващата част от публикациите по темата се разглеждат въпроси, свързани с хаотичната синхронизация. Това е явление, което може да възникне при подходящо свързване на две (понякога и повече) хаотични системи. При добре синтезирани управляващи функции динамиката на едната система е подчинена по строго дефиниран закон на динамиката на другата. Основната област на приложение на хаотичната синхронизация е в различни видове комуникационни системи или системи за криптиране на текст, изображения и видео, където псевдо-случайната природа на хаоса се използва за скриване и защитаване на полезната информация от неоторизиран достъп.

Най-разпространената форма на синхронизация между хаотични системи е тази, при която функциите на разсъгласуване представляват разликите между съответстващите си двойки променливи на състоянието на подлежащите на синхронизация системи. Когато двете хаотични системи са стартирани от различни начални условия и са свързани с такива управляващи функции, че функциите на разсъгласуване се установяват в нула, се казва, че между двете системи има идентична синхронизация.

Copyright © 2016 by Technical University of Sofia, Plovdiv branch, Bulgaria ISSN Online: 2535-0048

Друга форма на синхронизирано движение между две хаотични системи е тази, при която функциите на разсъгласуване представляват сумите от отделните двойки променливи на двете системи. На практика, ако тези функции се установят в нула, динамиката на всяка променлива на едната система ще е хаотична и ще представлява „огледален образ" на съответната променлива от другата система. Това явление се нарича антисинхронизация и има предимства пред идентичната синхронизация по отношение на по-голямата степен на защита на информацията в хаотичните комуникационни системи [2].

В настоящия доклад се предлага синтез на хаотични синхронизационни и антисинхронизационни системи за един от новите и по-малко познати модели на хаотични системи, който съдържа специфична нелинейност от тригонометричен тип. Синтезът на управляващите функции се основава на прилагането на втория метод за устойчивост на Ляпунов.

## 2. Хаотична система на Yu-Wang

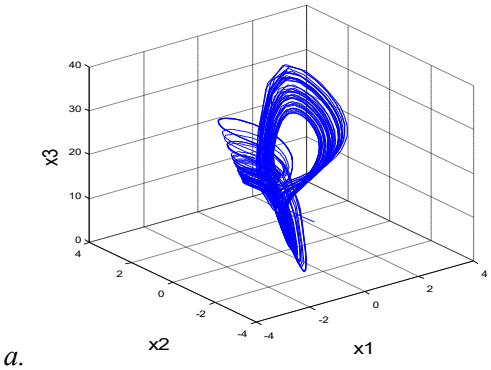
По-голямата част от известните модели на хаотични системи са от трети ред. Някои от тях са модели на реални системи от практиката, например от областите на електрониката, химията, физиката и дори икономиката. Друга част са само абстрактни математични модели, които могат да се разглеждат като своеобразни „генератори на хаос", който да се използва в приложения, изискващи хаотичен процес, например в комуникационни системи с хаотична защита на информацията. При тези системи на базата на математическата конструкция, генерираща хаос, се изгражда реална система.

Във всички хаотични модели задължително присъства поне един нелинеен елемент. В повечето хаотични модели от описаните по-горе два вида се срещат нелинейности предимно от типа $x_i x_j$, където $x_i$ и $x_j$ са променливи на състоянието на системата, или $x_i^p$, където най-често $p=2$ или $p=3$. През 2013 г. е предложен прост абстрактен математичен модел на автономна система със сложна хаотична динамика, която съдържа две нелинейности, едната от които е във вид на периодична функция [3,4]. Прието е системата да се нарича система на Yu-Wang по имената на нейните откриватели. Системата има две разновидности и може да се дефинира с общия запис:

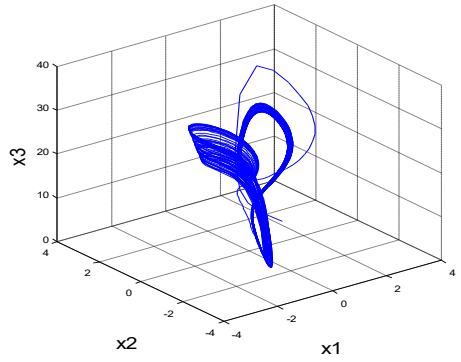
$$\begin{aligned} \dot{x}_1 &= a(x_2 - x_1), \\ \dot{x}_2 &= bx_1 - cx_1x_3, \\ \dot{x}_3 &= f(x) - dx_3, \end{aligned} \qquad (1)$$

където $f(x)=\sinh(x_1x_2)$ или $f(x)=\cosh(x_1x_2)$.

Номиналните стойности на параметрите на системата, за които системата има хаотична динамика, са $a=10, b=30, c=2, d=2.5$. При симулация на модела (1) с продукта MATLAB (Simulink) с начални условия: $x_1(0)=2$, $x_2(0)=1$, $x_3(0)=1$, избрани произволно, и $f(x)=\sinh(x_1x_2)$ се получава хаотичен атрактор, показан в пространството на състоянието на Фиг. 1*a*. На Фиг. 1*b* е показан атракторът на системата при същите начални условия и $f(x)=\cosh(x_1x_2)$.




*a.*

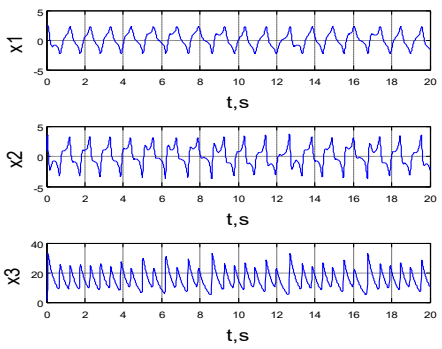



*b.*

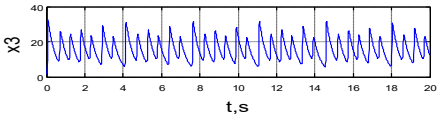
***Фиг. 1.*** *Атрактори на системата*

На Фиг. 2*a* са показани времевите характеристики $x_i(t), i=1\div3$ за първия вариант на системата с $f(x)=\sinh(x_1x_2)$, а на Фиг. 2*b* е показана динамиката на променливата $x_3(t)$ за втория вариант на системата с $f(x)=\cosh(x_1x_2)$, като останалите две променливи $x_1(t)$ и $x_2(t)$ практически не се различават от тези на Фиг. 1*a*.

При синтеза на синхронизационните схеми в следващите секции на доклада ще бъде разглеждан само първият вариант на системата с $f(x)=\sinh(x_1x_2)$.




*a.*




*b.*

***Фиг. 2.*** *Времеви характеристики* $x_i(t)$

### 3. Синтез синхронизационна система с идентична синхронизация между две системи на Yu-Wang

Нека са дадени две системи на Yu-Wang от вариант 1, свързани помежду си по следния начин:

$$\begin{aligned} \dot{x}_1 &= a(x_2 - x_1), \\ \dot{x}_2 &= bx_1 - cx_1x_3, \\ \dot{x}_3 &= \sinh(x_1x_2) - dx_3, \end{aligned} \tag{2}$$

$$\begin{aligned} \dot{\tilde{x}}_1 &= a(\tilde{x}_2 - \tilde{x}_1) + g_1(\mathbf{x}, \tilde{\mathbf{x}}), \\ \dot{\tilde{x}}_2 &= b\tilde{x}_1 - c\tilde{x}_1\tilde{x}_3 + g_2(\mathbf{x}, \tilde{\mathbf{x}}), \\ \dot{\tilde{x}}_3 &= \sinh(\tilde{x}_1\tilde{x}_2) - d\tilde{x}_3 + g_3(\mathbf{x}, \tilde{\mathbf{x}}), \end{aligned} \tag{3}$$

където $\mathbf{x} = [x_1 \ x_2 \ x_3]^T$, $\tilde{\mathbf{x}} = [\tilde{x}_1 \ \tilde{x}_2 \ \tilde{x}_3]^T$.

Системата (2) ще се нарича управляваща система в синхронизационната система, тъй като тя осигурява свързващия сигнал между двете системи, а системата (3) – подчинена. Видно е, че подчинената система не оказва влияние върху динамиката на управляващата система, тъй като връзката между двете е еднопосочна – от (2) към (3).

Функциите $g_i(\mathbf{x}, \tilde{\mathbf{x}}), i = 1 \div 3$ са управляващи функции към подчинената система, които трябва да бъдат синтезирани така, че между системите (2) и (3) да възникне и да се поддържа устойчива идентична синхронизация. Идентична синхронизация между две хаотични системи, например между системите (2) и (3), ще има, ако се изпълнява условието:

$$\lim_{t \to \infty} \mathbf{e}(t) = 0 \tag{4}$$

където $\mathbf{e} = [e_1 \ e_2 \ e_3]^T$, а

$$e_i = x_i - \tilde{x}_i, \ i = 1 \div 3 \tag{5}$$

са функциите на разсъгласуване между управляващата и подчинената системи.

На практика изпълнението на условието (4) при функции на разсъгласуване (5) ще означава, че системите (2) и (3) ще извършват идентични, и в същото време хаотични движения.

Системата от разсъгласуването между управляващата и подчинената системи се получава, като се извадят уравненията на системата (3) от съответните им уравнения на системата (2):

$$\begin{aligned} \dot{e}_1 &= \dot{x}_1 - \dot{\tilde{x}}_1 = \\ &= ax_2 - ax_1 - a\tilde{x}_2 + a\tilde{x}_1 - g_1(\mathbf{x}, \tilde{\mathbf{x}}) = \\ &= ae_2 - ae_1 - g_1(\mathbf{x}, \tilde{\mathbf{x}}), \\ \dot{e}_2 &= \dot{x}_2 - \dot{\tilde{x}}_2 = \\ &= bx_1 - cx_1x_3 - b\tilde{x}_1 + c\tilde{x}_1\tilde{x}_3 - g_2(\mathbf{x}, \tilde{\mathbf{x}}) = \\ &= be_1 - c(x_1x_3 - \tilde{x}_1\tilde{x}_3) - g_2(\mathbf{x}, \tilde{\mathbf{x}}), \\ \dot{e}_3 &= \dot{x}_3 - \dot{\tilde{x}}_3 = \\ &= \sinh(x_1x_2) - dx_3 - \sinh(\tilde{x}_1\tilde{x}_2) + d\tilde{x}_3 - g_3(\mathbf{x}, \tilde{\mathbf{x}}) = \\ &= \sinh(x_1x_2) - \sinh(\tilde{x}_1\tilde{x}_2) - de_3 - g_3(\mathbf{x}, \tilde{\mathbf{x}}). \end{aligned} \tag{6}$$

Изпълнението на условието за синхронизация (4) по същество е задача за стабилизиране на системата от разсъгласуването (6) в точката $\mathbf{e} = 0$ ($e_1 = e_2 = e_3 = 0$). Тази задача може да бъде решена с помощта на втория метод за устойчивост на Ляпунов, при който се търси функция на Ляпунов $V(\mathbf{e})$, която да отговаря на трите условия:

$$V(\mathbf{e}) > 0 \ \text{за} \ \forall \mathbf{e} \neq 0, \tag{7}$$

$$V(\mathbf{e}) = 0 \ \text{за} \ \mathbf{e} = 0, \tag{8}$$

$$\dot{V}(\mathbf{e}) < 0 \ \text{за} \ \forall \mathbf{e} \neq 0. \tag{9}$$

Ако бъде намерена функция $V(\mathbf{e})$, за която и трите условия (7)-(9) да се изпълняват, то според втория метод на Ляпунов системата ще се стабилизира в т. $\mathbf{e} = 0$.

При стартирането на двете хаотични системи (2) и (3) от различни начални условия функциите $e_i$ във всеки момент могат да приемат както положителни, така и отрицателни стойности. Тогава, за удовлетворяване на условията (7) и (8) функцията $V(\mathbf{e})$ следва да

бъде квадратична функция от променливите $e_i$, например от типа:

$$V(\mathbf{e}) = \frac{1}{2}(e_1^2 + e_2^2 + e_3^2). \qquad (10)$$

Изпълнението на третото условие ще се търси чрез подходящ синтез на управляващите функции към подчинената система $g_i(\mathbf{x}, \tilde{\mathbf{x}})$. Те трябва да бъдат така синтезирани, че за първата производна на функцията $V(\mathbf{e})$ да се получи отрицателно определен израз, например от типа:

$$\dot{V}(\mathbf{e}) = -k_1 e_1^2 - k_2 e_2^2 - k_3 e_3^2, \qquad (11)$$

където $k_i$ са положителни константи.

От (10) за първата производна на $V(\mathbf{e})$ следва:

$$\dot{V}(\mathbf{e}) = e_1\dot{e}_1 + e_2\dot{e}_2 + e_3\dot{e}_3. \qquad (12)$$

За да се приведе израза (12) към отрицателно определения израз (11), всяка от управляващите функции $g_i(\mathbf{x}, \tilde{\mathbf{x}})$ трябва да бъде така синтезирана, че за всяка от производните на функциите на разсъгласуване да се получи:

$$\dot{e}_i = -k_i e_i. \qquad (13)$$

Тогава, ако функциите $g_i(\mathbf{x}, \tilde{\mathbf{x}})$ се изберат както следва:

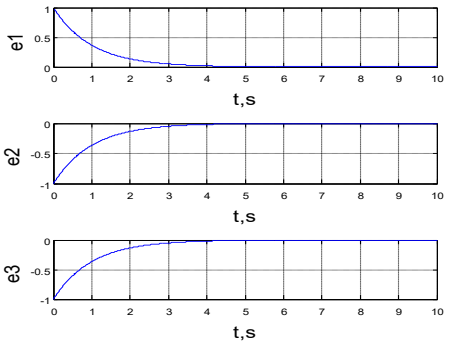
$$\begin{aligned} g_1(\mathbf{x}, \tilde{\mathbf{x}}) &= ae_2 - ae_1 + k_1 e_1, \\ g_2(\mathbf{x}, \tilde{\mathbf{x}}) &= be_1 - c(x_1 x_3 - \tilde{x}_1 \tilde{x}_3) + k_2 e_2, \\ g_3(\mathbf{x}, \tilde{\mathbf{x}}) &= \sinh(x_1 x_2) - \sinh(\tilde{x}_1 \tilde{x}_2) - de_3 + k_3 e_3, \end{aligned} \qquad (14)$$

след заместването им в уравненията на системата от разсъгласуването (6) ще се получи:

$$\begin{aligned} \dot{e}_1 &= -k_1 e_1, \\ \dot{e}_2 &= -k_2 e_2, \\ \dot{e}_3 &= -k_3 e_3, \end{aligned} \qquad (15)$$

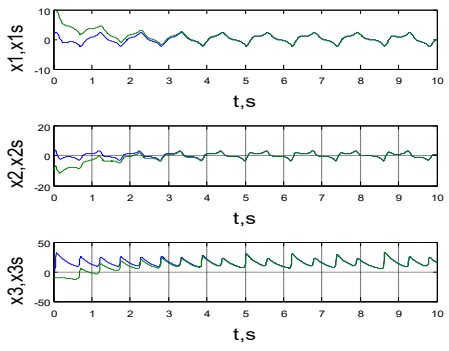
т.е. и трите уравнения стават от типа (13), което гарантира изпълнението и на третото условие за устойчивост по Ляпунов (9).

Хаотичната синхронизационна система между две системи на Yu-Wang (2)-(3) с управляващи функции към подчинената система (14) е тествана чрез симулационен модел в MATLAB (Simulink). Двете хаотични системи са стартирани от различни начални условия, съответно: $x_1(0) = 2$, $x_2(0) = 1$, $x_3(0) = 1$ за управляващата система и $\tilde{x}_1(0) = 1$, $\tilde{x}_2(0) = 2$, $\tilde{x}_3(0) = 2$ за подчинената система, като и двата набора начални условия са избрани произволно. И за трите константи $k_i$ е избрана стойност единица. На Фиг. 3 са показани получените при симулацията функции на разсъгласуване $e_i = x_i - \tilde{x}_i$, $i = 1 \div 3$. Вижда се, че след преходен процес (с еднаква продължителност и за трите функции) от 4s, се изпълнява условието за синхронизация (4).



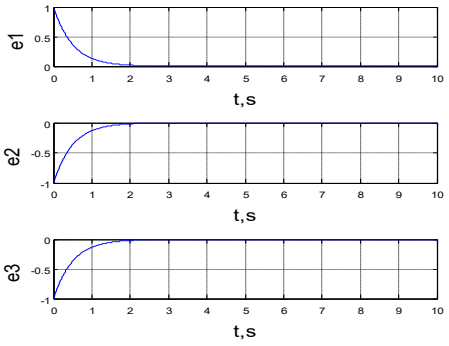

***Фиг. 3.*** *Функции на разсъгласуване* $e_i(t)$

На Фиг. 4 е показана съвместната динамика на променливите на управляващата и на подчинената системи $x_i, \tilde{x}_i$, $i = 1 \div 3$. За да се виждат по-добре разликите в състоянията на двете системи преди влизането им в синхронизационен режим втората система е стартирана с начални условия $\tilde{x}_1(0) = 10$, $\tilde{x}_2(0) = -10$, $\tilde{x}_3(0) = -10$. Вижда се, че след края на преходния процес състоянията на двете системи стават напълно идентични, като подчинената система започва да изпълнява същите хаотични движения като управляващата. Друга характеристика на хаотичната синхронизация, която може да се види от Фиг. 3 и Фиг. 4, е че независимо от значително по-големите разлики в началните условия при втория експеримент, големината на преходния процес се запазва непроменена – 4s.




***Фиг. 4.*** *Съвместна динамика на променливите на двете системи*

С помощта на коефициентите $k_i$ може да се регулира продължителността на преходния процес на синхронизацията. Например при $k_i = 2$ и начални условия на подчинената система, равни на тези от първия експеримент, продължителността на преходния процес вече е около 2s, както може да се види на Фиг. 5.




***Фиг. 5.*** *Функции на разсъгласуване* $e_i(t)$

**4. Синтез синхронизационна система с антисинхронизация между две системи на Yu-Wang**

Общата структура на хаотичната синхронизационна система при задачата за антисинхронизация е същата като тази в секция 3 на настоящия доклад, т.е. управляващата и подчинената хаотични системи на Yu-Wang се дефинират съответно с наборите уравнения (2) и (3). Двете системи ще бъдат в режим на антисинхронизация, ако отново се изпълнява условието (4), но вече за функции на разсъгласуване от типа:

$$e_i = x_i + \tilde{x}_i,\ i = 1 \div 3. \qquad (16)$$

Изпълнението на условието (4) при функции на разсъгласуване (16) ще означава, че системите (2) и (3) ще извършват еднакви по модул, но с противоположен знак хаотични движения, т.е. когато $e_i = 0$ $x_i = -\tilde{x}_i$.

В съответствие с (16), системата от разсъгласуването между управляващата и подчинената системи ще се получи, като се сумират съответните уравнения на системите (2) и (3):

$$\begin{aligned}
\dot{e}_1 &= \dot{x}_1 + \dot{\tilde{x}}_1 = \\
&= ax_2 - ax_1 + a\tilde{x}_2 - a\tilde{x}_1 + g_1(\mathbf{x}, \tilde{\mathbf{x}}) = \\
&= ae_2 - ae_1 + g_1(\mathbf{x}, \tilde{\mathbf{x}}), \\
\dot{e}_2 &= \dot{x}_2 + \dot{\tilde{x}}_2 = \\
&= bx_1 - cx_1x_3 + b\tilde{x}_1 - c\tilde{x}_1\tilde{x}_3 + g_2(\mathbf{x}, \tilde{\mathbf{x}}) = \\
&= be_1 - c(x_1x_3 + \tilde{x}_1\tilde{x}_3) + g_2(\mathbf{x}, \tilde{\mathbf{x}}),
\end{aligned}$$

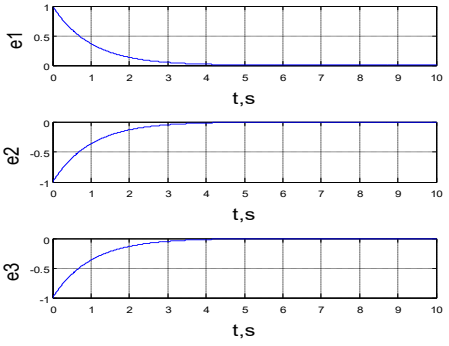
$$\begin{aligned}
\dot{e}_3 &= \dot{x}_3 + \dot{\tilde{x}}_3 = \\
&= \sinh(x_1x_2) - dx_3 + \sinh(\tilde{x}_1\tilde{x}_2) - d\tilde{x}_3 + g_3(\mathbf{x}, \tilde{\mathbf{x}}) = \\
&= \sinh(x_1x_2) + \sinh(\tilde{x}_1\tilde{x}_2) - de_3 + g_3(\mathbf{x}, \tilde{\mathbf{x}}).
\end{aligned} \qquad (17)$$

При избор на функция на Ляпунов (10), за да бъде първата й производна във вида (11), управляващите функции към подчинената хаотична система (3) трябва да бъдат както следва:

$$\begin{aligned}
g_1(\mathbf{x}, \tilde{\mathbf{x}}) &= -ae_2 + ae_1 - k_1e_1, \\
g_2(\mathbf{x}, \tilde{\mathbf{x}}) &= -be_1 + c(x_1x_3 + \tilde{x}_1\tilde{x}_3) - k_2e_2, \\
g_3(\mathbf{x}, \tilde{\mathbf{x}}) &= -\sinh(x_1x_2) - \sinh(\tilde{x}_1\tilde{x}_2) + de_3 - k_3e_3.
\end{aligned} \qquad (18)$$

При заместване на управляващите функции (18) в системата от разсъгласуването (17), тя отново добива вида (15), с което първата производна на функцията на Ляпунов е във вид (11), който удовлетворява третото условие за устойчивост по Ляпунов (9).

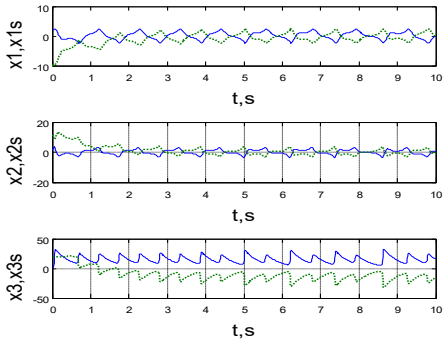
Синхронизационна система с анти-синхронизация между две системи на Yu-Wang (2)-(3) с управляващи функции към подчинената система (18) е тествана в MATLAB (Simulink). Началните условия са: $x_1(0) = 2$, $x_2(0) = 1$, $x_3(0) = 1$ и $\tilde{x}_1(0) = -10$, $\tilde{x}_2(0) = 12$. Константите $k_i$ са единици. На Фиг. 6 са показани получените при симулацията функции на разсъгласуване $e_i = x_i + \tilde{x}_i$, $i = 1 \div 3$. Вижда се, че продължителността на преходния процес е равна на тази при идентичната синхронизация при едни и същи константи $k_i$.




***Фиг. 6.*** *Функции на разсъгласуване* $e_i(t)$

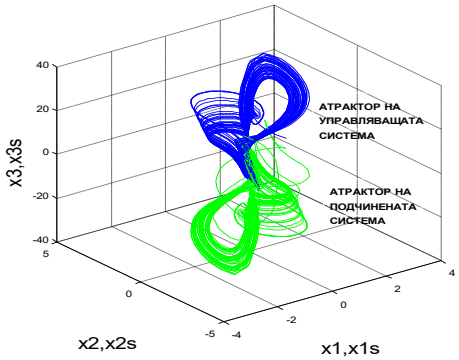
Антисинхронизационното движение на двете хаотични системи на Yu-Wang се илюстрира по-ефектно, ако се наблюдава съвместната динамика на променливите на управляващата и на подчинената системи $x_i, \tilde{x}_i,\ i = 1 \div 3$ (Фиг.7). Променливите на подчинената система са изобразени с прекъсната

линия. Вижда се, че след края на преходния процес състоянията на двете системи стават еднакви по модул, но с противоположен знак, т.е. динамиката на дадена променлива е „огледален образ" на съответстващата й променлива от другата хаотична система, като в същото време движението и на двете системи е хаотично.




***Фиг. 7.*** *Съвместна динамика на променливите на двете системи*

Друг начин за визуализация на анти-синхронизационната динамика на двете хаотични системи е чрез построяване на хаотичните им атрактори в едно общо пространство на състоянието (Фиг. 8). Вижда се, че подчинената система, която преди синхронизацията е имала хаотичен атрактор, идентичен на този на управляващата система (Фиг. 1*a*), сега има атрактор, който е симетричен спрямо трите оси на оригиналния.




***Фиг. 8.*** *Атрактори на системите при антисинхронизация*

По-аналогичен начин на този от т.3 и т.4 могат да се синтезират синхронизационна и антисинхронизационна системи на основата на другия вариант на базовата хаотична система с нелинейна функция в третото уравнение $f(x) = \cosh(x_1 x_2)$. За целта в управляващите функции за синхронизация (14) и антисинхронизация (18) функцията sinh се заменя с cosh. При симулациите се получават резултати, подобни на тези при първия вариант на хаотичната система.

## 5. Заключение

Синтезирани са хаотични синхронизационни системи с идентична синхронизация и антисинхронизация на основата на нов модел на хаотична система със специфична нелинейност, която води до по-сложна хаотична динамика. При използвания подход за синтез на управляващи функции според теорията за устойчивост на Ляпунов са получени успешно както синхронно, така и антисинхронно поведение на двете хаотични системи. При анти-синхронизацията подчинената система принудено сменя атрактора си и той вече е различен от оригиналния. При това двойката управляваща – подчинена системи могат да се разглеждат като една система от 6-ти ред с по-сложен хаотичен атрактор. Това, както и специфичната природа на избраната основна хаотична система могат да осигурят допълнителни предимства по отношение на сигурността при изграждането на хаотична комуникационна система на основата на синтезираните синхронизационни схеми.

## ЛИТЕРАТУРА

1. Carroll, T., L. Pecora (1991). Synchronizing chaotic circuits. *IEEE Transactions on Circuits and Systems-I*, volume 38 (4), pp. 453-456.
2. Emadzadeh, A., M. Haeri (2005). Anti-synchronization of two different chaotic systems via active control. *World Academy of Science, Engineering and Technology*, volume 6, pp. 62-65.
3. Yu, F., C. Wang (2013). Generation of a new three dimension autonomous chaotic attractor and its four wing type. *Engineering, Technology & Applied Science* Research, volume 3, pp. 352-358.
4. Umoh, E. (2014). Synchronization of chaotic flows with variable nonlinear hyperbolic functions via hybrid feedback control. *Proc. of Pan African Int. Conf. on Science, Computing and Telecommunications*. pp. 7011.

Контакти
Адрес: катедра "Автоматика, информационна и управляваща техника", Технически университет – Габрово, 5300 Габрово, ул."Хаджи Димитър" No 4.
E-mail: dchantov@abv.bg
E-mail: hsstoycheva@abv.bg

© International Scientific Conference on Engineering, Technologies and Systems
TECHSYS 2016, Technical University – Sofia, Plovdiv branch
26 – 28 May 2016, Plovdiv, Bulgaria

# ПРОЕКТИРАНЕ НА ХАОТИЧНИ СИНХРОНИЗАЦИОННИ СИСТЕМИ С РАЗЛИЧНИ ВИДОВЕ ИДЕНТИЧНА И НЕИДЕНТИЧНА СИНХРОНИЗАЦИЯ НА ОСНОВАТА НА МЕТОД С ЛИНЕЙНО-НЕЛИНЕЙНА ДЕКОМПОЗИЦИЯ

ДРАГОМИР ЧАНТОВ, ХРИСТИНА СТОЙЧЕВА

**Резюме:** *В доклада се предлага синтез на различни хаотични синхронизационни системи на основата на един базов модел на хаотична система, с цел получаване на идентична и различни форми на неидентична синхронизация, като изместена и осцилираща. Управлението се проектира на два етапа, като на първия се получава линейна система от разсъгласуването, което улеснява значително анализа й за устойчивост, а на втория се търси такова допълнително управление, което да осигури желания тип синхронизация.*

**Ключови думи:** *хаотични системи, синхронизация на хаотични системи, линейно-нелинейна декомпозиция*

# DESIGN OF CHAOTIC SYNCHRONIZATION SYSTEMS WITH DIFFERENT TYPES OF IDENTICAL AND NON-IDENTICAL SYNCHRONIZATION ON THE BASIS OF A LINEAR-NONLINEAR DECOMPOSITION APPROACH

DRAGOMIR CHANTOV, HRISTINA STOYCHEVA

**Abstract:** *In this paper synthesis of different chaotic synchronization systems on the basis of one particular chaotic model is proposed, with the aim of achieving identical and different types of non-identical synchronization, as marginal and oscillatory ones. The control is designed on two stages with the first stage yielding a linear error system, which significantly eases its stability analysis, and on the second stage such additional control is searched, that to ensure the desired type of synchronization*

**Key words:** *chaotic systems, chaotic synchronization, linear-nonlinear decomposition*

## 1. Въведение

При задачите за проектиране на хаотични синхронизационни системи обикновено се разглеждат две или повече хаотични системи, които могат да бъдат еднопосочно или двупосочно свързани. При първия случай, който е и по-разпространен, всяка система участва в управлението на следващата система във веригата, без да се

Copyright © 2016 by Technical University of Sofia, Plovdiv branch, Bulgaria ISSN Online: 2535-0048

влияе от нейната динамика. Често изграждащите синхронизационната схема хаотични системи са идентични, но с различни начални условия, а получената синхронизация между тях може да бъде идентична или неидентична. По-популярна е идентичната синхронизация, която се характеризира с нулеви функции на разсъгласуване или разлики между съответстващите си променливи на синхронизираните хаотични системи. По-малко изследвани са някои форми на неидентична синхронизация между идентични хаотични системи, като например изместената или осцилиращата хаотични синхронизации [1]. При изместената синхронизация поне една от функциите на разсъгласуване се установява в константа, различна от нула. При осцилиращата синхронизация поне две от функциите на разсъгласуване са периодични функции. Получаването на по-сложни от идентичната форми на синхронизация между хаотични системи се предпочита при синтеза на системи за защитено предаване на данни чрез хаотични сигнали, тъй като предлага по-големи възможности за защитата на данните.

В доклада се предлага синтез на хаотични синхронизационни схеми с идентична, изместена и осцилираща синхронизация на основата на прост модел на хаотична система от трети ред с един нелинеен елемент, открита през 2014 г. Тъй като желаният тип синхронизация зависи от собствените стойности на матрицата на състоянието на системата от разсъгласуването, се предлага управлението към подчинената хаотична система да е от две части, като първата има за цел да направи системата от разсъгласуването линейна. Така лесно и точно могат да се изчислят собствените стойности на матрицата на състоянието й и след анализ да се проектира второто управление, което да ги позиционира според желания тип синхронизация.

## 2. Методи за синхронизация на хаотични системи с линейно-нелинейна декомпозиция

При задачите за хаотична синхронизация най-често се разглеждат две идентични еднопосочно свързани нелинейни непрекъснати хаотични системи от вида:

$$\dot{\mathbf{x}} = \mathbf{f}(\mathbf{x}), \tag{1}$$

$$\dot{\widetilde{\mathbf{x}}} = \mathbf{f}(\widetilde{\mathbf{x}}, \mathbf{x}), \tag{2}$$

където $\mathbf{x}, \widetilde{\mathbf{x}} \in \Re^n$ са векторите на състоянието на системите.

Системата (1) се нарича управляваща, а системата (2) – подчинена. При задача за **идентична синхронизация** се търси такова управление към подчинената система, функция на променливите на управляващата система, че да се изпълнява условието:

$$\lim_{t\to\infty} \mathbf{e}(t) = 0, \tag{3}$$

където $\mathbf{e}(t) = \mathbf{x} - \widetilde{\mathbf{x}}$ се нарича вектор на разсъгласуване между системите (1) и (2).

Ако поне една от съставящите вектора **e** функции на разсъгласуване $e_i = x_i - \widetilde{x}_i$ вместо към нула клони към различна от нула константа, а останалите се установяват в нула, между системите (1) и (2) възниква **изместена синхронизация**.

Ако поне една (обикновено две) от съставящите вектора **e** функции на разсъгласуване $e_i = x_i - \widetilde{x}_i$ вместо да клони към нула се превръща в периодична функция, а останалите се установяват в нула, между системите (1) и (2) възниква **осцилираща синхронизация**.

Типът на синхронизирано движение се определя от системата от разсъгласуването, която се получава при изваждане на уравненията на системата (2) от тези на системата (1) и отчитане, че $\mathbf{x} - \widetilde{\mathbf{x}} = \mathbf{e}$:

$$\dot{\mathbf{e}} = \dot{\mathbf{x}} - \dot{\widetilde{\mathbf{x}}} = \mathbf{f}(\mathbf{x}) - \widetilde{\mathbf{f}}(\widetilde{\mathbf{x}}, \mathbf{x}). \tag{4}$$

Ако връзката между системите (1) и (2) е такава, че системата от разсъгласуването (3) е линейна система - $\dot{\mathbf{e}} = \mathbf{A}\mathbf{e}$, то типът на евентуалната синхронизация между системите може лесно да се определи по собствените стойности на матрицата **A**. Ако се синтезира такава връзка между (1) и (2), че всички собствени стойности на **A** да са с отрицателна реална част или реални отрицателни, между двете хаотични системи ще има идентична синхронизация. На практика това е условието за устойчивост на линейната система от разсъгласуването в т. $\mathbf{e} = 0$, която според (3) съответства на идентична синхронизация. Ако поне една от собствените стойности на **A** е равна на нула, а останалите са в лявата полуравнина на комплексната равнина, между (1) и (2) ще възникне изместена синхронизация. Ако измежду собствените стойности на **A** има двойка комплексно-спрегнати такива с нулева реална част, а останалите са в лявата полуравнина на комплексната равнина, между (1) и (2) ще възникне осцилираща синхронизация. Ако поне една от собствените

стойности на **A** е в дясната полуравнина на комплексната равнина, между (1) и (2) не може да има синхронизирано движение, тъй като системата от разсъгласуването става неустойчива.

Тогава при задача за получаване на желано синхронизирано движение между две хаотични системи трябва да се решат две подзадачи:

1. Синтез на такава връзка между управляващата (1) и подчинената (2) хаотични системи, че системата от разсъгласуването между тях да се получи линейна.

2. Синтез на допълнителна връзка между системите (1) и (2), чрез която да се манипулират собствените стойности на матрицата **A** според желания тип синхронизация.

Удобен инструмент за решаването на първата подзадача е прилагането на известния метод за синхронизация на хаотични системи с линейно-нелинейна декомпозиция [2]. При него системата (1) условно може да се представи във вида:

$$\dot{\mathbf{x}} = \mathbf{f}(\mathbf{x}) = \mathbf{A}\mathbf{x} + \mathbf{h}(\mathbf{x}), \qquad (5)$$

където $\mathbf{A}\mathbf{x}$ е линейната част на системата, а векторът $\mathbf{h}(\mathbf{x})$ съдържа само нелинейните елементи на функцията $\mathbf{f}(\mathbf{x})$.

Тогава, ако подчинената система (2) се синтезира във вида:

$$\dot{\tilde{\mathbf{x}}} = \mathbf{f}(\tilde{\mathbf{x}}, \mathbf{x}) = \mathbf{A}\tilde{\mathbf{x}} + \mathbf{h}(\mathbf{x}), \qquad (6)$$

т.е. свързващият елемент или управлението от (1) към (2) се явяват всички нелинейни елементи на базовата хаотична система, то за системата от разсъгласуването се получава:

$$\dot{\mathbf{e}} = \dot{\mathbf{x}} - \dot{\tilde{\mathbf{x}}} = \mathbf{A}\mathbf{x} - \mathbf{A}\tilde{\mathbf{x}} = \mathbf{A}\mathbf{e}, \qquad (7)$$

с което първата подзадача е решена.

Методът за хаотична синхронизация с линейно-нелинейна декомпозиция само осигурява линейността на системата от разсъгласуването, без да може да повлияе върху знака на собствените стойности на матрицата **A**. Така за даден модел на хаотична система при прилагането на този метод матрицата **A** може да има положителна собствена стойност и между системите да не може да възникне синхронизация, а при прилагането на метода за друг модел на хаотична система матрицата **A** може да има собствени стойности, които да отговарят на условието за един от трите типа синхронизация, описани по-горе.

Ако методът за хаотична синхронизация с линейно-нелинейна декомпозиция (5), (6) се съчетае с допълнителен управляващ сигнал към подчинената система [3] от типа:

$$\dot{\tilde{\mathbf{x}}} = \mathbf{f}(\tilde{\mathbf{x}}, \mathbf{x}) = \mathbf{A}\tilde{\mathbf{x}} + \mathbf{h}(\mathbf{x}) + \mathbf{B}(\mathbf{x} - \tilde{\mathbf{x}}), \qquad (8)$$

където $\mathbf{B}_{n\times n}$ е матрица с константи, то системата от разсъгласуването ще се получи във вида:

$$\dot{\mathbf{e}} = \mathbf{A}\mathbf{x} - \mathbf{A}\tilde{\mathbf{x}} - \mathbf{B}(\mathbf{x} - \tilde{\mathbf{x}}) = (\mathbf{A} - \mathbf{B})\mathbf{e}. \qquad (9)$$

От (9) се вижда, че при прилагането на допълнителното управление към подчинената система се запазва линейността на системата от разсъгласуването. В същото време чрез подходящ избор на ненулевите елементи на допълнителната матрица **B** може да се реши и подзадача 2, така че според избраните и получени чрез матрицата **B** собствени стойности на системата от разсъгласуването да се получи желания тип синхронизация между хаотичните системи. Този подход ще бъде илюстриран с помощта на модел на хаотична система от трети ред.

### 3. Синтез на синхронизационни схеми с идентична, изместена и осцилираща синхронизация за модел на Wu-Li

В [4] е предложен модел на хаотична система от трети ред с един нелинеен елемент, който се описва с уравненията:

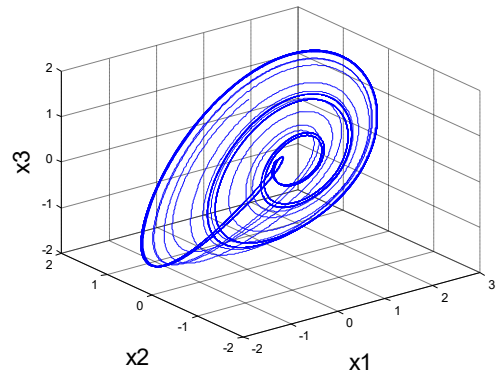
$$\begin{aligned} \dot{x}_1 &= -ax_2, \\ \dot{x}_2 &= x_3 / a, \\ \dot{x}_3 &= cx_1^2 - ax_2 - bx_3 - d, \end{aligned} \qquad (10)$$

където номиналните стойности на параметрите на системата са: $a = 1.2$, $b = 0.3$, $c = 0.3$, $d = 0.4$.

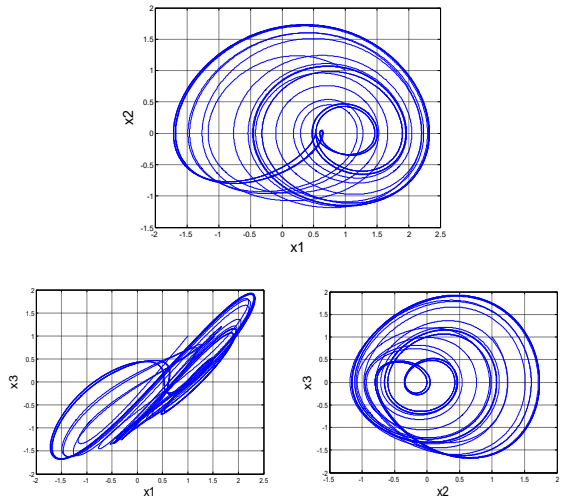
Моделът (10), известен като модел на Wu-Li, представлява един от най-простите модели на хаотични системи. При симулация на модела в MATLAB (Simulink) с начални условия: $x_1(0) = 1$, $x_2(0) = 1$, $x_3(0) = 1$, избрани произволно, се получава типичен хаотичен атрактор, показан в пространството на състоянието на Фиг. 1.

На Фиг. 2 са показани проекциите на хаотичния атрактор в трите фазови равнини: $(x_2, x_1)$, $(x_3, x_1)$ и $(x_3, x_2)$. Вижда се, че въпреки че моделът (10) на пръв поглед е съвсем елементарен и има само една квадратична нелинейност в третото уравнение, неговата

динамика се характеризира с висока сложност и атракторът му е типичен за хаотичните системи – голям брой орбити, разположени нагъсто в ограничена геометрична област в пространството на състоянието.




***Фиг. 1.*** *Атрактор на системата Wu-Li*




***Фиг. 2.*** *Проекции на хаотичния атрактор във фазовите равнини*

Нека моделът (10) се приеме за управляваща система в хаотична синхронизационна система. Тъй като моделът на Wu-Li съдържа само една нелинейност, синтезът на хаотична синхронизационна схема между два модела на Wu-Li по метода на линейно-нелинейната декомпозиция (5),(6) предполага максимално „икономична" връзка между управляващата и подчинената системи, като втората е:

$$\begin{aligned} \dot{\tilde{x}}_1 &= -a\tilde{x}_2, \\ \dot{\tilde{x}}_2 &= \tilde{x}_3 / a, \\ \dot{\tilde{x}}_3 &= cx_1^2 - a\tilde{x}_2 - b\tilde{x}_3 - d, \end{aligned} \tag{11}$$

т.е. връзката между системите (10) и (11) е само при нелинейния елемент на системата, където на мястото на първата променлива на подчинената система (11) се въвежда съответната променлива на управляващата система (10).

Системата от разсъгласуването, която се получава при изваждане на уравненията на системата (11) от тези на системата (10) с отчитане, че $e_i = x_i - \tilde{x}_i$, е:

$$\begin{aligned} \dot{e}_1 &= -ae_2, \\ \dot{e}_2 &= e_3 / a, \\ \dot{e}_3 &= -ae_2 - be_3, \end{aligned} \tag{12}$$

т.е. това е линейна система от вида (7) с матрица на състоянието:

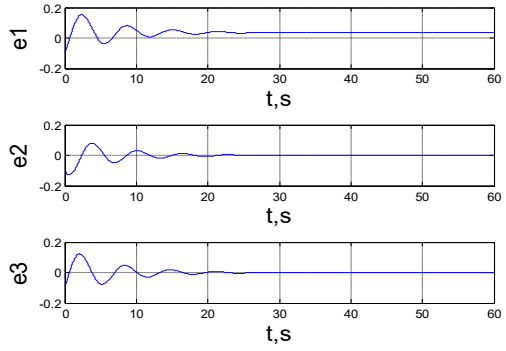
$$\mathbf{A} = \begin{bmatrix} 0 & -a & 0 \\ 0 & 0 & 1/a \\ 0 & -a & -b \end{bmatrix}. \tag{13}$$

Собствените стойности на матрицата (13) за номиналните стойности на параметрите, дадени по-горе, са:

$$\lambda_1 = 0,\ \lambda_{2,3} = -0.15 \pm 0.99\,j. \tag{14}$$

Тъй като едната собствена стойност на **A** е равна на нула, а другите две са с отрицателни реални части, се изпълнява условието за възникване на изместена хаотична синхронизация между управляващата и подчинената системи.

Функциите на разсъгласуване $e_i = x_i - \tilde{x}_i,\ i = 1 \div 3$, получени при симулация на хаотичната синхронизационна система (10), (11) в MATLAB (Simulink) за начални условия: $x_1(0) = 1$, $x_2(0) = 1$, $x_3(0) = 1$ за управляващата система и $\tilde{x}_1(0) = 1.1$, $\tilde{x}_2(0) = 1.1$, $\tilde{x}_3(0) = 1.1$ за подчинената система, са показани на Фиг. 3.

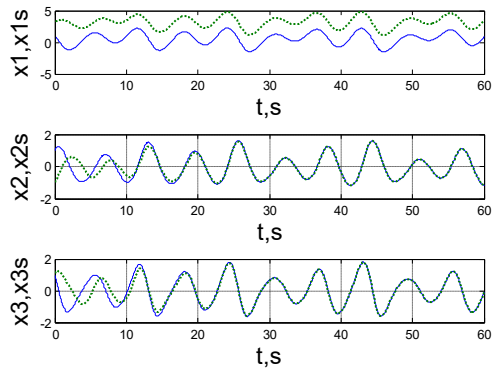



***Фиг. 3.*** *Функции $e_i(t)$ при изместена синхронизация*

Функцията $e_1(t)$ след преходен процес с продължителност от 20 s се установява на ниво 0.036. Функциите $e_2(t)$ и $e_3(t)$ след същия по продължителност преходен процес са

установяват в нула. Опитно е установено, че нивото, на което се установява функцията $e_1(t)$ зависи от началните условия $x_1(0)$ и $\tilde{x}_1(0)$, т.е. чрез избор на различни начални условия за първите променливи на двете системи може да се осигури различно изместване между $x_1(t)$ и $\tilde{x}_1(t)$.

На Фиг. 4 е показана съвместната динамика на променливите на управляващата и на подчинената системи $x_i, \tilde{x}_i$, $i = 1 \div 3$. На фигурата ясно се вижда, че след края на преходния процес динамиката на $\tilde{x}_1(t)$ повтаря хаотичния процес $x_1(t)$, но с константно изместване.




***Фиг. 4.*** *Съвместна динамика на променливите на двете системи*

Докато при модела на Wu-Li прилагането на метода за хаотична синхронизация с линейно-нелинейна декомпозиция директно осигурява получаването на изместена синхронизация, за получаването на идентична или осцилираща синхронизация е необходимо проектиране и на допълнително управление от вида (8).

Ако целта е получаване на идентична синхронизация между двете системи на Wu-Li, трябва да се синтезира такова допълнително управление към подчинената система от вида $\mathbf{B}(\mathbf{x}-\tilde{\mathbf{x}})$, че всички собствени стойности на матрицата на състоянието на системата от разсъгласуването да станат с отрицателни реални части. Анализът на базовата матрица на състоянието (13) показва, че собствената стойност $\lambda_1$ е равна на елемента $\mathbf{A}(1,1)$, тъй като останалите елементи в първия стълб на матрицата са равни на нула. Тогава ако този елемент не е нула, както е в (13), а например -2, то собствената стойност $\lambda_1$ също ще бъде равна на -2, а $\lambda_2$ и $\lambda_3$ няма да се променят.

Тогава матрицата **B** може да се избере във вида:

$$\mathbf{B} = \begin{bmatrix} b_{11} & 0 & 0 \\ 0 & 0 & 0 \\ 0 & 0 & 0 \end{bmatrix}, \qquad (15)$$

което съответства на следната подчинена система с допълнително управление:

$$\begin{aligned} \dot{\tilde{x}}_1 &= -a\tilde{x}_2 + b_{11}(x_1 - \tilde{x}_1), \\ \dot{\tilde{x}}_2 &= \tilde{x}_3 / a, \\ \dot{\tilde{x}}_3 &= cx_1^2 - a\tilde{x}_2 - b\tilde{x}_3 - d. \end{aligned} \qquad (16)$$

Системата от разсъгласуването и матрицата на състоянието й $\mathbf{A}-\mathbf{B}$ са съответно:

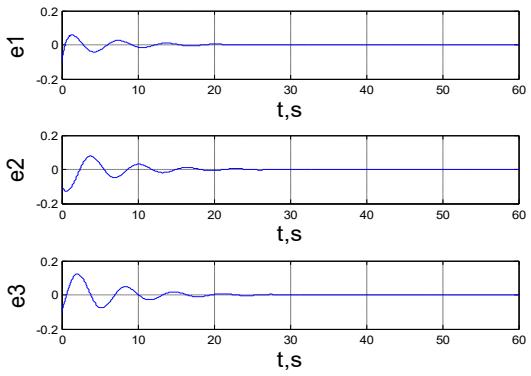
$$\begin{aligned} \dot{e}_1 &= -ae_2 - b_{11}e_1, \\ \dot{e}_2 &= e_3 / a, \\ \dot{e}_3 &= -ae_2 - be_3, \end{aligned} \qquad (17)$$

$$\mathbf{A}-\mathbf{B} = \begin{bmatrix} -b_{11} & -a & 0 \\ 0 & 0 & 1/a \\ 0 & -a & -b \end{bmatrix}. \qquad (18)$$

Собствените стойности на матрицата (18) за номиналните стойности на параметрите, и за $b_{11} = 2$, са:

$$\lambda_1 = -2, \ \lambda_{2,3} = -0.15 \pm 0.99\, j. \qquad (19)$$

Така с помощта на допълнителния управляващ сигнал към първото уравнение на подчинената система се осигурява изпълнението на условието за получаване на идентична синхронизация между хаотичните системи. Функциите $e_i = x_i - \tilde{x}_i$, получени при симулация на хаотичната синхронизационна система (10), (16) в са показани на Фиг. 5, като и трите се установяват в нула, което съответства на идентична синхронизация.




***Фиг. 5.*** *Функции $e_i(t)$ при идентична синхронизация*

Ако целта е получаване на осцилираща синхронизация между двете системи на Wu-Li, допълнителното управление към подчинената система трябва да е такова, че една от собствените стойности на матрицата на състоянието на системата от разсъгласуването да е отрицателна реална, а другите две да са комплексно спрегнати с нулева реална част. Анализът на базовата матрица на състоянието (13) показва, че собствените стойности $\lambda_2$ и $\lambda_3$ ще отговарят на горното условие, ако елементът $\mathbf{A}(2,2)$ е равен по модул и с обратен знак на елемента $\mathbf{A}(3,3)$. Тогава ако матрицата **B**, определяща допълнителното управление се избере във вида:

$$\mathbf{B} = \begin{bmatrix} b_{11} & 0 & 0 \\ 0 & b_{22} & 0 \\ 0 & 0 & 0 \end{bmatrix}, \qquad (20)$$

което съответства на следната подчинена система с допълнително управление:

$$\begin{aligned} \dot{\tilde{x}}_1 &= -a\tilde{x}_2 + b_{11}(x_1 - \tilde{x}_1), \\ \dot{\tilde{x}}_2 &= \tilde{x}_3 / a + b_{22}(x_2 - \tilde{x}_2), \\ \dot{\tilde{x}}_3 &= cx_1^2 - a\tilde{x}_2 - b\tilde{x}_3 - d, \end{aligned} \qquad (21)$$

системата от разсъгласуването и матрицата на състоянието ѝ $\mathbf{A}-\mathbf{B}$ ще бъдат съответно:

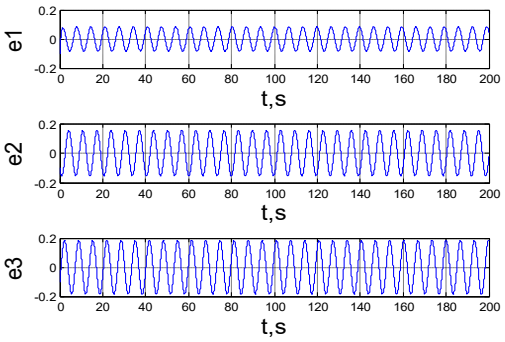
$$\begin{aligned} \dot{e}_1 &= -ae_2 - b_{11}e_1, \\ \dot{e}_2 &= e_3 / a - b_{22}e_2, \\ \dot{e}_3 &= -ae_2 - be_3, \end{aligned} \qquad (22)$$

$$\mathbf{A}-\mathbf{B} = \begin{bmatrix} -b_{11} & -a & 0 \\ 0 & -b_{22} & 1/a \\ 0 & -a & -b \end{bmatrix}. \qquad (23)$$

Собствените стойности на матрицата (23) за номиналните стойности на параметрите, за $b_{11} = 2$, и за $b_{22} = -b = -0.3$, са:

$$\lambda_1 = -2,\ \lambda_{2,3} = 0 \pm 0.95j, \qquad (24)$$

с което условието за възникване на осцилираща синхронизация между системите е изпълнено. Функциите $e_i = x_i - \tilde{x}_i$, получени при симулация на хаотичната синхронизационна система (10), (21) и показани на Фиг. 6, потвърждават наличието на осцилираща синхронизация.




***Фиг. 6.*** *Функции $e_i(t)$ при осцилираща синхронизация*

## 4. Заключение

Чрез представения в доклада подход за синтез на управление към подчинената хаотична система може да се получи желан тип синхронизирано движение за произволен модел на хаотична система. При системата на Wu-Li както схемата с изместена, така и тази с идентична синхронизация са с връзка между системите само по една променлива, т.е. връзката е максимално икономична.

## ЛИТЕРАТУРА

1. Krawiecki, A. *et.al.* (2000). Generalizations of the concept of marginal synchronization of chaos. *Chaos, Sol. & Fract.* vol.11, pp.1445-1458.
2. Yu, H., L. Yanzhu (2003). Chaotic synchronization based on stability criterion of linear systems, *Physics Letters A*, vol.314/4, pp.292-298.
3. Chantov, D. (2008). Modified linear-nonlinear decomposition method for chaotic synchronization. *Physics Letters A*, vol.372/36, pp.5783-5789.
4. Wu, Q., T. Li (2014). Analysis, circuit implementation and synchronization of a new chaotic system. *Proc. of the 33rd Chinese Control Conf.* 28-30.07.2014, Nanjing, China, pp.6070-6073.

Контакти
Адрес: катедра “Автоматика, информационна и управляваща техника”, Технически университет – Габрово, 5300 Габрово, ул.”Хаджи Димитър” No 4.
E-mail: dchantov@abv.bg
E-mail: hsstoycheva@abv.bg

© International Scientific Conference on Engineering, Technologies and Systems
TECHSYS 2016, Technical University – Sofia, Plovdiv branch
26 – 28 May 2016, Plovdiv, Bulgaria

# АВТОМАТИЧНО РЕГУЛИРАНЕ НА ПОСТОЯННОТОКОВО ЕЛЕКТРОЗАДВИЖВАНЕ С ПРЕОБРАЗУВАТЕЛ С ФАЗОВО УПРАВЛЕНИЕ

ДИМИТЪР СПИРОВ, ГЕОРГИ ТЕРЗИЙСКИ

**Резюме:** *Разработена и изследвана е система за фазово управление на постояннотокова машина с независимо възбуждане със затворен контур за управление на скоростта и подчинен контур за упраление на котвения ток. Захранването на постояннотоковата машина става от трифазен регулируем тиристорен изправител. Проектирани са регулатори за двата контура на регулиране, при удовлетворяване на зададените показатели. Получената система е моделирана в средата на Matlab/Simulink. Симулационните изследвания потвърждават работоспособността на разработения алгоритъм.*

**Ключови думи:** *постояннотокова машина, система за фазово управление, автоматично регулиране на координатите*

# CLOSED-LOOP PHASE CONTROLLED DC MOTOR DRIVE

DIMITAR SPIROV, GEORGI TERZIYSKI

**Abstract:** *A closed-loop phase-controlled dc motor drive with current and speed controllers is developed and investigated. A three-phase thyristor-controlled converter controls a dc motor. The design of the current and speed controllers is presented. The proposed drive system is modeled and its performance is simulated in Matlab/Simulink. The analysis presented is validated experimentally.*

**Key words:** *dc machine, phase-controlled system, closed-loop control*

## 1. Основни положения

Двигателите за постоянен ток с независимо възбуждане се използват за задвижване на много работни машини, които изискват плавно регулиране на скоростта в широк диапазон [1]. Двигателите със смесено и последователно възбуждане по правило се използват в отворените системи за електрозадвижване. Двигателите с независимо възбуждане са основа на затворените системи на регулируемите електрозадвижвания и се използват широко в тиристорни електрозадвижвания за постоянен ток.

При проектирането на затворените системи за управление с постояннотоков двигател основната задача е настройката на регулаторите, така че да удовлетворяват зададените показатели при регулиране на координатите на електрозадвижването, определени от технологичните изисквания [2, 3, 4].

При анализа на динамични системи от трети и по-висок ред определянето на зависимостите между показателите на качеството и параметрите на системата е значително по-сложно. Един от възможните варианти за решение на поставената задача е чрез използването на диаграмата на Вишнеградски [5]. Предложената диаграма дава възможност да се съди не само за устойчивостта, но и за някои основни показатели на качеството.

Други възможни варианти за решение на поставената задача е чрез използването на първи

Copyright © 2016 by Technical University of Sofia, Plovdiv branch, Bulgaria ISSN Online: 2535-0048

метод на Циглер и Николс, номограмите на Копелович и номограми дадени в [6]. Това са експресни методи за определяне на параметрите за настройка на регулатори по известни данни за преходната характеристика на обекта за управление [6].

Цел на настоящата работа е да се проектира затворена система за автоматично управление на постояннотокова машина с независимо възбуждане, захранвана от тиристорен регулируем изправител. Необходимо е да се изчислят коефицентите на регулаторите, така че да се удовлетворяват зададените показатели при регулиране на координатите на електрозадвижването.

## 2. Математически модели

Разработването на математическите модели и изследванията се извършват при общоприетите допускания и означения [7]. Системата уравнения, описваща електромеханичното преобразуване на енергията в постояннотоковата машина с независимо възбуждане се записва в следния вид:

$$u_a = e_a + R_a i_a + L_a \frac{di_a}{dt}; \qquad (1)$$

$$J_m \frac{d\omega_m}{dt} + B_l \omega_m = M_e - M_c. \qquad (2)$$

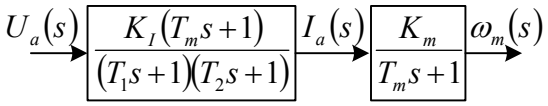
Където $J_m$ – инерционен момент на системата;

$B_l$ – коефициент на триене;

$M_e=K_{MФ}i_a$ – електромагнитен момент, $K_{MФ}=K_M Ф$ при $Ф=const.;$

$M_c=B_c\omega_m$ – съпротивителен момент на механизма, зависещ от $\omega_m$ с коефициент $B_c$.

На базата на този модел е получена структурната схема на постояннотоковата машина в операторен вид.




***Фиг. 1.*** *Структурна схема на постояннотоковата машина*

На фиг. 1 са въведени коефициентите $K_I=(B_l+B_c)/(k_1^2+R_a(B_l+B_c))$; $T_m=J_m/(B_l+B_c)$; $T_a=L_a/R_a$; $K_m=K_{MФ}/(B_l+B_c)$; $T_1=-1/\lambda_1$; $T_2=-1/\lambda_2$;

$$\lambda_1,\lambda_2 = -\frac{1}{2}\left(\frac{1}{T_m}+\frac{1}{T_a}\right) \pm \sqrt{\frac{1}{4}\left(\frac{1}{T_m}+\frac{1}{T_a}\right)^2 - \frac{k_1^2 + R_a(B_l+B_c)}{J_m L_a}};$$

Захранването на машината става от регулируем тиристорен изправител с предавателна функция:

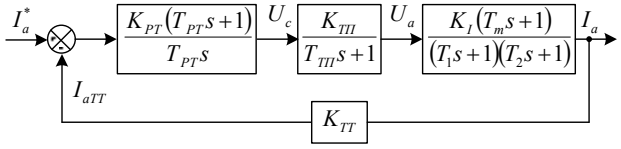
$$W_{TП}(s) = \frac{K_{TП}}{T_{TП}s+1}. \qquad (3)$$

Където $K_{TП}=3U_m/(\pi U_{cm})=1{,}35U/U_{cm}$; $U_{cm}$ – максимална стойност на управляващото напрежение $U_c$; $T_{TП}=(\alpha_T/2)/(360f_s)$, където $\alpha_T$ – ъгъл на отпушване между 2 тиристора, $f_s$ – честота на захранващата мрежа. Изходното постоянно напрежение може да се определи с израза [7]:

$U_a=3U_m\cos\alpha/\pi=1{,}35U\cos(\cos^{-1}(U_c/U_{cm}))$.

В системата за управление са въведени обратни връзки по ток и по скорост съответно чрез датчик на ток (токов трансдюсер) с предавателна функция $W_{TI}(s)=K_{TT}$ и датчик на скорост (тахогенератор) с предавателна функция $W_{TT}(s)=K_{TГ}$. На база на получената система е избран регулатор на ток с ПИ закон на регулиране и регулатор на скорост с ПИ закон на регулиране. Ограничението на зададената стойност на регулатора на ток се осъществява от лимитер.

На фиг. 2 е представен токовия контур на затворената система за управление на машината.




***Фиг. 2.*** *Структурна схема на токовия контур*

Предавателната функция на затворения токов контур е представена с изразра:

$$W_I(s) = \left(\frac{K_I K_{TT} K_{TП} K_{PT}}{T_{PT}}\right) \frac{(T_{PT}s+1)(T_m s+1)}{s(T_1 s+1)(T_2 s+1)(T_{TП}s+1)}. \qquad (4)$$

Ако приемем, че $(T_m s+1)\approx T_m s$ и $K=K_I K_{TT} K_{TП} K_{PT} T_m/T_{PT}$ и $T_{PT}=T_2$ получаваме предавателната функция в следния вид:

$$W_I(s) \approx \frac{K}{(T_1 s+1)(T_{TП}s+1)}. \qquad (5)$$

Характеристичното уравнение или знаменателя на предавателната функция приема вида:

$$H_I(s) = T_1 T_{TП} s^2 + (T_1 + T_{TП})s + K + 1. \qquad (6)$$

За да получим уравнението в стандартна форма разделяме двете страни на $K+1$:

$$H_{IC}(s)=\frac{T_1T_{TП}}{K+1}s^2+\frac{T_1+T_{TП}}{K+1}s+1. \qquad (7)$$

Получената система е от втори ред и се характеризира със свойствата на колебателно звено с времеконстанта на колебателното звено $T_0$ и коефицент на затихване $\xi$, представено със следния израз [8]:

$$H_{КЗ}(s)=T_0^2s^2+2\xi T_0s+1. \qquad (8)$$

Като приравним членовете пред различните степени на $s$, получаваме изрази за $T_0$ и $K$ във функция от коефициента на затихване $\xi$:

$$T_0=\frac{2\xi T_1T_{TП}}{T_1+T_{TП}}; \qquad (9)$$

$$K=\frac{(T_1+T_{TП})^2}{4\xi^2T_1T_{TП}}-1. \qquad (10)$$

За $K_{PT}$ получаваме израз, като заместим $K$ в (10):

$$K_{PT}=\frac{T_{PT}}{K_IK_{TT}K_{TП}T_m}\left[\frac{(T_1+T_{TП})^2}{4\xi^2T_1T_{TП}}-1\right]. \qquad (11)$$

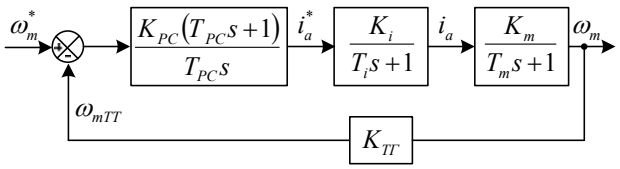
За избора на параметрите на регулатора на скорост токовия контур се представя с апроксимационен модел от първи ред [7]:

$$\frac{I_a(s)}{I_a^*(s)}=\frac{K_i}{T_is+1}, \qquad (12)$$

където:

$$K_i=\frac{K_{PT}K_{TП}K_IT_m}{T_{PT}+K_{PT}K_{TП}K_IT_mK_{TT}};$$

$$T_i=\frac{T_{PT}(T_1+T_{TП})}{T_{PT}+K_{PT}K_{TП}K_IT_mK_{TT}}.$$




***Фиг. 3.*** *Структурна схема на контура за регулиране на скоростта*

На фиг. 3 е представен контура за регулиране на скоростта на затворената система за управление на машината.

Предавателната функция на затворения контур за регулиране на скоростта е представена с израза:

$$W_\omega(s)=\left(\frac{K_{PC}K_iK_{MФ}K_{TT}}{T_{PC}(B_l+B_c)}\right)\frac{(T_{PC}s+1)}{s(T_is+1)(T_ms+1)}. \qquad (13)$$

Характеристичното уравнение или знаменателя на предавателната функция приема вида

$$H_\omega(s)=T_iT_mT_{PC}s^3+T_{PC}(T_i+T_m)s^2+ \\ +T_{PC}(K_mK_{PC}+1)s+K_mK_{PC}, \qquad (14)$$

където $K_m=K_iK_{TT}K_{MФ}/(B_l+B_c)$.

За да получим уравнението в стандартна форма разделяме двете страни на $K_mK_{PC}$:

$$H_\omega(s)=\frac{T_iT_mT_{PC}}{K_mK_{PC}}s^3+\frac{T_{PC}(T_i+T_m)}{K_mK_{PC}}s^2+ \\ +\frac{T_{PC}(K_mK_{PC}+1)}{K_mK_{PC}}s+1. \qquad (15)$$

Получената система е от трети ред и се характеризира със свойствата на последователно свързани колебателно и апереодично звена с времеконстанта $T_0$ и коефицент на затихване $\xi$, представени със следния израз [8]:

$$H_{КАЗ}(s)=T_0^3s^3+T_0^2(2\xi+1)s^2+ \\ +T_0(2\xi+1)s+1 \qquad (16)$$

Като приравним членовете пред различните степени на $s$, получаваме изрази за $T_0$, $K_{PC}$ и $T_{PC}$ във функция от коефициента на затихване $\xi$:

$$T_0=\frac{(2\xi+1)T_mT_i}{T_m+T_i}\sqrt[3]{\frac{(T_m+T_i)^2+(2\xi+1)T_mT_i}{(T_m+T_i)^2-(2\xi+1)T_mT_i}}; \qquad (17)$$

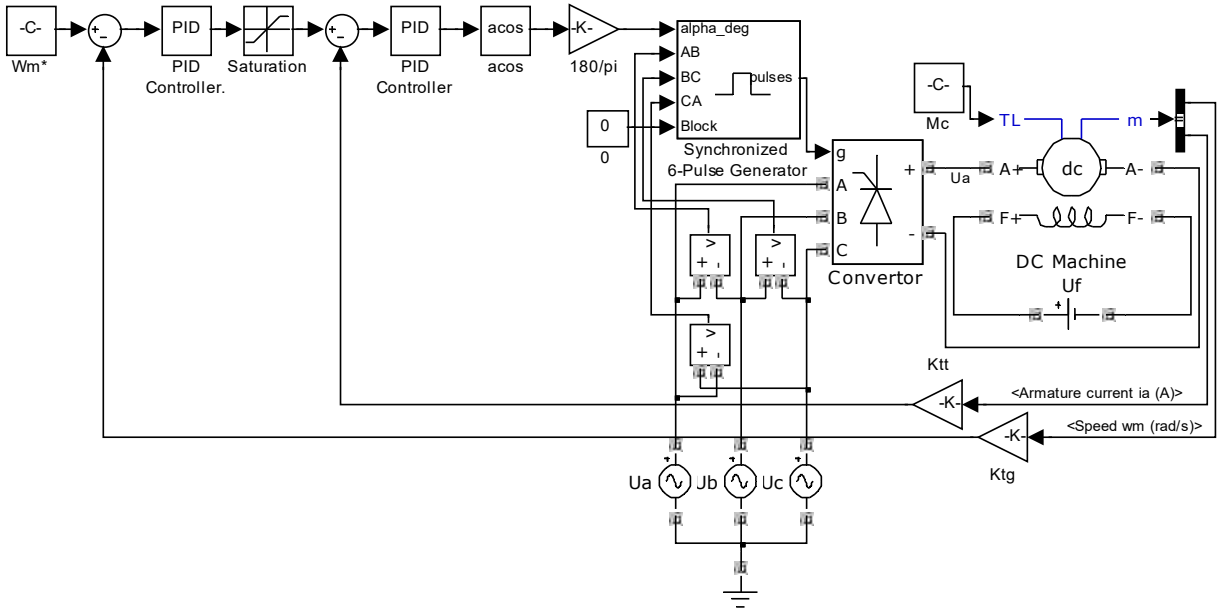
$$K_{PC}=\frac{(T_m+T_i)^2}{(2\xi+1)T_mT_iK_m}-\frac{1}{K_m}; \qquad (18)$$

$$T_{PC}=\frac{(2\xi+1)T_mT_i}{T_m+T_i}+\frac{(2\xi+1)^3T_m^2T_i^2}{(T_m+T_i)^3} \qquad (19)$$

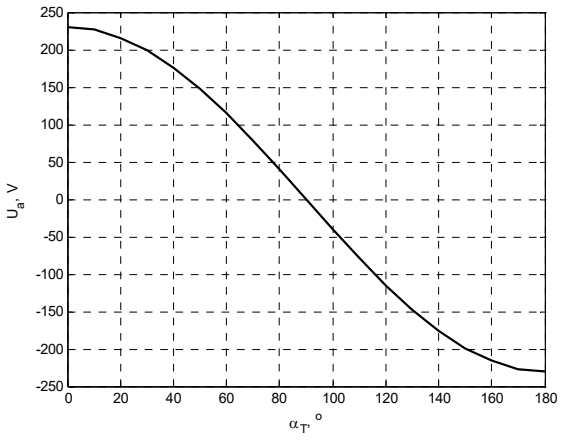
### 3. Симулационни резултати

Изследванията са проведени с постояннотоково електрозадвижване симулирано в средата на Matlab/Simulink. На фиг. 4 е представена симулационната схема на разработената система. Схемата съдържа постояннотоков двигател с независимо възбуждане тип П22-01 У4 с номинални данни 0,6kW, 230V, който задвижва механизъм с константен товар $M_c=M_n$. Постояннотоковата машина е симулирана чрез вградения в приложението „Sim-power system" на Matlab/Simulink модел „DC Machine". Техническите данни и параметри на машината са дадени в Приложение.

Постояннотоковата машина е захранена от трифазен регулируем тиристорен изправител „Universal Bridge", чиито управляващи импулси се формират от блока „Synchronized 6-Pulse Generator", моделирани в същото приложение на Matlab/Simulink. На входа на последния блок постъпва ъгъла на отпушване на тиристорите $\alpha_T$, който се формира от управляващото напрежение по израза $\alpha_T=cos^{-1}(U_c/U_{cm})$. Максималната стойност на изходното напрежение $U_{cm}=U_a$=230V се получава при $\alpha_T$=0˚, при $\alpha_T$=90˚, $U_a$=0V, а при $\alpha_T$=180˚, $U_a$=−230V. Характеристиката $U_a=f(\alpha_T)$ е представена на фиг. 5. Предавателния коефициент на токовия трансдюсер е $K_{TT}$=0,333, а предавателния коефициент на тахогенератора $K_{TI}$=0,549.




***Фиг. 4.*** *Симулационна схема на постояннотоково електрозадвижване*




***Фиг. 5.*** *Зависимост на $U_a=f(\alpha_T)$*

Параметрите на регулаторите са изчислени по изрази (11), (18) и (19) за $\xi$=0,99. Получените коефициенти са систематизирани в таблица 1.

Проведени са симулационни изследвания на получената система при задание на скоростта съответно $\omega_m^*$=(0,1; 0,5; 1)$\omega_{mn}$, и ограничение по ток $I_{am}$=(1,2; 1,5; 2)$I_{an}$.

***Таблица 1.*** *Изчислени коефициенти при $\xi$=0,99*

| | | | |
|---|---|---|---|
| Регулатор на ток | $T_0$ | $K_{PT}$ | $T_{PT}$ |
| | 0,0033 | 132,5 | 0,0279 |
| Регулатор на скорост | $T_0$ | $K_{PC}$ | $T_{PC}$ |
| | 0,0193 | 0,522 | 0,0202 |

В таблица 2 са систематизирани резултатите за пререгулирането $\Delta\omega_{m.max}^{*}=\Delta\omega_{m.max}/\omega_{m.ycm}$ за разглежданите случаи.

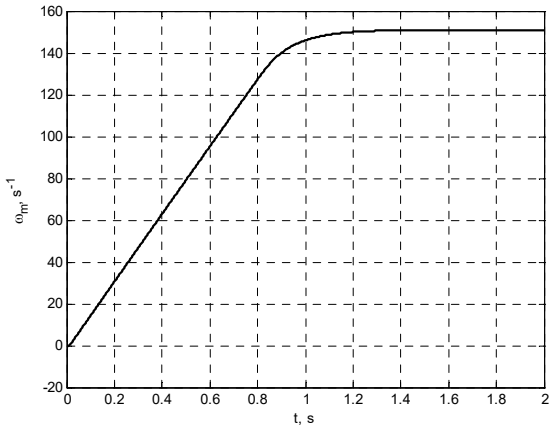
***Таблица 2.*** *Пререгулиране $\Delta\omega_{m.max}^{*}$ за разглежданите случаи*

| $I_{am}/I_{an}$ / $\omega_m^{*}/\omega_{mn}$ | 1,2 | 1,5 | 2 |
|---|---|---|---|
| 0,1 | 2,06 | 2,02 | 1,96 |
| 0,5 | 1,97 | 1,95 | 1,90 |
| 1 | 1,00 | 1,00 | 1,00 |

В таблица 3 са систематизирани резултатите за времето на преходния процес $t_{ПП}$ [$s$] за разглежданите случаи. За сравнение при директното пускане на двигателя, времето за пускане $t_{ПП}$=0,67s. Максималната стойност на пусковия ток $I_{a.max}$=17,69A=6,76$I_{an}$.

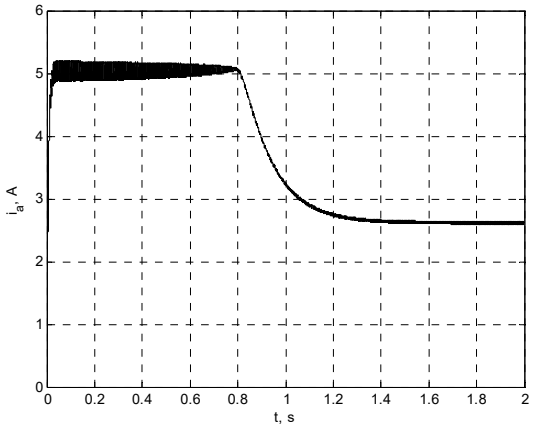
***Таблица 3.*** *Време на преходния процес $t_{ПП}$ [s] за разглежданите случаи*

| $I_{am}/I_{an}$ / $\omega_m^{*}/\omega_{mn}$ | 1,2 | 1,5 | 2 |
|---|---|---|---|
| 0,1 | 2,74 | 0,90 | 0,47 |
| 0,5 | 30,37 | 9,26 | 3,94 |
| 1 | 8,13 | 2,79 | 1,24 |

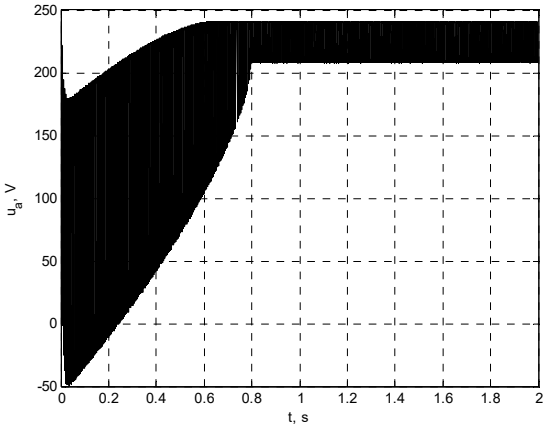



***Фиг. 6.*** *Зависимост на $\omega_m=f(t)$*

От таблица 2 се вижда, че пререгулирането $\Delta\omega_{m.max}^{*}$=1, зададено при проектирането на регулаторите чрез избора на коефициента на затихване $\xi$=0,99 се изпълнява само при задание на ъгловта скорост $\omega_m^{*}=\omega_{mn}$. При скорости под номиналната, максималната стойност на скоростта се увеличава повече от 2 пъти.




***Фиг. 7.*** *Зависимост на $i_a=f(t)$*




***Фиг. 8.*** *Зависимост на $u_a=f(t)$*

От таблица 3 се вижда, че ограничението на максималната стойност на котвения ток $I_a=I_{am}$ и конструктивното ограничение на максималната стойност на котвеното напрежение $U_a=U_{an}$ довеждат до увеличаване на времето на преходния процес при пускане до 12,13 пъти при $I_{am}/I_{an}$=1,2 и до 1,85 пъти при $I_{am}/I_{an}$=2 при задание за ъгловата скорост $\omega_m^{*}=\omega_{mn}$.

### 4. Заключение

В настоящия доклад е разработена и изследвана система за фазово управление на постояннотокова машина с независимо възбуждане със затворен контур за управление на скоростта и подчинен контур за упраление на котвения ток. В резултат от анализа на динамичната система са получени изрази за изчисляване на параметрите за настройка на ПИ-регулаторите на ток и на скорост. Изследванията, проведени със симулационния модел, разработен в средата на Matlab/Simulink, потвърждават работоспособността на разработения алгоритъм.

## ЛИТЕРАТУРА


1. Ключев, В. (1989). *Теория на електрозадвижването*, 544 с. ДИ „Техника”, София.
2. Singh, R., Pandey, A. K., Tech, M. (2012). Closed loop speed control of SEDC motor using three phase fully controlled bridge rectifier with inner current loop. *IJAET*, Vol. 3, Issue 2, pp. 559-567.
3. Pal, P., Dey, R., Biswas, R. K., Bhakta, S. (2015). Optimal PID controller design for speed control of a separately excited dc motor: a firefly based optimization approach. *IJSCMC*, Vol. 4, No. 4, pp. 39-48.
4. Dey, S., Malakar, S., Panda, M. (2014). Design of Optimized Speed Controller of DC Motor Using Chopper. *IJSER*, Vol. 3, Issue 6, pp. 32-38.
5. Наплатанов, Н. (1976). *Теория на автоматичното регулиране – том 1, Линейни системи*, ДИ „Техника”, София.
6. Хинов, Х. и др. (1978). *Автоматизация на производството – част 2. Автоматизация на технологични процеси*, ДИ „Техника”, София.
7. Krishnan, R. (2001). *Electric motor drives: modeling, analysis, and control*, Prentice Hall, New Jersey.
8. Драготинов, И., Ганчев, И. (2008). *Автоматизация на технологичните процеси*, УХТ - Пловдив.


## ПРИЛОЖЕНИЕ

Технически данни и параметри на постояннотоков електродвигател тип П22-01 У4:

$P_N$=0,6kW; $U_N$=230V; $U_f$=220V; $I_N$=2,61A; $n_N$=1450min$^{-1}$; $M_N$=3,34Nm $\eta$=75%; $J_m$=0,002kgm$^2$.

$R_a$=13Ω; $L_a$=0,297H; $R_f$=273,3Ω $L_f$=10,8H; $L_{af}$=1,61H.


Department of Electrical Engineering
University of Food Technologies – Plovdiv
26 Maritza Blvd.
4002 Plovdiv
BULGARIA
E-mail: dimitar_spirov@abv.bg
E-mail: georgi_terziyski@abv.bg

© International Scientific Conference on Engineering, Technologies and Systems
TECHSYS 2016, Technical University – Sofia, Plovdiv branch
26 – 28 May 2016, Plovdiv, Bulgaria

# DSP БАЗИРАНО АСИНХРОННО ЕЛЕКТРОЗАДВИЖВАНЕ С КВАЗИРЕЗОНАНСЕН ПРЕОБРАЗУВАТЕЛ

ДИМИТЪР СПИРОВ, НИКОЛАЙ КОМИТОВ

**Резюме:** *Разработено е DSP базирано асинхронно електрозадвижване с квазирезонансен преобразувател. За захранването на асинхронното електрозадвижване са използвани трифазен мостов инвертор и резонансна верига с три допълнителни ключа. Управлението на инвертора и резонансната верига става чрез развойната платка „TMS320C2000™ Experimenter Kit", изградена на базата на цифровия сигнален процесор (ЦСП) TMS320F2808, съвместим със Simulink®. Управляващата програма е разработена в Simulink®, а управляващите сигнали са подадени към инвертора чрез съгласуващата платка. Експерименталните резултати, получени с разработената система показват намаляване на загубите от превключване и повишаване на ефективността на асинхронното електрозадвижване.*

**Ключови думи:** *асинхронно електрозадвижване, квазирезонансен преобразувател*

# DSP BASED INDUCTION MOTOR DRIVE WITH QUASI-RESONANT CONVERTER

DIMITAR SPIROV, NIKOLAY KOMITOV

**Abstract:** *A DSP based induction motor drive with quasi-resonant converter is developed. The three-phase inverter bridge and resonant circuit switches are used for powering an induction motor drive. The „TMS320C2000™ Experimenter Kit" board built around the TMS320F2808 DSP controller is used to control the resonant circuit, inverter and motor. This platform is compatible with Simulink®, and includes six dual pulse PWM channels, 16 ADCs, and a speed encoder input. The control program is implemented in Simulink® and the switching signals are transferred to the inverter through an interface board. The experimental results show that a smaller switching loss and higher conversion efficiency are obtained by the proposed system.*

**Key words:** *induction motor drive, quasi-resonant converter*

## 1. Основни положения

Една от възможностите за подобряване на работоспособността и характеристиките както на захранващата схема, така и на товара е увеличаването на честотата на превключване на силовите преобразуватели. Повишаването на честотата на системите, захранвани от инвертор с широчинно-импулсна модулация (ШИМ) довежда до повишаване на загубите в силовите ключове и комутационни ударни натоварвания [1].

Създадени са множество схемни решения, които чрез един или друг метод осъществяват комутация при нулев ток и напрежение, но при ограничен диапазон на изменение на товара и за сметка на занижаване на к.п.д. при малки натоварвания [2].

Квазирезонансните инвертори се използват широко за захранване на асинхронни машини, въпреки техните недостатъци като наличието на високо напрежение в резонансната верига, което при някои от тях може да достигне до два пъти захранващото. При инверторите с паралелна резонансна верига и синхронизираните резонасни инвертори с постояннотокова връзка, "меката комутация" се

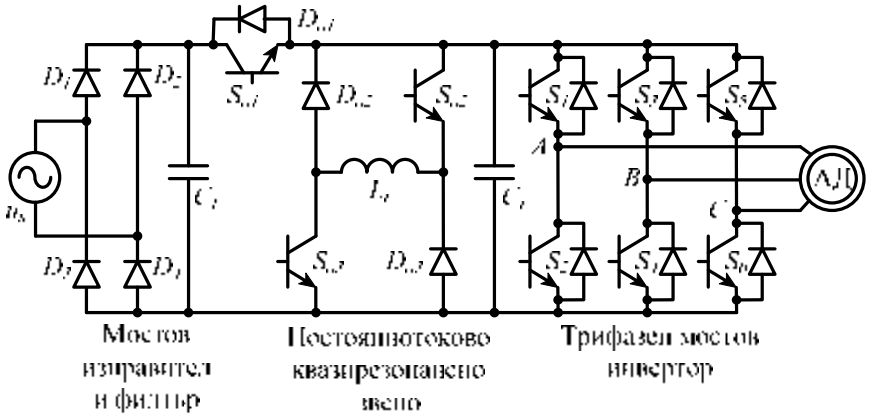
Copyright © 2016 by Technical University of Sofia, Plovdiv branch, Bulgaria ISSN Online: 2535-0048

осигурява от допълнителни ключове, чиито резонансни вериги са със сложни конфигурации и трудни за управление [3, 4]. Напрежението в резонансната верига достига до пикови стойности по-големи от захранващото напрежение, а тока през допълнителния ключ не достига нулеви стойности при установен режим, което води до увеличаване на загубите при провеждане. В [3] са разработени схеми за ШИМ, на базата на демпфери, които отстраняват до известна степен споменатите недостатъци. Разработените в [4] преобразуватели с "мека комутация" при включване при нулево напрежение изискват многократни преходи за постигане на желаното положение, освен това са необходими ограничителни диоди за да се избегне пренапрежение върху допълнителните резонансни ключове до нулирането на резонансния ток.

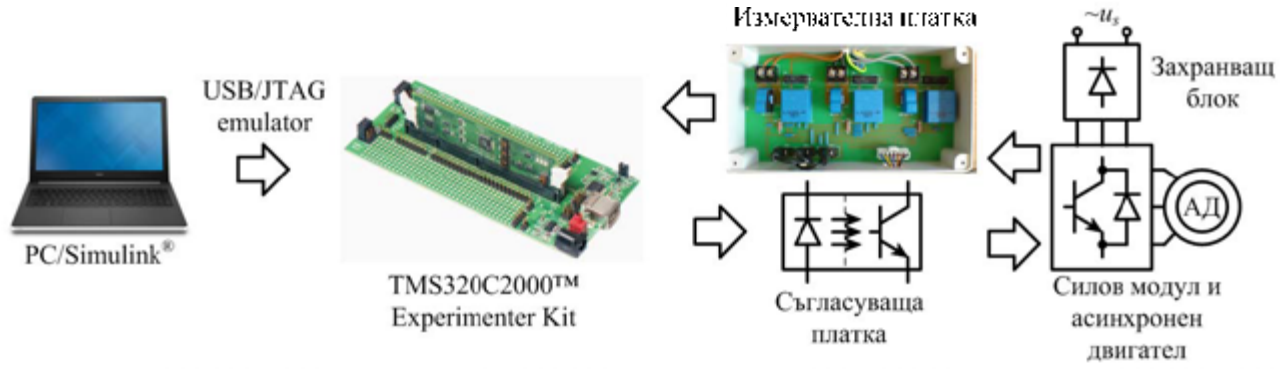
Целта на настоящия доклад е разработване и изследване на DSP базирано асинхронно електрозадвижване с квазирезонансен преобразувател. Необходимо е да се изследва ефективността и комутационните загуби на разработената система.

## 2. Управление на преобразувателя

Принципната схема на асинхронно електрозадвижване с паралелен квазирезонансен преобразувател с постояннотоково звено е представена на фиг.1 [5].




***Фиг. 1.*** *Принципна схема на квазирезонансен преобразувател*




***Фиг. 2.*** *Блок-схема на разработената система*

Схемата е захранена от монофазната мрежа $u_s$. Промелмивотоковото напрежение се изправя от диодния мостов изправител и се изглажда от филтровия кондензатор $C_f$. Допълнителното постояннотоково квазирезонансно звено (ДПКЗ) съдържа трите силови ключа $S_{a1}$, $S_{a2}$ и $S_{a3}$, трите диода $D_{a1}$, $D_{a2}$ и $D_{a3}$ и резонансните бобина и кондензатор $L_r$ и $C_r$. Трифазния мостов инвертор ($S_1$-$S_6$) осигурява трифазното напрежение за захранване на асинхронния двигател.

Импулсите за управление на силовите ключове се получават от управляващата платка „TMS320C2000™ Experimenter Kit". Платката „TMS320C2000™ Experimenter Kit" изпълнява функциите както на управляваща, така и на изчислителна платформа. Тази платка е изградена на базата на цифровия сигнален

процесор (ЦСП) TMS320F2808, съвместим със Simulink®, и включва шест двойки ШИМ канала (общо 12 канала), 16 аналого-цифрови преобразувателя (АЦП) и вход за енкодер за скорост. Процесора е 32-битов ЦСП с аритметика с фиксирана запетая, следователно могат да бъдат използвани блокове от Simulink® с дискретна математика и математика с фиксирана запетая.

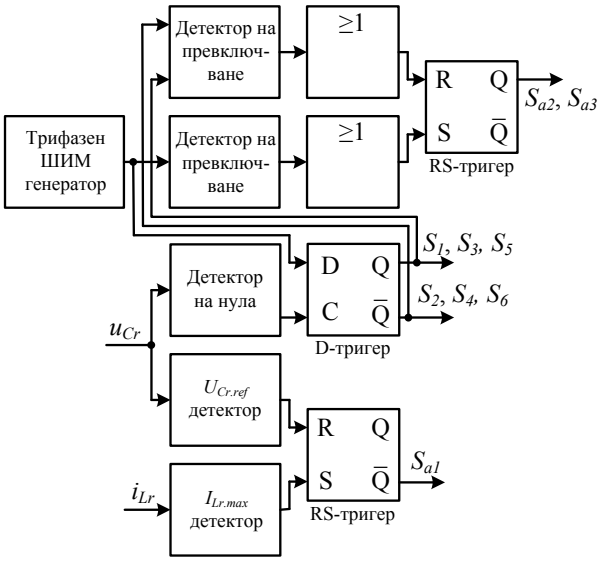
Както алгоритмите за управление, така и алгоритмите за изчислителната част използват информацията от сензорите за да осигурят необходимата обратна връзка. Информацията от директното измерване на напреженията и токовете чрез измервателната платка (фиг. 2) се използва от изчислителния алгоритъм на управляващата система. В токовата измервателна верига се използва токов тарнсдюсер, работещ на базата на ефекта на Hall тип LTS 15-NP. Грешката при измерване на токовия тарнсдюсер е под ± 0,2 % при 25 °C и честота до 100 kHz [6]. Трансдюсера използва еднополярно захранване +5V и може да измерва както постоянен, така и променлив ток. Изходната величина е повдигната на 2,5 V при нулев входен ток, което е половината от захранващото напрежение на трансдюсера. Максималната стойност от $0.625/I_{PN}$ ($I_{PN}$=15A) се получава при изходно напрежение, изчислено по израза $V_{out}=(0.625/I_{PN})I_P+2.5$.

В напрежителната измервателна верига се използва напреженов тарнсдюсер, работещ на базата на ефекта на Hall тип LV 25-P. Грешката при измерване на напрежителния тарнсдюсер е под ± 0,9 % при 25 °C [7]. Трансдюсера използва захранване ± 15V и може да измерва постоянно, променливо и импулсно напрежение. Максималната стойност се получава при изходно напрежение, изчислено по израза $V_{out}=0.01V_P$ ($V_{PN}$=400V).

Развойната платка „TMS320C2000™ Experimenter Kit" изисква напрежението на входовете на АЦП да са между 0 и 3 V. Изходът на АЦП е 12-битово цяло число с фиксирана запетая с обхват от 4095 при входен ток ± 12 A и входно напрежение ± 400 V максимална стойност.

В ЦСП е използвана математика с фиксирана запетая за осигуряване на максимална десетична точност. Библиотеката "Target for TI C2000" на Simulink разполага с модул "C28x IQmath" в който са поместени блокове с основни математически операции. Q стойността на IQ числото е бит пред който е поставена десетичната запетая.

Тъй като ЦСП F2808 е 32-битов с фиксирана запетая, типът данни, които се използват в Simulink-моделите са от вида "fixdt(1,32,19)" в Matlab номенклатурата, което отговаря на типа данни с фиксирана запетая. Диапазона на типа данни, посочен по-горе е от −4096 до 4095,9999980926514, а точността е $1{,}9073486328125\times10^{-6}$. Този диапазон е достатъчен за конкретното приложение, тъй като най-голямото възможно число е 4095, което се получава от 12-битовия АЦП. Точността е достатъчна, тъй-като е ограничена също така от 12-битовия АЦП. Честотата на часовника на ЦСП е 100MHz, а честотата за управление и изчисление е 2,5KHz.




***Фиг. 3.*** *Блок-схема на системата за управление*

На базата на анализа на работата на схемата [8] е разработена система за управление. При получаване на импулс за включване или изключване на инверторните ключове от системата за ШИМ се подава включващ импулс към паралелните ключове на допълнителната квазирезонасна верига $S_{a2}$ и $S_{a3}$. Токът на резонасната бобина $L_r$, започва да нараства и при достигането на граничната стойност $I_{Lr.max}$, се изключва последователния ключ на допълнителната квазирезонасна верига $S_{a1}$. Започва резонасно разреждане на кондензатора $C_r$ до напрежение $U_{Cr}$=0. В този момент се подават управляващи импулси към съответните ключове на инвертора и превключването им може да стане при нулево напрежение. След превключването на ключовете се подава импулс за изключване на $S_{a2}$ и $S_{a3}$. След изключването на $S_{a2}$ и $S_{a3}$, напрупаната енергия в $L_r$, предизвиква протичането на резонасен ток през обратните диоди $D_{a2}$ и $D_{a3}$ за зареждане на кондензатора $C_r$. Когато напрежението $u_{Cr}$ превиши захранващото напрежение $U_{DC}$, се включва обратния диод $D_{a1}$, който дава

възможност излишната енергия да се върне в мрежата. Ключа $S_{a1}$ се включва при нулево напрежение и схемата е подготвена за подаване на нов импулс за превключване на инверторните ключове. Схемата, представена на фиг. 3, осигурява това управление. Тя е разработена в Matlab/Simulink® и е компилирана в „TMS320C2000™ Experimenter Kit" чрез USB/JTAG емулатора, вграден в платката „TMS320C2000™ Experimenter Kit". Съгласуващата платка (фиг. 2) се използва за галванично разделяне на управляващата платка и силовия блок.

### 3. Експериментални резултати

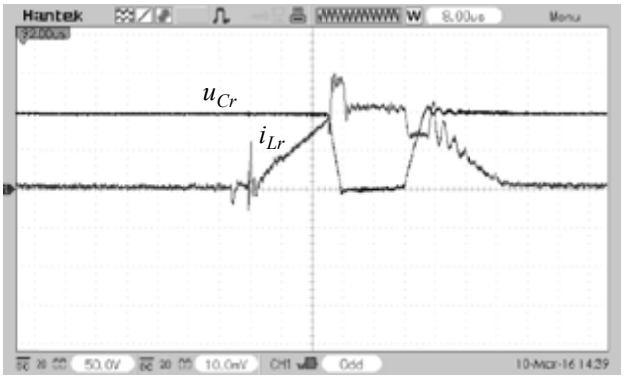
Разработеното DSP базирано асинхронно електрозадвижване с квазирезонансен преобразувател е изследвано експериментално с трифазен асинхронен двигател тип 4AO-80B-4D с номинални данни 0,75 kW, 380 V, 50 Hz, задвижващ механизъм с константен съпротивителен момент. Техническите данни и параметри на електродвигателя са дадени в Приложение.

Проектирането на предложения преобразувател включва избора на параметрите на $L_r$ и, $C_r$ така че да удовлетворяват поставените изисквания за *du/dt*, *di/dt* и пиковите стойности на тока и напрежението. Изразите са получени от диференциалните уравнения, описващи всеки интервал от работата на схемата [5]. На база на използваната методика, параметрите на елементите са избрани: $L_r$=560μH, $C_r$=100nF.

Управление на инвертора се осъществява въз основа на изискването при генерирането на сигнал за превключване на основните ключове, допълнителните вериги трябва да се включат, така че да предизвикат резонансен преходен процес. Превключването на ключовете на инвертора става, когато захранващото напрежение се установи на нула.

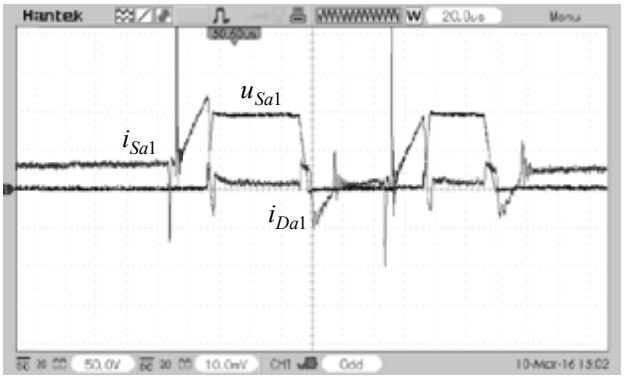
Изследванията са проведени при $U_{dc}$=100V. При измерването на тока е използвана токова сонда с коефициент 10mV/A.

На фиг. 4 са представени зависимостите на напрежението върху резонансния кондензатор $u_{Cr}$ и тока през резонансната бобина $i_{Lr}$ във функция от времето. От фигурата се вижда, че времето за спадане на $u_{Cr}$ до нула е $t_f$=3,77μs, времето за нарастване на $u_{Cr}$ до $U_{dc}$ е $t_r$=5,59μs, а времето през което $u_{Cr}$=0 е $t_z$=16,15μs. Като се има в предвид, че времето за изключване на силовите ключове, използвани в схемата по каталожни данни е $t_{OFF}$=3,5μs, то $t_z$ е достатъчно за превключване на силовите ключове при нулево напрежение. Тока през резонансната бобина достига максимална стойност $I_{Lr.max}$=3A.

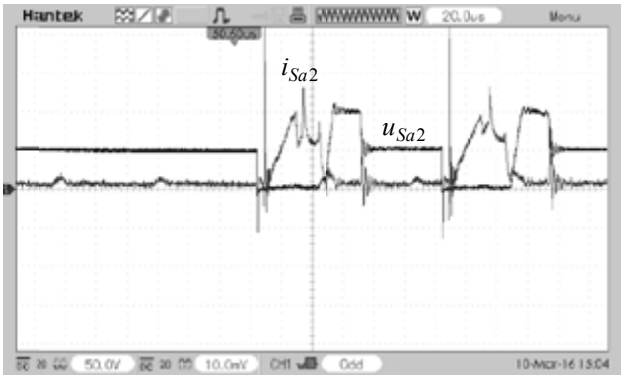



***Фиг. 4.*** *Зависимости на $u_{Cr}$, $i_{Lr}$=f(t)*

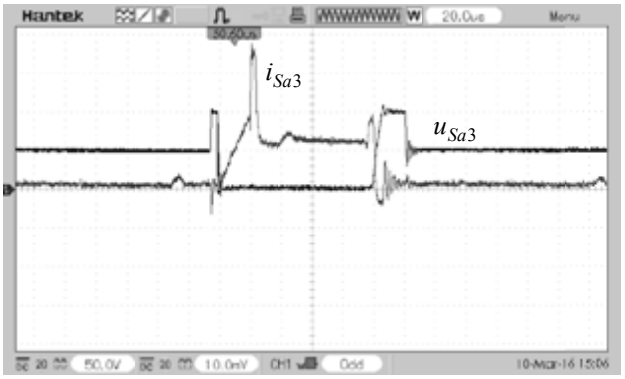
На фиг. 5, фиг. 6 и фиг. 7 са представени зависимостите на напрежението и тока на допълнителните ключове $S_{a1}$, $S_{a2}$ и $S_{a3}$. От фигурите се вижда, че и трите ключа се превключват с „мека комутация".




***Фиг. 5.*** *Зависимости на $u_{Sa1}$, $i_{Sa1}$, $i_{Da1}$=f(t)*

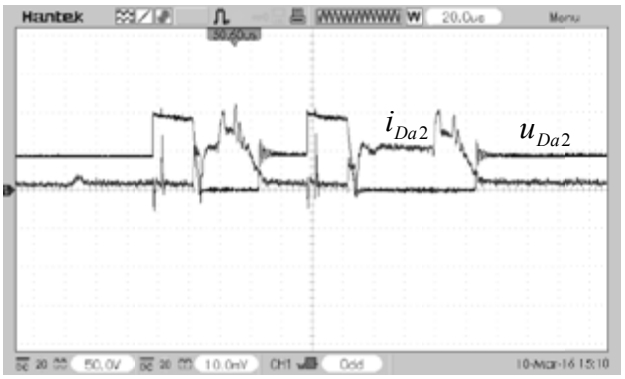



***Фиг. 6.*** *Зависимости на $u_{Sa2}$, $i_{Sa2}$=f(t)*




***Фиг. 7.*** *Зависимости на $u_{Sa3}$, $i_{Sa3}=f(t)$*

На фиг. 8 и фиг. 9 са представени зависимостите на напрежението и тока на допълнителните диоди $D_{a2}$ и $D_{a3}$.



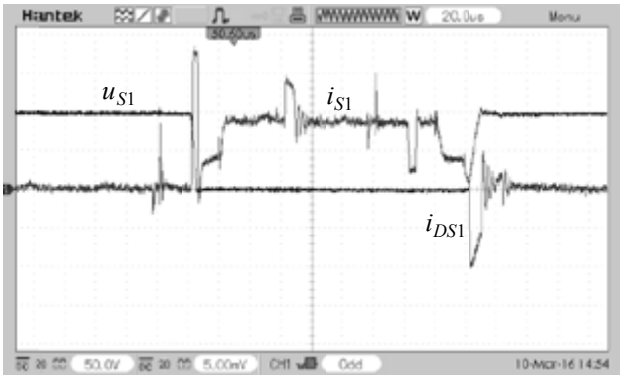

***Фиг. 8.*** *Зависимости на $u_{Da2}$, $i_{Da2}=f(t)$*



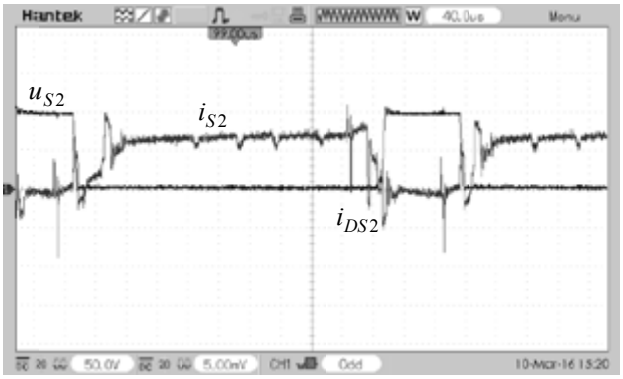

***Фиг. 9.*** *Зависимости на $u_{Da3}$, $i_{Da3}=f(t)$*

От фиг. 5 – фиг. 9 се вижда, че напрежението върху силовите прибори не превишава захранващото напрежение.

На фиг. 10 и фиг. 11 са показани зависимостите на напрежението и тока на една двойка транзистори на трифазния инвертор $S_1$ и $S_2$. От фигурите се вижда, че застъпването между напрежението и тока е минимално, т.е. ключовете се превключват с „мека комутация". Амплитудната стойност на тока през транзисторите е съответно $I_{S1max}$=1,85A и $I_{S2max}$=0,99A, или 2,12 и 1,5 пъти по голям от установения $I_{OS1}$=0,87A и $I_{OS2}$=0,66A.

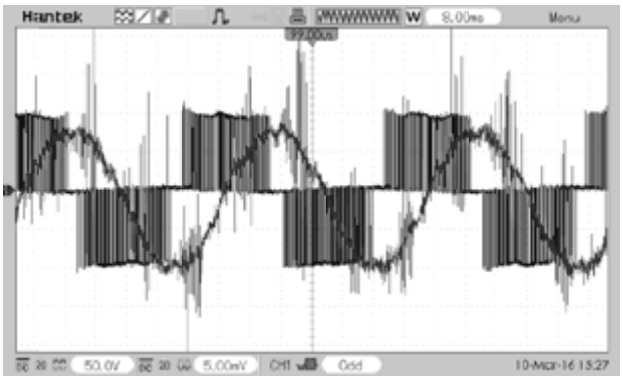



***Фиг. 10.*** *Зависимости на $u_{S1}$, $i_{S1}=f(t)$*




***Фиг. 11.*** *Зависимости на $u_{S2}$, $i_{S2}=f(t)$*

Фиг. 12 представя линейното напрежение на инвертора $u_{AB}$ и фазовия ток $i_A$. От фигурата се вижда, че тока има синусоидална форма.




***Фиг. 12.*** *Зависимости на $u_{AB}$, $i_A=f(t)$*

**4. Заключение**

Разработено е DSP базирано асинхронно електрозадвижване с квазирезонансен преобразувател. За захранването на асинхронното електрозадвижване са използвани трифазен мостов инвертор и резонансна верига с три допълнителни ключа. Управлението на инвертора и резонансната верига става чрез

развойната платка „TMS320C2000™ Experimenter Kit", изградена на базата на цифровия сигнален процесор (ЦСП) TMS320F2808, съвместим със Simulink®. Управляващата програма е разработена в Simulink®, а управляващите сигнали са подадени към инвертора чрез съгласуващата платка. Експерименталните резултати, получени с разработената система показват намаляване на загубите от превключване и повишаване на ефективността на асинхронното електрозадвижване.

## ЛИТЕРАТУРА


1. Chao, K., Liaw, C. (2001). Three-phase soft-switching inverter for induction motor drives. *IEE Proc. Elect. Power Appl*, Vol 148, No I, pp. 8-20.
2. Юдов, Д., и др. (1999). Повишаващ DC/DC преобразувател с подобрени енергетични показатели. *ANNUAL JOURNAL OF ELECTRONICS*, TU-Sofia, стр. 120-125.
3. McMurray, W. (1993). Resonant snubbers with auxiliary switches, *IEEE Trans. Ind. Appl*., pp. 355-361.
4. Vlatkovic, V., Borojevic, D., Lee, C. (1993). A new zerovoltage transition, three-phase PWM rectifiedinverter circuit, *IEEE Power Electron. Spec. Cons. Rec.*, pp. 868-873.
5. Cho, J.G., Kim, H.S., and Cho, G.H. (1991). Novel soft switching PWM converter using a new parallel resonant dc-link, *Proc. IEEE PESC*, pp. 241-247.
6. Current Transducer LTS 15-NP, Datasheet, LEM.
7. Voltage Transducer LV 25-P, Datasheet, LEM.
8. Kedarisetti, J. (2012). A Motor friendly Quasi-resonant DC-link Inverter, *Ph.D. dissertation*, Technische Universität Darmstadt, Darmstadt.


## ПРИЛОЖЕНИЕ

Технически данни на асинхронен електродвигател тип 4AO-80B-4D:

$P_N$=0,75kW; $U_N$=380V; $I_N$=2,1A; $n_N$=1400min$^{-1}$; $\eta_N$=71%; $cos\varphi_N$=0,70; $J_m$=0,00154kgm$^2$.


Department of Electrical Engineering
University of Food Technologies – Plovdiv
26 Maritza Blvd.
4002 Plovdiv
BULGARIA
E-mail: dimitar_spirov@abv.bg
E-mail: nikkomitov@abv.bg

© International Scientific Conference on Engineering, Technologies and Systems
TECHSYS 2016, Technical University – Sofia, Plovdiv branch
26 – 28 May 2016, Plovdiv, Bulgaria

# ОБУЧЕНИЕ НА СТУДЕНТИ ОТ ФАКУЛТЕТ АВТОМАТИКА И ЕЛЕКТРОТЕХНИЧЕСКИ ФАКУЛТЕТ ПО ДИСЦИПЛИНАТА „ОСНОВИ НА ИНЖЕНЕРНОТО ПРОЕКТИРАНЕ I“

ЛЮДМИЛА БАЛТОВА, ВАСИЛКА СТАНЧЕВА

**Резюме:** *В доклада са показани добрите практики разработени в катедра „Основни и технически средства за конструиране” на Машиностроителен Факултет в Технически Университет-София за обучение по дисциплината „Основи на инженерното проектиране I” за студенти от факултет Автоматика и Електротехнически факултет. Представени са начини за оценяване на усвоените знания и са показани и анализирани резултати от контролни работи по AUTOCAD и проектиране на детайл от натура, провеждани в края на първи семестър.*

**Ключови думи:** *обучение, качество на обучението, инженерно проектиране*

# LEARNING OF STUDENTS OF FAKULTY OF AUTOMATICS AND FACULTY OF ELECTRICAL ENGINEERING IN SUBJECT „FUNDAMENTALS OF ENGINEERING DESIGN“– PART I

LYUDMILA BALTOVA, VASILKA STANCHEVA

**Abstract:** *In this paper good practices for training students developed in the Department of Fundamentals and Techniques for Design in Mechanical Faculty at Technical University of Sofia are shown. Learning of students of Faculty of Automatics and Faculty of Electrical Engineering in subject „Fundamentals of Engineering Design“– part I are presented. The program for training the students in the subject is discussed, the means for assessment of the acquired knowledge are presented. In the paper are shown helpful applications which presents good practices for training students as measures to be applied to increase the knowledge and motivation.*

**Key words:** *education, quality of education, engineering design*

## 1. Основни положения

В катедра „Основни и технически средства за конструиране” на Машиностроителен Факултет в Технически Университет-София са разработени курсови задачи за увеличаване на практическите знания на студентите от I-ви курс на факултет Автоматика и Електротехнически факултет по дисциплината „Основи на инженерното проектиране“ I и II част (ОИП I, II).

Разработени са варианти на задания за контролни работи, които се използват в края на семестъра за проверка степента на усвояване на знанията.

Оценката на всеки студент се формира като се сумират точките получени от курсови задачи и контролни работи, направени през учебната година.

Учебника [1] и ръководството [2] съдържат теоритичната база от познания необходими за успешното изпълнение на курсовите задачи и контролните работи, както и справочна информация в приложенията.

В Табл. 1 са показани броя на точките приравнени към съответните годишни оценки.

Copyright © 2016 by Technical University of Sofia, Plovdiv branch, Bulgaria ISSN Online: 2535-0048

***Таблица 1.*** *Брой точки приравнени към съответна годишна оценка*

| **Бр. т-ки** | под 60 | от 60 т. до 69 т. | от 70 т. до 79 т. | от 80 т. до 90 т. | над 90 т. |
|---|---|---|---|---|---|
| **Год. оц.** | Слаб 2 | Среден 3 | Добър 4 | Мн.добър 5 | Отличен 6 |

## 2. Описание на курсови задачи

Курсовите задачи се изработват ръчно или с CAD продукт върху подходящи форматни листа /хартиен носител/ - А3, А4.

### 2.1. Курсова задача №1 "Проектиране и техническа документация на електрически схеми"

В тази кусова задача по зададени конструкторски документи се съставя силнотокова принципна електрическа схема (чертеж и списък на елементите). Съставя се схема на съединенията (скица). Прави се предложение за електротехническо табло (чертеж). Прави се инженерен анализ (главна функция, основни функции, допълнителни функции, добавяне на допълнителни елементи - записка).

### 2.2. Курсова задача №2 „Евристични методи I".

В тази курсова задача се търсят нови реализации, допълнителни функции или нов външен вид на технически обект по зададен евристичен метод (морфологичен анализ и синтез, фокусни обекти, емпатия - записка).

### 2.3. Курсова задача №3 „Проектиране на механични съединения".

В тази курсова задача се проектират липсващи детайли от зададено изделие, което е изобразено на чертеж на общия вид. Прави се инженерен анализ на изделието (главна функция, основни функции, функции на детайлите, детайли реализиращи основните функции, повърхнини на сглобяване на детайлите, ред на сглобяване, технология на изработване на един детайл - записка). Изготвя се част от конструкторската документация на изделието (чертеж и списък на съставните части). Накрая се представя предложение за изменение на сглобената единица (скица).

### 2.4. Курсова задача №4 „Модификация на електротехническа сглобена единица"

В тази курсова задача по зададена единица от натура се проектира модифицирана сглобена единица. Построяваше 3D модел на детайл от сглобената единица и се определят теоретично необходимите пресмятания и се прави конструктивна документация – записка. Накрая се разработва част от конструктивната документация (сборен чертеж, списък на съст. части и скици на 2 детайла).

## 3. Описание на лабораторни упражнения

Ръководството съдържа заданията за курсовите задачи, задачи и лабораторни упражнения, които студентите изпълняват през семетъра и обхващат материала, предвиден от учебната програма по дисциплината.

ЛУ №1 Проектират се силнотокови принципни електрически схеми, схеми на съединенията, ел. инсталации в плановете. Типове ел. елементи. Разположение на ел. елементите в електротехническо табло (ел. инсталация на помещение - скица).

ЛУ №2 Прави се автоматизирано изпълнение на силнотокова принципна електрическа схема (според зададен вариант) в среда на AutoCAD.

ЛУ №3 Проектират се ел. схеми, печатни платки и печатни възли.

ЛУ №4 Прави се автоматизирано изпълнение на принципна електрическа схема и се разработва модел на печатен възел в среда на Cadstar.

ЛУ №5 Проектиране, изобразяване и оразмеряване на детайли.

ЛУ №6 Евристични методи. Инженерен анализ на изделия.

ЛУ №7 Проектират се и се документират детайли (скица), а след това се прави и инженерен анализ.

ЛУ №8 Прави се автоматизирано изпълнение на чертеж на детайл от сглобена единица (според зададен вариант) в среда на AutoCAD.

ЛУ №9 Проектиране и документиране на типови съединения в електротехниката.

ЛУ №10 Проектира се и се документира електротехническа сглобена единица, прави се инженерен анализ и се представя модификация.

ЛУ №11 Прави се автоматизирано изпълнение на 3D модел на детайл в среда на SolidWorks (според зададен вариант).

## 4. Описание на контролни работи (КР)

### 4.1. КР1 Теоретичен въпрос с практическа насоченост.

Продължителност–45 мин., общо 2т – 4т: проектиране на силнотокови електротехнически схеми (2т); проектиране на детайли – изисквания към геометрията на повърхнините,

размери и грапавост (1т); проектиране и документиране на съединения на детайли (1т).

### 4.2. КР 2 Автоматизирано изпълнение в среда на AutoCAD.

Продължителност–2х45мин, общо 5т–9т: изобразяване на силнотокова принципна електрическа схема(2т – 4т); изобразяване на двумерен чертеж на детайл (3т – 5т).

### 4.3. КР 3 Проектиране на детайл от натура.

Продължителност–90 мин., общо 8т–12т: необходими и достатъчни изображения (7т); оразмеряване (3т); точностни характеристики и грапавост на повърхнините (1т); оформление на чертежа (1т).

За да може студентите да имат по-голям избор от дейности, успешната реализация на които ще увеличи получените точки, а оттам и крайната оценка, са разработени допълнителни задачи към КР3: частите на КР1; инженерен анализ (2 – 4 т.); предложение за модификация (2 – 4 т.); евристични методи - 2 бр. (2 – 4 т.).

## 5. Статистика и резултати

В Табл. 2 са показани броя на студентите от ФА и ЕФ, които са решили контролните работи в края на първи семестър за период от последните три учебни години.

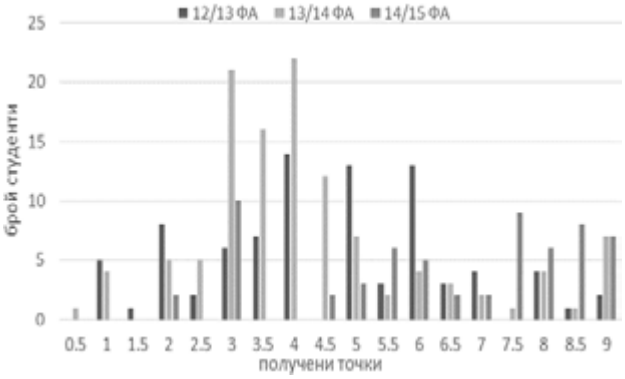
***Таблица 2.*** *Статистика*

| Година | Общ брой студ.-ФА | Общ брой групи-ФА | Общ брой студ.-ЕФ | Общ брой групи ЕФ |
|---|---|---|---|---|
| **12/13** | 107 | 8 | 83 | 6 |
| **13/14** | 130 | 10 | 162 | 12 |
| **14/15** | 76 | 10 | 98 | 7 |

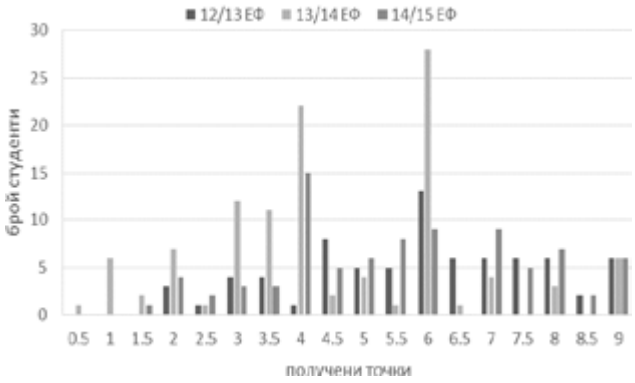
В Табл. 3 е сравнена успеваемостта на студентите от ФА и ЕФ при изпълнение на контролна работа с AUTOCAD за периода на поледните три учебни години.

***Таблица 3.*** *Брой точки от контролна работа на AUTOCAD разпределени по години*

| т-ки AUTOCAD | 12/13 ФА | 13/14 ФА | 14/15 ФА | 12/13 ЕФ | 13/14 ЕФ | 14/15 ЕФ |
|---|---|---|---|---|---|---|
| 0.5 | 0 | 1 | 0 | 0 | 1 | 0 |
| 1 | 5 | 4 | 0 | 0 | 6 | 0 |
| 1.5 | 1 | 0 | 0 | 0 | 2 | 1 |
| 2 | 8 | 5 | 2 | 3 | 7 | 4 |
| 2.5 | 2 | 5 | 0 | 1 | 1 | 2 |
| 3 | 6 | 21 | 10 | 4 | 12 | 3 |
| 3.5 | 7 | 16 | 0 | 4 | 11 | 3 |
| 4 | 14 | 22 | 0 | 1 | 22 | 15 |
| 4.5 | 0 | 12 | 2 | 8 | 2 | 5 |
| 5 | 13 | 7 | 3 | 5 | 4 | 6 |
| 5.5 | 3 | 2 | 6 | 5 | 1 | 8 |
| 6 | 13 | 4 | 5 | 13 | 28 | 9 |
| 6.5 | 3 | 3 | 2 | 6 | 1 | 0 |
| 7 | 4 | 2 | 2 | 6 | 4 | 9 |
| 7.5 | 0 | 1 | 9 | 6 | 0 | 5 |
| 8 | 4 | 4 | 6 | 6 | 3 | 7 |
| 8.5 | 1 | 1 | 8 | 2 | 0 | 2 |
| 9 | 2 | 7 | 7 | 6 | 6 | 6 |




***Фиг. 1.*** *Успеваемост на студенти от ФА при КР2 с AUTOCAD*




***Фиг. 2.*** *Успеваемост на студенти от ЕФ при КР2 с AUTOCAD*

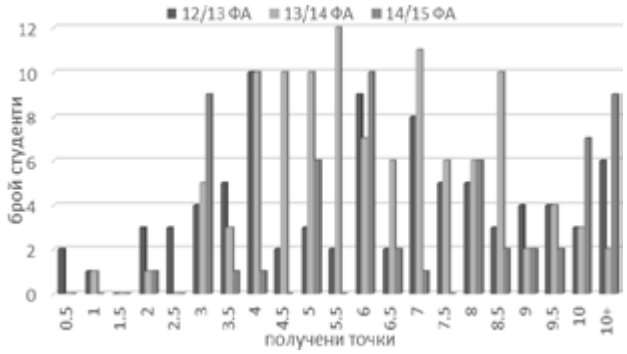
От Фиг.1 и Фиг.2 се вижда, че кривата на ФА е по-равномерна, т.е. по-голям брой студенти имат среден брой точки получени при изпълнение на КР2 с AUTOCAD.

В Табл. 4 е сравнена успеваемостта на студентите от ФА и ЕФ при изпълнение на контролна работа при проектиране на детаил от натура за периода на поледните три учебни години.

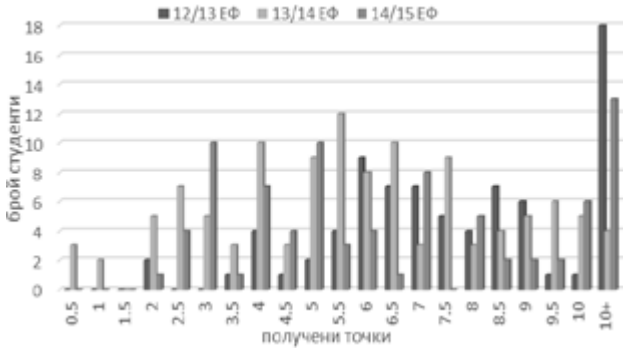
***Таблица 4.*** *Брой точки от КР на проектиране на детайл разпределени по години*

| т-ки детайл | 12/13 ФА | 13/14 ФА | 14/15 ФА | 12/13 ЕФ | 13/14 ЕФ | 14/15 ЕФ |
|---|---|---|---|---|---|---|
| 0.5 | 2 | 0 | 0 | 0 | 3 | 0 |
| 1 | 1 | 1 | 0 | 0 | 2 | 0 |
| 1.5 | 0 | 0 | 0 | 0 | 0 | 0 |
| 2 | 3 | 1 | 1 | 2 | 5 | 1 |
| 2.5 | 3 | 0 | 0 | 0 | 7 | 4 |
| 3 | 4 | 5 | 9 | 0 | 5 | 10 |
| 3.5 | 5 | 3 | 1 | 1 | 3 | 1 |
| 4 | 10 | 10 | 1 | 4 | 10 | 7 |
| 4.5 | 2 | 10 | 0 | 1 | 3 | 4 |
| 5 | 3 | 10 | 6 | 2 | 9 | 10 |
| 5.5 | 2 | 12 | 0 | 4 | 12 | 3 |

| | | | | | | |
|---|---|---|---|---|---|---|
| 6 | 9 | 7 | 10 | 9 | 8 | 4 |
| 6.5 | 2 | 6 | 2 | 7 | 10 | 1 |
| 7 | 8 | 11 | 1 | 7 | 3 | 8 |
| 7.5 | 5 | 6 | 0 | 5 | 9 | 0 |
| 8 | 5 | 6 | 6 | 4 | 3 | 5 |
| 8.5 | 3 | 10 | 2 | 7 | 4 | 2 |
| 9 | 4 | 2 | 2 | 6 | 5 | 2 |
| 9.5 | 4 | 4 | 2 | 1 | 6 | 2 |
| 10 | 3 | 3 | 7 | 1 | 5 | 6 |
| 10+ | 6 | 2 | 9 | 18 | 4 | 13 |




***Фиг. 3.*** *Успеваемост на студентите от ФА при КР3 – проектиране на детайл*




***Фиг. 4.*** *Успеваемост на студенти от ЕФ при КР3 – проектиране на детайл*

От Фиг.3 и Фиг.4 се вижда, че тенденцията на по-голям брой студенти получили средна оценка на КР3 – проектиране на детайл от натура се запазва и тук, което показва, че мотивацията при повече от студентите от ФА е по-голяма,отколкото при студентите от ЕФ.

Тъй като делът на показалите добро усвояване на необходимите знания и умения, е сравнително нисък се налага търсене на нови начини за мотивиране на студентите за показване на по-добри резултати. За тази цел е подходящо прилагането на входящ тест преди започването на съответното упражнение, с който да се проверяват знанията на студентите по задачите на упражнението. Студентите да се допускат до упражнение само при успешно решаване на входящия тест. Така ще се стимулира редовното учене и ще се намали риска от липса на мотивация на студентите.

## 6. Заключение

В доклада се разглежда обучението на студенти първи курс първи семестър от факултет Автоматика и Електротехнически факултет по дисциплината „Основи на инженерното проектиране I", разработена в катедра „Основни и технически средства за конструиране" на Машиностроителен Факултет в Технически Университет-София.

Описани са разработените курсови задачи, лабораторни упражнения и контролни работи.

Представена е статистика, включваща брой групи, брой студенти и резултати от контролни работи работи по AUTOCAD и проектиране на детайл от натура, провеждани в края на първи семестър на първи курс.

Направен е сравнителен анализ на разпределението на резултатите от контролните.

Показани са допълнителни задачи към КР3 като мерки, които се прилагат за намаляване на изоставането и за повишаване на знанията и мотивацията на студентите.

## ЛИТЕРАТУРА

1. Лепаров, М., Вичева, М., Георгиев М., (2015), *Основи на инженерното проектиране,* учебник за студенти от ФТК, ФКСУ, ФА, ФЕТТ и ЕФ на Технически Университет-София, трето преработено издание, издателство „Софттрейд", ISBN 978-954-334-082-8, София, 2015.
2. Станчева, В., Тодорова К., (2006), *Техническо документиране*, ръководство за упражнения на студенти от Електротехнически факултет, второ преработено и допълнено издание, под общата редакция на доц. д-р М. Георгиев, издателство „Софттрейд", ISBN-10:954-334-036-6, ISBN-13:978-954-334-036-1, София, 2006.

Контакти:
E-mail: lbaltova@tu-sofia.bg
катедра „Основи и технически средства за конструиране" при Машиностроителен факултет на Технически университет;
E-mail: vmartinova@tu-sofia.bg
катедра „Основи и технически средства за конструиране" при Машиностроителен факултет на Технически университет.

© International Scientific Conference on Engineering, Technologies and Systems
TECHSYS 2016, Technical University – Sofia, Plovdiv branch
26 – 28 May 2016, Plovdiv, Bulgaria

# SECTION 2 • СЕКЦИЯ 2

## ELECTRICAL ENGINEERING AND ENERGETICS ELECTRONICS; ELECTRONIC TECHNOLOGIES AND OPTOELECTRONICS

## ЕЛЕКТРОТЕХНИКА И ЕЛЕКТРОЕНЕРГЕТИКА; ЕЛЕКТРОНИКА И ОПТОЕЛЕКТРОНИКА

© International Scientific Conference on Engineering, Technologies and Systems
TECHSYS 2016, Technical University – Sofia, Plovdiv branch
26 – 28 May 2016, Plovdiv, Bulgaria

# OPTIMIZATION OF MULTI-LAYER LINEAR GRADIET INDEX ANTIREFLECTIVE BASED ON OXYNITRIDE SILICON

KADDOURI AMEUR MILOUD[1], KOUZOU ABDELLAH[2], HAFAIFA AHMED[2]

**Abstract:** *This paper deals with the comparative study between the performance of a multi-layers linear gradient index (MLLGI) antireflective coating (ARC) based on oxynitride silicon and that of a conventional single layer (SL) antireflective coating (silicon or silicon nitride) clearly shows the improvement made by the linear gradient index layers AR from point of view of the sensitivity, the thickness of the layers and the angle of incidence. This study allows to determining the optimal values of sensitive parameters (Thickness, index...) for the realization of gradient index ARC. It is proved in this study that multi-layers antireflective coatings with better efficiency under oblique incidence can be obtained with affordable methods of implementation.*

**Key words:** *antireflective coating (ARC), silicon oxynitride, linear gradient index, oblique incidence.*

## 1. Basics

The materials used for manufacturing solar cells (Si, GaAs, CdTe...) have high refractive indexes. Hence, the reflection losses are high. For silicon more than 35% of the incident light flux is reflected, which affects greatly the efficiency of photovoltaic devices [1]. To improve the efficiency of solar cells, anti-reflective layers (ARL) are generally used, they are deposited by different methods and following various designs. To achieve an antireflective coating (ARC) with graded index (GI), a deposit of a dielectric layer possessing a refractive index gradually decreasing from the substrate to the ambient medium can be used. Theoretically, if the index decreases gradually from ns (index of the substrate) to n0 (index of the ambient medium) the reflection will be null. Unfortunately, this cannot be achieved practically because the high refractive index materials are generally absorbent [2]. Indeed, it was proved previously in some published works that the use of oxynitride layers with graded index allows significantly to reduce the reflectance in the range of wavelengths where the monocrystalline silicon cell is sensitive [15-19 ]. In this paper the antireflection layers with linear gradient index that are achieved by PECVD silicon oxynitride (SiNxOy) are presented. Measures of reflectance factor were recorded . A theoretical model was developed to study the behavior of these AR layers at normal and oblique incidence [3]. The comparison between the theoretical curves and the experimental measurements of the reflectance factor has allowed to validate the model[4.14]. The use of this model permits the study of the parameters (thickness, optical indices) where the main aim is the optimization of their performances. the present paper contributes to the performance optimization of the linear gradient index antireflective layers. On the other side, the improvement that can be brought to the photovoltaic parameters of a conventional silicon solar cell including the photocurrent and energy efficiency has been studied.

## 2. Formatting

The use of antireflection coatings (ARC) on solar cells allows reducing the reflection losses and increasing the photocurrent (percentages of almost 50% [5,6]) and therefore, the short-circuit current. The open circuit voltage and the shape factor remain practically unchanged. Consequently, the energetic efficiency is improved in the same proportions as the photocurrent. For this reason, the ARC has to be optimized taking as a reference the illumination current, practically it is nearly equal to the short-circuit current [7.8]. To calculate the photocurrent, it is assumed that the ARC is deposited on a P + N monocrystalline silicon cell having a surface recombination velocity S = 106 cm / s, using the solar spectrum AM1.5, which is used

Copyright © 2016 by Technical University of Sofia, Plovdiv branch, Bulgaria ISSN Online: 2535-0048

for this kind of calculation. The photocurrent is then expressed as follows:

$$Jph = \int_{\lambda 1}^{\lambda 2} [1 - R(\lambda)] E(\lambda) S(\lambda) d\lambda \qquad (1)$$

S(λ) : spectral sensitivity (values published by M. Ogeret [7].

R(λ) : Reflection factor (calculated by the software achieved by the authors).

E(λ) : illumination spectrum AM1.5 [7].

For the integral calculation the Monte Carlo method is used [9]. The photocurrent depends on the domain of wavelengths used for the integration. However, for a silicon cell, generally the wavelength range of 300nm - 1100nm is used [7,8]. Preliminary calculations of the photocurrent of linear gradient ARC for a thickness of 260 nm, n = 2.0 to 1.5 and the photocurrent of a solar cell without ARC have showed an improvement of photocurrent of 35%. The parameters optimization has allowed certainly to obtain better results [12,13].

### 2.1. Level2 Sections

For second level of headings use „SectionL2" mark-up style.

## 3. Equations and symbols

Number The improvement in relative value of the photocurrent is due to the presence of the ARC which is presented as follows:

$$\frac{\Delta I}{I_0} = \frac{I_{PH} - I_0}{I_0} \qquad (2)$$

$I_{ph}$ : The photocurrent with ARC.

$I_0$ : The photocurrent without ARC.

The two currents are calculated from equation (1). The curves below show the relative increase of the photocurrent depending on the thickness of the multi-layer linear gradient ARC compared with traditional single-layer SiO2 and Si3N4. It is important to note that the photocurrent depends on the integration domain. However, the choice of 300nm to 1100nm range is more reasonable since it includes the entire sensitivity range of the silicon solar cell test. For single layer ARC it was verified that the maximum improvement of the photocurrent is obtained for thicknesses equal to the quarter of the wave length centered at λ = 600 nm (75 nm Si3N4 for n = 2.1 and 100 nm for SiO2 n = 1.5).

It is noted that the single-layer ARC Si3N4 gives good results for n = 2.1 which is closer to the optimum value (N0NS) 1/2 = 1.95. On the other side, it is noted that the photocurrent obtained with linear gradient ARC and the ARC Si3N4 are comparable. The photocurrent is improved by 40% which is a satisfactory result in comparison to the published results [10,11]. However, the gradient ARCs are less sensitive to an eventual error on the deposited thickness and/ or to a non-homogeneity on the surface of the deposited layers. This can be observed clearly on the very narrow peaks for the single layer ARC compared to the gradient ARC. It is also observed that the improvement of 40% remains effectively between 80nm and 160nm Fig. 1.

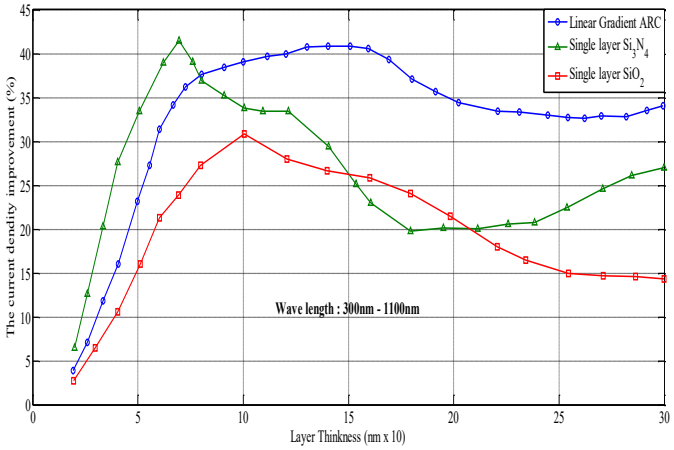



***Fig. 1.*** *The variation of the current density versus the thickness value*

## 4. Figures and tables

Figure 2. shows that greater is the variation of the gradient, the improvement of the photocurrent density in more better. This amounts is due to the fact that the reflectance factor is decreased.

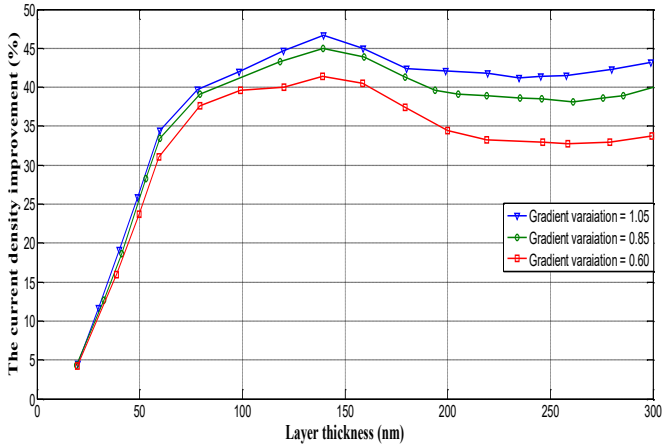



***Fig. 2.*** *The variation of the current density versus the thickness value*

### 5. References and citations

Taking the optimal values for each type of layers, their behavior face to the oblique incidence Fig 3. It appears that the gradient ARCs behave better under oblique incidence than the conventional single-layer ARC. For the ARCs Si3N4 and SiO2 the improvement decreases by more than 10% at 50 ° of incidence, while for the linear gradient ARC it decreases by only 3%.

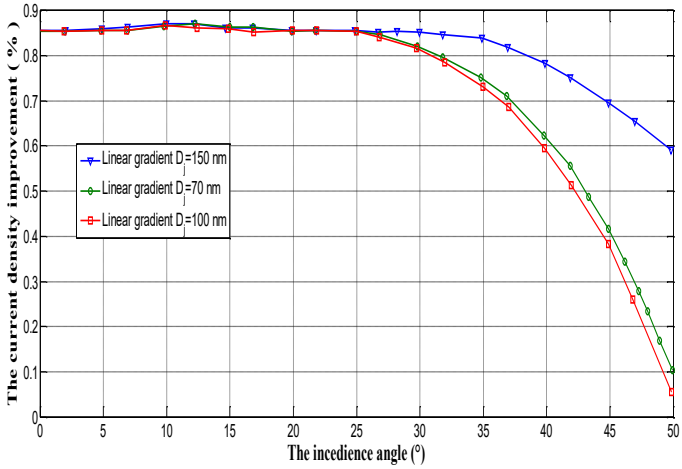



***Fig. 3.*** *The variation of the current density versus the incidence angle*

### 6. Conclusion

The study of the influence of each sensitive parameter of the linear gradient index ARC (including thickness, Δn gradient and angle of incidence) has been presented, where the main aim is to ensure their optimization design. The single layer linear gradient ARCs were compared to the widely used single layer ARC of type Si3N4 and SiO2 with quarter of the wave length. Based on the calculations performed at normal and oblique incidence leads to the following conclusions:

- The antireflective coating with graded index are less sensitive to a possible surface non-homogeneity and/or a gap on the deposited thickness. It was proved that the thicknesses between 100 nm and 200 nm gives nearly an over gain of 45% of the photocurrent in comparison a cell without antireflective coating.
- The linear graded index layers are less sensitive to the variation of the incidence angle which is generally the case of the solar cell practical operating conditions. This implies a considerable energy gain if it is used on the whole day. On the other hand, at an incidence angle of 50, the photocurrent lose is only 2.5% for the gradient antireflective coating compared to the photocurrent lose value of 10% of the conventional antireflective coating.

### REFERENCES


1. K. CHOPRA, ‘‘Solar selective coatings,’’ 3 rd workshop on thin films physics and technology, pp.306-311, 1999.
2. K. CHOPRA, ‘‘Solar selective coatings,’’ 3 rd workshop on thin films physics and technology, pp.306-311, 1999.
3. E. PELLETIER, ‘‘La réalisation des traitements optiques de surface,’’ Systèmes optiques, Ecole d’été – institut d’études scientifiques de Cargèse, Vol.I, PP 399-440, 1991.
4. J. VIARD, ‘‘Caractérisation des couches minces d’oxynitrures elaborées par PECVD,’’ Thése, Université de Montpellier. Science et Technologie, Février 1996.
5. A. M. KADDOURI, A. MAHDJOUB, S.CALLARD et J. JOSEPH , ‘’Etude des couches antireflets à base d’oxynitrure de silicium, ‘ 1st EEEC Laghouat 2000.
6. A.S. CALLARD, A. GAGNAIRE, J. JOSEPH, “ Fabrication and characterisation of graded refractive index silicon oxynitrid thin films, ” J.Vac.Sci.Technol. A, Vol.15, N°4, PP 2088-2094, 1997.
7. J. ZHAO, M..A. GREEN, ‘Optimized antireflection coatings for high-efficiency solar cells, ” IEEE Trans.Electron Devices, Vol.38, N° 8, PP 1925-1934, 1991.
8. M. ORGERET, ‘‘ Les Piles solaires : le composant et ses applications,’’ Ed Masson, 1985.
9. Z. CHAN, P. SONA, J. SALAMI, A. ROHAUGI, ‘‘ A Novel and effective PECVD SiO2/SiN antireflection coatings for solar cells,’’ IEEE Trans.Elec.Devi., Vol.40, n° 6, PP 1161-1165,1993.
10. M. EMINYON, K.RUBIN, ‘ Introduction à la simulation des systèmes physiques, ‘ Inter-editions, 1994.)
11. A.W. BLAKERS, M.J. STOCKS, ‘‘ Modelling the measurements of silicon solar cells under natural sunlight,’’ 14th Europeen P.V.Solar ener. Conf, Spain, 1997.
12. A. LAUGIER, ‘‘ Matériaux pour la conversion photovoltaïque,’’ Institut National des Sciences Appliquées de Lyon, 1983.
13. A.M.Kaddouri, A.Belaidi, "Optimisation des couches antireflets à gradient d'indice-comportement en incidence oblique", Conférence Internationale sur la Physique et

ses Applications, USTOMB Oran, Décembre 2003.
14. A.M.Kaddouri, A.Belaidi, "Optimisation des performances des couches antireflets à gradient d'indice linéaire a base d'oxynitrure de silicium", International Conference on Electrical/Electronics Engineering Communication & Physical systems, C U Saida, Mai 2004.
15. A.M.Kaddouri, A.Kouzou, A.Belaidi, "The study of the graded index anti-reflective coating based on silicon oxynitride", Journal of Optoelectronics and Advanced Materials, Vol.17, No.1-2, January-February.2015, p.50-61.
16. M.Beye, F.Ndiaye, A.S.Maiga, "Antireflection Coatings Combining Silicon Nitride with Silicon Nanoparticule", Journal of Engineering and Technology, Vol.1, Issue.2, 2014.
17. A.Alemu, A.Freundlich, N.Badi, C.Boney, A.Ben-saoula, "Low temperature deposited boron nitride thin filmsfor a robust anti-reflection coating of solar cells", Solar Energy Materials and Solar Cells, Vol.94, No.5, pp.921-923, 2010.
18. B.G.Lee, I.Skarp, V.Malinen, S.Li, S.Choi, H.M.Branz, in Proveeding of the IEEE Photovoltaic Specialists Conference, Austin, Tex, USA, 2012.
19. J.Kim, J.Park, J.H.Hong and all, "Double antireflection coating layer with silicon nitride and silicon oxide for polycristalline silicon solar cell", Journal of Electroceramics, Vol.30, No.1-2, pp.41-45, 2013.
20. M.Li, L.Zeng, Y.Chen, L.Zhuang, X.Wang, H.Chen, " Realization of colored multicrystalline silicon solar cells with SiO2/SiNx :H double layer antireflection coatings", International Journal of Photoenergy, Vol.30, Article ID 352473, 8 pages, 2013.
21.

Authors' contacts:
Address:
[1]Laboratoire des Science et Informatique des Matériaux (MSIL), ST Faculty, Djelfa University, Algeria

[2]Applied Automation and Industrial Diagnostics Laboratory (LAADI), Djelfa Universitydepartments of science and technology, Algeria
[2] University Amar Telidji of Laghouat

E-mail: amkaddouri@yahoo.fr
E-mail: kouzouabdellah@ieee.org

© International Scientific Conference on Engineering, Technologies and Systems
TECHSYS 2016, Technical University – Sofia, Plovdiv branch
26 – 28 May 2016, Plovdiv, Bulgaria

# VALIDATION OF A MODEL FOR GENERATION OF HOURLY AMBIENT TEMPERATURE TIME SERIES

DIMITAR DIMITROV, ATANAS ILIEV, NEVENKA KITEVA - ROGLEVA

**Abstract:** *Simultaneous solar radiation data and the ambient temperature hourly data time series are essential for photovoltaic systems analyses, as well as for the analyses for other power systems equipment. In this paper, a model for generation of hourly ambient temperature data for locations, where exist only the monthly mean temperature values and the corresponding hourly data of solar radiation on a horizontal surface. The validation of the model is carried out for the region of Skopje, R. Macedonia through statistical parameters comparison. Slight change of conversion factors is proposed.*

**Key words:** *ambient temperature, solar radiation, time series, statistical validation*

## 1. Introduction

The ambient temperature data series are important input for simulation of photovoltaic systems, load consumption, etc. [1-4]. Temperature variations are not so rapid, thus hourly temperature values are usually sufficiently short intervals for estimation for power consumption, performance analyses of renewable systems, etc. For that purpose, for more profound analyses, long-term hourly temperature time series are often required.

Time series of the ambient temperature are measured and recorded at many meteo-stations throughout the world. However, sets of monthly mean temperature data are available more often. On the other hand, for analyses of renewable energy systems simultaneous hourly data for solar radiation and the temperature are required as input

Having in mind the above, for that purpose, models for synthetic generation of hourly time series had been developed. The models for generation of hourly temperature time series had been reviewed in [5]. In [6] was concluded that the sufficient models should not only take into account the statistical and sequential properties of the temperature, but they should also involve the apparent cross-correlation between the solar radiation and the temperature. These models differ by their exactness, complexity, universality, required input data, etc.

The most known software package for generation of meteorological data, METEONORM (versions 2-4) [7], uses an updated model [8]. The model is based on the assumption that the temperature variation amplitudes during daytime are proportional to the corresponding daily global solar radiation amplitudes. Inputs in the model are hourly data of global solar radiation on a horizontal surface and monthly mean ambient temperature. Apart of these, the model uses conversion factors that depend on the meteorological and geographical characteristics of the location.

In this paper, validation of the updated Scartezzini's model is tested for the region of Skopje, R. Macedonia. The inputs are the measured data of global solar radiation on a horizontal surface and the calculated monthly mean ambient temperature for the same sequence of time. Version 5 and above of METEONORM [9], use another model, developed within the Project "SoDa" [10], but as explicitly reported, the quality of generated data is very similar to the data from the model used in the previous versions [7].

## 2. Generation of temperature time series

The ambient temperature data series contain deterministic and stochastic components. In the updated Scartezzini's model [7], the deterministic component is extracted from the hourly solar radiation time series. The solar radiation profile for each day is smoothed, stretched and time displaced using specific conversion factors that are typical for the location and the month. The stochastic component is a result of other (then solar radiation) influencing factors to the temperature.

The generated time series are composed of successively chained daily profiles. Each profile begins at sunrise hour and ends at sunrise hour in the following day. The profiles are joined in a way that the temperature at sunrise of ending profile is equalized to the temperature in the sunrise hour at

Copyright © 2016 by Technical University of Sofia, Plovdiv branch, Bulgaria ISSN Online: 2535-0048

the beginning of incoming profile. At the end of each month the generated time series are checked if they satisfy the allowed limits and constraints. If the conditions are satisfied the hourly time series are adjusted to the monthly mean, otherwise the generation process starts over again.

The hourly time series of solar radiation are also rarely available, thus their generation is required. In [11, 12] models for generation of these time series are presented.

### 2.1. Deterministic variations

The variation of the temperature, mainly, is determined by the variation of the solar radiation. However, due to the heating capacities of air masses, surrounding earth surface and objects etc., the thermal effects have greater inertia than the radiation effects. For that reason the temperature variations can't follow the immediate variations of the solar radiation (clouds covering the sun, etc). Also, as a consequence of greater inertia, the heating effect of solar radiation is felt with a delay. Namely, if the maximal solar radiation is at 12:00, the maximal temperature is (for example) at 15:00. Having in mind these, the modelled daily solar radiation profile is smoothed and time displaced. The smoothing is done by averaging the hourly solar radiation data for a given time interval (of several hours), centered in the considered hour. Its values may vary from 6 hours in winter up to 9 hours in summer months. Then the smoothed profile is displaced with a time lag of 2 or 3 hours. Both, the values of the smoothing interval and the time lag are site and monthly dependent conversion factors. The smoothed and time displaced daily solar radiation profile is then converted to a temperature by a stretching factor (another site and monthly dependent conversion factor).

The obtained profile gives the solar radiation dependent temperature component, but only from the sunrise the sunset hours. After the sunset, the temperature decreases depending on the time lag value. When the time lag is 2 hours, the temperature for the further hour continues to be derived from the daily temperature profile, and time lag of 3 hours – from the temperature profile for the next 2 hours after the sunset hour.

For each subsequent hour up to midnight, the temperature decrement is being reduced by a constant factor, which is between 1.15 and 1.5. After the midnight, a linear temperature decrement factor is assumed. This factor depends on the total solar radiation in the following day. When it exceeds 25 % of the daily extraterrestrial solar radiation (maximal possible radiation), the decrement factor is 1/2 of the temperature decrement at last hour before midnight, and when is below 25 % it is 1/3. However, from the measured data and a large number of temperature generation runs, it was concluded that the decrement factor of 1/1.5 is more suitable for the whole year when the total solar radiation exceeds 25 % of the daily extraterrestrial solar radiation.

### 2.2. Stochastic variations

The temperature variations that are not a direct consequence of the solar radiation (wind, rain, snow, dew, fog, etc.), are represented with stochastic processes [8]. There are two main components of the stochastic processes: hourly and daily perturbations.

The hourly perturbations $\Delta T_{AR}$ are generated by the following autoregressive process:

$$\Delta T_{AR}(h) = 0.7 \cdot \Delta T_{AR}(h-1) + 0.385 \cdot r \qquad (1)$$

where: $\Delta T_{AR}(h)$ is the perturbation of the temperature at hour $h$, $r$ is a normally distributed random variable with mean equal to 0 and standard deviation equal to 1.

The daily perturbations are represented by temperature differences from one midnight to the next $\Delta T_{mm}(n_d)$. The midnight-to-midnight temperature differences are obtained by a random process, which values have Gaussian distribution with the following mean value:

$$\Delta\overline{T}_{mm}(n_d) = \begin{cases} -0.01 + 0.05\sin\left[(n_d - 288)\dfrac{360}{365}\right], & H < 0.4H_0 \\ 0, & 0.4 \le H \le 0.8H_0 \\ 0.02 - 0.06\sin\left[(n_d - 288)\dfrac{360}{365}\right], & H > 0.8H_0 \end{cases} \qquad (2)$$

and the following standard deviation:

$$\sigma_{Tmm}(n_d) = 1 + \left\{2 + 2\sin\left[(n_d - 288)\frac{360}{365}\right]\right\}\sin^2(2\varphi) \qquad (3)$$

where: $n_d$ is the number of the day in the year, $H$ is the total daily global solar radiation on a horizontal surface, $H_0$ is the total daily extraterrestrial solar radiation on a horizontal surface, $\varphi$ is geographical latitude of the location.

The midnight-to-midnight temperature difference is assumed that linearly changes over the course of a day. Thus, the hourly temperature change for hour $h$ is:

$$\Delta T_{mm}(n_d, h) = \frac{h}{24}\Delta T_{mm}(n_d) \qquad (3)$$

### 2.3. Constraints and adjustments

Having in mind, that the generation process of hourly temperature time series depends on random numbers, it should be kept stabile and realistic under all possible conditions. This is done by application of few constraints and adjustments.

The first is month-to-month transition constrain. It is applied by superposing, to the generated temperature values, a supplementary midnight-to-midnight temperature trend $\Delta T_{sup}(h)$ during the first day of the month. With this trend is avoided, the midnight temperature difference between the first and the second day in the month $T_{mid}(1)$, to be higher than 4 °C from the monthly average temperature $\overline{T}_m$, i.e.:

$$\Delta T_{sup}(h) = \begin{cases} \frac{h}{24}\left(\overline{T}_m - 4 - T_{mid}(1)\right), & T_{mid}(1) < \overline{T}_m - 4 \\ 0, & \overline{T}_m - 4 \le T_{mid}(1) \le \overline{T}_m - 4 \\ -\frac{h}{24}\left(T_{mid}(1) - \overline{T}_m - 4\right), & T_{mid}(1) > \overline{T}_m + 4 \end{cases} \quad (4)$$

Other constrain relates to the average daily temperature values. These values should not deviate more than 10 °C from the monthly average temperature. If such value occurs, the process of generation starts over from the beginning of the month.

Also, the hourly temperature values are limited with minimum and maximum values around the monthly average temperature. These values are site dependent and they were extracted from long-term (more than 10 years) analyses of worldwide range of weather stations. Also, after occurring such value, the generation process starts over from the beginning of the month.

In temperate and cold climatic zones, in January and February, the generated minimum temperature data had been observed to be higher from the measured data. For that reason, so called "cold weather outbreaks", in the generation process within these months, are implemented. The outbreaks are applied by superposing a supplementary daily trend. The duration of the outbreaks is set to 4 days. The daily trend for the first day is another conversion factor, which has a negative value for the first day. In the second day, the daily trend is assumed to be 1/2 from the trend in the first day, and the third and fourth day the supplementary trend is –1/2 from the first day (it has a positive value). The appearance of the cold weather outbreaks is implemented as random event. For any single day, its probability is set to 5 %, so that in the first two months in the year the probability of appearance of cold weather outbreak is about 95 %. If no outbreaks are to happen up to the end of February, the generation process introduces one within these months, with a randomly chosen starting day.

The average value of the generated monthly temperature profiles should not deviated more than 4 °C than the monthly mean temperature. If this happen the generation process starts over from the beginning of the month. Otherwise all temperatures of the monthly profile are adjusted, so that the monthly average of generated temperature profile have exactly the same value as the monthly mean of the measured data. The adjustment is done in a way that all generated values are increased or decreased by the difference between the generated and measured monthly mean value. This may lead to a discontinuity at the beginning of the month. If the discontinuity is greater than 4 °C, the last two hours of the preceding month and the first two hours of the considered month are smoothed.

### 2.4. Location specific conversion factors and constraints

The generation process of hourly temperature time series, requires a number of conversion factors. They depend on the climatic sub-zone characteristics of the location and the period in the year. In [7] is given a review of climatic sub-zones. According to the meteorological and geographical characteristics the locations with similar characteristics belong to a same climatic sub-zone. In [7] are also given the conversion factors and some constraints for each corresponding climate sub-zone. Their values were extracted from long-term meteorological data analyses for a wide range of locations.

## 3. Validation of the model

The hourly time series of the global solar radiation on a horizontal surface and the ambient temperature, are measured for a period of 20 consecutive months. The measurements of the hourly solar radiation and the ambient temperature data, used for this paper, were measured at the Solar Energy Laboratory at the Faculty of Electrical Engineering and Information Technologies, University "Ss. Cyril and Methodius" in Skopje [14]. Within this period, due to technical problems, in the measured time series appeared several gaps. Since a continuum for at least the whole month is required for generation of the ambient temperature time series, there were successfully extracted months with uninterrupted time series. Hence, the generation of temperature time series was possible for the whole year.

***Table 1.*** *Conversion factors and constraints for a temperate elevated continental climate [7]*

| Month | I | II | III | IV | V | VI | VII | VIII | IX | X | XI | XII |
|---|---|---|---|---|---|---|---|---|---|---|---|---|
| Min. from average (°C) | -26 | -23 | -24 | -18 | -15 | -15 | -13 | -14 | -16 | -18 | -20 | -25 |
| Max. from average (°C) | 16 | 20 | 20 | 20 | 18 | 17 | 15 | 16 | 17 | 17(**20**) | 15 | 16 |
| Smoothing interval (h) | 7 | 7 | 8 | 9 | 9 | 9 | 9 | 9 | 9 | 8 (**9**) | 8 | 7 |
| Time displacing (h) | 2 | 2 | 3 | 3 | 3 | 3 | 3 | 3 | 3 | 3 | 2 | 2 |
| Stretching factor $\left(^{\circ}C/_{Wm^2}\right)$ (from the climatic sub-zone) | 0.028 | 0.026 | 0.024 | 0.021 | 0.017 | 0.016 | 0.015 | 0.018 | 0.022 | 0.025 | 0.027 | 0.028 |
| Stretching factor $\left(^{\circ}C/_{Wm^2}\right)$ (from the measured data) | 0.023 | 0.027 | 0.019 | 0.020 | 0.019 | 0.019 | 0.019 | 0.022 | 0.023 | 0.025 | 0.028 | 0.027 |

Skopje with its latitude of 42°N, longitude of 21.2°E, altitude of 250 m and other characteristics belongs to a temperate elevated continental climate sub-zone. The conversion factors and extreme temperature constraints for this climatic sub-zone are given in Table 1.

The measured data show a minor deviation from the characteristic values for the mentioned sub-zone. Namely, in October the maximal hourly temperature appeared to be 20 °C higher than the average. Also, for this month, the generation process shows that the smoothing interval is suitable to be 9. The reduction factor is taken to 1.15. The values of the stretching factor are given at the Tab. 1. Their values are close to those declared for the climatic sub-zone. The conversion factors with these corrections were used in further testing of the model's validation. A supplementary daily trend for cold weather outbreaks in January and February, for this climatic sub-zone, is –14.4 °C.

For the model validation, the generated and the measured temperature time series were compared. Despite the strong correlation between the solar radiation and the temperature, the ambient temperature has also a stochastic component. For that reason, the validation was done by comparing of some important parameters of time series. Since there were no long-term measured hourly time series of temperature and corresponding hourly time series of solar radiation, deeper statistical analyses could not have been done. Hence, some issues are subjectively assessed.

The monthly average temperature values are model's input. As was explained, the model adjusts the generated time series to have these monthly mean values. So, this parameter is automatically correct.

In Fig. 1, the hourly profiles of the measured and the generated time series for two months (June and January) are shown. As it can be seen, the generated time series fairly good follow the hourly variations of the temperature. Still, it is evident that the deviation of generated from the measured data is larger in January than in June. However, there is a good matching of the average hourly values from the generated and measured time series, which can be noted from the average daily temperature profiles given in Fig. 2. Nevertheless, there is a discrepancy between the average extreme (minimal and maximal) hourly values of the generated and measured data. Namely, the minimal hourly average of generated data is higher than the measured for 4 % for January and December, around 11 % for May, June, July and August, up to 16 % for March, from the measured average temperature amplitude.

The average daily temperature values of the measured (the thick line) and the generated values from five generating runs (other lines), for January and July, are given in Fig. 3. It can be seen that generating runs may differ, but still they are in reasonable limits. Larger deviations from the measured values are observed in winter months.

The distribution of measured and generated (5 runs) hourly temperature values are given in Fig. 4. There were also analyzed the generated (5 runs) minimal and the maximal temperature values (Fig. 5). The solid line represents the constraints imposed by the model. These values are obtained by appending the minimal and maximal temperatures (Table 2) to the monthly average temperature the values. Slight exceeding from these values is allowed after the adjustment to the monthly average temperature. The differences in minimal and maximal generated and measured exist because to the generation process are imposed the limits from the climatic sub-zone.

There were analyzed midnight-to-midnight temperature differences (Fig. 6). The average temperature difference is well reproduced for all months, while the standard deviation is acceptable for most months. The difference between standard deviation from the measured and the generated time series is higher for January, February, November and December.

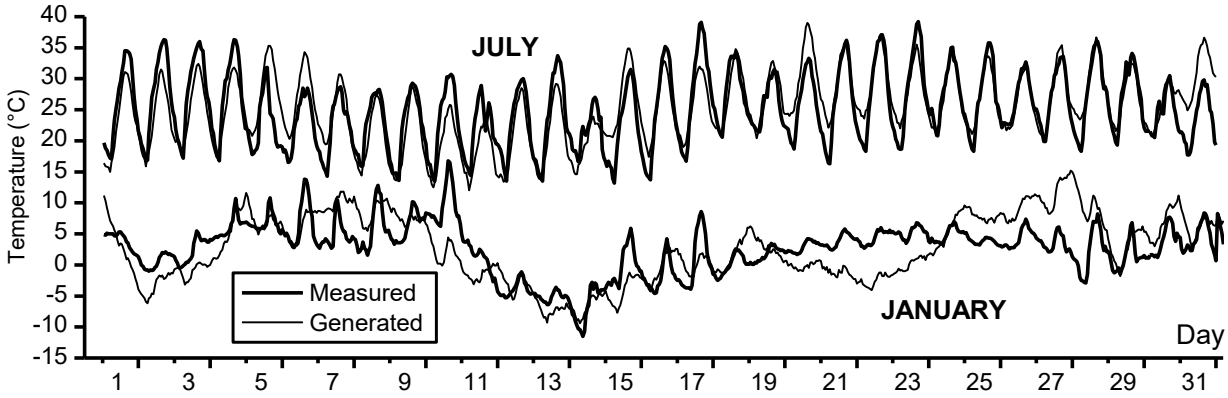



***Fig. 1.*** *Measured and generated hourly temperature values for June and January*

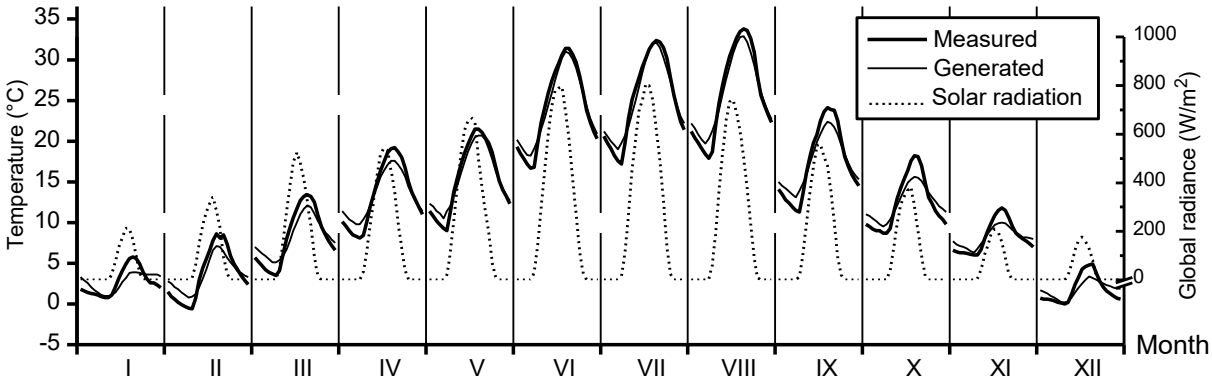



***Fig. 2.*** *Measured and generated daily average temperature daily profiles*

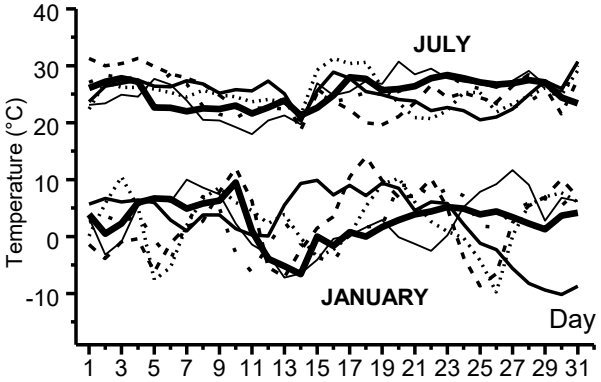



***Fig. 3.*** *Measured and generated average daily temperature values for Jul and January*

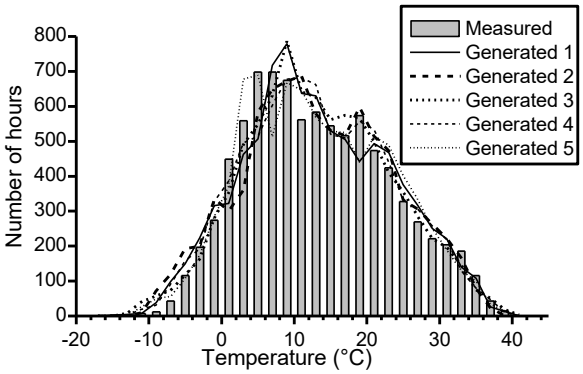



***Fig. 4.*** *Distribution of hourly values of measured and generated time series*

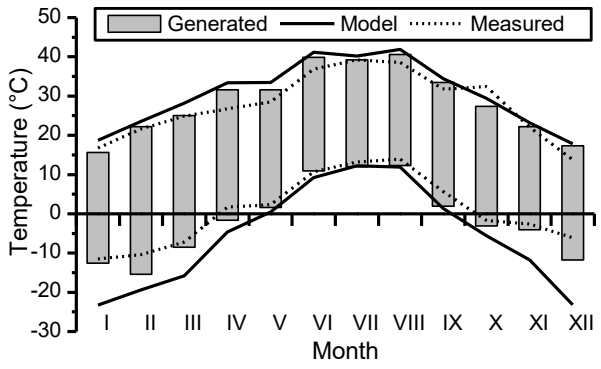



***Fig. 5.*** *Minimal and maximal hourly temperature values*

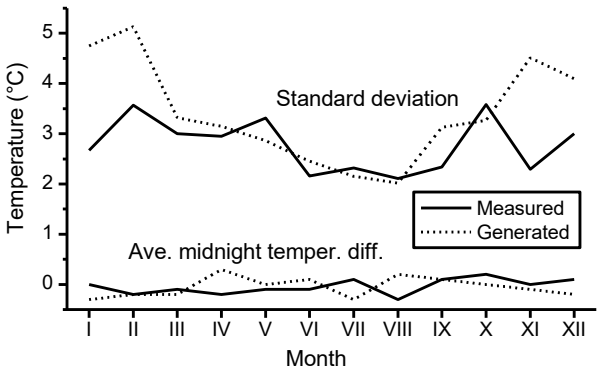



***Fig. 6.*** *Average and standard deviation of the midnight -to-midnight temperature differences*

## 4. Conclusion

In this paper the updated Scartezzini's model for generation of the hourly temperature values was elaborated. It was tested its validation for the region of Skopje. There were analyzed a number of parameters that are relevant for its assessment. The conclusions and remarks from this paper are very likely to be valid for locations with similar climatic characteristics as Skopje.

The comparing of the generated and measured temperature time series shows that the shapes of the generated temperature daily profiles were well represented. The deviations from the measured values were expected due to use of random components. However, it was evident that the amplitudes of the average hourly profiles of the generated time series are lower than the generated. In winter this deviation is unacceptably high and this is the weakest point of the model. This is likely because the generation process in winter months is very unstable and it is easy to get out of control. This probably may be improved by adding additional constraints, which likely can be identified from long-term measured data.

The distribution of generated hourly temperature values was generally acceptable. The hourly values of generated time series were within allowed minimal and maximal limits. The average midnight-to-midnight temperatures were well represented. The standard deviation of these values for summer months is good, but in winter months these values differ from the measured time series.

## REFERENCES


1. C. S. Chen et al., (1996). Determination of Customer Load Characteristics by Load Survey System at Thaipower. *IEEE Transactions on Power Delivery*, Vol. 11, No. 3, pp. 1430-1436,
2. D Dimitrov, V Glamocanin, J Pop-Jordanov, D Andonov, (1997). Simulated evaluation of grid-support photovoltaic systems regarding distribution loss reduction. Part 1: Contributions. CIRED. *14th International Conference and Exhibition on Electricity Distribution*, IEE Conf. Publ. No. 438.
3. D. Dimitrov, K. I. Kocev. (2002). An Approach to Assessment of the Power Loss Reduction in Distribution Networks with a Grid-Connected Photovoltaic System. *3rd Mediterranean Conference and Exhibition on Power Generation, Transmission, Distribution and Energy Conversion – MEDPOWER 2002, Athens, Greece*.
4. T. Markvart. (1994). *Solar Electricity*, John Wiley and Sons.
5. K. M. Knight, S. A. Klein, J. A. Duffie. (1991). A Methodology for Synthesis of Hourly Weather Data. *Solar Energy*, Vol. 46, No. 2, pp. 109-120, Elsevier Science.
6. D. Heinman, J. Schumacher. (1996). Synthesis of Hourly Ambient Temperature Time Series Correlated with Solar Radiation, *2nd ISES Europe Solar Congress, EuroSun'96*, Freiburg, Germany,
7. J. Remund, S. Kunz. (1997). *METEONORM, Global Meteorological Database for Solar Energy and Applied Climatology Version 3*. METEOTEST, Bern, Switzerland,
8. J.-L Scartezzini, M. N. Ferguson and F. Bochud. (1990). *Compression of multi-year meteorological data, Final Report*. OFEN Project EF-REN (90)009, Solar Energy and Building Physics Laboratory, Department of Architecture, Swiss Federal Institute of Technology, Lausanne, Switzerland.
9. J. Remund, S. Kunz. (2003). *METEONORM: Global Meteorological Database for Engineers, Planners, and Education, Version 5*. METEOTEST, Bern, Switzerland,
10. Project, "SoDa", DG "INFSO" IST-1999-12245, http://www.soda-is.com/. (last visited February 2016)
11. R. Aguiar, M. Collares-Pereira. (1992). TAG: A Time-Dependent, Autoregressive, Gaussian Model for Generating Synthetic Hourly Radiation. *Solar Energy*, Vol. 49, No. 3, pp. 167-174, Elsevier Science.
12. V. A. Graham, K. G. T. Hollands, (1990), "A Method to Generate Synthetic Hourly Solar Radiation Globally", Solar Energy, Vol. 44, No. 6, pp. 333-341, Elsevier Science,
13. "Providing information on Solar Radiation", http://www.helioclim.org/. (last visited February 2016)
14. D. Dimitrov, V, Stoilkov, A. Iliev. (2012): Solar Energy Labaratory – Summary of Ten Years Continous Experience, *Renewable Energy & Power Quality Journal*, No.10, ISSN 2172-038X.



University "Ss. Cyril and Methodius"
Faculty of Electrical Engineering & IT
Karpos bb, P.O. Box 574
1000 Skopje
Macedonia
E-mail: ddimitar@ feit.ukim.edu.mk
E-mail: ailiev@feit.ukim.edu.mk
E-mail: ailiev@feit.ukim.edu.mk

© International Scientific Conference on Engineering, Technologies and Systems
TECHSYS 2016, Technical University – Sofia, Plovdiv branch
26 – 28 May 2016, Plovdiv, Bulgaria

# МОДЕЛ НА МОНОФАЗЕН ДВУРОТОРЕН АКСИАЛЕН ГЕНЕРАТОР С РЕДКОЗЕМНИ МАГНИТИ

НИКОЛА ГЕОРГИЕВ

**Резюме:** *Изследва се монофазен синхронен шестнадесет полюсен генератор с аксиално магнитно поле и редкоземни магнити. Генераторът се състои от два ротора с по шестнадесет редкоземни магнита и един статор с дванадесет намотки. Съставена е еквивалентната магнитна верига на генератора. Извършена е симулация в приложението Schematics на OrCAD, като са изчислени основният магнитен поток и магнитните потоци на разсейване. С помощта на основния магнитен поток е пресметнато индуктираното фазово е.д.н. в една намотка, като са отчетени броят на навивките, чифтовете полюси на генератора, оборотите му и максималната стойност на магнитния поток. С помощта на получения израз за ефективната стойност на фазовото е.д.н. са пресметнати фазовите напрежения на генератора при режим на празен ход, както и мощността консумирана при активен товар. Направени са експериментални изследвания на изходните електрически параметри на разглеждания монофазен генератор в режими на празен ход и при активен товар. Сравнени са изходни характеристики получени от модела с тези от извършените експериментални измервания.*

**Ключови думи:** *монофазен синхронен генератор, аксиално магнитно поле, редкоземни магнити, модел*

# A MODEL OF A SINGLE-PHASE TWO-ROTOR AXIAL GENERATOR WITH RARE EARTH MAGNETS

NIKOLA GEORGIEV

**Abstract:** *This paper makes a study of a single-phase synchronous 16-pole generator with axial magnetic field and rare earth magnets. The generator consists of two rotors with sixteen rare earth magnets each and one stators with twelve windings. An equivalent magnetic circuit of the generator has been given. A simulation has been realized in the application Schematics (OrCAD), the main magnetic flux and the magnetic fluxes of dissipation have been calculated. The induced phase e.m.f. in one winding has been calculated by means of the main magnetic flux, taking into account the number of windings, the pole pairs of the generator, its revolutions per minute and the maximum value of the magnetic flux. Both the phase voltages of the generator at idle running and the power consumption at active load have been calculated with the help of the obtained expression for the r.m.s. value of the phase e.m.f. Experimental studies of the output electrical parameters of the considered single-phase generator at idle running and active load have been conducted. The output characteristics, obtained from the model, have been compared to those, from the experimental measurements.*

**Key words:** *single-phase synchronous generator, axial magnetic field, rare earth magnets, model*

Copyright © 2016 by Technical University of Sofia, Plovdiv branch, Bulgaria ISSN Online: 2535-0048

## 1. Introduction

Generators with NdFeB rare earth magnets have a simple and reliable construction and high power per unit of weight. The absence of both an excitation winding and current results in high efficiency in operation [1].

Initially the generators were made mostly with ferrite and alnico magnets, having significantly lower energy. The basic structure of the generators with axial magnetic field was unilateral: with a rotor and a stator and the bilateral structures appeared only recently – either with one rotor and two stators or with two rotors and a stator [2].

Paper [3] considers a single-phase generator, which is bilateral with two rotors and a stator, for which the flux linkage has been calculated by the finite elements method and then the r.m.s. value of the phase e.m.f has been defined. Similar are the models in [4], where the magnetic flux and the instant value of the e.m.f. have been calculated; and in [5], where the r.m.s. value of the stator e.m.f. has been defined.

This paper studies and models in Schematics (OrCAD) environment a low-power single-phase synchronous generator with axial magnetic field and rare earth magnets, consisting of two rotors and a stator.

## 2. Exposition

The considered single-phase axial generator consists of two rotors with sixteen rare earth magnets each and a stator with twelve windings connected in series.

Fig. 1 shows the construction scheme of the considered two-rotor single-phase generator with a view from the left, in which the following notations are used: by 1 the aluminum stator is denoted; 2 is the stator winding, 3 – the steel rotors; 4 – the rare earth magnets; and 5 is the shaft, driving the rotors.

In order to make an equivalent magnetic circuit it is necessary to define the e.m.f. $F$ and the equivalent magnetic reluctance $R_{\mu M}$ for one of the rare earth magnets [1]

$$F = R_{\mu M}.\Phi_r \,, \quad R_{\mu M} = \frac{l_M}{\mu_0.\mu_r.S_M} \quad , \tag{1}$$

where $l_M$ is the length of the average magnetic line of force through the magnet; $\mu_r$ and $\mu_0$ are the relative magnetic permeability and the air permeability, respectively, while $S_M$ is the cross-section of the magnet.

The magnetic flux in case of a short magnetic circuit can be calculated by means of the residual magnetic induction $B_r$ [1]

$$\Phi_r = B_r.S_M \quad . \tag{2}$$

Thus the equivalent circuit of the rare earth magnet is obtained.

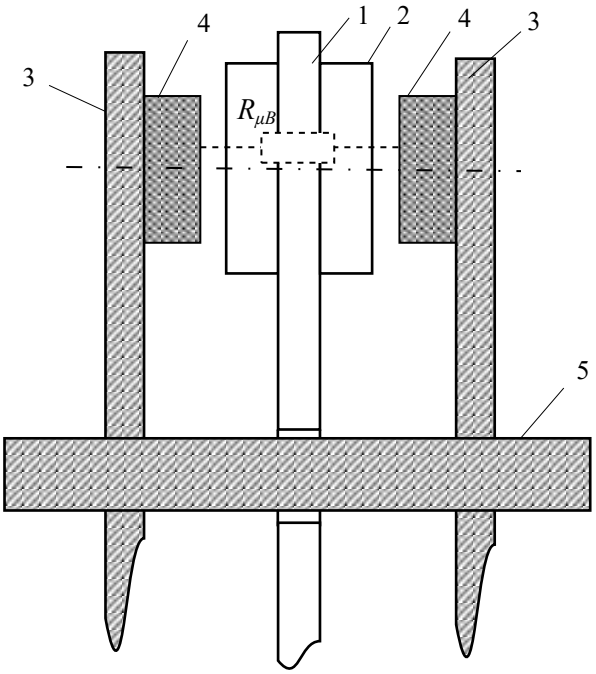



***Fig. 1.*** *Construction scheme of the two-rotor single-phase generator, a view from the left*

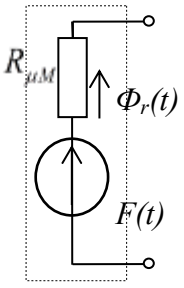



***Fig.2.*** *Equivalent circuit of the rare earth magnet*

Fig. 3 presents the equivalent magnetic circuit of the single-phase generator. $R_{\mu B}$ and $R_{\mu CT}$ represent the magnetic reluctances of the air gap and of the steel rotors. By means of the magnetic reluctance $R`_{\mu B}$ the losses from the dissipation of the magnetic flux between two neighboring magnets are defined, while $R``_{\mu B}$ shows the losses from the dissipation between the corresponding magnet and rotor

$$R_{\mu B} = \frac{l_B}{\mu_0 . S_B}, \quad R_{\mu CT} = \frac{l_{CT}}{\mu_0 . \mu_r . S_{CT}},$$
$$R'_{\mu B} = \frac{l'_B}{\mu_0 . S'_B}, \quad R''_{\mu B} = \frac{l''_B}{\mu_0 . S'_B}, \qquad (3)$$

where $l_B$, $l`_B$, $l``_B$, $l_{CT}$ are the lengths of the average magnetic lines of force through the air gaps and of the steel rotors, while $S_{CT}$ , $S_B$, $S`_B$, $S``_B$ are the cross-sections of the steel rotors and the air gaps.

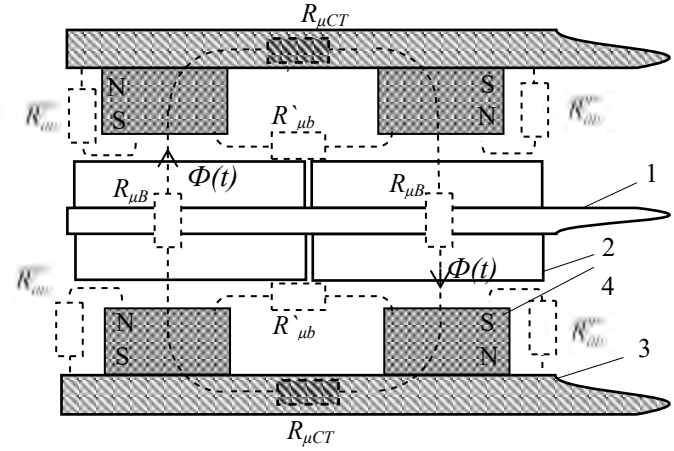



***Fig. 3.*** *Equivalent magnetic circuit*

By means of the equivalent magnetic circuit from Fig. 3, the full equivalent magnetic circuit of the single-phase generator is obtained - Fig. 4.

After calculating the magnetomotive voltages and the magnetic reluctances by (1), (2) and (3) and realizing a simulation in the application Schematics (OrCAD), the magnetic fluxes in the generator are obtained. In this case electromagnetic analogy is used, in which the sought magnetic fluxes correspond to the currents in the electric circuits. Therefore the dimensions of the calculated magnetic fluxes are in microamperes, not in microwebers - Fig. 5.

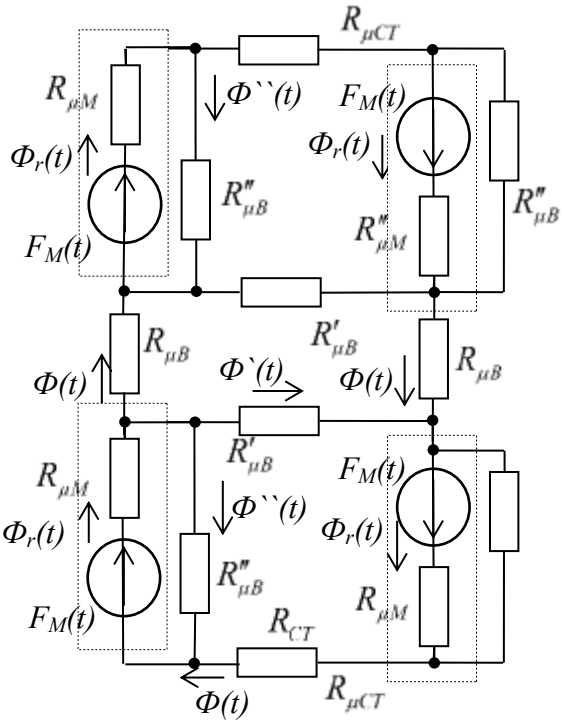



***Fig. 4.*** *Full equivalent magnetic circuit*

The performed simulation shows that 68% of the magnetic flux, created by the permanent magnets $\Phi_r(t)$ goes through the two coils of the single-phase generator $\Phi(t)$, and the remaining 32% are dissipation fluxes. The bigger dissipation flux is the one between two neighboring magnets $\Phi`(t)$, which is 59% from the losses. The smaller $\Phi``(t)$ (41%) is the magnetic flux of dissipation between the corresponding magnet and rotor.

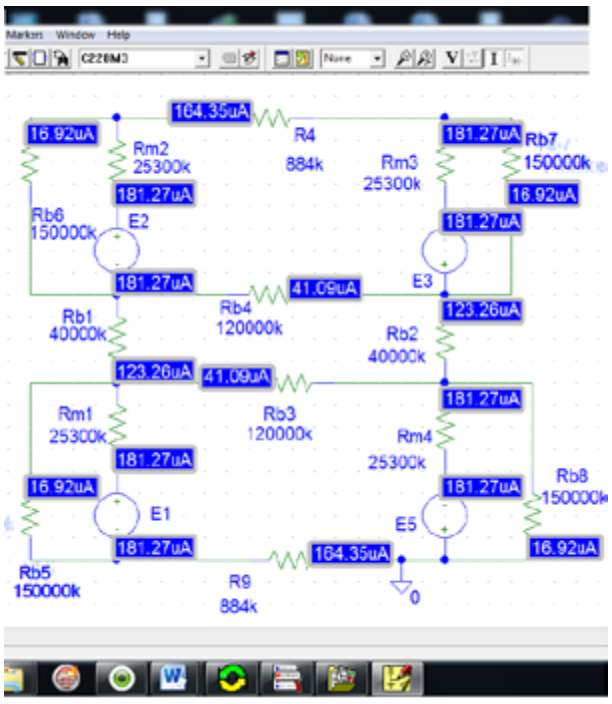



***Fig. 5.*** *Simulation scheme in Schematics*

By means of the calculated magnetic flux, going through the two windings of the single-phase generator $\Phi_m$=0,123 mWb, the r.m.s. value of the induced e.m.f. in one stator winding of the generator can be calculated

$$E_1 = \frac{\omega.W}{\sqrt{2}}\Phi_m \quad . \tag{4}$$

After expressing the circular frequency by means of the revolutions per minute and the number of pole pairs, it is obtained

$$\omega = \frac{2.\pi.p}{60}n \quad , \tag{5}$$

$$E_1 = \frac{W}{\sqrt{2}}\frac{2.\pi.p}{60}n.\Phi_m \quad . \tag{6}$$

Since the single-phase generator has 12 stator windings, connected in series, the full r.m.s. value of the phase e.m.f. is equal to

$$E_{12} = \frac{12.W}{\sqrt{2}}\frac{2.\pi.p}{60}n.\Phi_m \quad . \tag{7}$$

The formula, obtained this way, takes into account the number of turns in the stator winding, the number of generator poles and of the stator windings, the revolutions per minute and the maximum magnetic flux, going through one of the stator windings of the generator with rare earth magnets.

After using (7), the phase e.m.f. of the generator at idle running can be calculated. The equivalent electric circuit at idle running in a complex effective form is presented in Fig. 6, where by $R_{12}$ and $L_{12}$ the active resistance and the inductivity of the 12 stator windings are denoted respectively.

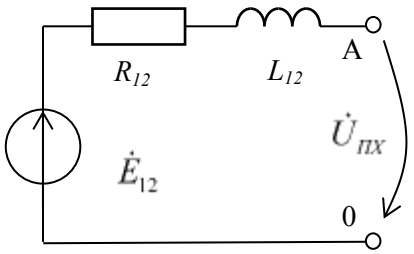



***Fig. 6.*** *Equivalent electric circuit at idle running*

In this case the r.ms.value of the phase voltage at idle running is equal to the phase e.m.f. of the generator

$$U_{ПХ}=E_{12} \quad . \tag{8}$$

Table 1 and Fig. 6 present the r.m.s. values of the calculated by the model phase voltage at idle running of the generator, and the measured phase voltage within a range of revolutions per minute from 0 до 1000 min$^{-1}$.

***Table 1.*** *Phase voltage, calculated by means of the model and measured experimentally*

| $n$, min$^{-1}$ | 0 | 200 | 400 | 600 | 800 | 1000 |
|---|---|---|---|---|---|---|
| $U_{mod}$, V | 0 | 23,1 | 42,4 | 68,3 | 89,2 | 122,2 |
| $U_{meas}$, V | 0 | 24,6 | 49,2 | 73,8 | 98,4 | 123 |

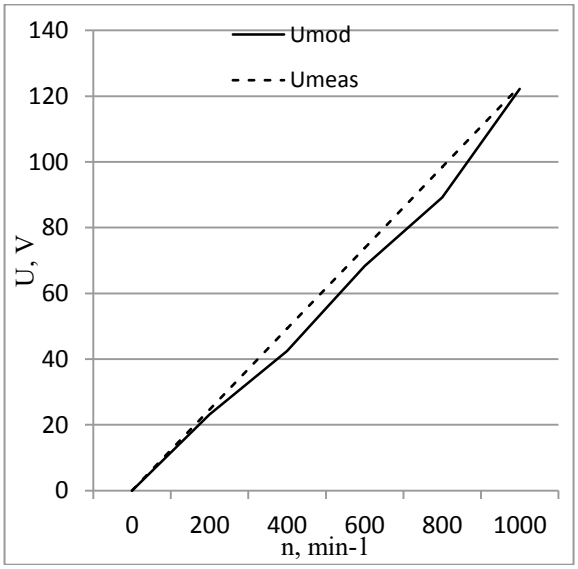



***Fig. 7.*** *Calculated by the model and measured in experiments phase voltage at idle running*

The maximum relative and fiducial errors for the voltages at idle running are correspondingly $\delta_{max}$=9,3% and $\gamma_{max}$=7,5%.

By using (7), the phase e.m.f. at active load can be calculated. In this case the active load resistance $R_T$ is also added to the equivalent electric circuit in a complex effective form - Fig. 8.

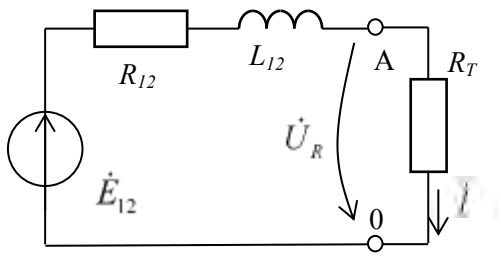



***Fig. 8.*** *Equivalent circuit at active load*

The r.m.s. value of the phase current is obtained by means of Kirchhoff's second law

$$I = \frac{E_{12}}{\sqrt{\left(R_{12} + R_T\right)^2 + \left(\omega.L_{12}\right)^2}} \quad . \qquad (9)$$

Thus the r.m.s. values of the voltage on the active load can be defined, as well as the active power, consumed by it

$$U_R = R_T I \quad , \quad P = U_R.I \quad . \qquad (10)$$

Table 2 and Fig. 6 give the r.m.s. values of both the calculated by the model and measured active power at active load of 5 Ω for revolutions per minute from 0 до 1000 $min^{-1}$.

***Table 2.*** *Calculated by means of the model and measured in experiments active power*

| $n$, $min^{-1}$ | 0 | 200 | 400 | 600 | 800 | 1000 |
|---|---|---|---|---|---|---|
| $P_{mod}$, W | 0 | 21,2 | 72,4 | 169,5 | 262,1 | 377,2 |
| $P_{meas}$, W | 0 | 19,2 | 67,7 | 161,3 | 253,5 | 363,1 |

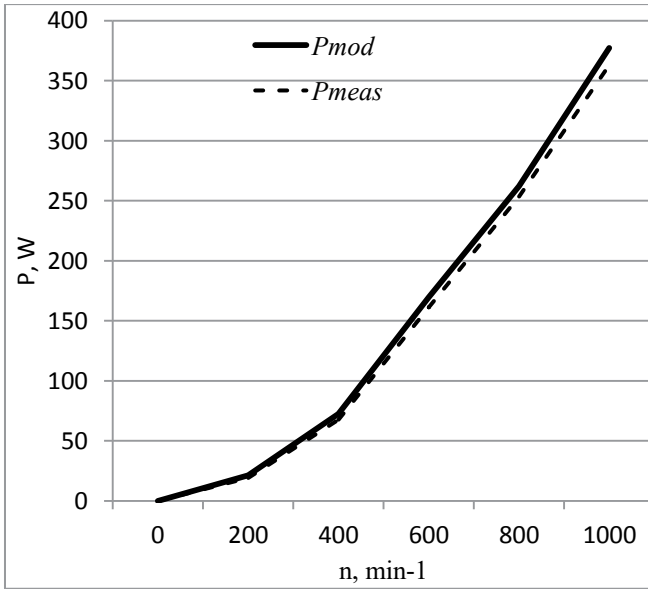



***Fig. 9.*** *Calculated and measured active power at active load $R_T$ =5Ω*

The maximum relative and fiducial errors for the voltages at active load $R_T$ =5Ω are correspondingly $\delta_{max}$=3,9% and $\gamma_{max}$=3,9%.

## 3. Conclusion

The following conclusions can be drawn based on the presented theoretical derivation, software simulation and experimental studies:

1. An equivalent magnetic circuit of the single-phase generator has been made, where the equivalent circuits of the rare earth magnets, the magnetic reluctances of the air gaps, the steel stator and the shaft have been taken into account. The magnetic reluctances, taking into consideration the losses from the dissipation of the magnetic flux between two neighboring magnets and between the corresponding magnet and the rotor have also been included in this circuit.

2. Electromagnetic analogy has been used and a simulation in the software application Schematics (OrCAD) has been realized, wherein the basic magnetic flux and the magnetic fluxes of dissipation have been calculated.

3. By means of the calculated basic magnetic flux, the induced e.m.f. in one winding has been calculated and then the phase voltage at idle running has been obtained.

4. An expression for the r.m.s. value of the phase e.m.f. has been obtained, in which the number of windings, of the pole pairs and of stator windings of the generator have been taken into account, as well as the number of its revolutions per minute and the maximum value of the magnetic flux in the middle of the corresponding winding.
5. The obtained model simulates with good precision the work of the studied single-phase generator with rare earth magnets, wherein the maximum relative and fiducial errors for the phase voltages at idle running are respectively $\delta_{max}$=9,3% and $\gamma_{max}$=7,5%, while for the power at active load they are correspondingly $\delta_{max}$=3,9% and $\gamma_{max}$=3,9%.
6. In order to reduce the maximum relative and fiducial errors, it is necessary to take into consideration both the asymmetries in the process of making the prototype of the generator, and the chatter from the rotation of the rotor.

**REFERENCES:**

[1] Mohammad, M. Sc. and Widyan, S. (2006). *Optimization, Construction and Test of Rare-Earth Permanent-Magnet Electrical Machines with New Topology for Wind Energy Applications,* 17-22. Fakultät IV –Elektrotechnik und Informatik der Technischen Universität, Berlin.

[2] Aritz, E. (2013). *Overview of Axial Flux Machines*. Electric Energy Magazine №4, Spain.

[3] Wang, R. and Kamper, M. (2005). *Optimal Design of a Coreless Stator Axial Flux Permanent-Magnet Generator*. IEEE Transactions on magnetics, vol. 41.

[4] Bolund, B. and Bernhoff, H. (2005). *Flywheel energy and power storage systems*. Renewable and Sustainable Energy Reviews.

[5] Wannakarn, P. and Kinnares, V. (2011). *Microcontroller based Grid Connected Inverter for Axial Flux Permanent Magnet Generator.* IEEE PEDS 2011, Singapore.

Department of Electrical Engineering
Technical University–Sofia, Branch Plovdiv
25 Tsanko Dystabanov St.
4000 Plovdiv
BULGARIA
E-mail: geotek@abv.bg

© International Scientific Conference on Engineering, Technologies and Systems
TECHSYS 2016, Technical University – Sofia, Plovdiv branch
26 – 28 May 2016, Plovdiv, Bulgaria

# ИЗЧИСЛЯВАНЕ НА МАГНИТНАТА ИНДУКЦИЯ ВЪВ ВЪЗДУШНАТА МЕЖДИНА НА ТРИФАЗЕН ДВУРОТОРЕН АКСИАЛЕН ГЕНЕРАТОР С РЕДКОЗЕМНИ МАГНИТИ

НИКОЛА ГЕОРГИЕВ

**Резюме:** *Извежда се формула за изчисляване на магнитната индукция в определена точка от въздушната междина, на двуроторен, аксиален, трифазен генератор с редкоземни магнити. С помощта на получената формула за магнитната индукция се изчислява основния магнитен поток, който преминава през намотките на статора. Така се пресмята и индуктираното е.д.н. в една намотка, а от там се получават фазовите електродвижещи напрежения и фазовите напреженията на трифазния генератор с аксиално магнитно поле, в режим на празен ход. Направени са експериментални изследвания на фазовите напрежения в режими на празен ход, които са сравнени с изчислените. Изчислената максимална магнитна индукция с предлаганата формула е сравнена компютърна програма изчисляваща също максималната индукция в точка от въздушната междина на двуроторен генератор.*

**Ключови думи:** *магнитна индукция, трифазен синхронен генератор, аксиално магнитно поле, редкоземни магнити, празен ход*

# CALCULATING MAGNETIC INDUCTION IN THE AIR GAP OF A THREE-PHASE TWO-ROTOR AXIAL GENERATOR WITH RARE EARTH MAGNETS

NIKOLA GEORGIEV

**Abstract:** *A formula for calculating the magnetic induction in a definite point of the air gap of a two-rotor axial three-phase generator with rare earth magnets has been derived. By means of the obtained formula the main magnetic flux, going through the windings of the stator, has been found. Thus the induced e.m.f. in one winding has also been calculated, from where the phase e.m.f. and the phase voltages of the three-phase generator with axial magnetic field have been obtained for the mode of idle running. Experimental studies of the phase voltages at idle running have been conducted and the results have been compared with the calculated values. The calculated by the proposed formula maximum magnetic induction has been compared with the result, obtained by means of a computer program, also calculating the maximum induction in a point of the air gap of a two-rotor generator.*

**Key words:** *magnetic induction, three-phase synchronous generator, axial magnetic field, rare earth magnets, idle running*

Copyright © 2016 by Technical University of Sofia, Plovdiv branch, Bulgaria ISSN Online: 2535-0048

## 1. Introduction

Axial generators with rare earth /NdFeB/ magnets, having power of up to 3 kW, are frequently used in practice due to: their simple, reliable and easy to produce construction, the lack of excitation winding and current, resulting in high efficiency in operation [1].

The magnetic attraction between the rotor and the stator is avoided in these generators and thus the resistive moment is reduced. These machines are much more efficient than the ones with radial magnetic field due to the lack of losses in the core [2].

In order to obtain the basic electrical parameters of the axial generators with permanent magnets, it is necessary to calculate the magnetic induction in the air gap. Under "air gap" the distance between the magnets of the rotor and the stator is understood for one-rotor type of generators, and between the magnets of the two rotors for two-rotor axial generators.

Paper [4] presents a formula for calculation of magnetic induction in a definite point of the air gap for a two-rotor axial generator with permanent magnets, in which the residual induction for the two magnets, as well as their dimensions, have been taken into account.

This paper derives a formula for calculating the magnetic induction in a particular point of the air gap in a two-rotor axial three-phase generator with rare earth magnets, taking into consideration the residual magnetic induction of the two magnets, their geometrical dimensions and the magnetic permeability of the air gap.

By means of the obtained formula for calculating the magnetic induction in a definite point of the air gap, the main magnetic flux, going through the stator windings is also calculated. Thus the induced e.m.f in one winding is found and thence the phase voltage of a three-phase, two-rotor, synchronous, 16-pole generator with axial magnetic field at idle running is obtained.

## 2. Exposition

The considered three-phase axial generator consists of two rotors with 16 rare earth magnets and 12 windings each, connected in a star - four for a phase.

Fig.1 shows the construction scheme with a view from the left and a magnetic circuit of the considered two-rotor, three-phase generator, in which the following notations are used: 1 – the aluminum stator; 2 – a winding; 3 – the steel rotors; 4 – the rare earth magnets; and 5 – the shaft, driving the rotors.

The magnetic reluctance of the air gap $R_{\mu B}$, the magnetic reluctance, which takes into account the dissipation $R'_{\mu B}$, the magnetic reluctance of the rare earth magnets $R_{\mu M}$, and the magnetic reluctance of the steel stators and the shaft $R_{\mu CT}$ are presented in Fig. 1.

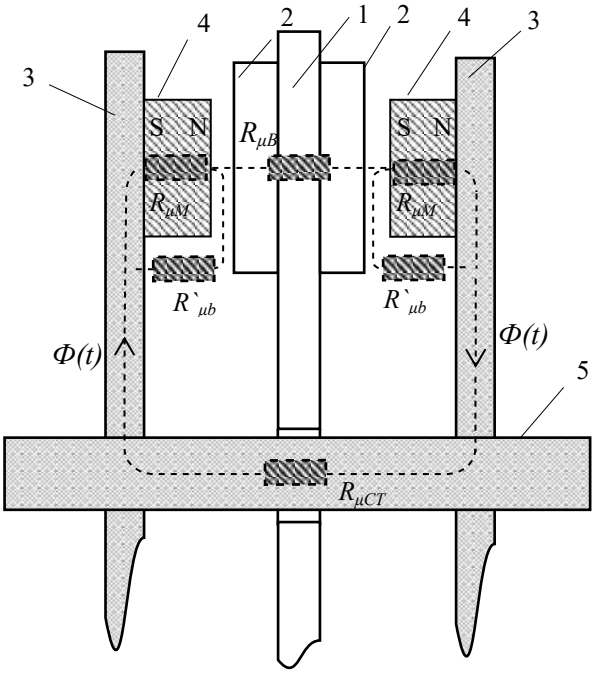



*Fig. 1. Construction scheme, a view from the left and magnetic circuit of the two-rotor three-phase generator*

For calculating the magnetic flux in the air gap, i.e., the one, going through one of the generator windings, the magnetomotive voltage $F$ and the equivalent magnetic reluctance $R_{\mu M}$ of one of the rare earth magnets are defined [1]

$$F = R_{\mu M}.\Phi_r \,, \quad R_{\mu M} = \frac{l_M}{\mu_0.\mu_r.S_M} \quad . \tag{1}$$

The magnetic flux in case of a short magnetic circuit can be found [1] in the following way

$$\Phi_r = B_r.S_M \quad , \tag{2}$$

and the magnetic reluctances of the air gap with the winding, of the steel and of the magnetic reluctance, which takes into account the dissipation, are

$$R_{\mu B} = \frac{l_B}{\mu_0 . S_B},$$
$$R_{\mu CT} = \frac{l_{CT}}{\mu_0 . \mu_r . S_{CT}},$$
$$R'_{\mu B} = \frac{l'_B}{\mu_0 . S'_B} \quad , \tag{3}$$

where:

$l_B$, $l_{CT}$, $l`_B$ are the lengths of the average magnetic lines of force through the air gap, the steel (the rotors and the shaft) and the fluxes of dissipation;

$\mu_r$ - the relative magnetic permeability;
$S_{CT}$ , $S_B$ , $S`_B$ – the cross-sections of the steel, of the air gap and the dissipation;
$B_r$ - the residual magnetic induction.

The equivalent magnetic circuit in an instant form at closing the magnetic flux, going through the shaft of the generator, is of the type.

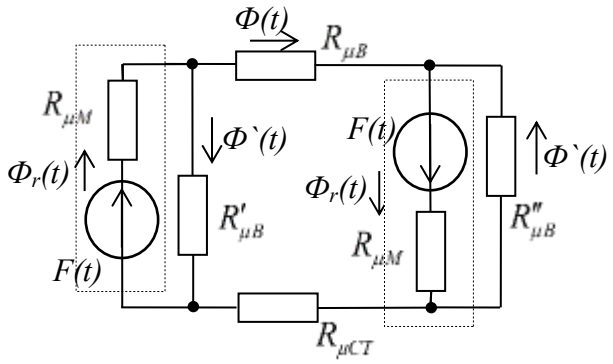



*Fig.2. Equivalent magnetic circuit*

By means of the magnetic reluctances $R`_{\mu B}$, the losses from the dissipation of the magnetic flux, created by the two magnets, are taken into consideration, but for a generator with two rotors and a small air gap they are much bigger and can be neglected. The magnetic reluctance $R_{\mu CT}$ can also be neglected since it is hundred times less than the one of the air gap in which the stator winding is located. Then the equivalent magnetic circuit is simplified in the following way:

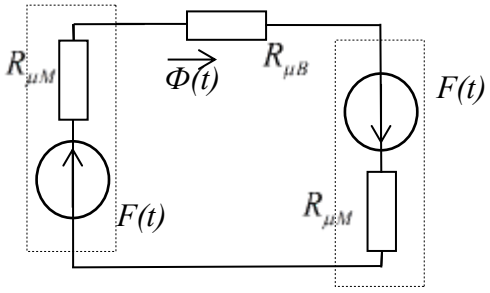



*Fig.3. Simplified magnetic circuit*

Using the obtained magnetic circuit – Fig.3 – and Kirchhoff's second law for magnetic circuits, it is found

$$\Phi(t) = \frac{2F(t)}{2R_{\mu M} + R_{\mu B}} \quad . \tag{4}$$

From the above expression the maximum value of the magnetic flux can be obtained

$$\Phi_m = \frac{2F_m}{2R_{\mu M} + R_{\mu B}} \quad . \tag{5}$$

The maximum value of the magnetic induction is equal to

$$B_m = \frac{\Phi_m}{S_B} = \frac{2F_m}{S_B\left(2R_{\mu M} + R_{\mu B}\right)} \quad . \tag{6}$$

By substituting (1), (2) into (6), it is obtained

$$B_m = \frac{2R_{\mu M} B_r S_M}{S_B\left(2R_{\mu M} + R_{\mu B}\right)} \quad ,$$
$$B_m = \frac{2B_r}{\frac{S_B}{S_M}\left(2 + \frac{R_{\mu B}}{R_{\mu M}}\right)} \quad . \tag{7}$$

After expressing the magnetic reluctances from (1) and (3), for the maximum value of the magnetic induction it is obtained

$$B_m = \frac{2.B_r}{2.\frac{S_B}{S_M} + \frac{l_B}{l_M}\mu_r} \quad . \tag{8}$$

In order to find the maximum value of the magnetic induction in any point $x$ of the air gap in the range from the surface of the magnet 0 to the middle of the air gap $l_B/2$, the above expression is changed in the following way

$$B_m = \frac{2.B_r}{2.\frac{S_B}{S_M} + \mu_r.\frac{l_B}{l_M}\left(1+\frac{x}{l_B}\right)} \quad . \tag{9}$$

The residual magnetic induction for the two magnets, the geometric dimensions of the magnets, their magnetic permeability and the magnetic reluctance of the air gap are taken into consideration by the obtained formula.

For the considered generator $l_B$=18 mm, $l_M$=10 mm, $x$=9 mm and $B_r$=1,2 T.

The table below gives the maximum induction for three points in the air gap of the generator, calculated both by the proposed formula and with the help of a computer simulation named "field calculator" [5].

***Table 1.*** *Maximum induction in three points of the air gap*

| $x$, mm | 5 | 7 | 9 |
|---|---|---|---|
| $B(x)$ , mT (Model) | 374 | 362 | 351 |
| $B(x)$ , mT ( Field Calc.) | 395 | 360 | 348 |

From Table 1 it can be seen that the maximum relative error is $\delta_{max}$=5,32%, and it is even smaller for the air gap $\delta_{max}$=0,86%. of the generator $x$=9. This confirms the adequacy of the proposed formula for calculating the maximum induction in any point $x$ in the air gap of a generator with permanent magnets.

By means of (9) the maximum value of the magnetic flux in the middle of the air gap can be found

$$\Phi_m = B_m.S_B = 139\,\mu Wb \quad . \tag{10}$$

The r.m.s. value of the induced e.m.f. in one winding with $W$ turns can be calculated by the following expression

$$E_1 = \frac{\omega.W}{\sqrt{2}}\Phi_m \, . \tag{11}$$

After expressing the circular frequency $\omega$ by means of the revolutions per minute $n$ and the number of pole pairs $p$, it is obtained

$$\omega = \frac{2.\pi.p}{60} n \, , \tag{12}$$

$$E_1 = \frac{W}{\sqrt{2}} \frac{2.\pi.p}{60} n.\Phi_m \, . \tag{13}$$

Since each phase consists of four stator windings, connected in series, then the full r.m.s. value of the phase e.m.f. is equal to

$$E_A = E_4 = \frac{4.W}{\sqrt{2}} \frac{2.\pi.p}{60} n.\Phi_m \quad . \tag{14}$$

Thus the final expression for the full r.m.s. value of the e.m.f. for the corresponding phase is obtained, in which the number of windings and of the pole pairs, as well as the maximum value of the magnetic flux in the middle of the corresponding stator winding have been taken into account.

Using (14), the phase voltages at idle running can be calculated (Fig. 4).

The r.m.s. value of the output voltage at idle running in this case is equal to the phase e.m.f. of the generator

$$U_{ПХ} = U_{AO} = E_A \quad . \tag{15}$$

Fig. 4 presents the electric circuit of the stator for phase A, wherein the phase active resistance $R_A$ and the inductive resistance $X_{LA}$ (expressed by the inductivity $L_A$) have not been taken into account at idle running.

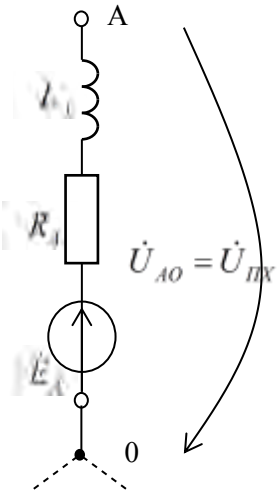



*Fig. 4. Electric circuit of phase A of the stator*

Table 2 and Fig. 5 present the r.m.s. values of both the calculated by the model phase voltage at idle running and the voltage, measured for the prototype of the generator for phase A, at a range of revolutions from 0 до 1000 $min^{-1}$.

***Table 2.*** *Measured and calculated by the model phase voltage*

| $n$, $min^{-1}$ | 0 | 200 | 400 | 600 | 800 | 1000 |
|---|---|---|---|---|---|---|
| $U_A = U_4$,V Meas. | 0 | 8,7 | 17,3 | 26,1 | 33,9 | 43 |
| $U_A = U_4$,V Mod. | 0 | 9,4 | 18,8 | 28,5 | 37,6 | 47 |

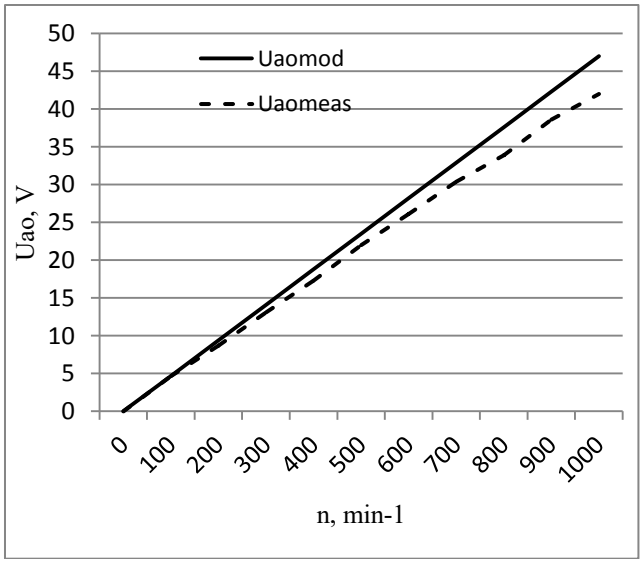



***Fig. 5.*** *Measured and calculated by the model phase voltage*

The maximum relative and fiducial errors at idle running are correspondingly $\delta_{max}$=8,5% and $\gamma_{max}$=8,5%. The errors have the same values due to the fact that the biggest differences between the measured and the calculated voltage at idle running are for the highest number of revolutions per minute at 1000 $min^{-1}$.

## 3. Conclusion

The following conclusions can be drawn based on the theoretical derivation and the experimental studies:

1. A formula has been obtained for calculating the magnetic induction in a certain point of the air gap in a two-rotor axial three-phase generator with rare earth magnets.
2. The derived formula takes into account the magnetic induction for the two magnets, their geometrical dimensions, their magnetic permeability and the magnetic reluctance of the air gap.
3. The adequacy of the proposed formula has been verified; the maximum relative error is $\delta_{max}$=5,32%, while for the air gap of the generator $x$=9 mm, where the middle of the stator winding is, it is even smaller $\delta_{max}$ =0,86%.
4. The maximum value of the basic magnetic flux, going through the stator windings can be defined by means of the proposed formula. Thus the induced e.m.f. in one winding is also calculated and thence the phase voltage at idle running is found.
5. The obtained formula simulates with good precision the work of the studied prototype of the three-phase generator, wherein the maximum relative and fiducial errors for the phase voltages at idle running are respectively $\delta_{max}$=8,5% and $\gamma_{max}$=8,5%.
6. In order to reduce the maximum relative and fiducial errors the asymmetries in the process of making the prototype have to be taken into consideration, as well as the chatter from the rotation of the rotor.
7. An expression for the full r.m.s. value of the e.m.f. for the corresponding phase has been obtained, in which the number of windings and of the pole pairs of the generator, together with its revolutions and the maximum value of the magnetic flux in the middle of the corresponding winding have been taken into consideration.

## REFERENCES


1. Mohammad, M. Sc. and Widyan, S. (2006). *Optimization, Construction and Test of Rare-Earth Permanent-Magnet Electrical Machines with New Topology for Wind Energy Applications,* 17-22. Fakultät IV – Elektrotechnik und Informatik der Technischen Universität, Berlin.

2. Gieras, J. F. and Wang, R. (2004). *Axial flux permanent magnet brushless machines*. Dordrecht, The Netherlands: Kluwer.

3. Kamper M.J. (2009). *Analisis and design of Axial flux permanent magnet wind generator system for direct battery charging application*. Stellenbosch University, Matieland, South Afrika.

4. Schroeler, K.H. (2010), *Permanent Magnets – materials and magnet system,* 5-6. IBS Magnet, vol. 13, Berlin.

5. www///Magnetic2Field Calculators and MagnetCalculationsMagnetSolutionsfromDexter-MagneticTechnologies.html



Department of Electrical Engineering
Technical University–Sofia, Branch Plovdiv
25 Tsanko Dystabanov St.
4000 Plovdiv
BULGARIA
E-mail: geotek@abv.bg

© International Scientific Conference on Engineering, Technologies and Systems
TECHSYS 2016, Technical University – Sofia, Plovdiv branch
26 – 28 May 2016, Plovdiv, Bulgaria

# ALGORITHMS AND PRINCIPLES FOR MONITORING SELECTED AUTOMATIC SYSTEM OR PARAMETERS

STEFAN BOBEV

**Abstract:** *In this article are presented algorithms and principles of configuring and managing the system charged with the task to oversee another electronic or automatic system. A original model that implements a specific assignment by programming from a very high level electronic monitoring system is described. The actual programming is drawing of a flowchart which realizes the assignment. This is possible by a specially developed for the needs of system design graphic editor, shaped in the form of a computer application.*

***Key words:*** *Electronic system, block algorithms for managing, process tracking, software design, automatic system.*

## 1. Introduction

According to the inquiry made on the information sources [1,2,3,4,5] for a system executing the function to track the performance of another electronic system, can be concluded that in all the indicated sources, and not only, there is a specific methodology for measurement and analysis. It is based on a selected, by the designers of the system, algorithm for operation. Noticeable is also the fact that in all commonly used monitoring systems, the working algorithm is fixed, and also the logic of tracking is uniquely determined according to the specific assignment.

This article aims to offer a original solution for an universal method in which to some extent the system for monitoring can be reconfigured in different topological work variations.

It is important to note that the working algorithm of tracking system itself is fixed by operations, but input / output connections between the already set for tracking parameters and logic in analyzing the data, are selected directly by the user. This author's decision is intended to be realized through the drawing of graphical block diagram rather than through writing a programming code, as in all mass development systems available on the market.

For this purpose, in the software of the monitoring system are written drivers in advance for a set of the most common peripheral modules for data collection by measuring electrical and non-electrical quantities.

The next unit which performs logical processing includes the commonly used mathematical functions and operators introduced software as functions in the program memory of the tracking system.

To enter and modify the algorithm for tracking according to the exposed original concept, a specially designed computer application is used. In the application's graphic editor each separate function or driver of the programming code are called by assigned to them I / O or logic blocks. A finished state of the working algorithm, on which the selected electronic system will be tracked, is given by drawing connections between the attached graphic blocks.

The design of an electronic system always goes through several key stages before reaching the physical realization of the device itself, as shown in [6]. These stages summarize the engineering work of the team responsible for the project. The proposed methodology examines the tracking system in a semi-finished state. This makes it an universal from the side of application into practice, as the logical connections are set according to the customer needs.

## 2. Concept of the chosen author's model for configuring the process

The design of a system for monitoring and control of another electronic system requires set of the important input / output parameters for the status of the tracked process. When the system, on which the monitoring will be performed, is specially set and the requested parameters are determined, the task can be practically executed. According to references cited above, such a tracking system is a

Copyright © 2016 by Technical University of Sofia, Plovdiv branch, Bulgaria ISSN Online: 2535-0048

standard electronic system comprising: sensors, power circuits, power supply, microcontroller displays and other peripherals devices for remote communication.

The differences come only from the wiring diagram and logical function that performs. A typical system of this kind is described in details in [7]. In order the system for monitoring and control to become more interesting and unified, it is a good option to have the possibility for configuring by the user. This requires the "design" method for configuring to be chosen. On the market electronic devices in semi-finished form are widely offered, reference may be made from [8,9]. At them is necessary to introduce the source code written by the user for an execution of a specific configuration, together with supplement of an extra external hardware. These are the so called "boards of Development". Their drawback is that the user should have profound programming knowledge and be familiar with the architecture of the developing environment with which he operates.

The selected author's design offers simple block configuration in which the user enters a logical block diagram of the electronic system that he wants to construct: implement the connections between the separate blocks, as it will be useful for him and sets operational parameters in them. Builds the electrical connection of the necessary external hardware for the designed model, in case of already set electric diagram, with labeled I / O ports.

Such as: displays, sensors, output drivers, relay outputs and more.

For this purpose, in a specially developed computer software there are written drivers to a selected set of hardware peripherals.

The following figure presents the author's model for the concept of the method.

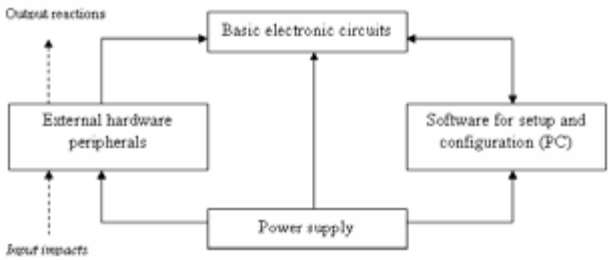



***Fig. 1.*** *Block diagram of the concept for monitoring*

The configuration of the system is done by a computer software. In it the user enters the whole block diagram of the device, then by the software it is translated into a source code that is programmed in the processor of the development board.

The external hardware periphery accepts the input parameters of the electronic system, which is tracked. In case of back-up function by the designed system through initiating reactions from power circuits, the control is taken or another process is controlled.

Close to this model, as you can see in [10.11], is the programming by ladder diagrams of programmable logic controllers (PLC), which uses an electric schemes with a set of software functions for configuring.

### 3. Computer software for system configuring according to the author's model

In the proposed author's methodology, computer software, which performs the programming of specific configuration, has the following basic components:

Work field - the logic diagram is drawn in it;

Menu for selection of "Input block" - here is the library with a possible range of input peripherals that can be used to measure various electrical and non-electrical quantities;

Menu for selection of "Output block" - The library of available output peripherals (for visualization, display and control);

Menu for selection of "Logical block" - contains a list of the introduced mathematical functions through which the input signals can be processed (addition, subtraction, comparison operators, amount module, multiplication, division);

Console for visualization of processed data measured by the development system (in numerical or graphical form);

Based on the described, the below mentioned author's figure presents the structure of computer software to adjust the designed system.

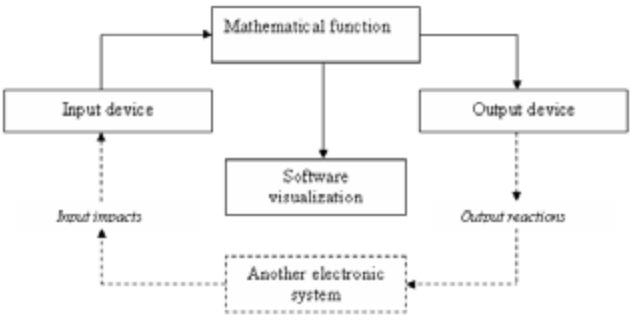



***Fig. 2.*** *Block diagram of the software for configuring and monitoring*

Logically the input impacts and the output reactions can be linked to another electronic system, in this way monitoring and back-up will be performed on it.

## 4. Operation of the system with the proposed working algorithm

According to the made review and selected principle, the work methodology of the tracking system can be summarized. It is divided into three phases:

Extract / calculating the value of the input blocks;

Implementation of the operations from the intermediate blocks;

Transfer of the result in the output blocks;

The block diagram created by the computer software is in non-volatile flash memory and is read when the system starts. During the first phase the values for all the input devices, sensors and input ports of the controller should be calculated. This is done consecutively, as the order is not important and is not determined by the visual arrangement in the computer software.

The second phase is the most difficult to execute. Intermediate blocks, in most of the cases are the most numerous and have multiple connections to each other, which requires a specific order of execution, because dependencies between them arise. Let's pay attention to the following case:



***Fig. 3.*** *Block structure of a tracked process*

Block A / B of Figure 3, shown in original PC application, can be calculated directly, because the first phase is completed and the values of the three input blocks from the left are known, but the block Compare cannot be completed without knowing the value of A / B. This requires, first, the appropriate order for execution of the intermediate blocks to be determined. If the blocks are presented as an oriented graph, multiple algorithms from the field of graph can be applied on them. Using topological sorting algorithm, as described in [9], a suitable order for execution of the entered blocks is opened. This methodology was chosen for software implementation at a low level in the proposed original approach for configuring the system by block modeling and high-leveled graphic editor.

In order to justify the choice of a low-level work cycle, should be briefly described, what are the main methods for presenting the data in the used an algorithm for topological sorting according to [12]. Graph is a data structure consisting of a number of vertices (nodes) and ribs. Each rib connects couple of vertices. When rib indicates separately connection and direction of possible movement, the rib is oriented. Oriented graph is the one which ribs are all oriented. An example is given in the following figure, according to the information source [12].



***Fig. 4.*** *Oriented graph*

Each vertex has a degree - it is the number of links to other vertices. In the oriented graphs vertices have 2 degrees - input and output, respectively, indicating the number of input and output ribs. The oriented graph is appropriate presentation for the blocks which should be arranged. Vertex of graph can present certain block, but rib - the connection between two blocks. The internal representation of a graph in a computer system according to [13] can be made in two ways - through matrix neighborhood or through an array of lists of the neighborhood. The choice of the method is evaluated by two criteria:

Required memory;

Difficulty of the operations execution: determining whether two vertices are adjacent and detection of all nodes adjacent to a certain node;

Matrix neighborhood quoted in [12] is appropriate way for presenting of a graph according to the second criterion. According to the first criterion (required memory), however, it is not appropriate, because graph with n top requires matrix with $n^2$ elements, moreover often the majority of them have zero values. This is a problem, because of the limited memory in the system.

Matrix neighborhood presenting Graph is a square matrix with size equal to the number of vertices. The numbers of rows and columns are the numbers of vertices. Matrix neighborhood for graph from the previous figure is as follows:

***Table 1.*** *Matrix neighborhood*

| | **0** | **1** | **2** | **3** | **4** | **5** | **6** | **7** |
|---|---|---|---|---|---|---|---|---|
| **0** | 0 | 0 | 1 | 0 | 0 | 0 | 0 | 0 |
| **1** | 0 | 0 | 0 | 0 | 0 | 1 | 0 | 0 |
| **2** | 0 | 0 | 0 | 0 | 0 | 0 | 0 | 0 |
| **3** | 0 | 0 | 0 | 0 | 1 | 0 | 0 | 0 |
| **4** | 0 | 0 | 1 | 0 | 0 | 0 | 0 | 0 |
| **5** | 0 | 0 | 0 | 1 | 1 | 0 | 0 | 0 |
| **6** | 0 | 1 | 0 | 0 | 0 | 1 | 0 | 1 |
| **7** | 1 | 0 | 1 | 0 | 0 | 0 | 0 | 0 |

**The array of lists** of the neighborhood contains "n" number of lists as "n" is the number of vertices. The list for each vertex contains vertices associated with it:

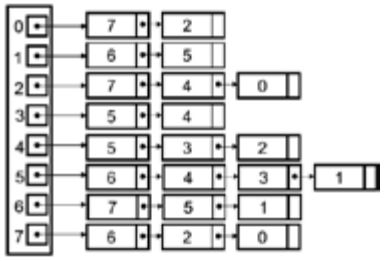



***Fig. 5.*** *An array of lists*

This way of presenting the graph is better in comparison with the first criterion. Each list of neighborhood contains as many elements as the number of output from the vertex ribs.

Regarding the second criterion, however, it is quite difficult to find the incoming neighbors of the vertices, and exactly this is the most important for the algorithm that uses the tracking system.

The practical implementation at the proposed approach for configuring is through the method of matrix neighborhood, as the sorting of the tasks is executed in the computer software, because is needed to be done only once. The higher request for memory is not a problem for modern computer system.

Graph's topological sorting according to [12] is an operation that is performed only for oriented acyclic graphs. As a result of the execution of this operation a row with number of vertices called topological order or topological arrangement. In the topological order the numbers of all vertices, direct predecessors of a certain vertex are numbers of the same peak. To graph often correspond some topological orders, but usually it is enough to find one of them.

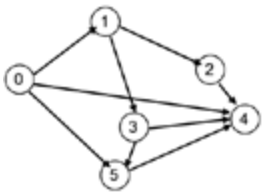



***Fig. 6.*** *Graph illustrating the topological sorting*

Topological order is obtained by the following algorithm:

If the graph has no vertices without predecessors, it is cyclical and cannot be subject to topological sorting;

One by one, in random, the vertices without predecessors are recorded in the topological order and deleted;

If there are still not deleted vertices, should pass towards operation 1, if all are deleted, the topological sorting is completed;

Let us apply this algorithm for the graph of Figure 7:

Without predecessors is vertex 0. To be recorded in the topological order and deleted;

Without predecessors is vertex 1. To be recorded in the topological order and deleted;

Now without predecessors are vertices 2 and 3. To be recorded in the topological order and to be deleted first vertex 2, then vertex 3, but it can be done in the reverse order.

After deleting the vertices 2 and 3 without predecessors remains the vertex 5. To be recorded in the topological order and deleted;

Now without predecessors is vertex 4. To be recorded in the topological order and deleted;

All vertices are deleted. A topological order for this graph is: 0, 1, 2, 3, 5, 4. The Graph is acyclic.

The discussed algorithm is simple and clear, but it is not a computer algorithm. According to [14] the computer algorithm should use the internal presentation of the graph, in this case the matrix of the neighborhood. If it is necessary to follow the described algorithm exactly, the matrix of the neighborhood must be changed after each deleting of a vertex. Thus, the formation of a topological order is accompanied by destruction of the matrix of the neighborhood, which is not desired.

In the presented method for configuring, another better algorithm is used. It uses two lists - for registration of the visited vertices and for the current number of predecessors of each vertex, as well as counter of the visited vertices. The algorithm consists of the following:

Sign up of all vertices as unvisited;

Detection of the entry grade of (the predecessors should be counted) each vertex;

All vertices without predecessors are sent to the queue waiting vertices;

One by one, the waiting vertices are taken from the queue, brought in the topological order, registered and counted as visited, the entry level of each of their heir is reduced, all the heirs left with an input level 0 are sent to the queue. This continues until there are waiting vertices in the queue. When the queue becomes empty, there are two options:

All the vertices are visited and the topological order is created;

Only a part of the vertices is visited - the graph is cyclical and defies topological sorting;

After displaying the appropriate sequence, the monitoring system executes the operations from

all blocks in that order. Thus, the result of each block is present.

In the third phase, the system displays the results in the devices, ports, or whatever else is set by the output blocks. For this purpose, each output block is reviewed, checked with which of the intermediate blocks is connected in order to take its score calculated in phase 2 and perform the relevant action.

The three phases are repeated in an infinite cycle. Some input devices such as sensors, have a requirement for minimum time to report, therefore the system has a setting for awaiting time until the next start of the execution of the phases.

### 5. Algorithms for operating system

Working algorithm according to which the operations will be executed should be brought. Original solution is selected to include a set of three phases grouped in separate algorithms. The main programming code or the so-called Main program calls in particular sequence each one of the three sub-programs. The functional-completed block algorithm ensures the realization of the block entered logic diagram in the graphic editor of the tracking system.

The methodology is presented in the following figures.

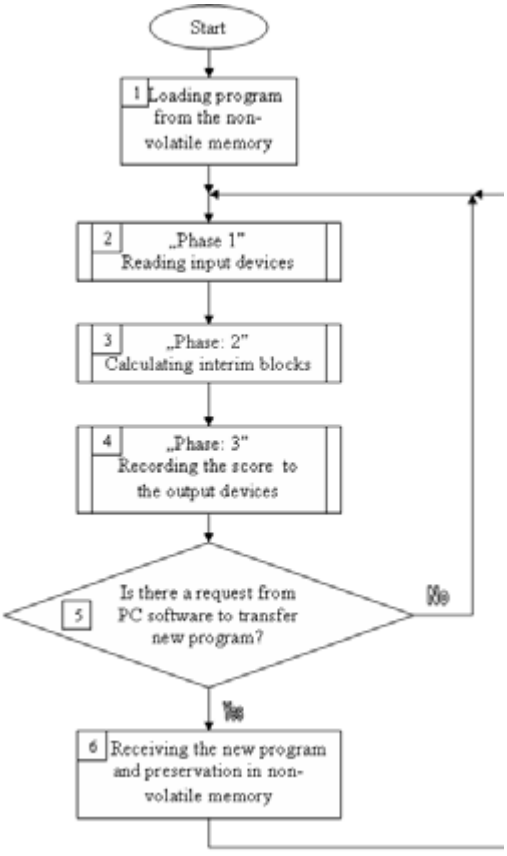



***Fig. 7.*** *„Main program"*

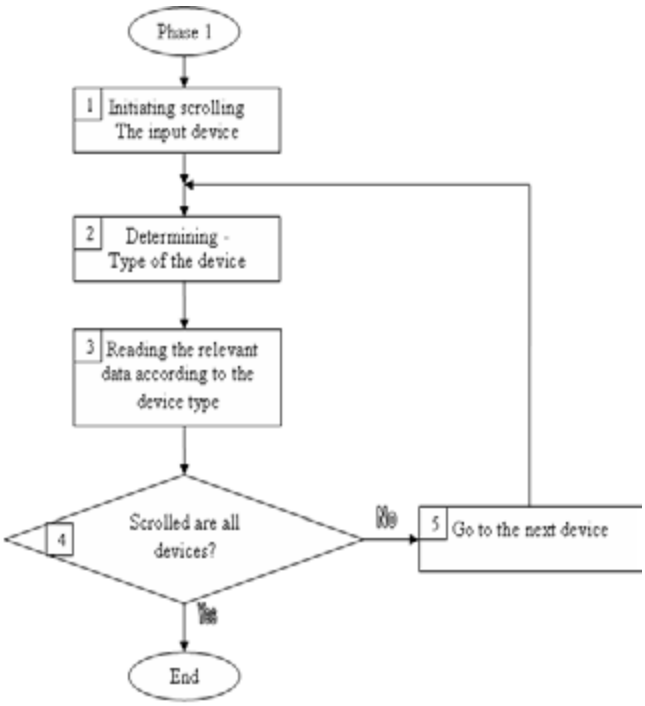



***Fig. 8.*** *„Phase 1"*

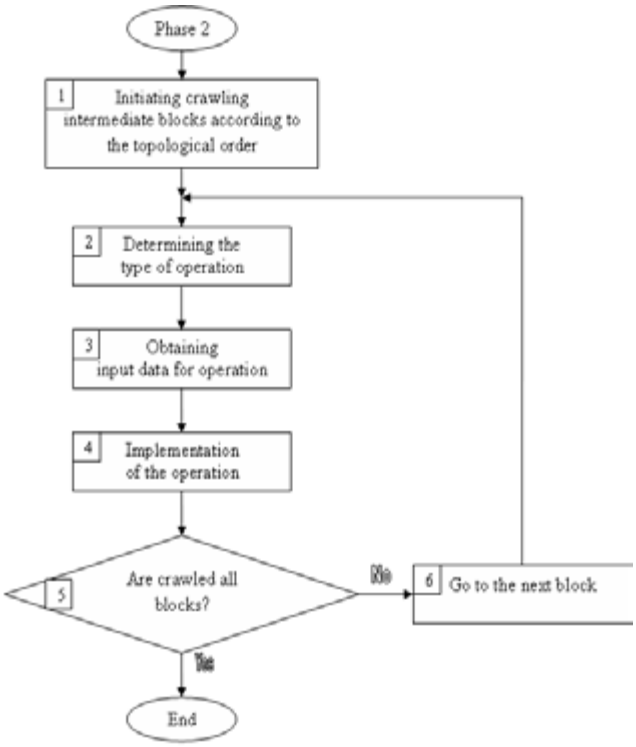



***Fig. 9.*** *„Phase 2"*

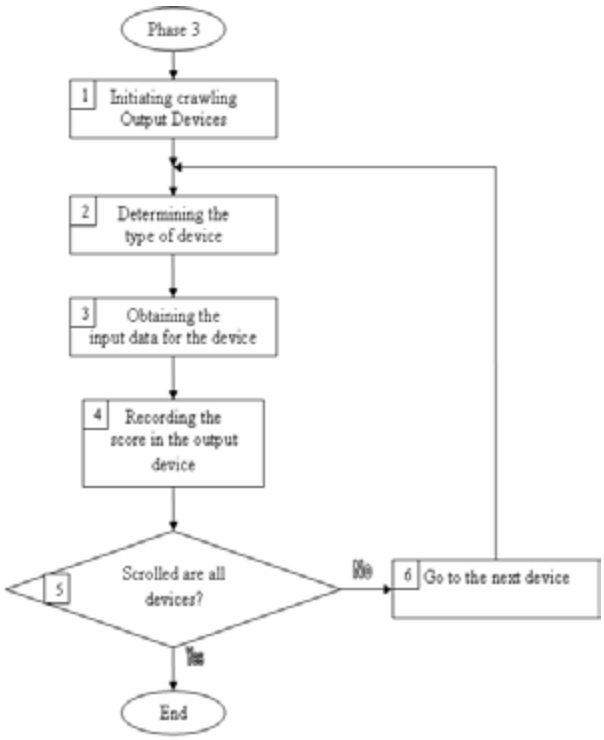



***Fig. 10.*** *„Phase 3"*

Based on the prepared block algorithms an electronic scheme is designed to realize them purely hardware. A software for realizing the chosen author's approach for tracking of the electronic automatic system is written. The physical realization of a working model functioning according to the set out methodology for monitoring aims to explore practically the behavior and the advantages that the chosen author's design gives.

## 6. Conclusion

In this article is described a original model for configuring of algorithm and construction in an electronic system designed for tracking another electronic system. On the basis of this, an universal internal scheme working algorithm for the system executing monitoring, is created. The presented algorithm is universal and is used in various fields of electronics and automation. The exposed concept could be applied successfully to complicated multi-module systems, which should be monitored, whether they function properly.

As a main benefits of the article can be indicated the following: Presented is the original model for user configuring of an electronic system during the tracking process, or another automatic system graphically, without the need of writing programming code by the user. In this way the user can create various complex configurations using multiple repeating the same software working algorithm. The approach of data sorting used in the computing systems is described by a specific example.

Disadvantages: The principle of operation is reviewed in general and does not affect the detailed features of the design of the proposed algorithms. The presented original model reduces the flexibility of the system logic at the expense of simple configuring.

## REFERENCES


1. Kenneth A. M. (2010), *Remote diagnostics and prognostics methods for complex systems,* Ford Global Technologies, Inc..
2. Muller A., Hauser G. (2011), *Diagnostic method for a process automation system,* Hauser Gmbh Co., Kg.
3. Hunsuke C., Danil V. P. (2008), *System and method for remote diagnosis and repair of a plant malfunction with software agents,* Toyota Engineering & Manufacturing North America, Inc..
4. David W. Jensen, James A. Marek (2009), *Prognostic processor system for real-time failure analysis of line replaceable units,* Rockwell Collins, Inc..
5. Chaucer C. (2003), *Real-time situation report system and method,* US patent 10/075,768.
6. Garywell S., Costas J. (2010), *Fundamentals of semiconductor manufacturing and process control,* IEEE Wiley Inter-science.
7. Bergstrom P. (2001)*, Making home automation communications,* IEEE, vol. 34, no.10, pp. 50 – 56.
8. Kenarov N. (2003): *PIC Microcontrollers part 2*, Young constructor, Varna.
9. Roy S. (2004), *Security technologies for manufacturing and control systems,* In-strum., Syst., Autom. Soc., Tech. Rep. ISA-TR99.00.01-2004
10. Grichnik A., Seskin M. (2006), *Diagnostic and prognostic method and system,* Caterpillar Inc..
11. Bolton D. (2006), *Process control fundamentals*, PAControl corporation.
12. David J. (2009) *A dynamic algorithm for topologically sorting directed acyclic graphs,* Department of computing imperial college, London.
13. Martin R. (2003), *Agile software development: principles, patterns, and practices*, Upper Saddle River, NJ, USA.
14. Miles R. (2011), *C# Programming*, second edition.



Department of Electronics
Technical University–Sofia
St.Kliment Ohridski Boulevard
Sofia 1756

© International Scientific Conference on Engineering, Technologies and Systems
TECHSYS 2016, Technical University – Sofia, Plovdiv branch
26 – 28 May 2016, Plovdiv, Bulgaria

# SPECIALIZED ELECTRONIC SYSTEM FOR TRACKING OTHER PROCESS, ELECTRONIC OR AUTOMATIC SYSTEM

STEFAN BOBEV

**Abstract:** *The developed an electronic system offers constructive and logical solution to the sample tracking, management or booking other electronic system or process. In the original idea is pledged an option for users to determine precise, logical connections between hardware and software blocks. The proposed algorithm is to do it so by drawing a block diagram and introducing operating parameters in it. All electronic devices of that type requires a new source code for different configuration, here it is not so. The example presents this constructed monitoring system used in a configuration for tracking other Ethernet based management system of a street lighting control. The idea is that the two systems operate independently of each other. The aim is to compare the received data, testing and exploring the presented method for configuring the specialized monitoring system. Also the article describes a simple example and configuration for monitoring the simple process. Presented an electronic system has its own computer software. In it the user has options for configuring and reporting the downloaded data.*

*The hardware configuration is constructed to explore the features and functionality of the proposed methodology for configuring. This author's model is described detailed in the article "Algorithms and principles for monitoring a selected automated system".*

**Key words:** *electronic system for tracking, automatic systems, process tracking, control and monitoring electric or physical parameters*

## 1. Introduction

From the reference made from various information sources cited under listed numbers [1,2,3,4,5] for available devices offered on the market that cover a wide range of possibilities (development systems, PLC, etc.). It is clear that all required the user to had knowledge of programming. The advertising presents all as "very easy to configure", people used them know that is not true. Here the developed system offers a facility in this direction, based on pure logic programming, when the user realizes a specific job for monitoring. Of course, any simplification of a system makes it less flexible. So it needs to properly weigh the advantages and disadvantages when choosing.

Currently the market is extremely rich oversaturated of any kind of monitoring devices, as it is evidenced by [6,7,8,9], therefore the proposed project can not claims the most effective and rational decision. But the fact is, that the proposed original method for configuring the tracking system does not occur in a similar type of electronic devices. Here the aim is to realizes and explores the conception for programming by the user with block diagrams.

## 2. The key features of the developed system

Pursuant to the foregoing, it is clear that a system for monitoring and control has all the basic components of an electronic automated system. Such are the power supply, main processor, peripherals, communication channels (wired and wireless) and others, as it is described in [10,11]. Presented system is structured modularly. It has a Master module and at least one slave module, who it serves a data collection. The main module coordinates the work between slave modules. By itself it could also carry out measurements and control

The basic idea used in the construction of the monitoring system is presented to the next author’s diagram.

Copyright © 2016 by Technical University of Sofia, Plovdiv branch, Bulgaria ISSN Online: 2535-0048

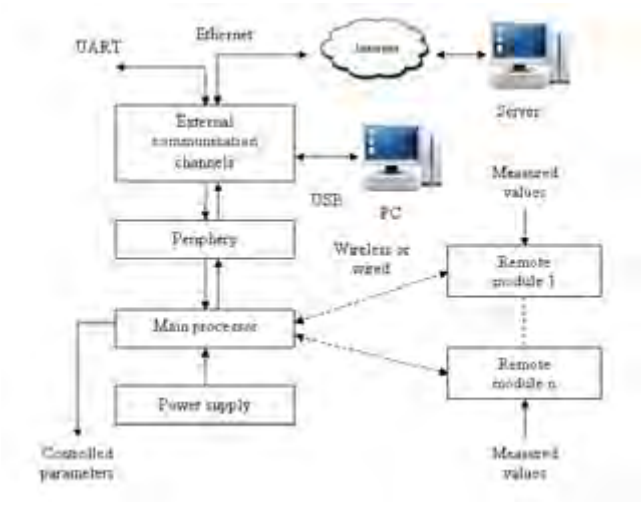



***Fig. 1.*** *Block diagram of the developed system for monitoring and control the other electronic systems*

Briefly, each block has the following function:

Main processor - It is a single-chip which together with its built-in peripherals performs all computing and matching operations;

Peripherals - these are all external integrated circuits and electronic elements, that complement the built-in hardware processor;

Channels for external communications - this includes connectors who realized connection with the physical environment from the printed circuit board to the external devices;

Power supply – it provides the necessary voltage for the main processor and the periphery;

Remote module - it incorporates the processor and outer periphery (sensors, interface ICs, power supply). The functional nature of this block is gathering information from a process or another system and transmission it to the main processor;

Personal computer (PC) - here is installed the specially developed software for system configuration and processing data, which is coming from the main processor. The actual configuration is done by executing the logic of work, realized in the form of a block diagram. In the processor has programmed software driver for each type of block and accordingly should be connected, and the necessary hardware. When configuration is selected and the operating parameters are set, the working process can start;

Server - this may be an ordinary PC, who has only accesses to the data stream from the module, without making any adjustments to the algorithm. For example this is web server or html page;

The first four units together form the Main module. Formed in this way the system has a universal character and may be used in various types of applications. The degree of universality depends on the installed sensors and drivers for these features. Accordingly, with more sensors could be expanded the functionality. The other function of a system also can maybe to manage a process and assume the control.

According to those both characteristics, the model is a hybrid.

**Advantages:**

Relatively inexpensive circuitry decision;

The user can to configure different algorithms for monitoring, without to have any knowledge of programming;

The system has its own configuration software;

**Disadvantages:**

The simplified configuration algorithm has a less programming flexibility;

The universality directly depends on the number of entered software drivers and the sensors connected to the system.

The aim is to leave open the model and allows to combining the advantages of different approaches for monitoring and control of the other electronic systems.

## 3. The model for tracking the management system of a street lighting

An example for test is implemented with the monitoring system of a street lighting control, in two ways. The monitoring methods are combined - software and hardware. The principle is presented at the next the figure.

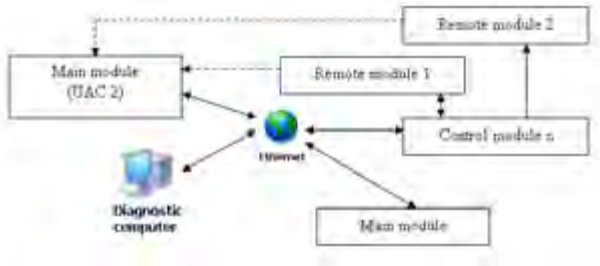



***Fig. 2.*** *Block diagram of the configuration for monitoring to management system of street lighting*

The developed monitoring system is tracking other electronic system for Ethernet based street lighting control. The components of the tracking system are used a "Master module (UAC2)" and two "Remote modules" of data collection. The other two presented block "Main Module" and "Control module" are from the system for street lighting control. Their purpose is as follows:

Main module – it coordinates work between individual control modules (one Master module can control up to 50 Control modules);

Control module – it implements specific management functions and collects statistical data (measurement the currents in phases, circuit for a phase-detection, light sensor, sensor for an open door, etc.);

The first remote module is placed in one of the Control module. It's taking signals from the designated control points and submitting them to the main module of the tracking system, through wireless radio channel. For comparison, the second Remote module takes information from duplicate sensors and transducers. It is placed near to the control unit and is connected to the power circuits. This method allows for precise localization the failure of a monitored system. For this purpose, in the computer for diagnosis are installed simultaneously two different software applications (The software who is used for system of street lighting control and the other which is for the monitoring system). The aim is to allow comparison of the data in real time.

## 4. Block diagram of the individual modules that build the submitted monitoring system

According to the information given in the preceding paragraph, here are shown the specific block diagrams, for each one of the designed modules.

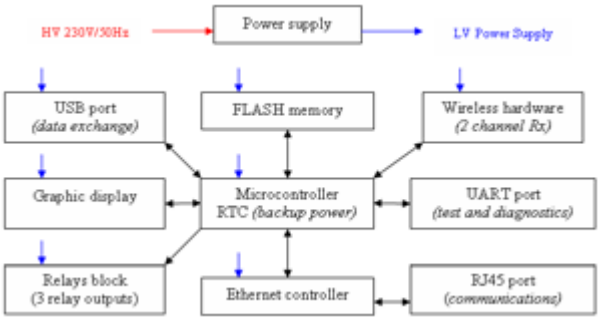



***Fig. 3.*** *Block diagram of the main module*

Remote modules, as mentioned, they have two configurations: The first one follows the management of street lighting control system (Remote Module 1), and the other one is with general purpose (Remote Module 2). The second configuration (Remote Module 2) has attached several different types of hardware peripherals for measuring electrical and non-electrical parameters. They, along with the integrated peripherals of the microcontroller form Universal module. The function of this module is for measuring and transmitting data to the main module (UAC2).

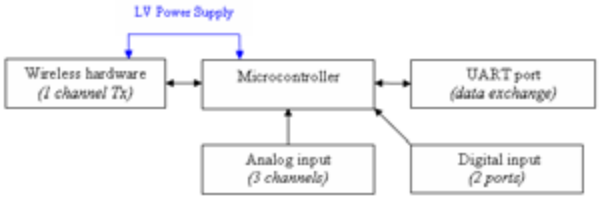



***Fig. 4.*** *Block diagram of the remote module 1*

Preference for the remote module is to have a lower consumption. This is achieved through built-in functionality of the hardware. The microcontroller PIC16F1827 is used. It has a function with a minimum consumption, according to the computational operations (nanoWatt XLP technology). Another approach, which is used, this is an alternation of cycles, when the data is sent from the individual sensors. The idea is that, at the same time is active only one sensor.

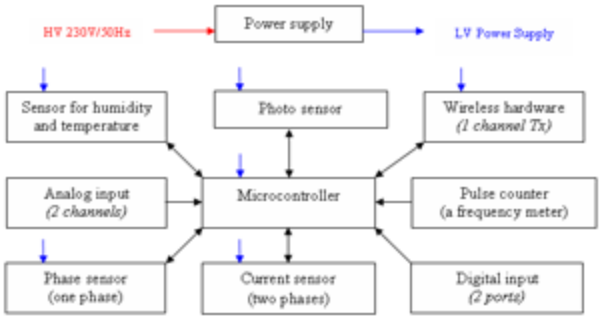



***Fig. 5.*** *Block diagram of the remote module 2*

Thus the developed monitoring system is designed as a multiprocessors system with data exchange through wireless channels. The wireless hardware is used in different communication channels, to avoid the conflict with a data transfer. The system uses the same carrier frequency of 2,4GHz. The standard wireless module nRF24 allows one receiver to captures up to six channels from different transmitters. For each group of six remote modules should be placed one receiver.

## 5. The developed hardware

The hardware is designed according to the exposed original idea for the tracking system. The modules have some degree of versatility, in terms of the software and also in the hardware configuration. The printed circuit board and the electronic circuits have been constructed on the model of the development board.

The structure of the wiring diagram for the main module combines selected microcontroller LPC2368FBD100. This processor and the integrated periphery are built in a single block. It is so-called "main processor". In this complex hardware block, the structure is displayed as a

general-purpose processor. Additional all connectors and bulky components are mounted externally. The power supply (AC230V / DC5V-1A), is also outside the main processor. The Main module can be powered also via USB cable from the PC.

The following figure shows a summary block diagram of the main module.

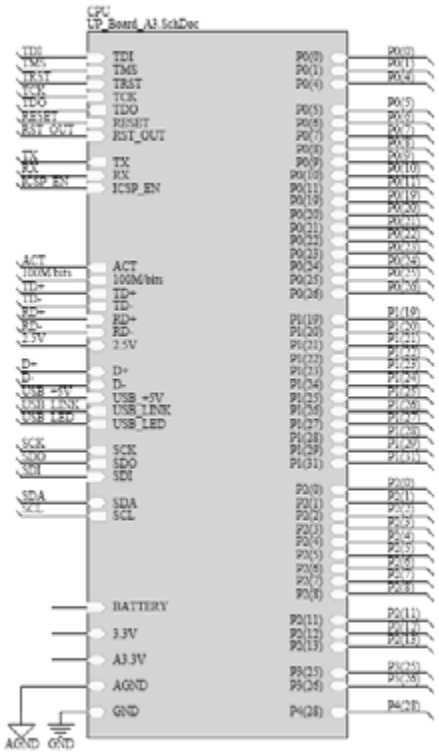



***Fig. 6.*** *Block diagram of the main module*

The designed circuit board from the main module provides connections to all ports of the controller with 2.5 mm pitch. For backup power to the embedded system clock is used super capacitor with a capacity of 1 farad. For the printed circuit board is used material FR4 with 1.5 mm thickness, the copper foil is 0.35 microns.

It is important to note that all the electronic components are placed only on the top layer.



***Fig. 7.*** *PCB main module - "top layer"*

The circuit diagram of the remote module is composed of the standard sensors, available on the market. A printed circuit board with the microcontroller has all external elements, necessary to establish the operating mode and programming. All other outer components are mounted to connectors for external periphery. The power supply unit is connected to the main module through socket.

In particular the prepared model is used for study the pledged author's model by tracking management system for street lighting, according to the block schemes described above. The installation of the remote modules is made as follows:

With the first remote module is captured signal from some control points. The registers of a microcontroller from the control system of a street lighting are reading with UART interface. This direct communication between the both processors is realized via conductors;

The second remote module, along with the needed sensors is installed in a separate box. In this condition it has access to the needed signals. In the same box is mounted and a scheme to generate pulses and analogue signal. With two potentiometers are regulated the voltage and frequency of the separate signals (digital and analog). The idea of the latter is to test the functionality by measurements of digital and analogue values.

In the next figure is represented management system of the street lighting, developed for the purpose of research. In It is installed the first remote module. The complex module is powered directly from the main power supply.



***Fig. 8.*** *Control module with mounted remote module inside it*

### 6. Computer software for configuration and measurements

For configuration the monitoring system and study of the proposed copyright model is used specially developed computer software runs on Windows OS. In order for fast and easy handling with the system setup are using special blocks, each of them has certain features, like the tracking

algorithm. The aim is to avoid programming code that repeatedly complicates and slows down the implementation of the required functionality. Each of these units has a number of inputs and / or outputs that are connected to the preceding or subsequent block. The blocks can be several types:

Data Sources - these blocks have one or more outputs, without inputs. They are two types - block constants that have numeric or boolean value, as well as blocks constituting an input device, such as a temperature sensor, or the periphery of the CPU, such as UART. They measure the value and then it is displayed on output;

Logic units - these blocks take one or more values to perform a logic operation on this value. They carry out the result into one or more outputs. Available are the follow units: compared operators <=>, logical AND, OR, NOT and others;

Blocks with mathematical operations - available are the following mathematical operations: addition, subtraction, multiplication, division and raising the degree. All from these blocks have two inputs and one output. The unit "absolute value" is available too. It has one input and one output;

Output blocks - these units have only one entrance. They are three types: output to a display - this block receives any type of data; exit to the port - it receives boolean value corresponding to the level which must be switched; output to the console - it receives any type of data too.

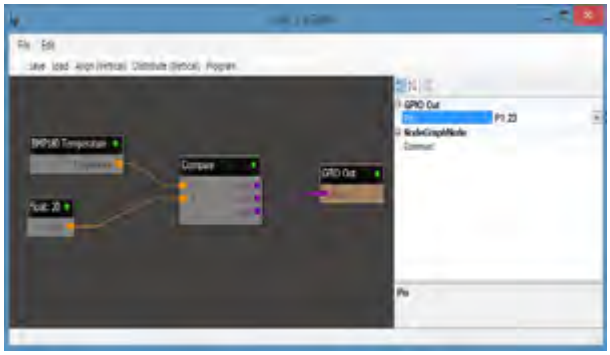


***Fig. 9.*** *View of computer software - a common type*

On this screen shot is shown a simple example in which the system receives data from the temperature sensor connected to it. This is BMP180. The purpose of the example is to demonstrate author's model for configuration the monitoring system.

The output from the temperature sensor is connected to the input of a block for comparison. On the other input of this block is connected constant value of 20. The output A<B of the logical block will has a value of 0, when the temperature detected by the sensor is above 20°C and 1 if it is below this temperature. This output is connected to the physical port from the main processor, which will switch to the corresponding logical level. In this case the selected port is P1_23.

Each of the blocks has a name and signal point in it. This point indicates whether the unit is connected properly or there is an error connecting. When the connection is wrong the point is red, and when all is properly connected - green. For properly connection, the block must have inputs and at least one output, to be connected with another block. There are exceptions, depending on the functionality of the block.




***Fig. 10.*** *Error connecting block "subtraction" because, as one gate is left open*

Each block can be configured by pressing with right click on it. With this function appears different parameters and can be configured the way it works.

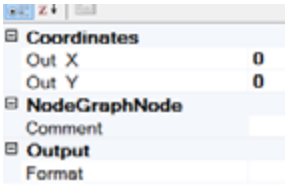



***Fig. 11.*** *Setting the block LCD Print*

In the unit "Display", with function "LCD Print" can be adjusted the coordinates of the display, the position where to displays an output text and format for the string. This function is made with identical style, same as "printf" from the standard C# library, reference may be made in [12].

When pressing and holding the mouse to one of the inputs / outputs appears connecting line that can be dragging to the input / output of another block. It thereby carries out the connection of the blocks.




***Fig. 12.*** *Connecting the blocks*

By pressing the right button on the blank space appears a context menu with a range of available blocks. They are divided into categories according to the function.

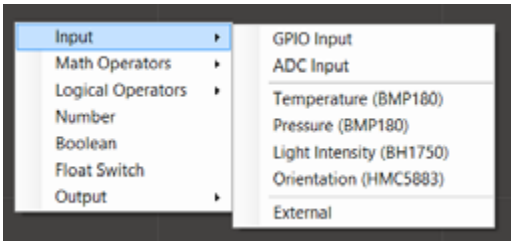



***Fig. 13.*** *Main menu and list of incoming blocks*

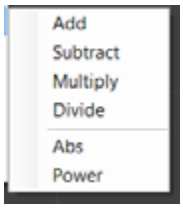



***Fig. 14.*** *Menu - Mathematical functions*

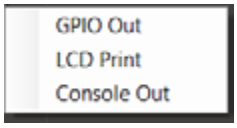



***Fig. 15.*** *Menu with output functions*

## 7. Conclusion

The article has all the key points relating to design a system for monitoring other electronic or automated systems.

The main purpose of the study is to prepare a specimen for examination and testing the author's model. It is associated with alternative configuration by the user, without software programming in different logical structures.

Specific examples are described in hardware configuration. They are management system for street lighting and an elementary example for monitoring the process (maintain temperature).

The benefits of the proposed development are:

**Advantages:** The simple logic which is proposed and hardware realization of a system for tracking other complex electronic or automatic system. The easy method is used for configuring the tracking system, without software programming. The system is organized to allow mounting of standard sensing circuits that are available on the market.

**Disadvantages:** The method for configuring the system decreases the flexibility of the hardware and thereby is limiting performance.

## REFERENCES

1. Teng J; Yuan C., Chen Y. (2004), *Integration of networked embedded systems into power equipment remote control and monitoring*, IEEE, vol. 15.
2. Lukas D., Johan K. (2010), *Methods and systems for fault diagnosis in observation rich systems*, IEEE, vol.80.
3. David P. Buse, (2010), *IP Network-based Multi-agent Systems for Industrial Automation: Information Management*, Condition Monitoring and control of power systems e-ISBN 978-1-84628-647-6, Springer-Verlag London Limited.
4. Shibu K. V. (2010), *Introduction to embedded systems*, McGraw-Hill Company.
5. Decotgnie J.-D., (2005), *Ethernet-based real-time and industrial communications*, Proceedings of the IEEE, vol. 93, No. 6.
6. Jen-Hao Teng; Chin-Yuan Tseng; Yu-Hung Chen, (2004) *Integration of networked embedded systems into power equipment remote control and monitoring*, IEEE, vol. 69.
7. Lin J.Y., Jin X.L., Mao Q.J., (2009), *Wireless monitoring system of street lamps based on Zigbee,* Proceedings of the 5th international conference on wireless communications, networking and mobile computing, Beijing, China. 24–26, pp. 1–3.
8. Unkle C., Richard M. (2006), *Method and apparatus for diagnosing difficult diagnose faults in a complex system*, GE Company.
9. Montreuil M., Fecteau K. (2013), *Electrical anomaly detection method and system*, Corporation Nuvolt Inc..
10. Buse D., Wu Q. (2010), *IP Network-based Multi-agent systems for industrial automation,* Condition monitoring and control of power systems e-ISBN 978-1-84628-647-6, Springer-Verlag London Limited.
11. Hespanha M., Joao P. (2007), *A survey of recent results in networked control systems*, Proceedings of the IEEE, pp138-162, vol.95, No.1
12. Miles R. (2011), *C# Programming*, second edition.

Department of Electronics
Technical University–Sofia
St.Kliment Ohridski Boulevard
Sofia 1756
E-mail: msbk@abv.bg

© International Scientific Conference on Engineering, Technologies and Systems
TECHSYS 2016, Technical University – Sofia, Plovdiv branch
26 – 28 May 2016, Plovdiv, Bulgaria

# FLUORESCENT SPECTROSCOPY APPLICATIONS IN VETERINARY MEDICINE AND HEALTHCARE

VANYA PLACHKOVA

**Abstract:** *For testing liquid samples from large and small sick ruminants was improved field method for fluorescence assay. In addition to samples from sick animals method is applicable for testing of raw milk that was taken directly from the manufacturer instead the commercially available. The specific method of fluorescent analysis described in this report is characterized by precision, fast response and easy feasibility. To confirm the efficacy of the fluorescence analysis for the detection of bacteria in ruminants and recognition of the different types of raw milk fluorescence analysis carried out with the help of a veterinarian. An essential point in the fluorescent analysis of samples from sick animals proved the fact of the companies establishing the presence of bacteria cause disease, which had no external symptoms in the animal. On the other hand important point in the testing of raw milk has proved that by fluorescence analysis can be obtained from samples of milk from one animal strain or mixed milk from more breeds. Fluorescence spectroscopy is used for analysis of olive oils and fruit juice too. It is shown that fluorescence spectroscopy is an efficient and fast method for analysis of purity and composition-native olive oil and juice, which are an integral part of healthy lifestyle. With fluorescent analysis we can easily ascertain the difference between pure olive oil and extra virgin olive oil. By fluorescence analysis is made easy and fast correlation between the purity of freshly squeezed fruit juice compared to those sold in markets*

**Key words:** *Fluorescence analysis, emission wavelengths, veterinary medicine, healthy food*

## 1. Introduction

The lack of methods for early diagnosis of animals is a major problem for farmers, which results in a reduction in population of animals. In order to prevent the serious disease spread an early diagnosis of the animal is required. Most drugs of the veterinary pharmaceutical industry are expensive for small and medium companies.

Besides that the drugs are expensive, they do not guarantee that the animal will recover. It turns out that despite the expensive drugs used to treat the animals they do not guarantee their rescue and livestock should be 'scrapped'. Therefore perfecting methods for early diagnosis of cattle is extremely important field of study. Early diagnosis of the problem animal diseases will allow increasing the benefits of livestock and reducing morbidity.

More and more often fluorescence spectroscopy gets used for analysis of milk products. In case of pre-prepared library of data, this method is fast and efficient. Unlike approved chemical tests for certification of agricultural products under fluorescent spectroscopy does not require additional supplies in the analysis of samples. In recent years there have been more yogurts, which are a mix example of cow and sheep's milk or sheep's and goat's milk or cow's and goat's milk. Therefore, attention was paid to an examination by fluorescence method of mixed milks.

Increasingly often are used impurities and substitutes for natural products in the food industry. By fluorescence analysis can be done easy diagnosis of the purity of the food product and its composition.

Copyright © 2016 by Technical University of Sofia, Plovdiv branch, Bulgaria ISSN Online: 2535-0048

## 2. Material and methods

### 2.1. F Field fluorescence measurements

Pattern of fluorescence spectroscopy is shown in Figure 1. Since fluorescence is often very weak, and in addition, in all directions, then in order not to saturate the receiver, the useful fluorescence signal is measured in a direction which is less than 45° relative to the excitation radiation.

Preferably the light source of the scheme is laser diode (LD) as the spectral width is very small. LED used in the experiment has a relatively wide spectral width of radiation from 30-40 nm and angular distribution of the radiation is in the range of large corner +/- 30°. It was selected to work with two laser diodes with one wavelength of 245 nm, which is used for the samples from infected animals, and the other 255 nm, which is used for the analysis of raw milk. Source analysis of samples from sick animals is chosen after preliminary investigations it was found that the bacteria in the body of cattle have low emission wavelength. Source analysis of samples of raw milk was selected after extensive tests were conducted and it was found that only at a wavelength of 255 nm and detects the difference in emission wavelengths between sheep and goat milk.

LEDs irradiate the sample and its emission wavelength is transmitted through the optical fiber to a CMOS detector. The sensitivity of the CMOS detector is in the range of 200 nm to 1100 nm. Its resolution is about $\delta\lambda = 5$ nm.

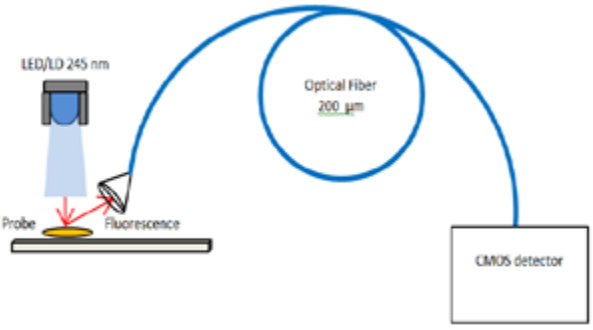



**Fig.1.** *Schematic of Field Fluorescence measurements.*

Fluorescence analysis was carried out at a dairy farm. It was decided to make field measurements, in order to avoid damage to the samples in transit and thus to ensure the more reliable fluorescence assay. With the above described production were studied various liquid samples from sick cows such as vaginal secretions, blood, nasal discharge and abscess, fluid samples from dead sheep sick of Pasteurella, a sample of the small intestine, colon sample. It was performed a fluorescence analysis of raw milk from sheep, goat, cow and mixed milk from several breeds of cows

### 2.2. Classical fluorescence spectroscopy

Fluorescence spectra were recorded using a Spectrometer - FluoroLog3 - TCSPC - Horiba Scientific. The Steady-state of Spectrometer is Broadband 450-W xenon arc lamp from UV to near-IR. The Resolution of FluoroLog3 is 0.2 nm. Of all the modern time-domain methods, including boxcar integration and streak cameras, TCSPC has by far the best dynamic range. Fixed-wavelength "Plug and Play" interchangeable NanoLED pulsed laser-diodes and LEDs. Wavelengths of 280, 340, 375, 405, 440, 473, 635, 650, 785 and 830 nm are available for laser-diodes. 370, 455, 465, 485, 560, 590, 605, 625 for LEDs.

Standard optical pulse durations are <200 ps (<100ps typical) for laser-diodes, <1.5 ns for LEDs.

### 2.3 Experimental set-up for the observation of fluorescence spectra

UV fluorescence spectroscopy was used to analyze and olive juice. The experimental set up is presented on Figure.2. Fluorescence spectra are recorded using fiber-optic spectrometer *Avantes 2048* with a spectral sensitivity within the 250 - 1100 nm range. The resolution of the spectrometer is $\delta\lambda$ 5 nm. An optical fiberwith a core diameter of 200 µm is used to bring light to the probe and to measure the scattered and fluorescent light. A collimator with a lens of an aperture D = 5 mm is used to gathermore light and focus it into a receiving fiber connected to the spectrometer. To block stray light, the cuvette holder is supplied with a cap.

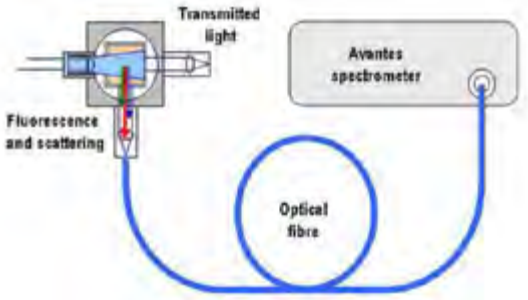



**Fig.2.** *Experimental set-up for the observation of fluorescence spectra.*

## 3. Results and discusions

### 3.1 Fluorescence spectroscopy of sheeps and cows

The excitation spectra for all studied samples of sick cows (blood sample, sample of the abscess, a sample of vaginal and nasal discharge) is 245 nm. Bacteria in the body of small ruminants have low emission wavelength. Recorded with the emission wavelengths set at: 590 nm for Fusobacterium necrophorum, 338 nm for Corynebacterium pyogenes, 579 nm for E. coli, 330 for S. Aureus, 700 for β-Hemolytic Stafilococcus, 350 for Streptococcus pyogenes and 448 for Mannheimia haemolytica

The excitation spectra for all studied samples of dead sheep (sample of the abscess open about lung cancer cient sample, a sample of colon) is 245 nm. Bacteria and nutrients in the body of small ruminants have low emission wavelength. Recorded with the emission wavelengths set at: 337 nm for Pasteurella multocida, 357 nm for sheep milk, 452 nm for β-defensin, 510 for lipopigment lipid, 400 for infusoria, 342 for pepsin and 475 for P-glycoprotein.

The aim of the study with sheep is bacterium Pasteurella multocida, which is responsible for the death of a sheep, other substances which are registered characterize the composition of the body of small ruminants.

The samples of sick cows were analyzed by veterinarian out at the dairy farm where the system for fluorescent analysis was positioned.

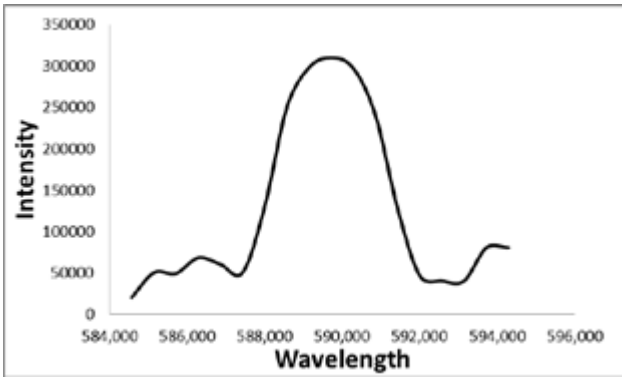



**Fig.3.** *Fluorescence spectroscopy of Fusobacterium necrophorum with emission wavelength of 590 nm at length of excitation λ = 245 nm.*

On Fig.3 and Fig.4 are clearly visible emission wavelengths of Fusobacterium necrophorum and Corynebacterium pyogenes, which were registered in the blood sample of one of the cows. Thus the diagnosis was confirmed by a veterinary specialist in emerging hoofed disease.

Sick sheep field autopsy was conducted by a veterinarian thus samples were procured for fluorescence spectroscopy.

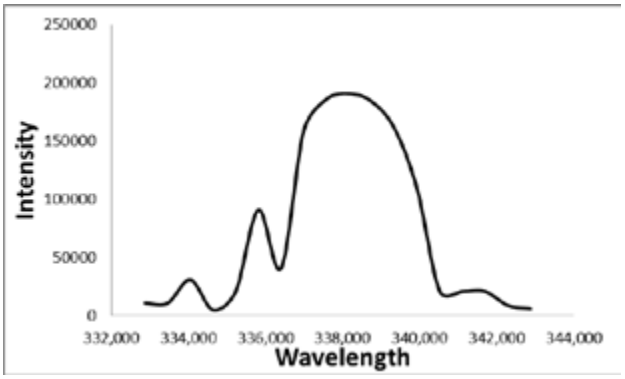



**Fig.4.** *Fluorescence spectroscopy of Corynebacterium pyogenes with the emission wavelength of 338 nm at length of excitation λ = 245 nm.*

On Fig.5 is clearly visible emission wavelength of Pasteurella multocida, which was recorded in a sample of abscess around the open areas of the lung of the animal. Thus the diagnosis was confirmed by a veterinary specialist for deadly fast growing Pasteurellosis disease, which is contagious to humans.

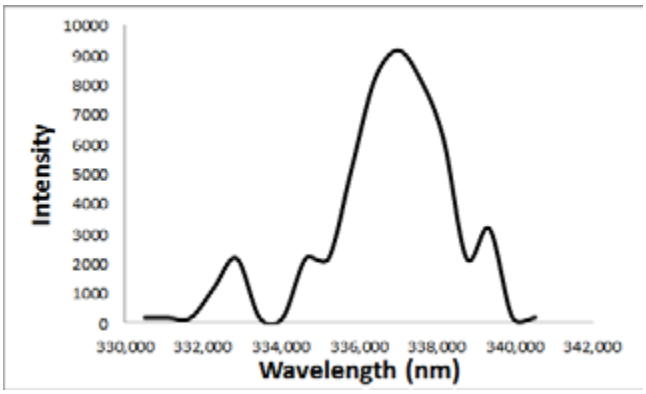



**Fig.5.** *Fluorescence spectroscopy of Pasteurella multocida with emission wavelength of 347nm at length of excitation λ = 245 nm.*

Pasteurella multocida was discovered by fast-acting fluorescent analysis as its emission wavelength have been previously studied by reference in specialized sources.

Other bacteria except Pasteurella multocida were not found, which means that the only disease in terms of fluorescence analysis is pasteurellosis. Besides samples of abscess was made and a

fluorescent analysis of liquid samples taken from small and large intestines.

### 3.2 Fluorescence spectroscopy of milk

For all studied samples of milk (cow milk, mixture cow milk, goat milk and sheep milk) the excitation wavelength is 255 nm. This is due to the fact that it only has a small difference in the peaks of fluorescence between goat and sheep milk. Records were made at the emission wavelengths set to: 343 nm for raw cow milk, 357 nm for sheep milk, 355 nm for goat milk and 366 nm for mixture cow milk.

Samples of small ruminants vary considerably in the emission wavelengths with that of the cow, which belongs to a class in cattle.

Consideration was given to a certain fluorescence spectroscopy test of mixed milks. The proportion of samples was 1:1, it is not currently performed fluorescence assay at various percentages of one or another type of milk. The excitation wavelength for all studied samples of mixture milk is 255 nm. The records with the emission wavelengths are set at: sheep + cow milk - 364 nm, sheep + goat milk - 360 nm, goat + cow milk - 354 nm.

Considerable attention was paid to an examination by fluorescence method of mixed milks presented on Fig.6 and Fig.7. Mixes a mixture of milk from large ruminant (cow) and retail (respectively goat and sheep) ratio of the samples was 1:1.

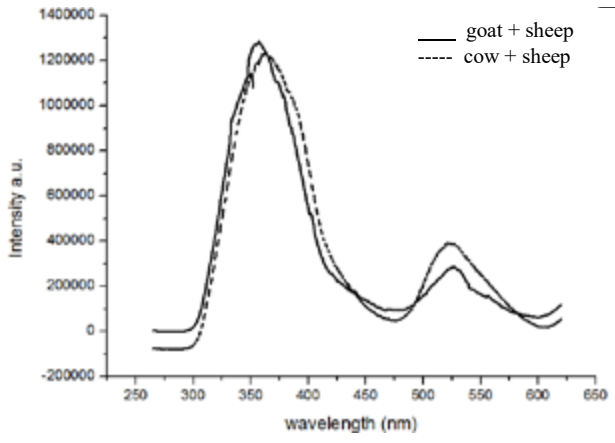



**Fig.6.** *Difference between the emission wavelength of goat + sheep and cow + sheep when irradiated at 255 nm.*

Currently made fluorescence assay at different rates contents of one or other type of milk. It turned out that the difference between the emission wavelength at various mixes is not so great as fluctuation between milk from a breed of cow milk from cows of several breeds. This means that in a blend of equal portions of the milk of the large and small ruminants is obtained more similar performance than mixing the milk from different breeds of cattle.

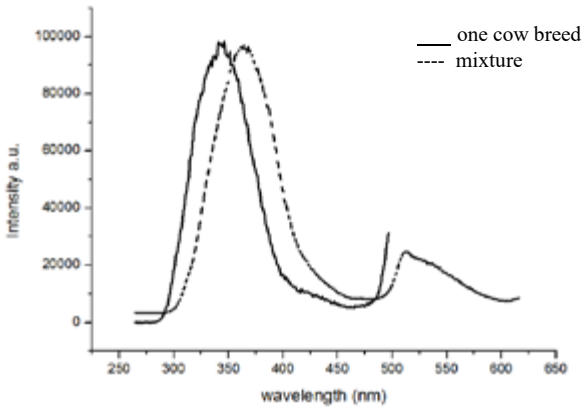



**Fig.7.** *Emission wavelength difference between one cow breed and cow mix when irradiated at 255 nm.*

Essential is the moment on Fig.7. In fluorescence diagnosis with respect to testing cow's milk is that the milk taken from a cow breed differs in wavelength of fluorescence with that which is a mixture of several breeds. This means that the method of fluorescence is suitable for determining the quality of milk for a selected breed.

### 3.2 Fluorescence spectroscopy of apple juice

Thirty two samples from fruit juices were investigated. They were from four different fruits and nine different well known brands that are widely distributed in the shop industry. The juices were drained using a juicer for 4 different fruits as it does not add additional impurities. In Fig. 8 we can see a difference between emission wavelength of freshly squeezed apple juice and emission wavelength of apple juice of market. At apple juice of market have two relatives emission wavelengths, which are located exactly on both sides of emission wavelength of freshly squeezed apple juice, this fact shows that the impurities that are added to the juice, which are commercially available are those which are close to the composition of freshly squeezed juice.

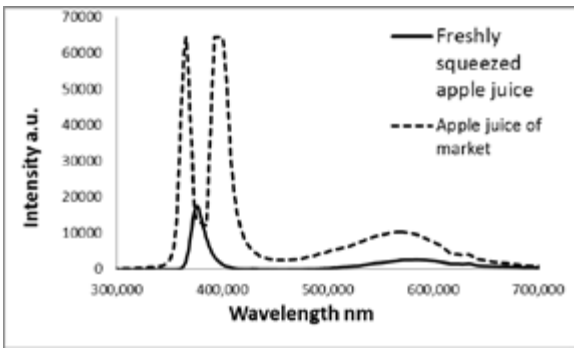



**Fig.8.** *Fluorescence spectroscopy apple juice for excitation at λ = 250 nm.*

### 3.4 Fluorescence spectroscopy of olive oil

Twenty four samples of different brands Spanish and Greek olive oils sold in supermarkets were investigated. The fluorescence of the samples was studied by exciting them with LEDs emitting at 370 nm, 395 nm, 425 nm and 450 nm. A 90◦ geometry of light detection in a 10×10 mm cuvette was used. Samples were studied without any preliminary solution.

The conclusion of the fluorescence analysis Pure olive oil there would be emission wavelength of colza. In physicochemical analyzes are difficult to distinguish between olive oil, which has impurities of colza and virgin olive oil. In Fig.9 is presented the difference between Pure olive oil and Extra virgin olive oil. There is a difference between the emission wavelength both types of olive oil.

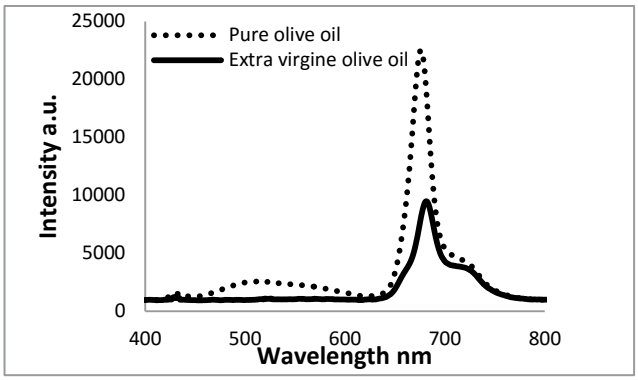



**Fig.9.** *Fluorescence spectroscopy olive oil for excitation at λ = 425 nm.*

## 4. Conclusions

Advanced is fast and easily accessible method for field fluorescence spectroscopy of liquid samples from cattle. The optimal wavelength for fluorescence analysis of diseased ruminants is 245 nm. The fluorescence method is suitable for early diagnosis of samples for the presence of bacteria in cattle and before the presence of symptoms of the disease, which causes the respective bacteria.

Bacterium Pasteurella multocida was detected by fluorescence analysis in the body of a sheep, which is dangerous for the human organism. By fluorescence analysis autopsies of sick animals can be avoided with harmless to the human organism method as most autopsies of animals are harmful to humans.

Optimal wavelength for fluorescence analysis of pure milk from ruminant animals is 255 nm. The fluorescence method is suitable for analysis of both individual samples of milk, and mixing samples (from different animals cow, goat or sheep). The fluorescence method is suitable for detection if milk from a cow breed or mix of several breeds (this would represent the interests for producers who select the breeds).

Optimal wavelength for fluorescence analysis of apple juice is 245 nm. At this wavelength differences are detected most easily in the composition of freshly squeezed juices and those that are available in stores. The method of fluorescent analysis of juices is fast and efficient. With a rich enough library can be done effective analysis of the purity of the natural juices offered by many companies. Samples of their products compared with freshly squeezed juice from the respective plate.

Optimal wavelength for fluorescence analysis of olive oil is 425 nm at this wavelength is most clear the difference between the composition of Pure olive oil and Extra virgin olive oil. Fluorescence analysis of olive oils is a fast and efficient way to establish the purity of olive oil.

Fluorescence analysis is a quick and efficient method for accurate analysis both in veterinary medicine and food industry. This method can successfully replace so far used chemical and physical methods. This is an easy and relatively inexpensive method of analysis, since it does not require additional supplies and one unit can check multiple samples. In most cases it has been shown that the fluorescence assay is more accurate than many of the physics-chemical assay, as impurities that are added in a product is similar in chemical composition to the natural, and only the fluorescence analysis can perform accurate and adequate contrast between the samples.

## REFERENCES

1. Nora E. Sobero´ n, Virginia S. Lioy, Florencia Pratto, Andrea Volante and Juan C. Alonso (2011) Molecular anatomy of the Streptococcus pyogenes pSM19035 partition and segrosome complexes Vol. 39, No. 7, 2624–2637 Nucleic Acids Research

2. Zhiyi Liu, Heng Shi 1, Le Liu, Sunan Deng, Yanhong Ji, Suihua Ma, Hui Ma and Yonghong He Line-Monitoring, Hyperspectral Fluorescence Setup for Simultaneous Multi-Analyte Biosensing *Sensors* 2011, *11*, 10038-10047

3. Pratto,F., Suzuki,Y., Takeyasu,K. and Alonso,J.C. (2009) Single-molecule analysis of protein·DNA complexes formed during partition of newly replicated plasmid molecules in Streptococcus pyogenes. J. Biol. Chem., 284, 30298–30306.

4. D. J. D'Amico 1 and C. W. Donnelly. Microbiological quality of raw milk used for small-scale artisan cheesenproduction in Vermont: Effect of farm characteristics and practices (2010) J. Dairy Sci. 93 :134–147

5. Maвmouri, O., Rouissi, H., Dridi, S., Kammoun, M., De Baerdemaeker, J., & Karoui, R. (2008). Mid infrared attenuated total reflection spectroscopy as a rapid tool to assess the quality of Sicilo–Sarde ewe's milk during the lactation period after replacing soybean meal with scotch bean in the feed ration. Food Chemistry, 106, 361–368.

6. Karoui, R., Dufour, E., & De Baerdemaeker, J. (2007). Monitoring the molecular changes by front face fluorescence spectroscopy throughout ripening of a semihard cheese. Food Chemistry, 104, 409–420.

7. Zhiyi Liu, Heng Shi 1, Le Liu, Sunan Deng, Yanhong Ji, Suihua Ma, Hui Ma and Yonghong He

8. Line-Monitoring, (2011) Hyperspectral Setup for Simultaneous Multi-Analyte Biosensing *Sensors 11*, 10038-10047

9. Pratto,F., Suzuki,Y., Takeyasu,K. and Alonso,J.C. (2009) Single-molecule analysis of protein·DNA complexes formed during partition of newly replicated plasmid molecules in Streptococcus pyogenes. J. Biol. Chem., 284, 30298–30306.

10. Dhammika N. Atapattu, Nicole A. Aulik, Darrell R. McCaslin, and Charles J. Czuprynski, Brief heat treatment increases cytotoxicity of *Microb Pathog*. (2009) *Mannheimia haemolytica* leukotoxin in an LFA-1 independent manner March, 46(3): 159–165

"Dept. Optoelectronics & Lasers", Techn. Univ.-Sofia, Branch Plovdiv and Scientific Laboratory "Quantum and Optoelectronics", R&D Devison,Techn.Univ.-Sofia
Phone (032/ 659 752 ):
E-mail: vania_plachkova@abv.bg

© International Scientific Conference on Engineering, Technologies and Systems
TECHSYS 2016, Technical University – Sofia, Plovdiv branch
26 – 28 May 2016, Plovdiv, Bulgaria

# ELECTRONIC CONVERTER FOR FIBER OPTIC THERMOMETER

SVETOSLAV IVANOV, YANKA IVANOVA

**Abstract:** *Fiber optic sensors working on reflectometric principle are used in sensors to measure temperature, liquid level and concentration of solutions. This article shows the results of research the created fiber optic thermometer for measuring temperature. Were tested transients in pulse optoelectronic transducer of temperature to analog signal. Optical receiver takes into account the difference between the amplitudes of the received signals from fiber optical sensor and a second optical fiber which transmits the optical signal directly from the source. A method is proposed for digital linearization of the transfer characteristic of the converter. Constructed fiber-optic thermometer allows measurement of temperatures ranging from 20 ° C to 150 ° C with a measurement accuracy of 1 ° C.*

**Key words:** *fiber optics, sensors, electronic transducers, temperature sensors.*

## 1. Basics

Fibers have many uses in remote sensing. Depending on the application, fiber may be used because of its small size, or because no electrical power is needed at the remote location, or because many sensors can be multiplexed along the length of a fiber by using light wavelength shift for each sensor, or by sensing the time delay as light passes along the fiber through each sensor. Lower temperature targets say from 100°C to 400°C can be measured by activating various sensing materials such as phosphors, semiconductors or liquid crystals with fiber optic links offering the environmental and remoteness advantages. For temperature measurement can be used fiber optic sensors working on reflectometric principle with external modulation of the luminous flux. At these sensors most commonly changes the amplitude of the intensity of the light pulses passing along the fiber [1,2]. On the basis of the U-a turn on reflectometric principle are created sensors for measuring liquid level, temperature and concentration of solutions. Have been created schemes for optical registration, which is carried converting light pulses into electrical impulses [3,4]. After that follows their demodulation of an amplitude detector. The resulting analog signal from the output of the detector enters the input of the analog-to-digital converter (ADC) [5,6]. In order to increase the measurement accuracy, typically puts additional linearization of the characteristic of the sensor. The purpose of the studies carried out and the results obtained is to create analog converter DC output signal proportional to the amplitude value of the electrical and light pulses respectively. Provided that the transmission characteristic of the sensor is a monotone increasing functional is possible a linearization of the measurement results in the entire temperature range.

## 2. Principle scheme of the electronic converter

The principle scheme of the created converter is shown in Figure 1. The generator G generates electrical impulses rectangular shape with constant frequency and constant duty cycle. These impulses controlled LEDs and amplitude detector. Light pulses passed through the optical fiber and modulated by sensitive element S, are input to a converter of current in voltage. As an optical receiver using a PIN photodiode. The electrical impulses from the output of converter to do the entrance of the detector. The input of the detector integrated circuit represents - *R1*, *C1*, whose output is connected to the input of the first circuit sample / hold S / H I. The output of the detector is an integrated circuit - *R2*, *C2*. The management of both schemes sample / hold (SH) is carried by the generator of electrical impulses. The first scheme remembers maximum output voltage from the

Copyright © 2016 by Technical University of Sofia, Plovdiv branch, Bulgaria ISSN Online: 2535-0048

output of integrated circuit during the pulse, received of its entrance. The second scheme (S / H II) is designed to maintain this peak value as a permanent signal at its output. The LED on the transmitter is connected via coupling with two quartz optical fiber FO1 and FO2. Optical fibers with gradient a refractive index higher with cross section 50 / 125μm. One fiber is connected to the sensor for measuring the temperature, and the other fiber carries light directly. By using these two fibers is removed the influence of the change of intensity of light output of the LEDs in the measurement process. The electronic converter amplifies the difference between the received signals of the two photodiodes. Optical fiber sensing element is a fiber with a U a turn contained within the sensor. Part of the surface of the U is the fold shucked optical sheath, the remaining optical core is placed in thermo-optical environment. The used thermal optical medium is a semi transparent polymer whose a refractive index higher is changed by temperature.

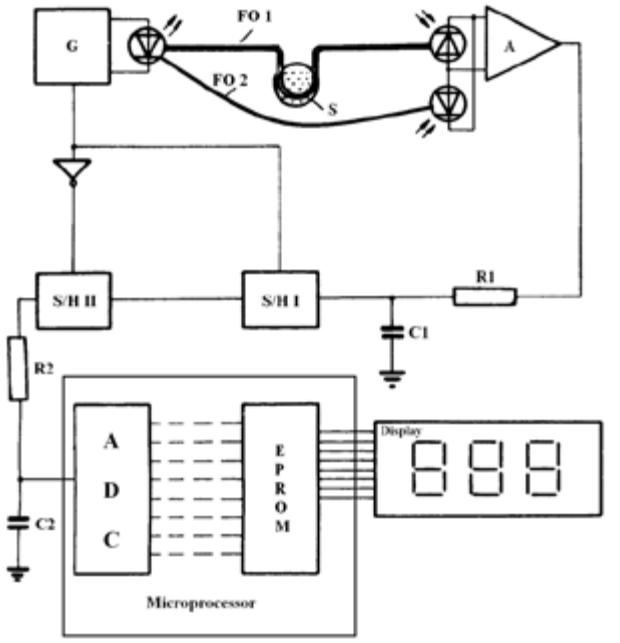



Fig. 1. Principle scheme of Research fiber optic thermometer

The input of the optical receiver is differential. It consists of two related cross and parallel PIN photodiodes. The two optical fibers coming from the transmitter and the sensor are connected to the respective photodiodes. The two optical fibers coming from the transmitter and the sensor are connected to the respective photodiodes.

### 3. Transient processes in the integrated circuit

Upon receipt of rectangular pulses with a constant frequency and constant duty cycle at the entrance of integrated circuit *R1*, *C1*, of its output is set transition process with permanent extreme values. The maximum value of the voltage $U_{max}$ charging the capacitor and the minimum value dilution $U_{min}$ are proportional to the amplitude of the input pulse. The maximum value of the voltage to which the capacitor is charged $U_{max}$ is the value which is maintained constant by scheme sample / hold to the output of the amplitude detector. This value is equal to:

$$U_{\max} = K.U_i \,, \qquad (1)$$

where: - $U_i$ is the amplitude value of the output voltage of the electronic converter

- coefficient $K = \left(1 - e^{-t_A}\right)$ (2)

The coefficient $t_A$ is expressed by the parameters of the received input pulses at the input of the amplitude detector in the following terms:

$$t_A = \frac{\alpha}{f.T_c} + \ln\left(\frac{1 - e^{\frac{1}{f.T_c}}}{1 - e^{\frac{1-\alpha}{f.T_c}}}\right), \qquad (3)$$

where: $\alpha$ - duty cycle of the pulses;

$f$ – the pulse frequency;

$T_c$ – the time constant of the integrating circuit $R_1$, $C_1$.

The coefficient $K$ represents the ratio of the transmission of the amplitude detector. Figure 2 shows a graph of the dependence of the coefficient $K$ of the transmission frequency of input pulses. The calculations are made at constant duty cycle of the input pulse $\alpha$ = 0,3 and time constant of the integrating circuit equal to $T_C$ = 0,027s.

Figure 3 graphically shows the dependence of the coefficient of transmission of the K from duty cycle of the received pulses, at a constant pulse frequency equal to 70Hz. The time constant of the integrating circuit is equal to the $T_C$ = 0,027s. Figure 3 graphically shows the dependence of the coefficient of transmission of the K from duty cycle of the received pulses, at a constant pulse frequency equal to 70Hz. The time constant of the integrating circuit is equal to the $T_C$ = 0,027s.

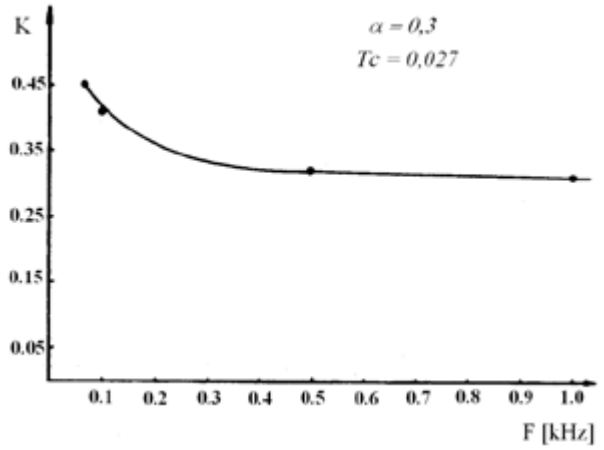



***Fig. 2.*** *Variation of the coefficient of transmission of the amplitude detector on the frequency of control impulses*

An advantage of the integrated circuit, as an input a step of the detector is that it greatly reduces the high frequency noise entering together with the signal at the input of the scheme.

The analyzes carried show that the ratio of the pulsation of the output voltage is equal to $K_P$=0,09%, with variation of output voltage in the range from 0.5 to 3,5V.

Analogue-to-digital converter is part of the microprocessor used for the linearization of the transfer characteristic of the sensor and the control of the digital indication.

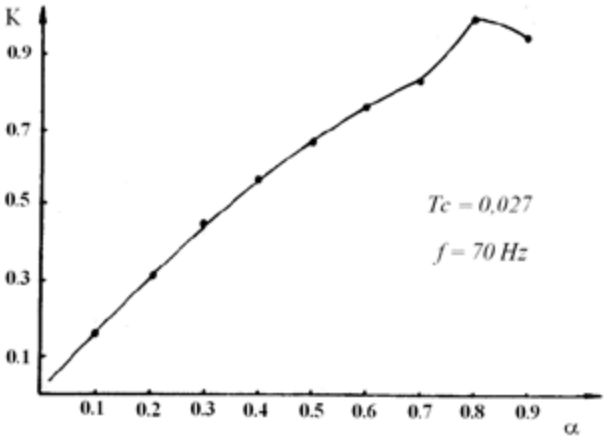



***Fig. 3.*** *Amending the coefficient of transmission of the duty cycle of the control pulses*

### 3. Block for digital linearization the characteristic

Digital code from the output of analog-to-digital converter (ADC) delivered to the address buses permanent memory (EPROM). Thus, by the generated address be addressed memory cell in which previously recorded actual value of the measured value. If we denote the value of the measured with $\theta$, and reading from the output of the ADC with $X$, the graph of the relationship $X = F(\theta)$ in a fiber-optic temperature sensor has the type shown in Figure 4. With the EPROM is realized inverse function $\theta = F^{-1}(X)$. In memory write any value of measured value $\theta_n$ is recorded in a range of cells in the memory addresses for $\theta_n$

$$\text{by address } \frac{x_n + x_{n-1}}{2} \text{ to } \frac{x_n + x_{n+1}}{2},$$

where $x_n = F(\theta_n)$, $x_{n-1} = F(\theta_{n-1})$ и $x_{n+1} = F(\theta_{n+1})$

The graph of the inverse function with the intervals, in which $\theta_n = const$ is shown in Figure 5. The determination of addresses, in which will record the measured value can be done and analytically;

$$x_n - \frac{1}{2.\theta'.(x_n)} < x < x_n + \frac{1}{2.\theta'.(x_n)} \quad (4)$$

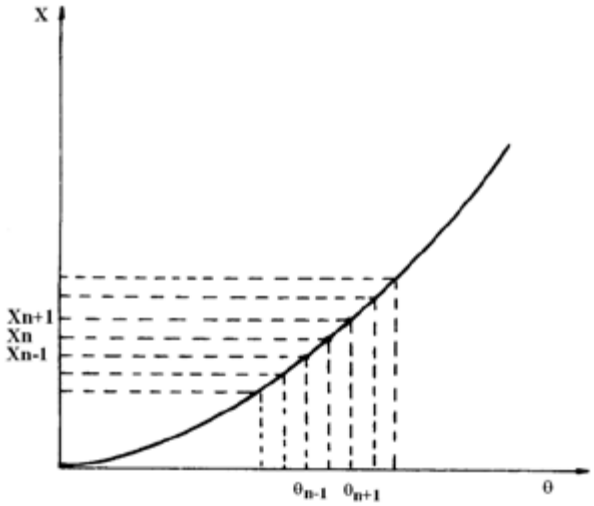



***Fig. 4.*** *Amending the output data of the ADC as a function of temperature*

The latter inequality determines the range of address values $x$, in which must be recorded value $\theta_n$ for respectively $x_n$. Thus the maximum value of the absolute error of the entire measurement interval will be constant and equal to half of the smallest significant digit in the measurement.

Constructed fiber-optic thermometer permits measuring temperatures ranging from 20° C to 150 ° C. The accuracy of measurement is 1° C. Scheme linearization the characteristic allows the

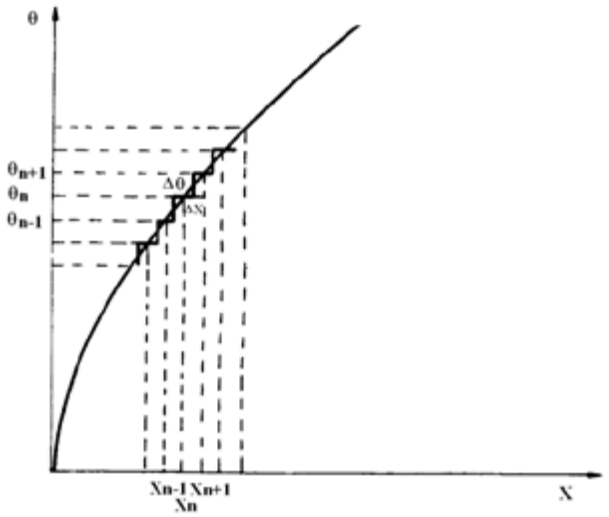



***Fig. 5.*** *Graph of the inverse function of measuring temperature*

sensor to achieve absolute error in the entire measuring range ± 0,5 ° C.

The percentage error at maximum measured value 150 ° C, is equal to 0.033%.

## 4. Conclusion

In constructing a detector for an amplitude modulated pulses with success may be used extreme values of transients in an integrating circuit. The maximum value of the output from the integrated circuit can be established as a permanent signal with the use of two series-connected circuits - "sample / hold". The theoretical calculations and experimental results prove the constant coefficient of transmission of the detector and low ripple output voltage detection pulses with a constant frequency and constant duty cycle.

In digital circuits for linearization of the characteristics of the sensors is appropriate to use an EPROM memory. If the characteristic is strictly increasing or strictly decreasing function, it is possible linearization, to give the a constant absolute error of measurement over the entire range.

Constructed optoelectronic transducer is attached to fiber-optic thermometer that measures temperatures ranging from 20 ° C to 150 ° C. The characteristic of the sensor is linear and is a strictly growing function. The resultant absolute error is ± 0,5 ° C in the entire interval measurement.

## REFERENCES

1. K.T. Grattan, T. Sun, Dr (2000), Fiber optic sensor technology: an overview, Sensors and Actuators A: Physical**,** Volume 82, Issues 1–3, 15 May 2000, Pages 40–61.
2. Feng, X., Zhang, X., Sun, C., Motamedi, M., and Ansari, F., Stationary Wavelet Transform Method for Distributed Detection of Damage by Fiber-Optic Sensors (2014), Journal of Engineering Mechanics , April 2014, Vol. 140, No. 4
3. International Electrotechnical commission. *Calibration of Optical Time-Domain Reflectometers (OTDR)-Part 2: OTDR for Multimode Fibres*; Nr. 61746-2; International Electrotechnical commission: Geneva, Switzerland, 2010.
4. Koyamada, Y.; Eda, Y.; Hirose, S.; Nakamura, S.; Hogari, K. Novel fiber-optic distributed strain and temperature sensor with very high resolution. *IEICE Trans. Commun.* **2006**, *E89-B*, 1722–1725.
5. Nazarathy, M.; Newton, S.A.; Giffard, R.P.; Moberly, D.S.; Sischka, F.; Trutna, W.R., Jr.; Foster, S. Real-time long range complementary correlation optical time domain reflectometer. *J. Lightw. Technol*. **1989**, *7*, 24–38.
6. Anderson, D.; Bell, F. *Optical Time Domain Reflectometry*; Tectronix: Beaverton, OR, USA, 1997; p. 61.

Authors' contacts Address:
E-mail: etehsv@gmail.com
E-mail: yankakiss777@abv.bg

© International Scientific Conference on Engineering, Technologies and Systems
TECHSYS 2016, Technical University – Sofia, Plovdiv branch
26 – 28 May 2016, Plovdiv, Bulgaria

# ON ADVANTGEOUSLY USE OF GAUSSIAN BEAM END DIODE LASER PUMPING OF ND:YAG LASER IN TWO-WAVELENGTH COAXIAL ARCHITECTURE

MARGARITA DENEVA

**Abstract:** *We propose to take advantage of the specific light intensity distribution in the pump beam when the cylindrical active Nd:YAG rod laser is end-pumped by a Gaussian beam diode laser to create a new effective two-wavelength laser. The essentially high pump intensity in the central part of the rod increases the pump power density there ~ 3-4 times (depending of chosen radius) in comparison with the peripheral rod part. The increasing strongly favorites the generation of weaker lasing lines in the axial part. This advantage is utilized by employing coaxial two-channel laser architecture, where the optically separated axial and peripheral parts of the rod generate each in its own spectrally selective resonator. Beside the competition-less generation at two wavelengths (lines), other specific and essential advantages of the proposed laser solution are: i) to produce emissions at a weeker line (generated in the axial part) and at a stronger line (in peripheral part), simulataneously and with equalized energy without loss of pump energy for the equalisation; ii) the two emissions are produced and emitted naturally in coaxial beams using the full rod volume. Exept the argumented proposal, we considered in details theoretically the action of such laser on the example of generation of the pair lines - of the weaker at 1.36 um and the strongest at 1.06 μm respectively and show the expected advantages. Such laser can be applied effectively for generation of pair of Nd:YAG lines from 1.06, 1.32, 1.34, 1.36 and 1.44 μm and also for the generation in other materials (including Q-switching).*

**Keywords:** *Gaussian beam diode pumped laser, two-wavelength generation, Nd:YAG laser, coaxial geometry laser architecture, independent generation control*

## 1. Basics

In spectroscopic and optical instrumentations laser light at two or more wavelengths, in particular, at two different emission lines (or colors) and with tunability are employed. Such light is of essential interest in space composition determination by the technique of Differential Absorption Spectroscopy (DAS), including distant monitoring of gas pollutants and aerosols in the atmosphere (LIDAR) [1-5], in spectroscopy, in nonlinear optics [6-8], in metrology [9], in bio-medical investigations and treatments [10]. The superposition of the beams of two lasers is a simplest way to obtain two-wavelength laser light [11]. However, such a realization need two lasers, special filters for neighboring wavelengths and is difficult for synchronization of two sub-systems for operation using two nanosecond-timed Q-switchers.

A simpler and cheaper way to obtain controlled two-wavelength laser emission is to use a single laser that generates the two wavelengths in a single exciting pulse or in CW emission – i.e. so-called two-wavelength (dual line, dual color) laser with a flashlamp (for high energy output) or diode pumping. The detailed review of such lasers is given in [12]. The diode pumping is of essential interest assuring compact technical solutions and high energetical effectiveness for CW and pulsed regime [13-15]. Especially, high simplicity, compactness and effectiveness are for the case of so-called diode laser end-pumped Nd:YAG cylindrical laser. Such pumping consists of introduction of the entire pump light into the crystal and along its axial rod direction.

One effective way to produce the two emissions is to use a single laser rod, in which each wavelength is generated in separated pumped parts of the rod volume. The dual-wavelength generation

Copyright © 2016 by Technical University of Sofia, Plovdiv branch, Bulgaria ISSN Online: 2535-0048

in separated parts has the advantage to avoid so-called "wavelength competition effect" that is typical and leads to a problem when the two wavelengths are generated in common parts of the rod [16, 17, 14]. Our scientifique group, on the base of new development of our patented principle, has developed and published an effective, coaxial geometry, flash-lamp pumped two-wavelength Nd:YAG laser [12]. We have used the focalizing effect of the cylindrical rod of the side pumped flash-lamp light and have shown the effectiveness of apllication of the coaxial two-channel architecture for the case.

The aim of this work is to introduce and show the attractiveness and usefulness of the application of the coaxial geometry laser solution for the case of the diode end-pumped beam with Gaussian distribution. The combination of this two circumstances strongly favorites the creation of effective laser of the noted type as we shell show in the work.

## 2. Principle and scheme of the proposed laser

The basic optical scheme of the proposed Nd:YAG two-wavelength coaxial-geometry laser pumped by diode laser with Gaussian beam is given in Fig. 1.

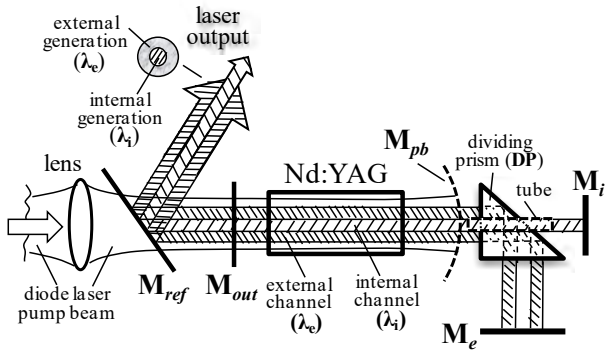



**Fig. 1.** *Optical scheme of the laser with channel separator prism SPr with hole.*

In the description of the principle and in the consideretaion,given below, we use the following combination of elements for the Nd:YAG diode pumped set-up: Nd:YAG cylindrical rod with diameter $d = 0.5$ cm, length $l = 0.5$ cm and concentration of $Nd^{3+}$-ions of 0.6 at %. (in the scheme in the figure - Nd:YAG). Note that in the consideration we will use the parameters of our available specialized laser crystal designed for the diode pumping. The pumping is by the pulses of diod laser at 0.808 μm with Gaussian intensity distribution and energy of 120 mJ and pulse duratin of ~ 200 μs. The input pump beam passes through lens with sutable focal length to form the spot at the antrance of the Nd:YAG rod with diameter of ~ 0.5 cm, containing ~ 99 % of the incident beam power $P_{tot}$ (i.e. 1.6 time higher than the Gaussian radius in this cross-section following, e.g. [13]). The length of the lens assures the Relay length essentially larger than the rod length *l*. Thus we can consider the beam rays propagation into the crystal as near parallel to the cristal axis. Before to enter into the rod, the pump beam passes through declined at ~35° multichroic mirror $M_{ref}$ (with reflectivity 0.86 for 1 - 1.4 μm, and ~ 0.1 for 0.808 μm). The Nd:YAG laser output mirror $M_{out}$ is also multichroic (reflectivity 0.86 for 1.32 - 1.36 μm and 0.1 for 1.06 μm and R~ 0.1 for 0.808 μm). At the oposite end of the crystal is sutably adjusted near-plane multichroic miror $M_{pb}$ with radius of curvature few meters (reflectivity ~ 0.1 for 1- 1.4 μm and ~ 0.86 for 0.808 μm). The generation at the two wavelengths (scheme in Fig.1) is produced in two coaxially disposed and optically separated parts of the described Nd:YAG laser rod, for each part being formed own spectrally-selective resonator with length of each $L \approx 10$ cm. As symplest optical separation of the two rod parts with their resonators (hatched differently in Fig.1) is used a dividing rectangular prism (DP). It is with 0.38 cm diameter bore hole and length of 0.4 cm through the cathetus and the axis, coinciding with the rod axis. In the hole a very thin (~0.1 mm wall) metal tube with 2 cm length is introduced, which detail assures very good separation of both channels as we have shown in our previous work [12]. The prism is declined at ~5° with respect to the crystal axis to avoid the back Fresnel's reflection. In the external, perepherial part of the active rod and its resonator (external channel), the light at the first wavelength $\lambda_e$ is generated. The second wavelength $\lambda_i$ is obtained in the coaxial, round cross section, internal rod part, and its corresponding resonator (internal channel). We will consider here the scheme in simplest manner with two flat-flat Selective Mirror Resonators (SMRs) using, as the common output coupler, the multichroic mirror $M_{out}$. The end mirror $M_e$ of the external resonator for generation at $\lambda_e = 1.06$ μm is with $R_e$=0.99 for 1.06 μm and the end mirror $M_i$ of the internal resonator for generation at $\lambda_i$=1.36 with $R_i$ =0.99 for 1.36 μm. The last mirror is with less than 0.70 reflectivity for the other wavelength and AR ends coated for the 1.06 μm. By replacing both end mirrors with sutable reflectivity we can change the generated line in the corresponding channel (if the pumping is sufficient). The ends of the crystal is specially AR coated for the wavelengths in the range 0.9 - 1.4 μm. As we have realized for the case of flashlamp pumping coaxial geometry laser [12], the end mirrors $M_i$ and $M_e$ can be replaced

with sutable prism-selective blocks and for sufficently pumping energetic characteristic may obtain in each channel tunable generation.

### 3. Theoretical modeling and treatment of the two-wavelength operation of the proposed laser

Due to essential difference for the spectroscopic data for Nd:YAG absorption cross section at 0.808 μm, we have realized our proper estimation of our crystal absorption. We measured the absorption of the crystal for 0.594 μm wavelength of our yellow He-Ne laser. Taking the measured absorption and the graphs of the absorption of Nd:YAG as a function of the wavelength, given in the representative literature [13, 14], we have evaluated that for our crystal the absorption coefficient for pumping wavelength of 0.808 μm is 3.9 $cm^{-1}$. Having all nessesary data, given already, we have used the following approach. Firstly, we have calculated, in our point of view - corectly, the pumped power distribution in the laser rod.

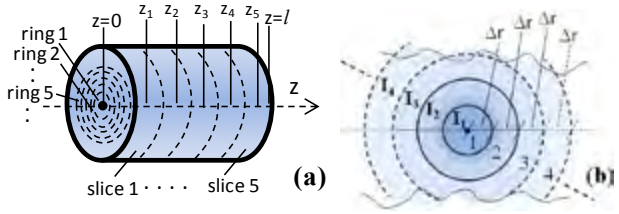



***Fig.2.*** *Schematic Nd:YAG rod division: (a) longitudinal in slices (b) and radially in rings (b); z=0 and z=l are the front and rear surfaces of the crystal, respectively.*

Schematically for the theoretical treatment, the Nd:YAG rod is divided radially at rings and longitudinally in slices. This division is clarified in Fig. 2. The cross-section of the rod is divided at 8 rings with equal increasing radii for each sequent by Δr (see Fig.2b). Along the axis Z of the crystal the division is at 5 slices each with equal length $\Delta l = l/5$. For our treatment we consider the cylindrical Nd:YAG crystal with concentration ~0.6% $Nd^{3+}$-ions, length of 0.5 cm and cross-section diameter of 0.5 cm. Respectively we have $\Delta l$=0.1 cm and Δr = 0.0625 cm. In considered by us case, the pumping diode laser power is 120 mJ in a near rectangular pump pulse with duration of ~200 μs. The pump beam is focalized with appropriate lens in manner that the focalized total beam power drops at the ends of the Nd:YAG rod down to 2% (ratio of the rod diameter and pump Gaussian beam diameter is ~1.6). Thus, in practice the total pump power is used to pump the crystal.

We will provide a theoretical consideration for the noted already data. The aim of our consideration will be to find the limits of the ring around the optical axis, where the output energy at the wavelength 1.36 μm is comparable with this one generated at 1.06 μm in the external rings. We expect that it is possible due to the essentially different cross-section of the stimulated emission for the two wavelengths and the difference in the pumping power (intensity) in the central axial part and peripheral part of the crystal.

Let's first consider the distribution of the pumping for each cylinder formed by border lines parallel to the axis of the crystal and closed by the pair of rings at the front and rear sections of the crystal (partial cylinders).

The maximal intensity $I_0$ in the center of the beam at the entry plane of the rod was calculated on the base of well known relation:

$$I_0 = \frac{2P^{\max}}{\pi \cdot \omega^2} \qquad (1)$$

where $P^{max}$ is the maximal pump power in the pulse and $\omega$ is the Gaussian radius of the pump beam. The intensity for each partial cylinder is calculated for the middle of the ring radius ($r_i = (2 \cdot i - 1) \cdot (\Delta r/2)$, $r = 1, 2 \ldots 8$) and is assumed to be homogeneous for the ring. The points on the graphics in Fig.3 present the values for the corresponding rings.

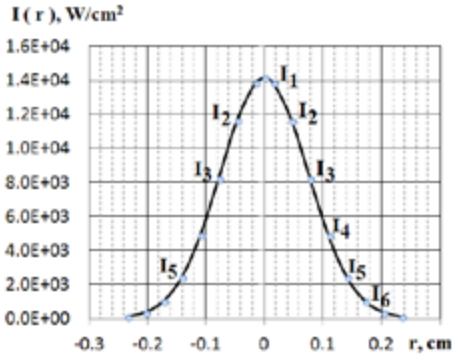



***Fig.3****. Calculated distribution of the initial intensity ($I_i$) in cross-section at the entrance for the corresponding ring (i – see Fig.2), on the axis X is given the distance* ***r*** *from the center (r=0) of the beam cross-section.*

The distribution of the pump power for each ring, the area of the corresponding ring and pump intensity are presented in Fig. 4.

In the calculations for propagation along the Z axis, we have used the Bouger's law, taken into account the effect of absorption saturation. We have evaluated the change of the pump intensity correspondingly for each ring, slice by slice – forward and backward after reflecting by the mirror $M_{pb}$. For each slice we sum forward and backward values, accepting that for any ring of the slice the

intensity is constant, equal to this one at the half length of the slice. We assume a total input in the

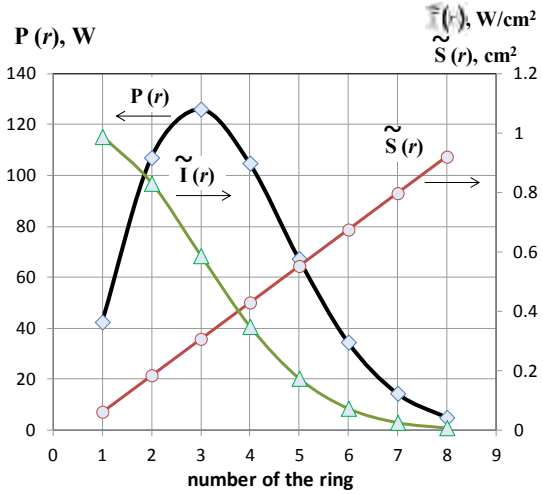



***Fig. 4.*** *The pumping power P(r) corresponding to each ring. The corresponding starting pump intensity I (r) and the area S (r) of the ring are also given. Here* $\tilde{I}(r) = I(r)/1.4\cdot10^4$ *and* $\tilde{S}(r) = S(r)\cdot 20\cdot$

crystal pump power $P_{tot}$≈100 mJ / 200 μs, Gaussian beam intensity distribution. In Fig. 2(a) $z_i$ ($i$ = 1, 2, …5) corresponds to the middle of the length's slice, where the result intensity is calculated. The values of the obtained intensity $I_{r,Zi}$ for the first five rings, where generations exist, are presented in Fig.5.

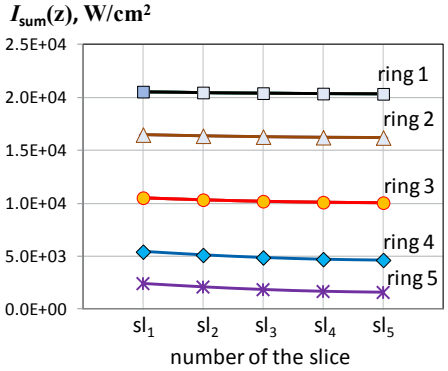



***Fig. 5.*** *The result pump intensity for the first five rings obtained after summing the forward and backward values, calculated slice by slice. On axis X are plotted the number of the slice* $sl_i$, *i=1,2..5 (in the middle in which the results are obtained).*

The calculation graphics given in Fig.5 show for each partial cylinder practically the same sum pump power (and energy) - uniformity both in slices and in the cross section – i.e. in the corresponding ring. This uniformity determines the fact that we can accept homogeneity of the pumping with different energy density for the partial cylinders (the change in the intensities from the firs to the last slice for the corresponding cylinder is of order of some percentages and practically could be accepted as constant for each ring). On this base, we can calculate the generation for each partial cylinder applying the set of rate differential equations [14] adapted for the case, presented in next point. The considerable difference in the pump power for the rod parts around the axis and in the peripheral areas, enabling us to expect generation at weak lines (with smaller values of the emission cross-section) comparable to that at the stronger lines, including the main 1.06 μm, when it is generated in peripheral part of the crystal. In the analysis below, we show this possibility in the case of the line 1.36 μm, generated in near axial part and the line 1.06 μm generated in the peripheral part of the crystal.

## 4. Analysis of the laser generation

Taking the obtained results for the approximately constant value of the pump energy into slices along the axis of the crystal – i.e. possibility to assume homogeneity of the excitation (with different energy density for the corresponding ring), we apply the adapted set of differential rate equations [14] for the analysis. The adapted system that describes our case and assumed parameters is:

$$\begin{cases} \dfrac{dN_2}{dt} = R_p^{(e,i)}(t) - B^{(e,i)}\cdot q^{(e,i)}\cdot N_2 - \dfrac{N_2}{\tau} \\ \dfrac{dq^{(e,i)}}{dt} = Va^{(e,i)}\cdot B^{(e,i)}\cdot q^{(e,i)}\cdot N - \dfrac{q^{(e,i)}}{\tau_c^{(e,i)}} \end{cases} \qquad (2)$$

with $P_{out}^{(e,i)}(t) = \left(\gamma_{out}^{(e,i)}\cdot c/2L'\right)\cdot h\nu^{(e,i)}\cdot q^{(e,i)}(t)$ (3)

Here $B^{(e,i)} = \sigma_{21}^{(e,i)}\cdot l\cdot c/V_a^{(e,i)}\cdot L'$, s$^{-1}$; $\sigma_{21}^{(e)}$= 2.8×10$^{-19}$ cm$^2$; $\sigma_{21}^{(i)}$= 0.6×10$^{-19}$ cm$^2$ – emission cross-section of the Nd:YAG laser crystal for $\lambda_e$ = 1.06 μm and $\lambda_i$ = 1.36 μm [12], $l$ – crystal length; $c$ = 3×10$^{10}$ cm/s is the light velocity; L' = 10.42 cm is the optical length of the resonator. The lifetime of the upper laser level is $\tau$ = 230 μs. The term in (3) $h\nu^{(e,i)}$~10$^{-18}$ J is the energy of the generated photons for the corresponding wavelength. The dumping time of the photon in the resonator is $\tau_c^{(e,i)} = L'/c\cdot\gamma^{(e,i)}$, where $\gamma^{(e,i)}$ describes the loss in the corresponding resonator following Ref. [14] accounting the corresponding considered ring (partial cylinder). The calculations are for the laser and pumping parameters, given already. The total number of active Nd$^{3+}$ ions/cm$^3$ used in the calculations is 6.9×10$^{19}$ cm$^{-3}$ (for 0.6 % Nd$^{3+}$). The pump rate $R_p^{(e,i)}(t) = P_p^{(e,i)}(t)/\left(h\cdot\nu^{(e,i)}\right)\cdot V_a^{(e,i)}$ is defined on the base of the part of the optical pumping power

that corresponds to the considered ring and wavelength. According our data, the obtained pump power for each ring is plotted in graphics in Fig.5. The pump power is a function of the area and the intensity in the ring. $R_p^{(e,i)}$ is related to the temporal shape of pump energy in combination with the diode pump pulse shape. Our oscilloscope observation shows that the pump pulse can be well approximated by a trapezoide shape with a rise time of 100 ns, near-plateau part of 200 μs and fall time of 100 ns. $V_a^{(e,i)}$ is the active volume of the considered ring for the generation of the corresponding wavelength. In the calculations we have taken the geometrical data for each ring derived from the description of the laser rod separation given above.

The system is solved using the Runge-Kutta method. For the solutions we take, as initial conditions N = 0 and $q^{(e,i)}$ = 1. Due to the practically rectangular pump pulse, the pump power in each cylindrical part during the pumping is constant. The system (2-3) is solved independently for the generation in the other considered coaxial parts. From the solution of the system, we obtain the temporal shape of the laser output power and its integration gives the output energy [14]. For the used parameters, described above, generation in five rings in total is obtained – in the first three rings the 1.36 μm wavelength is generated, and for the next two rings a generation for the 1.06 μm wavelength is produced. The type of the generations for two of the rings is presented in Fig.6.

The output energy for the wavelengths and for the corresponding partial cylinder is plotted in Fig.7.

The total output energy produced for the 1.36 μm wavelength is ~ 17 mJ and for the 1.06 μm wavelength is ~ 15 mJ. Thus, as we have shown, it is really possible to obtain practically equal energetic characteristics of both generations.

## 5. Discussion and Conclusion

In the work we have shown the possibility to use the specific light intensity pump beam distribution in the Gaussian beam in combination with coaxial geometry to obtain a new effective two-wavelength laser. Following our theoretical modeling and computer analysis, we have shown the potentiality for efficient two-wavelength laser operation in the Nd:YAG crystal at an weak and the strongest wavelengths with practically equal output energies. The weak line is generated in near axial part, where naturally the pump energy density is higher than the one in the peripheral part, where the

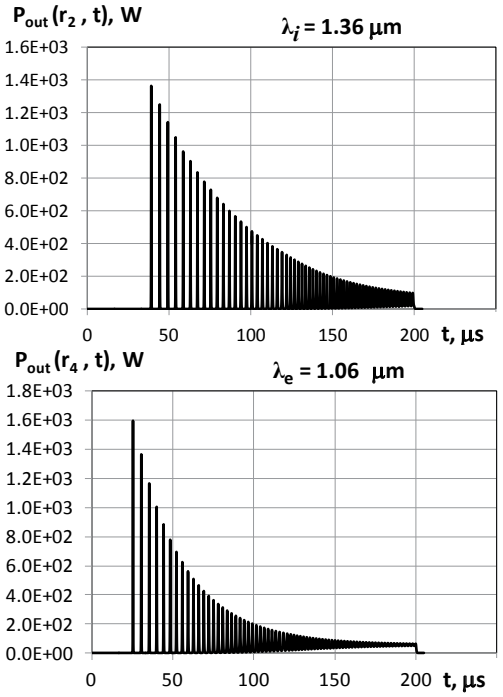



***Fig. 6.*** *The temporal generation in the second and in the forth ring of the active medium for both wavelengths – 1.36 μm and 1.06 μm, respectively.*

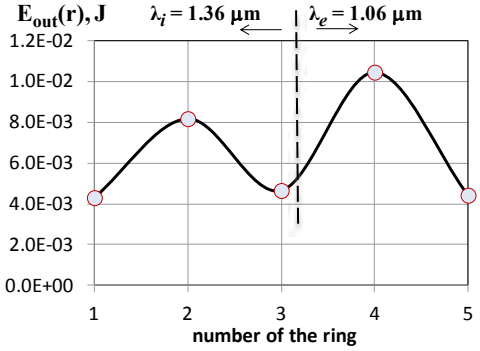



***Fig. 7.*** *Distribution of the calculated output energy for each partial cylinder for both wavelengths.*

strong line is generated (difference of the pump energies ~ 3-4 times). On the base of the applied approach for calculation, it was obtained the limits of the size in the laser crystal where the two noted outputs are energetically equal. The case considered as an example is for the lines 1.36 μm and 1.06 μm. The analysis shows that equality of the energies for both lines can be achieved for the axial part with a diameter 0.38 cm (generation at 1.36 μm) for the whole diameter of the crystal of 0.5 cm and the other line – strongest 1.06 μm line, is generated in the remaining peripheral part. This advantage is utilized employing coaxial two-channel laser architecture, where the optically separated axial and peripheral parts of the rod generate each in its own spectrally selective resonator. Beside the absence of wavelength-competition effect [16,17], which strongly worses the two-wavelength generation, the practically equal energy emission at the weeker

and the strongest line can be produced simulataneously without loss of pump energy for the equalisation. The two emissions are produced and emitted naturally in coaxial beams using the entire rod volume. Such Gaussian beam diode pumped laser can be applied effectively for generation of different pair of Nd:YAG lines with noted advantages. The technique developed in the work can be applied also for other materials used as active medium, also for other type of suitable beam distribution for longitudinal pumping.

**Acknowledgements**

This work was supported partially by the contracts DNTS/Austria 01/3 (Project No. BG 07/2013) and DRILA 01/7-19 (TR PHC RILA 2011 projet No. 25197 VB France) and the Technical University of Sofia, Branch Plovdiv - R&D Laboratory "Quantum and optoelectronics". M.D. thanks to Photonics Institute, Vienna University of Technology for the possibility to carry out joint work in their laboratories.

## REFERENCES

1. Spinhirne, J.D., Chudamani, S., Cavanaugh, J.F., Buffon, J.L. (1997). Aerosol and cloud backscatter at 1.06, 1.54, and 0.53 μm by airborne hard-target-calibrated Nd:YAG/ methane Raman lidar. *Applied Optics.* 36(15), 3475-3490
2. Zanzottera, E. (1990). Differential absorption lidar techniques in the determination of trace pollutants and physical parameters of the atmosphere. *Crit. Rev. Anal. Chem.* 21, 279-319
3. Vaicikauskasa, V., Kuprionisb, Z., Kaucikasa, M., Svedasa, V., Kabelkaa, V. (2006). Mid-infrared all solid state DIAL for remote sensing of hazardous chemical agents, Proc. of SPIE. 6214, 62140E
4. Farley, R.W., Dao, P.D. (1995). Development of an intracavity summed multiple-wavelength Nd:YAG laser for a rugged, solid-state sodium lidar system. *Appl. Opt.* 34, 4269-4273
5. Demtröder, W. (2003). *Laser spectroscopy: basic concept and instrumentation*. 3th ed. Springer, Germany
6. Rico, M.L., Valdes, J.L., Martinez-pastor, J., Capmany J. (2009). Continuous-wave dual-wavelength operation at 1062 and 1338 nm in $Nd^{3+}$:$YAl_3(PO_3)_4$ and observation of yellow laser light generation at 592 nm their self-sum-frequency-mixing. *Optics Communs.* 282(8), 1619-1621
7. Saha, A., Ray, A., Mukhopandhay, S., Datta, P.K., Saltiel, S.M. (2007). Littrow-type discretely tunable, Q-switched Nd:YAG laser around 1.3 μm. *Appl.Phys.* B 87, 431-436
8. Zhao, L.N., Su, J., Hu, X.P., Lv, X.J., Xie, Z.D., Zhao, G., Xu, P., Zhu, S.N. (2010). Single-pass sum-frequency-generation of 589-nm yellow light based on dual-wavelength Nd:YAG laser with periodically-poled $LiTaO_3$ crystal. *Opt. Express.* 18(13), 13331–13336
9. Dandliker, R., Thalmann, R., Prongue, D. (1988). Two-wavelength laser interferometry using superheterodine detection. *Optics Letters.* 13(5), 339-341
10. Devaux, B.C., Roux, F.X. (1996). Experimental and Clinical Standards and Evolution of Lasers in Neurosurgery. Acta Neurochirurgia, the Europ. J. Neurosurgery. 138, 1135-1147 & the literature cited there in.
11. Tankovich, N., Lukashev, A. (2003). United states patent, Pat.No. US 6,613,042 B1, Sep. 2
12. Deneva, M., Nenchev, M., Wintner, E., Topcu S. (2015). Coaxial-geometry tunable dual-wavelength flashlamp-pumped Nd:YAG laser. *Opt.Quant.Electron*. 47:3253–3271; DOI 10.1007/s11082-015-0205-3
13. Koechner, W. (2005). *Solid-State Laser Engineering*, 6 revised and updated edition, Springer, Berlin
14. Svelto O. (2010). *Principles of lasers*, 5th ed. Springer Science+Business Media, LLC 2010, ISBN 978-1-4419-1301-2 (e-ISBN 978-1-4419-1302-9)
15. Ifflander, R. (2001). *Solid-State Lasers for Materials Processing*, Springer-Verlag Berlin. Heidelberg, New York, series in Optical Sciences. ISSN0342-4111,ISBN3-540-66980-9
16. Louyer, Y., Wallerand, J.-P., Himbert, M., Deneva, M., Nenchev, M.: Two-wavelength passive self injection controlled operation of a diode pumped cw Yb:doped crystal lasers. Appl. Opt. 42(27), 5463-5476 (2003).
17. Deneva, M., Uzunova, P., Nenchev, M.: Tunable subnanosecond laser pulse generation using an active mirror concept. *Opt Quant Electron.* 39, 193-212 (2007).

Author's contact
Address:
Technical University of Sofia, Branch Plovdiv
Dept. "Optoelectronics and Laser Engineering" and R&D Laboratory "Quantum and Optoelectronics"
25 Tsanko Diustabanov St.
4000 Plovdiv, Bulgaria

E-mail: mdeneva@yahoo.com
deneva@tu-plovdiv.bg

© International Scientific Conference on Engineering, Technologies and Systems
TECHSYS 2016, Technical University – Sofia, Plovdiv branch
26 – 28 May 2016, Plovdiv, Bulgaria

# LIGHT BASED TECHNIQUES AS POSSIBILITY TO SOLVE THE POLLUTION PROBLEMS IN LASER IGNITION COMBUSTION OF GASEOUS MATER. A PILOT STUDY

MARGARITA DENEVA[1] MARIN NENCHEV[1], NADEJDA KAYMAKANOVA[1], ERNST WINTNER[2], MARK HIMBERT[3]

**Abstract:** *The work concerns the physics and techniques of laser ignition combustion of gaseous matter, in particular oriented to an important practical case – application in internal combustion engines. The problem, in the general case, is related to the formed micro-particles by the combustion that can pollute the entry windows for the laser ignition beam and also, to absorb and disperse the last in its trajectory. On the base of our new experimental results (completed with theoretical estimations) we propose and develop, with necessary argumentation, the principle of two techniques for solution of the noted problem (as a minimum – for the case of relatively low polluting fuel). The developed principle is based on the use of complex laser pulses, each pulse is with specially formed in cross-section two beams with convenient temporal, spatial and energy control. As we have shown on the base of our investigation, applying such pulses, we can realize that their light pressure is able to drive out the polluting particles away from the acting laser beam trajectory and the window. We present also some properties of the developed special type of Nd:YAG laser (on the base of our patented approach) suitable for the discussed applications.*

**Keywords:** *laser ignition combustion of gaseous matter, internal combustion engines, micro-particles pollution, laser light pressure*

## 1. Introduction.

**General.** The work concerns the physics and techniques of laser ignition combustion of gaseous matter, in particular oriented to an important practical case – application in internal combustion engines [1-3]. In this type ignition systems, a powerful laser beam is focused in the gas-fuel mixture in the engine cylinder and initiates an electric discharge and respectively an combustion, analogously to the use of the traditional electric sparking plugs [1,2]. This technique, in present, is from resurgent interest, due to its specific advantages and the essential progress of laser techniques.

At the present time, such laser ignition technique is with real practical applicability in combustion engines using gas mixtures that provide negligible polluting products by the explosion. In the literature are described practical applications of the laser ignition in high dimension engines with large (tens or more liters) working volumes, which employ gases, such as methane, the last producing negligible pollutions as fuel [3].

As it is discussed in the literature [e.g. 1], the laser ignition presents some useful advantages and potential. This justifies the work for its development. Note some of them such as: to affects advantageously the ignition of very lean mixtures – the COV-pi value for NOx emission level < 200 mg/Nm³ is definitely below the curve for a corresponding electrical ignition system; generally, laser ignition tends to yield better smoothness of engine operation, also - for easier correction the moment and the point of the ignition spark, shorter ignition delays leading to shorter burning times and reducing losses (as a potential benefit of laser ignition); light weight of the ignition system and its long life, and especially - the ability to change and regulate the precise and technically highly simplified depth of occurrence of the ignition spark by changing the focus of the beam. The influences of the water vapor and humidity is decreased.

**Problem.** To extend the applicability of the method for laser ignition, common and essential problem that must be solved is the cleaning or better – to preserve the light input windows from the

Copyright © 2016 by Technical University of Sofia, Plovdiv branch, Bulgaria ISSN Online: 2535-0048

deposition of the products, formed from the fuel combustion in the cylinders. Also, the problem with the pollutants is additionally complicated due to the partially decreasing of the intensity of the laser beam (end part) in the cylinder related with their absorption and scattering. The existence of residual pollutions in the formation of the gas-fuel in the subsequent engine cycle, as addition, decreases the intensity of the igniting laser beam. The use of fuels that produce undesired pollutants is typical case for the traditional combusting engines in the cars.

In practice, however, the decisions of the noted problems with pollutions, for the general case, are far from trivial. The simplest idea to clean the window by directly use of simple ignition laser beam is not convenient due to its drastically no suitable parameters for such purpose, as we also will show below.

**Aim of the work.** The present work gives a pilot study - principle, experiment, theoretical evaluations, concerning the development of general technique for solution of the discussed already problem of the pollution by the products of the fuel burning. The developed principle is to use for the ignition the laser pulses, wherein each pulse is specially formed in cross-section as a coaxial or parallel combination of two light beams with appropriate intensity, temporary and energetically parameters and directed in convenient manner to the window. As we show mainly on the experimental study (and partially, in the explications - by the theoretical estimation), such pulses are suitable to offer wanted effect. The potential for real application, in any case, is for the internal combustion engines that work with fuel, producing relatively low pollutants (e.g. without mixing of benzine and engine oil etc.).

**2. Experimental results and theoretical evaluations – base of the proposition.**

Generalized schematic picture of the working cylinder of combustion engine with laser ignition system is given in Fig.1. Schematically on the picture is presented also the pollutant particles of the combustion after electric discharge, the last being produced by the focalized laser beam (the notations are given in the picture). In the focal region the ignition beam light intensity must be of order $10^{11}$-$10^{13}$ W/cm$^2$ (~$10^8$-$10^9$ W/cm$^2$ on the entrance window; partially focalization).

Due to that here we plan to present a general study for the discussed in point I question, the consideration will be on the modeling, using the clearly evident and simplified examples.

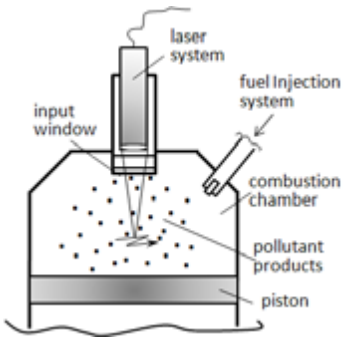
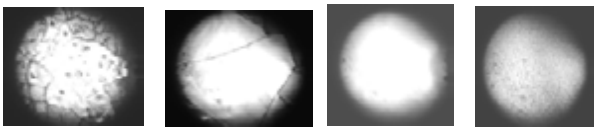



**Fig. 1.** *Schematic picture of the working cylinder of combusting engine with laser ignition system.*

The results, on the one hand give new specific scientific knowledge, on the other hand they can be used as a starting base-principle for further more detailed and concrete technical development of pollutant problem solutions. For this study we have modeled in the experiments the impurity with black thin layers on glass or quartz plates. The layers were produced by a smoke of burning paraffin candle (note that the paraffin frequently can be one of the components of the fuel). The thickness of the layer using microscope measurement is evaluated to be ~ 30-70 μm. As it is expected, the acting of the light depends strongly on the power density and energy density; however we have found the quantitatively such dependences.

Typical results - examples of this study are shown in Fig.2. The beam of Nd:YAG laser, needed for combustion, illuminates the layer with high power density light (on the window of ~ $10^7$W/cm$^2$; 50-100 mJ/ 70 ns; 0.4 cm illuminated area). Such illumination strongly changes the layer and the support and they become definitely nontransparent. We relate this with fusion and crystallization and besides these factors with the thermo-ablation. The damage of the glass or quartz support surface is relatively low, however no reversible. For the clean support the beam with such power density passes without damages. The typical microscope picture of the plate surface in this case is shown in Fig. 2(a). Thus, the self-cleaning of the strongly polluted input window by the ignition pulses themselves is unrealizable.

In the series of the experimental studies, by varying the illumination laser beam energy, we have found that for the parameters, corresponding to the free lasing, i.e. ~ 0.7 J/350 μs (~ 5.5 J/cm$^2$;~ 16 kW/cm$^2$) can be estimated parameters allowing good cleaning of the windows. The series of the microscope (low magnification) photographs are shown in Fig.2 (a), (b), (c) with given in the figure



(a) (b) (c) (d)

for a-d. [I---------I 4 mm], spot diameters ~ 4mm



(e) (f)

for e – [I------I 4mm], the spot diameter ~ 4 mm.

**Fig. 2.** *Photographs of the cleaned areas of a layer for different illuminating beam parameters. In (a)- for high power Q-switched beam (~10 MW/cm$^2$; ~70ns); (b,c,d) - for free lasing (~ 0.3-1.5 J, ~ 350 μs) with illumination:(b)~35 kW/cm$^2$;~12 J/cm$^2$ (c)~ 16 kW/cm$^2$;~5,5J/cm$^2$;(d)~7kW/cm$^2$; ~2.5J/cm$^2$. In Fig.2 is shown the cases around the optimum of the cleaning, being best for the central spot where the conditions are as this one for Fig.2(c).Below the glass is disposed text with letters. Fig.2(f) shows the case of very regular crystallization (good picture, however worst cleaning).*

text values. The good cleaning is shown in Fig.2(c). For energy and power density of ~ 10 J/cm$^2$ and ~30 kW/cm$^2$ we obtain very clear picture of crystallization (f).

Thus, for high power densities are typically highly prominent disturbances of the polluted window (power density of ~ $10^8$-$10^{10}$ W/cm$^2$ on the transparent material, especially with layer of absorption impurities). To considerably lower values (~ 30 kW/cm$^2$, respectively close to the free generation at ~ 0.3-1 J / 350 μs) the destruction is strongly reduced. Also, for suitable pulses in this order of the beam parameters, an acceptable cleaning of the impurities can be achieved, as it is shown in Fig.2(c). Measured light losses for the optimal case after the cleaning are ~5% and are related with some remaining dots on the layer. The question of damage of the windows, covered by pollutants (also in minimal quantities) is specific to each case and information in the literature is missing or presents individual situation. In any case, the obvious requirement is that the power density and energy of the passing radiation through the window must not exceed the passport data threshold of laser destruction. For the pure glass (quartz) window by catalog data typical threshold is 2-5 J/cm$^2$ for 10 ns (~$10^9$ W/cm$^2$) pulse, in particular for standard quality optical glass B7. Note that the laser ignition power in the focal region is ~ $10^{12}$ W/cm$^2$ inside the working gas [3] and is essentially smaller (not focalized) at the window. The dependence of the damage threshold by the light power density is related with square root of the pulse length. Our experiments have as aim outlining the general nature of the processes and expected advancement of the idea to propose approach for solution of the pollution problem. From the presented results we make the important conclusion that the cleaning of the impurities in the considered by us case need a relatively low power and energy density (~20 kW/cm$^2$; ~ few joules J/cm$^2$) light. This power correspond well to the free lasing operation of the widely used for the combustion motors ignition Nd:YAG lasers, especially in compact realization with diode pumping [5].

On the base of the presented above results, it seems that can be applied a simplest solution for laser ignition using the formed pulse that is composed by preliminary free generation and following ignition pulse. Both generations are with parameters, mentioned already and propagate in common beam. However, the cleaned particles are directed along ignition beam trajectory, thus providing energy losses for it. We propose other solution that avoids this problem. The solution is based on the experimental results given above in this point and these ones - below.

The ideas and the results of the continuation of the experiments are clarified by the series of the pictures and photographs shown in Fig.3 and Fig.4. During our experiments, described in Fig.2, we have observed other important peculiarity of the layer cleaning. Schematically our observation is illustrated in Fig.3. In Fig.3(a) we present the case of illumination of glass-plate with thin black paraffin layer and for the case of low power incident laser beam (~ kW), acting relatively long time - of hundred microseconds. The illuminated layer area (with $\varnothing$ ~ 0.1 cm- diameter) for such power is manly fused and vaporized and is also accompanied with poorly developed photo-ablation (following the microscope observations). The particles are dispersed in all directions – in near spherical diagram of motion. The essentially most interesting are the cases of illumination with laser beam ($\varnothing$ ~0.1 cm) having moderately high energy and power of free lasing: E ~ 0.5 – 1,5 J, $\tau$ ~ 100-400 μs (Fig.3-b,c). In the last case the cloud of the thrown out particles is transformed into a sharp torch around the axis of the incident beam.

The results of the detailed experimental investigations are illustrated in the Fig. 4. We have used combination of layered glass plate (GPPL in the Figure) and clean parallel indicated (marking) glass plate (MGP). The two plates are at distance of 0.7 cm each other. For the illumination with laser beams with parameters as these ones, described for Fig.3 (b) and (c), we obtained experimental results,

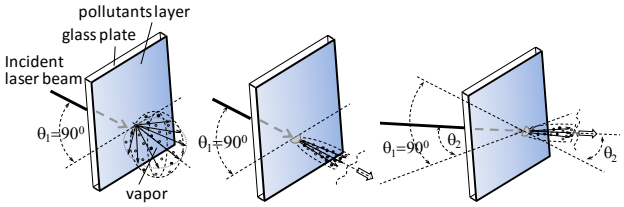



**Fig. 3.** *The qualitative schematic of the trowning out particles motion, following the preliminary experiments in Fig.2 .For illumination with free generation beam heaving: (a) low power(~ 1-2 kW/cm$^2$) and energy* **;** (b) *for moderate power (~ 20 kW/cm$^2$)and falling at 90$^o$ and* (c) with *moderate power (~20 kW/cm$^2$) and energy at angle* $\theta_2 \neq 90^o$.

corresponding qualitatively to the estimated one (the discussion to Fig.3). Here and below we note the formed vapors and thermo-ablation micro-particles by the illuminating beam for simplicity with "vapor" or "pollutant particles".

The most important experimental results is the observation that the motion of the vapor is really in the sharp torch close to the direction of the laser beam. This is illustrated in the photograph in Fig. 4(b)-(c) which shows the cleaned spots on the layer and the formed spots on the marking plate. The acting beam is from Nd:YAG, 1.06 μm wavelength, free lasing laser, traced by pilot red He-Ne laser beam. The energetic parameters of the illumination is ~ 0.5J/350 μs, ~ 30 kW/cm$^2$, ~ 15 J/cm$^2$, spot diameter on the layer ~ 0.1 mm. The photograph in Fig.4(b) illustrates the situation when the glass-plates composition is tilted at angle of ~ 20$^o$ with respect to the incident laser beams. The red color of the spot on the indicated glass plate is formed by the dispersed beam red light of the pilot He-Ne laser. Note that both beams propagate in completely superimposed trajectories. It can be seen that on the indicated glass plate the spot, formed by the vapors, coincides with the incident beam place (make evident by the diffusion of He-Ne beam).

To be more clear the last situation, the ensemble of both plates is turn to be perpendicular to the incident beams as it is shown in Fig.4(c) .The Nd:YAG laser beam is stopped and illumination is only by the pilot He-Ne laser beam. The deviation of the spot formed by the vapors from the direction of the He-Ne laser beam and the measurement show that really the vapors follow the Nd:YAG beam direction. We have investigated the obtained spots of vapors using appropriate microscope. The microscope photograph of part of the spot is given in Fig.5. The evaluation of the averaged dimension of the particles in the spots shows manly the presence of particles with diameters of ~ 0.5 μm, also the particles with smaller than these diameters (difficult to be measure with our technique) and

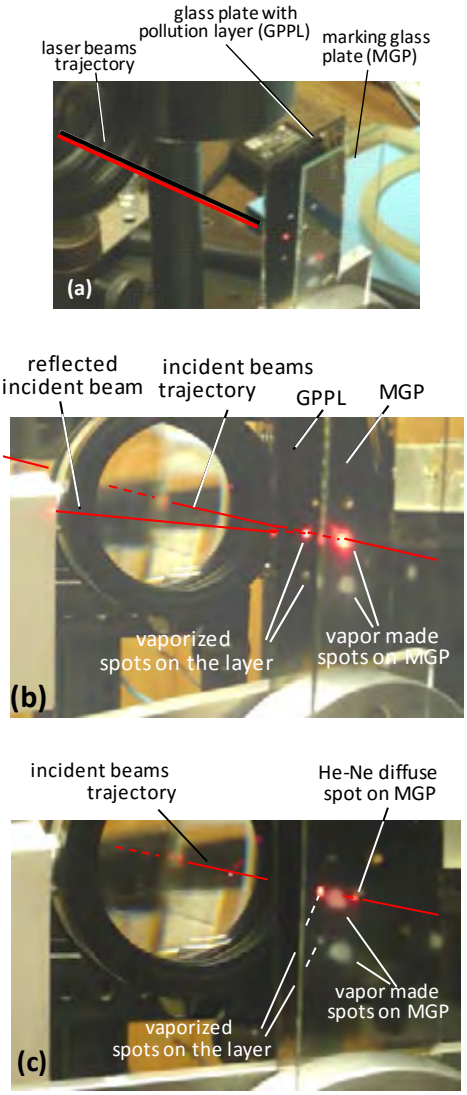



**Fig.4.** *Schematic of the determination of the particles motion. (a) actual photograph of the experimental arrangement;(b) case of beams at incident angle ≠ 0 on the plates (He-Ne and Nd:YAG); (c) case of perpendicularly tilted to the beams plates system, Nd:YAG stopped (see the text).*

negligible percentage of particles of ~1-2 μm. This gives us the idea that the pollutant particles are obtained by vaporization in combination with thermo-ablation (noted existence of small number of particles with higher diameter). However, following our investigation, practically we can accept that the average particle diameter is 0.5 μm.

**Discussion:** The realistic physical idea for the motion of the "vapors" can be related with the light pressure of the Nd:YAG acting beam. Using the estimated value of particle diameters, we will consider the particles as spheres with diameter of 0.5 μm and we will analyze the effect of the light pressure. Let's estimate the momentum, created on each particle by the light photons momentums that act on this particle. For the laser spot on the layer we have measured the diameter of ~ 0.1 cm

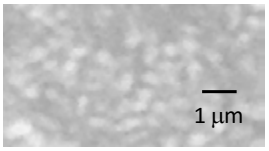



**Fig.5.** *Photograph of the produced particle, thrown out by the beam illumination of the layer.*

(partially focalized illuminating beam). The laser wavelength is 1.06 μm, the case that we consider is for the energy in the incident 1 J and the pulse duration 350 μs. This corresponds to energy density in the illuminating area $1.3x10^{6}$ J/m$^2$. Thus, the number of the incident photons of m$^2$, each with energy of $3x10^{-19}$ J is $0.4x10^{25}$photons/m$^2$. The volume of the particle-sphere is $0.65x10^{-19}$ m$^3$. We take into account that our experimental observation shows both the produced particles float in the air and also the specific mass of the paraffin is ~ (0.8-0.9)$x10^3$ kg/m$^3$. Taken into account this observation we can accept reasonably that the specific mass of the pollution particle space is ~2- $5.10^3$ kg/m$^3$. As below we will see, the relatively large variation of this value (1-7 kg/m$^3$) is not critical for the proposal. Thus, taken the mass density to be $5.10^3$ kg/m$^3$ the mass of the particle is $3.25x10^{-16}$ kg. The cross-section of the particle for the illuminated photons can be accepted to be equal of the main circle of the sphere and respectively with area of $0.2x10^{-12}$ m$^2$. Thus, any particle accepts, during the illumination, portion of $8x10^{11}$ photons. The momentum of each photon is $p=h/\lambda$ equal to $6.6x10^{28}$ kg.m/s and, accepting correctly that the all illuminating the particle photons move in the same direction and also are absorbed by this particle, we obtain that the sum momentum received by the particle by the laser illumination is ~ $0.53x10^{-15}$ kg.m/s. The average speed, can be calculated to be ~2 m/s, using $m.v = 0.53x10^{-15}$ kg.m/s and with the calculated above mass of the particle. If the energy in the area of the layer illumination is 3 J, the speed will be 6 m/s and in acceptance for the specific mass of ~ 2 $.10^3$ kg/m$^3$, the speed must be ~16 m/s. Also, what is very important, the obtained pulse momentum is directed toward to the direction of the beam propagation, and the particles move in direction of the beam. From our discussion we can conclude that the light pressure is the main factor of their motion. Possible influences can have also the pressure of more intensively formed drops in direction of the incident powerful beam (thermo-ablation, vaporization). The particles motion is impeded with the increasing of the gas pressure; however this is favorable condition for our aim. In any case, the described above experimental result is really obtainable. It can be considered as an important observation and base of useful technical solution.

### 3. Principles of the schemes of light cleaning and preserving the input window.

Two schemes, proposed on the base of the described experimental results and the discussion in the previous section are shown in Fig.6 and Fig.7.

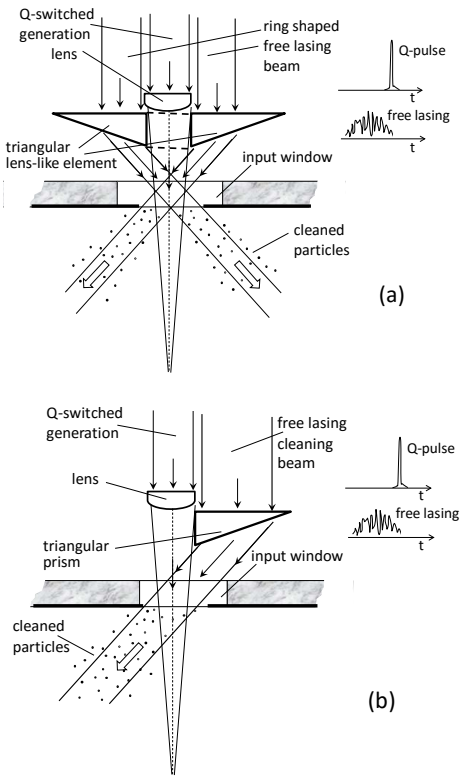



**Fig.6.** *Schematic of light cleaning and preservation arrangement with **(a)** coaxial beams and **(b)** with parallel beams.*

In both schemes a single, two channels laser beam with independently controlled light in each channel (temporally, energetically) is used. The light in the external channel is with suitable parameters (free lasing) for cleaning the window and in the other – internal - for fuel combustion ignition (Q-switching); the two emissions are with suitable temporal disposition. Fig. 6(a) clarifies the principle of the laser ignition engine with two coaxially disposed beams - the external-cleaning (from the external free lasing) and the other - Q switched by the internal axial channel. The Fig.6(b) gives the case with closely parallel beams. The optical focalizing system on the ~ 3-4 mm window in Fig.6 consist of prismatic lens-like element that directs the external beam on the window and pushes the evaporated pollution particles outside the projection of the window. The flat-concave lens focalizes the igniting beam inside the fuel. Thus, the vapor particles are pushed outside the ignition beam

trajectory. The estimations take into account that the normal combustion ignition forms the wave of the combustion that moves with ~ 20-40 m/s. Applying theoretical evaluation as the given one above in this point, it can be predicted the reality of the possibility for the two momentum to can quench each other or its sum to be momentum, directed outside the window projection (see the Fig.7).

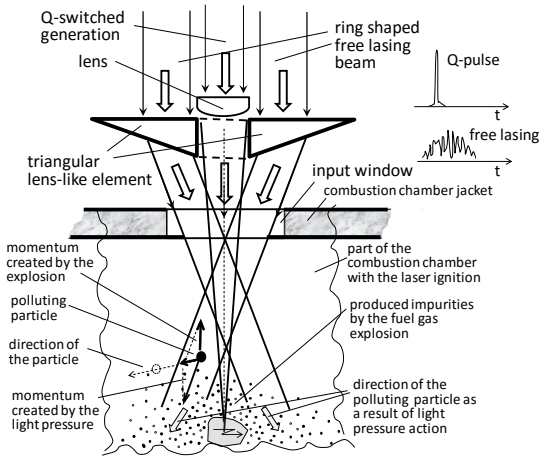
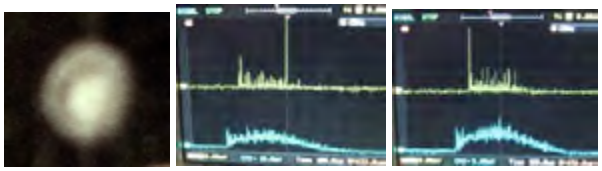



**Fig.7.** *Principle with light-pressure window preservation*

Such lasers with two-channel geometry for coaxial [3] and parallel [4] output beams (from single rod) are realized by us on the example of Nd:YAG rod. A solution, using the specific properties of the Gaussian beam in combination with coaxial laser geometry, is proposed for diode end-pumped Nd:YAG laser [5]. Each channel generates and is controlled independently. One example, of the laser spots with coaxial beams, is shown in Fig.8(a). In Fig.8(b) are shown the oscilloscope traces (50μs/div) of two convenient temporally emissions for realization of the schemes.



(a) (b)

**Fig.8**. *(a) laser spots in coaxial beams; (b) oscilloscope traces of the convenient emissions.*

For both photographs, the bottom oscilloscope traces are for the free lasing and the top one –for the Q-switched ignition pulse, the last accompanied with free lasing that help for cleaning or suppression of the formed particle. It is easy to change the type of emission of each of the channels. The preliminary (laboratory modeling) tests, using these lasers, prove the expected possibility to surmount the discussed problem.

## 4. Conclusion

In the work we have presented the experimental results, accompanied with theoretical evaluation, related with the controlled cleaning by the laser light of thin layers of pollutants on the transparent supports. The work is especially to look to the laser ignition in internal combust engines. From our study we have made the essential conclusion about the possibility to use the laser light pressure in needed manner for cleaning – with deviation of the formed pollutant particles that the last do not disturb the entry of the ignition laser beam. On the base of the results we have proposed with the argumentation two types of schemes for suitable laser-optical arrangement for laser ignition of the combustion in gaseous matter, including the laser ignition in engines.

## REFERENCES


**1.** Wintner, E., Deneva, M., Nenchev, M. (2014). Laser Ignition of Engines – A Contribution to Environmental Protection and a Challenge to Laser Technology", *Ann. J. Electron.,* 1-8 ISSN 1314-0078ET and the literature cited therein.

**2.** Dale, J.D., Smy, P.R., Clements, R.M. (1978). *Laser ignited internal combustion engine – an experimental study*; SAE Congress, paper 780329, Detroit

**3.** Deneva M., Nenchev M., Wintner E., Topcu S. (2015). Coaxial-geometry tunable dual-wavelength flashlamp-pumped Nd:YAG laser *Opt. Quant. Electron.,* DOI 10.1007/s11082-015-0205-5

**4.** Kissov H., Deneva, M., Nenchev, M. (2013). Development of a tunable, competition less flash-lamp pumped Nd:YAG laeser generated of a chosen pair of two lines*, Proc. SPIE*, 8770-50, 1-7

**5.** Deneva M., On advantageously use of Gaussian beam end diode laser pumping of Nd:YAG laser in two-wavelength coaxial architecture, *Techsys'2016*, submitted for publication.



M. Deneva, M. Nenchev, N. Kaymakanova are with "QOE" Laboratory, R&D Dept., Technical University of Sofia and OELE, Plovdiv, BG;
e-mail: mdeneva@yahoo.com
E.Wintner is with Vienna University of Technology, Photonics Institute, Gusshausstr. 25-29, 1040 Vienna, Austria;
e-mail: ernst.wintner@tuwien.ac.at, Austria;
M.Himber is from CNAM, Université CNAM, Institut de métrologie, Paris, France.

© International Scientific Conference on Engineering, Technologies and Systems
TECHSYS 2016, Technical University – Sofia, Plovdiv branch
26 – 28 May 2016, Plovdiv, Bulgaria

# DEVELOPMENT OF THE THERMO-SENSITIVE PAPER APPLICATION AS METHOD FOR LASER BEAM SPOT STUDY

MARGARITA DENEVA, MARIN NENCHEV, VALKO KAZAKOV, NADEJDA KAYMAKANOVA

**Abstract:** *We present a detailed investigation and development of thermo-sensitive paper application as a method, which in strongly defined conditions can be successively used for laser beam spot study. This old technique is applied in the literature and in the laboratory practice only for visual illustration of the laser beam spot by the whitening of the incident area of black thermo-sensitive paper, with accidentally taken sensitive materials. However, looking in details, in competition with the modern electronic beam scope techniques, it presents some essential advantages. As it can be expected and we have marked in our experiments – it cannot be spectrally sensitive in very large range, as example - from UV to IR; also the registration cannot be disturbed by different noise sources; as addition, it is extremely cheap and accessible. In our knowledge in the literature has not systematic study of the possibility of this simplest method. This work presents results of the detailed and systematic study of the noted technique-method. We have shown that using appropriate, well defined and reproducible as production sensible materials in combination with their precise known reaction to the laser light with specific parameters and using standard computer treatment, the noted advantages of this technique can be successfully employed for laser spot parameters investigation.*

**Key words:** *laser spot study, thermo-sensitive paper*

## I. Introduction. General aim of the work.

The aim of the work is detailed investigation and development of the practical application of **T**hermo-**S**ensitive **P**aper **R**egistration **T**echnique (TeSPeRT) for laser spot imaging. This method, as we show, in strongly defined conditions, can be successfully used for laser beam energetic parameter study. The base of the technique, as a rule, is the whitening in the laser beam incident area of the black thermo-sensitive paper. This old technique [1,2] is used in the literature and in the laboratory practice only for visual illustration (including also successfully - for the interesting cases) of the laser spot. The reported applications are used accidentally taken sensitive materials and without conclusion about energetic characteristics of the spot. However, looking in details, this technique presents some essential advantages in competition with the modern electronic beam-scope apparatus. First of all, as it can be expected and we have marked in our experiments with two-wavelength lasers [3], few properties can be marked: a correct registration cannot be spectrally sensitive in very large range, as example - from UV to IR (e.g. 0.3-3 μm and longer); secondly, the registration cannot be disturbed by the electromagnetic noise and third - as addition it is extremely cheap. In our knowledge, (according to our research) no systematic and detailed study of this technique is given in the literature. It was neglected especially due to the facilitated accessibility of the modern electronic beam-scope apparatus. Thus we formulate the aim of the work to study in detail the technique of beam profile registration using a black thermo-sensitive paper.

## II. Experimental investigations and results.

Following our preliminary observations we have planned to: 1) study the reaction between different strongly defined blacked-out paper sheets and the laser beam illumination and to choose more convenient and widely obtainable combination; 2) study the reaction of the registration on the illuminating beam energetic and temporal parameters to find the range of the linear widening; 3) study the dependence from the beam wavelength.

First point of our investigation is related to testing of series of blacked-out materials on the illuminating beam reaction. We have found that very suitable material for the marking is the tracing

Copyright © 2016 by Technical University of Sofia, Plovdiv branch, Bulgaria ISSN Online: 2535-0048

paper blacked one (1Xe) or two (2Xe) times through the copy machine. The copy machine used was standard xerography type action Konica Minolta Dialfa Di 5510. The blacking-out was by copying of the black paper at normal blacked position for the machine option. We do not observe noticeable difference comparing few tracing papers of different producers and also the blacking by the different copiers of the noted before types (Sharp-MX-3500, Toshiba 2500c) for normal blacking operation. The transmission of the pure tracing paper is measured to be ≈ 50% when the paper is placed closely to the entrance of the light power meter (Thorlabs SN6050506); in this manner the measured with flat and large entrance of 2 cm diameter accept all the diffused light. He-Ne yellow (0.595 μm) laser beam with incident diameter on the paper of ~ 2 mm and power of 3.6 mW is used. For the 1Xe and 2Xe blacked paper the transmissions are ≈ 9 % and ≈ 6% respectively. As we show below, the use of 2Xe paper is an optimal case. The illumination by the laser beam was from the not blacked layered side of the sheet. When it was from the layered side, the spot image frequently was not pure, having 'moustaches', probably produced by the reinjection of the part of the vaporizing (or/and thermo-ablating) micro-particle by the incident beam light pressure.

We combine this registration with tracing of the whitening spots from the paper by computer scanner and computer treatment of the image. The treatment includes two type of manipulation with adapted standard programs. The first treatment was the tracing of the whitening along the beam spot diameter in 2D image. The other - second treatment was to create 3D images of the whitening_in any point of the spot.

In the study we have used our two homemade flash-lamp pumped lasers – Nd:YAG and Nd:Glass. The first laser (I) produces a controllable energetically emission at 1.06 μm or at 1.36 μm. The output energy can be varied from 0.1 J to 1.5 J in pulse duration approximately 350 μs. The spot in cross section of the emitted beam is with good approximation in circle with diameter at the laser output of ~ 0.7 cm. The second laser (II) produces a beam with cross section spot of 1 cm at the laser output variable between 8 and 10 J with pulse duration of 3 ms and the laser oscillate at the wavelength 1.06 μm. Simultaneously with the spot registration we have measured the laser output energy (FIELDMAX energy meter, Coherent, USA) is used, furthermore a two-channel storage 200 MHz oscilloscope RIGOL DS1202CA (USA) and light detectors with resolution better than 5 ns (R108BG). Both lasers are multi-mode and operate in plane-plane mirrors resonators.

The typical case of spot registration and computer treatment are presented in Fig,1. The spots are formed by the beam from Nd:YAG laser (I, 1.06 μm) at the 2Xe paper. The illuminating energies that are varied by the pumping are given in the figure. The averaged energy densities for the spots are in the limits from 0.4 to 0.65 J/cm$^2$. The ratio (measured energy)/(calculated volume in arbitrary units) for the spots are:1-(0.71J)/(1x); 2-(0.43J)/(0.61x);3-(0.45)/(0.62x); 4-(0.63J)/(0.89); 5-(0.72J)/(1.03);6-(0.49)/(0.73). The volumes are calculated using corresponding for this operation computer program. The analytic calculation of the volume, using the tracing curve in Fig.1(c) and

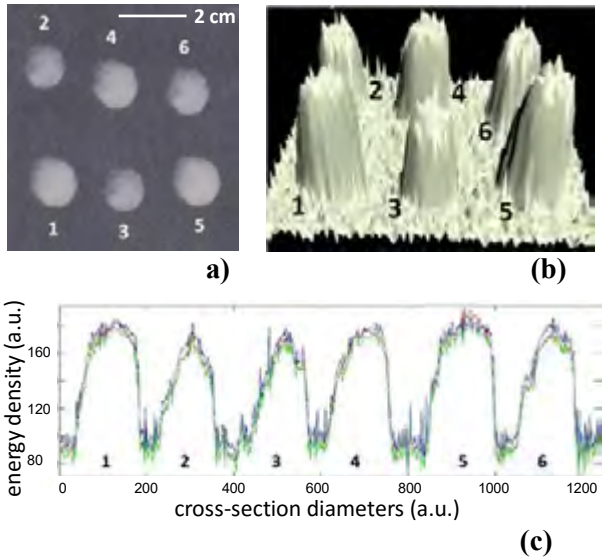



**Fig.1.** *Photographs of the beam spots on the paper (2Xe) (a); the 3D computer imaging (b), and 2D tracing curves along the spot diameter (c).*

accepting the symmetry in rotation, gives very close results as these ones for Fig.1(b). The ratios energy/volumes for any spots pairs can be marked to be equal. This signifies linearity of the whitening with the laser energy density in the considered energy range 0.4– 0.8 J (energy density ~ 0.4 to 0.65 J/cm$^2$).

From the experimental results as those shown in Fig.1 and from general reasons, we conclude that it is correct to relate the distribution of the whitening in the spots with corresponding energy density distribution. Let's take the schematic for the analysis as this one given in Fig.2. Note the energy density distribution with $\mathbf{w_E\ (x,y)}$ where **X,Y** are the axis in the plane of the spot and $\mathbf{w_E\ (x,y)}$ is in the **Z** axis. Let's accept that the whitening $\mathbf{w_h\ (x,y)}$ in relative units is proportional to the $\mathbf{w_E\ (x,y)}$, **i.e.** $\mathbf{w_h(x,y) = k_1.w_E\ (x,y)}$, where $\mathbf{k_1}$ is the coefficient of the proportionality. The volume in a.u., limited by the function $\mathbf{w_h\ (x,y)}$, is**:**

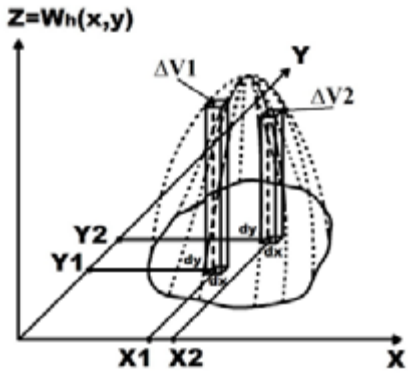



**Fig.2.** *To the calculation of the relation beam illumination energy - volume of the spatial figure, limited by the whitening*

$$V = \sum \Delta V_i \text{ and } V = \int\limits_{x}\int\limits_{y} k_1 \cdot w_E(x,y)dxdy = k_1 \cdot E_{jb}, \quad (1)$$

as the volume under surface $\mathbf{w_h}$ **(x,y)** is accepted to be proportional of the energy $\mathbf{E_{ib}}$ in the illuminating beam. This is the case in Fig.1, for the given limits the linearity presents.

Following the above explanation, one of the questions concerning the use of the TeSPeRT for laser beam energetic parameters determination is to investigate the linearity of the whitening of the paper as a function of the laser energy density in the spot. For this purpose, we investigate the formed laser spot on the 2Xe paper using the Nd:YAG laser II - with output 8-10 J. The multimode operation gives a relatively uniform illumination and we can use an averaged energy distribution in the spot.

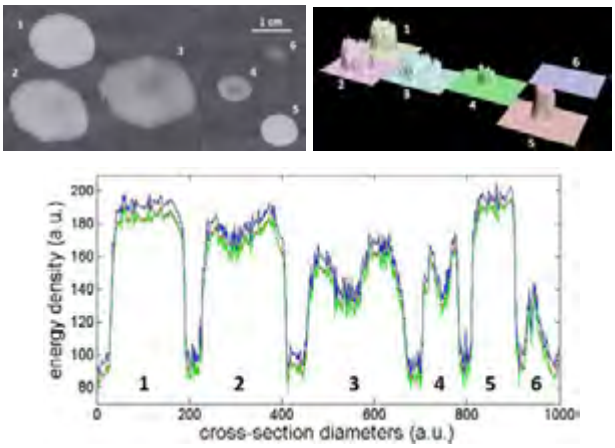



**Fig.3.** *To the determination of the averaged whitened function* $\boldsymbol{w_h}$ ***(x,y)*** *as averaged energy density in the spot. The spot photographs (a), 3D image (b) and 2D tracing curves along the spot diameters (c).*

The illuminating average energy density is for the spot noted in (1) - 4.3 J/cm$^2$; (2) - 3.3J/cm$^2$; (3) - 2.2 J/cm$^2$; (4) - 1.5 J/cm$^2$; (5) - 6.2J/cm$^2$. For the spots 1:2 – the measured energy ratio 8J/ 8J = 1; computer treatment obtained volume ratio is 0.94. Respectively, for the spots 1:3 - 8J/9.2J = 0.87; for 2:3 = 8J/ 9.2J = 0.87. In other words, the difference between the measured energy ratio and this one obtained by the spot treatment is ~ 10% (probably due to the precision of our home made thermo-electric bridge meter, convenient for the energy measurement of long pulses ~ few ms).

As it is seen from Fig.2(b) and Fig.2(c) – the saturation effect starts for the spot (1) and is clearly evident for the spot (5). Thus the energy density of ~ 4 J/cm$^2$ is upper limit of the correct registration for this paper and pulse length (~350μs). As a low limit for the reliable registration we accept ~ 0.2 J; (~0.5 J/cm$^2$), that is illustrated in Fig.3 (spot 5). A typical transmission of the saturation whitened spot area is ≈18 %. The testing experience has shown us that the transmission of the whitened spot (i.e. the bleaching) cannot be applied for energy density evaluation; there is no proportionality as this one for the whitening that was observed. We relate the explanation with the shown below whitening by the appearance of white products by the burning of the black layer by laser irradiation. Note that, for the 1Xe and 2Xe paper the limits are not essentially different, being a little smaller for 1X. The saturation effect for 3Xe paper is high, however the registrations of the low energy density spots (0.3-0.4 J) are not reliable; also such layering is practically very difficult. Thus, our observation shows that for moderate energy density 2Xe paper is well suitable. If the pulse is with high energy density, the latter can be decreased by filter.
Other question is the dependence of the pulse power density. For this purpose we have used the passive Q-switched operation of the laser (I) with output (and illuminating) energy of 0.5 J and pulse length of ~ 1 μs. The energy density was ~ 2 J/cm$^2$ and power density ~4 MW/cm$^2$. We compare the spot parameters on the paper 2Xe with this one for the free lasing of 2 J/cm$^2$ and pulse of ~350 μs.

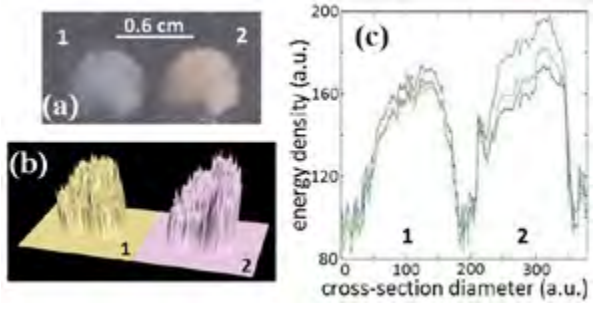



**Fig.4**. *Spot photographs (a) and theirs computer 3D (b) and 2D (c) treating for the Illumination by the free lasing (1) and Q-switched pulse (2).*

The difference of the reaction is in the little coloring of the Q-switched marked spot in red, probably related with additional products of paper burning (see below) and the increased transmission of the paper area at the spot (~2 times, in general, also low ≈ 25 %.). However, the ratio (energy)/(volume of bleaching) is not essentially different that this one, obtained for the free generation (Fig.3). Thus, the TeSPeRT, as we have sowed, is applicable also for the case of relatively long Q-switched pulses (~ 1-10 μs; ~ 1 MW). For shorter and high power pulses the additional investigations are needed. The described above observation shows that the main factor for the whitening is the energy density (for the moderate pulses duration of our investigation (~1 μs - 3 ms).

Other important investigation is the dependence of the wavelength of the illuminated beam. Using our laser (I) we have produced free-lasing generation at the wavelength λ = 1.06 μm and at λ =1.36 μm and have studied the paper recording reaction. Fig.5 illustrates the spots and their diametric tracing, for the illumination with 1J energy beam at λ = 1.06 μm (left spot and trace) and for 0.56 J at λ =1.36 μm. The study shows good coincidence of the ratios energy/energy and volume/volume for the two wavelengths, that shows the expected wavelength independence (investigation for the range 0.53 μm- 1.36 μm).

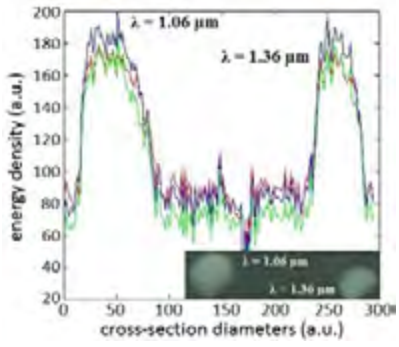



**Fig.5.** *Spot photographs (inside) and their computer 2D treating (curves) for the Illumination by the λ = 1.06 μm wavelength laser pulse with energy 1.1J and for λ =1.36 μm with pulse energy 0.56 J.*

The investigation shows, as already mentioned that the whitening results from changing the structure of the illuminated area of the black-out xerox layer. The small black composite of the layer (dimension of ~ 10-20 μm) is transformed to be white in colour. A little decrease of its dimension is observed. Also some part of black material of the layer was knocked out under thermo-bleaching by the incident beam. The main reason of the whitening is the first mechanism. This is proved by our experiment with treatment of the whitened spot in condition of photographing (our computer scanning) the spot on black and white background. Not essential difference was observed.

In Fig.6, as illustration of our observations, is plotted the microscope photograph of the black layer (2Xe) on the tracing paper before and after the laser beam illumination. The similar picture is observed also for 1Xe paper. The discussed bleaching effect for the composites of the layer can be observed.

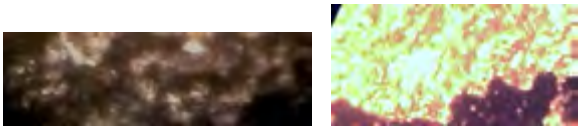


**Fig.6.** *Microscope photograph of the black layer on the tracing paper (2Xe) before and after the laser beam illumination.*

## III. Conclusion

In the work we present results from detailed and systematic study of the of thermo-sensitive paper registration (TeSPeRT) in laser technique. We have shown that using appropriate, well defined and reproducible as production sensible materials in combination with their precise known reaction to the laser light with specific parameters and using standard computer treatment, this technique can be successfully employed for laser spot parameters investigation. Its essential advantages that can be marked by our study are: determination of the energy distribution in the laser spot; comparison of the energies of two pulses; having an etalon spots in order to evaluate correctly the laser pulse energy; no spectral and noise sensitivity. In addition, this technique is extremely cheap and accessible.

**References:**

1. Ifflander, R. (2001). *Solid-State Lasers for Materials Processing*. Springer-Verlag Berlin. Heidelberg, New York, series in Optical Sciences. ISSN0342-4111, ISBN 3-540-66980-9 (2001).
2. Carlos B. Roundy, Spiricon, Inc., http://aries.ucsd.edu/LMI/TUTORIALS/profile-tutorial.pdf, Beam Profile Measurements and the literature therein.
3. Deneva M., Nenchev M., Wintner E., Topcu S. (2015). Coaxial-geometry tunable dual-wavelength flashlamp-pumped Nd:YAG laser. *Opt. Quant. Electronics*, DOI 10.1007/s11082-015-0205-5 online publ.

M. Deneva, M. Nenchev, V. Kazakov, N. Kaymakanova are with "QOE" Laboratory, R&D Dept., Technical University of Sofia and OELE, Plovdiv, BG; e-mail: mdeneva@yahoo.com

© International Scientific Conference on Engineering, Technologies and Systems
TECHSYS 2016, Technical University – Sofia, Plovdiv branch
26 – 28 May 2016, Plovdiv, Bulgaria

# PERFORMANCE SENSING SOLUTIONS FOR A GREEN ENVIRONMENT DESIGNED IN BULGARIA

PETAR MITSEV, ANGEL TANEV, TSVETELINA LAZAROVA

**Abstract:** *This paper presents novel green automotive platinum sensing technology. In recent years, worldwide emissions legislation has been introduced and is rapidly becoming more stringent. With alternative vehicular propulsion methods far from becoming mainstream reality, leading automotive providers have intensified efforts in the direction of reducing the harmful footprint of their products. This is being accomplished via smaller, more optimally designed internal combustion engines, necessitating an increased and higher-performance sensor content per vehicle. This paper elaborates on temperature sensor application in automotive exhaust gas performance sensing.*

**Key words:** *automotive exhaust gas, platinum temperature sensor, materials technology*

## 1. Introduction

The growing environmental awareness within society has necessitated an immediate and effective solution towards air pollution reduction and control [6]. A large portion of the latter is produced every day by the global vehicle fleet, responding to the ever-growing transportation needs of an expanding world population, with automotive being among the three major energy consumer sectors. The above requires a greater degree of sensing, operating under harsher application conditions, prompting the need for novel sensor technology.



***Fig. 1.*** *Automotive sensors: general view [11]*

## 2. Theoretical Background

In practice, there are 3 sensor technologies that are viable in vehicle exhaust: thermocouples, thermistors, and resistance temperature detectors (RTD). Each of them have their own advantages and disadvantages, and will be considered in brief detail.

Thermocouples are formed by welding two dissimilar metals together forming a bimetallic junction that produces a temperature-dependent voltage as a result of the thermoelectric effect [17].
For a vehicle application, a type K (chromel-alumel), type R or S (platinum-rhodium) or type N (Nicrosil-Nisil) would be used for the range of temperatures previously mentioned. Thermocouples can be relatively low cost sensors (for example, using type K) as compared with thermistors or RTDs. However, the electrical system is significantly more expensive since there must be introduced a compensation for voltages produced whenever there is a change in wire material (often called cold-junction compensation).
Thermocouples can be made with very little mass which allows for a fast response with changing temperature. In order for the sensor to minimize drift and be reliable in a vehicle exhaust environment however, the thermocouple must be protected by a sheath, and therefore they are made thicker. Thus much of the fast response advantage is reduced.
Thermistors are made from various nonmetallic conductors (i.e. metal oxides). The types of thermistors found in a vehicle exhaust environment will typically produce a negative temperature coefficient (NTC), meaning the resistance will decrease with increasing temperature. Thermistors offer a high sensitivity over a smaller range in

Copyright © 2016 by Technical University of Sofia, Plovdiv branch, Bulgaria ISSN Online: 2535-0048

temperature than either thermocouples or RTDs [17].

At 0°C the resistance can be over 100000 Ω, at 200°C: 200 to 500 Ω, and at 800°C 50 Ω. Therefore, thermistors can achieve very high sensitivities over a particular range of temperatures. However, achieving nearly the same accuracy over a large range in temperatures is not possible (unless several pull up resistors are used) due to the highly nonlinear characteristic response. Thermistors can be made with a very small thickness for quick response. However, they are not able to withstand even mild vehicle exhaust environments without being protected by a metal or ceramic insulated sheath thus causing the sensor response to be relatively slow.

Tolerance of a thermistor depends on its intended range of use. For example, thermistor tolerances in manifold air temperature sensors (MAT) or coolant sensors are very tight over the relatively narrow range of measurement (ex. 0.6°C from 0° to 100°C). However in a vehicle exhaust that can vary between -40°C and 1000°C, thermistors have a fairly poor tolerance depending on the temperature range (2% to 6% of temperature). As previously described, thermistors typically have a very high resistance below T=100°C. This makes it difficult to meet requirements of being able to read the sensor at temperature -40°C, or being able to perform OBD (On-Board Diagnostics) start up diagnostics at 20°C.

Table 1 shows a summarized comparison of the three different sensor types. The RTD is the most accurate of the three sensor types over the entire measurement range over time. It is important to note that zero hour accuracy is only one portion of total accuracy; how the sensor performs in the application over time at temperature is vital [17].

Figure 2 [13,14,15,16] shows two thermistors and a typical RTD designed for vehicle exhaust use (thermocouples are not shown since they generate an output voltage instead of measuring a resistance). As can be seen from the graph, the thermistors show a very non-linear curve as compared to the RTD. Further, there is a significant difference between the two different thermistor manufacturers, with one not being practical for measuring temperatures below 100°C. The tolerances indicated on the graph show that the RTD has a much tighter tolerance than thermistors over the measurement range.

***Table 1***. *Comparison of three sensor technologies*

| Characteristic | Thermocouple | Thermistor | RTD |
|---|---|---|---|
| Linearity | Poor | Poor | Good |
| Accuracy | Fair | Fair to poor | Excellent |
| Sensitivity<br><600°C<br>>600°C | <br>Poor<br>Poor | <br>Excellent<br>Fair | <br>Good<br>Good |
| Signal Level<br><600°C<br>>600°C | <br>Poor<br>Poor | <br>Excellent<br>Fair | <br>Good<br>Good |
| Response time | Poor (3 mm dia) | Poor | Good (No sheath) |
| System Complexity | Poor | Good | Excellent |
| Standardized output signal | Excellent | Poor | Good |
| -40°C measurement | Excellent | Poor | Excellent |
| 20°C OBD II measurement | Excellent | Poor | Excellent |

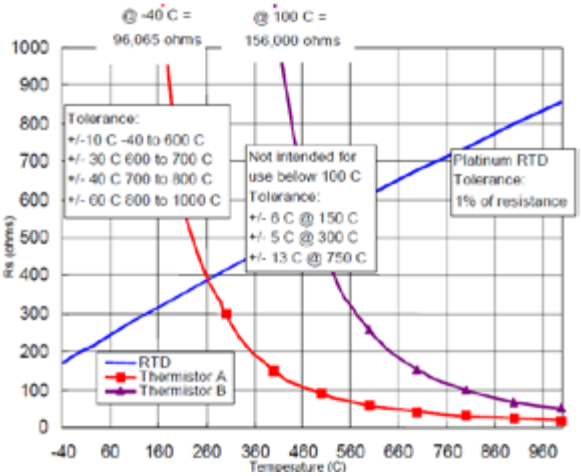



***Fig. 2.*** *Comparison of three sensors technologies.*

Resistance Temperature Detectors (RTDs) operate through the principle of electrical resistance change in metal thermistors. Platinum is the most widely specified RTD element type although nickel, copper, and Balco (nickel-iron) alloys are also used. Platinum is popular due to its wide temperature range, accuracy, stability, as well as the degree of standardization among manufacturers, thus interchangeability. RTDs are characterized by an almost linear positive change in resistance with respect to temperature. They exhibit the most linear signal with respect to temperature of any electronic sensing device [1].

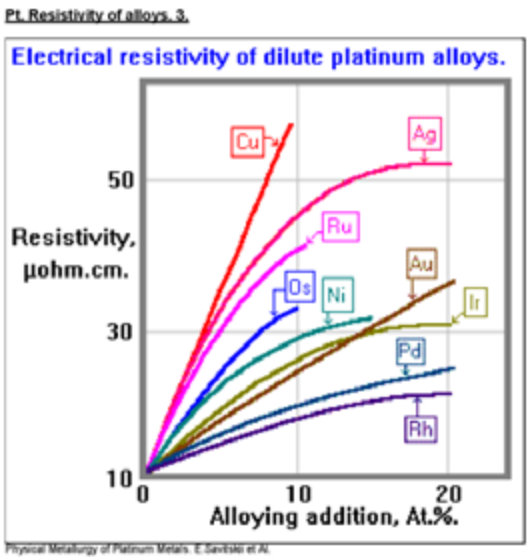



***Fig. 3.*** *Resistivity of various Pt alloys [6].*

The platinum and copper RTDs are most commonly used [1]. In general, RTDs are employed over the wide temperature range from –260°C up to 850°C, and some of these RTDs are applied up to 1200 °C [1].

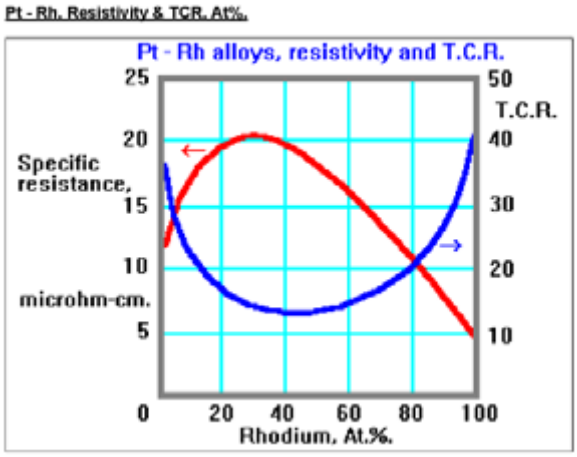



***Fig. 4.*** *Effect of Rh addition on Pt TCR [12].*

The effect of adding rhodium over the platinum's temperature coefficient of resistance (TCR) is given on Fig.4. The quantity of rhodium (Rh) in the Pt-Rh alloy is less than 1%. This is commonly used to control the TCR value.

The resistance vs. temperature equation is shown below, which is represented by the best-fit quadratic equation of the measured data [2]:

$$R(T) = R_0\left(1 + \alpha T + \beta T^2\right) \qquad (1)$$

where:
R(T)- sensor resistance [Ω] vs Temp(°C),
α is a slope of $R/R_0$ vs T line,
β is a non-linear (quadratic) term.

For a standard Pt RTDs, the coefficients $\alpha$ (slope) and $\beta$ (quadratic term) are summarized in Table 2:

***Table 2****. Pt RTD international standards.*

| Standard | Temperature coefficient of resistance, (TCR) | $\alpha$ | β |
|---|---|---|---|
| | $[°C]^{-1}$ | $[°C]^{-1}$ | $[°C]^{-2}$ |
| DIN 43760 | 0.003850 | $3.9080 \cdot 10^{-3}$ | $-5.8019 \cdot 10^{-7}$ |
| American | 0.003911 | $3.9692 \cdot 10^{-3}$ | $-5.8495 \cdot 10^{-7}$ |
| ITS-90 | 0.003926 | $3.9848 \cdot 10^{-3}$ | $-5.870 \cdot 10^{-7}$ |
| IEC 60751:2008 | 0.003851 | $3.9083 \cdot 10^{-3}$ | $-5.775 \cdot 10^{-7}$ |

The standard IEC 751 sets two tolerance classes for the interchangeability of platinum Pt RTDs [1]:

Class A: $Tolerance\ (°C) = \pm(0.15 + 0.002|t|)$
Class B: $Tolerance\ (°C) = \pm(0.3 + 0.005|t|)$

where: $|t|$- absolute temperature in °C.

Class A applies to temperatures from –200°C to 650°C, and only for RTDs with three or four-wire configurations. Class B covers the entire range from –200°C to 850°C.

The Platinum resistance as a function of measured temperature is shown on Fig.5. The function is almost linear over a wide range of temperatures (up to 850°C). The resistance at 0°C is $R_0 = 200\,\Omega$.

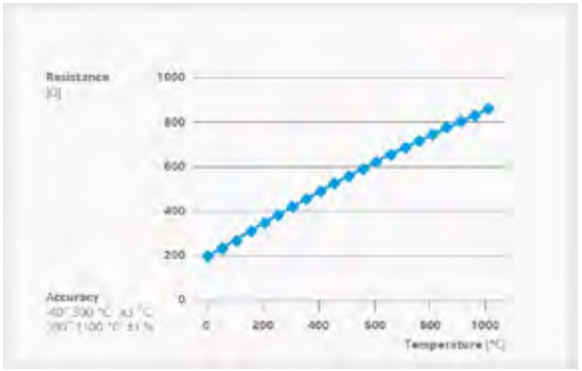



***Fig. 5.*** *R=f(T) function [7]*

To accomplish the above, design engineering is involved along the scale axis, via different disciplines, shown below on Fig.6 [3,4,5,18]:

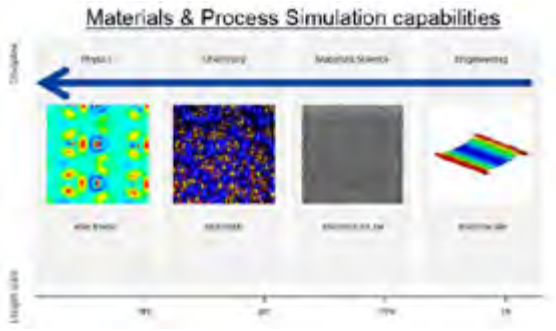



***Fig. 6.*** *Physical scale versus scientific disciplines, used in sensor design [8].*

### 3. Application

The technology, described in this paper, is used to satisfy the world's growing need for safety, energy efficiency and a clean environment. Incorporation examples are provided below (see Fig.7):



***Fig. 7.*** *Areas of application [9]*

Due to the increased atutomotive systems introduction together with their complexity, sensor content per vehicle is increasing (Fig.8, top):

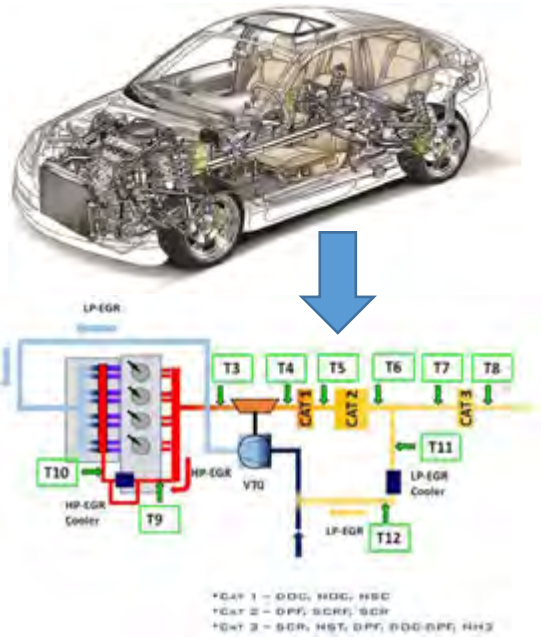



***Fig. 8.*** *Temperature sensor positions along the exhaust tract [10]*

Typically, several exhaust gas temperature sensors are positioned along the thermodynamic chain (Fig.8, bottom). For example, diesel trucks- starting with the 2007 model year- used for on highway applications are required to have an exhaust treatment system to reduce emissions, specifically large particulate matter. The diesel particulate filter (DPF) is a component of the system. DPFs are designed to physically filter particulate matter (soot). A regeneration process removes the accumulated soot from the filter.

### 4. Conclusion

In this paper, the application of automotive exhaust gas temperature sensing, along the length of the thermodynamic tract, has been described. The influence of metal alloy composites on resistivity and the temperature coefficient of resistivity, thus sensor signal, has been elaborated. The physical scale to scientific discipline design implications has been discussed, providing for performance sensors of increased stability and reliability.

### REFERENCES


1. Adler B., *Reliability Aspects of Temperature Measurement*, Moore Industries-International, Inc., North Hills, CA 91343.
2. http://www.ni.com/tutorial/7115/en/
3. Fischer et al. (2001). Practical Experience with New Oxide Dispersion Hardened Platinum Materials, Tucson, Arizona, USA, June 9-12, 2001.
4. Jose´ S. Moya, Sonia Lopez-Esteban, Carlos Pecharroma´n (2007). The challenge of ceramic/metal microcomposites and nanocomposites, *Progress in Materials Science 52*, 1017–1090.
5. Ke Fan, Min Liu, Tianyou Peng, Liang Maa, Ke Dai (2010). Effects of paste components on the properties of screen-printed porous TiO2 film for dye-sensitized solar cells, *Renewable Energy 35*, 555–561.
6. Savitski E. et al (1978). Physical Metallurgy of Platinum Metals.
7. Kyocera Pt 200 RTD product datasheet
8. Materials Design MedeA product presentation
9. Sensata Technologies Inc
10. Sensata Technologies Inc
11. Sensata Technologies Inc
12. The PGM database, www.pgmdatabase.com
13. Desmarais R., et al. (2001), "How to Select and Use the Right Temperature Sensor", Sensors Magazine.
14. LeGare J., et al. (1995), "Temperature Sensors for On-board Diagnosis of LEV/ULEV Systems", Automotive Engineering.

15. Mathews D., (2000), “Choosing and Using a Temperature Sensor”, Sensors Magazine.
16. Volbrecht A., (1998), “Temperature Measurement: Making Sense of it All”, Sensors Magazine.
17. Nelson C., et al., (2004), The Development of a RTD Temperature Sensor for Exhaust Applications, Delphi Corporation, SAE International.
18. Petrov, N. I., (2007), Reliability’s investigations of risk technical systems. Yambol, Bulgaria: Publishing House “Jelio Uchkov”.

Authors’ Contacts:
Address: Sensata Technologies, Sofia.
Petar Mitsev, e-mail: pmm@sensata.com
Angel Tanev, e-mail: a-tanev@sensata.com
Tsvetelina Lazarova, e-mail: tlazarova@sensata.com

© International Scientific Conference on Engineering, Technologies and Systems
TECHSYS 2016, Technical University – Sofia, Plovdiv branch
26 – 28 May 2016, Plovdiv, Bulgaria

# ЕНЕРГИЙНИ ХАРАКТЕРИСТИКИ НА ЗЕЛЕ С ДОБАВЕН БИОВЪГЛЕН.

СЕВДАЛИНА МАНОЛОВА, СТАНИМИР СТОЙНОВ, ИВАНКА МИТОВА, АНГЕЛИНА МИКОВА, ПЕТРА АЛЕКСАНДРОВА, ГЕОРГИ СТОИМЕНОВ

**Резюме:** *В работата се изследва влиянието на биовъглена върху топлотворната способност на биомаса от зеле като суровинен енергиен източник. Използвано е микровълново сушене на пробите биомаса. Получени са данни за енергийна стойност и енергийна плътност на биомасата при различна влажност на биомасата.*

**Ключови думи:** *биомаса, микровълново сушене, енергийна стойност, енергийна плътност*

# ENERGY CHARACTERISTICS OF CABBAGE WITH ADDED BIOCHAR

SEVDALINA MANOLOVA, STANIMIR STOJNOV, IVANKA MITOVA, ANGELINA MIKOVA, PETRA ALEXANDROVA, GEORGI STOIMENOV

**Abstract:** *The present paper examines the impact of biochar on the heating value of biomass of cabbage as raw energy.* Used is microwave drying of the samples of biomass. Data have been obtained for the energy value and energy density of biomass at different humidity of biomass.

**Key words***: biomass, microwave drying, energy value, energy density*

## 1. Въведение

Възможностите за енергийно използване на биомасата са многостранни. Като енергоносители на биоенергия служат биогенни горива, които се получават чрез едно или повече преобразувания на биомасата [6, 7, 8]. В резултат на пиролизата, преобразуването на биомасата в устойчив източник на органичен въглерод - биовъглен (БВ), има разнообразно приложение – отопление, при компостирането, за подобряване на свойствата на почвата, растежа на растенията и тяхната енергийна стойност [3, 5, 9, 10, 11].

В работата се изследва влиянието на биовъглена върху топлотворната способност на биомаса от зеле, при различна влажност на биомасата.

## 2. Методика на изследването

За целта на изследването са използвани проби от зеле, от проведени опити в ИПАЗР ”Н. Пушкаров” през 2015г, в две фитокамери с нисък енергиен разход. Фитокамерите осигуряват температурен режим, съответно 12°C и 23°C, максимално осветление от 23 000 lx по зададена програма ден/ нощ: 12h/12h. Растенията са отгледани в съдове от 500g с торови норми $N_{150}P_{100}K_{126}$ и биобъглен БВ-6 g/kg в три повторения за варинти, показани на табл.1. Използван е лесно приложим метод за получване на биовъглен (БВ) и разтрошаването му преди внасянето му в почвата.

***Таблица 1.***

| № вариант | Торене | Температура | поливане |
|---|---|---|---|
| 1 | БВ+ NPK | $I_{кам}$= 12ºC | ежедневно |
| 2 | БВ+ NPK | $I_{кам}$= 12ºC | през ден |
| 3 | БВ+ NPK | $I_{кам}$= 12ºC | през 2 дни |

Copyright © 2016 by Technical University of Sofia, Plovdiv branch, Bulgaria ISSN Online: 2535-0048

| | | | |
|---|---|---|---|
| 4 | NPK | I $_{кам}$= 12ºC | ежедневно |
| 5 | NPK | I $_{кам}$= 12ºC | през ден |
| 6 | NPK | I $_{кам}$= 12ºC | през 2 дни |
| 7 | БВ+ NPK | II $_{кам}$= 23ºC | ежедневно |
| 8 | БВ+ NPK | II $_{кам}$= 23ºC | през ден |
| 9 | БВ+ NPK | II $_{кам}$= 23ºC | през 2 дни |
| 10 | NPK | II $_{кам}$= 23ºC | ежедневно |
| 11 | NPK | II $_{кам}$= 23ºC | през ден |
| 12 | NPK | II $_{кам}$= 23ºC | през 2 дни |

Енергийният еквивалент на биомасата е определена с калориметричен метод. Използуван е бомбов калориметър - система Gallenkamp. Всяко определение е извършено в трикратна повторност при допустима грешка от 2%, след изсушаване на пробите при 60°C. Получените резултати са преизчислени към абсолютно сухо вещество без да се отчита ендотермичния ефект на хигроскопичната влага.

За сушене на пробите биомаса е използван микровълнов метод, при високоинтензивно нагряване с честоти 2,45 GHz и дължина на вълната λ =12,23 cm.

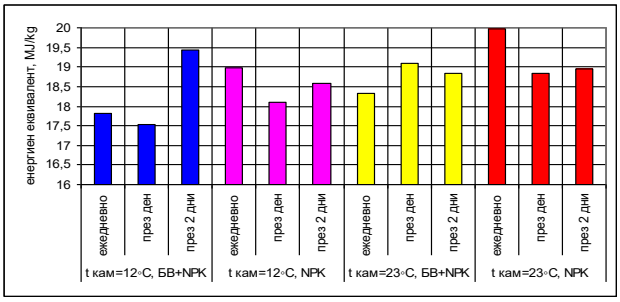
Като оптимални параметри на микровълново облъчване (МВО) са получени ниво на мощност 800 W, с времетраене 60 s, време за релаксация извън камерата 5 min.

Последователността на експеримента включва овлажняване за 2 часа на пробите биомаса в определените варианти, в три повторения, поставяне на пробите в цилиндрични пръстени, претегляне, микровълново облъчване, престой извън камерата, отново претеглене и повтаряне на процеса. Броя на микровълновите облъчвания се повтаря до достигане на постоянна стойност на суха маса, с влажност при атмосферни условия. Следена е температурата в централна точка на пробата. За времето извън камерата, загубата на маса на пробата продължава, съпроводено с намаляване на температурата на биомасата. Загубата на влага е определена чрез тегловен метод. Използвана е цифрова везна с чувствителност 0.01g.

Калоричността на биомасата е определена с изчислителен метод за получаване на данни за долна топлина на изгаряне при различни влажности на масата [1, 12].

## 3. Резултати и обсъждане

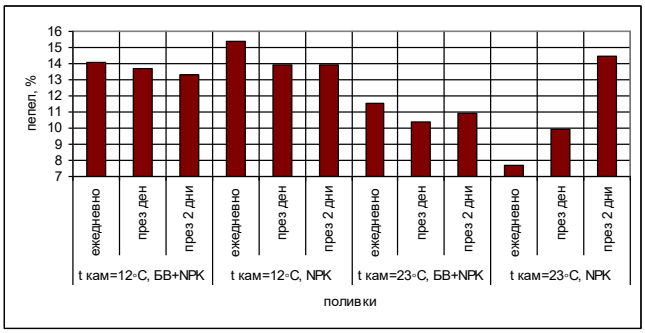
На фиг1 и фиг2 са представени средни стойности на експериментално установените енергийни еквиваленти и съдържание на пепел на биомасата по варианти.




***Фиг. 1.*** *Енергиен еквивалент на биомаса по варианти*

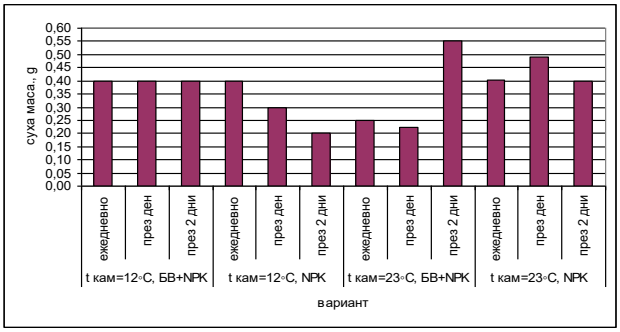
По отношение на фактора температура, стойностите за енергиен еквивалент са по-високи при $t_{кам}$=23°C и са в диапазона 18,34 MJ/kg - 19,96 MJ/kg, с максимум за вариант с ежедневно поливане и торене само с NPK.

При $t_{кам}$=12°C енергийното съдържимо е в диапазона 17,54 MJ/kg до 19,43 MJ/kg при вариант с БВ и поливки през 2 дни.




***Фиг. 2.*** *Съдържание пепел по варианти*

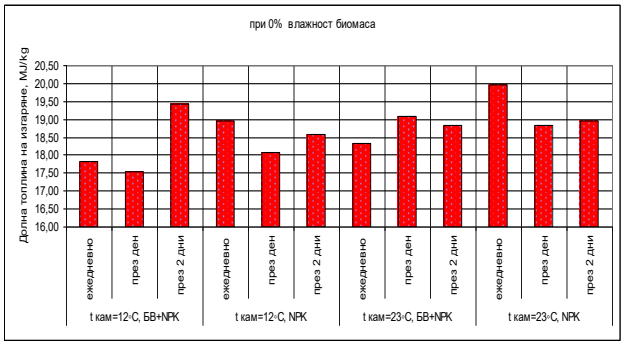
Съдържанието на пепел в биомасата при $t_{кам}$=23°C е значително по-малко от това при $t_{кам}$=12°C, където не се наблюдват съществени различия по отношение на поливки и торене.



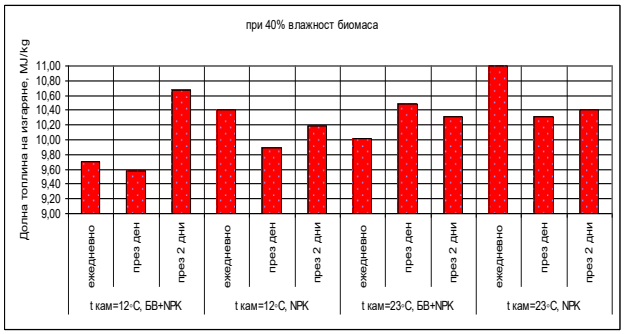

***Фиг. 3.*** *Суха маса след микровълново облъчване по варианти*

При по- ниската температура на отглеждане на зелето добавянето на биовъглен увеличава сухото вещество. При $t_{кам}$=23˚C съществено увеличение на сухото вещество се наблюдава при вариантите без БВ, с изключение на вариант с БВ и поливане през 2 дни, показващ най-висока стойност на сухо вещество

На фиг.4 и фиг.5 е илюстрирана получената долна топлина влажност на изгаряне, съответно при 0% и 40% на биомасата, за вариантите на отглеждане.




***Фиг. 4.*** *Долна топлина на изгаряне при 0% влажност на биомасата*

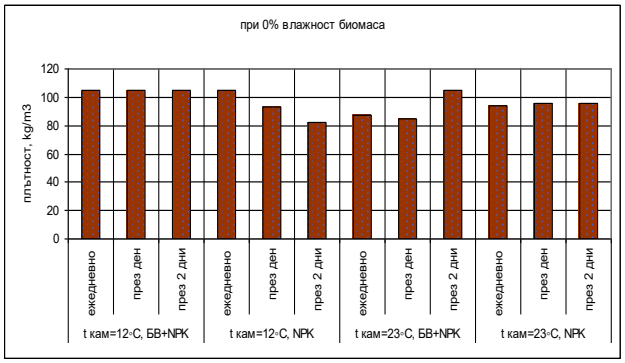



***Фиг. 5.*** *Долна топлина на изгаряне при 40% влажност на биомасата*

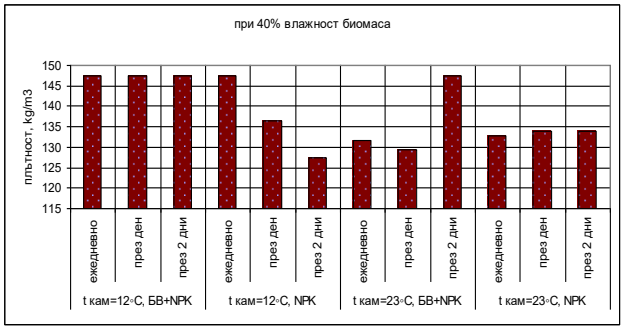
При 0% влажност на биомасата, за контролата (вариантите без биовъглен), и при двете температури на отглеждане, стойностите за долна топлина на изгаряне са по-високи при ежедневно поливане, съответно 19,96 MJ/kg при $t_{кам}$=23˚C и 18,97 MJ/kg при $t_{кам}$=12˚C. За вариантите с биовъглен, долната топлина на изгаряне е с най-висока стойност при вариант с поливане през два дни- 19,43 MJ/kg.

При 40% влажност на биомасата долната топлина на изгаряне показва същата тенденция като при абсолютна влажност на биомасата, със стойности съответно -за контрола, при $t_{кам}$=23˚C и ежедневно поливане -11,00 MJ/kg, и за вариант с БВ, при $t_{кам}$=12˚C, поливане през два дни- 10,67 MJ/kg.

На фиг. 6 и фиг.7 е илюстрирана плътността на биомасата при влажност 0% и 40%.



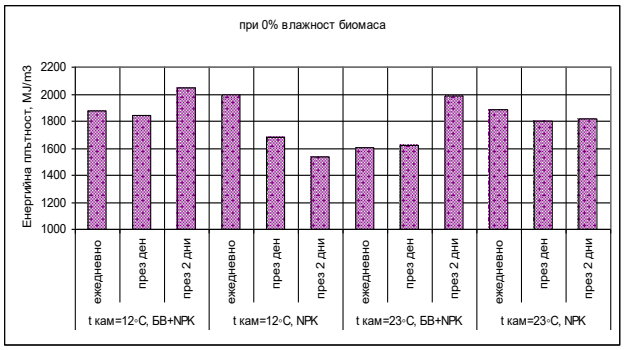

***Фиг. 6.*** *Плътност при 0% влажност на биомасата*



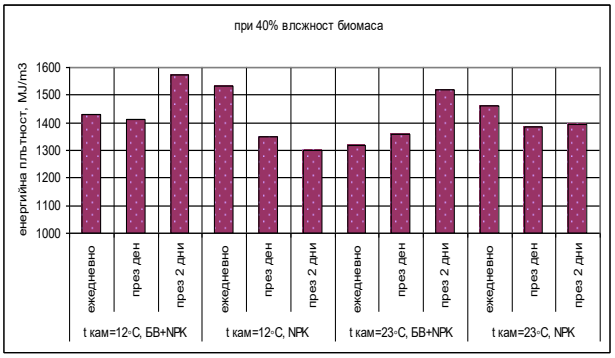

***Фиг. 7.*** *Плътност при 40% влажност на биомасата*

Плътността на биомасата при 0% влажност е сравнително постоянна за различните варианти, с малко по-високи стойности при по-ниската температура и добавен биовъглен- 105kg/m$^3$. Тази тенденция е силно изразена при влажност 40%, както и за вариант с биовъглен, при $t_{кам}$=23˚C, поливане през два дни -147 kg/m$^3$.

На фиг. 8 и фиг.9 е показана енергийната плътност при 0% и 40% влажност на биомасата.




***Фиг. 8.*** *Енергийна плътност при 0% влажност на биомасата*

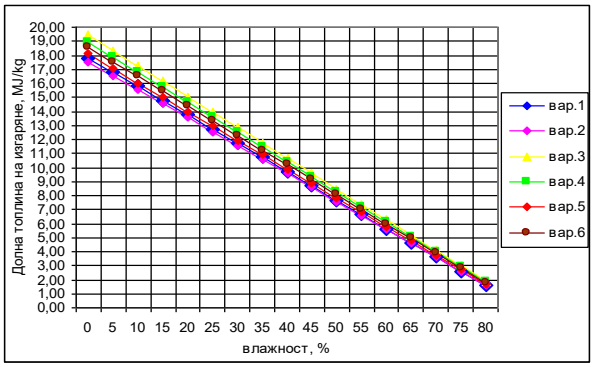



***Фиг. 9.*** *Енергийна плътност при 40% влажност на биомасата*

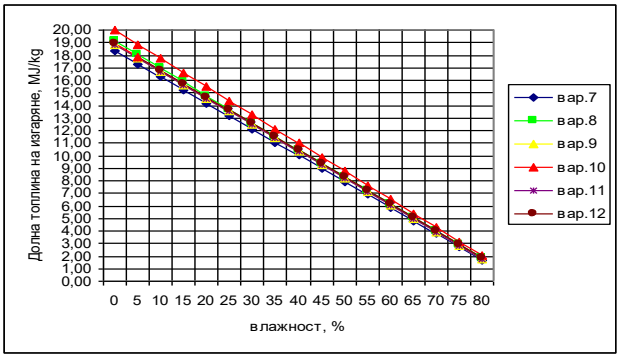
При 0% влажност на биомасата, резултатите за енергийна плътност, за контролата и при двете температури на отглеждане показват по-високи стойности при ежедневно поливане в сравнение с другите варианти на поливане. Енергийната плътност за варианти с добавен биовъглен е по-голяма при поливане през два дни, в сравнение с другите варианти на поливане, като данните са съответно 2046 MJ/m$^3$ при $t_{кам}$=12˚C и 1984 MJ/m$^3$ при $t_{кам}$=23˚C.

При 40% влажност тенденцията се запазва, като данните за енергийна плътност при вариант, с биовъглен, поливане през два дни са 1573 MJ/m$^3$ при $t_{кам}$=12˚C и 1521 MJ/m$^3$ при $t_{кам}$=23˚C.

На фиг.10 и фиг.11 е показана функционалната зависимост на долна топлина на изгаряне от влажност на биомасата, а на фиг.12 и фиг 13 зависимостта на плътност на биомасата от влажността й, за дипазона от 0% до 80%, през интервал 5%.

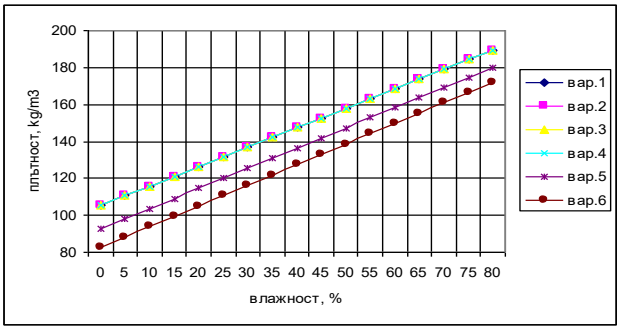



***Фиг. 10.*** *Зависимост на долна топлина на изгаряне от влажността на биомасата, при $t_{кам}$=12˚C, за варианти от 1* до 6.

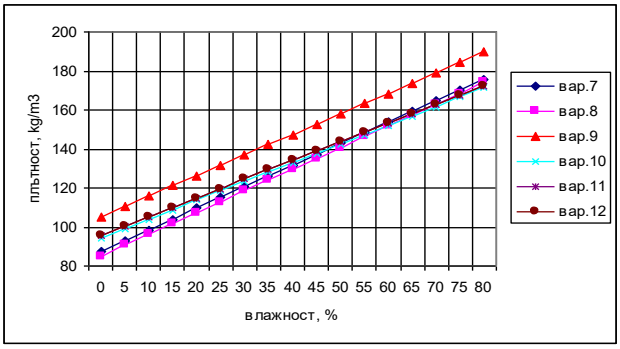



***Фиг. 11.*** *Зависимост на долна топлина на изгаряне от влажността на биомасата, при $t_{кам}$=23˚C, за варианти от 7 до 12.*

С увеличаване влажността на биомасата, долната топлина на изгаряне намалява както следва: за вариант при $t_{кам}$=23˚C, без биовъглен, ежедневно поливане –от 19,96 MJ/kg при 0% до 2,04 MJ/ kg при 80%; за вариант при $t_{кам}$=12˚C, с биовъглен, поливане през два дни–от 19,43 MJ/ kg при 0% до 1,91 MJ/ kg при 80%.




***Фиг. 12.*** Зависимост на плътността на биомасата от влажността й, при tкам=12°C, за варианти от 1 до 6.

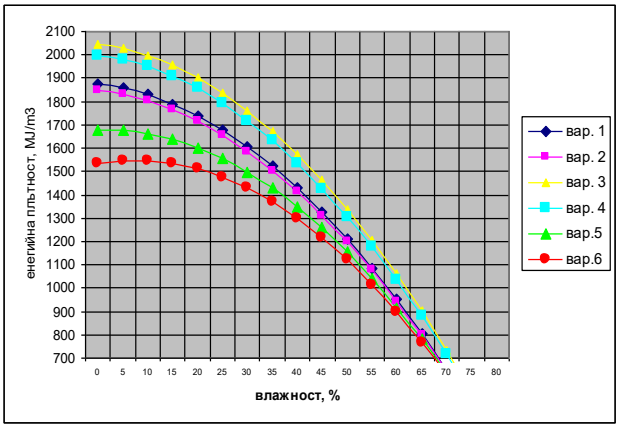



***Фиг. 13.*** *Зависимост на плътността на биомасата от влажността й, при $t_{кам}$=23˚C, за варианти от 7 до 12.*

С увеличаване влажността на биомасата от 0% до 80%, плътността й се увеличава, например -за вариант при $t_{кам}$=12˚C, с биовъглен,

поливане през два дни– от 105 kg/m$^3$ до 190 kg/m$^3$.

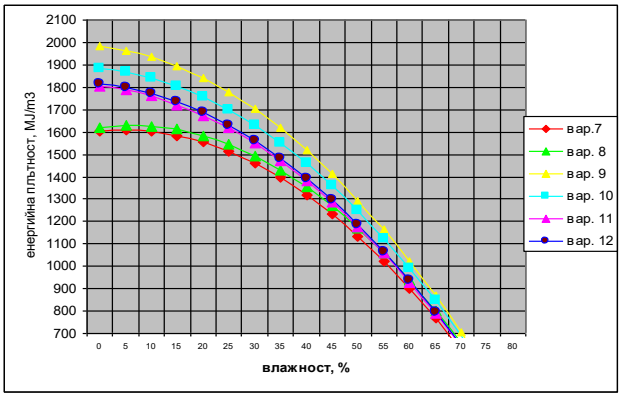
На фиг.12 и фиг.13 е показана зависимостта на енергийна плътност от влажност на биомасата в доапазон от 0% до 80%.




***Фиг. 14.*** *Зависимост на енергийна плътност от влажността на биомасата, при $t_{кам}$=12°C, за варианти от 1 до 6.*

С увеличаване на влажността на биомасата енергийната плътност намалява, като в диапазона от 0% до 40% различията във вариантите са ясно изразени.

Енергийната плътност за вариант при $t_{кам}$=12°C, с биовъглен, поливане през два дни намалява от 2046 MJ/m$^3$ при 0 % влажност до 362 MJ/m$^3$ при 80 % влажност; за вариант при $t_{кам}$=12°C, без биовъглен, поливане през два дни енергийната плътност намалява от 1536 MJ/m$^3$ при 0 % влажност до 308 MJ/m$^3$ при 80 % влажност.




***Фиг. 15.*** *Зависимост на енергийна плътност от влажността на биомасата, при $t_{кам}$=23°C, за варианти от 7 до 12.*

При $t_{кам}$=23°C енергийната плътност за вариант с биовъглен, поливане през два дни намалява от 1984 MJ/m$^3$ при 0 % влажност до 341 MJ/m$^3$ при 80 % влажност; за вариант с биовъглен, ежедневно поливане енергийната плътност намалява от 1603 MJ/m$^3$ при 0 % влажност до 299 MJ/m$^3$ при 80 % влажност.

## 4. Заключение

От направения анализ се установява, че внасянето на биовъглен в почвата се отразява благоприятно по отношение на нарастване на енергийните показатели на биомасата. Най-силно това влияние е изразено при условията на ограничено подаване на вода и при двата температурни режима, като стойностите са по-високи при по- ниския температурен режим.

Получените стойности за калоричност и енергийна плътност, при различно влагосъдържание, са важен критерий при оценка на качеството на биомасата.

Получените резултати са основа за по-нататъшни изследвания за въздействие на биовъглена в контекста на цялостния ефект от приложението му върху типове почва, растения и климатични въздействия в дългосрочен план.

## ЛИТЕРАТУРА


1. Йосифов Н. (2006). Суровинен ресурс и характеристика на биогенните горива от растителна биомаса. *Топлотехника за бита*, бр. 1, 25-37.
2. Brandstaka, T. and Other. (2010). Biochar Filter: Use of Biochar in Agriculture as Soil Conditioner. *Report for BSAS Commitment 2010*, 22 pp.
3. Biederman L., S. Harpole (2013). Biochar and its effects on plant productivity and nutrient cycling: a meta-analysis. *GCB Bioenergy (2013)* 5, 202–214.
4. Burdo O., and Other. (2012). Raw material dewatering electromagnetic technologies. *Problemele energeticii regionale* 1 (18), 78-86.
5. Carter S. and Other. (2013). The Impact of Biochar Application on Soil Properties and Plant Growth of Pot Grown Lettuce (Lactuca sativa) and Cabbage (Brassica chinensis). *Agronomy 2013*, 3, 404-418.
6. Dimitrova B. and Other. (2011). Equipment and Technologies for Treatment of Biomass. *Journal of the Technical University Sofia, branch Plovdiv "Fundamental Sciences and Applications"*, Vol.

16, International Conference Engineering, Technologies and Systems TechSys 2011.
7. Mcelligott K. and Other. (2011). Bioenergy Production Systems and Biochar Application in Forests: Potential for Renewable Energy, Soil Enhancement, and Carbon Sequestration. *Research Note RMRSRN-46. Fort Collins, USDA Forest Service*: 14.
8. Park J.,Y. Lee, C. Ryu'. (2014). Slow Pyrolysis of Rice Straw: Analysis of Products Properties, Carbon and Energy Yields. *Bioresource Technology*, Vol 155, 63–70.
9. Iswaran V. and Other. (1980). Effect of charcoal, coal and peat on the yield of moong, soybean and pea. *Soil Biology and Biochemistry* 12:191-192.
10. Kristin M. and Other. (2011). Bioenergy Production Systems and Biochar Application in Forests: Potential for Renewable Energy, *Soil Enhancement, and Carbon Sequestration. Research Note RMRS-RN-46. 2011*.
11. Srinivasarao Ch. and Other. (2013). Use of Biochar for Soil Health Enhancement and Greenhouse Gas Mitigation in India: Potential and Constraints. *NICRA Bulletin 1/2013*.
12. Yamamoto, H., J. Fujino, K. Yamaji. 2001. Evaluation of Bioenergy Potential with a Multiregional Global land use and Energy Model. Biomass Bioenergy 21 (3), Pp.185-203.

Контакти:
Department of Soil Physics
Institute of Soil Science, Agrotechnology and Plant Protection
"Nikola Poushkarov" (ISSAPPNP)
7, Shosse Bankya str. 1080 Sofia, Bulgaria

Assoc. Prof. Dr. Sevdalina Manolova
E-mail: sevdalina_manolova@abv.bg
Mobile: +(359) 887489001

© International Scientific Conference on Engineering, Technologies and Systems
TECHSYS 2016, Technical University – Sofia, Plovdiv branch
26 – 28 May 2016, Plovdiv, Bulgaria

# СПЕЦИФИЧНИ ОСОБЕНОСТИ ПРИ ПРОЕКТИРАНЕ НА ФАСАДНИ / ПОКРИВНИ ФЕЦ

АЛЕКСАНДЪР АНГЕЛОВ

**Резюме:** *В доклада се разглежда въпроса за използването на смесен тип ФЕЦ, съставени от фасадна и покривна част, за осигуряване на част от потреблението в жилищна сграда. Разгледани са различни типове фотоволтаични модули подходящи за използване при изграждането на фасадни/покривни ФЕЦ, различна ориентация на модулите, проведено е симулационно изследване и е направлен анализ на получените резултати.*

**Ключови думи:** *фасадни/покривни ФЕЦ, типове фотоволтаични модули*

# SPECIAL FEATURES DESIGN OF FACADE/ROOF PV PLANT

ALEXANDER ANGELOV

**Abstract:** *The report addresses the use of mixed PV composed of facade and roof part, to provide part of the consumption in residential building. Many different types of photovoltaic modules suitable for use in building facade / roof PV plant different orientation of the modules conducted a simulation study and directions analysis of results.*

**Key words:** *facade / roof PV, tips photovoltaic modules*

## 1. Въведение

### 1.1. Развитие на електроенергетиката в България

Устойчивото енергийно развитие, свързано с намаляването на емисиите на парникови газове, е изведено като център на енергийната политика на Република България [4]. Според [4,5,6] използването на ВЕИ се разглежда като един от основните фактори за преминаване към нисковъглеродна икономика.

Благодарение на високите преференциални цени за изкупуване на електроенергията (ЕЕ) произведена от ФЕЦ, приети от ДКЕВР [15-21] в периода 2006 – 2013 бяха изградени ФЕЦ с обща мощност 1012 MW [7]. Основна част от тях отдават ЕЕ към електроенергийната система (ЕЕС). Тази мощност надхвърля заложените в [8] мощност от 600 MW, която гарантира качеството на управление и сигурносттана електроенергийните доставки до 2020г.

Затова временно се преустанови присъединяването към преносната и разпределителните електрически мрежи на нови обекти за производство на електрическа енергия от възобновяеми източници [9]. Ограничението за присъединяване на ВЕИ не се прилага:

а/за обекти с обща инсталирана мощност до 30 kW включително, които се предвижда да бъдат изградени върху покривни и фасадни конструкции на присъединени към електроразпределителната мрежа сгради и върху недвижими имоти към тях в урбанизирани територии;

б/за обекти с обща инсталирана мощност до 200 kW включително, които се предвижда да бъдат изградени върху покривни и фасадни конструкции на сгради за производствени и складови дейности присъединени към електропреносната или електроразпределителната мрежа в урбанизирани територии [9].

Copyright © 2016 by Technical University of Sofia, Plovdiv branch, Bulgaria ISSN Online: 2535-0048

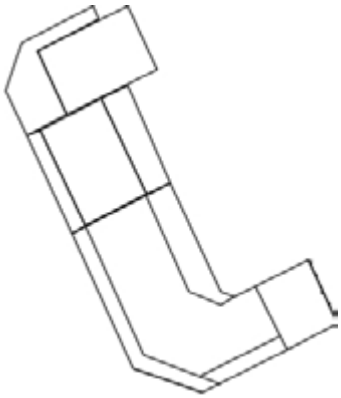
### 1.2. Нормативно стимулиране на енергийна ефективност

При изграждане на нови или при реконструкция, основно обновяване, ремонт или преустройство на съществуващи сгради се въвеждат в експлоатация инсталации за производство на енергия от възобновяеми източници, когато това е технически възможно и икономически целесъобразно [10].

С [11] се определят минималните изисквания за енергийна ефективност на жилищни сгради и на сгради за обществено обслужване. За оптимизиране на годишния разход на енергия при съвместното функциониране на системите за отопление /охлаждане/вентилация проектите на тези системи се изработват въз основа на изчисленията за годишен разход на енергия и енергийния баланс на сградата в част "Енергийна ефективност" [11].

### 2. Обект на изследване

На фиг.1 е показана покривната част на обекта, за когото се прави изследването.



***Фиг. 1.*** *Скица на разглеждания обект*

Сградата е във фаза на проект и е предвидено да се състои от апартаменти и търговски обекти, намиращи се в приземния етаж. Сградата не е разположена в район с централно топлофициране. Поради тази причина се приема, че за осигуряване на температурния комфорт в стаите и помещенията ще се използва отоплителни и климатични уреди. Част от климатизацията на търговските обекти ще се осъществява от чилъри, които ще доведат до намаляване на потреблението на ЕЕ в тези места.

По първоначални изчисления общото годишно потребление на ЕЕ ще бъде около 300 000 kWh. Според нормативната уредба за енергийно ефективна сграда се приема тази, която може да покрие 50% от собствената си консумация чрез използване на ВЕИ. В проекта е заложено локалният ВЕИ да бъде ФЕЦ.

### 3. Фотоволтаична централа

Фотоволтаичната централа трябва да бъде разположена върху всички свободни части, които имат подходяща ориентация. При първоначално определяне това са места с обща площ от 1 715 $m^2$, включваща покривна и фасадна част като разпределението е следното:

- покрив/югозапад – 883 $m^2$;
- покрив/юг – 182 $m^2$;
- покрив/югоизток – 290 $m^2$;
- фасада/югозапад – 250 $m^2$;
- фасада/югоизток – 110 $m^2$.

За да може да бъде усвоена цялата слънчева енергия падаща върху модулите, те трябва да бъдат разположени перпендикулярно на падащатата слънчева светлина. Поради годишното движение на слънцето ъгълът на наклона на модулите също трябва да се изменя. При стационарните ФЕЦ се избира оптимален ъгъл, при който целогодишното производство на ЕЕ е най-голямо.

Модулите, които са разположени по покривните части на сградата ще бъдат наклонени под ъгъл, който позволява по-голяма част от слънчевата светлина, която пада върху модулите, да бъде използвана за производство на електрическа енергия. Намирането на този ъгъл е решение на оптимизационна задача, която трябва да покрие следните условия:

а/площта върху, която ще бъде разположена централата не трябва да надвишава предварително определената площ;

б/произведеното количество ЕЕ да бъде възможно най-голямо.

При фасадното разположение на модулите няма възможност за търсене на оптимален ъгъл на наклона – монтирането на модулите е вертикално. По този начин голяма част от слънчевата енергия, която пада се отразява и не се преобразува в електрическа. Така разположените модули ще произвеждат по-малко енергия, отколкото ако същия тип модули са разположени на покрива. Поради тази причина, първоначално не може да се оцени еднозначно кой тип модул е най-подходящ при такова смесено разположение.

Поради бурните темпове на развитие на ВЕИ сектора, особено на фотоволтаичния, през последните години е налице голямо разнообразие на предлаганите продукти. Фотоволтаичните модули могат да се разделят на три основни групи според технологията на производство - монокристални, поликристални и тънкослойни

модули. За целите на изследването ще бъде разгледан по един модул от всяка група, като многообразието на модулите във всяка една от групите ще бъде пренебрегнато.В Таблици 1, 2 и 3 са посочени техническите данни на фотоволтаични модули, които ще се използват в проучването [12, 13, 14].

***Таблица 1.*** *Технически параметра на монокристален модул*

| **Монокристален модул** | |
|---|---|
| Мощност при MPP | 260 Wp |
| Ток на к.с. | 9.05 A |
| Напрежение на п.х. | 37.7 V |
| Ток при MPP | 8.56 A |
| Напрежение при MPP | 30.4 V |
| КПД | 15.6 % |
| Температурен коефициент на ток на к.с. | +0.06 %/$^0$C |
| Температурен коефициент на напрежение на п.х. | -0.34 %/$^0$C |
| Температурен коефициент на мощност при MPP | -0.44 %/$^0$C |

***Таблица 2.*** *Технически параметри на поликристален модул*

| **Поликристален модул** | |
|---|---|
| Мощност при MPP | 260 Wp |
| Ток на к.с. | 9.15 A |
| Напрежение на п.х. | 37.77 V |
| Ток при MPP | 8.53 A |
| Напрежение при MPP | 30.46 V |
| КПД | 15.6 % |
| Температурен коефициент на ток на к.с. | +0.04 %/$^0$C |
| Температурен коефициент на напрежение на п.х. | -0.30 %/$^0$C |
| Температурен коефициент на мощност при MPP | -0.41 %/$^0$C |

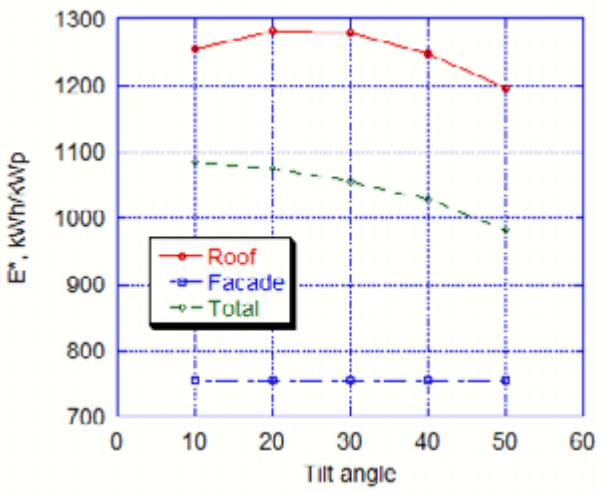
За направа на симулациите за различните типове фотоволтаични модули ще се използва специализирания софтуер PVSOL.

***Таблица 3.*** *Технически параметри на тънкослоен модул*

| **Тънкослоен модул** | |
|---|---|
| Мощност при MPP | 122.5Wp |
| Ток на к.с. | 1.93 A |
| Напрежение на п.х. | 87.0 V |
| Ток при MPP | 1.76 A |
| Напрежение при MPP | 69.9 V |
| КПД | 17.01 % |
| Температурен коефициент на ток на к.с. | +0.04 %/$^0$C |
| Температурен коефициент на напрежение на п.х. | -0.28 %/$^0$C |
| Температурен коефициент на мощност при MPP | -0.29 %/$^0$C |

## 4. Резултати и изводи

На фиг.2 е показано измененито на специфичното производство на ЕЕ от ФЕЦ с поликристални модули при покривна ФЕЦ със смесена ориентация, при покривна ФЕЦ с южна ориентация и покривна/фасадна ФЕЦ със смесена ориентация спрямо наклона на модулите.




***Фиг. 2.*** *Специфичното производство на ЕЕ от ФЕЦ*

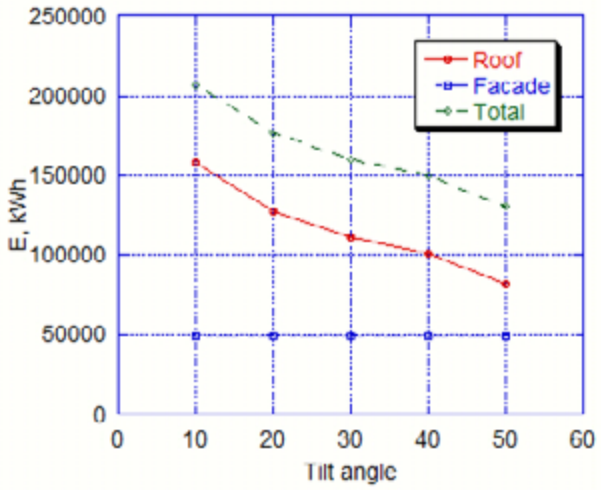
На фиг.3 е показано разпределението на произведената ЕЕ от ФЕЦ с поликристални модули при покривна част, при фасадна част и при общата мощност спрямо наклона на модулите.

На фиг.4 е показано дялово разпределение на произведената ЕЕ от ФЕЦ с поликристални модули между покривна и фасадна част спрямо наклона на модулите.

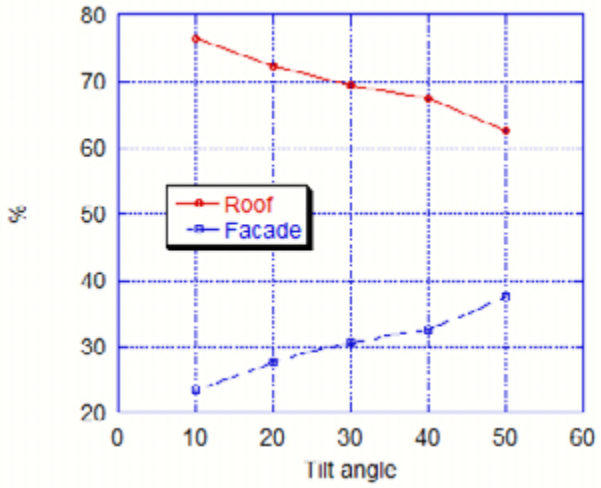
От фиг.2, фиг.3 и фиг.4 могат да се направят следните изводи:

- Наблюдава се значителна разлика във влиянието, което оказва ъгълът на наклона на модулите при централи с покривна и фасадна част и само покривна част, т.е. определянето на оптималния ъгъл;
- Съществено влияние върху цялостната ефективност на централата дава делът на произведената ЕЕ от фасадна част на централата. Колкото тя е по-малка, толкова ефективността на централата е по-висока.

На фиг.5 е показано сравнението на инсталираните мощности на цялата централас поликристални модули при ориентация на модулите спрямо разположението на сградата и насочени на юг спрямо наклона на модулите.




***Фиг. 3.*** *Разпределение на произведената ЕЕ*

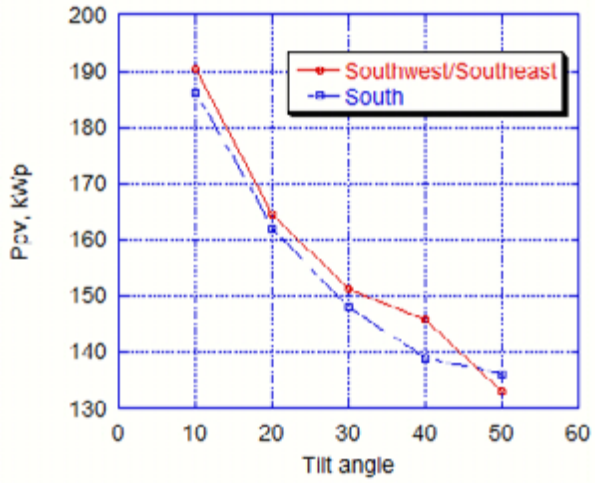



***Фиг. 4.*** *Дялово разпределение на произведената ЕЕ*

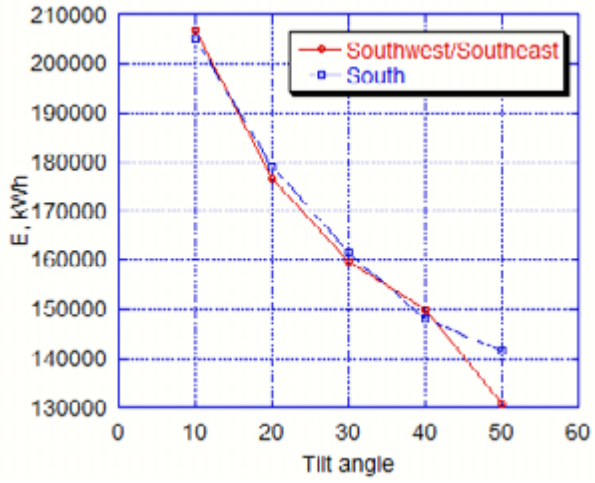
На фиг.6 е показано сравнението на произведената ЕЕ на цялата централа с поликристални модули при ориентация на модулите спрямо разположението на сградата и насочени на юг спрямо наклона на модулите.

От фиг.5 и фиг.6 могат да се направят следните изводи:

- Инсталираната мощност на ФЕЦ при ориентация на модулите на юг е по-малко, поради непълното уплътняване на площтите;
- Произведена ЕЕ при двата варианта на ориентация е сходна. Това се дължи на по-високото специфично производство на ЕЕ на модулите, които са ориентирани на юг.




***Фиг. 5.*** *Инсталирана мощност на ФЕЦ спрямо ориентация на модулите*



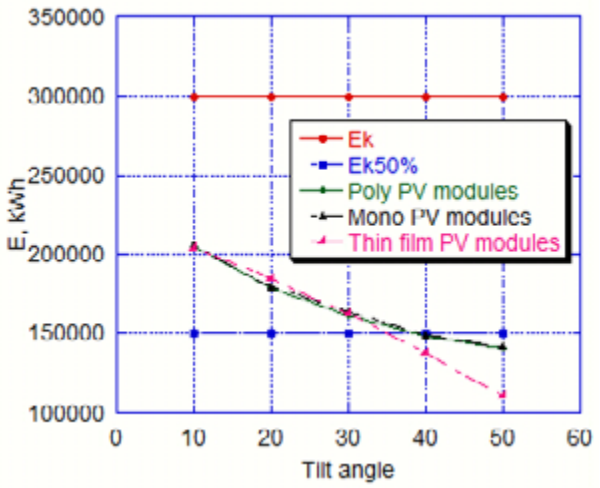

***Фиг. 6.*** *Произведена ЕЕ от ФЕЦ спрямо ориентация на модулите*

Резултатите от направените симулации за другите два типа модули са сходни с тези на поликристалния модул. Този извод се отнася и за четирите групи изследвания:

- специфичното производство на ЕЕ от ФЕЦ, дадени на фиг.2;
- дялово разпределение на произведената ЕЕ (фиг.3 и фиг.4);
- инсталирана мощност на ФЕЦ спрямо ориентация на модулите (фиг.5);
- произведена ЕЕ от ФЕЦ спрямо ориентация на модулите. (фиг.5).

На фиг.7 са показани графиките на очакваното потребление на сградата, критерият за енергийна ефективност на сградата и произведената ЕЕ от ФЕЦ при трите типа модули От фиг.7 могат да се направят следните изводи:

- Количеството произведена ЕЕ и трите типа модули е съизмерима;
- При така зададените условия – свободна площ и дял на покриване на потреблението, централата покрива тези изисквания, независимо от избрания тип модул.




***Фиг. 7.*** *Потребена и произведена ЕЕ*

В Таблици 4, 5 и 6 са посочени обобщените стойности на направеното изследване, относно производството на ЕЕ от различните типове модули, получени на наклон на модулите от $10^0$ и ориентация на модулите съвпадаща с тази на сградата.

## 5. Заключение

От направеното изследване могат да се направят следните заключения:

Когато има ФЕЦ от смесен тип, покривна и фасадна, е желателно да се избира по-малък ъгъл на наклона на модулите. По този начин инсталираната мощност на покривната част ще бъде по-голяма. Това ще доведе до по-голямо количество произведена ЕЕ, което ще намали делът на фасадната част, която е с по-лоши показатели. По този начин ще увеличи ефективността (специфичното производство) на цялата централа;

Когато няма определени архитектурни особености (например наличие на наклон по посока на разположение на сградата), които биха довели до допълнително усложняване и оскъпяване на централата се препоръчва ориентацията на модулите да бъде изцяло към юг. От представените графики следва, че количеството произведена ЕЕ е приблизително еднакво при двата вида разположение. Поради по-високото специфично производство при ориентация на юг инсталираната мощност на централата ще бъде по-малка. Това ще доведе до намаляване на първоначалната инвестиция и съкращаване на сроковете за изграждане на централата.

***Таблица 4.*** *Обобщени данни за монокристален модул*

| **Монокристален модул** | |
|---|---|
| Инсталирана мощност | 190.58 kWp |
| Очаквано годишно производство на ЕЕ | 208 120 kWh |
| Очаквано годишно специфично производство на ЕЕ | 1092.04 kWh/ kWp |

***Таблица 5.*** *Обобщени данни за поликристален модул*

| **Поликристален модул** | |
|---|---|
| Инсталирана мощност | 190.58 kWp |
| Очаквано годишно производство на ЕЕ | 206 798 kWh |
| Очаквано годишно специфично производство на ЕЕ | 1085.10 kWh/ kWp |

***Таблица 6.*** *Обобщени данни за тънкослоен модул*

| **Тънкослоен модул** | |
|---|---|
| Инсталирана мощност | 178.97 kWp |
| Очаквано годишно производство на ЕЕ | 200 464 kWh |
| Очаквано годишно специфично производство на ЕЕ | 1 120.08 kWh/ kWp |

Независимо от типа на модула очакваната произведена ЕЕ от ФЕЦ е не по-малко от 200 000 kWh, а очакваното потребление - 300 000 kWh. Това показва, че на етап проектиране за тази сграда, ЕЕ произведена от ФЕЦ осигурява повече от 60% от собствената ѝ консумация. Всички типове модули покриват поставените критерии за енергийно ефективна сграда. Но не може да се определи еднозначно кой тип модул е най-подходящ. Ако критерият за избор е най-високо специфично производство – най-подходящ за използване са тънкослойните модули. Но общото количество производство на ЕЕ е по-ниско спрямо останалите варианти, а това е един от основните критерии. От резултатите се вижда, че най-голямо годишно производство се получава при използване на монокристални модули. Недостатъкът им е по-високата цена спрямо поликристалните модули, за една и съща мощност (Цената на монокриталния модул, предлагана от един и същи търговски представител, е 0.85 €/Wp, а на поликристалния модул е 0.78 €/Wp.). От друга страна годишно произведената ЕЕ от поликристалните модули е съизмерима с тази на монокристалните. Като се отчете, че поликристалните модули са по-евтини от монокристалните може да се направи извода, че най-подходящи за използване при изграждане на смесени (покривни и фасадни) ФЕЦ са поликристалните модули;

## ЛИТЕРАТУРА


1. Ангелов, А., Шакев, Н., Ганев, Г., Прогнозиране на потреблението на електрическа енергия на обществен обект, 2015.
2. Министерство на енергетиката, *Бюлетин за състоянието и развитието на енергетиката на Република България,* 2015
3. Георгиев, А., *Статистически данни и показатели за електропроизводството в България през 2014 г.*, 2015
4. Енергийна стратегия на Република България до 2020 г. за надеждна, ефективна и по – чиста енергия
5. Киряков, В., Петрова, Б., Меркулов, М., Стамболийски, Н., 2010, Бъдещо развитие на ВЕИ в енергийната система на България в съответствие с Директива 2009/28/ЕО
6. Европейска комисия, Доклад за напредъка в областта на енергиятя от възобновяеми източници, 2015
7. www.seea.government.bg
8. План за развитие на преносната електрическа мрежа на Българияза периода 2010 – 2020
9. Решение №ЕМ-01 от 29.06.2012 на Държавната комисия за енергийно и водно регулиране
10. (4) Закон за енергия от възобновяеми източници, Обн., ДВ, бр. 56 от 24.07.2015, в сила от 24.07.2015
11. Наредба №7 от 2004г. за енергийна ефективност на сгради, Обн., ДВ, бр. 27 от 2015, в сила от 15.07.2015
12. www.q-cells.com
13. http://www.winaico.com
14. www.firstsolar.com
15. Решение №Ц-033 от 29.12.2006 на Държавната комисия за енергийно и водно регулиране
16. Решение №Ц-015 от 31.03.2008 на Държавната комисия за енергийно и водно регулиране
17. Решение №Ц-04 от 30.03.2009 на Държавната комисия за енергийно и водно регулиране
18. Решение №Ц-018 от 31.03.2010 на Държавната комисия за енергийно и водно регулиране
19. Решение №Ц-010 от 30.03.2011 на Държавната комисия за енергийно и водно регулиране
20. Решение №Ц-18 от 20.06.2011 на Държавната комисия за енергийно и водно регулиране
21. Решение №Ц-28 от 29.08.2012 на Държавната комисия за енергийно и водно регулиране



Контакти
E-mail: a_angelov.82@abv.bg

© International Scientific Conference on Engineering, Technologies and Systems
TECHSYS 2016, Technical University – Sofia, Plovdiv branch
26 – 28 May 2016, Plovdiv, Bulgaria

# SECTION 3 • СЕКЦИЯ 3

## INFORMATICS AND COMPUTER SYSTEMS AND TECHNOLOGIES

## ИНФОРМАТИКА И КОМПЮТЪРНИ СИСТЕМИ И ТЕХНОЛОГИИ

© International Scientific Conference on Engineering, Technologies and Systems
TECHSYS 2016, Technical University – Sofia, Plovdiv branch
26 – 28 May 2016, Plovdiv, Bulgaria

# GENERATOR OF NETWORK DoS ATTACKS

VENETA ALEKSIEVA, IVAYLO ZHELYAZKOV

**Abstract:** *This paper presents a system for generation of network DoS attacks, using protocols of TCP / IP suite - UDP, TCP and ICMP. The purpose of the developed system is for education and it offers versatile tools for simulating different types of attacks. DoS attacks with various parameters are implemented. There are presented results of experimental research.*

**Key words:** *DoS attack, UDP attack, TCP attack, ICMP attack, Syn flood attack*

## 1. Introduction

Network Denial of Service (DoS) attacks do not aim penetration, establishing control over data or eavesdrop on communication. Their task is to cause a collapse in network devices or servers, thus compromising the whole system or only a range of services, making them unavailable to the legitimate users.

Statistics provided by Kaspersky Lab [1] present that DDoS in 2015 has decreased by 11% in comparison to 2014. But during the first quarter of 2015 they are 23,095 and most of the attacks are carried out on the territory of China, the US and Canada. The longest attack was 140 hours. Financial institutions, banks and large companies in the energy sector have registered loss of over $ 12 million annually. It directs insurers to offer insurances against hacker attacks. In 2015 the company Loyd British Insurance [2] has registered an increase in the amount of revenue as a result of the conclusion of insurance policies with companies to cover the risks of hacking, worth 2.5 billion dollars. Globally, the cost of cyber security is 77 billion dollars in 2015 and to 2020 worldwide companies expect to invest about 170 billion dollars to protect their data.

There are many tools and technologies, whose task is to identify and block various types of attacks [3,4] - antivirus programs, firewalls, static ARP tables, physical firewall devices, expensive specialized equipment like Cisco Guard XT 5650, FortiDDoS-400B, FortiDDoS -2000B and others. To respond effectively to these suspicious activities to computer or network resources, it is needed to know the nature of the attacks.

The proposed generator simulates various network attacks with different parameters. This allows to study the effectiveness of various protection tools against these threats.

## 2. Related Works

Most of the realizations of network DoS attacks use high-level languages like C and C++, because they have tools to work with sockets (in particular raw sockets). With these tools the programmer constructs own TCP/IP headers of messages that will attack a system. The operating system Windows and many modern Linux distributions impose a number of restrictions on the use of raw sockets on kernel level. For example, the raw sockets are prohibited in versions of Windows after XP, and Server-oriented versions after Server 2008R2, as in many of the latest versions of popular Linux distributions such as Ubuntu, Debian, Fedora. The idea is similar at all - do not allow the operating system to become the conductor of this type of action or impose a number of restrictions against malware to fulfill its purpose. The weaknesses and shortcomings in the TCP / IP stack and the freedom that has the system programmer on the form and content of IPv4 packets is a precondition for abuse. The flexibility of programming languages is large enough to allow the development of algorithms that dynamically change the parameters of the IPv4 packets, which are the attacked victims. This obstructs prevention and localization of beginning stages of the DoS attack.

There are many solutions to generate DoS attacks for testing purposes under Windows, for example:

- LOIC (implements attacks on TCP/ HTTP/ UDP/ ICMP) [5]
- XOIC (implements attacks on TCP/ HTTP/ UDP/ ICMP) [6]
- PyLoris (implements attacks HTTP, which used SSL, SOCK Proxy) [7]

They have some disadvantages, as low efficiency, inability to replace addresses of packets (limits after Windows XP SP2 and Server 2008R2).

Copyright © 2016 by Technical University of Sofia, Plovdiv branch, Bulgaria ISSN Online: 2535-0048

In most decisions is absent an option for simulation of attack from more than one source simultaneously.

The generators of network attacks under Linux offer more variety and efficiency than generators under Windows and they offer the possibility to replace addresses, for example:

- hping3 (implements attacks on TCP/ HTTP/ UDP/ ICMP, pack dumping, port scanning, transporting files regardless of the aggressive policy of firewalls) [8]
- GoldenEye (implements attacks on HTTP) [9]
- PyLoris (implements attacks on TCP/ HTTP/ UDP/ ICMP) [10]

They generate packets with static content that is easily recognizable from firewalls. Other disadvantage is that they are so tightly specialized.

## 3. DoS attacks imlemented in the proposed generator

For realization of the proposed generator of DoS attacks is selected operation system - Kali Linux 2.0 sana, because it is optimized for performing penetration tests and many of the restrictions imposed by other popular Linux distributions and in most versions of Windows (except Windows XP / 2000 / Server 2000/2008), with respect to the RAW socket, are absent. The selected programming environment is Code Blocks 10.05, with the compiler GNU GCC.

To prevent possible abuse with this proposed noncommercial generator many restrictions are implemented as:

- Prohibition of multiple instantiation of software – starting it in parallel processes;
- Limit the maximum number of simultaneously working threads to 500. Each tread after 500 will wait in the FIFO queue to be started;
- The number of implementations of various types of attacks is reduced to four most popular attacks - flood with UDP packets, flood with TCP packets, flood with ICMP packets (there are two realizations - Ping of Death and broadcast attacks), flood with TCP SYN messages;
- The maximum total number of bytes sent to the "victim" will be limited to a maximum value of type unsigned long, regardless of the duration of the attack;
- Maximum size of a single ICMP packets is 64 bytes;
- The data buffer of UDP and TCP packets is limited to 27 bytes.

The proposed generator of DoS attacks provides the following features:

- set of popular DoS attacks to perform simulation tests;
- set of tools for customizing the parameters of the attack;
- tools for automated tests in order to re-simulation of various scenarios with minimal user intervention;
- good performance and high level of control on the performed tests;
- low system requirements;
- the most simple and intuitive set of commands;
- creation of log files for analysis.

Figure 1 presents the general algorithm for generating of each attack. The particular specificity of each attack is described below.

### 3.1. UDP/ TCP flood attack

These attacks use protocol 17 (UDP - User Datagram Protocol) or protocol 6 (TCP - Transmission Control Protocol). They generate packets, whose data content consists from a random combination of letters and numbers. The length of payload data may vary between 10 and 27 characters. The source IP address and the source port number in the IP header may be user defined or randomly generated.

### 3.2. ICMP flood attack

This attack uses protocol 1 (ICMP- Internet Control Message Protocol) with generation of echo-packets. The size of a regular ICMP Echo-Request packet is 32 bytes. It seems as ICMP Echo-Request packet of ping communication.

Most of the computer systems cannot process a packet that exceeds the maximum size accepted for IPv4 protocol - 65535 bytes due to the small size of echo packets used in the attack was fixed on 64 bytes as payload part will contain randomly generated data. The algorithm of conducting of this attack is similar to the previous one, but before check the *timeout* is added *sockopt broadcast*.

### 3.3. SYN flood attack

This attack uses protocol 6 (TCP - Transmission Control Protocol). It generates SYN (synchronization) packets to user-defined destination port of attacked server or to its random port. The attack uses the weaknesses in the three way handshake communication mechanism. When the victim received SYN message, it responds with a SYN/ACK (synchronization acknowledged) message for each open port and it waits for ACK (acknowledged) packets from bogus clients.

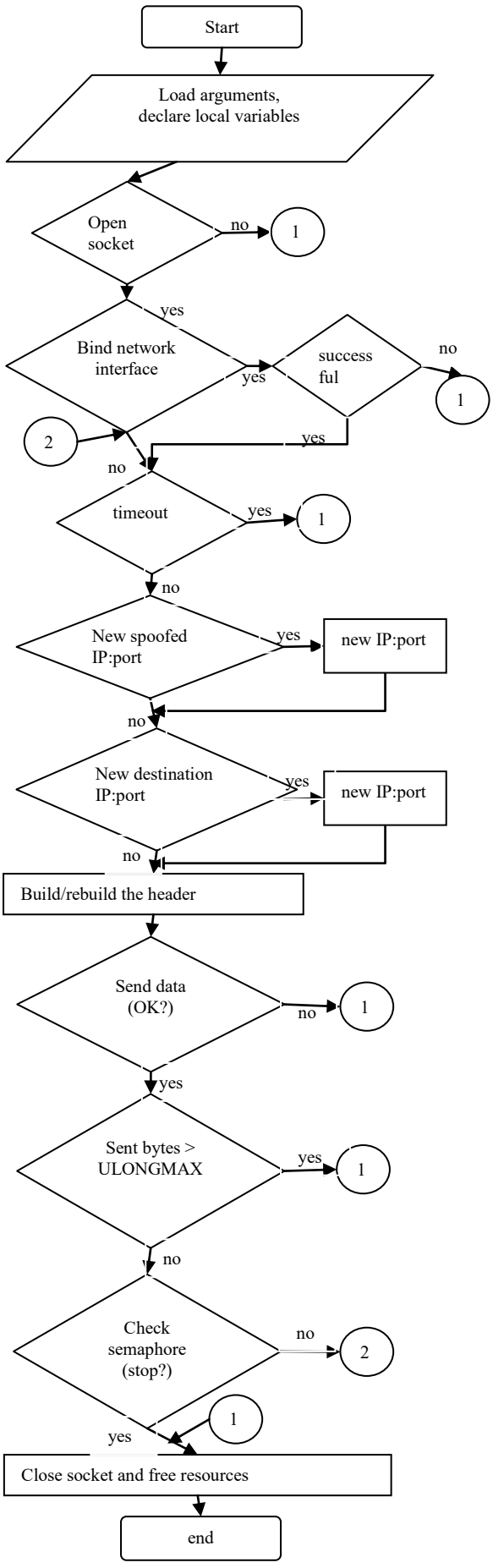



***Fig. 1.*** *UDP/TCP Flood Attack*

Thus the attacker forces the server to allocate a large number of resources for each of the open connections for nonexistent clients in the extremely short period of time. So, the attacked host cannot service their regular customers during the *timeout* and deprives them of the provided service.

Figure 2 presents the console application of the proposed generator of DoS attacks. There are presented different options for generating of different attacks.

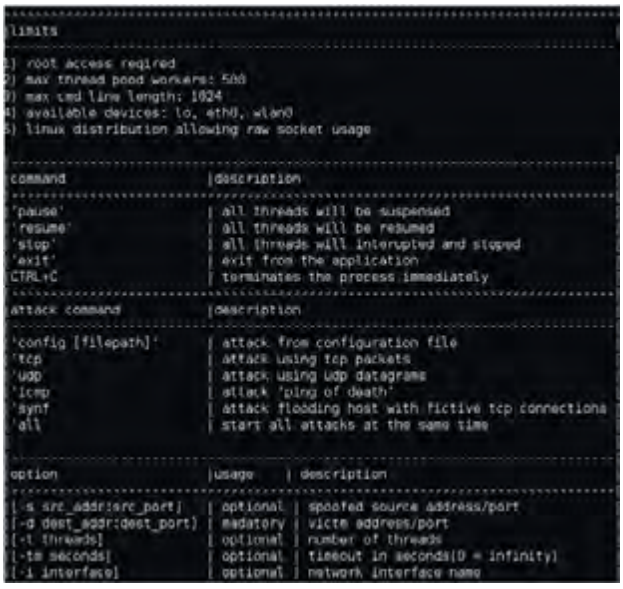



***Fig. 2.*** *The Parameters for Generating an Attack*

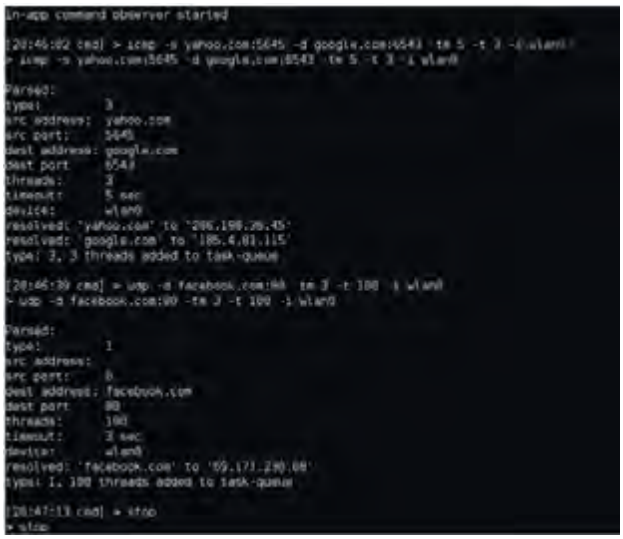



***Fig. 3.*** *Attacks Examples*

The executed attack can be stopped for a certain period ( '*pause*'- blocks all running threads in the pool), to be recovered (' *resume*'- restarts all blocked threads in the pool), fully stopped ( '*stop*'- terminates to execute of all threads in the pool and releases used resources). There are two ways to finish work with the application – choice '*exit*' or immediate close process with a keyboard shortcut

*'CTRL + C'*. The attacks can be run separately, but it is possible to activate them simultaneously.

Figure 3 presents the screenshot from ICMP flood attack and UDP attack to popular sites.

## 4. Experimental results

Tests are provided in two similar experimental situations - the attacked machine at the first situation is running under Linux Slackware, and at the second - under Windows 7. Tests are provided in the local Ethernet network.

### 4.1. Test 1

The victim (the host under attacks): CPU Intel Core2Duo T7700 2x2.40 GHz; RAM(physical) 2.00GB ddr2 ; OS Slackware 32-bit; interface eth0 192.168.0.213;

The attacker (the host who execute attacks): CPU Intel Core i7 vPro 4x2.13 GHz; RAM(physical) 4.00GB ddr3; OS Kali Linux 2.0 sana 64-bit; interface eth0 192.168.0.233.

#### 4.1.1. Attack 1. UDP

The attacker generates UDP packets with replaced IP/port in the UDP header. The aim of the attack is to check for a short period of time with what quantity of packets can be overload communication channel.

The result is presented on Fig.4. The source is only one with IP 2.5.11.17 and number of port 29686. Average 7538560 byte/s (or 188464 packets) reach to victim during 1 second on communication channel.

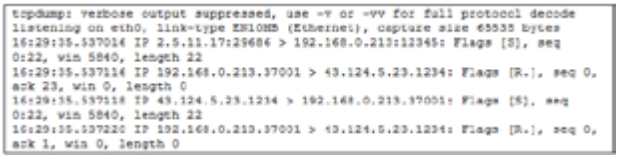



***Fig. 4.*** *Screenshot from tcpdump -i eth0, started on the host under UDP flood attack*

#### 4.1.2. Attack 2. TCP

The attacker generates TCP packets with SYN = 1, with replaced IP/port in the TCP header. The aim of the attack is to check for a short period of time with what quantity of packets can be overload communication channel. In addition it checks whether the attacked machine attempts to return ACK = 1.

The result is presented on Fig.5. The source is only one with IP 43.124.5.23 and number of port 1234. Average 21976971 byte/s (or 430921packets) reach to victim during 1 second on communication channel.

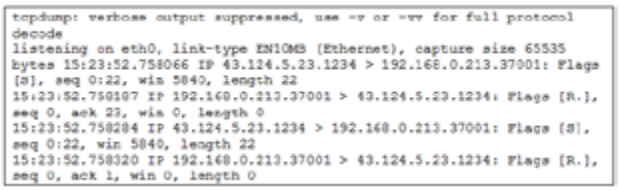



***Fig. 5.*** *Screenshot from tcpdump -i eth0, started on the host under TCP flood attack*

#### 4.1.3. Attack 3. ICMP

The attacker generates ICMP packets with replaced IP in the ICMP header. The aim of the attack is to check for a short period of time with what quantity of packets can be overload communication channel.

The result is presented on Fig.6. The source is only one with IP 43.24.52.40. Average 69200 byte/s reach to victim during 1 second on communication channel.

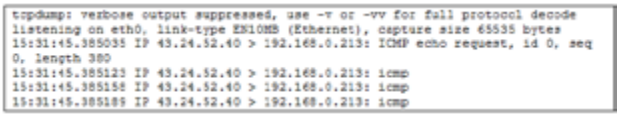



***Fig. 6.*** *Screenshot from tcpdump -i eth0, started on the host under ICMP flood attack*

#### 4.1.4. Attack 4. SYN Flood

The attacker generates TCP packets without payload, with SYN = 1 and with replaced IP/port in the TCP header. The aim of the attack is to check for a short period of time with what quantity of SYN packets can be overload communication channel. In addition it checks whether the attacked machine attempts to return ACK = 1.

The result is presented on Fig.7. Less than 1 second 756 TCP SYN packets reach to victim, each of them is from different source.

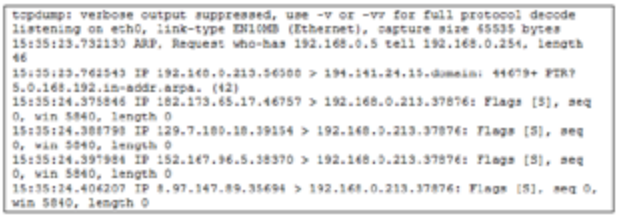



***Fig. 7.*** *Screenshot from tcpdump -i eth0, started on the host under SYN flood*

### 4.2. Test 2

The victim (the host under attacks): CPU Intel Core2Duo T7700 2x2.40 GHz; RAM(physical) 2.00GB ddr2RAM(total virtual)

4.00GB; OS Windows 7 Enterprise 32-bit; interface eth0 192.168.0.16;

The attacker (the host who execute attacks): CPU Intel Core i7 vPro 4x2.13 GHz; RAM(physical) 4.00GB ddr3; OS Kali Linux 2.0 sana 64-bit; interface eth0 192.168.0.233.

#### 4.2.1. Attack 1. UDP

The result is presented on Fig.8. The source is only one with IP 12.5.32.56:45464. During 1 second to the victim reach average 7461467 byte/s (or 181987 packets).

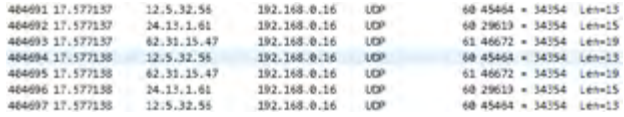


***Fig. 8.*** *Screenshot from Wireshark, started on the host under UDP flood attack*

#### 4.2.2. Attack 2. TCP

The result is presented on Fig.9. The source is only one with IP 76.41.16.45:46672. During 1 second to the victim reach average 10386417 byte/s (or 185471 packets).

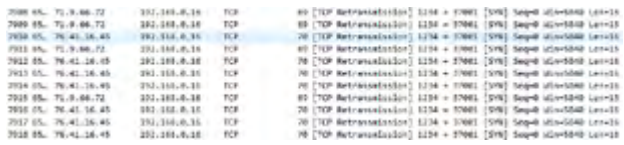


***Fig. 9.*** *Screenshot from Wireshark, started on the host under TCP flood attack*

#### 4.2.3. Attack 3. ICMP

The result is presented on Fig.10. The source is one with IP 4.19.25.41. Less than 1 second to the victim reach 69200 bytes.



***Fig. 10.*** *Screenshot from wireshark, started on the host under ICMP flood attack*

#### 4.2.4. Attack 4. SYN Flood

The result is presented on Fig.11. Less than 1 second to the victim reach 432 TCP SYN packets, each of them is from different source.

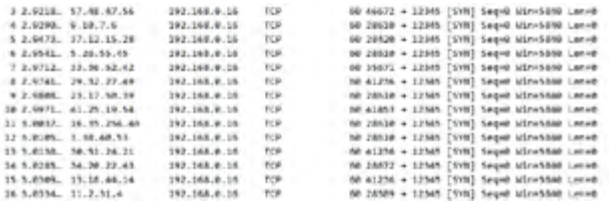


***Fig. 11.*** *Screenshot from wireshark, started on the host under SYN flood attack*

The results for both tests are similar - in UDP and ICMP attacks the observed total number of B/s are very close. However during TCP Flood and SYN Flood attacks, where the used protocol is TCP, it is observed discrepancy approximately twice the volume of records. It is important to point that during the tests the firewall of victim is “on”. The probable cause for the discrepancy in results is precisely defined restrictive policy that is imposed over the incoming data flow.

## 5. Conclusion

This paper presents a generator of DoS attacks. There are implemented and tested four attacks - UDP attack, TCP attack, ICMP attack, SYN flood attack.

The main goal of the future work is to extend functionality, providing this program with more popular types of attacks as HTTP flooding, which received popularity in recent years with attacks on various public websites and web services, TCP Session Hijacking and ARP poisoning, because they are in the root of different *man in the middle* attacks – rerouting, change / replacement of packages or sniffing, etc.

The possibility of multiple instantiation of the program on single machine would also be a good step for future work. Multiprocessing start of attacking program would allow more realistic simulation of DDoS attack, launched from a single machine, but in the same time this would allow to control synchronization of execution of DoS attacks from several machines, which work in parallel in master-slave mode (DDoS attack).

## REFERENCES


1. Kaspersky Lab, Kaspersky DDoS Intelligence Report for Q4 2015, (2016), https://securelist.com/analysis/quarterly-malware-reports/73414/kaspersky-ddos-intelligence-report-for-q4-2015/
2. LLOYD’S, (2016), www.lloyds.com/
3. Mirkovic J, S. Dietrich, D. Dittrich, P. Reiher, “Internet Denial of Service: Attack and Defense Mechanisms”, Prentice Hall 2004, ISBN: 0-13-147573-8

4. Zargar S.T., J. Joshi, D. Tipper, “A Survey of Defense Mechanisms Against DDoS Flooding Attacks”, IEEE Communications Surveys & Tutorials, Vol. 15, Issue: 4, 2013, pp. 2046 – 2069, ISSN:1553-877X.
5. https://sourceforge.net/projects/loic/
6. https://sourceforge.net/projects/xoic/
7. https://sourceforge.net/projects/pyloris/
8. www.hping.org/download.html
9. golden-eye.soft112.com
10. pyloris.soft112.com

Address:Technical University of Varna,
Str. „Studentska”1
Phone: 052/383 439
E-mail: valeksieva@tu-varna.bg
E-mail: ijelqzkov@live.com

© International Scientific Conference on Engineering, Technologies and Systems
TECHSYS 2016, Technical University – Sofia, Plovdiv branch
26 – 28 May 2016, Plovdiv, Bulgaria

# DEVELOPING OF A LIBCLOUD DRIVER FOR OWNCLOUD

SIMEON TSVETANOV

**Abstract:** *Apache Libcloud [1] is a Python library that abstracts the differences between cloud providers and allows unified access to different cloud resources through an easy to use API. Although Libcloud supports impressive number of providers and methods [3], it doesn't support the popular storage platform ownCloud [2] and that was the motivation for developing a Libcloud driver for ownCloud.*

**Key words:** *Cloud Technologies, Libcloud, owncloud, Webdav.*

## 1. Introduction

Cloud storages are kind of online storage sites where the data is stored in data centers. The hosting companies operate with large data centers, so people who need to store their data, purchase or rent a storage capacity of them. People or organizations hire or purchase cloud space in order to store customers, user or corporate data. On the other hand, cloud customers can use the storage to store their provided applications. Data in the cloud space can be accessed through APIs or through a web-based system for managing content [4].

Grid and cloud technologies provide an abstraction of the computational resources and make the access to them much easier, but users still face the problem of interacting with the different interfaces of the different service providers. Libcloud aims to solve this problem by providing unified interface for most of the cloud service providers, fig 1.

Driven by increasing demand for standards in cloud technologies [5] Apache Libcloud supports more than 30 cloud providers including Amazon EC2 (Elastic Cloud Compute), Rackspace Cloud, Terremark, IBM Cloud, GoGrid Linode, etc.

Libcloud acts as a driver in order to abstracts the differences between cloud providers and to allow unified access to different cloud resources. Provided services are divided into the following categories:

- Compute – allows the user to manage cloud and virtual servers offered by different providers;
- Cloud Storage - services such as Amazon S3 and Rackspace CloudFiles;
- Load Balancers as a Service - services such as Amazon Elastic Load Balancer and GoGrid Load Balancers;
- DNS as a Service - services such as Amazon Route 53 and Zerigo;
- Container - to install and deploy containers onto container based virtualization platforms;
- Backup - to manage Backup as a Service and services such as EBS Snaps, GCE volume snap and dimension data backup.

Some frequently used term in Libcloud:

**Node** - represents a cloud or virtual server.
**NodeSize** - represents node hardware configuration. Usually this is amount of the available RAM, bandwidth, CPU speed and disk size.
**NodeImage** - represents an operating system image.
**NodeLocation** - represents a physical location where a server can be.
**NodeState** - represents a node state. Standard states are: running, stopped, rebooting, terminated, pending, and unknown.
**KeyPair** - represents an SSH key pair object.
**StorageVolume** - represents a storage volume
**VolumeSnapshot** - represents a point in time snapshot of a StorageVolume

Most users have long been looking carefully which is the largest, free and qualitative package with cloud services that can be used. The right choice of provided services is important because of subsequent difficulties in migration from one cloud provider arise the need to restructure files and there are enormous effort needed for migration.

OwnCloud [6] is a suite of client-server software for creating file hosting services and using them. OwnCloud is functionally very similar to the widely used Dropbox, with the primary functional difference being that OwnCloud is free and open-

Copyright © 2016 by Technical University of Sofia, Plovdiv branch, Bulgaria ISSN Online: 2535-0048

source, and thereby allowing anyone to install and operate it without charge on a private server.

Its open architecture and APIs allow IT to easily add corporate branding, and extend core functionality as needed to meet the company's evolving needs. From enterprise directories to SAML, SharePoint or Windows network drives, ownCloud allows you to leave data where it lives while exposing secure access to users on any device.




***Fig. 1.*** *Accessing different cloud providers through Libcloud API*

OwnCloud is in the top of any competitive analysis and has been preferred for self-hosted storage platform, but that opens the issue about the integration with the rest of the system, fig 2.

## 2. Design of the Libcloud driver

Before starting with the implementation of the new driver, some investigation about the possible ways to interact with ownCloud is needed.

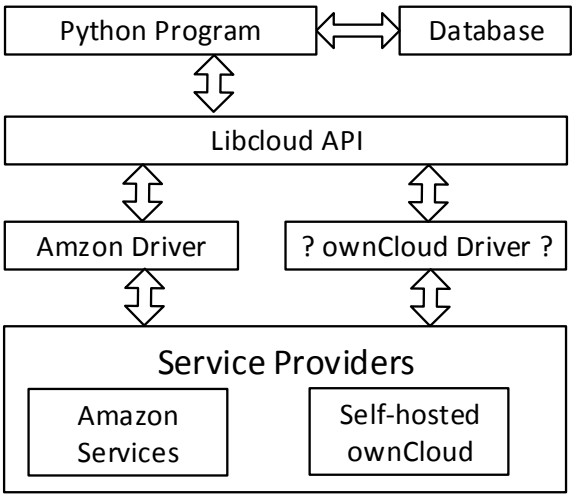



***Fig. 2.*** *Global view of the system is showing where the new ownCloud driver is required*

OwnCloud is written in PHP and has a local database for storing the whole file structure and the application.

The platform support WebDAV [7] protocol for file transfer that could be used for desired interaction. Web Distributed Authoring and Versioning (WebDAV) is an extension of the Hypertext Transfer Protocol (HTTP) that allows clients to perform remote Web content authoring operations. It provides a framework for users to create, change and move documents on a server; typically a web server or web share. The most important features of the WebDAV protocol include the maintenance of properties about an author or modification date, namespace management, collections, and overwrite protection.

To use its features, a new Libcloud module for WebDav communication is needed. Then the developed driver could use that WebDAV module in order to provide the required functionality.

This approach allows Libcloud to interact with any ownCloud server and with minor modification to any server supporting WebDav protocol.

## 3. Development of the new driver

The first step of developing the new driver is to install Libcloud. The library is available on PyPi [8] and could be easily installed using pip.

*pip install apache-libcloud*

Then a new module for WebDAV interaction (presented in webdav.py file) has to be added in libcloud/utils folder.

Next step is to create a driver which uses the already created WebDav module in order to send requests to the server. The driver file is called

owncloud.py and has to be added in libcloud/storage/drivers folder.

Then is time to bind the driver with the appropriate provider by adding the following lines in libcloud/storage/providers.py

*Provider.OWNCLOUD:*
*('libcloud.storage.drivers.owncloud',*
*'OwnCloudStorageDriver'),*

Here is the list of affected files.
New files:
**webdav.py** file in libcloud/utils folder
**owncloud.py** file in libcloud/storage/drivers folder
Modified:
libcloud/storage/**providers.py** added entry for owncloud as a provider

The code is available on Github https://github.com/hpcbg/libcloud under GNU GPL.

This is how to create new Libcloud driver in general and it particular to create one for interaction with any server that supports WebDAV. The new driver could be used in a standard manner and users just need to provide the appropriate credentials to get access to the files.

## 4. Testing and experiments

OwnCloud could be installed on a standard LAMP [9] server in order to use its embedded WebDAV functionality.

First test is just to list the files on the server WebDAV directory.

```
from pprint import pprint
# Obtain reference to the provider driver
from libcloud.storage.types import Provider
from libcloud.storage.providers import get_driver
OwnCloudFiles=get_driver(Provider.OWNCLOUD)
# Instantiate the driver with your provider credentials
driver=OwnCloudFiles('example.com', 'username', 'password')
# Start using the driver
basePath='/owncloud/remote.php/webdav'
containers=driver.list_all(basePath)
pprint(containers)
```

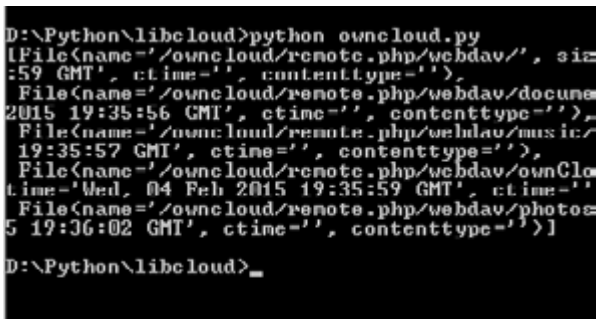



***Fig. 3.*** *Listing the files on the server*

Second test is to create new directory.

```
containers=driver.create_directory(basePath+'/test')
containers=driver.list_all(basePath)
pprint(containers)
```




***Fig. 4.*** *Creating new test directory*

Third test is to check the existence of a file.

```
exists = driver.check_exists(basePath+'/music')
pprint(exists)
exists = driver.check_exists(basePath+'/music2')
pprint(exists)
exists=driver.check_exists(basePath+'/UserManual.pdf')
pprint(exists)
```

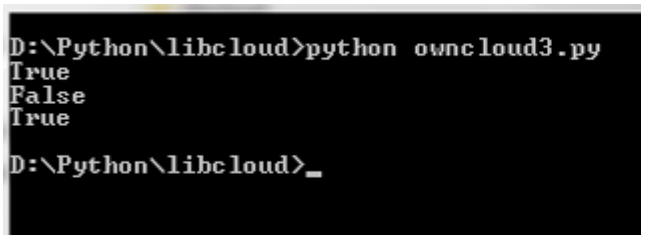



***Fig. 5.*** *Check the existence of a file.*

As is shown on the picture above the program check the existence of a file and return True or False if it exist or not.

Those were just simple examples of some basic features in order to present the idea of using the unified interface to access remote information resources.

The driver is used in standard way witch make it easy to write less code using Python language and Libcloud library to access file from the remote server.

## 5. Conclusion

The paper presents the development of a new driver which extends Libcloud library in order to access files on ownCloud server.

This approach extends the Libcloud functionality allowing unified access to different cloud resources through an easy to use API. Users might manipulate impressive number of providers and methods, but also can access the popular storage platform ownCloud using developed driver.

Experiments proved the correct work of the basic functionality for manipulating files like: create, rename, delete, upload, etc.

The developed driver allows Libcloud to interact with any ownCloud server and with minor modification to any server supporting WebDav protocol. The new driver could be used in a standard manner and users just need to provide the appropriate credentials to get access to the files.

## REFERENCES


1. https://libcloud.apache.org
2. https://owncloud.org/
3. https://libcloud.readthedocs.io/en/latest/supported_providers.html
4. Tsvetanov, S., Doundakova, I., “Cloud Storage Integration Platform”, International Scientific Conference Computer Science’2015, September 8-10, Durres, Albania.
5. Edmonds, A., Metschm, T., Papaspyrou, A., Richardson, A., Toward an Open Cloud Standard, IEEE Internet Computing, Issue No.04 - July-Aug. (2012 vol.16), pp: 15-25,
6. https://owncloud.com/owncloud-architecture-overview/
7. http://www.webdav.org/specs/rfc2518.html
8. https://pip.pypa.io/en/stable/
9. https://doc.owncloud.org/server/8.0/admin_manual/installation/source_installation.html



Author’s contacts
Address:
Sofia 1756, 8 Kliment Ohridski blvd.
E-mail: s_tsvetanov@tu-sofia.bg

© International Scientific Conference on Engineering, Technologies and Systems
TECHSYS 2016, Technical University – Sofia, Plovdiv branch
26 – 28 May 2016, Plovdiv, Bulgaria

# GENERATING 2D GAUSSIAN KERNELS FOR THE PURPOSE OF STUDYING FPGA-BASED LINEAR SPATIAL FILTERS

IVAN KANEV, PETYA PAVLOVA, DIMITRE KROMICHEV, JORDAN GENOFF

***Abstract*** *This paper presents one approach to generating normalized 2D Gaussian kernels. Defined are the conditions for determining the coefficients of the kernels. Selected is an approach through which the kernel coefficients are represented as positive integers. This approach aims at speeding up the time to calculate the linear spatial filters (LSF) and reducing the number of logic elements. An algorithm for generating 2D Gaussian kernels is proposed. The studies are conducted using the software tool "Gaussian Kernel Generator (GKG)". As a result of the studies, the Gaussian kernel coefficients, which are represented as real and integer numbers, are determined on the basis of the preset criteria. The obtained results can be employed in designing and studying LSF through using FPGA platforms.*

***Keywords:*** *linear spatial filters, LSF, weighted average, normalized Gaussian 2D Kernel, VHDL, FPGA*

## 1. Introduction

Filtering of images by employing linear spatial filters (LSF) is one of the basic tools used in image processing. [1]. The development of Field Programmable Gate Arrays (FPGA) and ASIC technologies suggests a new modern approach to the hardware realization of LSF [4]. The filtering of an input image $p(x,y)$ of raster size $M \times N$.

Results in computing new values for the gradations of each pixel - $g(x,y)$ depending on the gradations of the pixels around it. The filtering effect is determined by the mask of weighted coefficients $w(a,b)$ defined within a window of neghbourhood of size $S \times S$, where $S$ is an odd number and $S \geq 3$, and the mask contains finite number of elements [2]. One of the most commom LSF is the weighted average filter which is defined by the following expression [3]:

$$g(x,y) = \frac{\sum_{a=-k}^{k} \sum_{b=-k}^{k} w(a,b) \bullet p(x+a, y+b)}{\sum_{a=-k}^{k} \sum_{b=-k}^{k} w(a,b)}, \quad (1)$$

where

$$k = \frac{S-1}{2}, \; k = \{1, 2, ..\}; \quad (2)$$

$$x = 0, 1, 2, .., M-1; \quad (3)$$

$$y = 0, 1, 2, .., N-1. \quad (4)$$

In (1) $x, y$ are used to denote the global coordinates of pixels in the input image $p(x,y)$, and $a,b$ denote the relative coordinates of the same image within the window of size $S \times S$.

Most often the realization of $w(a,b)$ is based on a normalized Gaussian 2D operator, also designated as Gaussian kernel. [3].

The normalized Gaussian 2D operator is defined by the following expression:

$$w(a,b) = \frac{1}{2\pi\sigma^2} exp\left(-\frac{a^2+b^2}{2\sigma^2}\right). \quad (5).$$

where

$$-k \leq a,b \leq k. \quad (6)$$

Designing LSF by employing VHDL or Verilog demands the generation of Gaussian kernels to be used in the study of components utilized in the realization of FPGA platform based filters. This way, the selection of conditions for generating Gausian kernels

Copyright © 2016 by Technical University of Sofia, Plovdiv branch, Bulgaria ISSN Online: 2535-0048

focuses on the tool set to be used in defining the parameters of components through which the filters will be realized.

To achieve this objective, the following tasks are to be performed:

- to conduct studies focused on the Gaussian kernel generation; the aim is defining basic parameters of the components;
- to define an algorithm for generating test Gaussian kernels;
- to conduct studies utilizing tools for Gaussian kernel generation

**2. Gaussian kernel generation**

The normalized Gaussian 2D operator being used, the Gaussian kernel weighted coefficients are a function of two arguments - $k$ and $\sigma$. Taking into account that $k$ are calculated in advance (2), for a certain $k$ the function (5) depends only on $\sigma$.Let us analyze two specific cases in defining the values of weighted coefficients in (5) within the limits of $a$ and $b$ :

1. Let us assume that

$a,b = k$ (or $a$ and $b$ = - $k$), then

$$w(k,k) = \frac{1}{2\pi\sigma^2} exp - \frac{k^2}{\sigma^2}, \qquad (7)$$

and the function (5) has a minimum.

2. Let us assume that

$a,b = 0$, then

$$w(0,0) = \frac{1}{2\pi\sigma^2} \qquad (8)$$

function (5) has a maximum.

From (6) and (7) a conclusion can be easily arrived that the descrete values of $w(a,b)$ (5) for $\sigma > 0$ are confined within the interval

$$0 < w(a,b) < 1 \qquad (9)$$

and are positive real numbers.

In this study, the Gaussian kernel generation is to be realized under the following conditions:

#1. For the purpose to avoid calculating $w(a,b)$ (5) using components represented by floating point numbers, Gaussian kernel coefficients have to be represented as popsitive integers. This will speed up the computation time and reduce the number of logical elements being used.

#2. Filtering through the use of weighted average filter requires that all the pixels of the input image should take part into the computation of the image being filtered. This condition implies that all the coefficients of the Gaussian kernels are different from zero.

Let us use $w_{int}(k,k)$ to denote the minimum value of the function (5), represented as a positive integer.

Let us assume that the following dependence is valid:

$$w_{int}(k,k) = \lfloor w(k,k).V_{int} \rfloor = C_{min}, \qquad (10)$$

where:

$V_{int}$ ,

is a coefficient which calculates the function (5) down to positive integers;

$C_{min}$,

$C_{min} = \{1,2,..\}$ is a constant defining the concrete value of $w_{int}(k,k)$.

Then for the conditions #1 and #2 to be fulfilled, for a certain $C_{min}$, it is enough to define such a value of $V_{int}$, that is capable of satisfying the equality (9).

This statement can be supported by the following arguments:

Let us use $w_{int}(a,b)$ to denote the Gaussian kernel coefficients calculated down to positive integers. Then

$$w_{int}(a,b) = \lfloor w(a,b).V_{int} \rfloor \geq C_{min}, \qquad (11)$$

By which the conditions #1 and #2 are satisfied due to the fact that all the Gaussian kernel weighted coefficients are positive integers, different from zero.

### 3. Algorithm for test Gaussian kernel generation

VHDL and Verilog require that the filter description should contain the definition of the signal width in bits which allows for its components to be parameterized. Let us use $2^m, 2^{m+1}$ to define the interval of possible solutions, where $m, m+1$ denote the number of binary digits within the interval containing the possible solution.

***Start of the algorithm***

Input parameters: $k$ (2); $C_{min}$ (10).

*Step #1. Defining the initial value of m.*

For a $k$, $m$ can be defined by comparing the number of binary combinations within the interval

$$2^m, 2^{m+1} \tag{12}$$

to the number of the elewments in the Gaussian kernel (5).

Let us have

$$2^m \geq (2k+1)^2, \tag{13}$$

then

$$m = \left\lceil log2(2k+1)^2 \right\rceil. \tag{14}$$

*Step #2. Defdining $V_{int}$ and $V_R$*

$V_{int}$ can be defined on the basis of the upper limit of the interval which can contain the possible solution:

$$V_{int} = 10^{\left\lceil log(2^{m+1}+1) \right\rceil} \tag{15}$$

Let us use $V_R$ to denote the reciprocal value of $V_{int}$ normalized to $V_{int}$

$$V_R = \frac{C_{min}}{V_{int}}. \tag{16}$$

$V_R$ is introduced for trhe purpose of computing the Gaussian kernels within the interval denoted by (13). This approach allows an evaluation of the error resulting from calculating the Gaussian kernel coefficients from real numbers down to integers.

*Step #3. Defining $\sigma_L$ for the lower limit of the interval.*

Let us use $w_L(0,0)$ to denote the maximum value of the Gaussian function for the lower limit of the interval assuming that:

$$w_L(0,0) = 2^{m+1}.V_R. \tag{17}$$

Then from (7) $\sigma_L$ for the lower limit of the interval can be defined:

$$\sigma_L = \frac{1}{\sqrt{2\pi.2^{m+1}.V_R}}. \tag{18}$$

*Step #4. Defining $\sigma_H$ for the upper limit of the interval.*

Let us use $w_H(0,0)$ to denote the maximum value of the Gaussian function for the upper limit of the interval assuming that:

$$w_H(0,0) = 2^m.V_R, \tag{19}$$

Then from (7) $\sigma_L$ for the upper limit of the interval can be defined:

$$\sigma_H = \frac{1}{\sqrt{2\pi.2^m.V_R}} \tag{20}$$

*Step #5. Defining $w(a,b)$* and $w_{int}(a,b)$.

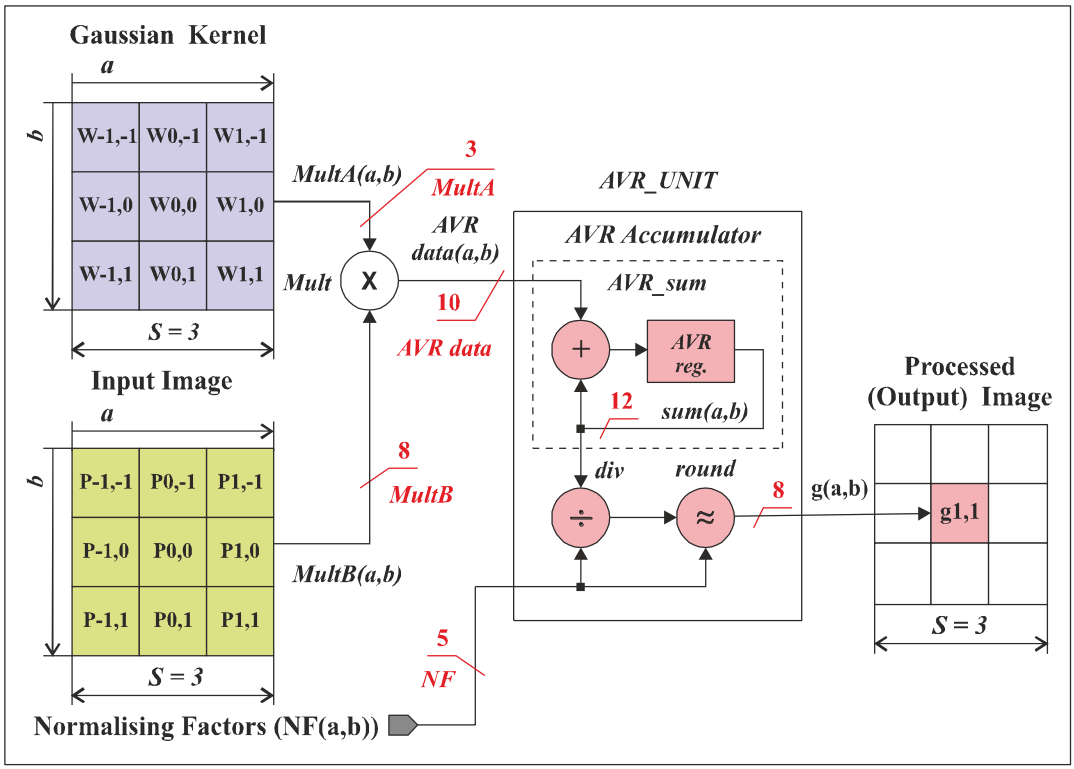



***Fig. 1.*** *Conceptual model of FPGA-based weighted average filter k=1*

Within the interval

$$\sigma_L \le \sigma \le \sigma_H \tag{21}$$

a value of $\sigma$ for which

$$w(k,k) = V_R \tag{22}$$

is sought.

If the equality is not satisfied, the algorithm is repeated from *step #2* for $m = m+1$. Otherwise the calculated value for $\sigma$ is used to compute $w(a,b)$ (5) and the Gaussian kernel integer coefficients:

$$w_{\text{int}}(a,b) = \lfloor w(a,b).C_{\text{int}} \rfloor. \tag{23}$$

**End of algorithm**

## 4. Conceptual model and operations for the hardware realization of weighted average filters

Defining the conceptual module of the components used in the hardware realization of weighted average filters is the first very important step for their complete study and development. The conceptual model (Figure 1) has to suggest solutions to the following problems: the basic operations by which the components will be realized; the subcomponents that will be used in the realization of these operations; definitions of the signals that connect different subcomponents.

The hardware realization of the weighted average filters can be achived through employing the following operations:

Multiplying the elements characterized by the same coordinates in the Gaussian Kernel and Input Image matrices. Generally, this operation is determined by the following dependence:

$$AVRdata(a,b) = w(a,b).p(a,b). \tag{24}$$

Operation (24) can be realized in terms of subcomponent for hardware multiplication *Mult*, embedded in FPGA. If we assume that the coefficients of weights $w(a,b)$ and the cuirrent pixels $p(a,b)$, are stored in memories, then (24) can be presented in the following way:

$$AVRdata(a,b) = MultA(a,b).MultB(a,b). \tag{25}$$

The products $AVRdata(a,b)$ define an input data flow which is used in the component AVR_UNIT computations that are to follow.

1. Summation of products $AVRdata(a,b)$. The operation $sum(a,b)$ in component $AVR\_UNIT$ computes the dividend of the filter (1):

$$sum(a,b) = \sum_{a=-k}^{k} \sum_{b=-k}^{k} AVRdata(a,b). \quad (26)$$

Operation $sum(a,b)$ is realized by subcomponent $AVR\_Accumulator$ which includes adder $AVR\_sum$ and register $AVR\_reg$. The adder receives the current value of $AVRdata(a,b)$ and the current value of $AVR\_reg$ as operands. All the values $AVRdata(a,b)$ having been added up, the output value of $sum(a,b)$ is stored in the register $AVR\_reg$.

2. Normalization of filter pixels $g(a,b)$. This operation is aimed at equalizing the pixel width in the input image and the pixel width in the filtered image. Generally, this operation is determined by the following expression:

$$g(a,b) = div + round, \quad (27)$$

where :

$$div = \frac{sum(a,b)}{NF(a,b)}, \quad (28)$$

is an operation by which the filtered pixels are normalized through employing division;
$NF(a,b)$ is normalization factor, and

$$NF(a,b) = \sum_{a=-k}^{k} \sum_{b=-k}^{k} w(a,b); \quad (29)$$

*round* is a factor used to perform rounding over the result of operation $div$.

## 5. Rules for calculating the width of signals and subcomponents

The integer coefficients of Gaussian kernel having been defined, it is possible for the width of signals: $MultA(a,b)$; $MultB(a,b)$; $AVRdata(a,b)$; $NF$; $sum(a,b)$, and the normalization factor of the output function $NF_{int}(a,b)$ to be calculated (Fig.1). Defining the width of signals is required in the designing of weighted average LSF with VHDL or Verilog.

#1. Let us use $MultA$ to denote the width of saignals $MultA(a,b)$ (25), and $w_{\max}$ to denote the central element value in the weighted coefficients matrix:

$$w_{max} = \lfloor w(0,0).C_{int} \rfloor, \quad (30)$$

then:

$$MultA = \lceil log_2(w_{max} + 1) \rceil. \quad (31)$$

#2. Let us use $MultB$ to denote the width of saignals $MultB(a,b)$ (25), and $p_{\max}$ to denote maximum value of pixels in the input image.

Then:

$$MultB = \lceil log_2(p_{max} + 1) \rceil. \quad (32)$$

For the purposes of this study, it is assumed that the input image pixels are confined to the interval:

$$0 \le p(a,b) \le p_{max}, \quad (33)$$

where $p_{max} = 255$.

#3. Let us use $AVRdata$ to denote the width of signals $AVRdata(a,b)$,

then:

$$AVRdata = \lceil log_2((p_{max} + 1).(w_{max} + 1)) \rceil. \quad (34)$$

#4. Let us use $NF$ to denote the width of signals $NF_{\text{int}}(a,b)$, where:

$$NF_{int}(a,b) = \sum_{a=-k}^{k} \sum_{b=-k}^{k} w_{int}(a,b), \quad (35)$$

is the value of normalization factor of the filtered pixel (29), computed by utilizing the Gaussian kernel integer coefficients.

Then:

$$NF = \lceil log_2(NF_{int}(a,b)) \rceil. \quad (36)$$

#5. Let us use $sum$ to denote the width of saignals $sum(a,b)$ (26).

Then:

$$sum = \lceil log_2(NF_{int}(a,b).(p_{max} + 1)) \rceil. \quad (37)$$

## 6. Results

On the basis of the algorithm for generating test Gausian kernels, a Gaussian kernel generator (GKG) has been proposed.

For certain $k$ and $C_{\min}$, the employing of GKG presents the following results:

- The value of $\sigma$, for which $w(k,k)=V_R$, is computed
- The weighted coefficients of test Gaussian kernels $w(a,b)$, represented by integers, are generated.
- The weighted coefficients of test Gaussian kernels $w_{\text{int}}(a,b)$, calculated down to positive intrgers, are generated. For the graphical representation of $w_{\text{int}}(a,b)$, GKG generates a 3D figure.
- The normalizaqtion factor integer value $NF_{int}(a,b)$ is computed.
- The width of signals *MultA* (32) ; *MultB* (33); *AVRdata* (35); $NF$ (36); $sum$ (38) is calculated. The normalization factor of the filtered pixel $NF_{\text{int}}(a,b)$ is computed.
- A file containing the weighted coefficients of Gaussian kernels $w_{\text{int}}(a,b)$ is generated. This file is used by FSM ROMizer [6] for the purpose of designing of ROM-based FSMs that control components involved in the realization of weightewd average filters.

The following tables and figures present the results, obtained by employing GKG for $k=\{1,2,3\}$ and $C_{\min}=1$:

### 6.1. Test kernels:

$k=1,\ NF_{int}(a,b)=\{9,10,16\}$

Table 1

Test kernel Box Filter- $k=1$; $NF_{int}(a,b)=9$

| a/b | -1 | 0 | 1 |
|---|---|---|---|
| -1 | 1 | 1 | 1 |
| 0 | 1 | 1 | 1 |
| 1 | 1 | 1 | 1 |

Table 2

Test kernel - k = 1, $NF_{int}(a,b)=10$.

| a/b | -1 | 0 | 1 |
|---|---|---|---|
| -1 | 1 | 1 | 1 |
| 0 | 1 | 2 | 1 |
| 1 | 1 | 1 | 1 |

Table 3

Test kernel $k=1$; $NF_{int}(a,b)=16$.

| a/b | -1 | 0 | 1 |
|---|---|---|---|
| -1 | 1 | 2 | 1 |
| 0 | 2 | 4 | 2 |
| 1 | 1 | 2 | 1 |

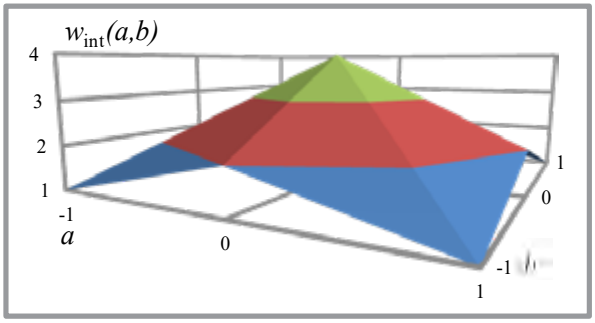



***Fig. 2.*** *Graphical representation of function* $w_{\text{int}}(a,b)$ *: k = 1;*

### 6.2. Generating Gausian kernels with GKG– *k = 2*

Table 4

Conditions for Generating test Gaussian kernels – *k =2*

| $k$ | $C_{\min}$ | $m$ | $V_{\text{int}}$ | $\sigma$ |
|---|---|---|---|---|
| 2 | 1 | 7 | 1000 | 0,86447891 |

Table 5

Test Gaussian kernels for $k=2$ – discrete values of function $w(a,b)$ (5) represented by real numbers

| a/b | -2 | -1 | 0 | 1 | 2 |
|---|---|---|---|---|---|
| -2 | 0,001008740 | 0,007507216 | 0,014657011 | 0,007507216 | 0,001008740 |
| -1 | 0,007507216 | 0,055869961 | 0,109079929 | 0,055869961 | 0,007507216 |
| 0 | 0,014657011 | 0,109079929 | 0,212966514 | 0,109079929 | 0,014657011 |
| 1 | 0,007507216 | 0,055869961 | 0,109079929 | 0,055869961 | 0,007507216 |
| 2 | 0,001008740 | 0,007507216 | 0,014657011 | 0,007507216 | 0,001008740 |

Table 6

Test Gaussian kernels for $k=2$ – discrete values of function $w(a,b)$ (5) represented by integers.

| a/b | -2 | -1 | 0 | 1 | 2 |
|---|---|---|---|---|---|
| -2 | 1 | 8 | 15 | 8 | 1 |
| -1 | 8 | 56 | 109 | 56 | 8 |
| 0 | 15 | 109 | 213 | 109 | 15 |
| 1 | 8 | 56 | 109 | 56 | 8 |
| 2 | 1 | 8 | 15 | 8 | 1 |

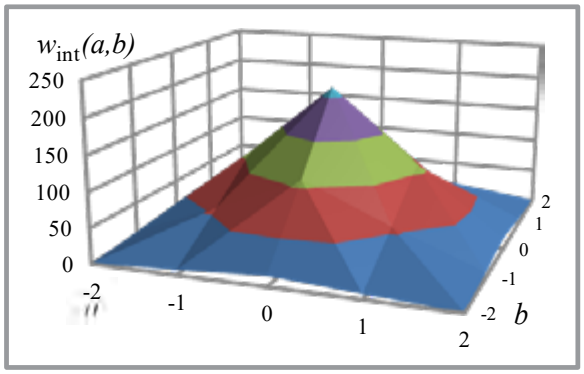



***Fig. 3.*** *Graphical representation of function* $w_{int}(a,b)$ - k = *2*

### 6.3. Generating Gausian kernels with GKG – *k = 3*

Table 7

Conditions for Generating test Gaussian kernels - $k = 3$

| $k$ | $C_{\min}$ | $m$ | $V_{\text{int}}$ | $\sigma$ |
|---|---|---|---|---|
| 3 | 1 | 9 | 10000 | 1,12344622 |

Table 8

Test Gaussian kernels for $k=3$ – discrete values of function $w(a,b)$ represented by real numbers .

| a/b | -3 | -2 | -1 | 0 | -1 | -2 | -3 |
|---|---|---|---|---|---|---|---|
| -3 | 0,000100890 | 0,000731292 | 0,002400131 | 0,003566836 | 0,002400131 | 0,000731292 | 0,000100890 |
| -2 | 0,000731292 | 0,005300675 | 0,017397039 | 0,025853740 | 0,017397039 | 0,005300675 | 0,000731292 |
| -1 | 0,002400131 | 0,017397039 | 0,057097812 | 0,084853060 | 0,057097812 | 0,017397039 | 0,002400131 |
| 0 | 0,003566836 | 0,025853740 | 0,084853060 | 0,126100135 | 0,084853060 | 0,025853740 | 0,003566836 |
| -1 | 0,002400131 | 0,017397039 | 0,057097812 | 0,084853060 | 0,057097812 | 0,017397039 | 0,002400131 |
| -2 | 0,000731292 | 0,005300675 | 0,017397039 | 0,025853740 | 0,017397039 | 0,005300675 | 0,000731292 |
| -3 | 0,000100890 | 0,000731292 | 0,002400131 | 0,003566836 | 0,002400131 | 0,000731292 | 0,000100890 |

Table 9

Test Gaussian kernels for $k = 3$ - discrete values of function $w(a,b)$ represented by integers

| a/b | -3 | -2 | -1 | 0 | -1 | -2 | -3 |
|---|---|---|---|---|---|---|---|
| -3 | 1 | 7 | 24 | 36 | 24 | 7 | 1 |
| -2 | 7 | 53 | 174 | 259 | 174 | 53 | 7 |
| -1 | 24 | 174 | 571 | 849 | 571 | 174 | 24 |
| 0 | 36 | 259 | 849 | 1261 | 849 | 259 | 36 |
| -1 | 24 | 174 | 571 | 849 | 571 | 174 | 24 |
| -2 | 7 | 53 | 174 | 259 | 174 | 53 | 7 |
| -3 | 1 | 7 | 24 | 36 | 24 | 7 | 1 |

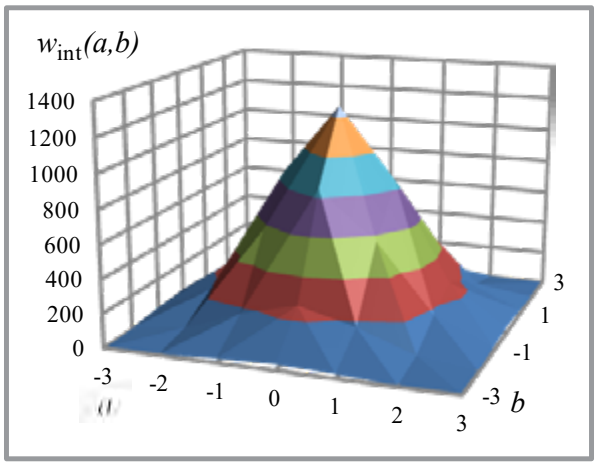



***Fig. 4.*** *Graphical representation of function* $w_{\text{int}}(a,b)$ - k = *3*

Table 10

Signal width and values of the filtered pixel normalization factor

| *k* | 1* | 1 | 2 | 3 |
|---|---|---|---|---|
| *MultA* | 1 | 3 | 8 | 11 |
| *MultB* | 8 | 8 | 8 | 8 |
| *AVRdata* | 8 | 10 | 16 | 19 |
| *Sum* | 12 | 12 | 18 | 22 |
| *NF* | 4 | 5 | 10 | 14 |
| $NF_{\text{int}}(a,b)$ | 9 | 16 | 993 | 9974 |
| *Remark*: Box mask* | | | | |

An example for using the data in Table 10 for $k$=1 are presented in Fig. 1.

## 7. Conclusion

The studies conducted in this paper are focused on generating Gaussian kernels for the purpose of determining basic parameters of the components used in the realization of FPGA-based LSF**.** An original algorithm for generating Gausian kernels is proposed. A conceptual model of FPGA-based LSF is defined. Defined are the signals and components needed for the hardware realization of LSF. A Gaussian kernel generator (GKG) is proposed. GKG is utilized to calculate the width of the signals defined in the conceptual model. The results obtained are employed in the designing and studying of FPGA-based linear spatial filters [6]

## References

[1] Ganguly S. et al., Automatic Analisys of Smoothing Techniques by Simulation model Based Real-Time System for Processing 3D Human Faces, International Journal of Embedded Systems and Applications (IJESA) Vol.4,No.4, 2014

[2] Gonzalez R., Woods R., Digital Image Processing, Prentice Hall, 2008

[3] Hanumantharaju M. C. et al, Design of Novel Algorithm and Architecture for Gaussian Based Color Image Enhancement System for Real Time Applications Advances in Computing, Communications and Informatics (ICACCI) International Conference , 2013

[4] Uwe Meyer-Baese, Digital Signal Processing with Field Programmable Gate Arrays *(FPGA),* 4th Edition, ISBN 978-3642453083 , Springer, 2014

[5] Bailey D. G.,Design for Embedded Image Processing on FPGAs, First Edition. John Wiley & Sons (Asia) Pte Ltd. Published by John Wiley & Sons (Asia) Pte Ltd. ISBN: 978-0-470-82849-6, 2011

[6] Kanev I., An Approach to FPGA- based Design of Weighted Average Linear Spatial Filters, Journal of the Technical University – Sofia Plovdiv branch, Bulgaria "Fundamental Sciences and Applications" Vol. 21, pp 263-268 ISSN1310-8271, 2015.

Department of Computer Systems and Technologies, Technical University - Sofia, Branch Plovdiv 25 Tsanko Dyustabanov Str.
Email: itkanev@yahoo.com
Email: p_pavlova@tu-plovdiv.bg
Email: jgenoff@tu-plovdiv.bg
University of Plovdiv "Paisii Hilendarski", Tzar Assen str. 24
Email: dkromichev@yahoo.com

© International Scientific Conference on Engineering, Technologies and Systems
TECHSYS 2016, Technical University – Sofia, Plovdiv branch
26 – 28 May 2016, Plovdiv, Bulgaria

# LOOK-UP TABLE-BASED MICROPROCESSOR ENERGY MODEL

LUBOMIR BOGDANOV

**Abstract:** *The following paper discusses the creation of an energy model of a single-core, single-threaded, deeply-embedded microprocessor for the needs of an Instruction Set Simulator (ISS) called Powot Simulator. The modeled architecture is ARM Cortex-M4 but the measurement methods used are universal and can be applied to others as well. The main goal of the research is simplicity and therefore a look-up table of the target ISA with energy costs is implemented.*

**Key words:** *energy model, microprocessor, embedded systems, look-up table*

## 1. Introduction

Estimation of the consumed energy at early stages of the development is important in embedded systems with battery supplies and eco-friendly equipment. Developers use various kinds of simulators like gem5, SimplePower, Wattch, SESAME, etc. Some of them allow performance simulations, others – energy, and sometimes we see both. In [1] we proposed an Instruction Set Simulator (ISS) called Powot Simulator for estimating the energy consumption of a microcontroller that executes single-threaded, OS-less C program. The model used there is fairly simple – an energy value is assigned to each instruction's mnemonic. The only parameters that are varied are:

- Microprocessor frequency
- Number of instruction operands.

Those parameters were called model domains. They reflect the set of possible energy consumptions depending on the user-defined system frequency and compiler generated assembler instructions with different number of operands (respectively – different addressing modes).

For a first version of the ISS, the model complexity was enough. The ISS estimated the energy consumption on a function call basis. However, with the release of Powot Simulator version 2 the energy evaluation is statement-based. In other words, the analysis takes place inside each C function. The modeling detail has to be increased with additional information about Dynamic Frequency Scaling (DFS) and Dynamic Voltage Scaling (DVS) APIs that separate code in different frequency and voltage regions (or domains). To make the simulator better, other domains are introduced as well – memory, temperature and instruction type. This leads to rethinking the model concept – the new simulator version requires a new energy model.

## 2. Related work

Energy modeling in embedded systems is done in different levels of abstraction [2] – starting from the highest, ESL, and going down to the lowest transistor-level. In [3] the energy simulation takes place at the highest level. The environment used is called SESAME and the purpose of the research is to speed-up energy simulation. This would allow faster Design Space Exploration (DSE) of the developed system. The technique used is called signature-based power modeling. The application, architecture and mapping are separated. Application events such as process execution and process communication are reflected in the architecture specification with event tables containing timing values. Those tables are expanded to support energy simulation as well. However if the power/energy measurements are done for a specific hardware configuration, the energy model would be valid only for that hardware.

To work around this problem an Abstract Instruction Set (AIS) is used that is later tied to a wide range of microprocessors. In a case study, examples with two microprocessors were given – PowerPC and ARM. Interconnects and dedicated hardware components were not considered at the time of writing of that paper. The microprocessor energy model included information for a dynamic pipeline, read/write accesses to memory, statistics about ALU/register file/cache accesses during application events, leakage power, buses (represented as a set of wires and their respective capacitances), clock and respective buffers (using

Copyright © 2016 by Technical University of Sofia, Plovdiv branch, Bulgaria ISSN Online: 2535-0048

analytical methods). The main memory was not modeled. Due to the bigger set of parameters used, we could say that this is fine-grained, high-level energy model of a microprocessor. The model results yielded 5 – 10% simulation error on average to the simulator Wattch. Wattch is an ISS simulator and is at lower level of abstraction which means – it would take greater time for simulation.

In [4] a pipeline-aware ISS is developed for VLIW processors. Due to the specific type of core the following parameters were taken into account: instruction ordering, pipeline stall probability, instruction cache miss probability, power consumption of different stages of the pipeline. It is an analytical model that makes the link between the instructions and the different functional units of the core. The simulator that uses this model is cycle-accurate and gives average error of 4.8% compared to a gate-level simulator.

In [5] an interesting case of a temperature model of a microprocessor is presented. The model is analytical. It is implemented with a C structure. The structure contains parameters such as object geometry, material properties, boundary conditions, etc. The model is used to measure the different effects of the temperature over time in a microprocessor package. To do this, space and time convolutions of plane-generated temperature and power density are used with the help of FFT to speed up the computations. As a conclusion, the temperature consists of two components – total power dissipation of the chip and power density at certain point. The power dissipation on the other hand depends on leakage currents and user-program activity.

A very good guide to designers of microprocessor models is [6]. All of the parameters that could add up to the energy consumption are explained: analytical power models (that include formulae for sub-threshold and gate leakage), thermal models (steady-state, dynamic and adaptive analysis), leakage-temperature model, reliability models (including the effects of electromigration, thermal cycling, time-dependent dielectric breakdown, stress migration), system frequency models and chip technology variation.

A pipelined microprocessor model is described in [7]. In it the core is separated in two parts – datapath and control path. The datapath is represented with high-level, multi-bit modules and buses which yields fast simulation times. The control path is modeled with behavioral HDL code. According to [7] the pipeline must take into account effects such as stalling, squashing and bypassing.

In [8] an entire modeling and validation environment, called MMV, is proposed. The microprocessor (and even the whole system) is modeled using UML diagrams. On architectural level the processor consists of core (described in RTL), main memory and ISA. The ISA model includes information about each instruction. The fields that describe it are: group (or instruction category that could be data transfer, arithmetic, etc), if-else-block (describes a conditional behavior of the instruction), operands (to hold the data to be processed) and addressing mode type of the operands.

### 3. Energy measurement setup

The energy model proposed in this paper is far less complex than the models described in the previous section. No analytical description of any part of the system is needed. The microprocessor is considered a black box. The energy consumed by each instruction is measured as the average current consumption Idd, multiplied by the time for its execution, multiplied by the voltage Vdd (which is held constant in our case). Idd is measured with a shunt resistor and differential amplifier that will introduce error since there will be a voltage decrease of the microcontroller supply. The time window is measured with the help of a free GPIO pin that is toggled before and after the execution of the instruction. The microprocessor of interest is ARM Cortex-M4 implemented on a Texas Instruments' Tiva TM4C123G deeply-embedded microcontroller. A development board with the needed setup is available from TI and is shown in Fig. 1. The compiler used is arm-none-eabi-gcc.

There are, however, some considerations that are worth noting. First of all, the energy consumed in the period 0 ÷ T is an integral of the power consumption during this period. On the other hand, with this setup, we are measuring the average current Idd. This will introduce some error. True energy measurements are possible with equipment

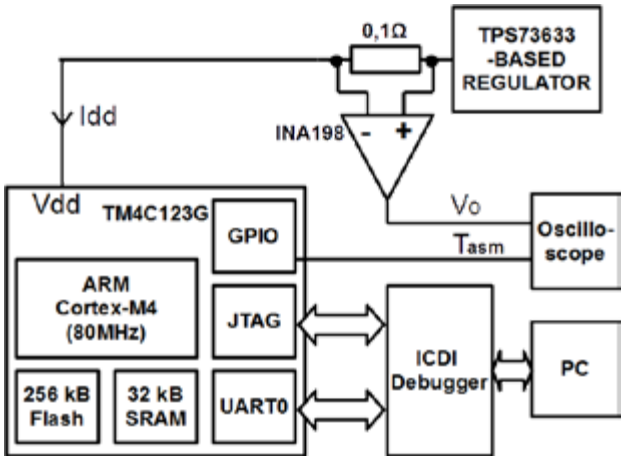



***Fig. 1.*** *Experimental Setup for ISA Energy Measurments*

that is cycle-accurate which requires fast differential amplifier, fast GPIO pin and good oscilloscope. To simplify the setup, no such equipment is used.

The settle time of the output for input change from 10 mV to 100 mV of the sense amplifier INA198 is provided in the datasheet as:

$$T_{SETTLE} = 2\mu s \quad (1)$$

meaning that the microprocessor current consumption should remain unchanged for time greater than 2 µs, otherwise the Idd measurements won't be correct. In our case we have chosen the code:

```
while(1){
        set_gpio(1);
        for(...){
                __asm(…);
        }
        set_gpio(0);
        delay_ms(50);
}
```

for the base energy estimation, where the high-lighted code should be greater than $T_{SETTLE}$. We have chosen this time to be equal to or greater than 100 µs which was done experimentally and yielded the number 1326 loop iterations. Adding the instruction under test with the inline assembly macro __asm( ); will increase this time even more.

In order to reduce the overhead of the for( ) loop, the latter was substituted with code in inline assembler. The code of interest was:

```
__asm("        mov     r10, #1326  \n");
__asm("loop:   subs    r10, r10, #1 \n");
//Instruction under test
__asm("        add     r9, r7, r8      \n");
__asm("        subs    r10, #0         \n");
__asm("        bne     loop            \n");
```

This, however, led to a problem – the time window of the tested instruction is almost always smaller or comparable with the other 4 loop instructions. Even though it is possible to make such measurements, the chosen approach is different. The instruction under test (the high-lighted line in the example above) is duplicated 20 times. This way the time window of interest is much bigger than the time window of the auxiliary code. A graph of the execution time of an ARM Cortex-M4 "add" instruction is shown in Fig. 2.

After setting up all hardware and software, the energy measurements were performed for most of the ARM Cortex-M4 ISA. Pseudo instructions were also measured because the object file of a program may contain some of them.

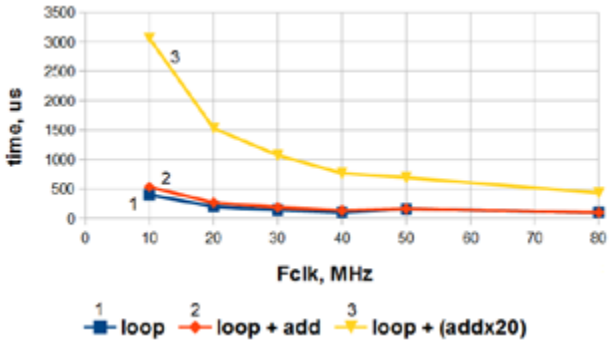



***Fig. 2.*** *Execution time of an empty loop, loop + add instruction, and loop + 20 add instructions*

## 4. Energy model file format

The energy model file format is intended to be simple in order to help improve the proliferation of Powot Simulator in industry. It is a human-readable text file that contains a look-up table for each instruction from the target ISA. Therefore any description language is not necessary – there is no need for conditional and functional description. All the information is available to the simulator.

The text file can contain '#' for line comments, like many other configuration files. The comment span is up to the end of line. Any line that contains '#' is considered a comment, therefore this symbol should not be used for model data. Users can use as much comments as they want – this won't affect the parsing of the file (which is done once at simulator start up).

The Powot Simulator model file is a TAB-separated file that consists of two columns – a tag and a parameter:

[TAG]['\t'][PARAM]

Each parameter can be expanded to multiple parameters by using TAB:

[TAG]['\t'][PARAM1]['\t'][PARAM2]…

There are special tags that describe set of domains and therefore require a respective terminating tag. The syntax is:

[DOMAIN_START]

…..

[DOMAIN_END]

The model file begins with a tag [METRICS] that tells the simulator in what units is the data in the look-up table. If, for example, the current is in mA, time is in ms and voltage is in V, then the base energy will be in µJ.

Following is the [DIVISOR] tag. It tells the simulator to divide the energy units by a specific number. The idea is to make the model more flexible. The energy representation can be changed easily without the need to rewrite the whole model file.

Next is a domain description header that contains informative data to the user. It can be accessed through a special command line parameter passed to the simulator. It is advisable to always include such a header because the first entry of each domain is considered a default entry for the code analysis, if no specific parameters are set from the command line.

Currently the supported domains are the following. We start with address map description of the target microcontroller:

[ADDR][‘\t’][MEM_NAME][‘\t’]
[ADDR_START] [‘\t’][ADDR_STOP]

where the memory name [MEM_NAME] could be FLASH, SRAM, FRAM, EEPROM, etc. Then the start and end address of this region is specified with [ADDR_START] and [ADDR_STOP]. Special function register could also be placed here but peripheral simulation, up to this date, is not possible.

Various other domains are declared with a single tag and one or more parameters following it. The supported domains are:

- [TEMPERATURES]
- [VOLTAGES]
- [FREQUENCIES]
- [OPERANDS]

where the first three are fully supported, while the operands tag can only specify the number of instruction operands and not the addressing mode.

After the declaration of the domains contained in this file, a declaration of DFS and DVS supported APIs is placed. This is very important improvement in the model – it allows us to detect parts of code with dynamic frequency-voltage scaling. The tags are named:

- [DFS_API_START] and [DFS_API_END]
- [DVS_API_START] and [DVS_API_END]

In between the tags there should be a declaration of the change in state that the API forces and the energy cost of the API itself in the following format:

- [FREQUENCY][‘\t’][TIME][‘\t’] [ENERGY]
- [VOLTAGE][‘\t’][TIME][‘\t’] [ENERGY]

where the “time” parameter shows the latency of the API call and is included in case we want to turn the energy simulator into a performance simulator in the future.

Next the main part of the model file is included – the look-up energy table of each instruction. The format is the following:

- [INSTR] – the instruction mnemonic, for example add, nor, movs, etc
- [TYPE] – the type of instruction. Currently this is just a string of type: mem (memory access), datap (data processing), sat (saturation), contr (control and branch), misc (miscellaneous). In the future with the help of this tag we would be able to tell whether the code accesses peripheral and if so, will invoke separate simulation for that peripheral
- Domain data – energy data for each domain.

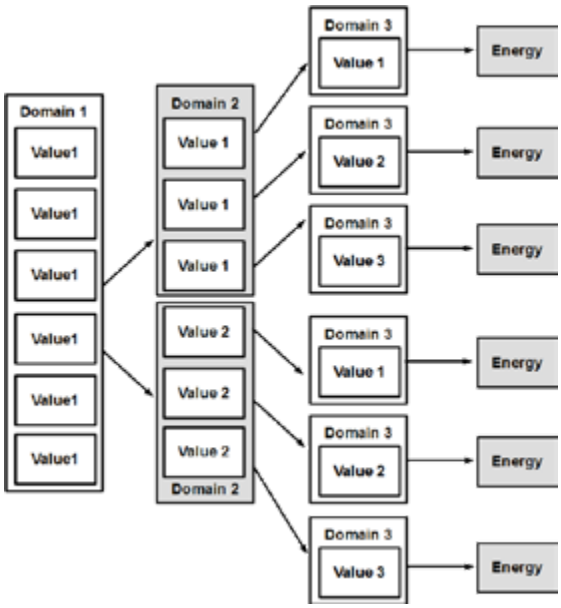



***Fig. 3.*** *Structure of the look-up energy table of an instruction*

The energy data is entered in a tree-like manner as shown in Fig. 3. The more domains we add, the more energy measurements have to be performed. Alternatively the process will be automated in the future with the help of specialized energy profiling equipment.

## 5. Instruction types

Measuring different types of instructions requires augmenting the original software described in the experimental setup section. Some of the instructions simply cannot be put inside a loop. Such examples are branch and table instructions, as well as instructions that change processor state. There are instructions that were not modeled due to their dependence on external (to the microprocessor) events such as WFI and WFE that put the microprocessor in a sleep state.

The registers that are used by the instruction under test are initialized prior to entering the measurement loop. Due to the opulent number of instruction types, the initialization procedure differs.

According to [9] the Cortex-M4 instruction set can be divided in 9 groups: memory access, data processing, multiply and divide, saturating, packing and unpacking, bitfield, branch and control, floating-point and miscellaneous instructions. Not all types are presented in this paper. Only the special cases are shown here.

### 5.1. Branch instructions

Measuring branches like “b” and “bl” was implemented with an additional “nop” instruction at the branch address. This means that from the measured energy we have to subtract the energy of the “nop” (measured separately) and that would give us the base energy cost of the branch instruction itself. The chosen code was:

```
__asm("                bl test_loop1");
__asm("test_loop1:     nop");
__asm("                bl test_loop2");
__asm("test_loop2:     nop");
…
__asm("                bl test_loop20");
__asm("test_loop20:    nop");
```

The same scenario was implemented with the table instruction “tbb”. The only difference is that the initialization must include loading of the first table label and specifying zero offset:

```
__asm("ldr r7, #Table1");
__asm("mov r8, 0x00");
```

### 5.2. Conditional instructions

The Cortex-M4 implements conditional instruction execution in a so-called IT block. This is done for better high-level language support. Modeling instruction blocks with look-up tables is not possible because the number of instructions inside the block, as well as their type, can vary and this would introduce too much combinations. That part of the model is not well defined – only one IT block was measured. The users will have to either provide their own measurements or just copy the available block and change the instructions. The only measured block is:

```
__asm("itte      ne");
__asm("andne  r7,r7,r8");
__asm("addsne r9,r9,#1");
__asm("moveq  r9,r10");
```

### 5.3. Stack-related instructions

An interesting case are the stack-related “push” and “pop” instructions. Since they place and retrieve data from the stack, the latter has to be increased drastically due to the chosen loop repetition number. The number 1326 means that 1326 32-bit values will be pushed on the stack, which is approximately 5 kB. For this type of microcontrollers this value is big but since no other complex code is being executed, that is no problem and the stack is resized to this value.

In order to make multiple loop measurements the “push” and “pop” instructions are used in pairs. The GPIO pin toggling is set to measure only one of the two instructions at a time. Due to memory constraints, only one instance is placed inside the loop.

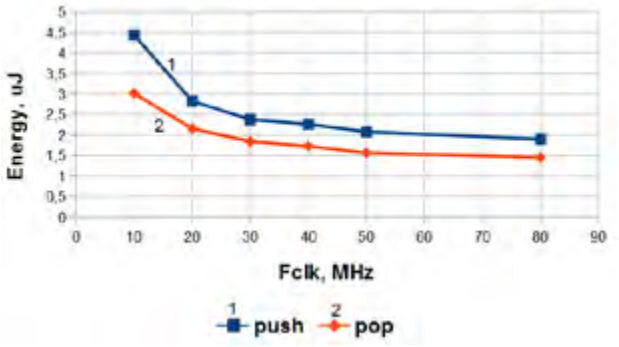



***Fig. 4.*** *Energy consumption of push and pop instructions (executed 1326 times)*

The base energy cost measurements showed that there is a noticeable difference between those two instructions. This effect is shown in Fig. 4.

### 5.4. Supervisor call instruction

The “svc” instruction is used with embedded OS whenever there is need to request privileged operations or system resources. An effect of this instruction is that an interrupt is generated. To cope with it an empty interrupt handler “void SVCIntHandler(void) { }” was added. All of the handler’s prologue and epilogue instructions were extracted from the C code and their base energy values (previously measured) were assigned. This way we can subtract the handler’s energy overhead and find the real energy cost of the “svc” instruction.

## 6. Experimental results

The final energy file of a Tiva TM4C123G microcontroller consists of 116 measured instructions. A total of 6 values were considered for the frequency domain. One value is for temperature and voltage domains. Most of the instructions have one value for the memory domain but some selected ones were measured with two values – FLASH and SRAM. Six DFS APIs were included.

Fig. 5 presents frequency domain data of 25 Cortex-M4 instructions. Most of the instructions exhibit same energy curves but some, like the “isb”, have nonlinearities between 40 and 50 MHz. Those effects are due to the presence of Flash buffers that turn on at system clock of 40 MHz or higher. Such details can aid energy optimizations of code.

## 7. Conclusion

With the help of the ISS energy model simulations with relative error of 5 % is achievable. However absolute error of 20 – 30 % and more was measured due to the simple and basic method used for the measurements. Future research area would be to automate the process and make cycle-accurate

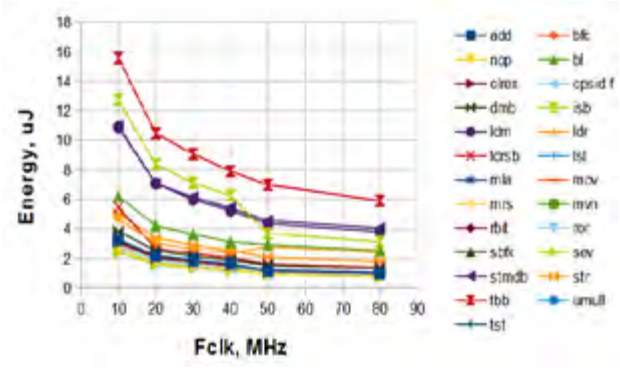



***Fig. 5.*** *Energy consumption of 25 ARM Cortex-M4 instructions (executed 1326 times from flash, on a TM4C123G)*

energy measurements that should increase accuracy and speed-up model development.

## REFERENCES


1. Bogdanov, L. V. and Ivanov, R. M. (2013). Microprocessor Power Modeling and Simulator Implementation, *IX Национална Студентска Научно-техническа Конференция: Сборник с доклади*, pp. 67 – 73, Technical University – Sofia, Sofia.
2. Young-Hwan, P., Pasricha, S., Kurdahi, F., Dutt, N. (2011). A Multi-Granularity Power Modeling Methodology for Embedded Processors, *IEEE Transactions on very large scale integration (VLSI) systems, Vol. 19, pp. 668 – 681, IEEE Xplore, 2011.*
3. Stralen, P. and Pimentel, A. (2010). A High-level Microprocessor Power Modeling Technique Based on Event Signatures. *Journal of Signal Processing Systems*, Volume 60, pp. 239 - 250.
4. Zaccaria, V., and Other(2004). *Power Estimation and Optimization Methodologies for VLIW-based Embedded Systems*, Chapter 4. Kluwer Academic Publishers, Dordrecht.
5. Michaud, P. and Sazeides, Y. (2007). ATMI: Analytical Model of Temperature in Microprocessors. *Proc. MoBS*, pp. 1 – 10.
6. Brooks, D., Dick, R., Joseph, R. Shang, L (2007). *Power, Thermal, and Reliability Modeling in Nanometer-Scale Microprocessors*, Volume 27, Issue 3, pp. 49 – 62, IEEE, Micro, IEEE.
7. Campenhout, D. (1999). *Functional Design Verification for Microprocessors by Error Modeling*, Chapter 4, pp. 83 – 89. Dissertation, The University of Michigan.
8. Sreekumar, V. K., and Other(2007). Model Based Test Generation for Microprocessor Architecture Validation. *VLSI Design*, pp. 465 – 472.
9. *Cortex-M4: Generic User Guide*, ARM Limited, (2010).



Contacts:
Address: Boul. St. Kliment Ohridski №8, Technical University – Sofia, Rectorate, lab. 1362, Sofia, Bulgaria
Phone: +359 2 9653362
E-mail: lbogdanov@tu-sofia.bg

© International Scientific Conference on Engineering, Technologies and Systems
TECHSYS 2016, Technical University – Sofia, Plovdiv branch
26 – 28 May 2016, Plovdiv, Bulgaria

# BIG DATA IN BIOINFORMATICS

DOBRINKA PETROVA

**Abstract:** *The paper is primarily dedicated to big data challenge in bioinformatics. The term 'big data' is defined, considering its characteristics, problems that arise and general solutions for them. The growth of big biological data is discussed in details, providing digits and outlining trends. Big data problems in bioinformatics are discussed, as well as solutions for them, concerning storage, processing, analysis and knowledge extraction.*

**Key words:** *bioinformatics, big data, biological databases, high performance computing*

## 1. Big data

### 1.1. Definitions and characteristics

According to a formal definition, proposed soon in [1], big data represents the information assets characterized by such a high volume, velocity and variety to require specific technology and analytical methods for its transformation into value. This statement is based upon some widely accepted former explanations of big data, described in terms of its characteristics and the challenges it presents. In 2001, Doug Laney defined data growth and management challenges as being three-dimensional, addressing volume, velocity and variety of data [2]. Volume refers to the size of the data. Velocity addresses the speed at which data can be produced, transferred and analyzed. It also refers to the rate of change of data. Variety is determined by the range of data types and sources. This concept, known as the "3 V's" has been updated [3] and extended to 4 or even 5 V's [4], adding Value and Veracity to big data characteristics. Including the last 'V' – veracity, introduces the question of trust and uncertainty of data and the outcome of its analysis.

No matter which definition of the term "big data" is used, it generally refers to data that is too big or too complex to process on a single machine [5]. Living in an age where data is growing orders of magnitude faster than ever before, such "too big" and "too complex" data does not represent just an abstract problem. According to International Data Corporation, the digital universe — the data we create and manipulate, is doubling in size every two years, and by 2020 will reach 44 zettabytes, or 44 trillion Gbytes [6]. The digital universe is diverse — created by the millions of digital cameras, sensors and devices connected over the Internet, as well as the Large Hadron Collider (LHC) at CERN [7] for example. The volume of data produced at the LHC presents a considerable processing challenge – approximately 600 million times per second particles collide within the LHC, which equals to 30 Petabytes (PB) of data for a year.

### 1.2. Problems, initiatives and solutions

The primary goal while collecting, storing, processing and analyzing big data is to extract significant information from it. According to Cox and Ellsworth [8], two distinct problems may arise here based on big data collections or big data objects. Big data collections are aggregates of many data sets that are individually manageable, but as a group are too large to fit on disk. Typically they are multisource, often in disparate formats, distributed among multiple physical sites, and stored in different types of data repositories. Big data objects are single source objects that are too large to be processed by standard algorithms and software on available hardware.

Aiming to make the most of the fast-growing volume of digital data and to solve the problems appeared, USA Administration announced $200 million in a "Big Data Research and Development Initiative" [9] in 2012. In the same year Research Councils UK presented their strategic framework "Investing for Growth: Capital Infrastructure for the 21st Century" [10]. Vital part of it is the innovation "Big Data and Energy Efficient Computing" with a total sum of £189 million to invest. Universities [11], [12], [13] and associations [14] also launched their research initiatives focused on big data problem.

Diverse solutions for storing, processing and analyzing big data are proposed as a result from the initiatives and investigations. Cloud computing as a model for enabling ubiquitous, convenient, on-demand network access to a shared pool of configurable computing resources [15] is a promising solution for both storage and analysis of

Copyright © 2016 by Technical University of Sofia, Plovdiv branch, Bulgaria ISSN Online: 2535-0048

big data. There are proposals – such as Hadoop Distributed File System (HDFS) [16], which concern the storage and management of huge amount of information at the file system level. HDFS is a Java-based file system that provides scalable and reliable data storage of large files across multiple machines. A solution at a higher level for storage and management of unstructured big data are NoSQL (non-relational) databases. They are preferred in some cases, aiming to overcome the limitations of relational databases.

Massive parallelism, both in storage and computation, is searched and investigated to solve the problems, associated with big data. Proposed by Google, MapReduce [17] is a programming model for processing and generating large data sets. Programs written in this functional style are automatically parallelized and executed on a large cluster of commodity machines. HDFS along with MapReduce are modules in Apache Hadoop – open source framework for distributed processing of large data sets across clusters of computers. Apache Spark [18] is another open source cluster computing framework for large-scale data processing, based on DAG (Direct acyclic graph) execution engine.

Along with open source solutions, some of the major vendors as Oracle [19], IBM [20] and Microsoft [21] propose business-oriented solutions for big data storage and manipulation.

Machine learning, as well as cloud computing, takes place in big data analysis. Supervised, unsupervised, and hybrid machine learning approaches are widely used tools for descriptive and predictive analysis of big data [22]. Systems for distributed machine learning are proposed, such as PaDDMAS [23], MLbase [24] and GraphLab [25] – implemented on the cloud.

Maybe one of the best strategies for management of big data is used at CERN. The huge amount of data, produced by the LHC, is reduced with more than 99% in a two-stage process before the real storing and analysis to take place. Then, the data is recorded and processed onto the world's largest computing grid, whose mission is to provide computing resources to store, distribute and analyse the data generated by the LHC.

Next sections of the paper are dedicated to big data challenge in the field of bioinformatics. Section 2.1 provides background on the problems that arise; while in section 2.2 existing solutions are examined and discussed.

## 2. Big data in bioinformatics

### 2.1. Bio data in digits and trends

As a result from many projects and initiatives in bioinformatics, the volume of biological data is increasing extremely fast – it is doubling every 9 months [26]. According to the 2016 Database Issue of Nucleic Acids Research [27] Molecular Biology Database Collection consists of 1685 databases.

European Bioinformatics Institute (EMBL-EBI) [26] maintains the world's most comprehensive range of freely available, up-to-date biological databases – from raw DNA sequences to curated proteins, chemicals, structures, systems, pathways, ontologies, etc. Total disc storage at EMBL-EBI is 75 PB as of December 2015, where the actual total volume of all data resources is about 30%. The largest part of data, accumulated at EMBL-EBI are sequences. European Nucleotide Archive [28], respectively, is the resource at EMBL-EBI with the largest storage capacity, required to store the collection of more than 724 million DNA and RNA sequences. 54,3% of them are assembled sequences from Whole Genome Shotgun projects (WGS) [29] and more than 25% arrive from the partners in the International Nucleotide Sequence Database Collaboration [30] – GenBank [31], the European Molecular Biology Laboratory [32] and DNA DataBank of Japan [33] which exchange data on a daily basis.

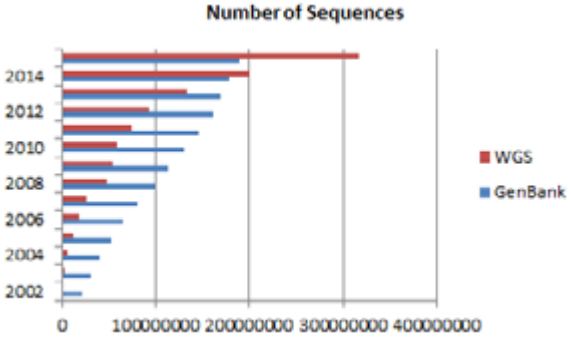



***Fig. 1.*** *Number of sequences in GenBank and WGS*

Fig. 1 and fig. 2 show the rates, at which entries of WGS and GenBank (an annotated collection of all publicly available DNA sequences) are submitted since 2002 till present [34]. The number of sequences (fig. 1) from WGS is increasing with an exponential rate and reaches 317.1 million at the end of 2015, which comprises 58,3% growth per last year.

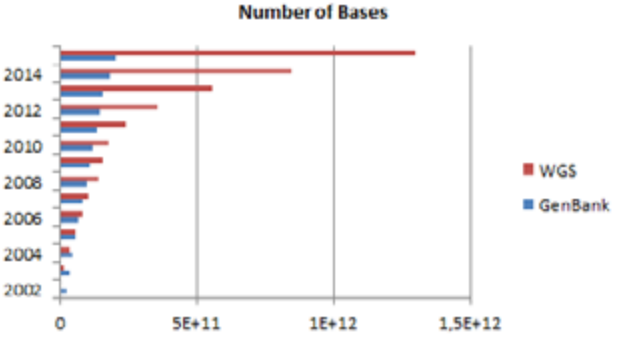



***Fig. 2.*** *Number of bases in GenBank and WGS*

The number of bases (fig. 2) from WGS follows the same dependences – it is increased with more than 53% for 2015. The growth of GenBank for the last year is 10.3% for bases and 5.5% for sequences, corresponding to 204 billion bases and more than 190 million sequences, stored in this data repository. According to [34], from 1982 till present, the number of bases in GenBank has doubled approximately every 18 months. In table 1, along with GenBank, are presented selected databases – representatives in five categories with publicly available statistics. The number and type of stored entries are given for each database, and growth per last year is calculated.

***Table 1.*** *Biological databases statistics*

| ***Database name*** | ***Entries*** | ***Growth*** |
|---|---|---|
| Nucleotide Sequence Database | | |
| GenBank [31] | 204 billion bases | 10.3 % |
| | 190 million sequences | 5.5 % |
| RNA sequence database | | |
| RNAcentral [35] | 9321083 sequences | 14 % |
| Protein sequence databases | | |
| UniProtKB [36] | | |
| • TrEMBL | 59718159 sequences | 10% for last month |
| • Swiss-Prot | 550299 sequences | |
| Protein structure database | | |
| PDB [37] | 115918 structures | 8.8% |
| Microarray data and other Gene Expression databases | | |
| • Gene Expression Omnibus [38] | 1727633 samples | 26.5% |
| • ArrayExpress [39] | 1911539 assays | 18% |

The most significant growth of deposited entries can be seen for UniProtKB/TrEMBL – for the first month of 2016 year it is 10% and the number of protein sequences reaches almost 60 million [36]. The increasing rate of GEO [38] is also noticeable – 26.5% for the last year and more than 1.7 million samples from 65500 series and 15443 platforms. The other microarray database, mentioned in table 1 – ArrayExpress [39] achieves 18% growth with 63530 experiments up to date and 40.34 TB of archived data.

According to [40] the cost of generating data is falling and it enables researches and corresponding projects to produce more data. So, one of the major bottlenecks in life science research today is not generation, but storage of biological big data sets. Solutions are also required for transforming big data stored in heterogeneous and different-in-nature sources into a structured well-interpretable format for further manipulation. Applications are needed that will process in parallel large and often distributed data sets for target data analysis and knowledge extraction.

### 2.2. Solutions for big data problem

General solutions for 'big data' problem are applicable in the field of bioinformatics too. In this section are briefly discussed bioinformatics applications and projects and the approaches, which they use to effectively store, process and analyze big biological data.

#### 2.2.1. Storing big data in bioinformatics

Cloud computing is one of the most popular solutions, which promises to address not only storage, but also acquisition and analysis issues of big biological data. By storing on the cloud large data sets, which previously required hours to locate, download and analyze, they become quickly and easily accessible (with their last updates) to a wide range of devices connected over the Internet and can be seamlessly integrated into cloud-based applications for data analysis. The world's largest set of data on human genetic variation, produced by the international 1000 Genomes Project [41], is publicly available on the Amazon Web Services (AWS) cloud [42] since 2012. AWS provides a centralized repository of many other public biological data, including archives of GenBank, Ensembl project [43], Unigene [44], etc.

Another approach to manage the storing of huge amount of data, growing faster than the storage available is to compress the data. There is a variety of standard data compression algorithms, but they are not efficient enough in compressing biological data. In 2011, the Pistoia Alliance [45], supported by AWS, initiated a competition to award US$15,000 to the developer of the best novel open-source compression algorithm for Next Generation Sequencing (NGS) data. The winner proposed a cluster of algorithms [46] that all delivered high performance in terms of compression ratio,

compress and decompress time. In [47] for large-scale compression of genomic sequences the Burrows–Wheeler transform is applied, in [48] the compression is based on cascading Bloom Filters.

The European Bioinformatics Institute uses CRAM [49] as a compression technique to handle nucleotide data on a very large scale. But, to address the challenge of storing exponentially growing biological data in a storage capacity, growing in linear fashion, at the beginning of 2016, EMBL-EBI defines the task for developing novel compression methods as an important part of institute's work [50].

### 2.2.2. Processing and analysis of big data in bioinformatics

Big biological data are challenge not only for storing, but also for processing and analyzing in order to turn them into real knowledge. Various high-performance computing techniques are applied in dealing with the huge amount of data. Examples include cluster computing ([51], [52]), grid [53] and on-chip supercomputing [54]. Cloud computing, often in conjunction with Hadoop and MapReduce, is also a widely used solution for big data analysis in bioinformatics. There are a variety of software tools in bioinformatics, developed as Software as a service (SaaS), Platform as a Service (PaaS) and Infrastructure as a Service (IaaS).

SaaS is a software model, in which the capability provided to the consumer is to use the provider's applications running on a cloud infrastructure. In this way, SaaS eliminates the need for local installation and facilitates remote access to cloud-based software services. Among the examples of SaaS are: Hadoop implementation of BLAST – CloudBLAST [55], scalable software pipeline for whole genome resequencing analysis – Crossbow [56], cloud computing tool for calculating gene expression in large RNA-seq datasets – Myrna [57] and highly sensitive read mapping with MapReduce – CloudBurst [58].

PaaS provides the capability for users to deploy applications onto the cloud infrastructure, where computer resources scale automatically and dynamically to match application demand. Eoulsan [59] is such a framework (based on Hadoop) for high throughput sequencing analyses. BioPig [60] is also Hadoop-based framework for genomic data analysis. Galaxy Cloud [61] is a cloud-based Galaxy for large scale data analyses. CloudGene [62] is a platform for MapReduce programs on private and public clouds.

IaaS as a model offers a full computer infrastructure – physical or virtual machines, and provisions processing, storage, networks, and other fundamental computing resources. Cloud BioLinux [63] is a publicly accessible virtual machine that enables scientists to quickly provision on-demand infrastructures for high-performance bioinformatics computing. Cloud Virtual Resource (CloVR) [64] is also implemented as a single portable virtual machine. It provides several automated analysis pipelines for microbial genomics, whole genome and metagenome sequence analysis. Bionimbus [65] is a cloud-based infrastructure for managing, analyzing and sharing genomics datasets.

The Embassy Cloud [50], launched in 2013, is an IaaS that enables groups to work in private, secure, virtual-machine-based workspaces hosted within EMBL-EBI's data centres. Virtual machines and analysis pipelines are accessible from anywhere with an Internet connection for external groups that are collaborating with EMBL-EBI teams, but the aim is to expand service to be widely available.

Along with analysis, supported by HPC techniques, Semantic Web technologies and ontologies are applied in order to extract real knowledge from diverse and heterogeneous big biological data. The development of metadata for biological information on the basis of Semantic Web standards is regarded as a promising approach for a semantic-based integration of biological information [66]. Ontologies, on the other hand, organize the information in a hierarchical structure, thus dealing with its heterogeneity and integration [67], and providing suitable representation of biological data for effective quering and analysis.

## 3. Conclusion

As a result from many projects and initiatives, and due to the falling cost of the experiments, biological data have grown in a steady exponential fashion, thus defining the big data challenge in bioinformatics. The huge amounts of biological data – heterogeneous and often distributed, bring up the questions of their storage, processing, analysis and knowledge extraction.

Compression is one of the approaches, used to resolve the important issue of the storage of data on a very large scale. Cloud computing is a popular solution, which addresses not only storage, but also acquisition and analysis issues of distributed big biological data. Other high-performance computing techniques – such as cluster computing, grid and on-chip supercomputing are also applied in dealing with processing and analysis of biological data. Semantic Web technologies and ontologies are used for knowledge extraction, addressing the diversity and heterogeneity of big biological data.

Considering the rapid changes in biological field due to technological advances, which produce more data in diverse formats, faster than before, the problems of storing, processing and analyzing them

are still important and awaiting their diverse solutions.

## REFERENCES


1. De Mauro, A., Greco, M. and Grimaldi, M. (2014). What is Big Data? A Consensual Definition and a Review of Key Research Topics. *AIP Conference Proceedings,* 1644, p. 97-104.
2. Laney, D. (2001). 3D data management: Controlling data volume, velocity and variety. *META Group Research Note*.
3. Beyer, M. A. and Laney, D. (2012). The Importance of 'Big Data': A Definition. *Gartner*.
4. Demchenko, Y., Grosso, P., de Laat, C. and Membrey, P. (2013). Addressing big data issues in scientific data infrastructure. *In: 2013 International Conference on Collaboration Technologies and Systems (CTS)*, San Diego, IEEE, p 48–55.
5. Landset, S., Khoshgoftaar, T. M., Richter, A. N. and Hasanin T. (2015). A survey of open source tools for machine learning with big data in the Hadoop ecosystem. *Journal of Big Data*.
6. Turner, V., Reinsel, D., Gantz, J. F. and Minton, S. (2014). The Digital University of Opportunities: Rich Data and the Increasing Value of the Internet of Things. *IDC White Paper,* http://idcdocserv.com/1678
7. http://home.cern/topics/large-hadron-collider
8. Cox, M. and Ellsworth, D. (1997) Managing big data for scientific visualization. *ACM Siggraph '97 course #4 exploring gigabyte datasets in real-time: algorithms, data management, and time-critical design*.
9. https://www.whitehouse.gov/sites/default/files/microsites/ostp/big_data_press_release_final_2.pdf
10. http://www.rcuk.ac.uk/research/infrastructure/big-data/
11. http://www.bigdata.cam.ac.uk/
12. http://bigdata.csail.mit.edu/
13. http://vcresearch.berkeley.edu/
14. http://bigdata.ieee.org/
15. Mell, P. and Grance, T. (2011). The NIST Definition of Cloud Computing. *National Institute of Standard and Technology, U. S. Department of Commerce.*
16. HDFS - https://hadoop.apache.org/docs/r1.2.1/hdfs_design.html
17. Dean, J., and Ghemawat, S. (2008). MapReduce: simplified data processing on large clusters. *Commun. ACM* 51, 1, 107-113.
18. Apache Spark - http://spark.apache.org/
19. Oracle: Big Data for the Enterprise. (2013).
20. http://www03.ibm.com/software/products/en/category/bigdata
21. http://enterprise.microsoft.com/en-us/
22. Kashyap, H., Ahmed, H.A., Hoque, N., Roy, S., and Bhattacharyya, D.K. (2014). Big Data Analytics in bioinformatics: A Machine Learning Perspective. arXiv:1506.05101v1
23. Rana, O., Walker, D., Li, M., Lynden, S., and Ward, M. (2000). PaDDMAS: parallel and distributed data mining application suite. *Parallel and Distributed Processing Symposium, 2000. IPDPS 2000. Proceedings. 14th International*, Cancun, 2000, 387-392.
24. Kraska, T., Talwalkar, A., Duchi, J. C., Griffith, R., Franklin, M. J., and Jordan, M. I. (2013). Mlbase: A distributed machine-learning system. *CIDR 2013*.
25. Low, Y., Bickson, D., Gonzalez, J., Guestrin, C., Kyrola, A., and Hellerstein, J.M. (2012) Distributed GraphLab: a framework for machine learning and data mining in the cloud. *Proc. VLDB Endow.* 5, 8, 716-727.
26. http://www.ebi.ac.uk
27. Rigden, D. J., Fernandez-Suarez, X. M. and Galperin, M. Y. (2015). The 2016 database issue of Nucleic Acids Research and an updated molecular biology database collection. *Nucleic Acids Research,* 44 (D1): D1-D6.
28. Gibson,R., Alako,B., Amid,C., Cerdeno-Trarraga,A., Cleland,I., Goodgame,N., ten Hoopen,P., Jayathilaka,S., Kay,S., Leinonen,R. et al. (2016). Biocuration of functional annotation at the European Nucleotide Archive. *Nucleic Acids Res*earch, 44.
29. http://www.ncbi.nlm.nih.gov/genbank/wgs
30. INSDC - http://www.insdc.org/
31. Benson, D.A., Cavanaugh, M., Clark, K., Karsch-Mizrachi, I., Lipman, D.J., Ostell, J. and Sayers, E.W. (2013). GenBank. *Nucleic Acids Research*, 41(D1):D36-42.
32. http://www.embl.org/
33. http://www.ddbj.nig.ac.jp/
34. http://www.ncbi.nlm.nih.gov/genbank/statistics
35. http://rnacentral.org/about-us#growth-chart
36. http://www.ebi.ac.uk/uniprot/TrEMBLstats
37. http://www.rcsb.org/pdb
38. Barrett, T., Wilhite, S.E., Ledoux, P., Evangelista, C., Kim, I.F., Tomashevsky, M,, Marshall, K.A., Phillippy, K.H., Sherman, P.M., Holko, M., Yefanov, .A, Lee, H., Zhang, N., Robertson, C.L., Serova, N., Davis, S. and Soboleva A. (2013). NCBI GEO: archive for functional genomics data sets--update. *Nucleic Acids Research,* 41: D991-5.
39. Kolesnikov, N. et al. (2015). ArrayExpress update-simplifying data submissions. *Nucleic Acids Research*, doi:10.1093/nar/gku1057

40. http://www.ebi.ac.uk/about/brochures
41. McVean et al. (2012). An integrated map of genetic variation from 1092 human genomes. *Nature* 491, pp.56-65.
42. http://aws.amazon.com/public-data-sets/
43. Flicek, P., et al. (2014). Ensembl 2014, *Nucleic Acids Research* 42 Database issue: D749-D755.
44. Pontius, J.U., Wagner, L., and Schuler, G.D. (2003). UniGene: a unified view of the transcriptome. In: *The NCBI Handbook*. Bethesda (MD): NCBI.
45. http://www.pistoiaalliance.org/projects/sequence-squeeze/
46. Bonfield, J.K., and Mahoney, M.V. (2013). Compression of FASTQ and SAM Format Sequencing Data. *PLoS ONE* 8(3): e59190.
47. Cox, A.J., Bauer, M.J., Jakobi, T., and Rosone, G. (2012). Large-scale compression of genomic sequence databases with the Burrows-Wheeler transform. *Bioinformatics*, 28(11):1-6.
48. Rozov, R., Shamir, R., and Halperin, E. (2014). Fast lossless compression via cascading Bloom filters. *BMC Bioinformatics* 15(Suppl 9):S7
49. Hsi-Yang Fritz,M., Leinonen,R., Cochrane,G. and Birney,E. (2011) Efficient storage of high throughput DNA sequencing data using reference-based compression. *Genome Research*, 21, 734–740.
50. Cook, C. E., Bergman, M. T., Finn, R. D., Cochrane, G., Birney, E., and Apweiler, R. (2016). The European Bioinformatics Institute in 2016: Data growth and integration. *Nucleic Acids Research* 44 (D1): D20-D26.
51. BioHPC - http://biohpc.org/info_arch.aspx
52. Elixir - http://www.elixir-europe.org/
53. Kertesz, A., Otvos, F., Kacsuk, P. (2013) A Case Study for Biochemical Application Porting in European Grids. *Concurrency and Computation: Practice and Experience*, 26(10):1730–1743.
54. http://www.nvidia.com/object/bio_info_life_sciences.html
55. Matsunaga, A., Tsugawa, M. and Fortes, J, (2008). CloudBLAST: Combining MapReduce and Virtualization on Distributed Resources for Bioinformatics Applications. *In eScience, 2008, IEEE Fourth International Conference on eScience*, pp.222-229.
56. Langmead, B., Schatz, M.C., Lin, J., Pop, M,, Salzberg, S.L. Searching for SNPs with cloud computing.*Genome Biol* 10:R134
57. Langmead, B., Hansen, K., and Leek, J. Cloud-scale RNA-sequencing differential expression analysis with Myrna. *Genome Biology* 11:R83.
58. Michael C. Schatz. (2009). CloudBurst: highly sensitive read mapping with MapReduce. *Bioinformatics,* 25 (11): 1363-1369.
59. Jourdren, L., Bernard, M., Dillies M.A., and Le Crom, S. (2012). Eoulsan: A Cloud Computing-Based Framework Facilitating High Throughput Sequencing Analyses. *Bioinformatics* 28 (11): 1542-1543.
60. Nordberg, H., Bhatia, K., Wang, K., and Wang, Z. (2013). BioPig: a Hadoop-based analytic toolkit for large-scale sequence data. *Bioinformatics* 29(23):3014–3019.
61. Afgan, E., Baker, D., Coraor, N., Goto, H., Paul, I. M., Makova, K. D., Nekrutenko, A., and Taylor, J. (2011). Harnessing cloud-computing for biomedical research with Galaxy Cloud. Nature Biotechnology, 29(11), 972–974.
62. Schonherr, S., Forer, L., Weißensteiner, H., Kronenberg, F., Specht, G., and Kloss-Brandstätter, A. (2012). Cloudgene: a graphical execution platform for MapReduce programs on private and public clouds. *BMC Bioinformatics* 13:200.
63. Krampis, K, Booth, T., Chapman, B., Tiwari, B., Bicak, M., Field, D., and Nelson, K. (2012). Cloud BioLinux: pre-configured and on-demand bioinformatics computing for the genomics community. *BMC Bioinformatics* 13:42.
64. Angiuoli, S.V., Matalka, M., Gussman, A., Galens, K., Vangala, M., Riley, D.R., Arze, C.,White, J.R., White, O., and Fricke, W.F. (2011). CloVR: a virtual machine for automated and portable sequence analysis from the desktop using cloud computing. *BMC Bioinformatics*, 12:356.
65. Heath, A. P., Greenway, M., Powell, R., Spring, J., Suarez, R., Hanley, D., and Grossman, R. L. (2014). Bionimbus: a cloud for managing, analyzing and sharing large genomics datasets. *Journal of the American Medical Informatics Association : JAMIA*, 21(6), 969–975.
66. Cannata, N., Schröder, M., Marangoni, R., and Romano, P. (2008). A Semantic Web for bioinformatics: goals, tools, systems, applications. *BMC Bioinformatics*, 9 (4):S1.
67. Blake, A., Bult, C. (2006). Beyond the data deluge: data integration and bio-ontologies. *Journal of Biomedical Informatics*, 39 (3), 314–320.



Authors' contacts:
Dobrinka Petrova
63 Sankt Peterburg Blvd, Plovdiv, Bulgaria
Phone: 032/ 659 727
E-mail: dpetrova@tu-plovdiv.bg

© International Scientific Conference on Engineering, Technologies and Systems
TECHSYS 2016, Technical University – Sofia, Plovdiv branch
26 – 28 May 2016, Plovdiv, Bulgaria

# DDOS ATTACKS AS THE CYBER-WARFARE TOOLS

TARIK YERLİKAYA, ŞENOL ŞEN

***Abstract:*** *DDOS attacks are one of the most fundamental problems of the present and future of the Internet. As the number of computers connected to the Internet increased, these threats will continue to increase exponentially. Today, the importance of this topic is understood more clearly after the corporates suffered from DDOS attacks with the occurrence of moral and material results. Therefore DDOS attacks are one of the first subject must be taken precautions in the business continuity projects that more focusing and often speaking. DDOS attacks, in other words Distributed Denial of Service attacks, completely target the Accessibility component of Information Security. At first, these type of attack was arisen DOS, it means an attack from a single source towards the target, and then in time it was shaped an attack from multiple sources toward the target for increasing its effect. DDOS threat that is insoluble since the internet first came out is a serious problem and not possible to solve in a long time with the TCP/IP protocol. The main objective of DDOS attacks is to disable the target and two things can be done: sending more traffic than the amount of bandwidth owned by the target system and loading bandwidth or exploiting the target system's resources in a way not available to other users.In this study DDOS attack types using a cyber-warfare in today's world and precautions while these attacks occurred are investigated. Also an example application is carried out for these attacks.*

***Key words:*** *DDOS, cyber warfare, security.*

## 1. Introduction

DOS and DDOS attacks are one of the most fundamental problems of the present and future of the Internet world. As the number of computers connected to the Internet increases, these threats will continue to increase as well. DOS (Denial of Service) is to prevent the system or services from offering service for the users whom it is supposed to serve or to slow them down by overloading. Generally, if the assailers can not get an unauthorized access to a system, they try to harm the system via a DOS attack [1].

Initially emerging only as DOS (Denial of Dervice), that is emerging from an attack to the target from a single source, this attack type, in order to gain more severity, has turned into an assault in which one single source becomes the target of many sources. DDOS (Distributed Denial of Service) attack, intends to provide a basis for Trojan or similar harmful softwares to attack to the target system through multitude of systems. These systems which attack involuntarily are called zombie. This threat which could not have been solved since the first days of Internet, is a problem that will not be able to be solved for a very long time due to already used TCP/IP protocol. In DDOS attacks, the main purpose is to render the system useless. In relation with the attack performed, the effects of DOS might be resulted with one of the items below [2];

- Inaccessibility of the web page
- Late response time of the web page/services to the commands
- Lagging in web performance
- Performance CPU/RAM problems in operation systems
- Failure of warning systems.

## 2. DDOS Types

The main purpose in DOS attacks is to render the target useless by attacking extensively and coordinately to the services of the system. There are two things to do in order to achieve this: to fill the bandwith by sending more traffic than the bandwith amount which the target system has or to consume the sources of the target system in a way in which they would become unusable for other users. Even though the first method comes to the minds of many people when DOS is mentioned, the real dangerous DDOS type is the second type of source consumption. In order to realize the first method, the attacker needs to work in an organized

Copyright © 2016 by Technical University of Sofia, Plovdiv branch, Bulgaria ISSN Online: 2535-0048

way and to have a strong botnet. Yet, in source consumption attacks, which is the second method, when the attacker has 1/10th of the target system's bandwith, he can perform a successful DOS attack. Resulting from the inability of present - day network devices' to provide a healthy protection against DOS, this problem is going to be one of the troubling subjects in the future, too [1].

DDOS according to their executions:

- Synflood
- Udpflood
- Ack flood
- HTTP GET flood
- DNS flood
- Teardrop
- Ping of death [3].

### 3. TCP (Transmission Control Protokol) Information

TCP protocol has been written in order to provide dissipationless data transmission in packet switched computer communication on computer networks. Located on the 4th layer according to OSI layer, TCP is the most frequently used protocol in today's internet world. It has a quite complicated structure compared to the neighbouring protocol UDP, which is situated on the same layer. Protocols such as HTTP, SMTP, POP3, HTTPS all use TCP as infrastructure [1].

TCP connections are run with flags. Flags have the status to identify condition in TCP connections. In other words logging in, data transfer, confirmation mechanism and logging off tasks are realized via the flags (SYN, ACK, FIN, PUSH, RST, URG are the types of flags). On the other hand, UDP does not have such a mechanism.

On UNIX/Windows systems the most detailed information related to connections is acquired through netstat (Network statistics) command. By using Netstat, we can see all the information related with TCO, UDP connections. In TCP, there are quite many cases belonging to the connection. Below are some of the various cases that can be seen through netstat on TCP connections:

CLOSE WAIT, CLOSED, ESTABLISHED, FIN_WAIT_1, FIN_WAIT_2, LAST_ACK, LISTEN, SYN_RECEIVED, SYN_SEND and TIME_WAIT [4].

#### TCP Session Login

If to give example over http which is used for browsing web pages, in order to access a web page and see its contents, primarily, TCP login session process (triple hand shake) has to be realized. After this step is completed, the commands which are needed to display the contents of the web page are sent to the system.

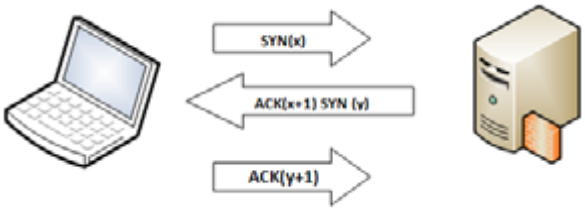



***Fig. 1.*** *TCP session login*

If an already functioning TCP port is open, as a respond to the incoming SYN packet, ACK+SYN packet is sent in return. Of the packets sent in return, ACK is affirmation packet, SYN is demand start packet of the service side. If the port is closed, RST turns back, in order for SYNflood attack to be successful, the port must be open and must be in LISTEN mod [5].

An average TCP header would be 60 Byte, and the SYN+ACK answer sent in return would be around 60 Byte, and in related to its configuration the system receiving SYN packet, until receiving the last ACK packet sends SYN+ACK packet 5-6 times, and this process lasts like 3 minutes.

When SYN packet arrives a TCP port in Listen mod, it changes to SYN_RECEIVED status and until the last ACK packet arrives it holds the data in a data structure. This data structure is named as TCB (Transmission Control Block). Though TCB value varies in relation to the operating system, it consumes a memory of 280 - 1300 byte in the system in general. (TCB: The amount of memory that SYN packet consumes in the system until the triple hand shake is completed) [1].

Operating systems restrict the maximum memory amount TCBs use in order to prevent memory insufficiency resulted from excess demands.

### 4. SynFlood Attacks

Syn Flood attack, simply put, is realized when SYN packets sent to an open port exceed the capacity of the target system. Here, the "capacity" definition is crucial. Technically, this capacity is named as Backlog Queue.

Operating systems use an area from the memory until the moment when triple handshake is completed in return for the each SYN packet, this area is called as TCB (Transmission Control Block) and the total of these areas is called as backlog queue.

In other terms, the amount of how much an operating system can hold as half - open is determined by backlog queue datastructure. This value is present in each operating system and is a low value (around 256) as a pre - determined structure. During SYNFlood attacks, additional

measure can be taken by increasing the value against the attack.

In Synflood attacks, it is all about the filling of backlog queue and the refusal of newly received connections. It means that, the bigger the backlog queue value is, the more half - open (SYN packet) connection can be accepted.

When the backlog queue is full, the operating system can not accept new connection, and in the meantime the ones who try to connect to the server fail. Thus, SYN Flood attack occurs.

Here is an example to show how the systems which do not have the necessary precautions stand weak against Synflood:

A system can be rendered nonfunctional, when 2000 SYN packets are sent to a system whose backlog queue value is 2000. 2000 SYN packets are equal to 2000*60 byte= 120.000 byte; and this is around 1000Kbps~ 1Mbps; a value which is close to the line capacity most of the ADSL users have in our present day.

Nonfunctionality is in parallel to the timeout values of the packets arriving the related port. In case of sending the same amount of packets each 60 seconds, the system could be rendered totally inaccessible.

### 5. SYNflood Tests via Hping

Before Syn Flood attacks are directed to your systems, configuring your own systems against such attacks and testing them would give you an idea about what kind of a situation we might be in the face of a such attack.

Hping is TCP/IP production medium. By using - flood and rand - source features of Hping, SYN Flood attack simulation can be made in great quantities [6].

We applyed the SYNflood attact, from a spoofed IP adress, with hping commands to server running Windows 2012 with ISS IIS (Internet Information Service). When the attack starts, the status of CPU is reaching to 100 %. while the status of CPU is %8 before the attack start.

The following commands are used.

```
# hping3 --rand-source –p 80 -S target_IP --flood
```

By using the similar mediums, according to the owned traffic amount you can produce and send SYN packets in high numbers. If it is considered that SYN packet is around 60 byte, with 50Mb line, 100.000 SYB packet could be produced and sent in a second, and this value would fill the number of connection limit which many firewall have in short time [1].

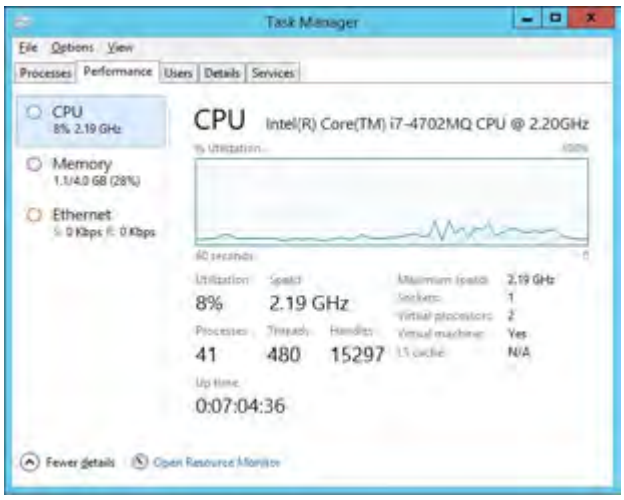



***Fig. 2.*** *CPU status before SYNflood*

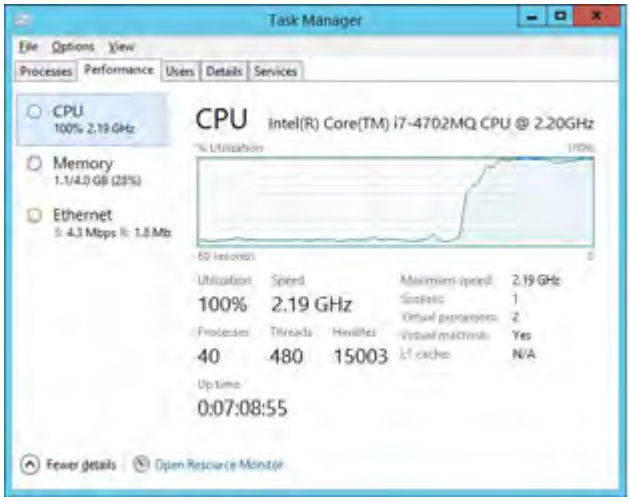



***Fig. 3.*** *CPU status during SYNflood*

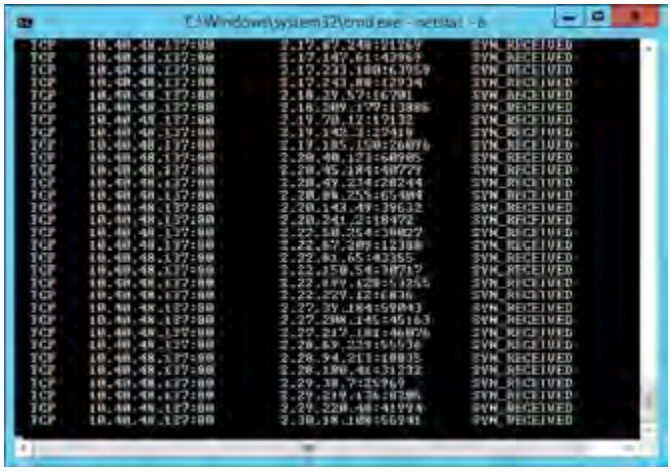


***Fig. 4.*** *Netstat command output*

Synflood attacks can be seen using the appropriate paramaters with netstat command, at the linux and windows operating systems. The SYNflood attack coming from different IP to port

80 on our server, can clearly seen at Figure 4.

During SynFlodd attacks, if the source ip addresses are chosen from the open ip addresses in the internet, the affect would be low. Because, server would respond with SYN+ACK in return against SYN packet which would be sent by spoofing of an open ip address, and this answer would come to the spoofed machine, and since the machine has not sent such a packet before, it would cause the connection to drop quickly by sending RST packet.

## 6. Conclusion

DoS and DDoS usually preferred by beginners, very well organized virtual attackers who controls botnets and zombies, by social groups and states as the preferred political and commercial low density real battle tactics.

In today still there is not 100% solution against DDoS attacks. However, it is possible to gain defense power against attacks with very good network analysis and IP traffic results with data mining study, controlledly change of TCP / IP and other protocol parameters. Controlling network traffic, logging, recording and analysis of the packages are critical for defense. We can analyze well the package anomalies with mostly open source coded softwares like; tcpstat, tcpdstat, tcptra of tcpdump, the ourmo, argus, urlsnorf, snort, cut, grep, etc.. and with solutions that we use for IPS.

In case of performing studies below for related systems, we can get through minimum casualty against DDOS attacks [2].

- Performance improvements need to made in Web server software
- Load-balancing systems (Loadbalancer) and reverseproxy (Nginx) should be used to meet requests more comfortable and that can take into memory when needed.
- With Firewall / IPS, maximum number of requests and packages (that could come from a particular source) limits must be restricted.
- During attacks if specific data field (User-Agent, Referer, etc.) could be identify by examining logs, by writing custom IPS signatures, packages with these data fields can be prevented.
- Web server supported DoS protection modules can be used. (Eg, Apache Mod_dosevasiv), Most of the mid-level DoS attacks could be prevented easily with this well-structured module.
- In attacks like TCP SYN, ACK, GET floods (flood), with saving and analyzing the contents of incoming packages, we can gain time for defense. In this way, attack information such as true / fake IP address source, intensity and geographical location can be determined.

Stress testing to servers, applications and network access devices, could let us know the limits of endurance of the system against possible attacks.

## REFERENCES


1. Önal, H., *DOS / DDOS attacks, Defense Ways and Proposed Solutions*, www.bga.com.tr.
2. Ceylan C., *DDoS attacks on the Internet as a Tool to Stop Cyber War*, http://www.bilgiguvenligi.gov.tr/.
3. Burlu K.,(2013),*The Dark Side of Computing*, 186-199, Nirvana, Ankara
4. *TCP (Transmission Control Protocol)*, https://tr.wikipedia.org/wiki/TCP.
5. *TCP-rfc793*, https://tools.ietf.org/html/rfc793
6. *Hping*, http://www.hping.org/.



Contacts:
TRAKYA UNIVERSITY
22180 EDIRNE
e-mail: tarikyer@trakya.edu.tr
e-mail: senolsen@trakya.edu.tr

© International Scientific Conference on Engineering, Technologies and Systems
TECHSYS 2016, Technical University – Sofia, Plovdiv branch
26 – 28 May 2016, Plovdiv, Bulgaria

# IMPLEMENTATION AND ENCRYPTION TIME MEASUREMENT OF SKIPJACK

YASIN AKMAN

**Abstract:** *Cryptographic algorithms can be used to protect electronic data. Skipjack is a secret key encryption algorithm for the transmission of information, developed by the National Security Agency (NSA) in the USA. In this paper the structure of Skipjack encryption algorithm is examined. Subsequently, encryption time of the Skipjack encryption algorithm is measured.*

**Key words:** *Skipjack, Encryption Time, Implementation,*

## 1. Introductions

In April 1993, the USA administration announced a proposed encryption technology that, according to the announcement "will bring the Federal Government together with industry in a voluntary program to improve the security and privacy of telephone communication while meeting the legitimate needs of law enforcement." Then, in July 1993, a more formal announcement appeared in the Federal Register as a request for comments on a proposed Federal Information Processing Standard. The overall approach was initially referred to as Clipper, whereas the specific encryption algorithm is known as Skipjack[1][2][3].

The Skipjack algorithm was classified. After much debate, Skipjack was declassified and its description was made public on the web site of National Institute of Standards and Technology (NIST) in June 1998[4].

## 2. Skipjack

Skipjack is an iterative block cipher encryption algorithm with 32 rounds that transforms a 64-bit input block into a 64-bit output block. However, its key length is 80 bits.

The Skipjack encryption algorithm has two different types of rounds, called Rule-A and Rule-B. The algorithm consists of first applying 8 Rule-A rounds, then 8 Rule-B rounds, once again 8 Rule-A rounds and finally 8 Rule-B rounds. Block diagrams of Rule-A and Rule-B are shown in Fig.1 and Fig.2 (Counter is round number).

Also, Skipjack has modes of operation; Output Feed-back (OFB) Modes, Cipher Feed-back (CFB) Modes, Codebook and Cipher-Block Chaining (CBC).

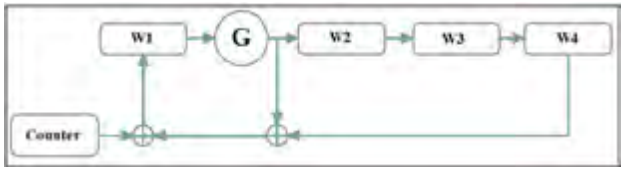



***Fig. 1.*** *Rule-A*

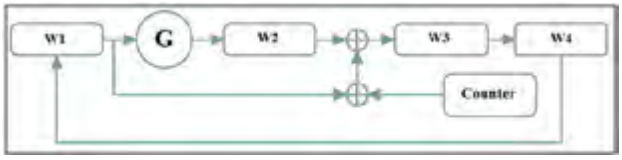



***Fig. 2.*** *Rule-B*

The original definitions of Rule-A and Rule-B are given in Fig.3 and Fig.4 respectively.

$$\begin{aligned} w_1^{k+1} &= G^k(w_1^k) \oplus w_4^k \oplus counter^k \\ w_2^{k+1} &= G^k(w_1^k) \\ w_3^{k+1} &= w_2^k \\ w_4^{k+1} &= w_3^k \end{aligned}$$

***Fig. 3.*** *Rule-A*

$$\begin{aligned} w_1^{k+1} &= w_4^k \\ w_2^{k+1} &= G^k(w_1^k) \\ w_3^{k+1} &= w_1^k \oplus w_2^k \oplus counter^k \\ w_4^{k+1} &= w_3^k \end{aligned}$$

***Fig. 4.*** *Rule-B*

Copyright © 2016 by Technical University of Sofia, Plovdiv branch, Bulgaria ISSN Online: 2535-0048

***Table 1.*** *F-Table*

| | x0 | x1 | x2 | x3 | x4 | x5 | x6 | x7 | x8 | x9 | xA | xB | xC | xD | xE | xF |
|---|---|---|---|---|---|---|---|---|---|---|---|---|---|---|---|---|
| **0x** | a3 | d7 | 09 | 83 | f8 | 48 | f6 | f4 | b3 | 21 | 15 | 78 | 99 | b1 | af | f9 |
| **1x** | e7 | 2d | 4d | 8a | ce | 4c | ca | 2e | 52 | 95 | d9 | 1e | 4e | 38 | 44 | 28 |
| **2x** | 0a | df | 02 | a0 | 17 | f1 | 60 | 68 | 12 | b7 | 7a | c3 | e9 | fa | 3d | 53 |
| **3x** | 96 | 84 | 6b | ba | f2 | 63 | 9a | 19 | 7c | ae | e5 | f5 | f7 | 16 | 6a | a2 |
| **4x** | 39 | b6 | 7b | 0f | c1 | 93 | 81 | 1b | ee | b4 | 1a | ea | d0 | 91 | 2f | b8 |
| **5x** | 55 | b9 | da | 85 | 3f | 41 | bf | e0 | 5a | 58 | 80 | 5f | 66 | 0b | d8 | 90 |
| **6x** | 35 | d5 | e0 | a7 | 33 | 06 | 65 | 69 | 45 | 00 | 94 | 56 | 6d | 98 | 9b | 76 |
| **7x** | 97 | fc | b2 | e2 | b0 | fe | db | 20 | e1 | eb | d6 | e4 | dd | 47 | 4a | 1d |
| **8x** | 42 | ed | 9e | 6e | 49 | 3c | cd | 43 | 27 | d2 | 07 | d4 | de | c7 | 67 | 18 |
| **9x** | 89 | cb | 30 | 1f | 8d | c6 | 8f | aa | c8 | 74 | dc | c9 | 5d | 5c | 31 | a4 |
| **Ax** | 70 | 88 | 61 | 2c | 9f | 0d | 2b | 87 | 50 | 82 | 54 | 64 | 26 | 7d | 03 | 40 |
| **Bx** | 34 | 4b | 1c | 73 | d1 | c4 | fd | 3b | cc | fb | 7f | ab | e6 | 3e | 5b | a5 |
| **Cx** | ad | 04 | 23 | 9c | 14 | 51 | 22 | f0 | 29 | 79 | 71 | 7e | ff | 8c | 0e | e2 |
| **Dx** | 0c | ef | bc | 72 | 75 | 6f | 37 | a1 | ec | d3 | 8e | 62 | 8b | 86 | 10 | e8 |
| **Ex** | 08 | 77 | 11 | be | 92 | 4f | 24 | c5 | 32 | 36 | 9d | cf | f3 | a6 | bb | ac |
| **Fx** | 5e | 6c | a9 | 13 | 57 | 25 | b5 | e3 | bd | a8 | 3a | 01 | 05 | 59 | 2a | 46 |

G is a four-round Feistel permutation whose F function is defined as an 8x8-bit S box, called F-Table, and each round of G is keyed by eight bits of the key[5]. Schematic of G permutation is shown in Fig.5.

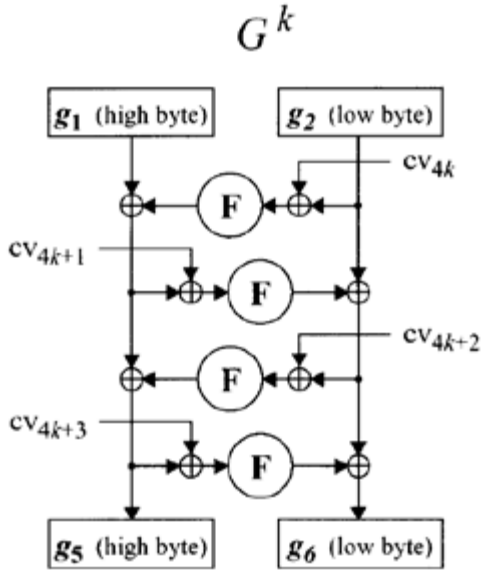



***Fig. 5.*** *G permutation*

The key schedule of Skipjack takes a 10 byte key, and uses four of them at a time to key each G permutation. The first four bytes are used to key the first G permutation, and each additional G permutation is keyed by the next four bytes cyclically, with a cycle of five rounds[5].

F-Table is given Table 1 in hexadecimal notation. The high order 4 bits of the input index the row and the low order 4 bits index the column. For example F(A9)=82.

### 3. Encryption Time Measurement Of Skipjack

The Skipjack encryption algorithm is coded by Eclipse Europa using C programming language and GCC is used as the compiler.

The qualifications of the operating computer on which the time is measured are shown in Table 2.

***Table 2.*** *Qualifications of computer*

| | **Qualifications** |
|---|---|
| **Processor** | Intel Core i7-2670 (6MB Cache, up to 3.1 GHz) |
| **Operating System** | Ubuntu 12.04 LTS |
| **Memory** | 6GB DDR3 SDRAM at 1333Mhz |
| **Hard Drive** | 5400 Rpm SATA (650GB) |

Plaintext input and cryptovariable values are extracted from NIST-SKIPJACK and KEA algorithm specification[4]. The same ciphertext output values are obtained, as shown in Table 3.

***Table 3.*** *input, cipher key, output values*

| | **Values** |
|---|---|
| **Plaintext input** | 33221100ddccbbaa |
| **Cryptovariable** | 00998877665544332211 |
| **Ciphertext Output** | 2587cae27a12d300 |

The time measurement result are shown in Fig.6.

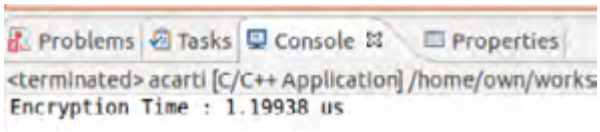



***Fig. 6.*** *Encryption time of Skipjack on computer*

## 4. Conclusion

In this work, I aimed to measure the encryption time of Skipjack encryption algorithm.

Consequently, I measured the encryption time on the computer of which the qualifications are given in Table 2. During the encryption process the best performance of the computer was 1.19938 µs.

## REFERENCES

1. Kyungdeok H., Wonil L., and Other (2002). Saturation Attacks on Reduced Round Skipjack. *Fast Software Encryption*, pp:100-111, Springer
2. Diffie W., Landau S., (1998). Privacy on the Line, MIT Press
3. Schneier B., Banisar D., (1997). The Electronic Privacy Papers, Wiley, New York
4. NIST (1998). "SKIPJACK and KEA algorithm specification." *Technical Report 2.0* http://csrc.nist.gov/groups/ST/toolkit/documents/skipjack/skipjack.pdf
5. Biryukov Alex (2011), Skipjack, *"Encyclopedia of Cryptography and Security"*, pp:1220-1221, Springer, http://link.springer.com/referenceworkentry/10.1007/978-1-4419-5906-5_616

Yasin AKMAN
Computer Programming Department /
Selcuk University / TURKEY
E-mail: yasinakman@selcuk.edu.tr

© International Scientific Conference on Engineering, Technologies and Systems
TECHSYS 2016, Technical University – Sofia, Plovdiv branch
26 – 28 May 2016, Plovdiv, Bulgaria

# COMMUNICATION SYSTEM FOR LAN SERCHING

HRISTO VALCHANOV

**Abstract:** *The resource sharing in local networks allows efficient use of information. The built in Windows 7 search system does not have possibility to search within the local network. This paper presents a communication system for distributed indexing and searching in a local Windows network. The indexing process can be performed both in operational memory and in disk storage. Access to the system's functionality is organized on the basis of user groups. The experimental studies and comparative analysis are presented.*

**Key words:** *Windows Search, Distributed Search, Indexed Search*

## 1. Introduction

One of the advantages of local networks is the sharing of resources between users. The development of computer technologies and systems creates the need for development of systems for searching and information retrieval [1].

The Windows operating system is widely used in the world. One of its service, which is a system component after Windows Vista, is an indexing service (Windows Search Indexer). It speeds up the built-in file search system on the local machine. Despite the improved functionality this system has a number of disadvantages. One major limitation is that it does not support indexing and searching in a local network of Windows-based computers. Partially possibility is provided through the use of obvious configured by the user shared resources. For indexing them, however, they must be previously turned in offline mode, which excludes them from sharing mechanism during this period. Excluding the sharing service from a single user (Network Discovery and File and Printer Sharing) eliminates the ability other users to search for the previously shared resources.

There are a number of free alternative tools of indexing and searching in Windows. Some tools, like grepWin, MasterSeeker, FileSeek and Listary [2], despite their enhanced functionality, are intended solely for desktop search. There are also tools that provide indexing and search in shared drives on a network. Accelerated indexing and search is provided by Locate32 [2]. The disadvantage of the software is the lack of search in the contents of the file. LanHunt [3] is a Java-based application using the database index, which speeds up the search process, but the search is provided only by single words. Other free and flexible applications are LanSearch Pro [3] and EveryThing [4]. Despite their rich functionality, the searching is limited to only the name or file type. A characteristic of search LAN applications is that they are based entirely on the sharing system of Windows. Excluding the sharing service limits their functionality only to a desktop indexing and search.

This paper presents the architecture of the communications subsystem of a distributed environment for indexing and searching in a local Windows network.

## 2. System for indexing and searching

The system for indexing and searching has distributed architecture. It consists of multiple search engines (SE) that are installed as a service on all machines in the local network involved in the process of searching for information. Each SE operates independently of the others and indexes the information on the local machine.

On Figure 1 is shown the structure of a SE.

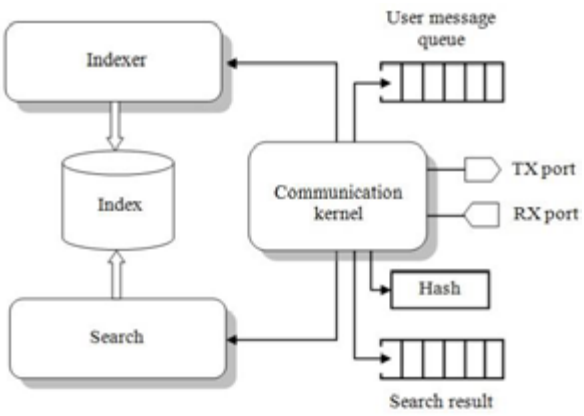



***Fig.1**. Structure of a SE*

Copyright © 2016 by Technical University of Sofia, Plovdiv branch, Bulgaria ISSN Online: 2535-0048

With indexes is accelerated the speed of searching for information in single or in multiple documents. The indexing is based on the inverted index concept [5]. It is a list (dictionary) of found terms (words) and for each word is built a list of file identifiers (postings), which contain this term. For each word is maintained its position and frequency of occurrence in each file. Thus allows searching by phrases and sorting the results.

In order to effectively use of the resources of the machine, the construction of indexes was implemented in two ways: in the RAM memory and on the disc.

When the index is building in RAM, the dictionary is implemented as a modified binary tree. Each node has subnodes for the symbols of the alphabet. The goal of this method is to accelerate the process of indexing.

The index building in a disk memory is effective on large collections. The difference lies in the use of buffer with a fixed size, which stores the posting lists. When the buffer is full, it is stored on the disk and the indexing process continues. After completing the indexing process the dictionary must be sorted. Due to its inability to load in the computer memory, an external sorting is applied. To speed up the search process after completion of the sorting, a map of sorted indexes is created. It contains all the initial letters of the dictionary and their start and end positions in the index file.

The search module processes the received queries, which can be submitted both locally or received over the network from other machines. Upon receipt of a query it is filtered and checked for the presence of logical operators, mask terms or phrases. Then each term of the query is checked for presence in the list with built indexes.

The system allows execution of several types of queries: searching by a word, by a part of a word (searching with a mask), searching by a phrase and complex logical expressions.

## 3. Communication subsystem

The communication subsystem ensures exchange of information between started on separate machines SE. This exchange involves the transmission of search queries to all machines and sending the resulting search results. These actions suggest a high load on the network. In terms of network performance an important issue is the choice of suitable transport protocol. One way to achieve this is to send the search query for processing to all SE using multicast delivery.

The current implementation of the proposed communication system is based on Winsock2 multicast [8]. The nature of the exchanged data (words, phrases, search results in the form of paths to files and files themselves) requires to be delivered reliably. The integrated in Winsock2 multicast protocol for reliable delivery is Pragmatic General Multicast protocol (PGM) [9]. The PGM is a transport layer protocol for reliable multicast for applications that require ordered or disordered, without duplicates delivery of data from multiple sources to multiple recipients. The PGM ensures that a group recipient will receive any data packets or it is able to detect unrecoverable data packet loss.

The communication subsystem (Figure 1) consists of several basic components:

- Communication kernel - the core that provides basic functionality.
- User message queue - a synchronized queue of messages that are intended to send or process.
- Search result – a buffer to store search results.
- Hash – a hash buffer used in the phases of the authentication process.
- RX, TX port – PGM sockets for message receiving and sending through the network.

### 3.1. Users and groups

The used for communication multicast address is fixed and common to all instances of the application. In this form each user could participate in searches. In a real environment, this is insufficient. In order to divide users into subsets and limit searches to within a given subset the mechanism of the groups was introduced. Each user can be member of one or several groups.

### 3.2. Security of the communications

The concept of group allows flexibility in limiting the perimeter of searching, but by itself does not provide protection from reading the data which are transmitted from machines outside the group. For providing such a protection the concept for multicast encryption is used [10]. Unlike classical scheme instead of having one key for the overall multicast group, now is introduced one key for each of group, called a group key. Any user who wants to do a search, is obliged to use appropriate group key to encrypt messages sent.

Maintaining the group keys and information about membership in groups is implemented by a special centralized component - authenticator (Figure 2). It is located in the global system space – it is not a member of any group and accepts all messages in the multicast group but handles only those that are related to its role.

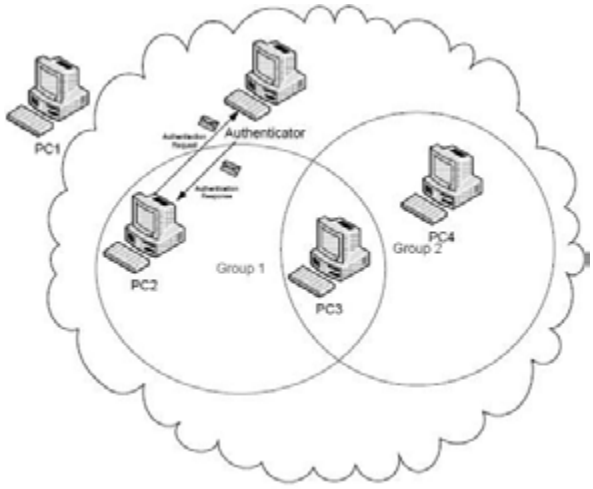



***Fig. 2.*** *Groups and authentication*

### 3.3. The encryption system

The encryption system consists of a library that provides cryptographic functions and a module for generating the key pairs. It is implemented on the basis of Cryptography API Next Generation (CNG) [11]. In the current implementation are used integrated in the program code keys. As a future development is provided keys generation as a random sequence of symbols in the authenticator and verifying them that are unique among the current set of generated group keys.

## 4. Experimental study and results

The goal of the study is to explore the functionality of the proposed system in a real local network and to compare its performance with that of the built-in Windows system for indexing and searching. The experiments were carried out in a local network, including four separate clients and an authenticator machine. The computers are running Windows 7 Enterprise operating system.

Two test groups are performed - indexing and search queries.

- Indexing. Three types of indexing are tested: indexing in RAM, indexing in disc memory and Windows Indexing.
- Processing of search queries. Four query types are tested:
  - Searching by a term – *term*;
  - Searching by a mask – *term**;
  - Searching by a phrase – *term1 term2*;
  - Logical searching in the form *term1 AND term2 OR term2*.

The system load is very high for Microsoft indexing and indexing in RAM. For RAM indexing all indexes are stored in memory, leading to high load, while for Microsoft has no information how the indexes are built.

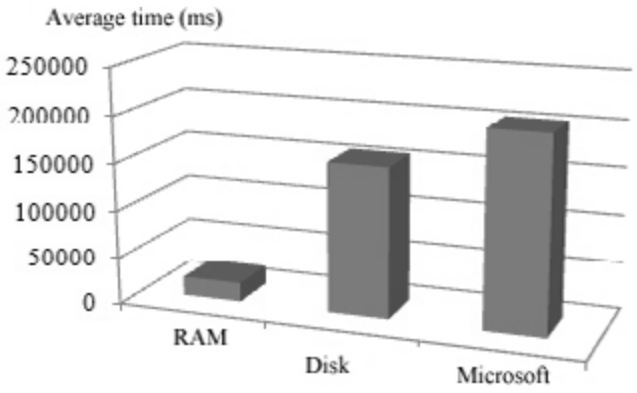



***Fig.3****. Average indexing time*

On Figure 4 are shown the results of the processing of queries. When comparing the averages of the results it is observed that the processing of queries with a mask in the operating memory (a tree) is performed two times faster than in disk memory (by repeatedly loading the vector buffer) and the greatest time has the Microsoft search.

For searching for a single word and for logical expressions again the best results gives the search in RAM. The algorithm with the vector buffer is slower, while Microsoft implementation is two times slower than the disk search. When searching a phrase the search algorithm with tree answers twelve times faster than searching with vector buffer. The Microsoft search again has the highest average time.

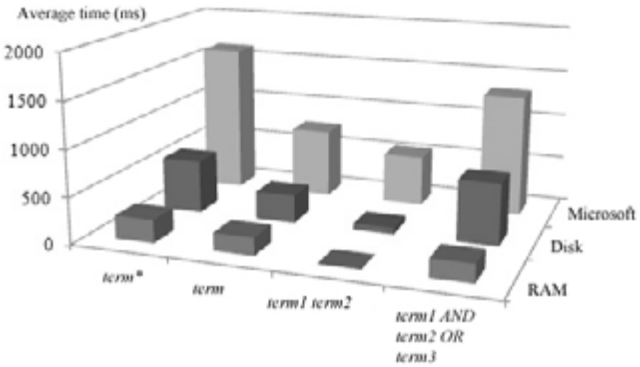



***Fig. 4.*** *Average time for query processing*

## 5. Conclusions

This paper presents a communication subsystem of a distributed environment for indexed search in a local Windows network. The process of indexing can be performed both in operational and in disk memory. An experimental comparisons and evaluations of the two methods for indexing are performed. The proposed search system was compared with the built into the Windows 7 system

for indexing and searching. The results indicate that it has reached a performance boost from the existing implementation in Windows.

Goal of a future work is to develop a hybrid indexing algorithm and automatically to generate keys for authentication.

## REFERENCES


1. Baeza R., Ribeiro B. (2011). *Modern Information Retrieval: The Concepts and Technology behind Search*. Addison-Wesley.
2. Five Alternative Search Tools for Windows. (2015). http://www.thewindowsclub.com/windows-search-alternative-tools.
3. Tools to Search Any Files in LAN. (2016). https://www.raymond.cc/blog/search-find-and-locate-any-files-on-local-area-network-shared-folders/.
4. EveryThing Search Engine. (2016). http://www.voidtools.com/.
5. Buettcher S., C. Charles. (2010). *Information Retrieval: Implementing and Evaluating Search Engines*. The MIT Press.
6. Flex Lexycal Analyzer. (2016). http://flex.sourceforge.net.
7. BulStem. (2016). http://lml.bas.bg/~nakov/bulstem/.
8. Microsoft. Windows Socket 2 Architecture. (2016). https://msdn.microsoft.com/en-us/library/windows/desktop/ms740650%28v=vs.85%29.aspx.
9. PGM Reliable Transport Protocol. (2016). https://tools.ietf.org/html/rfc3208.
10. Shoufan A. (2012). *High Performance Group Key Management*. Akademikerverlag.
11. Cryptography API Next Generation. (2016). https://msdn.microsoft.com/.



Authors' contacts:
Technical University of Varna
Varna, 1, Studentska Str.
E-mail: hristo@tu-varna.bg

© International Scientific Conference on Engineering, Technologies and Systems
TECHSYS 2016, Technical University – Sofia, Plovdiv branch
26 – 28 May 2016, Plovdiv, Bulgaria

# CANNY EDGE DETECTION: A SURVEY

DIMITRE KROMICHEV

**Abstract:** *Edge detection has long acquired the importance of being an indispensible digital image processing tool. Among the numerous edge detectors, the algorithm proposed by John Canny has focused well deserved attention on the basis of its being precise and effective yet computationally complicated and particularly difficult for hardware implementation. The paper presents a survey of the essential views, approaches and concepts focused on Canny edge detection with respect to categorization, comparative evaluation, advantages and disadvantages, modification, and FPGA implementation.*

**Key words**: *Canny edge detection, categorization, comparative evaluation, advantages and disadvantages, modification, FPGA implementation.*

## 1. Introduction

Edge detection is a widely used low level digital image processing technology. John Canny's algorithm [8] has been extensively studied, scrutinized and subjected to various analyses focused on the multilateral aspects of its capabilities and implementation.

This paper is a literature survey of Canny edge detection. The objective is to present the essential views, approaches and concepts regarding the characteristics, functionalities and realization of the Canny algorithm. The task is to exhibit the publications' basic points related to Canny edge detection categorization, comparative evaluation, advantages and disadvantages, modification, and FPGA implementation.

## 2. Categorization of Canny edge detection

1) Gaussian edge detector: characterized by using probability for finding error rate and localization, and by employing noise reduction by smoothing the image through convolving it with the derivative of Gaussian function [27], [33], [34], [36].
2) Gradient based edge detector (equivalent designations: first order edge detector [42]; first order derivative of Gaussian function operator [25]; first order derivative based edge detection [24]): it detects the edges by computing the maximum and minimum in the image first derivative which assumes a local maximum at an edge [30], [37].
3) Laplacian based edge detector (equivalent designation: second derivative-based edge detector [21]). Canny is placed in one classification category with the Laplacian of Gaussian (LoG) operator, the latter being defined as working on zero crossings in the second derivative to detect edges [9].
4) Optimal edge detector. One approach is based strictly on results. Canny is the finest edge detection algorithm as compared to first and second order derivative operators; it is the sole representative in this category [2]. Second approach is based on detecting the point whose second derivative is 0 as a way of detecting edges. Canny is put into one category with Marr-Hildreth operator [32].

## 3. Comparative evaluation of Canny edge detection

In [17], Robert, Sobel, LoG and Canny are compared, and performance is evaluated in terms of signal-to-noise ratio (SNR). Canny results are the best. Canny is more resistent to noise, much more adaptive, provides good localization, detects sharper edges, and demonstrates less false edges. Canny presents good edge detection but poor SNR. In [37], Canny *algorithm* is compared to LoG, Robert. Sobel *techniques.* Canny performance depends heavily on adjustable parameters: σ - the standard deviation of Gaussian function controlling the filter

Copyright © 2016 by Technical University of Sofia, Plovdiv branch, Bulgaria ISSN Online: 2535-0048

size, and the two thresholds. The larger the filter size, the less accurate edge localization. Smaller σ values imply a smaller filter maintaining finer edges. Canny is tailored by adjusting these parameters to adapt to different environments. Canny is computationally more expensive but performs better under almost all scenarios**.** In [34], Canny, LoG, Robert. Sobel are compared. The best results are shown by Canny although LoG shows similar results but with less defined edges. Canny is the best due to the adjustable parameters affecting computation time and effectiveness: 1) Gaussian filter size: smoothing directly affects the detection results for small, sharp lines; 2) two thresholds allow more flexibility than a single threshold - threshold set too high can miss important information while, on the other hand, a threshold set too low will falsely identify irrelevant information (such as noise) as important. In [13], Sobel, Robert, Canny, LoG are compared. Experimental results based on images of size 700x523 show that the edge map of Canny and LoG are almost similar. Canny's performance is optimal. In [24] , comparative qualities of Robert, Sobel, LoG, Canny are evaluated. Under noisy conditions Canny yields the best results due to its accounting for regions in an image. Canny's yielding thin and precise edges are among the positives of its superior performance. As to statistical evaluation of edge maps, Canny reports the highest number of detected edge pixels. The edge pixels frequency analysis defines Canny as the best. The statistical analysis shows it is Canny that is much more suitable for detecting both strong and weak edges in complicated images. In [21], Canny, LoG, Robert. Sobel are experimentally compared. The conclusions: Canny algorithm is the best due to its ability to filter noise, maintain the integrity of valid edge data, and ensure high positioning accuracy. Canny is prioritized to the other algorithms employing differential operation for its good noise resistence and ability to detect true weak edges. In [26], the characteristics of Marr-Hildreth and Canny are analyzed. Although superior to the other Gaussian-based algorithms such as Marr-Hildreth, the Canny marks a point as an edge if its amplitude is larger than that of its neighbors without checking whether the differences between this point and its neighbors are higher than what is expected for random noise. Canny is slightly more sensitive to weak edges, and more susceptible to spurious and unstable boundaries wherever there is an insignificant change in intensity (e.g., on smoothly shaded objects and on blurred boundaries)**.** In [28], the experimental comparison of Roberts, Sobel, Kirsch, Robinson, Marr-Hildreth, LoG, and Canny shows that Marr-Hildreth, LoG and Canny present almost the same edge maps. Yet Canny result is superior to all other results. In [7], the following criteria are applied to evaluate the efficiency of Roberts, Sobel, Kirsch, Robinson, Marr-Hildreth, LoG, Canny 1) False Acceptance Rate (FAR), or False Match Rate - number of times edges are inaccurately positively matched; 2) False Rejection Rate (FRR), or False Non-match Rate - the number of times an edge should be identified positively instead of rejected. Combination of FAR and FRR determines the edge detection that is more useful for a particular type of image. Performance of an edge detection system can be summarized using the measures based on Receiver Operating Characteristics (ROC), or Receiver Operating Characteristics Area (ROCA). The lower the value of ROCA, the better the results of the output image. ROCA can be calculated by mapping FAR and FRR of a particular edge detection of an image - here the lowest value of ROCA is to be defined as the best result. Experiments show Canny results as the best. On that basis, the Canny result is selected as a model image.Then the model image is compared with the results of the other edge detection techniques with respect to FAR, FRR, ROCA, and computation time. The lowest value of ROCA is in Canny. Robinson and Canny have the second longest computation time of all techniques. In [5], compared are the following categories of edge detectors: gradient based (Sobel), Laplacian based (LoG, Canny), and non-derivative based (SUSAN). They are applied to real life images and results are analyzed qualitatively. Canny successfully uses the first derivative of a Gaussian approximation as a reliable tool for achieving better results. Canny can also be sensitive to weak edges, and define fake and unstable boundaries as edges, thus leading to a corrupted edge map. With low Gaussian smoothing Canny presents many wrong edges, and misses many edges if the Gaussian smoothing is increased. Canny is superior to Sobel and LoG but the non-derivative based SUSAN shows the best results even in the presence of noise**.** In [50] Canny, Kirsch, Rothwell, Sobel, Laplace and SUSAN are experimentally compared on the basis of 45,032 UK images containing license plates at 720×288 resolution captured under various illumination conditions. The conclusion: Canny yields highest plate detection ( 98.2%), and longest average processing time per image of 56.4 ms**.** In [29], Marr-Hildreth, Canny, Boolean, Multi-flash, and Euclidian distance/vector angle edge detectors are compared on the basis of the following set of criteria: 1) the probability of a false positive (falsely marking an edge); 2) the probability of a false negative (failing to mark an edge); 3) the error in estimating the edge angle; 4) the mean square

distance of the edge estimate from the true edge; 5) the algorithm's tolerance to distorted edges and features such as corners and junctions. Canny presents the thinnest edges but becomes fairly confused at corners due to the Gaussian smoothing. Also, since the direction of the edge changes instantly, corner pixels look in the wrong directions for their neighbors. Canny correctly marks the edge locations and presents nice outlines of the objects. Boolean detector performs surprisingly similarly to the Canny even though they are drastically different approaches. Canny is still preferred since it provides single pixel thick, continuous edges. In [44], Sobel, LoG, Canny, Rothwell, and Edison detector are compared. The desirable features for a good edge detection evaluation are proposed to be: 1) generality: evaluation measure should be well quantified yet generally applicable; 2) objective evaluation: the evaluation measure should be *objectiv*e to avoid possible inconsistency in subjective evaluation; 3) real image: real (noisy) images should be used for evaluation, as prior studies has revealed that conclusions drawn from synthetic images are usually not applicable to real images; 4) large data set: a convincing edge-detection evaluation should be conducted in a large set of real images and the results should be drawn through statistical analysis. The outstanding feature of Canny is its hysteresis with high threshold helping remove false positives and low threshold helping improve the edge-location accuracy. In general, the Canny edge detector has a tendency to detect long edges, which usually improves its performance in *subjective* evaluations. The *objective* evaluation on the basis of 1030 real images show that the overall performance of the five edge detectors is very similar. The performance difference is marginal and there is no obvious winner. The evaluated algorithms in fact complement each other. In [47], presented is comparison of Canny, Sobel and Roberts being used in an FPGA-based road lane detection system. The experimental results on the basis of a number of road images of size of 640×480 show that the Roberts demonstrated the fastest speed performance – it is 3.14 times faster than Canny. Roberts is also the most accurate in detecting the lines of the actual road lanes. Canny is the most time consuming process, and gives too many lines outside the road lane**.**

## 4. Advantages and disadvantages of Canny edge detection

In [43], Canny advantages are the smoothing (detecting of errors is effective by using probability), the improvement of SNR realized by the non-maximum suppression, and the better detection of edges especially in the presence of noise through hysteresis. The two major disadvantages are the gradient computation to define the angle of suppression, and the complex computations taking a lot of time. In [20], [27], [37], [40], the main advantages of Canny are the using of probability for detecting error rate and localization, improving SNR, better detection, insensitiveness to noise. The disadvantages are expensive computation, false zero crossing, a lot of time, complexity. In [14], Canny has two main drawbacks: 1) it cannot detect simultaneously step edges at two very different scales; 2) junctions cannot be properly detected and are often broken in distinct segments. Also, Canny's edge maps are more dense near sharp edges and almost empty near smooth edges, In [12], it is shown that Canny has the advantages of : removing the noise by smoothimg, enhancing the signal as to SNR, being adaptive and capable of removing streaking. The disadvantages are: difficult for real time realization, takes a lot of time, same thresholds cannot work with all images, complex computations. In [6], the analysis shows that although Canny is more resilient to noise, its performance is still not satisfactory when the noise level is high. There are many cases wherein sharp changes in color intensity do not match the object boundaries - surface marking, recording noise and uneven lighting conditions. In [41], it is pointed out that Canny loses some real edges in the input image. It is likely to compute the suitable thresholds after many trial-and-error calculations but, in real time, the high and low thresholds generally change with respect to the scene and brightness variations. In [22], it is underlined that Canny's approach of classifying a pixel as an edge on the basis of gradient magnitude of a pixel being larger than those of the pixels at both its sides in the direction of maximum intensity change results in some important edges to be missed. In [45], two shortcomings of Canny are analyzed: 1) the thresholds of the algorithm need to be calculated and set manually; 2) the algorithm takes a lot of time to execute and cannot be implemented in hardware in real time. In [23], several practical limitations of Canny are presented: 1) close edges may affect each other especially when the standard deviation of the Gaussian function is too large which results in inaccurate locations and edge losses; 2) hysteresis requires not only trial and error adjustment of two thresholds but also controlling the imaging environment to assure validity of the pre-adjusted thresholds; 3) after detection the edges look like a loop; 4) expensive and complex computation; 5) false zero crossing; 6) time consuming; 7) the corner pixels look in the

wrong directions for their neighbors, leaving open ended edges and missing junctions. In [46], two flaws in Canny are exposed: 1) Canny's derivation of localization criterion is incorrect; 2) much more serious, the Canny criteria yield a too wide optimal edge detector.

## 5. Modified Canny edge detection

In [48], proposed is a modification of the Canny algorithm on the basis of employing curvature models for the purpose of recovering reliable edges that have been missed in the gradient computations. Typically, smoothing the image prior to edge detection leads to a trade-off between detecting weak and noisy edges, and oversmoothing genuine edges. The presented method uses local curvature consistency to adaptively control the smoothing of gradient estimates. The underlying goal is to use the local variation in curvature labels to control the degree of smoothing applied to the gradient field. It is demonstrated that this accomplishes the dual tasks of improving the curvature labeling of the image, and achieving modified gradient estimates that can be used with the Canny edge detector to compute an improved set of edge contours. The approach aims to adjust the gradient estimates in such a fashion as to increase the consistency of the neighbourhood curvature labels. The modification essentially relies on using a curvature consistency process to adjust the gradient direction estimates prior to computing the zero crossings in those directions. This approach yields improvements over the standard Canny edge detector in terms of progressively removing noisy edges whilst retaining the strong edges in an image. This is accomplished by adjusting the gradient estimates to reduce the differences between shape-index labels of neighbouring pixels. The adaptively-smoothed gradient field can be used as the basis for a modified version of the Canny algorithm, by computing the second derivatives in the adjusted gradient directions which are calculated through using curvature consistency. In [15],[39], a bilateral filter is used instead of Gaussian filter to reduce probability of false edges detection. Also, OTSU method is used for adaptive thresholding on the basis of maximizing the separability of the resultant classes of gradient magnitude. OTSU's method computes two thresholds: T1 (high) and T2 (low). Then a point P (i, j) is fixed as a candidate pixel. The gradient G (i, j) of this pixel is calculated. The result is: 1) If G (i, j) > T1 then P (i, j) is definitely an edge point; 2) If G (i, j) < T2 then P (i, j) is not an edge point. In [25], the most appropriate maximum threshold value is calculated by OTSU on the basis of the gradient histogram. This value is used as the exact high threshold in hysteresis. The low threshold is equal to the high threshold value multiplied by 0.5. In [32], proposed is an improved Canny algorithm aimed at avoiding the need of manual setting of the thresholds. For the purpose, the OTSU method is applied to achieve the adaptive calculation of the high and low thresholds by basically splitting all the image pixels into two classes, and compute the best threshold value through the variance maximum value between the two classes. The approach here is to select a threshold which minimizes the within-class variance or maximizes the between-class variance. Such a threshold can both suppress noise and retain the fine edges. In [18], the Gaussian smoothing module is replaced by B-spline function computing the gradient amplitude in 3×3 neighborhoods; using the gradient histogram to compute and select the two thresholds. On an experimental basis, a conclusion is drawn that the proposed modified Cany algorithm significantly improves the accuracy of edge localization and provides a much better level of denoising with different images. In [10], the modification impacts computation of high and low thresholds to enable parallel processing. The input image is divided into m×m overlapping blocks. The adjacent blocks overlap by (L − 1)/2 pixels for a LxL gradient mask. Uniformly quantized gradient magnitude histograms are computed on overlapped blocks. An intermediate classification threshold is calculated based on a set of pixels with gradient magnitudes larger than a defined value. The high threshold is computed on the basis of the histogram. The lower threshold is the 40% of the higher threshold as in the standard Canny. In [19], two basic modifications are proposed: 1) Switching based on four directional Laplacian operators and taking into account the continuity in edge direction to remove the impulsive noise; then Gaussian filter is employed to smooth the other types of noise;
2) Gradient magnitude histogram concavity analysis for automatically selecting the high and low thresholds is introduced**.** In [3], on the basis of the statistical fact that in gradient magnitude histograms after non-maximum suppression edge pixels present a series of smaller peaks wherein each peak defines a class of edges having similar gradient magnitudes, it is proposed that the high threshold of Canny should be selected between the largest peak and the second largest edge peak. A non-uniform quantizer to discretize the gradient magnitude histogram is proposed to to compute the high threshold value. The quantizer needs to have more quantization levels in the region between the largest peak and the second largest peak, and few quantization levels in other parts**.**

## 6. FPGA implementation of Canny edge detection

In [9], Canny is implemented on Xilinx Spartan 3E FPGA. A 128x128 image is stored in Block ROM prior to applying Canny. Here single port Block ROM is used which can support up to 360Kbits. The width and depth of the design is user defined. The pixel values stored in the Block Memory are the inputs to Canny edge detection algorithm. A 3x3 Gaussian filter is used for smoothing based on two FIFO buffers with the depth of one image row pixels. The pixels are used as arrays of values which are stored in a text file. This text file data is used as input during the smoothing process. Size of the filter is selected with respect to the fact that as the size increases filter becomes less sensitive to noise. The architecture of non-maximum euppression block consists of window 3x3 unit, selector unit, arithmetic and comparator unit. Window 3×3 unit holds the 8 pixel values at a time and feeds the input to the selector unit and the middle value is input to the comparator unit. In the selector block angle is calculated at each pixel location simultaneously after the calculation of gradient of an image. Hysteresis thresholding relies on a moving window, two comparators, FIFO buffer and OR gates. In [1], [4], [35], a distributed Canny is implemented on Xilinx Virtex-5 FPGA. It is characterized by significantly reduced memory requirements, higher speed, and increased throughput with no loss in edge detection performance. Performing the Canny algorithm at the block level would speed up the edge detection but it would also result in lost of significant edges in high detailed regions and surplus edges in texture regions. Images consist of a mix of smooth region, texture region and high detailed regions and such a mix of regions cannot be available locally in every block of the entire image. In the distributed Canny algorithm there is no dependency between the various blocks, so the image can be divided into blocks and each block can be processed in parallel. The input image is divided into mxm overlapping blocks. The adjacent blocks overlap by (L – 1)/2 pixels for a gradient mask LxL. For each block, only edges in the central n× n (where n = m + L – 1) non-overlapping region are included in the final edge map. The resultant block-based algorithm has significantly faster In addition to that, quantitative conformance evaluations and subjective tests show that the edge detection performance of the proposed algorithm is better than the standard frame-based Canny, especially for noisy images. A low-complexity 8-step non-uniform gradient magnitude histogram is used to compute block-based hysteresis thresholds. The computational cost of the proposed algorithm is very low compared to the standard Canny edge detection. Simulation results show a 512x512 image is processed in 0.287 ms at a clock rate of 100 MHz. In [49], a novel distributed Canny is implemented on Xilinx Virtex-5 FPGA. It computes edges of multiple blocks at the same time. An adaptive technique calculates the high and low thresholds of the entire image while only processing the pixels of an individual block. The advantages are: higher speed, better edge detection performance, and pipelining of computations. The proposed algorithm is scalable and has very high detection performance. The implementation results show 64% slice utilization and 87% BRAM memory utilization. The proposed FPGA implementation takes only 0.721ms (including the SRAM read/write time and the computation time) to detect edges of 512x512 images at clock rate of 100MHz. In [16], a novel Xilinx Spartan-6 FPGA implementation of Canny takes advantage of 4-pixel parallel computation. It is a pipelined architecture that uses on-chip BRAM memories to cache data between the different stages. The computation time achieved is 3.09 ms for 1280x960 images. For the pixel input a specialized cache is used. Five cache memory elements are employed, each one storing the data of one image line. The on-chip BRAMs are utilized for fast computations. Double thresholding is executed by a double comparator with the data being stored in a specialized cache for the hysteresis thresholding with a size of 1 x image width x 2 bits. The comparison is achievable as long as a second pass is executed with the pixels read in the opposite direction. The comparison is also executed for 4 pixels in parallel. The computed data from pass # 1 of hysteresis is still 2 bits for each pixel and it is stored in an external onboard memory. In [11], Canny architecture is implemented on Xilinx Virtex 5 FPGA. Gaussian filter being separable, the implementation of the 2-D convolution is achieved using row and column 1- D convolutions. For accessing all the pixels in the neighborhood for non-muximum suppression two FIFO bufferes are employed. For the two thresholds an 8-step non-uniform quantizer is employed to obtain the discrete histogram for each processed block. The block-based hysteresis thresholds (high threshold ThH and low threshold ThL) are computed. In [38], the implementation is on Xilinx Vertex-4 FPGA. Canny is implemented at block level without any loss in edge detection performance. The modified Canny adaptively computes the edge detection thresholds based on the block type and the local distribution of the gradients in the image block. The input image is divided into m*x*m overlapping blocks which are processed independent of each other. For an LxL

gradient mask, the mxm overlapping blocks are obtained by first dividing the input image into nxn non-overlapping blocks and then extending each block by (L + 1)/2 pixels along the left, right, top, and bottom boundaries, respectively. Steps 1 to 3 and Step 5 of the distributed Canny are the same as in the standard Canny except that these are now applied at the block level. Step 4, which is the hysteresis high and low thresholds calculation, is modified to enable parallel block-level processing without degrading the edge detection performance. 512x512 image is processed in 0.28ms at a clock rate of 100 MHz.

## 7. Conclusion

The two basic techniques taken into account in the categorization of Canny are Gaussian filtering and differentiation. Canny is experimentally concluded to be the best algorithm when compared to Robert, Sobel, and LoG with respect to noise resistence, adaptivity, localization, sharper edge detection, false edges, SNR, impact of adjustable parameters on overall performance and effectiveness, quality of edges, computatrional complexity, computation time. On experimental basis, it is shown that Marr-Hildreth, LoG and Canny present almost the same edge maps, yet generally Canny is prioritized. It is pointed out that the non-derivative based SUSAN's results are better than Canny's even in the presence of noise. Boolean detector performs surprisingly similarly to Canny even though they are very different approaches. Canny is still preferred for its single pixel thick, continuous edges. Contrary to *subjective* evaluations, the *objective* evaluation of Sobel, LoG, Canny, Rothwell, and Edison detector show that the overall performance of the five edge detectors is very similar. Canny's main advantages are: smoothing; SNR improvement; better detection; noise resistence. The disadvantages are: expensive computations; false zero crossing; a lot of time; complexity; lack of capability to properly detect junctions; difficulties with real time realization and hardware implementation. Canny is modified by replacing Gaussian filtering with: curvature consistency based adaptive smoothing technique; bilateral filtering; B-spline function; median filter based on four directional Laplacian operators followed by Gaussian filter. Another set of modifications focuses on computing the two thresholds by employing: OTSU method; gradient magnitude histogram concavity analysis; non-uniform quantizer to discretize the gradient magnitude histogram. The vast majority of FPGA implementations are on Xilinx FPGAs. Clock rates do not exceed 100 MHz. Main focus is on the distributed architecture aimed at reduced memory, higher speed, and increased throughput as well as novel architectures utilizing 4-pixel parallel calculations and on-chip BRAM memories to cache data between the different pipelined stages.

## REFERENCES


1. Aasiya anjum and Sanjay asutkar (2015). FPGA Implementation of Efficient Edge Detection Using Canny Algorithm, *International Journal on Recent and Innovation Trends in Computing and Communication*, Vol. 3 (2), pp. 20-22
2. Aniket A. Ingle and Vrushali G. Raut (2014). Hardware Software Cosimulation of Edge Detection for Image Processing System Using Delay Block in XSG, *International Journal of Research in Engineering and Technology*, Vol. 3 (5), pp. 549 - 553
3. Anupsingh Ramprakashsingh Rajput and Samina Jafar (2013). Improved Distributed Canny Edge Detector in VHDL, *International Journal of Electrical, Electronics & Communication Engineering*, Vol. 3 (6), pp. 291-295
4. Aravindh G. and Manikandababu C. S. (2015), Algorithm and Implementation of Distributed Canny Edge Detector on FPGA, *ARPN Journal of Engineering and Applied Sciences*, Vol. 10 (7), pp. 3208-3216
5. Ayaz Akram and Asad Ismail (2013). Comparison of Edge Detectors, *International Journal of Computer Science and Information Technology Research* (IJCSITR), Vol. 1 (1), pp. (16-25)
6. Bijay Neupane, Zeyar Aung and Wei Lee Woon (2012). A New Image Edge Detection Method using Quality-based Clustering, *Proceedings of the IASTED International Conference Visualization, Imaging and Image Processing*, pp. 20-26
7. Bhabhor C. H. and Upadhyay (2013). Performance Analysis of Various Edge Detection Techniques for Image Segmentation, *International Conference on Research & Development in Engineering, Technology & Sciences,* Vol. 2 (1), pp. 400 – 405
8. Canny J. (1986). A Computational Approach to Edge Detection‖, *IEEE Transaction on Pattern Analysis and Machine intelligence*, No. 6, pp. 679-698
9. Chaithra N. M. and Ramana Reddy K. V. (2013). Implementation of Canny Edge Detection Algorithm on FPGA and displaying Image through VGA Interface*, International Journal of Engineering and Advanced*

*Technology (IJEAT,* Volume 2 (6), pp. 243-247
10. Chandrashekar N.S. and Nataraj K.R. (2013). Design and Implementation of a Modified Canny Edge Detector Based on FPGA, *International Journal of Advanced Electrical and Electronics Engineering*, (IJAEEE), Vol. 2 (1), pp. 16-21
11. Chandrashekar N.S. and Nataraj K.R. (2013). NMS and Thresholding Architecture used in FPGA based Canny Edge Detector for Area Optimization, *Proceeding. of International Conference on Control, Communication and Power Engineering*, pp. 80-84
12. Diya Chudasama, Tanvi Patel, Shubham Joshi and Ghanshyam I. Prajapati (2014). Survey on Various Edge Detection Techniques on Noisy Images, *International Journal of Engineering Research & Technology*, Vol. 3 (10), pp. 705-709
13. Fari Muhammad Abubakar (2012) Study of Image Segmentation by Using Edge Detection Techniques, *International Journal of Engineering Research & Technology* (IJERT) Vol. 1 (9), pp. 1-8
14. Felice Andrea Pellegrino, Walter Vanzella, and Vincent Torre (2004), Edge Detection Revisited, IEEE *Transactions on Systems, Man, and Cybernetics—Part B: Cybernetics*, Vol. 34, (3), pp.1500-1518
15. Gao Jie and Liu Ning (2012). An improved adaptive threshold canny edge detection algorithm, *IEEE Transactions, International Conference on Computer Science and Electronics Engineering* (ICCSEE),, Vol. 1, pp.164-168
16. Gentsos C., Sotiropoulou C., Nikolaidis S., and Vassiliadis N. (2010), Real-time canny edge detection parallel implementation for FPGAs, *17th IEEE International Conference on Electronics, Circuits, and Systems* (ICECS), pp. 499 – 502
17. Gurjeet Singh and Er. Harjinder singh (2014). Study and Comparison of Various Techniques of Image Edge Detection, *International Journal of Engineering Research and Applications* Vol. 4, pp.908-912
18. Jun Li and Sheng Ding (2011). A Research on Improved Canny Edge Detection Algorithm, *Proceedings of International Conference on Applied Informatics and Communication*, Part V, pp. 102-108
19. Jun Zeng and Dehua Li (2011). An Adaptiv Canny Edge Detector using Histogram Concavity Analysis, *International Journal of Digital Content Technology and its Applications*. Volume 5 (6), pp. 172-181
20. Indrajeet Kumar, Jyoti Rawat, Bhadauria H.S. (2014). A Conventional Study of Edge Detection Technique in Digital Image Processing, *International Journal of Computer Science and Mobile Computing*, Vol.3 (4), pp. 328-334
21. Li Bin and Mehdi Samiei yeganeh (2012), Comparison for Image Edge Detection Algorithms, *IOSR Journal of Computer Engineering* (IOSRJCE), Vol. 2 (6), pp. 1-4
22. Lijun Ding and Ardeshir Goshtasby (2001), On the Canny edge detector, *Pattern Recognition*, Volume 34 (3), March 2001, pp. 721–725
23. Mahbubun Nahar and Md. Sujan Ali (2014). An Improved Approach for Digital Image Edge Detection, *International Journal of Recent Development in Engineering and Technology*, Volume 2 (3), pp. 14-20
24. Mamta Juneja and Parvinder Singh Sandhu (2009). Performance Evaluation of Edge Detection Techniques for Images in Spatial Domain, *International Journal of Computer Theory and Engineering*, Vol. 1 (5), pp. 614-621
25. Mei Fang, GuangXue Yue and Qing Cang Yu (2009). The Study on An Application of Otsu Method in Canny Operator, *Proceedings of the 2009 International Symposium on Information Processing* (ISIP'09), pp. 109-112
26. Mitra Basu (2002) Gaussian-Based Edge Detection Methods — A Survey, *IEEE Transactions On Systems, Man, And Cybernetics*, Part C: Applications And Reviews, Vol. 32 (3), pp. 252-260
27. Mohsen Sharifi, Mahmoud Fathy and Maryam Tayefeh Mahmoudi (2012), A Classified and Comparative Study of Edge Detection Algorithms, *Proceedings of the International Conference on Information Technology: Coding and Computing* (ITCC.02), pp. 117-120
28. Muthukrishnan.R and M.Radha (2011). Edge Detection Techniques for Image Segmentation, *International Journal of Computer Science & Information Technology* (IJCSIT), Vol 3 (6), pp. 259-266
29. Nadernejad E.,Sharifzadeh S. and Hassanpour H. (2008). Edge Detection Techniques: Evaluations and Comparisons, *Applied Mathematical Sciences*, Vol. 2, (31), pp. 1507-1520
30. Nidhi Chandrakar and Devanand Bhonsle (2012), Study and Comparison of Various Image Edge Detection Techniques, *International Journal of Management, IT and Engineering*, Vol. 2 (5), pp. 1-12
31. Parminder Kaur and Ravi Kant (2014), A

Review on: Comparision and Analysis of Edge Detection Techniques, *International Journal of Engineering Research and General Science*, Volume 2 (3) pp. 102-109
32. Ping Zhou, Wenjun Ye, Yaojie Xia and Qi Wang (2011), An Improved Canny Algorithm for Edge Detection, *Journal of Computational Information Systems*, Vol. 7 (5), pp. 1516-1523
33. Pooja Ameta and Mahesh Kumar Porwal (2015). A Review on Edge Detection Technique, *International Journal of Advanced Engineering Research and Science* (IJAERS), Vol 2 (4), pp. 48-53
34. Poonam Dhankhar and Neha Sahu (2013). A Review and Research of Edge Detection Techniques for Image Segmentation, *International Journal of Computer Science and Mobile Computing*, IJCSMC, Vol. 2 (7), pp.86 – 92
35. Xu, Chakrabarti C., Karam L. J. (2011), A distributed Canny edge detector and its implementation on FPGA, *Digital Signal Processing Workshop and IEEE Signal Processing Education Workshop* (DSP/SPE), pp. 500 – 505
36. Rajwinder Kaur, Monika Verma, Kalpna and Harish Kundra (2014), Classification of Various Edge Detectors, *International Journal of Computer Science and Information Technology* (IJCSIT) Vol. 2 (5), pp.16-23
37. Raman Maini, Himanshu Aggarwal (2009). Study and Comparison of Various Image Edge Detection Techniques, *International Journal of Image Processing* (IJIP), Vol. 3 (1), pp. 1-12
38. Ramgundewar, Pallavi, Hingway, S .P. and Mankar, K. (2015). Design of modified Canny Edge Detector based on FPGA for Portable Device, Journal of The International Association of Advanced Technology and Science, Volume 16 (2), pp. 210-214
39. Rashmi, Mukesh Kumar, Jaiswal A.K, and Rohini Saxena (2013). Performance Analysis of Adaptive Canny Edge Detector Using Bilateral Filter, International Journal of Innovative Research in Computer and Communication Engineering Vol. 1, (4), pp. 930 – 936
40. Rathod M. (2014). Edge Detection in VHDL, *International Journal of Engineering Development and Research*, Vol. 2 (1), pp. 1095-1099
41. Sheffali Bamba (2014). Analysis of Edge Detection Techniques for Complex Background Images, *International Journal of Science and Research* (IJSR), Volume 3 (5), pp. 1649-1654
42. Shraddha S Aher (2015). Analysis of different algorithms on edge and corner detection, *International Journal of Multidisciplinary Research and Development*, Vol. 2 (6), pp. 99-102
43. Shrivakshan G.T. and Chandrasekar C. (2012). A Comparison of Various Edge Detection Techniques Used in Image Processing, *International Journal of Computer Science*, Vol. 9 (5) No 1, pp. 269-276
44. Song Wang, Feng Ge, and Tiecheng Liu (2006). Evaluating Edge Detection Through Boundary Detection, *EURASIP Journal on Applied Signal Processing*, Vol. 2006, pp. 1–15
45. Wenhao He and Kui Yuan (2008). An improved Canny edge detector and its realization on FPGA, *Intelligent Control and Automation*, pp. 6561–6564
46. William McIlhagga (2011). The Canny Edge Detector Revisited, *International Journal of Computer Vision*, Vol. 91 (3), pp. 251-261
47. Worawit Phueakjeen, Nattha Jindapetch, Leang Kuburat and Nikom Suvanvorn (2011). A study of the edge detection for road lane, *8th International Conference on Electrical Engineering, Electronics, Computer, Telecommunications and Information Technology* (ECTI-CON), pp. 995 – 998
48. Worthington, P.L (2002). Enhanced Canny edge detection using curvature consistency, *Proceedings. 16th International Conference on Pattern Recognition*, vol.1, pp. 596–599
49. Veeranagoudapatil, Chitra Prabhu (2015). Distributed Canny Edge Detector: Algorithm & FPGA Implementation, *International Journal for Research in Applied Science & Engineering Technology* (IJRASET), Vol. 3 (5), pp. 586-588
50. Zuwena Musoromy, Soodamani Ramalingam and Nico Bekooy (2010). Edge detection comparison for license plate detection, *11th International Conference on Control Automation Robotics & Vision* (ICARCV), pp. 1133–1138

University of Plovdiv
Plovdiv 4000
24 Tzar Asen Street
e-mail: dkromichev@yahoo.com

© International Scientific Conference on Engineering, Technologies and Systems
TECHSYS 2016, Technical University – Sofia, Plovdiv branch
26 – 28 May 2016, Plovdiv, Bulgaria

# TECHNOLOGY OF COMPUTATIONS IN CANNY EDGE DETECTION FOR FPGA IMPLEMENTATION

DIMITRE KROMICHEV

**Abstract:** *Precise and effective, Canny edge detection is computationally complicated and difficult for a fast hardware realization. This paper is focused on the technology of computations in John Canny's algorithm aimed at a speed optimized FPGA implementation. Each computational module is scrutinized in terms of memory utilization, organization of computations, and integer arithmetic speed. Proposed are new techniques and algorithms to accomplish the goal of speeding up Canny edge detection execution with respect to FPGA characteristics and functionalities.*

**Key words:** *Canny edge detection, FPGA, speed, technique, algorithm*

## 1. Introduction

John Canny's algorithm [6] has gained the recognition of being the standard gauge for the edge detection segment of digital image processing. It is a low level filtering technology intended to be used in software. Field Programmable Gate Array (FPGA) has been increasing its market share over the last two decades. One of the basic requirements for an FPGA-based hardware implementation of Canny edge detection is speed.

Described in the literature are several approaches addressing the Canny algorithm's being difficult for a fast execution on FPGA: 1) Split Canny [10]. It uses input image fragmentation for fast Gaussian smoothing and pipelining effectiveness. In terms of the speed parameter, the design flaws are: both on-chip and external memory data transfers; a substantial quantity of repeated computations for fragment boundary pixels; recursive computations in hysteresis thresholding. 2) Distributed Canny [9]. It attemps to spare the on-chip memory at the expense of a constant throughput through performing the computations at block level. Design flaws: parallel computations speed is eroded by excessive processed image defragmentation calculations; recursive computations. 3) Area optimized Canny [8]. It is mainly concentrated on a new architecture of the non-maximum suppression and hysteresis thresholding modules. Design flaws: sequential multiplications; recursive computations. 4) Modified Canny [7].The image is partitioned into q sub-images and each sub-image is further divided into p m×m blocks.The architecture consists of q processing units. Design flaws: heavy demands on memory; recursive computations.

The objective of this paper is to present the technology of fast Canny edge detection computations in compliance with FPGA characteristics. The task is to scrutinize the Canny algorithm speed optimization capabilities proposing new computational techniques and algorithms as ell as an effective utilization of the fastest FPGA memory. The targeted hardware is Altera FPGAs. Relevant to the analyses and conclusions arrived at in this paper are only gray scale images.

## 2. Computations in the Canny algorithm Modules

### 2. 1. Gaussian smoothing

Gaussian weighted average filtering is a representative of linear spatial filtering

$$v(m,n) = F[u(m,n)] \quad , \qquad (1)$$

where

u(m,n) is the input image,
v(m,n) is the output (filtered) image,
F is the filtering function

If F is defined as a ZxZ neighborhood operation (Z is an odd number and Z 3), Gaussian

Copyright © 2016 by Technical University of Sofia, Plovdiv branch, Bulgaria ISSN Online: 2535-0048

smoothing is:

$$v(m,n) = \frac{1}{s}\sum_{k=-w}^{w}\sum_{l=-w}^{w} g(k,l)u(m+k,n+l) \quad , \qquad (2)$$

where

u(m,n) is the input image,
v(m,n) is the filtered image,
$w = \frac{z-1}{2}$ , w = {1,2,..},
g(k,l) is the Gaussian filter (k = Z, 1 = Z) ,
s is the sum of all coefficients in the mask (*normalization factor);* the coefficients are integers based on the binominal series.

### 2. 1. 1. Memory utilization

For the FPGA-based Canny algorithm to start being executed, an exact number of 8-bit values need to be available for smoothing in at least one of the memories on the FPGA board. On-chip memory is the fastest memory on the Altera FPGAs [1],[2],[3],[4]. Consequently, the highest frequency this memory can be read from presents the upper speed limit the execution of computations can eventually approximate to. The image matrix pixels are loaded into the memory sequentially, i.e. row by row. From (2), and taking into account the technical characteristics of the Altera FPGA on-chip memory operations, if the Gaussian filter is of size ZxZ, and the image is of size MxN, the exact number of available pixels required for the Gaussian smoothing module to commence the linear spatial filtering operations should be:

$$(Z-1)*N + (Z+1) \qquad (3)$$

Parallelism in the execution of instructions, which, in terms of speed, is a great advantage of the FPGA-based hardware implementation over the software implementation, provides the capability of all the pixels under the Gaussian mask being accessible within a single clock cycle.

On-chip memory on Altera FPGAs is limited in quantity, and Canny edge detection is a rather complicated algorithm, requiring a serious amount of storage space. Consequently, it is quite inefficient for the whole image to be stored into memory prior to starting Gaussian filtering. The continuous execution of smoothing is guaranteed, if the memory contains only those rows of the image matrix that are currently involved in the computations. The image rows needed for the Gaussian smoothing are loaded in Dual-port RAMs. The depth of a single Dual-port RAM depends on the restrictions imposed on the memory organization by Altera. If a Dual-port RAM's depth is equal or bigger than the number of columns in the image matrix, then the number of all the Dual-port RAMs providing a single clock access to all the pixels under the Gaussian mask of size ZxZ is:

$$(Z*Z+1)/2 \ . \qquad (4)$$

The condition expresssed by (3) being satisfied, and the filtering of the pixel with image matrix coordinates ((Z-1)/2,(Z-1)/2) having been started, the next 8-bit value belonging to the row of highest ordinal number that is currently under the Gaussisan mask is simultaneously loaded into Dual-port RAM. In this way, the next pixel is immediately available for smoothing, and consequently the Gaussian filtering computations are guaranteed to be continuously executed. All the pixels in the image matrix row of number (Z-1)/2 having been filtered, the smoothing continues with the first subject to being filtered pixel from the image matrix row of number (Z+1)/2. For the computational process to be continuous, while the pixels from the image matrix row of number (Z-1)2 are being filtered the pixels belonging to image matrix row of number Z need to be sequentially stored in Dual-port RAMs whose exact number is presented by the expression

$$(Z+1)/2 \ . \qquad (5)$$

When image matrix row of number (Z+1)/2 starts being filtered the Dual-port RAMs containing the input image matrix row of number 0 are not relevant to the Gaussian smoothing computations any more. So, every clock cycle these pixels are sequentially overwritten by the pixel values of the input image matrix row of number (Z*2+2)/2. For one thing, this technique of revolving Dual-port RAMs and storing one image row through replacing another that is not usable spares the fastest memory on the Altera FPGAs, thus providing the opportunity images of different sizes to be processed by the FPGA implemented Canny edge detection. The total number of Dual-port RAMs required for the Gaussian smoothing module is:

$$(Z*Z+1)/2 + (Z+1)/2 \ . \qquad (6)$$

### 2. 1. 2. Organization of computations

With all the pixels under the Gaussian mask being accessible within a single clock cycle, the available built-in hard multipliers providing the fastes multiplication on the Altera FPGAs (Altera LPM_MULT function [5]) are employed for the

execution of convolution. The next step consists of each multiplication result being divided by the normalization factor. The quotients obtained are 8-bit in width which is an important fact with respect to the characteristics of computations on the Altera FPGAs. The last step is addition of the division results to calculate the final value of the Gaussian smoothed image pixel. For the purpose of execution speed optimization, the parallel adder is used (Altera PARALLEL_ADD function [5]), taking the advantage of maximum speed of arithmetic operations on the Altera FPGAs being guaranteed for input data width of 8 bits [5].The output of the parallel adder is the filtered pixel.

### 2. 1. 3. Integer arithmetic speed

While addition and multiplication are the two fastest representatives of integer arithmetic on the Altera FPGAs [1],[2],[3],[4], in terms of speed, division is definitely a weak point. Using a divider by employing the Altera LPM_DIVIDE function [5] will immensely erode the speed parameter of Canny's algorithm execution. Consequently, the conventional integer division has to be replaced with a technique capable of reducing the computational time and guaranteeing the same accuracy of results. The algorithm of this technique encompasses the following sequence of steps: **1)** Defining the positive integer that serves as divisor in the conventional division. In this case, it is the normalization factor of the Gaussian filter. **2)** Experimentally, an appropriate value equal to a power of 2 is selected. This value is divided by the integer number from *step 1)* . **3)** Only the integer part of the division result calculated in *step 2)* is taken. **4)** The number that will be divided is multiplied by the integer number from *step 3)* . **5)** From the result calculated in *step 4)*, a sequence of bits (starting with LSB and going leftwards) is dropped out. The number of the dropped out bits is equal to the number of the power of 2 selected in *step 2)*. **6)** The value of MSB of the bits that are dropped out in *step 5)* is added to the value represented by the remaining bits in the multiplication result calculated in *step 4)* after the sequence of bits is dropped out in *step 5)*. The positional number of this bit in the multiplication result calculated in *step 4)* is equal to: [the number of the power of 2 selected in *step 2)*] – 1. **7)** The result of addition in *step 6)* is the quotient.

The normalization factor is a filter specific constant. It has to be different from a power of 2. If it is equal to some power of 2, only the operation bit slicing (*steps 5), 6),* and *7*) of the algorithm) is relevant to the calculations.

To apply this technique, all the coefficients in the Gaussian filter should have been multiplied by the integer number calculated in *step 3)* prior to starting the Canny edge detetion computations. Thus, a Gaussian mask is modified with respect to coefficients' values, remaining the normalization factor unchanged.

Being based on two of the five fastest operations on Altera FPGAs [1],[2],[3],[4], the presented technique guarantees the utmost speed. Combined with the other two most advanced in terms of speed arithmetic operations – addition and multiplication, this technique provides for a maximum speed of Gaussian smoothing computations.

## 2. 2. Computation of orthogonal gradients

### 2. 2. 1. Memory utilization

Gaussian filtering having been applied, the total number of pixels in the input image is reduced, and the total number of filtered image pixels is :

$$M*N - \{[M - (Z-1)] * (Z-1) + N * (Z-1)\}. \quad (7)$$

The exact number of available Gaussian smoothed pixels required for this module to commence the parallel computations of the vertical and horizontal gradients applying the two Sobel filters (Fig. 1.)

| | | |
|---|---|---|
| -1 | 0 | 1 |
| -2 | 0 | 2 |
| -1 | 0 | 1 |

Gx

| | | |
|---|---|---|
| -1 | -2 | -1 |
| 0 | 0 | 0 |
| 1 | 2 | 1 |

Gy

***Fig. 1***. Sobel masks for *x* and *y*

should be:

$$2*(N-(Z-1)) + 4 . \quad (8)$$

As with Gaussian smoothing module, the filtered fixels are stored in revolving Dual-port RAMs for the purposes of guaranteeing the access to all the pixels under the Sobel masks within a single clock cycle, thus emplpoying pipelining of computations, and saving memory. The total number of Dual-port RAMs utilized in this module is 7.

### 2. 2. 2. Organization of computations

As gradient filters, the two Sobel masks have positive and negative coefficients. If in a 3x3 neighborhood C(*x,y*) is the central pixel, and the numbers of neighboring pixels are as shown (Fig. 2.) ,

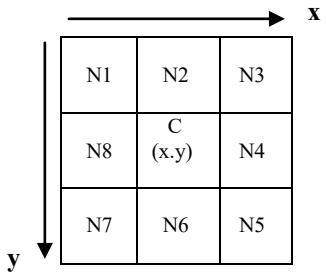



***Fig. 2.*** 3x3 neighborhood pixels

the equations used to calculate the *x* gradient and the *y* gradient for C(*x,y*) are:

$$G_x = \frac{(N_3 + 2N_4 + N_5) - (N_1 + 2N_8 + N_7)}{4} \quad (9)$$

$$G_y = \frac{(N_7 + 2N_6 + N_5) - (N_1 + 2N_2 + N_3)}{4} \quad (10)$$

There are two important facts here:
1) Division by the sum of positive coefficients in the Sobel masks avoids the need for scaling; 2) The difference in signs of the values calculated for both gradients is applied in the speed optimization of gradient direction computations.

### 2. 2. 3. Integer arithmetic speed

The multipliers and the divisors being a power of 2, integer arithmetic guarantees a maximum speed of computations in this module.

## 2. 3. Computation of gradient magnitude and gradient direction

### 2. 3. 1. Memory utilization

The orthogonal gradients having been computed, the total amount of pixels to be used in calculating the magnitude and direction of the gradient is:

$$M*N-\{[M-(Z+1)] * (Z+1) + N * (Z+1)\}. \quad (11)$$

Mathematically, gradient magnitude $G_M$ is computed using

$$G_M = \sqrt{G_x^2 + G_y^2} \quad (12)$$

and gradient direction $G_D$ is computed using:

$$G_D = \tan^{-1}\left(\frac{G_y}{G_x}\right) \quad (13)$$

There is no need for memory storage of a certain number of pixels processed in the prevoius computational module for the computations in (12) and (13) to start being executed. The pairs of pixel values computed in (9) and (10) are immediately pipelined and processed in (12) and (13). Consequently, no Dual-port RAMs are utilized in this module.

### 2. 3. 2. Organization of computations

Altera provides a specialized integer square root function – ALTSQRT [5]. Although the 8-bit input data width is advantageous to the speed parameter, the maximum clock rate the function can be executed at [5] is not campatible with the accomplishment of the speed optimization goal. That is why, (12) is replaced by the approximation

$$|G_M| = |G_X| + |G_Y|, \quad (14)$$

the latter being functional insomuch as it does not distort the local maximum calculations in the computational module to follow.

The hardware implementation of (13) erodes very seriously the speed of Canny edge detection. To overcome this hurdle, (13) is replaced by computing the ratio between *Gy* and *Gx*. The ratio is calculated on the basis of two reference points and the signs of *Gy* and *Gx*. One of the reference points is used to represent an angle of 22.5°, and the other - 67.5°. The most appropriate approximation to angle 22.5° is the fraction $\frac{2}{5}$ ($\tan^{-1}\left(\frac{2}{5}\right)$ = 21.8014094°), and to angle 67.5° - the fraction $\frac{5}{2}$ ($\tan^{-1}\left(\frac{5}{2}\right)$ = 68.1985905°) . In this way, the gradient direction calculation is based on:

**1)** $Gy > 0$ & $Gx > 0$
$Gy < 0$ & $Gx < 0$
If $|Gx|*2 \geq |Gy|*5$ $G_D$ = **0**
If $|Gx|*2 < |Gy|*5$ & $|Gx|*5 > |Gy|*2$ $G_D$ = **45**
If $|Gx|*5 \leq |Gy|*2$ $G_D$ = **90**

**2)** $Gy > 0$ & $Gx < 0$
$Gy < 0$ & $Gx > 0$
If $|Gx|*2 \geq |Gy|*5$ $G_D$ = **0**

If |Gx|*2 < |Gy|*5 & |Gx|*5 > |Gy|*2 $G_D$ = **135**
If |Gx|*5 |Gy|*2 $G_D$ = **90.** (15)

### 2. 3. 3. Integer arithmetic speed

Employing (14) in computing the gradient magnitude guarantees a maximum speed of execution. Although (15) is much faster than (13), the comparison functions on the Altera FPGAs cannot match addition and multiplication in terms of speed. Consequently, there is a speed incongruity between the two parallelly executed computations. It is the speed of (15) that to a great extent determines the general speed characteristics of this module. There is an input image size dependable compensation for the comparison functions being slower – the essence of FPGA computations in the next module demands that the number of values representing the magnitudes should exceed the number of values representing the directions by a whole image row. Consequently, the larger the number of columns in the input image matrix, the narrow the gap between the comparative speeds of gradient magnitude and direction calculations.

## 2. 4. Non-maximum suppression

### 2. 4. 1. Memory utilization

Computing the local maximum being based on comparing one magnitude with two adjacent magnitudes positioned along the direction of the gradient, the exact number of calculated magnitudes required for this module to start executing is

$$2*(N-(Z+1)) + 4, \quad (16)$$

while the exact number of calculated directions is estimated to be

$$(N-(Z+1)) + 4. \quad (17)$$

They are to be stored in separate revolving Dual-port RAMs whose total number in this module is 10.

### 2. 4. 2 . Organization of computations

Non-maximum suppression is based on:

M(x,y) = M(x,y) only for
[M(x,y)>M_1(x1,y1) & M(x,y)>M_2(x2,y2)];
M(x,y) = 0 in all the other cases, (18)

where

M(x,y) is a pixel possibly belonging to the edge, M_1(x1,y1) and M_2(x2,y2) are the magnitudes of the two adjacent pixels positioned along the gradient direction.

### 2. 4. 3. Integer arithmetic speed

The overall speed performance in this module is influenced by two factors: 1) the rate of loading the calculated in the previous module gradient direction values in the Dual-port RAM; 2) comparison functions are the indispensible integer arithmetic here, and taking into account that the total number of their execution is a constant, it is the maximum clock rate for input data width of 8 bits that is of crucial importance.

## 2. 5. Hysteresis thresholding

### 2. 5. 1. Memory utilization

The result of this module computations being the final edge detected image, it is required that there be available on-chip memory to store

$$M*N-\{[M-(Z+3)] * (Z+3) + N * (Z+3)\} \quad (19)$$

pixels. So far in the computational process, the appropriate pipelining techniques based on the revolving Dual-port RAMs, has left enough storage space for all these pixels to be stored into the fastest memory on Altera FPGAs.

### 2. 5. 2. Organization of computations

Each pipelined magnitude being compared to the two calculated in advance threshold values (high - *T1*, and low - *T2*), the essential concentration here is the determining of connectivity/non-connectivity with respect to *T1*. The algorithm focuses on several steps:
**1)** A 3x3 window centered around each pixel satisfying the condition *T1>GM>T2* is used. All the eight neighbouring magnitudes are tested with respect to *T1*. **2)** If there is a value bigger than *T1*, this pixel is defined as an edge and its coordinates in the image matrix are stored in a separate memory buffer to avoid redundant double check of five magnitudes when the window moves on to the next pixel. **3)** If none of the neghbouring magnitudes is bigger than *T1*, but at lest one falls between *T1* and *T2*, then only the peripheral magnitudes of a 5x5

window are checked for values bigger than *T1*. **4)** If such a value is available, then the pixel is an edge. **5)** If one or more of these sixteen peripheral magnitudes in the 5x5 window falls between *T1* and *T2*, then its (their) coordinates are stored in another memory buffer. If such a value is not available, then the pixel is not an edge. **6)** The described procedure is repeated for the next pixel in the image row, taking into account that from the second pixel downwards the contents of the two memory buffers are constantly checked. The second buffer contains those pixels which can eventually be nominated for edge pixels on the basis if indirect connectivity.

In terms of speed, two advantages are achieved: total avoidance of recursive computations, and immense reduction of the calculations based on the comparison functions to define the edge/non-edge status of a single pixel.

### 2. 5. 3. Integer arithmetic speed

In this module, too, the comparison functions are the indispensible integer arithmetic. For the purpose of speed optimization, the accomplishable goal here is their reduction to the bare minimum on the platform of the appropriate computational algorithm implementing the hysteresis thresholding.

## 3. Conclusion

The technology of Canny edge detection computations for implementatation on Altera FPGAs has been analyzed in this paper. The computational modules of John Canny's algorithm are scrutinized on the platform of memory utilization, organization of computations, and integer arithmetic for the purpose of optimizing the speed parameter. This goal is accomplished by employing a set of approaches: optimized memory utilization in terms of revolving Dual-port RAMs; fast technology for Gaussian smoothing employing a novel organization of computations combined with a new advanced integer division replacing technique; avoiding additional scaling calculations to prevent eroding the speed in the Sobel filtering module; defining a new algorithm for computing the gradient direction; new computational mechanism for the hysteresis thresholding algorithm aimed at total avoidance of recursion as well as maximum reduction of the number of times the comparison functions, which are much slower than the other Altera FPGA integer arithmetic, are used. The proposed technology of computations is a solid basis for an advanced computational architecture of FPGA-based Canny algorithm focused on speed.

## REFERENCES


1. Altera Corporation. Cyclone IV Device Handbook, Volume 1, 2014
2. Altera Corporation. Cyclone V Device Handbook, Volume 1, 2014
3. Altera Corporation. Stratix III Device Handbook, Volume 1, 2014
4. Altera Corporation. Stratix IV Device Handbook, Volume 1, 2014
5. Altera Corporation. Integer Arithmetic IP Cores User Guide, 2014
6. Canny, J. F. (1986). A computational approach to edge detection, *IEEE Transactions on Pattern Analysis and Machine Intelligence*, 8, pp. 679-698
7. Chandrashekar N.S. and Nataraj K. R. (2013). Design and Implementation of a Modified Canny Edge Detector based on FPGA, *International Journal of Advanced Electrical and Electronics Engineering,* (IJAEEE), Vol.2, (1), pp. 17-21
8. Chandrashekar N.S. and Nataraj K.R. (2013). NMS and Thresholding Architecture used for FPGA based Canny Edge Detector for Area Optimization, *Proceeding. of International Conference on Control, Communication and Power Engineering,* pp. 80-84
9. Divya. D. and Sushma P. S. (2013). FPGA Implementation of a Distributed Canny Edge Detector, *International Journal of Advanced Computational Engineering and Networking*, Vol. 1, (5), pp. 46-51
10. Shamlee V. and Jeyamani (2014). A Split Canny Edge Detection: Algorithm and its FPGA Implementation. *International Journal of Science and Research* (IJSR), Vol. 3 (11), pp. 1198-1205



University of Plovdiv
Plovdiv 4000
24 Tzar Asen Street
e-mail: dkromichev@yahoo.com

© International Scientific Conference on Engineering, Technologies and Systems
TECHSYS 2016, Technical University – Sofia, Plovdiv branch
26 – 28 May 2016, Plovdiv, Bulgaria

# ESTIMATING IMPACT OF IMAGE PARAMETERS ON METHOD FOR TRACKING AND MAPPING A MOTION IN SOLAR CORONA

DIMITAR GARNEVSKI

**Abstract:** *Development of methods for astronomical image processing can require input images with certain quality and properties. Due to the imperfection of sensors, optics, transmission protocols or limitation of storage capacity or atmosphere distortion input images can contains undesired artifacts or can be with inappropriate parameters. In this paper we perform estimation of image properties like bit depth in image (monochrome or color image), compression level (in JPEG image) and raster size. We execute selected algorithm for tracking and mapping a motion against number of test images with different characteristics and estimating result of algorithm execution. As the result of the study we create accuracy limits of the image parameters and define eligibility criteria for the images which can be used by algorithm. By defining of accuracy limits and eligibility criteria of images we can create algorithm which will be used for image pre-selection in methods for tracking and mapping a motion or other image processing algorithms with similar image quality requirements.*

**Key words:** *image processing, image quality, JPEG, bit-depth, compression, raster*

## 1. Introduction

In implementation of algorithms for image processing often must be pledged requirements for the quality of the input images so as to produce most effective result from the execution of the algorithm. In some cases we have a particular set of captured images from which must selected only those that are appropriate for a defined algorithm. In this study was used a stochastic approach to estimate the influence parameters of input images on performance of the algorithm for tracking and mapping a motion. By examining the influence of a group of selected parameters of the image will be formed requirements to the quality of images that can be used as well to define accuracy limits and eligibility criteria of images we can create algorithm which will be used for image pre-selection in methods for tracking and mapping a motion or other image processing algorithms with similar image quality requirements.

## 2. Method for tracking and mapping a motion

The method for motion tracking and mapping, based on solar corona images [3] proposes an ability for modeling the dynamical changes in solar prominences during its evolution. However, to obtain a correct model for image processing we have to ensure an optimal accuracy and reliability of the extracted features, fixed as 2D compass directions of layers. The test has been conducted on sequences of images that include several elements – an artificial moon visible as a black half circle, the solar corona with bright prominences above the moon and near them – background of a shining Earth atmosphere. A correction for Earth rotation was also applied, using some static elements in the images as a reference.

The method supposes a usage of calculating techniques that ensure at first - an optimal time-period for image sequences processing commensurable with the time period of the fastest developing parts of the prominence (several minutes), and second - a presentation of the lightness information independent from the sensor of particular coronagraph and image file format.

Block scheme of the algorithm is represented at Fig. 1. All operations over input images sequence can be separated into two steps. At the first step we perform pre-processing: algorithm estimates photo-spherical shining and removes it. A Gauss filtration and image sharpening were also applied. At the second step method calculates image gradients and performs a map of motions [5].

Copyright © 2016 by Technical University of Sofia, Plovdiv branch, Bulgaria ISSN Online: 2535-0048

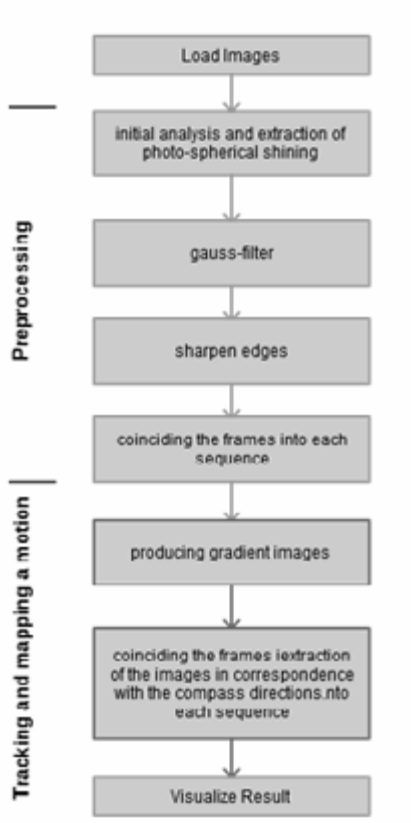



***Fig. 1.*** *Method for tracking and mapping a motion*

## 3. Digital images

An image may be defined as a two-dimensional function f (x, y), where x and y are spatial (plane) coordinates, and the amplitude off at any pair of coordinates (x, y) is called the intensity or gray level of the image at that point. When x, y, and the amplitude values off are all finite, discrete quantities, we call the image a digital image.

The color depth measures the amount of color information available to display or print each pixel of a digital image. A high color depth leads to more available colors, and consequently to a more accurate color representation. For example, a pixel with one bit depth has only two possible colors: black and white. A pixel with 8 bits depth has 256 possible values and a pixel with 24 bits depth has more than 16 million of possible values. Usually, the color depths vary between 1 and 64 bits per pixel in digital images. The color models are used to specify colors as points in a coordinate system, creating a specific standard. In the following, the most common color spaces are briefly presented.

The RGB (Red, Green, and Blue) color space is one of the most used color spaces, specially for 8 bit digital images. The RGB is an additive model where the red, green, and blue colors are combined on different quantities or portions to reproduce other colors. The pixels of an image represented in the RGB model have usually 8 bits depth, resulting in 256 possible intensities, i.e., the range of [0, 255] for each color.

In the context of digital images, an image format is a common manner to organize and store image data. The format defines how the data are arranged and the used compression type or level. Generally speaking, raster graphics or bitmap files (map of bits), contain a representation of a graphic stored as pixels at a fixed resolution. A common example is a digital photo or a scanned image. Some of the most usual raster formats are GIF, JPEG, PNG, TIFF, and BMP [8].

### 3.1. Image zooming

Zooming requires two steps: the creation of new pixel locations, and the assignment of gray levels to those new locations. In order to perform gray-level assignment for any point in the overlay, we look for the closest pixel in the original image and assign its gray level to the new pixel in the grid. [2]

### 3.2. Image shrinking

Image shrinking is done in a similar manner as just described for zooming. The equivalent process of pixel replication is row-column deletion. For example, to shrink an image by one-half, we delete every other row and column. We can use the zooming grid analogy to visualize the concept of shrinking by a no integer factor, except that we now expand the grid to fit over the original image.[2]

## 4. JPEG Compression

JPEG is currently a worldwide standard for compression of digital images. The standard is named after the committee that created it and that continues to guide its evolution. This group, the Joint Photographic Experts Group (JPEG), consists of experts nominated by national standards bodies and by leading companies engaged in image-related work. The key features of the lossy JPEG standard are as follows.

- Both sequential and progressive modes of encoding are permitted. These modes refer to the manner in which quantized DCT coefficients are encoded. In sequential coding, the coefficients are encoded on a block-by-block basis in a single scan that proceeds from left to right and top to bottom. In contrast, in progressive encoding only partial information about the coefficients is encoded in the first scan followed by encoding the residual information in successive scans.
- Low complexity implementations in both hardware and software are feasible.
- All types of images, regardless of source, content, resolution, color formats, etc., are permitted.

- A graceful tradeoff in bit rate and quality is offered, except at very low bit rates
- A hierarchical mode with multiple levels of resolution is Bit resolution of 8-12 bits is permitted.
- A recommended file format, JPEG File Interchange Format (JFIF), enables the exchange of JPEG bit streams among a variety of platforms.

The JPEG standard is intended for the compression of both grayscale and color images. In a grayscale image there is a single "luminance" component. However, a color image is represented with multiple components and the JPEG standard sets stipulations on the allowed number of components and data formats. The standard permits a maximum of 255 color components, which are rectangular arrays of pixel values represented with 8-to 12-bit precision. For each color component, the largest dimension supported in either the horizontal or the vertical direction is 216 = 65,536. All color component arrays do not necessarily have the same dimensions. Assume that an image contains K color components denoted by C, n = 1,2, . . . , K. Let the horizontal and vertical dimensions of the nth component be equal to X, and Y, respectively. Define dimensions Xm, Ym, and Xmin, Y,in as

$$X_{\max} = \max_{n=1}^{K}\{X_n\}, \quad Y_{\max} = \max_{n=1}^{K}\{Y_n\}, \qquad X_{\min} = \min_{n=1}^{K}\{X_n\}, \quad Y_{\min} = \min_{n=1}^{K}\{Y_n\} \tag{1}$$

With lossy compression, the amount of distortion introduced in the image is inversely related to the number of bits (bit rate) used to encode the image. The higher the rate, the lower the distortion. Naturally, for a given rate we would like to incur the minimum possible distortion. Similarly, for a given distortion level, we would like to encode an image with the minimum rate possible. Hence lossy compression techniques are often studied in terms of their rate-distortion performance, i.e., the distortion they introduce at different bit rates. The rate-distortion performance of JPEG is determined mainly by the quantization tables. As mentioned before, the standard does not recommend any particular table or set of tables and leaves their design completely to the user. While the image quality obtained from the use of the "default" quantization tables is very good, there is a need to provide flexibility to adjust the image quality by changing the overall bit rate. In practice, scaled versions of the "default" quantization tables are very commonly used to vary the quality and compression performance of JPEG. For example, the popular IJPEG implementation, freely available in the public domain, allows this adjustment through the use of quality factor Q for scaling all elements of the quantization table. [1] The scaling factor is then computed as

$$scale\ \ factor = \begin{cases} \dfrac{5000}{Q}, & for\ \ 1 \le Q < 50 \\ 200 - 2 * Q, & for\ \ 50 \le Q \le 99 \\ 1, & for\ \ Q = 100 \end{cases} \tag{2}$$

## 5. Estimation process

Entire process of estimation of quality and properties of input images which will be used by method for tracking and mapping a motion can be separated into following steps:

- Selection of input images
- Generation of test images sequences
- Apply of method for tracking and mapping a motion on input sequences
- Store motion map on file system
- Compare histograms of motion map and reference by correlation and intersection methods

As input for our research we use RGB images with size 1728 x 1152 pixel captured with coronagraph. Input images were captured in time interval and contains differences due motion of solar material.

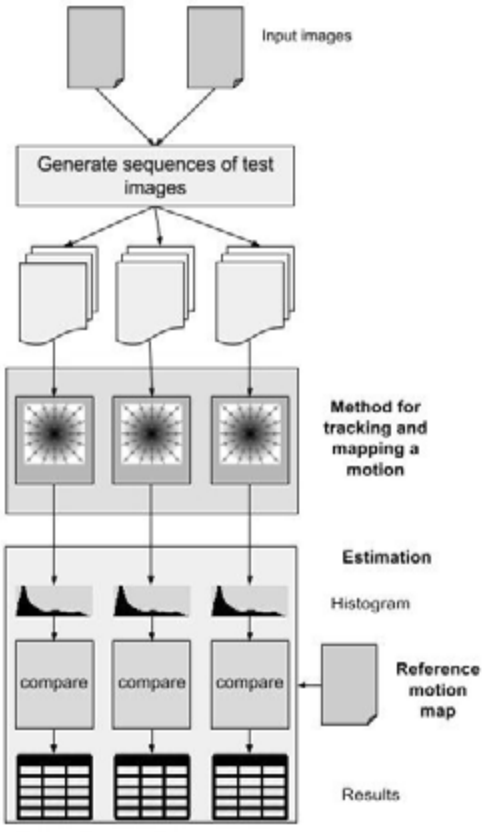



***Fig. 2.*** *Image estimation process*



***Fig. 3.*** *Input image*

### 6. Estimation of bit-depth influence

In Table 1 are shows results from histogram comparison of motion maps which were generated on gray-scale input images with different bit-depth.

***Table 1.*** *Histogram compare of motion map depending on bit-depth — gray-scale*

| | Low bits | | High bits | |
|---|---|---|---|---|
| **bits** | **Correl.** | **Intersect.** | **Correl.** | **Intersect.** |
| 4 | 0.999983 | 5.597783 | 0.640083 | 1.015218 |
| 5 | 0.999996 | 5.614305 | 0.643906 | 1.035348 |
| 6 | 1.000000 | 5.623490 | 0.695268 | 1.348076 |
| 7 | 1.000000 | 5.626739 | 0.730155 | 1.587119 |
| 8 | 1.000000 | 5.626779 | 0.730155 | 1.588119 |

During estimation process were used gray-scale images with 5 to 8 bit depth for both - low and high part of pixel bit.

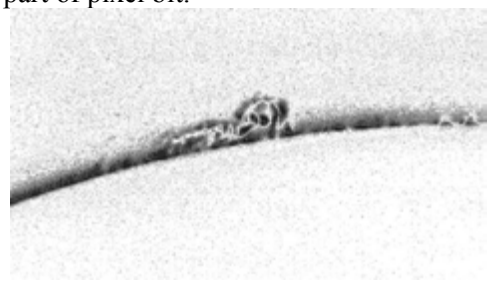


***Fig. 4.*** *Motion map gradients – high bits – gray-scale*

At Fig. 4 and Fig. 5 are shown result motion maps of two inputs set containing gray-scale images with 7 bit depth. In bit-depth range from 5 to 8 generated map in high and low bits are almost identical. But in small bit-depth we have significant amount of lost details. Image shown on Fig. 5 which was generated on lower bits in pixel visually contains more fine details.

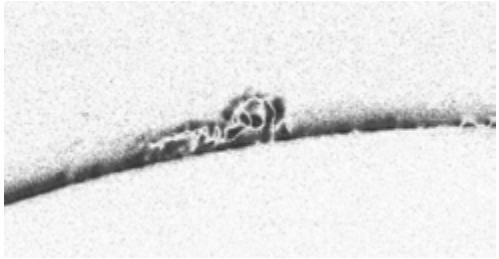


***Fig. 5.*** *Motion map gradients – low bits – gray-scale*

In Table 2 are shows results from histogram comparison of motion maps which were generated on color input images with different bit-depth.

***Table 2.*** *Histogram compare of motion map depending on bit-depth — color*

| | Lower bits | | Higher bits | |
|---|---|---|---|---|
| **bits** | **Correl.** | **Intersect.** | **Correl.** | **Intersect.** |
| 4 | 0.999786 | 7.519207 | 0.513051 | 1.120022 |
| 5 | 0.999999 | 7.510696 | 0.528951 | 1.204329 |
| 6 | 1.000000 | 7.515206 | 0.545791 | 1.276092 |
| 7 | 1.000000 | 7.518377 | 0.753839 | 2.153798 |
| 8 | 1.000000 | 7.519514 | 1.000000 | 7.519514 |

Motion maps shown on Fig. 6 and Fig. 7 were generated with 6 bit depth with high order bits and low order bits respectively. As you can see usage or high order bits saves common information about motion and reduces minor artifacts.

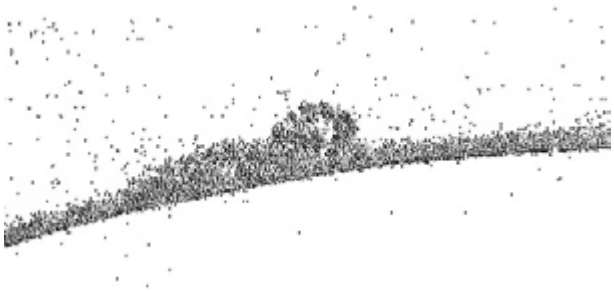


***Fig. 6.*** *Motion map gradients - color – 6 high bits*



***Fig. 7.*** *Motion map gradients - color – 6 low bits*

### 7. Estimation of compression level influence

Compression level dependency estimation was performed with two types of images with same raster size – 8-bit color and 8-bit grayscale. For tests were used two input images and OpenCV library [7] by which was generated set of test images with different compression level. In Table 3 are shown results from motion maps histogram compassion of generated input set and original input images. First column of the table shows compression level of images in set where 10 is maximum compression and 100 is image without compression.

***Table 3.*** *Histogram compare (correlation and intersection) of motion map depending on compression level (CL) (10 – max compression, 100 – without compression)*

| | 8-bit color | | 8-bit grayscale | |
|---|---|---|---|---|
| **CL** | **Correl.** | **Intersect.** | **Correl.** | **Intersect.** |
| 10 | 0.519408 | 1.110923 | 0.634735 | 1.070910 |
| 20 | 0.607175 | 1.452810 | 0.643763 | 1.235687 |
| 30 | 0.533697 | 1.159272 | 0.637421 | 1.111867 |
| 40 | 0.534448 | 1.162480 | 0.637105 | 1.099990 |
| 50 | 0.544669 | 1.195866 | 0.639732 | 1.131089 |
| 60 | 0.641407 | 1.662656 | 0.643571 | 1.254978 |
| 70 | 0.567252 | 1.276844 | 0.643384 | 1.168477 |
| 80 | 0.621592 | 1.522236 | 0.670619 | 1.311020 |
| 90 | 0.854473 | 3.516023 | 0.657837 | 2.468472 |
| 100 | 0.998354 | 6.928975 | 0.693442 | 2.907942 |

Fig. 8 and Fig. 9 shows result motion maps of respectively color and gray-scale images with identical compression level - 80. Both images preserve significant amount of details and successfully can be used with algorithm for tracking and mapping a motion. Images with compression levels below 80 have loses in details which don't contains information of particles motion but common details which contains motion data are still preserved.



***Fig. 8.*** *Motion map of 8-bit color image at compression level 80*



***Fig. 9.*** *Motion map of 8-bit gray-scale image at compression level 80*

At levels of compression smaller than 80 main losses in the area with little change of the image parameters. The part of the image containing the changes in gradient is preserved, but with reduced resolution

## 8. Estimation of raster size influence

In Table 4 are shows results from histogram comparison of motion maps which were generated on color input images with different sizes. Scale factor in first column of the table represents scale by which original input image with size 1728 x 1152 pixels was scaled down.

***Table 4.*** *Histogram compare (correlation and intersection) of motion map depending on scale factor*

| Scale factor | Correlation | Intersection |
|---|---|---|
| 1/2 | 0.942206 | 4.378632 |
| 1/3 | 0.961200 | 4.885306 |
| 1/4 | 0.921623 | 4.005298 |
| 1/5 | 0.942047 | 4.347442 |
| 1/6 | 0.930380 | 4.099806 |
| 1/7 | 0.945862 | 4.462879 |
| 1/8 | 0.940795 | 4.371694 |
| 1/9 | 0.959371 | 4.861311 |

As is shown on Fig. 10 and Fig. 11 we can use image with 1/2 size of original in each direction and preserve amount of details in result motion map.



***Fig. 10.*** *Motion map of 8-bit color image at scale factor 1/2*



***Fig. 11.*** *Motion map of 8-bit color image at scale factor 1/4*

## 9. Conclusions

After this research we can make the following conclusions about the quality of the images and their parameters that can be used for tracking and mapping a motion algorithm.

- Use of gray images leads to loss of fine detail, whether used high or low bits in representation of the value of pixels.
- Using of gray-scale images generate areas with significant changes in the movement of the particles (differences in gradations), which can be used to illustrate the general movement. In this case it is more appropriate use of high bits (6 or 7) in pixels of grayscale images.
- Usage of color images with depth less than 6 bit it's not suitable due lost of important details in motion map. In case of color images with 6 bit depth and usage of low part of the original pixel correlation of motion map is 1 and intersection is close to reference images - motion is almost identical to the reference motion map.
- It is appropriate use of compressed images with level of compression greater than 80, in this case the result of applying the algorithm to the compressed image is identical to that of the original image without any compression.
- At reducing the size of the image algorithm generate unwanted artifacts that deteriorate output map the change in parameters in the image.

Finally we can define following requirements to the input images:

- color image with at least 6 bit depth from low bits in pixel
- gray-scale images can be used with at least 6 bit depth, but only in cases when result motion map can be without fine details
- compression level at least 80 - for color an gray-scale images
- minimal size of the image 1000 x 500 pixels

Based on the requirements described above can be implemented automated method for estimation and pre-selection of images which will be processed by the algorithm.

## REFERENCES


1. Al Bovik. (2004). *Handbook of image and video processing*, Academic Press. Canada.
2. Rafael C. Gonzalez Richard E. Woods (2002) *Digital Image Processing*, 2nd Edition, Prentice Hall
3. Petya Pavlova, Elena Duncheva, Kostadinka Koleva (2010). Method for tracking and mapping a motion based on images of the solar corona. *Proceedings of the VII Bulgarian-Serbian Astronomical Conference (VII BSAC)*, Chepelare, Bulgaria.
4. Petya Pavlova, Kristina Staneva (2005). Dependence of the Colour in Computer Models on the Colour-reproducing Signals Discretization. *E+E*.
5. Petya Pavlova, Dimitar Garnevski, Kostadinka Koleva (2016). Optimization of a motion tracking and mapping method based on images of the solar corona. *Bulgarian Astronomical Journal, Volume 24*
6. S. G. Hoggar, *Mathematics of digital images. Creation, Compression, Restoration, Recognition*, Cambridge
7. *http://opencv.org/,* OpenCV (Open Computer Vision) Reference
8. Frery A. C, Perciano T. (2013*). Introduction to Image Processing Using R*, Chapter 2, Springer



Department of Electrical Engineering
Technical University–Sofia, Branch Plovdiv
25 Tsanko Diustabanov St.
4000 Plovdiv
E-mail: garnevsky_dm@abv.bg

© International Scientific Conference on Engineering, Technologies and Systems
TECHSYS 2016, Technical University – Sofia, Plovdiv branch
26 – 28 May 2016, Plovdiv, Bulgaria

# ПАРАЛЕЛНА РЕАЛИЗАЦИЯ НА АНИЗОТРОПНА ДИФУЗИЯ

ДИМИТЪР ГЪРНЕВСКИ

**Резюме:** *Въведения от Perona и Malik метод за анизотропна дифузия позволява извършването на филтрирането на шумовете като същевременно запазва контурите на обектите в изображението, за разлика от изотропна дифузия която не отчита границите на обектите. В текущата работа е представена OpenCL реализация на метода и влиянието му върху целеви изображения.*

**Ключови думи:** *обработка на изображения, филтриране, Гаусов филтър, анизотропна дифузия, паралелни изчисления, оптимизация, OpenCL*

# PARALLEL IMPLEMENTATION OF ANISOTROPIC DIFFUSION

DIMITAR GARNEVSKI

**Abstract:** *Introduced by Perona and Malik anisotropic diffusion method to allow for filtering of noise while preserving contours of the objects in an image, unlike the isotropic diffusion that does not take into account the boundaries of the objects. In current work is represented OpenCL implementation of the method and its impact on the target images.*

**Key words:** *image processing, filtering, Gaussian kernel, anisotropic diffusion, parallel computing, optimizations, OpenCL*

## 1. Въведение

Методите за напреднала обработка на изображения като разпознаване на контури и посоки на движението на обектите изискват предварителна обработка на входните изображения. В определени случаи използването на Гаусов филтър не е достатъчно и се налага използване на филтри които да предпазят от размиването на контурите на обектите в изображението като същевременно премахват шумовете. В този случай е удачно прилагането на анизотропен филтър представен от *Perona* и *Malik* [1].

## 2. Анизотропна дифузия

*Perona* и *Malik* въвеждат *flux* функция, целта на която е да ограничи процеса на дифузията до съседни хомогенни региони, но не и през границите им. Топлинното уравнение което изразява горното се дефинира със:

$$\frac{\partial I}{\partial t} = c(x, y, t)\Delta I + \nabla c \cdot \nabla I \quad (1)$$

където $c$ е предложената *flux* функция, която контролира нивото на дифузията във всяка точка на изображението. Изборът на $c$, така че да следва нивата на градиента в дадената точка предизвиква забавянето на процеса на дифузия при достигането на границите на региона. При достигане на границите на изображението може да бъде предизвикана инверсна дифузия която ще подобри ръбовете.

*Perona* и *Malik* предлагат следните две *flux* функции:

$$c\left(\left\|\nabla I\right\|\right) = e^{-\left(\left\|\nabla I\right\| / K^2\right)} \quad (2)$$

$$c\left(\left\|\nabla I\right\|\right) = \frac{1}{1 + \left(\frac{\left\|\nabla I\right\|}{K}\right)^2} \quad (3)$$

Copyright © 2016 by Technical University of Sofia, Plovdiv branch, Bulgaria ISSN Online: 2535-0048

Двете *flux* функции предлагат различен баланс между запазване на ръбовете и заглаждане на хомогенните региони. Първата дава предимство на ръбовете с висок контраст пред такива с нисък, а втората дава предимство на големите региони пред малките. И двете се управляват от свободен параметър *k*, който дефинира "силата" на ръбовете, на база на която се определя валиден регион от изображението.

Дискретното решение на анизотропния филтър може да бъде представено чрез *FTCS (Forward-Time Central-Space)* метода по следния начин

$$I_{i,j}^{t+1} = I_{i,j}^{t} + \lambda \begin{bmatrix} c_N \cdot \nabla_N I + c_S \cdot \nabla_S I \\ + c_E \cdot \nabla_E I + c_W \cdot \nabla_W I \end{bmatrix}_{i,j}^{t} \quad (4)$$

където означенията *[N, S, W, E]* съответстват на пикселите отгоре, отдолу, вляво и вдясно спрямо пиксела, който се разполага на позицията *(i, j)*. Т.к. *c* се базира на промяната на градиента, не е от значение дали се използва прав или обратен градиент [1][2][3][4].

### 3. Платформа OpenCL

*OpenCL* представлява първи отворен стандарт за междуплатформено паралелно програмиране върху съвременните процесори в персоналните компютри, сървъри и ръчни/вградени устройства. Той е създаден за да позволи разработване на преносими приложения за системи с хетерогенни компютърни устройства. Под процесор се разбира не само *x86* базиран такъв, а и графичния ускорител, *DSP (Digital Signal Processor)*, *Cell Broadband Engine* и т.н. Стандартът е разработен и се поддържа от Khronos Group при участие на водещи фирми в областта на компютърната техника и електроника.

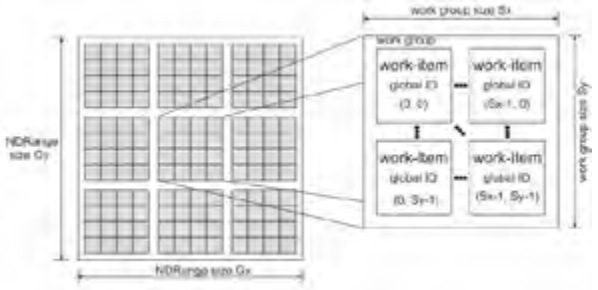
*OpenCL* представлява завършен *framework* състоящ се от езика *OpenCL C*, който поддържа паралелизма и *API* , което дава възможност приложението да използва едно или няколко устройства налични в системата и поддържащи *OpenCL*.

*OpenCL* има по-сложен модел на платформата и по-сложен модел за управление на устройствата, което се дължи на поддръжката на множество платформи и производители. Реализациите му вече съществуват за *AMD ATI* и *NVIDIA GPU*, както и за *x86* фамилията процесори. Също така се предвиждат бъдещи реализации за *DSP (Digital Signal Processor)* и *FPGA (Field-Programmable Gate Array)*. Сложността на програмирането с *OpenCL* се дължи точно на разнообразието на хардуера и в това, че много от съществуващи допълнения са специфични за конкретните устройства. Последното налага избягване на опционалните черти на платформата с цел създаване на истински платформено-независим преносим код. Също така поради изброените по-горе причини не трябва да се очаква, ще бъде постигната максималната производителност при всяко едно от използваните устройства




***Фиг. 1.*** *Архитектура на OpenCL*

*OpenCL* използва модела на паралелизма при дани, който директно съответства на този в *CUDA*. Програмите се състоят от две части: *kernel* функция, което се изпълнява върху едно или повече *OpenCL* устройства и *host* програма, която управлява изпълнението на *kernel* функциите. Предаването на работата за паралелно изпълнение става чрез зареждането на функциите от *host* програмата. След като ядрото е заредено кодът му се изпълнява от работни единици *(work items)*, които по същество представляват нишки.




***Фиг. 2.*** *NDRange и работни групи*

Използва динамичен модел на компилиране подобно на *OpenGL* и *DirectX*, т.е. компилирането на *OpenCL C* кода става преди той да се изпълни от изчислителното устройстово по време на изпълнение на програмата. Първоначално той се компилира до междинен код *(Intermediate Representation)*, а след което до машинен код на съответното устройство. Взаимодействието с *OpenCL* устройството се осигурява чрез драйвъри. За тази цел *AMD* осигурява библиотека от такива

наречена *AMD CAL (AMD Compute Abstraction Layer)*, която осигурява интефейс за съвместимост с устройствата, като едновременно с това се запазва възможностите за оптимизиране на кода [7][8].

### 4. Реализация на филтъра на OpenCL

Филтърът се реализирина с помощта на езика *C* и *OpenCL C* и се оптимизира за изпълнение върху *CPU*. Частта на филтъра, реализирана с помощта на *OpenCL* състои от двете *flux* функции, имплементирани като отделни *kernel* методи на *OpenCL C* и *kernel* фукнкция на самия анизотропен филтър.

Като вход на филтъра се използват цветни некомпресирани *BMP* изображения с дълбочина 8 бита.

Като целево устройство, върху което ще се изпълнява филтъра се разглежда *CPU*. Поради това се използва оптимизация с помощта на векторните типове (*uchar4* и *float4*), предлагани в *OpenCL* и организация на блоковете изпълняваните нишки по редове на изображението, като максималния брой нишки в една работна група е 256. Използването на векторти типове данни като *uchar4* и *float4* позволява едновременен достъп до всички цветови компоненти на пиксела [6].

### 5. Филтриране на изображения

В таблиците от 1 до 4 са представени резултати от филтриране на изображения с помощта на анизотропен филтър, като се изполва контрастно изображение на пръстов отпечатък и изображение на слънчево изригване.

***Таблица 1.*** *Анизотропно филтриране - exponential flux*



*Оригинал* *4 итерации* *8 итерации*

*16 итерации* *32 итерации* *64 итерации*

***Таблица 2.*** *Анизотропно филтриране - quadratic flux*



*Оригинал* *4 итерации* *8 итерации*

*16 итерации* *32 итерации* *64 итерации*

***Таблица 3.*** *Анизотропно филтриране - exponential flux*



*Оригинал* *4 итерации* *8 итерации*

*16 итерации* *32 итерации* *64 итерации*

***Таблица 4.*** *Анизотропно филтриране - quadratic flux*



*Оригинал* *4 итерации* *8 итерации*

*16 итерации* *32 итерации* *64 итерации*

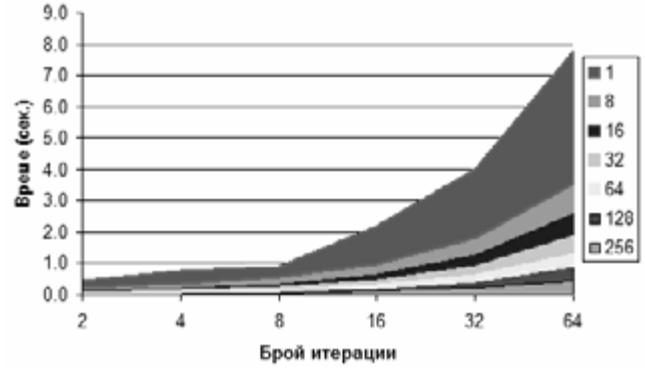
Във филтрираните изображения ясно се наблюдава запазване на контурите при използване на *quadratic flux*.

### 6. Производителност

За изследване на производителността на филтъра са използва предварително избрано изображение в *BMP* формат с размери 1024 x 1024 пиксела. Тестването на алгоритъма се осъществава върху *Intel Core i5* процесор който поддържа *SSE 4.1, SSE 4.2* и *AVX* инструкции за работа с вектори. Оптималния размер на работната група, която може ефективно да изпълнява операциите върху реда с пикселите на изображението е 256. В Таблицата 5 са представени времената на изпълнение на алгоритъма върху избраното изображение при различен брой итерации с намаляващ размер на работната група в намаляващ ред. Размерът на работната група = 1, който отбелязан на последния ред съотвества на 1 изпълнявана нишка, т.е. може да се разглежда като серийно изпълнение на алгоритъма, въпреки че се извършва чрез платформата *OpenCL*.

***Таблица 5.*** *Времена на изпълнение (сек.) на алгоритъма за брой итерации при определен размер на работната група (брой нишки)*

| | Брой итерации | | | | | |
|---|---|---|---|---|---|---|
| **WG** | **2** | **4** | **8** | **16** | **32** | **64** |
| **256** | 0.027 | 0.039 | 0.065 | 0.116 | 0.218 | 0.430 |
| **128** | 0.028 | 0.058 | 0.075 | 0.128 | 0.239 | 0.485 |
| **64** | 0.030 | 0.055 | 0.078 | 0.137 | 0.245 | 0.482 |
| **32** | 0.035 | 0.054 | 0.088 | 0.158 | 0.288 | 0.569 |
| **16** | 0.057 | 0.075 | 0.100 | 0.187 | 0.354 | 0.678 |
| **8** | 0.060 | 0.095 | 0.168 | 0.244 | 0.461 | 0.921 |
| **1** | 0.197 | 0.356 | 0.312 | 1.202 | 2.202 | 4.208 |




***Фиг. 3.*** *Времена на изпълнение (сек.) на алгоритъма за брой итерации при определен размер на работната група (брой нишки)*

Както се вижда от данните посочени в Таблицата 5 и представени на Фиг. 3 най-добри резултати от изпълнението се постигат при използване на работна група с размер 256.

### 7. Заключение

Методът за анизотропното филтриране на изображения е много близък като резултат до добре познатия Гаусов филтър, но поради използването на *flux* функция, която ограничава ефекта върху хомогенните региони и извършва подчертаването на границите между тези региони, той има определени предимства при премахване на шума и възстановяване на изображения.

Сложността на филтъра и респективно наличието на повече изпълними операции в него може да бъде успешно компенсирано чрез използване на съвременни платформи за паралелно програмиране като *OpenCL*. Дори и чрез използването им върху *CPU* се постигапълното използване на операциите върху вектори, които са ефективно реализирани в съвременните *CPU*.

### ЛИТЕРАТУРА


1. Perona, P. and J. Malik, *Scale-space and edge detection using anisotropic diffusion*, Proceedings, IEEE Computer Society workshop on Computer Vision, 1987, pp. 16-27
2. Black, M., G. Sapiro, D. Marimont, and D. Heeger, *Robust anisotropic diffusion*, IEEE Transactions on Image Processing Volume 7, PP 421-432, 1998
3. Datar M., *Anisotropic Diffusion*, University of Utah
4. Rafael C. Gonzalez Richard E. Woods (2002) *Digital Image Processing*, 2nd Edition, Prentice Hall
5. Al Bovik. (2004). *Handbook of image and video processing*, Academic Press. Canada.
6. David B. Kirk, Wen-mei W. Hwu *Programming Massively Parallel Processors*
7. Benedict Gaster, Lee Howes, *Heterogeneous Computing with OpenCL*
8. *OpenCL 1.2 Reference,* www.khronos.org



Department of Electrical Engineering
Technical University–Sofia, Branch Plovdiv
25 Tsanko Diustabanov St.
4000 Plovdiv
E-mail: garnevsky_dm@abv.bg

© International Scientific Conference on Engineering, Technologies and Systems
TECHSYS 2016, Technical University – Sofia, Plovdiv branch
26 – 28 May 2016, Plovdiv, Bulgaria

# КОД НА ХЕМИНГ И EXCEL ПРИЛОЖЕНИЕ ЗА ГЕНЕРИРАНЕ И КОДИРАНЕ

МАРИН ЦВЕТКОВ МАРИНОВ, ЛОРА ЛЮБОМИРОВА МАРИНОВА

**Резюме:** *Във връзка с по-удобното и надеждно представяне, обработка и съхранение на информацията в електронни устройства се използват различни кодирания, най-подходящи за съответните цели и операции. В настоящата разработка е разгледан код на Хеминг, който е пример за код с излишък, чието основно преимущество е откриване на грешки при предаване на данни и при определени условия, възможност за възстановяване на загубени данни. Представено е приложение на Excel за кодиране на двоични числа с код на Хеминг.*

**Ключови думи:** *машинни кодове, машинно представяне на данни, код на Хеминг, кодове с излишък, откриване на грешки, възстановяване на данни, бройни системи, булева алгебра, логически операции.*

# HAMMING CODE AND EXCEL APPLICATION FOR GENERATION AND ENCODE

MARIN MARINOV, LORA MARINOVA

**Abstract:** *In reference to the more convenient and reliable presentation, processing and storage of information in electronic devices different encodings are used according to the relevant objectives and operations. In this article is reviewed Hamming code, an example of redundant code, which main advantage is the detection of errors in data transmission and, under certain conditions, the potential to recover lost data. It is presented an Excel application for coding of binary code with Hamming code.*

**Key words:** *machine code, machine presentation of data, Hamming code, error-detecting codes, data recovery, numeral systems, Boolean algebra, logical operations.*

## 1. Въведение

Във връзка с по-удобното и надеждно представяне, обработка и съхранение на информацията в електронни устройства се използват различни кодирания, най-подходящи за съответните цели и операции. В настоящата разработка е разгледан код на Хеминг, който е пример за код с излишък, чието основно преимущество е откриване на грешки при предаване на данни и при определени условия, възможност за възстановяване на загубени данни.

„Ръчните" изчисления и операции в различни бройни системи са по-бавни, трудоемки и с повишена вероятност от грешки.

С представените приложения на Excel се кодират зададени или генерирани двоични числа в код на Хеминг. MS Excel е избран като стандартно, разпространено офис-приложение, съдържащо необходимите функции, математически апарат и с необходимите възможности за прегледно представяне на данните.

## 2. Теоретична обосновка

### 2.1. Контрол и корекция на информацията.

При четене, запис и предаване на информация има въздействия (шумове), които изкривяват и дори унищожават информацията. Шумовете са различни по произход и начин на

Copyright © 2016 by Technical University of Sofia, Plovdiv branch, Bulgaria ISSN Online: 2535-0048

въздействие: токови удари, електромагнитни въздействия, дефекти в носителите и др. Шумовете могат да се класифицират в две групи:

- детерминирани (определени). Отстраняват се чрез методи, които се залагат в апаратурите за запис и четене т.е. хардуерно;
- случайни. Появяването им има вероятностен характер. По принцип са неотстраними хардуерно. За отстраняването им се използва специално кодиране на информацията.

Откриването на грешки се гради върху идеята, че от всички кодови комбинации в даден код, N0, се използват само една част, N < N0. Използваните кодови комбинации се наричат разрешени, а неизползваните – забранени. Грешката се открива ако в резултат на шумовото въздействие от разрешена кодова комбинация се получи забранена.

Кодове за откриване на грешка, изискващи предаването на информацията по канала за връзка да бъде повторено, се наричат контролиращи кодове. Процесът по откриване на грешката и повторно предаване на информацията по канала за връзка в случай на грешка се нарича контрол на информацията.

Кодове, чрез които се коригира грешка се наричат коригиращи кодове. Това в общия случай се извършва без да е необходимо повторно предаване на информацията по канала за връзка. Процесът по откриване и корекция на грешката се нарича корекция на информацията. Тези кодове изискват по-голям излишък и се използват там, където средата е силно зашумена (малка е вероятността да бъде прочетена правилно информацията) и където се търси по-голямо бързодействие (няма време за повторно предаване).

Коригиращите и контролиращите кодове се делят на две групи:

- разделими, кодовата дума на които се дели на две полета (части) – информационно и контролно, които могат да се отделят.
- неразделими, кодовата дума няма отделни части.

### 2.2. Коригиращи кодове.

Важна характеристика на всеки код е т.н. **кодово разстояние, D,** което се изразява като различие между две кодови думи.

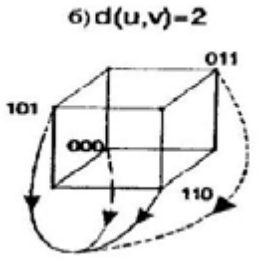
Най-разпространената мярка за разстояние между кодови думи е ***кодово разстояние по Хеминг***, което се дефинира като **разлика в съдържанието на разрядите на две кодови думи** – D(u, v).

Нека u=11010, а v=1**0**0**0**1 – вижда се, че разлика има в **три разряда** т. е. D(u, v)=3.

**Най-малката разлика в разрядите на две кодови думи (два кодови вектора) за цялото кодово пространство се дефинира като минимално кодово разстояние по Хеминг – Dmin. Този параметър показва ефикасността на кода за откриване и коригиране на грешки**.

Примери: Нагледен начин за представяне на кодовите думи е обемният, при който на всяка дума се съпоставя точка от "n" мерното пространство. Кодовите думи са разположени във върховете на куб.

А) $D_{min}$ = 1. Този код няма никаква възможност за откриване на грешка, защото при всяка грешка ще се попадне в друга разрешена комбинация.



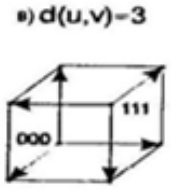

**Фиг. 1.**

**Таблица 1.**

| | | | | | | | | |
|---|---|---|---|---|---|---|---|---|
| X | 0 | 0 | 0 | 0 | 1 | 1 | 1 | 1 |
| Y | 0 | 0 | 1 | 1 | 0 | 0 | 1 | 1 |
| Z | 0 | 1 | 0 | 1 | 0 | 1 | 0 | 1 |

Б) $D_{min}$ = 2. От възможните 8 кодови думи са използвани 4, подбрани

така, че кодовото разстояние между две кои да е от тях да бъде 2. Този код има възможност за откриване на еднократна грешка, но не и за корекция.

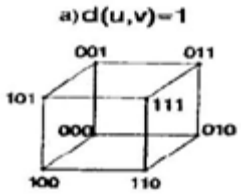



**Фиг.2.**

**Таблица 2**.

| | | | | |
|---|---|---|---|---|
| X | 0 | 0 | 1 | 1 |
| Y | 0 | 1 | 0 | 1 |
| | 0 | 1 | 1 | 0 |

В) $D_{min}$ = 3. От всички кодови комбинации са избрани 2. Съществува възможност за откриване на двукратна грешка и корекция на еднократна.




•

**Фиг.3**

Условието да бъде коригирана t-кратна грешка се дава чрез израза:

$$D_{min} \geq 2t+1, \quad (1)$$

• където t е кратността на грешката при корекция.

• Условието да бъде гарантирано откриването на t-кратна грешка се дава чрез израза:

$$D_{min} \geq t+1, \quad (2)$$

• където t е кратността на грешката при контрол.

### 2.3. Коригиране на грешка.

Коригирането на грешка първоначално изисква наличието на статистическите и аналитични изчисления, при каква максимална дължина на съобщението може да се получи не повече от една грешка.

За примера се приема, че при изпращането на съобщение с дължина 20 или по-малко нули и единици е възможно само на едно единствено място да се получи грешка. Нулата да бъде заменена с единица или обратно. Изключва се възможността за две и повече грешки.

Ако съобщението се състои от 4bit-а, въпросът е: „***Може ли да се допълни четири-символното съобщение с допълнителна информация, с която да се установи има ли грешка и ако има – да се поправи?***"

Един от възможните начини е три пъти да се изпрати съобщението с дължина 4bit.

**Таблица 3**. *Информативна част на съобщението*

| 1 | 2 | 3 | 4 |
|---|---|---|---|
| 0 | 1 | 1 | 1 |

**Таблица 4**. *Изпратено кодирано съобщение*

| 1 | 2 | 3 | 4 | 5 | 6 | 7 | 8 | 9 | 10 | 11 | 12 |
|---|---|---|---|---|---|---|---|---|---|---|---|
| 0 | 1 | 1 | 1 | 0 | 1 | 1 | 1 | 0 | 1 | 1 | 1 |

Полученото съобщение е с дължина 12 и в него е възможна една грешка, например в девета позиция.

**Таблица 5.**

| 1 | 2 | 3 | 4 | 5 | 6 | 7 | 8 | 9 | 10 | 11 | 12 |
|---|---|---|---|---|---|---|---|---|---|---|---|
| 0 | 1 | 1 | 1 | 0 | 1 | 1 | 1 | 1 | 1 | 1 | 1 |

За да се коригира грешката, съобщението се разделя на три части и се подреждат една под друга.

**Таблица 6.**

| 1 | 2 | 3 | 4 |
|---|---|---|---|
| 0 | 1 | 1 | 1 |
| 0 | 1 | 1 | 1 |
| 1 | 1 | 1 | 1 |
| 0 | 1 | 1 | 1 |

Грешка при предаването се открива, когато два от символите в колоната съвпадат, а третия се различава, както е в първа позиция. Правилният символ се среща два пъти – в случая нула.

### 2.4. Код на Хеминг.

Хеминг е открил код с минимална дължина на съобщението, което трябва да бъде изпратено, за да се открият и коригират грешките.

Ричард Уесли Хеминг (1915 –1998) започва изследователската си кариера в лабораторията на Бел, където открива коригиращия грешките код, носещ неговото име.

Кодът на Хеминг е един от най-известните систематични кодове за коригиране на единични грешки и има минимално кодово разстояние $d_{min}=3$.

Кодът на Хеминг се строи по такъв начин, че към началните информационни разряди се добавят известен брой контролни разряди, които се формират преди предаване на информацията на базата на определяне на четността на сумата на единиците в съответни групи информационни разряди.

След приемане на информацията контролната апаратура образува от получените информационни и контролни разряди т.нар. коригиращо число на базата на аналогично преброяване на единиците. При липса на грешка коригиращото число е равно на нула. При грешка стойността му посочва мястото на грешката - двоичния номер на грешния разряд в думата. Грешният разряд автоматично се коригира чрез инвертиране на стойността му.

#### 2.4.1. Кодиране с код на Хеминг.

Кодът на Хеминг е с $D_{min}=3$ и следователно може да открива двукратни грешки и да коригира еднократни.

**Таблица 7.**

| | | k1 | k2 | k3 | k4 | n | 2^n |
|---|---|---|---|---|---|---|---|
| 0 | 00000000 | | | | | 0 | 1 |
| 1 | 00000001 | x | | | | 1 | 2 |
| 2 | 00000010 | | x | | | 2 | 4 |
| 3 | 00000011 | x | x | | | 3 | 8 |
| 4 | 00000100 | | | x | | 4 | 16 |
| 5 | 00000101 | x | | x | | 5 | 32 |
| 6 | 00000110 | | x | x | | 6 | 64 |
| 7 | 00000111 | x | x | x | | 7 | 128 |
| 8 | 00001000 | | | | x | 8 | 256 |
| 9 | 00001001 | x | | | x | | |
| 10 | 00001010 | | x | | x | | |
| 11 | 00001011 | x | x | | x | | |
| 12 | 00001100 | | | x | x | | |
| 13 | 00001101 | x | | x | x | | |
| 14 | 00001110 | | x | x | x | | |
| 15 | 00001111 | x | x | x | x | | |
| 16 | 00010000 | | | | | | |

При кодирането трябва да се получат контролните разряди. Те се намират в позициите на думата W*, които са точни степени на 2 / $2^0$=1поз., $2^1$=2поз, $2^2$=4поз и т.н./. Контролните разряди се получават като се приравнят горните изрази на "0" и се изразят членовете, точни степени на 2 / $W_1$, $W_2$, $W_4$, $W_8$…./.

$к_1 \rightarrow W_1 = W_3 \oplus W_5 \oplus W_7 \oplus W_9 \oplus \ldots$ всички разряди през един;

$к_2 \rightarrow W_2 = W_3 \oplus W_6 \oplus W_7 \oplus W_{10} \oplus \ldots$ всички разряди през 2 по 2;

$к_3 \rightarrow W_4 = W_5 \oplus W_6 \oplus W_7 \oplus W_{12} \oplus W_{13} \oplus \ldots$ всички разряди през 4 по 4

$к_4 \rightarrow$ всички разряди през 8 по 8

Броят на контролните разряди "к" зависи от броя на информационните разряди "n" и се изчислява по формулата:

$$2^k \geq n + к + 1 \qquad (3)$$

Позициите на контролните разряди са строго фиксирани.

### 2.4.2. Пример - кодиране:

Информативната част на съобщението е с дължина n=4. От формулата се изчислява, че $2^3 \geq 4 + 3 + 1$, изпратеното съобщение ще е с дължина m=7. Същото се вижда и от табл. 7.

Позициите с номера, които не са степени на две (3, 5, 6, 7) са за самото съобщение, а позициите с номера степените на двойката (1, 2, 4) са служебни.

---

Попълват се позициите за съобщението, а служебните остават свободни:

**Таблица 8.**

| 1 | 2 | 3 | 4 | 5 | 6 | 7 |
|---|---|---|---|---|---|---|
| | | 0 | | 1 | 1 | 1 |

---

Построява се матрица представляваща числата от 1 до 7 в двоична бройна система (извадка от табл. 7). Това са трибуквени думи от азбуката {0,1} , подредени лексикографски (както в речник). Номерата на редовете са отляво.

**Таблица 9.**

| | | | |
|---|---|---|---|
| 1 | 0 | 0 | 1 |
| 2 | 0 | 1 | 0 |
| 3 | 0 | 1 | 1 |
| 4 | 1 | 0 | 0 |
| 5 | 1 | 0 | 1 |
| 6 | 1 | 1 | 0 |
| 7 | 1 | 1 | 1 |

---

**Таблица 10.**

Редът с номер 1 е равен на сумата по модул две от трите реда с номера 3 , 5 и 7; [1]=[3] ⊕ [5] ⊕ [7], защото (001)= (011) ⊕ (101) ⊕ (111).

$$\begin{array}{rc} & 0\ 1\ 1 \\ \oplus & 1\ 0\ 1 \\ \hline & 1\ 1\ 0 \\ \oplus & 1\ 1\ 1 \\ \hline & 0\ 0\ 1 \end{array}$$

С аналогични изчисления проверяваме, че:

[2]=[3] ⊕ [6] ⊕ [7] ⇔ (010)= (011) ⊕ (110) ⊕ (111)

[4]=[5] ⊕ [6] ⊕ [7] ⇔ (100)= (101) ⊕ (110) ⊕ (111)

---

Сега служебната позиция с номер 1, по подобие на равенството [1]=[3] ⊕ [5] ⊕ [7] се попълва със сума по модул две от числата, стоящи на позиции 3, 5 и 7: 0 ⊕ 1 ⊕ 1=0

**Таблица 11.**

| 1 | 2 | 3 | 4 | 5 | 6 | 7 |
|---|---|---|---|---|---|---|
| 0 | | 0 | | 1 | 1 | 1 |

---

Позицията с номер 2, по подобие на равенството [2]=[3] ⊕ [6] ⊕ [7] се попълва със сумата от числата, стоящи на позиции 3, 6 и 7: 0 ⊕ 1 ⊕ 1=0

**Таблица 12.**

| 1 | 2 | 3 | 4 | 5 | 6 | 7 |
|---|---|---|---|---|---|---|
| 0 | 0 | 0 | | 1 | 1 | 1 |

---

Позицията с номер 4, по подобие на равенството [4]=[5]⊕[6]⊕[7] се попълва със сумата от числата, стоящи на позиции 5, 6 и 7: 1⊕1⊕1=1

**Таблица 13.**

| 1 | 2 | 3 | 4 | 5 | 6 | 7 |
|---|---|---|---|---|---|---|
| 0 | 0 | 0 | 1 | 1 | 1 | 1 |

**Това е кодираното съобщение.**

### 2.4.3. Декодиране на код на Хеминг.

**При декодирането** се образува двоично число "А", наречено контролно. Ако "А" е "0"- няма грешка, ако е различно от нула-показва позицията, в която има грешка.

Разрядите на контролното число се получават с помощта на операцията сума по модул 2 от разрядите на получената по канала за връзка дума W*, като се използва определен алгоритъм.

**Алгоритъм за получаване на контролното число А**=$a_1$ $a_2$ $a_3$ ……..$a_k$ от кодовата дума W*=$W_1$

$W_2$…….$Wl_{-1}$ $W_l$:

$a_1=W_1 \oplus W_3 \oplus W_5 \oplus W_7 \oplus W_9 \oplus$ ……всички разряди през един;

$a_2=W_2 \oplus W_3 \oplus W_6 \oplus W_7 \oplus W_{10} \oplus$…… всички разряди през 2 по 2;

$a_3=W_4 \oplus W_5 \oplus W_6 \oplus W_7 \oplus W_{12} \oplus W_{13} \oplus$… всички разряди през 4 по 4

$a_4=W_8 \oplus W_9 \oplus W_{10} \oplus$…… всички разряди през 8 по 8;

.

. $a_k$

Получават се "к" равенства, така се получават всички разряди на числото "А".

### 2.4.4. Пример - декодиране:

При получаването на данните се извършва проверка по правилата

[1]=[3] ⊕ [5] ⊕ [7]  [2]=[3] ⊕ [6] ⊕ [7]  [4]=[5] ⊕ [6] ⊕ [

за контролните позиции и ако и трите равенства са изпълнени кодираното съобщение е прието вярно.

Но интересното е, че ако не е така, може да се намери позицията, в която има грешка. Ако например е сгрешен 5-ти bit и вместо 1 е получена 0.

**Таблица 14.**

| 1 | 2 | 3 | 4 | 5 | 6 | 7 |
|---|---|---|---|---|---|---|
| 0 | 0 | 0 | 1 | 0 | 1 | 1 |

**Таблица 15.** *Извършва се проверка на контролните позиции по познатото правило.*

| 1 | 2 | 3 | 4 | 5 | 6 | 7 |
|---|---|---|---|---|---|---|
| 0 | 0 | 0 | 1 | 0 | 1 | 1 |
| 1 | 0 | | 0 | | | |

Намира се сумата по модул 2 на съдържанията на получените и изчислените контролни позиции.

**Таблица 16.**

| | | | |
|---|---|---|---|
| ⊕ | 0 | 0 | 1 |
| | 1 | 0 | 0 |
| | 1 | 0 | 1 |

**Обръщат се получените цифри** ( в случая числото е същото) – 101 **и това е номерът на сгрешената позиция в двоична бройна система**.

$101_{(2)} = 5_{(10)}$ - Грешната позиция е с номер 5 и информативното съобщение не е 0011 а 0111.

Пример за декодиране и откриване на грешка в полученото съобщение:

**Таблица 17.**

| 1 | 2 | 3 | 4 | 5 | 6 | 7 |
|---|---|---|---|---|---|---|
| 0 | 0 | 0 | 1 | 1 | 0 | 1 |
| 0 | 1 | | 0 | | | |

**Таблица18.**

| | | | |
|---|---|---|---|
| + | 0 | 0 | 1 |
| | 0 | 1 | 0 |
| | 0 | 1 | 1 |

Изчислените контролни суми и сумата от съдържанията на контролните позиции показват, че грешното число е $110_{(2)} = 6_{(10)}$ в десетична бройна система. Там е грешката и информативното съобщение е 0111.

**Това е направил Ричард Уесли Хеминг!**

### 2.5. Интегрални схеми, реализиращи код на Хеминг

Съществуващите интегрални схеми, реализиращи код на Хеминг, могат да се разделят според разрядността си:

- 8 битови - 74636 и 74637;
- 16 битови - 74616, 74617, 74630 и 74631;
- 32 битови - 74632, 74633, 74634 и 74635.

### 2.6. Приложение на кода на Хеминг

Кодът на Хеминг се използва за контрол и корекция на грешки в запомнящия масив на ОП на компютрите**. При запис** в масива информацията се кодира, т.е. към нея се добавя **k**-разрядна контролна дума, която се записва заедно с основната. **При четене** на n-разрядната дума от паметта се извършва декодиране, при което се коригират единичните грешки, а двойните се откриват.

## 3. Приложение на EXCEL за работа с кодове на Хеминг.

С приложението на Excel се решават следните типове задачи:

1) Изчислява се колко бита е дължината на кодирано съобщение по зададен брой информационни битове.
2) Кодират се зададени числа с код на Хеминг.
3) Проверяват се кодирани числа съдържат ли грешка.




**Фиг. 4**

За да се генерират нови стойности се посочва между етикети на редове или колони и когато показалецът на мишката е като на картината - вертикална чертичка с разнопосочни хоризонтални стрелки - се кликва с ляв бутон на мишката.




**Фиг. 5** Кодиране с код на Хеминг на двоично число въведено в зелените клетки.

Таблицата за генериране на числа е съставена от еднотипни блокове. Относителните адреси са зададени, така че в зависимост от необходимостта може да се генерират неограничен брой числа и кодове, а информацията за междинните операции в решението може да бъде визуализирана или скрита.




**Фиг. 6**

## 4. Заключение

Представената разработка синтезира и доразвива съществуващата информация по темата. Демонстрират се основните идеи, принципи и стъпки при теоретичната обосновка, кодирането и възможностите за коригиране на грешки в предадените данни.

Приложенията са създадени на базата на практическата необходимост за решаване и анализиране на изброените типове задачи.

## ЛИТЕРАТУРА


1. Гарванов, Ив. (2014). *Компютърни архитектури.* София.
2. Мюллер, Скотт. (2011). *Модернизация и ремонт ПК*. изд. "И. Д. Вильямс", 19-е издание. Москва.
3. Романски, Р. и Нониска, Ир. (2010). *Информатика (информационна техника, системи и технологии).* Издателство на Технически университет – София. София.
4. Романски, Р. и Недев, С. (2009). *Ръководство за лабораторни упражнения по Основи на компютърната техника*. изд. „Кинг”.
5. Таненбаум, Э. и Остин, Т. (2013). *Архитектура компьютера.* изд. "Пиер", 6-е издание. Москва.
6. Хеминг, Р.В. (1983). *Теория кодирования и теория информации.* изд. „Радио и связь”. Москва.



Контакти
E-mail: m.marinov1516@gmail.com
E-mail: lek_iv5@abv.bg

© International Scientific Conference on Engineering, Technologies and Systems
TECHSYS 2016, Technical University – Sofia, Plovdiv branch
26 – 28 May 2016, Plovdiv, Bulgaria

# ОБОБЩЕНО МРЕЖОВ МОДЕЛ ЗА ИЗСЛЕДВАНЕ НА ПОВЕДЕНИЕ НА СЪТРУДНИЧЕСТВО МЕЖДУ ИНТЕЛИГЕНТНИ ВИРТУАЛНИ АГЕНТИ

ДИЛЯНА БУДАКОВА, РУМЕН ТРИФОНОВ, НИКОЛА ЦАЙКИН

**Резюме:** *В тази статия се представя обобщено мрежов модел (ОММ) за изследване поведение на сътрудничество между интелигентни виртуални агенти (ИВА). ОММ е съставен от три подмрежи: за извличане на правилата на сценария и когнитивен анализ; за планиране и анализ; и за изпълнение на задачите според направения план. Експериментите показват, че когато ИВА се съобразяват с плановете си успяват да ги реализират и предотвратяват възникването на конфликтни ситуации.*

**Ключови думи:** *сътрудничество, интелигентни виртуални агенти, обобщени мрежи*

# GENERALIZED NET MODEL FOR COOPERATIVE BEHAVIOR INVESTIGATION BETWEEN INTELLIGENT VIRTUAL AGENTS

DILYANA BUDAKOVA, RUMEN TRIFONOV, NIKOLA TSAIKIN

**Abstract:** *This paper presents a generalized net model (GNM) for studying the behavior of collaboration (cooperation) between intelligent virtual agents (IVA). The model is composed of two sub-nets for: deriving the rules of the scenario and cognitive analysis; executing the tasks in accordance with the plan. The experiments show that when the IVA follow their plans, they manage to realize them and to prevent themselves from conflict situations occurrence.*

**Key words:** *cooperative behavior, intelligent virtual agents, generalized net, cognitive*

## 1. Въведение

Редица източници посочват, важността да се разберат основните и спомагателните механизми, които играят роля и благоприятстват процеса на сътрудничество между хората и групите от хора. [2,3,5,9]. Съществуват емпирични изследвания, които потвърждават, че основни фактори, който карат хората да си сътрудничат са страхът от наказание, очакванията, че ще постигнат по-големи печалби заедно [2,3], хуманното желание да помогнат. Сътрудничество и конкуренция между групи хора може да се наблюдава в академичните изследователски екипи, в армията, при спортните отбори и др.[9].

При моделирането на интелигентни виртуални агенти (ИВА) също целта е да се изгради доверие и сътрудничество между ИВА и потребителите [6,7,8,10,15]. ИВА са програмно реализирани, автономни агенти, с графично построено човешко лице (често и тяло) и съществуват в 2D или 3D виртуална среда [11]. Те притежават възможности интелигентно да взаимодействат със заобикалящата ги среда в това число както и с други ИВА, така и с потребителите на съответното програмно приложение.

В тази статия се представя обобщено мрежов модел (ОММ) на програмна система със сценарий за изследване на поведение на сътрудничество между ИВА с когнитивна PRE-ThINK архитектура [4]. Системата поддържа релационна база данни и база знания. Компонентите на PRE-ThINK архитектурата принципи, наблюдения и знания се реализират по

Copyright © 2016 by Technical University of Sofia, Plovdiv branch, Bulgaria ISSN Online: 2535-0048

процедурен и декларативен начин, докато компонентите мисли, действия, емоции, потребности и рационалност се представят с релационна база данни със съответните таблици и релации между тях. Този начин на представяне позволява лесно да се добавят или изтриват: действия за решаване на проблемна ситуация; мисли за всяко възможно действие; аргументи за всяка мисъл; емоционални, рационални и потребностни оценки за всяка релация „мисъл-действие“.

## 2. Сценарий и възможности за моделиране

Според предложения в [4] сценарий два ИВА са моделирани да бъдат в ролята на студенти, които едновременно с това работят във фирма. Те имат определен брой задачи с различна сложност всеки ден. ИВА могат да получат бонус ако успеят да изпълнят точно определен брой сложни задачи. За да им остане достатъчно време за изпитите и срещите с приятели, те трябва да изпълнят норматива си с лесни задачи. Тези конфликтни ситуации предизвикват смесени емоции у ИВА и те трябва да намерят възможно най-доброто решение.

Обобщените мрежи са гъвкав и подходящ математически апарат за моделиране [1]. Големите възможности и свобода, които предлагат, са причина да бъдат предпочитани и да бъдат избрани тук за моделирането на поведение на сътрудничество между ИВА.

Един алтернативен модел, който бихме искали да построим и да сравним с предложения тук е Бейсов мрежов модел за изследване на сътрудничество между ИВА. При Бейсовите мрежови модели [12,13] основна роля играят причинно-следствените връзки, но разбирането точно какво се случва не е пълно и е необходимо ситуацията да се опише с вероятности. Когато е необходимо да се предсказват събития, които се развиват във времето, чрез други събития, които се наблюдават пряко може да се построят скрити вероятностни Марковски модели [14]. Всеки алтернативен модел помага да се изгради различна представа за разглеждания проблем и да се видят негови предимства и недостатъци от различна гледна точка [10,15].

## 3. Обобщен мрежов модел за изследване на поведение на сътрудничество между ИВА

Обобщеният мрежов модел за изследване на поведение на сътрудничество между ИВА, предложен тук, се представя с множеството A преходи на мрежата: $A= \{r_1, r_2, r_3, r_4, r_{p1}, r_{p2}, r_{p3}, r_{z1}, r_{z2}, r_{z3}\}$.

Приема се, че поведението на ИВА в този конкретен сценарий е последователност от три основни етапи представени с три подмрежи: Подмрежа 1 (фиг.1) е ОММ за извличане на правила за вземане на решения, който се реализира с преходите: $r_1$ – хипотетичен избор на един от ИВА на лесна или трудна задача, $r_2$ – хипотетичен избор на втория ИВА на лесна или трудна задача за деня на базата на избора на първия агент, $r_3$ – извличане на правилата според зададената от сценария матрица с печалбите и загубите (PayOff Matrix), $r_4$ – PRE-ThINK когнитивен анализ на ситуацията и избор на най-доброто решение; Обратните връзки в преходите позволяват многократно хипотетично обхождане на всички варианти на избор на трудни или лесни за реализиране задачи от ИВА в съответствие с ангажиментите, които е възможно да имат.

Извлечените по този начин правила и планирани действия се преобразуват до мисли оценени от емоционална, рационална и потребностна гледна точка. След анализа се избира и се предприема най-добрия вариант за действие в съответствие с текущите приоритети на ИВА. Променя се емоционалното състояние на агента и се генерират мисли към другия агент. Те могат да са мисли на благодарност, одобрение или молба за преразглеждане на избраното действие, укор и други. Обучение на ИВА може да се реализира когато ИВА самостоятелно построяват матрицата на печалбите и загубите за даден сценарий или разширяват, съкращават и редактират стойностите и. Тази матрица се реализира чрез предикатите дадени на (фиг.2). PRE-ThINK анализ се реализира с предикатите на преход $r_4$ : $w_{10\ 16}$, $w_{11\ 16}$, $w_{12\ 12}$, $w_{13\ 13}$, $w_{14\ 14}$, $w_{15,15}$

Подмрежа 2 (фиг.3 ) представлява ОММ за планиране на задачите за седмицата, който се реализира с преходите: $r_{p1}$ – преход за споделяне на ангажиментите през седмицата , $r_{p2}$ – преход за предварително преразпределяне на задачите за следващата седмица според откритите конфликтни ситуации, $r_{p3}$ – преход за проверка дали има още дни от седмицата с конфликтни ситуации. Ако има то отново се активира преход $r_{p2}$, иначе се преминава към Подмрежа 3. Планирането на седмичното натоварване се реализира с предикатите представени на (фиг. 4).

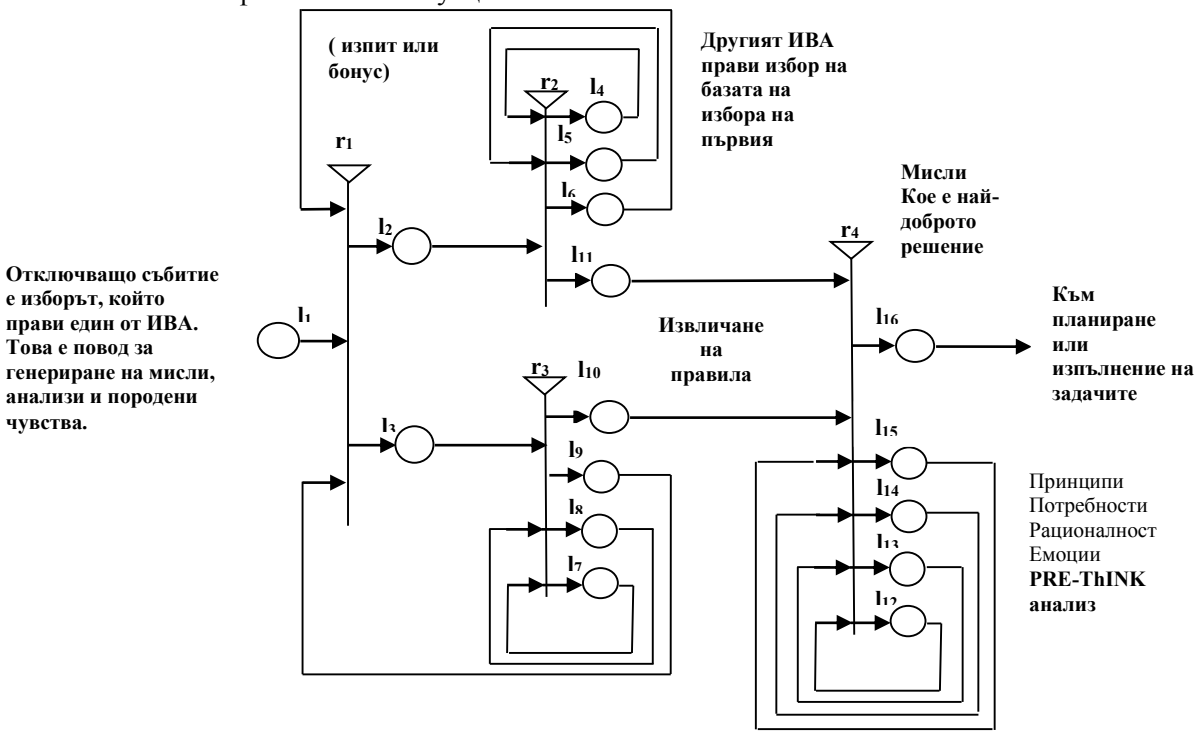
Подмрежа 3 (фиг. 5) е ОММ за реализиране на задачите през седмицата според направения от Подмрежа 2 план.Този ОММ включва преходите: $r_{z1}$ – ИВА получават най-оптималният план за разпределение на задачите за седмицата, $r_{z2}$ – избор на задача за изпълнение и проверка за край на задачите от списъка със задачи за текущия ден.

$r_{z3}$ – преход за изпълнение на избраната задача. Преходите са синхронизирани по време с ОММ за протичане на времето. Съхранява се историята на изпълнените задачи. Реализира се обратна връзка към същия преход до приключване на изпълнението на съответната задача или към предишния преход до приключване на задачите за седмицата. Има връзка с ОММ за когнитивен PRE-ThINK анализ. За целите на този модел подмрежа 3 се реализира с предикатите описани на (фиг.6).

## 4. Външни и вътрешни ядра в предложения ОММ.

Мислите на агента относно: анализа на възникналите конфликтни ситуации и възможностите за решаването им; мислите относно състоянието и желанията на ИВА; ангажиментите на ИВА за седмицата; задачите за изпълнение; ще наречем външни ядра. Моделът позволява да се реализира конкуренция и взаимодействие между ядрата-мисли, между ядрата-ангажименти и ядрата-задачи на ИВА.

Всяка система има индивидуални знания, които определят възможностите и за анализ на ситуацията. Ролята на притежаваните от конкретната система знания при етапите на анализ се моделира чрез включването на съответната обратна връзка и вътрешните ядра.




***Фиг. 1.*** *Подмрежа 1. Обобщено мрежов модел на матрицата, която представя печалбите и загубите, които ще имат ИВА при избор на действие според сценария.. Реализира се анализ на ситуацията, извличане на правило, когнитивен анализ и вземане на решение за избор на действие.*

$r_1$ =

| | $l_2$ | $l_3$ |
|---|---|---|
| $l_1$ | $w_{1\,2}$ | $w_{1\,3}$ |
| $l_6$ | $w_{6\,2}$ | false |
| $l_9$ | false | $w_{9\,3}$ |

фиг. 4а

$r_2$ =

| | $l_4$ | $l_5$ | $l_6$ | $l_{11}$ |
|---|---|---|---|---|
| $l_2$ | $w_{2\,4}$ | $w_{2\,5}$ | $w_{2\,6}$ | false |
| $l_4$ | false | $w_{4\,5}$ | $w_{4\,6}$ | $w_{4\,11}$ |
| $l_5$ | $w_{5\,4}$ | false | $w_{5\,6}$ | $w_{5\,11}$ |

фиг. 4а

$r_3$ =

| | $l_7$ | $l_8$ | $l_9$ | $l_{10}$ |
|---|---|---|---|---|
| $l_3$ | $w_{3\,7}$ | $w_{3\,8}$ | $w_{3\,9}$ | false |
| $l_7$ | false | $w_{7\,8}$ | $w_{7\,9}$ | $w_{7\,10}$ |
| $l_8$ | $w_{8\,7}$ | false | $w_{8\,9}$ | $w_{8\,10}$ |

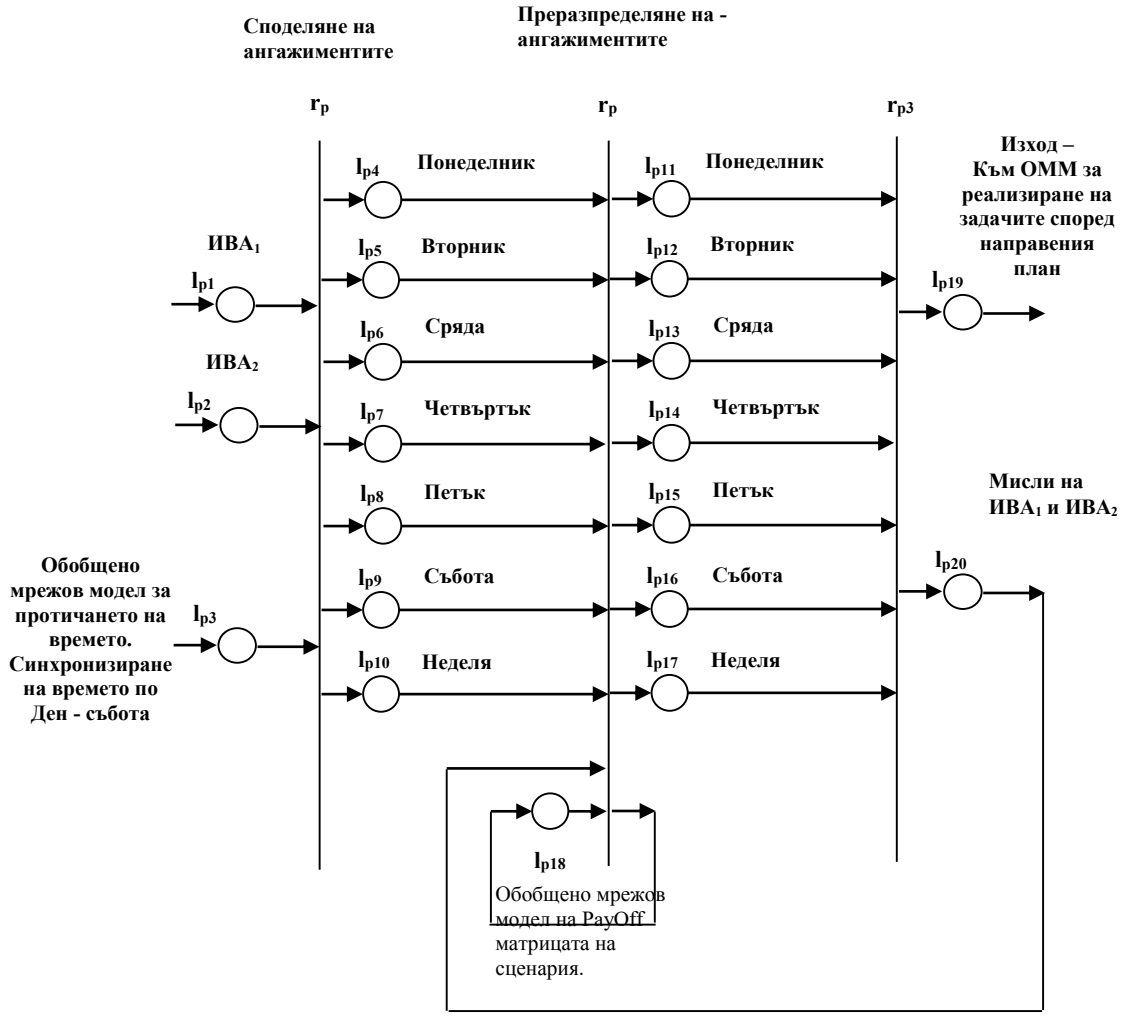
фиг. 4а

$r_4$ =

| | $l_{12}$ | $l_{13}$ | $l_{14}$ | $l_{15}$ | $l_{16}$ |
|---|---|---|---|---|---|
| $l_{10}$ | false | false | false | false | $w_{10\,16}$ |
| $l_{11}$ | false | false | false | false | $w_{11\,16}$ |
| $l_{12}$ | $w_{12\,12}$ | false | false | false | false |
| $l_{13}$ | false | $w_{13\,13}$ | false | false | false |
| $l_{14}$ | false | false | $w_{14\,14}$ | false | false |
| $l_{15}$ | false | false | false | $w_{15\,15}$ | false |

фиг. 4а

***Фиг. 2.*** *Индексирани матрици на преходите на подмрежа 1. ОММ на матрицата за печалби и загуби (PayOff matrix) на сценария*




***Фиг. 3.*** *Подмрежа 2. Обобщено мрежов модел за планиране на ангажиментите за седмицата от ИВА1 и ИВА2, така че да се предотвратят конфликтите на работното място.*

$r_{p1}$ =

| | $l_{p4}$ | $l_{p5}$ | $l_{p6}$ | $l_{p7}$ | $l_{p8}$ | $l_{p9}$ | $l_{p10}$ |
|---|---|---|---|---|---|---|---|
| $l_{p1}$ | $W_{p1\ p4}$ | $W_{p1\ p5}$ | $W_{p1\ p6}$ | $W_{p1\ p7}$ | $W_{p1\ p8}$ | $W_{p1\ p9}$ | $W_{p1\ p10}$ |
| $l_{p2}$ | $W_{p2\ p4}$ | $W_{p2\ p5}$ | $W_{p2\ p6}$ | $W_{p2\ p7}$ | $W_{p2\ p8}$ | $W_{p2\ p9}$ | $W_{p2\ p10}$ |
| $l_{p3}$ | $W_{p3\ p4}$ | $W_{p3\ p5}$ | $W_{p3\ p6}$ | $W_{p3\ p7}$ | $W_{p3\ p8}$ | $W_{p3\ p9}$ | $W_{p3\ p10}$ |

фиг. 6а

$r_{p3}$ =

| | $l_{p19}$ | $l_{p20}$ |
|---|---|---|
| $l_{p11}$ | $W_{p11\ p19}$ | $W_{p11\ p20}$ |
| $l_{p12}$ | $W_{p12\ p19}$ | $W_{p12\ p20}$ |
| $l_{p13}$ | $W_{p13\ p19}$ | $W_{p13\ p20}$ |
| $l_{p14}$ | $W_{p14\ p19}$ | $W_{p14\ p20}$ |
| $l_{p15}$ | $W_{p15\ p19}$ | $W_{p15\ p20}$ |
| $l_{p16}$ | $W_{p16\ p19}$ | $W_{p16\ p20}$ |
| $l_{p17}$ | $W_{p17\ p19}$ | $W_{p17\ p20}$ |

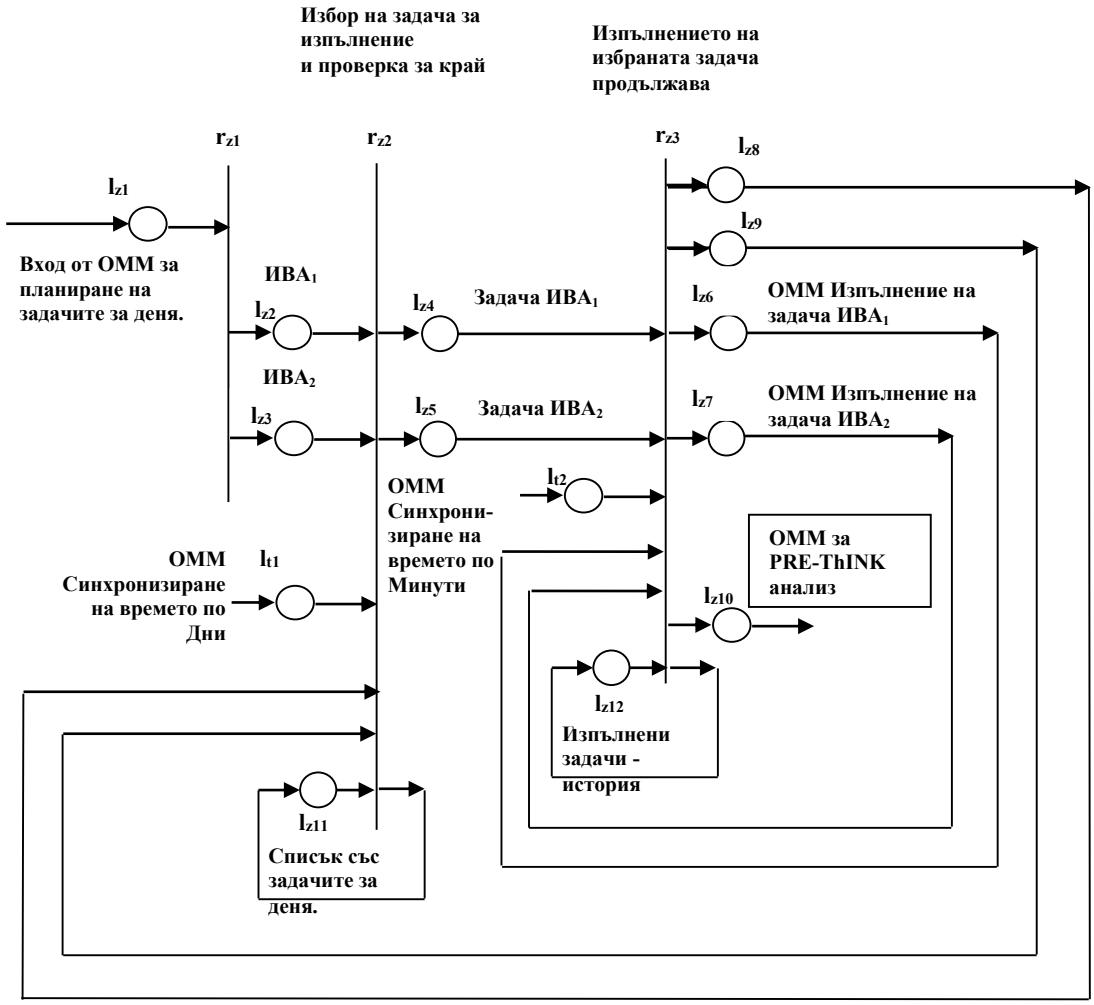
фиг. 6в

$r_{p2}$ =

| | $l_{p11}$ | $l_{p12}$ | $l_{p13}$ | $l_{p14}$ | $l_{p15}$ | $l_{p16}$ | $l_{p17}$ | $l_{p18}$ |
|---|---|---|---|---|---|---|---|---|
| $l_{p4}$ | $W_{p4\ p11}$ | $W_{p4\ p12}$ | $W_{p4\ p13}$ | $W_{p4\ p14}$ | $W_{p4\ p15}$ | $W_{p4\ p16}$ | $W_{p4\ p17}$ | false |
| $l_{p5}$ | $W_{p5\ p11}$ | $W_{p5\ p12}$ | $W_{p5\ p13}$ | $W_{p5\ p14}$ | $W_{p5\ p15}$ | $W_{p5\ p16}$ | $W_{p5\ p17}$ | false |
| $l_{p6}$ | $W_{p6\ p11}$ | $W_{p6\ p12}$ | $W_{p6\ p13}$ | $W_{p6\ p14}$ | $W_{p6\ p15}$ | $W_{p6\ p16}$ | $W_{p6\ p17}$ | false |
| $l_{p7}$ | $W_{p7\ p11}$ | $W_{p7\ p12}$ | $W_{p7\ p13}$ | $W_{p7\ p14}$ | $W_{p7\ p15}$ | $W_{p7\ p16}$ | $W_{p7\ p17}$ | false |
| $l_{p8}$ | $W_{p8\ p11}$ | $W_{p8\ p12}$ | $W_{p8\ p13}$ | $W_{p8\ p14}$ | $W_{p8\ p15}$ | $W_{p8\ p16}$ | $W_{p8\ p17}$ | false |
| $l_{p9}$ | $W_{p9\ p11}$ | $W_{p9\ p12}$ | $W_{p9\ p13}$ | $W_{p9\ p14}$ | $W_{p9\ p15}$ | $W_{p9\ p16}$ | $W_{p9\ p17}$ | false |
| $l_{p10}$ | $W_{p10\ p11}$ | $W_{p10\ p12}$ | $W_{p10\ p13}$ | $W_{p10\ p14}$ | $W_{p10\ p15}$ | $W_{p10\ p16}$ | $W_{p10\ p17}$ | false |
| $l_{p18}$ | false | false | false | false | false | false | false | $W_{p18\ p18}$ |
| $l_{p20}$ | $W_{p20\ p11}$ | $W_{p20\ p12}$ | $W_{p20\ p13}$ | $W_{p20\ p14}$ | $W_{p20\ p15}$ | $W_{p20\ p16}$ | $W_{p20\ p17}$ | false |

фиг. 6б

***Фиг. 4.*** *Индексирани матрици на преходите на подмрежа 2 за планиране на ангажиментите за седмицата на ИВА*




***Фиг. 5.*** *Подмрежа 3. Обобщено мрежов модел на подмрежата за изпълнение на задачите за всеки ден според направения план. След всяка изпълнена задача и след изпълнението на задачите за деня се прави анализ-равносметка на текущата ситуация от ИВА1 и ИВА2 с помощта на възможностите, които предоставя PRE-ThINK когнитивният анализ.*

$r_{z1}$ =

| | $l_{z2}$ | $l_{z3}$ |
|---|---|---|
| $l_{z1}$ | $w_{z1\ z2}$ | $w_{z1\ z3}$ |

фиг. 8а

$r_{z2}$ =

| | $l_{z4}$ | $l_{z5}$ | $l_{z11}$ |
|---|---|---|---|
| $l_{z2}$ | $w_{z2\ z4}$ | false | false |
| $l_{z3}$ | false | $w_{z3\ z5}$ | false |
| $l_{t1}$ | $w_{t1\ z4}$ | $w_{t1\ z5}$ | false |
| $l_{z8}$ | $w_{z8\ z4}$ | false | false |
| $l_{z9}$ | false | $w_{z9\ z5}$ | false |
| $l_{z11}$ | false | false | $w_{z11\ z11}$ |

фиг. 8б

$r_{r3}$ =

| | $l_{z6}$ | $l_{z7}$ | $l_{z8}$ | $l_{z9}$ | $l_{z10}$ | $l_{z12}$ |
|---|---|---|---|---|---|---|
| $l_{z4}$ | $w_{z4\ z6}$ | false | $w_{z4\ z8}$ | false | $w_{z4\ z10}$ | false |
| $l_{z5}$ | false | $w_{z5\ z7}$ | false | $w_{z5\ z9}$ | $w_{z5\ z10}$ | false |
| $l_{t2}$ | $w_{t2\ z6}$ | $w_{t2\ r7}$ | $w_{t2\ z8}$ | $w_{t2\ z9}$ | $w_{t2\ z10}$ | false |
| $l_{z6}$ | $w_{z6\ z6}$ | false | false | false | $w_{z6\ z10}$ | false |
| $l_{z7}$ | false | $w_{z7\ z7}$ | false | false | $w_{z7\ z10}$ | false |
| $l_{z12}$ | false | false | false | false | false | $w_{z12\ z12}$ |

фиг. 8в

***Фиг. 6.*** *Фиг. Индексирани матрици на преходите на подмрежа 3 за изпълнение на задачите от ИВА.*

### 5. Експерименти и дискусия

Проведени са два експеримента за 10 работни дни, при липса на комуникация между агентите и при взаимно съобразяване с плановете и ангажиментите си. При двата експеримента се наблюдава броя изпълнени задачи от ИВА; продължителността на работа на агентите измерена в часове; промяната на емоционалното състояние на ИВА в зависимост от това дали са реализирали всички заявени ангажименти за всеки експериментален ден. При липса на комуникация много по-често се оказва, че агентите се конкурират за получаването на бонуси или се налага да си тръгнат от работа преди да са изпълнили нормата си, в резултат на което напрежението между тях нараства. Обратно, ИВА успяват да преразпределят ангажиментите си и да получат повече бонуси без да се конкурират както и да изпълнят повече задачи на работното си място когато взаимно се съобразяват с плановете си. Решаването на повечето възможни конфликтни ситуации води до намаляване на безпокойството у ИВА.

### 6. Заключение

Сътрудничеството е сложно социално поведение, което изисква емпатия и предварително обмисляне. То е свързано с планиране и вземане на решения в сложни ситуации, при които възникват смесени емоции. В тази статия е представен обобщено мрежов модел за изследване поведение на сътрудничество между интелигентни виртуални агенти (ИВА). Обобщеният мрежов модел е представен с три подмрежи съответно за извличане на правилата на сценария и когнитивен анализ; за планиране и анализ; и за изпълнение на задачите според направения план. Интелигентните виртуални агенти с PRE-ThINK архитектура успяват да разпределят задачите на работното си място. Когато взаимно се съобразяват с плановете си през седмицата те успяват да ги реализират като предотвратяват възникването на конфликтни ситуации.

### ЛИТЕРАТУРА


1. Atanassov K. (1992). *Applications of generalized nets.* World Scientific Publ. Co., Singapore.
2. Gintis H., Bowles S., Boyd R.and Fehr E., (2005) "*Moral sentiments and material interests*" The foundations of cooperation in economic life., Cambridge, MA: MIT Press,.
3. Sabater J., Sierra C. (2005), "*Review on computational trust and reputation models*," Artificial Intelligence Review, 2005, pp. 33—60.
4. Budakova D., Dakovski L., Trifonov R. (2015), *Modeling and Studying Cooperative Behavior between Intelligent Virtual Agents by Means of PRE-ThINK Architecture*, Cognitive 2015, March 22 - 27, 2015 - Nice, France, ISBN: 978-1-61208-390-2, ISSN: 2308-4197, 2015, pp. 115-122.
5. Burton-Chellew M. N., Ross-Gillespieb A., West S. A. (2010), "*Cooperation in humans: competition between groups and proximate emotions, Evolution and Human Behavior*", Elsevier, 31, pp. 104–108.
6. de Melo C. M., Zheng L., J. Gratch (2009) "*Expression of Moral Emotions in Cooperating Agents*", Intelligent Virtual Agents, Amsterdam, Sep. 2009, pp. 14-16.
7. de Melo C. M., Carnevale P., and Gratch J. (2012) "*The Impact of Emotion Displays in Embodied Agents on Emergence of Cooperation with People*" Teleoperators and Virtual Environments, vol. 20, no. 5, 2012, pp. 449-465.
8. Niewiadomski R., Ochs M. and Pelachaud C. (2008), *"Expressions of empathy in ECAs,"* IVA'2008, Tokyo, Japan, LNAI, Vol. 5208, 2008, pp. 37-44.
9. Puurtinen M. and Mappes T., (2009) "*Between-group competition and human cooperation*" Royal Society B-Biological Sciences, 276(1655), 2009, pp.355−360.
10. Sun R. (2009) "*Motivational representations within a computational cognitive architecture*" Cognitive Computation, Vol.1, No.1, 2009, pp. 91-103
11. http://iva2006.ict.usc.edu/index_scope.htm
12. http://www.cogsci.northwestern.edu/Bayes/Pearl_1988.pdf Judea Pearl, 1988.
13. http://www.cs.ubc.ca/~murphyk/Bayes/Charniak_91.pdf Euhene Charniak, *Bayesian Networks without tears*, info@aaai.org http://www.aaai.org
14. https://en.wikipedia.org/wiki/Hidden_Markov_model
15. (http://www.cogsci.rpi.edu).



Адрес: Технически Университет-София, Технически Университет-София, Филиал Пловдив, бул.„Санкт Петербург“ 61, Катедра Компютърни системи и технологии, Пловдив

E-mail: dilyana_budakova@yahoo.com
E-mail: r_trifonov@tu-sofia.bg
E-mail: tsaikin@au-plovdiv.bg

© International Scientific Conference on Engineering, Technologies and Systems
TECHSYS 2016, Technical University – Sofia, Plovdiv branch
26 – 28 May 2016, Plovdiv, Bulgaria

# МОДЕЛИРАНЕ НА СОЦИАЛНО ПОВЕДЕНИЕ С ИНТЕЛИГЕНТНИ ВИРТУАЛНИ АГЕНТИ С КОГНИТИВНИ АРХИТЕКТУРИ

НИКОЛА ЦАЙКИН, ДИЛЯНА БУДАКОВА

**Резюме:** *В изследванията се откриват и измерват проявите на емоции и социален отклик у хората при тяхното общуване с други хора или с изкуствени агенти. Тези прояви се възприемат като неявен канал за информиране за вътрешната нагласа и намерения на отсрещния - ефекта backchanel. Този канал се възприема като относително по-автентичен и неманипулируем от вербалната декларация. Направен е и обзор на стратегиите за вземане на решение при хората и тяхното прилагане в изкуствените агенти. Некомпенсаторните стратегии са по-използвани от хората защото са по-бързи и достатъчно правилни като резултат. Те се реализират като евристики и заедно с другите правила за емоционална оценка се съхраняват в модулите за дългосрочна памет на когнитивните архитектури.*

**Ключови думи:** *емоции, когнитивни архитектури, агенти*

# MODELLING OF SOCIAL BEHAVIOR WITH INTELLIGENT VIRTUAL AGENTS WITH COGNITIVE ARCHITECTURES

NIKOLA TSAIKIN, DILYANA BUDAKOVA

**Abstract:** *Researches find out and measure the manifestations of emotions and social response in people in their communication with other people or with artificial agents. These manifestations are seen as an implicit channel for information about internal attitudes and intentions of the other person - the backchannel effect. This channel is perceived as relatively more authentic and unsusceptible to manipulations from the verbal declaration. An overview of people's decision-making strategies and their application in artificial agents has been made. Non-compensatory strategies are more often used by people because they are faster and correct enough as a result. They are realized as heuristics and together with the other rules for emotional evaluation are stored in the modules for long-term memory of cognitive architectures.*

**Key words:** *emotions, cognitive architectures, agents*

## 1. Увод

Моделрането на емоционални състояния чрез инструментариума на информатиката е предизвикателство в много аспекти. Емоциите, в контекста на социалното взаимодействие, сами по себе си се изучават от науката психология, която изследва човешкото поведение. С развитието си изкуствения интелект винаги се стремял да достигне функционалност и резултати съизмерими с естествената интелигентност на човека. В книгите и филмите, които отразяват очакванията на хората от изкуствената интелигентност откриваме два вида прояви на такава. Роботите в повечето случаи са хуманоидни и имат социални аспекти в поведението си, демонстрирайки разпознаване и проява на човешки емоции. Другата проява е на експертност, при която без много емоции, компютъра изчислява алтернативи. По-надолу ще свържем тези два вида прояви с компенсаторните и некомпенсаторни стратегии за вземане на решения.

Copyright © 2016 by Technical University of Sofia, Plovdiv branch, Bulgaria ISSN Online: 2535-0048

## 2. Изучаване на проявата на емоции

Заглавието на [1] започва така: „Това е просто компютър", или перефразирано: „Какво толкова! Това е само машина." и продължава: „Виртуалните интервюиращи предразполагат към повече откровенност (у хората)." Започвам това ревю с концепцията „Ethopoeia", че социалните признаци, дори когато идват от осъзнато неодушевени обекти, предизвикват социален отклик у хората. В тази статия е направено изследване как хората възприемат виртуален, графично изобразен субект (ВС), който ги интервюира по медицински въпроси. Някои от участниците са подведени да повярват, че ВС е с изкуствен интелект, а не аватар, контролиран от оператор. Статистическата обработка на резултатите показва, че хората, които са вярвали, че общуват с автономен ВС, а не с аватар са по-склонни да разкриват подробности за себе си. Това е предизвикан социален отклик чрез емоционални и социални знаци. Използван е софтуера CERT за измерване на лицевата експресия на участниците: ширина на усмивката, вежди и др.

В [2] е приложен двувекторен подход 2x2 за да се измери социалния отклик и да се провери концепцията „Ethopoeia". Единия вектор е ефекта на агентността, дали е аватар на човек или е изкуствен агент. Втория вектор е нивото на социалните знаци: графично изобразен ВС или просто текст чат. И в четирите случая участниците са общували по едни и същи въпроси със система, контролирана от оператор, а определена група е подведена да вярва, че общува с изкуствен интелект. Участниците са почуствали повече социално присъствие при осъзнато общуване с аватар. Хората възприемат човека като по-способен на емоционално общуване от компютъра. Това е ефекта на агентността, който в [3] е определен като: 1) способност да се планира; 2) способност за емоционална чувствителност. Когато се сравняват резултатите по вектора на социалните знаци между ВС и чата, ВС е предизвикал повече усещания, независимо дали е приеман като аватар или агент, заради графичното предаване на жестове, мимики и др. в така наречения „невербален танц".

В [4] се оценява съответствието между докладвана и измерена емоция, изразена с усмивка. Усмивката се измерва чрез софтуер OKAO Vision system, разпознавайки 16 лицеви точки и като краен резултат степен на усмивката от 0-100%. Отчетените разлики между измерената и почувствана емоция зависят от обстоятелството победа/ загуба и проявената емпатия към опонента - приятел/ непознат. Анализът показва по-голямо съответствие между измерените последователности от изражения и дейстствителното състояние на победа/ загуба срещу приятел/ непознат, отколкото спрямо докладваните емоции от участниците. Това показва, че емоционалните експресии са по-автентични от осъзнатите и докладвани чувства и нагласи.

Друг софтуер за анализ на лицева емоционална експресия е ACUME, представен в [5]. В него се разпознават 54 лицеви точки и разстояния (FACS – Facial Action Coding System), въз основа на които се определят 27 лицеви действия (AUs – Action Units). В изследването 66 участника са гледали откъси от филми със силна експресия на 6 основни емоции. Измерва се появата на тези AUs по лицата на участниците и се създават статистически биграми за появата на AUs за различните емоции. В [6] от тези AUs, чрез Скрит Марков Модел (HMM) и Динамично Баезиево Разпределение се разпознават основни емоционални състояния на участниците.

В [7] се доказва, че графичното изобразяване на повече части от тялото на ВС и неговите движения носи по-богата гама от емоционални послания. Сравнението е между ВС с цяло тяло и такъв само с лице. Това отваря допълнителен неявен канал на информираност (backchannel), предаващ послания чрез емоционални състояния, проявени чрез езика на тялото. Както бе коментирано по-горе за [4], емоционалната експресия е относително по-автентичен индикатор за нагласата на отсрещния от неговата вербална декларация. Използването на тази невербална информация като неявен канал за информиране (НКИ) е застъпено и в [8], където система с ВС се използва за тренажор за социални умения по сценарий за интервю за работа. Акцентира се както върху наблюдаването на езика на тялото на ВС, така върху измерването на жестовете на човека потребител и анализирането им като обратна връзка.

Систематизирането на тези експресии е важно за програмирането им в поведението на изкуствени агенти със социално поведение, така че да отразяват правилно оценката и намерението на агента. Човека, като участник в такава интеракция умее да разчита и интерпретира емоционалната експресия и ако тя не е коректна той ще се почувства подведен и ще оттегли доверието си от системата.

## 3. Систематизиране на емоции

В [9] е направен обзор на методите и насоките за моделиране на емоции чрез

изчислителни процеси. В раздел 2.2 се отчитат постиженията на психологията като наука, която разглежда емоциите в целия им спектър в човешкото поведение. Разгледана е необходимостта за нуждите на компютърното моделиране да се направи редукция на този широк спектър до малък брой базови състояния. В раздел 2.2.1 е направен опит да се даде дефиниция за емоция през призмата на моделирането. Дефинирани са два аспекта: 1) Емоцията е реакция на перцепция от външната среда или на съждение, съсдадено вътре в когнитивната архитектура, еквивалентно на въображение или мисъл; 2) Емоцията има характеристика по-скоро на субективна проява на агент, отколкото на обективна реакция по общовалидни правила. В 2.2.4 е направена класификация на хипотезите за ефекта от емоциите: 1) Като послание с информация за други околни агенти, вербално или невербално – ефекта НКИ; 2) Пренасочване на вниманието на агента към важни източници на информация; 3) Мотивационна функция чрез приоритизиране на целите и инициирането на нови такива.

В [10] са разгледани изчислителни модели на емоциите и е направен опит да се представят концептуалните различия в по-обща терминология и да се предостави инструмент за сравняване на различните конкурентни модели.

### 4. Вземане на решения под афект.

„Упоритостта предполага готовност за понасяне на щети” [11]. В това изследване участниците играят елементарна игра едни срещу други с финансови стимули. За да бъдат доведени до състояние на упорство, в някои случаи играта се манипулира в полза на опонента. Лицевата експресия на участниците се записва и анализира. Направени са и анкети за изпитаните емоции. Изследва се склонността да се влагат усилия дори когато загубата е очевидна. Резултатите показват, че загубилите са положили повече усилия. Друг резултат от анкетите и анализа на усмивките е че упоритостта се съчетава с повече положителни емоции отколкото с отрицателни. Получените данни са полезни при програмиране на качеството упоритост в изкуствени агенти.

В статията [12] участниците в експеримента трябва да водят морално натоварени преговори с финансови предложения. В интерфейса на постановката участникът избира от няколко графично представени типови емоции, с която да се представи на опонента и съответно вижда неговия избор. Емоциите са представени с рисувани лица. Моралната натовареност е представена чрез контекста „моето семейство” и „другото семейство”. Резултатите показват, че тъгата предизвиква по-щедри предложения, а гневът обратното. Също така емоциите водят до предизвикване на същата емоция у отсрещния.

В [13] е разгледана способността на емоцията да предизвика самозаблуда, добавяйки новогенерирани фактори в процеса на вземане на решения. В [14] е дефинирана трансформираща функция, която разграничава обективната и субективна различимост на факторите при вземане на решение под риск. Тя има участък за деформацията на субективната различимост при очаквана печалба и съответно при очаквана загуба. В [15] са извлечени няколко конфигурации на тази функция в участъците за печалба и загуба, които съответстват на базовите емоции и показват как те променят субективната различимост на тези фактори.

### 5. Когнитивни архитектури

От когнитивните архитектури най-напред ще спомена онази, която като основа се стреми да обясни и да представи в модел естествените когнитивни процеси в човешкия мозък и след това на тази база да предложи архитектура, удобна за компютърно моделиране и обработка на знанията, формализирани според методологията на информатиката. Както бе споменато в увода върхова цел на изкуствения интелект е имитация и функционалност като на естествения ум на човека. Намирането на решения на конкретни приложни проблеми е перспективно но не чак толкова престижно направление в тази област. Когнитивната архитектура ACT-R [16] се състои от модули, които са съответствие на определени части на естествения мозък, за които е изследвано че имат съответсващи функции. Модулите са: моторни, за възприятие, за цели, декларативна памет и други. Генерират се информационни пакени – chunks (буци), които се обработват от продукционна система, базирана на правила от декларативната памет. За всеки от модулите в архитектурата са дадени латинските наименования на съответните части на мозъка. ACT-R, като замисъл е теория за обяснение на работата на ума. Създават се времеви диаграми, където се проследява обмена на информация между отделните модули и се прави оценка на необходимото време за вземане на решение.

В когнитивната архитектура Soar основна роля имат модулите на краткосрочната и дългосрочната памет (short term memory –

STM и long term memory – LTM). В краткосрочната се изграждат символни структури с атрибути, отразяващи текущата ситуация, целите и прогреса на постигането им. В LTM се съхраняват процедури от правила и оператори, които добавят цели, обработват съдържанието на STM и генерират изходни действия. Архитектурата работи чрез цикъл на Soar: въвеждане на данни от входния интерфейс; задействат се правила от LTM, които модифицират структурите в STM; определят се операторите, които магат да бъдат изпълнети; процедура за решение определя кои оператори да се изпълнят; изпълнение чрез мотириката на исходния интерфейс. Базовия метод на учене, т.е. създаване на нови процедури в LTM е chunking (извличане на буци). Когато е налице постината цел или подцел, структурата в STM се конвертира в правило и се добавя към LTM.

В [17] архитектурата Soar се разширява с допълнителни модули и раздели в LTM. Те добавят още три метода на учене с възможности, които не могат да се реализират чрез chunking. Като цяло chunking се оценява като твърде реактивен метод за учене. Добавени са semantic, episodic и Reinforcement learning. Модула Appraisal Detector, който позволява Reinforcement learning, оценява структурата в STM и генерира стимули за награда/санкция , които се използват за извличането на нови правила, водещи до положителни резултати. Тук, чрез Appraisal Detector е предвидена възможността да се кодират емоциите и тяхното влияние върху оценката, чрез добавяне на структура за емоция към STM. Това прави Soar удобна за програмиране на емоции без допълнителни модификации.

В архитектурата PRE-ThINK [18] отчитането и симулирането на емоции има ключова роля в поведението на изкуствения агент. На база на OCC мадела, емоциите се представят като нужди и мотиватори за действие, които от своя страна се приоретизират и етикират с коефициенти според теорията на Maslow. Текущата ситуация се отразява въз основа на принципи и правила, които генерират мисли със съответната емоция като атрибут. Всяка мисъл е условие за предприемане на действие. Създава се „мисловен баланс”, при който всяко действие формира набор от текущите мисли, които могат да го предизвикат. Отделните набори се оценяват по формула и действието с най-висока оценка се изпълнява. Процесът на учене се осъществява от модул за проследяване, който генерализира тенденции в мисловния баланс и създава нови принципи.

В обзора [9] е разгледана архитектурата BDI – belief desire intension (вярвания, желания, интензивност), която е формализирана агентна логика с включване на емоции и социален афект. Тя е по абстрактна от ACT-R и Soar. Няма отделни видове модули памет и се състои от пет стъпки: 1) перцепция; 2) обновяване на текущата база от вярвания и желания; 3) генериране на опции или планове; 4) избор на план и генериране на интензивност; 5) изпълнение. Освен ACT-R и Soar в раздел 4 са разгледани и други архитектури, като са направени и сравнителни анализи. Едно от обобщенията, които могат да се направят е че емоциите се кодират в набора от генерални правила и се съхраняват в модули от тип LTM.



***Фиг. 1.*** *ВС на SimSensei Kiosk*

В статията [19] е представена системата SimSensei Kiosk, която визуализира ВС с изобразено цяло тяло като на фиг.1. и се прилага за интервюиране на пациенти с PTSD. Като входни данни системата разпознава естествена реч на определено ниво и анализира визуално поведението на пациента. Измерват се атрибути на лицевата експресия като ширина на усмивката и други движения на части от лицето чрез локализиране и проследяване на контролни точки по него. Също чрез контролни точки на тялото се засичат някои от движенията му. Cerebella е платформа, която анализира връзката между вербалните когнитивни процеси и невербалното поведение, изразено чрез езика на тялото (НКИ). Платформата се използва както за наблюдение на пациента, така и за формиране на движенията на ВС. Управлението на диалога се реализира чрез набор от готови граматически конструкции и изречения, приоритизирани и подредени в сценарии.

### 6. Компенсаторни и некомпенсаторни стратегии за вземане на решение

В изследването (20) се сравняват три статегии за вземане на решение чрез когнитивната архитектура ACT-R. Участниците в експеримента са инструктирани да направят разграничително решение по строго определен алгоритъм, съответстващ на изследваната

стратегия. Стратегиите са: TTB take the best (вземи най-доброто); TLL talling (етикиране); WLM weighted-linear model (тегловен модел).

Участниците трябва да запомнят 4 атрибута с коефициенти за 8 града или 64 факта за да направят решение в полза на един от двата града чрез сравнение на атрибутите. TLL и WLM са определени като компенсаторни, защото алгоритмите им изискват да се отчетат и четирите факта за града и при изчисляване на разграничителната оценка фактите с обратен знак на коефициентите се компенсират. TTB е некомпенсаторна, защото обхождането на фактите спира при намирането на първия такъв с достатъчно висок разграничаващ коефициент. Най-общо казано компенсаторните стратегии правят изчислителен анализ на всички известни атрибути на алтернативите, които трябва да бъдат разграничени. Некомпенсаторните стратегии (НКС) търсят първия достатъчно силен разграничителен критерий.

В статията [21] се изследва вземането на решения, звързани с риск. Участниците избират между две лотарийни алтернативи с вероятности. Резултатите показват, че само 5% от участниците са изчислявали математически вероятностите, за да изберат по изгодната сума. Повечето са избирали според сравнителни оценки от типа „съразмерно" и „много по-голямо/ малко" което се явява прилагане на разграничителен критерий (НКС). В изследването [22] също се прави извод, че НКС отговарят в много по-голяма степен на човешките решения. Показани са парадигмите „елиминиране чрез разпознаване" и „от разпознаване до решение". Базирани са на разпознавателни евристики (RH), които се използват в голяма степен в механизма, по който хората разграничават между алтернативи.




***Фиг. 2.*** *Сравнение на коректността на резултатите при различни стратегии.*

В статията озаглавена "За добро решение не е необходимо комплексен когнитивен процес" [23] също се прави сравнение между стратегии с RH и такива с изчислителен анализ. Аналитичната стратегия се представя отлично на обучаващите примери, но е по неадекватна на нови примери от същата среда, както е показано на Фиг.2, която е от статията.

## 7. Заключение

По отношение на когнитивните архитектури емоциите се кодират като RH в набора от генерални правила и се съхраняват в модули от тип LTM. Тези RH се активират в два случая: когато разпознават емоция в друг агент и при оценка на текуща ситуация. И в двата случая се генерира емоция [2, 5, 12], която влияе на когнитивния процес.

НКС са най-подходящи за процесиране на емоции, заради същността на емоциите като условни разпознавателни критерии. Състоянията на афект изкривяват когнитивния процес, но също така НКС осигуряват по-правилни разграничения при променена и рискова среда. Трансформиращата функция в [14] изкривява обективната различимост, която обаче е оптимизирана за позната среда. При променена среда субективната различимост има потенциал да генерира по-правилно решение. Друг пример е упорството [11], което предизвиква влагане на усилия и при очевидна загуба. Но при наличие на скрит фактор в една непозната среда усилията може и да се увенчаят с успех. Това е евристика.

Компютърът отдавна е победил човека на шах, но там имаме ограничена и прозрачна топология и краен брой фигури с пределно изяснена функционалност. Рутинно грубия аналитичен подход може да изчисли всички алтернативи на тази прозрачна среда. В реалната среда на хората обаче основен фактор са намеренията на човека и непрозрачните му мотиви. Ако искаме да вмъкнем изкуствените агенти в този непредвидим социум трябва да ги програмираме да разчитат и излъчват правилните емоционални сигнали.

## ЛИТЕРАТУРА

1. Lucas, G., Gratch, J., King, A. and Morency, L. It's Only a Computer: Virtual Humans Increase Willingness to Disclose. *Journal of Computers in Human Behavior*. v37. 2014. 94-100
2. Appel, J., Pütten, von der, A., Krämer, N., and Gratch, J. Does humanity matter? Analyzing the importance of social cues and perceived agency of a computer system for the emergence of social reactions during human-computer interaction. *Advances in Human-Computer Interaction*. 13, 2012

3. Melo, de, C., Gratch, J., and Carnevale, P. The Importance of Cognition and Affect for Artificially Intelligent Decision Makers *AAAI,* 336-342, 2014
4. Gratch, J., Cheng, L., Marsella, S. and Boberg, J. Felt emotion and social context determine the intensity of smiles in a competitive video game. *10th IEEE International Conference on Automatic Face and Gesture Recognition.* Shanghai 2013
5. McDuff, D., Kaliouby, R., Kassam, K., Picard, R., Acume: A new visualization tool for understanding facial expression and gesture data**,** *9th IEEE International Conference on Automatic Face and Gesture Recognition* Santa Barbara, CA, USA, 21-25, 2011.
6. Baltrusaitis, T., McDuff, D., Banda, N., Mahmoud, M., Kaliouby, R., Robinson, P., Picard, R. Real-time inference of mental states from facial expressions and upper body gestures**,** *9th IEEE International Conference on Automatic Face and Gesture Recognition and Workshops*, Santa Barbara 21-25, 2011.
7. Huang, L., Morency, L., Gratch, J. Parasocial Consensus Sampling: Combining Multiple Perspectives to Learn Virtual Human Behavior. *9th International Conference on Autonomous Agents and Multiagent Systems.* Toronto, Canada, 2010.
8. Hoque, M. Computers to Help with Conversations: Affective Framework to Enhance Human Nonverbal Skills**,** MIT PhD Thesis, 2013.
9. Reisenzein, R., Hudlicka, E., Dastani, M., Gratch, J., Hindriks, K., Lorini,E., and Meyer, J. Computational Modeling of Emotion: Towards Improving the Inter- and Intradisciplinary Exchange. *IEEE Transactions on Affective Computing*, 2013, pp. 246-266
10. Marsella S., Gratch J. and Petta P. Computational Models of Emotion. In Scherer K., Bänziger T., & Roesch E. (Eds.) A blueprint for a affective computing: A sourcebook and manual. Oxford University Press, 2010
11. Lucas, G., Gratch,J., Cheng, L. and Marsella, S. When the going gets tough: Grit Predicts costly perseverance. *Journal of Research in Personality*. 59 (2015) 15–22
12. Dehghani, M., Carnevale, P. and Gratch, J. Interpersonal effects of expressed anger and sorrow in morally charged negotiation. *Judgment and Decision Making*. 9(2). 2014
13. Ito, J., Pynadath, D., and Marsella, S. Modeling self-deception within a decision-theoretic framework. *Autonomous Agents and Multi-Agent Systems 20*, 1 (May 2010), 3–13.
14. Ahn, H. and Picard R., Modeling Subjective Experience-based Learning under Uncertainty and Frames, Conference on Artificial Intelligence (AAAI-14), Québec, 2014.
15. Ahn, H. Modeling and Analysis of Affective Influences on Human Experience, Prediction, Decision Making, and Behavior, MIT PhD Thesis, September 2010.
16. Anderson, J., Bothell, D., Byrne, M., Douglass, S., Lebiere, C., Qin, Y. An Integrated Theory of the Mind. *Psychological Review*, Vol 111(4), Oct 2004, 1036-1060.
17. Laird, Extending the Soar Cognitive Architecture, *Artificial Intelligence and Applications*, 2008.
18. Budakova D. Behavior of home care intelligent virtual agent with PRE-ThINK architecture. *ICAART 2011 - Proceedings of the 3rd International Conference on Agents and Artificial Intelligence*, 2, 28-30,
19. DeVault, D., Artstein, R., Benn, G., Dey, T., Egan, A., Fast, E., Georgila, K., Gratch, J., Hartholt, A., Lhommet, M. SimSensei: A Virtual Human Interviewer for Healthcare Decision Support. *13th International Conference on Autonomous Agents and Multiagent Systems*. Paris, 2014
20. Dimov, C., Marewski, J., and Schooler, L. Constraining ACT-R models of decision strategies: An experimental paradigm, Cognitive Science Society, 2013, 2201-2206
21. Cokely, E., & Kelley, C. Cognitive abilities and superior decision making under risk: A protocol analysis and process model evaluation. Judgment & Decision Making, 2009, 20-33
22. Marewski, J., Gaissmaier, W., Schooler, L., Goldstein, D., & Gigerenzer, G. (2010). From recognition to decisions: Extending and testing recognition-based models for multialternative inference. *Psychonomic Bulletin & Review, 3*, 287-309.
23. Marewski, J., Gaissmaier, W., Gigerenzer, G. Good judgments do not require complex cognition. *Cognitive Processing*, 2010, 103-121.



Контакти:
1. Аграрен Университет – Пловдив;
E-mail: tsaikin@au-plovdiv.bg
2. Технически Университет – София,
Филиал Пловдив;
E-mail: dilyana_budakova@yahoo.com

© International Scientific Conference on Engineering, Technologies and Systems
TECHSYS 2016, Technical University – Sofia, Plovdiv branch
26 – 28 May 2016, Plovdiv, Bulgaria

# НЯКОИ ПОДХОДИ ЗА ИНТЕГРИРАНЕ НА ИМИТАЦИОННО МОДЕЛИРАНЕ В ОБУЧЕНИЕТО

СВЕТЛАНА ВАСИЛЕВА, ДЕЛЯН ВАСИЛЕВ

**Резюме:** *В доклада се разглеждат някои аспекти на приложението на средата за имитационно моделиране GPSS World и нейните надстройки – Разширения редактор и Универсалния редактор на формите за създаване на демонстрационни модели и използването им в обучението на студенти. Класическото приложение на имитационното моделиране е за изследване на различни системи. Но „прозорците за наблюдение“ на симулациите в GPSS World и споменатите нови редактори към системата разкриват нови разширени възможности на GPSS за интегриране на имитационното моделиране в учебния процес. В доклада са представениы примери за използване на имитационни модели и демонстрационните възможности на GPSS World, Разширения редактор и универсалния редактор на формите в учебни материали по Операционни системи и Бази от данни.*

**Ключови думи:** *имитационни модели, синхронизация процеси, управление на транзакции, GPSS, Разширен редактор, Универсален редактор на формите*

# SOME APPROACHES TO INTEGRATION SIMULATION MODELING IN EDUCATION

SVETLANA VASILEVA, DELYAN VASILEV

**Abstract:** *The paper discusses some aspects of the implementation of environment for Simulation modeling GPSS World and its extensions - Extended editor and Universal editor of forms to create demonstration models and their use in the training of students. The classic use of simulation modeling is to study the variety of systems. But "observation windows" of simulations in GPSS World and cited new editors reveal new advanced capabilities of GPSS to integrate imitation modeling in the learning process. The report gives examples of the use of the imitation models and demonstration capabilities of GPSS World, the Extended editor and the Universal editor of forms in teaching materials Operating Systems and Databases.*

**Key words:** *simulation models, process' synchronization, transaction concurrency control, GPSS, Extended editor, Universal editor of forms*

## 1. Основни положения

Компютърното моделиране намира приложение във всички сфери на човешката дейност - от модели на технически, технологични и организационни системи до проблеми на развитието на човечеството. Имитационното моделиране (ИМ) е едно от най-популярните средства от системите за моделиране. ИМ позволява да се изследват системи за масово обслужване (СМО) при различни типове входни потоци и интензивности на постъпване на заявките на входовете на системите и определяне на основните характеристики на същите. Една от най-използваните системи за имитационно моделиране – GPSS World предоставя на потребителите средства за взаимодействие със системата в процеса на симулационните изследвания и програмни средства, реализиращи непосредствено процеса на изпълнение на модела, такива като: интерпретатор, моделен часовник, управление на списъците от събития и др. [1] Като обекти на езика GPSS [2] се използват аналози на такива стандартни компоненти на СМО, като заявки, обслужващи прибори, опашки и други. [3] Достатъчният набор от подобни компоненти позволява да се конструират сложни симулационни модели, при запазване на привичната терминология на СМО. GPSS е

Copyright © 2016 by Technical University of Sofia, Plovdiv branch, Bulgaria ISSN Online: 2535-0048

език за моделиране, който се използва за построяване на събитийни дискретни имитационни модели и провеждане на експерименти на компютър ([2], [3] и др.) Това предполага използването на средата на GPSS и в учебния процес за демонстрация на работата на изучавани системи и за разработване от самите студенти на модели за управление и работа на различни системи (Компютърни системи [4], Комуникационни системи [5], Бази от данни [6], Grid системи [7] и други).

Основното и ефективното приложение на ИМ е при изследването на различни СМО, но симулационното моделиране може успешно да се използва и като средство за обучение, особено по дисциплини (Операционни системи, Паралелно програмиране [8] и други, Бази от данни [6], Grid системи [7]), в съдържанието на които се изучават теми по управление на едновременната работа на процеси (транзакции) и други такива, описвани в термините на СМО като заявки за обслужване.

Представените в доклада средства на GPSS показват различни възможности ИМ да бъде интегрирано в учебни материали под формата на: текстови модели, които да бъдат стартирани в средата на GPSS World или Разширения редактор на GPSS модели; филми-записи на симулации; 2-D анимация и др.

## 2. GPSS World - възможности за моделиране и визуализация на алгоритми за синхронизация

Базовите компоненти на GPSS World са транзакти и блокове, които представляват съответно динамичните и статичните обекти на моделираната система [2], [3] и [5]. Основен принцип на работата на имитационния модел под управлението на симулатора е преместването на GPSS транзактите от блок към блок и предаване на управлението в моделно време.

Прозорецът на блоковете и другите прозорци за визуализация в средата на GPSS World предоставят отлични възможности за наблюдаване работата на моделираните системи. С помощта на командата *Simulation Window* от менюто Window се избира кои прозорци да бъдат показани на екрана, за да се наблюдава симулацията [2]:

- *Blocks Window* – прозорец на блоковете – различен режим на работа за кратка или детайлизирана справка по време на симулация, съдържаща информация за етикети и имена на блоковете, брой вхождения в съответния блок, журнал с хронологично проследяване на действията по блокове в моделното време;

- *Facilities Window* – прозорец на едноканалните устройства (фиг. 1, долу вляво) – информация за: Номер/име на устройството; Брой влезли транзакти; Коефициент на използване; Средно време на пребиваване на транзакт в устройството; Брой транзакти, очакващи специални условия; Брой транзакти, изчакващи заемането на съответното устройство и др.;

- *Matrix Window* – прозорец на матрица (фиг. 1 – двата прозореца вдясно) – резултати в стойности на общия за транзактите ресурс и тяхната съпоставка при зададени единици моделно време;

- *Plot Window* – прозорец на диаграма на функция или израз. Може да се използва за проследяване на стойностите на произволно съставени изрази;

- *Logicswitches Window* – прозорец на логическите ключове;

- *Queues Window* – прозорец на опашките. Показва информация за: Номер/Име на опашката; Максимална дължина на опашката; Текуща дължина на опашката; Общ брой вхождения; Средна дължина на опашката; Средно време на изчакване на транзактите в опашката и други;

- *Savevalues Window* – прозорец на съхраняваните стойности (фиг. 1 панелът горе вляво). Може да се наблюдава всяка промяна на променливите (обикновено броячи), дефинирани в модела;

- *Storages Window* – прозорец на многоканалните устройства (фиг. 1, панелът вляво по средата). По време на симулация в него може да се види всяка промяна на: броя свободни единици от капацитета на всяко от многоканалните устройства; минималния и максималния използван капацитет на устройството; броя вхождения в съответното многоканално устройство и др.;

- *Table Window* – прозорец на таблица - диаграма на честотно разпределение на табулираните транзакти в дефинирана в модела таблица. Прозорецът на избраната таблица представя динамична хистограма, която е изключително полезна за показване на обслужени/постъпили транзакти, на честотно разпределение и други характеристики.

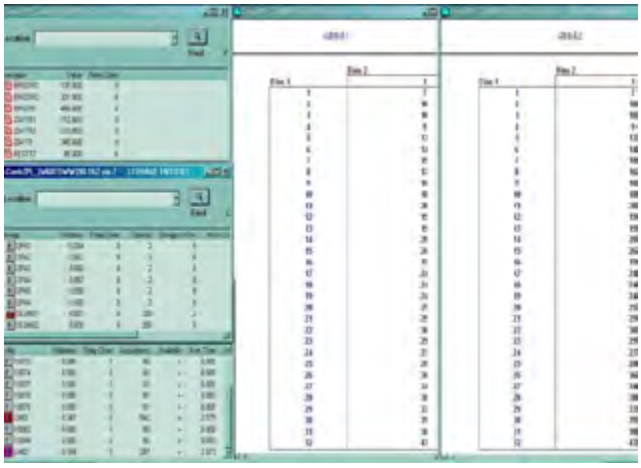
На фиг. 1 е показано как може да се отворят и подредят на екрана няколко различни прозореца от изброените по-горе и в тях да се наблюдава работата на моделираната система. В примера е показан комбиниран прозорец за наблюдаване на симулация на Централизирана

Двуфазна блокировка с вграден механизъм на хронометраж (такива алгоритми се изучават в темите Алгоритми за управление на транзакции и Разпределени системи за управление на бази от данни по дисциплини като Бази от данни).

Моделиращият алгоритъм, кадър от който е демонстриран на фиг.1 е описан подробно в [9]. В примера на фиг. 1 „комбинираният прозорец" дава възможност да се наблюдават:

- Стойностите на елементите на матриците *GBDA1* и *GBDA2*. Матриците моделират локалните бази от данни, в които се съхраняват двете копия на елементите от данни. В прозорците на матриците *GBDA1* и *GBDA2* могат да видят синхронното обновяване на стойностите на локалните копия на всеки елемент от данни. Първата колона на матриците *GBDA1* и *GBDA2* са номерата на елементите от данни, а втората колона – стойността на копието на елемента от данни;

- Прозорецът на съхраняваните стойности горе вляво на фиг. 1 дава възможност да се наблюдават броячите: *BROITR1* и *BROITR2* – брой генерирани транзакти, обработващи съответно 1 и 2 елемента, *BROITR* – общ брой генерирани транзакти, *ZAVTR1* и *ZAVTR2* – брой напуснали модела транзакти, обработили съответно 1 и 2 елемента от данни, *ZAVTR* – общ брой транзакти, напуснали модела, *RESTRT* – брой рестартирани транзакти.



***Фиг. 1.*** *Комбиниран прозорец за демонстрация изпълнението на моделиращ алгоритъм*

### 3. Моделиране и демонстрация на алгоритми за синхронизация с Разширения редактор на GPSS World

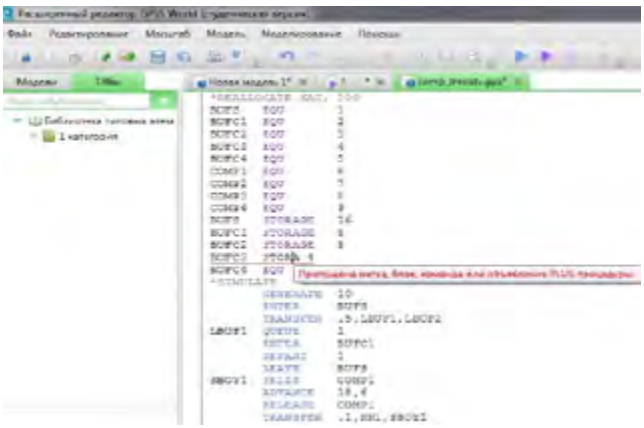
Показаният на фиг. 1 комбиран прозорец за наблюдаване на симулация се аранжира ръчно от преподавателя и това представлява известно неудобство, а и поставя допълнителни изисквания при подготовката на учебните модели. В Разширения редактор на GPSS модели, обаче, се автоматизират повечето операции и действия на изследователя и преподавателя при провеждане на целия цикъл от имитационни изследвания [1] и [10].

Многофункционалният текстов редактор на GPSS моделите (в състава разширения редактор), прави работата с моделите още по-удобна. С текстовия редактор, преподавателят може да създава елементарни модели и библиотеки от готови елементи. Други удобства, предоставяни от Редактора за разработчика на модели са: Наименованията на блоковете и командите, служебните думи на вградения език PLUS, коментарите и текстовите лексеми се показват на екрана с различни цветове за по-добра нагледност на текста на модела; Командите и блоковете, аргументите и коментарите автоматично се подравняват за по-лесно разпознаване при четене; Въвеждането на текста на модела се съпровожда с контекстна подсказка, описваща текущия операнд, или аргумент на функция и списък с подходящи значения, както е демонстрирано на фиг. 2 (това е много удобно за студентите, а и за преподавателя, който обикновено не е специалист по ИМ) [1], [10]. Всички тези и други удобства за преподавателя, използващ ИМ, предоставяни от текстовия редактор на моделите инициира приложението на Разширения редактор в обучението по технически дисциплини като споменатите по-горе: Операционни системи, Компютърни системи, Grid системи и др.



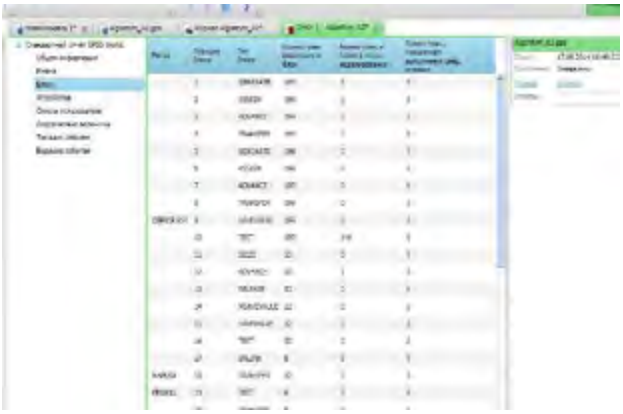
***Фиг. 2.*** *Модел в прозореца на Текстовия редактор с контекстно подсказване*

Друга възможност, подпомагаща приложението на Разширения редактор в учебния процес е, че Редакторът автоматично открива и отбелязва структурните грешки в модела (фиг. 3). Операторите, в които има грешки се подчертават с червена линия, а самите грешки се изобразяват при доближаване указателя на мишката.



***Фиг. 3.*** *GPSS модел в средата на текстовия редактор с маркирана грешка в модела*

След създаването на модела, може да се изпълни моделирането. По време на моделирането се вижда журнала, а след края на моделирането – стандартен отчет, показан на фиг. 4.



***Фиг. 4.*** *Отчет от моделиране на алгоритъма Декер в прозореца на Разширения редактор (GPSS моделът е представен в [8])*

В Разширения редактор за търсене на грешки в модела в вградена подсистема за трасировка. [1], [10] Механизмът, позволява да се събират данни за движението на транзактите и измененията в обектите на модела по време на изпълнението му. Това може да се използва както за настройка на модела, така и за създаване на филми (например с CamStudio Recorder). Една от възможностите на механизма за трасировка на модела е търсене на транзакт по номера или стойността на негов параметър и проследяване само на неговото придвижване в модела.

На фиг. 5 е даден пример с прозорец от трасировката на модел на алгоритъма на Декер (показан в [8]) в средата на Разширения редактор. В сравнение с прозореца на трасировката на класическата GPSS World (фиг. 6) тук автоматично се показва прозореца на съхраняваните величини (Savevalues) и на матриците (в долния десен ъгъл на фиг. 5). Автоматично се показва и номера на транзакта обслужван в даден момент от моделното време (в горния десен ъгъл). Визуализират се и значенията на параметрите на обслужвания транзакт, моделиращ процес (фиг. 5 вляво).



***Фиг. 5.*** *Трасировка на модел в прозореца на Разширения редактор*

## 4. Интегриране на симулационни модели в електронни учебни пособия

Електронните учебници дават огромни възможности за вграждане на имитационните модели, разработени в средата на GPSS World или Разширения редактор. На фиг. 6 е показано вграждане на „учебен филм”, записан с програмата CamStudio на основата на комбиниран прозорец за наблюдение на симулация на Централизирана Двуфазна блокировка с вграден механизъм на хронометраж [9]. Във филма: • Двата панела вляво са споменатите в раздел 2 матрици *GBDA1* и *GBDA2*; • В горния десен панел са показани първите 3 колони на таблицата на блокировките, представена в модела с матрицата *LTA* [9] за първите 20 елемента от данни (колоните показват стойностите на: тип на блокировката, с която е зает елемента; номер на транзакта, блокирал елемента; номер на сайта, генерирал транзакта); • Долният десен панел (фиг. 6) визуализира по време на симулация диаграмата на честотното разпределение на времето за обслужване на транзактите в модела. Филмът на фиг. 6 заснема изпълнението на същия модел като на фиг. 1, но от „друг поглед” (отново ранжиран ръчно от преподавателя).

На фиг. 7 е показана симулация на метода за процесна синхронизация „Писатели - Читатели”. Филмът е вграден в електронен учебник по Операционни системи и представлява запис на трасировка на модела в средата на Разширения редактор.

Моделиращият алгоритъм е описан в [12]. Направени са някои модификации за целите на представянето на модела във Форма за проследяване динамиката на експеримента (показана на фиг. 9) в Универсалния редактор на формите [13]. Този редактор предоставя още по-богати възможности за създаване на учебни филми на базата на форми за 2-D анимация и др.



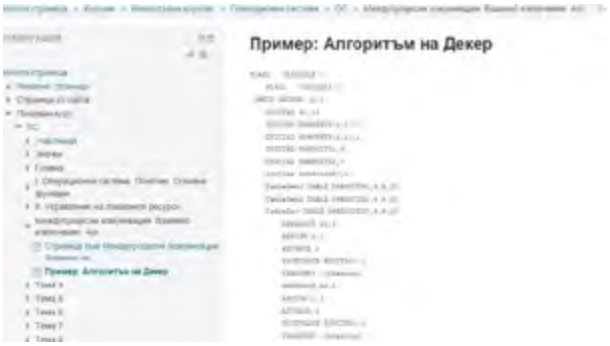
***Фиг. 6.*** *E-Textbook page with embedded Combined window to the windows for demonstration and tracing of transaction execution*



***Фиг. 7.*** *Страница от Е-учебник с вграден запис на симулация на процесна синхронизация по метода "Писатели-Читатели"*

В прозореца на променливите в десния панел (фиг. 7) може да се наблюдават стойностите на: брояча на генерираните в модела писатели NumProd; брояча на генерираните читатели NumRead; брояча на завършилите писатели EndProd; брояча на завършилите читатели. А в левия панел може да се наблюдава обслужването на процесите.

Друга възможност за интегриране на имитационното моделиране в електронен учебник е публикуването на целия текст на съответния GPSS модел, както е показано на фиг. 8. Студентите могат да копират текста на GPSS кода в средата на Разширения редактор и могат след това да стартират и наблюдават симулацията в режим на трасировка със скорост, каквато би им била удобна според индивидуалните възможности на съответния студент. Освен скоростта на наблюдаване работата на моделираната система, този начин дава възможност студентите да правят промени в модела и да наблюдават симулациите при различни начални параметри.




***Фиг. 8.*** *Програмен код на GPSS модел на алгоритъма на Декер, включен в Е-учебник*



***Фиг. 9.*** *Форма на Динамиката на хода на експеримента, проектирана в Универсалния редактор на формите*

Демонстрационните материали, показващи работата на системите при различни алгоритми за синхронизация (и не само) могат да бъдат включени в електронни учебници и като хипер връзки към съответните материали. Филми като демонстрираните на фиг.6 и фиг. 7, са с голям размер на файловете и това може да бъде проблем. Затова може да се използват възможностите на облачните системи, като например OneDrive, Dropbox и др. Преподавателят, след като е записал филм може да го копира в облака и след това да добави хипер връзката в съответното място в учебника.

## 5. Заключение

Автоматизираното създаване на симулационни модели в Разширения редактор на GPSS World, „стандартния комбиниран

прозорец" за наблюдение изпълнението на модела и удобният графичен интерфейс на Редактора, го правят изключително подходящ за учебни демонстрации на работата на различни системи. А с формите, които може да се създават в средата на Универсалния редактор на формите демонстрационните материали биха могли да бъдат още по-атрактивни и информативни за студентите. Записаните на филми симулации представят работата на моделираните системи при различни режими, почти реално „в действие". А вграждането в електронни учебници (в online курсове или в учебни помагала, реализирани на CD, DVD и др.), предоставя възможности за асинхронно разпространение/доставяне на същите чрез e-mail, облачни системи, обикновена поща и др.).

Не на последно място, чрез създаването на коплексни (изискващи интеграция на различни дейности и съответно участници) учебни материали по различни дисциплини студентите могат да бъдат привличани за реално участие в проекти. Проекти, в които да решават реални практически проблеми, с което да се подготвят за бъдещата си реализация като специалисти и не по-маловажно – да се учат да работят в екип

## ЛИТЕРАТУРА


1. Власов, С., Девятков, В., Исаев, Ф., Федотов, М. (2012) Имитационные исследования с использованием GPSS World – новые возможности. *Автоматизация в промышленности*, No 7, с. 3–8.
2. Minuteman Software. (2010) *GPSS World Tutorial Manual*. http://www.minutemansoftware.com/tutorial.
3. Томашевский, В., Жданова Е. (2003) *Имитационное моделирование в среде GPSS*. Бестселлер, Москва.
4. Романски, Р. (2012) *Компютърно моделиране*. http://www.tu-utc.com/Webpages/E_learning/CompModelirane/KMod-Labs.
5. Компьютерное моделирование. (2013) http://www.intuit.ru/studies/courses/643/499/lecture/6490
6. Vasileva, S. and Kulchiar, A. (2014) Options of GPSS World for integrated demonstration models in the educational process. *Proceedings of 2014 Science and Information Conference SAI 2014*, London, United Kingdom, pp. 933-937.
7. Георгиев, В. *Grid системи*. Симулационно моделиране с GPSS. http://ci.fmi.uni-sofia.bg/VasilGeorgiev/datagrid/grids13.pdf.
8. Vasileva, S. and Kapinchev, K. (2012) Some Simulation Models of Process' Synchronization for Educational Purpose. *International Conference on Application of Information and Communication Technology and Statistics in Economy and Education– 2012*, UNWE, Sofia, Bulgaria, pp. 474-483.
9. Vasileva, S. (2013) An algorithm modelling centralized two-phase locking with integrated mechanism of timestamps. *Journal of the Technical University Sofia, branch Plovdiv. "Fundamental Sciences and Applications"*, Vol. 19(1), International Conference Engineering, Technologies and Systems TechSys 2013, pp. 237-242.
10. Федотов, М., В. Девятков. (2013) САИИ для профессионалов – развитие возможностей расширенного редактора GPSS World. *Сборник докладов шестой всероссийской научно-практической конференции „Имитационное моделирование. Теория и практика" (ИММОД-2013)*. Том 1, Изд. ―ФЭН" Академии наук РТ, Казань, 2013. С. 356-360.
11. Информатика–лекции и материали. http://www.bg-informatika.com/2011/07/22.html.
12. Popov, G. (2007) GPSS as Tool for Decision of Classical Task in Operation System, *Academic Journal Mechanics.Transport. Communication (MTC AJ)* No 3,2007,article No 0186, pp. VIII-47 – VIII-49 (http://www.mtc-aj.com)
13. Исаев, Ф., В. Девятков. (2013) Основные возможности универсального редактора форм для GPSS World. Сборник докладов шестой всероссийской научно-практической конференции „Имитационное моделирование. Теория и практика" (ИММОД-2013). Том 2, Изд. "ФЭН" Академии наук РТ, Казань, с. 149-154.



-Контакти:
Адрес Висше училище по мениджмънт, Оборище 13А, 9000 Варна
Рамсофт ЕОД, пл. Свобода 6, 9300 Добрич
E-mail: svetlanaeli@abv.bg
E-mail: delyan.vasilev@iit13.eu

© International Scientific Conference on Engineering, Technologies and Systems
TECHSYS 2016, Technical University – Sofia, Plovdiv branch
26 – 28 May 2016, Plovdiv, Bulgaria

# SECTION 4 • СЕКЦИЯ 4

## MECHANICAL ENGINEERING;
## MECHANICAL AND INSTRUMENT ENGINEERING

## МАШИНОСТРОИТЕЛНА ТЕХНИКА И ТЕХНОЛОГИИ;
## МАШИНОСТРОЕНЕ И УРЕДОСТРОЕНЕ

© International Scientific Conference on Engineering, Technologies and Systems
TECHSYS 2016, Technical University – Sofia, Plovdiv branch
26 – 28 May 2016, Plovdiv, Bulgaria

# MECHANICAL AND TRIBOLOGICAL PROPERTIES OF AlN HARD FILMS DEPOSITED BY REACTIVE MAGNETRON SPUTTERING

NIKOLAY PETKOV[1], TOTKA BAKALOVA[2], TETIANA CHOLAKOVA[1], LUKÁŠ VOLESKÝ[2], PETR LOUDA[2]

**Abstract:** *Aluminium nitride films with a thickness of 2 μm are grown on high speed steel and Si (100) substrates by DC magnetron sputtering at 200°C in a gas mixture of argon and nitrogen, using a pure aluminium target. The influence of process parameters on the mechanical and tribological properties of deposited AlN films was studied. The surface topography of the AlN is investigated by atomic force microscopy in contact mode and an average surface roughness of 52nm is obtained. Mechanical properties of the films are exanimated by nanoindentation and microscratch techniques. The best samples showed the nanohardness of 28 GPa, elastic modulus of 437 GPa and good adhesion to the high speed steel substrates. Using a Multi-Specimen Test System in ball-on-disc mode at the room temperature are evaluated the friction coefficient and the wear rate of AlN. The calculated wear rate of the AlN films is $1.22\times10^{-3}$ $mm^3N^{-1}m^{-1}$ and the coefficient of friction is 0.31.*

**Key words:** *reactive magnetron sputtering; AlN thin films; mechanical properties; tribological properties.*

## 1. Introduction

Aluminum nitride (AlN) has many attractive properties including high thermal and chemical stability, high electrical resistivity, low dielectric contact, high thermal conductivity, high hardness, good mechanical strength, high melting point, high acoustic velocity, good dielectric properties and transparency in the visual and infrared region [1-4]. Because of these properties AlN film have application in various industries as microelectronics, optoelectronics, mechanical engineering, in passivation of thin films, insulator layers, optical sensors in the ultraviolet and hard coatings [1-3].

This paper presents some results of the mechanical and tribological properties of AlN thin films obtained by reactive magnetron sputtering deposition.

## 2. Experimental details

AlN coatings were grown onto steel (ISO 4957, HS6-5-2C) and Si (100) substrates by reactive DC magnetron sputtering technique. The substrate holder was located at 10 cm from the target. Prior to deposition process, the samples were cleaned in ultrasonic bath at the temperature of 60˚C in acetone (8 min) followed by 8 min in isopropanol. After this, the samples were mounted in the PVD chamber, in order to suffer a sputter-cleaning process. Before each deposition, the substrates were sputtered-cleaned at an argon atmosphere for 15 min. The bias voltage with the values of 900V (sample1) and 600 V (sample 2) was applied by a r.f. source (13.56 MHz) for two different series of samples in order to investigate its influence on the layer properties.

After the cleaning, samples were submitted to the coating process. The AlN films were obtained by sputtering of pure Al (99.99%) target in $Ar/N_2$ atmosphere. Deposition chamber was evacuated at $4.6 \times 10^{-3}$ Pa before the film growth process by a turbomolecular pump.

Technological conditions of the deposition process for the two series of samples presented the best properties were: working pressure of 0.8 Pa, the ratio of working gases in the chamber $Ar:N_2$/7:3; magnetron power supply of 600 W and negative substrate bias voltage of 75V. The samples temperature was not higher than 200°C.

The influence of some the sputtering conditions, such as the $N_2$ concentration in the sputtering atmosphere, the bias voltage and the distance between the target and the substrate over the AlN films properties are investigated.

Properties of the deposited films are exanimated by the next techniques:

Copyright © 2016 by Technical University of Sofia, Plovdiv branch, Bulgaria ISSN Online: 2535-0048

Thickness of the AlN films is confirmed using a "stylus" profilometer by measuring the difference in height of the step between an uncoated part and a coated part on Si substrate, provided by the profile scan.

The surface topography of the AlN is investigated by atomic force microscopy in contact mode. The surface area used for the AFM analysis was 10µm×10µm. Two main parameters were analysed: average roughness (Ra) and root mean square roughness (Rms).

The hardness and the elastic modulus were measured by CSM Instruments nanoindentation technique with a trigonal shaped Berkovitch indenter and calculated from the loading–unloading curves. The Berkovitch tip area function was estimated with the Oliver–Pharr method.

The adherence strength evaluation is carried out with a Micro Scratch tester equipped with a diamond tip (Rockwell, radius 120º).

The tribological properties (wear and friction) are studied using CETR UMI Multi-Specimen Test System in ball-on-disc mode at a room temperature in dry friction conditions. The wear scars of the balls and tracks on the samples are observed with light optical microscope (LM) Carl ZEISS Axiolmager M2**.**

## 3. Results and discussion

### *3.1. Surface morphology*

Surface topography of coating is examined with an atomic force microscopy (AFM) in contact mode. Fig. 1 shows the result from scan area 10 x 10 µm$^2$. The AFM analysis indicated that the coatings are dense, with an average surface roughness (Ra) of 52 nm and the root mean square (Rms) roughness of 71 nm.

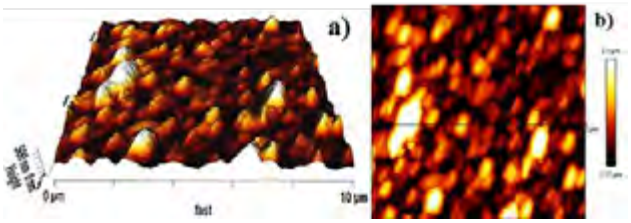



***Fig. 1.*** *(a) 2-D and (b) 3-D AFM image of surface topography of AlN thin films.*

### *3.2. Nanoindentation*

The CSM Instruments Indentation Tester for hardness estimation of the AlN coating surface is used. Measurement of nanohardness is made with a diamond indenter prism of Bercovich, with loads in the range of 1-500 mN. Maximum penetration depth during measurement is not more than 10% from the coating thickness. Table 1 present the measurement results of nanohardness (H), Young modulus (E), and calculated result of plasticity index [11] *H/E* and coating's resistance to plastic deformation [11] $H^3/E^2$.The measured hardness value of AlN coatings is agree with previous reports, between 13 and 37 GPa [1, 5-9].

***Table 1.*** *Mechanical properties of the best AlN samples.*

| Sample, No | H[GPa] | E [GPa] | $H^3/E^2$ | *H/E* |
|---|---|---|---|---|
| #1 | 28.25 | 437 | 0.118 | 0.065 |
| #2 | 22.33 | 249 | 0.180 | 0.090 |

### *3.3. Scratch test analysis*

Scratch tests were carried out in order to evaluate the adhesion between the film and the substrate. The adhesion properties of AlN coatings can be characterized by the following two stages: the first, $L_{C1}$, with the lower critical load, defined as the load where first cracks occurred (cohesive failure); and the second, $L_{C2}$, with the upper critical load, which shows the first delamination when the scratch track occurred (adhesion failure).The failure mechanisms were analyzed by optical microscopy, observing carefully the scratch grooves. Each failure mechanism was identified and measured the corresponding distance to the start point, in order to observe the corresponding normal load in the range of 0–100 N. Figure 2 presents the scratch test results for the #2.

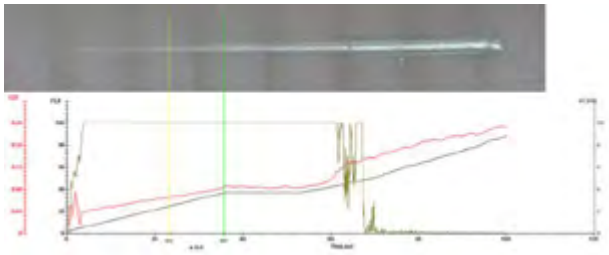


***Fig. 2.*** *Image of the micro-scratch test results of the #2 with marked $L_{C1}$ and $L_{C2}$.*

The first cohesive and adhesive failures were registered at 9.6 N and 21.6 N, respectively for the #1 and at 23.3 N and 35.7 N, respectively for the #2.The investigation of mechanical properties of the AlN revealed, that the value of bias voltage on the stage "substrate cleaning" have influence over the film hardness and adhesion.

### *3.4. Tribology*

The tribological properties (wear and friction) were studied using a ball-on-disk rotating tribometer. The ball material was steel by AISI 420Cwith diameter of 6.35 mm. Used test parameters are: load force of 5N, sliding circumference radius of 4 mm and sliding speed of 60 rpm. The surface of sample after tribology test was scanned with profilometer. Recording of images from a light optical microscope is obtained

by CCD camera. The scanned data can then archive, analyze and modify by the software. The goal of data software analysis is the processing of visual information, elimination of random errors and extraction of typical features characterizing the image. [12]

### 3.4.1. Coefficient of friction

Coefficient of friction is a value that shows the relationship between the force of friction between two objects and the normal force between the objects. Therefore, its value is correct only for the friction pair for which is determinate. Here the friction pair are: (1) the uncoated steel substrate and steel ball, and (2) the AlN coating, deposited on the steel substrate, and steel ball. Fig. 3 shows the evolution of the friction coefficient results during the ball-on-disk tribology test in the case of dry friction. Curve 1 present the friction evolution between the AlN coating and ball. The coefficient of friction is around 0.31, and the coating endurance is 40 cycles (40 s) of dry friction in these circumstances. For comparison, Wu and co-authors are reported a friction coefficient value of 0.3235 for single AlN layer, in the case of 3 mm GCr15 steel ball counter body[7]. Curve 2 (Fig. 3) present friction between uncoated sample and ball. The coefficient of friction between those two parts is around 0.15, and the surface endures 130 cycles (130 s) of dry-friction in these circumstances.

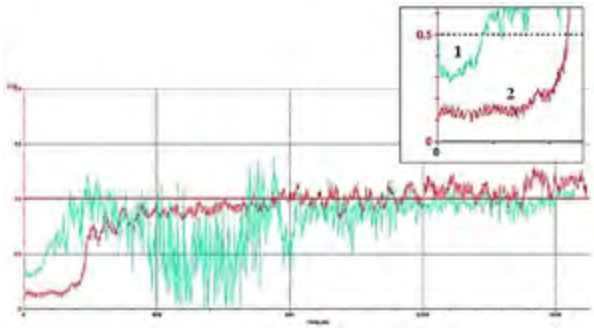



***Fig. 3.*** *Friction curves of the AlN coating sample 1 (1) and steel substrate (2) sliding against steel ball at 25°C.*

### *3.4.2. Wear rate*

Transferred material from ball to the coated surface and from coating to the ball surface, during tribology test ball-on-disc, makes difficult to measured wear of the coating. Therefore, wear of the counter body (ball) is measured and is being reported. The estimation of ball wear is made by Eq. (1) according standard EN 1071-13:2010.

$$V = \frac{\pi A^3 B}{32D} \quad (1)$$

where $V$ is wear volume in mm$^3$, $A$ is measuring wear scar diameter in direction of erasure in mm, $B$ is measuring wear scar diameter in direction perpendicular of the erasure in mm, and $D$ is the ball diameter in mm.

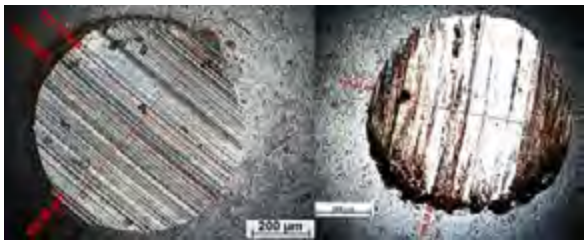



***Fig. 4.*** *Wear scar of the ball used for ball-on-disc test on sample with AlN coating (left) and on the uncoated sample (right).*

Diameter values on the wear scar are measured by LM. Fig. 4 (left) presents wear scar photography of the ball from ball-on-disc test made over the AlN coated sample. The average value of the measured wear scar diameter in direction of erasure is A = 756.56 µm, and the measured wear scar diameter in direction perpendicular of the erasure is B = 830.98 µm. Therefore, the calculated value of ball wear by is V = $5.56 \times 10^{-3}$ mm$^3$. Fig.4 (right) presents wear scar photography of the ball from ball-on-disc test made over the uncoated sample. The measured values of the diameters are A = 750.71 µm and B = 786.17 µm. Therefore, the calculated value of ball wear by is V = $5.14 \times 10^{-3}$ mm$^3$.

Wear rate estimation of the coating is made by the follow equation [10]:

$$\text{wear rate} = \frac{\text{wear volume}}{\text{load} \times \text{sliding distance}} \quad (4)$$

where sliding distance is in m, load in N, and wear volume (in mm$^3$) of the coating is calculated as follow:

$$V = Sh \quad (5)$$

$$S = 2\pi R_s d_s \quad (6)$$

where $h$ is the penetration depth (or layer thickness), $S$ is the track area, $R_s$ is the sliding circumference radius, and $d_s$ is the averagetrack width.

Thickness of AlN coating is 2 µm. Average track width is 0.61 mm (Fig. 5).Therefore, the calculated wear volume of the AlN coating is $30.662 \times 10^{-3}$mm$^3$. Sliding distance is equivalent of 200 cycles, consequently, the calculated wear rate of the AlN coating is $1.22 \times 10^{-3}$ mm$^3$N$^{-1}$m$^{-1}$.

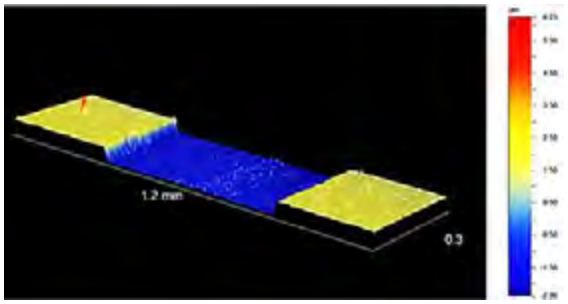



***Fig. 5.*** *The wear track profile of the sample with AlN coating (sliding with steel ball), 3Dimage.*

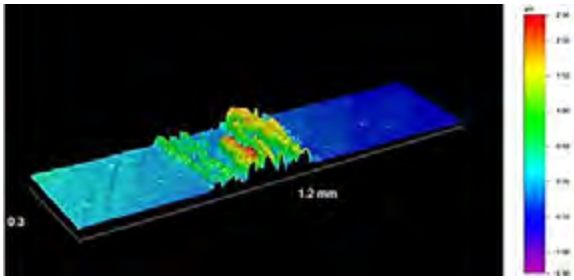



***Fig. 6.*** *The wear track profile from the ball-on-disc test on the sample without coating, 3D image.*

Fig. 5 presents the profile of the track on the sample with AlN coating after ball-on-disc test with measured track width value by mechanical profilometer. Fig. 6 presents the profile of the track on uncoated sample after ball-on-disc test with measured tracks width value by mechanical profilometer. High speed steel (ISO 4957) has a significantly higher wear resistance compared with steel AISI420, due to the high percentage of carbon (C) and a high proportion of tungsten (W). This effect is observed in Fig. 6.

### 4. Conclusions

AlN thin films were deposited on HSS and silicon substrates by DC reactive magnetron sputtering in a gas mixture of argon and nitrogen. The AlN coatings are dense, with an average surface roughness of 52 nm. The samples have shown good adhesion to the high speed steel substrates, high value of hardness, low coefficient of friction and good adhesion properties. An in-depth study of the tribological properties of these coatings revealed that AlN films have higher wear resistance in comparison to high speed steel substrates. It has been found that the bias voltage applied to the substrate during the cleaning affects the properties of the layer.


### ACKNOWLEDGEMENT

The paper was supported in part by the project LO1201 through the financial support of the Ministry of Education, Youth and Sports in the framework of the targeted support of the "National Programme for Sustainability I" and the OPR&DI project "Centre for Nanomaterials, Advanced Technologies and Innovation" registration number CZ.1.05/2.1.00/01.0005.


### REFERENCES


1. L. Yate, J.C. Caicedo, A. Hurtado Macias, F.J. Espinoza-Beltran, G. Zambrano, J. Munoz-Saldana, P.Prieto, Surf. & Coat. Technology **203**, 1904 (2009)
2. K. Tonisch, V. Cimalla, Ch. Foerster, H. Romanus, O. Ambacher, D.Dontsov, Sensors and Actuators A **132**, 658 (2006)
3. S. Venkataraj, D. Severin, R. Drese, F. Koerfer, M. Wuttig, Thin Solid Films **502**, 235 (2006)
4. F. Hajakbari, A. Hojabri, M.M. Larijani, Journal of Applied Chemical Research, 8, **3**, 45 (2014)
5. T.A. Rawdanowicz, V. Godbole, J. Narayan, J. Sankar, A. Sharma, Compos. Part B **30**, 657 (1999)
6. A.L. Ji, L.B. Ma, C. Liu, C.R. Li, Z.X. Cao, Diamond Relat. Mater. **14**, 1348 (2005)
7. Z.G.Wu, G.A. Zhang, M.X.Wang, X.Y. Fan, P.X. Yan, T. Xu, Appl. Surf. Sci., **253**, 2733 (2006)
8. X.Wang, A. Kolitsch, F. Prokert,W. Möller, Surf. Coat. Technol. **103–104** 334 (1998)
9. J.H. Lee, W.M. Kim, T.S. Lee, M.K. Chung, B. Cheong, S.G. Kim, Surf. Coat. Technol. **133 - 134**, 220 (2000)
10. K. Singh, P.K. Limaye, N.L. Soni, A.K. Grover, R.G Agrawal, A.K. Suri, Wear, **258**, 1813 (2005)
11. A. Leyland, A. Matthews, Wear, **246**, 1 (2000)
12. T. Bakalova, T., L. Volesky, P. Loudaand Z. Andrsova. The Use of Optical Microscopy to Evaluate the Tribological Properties. Manufacturing technology. Vol. 1, N. 3. pp. 256 – 261. ISSN 1213-2489 (2014).



Central Laboratory of Applied Physics, Bulgarian Academy of Sciences, 61, St. Peterburg Blvd. 4000 Plovdiv, Bulgaria,
E- mail: petkovnik@gmail.com
E- mail: ipfban-dve@mbox.digsys.bg

Institute for Nanomaterials, Advanced Technologies and Innovation, Technical university of Liberec, Studentská 1402/2, 461 17 Liberec 1, Czech Republic,
E-mail: totka.bakalova@tul.cz
E-mail: lukas.volesky@tul.cz
E-mail: petr.louda@tul.cz

© International Scientific Conference on Engineering, Technologies and Systems
TECHSYS 2016, Technical University – Sofia, Plovdiv branch
26 – 28 May 2016, Plovdiv, Bulgaria

# DEPOSITION OF AlCN THIN FILMS BY REACTIVE DC MAGNETRON SPUTTERING AND TRIBOLOGY

NIKOLAY PETKOV[1], TOTKA BAKALOVA[2]

**Abstract:** *The process of friction between two solid surfaces is inevitably accompanied by the occurrence and energy losses. If the surfaces are separated by a layer of dissimilar material, the friction process also takes place within the layer, and the wear of the surface and possibly the energy losses due to friction are reduced considerably. AlCN films with differing composition are deposited on the samples from high-speed steel by reactive DC magnetron sputtering of pure Al (99.99%) with various different gas ratios of $N_2$ and $CH_4$. The deposition chamber, before films growth processes, is evacuated up to approximately 5.2 $\times 10^{-3}$Pa by a turbomolecular pump. During the deposition process and Ar plasma cleaning process the bias voltage is applied with r.f. source (13.56 MHz).Tribological testing (EN1071-13:2010) is conducted with a constant load of 5 N at room temperature and humidity of 40 ± 2 %, by using a ball made from steel ISO 683/13 (X105CrMo17) with a diameter of 6.350 mm.*

**Key words:** *thin films, magnetron sputtering, tribology, coefficient of friction, wear*

## 1. Introduction

Covalent compounds comprising light elements have excellent chemical and mechanical stability, due to the small atomic radius and strong interatomic bonding [1, 2]. Carbides, nitrides and aluminium have attracted considerable interest from multidisciplinary researchers and have found extensive applications in various industry branches [1-6]. In recent years, the research work has been shifting gradually, but steadily, from the binary materials to ternary ones [1, 2, 6].

Tribology is the study of the thermal, mechanical and chemical interactions that occur in mutually acting solid surfaces and their surroundings. Tribology should be understood as an interdisciplinary field of study. An explanation of the various scientific disciplines is often essential for an understanding of tribological problems. [7-9]

During relative movement between solid bodies, friction and wear are an inevitable occurrence. Both a low friction coefficient and low wear are desirable for most systems; this is associated with ensuring the reliable working of the system and less energy consumption, which leads to an extension of lifespan. Some systems require a high friction coefficient (e.g. a tyre on the road) and some systems require even higher wear (e.g. pencils), but most effort is focused on developing application systems with a low a friction coefficient and minimal wear. [7- 9] Wear is usually defined as "damage to the hard surface comprising a progressive loss of material due to relative movement between the surface and the surface of another material or substance" [10].

Two solid bodies mutually deform each other if they come into contact. Deformation in the first body occurs as a result of mechanical resistance of the second body and vice versa. An important factor is whether or not the solid body comes into contact with the entire surface, partially or the surfaces are in a non-conforming contact. Contact interactions are further complicated by surface roughness. The development of structures of various mechanical systems is associated with the selection of suitable materials with specific properties. Friction and wear depend on many parameters and conditions, including: material pairing, contact geometry, applied normal load, contact pressures, relative sliding speed, material surface topography and roughness, environment, temperature, chemical interactions, sliding direction (unidirectional, reciprocating, random, etc.) [7-9]

Many mechanical systems need to work in various different environments. Some components must provide reliable wear and friction against several different types of materials. [10]

In this work are studied the mechanical and tribological properties of the AlCN thin films, with different compositions, deposited by the reactive

Copyright © 2016 by Technical University of Sofia, Plovdiv branch, Bulgaria ISSN Online: 2535-0048

DC magnetron sputtering as bias polarization voltage is applied by r.f. source.

## 2. Experimental information

Experiments are carried out in cooperation between the Central Laboratory of Applied Physics, Bulgarian Academy of Sciences and the Institute for Nanomaterials, Advanced Technology and Innovation, Technical University of Liberec (TUL).

Polished discs (Ø 20 mm × 5 mm thick) of EN ISO HS 6-5-2 tool steel are used as the substrate material. It is a high-speed Mo-W steel with high toughness. The chemical composition of the EN ISO HS 6-5-2 steel [wt %] is: C 0.80–0.90; Mn max. 0.45; Si max. 0.45; P max 0.035; S max 0.035; Cr 3.80–4.60; Mo 4.50–5.50; W 5.50–7.00; V 1.50–2.20.

AlCN films with differing composition are deposited on the samples from high-speed steel by reactive DC magnetron sputtering of pure Al (99.99%) with various different gas ratios of $N_2$ and $CH_4$. Fig. 1 shows the substrate holder located at 10 cm from the magnetron target (left) and shape of the plasma during deposition process (right).

Vacuum chamber, before films growth processes, is evacuated up to approximately $5.2 \times 10^{-3}$ Pa by a turbomolecular pump. During the deposition process and Ar plasma cleaning process the bias voltage is applied with r.f. source (13.56 MHz).



***Fig. 1.*** *The substrate holder location and plasma in vacuum chamber during deposition process.*

Table 1 shows the gas flow ratio between the reactive gasses. Gas flow ration between Ar and the reactive gasses during deposition processes is 7/3. To achieve good adhesion to the substrate cleaning in a glow discharge of argon for 30 min at chamber pressure of 4 Pa and negative bias voltage of 900 V is performed, followed by deposition of a contact transition layer of AlN. Parameters of the deposition processes are: working chamber pressure of 0.7 Pa, magnetron power of 600W, negative bias voltage of 75V, and deposition time of 40 min. Sample temperature, during deposition is not higher than 200°C.

Prior to deposition process, the samples were cleaned in ultrasonic bath at the temperature of 60˚C in acetone (8 min) followed by 8 min in isopropanol.

***Table 1.*** *Gas flow ration*

| *Type of coatings* | AlCN-1 | AlCN-2 | AlCN-3 |
|---|---|---|---|
| $N_2/CN_4$ | 5/1 | 2/1 | 1/1 |

Using CSM Instruments nanoindentation technique with a trigonal shaped Berkovitch indenter, the hardness and the elastic modulus were measured and calculated from the loading–unloading curves. The Berkovitch tip area function was estimated with the Oliver–Pharr method.

The adherence strength evaluation is carried out with a Micro Scratch tester equipped with a diamond tip (Rockwell, radius 120º).

Using CETR UMI Multi-Specimen Test System in ball-on-disc mode at a room temperature in dry friction conditions are studied the layers tribological properties (wear and friction). The wear scars of the balls and tracks on the samples are observed with light optical microscope (LM) Carl ZEISS Axiolmager M2**.**

## 3. Results and Discussion

### 3.1. Mechanical properties

Evaluation of the thin films thicknesses*d* is made by calottes. The diameter of used ball for this purpose is 30 mm, and the thickness results are given in Table 2.

The CSM Instruments Indentation Tester for hardness estimation of the AlCN thin films surfaces is used. Measurement of nanohardness is made with a diamond indenter prism of Bercovich and loads in the range 1-500 mN. Maximum penetration depth during measurement is not more than 10 % from coating thickness. Table 2 shows the results from measurement of nanohardness *H*, elastic module *E*, and calculated ratio of plastic deformation *H/E* between them. This ration gives information for wear resistance of the thin films [11].

***Table 2.*** *Thickness d, Nanohardness H, elastic module E, and plastic deformation H/E*

| *Type of coatings* | d [μm] | H[GPa] | E[GPa] | *H/E* |
|---|---|---|---|---|
| AlCN-1 | 1.236 | 14 | 125 | 0.112 |
| AlCN-2 | 1.225 | 12 | 499 | 0.024 |
| AlCN-3 | 1.115 | 7.7 | 197 | 0.039 |

High *H/E* ratio is often a reliable indicator of good wear resistance in a coating, with the caveat that super- or ultra-hardness should not be pursued at the cost of extreme elastic property mismatch

between coating and substrate, since this will restrict the practical applicability of such coatings. Regardless of such factors, the reliability of the data employed to calculate *H/E* values needs to be assured, if the theoretical benefits of coating materials are to be translated into 'real' industrial applications. [12]

### 3.2. Scratch test analysis

Bruker's UMT-1 micro-mechanical test instrument platform provides ultimate flexibility in indentation and scratch testing.

Progressive Load Scratch Test: A stylus is moved over a specimen surface with a linearly increasing load until failure occurs at critical loads (Lci). Normal force and tangential force are recorded. The failure events are examined by an optical microscope. Lc is a function of coating-substrate adhesion, stylus-tip radius, loading rate, mechanical properties of substrate and coating, coating thickness, internal stress in coating, flaw size distribution at substrate-coating interface, and friction between stylus-tip and coating. Figure 2 presents the scratch test results for the AlCN-1.

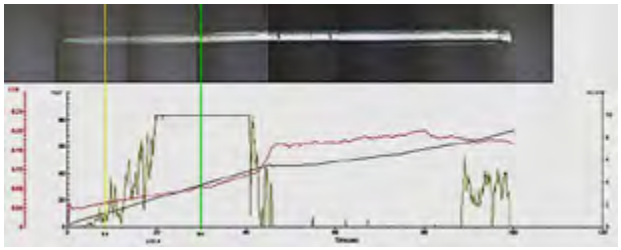


***Fig. 2.*** *Image of the scratch test results of the AlCN-1 with marked $L_{C1}$ and $L_{C2}$*

Scratch test technique is carried out to characterize film adherence strength. The adhesion properties of AlCN thin films is characterized by the following two stages: (1)$L_{C1}$, with the lower critical load, defined as the load where first cracks occurred (cohesive failure); and (2)$L_{C2}$, with the upper critical load, which shows the first delamination when the scratch track occurred (adhesion failure). The thin film adhesion scratch tests disclose the cohesion and adhesion properties of the tested coating. In virtue of the tests carried out, it is found that the critical load $L_{C1}$ fitted within the range 5 – 11 N, and $L_{C2}$ fitted within the range 18 – 31 N (Table 3).

### 3.3. Tribology measurement

Tribological testing is carried out in the Laboratory of Preparation and Analysis of Nanostructures at the Technical University of Liberec. Tribological testing (EN1071-13:2010) is conducted with a constant load of 5 N at room temperature and humidity of 40 ± 2 %, by using a ball made from steel ISO 683/13 (X105CrMo17) with a diameter of 6.350 mm, and follow chemical composition [wt %]: C 0.95 - 1.20; Si max 1.0; Mn max 1.0; P max 0.040; S max 0.015; Cr 16.0 – 18.0; Mo 0.40 – 0.80 (57–60 HRc). Radius, of the circle along the "ball" body is moving, is 4 mm.

The basis of the tribological measurements is the "ball-on-disc" testing method. Fig. 3 shows schematically "ball-on-disc" configuration. The measurement involves the injection of fixed attachments of the test piece ("ball") in the form of balls of the chosen material defined as the force to drive (the test sample).An essential part of the test measurement is a friction sensor. The coefficient of friction (CoF) between the unit and the disc is determined during the test measurement.

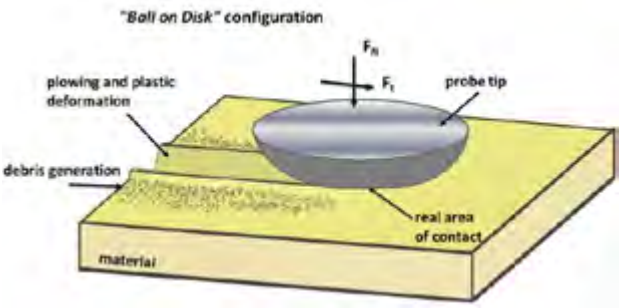



***Fig. 3.*** *Schematic representation of "ball-on-disc" configuration[7]*

Fig. 4 presents graphically the measured dry friction coefficients, and their numerical values are given in Table 3.

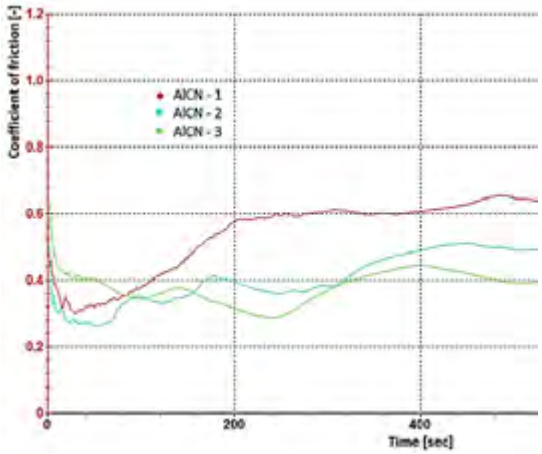



***Fig. 4.*** *Dry friction coefficients of AlCN thin films*

The optical microscope Zeiss AXIO Imager M2 is employed to evaluate the scar size on the steel balls. Attrition can be defined as a progressive loss of material due to relative movement between both surfaces. The result is a specific amount of ploughed material, in some cases also plastic deformation or displacement of the disc material due to side forces acting on the ball.

Evaluation of wear of the friction pairs of the ball against the steel is performed according to standard EN 1071-13:2010, as calculation of wear volume $V_{pin}$ [mm$^3$] of the balls is made by Eq. (1). Where $A$ [mm] is measuring wear scar diameter in direction of erasure, $B$ [mm]is measuring wear scar diameter in direction perpendicular of the erasure, and $D$ [mm]is the ball diameter.

$$V_{pin} = \frac{\pi A^3 B}{32D} \quad (1)$$

***Table 3.*** *CoF and adhesion properties of AlCN thin films, and wear volume of the balls*

| *Type of coatings* | CoF [-] | $V_{pin}\times10^{-3}$ [mm$^3$] | $L_{C1}$ [N] | $L_{C2}$ [N] |
|---|---|---|---|---|
| AlCN-1 | 0.354 ± 0.038 | 1.105 | 11 | 31 |
| AlCN-2 | 0.317 ± 0.040 | 0.585 | 5 | 18 |
| AlCN-3 | 0.336 ± 0.081 | 0.870 | 6.5 | 26 |

## 4. Conclusions

The experiments describe the mechanism of the process of interaction of the friction elements and their wear. The described experiments simulate the processes during machine cutting and enable us to predict the behaviour of materials during their practical application.

In this material are presented and studied AlCN thin films deposited by reactive DC magnetron sputtering as the bias polarization voltage is applied by r.f. source. The measured nanohardness of this layers are commensurate with result presented in Ref. [6], but are too far from reported 53.4 GPa in Ref. [1].

The study shows that the changes in gas flow mixture at the deposition process have influence over mechanical and tribologycal properties of the thin films, as decrease of CoF, hardness and value of ratio *H/E*. Notably, that the observed differences in the thickness are inessential.

## ACKNOWLEDGEMENT

The paper was supported in part by the project LO1201 through the financial support of the Ministry of Education, Youth and Sports in the framework of the targeted support of the "National Programme for Sustainability I" and the OPR&DI project "Centre for Nanomaterials, Advanced Technologies and Innovation" registration number CZ.1.05/2.1.00/01.0005.

## REFERENCES

1. A.L. Ji., L.B. Ma, C. Liu, C.R. Li, Z.X. Cao, Diamond & Related Materials 14, 1348 (2005)
2. A.L. Ji., L.B. Ma, C. Liu, P. Zheng, C.R. Li, Z.X. Cao, Applied Physics Letters 86, 021918 (2005)
3. A. Lousa, S. Gimeno, J. Vac. Sci. Technol., A, Vac. Surf. Films 15 (1) (1997) 62.
4. C.M. Zettering, M. Ostling, K. Wongchotigul, M.G. Spencer, X. Tang, J. Appl. Phys. 82 (6) (1997) 2990.
5. J.H. Xu, L.H. Yu, I. Kojima, J. Appl. Phys. 94 (10) (2003) 6827.
6. L. Yate, J.C. Caicedo, A. Hurtado Macias, F.J. Espinoza-Beltran, G. Zambrano, J. Munoz-Saldana, P.Prieto, Surf. & Coat. Technology 203, 1904 (2009)
7. Bakalova, T., aj. Nanoadditives SiO2 and TiO2 in Process Fluids. Manufacturing technology. 1. vyd. Ústí n. L.: J. E. Purkyne University in Usti nad Labem, 2015, vol. 4. pp. 502 – 508, ISSN 1213-2489.
8. K. Holmberg, A. Matthews: Coatings Tribology: Properties, Mechanisms, Techniques and Applications in Surface Engineering. 2nd ed. Boston: Elsevier Science, xv, 560 p., [3] p. of plates. Tribology and interface engineering series, 56. ISBN 9780444527509, 2009.
9. Burakowki, T., Wierzchon, T. (1999). Surface engineering of metals, CRC Press LLC, ISNB 0–8493–8225–4, New York.
10. Shaji, S., Radhakrishnan, V., (2003). Application of solid lubricants in grinding: investigations on graphite sandwiched grinding wheels. Mach. Sci. Technol. 7, 137-155.
11. J. Musil, RSC Adv., 2015, 5, 60482
12. A. Leyland, A. Matthews, Wear, **246**, 1 (2000)

Central Laboratory of Applied Physics, Bulgarian Academy of Sciences, 61, St. Peterburg Blvd. 4000 Plovdiv, Bulgaria, E-mail: petkovnik@gmail.com

Institute for Nanomaterials, Advanced Technologies and Innovation, Technical university of Liberec
Studentská 1402/2, 461 17 Liberec 1, Czech Republic, Phone: +420 485353818, E-mail: totka.bakalova@tul.cz.

© International Scientific Conference on Engineering, Technologies and Systems
TECHSYS 2016, Technical University – Sofia, Plovdiv branch
26 – 28 May 2016, Plovdiv, Bulgaria

# DEVELOPMENT OF SPECIALIZED HOLDERS FOR BEARING BALLS AND ROLLERS COATING BY PVD METHODS

VIKTOR KOPANOV, STANISLAVA RABADZHIYSKA

**Abstract:** *Two types of specialized holders for coating deposition on details as bearing balls and rollers were developed for Cathodic arc deposition (CAD) and Unbalanced magnetron sputtering (UBMS) equipment. It is important to achieve maximum coating uniformity on the components surface.*

**Key words:** *specialized holders, bearing balls, rollers, one axial and biaxial rotation*

## 1. Introduction

One of the main aspects in transport and energetics equipment is the effective torque transmission. It is known that the main losses at power transmission are in the bearings and gears (reduction gears). Another problem which occurs during the components and systems exploitation is balls wearing out [1, 2]. It is necessary to extend the life-time of the components and systems in use. Losses decrease and resource increase are foreseen when the details are designed. This gives an opportunity for an additional optimization of bearing lubrication and cooling [3]. For this purpose physical vapour deposition (PVD) coatings can be successfully deposited on bearings details and gears. For example, the superhard multilayer nanocomposite coatings can be deposited on balls, rollers, bearing inner and outer rings. The change of the surface characteristics of the details, such as decrease of the coefficient of friction and hardness increase, are methods, which solve problems as indices bearing balls stability at a low quantity of lubricant-cooling liquid and reversing loadings at torque transmission [4]. Different coatings as diamond-like carbon are of interest for use in industrial applications. Multilayer coatings as CrAlN/TiAlN and different carbo nitrides such as TiCN, CrCN have good exploitation properties [5].

Deposition of thin films by PVD techniques has found widespread use in many industrial sectors [6]. A number of special devices were worked out for coating bearing balls with single and multilayer coatings [7]. The described equipment is suitable for large-scale production but the high cost and very complex construction make them incompatible for scientific needs. It is appropriate for magnetic and non-magnetic details with spherical shape. Depending on that what the material of the balls is, the construction can consist electromagnets, reduction gears, endless magnetic belt and angle situated set of rotating plates with slots.

The aim of this study is development of specialized sample holders for deposition of coatings on details as bearing balls and rollers by cathodic arc deposition (CAD) and unbalanced magnetron sputtering (UBMS) equipment. It is important to achieve a maximum coating uniformity on the component surface. It can perform by a continuously movement (rotation) of the details around one or many axes [8]. Different specialized holders were developed. Each of them is characterized by its functionality, the details which will be coated, the complexity level of the construction and special requirements. When the bearing balls and rollers rotate, they are constantly in a contact with different surfaces of the holder. This ensures a reliable electric contact to the coated details and thus provides, a bias voltage which results in high coating uniformity.

## 2. Description of the holders

Two types of specialized holders were developed. The holders were made of a high quality stainless steel SS 304. The first one was created for a work together with an available holder to the CAD equipment Platit $\pi^{80+}$ (company Platit, Switzerland). After constructional modifications, this holder can be successfully used during coating deposition in UBMS equipment UDP850-4 (company Teer Coatings, England). Fig.1 shows a common view of a specialized holder for the Platit $\pi^{80+}$ equipment, designed for one axial and biaxial rotation. The second holder has a simple construction which is easy to make and all-purpose.

Copyright © 2016 by Technical University of Sofia, Plovdiv branch, Bulgaria ISSN Online: 2535-0048



***Fig. 1.*** *A picture of specialized holder for Platit $\pi^{80+}$ equipment for CAD, designed for one axial and biaxial rotation*

It can be used in both equipment depending on the technological parameters.

Fig.2 illustrates a specialized holder for Platit $\pi^{80+}$ equipment which is designed for one axial rotation. In Fig.3 it is shown a plate holder that provides biaxial rotation and is suitable for application in Platit $\pi^{80+}$ and UDP 850-4.



***Fig. 2.*** *A picture of specialized holder for Platit $\pi^{80+}$ equipment by CAD, designed for one axial rotation*

The first holder provides a maximum coating uniformity on the balls. It consists of a base and a bottom, which are welded in between them. The bottom radius assists the bearing ball continuously movement on the surface. As a result of the carousel movement and a specific geometry of the bottom it gets the ball oscillation around the balance position without motion which is the lowest point of the bottom. A sketch of holder is presented in Fig. 4.



***Fig. 3***. *A picture of specialized holder for Platit $\pi^{80+}$ equipment by CAD, designed for biaxial rotation*

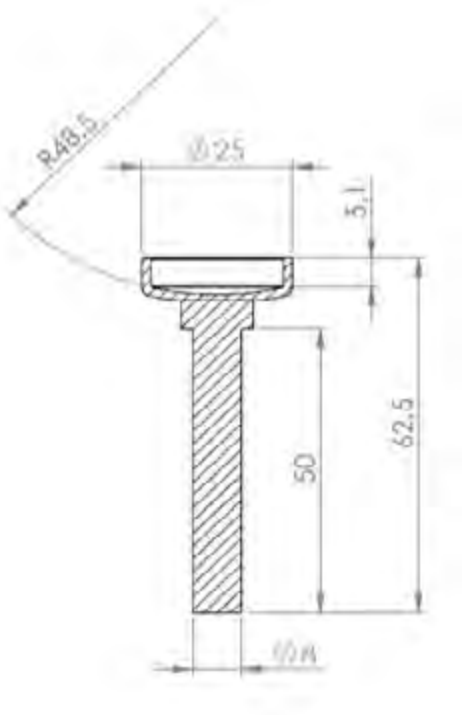



***Fig. 4***. *A sketch of a holder for balls*

The second holder contains metal plates with definite sizes and many holes, which were put in grid baskets. Maximum three balls could be placed in the baskets. The plates can provide to the details one axial or biaxial rotation in common with the equipment carousel depending of the sizes and construction them. Schematic illustrations of stainless steel plates with different sizes and a number of holes which can be used depending on technological requirements are presented in Fig.5 and Fig. 6.

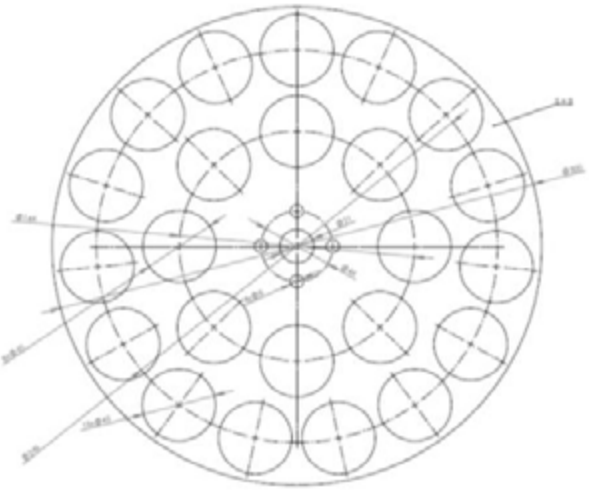


***Fig. 5.*** *A sketch of plate with 23 holes*

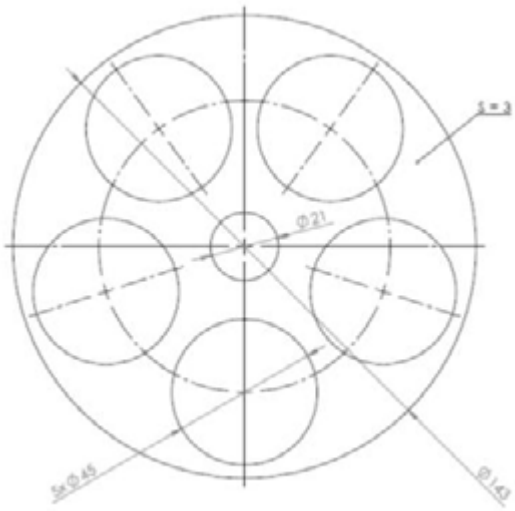


***Fig. 6****. A sketch of plate with 5 holes*

## 3. Results

The developed specialized holders are already in an operation together with the available high technological equipment at the Central Laboratory of Applied Physics in Plovdiv. The coated balls have a high quality and it is expected to have a good uniformity of the coating thickness because of a provided great number of rotation axes during the process. Fig. 7 illustrates the bearing balls and rollers which are coated with TiCN. For further experimental needs in inner and outer bearing rings were coated with TiCN (Fig. 8). Mentioned components as TiCN coated bearing balls and rings are already in use as a part of experimental bearing assembly integrated at CAD and UBMS equipment at CLAP.



***Fig. 7.*** *A picture of balls and rollers, coated with TiCN*



***Fig. 8.*** *A picture of inner and outer rings, coated with TiCN*

## 4. Conclusion

Specialized sample holders for details coating as bearing balls and rollers has been developed for Cathodic arc deposition (CAD) and Unbalanced magnetron sputtering (UBMS) equipment. A good coating quality on the components surface was achieved. It was performed by a continuously movement (rotation) around one or many axes of the coated balls, provided by the developed holders. They are characterized with different constructions that depend on technological needs. The devices are low-cost and effective in use, and in the same time cover the requirements of high technological processes as PVD. The coated bearing balls and rings, which are in use, show excellent work properties. They are working in hard conditions as excessive heat and without cooling and lubrication. Components of the bearing assembly with coating have longer service life, minimize the friction and noise, greater thermal and corrosion resistance.

## REFERENCES


1. Chang C., Chen H., Lee J., Duh J. (2015). *Surface & Coatings Technology 284*, 273-280.
2. Chen H., Chan Y., J. Lee, Duh J. (2010). *Surface & Coatings Technology 205*, 1189-1196.
3. Chen H., Chan Y., Lee J., Duh J. (2011). *Surface & Coatings Technology 206*, 1571-1580.
4. Lukaszkowicz K., Sondor J., Balin K., Kubacki J. (2014). *Applied Surface Science 312*, 126-135.
5. Li W., Liu P., Zhu X., Pan D., Zhang K., Xinkuan L. (2015). *Journal of Alloys and Compounds* 650, 592- 611.
6. Mishev G., Dishliev S., Rupetsov V. (2014). Increase the wear resistance of injection molds using PVD coatings. *Tribological Journal BULTRIB*, vol. IV, 147-154 (in Bulgarian).
7. Иващенко, С. А. (2001). *Газотермические и вакуумно-плазменные покрытия со специальными физико-механическими свойствами*, 214. УП „Технопринт", Минск.
8. Pashinski Ch. (2013). Algorithm and program for synthesis of carousels for PVD technology. *International Journal of Scientific & Engineering Research*, vol. 4, iss. 6, 870-876.



Contacts
Central Laboratory of Applied Physics,
Bulgarian academy of sciences
Address: 61 Sankt Peterburg Blvd. 4000,
Plovdiv, Bulgaria
Phone: 0878 195 325
E-mail: viktorkopanov@abv.bg
E-mail: s1983@abv.bg

© International Scientific Conference on Engineering, Technologies and Systems
TECHSYS 2016, Technical University – Sofia, Plovdiv branch
26 – 28 May 2016, Plovdiv, Bulgaria

# EXPERIMENTAL COMPARISON OF WEAR RESISTANCE AND CYCLIC LOADING TO BENDING BETWEEN CYCLOID AND INVOLUTE GEARS

DIMITAR PETROV, PETKO DOBREV, STANISLAV ALEXIEV

**Abstract:** *The reasoning for the proposed replacement of involute gears with cycloid is given. The experimental results obtained from comparative tests between cycloid and involute plastic gears in terms of load capacity, wear resistance, temperature on pitch point and noise emission are reported. Some conclusions with respect of the derived experimental results are made.*

**Key words:** *cycloid gears, involute gears, plastic spur gears, wear, pitch line fracture*

## 1. Introduction

The use of plastic gears is already widely spread in many industries and applications, which is on account of their beneficial properties – low cost; light weight and low inertia; capability to absorb shock and vibration; noiselessness; their tolerances often less critical in comparison of metal gears; their ability to operate under dry (not lubricated) conditions; etc. [1]. However, when using plastic gears (comparatively with metal gears) should be taken into account such their shortcomings as lower strength parameters concerning broken teeth from bending fatigue, greater wear and lower contact resistance of the tooth flanks, greater thermal expansion and contraction, greater absorption moisture, etc.

Up to now a lot of investigations are made to improve load capacity and durability to wear of the plastic gears. For improving the capacity to cyclic loading of the plastic gears are used different measures – appropriate choice of a module, pressure angle or number of teeth [2]. These measures have controversial effect, which effect depends by the type of the plastic - hard thermoplastic or elastic thermoplastic. Another approach is, for example, the use of advanced plastics or reinforced plastics with appropriate fillers (carbon or glass fiber) - but this is linked to increased costs of the final product. The latter approach is used successfully to improve the durability to the wear [3]. And other techniques are used to improve durability against wear of gears - Rao et al [4] looked at the effect of poly-tetra-fluoro-ethylene (PTFE) as an internal lubricant on the friction and wear of filled and unfilled PA66 and polyacetal; Akkurt [5] examined the effect of the surface roughness of steel gears running against polymer (acetal) gears; by K.D.Dearn, T.J.Hoskins, D.G.Petrov et al [6] have investigated the possibilities of using a series of solid lubricant coatings deposited on flanks of the polymer gear teeth.

Stanislav Aleksiev et all [7] have proposed substitution of the involute profile of teeth with cycloid profile for plastic gears to improve the load capacity and the durability to wear and have made an attempt to justify theoretically, in their opinion, the advantages of cycloid profile in comparison with the involute profile. For this purpose, two gear pairs with two identical spur gears with number of teeth z=17 and module m=1 mm are theoretically compared - one gear pair with involute profile and the other - with cycloid profile. Here is found by simple calculating, that the sliding velocity between meshing teeth profiles in the case of using of cycloid profiles is less than the case of using of involute profiles. The second reason for less wear of the cycloid gears is the presence of smaller contact stresses in comparison with the such contact stresses of involute gears, because of fact that in the cycloid gears the contact take place between a convex flank and concave surface, whereas in involute gears, the convex surfaces are in contact [7, 8]. In [7] it is further maintained that the teeth's strength against bending in the cycloid gears will be greater than that of the involute gears, due to thicker root at the base of the tooth.

The purpose of this work is to report about the experimental results derived in the comparative tests in respect of load capacity and resistance to wear of plastic spur gear wheels - the half of plastic

Copyright © 2016 by Technical University of Sofia, Plovdiv branch, Bulgaria ISSN Online: 2535-0048

spur gear wheels are made with cycloid profile of the teeth, the second half are made with involute profile. These comparative tests have been made to ascertain experimentally the correctness of the suppositions given in [7].

## 2. Materials and basic parameters of the gear wheels, test rig, experimental methodology and conditions

All the studied plastic spur gears were made by typical for that purpose material polyamide PA 6. The target applications of that material are transportation, mechanical engineering, automotive industry, conveyor technology, packaging and paper machinery, textile industry. Because of its main features as high strength, good slide and wear properties, good machinability, resistance to many oils, greases and fuels, low cost, it is widely used for manufacturing of gears. The main mechanical properties (as density 1.19 g/cm$^3$, ball indentation hardness - 175 MPa (at norm ISO 2039-1), modulus of elasticity (tensile test) - 3900 MPa (at norm DIN EN ISO 527-2), tensile strength - 79 MPa (at norm DIN EN ISO 527-2), impact strength (Charpy) - 53 kJ/m2 (at norm DIN EN ISO 179-1eU)) and thermal properties (melting temperature - +221°C (at norm DIN 53765), long term service temperature - +100°C, short term service temperature - +160 °C) of polyamide PA 6 could be found in [14].

The studied plastic spur gears were made by means of cutting – four involute gears (fig.1) were made on hobbing milling machine (machining with hob cutter), and four cycloid gears were made on CNC milling machine by means of end milling cutter. Except their profile, all the gears have steel insertion (fig.2) and similar parameters - number of teeth z = 15, module m = 4 mm, width of the tooth crown b = 18 mm, profile angle of pitch circle $\alpha_w$ = 20°.

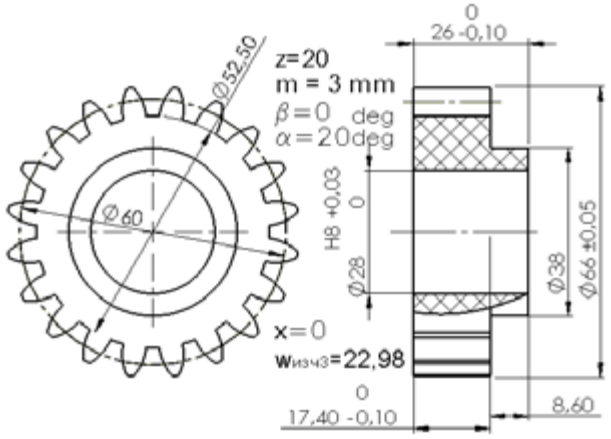



***Fig. 1.*** *Sketch of plastic gears.*

The photo of the test rig used for the tests and its scheme are shown on fig.3 and fig.4. It is a closed loop rig designed specifically for testing polymer gears and is described in [9, 10]. One gearbox (Master Gearbox) contains identical metal gears, which do not require replacement, while the polymer test gear pair forms the opposing set. The power to drive the arrangement is that which is needed to overcome the gear sliding and bearing losses in the system. When the motor is switched on the reactive forces between the test gears balance the externally applied torque and the bearing block and loading arm are maintained in balance. When using a closed loop system the torque is normally wound-in but for plastic gears wear and tooth deformations would mean that the torque would change (reduce) with time. Using a pivot block and load arm to load the gears ensured that the test gears were subjected to a constant load throughout the test. As the test gear wear, the bearing block rotates about the pivot. Quite large rotations are allowed, and, because of this and the associated differential movement, the closed loop drive shafts are free to slide axially and are fitted with universal joints.



***Fig. 2.*** *Plastic gears with steel insertion.*



***Fig. 3.*** *Photo of the test rig.*

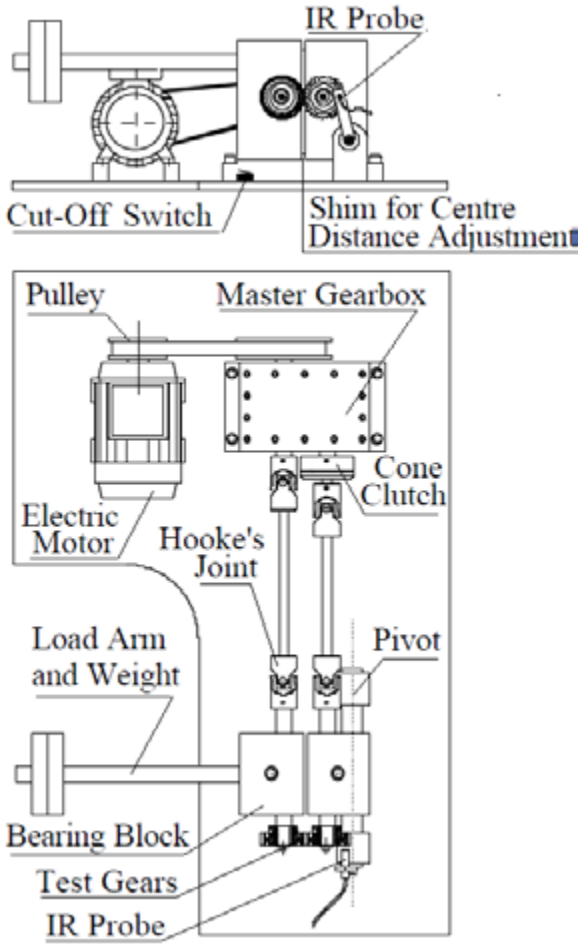



***Fig. 4.*** *The scheme of the test rig.*

Two pairs of gears (one with involute gears and the other with the cycloid gears) were tested to ultimate load (calculated for involute gears for 1500 load cycles) of 25,2 Nm, and similar other two pairs of gears were tested at lower load of 18,9 Nm for testing of wear resistance. The tests were conducted at dry running (without lubrication) and at 1000 rev/min$^{-1}$. Wear of the test gears was measured by mass loss using an electronic precise analytical balance [15] - model TP-214 (weighting capacity - 210 g, readability - 0,1 mg, repeatability - ≤ 0,1 mg, linearity - ≤ 0,2 mg). To do this the meshing gears were stopped periodically, (noting their relative positions), then removed and after weighing they were replaced as closely as possible to the original positions. To account for changes in moisture content of the test gears, the mass of a control gear, mounted on the pivot block assembly during running, was measured at the same time as the test gears. Relative wear (as a percentage mass loss, *R%*) was calculated using equation(1)

$$R\%_i = \frac{\left(\frac{Q_i}{Q_0}.P_0 - P_i\right)}{P_0}.100\% \qquad (1)$$

Where: $P_0$ - original gear mass; $P_i$ – current gear mass; $Q_0$ - original control gear mass; $Q_i$ - current control gear mass; $R\%_i$ – current relative mass loss.

The temperature at the pitch point of the gears was continuously measured using non-contacting infra-red thermocouple and the data stored on a computer. In such non-contacting manner was measured the noise from tested running gears (with portable sound-level meter GM1351 – measuring range: 30 – 130 dB; accuracy: ±1.5dB (94dB at 1kHz); frequency response: 31.5Hz-8.5kHz).

### 3. Experimental results

Fig.5 shows the relative loss of mass (the relative wear) against the number of cycles for the four tested polyamide gears – two pairs of cycloid gears and another two pairs of involute gears (respectively from each type of gears (involute and cycloid) the one pair loaded with 25,2 Nm and the other pair loaded with of 18,9 Nm). Note that each point on the graphs represents the average of relative mass losses of the drive gear and the driven gear that have been measured simultaneously after given number of cycles. The sharp jumps at the end of the curves for greater load of 25,2 Nm correspond to the fracture of one and then of a second tooth of the drive gear in each gears pair - involute and cycloid.

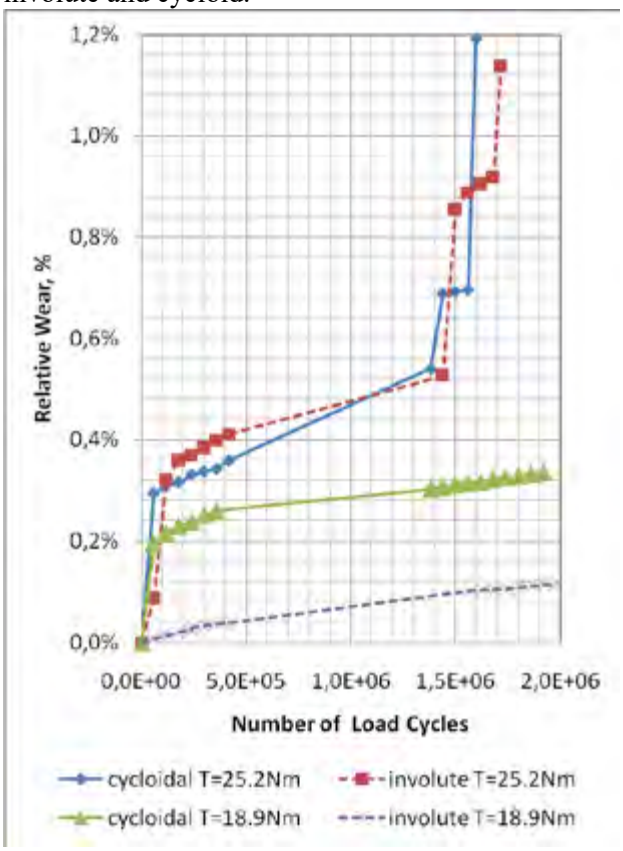



***Fig. 5.*** *Relative Wear, % - load cycles.*

It could be seen that there are not big differences in curves for loading with 25,2 Nm – the behaviors of the cycloid gears and involute gears are identical. Both gears suffered fractures of teeth after approximately $1{,}5\times10^6$ cycles. On the other hand, in the case of lower (of 18,9 Nm) load, involute gear showed less wear over the time than the cycloid gear.

The fractures of teeth in both cases of (involute and cycloid) gears occurred on the drive gear, not on driven gear and in addition of that they occurred higher on the tooth, not on the root of the tooth. The fractures on the drive involute gear wheel happened near the pitch circle (Fig.6), on the drive cycloid gear wheel happened little lower (Fig.7) and they for both had fatigue nature (Fig.8).



***Fig. 6.*** *Pitch line fractures for involute gear.*

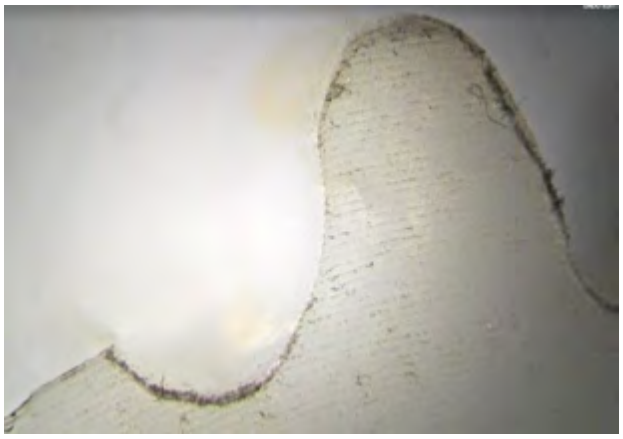


***Fig. 7.*** *Fracture and wear on cycloid gear wheel.*

In our opinion the causes for breaking teeth on drive gear wheels are complex – excessive wear, pitting, cracking at pitch circle (fig.9). Sliding forces always act away from the pitch point on the drive gear and towards the pitch point on the driven gear. So, sliding forces (fig.10) make wear and in addition push material away from the pitch point on the driving tooth (a), leaving a small pit or push material towards the pitch point on the driven leaving a small tip (b) [11,12]. This pit is the most probably the cause (concentrator of stresses) for cracking and breaking tooth on pitch line (so-called "pitch line fracture" [12]) for drive gear.



***Fig. 8.*** *Pitch line fracture with a fatigue character of a tooth for involute gear.*

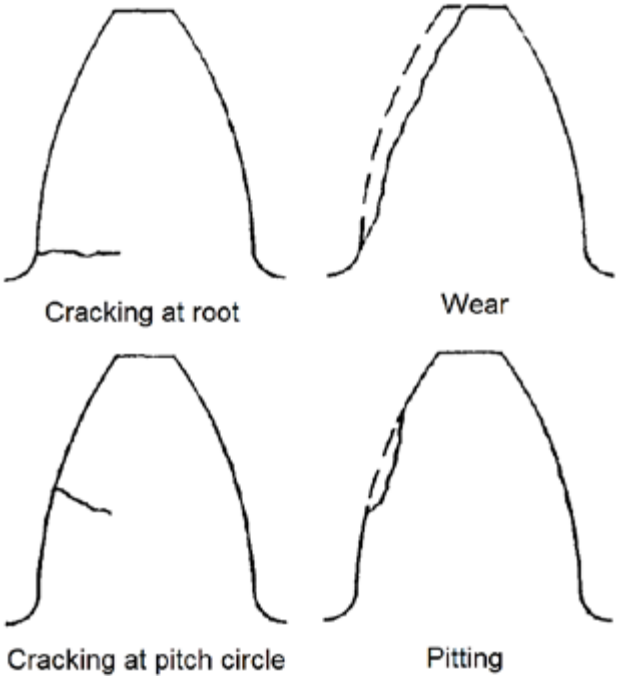



***Fig. 9.*** *Modes of failure that commonly occur in plastic gears – after Walton D. & Shi Y. W.[13].*



***Fig. 10.*** *Wear profiles on plastic gear flanks for (a) the driver and (b) the driven gears.*

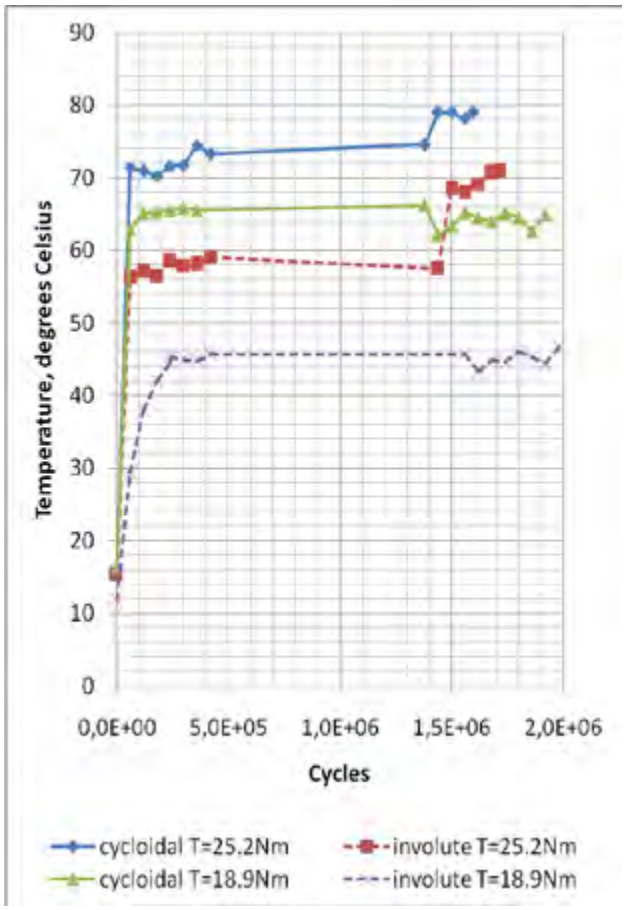



***Fig. 11.*** *Temperature curves.*

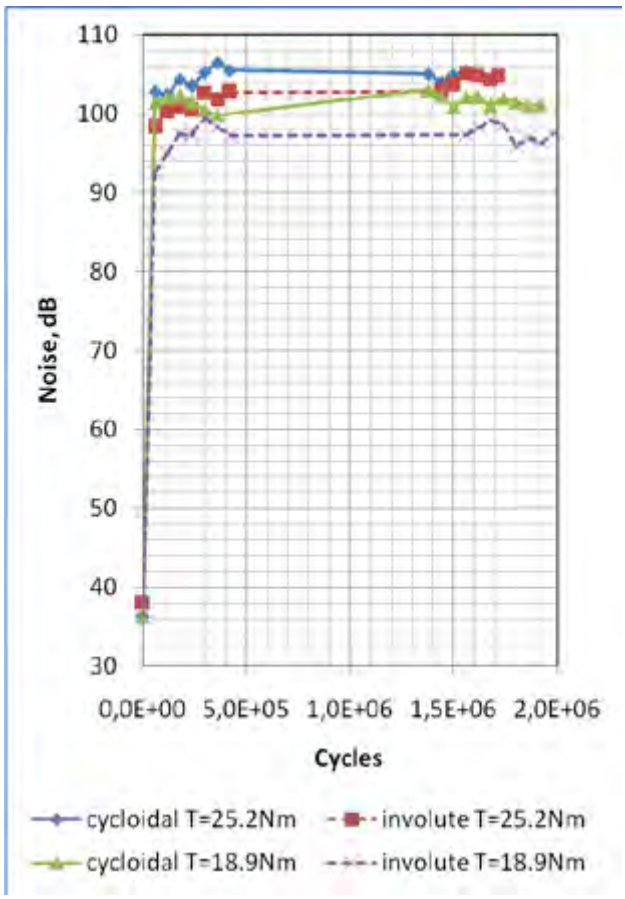



***Fig. 12.*** *Noise curves.*

On fig. 11 and fig.12 are shown the curves of all four gears for measured temperature on pitch point and for measured noise from gears. Again the involute gears had better performance than cycloid – with lower temperature and noise emissions.

## 4. Conclusion

Contrary to the assumptions in [7], experimental results derived by us did not prove the expectations about greater long-term resistance to wear and against cyclic loading of the cycloid gears in comparison of involute gears.

In the extreme test the cycloid gear suffered breaking of teeth a little earlier than the corresponding involute gear, while in the lighter test the cycloid gear showed more wear than the involute gear did.

This was confirmed and by the results of measuring the temperature at pitch point and the noise emission. In the our experimental tests, the cycloid gears have showed emissions of more heat as well as of more noise, which was an indirect evidence of a presence of more intense wear and of more vibrations causing noise with sound frequencies.

These results can be explained by the fact that the work of cycloid gears is more dependent of the accuracy of their manufacturing and much more sensitive to the observance of the exactness of center distance, than the same is for the involute gear drives.

The observed from us fractures of teeth near the pitch circle are specific and characteristic to the plastic gears. The reason for their (of pitch line fractures) occurrence is still unclear and is the subject of research. In our opinion, the appearance of these fractures in the vicinity of the pitch circle is due to the formation of a typical groove (fig.10) under the effect of the sliding forces and in the absence of lubrication on the flanks of the teeth of the drive gear. This groove (fig.13) is a concentrator of stresses - here begins the appearance of cracks at the line near the pitch circle ending with a fracture of the tooth.

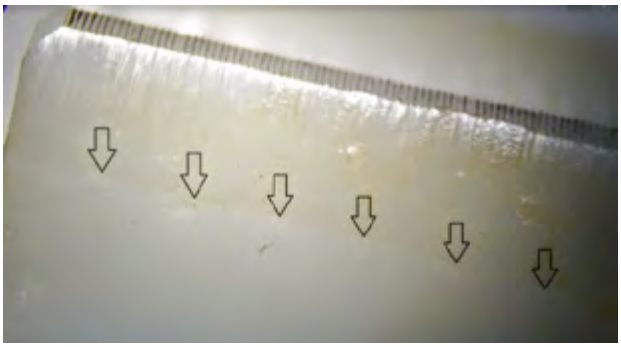


***Fig. 13.*** *Furrow on the flank of tooth of drive gear.*

**5. Acknowledgments**

The publication of the results of these experimental studies is thanks to funds received on the basis of a research project № 152ПД0016-24 to aid the PhD student and funded by subsidy for scientific research at the Technical University – Sofia, branch Plovdiv.

## REFERENCES

1. http://plastics.dupont.com/plastics/pdflit/americas/markets/*gears*.pdf.
2. Rudy Walter, (2004), *Engineering Principles for Plastic Gears,* Gear Solutions, gearsolutionsonline.com, pp 24 - 35
3. H. Voss and K. Friedrich., (1987), On the wear behaviour of short-fibre-refinforced PEEK composites. *Wear* 116, pp 1-8,
4. M. Rao, C. J. Hooke, S. N. Kukureka, P. Liao and Y. K. Chen, (1998), The effect of PTFE on the friction and wear behaviour of polymers in rolling-sliding contact. *Polymer Engineering and Science*, Vol. 38, No. 12, pp 1946-1958.
5. S. Akkurt, (1995), On the effect of surface roughness on wear of acetal-metal gear pairs. *Wear* 184, pp 107-109
6. K.D.Dearn, T.J.Hoskins, D.G.Petrov, S.C.Reynolds, R.Banks,(2013), Applications of dry film lubricants for polymer gears, *Wear*, Volumes 298–299,2 15 February 2013, Published by Elsevier B.V., Pages 99–108
7. Stanislav Aleksiev, Miroslav Aleksiev, Theoretical justification for the selection of curves engage manufacturing of gears from polymer material, *Tribological Journal BULTRIB* (Volume V, Number 05 (05) 2015), ISSN: 1313-9878, Printing House of the Technical University, Sofia, Bulgaria, pp 291-295 (in Bulgarian).
8. R.S. Khurmi & J.k. Ghupta, (2005), A Textbook of Machine Design (S.I. Unit), Eurasia Publishing House (PVT.) LTD., Ram Nagar, New Delhi – 110 055, pp 1031-1032.
9. Mao K., (1993), *The performance of dry running non-metallic gears*. PhD thesis, Birmingham University, pages 52-66.
10. A.B.Cropper, (2003), *The failure mode analysis of plastic gears*, PhD thesis, Birmingham University, pages 233-260.
11. Tsukamoto N, (1979), Investigation about the strength of plastic gears, 1st report; the strength of nylon gears which have counter-crowning, *Bulletin of JSME*, Nov, Vol.22, No 173.
12. White John,(1998),*The design and evaluation of polymer composite spur gears*, PhD thesis, Birmingham University, pages 52-66.
13. Walton D, Shi Y.W., (1989), A comparison of ratings for plastic gears, Proc. IMechE Part C: *Journal of mechanical engineering science*, Vol. 203, pp. 31-38.
14. http://www.ensinger-online.com/my/materials/engineering-plastics/polyamides/#c49084
15. http://www.denverinstrumentusa.com/media/pdf/Op-Man-Timberline-Series-balances.pdf

Address: Technical University - Sofia, Plovdiv Branch, 25 Tsanko Diustabanov St, 4000 Plovdiv, Bulgaria
E-mail: dimgog@abv.bg
E-mail: eng.dobrev@mail.bg
E-mail: stanislav_al@abv.bg

© International Scientific Conference on Engineering, Technologies and Systems
TECHSYS 2016, Technical University – Sofia, Plovdiv branch
26 – 28 May 2016, Plovdiv, Bulgaria

# INVESTIGATION OF THE EFFECTS OF CUTTING TOOL, CUTTING SPEED AND MATERIAL TYPE ON SURFACE ROUGHNESS

CENK MISIRLI[1], MEHMET CEVİZ[2]

***Abstract:*** *Every producer try to find a solution that is cheaper and more durable for products which they want to produce so they aim to decrease intensionally tool changing cost and period. In this work, the manufacturing steel has been machined on a CNC lathe without cutting fluid, at various cutting speed and feed rate values with a constant depth of cut. Effect of cutting speed and feed rate on surface rougness were investigated by machining the manufacturing steel by a carbide insert without coating. In the experiments three different feed rate values between 0.1,0.2,0.3 mm/dev and three different cutting speed settings 100, 180 and 280 m/dak were used and the manufacturing steel (Ç1050) that is known mechanics and chemical properties was processed. In this experiment, total 27 pieces were turned. Surface roughnesses that was found were measured and wearing rate of cutting tools was investigated. In this way , Surface roughnesses and optimum cutting parameters for the manufacturing steel was determined.In this article Optimum cutting parameters and minimum surface roughnesses were tried to determine for selected material and cutting tip.*

**Key words:** *Cutting tool, Cutting Speed, Surface Roughness, Depth of Cut*

## 1. Introduction

The proper selection of cutting tools and process parameters is essential to achieve the desired quality of surface finish. Optimization seeks to maximize the performance of a system, part or component, while satisfying design constraints. So that, the process parameters need to be optimized to obtain the desired surface finish[1]. Nowadays in machinability process of metals, Various experiments are carried out to create same quality product. In terms of surface roughness and cutting force, Cutting parameters which are used on machinability of metals are of capital importance. In terms of quality machined surface structure is one of significant criterions[2]. From the literature reviewed, it has been observed that there is a disagreement between researchers about the use of coolants in hard turning. With this view, in the present work, cutting parameters under dry and minimum quantity lubrication were optimized to address the widely debated topic of application of coolants in hard turning[3]. Machining is a way which has been being applied for years and Today, It preserve its importance as well. In turning which is a common section of machining, machining parameters are the leading of factors that affect directly product quality[4]. Two types of coated cemented cardide inserts were used, various combinations of side cutting edge angles (SCEAs), cutting speeds and feedrates were tested at a constant depth of cut. Cutting results indicate the SCEA, together with cutting speed and federate, do play a significant role in determining the tool life of an inset when machining Inconel 718 [5]. The correlations between the cutting parameters and the performance measures, namely, three components of cutting force, surface roughness and tool life were developed based on experimental observations[6].

## 2. Experimental work

Total 27 manufacturing steel samples have been considered for this work to show the alteration of surface roughness under different parameters. First of all prepared samples were investigated with spectral analysis and Material combinations and mechanical properties which were determined of these sample are shown in Table 1. and Table 2.

Copyright © 2016 by Technical University of Sofia, Plovdiv branch, Bulgaria ISSN Online: 2535-0048

***Table 1.*** *Chemical composition of test sample (%)*

| S | P | Mn | Si | C |
|---|---|---|---|---|
| **0,045** | 0,035 | 0.718 | 0.158 | 0.472 |

***Table 2.*** *Machanical properties of test sample*

| Breaking elongation %5d | Yield strength Mpa | Tensile strength Mpa | Hardness HB |
|---|---|---|---|
| **28** | 400 | 459,5 | 128 |

### 2.1. Cutting Tool Selection and Properties

Cutting edge was selected from catalog which belong to Sandvik firm for manufacturing steel. Cutting edge angle was determined as triangle for every cutting tool. Selected cutting edge and properties were described below;

ISO standard: TCMX 09 02 02-WF

ANSI standard: TCMX 1.8(1.5)0-WF

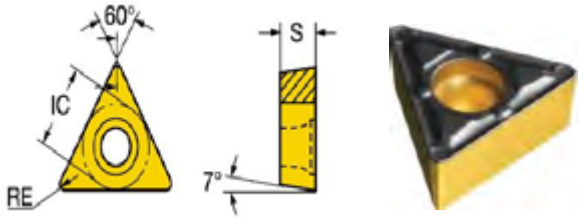



***Fig. 1.*** *KTCMX-WF Cutting edge dimensions and shape*

### 2.2. Preparation of Test Samples and Selection of Parameters

In a machning process, the most significant factor of machinability is surface sensitivity of workpiece. Therefore surface roughness that will be determined must be investigated under independent conditions from each other. With priority these independent conditions are feed rate, cutting speed and depth of cut. Experimental studies are required in order to investigate these parameters. İn this context, because of the experiment which will be executed without coating carbide cutting tool (TCMX-WF) , three different cutting speed (100, 180, 280 m/min) , three different feed rate (0,1-0,2-0,3 mm/dev) and 1mm constant depth of cut were selected. Test samples were machined and average surface roughnesses were measured.



***Fig. 2.*** *Before machining test samples*



***Fig. 3.*** *During machining a picture*



***Fig. 4.*** *Machined test samples*

In the experiment made, totally, 27 workpieces were machined by turning three test samples with each of cutting edges of cutting tool. In this way, optimum cutting parameters were designated for selected cutting tool as well.

### 2.3. Surface Roughness Measurement

In assignation surface roughnesses of test samples, MARSURF M400 measuring device of surface roughness was utilized. Roughness values were measured for three varied values of each of these parameters. 1 mm length of cut, 6mm sampling length and 15±1 ºC ambient temperature were selected so as to surface roughness. Measuring device used is shown in fig. 5.



***Fig. 5.*** *Measurement of surface roughness*

### 3. Results and Discussion

Average surface roughnesses found are shown in Table 3. and Fig. 6.

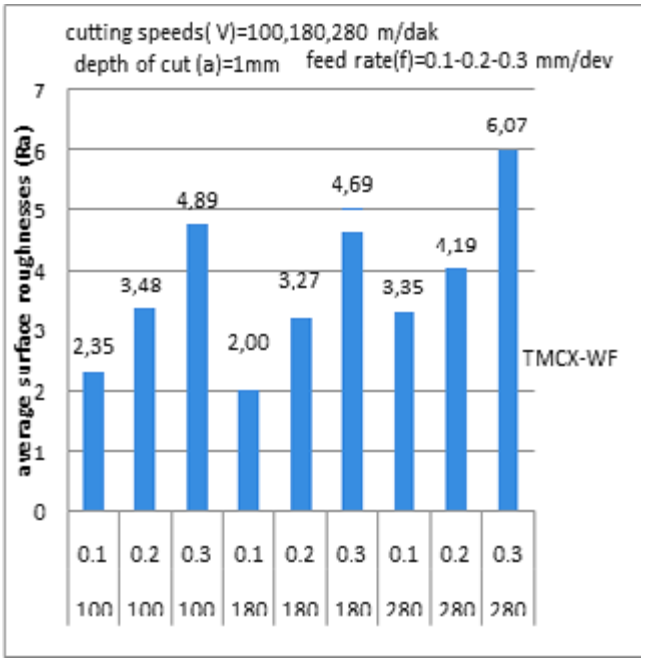



***Fig. 6.*** *Surface roughnesses dependent on cutting speed and feed rate*

According to feed rate (0,1-0,2-0,3 mm/dev) consideration;

When average surface roughness is investigated, it is seen that surface roughness increase as feed rate increase. There is a direct proportion between feed rate and surface roughness as it is seen in table. As it is understood, A way of roughness reduction is to decrease feed rate. In other words, in the experiments made, minimum surface roughness was seen to have been obtained with 0,1 mm/dev feed rate. In test samples which were machined with 1 mm constant depth of cut for TCMX-WF carbide cutting tool, while feed rate increased 100% ,surface roughness increased between 51,15% and 209,18% .

***Table 3.*** *According to constant depth of cut Surface roughnesses with TCMX-WF cutting edge*

| Cutting tool | Cutting speed m/min | Constant depth of cut (mm) | feed rate mm/dev | Average Surface roughnesses |
|---|---|---|---|---|
| TCMX-WF | v | a | f | Ra |
| | 100 | 1 | 0.10 | 2.35 |
| | | 1 | 0.20 | 3.48 |
| | | 1 | 0.30 | 4.89 |
| | | | | |
| | | | | |
| TCMX-WF | 180 | | | |
| | | 1 | 0.10 | 2.00 |
| | | 1 | 0.20 | 3.27 |
| | | 1 | 0.30 | 4.69 |
| | | | | |
| | | | | |
| TCMX-WF | 280 | 1 | 0.1 | 3.35 |
| | | 1 | 0.20 | 4.19 |
| | | 1 | 0.30 | 6.07 |
| | | | | |

According to cutting speed (100, 180, 280 m/min) consideration;

Minimum average surface roughness was seen to have been turned with 180 m/min cutting speed and İt is seen that average surface roughness decrease as cutting speed increase until 180 m/min. Another way of roughness reduction is to increase to a certain extent, which this is the most common known method.

However, As it is seen in Fig. 7, It is understood that surface roughness increase after cutting speed exceed 180 m/min.

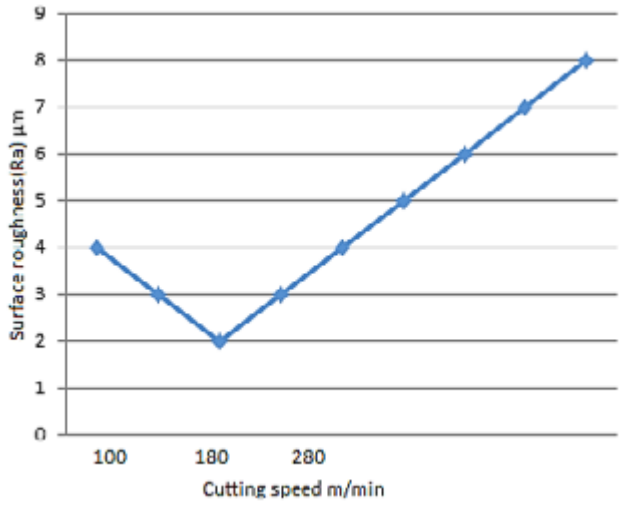



***Fig. 7.*** *Effect to surface roughness of wear which occurs on without coating cutting tool[6]*

The reasons for the increase in surface roughness are high temperature occurring dependent on friction, wear occurring on shear edge of cutting tool and vibration. Notch and Flank wears Which consisted of high cutting speed were enlarged sixty times by using optical microscope and were shown in Fig. 8.




***Fig. 8.*** *Notch and Flank Wear*

## REFERENCES

1. Korkut, I., Kasap, M., İ. Çiftçi, I., Seker, U. (2004). Determination of optimum cutting parameters during machining of AISI 304 austenitic stainless steel. *Materials & Design.*
2. Özer, L., Tosun, N., İnan, A. (2000). Östenitik Manganlı Çeliğin Sıcak Talaşlı İşlenmesinde Yüzey Pürüzlülüğünün İncelenmesi. *Turkish journal of engineering and environmental sciences*, 24, 287-296.
3. Diniz, A. E., Ferreira, J. R., Filho, F. T. (2003). Influence of refrigeration/lubrication condition on SAE 52100 hardened steel turning at several cutting speeds. *International Journal of Machine Tools and Manufacture*, 43, 317–326.
4. Ay, M., Turhan, A. (2010). Tornalama İşleminde Kesme Parametrelerinin ve İş Parçası Uzunluğunun Yüzey Pürüzlülüğüne Etkilerinin İncelenmesi. *Electronic jJournal of Machine Technologies.*
5. Rahman, M., Seah, W. K. H. and Teo, T. T. (1997). The machinability of Inconel 718. *Journal of Materials Processing Technology*, Vol. 63, pp. 199-204.
6. Feng, C. (2002). Development of Emprical Models For Surface Roughness Prediction in Finish Turning. *Internatianal Journal of Advanced Manufacturing Technology*.

Authors' contacts :
Adress : Trakya Uni. Mech. Eng. Dep.
22180 EDIRNE
Tel: +905332353511
E-mail : cenkm@trakya.edu.tr

© International Scientific Conference on Engineering, Technologies and Systems
TECHSYS 2016, Technical University – Sofia, Plovdiv branch
26 – 28 May 2016, Plovdiv, Bulgaria

# 5083 ALUMINUM HEAT TREATMENT

CEM MISIRLI, CENK MISIRLI

***Abstract:*** *As the time goes on, where the demand for lighter, more durable, recyclable and replaceable materials are increasing due to the fact of economical and technical considerations. Aluminum and its alloys are used widely because of their specific gravity, good mechanical properties and the reason that they are easy to find. Because of these reasons in studies and investigations regarding to achieve beter and optiumum material and its alloys AA 5083 aluminum is special series of the aluminum parts. This series's corrosion resistance and welding ability are very good. It's fatigue strength value is high. Cold shaped of these series is good at soft tempering form. Thin and mixed parts of AA 5083 aluminum is hard to extrusion. In this operation, microstructures of the AA 5083 aluminum alloy depending on heat treatment of the changes, and these changes determine the effect of extrusion parameters.*

**Key words:** *5083 Aluminum Alloy, Microstructure, heat treatment, hardness*

## 1. Introduction

Iron outstanding material properties together with the most aluminum alloys and non-ferrous metals production of these materials have led to be sought by customers in many different application areas. Outstanding material readily available outside the specifications of raw materials, are other reasons to be advanced production techniques of the high and low price of aluminum consumption.

To make many metal alloys of aluminum provides to obtain the necessary characteristics for specific applications.One of the most important characteristics of the aluminum-based material, strength corresponding to the low density / density ratio is high.The mechanical properties of the metal microstructure, which in the composition of the material, the heat treatment after the gelation and solidification process and is based on mechanical shaping process.

Aluminum and most alloys of it are readily more deformable than the other materials. Commercially pure aluminum lightweight, ductile, soft, machinability and corrosion resistance of a material is high. Although pure aluminum is very soft material, strength, applying cold forming process can be significantly increased. Another way to increase the strength to make the solid solution hardening of magnesium, silicon, copper, zinc, is to make the alloying elements such as manganese with.

By heat treatments to be applied is obtained by forming a high resistance values age hardening. High-purity aluminum pull strength of about 50 MPa while pulling the aged state in the case of Al-alloy znmgcu1.5 reaches its strength 600-700 MPa. Aluminum and aluminum alloys for applications such as spacecraft and aircraft construction are also important in the light of my next of these properties that are very important. Because it is easily formed and aluminum alloys are commonly used in the extrusion industry.

Other important features of the thermal and electrical conductivity of aluminum is high, lack of magnetism property after the high corrosion resistance and mechanical shaping clean surface can be obtained. To be important for specific applications in the electrical and electronics industry is magnetic.

High corrosion resistance thanks to the fresh and salt water, can be used easily in many different environments, such as various chemicals and air, with anodic coating is formed decorative products. The aim of the anodic coating, through the thickening of the oxide layer is formed on the aluminum surface is to increase the corrosion resistance of the material. The cleanliness of the surface after mechanical shaping is one of the important factors that determine the quality of the anodic coating. Good extrusion feasibility, after mechanical forming to obtain clean surfaces, aluminum and aluminum alloys with a combination of corrosion resistance and compliance features in air anodic coating has gained importance in architectural applications.

Copyright © 2016 by Technical University of Sofia, Plovdiv branch, Bulgaria ISSN Online: 2535-0048

Aluminum-magnesium (Al-Mg) or aluminum-magnesium (Al-Mg) alloy, is also known as the 5000 series alloys. Because of high tensile strength, dimensional stability and workability are quick feature. Drilling and turning can be done easily, sawdust enough during these operations, mining without distortion. Without distortion based on plasma are welding. As the surface appear very bright, it does not require much processing. S-aımg 4.5 Mn (5183) can be easily welded using the electrode. It shines very well. Anodizing (non-decorative) can be done. It retains its properties at low temperatures. It is resistant to sea water and corrosion.

In this study, the most commonly used alloys from the 5083 's specifications to supply the aluminum alloy on the market as appropriate in shaped aluminum alloy extrusion, and changes in the microstructure was examined depending on the applied heat treatment. In laboratory conditions, product quality deterioration without the high production rate to be applied to determine the optimum microstructure can be obtained homogenization temperature and above in order to select the cooling rate to be applied after homogenisation the duration of homogenization, followed cooling test was conducted, which occur after each test microstructures examined material depending on the process conditions applied heat exchange between the metal compound material is determined. When results are evaluated, it was conducted a series of experiments to demonstrate the effect of extrusion extrusion feasibility of this study.

## 2. Aluminum Alloy and Classification

Aluminum alloy mechanical varies depending on the physical and chemical properties and microstructure of alloy elements. The most important alloying elements are participating aluminum copper, manganese, silicon, magnesium and zinc.

Wrought aluminum alloys and cast alloys are divided into two groups. Forged alloys, plastic deformation capability that are good can be shaped easily. Aluminum forging and heat treatment can be applied to a large portion of the cast alloy.

According to the American troops aluminum, aluminum wrought alloys are classified into four letters. This classification is as follows:

**1XXX:** Pure aluminum. It is often used in the electrical and chemical industries.

**2XXX:** Al-Cu alloys. Main alloying elements is copper. Other alloying elements may also be present including especially magnesium, it is used widely in the desired high strength aerospace industry.

**3XXX:** Al-Mn alloys. Main alloying element manganese. Pipe, tank, and is used in architectural applications.

**4XXX:** Al-Si alloys. Main alloying elements are silicon. Low coefficient of thermal expansion are high wear resistance and corrosion resistance alloy. in welded structures in plate production it is used in the production of auto parts.

**5XXX:** Al-Mg alloys. Main alloying element is magnesium. Of magnesium ratio increases hardness and strength increases but the ductility decreases. Marine corrosion resistance is high is used in the manufacture of the structure to run in this environment.

**6XXX:** Al-Mg-Si alloys. Main alloying elements are magnesium and silicon. These alloys are formed with high ability often used in the manufacture of the parts produced by extrusion.

**7XXX:** Al-Zn alloys. The main alloying elements copper, magnesium, chromium and zirconium alloy element addition. 7XXX series, the one with the highest strength of the aluminum alloy. Aircraft parts and other places used in the construction of high strength is desired.

**8XXX:** Al-Li alloys: lithium is the main alloying element can be made of tin plugin. In particular, this material being used in aircraft and space structures, has good fatigue resistance and good toughness properties. But compared to other Al alloys have high production costs.

### 2.1. Heat Treatment of Aluminum Alloys

Heat treatment made from an aluminum alloy to be applied in different ways and applied to his writing process with alloy numbers TX symbols. This process is expressed as follows:

O: Annealed, F: As produced, H: Hardened, T: thermal processing subjected

T1: cooled after hot forming processes and of course left to aging.

T2 cooled after hot forming processes, cold formed and of course left to aging.

T3: The process of getting a solution made of cold-formed, and of course has been allowed to age. T4: the process of getting the solution is made and of course left to aging.

T5: Cooled after hot forming process and made artificial aging

T6: The process of getting the solution is made and made artificial aging.

T7: The process of getting the solution is made and carried over aging.

T8: Take the solution has been carried out, made of cold-formed and artificial aging.

T9: Take the solution process is applied and made artificial aging and cold formed.

T10: Cooled after hot forming process, made of cold-formed and artificial aging.

### 2.2. Corrosion of Aluminum and its Alloys

Low specific gravity, a good conductor of electricity and heat ability, mechanical strength may be sufficient numbers and good plastic shaped aluminum having the ability to be used in various corrosive environments. in particular corrosion resistance is sought, no aluminum purity of less than 99.5% because the alloying is necessary but generally made to improve the mechanical properties of aluminum, corrosion resistance of aluminum alloys is lower than that of pure aluminum.

•Aluminum The resistance to many corrosive environments, formed on the surface depending on the current conditions is due to the amorphous or crystalline aluminum oxide layer.

•It is much more amorphous surface film in the atmosphere, in water and water vapor is more crystalline structure is formed at the surface. What is more homogeneous layer consisting of highly resistant to corrosion under the same conditions is also so good.

•Aluminium materials are highly resistant to corrosion in the atmosphere.

•In the industrial atmosphere (SO2, dirt, dust) and the corrosive effect results after thirty years in the marine atmosphere, reduction in strength aluminum materials, is approximately 9-13%.

## 3. Experimental Study

### 3.1. Materials used in the experiments

This section of the 5083 quality aluminum alloy development and surface characteristics of the homogenization process are described in the previous section in order to investigate the mechanical behavior and the pieces were informed about the issue of preparation for this process.

13 mm thick seams are cut from the as-cast cylindrical billet of 110 mm diameter were used in the experiment homogenisation. In high temperature oven in which the homogenisation process, the sample temperature was measured by thermocouple inserted into a hole drilled into the test specimen is drawn with a chart recorder during the sample heating process. Sample temperature of +4 °C were found to show change. 5 °C intervals eight temperatures between 490 ºC and 530 °C in homogenisation experiments were performed. In each temperature ½, 1, 2, was tested five times selected as 4 and 6 hours. In order to be close to industrial applications, samples were heated to the homogenization temperature 6 hours. The temperature and time are removed at the end of the cooling air from the oven samples hardness was measured.

Rockwell hardness measurements are made at Universal hardness tester. The average of 3-4 readings for each sample when measured by the Rockwell hardness value was taken as the E grade.

Optical microscopy and Scanning Electron Microscope (SEM) investigations to the edge of the index and the middle two samples were taken, were polished mechanically mounting buried. 1 ml HF etching (48%) + 200 ml of water was used. Samples for SEM examination 200 mm Edwards high vacuum coating equipment. Thickness is covered with carbon film. SEM examination of 840 Jeol scanning electron microscopy and microanalysis associated Tracer Northern TN-2000 system is used.

Transmission Electron Microscopy (TEM) for the preparation of samples using a diamond saw running at slow speed drive 500 .mu.m. slice cut from 3mm thick. Diameter discs were removed, these discs are mechanically 250 μm. Thickness is thinned. The electrolytic polishing method is used for final refining. Tenupol $NHO_3$ 30% + 70% methanol was used as the electrolytic solution in the electrolytic polishing apparatus and diluted samples by passing a current of 1.8-30 °C ambient temperature. TEM examination was carried out in a Jeol 100C Transmission Electron Microscopy.

After homogenization the size and distribution of precipitates in the air in the structure of the cooled sample analyzes were performed with the SEM attached Tracer Northern TN-1310 system. Again matrix solutionizing selective metal dissolving process to keep in solution from compound was applied to determine the variation of heat treatment conditions of the precipitate. Electrolytically performed and as electrolyte 15 g of 8-hydroxyquinoline in 80 ml of chloroform, 60 g of benzoic acid and 200 ml of methanol in the procedure used, 100 A/m² current applied and the counter electrode was used as the material itself. particles of the resulting solution was precipitated by centrifugation, the precipitate was washed 4 times with chloroform and methanol 1 time the precipitation with each washing process again applied in step centrifugation. The resulting precipitate was limited in miltar distributing slide taken on in ethanol and Philips X-ray phase analysis was performed using Co tube diffractometer apparatus. on my material and the analysis made of any of the major impurities of iron or other alloying elements forming precipitates peak was observed.

Here also used for selective dissolution of the electrolyte to be suitable, the disentanglement was also concluded to be successful.

Be done by electron diffraction phase analysis has been taken with a ultrasonic blender in order to precipitate with ethyl alcohol and the carrier carbon film coated copper grids were dipped in the suspension allowed to dry. Thus prepared TEM samples were analyzed using a Jeol still 100C Transmission Electron Microscopy voltage of 100 keV.

After homogenization for a small oven suitable microstructure of the brick with the cooling operation is performed in order to determine the cooling rate can be achieved by an arrangement in open hole is provided. It is placed over the small brick in the middle of the piping system it was cooled by spraying with air or water passing through the tubes. Cool down while K-type buried in the center of the index (kormelalumel) with the help of thermocouple temperature was recorded continuously.

Wedges heated at high temperature electric resistance furnace to the extrusion temperature and the temperature were measured by a K-type thermocouple. Experiments wedge sleeve and the initial temperature of the mold is kept constant. The method used to maintain constant temperature of the wedge, the wedge is heated up to 500 °C was continued off and temperature measurements from the oven. Placed in the casing when the temperature of temperature 375 °C fall until it drops to 360 °C the time was determined. It takes 25 seconds Extrusion experiments after 25 seconds after the wedges inserted into the sleeve printed and thus the starting temperature of the extrusion is provided to be fixed in all experiments.

To examine the effect on the suitability for extrusion of homogenization temperature, homogenized for 6 hours at the lowest temperature of 7 °C/min to the cooled slab extrusion experiments were carried out.

## 4. Conclusion

Purchased commercially and produced by continuous casting and AA 5083 according to the standards that are in the structure after breakdown of reported aluminum alloy all βalfe phase preferred for extrusion α-AlFeSi possible to convert the phase. This conversion is implemented at 490 ° C for 5 hours while completing the experimental conditions, 490 °C for 2 hours, 510 °C is complemented ½ hour. However, after 10 hours, the longest period of time even if applied at temperatures less than 590 ° C the conversion was not complete.

During the heat treatment to be used in the most important part of dimensional change in the extrusion AlFeSi phase occurs during heating of the slab to the homogenization temperature. It was concluded therefore conclude that there is a relationship between the size change phase transformation.

Mg along the feasibility of the extrusion of aluminum alloys used in the study and for the formation phase which Mg2'N to determine the hardenability in the structure after casting the material in the four Al-Mg-Fe phase and in a short time can pass through solid solution Si should be in solid solution. Therefore, the heat treatment process is applied sufficient to combine with Mg Si right must take in solid solution. Therefore, 490 ° C and long-term heat treatment at temperatures above not only for the conversion of α-β-Alfes Alfes Si is required to pass from solid solution.

The Mg and Si in solid solution combine to create $Mg_2Si$ solution to be provided that the formation of the desired microstructure in the same controlled cooling can be realized by applying a rapid cooling sample aging process. Thus a more economical production.

While performing at low load extrusion billets suitable microstructure is obtained through thermal treatment, it will also be provided to reach the maximum yield strength.

During the experiments the applied cooling speed for decreasing the cooling rate of a microstructure suitable for extrusion was concluded to be obtained. However, in case of very reduced cooling rate $Mg_2Si$ deposits will cause an error in widening the extrusion. Therefore, in practice, the slowest cooling rate of 3 °C applied in this study / min is well below should not ynyl.

A 5083 and contained in the alloy according to the alloy and β-AlFeSi phase of known positive effect on the conversion of Mn is concluded to be included in this phase.

## 5. Figures and tables



***Fig. 1.*** *where the homogenization heat treatment furnace*

***Table 1.*** *The composition of the materials used in the experiments*

| Fe % | Si % | Mn % | Mg % | Cu % | Ti % | Al % |
|---|---|---|---|---|---|---|
| 0.50 | 1.00 | 0.70 | 4.50 | 0.10 | 0.10 | Remaining |

## REFERENCES


1. Deliküçük, Y., "Al-Mn Alloys Operations feasibility Effects of Annealing Parameters." Master's Thesis. Selcuk University FBA. Konya, 1989, p.86
2. T.S.E., TS 140 EN ISO 6508-1, Metallic materials-Rockwell hardness test
3. Petch, N.J., Iron Stell Inst., 1953, 174, 25
4. Onurlu, S., "Homogenization of the 6063 Effect of Microstructure and Properties of Aluminum Alloys" ITU Ph.D. Institute of Science and Technology, Istanbul, 1993
5. Şimşek, A.T., "Al-Mn aluminum ingot homogenization of ductility and formability Effects in Alloys", II.Alumium Industry Conference Proceedings, 1984, s.335-349

© International Scientific Conference on Engineering, Technologies and Systems
TECHSYS 2016, Technical University – Sofia, Plovdiv branch
26 – 28 May 2016, Plovdiv, Bulgaria

# INFLUENCE PRESSURE OF ASSISTED GAS ON LASER CUTTING PROCESS BY MELTING

LYUBOMIR LAZOV, HRISTINA DENEVA

**Absract**: *Pressure influence of assisted gas nitrogen in laser cutting process through melt of lamellae for electric motors, is presented in this study. Experiments have been made by a laser technological system TruLaser 1030 and a Yb: YAG laser source TruDisk 2001. In experimental series the gas pressure p is changed by interval (4 ÷ 20) bar via step Δp = 2 bar. It has been described and analyzed the influence of gas pressure p on input cut widths and output cut widths b = b (p), as well as cut angle deviation α by pressure α = α (p). Samples with 0,35 mm and 0,50 mm thickness from two grades steels M250-35A and M530-50A have been studied too.*

**Key words:** *laser cutting by melting, sheet steel, pressure of assisted gas*

# ВЛИЯНИЕ НА НАЛЯГАНЕТО НА ПОМОЩНИЯ ГАЗ ВЪРХУ ПРОЦЕСА НА ЛАЗЕРНО РЯЗАНЕ ЧРЕЗ ТОПЕНЕ

ЛЮБОМИР ЛАЗОВ, ХРИСТИНА ДЕНЕВА

**Резюме:** *В изследването се разглежда влиянието на наляганетo p на помощен инертен газ азот при процеса на лазерно рязане чрез топене на ламели за електромотори. Експериментите са проведени с лазерна технологична система TruLaser 1030 и Yb:YAG лазерен източник TruDisk2001. В експерименталните серии наляганетo на газа се променя в интервала p (4 ÷ 20) bar със стъпка Δp = 2 bar. Показано и анализирано е влиянието на наляганетo p върху широчините b на входа и изхода на сряза b = b (p) и отклонението от успоредност на срещуположните стени на сряза α = α (p). Изследвани са образци с дебелини 0,35 mm и 0,50 mm от две марки стомани M250-35A и M530-50A.*

**Ключови думи:** *лазерно рязане чрез топене, листова стомана, налягане на помощния газ*

## 1. Introduction

Laser technologies are the most rapidly developing industrial technologies of the 21st century. Because of a number proven its advantages [1] such as high efficiency, reliability, move quickly and environmental purity of the process, almost no sector of industry (machine engineering, aircraft construction, electrical engineering, electronics, etc.) in which laser technologies has not been used [2].

Laser cutting is one of the first industrial laser applications immediately after its discovery [3, 4]. Laser cutting of materials is distinguished by traditional cutting methods because of its specifics: a high concentration of energy in a small area; locally and selectively effects of radiation; minimal impact of laser radiation on adjacent areas, etc. [5].

In recent years, laser cutting technologies are imposed and in automotive industry. With the development of electrical vehicles production this trend will increasingly strengthen. For example, American manufacturer of Tesla Motors reported that he has the best quarterly results in his history and in the first quarter of 2015, 10 030 cars have been made. Over the same quarter of the last year this represents an increase of 55 %. [6].

Copyright © 2016 by Technical University of Sofia, Plovdiv branch, Bulgaria ISSN Online: 2535-0048

Many advantages to this type of car such as reduction of harmful emissions into the environment (greenhouse effect) and energy efficiency assign to electric cars a leading place in the new history of automotive industry.

Basic module in this type car is an electric motor. Laser technology is appeared as a new technology that can meet the needs for rapidly designing, developing and testing of new constructions motors. Laser cutting of lamellae for rotor and stator packages is not only an energetically and economically advantageous solution, but it offers a higher quality and flexibility when solving new constructive ideas.

To realize a qualitative technological process of laser cutting together with selecting of laser source, in treatment zone it is important and the selection of suitable auxiliary gas, gas nozzle and gas pressure.

Pilot experimental studies are required to performing when we discuss the complexity of physical processes that occur in each specific case of laser application [7]. In practice three methods of laser cutting (oxygen, through melting, sublimation) are known and they happening at different temperatures, as well as they differed with their technological parameters and characteristics (figure 1). For cutting of thin metal sheets in the industry have been mostly used disc Nd:YAG and Yb:YAG lasers, providing power densities from $10^7$ W/cm$^2$ to $10^8$ W/cm$^2$, sufficient to implement laser cutting process through melting.

Metal in the treatment zone is melted and ejected under the influence of inert gas flow which is directed to cutting area (figure 2). Simultaneously the gas puts pressure onto melts as well as hinders oxidation process and cools the processing area as helping to avoid forming a large heat affected zone around cut edge.

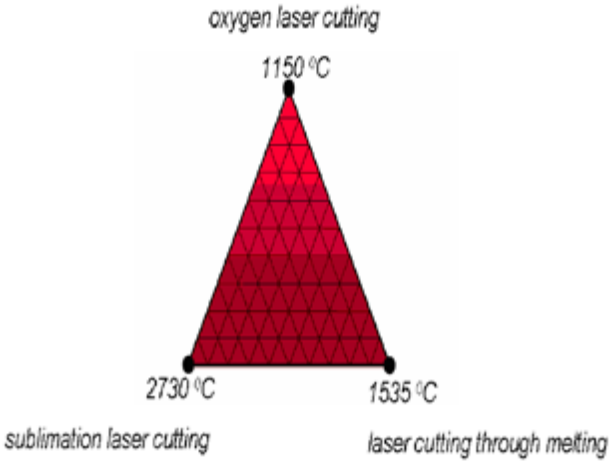



***Figure. 1***. *Laser cutting methods (indicated temperatures are for steel)*

Criteria defined quality of the process are [8]:

- deviation from the required profile and dimensional tolerances;
- perpendicularity and angularity deviations of cut faces (DIN EN ISO 9013:2003-7);
- widening of kerf;
- roughness of the kerf;
- lack of slag.

They are dependent on some factors. The main of them are: material properties; characteristics of a laser source; cutting speed; passing of an auxiliary gas, focus position, etc. (figure 3) [9, 10].

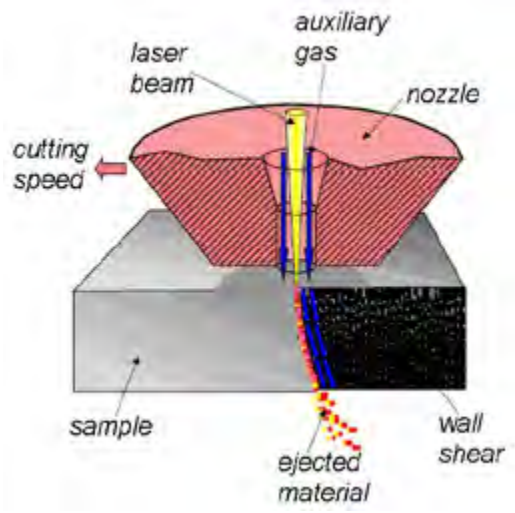



***Figure. 2.*** *Principle scheme of laser cutting by melting*

Actually, in the scientific literature there are a limited number of studies and analyzes for the processes as well as the efficiency to removing of melt from channel zone and formation of slag. So in this regard it is important to do detailed scientific oriented experimental and theoretical researches.

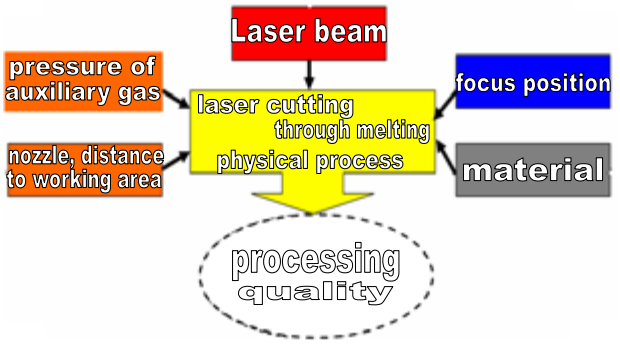



***Figure. 3.*** *Factors influencing on physical process laser cutting by melt*

Many of the factors influencing on laser cutting process and processing quality as well as the factors with gas passing are connected and grouped [11]. To this group belong:

- Correct selection of the auxiliary gas;
- Gas pressure;
- Nozzle diameter;
- Distance to the working surface.

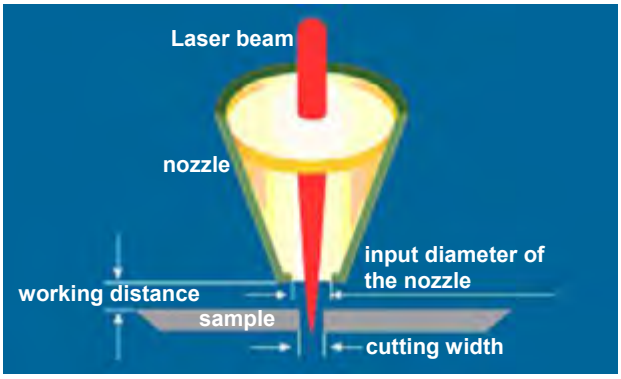



***Figure. 4.*** *Scheme nozzle and working distance from it to the treatment zone*

The choice of optimum operating mode to submission of the auxiliary gas during the technological process is crucial for the quality in laser cutting process through melting. Two factors influence on forming of gas flow. From the one side are nozzle type and form, as the other one is distance between nozzle and working surface (figure 4). In modern technological system this distance is controlled by special sensor with aim to keep up optimum mode of treatment although possible defects on metal surface sheet.

Nozzle type for laser cutting through melting is different by these for technological operations as welding and hardening. In this kind of operation is important the nozzle diameter to be elected so that it is correspond with cutting width in the material. Only a certain portion of gas flow entering through nozzle is directed and came into the groove of cutting area. The distance from the nozzle end to the working surface is chosen depending on the design of the nozzle itself (its diameter). In the most general case it must be less than diameter of the nozzle itself, in order to avoid advent of turbulence and decreases of the pressure. For smaller distances itself slit is appeared as additional small nozzle, that has a favorable influence on the processing quality.

When cutting of thin sheet material having a thickness up to 1 mm with a good approximation, it may be considered that the parameters of gas stream are remained constant. In this case, a pressure gradient $\frac{\partial p}{\partial z}$ along the channel cut in realization of an isentropic process is given by the equation

$$\frac{\partial p}{\partial z} = \frac{p_{in} - p_a}{h}, \qquad (1)$$

where $p_{in}$ is gas pressure on the enter,
$p_a$ – atmospheric pressure,
$h$ – thickness of the sheet.

When it comes to work with larger distance between the nozzle and working surface it is necessary the nozzle to be special designed for this purpose. Particularly this concern about the cases of gas pressures higher than 2 – 3 bar. Standard nozzles are with a diameter of 0,8–3,0 mm, as working distance is kept in the range of 0,5–1,5 mm.

## 2. Results

To investigate the influence of auxiliary gas pressure (nitrogen) on the geometry and cutting quality were done series experiments in the range from 4 bar to 20 bar by step 2 bar. Experiments were performed of prior prepared samples of electrical steel M250-35A and M530-50A. Technological parameters in laser cutting process through melting which in the course of studying remain constant, are given in table 1.

***Table 1.*** *Technological parameters of laser system TruLaser 1030 when is studied the pressure influence p*

| Parameter | Value |
|---|---|
| Power of laser radiation $P$ | 2 000 W |
| Cutting speed $v$ | 50 m/min |
| Impulses frequency $\nu$ | 20 000 Hz |
| Nozzle diameter | 1,7 mm |
| Defocus position $\Delta f$ (0.35 mm) | - 1,85 mm |
| Defocus position $\Delta f$ (0.50 mm) | - 2,00 mm |

When realize the cutting process by melting in the processing area it can be observed a cut angle deviation (figure 5). To investigated this phenomenon we used a developed by us methodic based on Standards DIN EN ISO 9013:2003-7 and DIN EN ISO 12584 [12]. The cut angle deviation is defined with

$$\mathrm{tg}\alpha = AB/AC, \qquad (2)$$

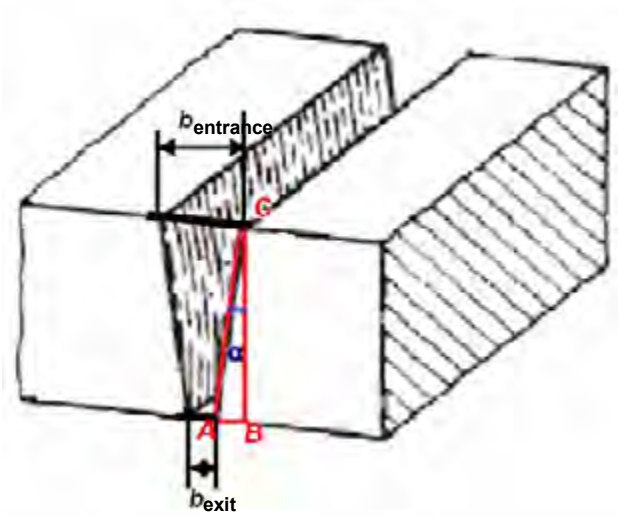



***Figure. 5.*** *A scheme of cut geometry, α is a cut angle deviation*

### 2.1. Results of the study on dependence $b = b\,(p)$

Intervals of measured values cutting widths $b_{entrance}$ and $b_{exit}$ in research range of gas pressure, are shown in table 2.

***Table 2.*** *Intervals of alteration in cutting width when study b = b (p)*

| material | $b_{entrance}$, μm | $b_{exit}$, μm |
|---|---|---|
| M250-35A | 273÷283 | 182÷192 |
| M530-50A | 278÷288 | 180÷190 |

The results obtained for functional dependences of entrance width $b_{entrance}$ and exit width $b_{exit}$ by pressure of inert gas $p$ about samples of two blade steels, are shown respectively in figure 6 (a) and figure 6 (b).

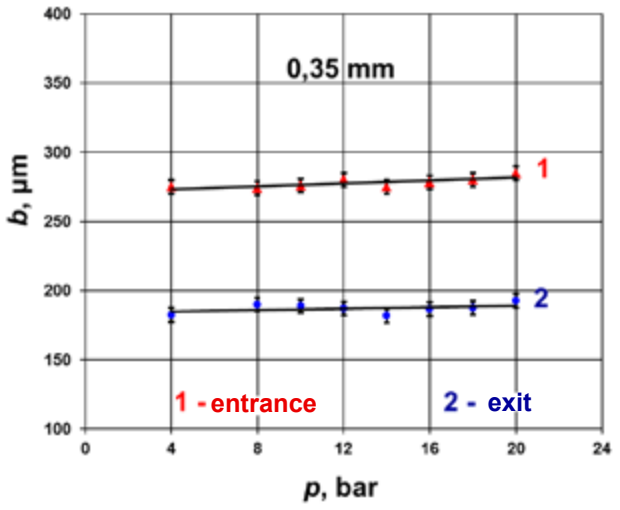



***Figure 6 (a)***

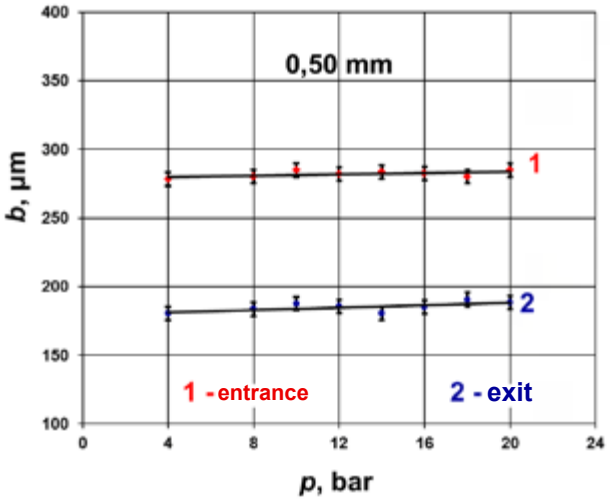



**Figure 6 (b)**

***Figure. 6.*** *(a), (b) Experimental dependences $b_{entrance} = b_{entrance}\,(p)$ and $b_{exit} = b_{exit}\,(p)$ when cutting of steel samples M250-35A and M530-50A*

### 2.2. Results of the study on dependence $\alpha = \alpha\,(p)$

In the present study is shown and the influence of the auxiliary gas pressure alteration $p$ upon $\alpha$ – cut angle deviation. When is carried out the experimental series the gas pressure $p$ is changed in specified above interval, as well as the values given in table 1 were kept constant, too.

The results obtained for functional dependences $\alpha = \alpha\,(p)$ for two type sheet material with thickness 0,35 and 0,50 mm, are shown respectively in figure 7 a and figure 7b.

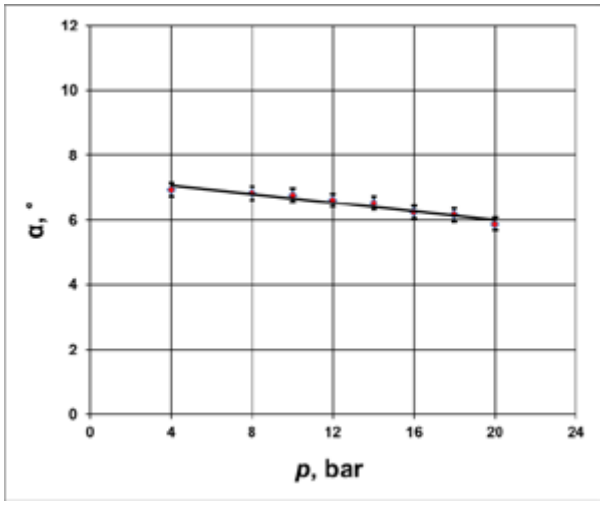



***Figure 7 (a)***

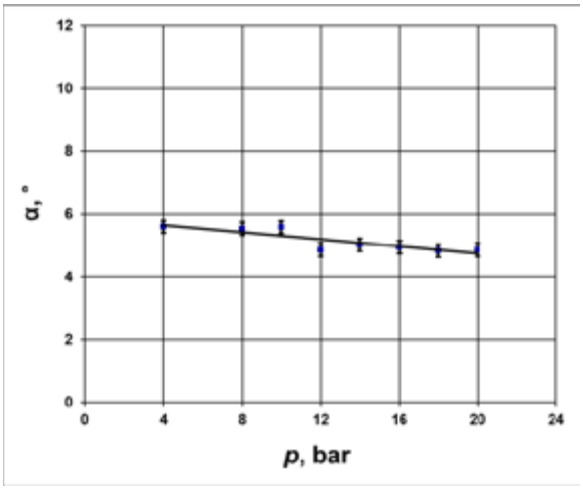



***Figure 7 (b)***

***Figure. 7.*** *(a), (b) Graphics of experimental dependence α = α (p) when cutting of samples M530-50A and M250-35A*

### 3. Discussion

From the obtained results it can be drawn the following conclusions:

✓ Pressure alteration $p$ of the auxiliary gas in the interval 4 ÷ 20 bar does not lead to a significant change in cutting widths $b$ both the entrance and the exit. Changing cutting width on the entrance $\Delta b_{entrance}$ and the exit $\Delta b_{exit}$ in the considered range of the pressure is on the order ± 5 μm about the samples of two steel grades. Maximum deviation of $\Delta b$ is on the order of accuracy measurement.

✓ Rapidity with which is changed the cutting width on the entrance $\Delta b_{entrance}$ by gas pressure $p$, is:

- $\Delta b_{entrance}/\Delta p$ = 0,56μm/bar for M250-35A;
- $\Delta b_{entrance}/\Delta p$ = 0,50μm/bar for M530-50A.

✓ Rapidity with which is changed the cutting width on the exit $\Delta b_{exit}$ in function of gas pressure $\Delta p$, is:

- $\Delta b_{exit}/\Delta p$ = 0,38 μm/bar for samples of M250-35A,
- $\Delta b_{exit}/\Delta p$ = 0,31 μm/bar for samples of M530-50A.

Larger values of the ratio $\Delta b_{entrance}/\Delta p$, than those of $\Delta b_{exit}/\Delta p$ are due to the fact that the processing were realized from surface heat source and absorbed laser radiation has a Gaussian intensity distribution. Difference in the values of the ratio $\Delta b_{entrance}/\Delta p$ and $\Delta b_{exit}/\Delta p$ about both types of material is explained by the varying thickness of the samples.

✓ Increasing pressure values of the auxiliary gas nitrogen from 4 bar to 20 bar with step 2 bar leads to decrease of cut angle deviation by about 1 º in samples of both types steel.

✓ The alteration of gas pressure $\Delta p$ does not affect significant of the rapidity, with which varies the cut angle deviation $\alpha$. Rapidity with which is changed the cut angle deviation $\Delta\alpha$ in dependence of pressure $p$, is:

- $\Delta\alpha/\Delta p$ = 0,066 º.bar-1 for samples of steel M250-35A,
- $\Delta\alpha/\Delta p$ = 0,064 º.bar-1 for samples of steel M530-50A.

✓ Optical analyses of the processing area showed that at values of the pressure $p$ less than 8 bar cutting quality is getting worse. Below this gas pressure at the set out experimental technological parameters it is impossible to be disposed entirely and molten material from the processing area. The molten material is postponed on the output kerf as thus forming drops and other imperfections.

✓ In this study as a recommended mode of cutting through melting it may be indicated the interval $p$ = (10 ÷ 14) bar (good results are obtained at values greater than 14 bar, but from the viewpoint of economic efficiency, it is not necessary to be carried out the cutting process of lamellae with bigger values of the pressure by these).

### 4. Conclusion

Performed experiments and analyses were confirmed the complexity of the physical picture and the phenomena associated with the dynamics and discarded products from the processing cutting area. Important factors having a direct impact on the quality of treatment are proved: the value of the gas pressure; optimization of the distance from the edge of the nozzle to the work surface; the diameter of the nozzle, etc. It is interesting to analyze the obtained optimal values for the role of the auxiliary gas pressure in the present investigation by series of tests in different laser powers and cutting speeds. Such researches will complete and enrich the picture of laser interaction on the substance and finally will optimize the entire technological process in widely limits. The complexity of physical model as well as the practical needs imposed a high activity of scientific researches in this direction.

### REFERENCE

1. www.teslamotors.com

2. Dinev, S., *Lasers in modern technologies*, ALFA, Sofia, 1993 (Bulgarian).

3. Parfenov, V. A., *Lasernaq mikroobrabotka materialov*, SPbGƏTU „ЛЭТИ“, St.Petersburg, 2011 (Russian).

4. Steen W. M., *Laser Material Processing*// Third Edition, L.: Springer, 2003.

5. Golubev, V. S., *Lasernae makrotechnologii: sovremennoe sostoanie i tendentcii razvitiq, Perspektivnae materiala*. 2005, № 1. C. 5-12 (Russian).

6. Giovanni Tani, Luca Tonissani, Giampaolo Campana, Prediction of melt geometry in laser cutting, *Applied surface science* V 208-209 (2003), pp. 142-147.

7. Giovanni Tani, Luca Tomesani, Giampaolo Campana, Alessandro Fortunato, Quality factors assessed by analytical modelling in laser cutting Thin Solid Films, *Applied surface science* 453 –454 (2004) pp. 486–491.

8. Wolfgang Schulz, Vadim Kostrykin, Markus Nieben, Jan Michel, Dirk Petring, Ernst W Kreutz and Reinhart Poprawe, Dynamics of ripple formation and melt flow in laser beam cutting, J. Phys. D: *Appl. Phys.* 32 (1999) pp. 1219–1228.

9. Schuöker, D. Dynamic Phenomena in Laser Cutting and Cut Quality. *Applied Physics*, 1986, B 40, pp. 9 -14.

10. Veiko, V. P., *Tehnologicheskie lasera i lasernoe izluchenie*, St. Petersburg, ITMO, 2007, 52c (Russian).

11. Lee Mein Wee, Lin Li An analytical for striation formation in laser cutting, *Applied Surface Science*, 2005.

12. http://www.din.de/cmd?level=tpl-home&contextid=din&languageid=en

Contacts
Lyubomir Lazov, Hristina Deneva
Faculty of Engineering,
Rezekne Academy of Technology, Latvia
Atbrīvošanas aleja 90, Rezekne, Latvia
e-mail: llazov@abv.bg, hdeneva@abv.bg

© International Scientific Conference on Engineering, Technologies and Systems
TECHSYS 2016, Technical University – Sofia, Plovdiv branch
26 – 28 May 2016, Plovdiv, Bulgaria

# EXPERIMENTAL DETERMINING OF THE ELASTICITY MODULE OF POLYMER CONCRETE COMPOSITES

ILIA POPOV, PEPO YORDANOV, SABI SABEV

**Abstract:** *This study reviews the test method of bending intended for quantitative determination of the module of linear deformation – E of gamma polymer concrete composites. The experimental samples have the form of rectangular parallelepiped (beam type). A testing table for bending is described.*

**Keywords:** *polymer concrete composites, module of linear deformation, regression analysis.*

## 1. Introduction

The higher requirements towards the accuracy of dimensions and forms of the details processed on metal cutting machines (MCM), and especially of these on MCM with CPU are major reason for increasing the quality parameters, efficiency and reliability of the metal cutting machines. In this line of thought, the dynamic processes are considered as priority in the structural design and calculation of the MCM.

The conventional approach used until recently for analysis of the static and dynamic behavior of the body parts of the support system of the MCM, in which the deformation, pressures and dynamic parameters in them are determined, always included the preparation of a kind prototype and its testing as well. The physical prototyping and testing require lots of time and resources. All this reflects on the productivity, quality, accuracy, and cost price of the production.

Due to the widespread application of the computer equipment and automation of the engineering labour in machine building sector, virtual prototyping became possible. In it, the product is designed immediately through a 3D (three-dimensional) prototype with high level of complexity. For the different virtual tests, of specific importance are the quantitative values of the material constants of the structural material of the product. These values are necessary as input data for the various software products for engineering analysis. In this regard, the **intention** of this study is: To determine the modules of elasticity of gamma polymer concrete composites, made in the Test and Research Laboratory of Technical University – Sofia, Plovdiv Branch. The same will be used as structural material for body and body parts in production equipment.

## 2. Theoretic prerequisites

One of the approaches in testing the technical polymer composites is through bending test [1]. The simplest case of bending is the pure bending. In this instance, prevailing normal stresses from bending moment is applied at the cross-sections of the sample type "beam".

Fig. 1 shows the three-point loading of the beam, with bending force *P* and distance between the supports – *l*.

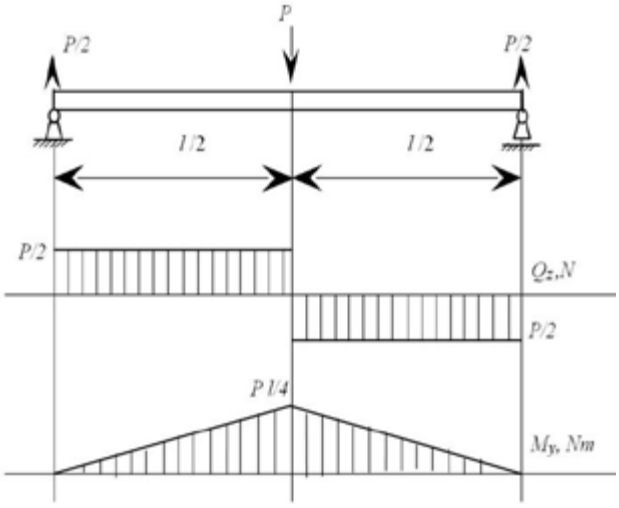



***Fig. 1**. Diagrams in the cases of bending*

Copyright © 2016 by Technical University of Sofia, Plovdiv branch, Bulgaria ISSN Online: 2535-0048

From the theory of bending [2, 3] it is known that the deformation $f$ of a beam lying on two supports and loaded with focused static force $P$ is equal to:

$$f = \frac{Pl^3}{48EJ_y} \quad (1)$$

On this grounds we express the force $P$:

$$P = \frac{48EJ_y}{l^3}.f\ , \quad (2)$$

where:

$EJ_y$ - is the linear hardness of bending;

$E$ – module of linear deformations;

$J_y$ - moment of inertia versus the central axis of inertia $y$. For the rectangular cross section it is equal to:

$$J_y = \frac{b.h^3}{12} \quad (3)$$

After substituting (3) in (1) and (2), the following result is obtained:

$$f = \frac{Pl^3}{4Ebh^3}, \qquad P = \frac{4Ebh^3}{l^3}.f\ . \quad (4)$$

The diagram of the functional dependence between the loading force $P$ and the bending flexure (deformation) of the sample body $f$ is shown on Fig.2.

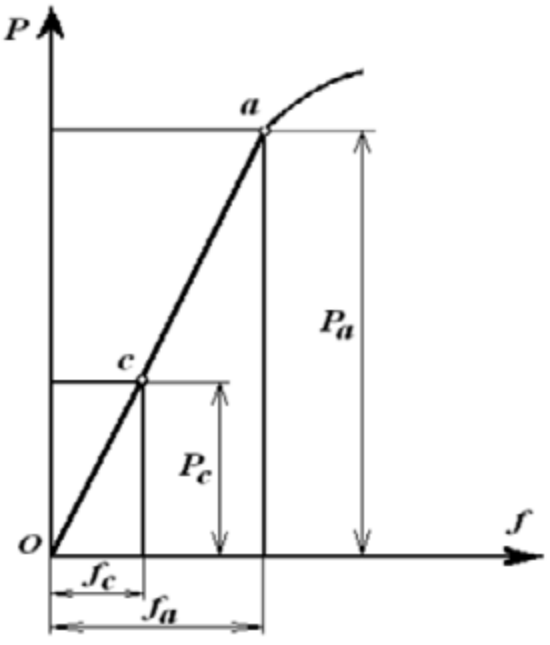



***Fig. 2.*** *Functional dependence between P and f*

Regarding the boundary of proportionality, where the Hooke's law applies, we can correctly write down that:

$$P_a = \frac{4Ebh^3}{l^3}.f_a\ , \quad (5)$$

$$P_c = \frac{4Ebh^3}{l^3}.f_c \quad (6)$$

and $$P_a - P_c = \frac{4Ebh^3}{l^3}.(f_a - f_c) \quad (7)$$

On the grounds of (7) we draw the dependency for the module of linear deformation – $E$:

$$E = \frac{(P_a - P_c)l^3}{4bh^3(f_a - f_c)} \quad (8)$$

### 3. Methodics of the experiment

On the grounds of the bending test standard [1, 4] and the above clarified algorithm for determining the module of linear deformation a laboratory table is designed and made. The sample bodies will be loaded with fixed forces as follows: *200 N, 300 N, 400 N* and *500 N*. Thus three force differences are formed. Respectively, at each loading, the bending flexure of the respective sample will be measured. The obtained results will be processed with the help of the statistical program Minitab 17.

The sample bodies for experimental determining of the module of the linear deformations of polymer concrete composites (15 composites) have the form of rectangular parallelepiped (beam), with dimensions 30x30x350 mm. The form and dimensions are consistent with the generally accepted standardization regulations.

The table for determining the module of linear deformation in bending is shown on Fig.3 and Fig.4. The tested polymer concrete sample 4 is placed freely on the supports 2. They are fixed between the sides 1 through bolts 21. The supports are made of steel (ANSI 304) with diameter $\phi 30$, consistent with the requirements of the standard [1], and they are positioned at $l = 320\,mm$ one from the other. The loading is dome though ball screw and nut transmission 7-14, transmitting the loading to

the sample with the help of the steel (ANSI 304) support 6, with diameter $\phi 30$.,

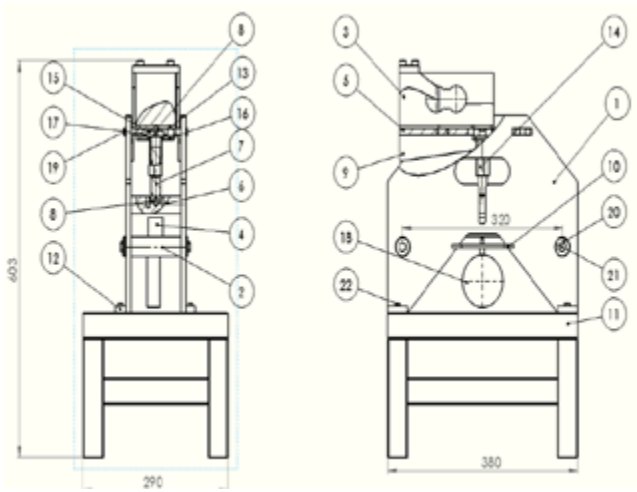


***Fig.3***. *Testing table*

The loading force is measured by a tensiometer (sensor) 3, model "1-PW12BC3/300k-C" by the American company "HBM", with sensitivity $2mV/V$ and maximum loading up to $3kN$. It is connected to a standard terminal ST150 of the German company BIZERBA, Fig.4.

The deformations of the samples are measured by a micrometer 18 (range $1mm$ and separating capacity $1\mu m$), mounted on a stand 10.




***Fig.4.*** *Testing table*

***Table 1*** *Bending flexure $f$ in $\mu m$*

| № specimen | Value $E$ | | | | | | |
|---|---|---|---|---|---|---|---|
| | Load $N$ | | | | Received $E \times 10^9 Pa$ | | |
| | *200* | *300* | *400* | *500* | $E_1$ | $E_2$ | $E_3$ |
| 1.1 | 57 | 95 | 135 | 174 | 25,50 | 24,22 | 24,84 |
| 1.2 | 55 | 97 | 138 | 180 | 23,07 | 23,63 | 23,07 |
| 1.3 | 60 | 105 | 145 | 184 | 21,53 | 24,22 | 24,84 |
| 2.1 | 56 | 105 | 155 | 205 | 19,77 | 19,38 | 19,38 |
| 2.2 | 68 | 118 | 170 | 218 | 19,38 | 18,63 | 20,19 |
| 2.3 | 75 | 122 | 175 | 232 | 20,61 | 18,28 | 17,00 |
| 3.1 | 25 | 44 | 57 | 77 | 50,99 | 74,53 | 48,44 |
| 3.2 | 34 | 53 | 75 | 105 | 50,99 | 44,04 | 32,30 |
| 3.3 | 58 | 95 | 134 | 168 | 26,19 | 24,84 | 28,50 |
| 4.1 | 62 | 112 | 160 | 216 | 19,38 | 20,19 | 17,30 |
| 4.2 | 58 | 100 | 155 | 207 | 23,07 | 17,62 | 18,63 |
| 4.3 | 72 | 121 | 172 | 220 | 19,77 | 19,00 | 20,19 |
| 5.1 | 75 | 130 | 194 | 252 | 17,62 | 15,14 | 16,70 |
| 5.2 | 67 | 125 | 184 | 234 | 16,70 | 16,42 | 19,38 |
| 5.3 | 65 | 125 | 184 | 245 | 16,15 | 16,42 | 15,88 |
| 6.1 | 88 | 152 | 235 | 310 | 15,14 | 11,67 | 12,92 |
| 6.2 | 95 | 178 | 257 | 342 | 11,67 | 12,26 | 11,40 |
| 6.3 | 98 | 170 | 257 | 350 | 13,46 | 11,14 | 10,42 |
| 7.1 | 70 | 122 | 195 | 258 | 18,63 | 13,27 | 15,38 |
| 7.2 | 80 | 140 | 195 | 275 | 16,15 | 17,62 | 12,11 |
| 7,3 | 76 | 140 | 210 | 280 | 15,14 | 13,84 | 13,84 |
| 8.1 | 90 | 158 | 227 | 296 | 14,25 | 14,04 | 14,04 |
| 8.2 | 100 | 170 | 240 | 305 | 13,84 | 13,84 | 14,91 |
| 8.3 | 80 | 155 | 222 | 295 | 12,92 | 14,46 | 13,27 |
| 9.1 | 74 | 122 | 173 | 237 | 20,19 | 19,00 | 15,14 |
| 9.2 | 72 | 131 | 185 | 241 | 16,42 | 17,94 | 17,30 |
| 9.3 | 68 | 126 | 185 | 240 | 16,70 | 16,42 | 17,62 |
| 10.1 | 71 | 141 | 200 | 263 | 13,84 | 16,42 | 15,38 |
| 10.2 | 57 | 118 | 170 | 232 | 15,88 | 18,63 | 15,63 |
| 10.3 | 65 | 118 | 185 | 240 | 18,28 | 14,46 | 17,62 |
| 11.1 | 68 | 127 | 186 | 241 | 16,42 | 16,42 | 17,62 |
| 11.2 | 75 | 135 | 200 | 265 | 16,15 | 14,91 | 14,91 |
| 11.3 | 75 | 138 | 204 | 265 | 15,38 | 14,68 | 15,88 |
| 12.1 | 74 | 138 | 201 | 275 | 15,14 | 15,38 | 13,09 |
| 12.2 | 98 | 160 | 225 | 310 | 15,63 | 14,91 | 11,40 |
| 12.3 | 80 | 155 | 227 | 308 | 12,92 | 13,46 | 11,96 |
| 13.1 | 57 | 115 | 155 | 232 | 16,70 | 24,22 | 12,58 |
| 13.2 | 66 | 113 | 167 | 225 | 20,61 | 17,94 | 16,70 |
| 13.2 | 60 | 110 | 160 | 215 | 19,38 | 19,38 | 17,62 |
| 14.1 | 60 | 96 | 138 | 174 | 26,91 | 23,07 | 26,91 |
| 14.2 | 61 | 98 | 132 | 170 | 26,19 | 28,50 | 25,50 |
| 14.3 | 52 | 92 | 130 | 168 | 24,22 | 25,50 | 25,50 |
| 15.1 | 52 | 112 | 154 | 221 | 16,15 | 23,07 | 14,46 |
| 15.2 | 68 | 123 | 195 | 256 | 17,62 | 13,46 | 15,88 |
| 15.3 | 70 | 132 | 195 | 260 | 15,63 | 15,38 | 14,91 |

## 4. Experimental results

The obtained experimental results for the modules of linear deformations of the polymer concrete composites are grouped in Table 1, where *E1, E2, E3*, are respectively the calculated values on the boundary of proportionality for the three force differences.

## 5. Processing of results

The experimental polymer concrete composites are multicomponent systems with interdependent and bilaterally limited components due to which the regression models represent the so called aligned (canonical) polynomials.

The mathematical and statistical processing is made with the software product MINITAB 17. For the mathematical description of the target function $\hat{y}$ - (the module of linear deformation $E$) an aligned model of third power of the following type is used:

$$\hat{y} = \sum_{i=1}^{q} b_i x_i + \sum_{i=1}^{q-1} \sum_{j=i+1}^{q} b_{ij} x_i x_j + \sum_{i=1}^{q-2} \sum_{j=i+1}^{q-1} \sum_{l=j+1}^{q} b_{ijl} x_i x_j x_l$$

The data in Table 1 is processed and the following regression model was obtained:

$$\begin{aligned}\hat{y} = {} & 9724x_1 + 6724x_2 + 42976x_3 + 298x_4 - 67885x_1x_2 - \\ & - 296035x_1x_3 - 13601x_1x_4 - 30676x_2x_3 - 8560x_2x_4 - \\ & - 47173x_3x_4 + 538594x_1x_2x_3 + 76319x_1x_2x_4 + \\ & + 319844x_1x_3x_4 - 81458x_2x_3x_4\end{aligned}$$

| | Sum of the squares | Degrees of freedom | Dispersion assessment |
|---|---|---|---|
| Regression | $Q_R = 2280{,}9$ | $v_R = 13$ | $s_R^2 = 175{,}454$ |
| Error | $Q_{rez} = 515{,}21$ | $v_{rez} = 31$ | $s_{rez}^2 = 16{,}620$ |
| Total | $Q_O = 2796{,}1$ | $v_O = 44$ | |

***Model adequacy:***

The coefficient of determination is calculated, namely $R^2 = 81{,}57\%$, while the corrected coefficient of determination has the following value $R_{adj}^2 = 73{,}85\%$. In order to check the significance of $R^2$ a value has been calculated, having Fisher's distribution:

$$F = \frac{s_R^2}{s_{rez}^2} = \frac{175{,}454}{16{,}620} = 10{,}556 \qquad (9)$$

In Table [5] with Fisher's distribution $F_T$ was calculated with significance level $\alpha = 0{,}05$ and degrees of freedom $v_R = 13$ $v_{rez} = 31$:

$$F_T = F(0{,}05;13;31) = 2{,}04 \qquad (10)$$

As $F > F_T$ $(10{,}556 > 2{,}04)$ a conclusion can be made that $R^2$ is significant.

In order the coefficient to be significant, the following have to be valid $|t_i| \geq t_T(\alpha; v_{rez})$. In Table [6] with Student's distribution, with level of significance $\alpha = 0{,}05$ the following was reported $t_T = (0{,}05;31) = 1{,}695$. On the basis of a comparison of $t_T$ with the values of Table 2, the conclusion can be made that almost all coefficients are insignificant with the exception of one.

***Table 2*** *Quote from the report*

| Term | Coef | SE Coef | T | P | VIF |
|---|---|---|---|---|---|
| C2 | 9724 | 7026 | * | * | 2655742 |
| C3 | 6724 | 10240 | * | * | 3605541 |
| C4 | 42976 | 23993 | * | * | 1039105 |
| C5 | 298 | 361 | * | * | 188941 |
| C2*C3 | -67885 | 77682 | -0,87 | 0,389 | 4122959 |
| C2*C4 | -296035 | 189561 | -1,56 | 0,129 | 1289979 |
| C2*C5 | -13601 | 10693 | -1,27 | 0,213 | 3250748 |
| C3*C4 | -30676 | 79938 | -0,38 | 0,704 | 147043 |
| C3*C5 | -8560 | 15280 | -0,56 | 0,579 | 4166049 |
| C4*C5 | -47173 | 29342 | -1,61 | 0,118 | 793799 |
| C2*C3*C4 | 538594 | 179541 | 3,00 | 0,005 | 14755 |
| C2*C3*C5 | 76319 | 106550 | 0,72 | 0,479 | 3982846 |
| C2*C4*C5 | 319844 | 239754 | 1,33 | 0,192 | 1042070 |
| C3*C4*C5 | -81450 | 106550 | -0,76 | 0,450 | 129269 |

The analysis of the residuals is made by means of the charts of standardized residuals, Fig.5.

Fig. 5 clearly shows the presence of two mistakes: Observation no. 7 and no. 9. The experimentally measured values of the controllable parameter are: $y_7 = 57{,}99$ and $y_9 = 26{,}51$, while the forecasted values of the model are: $y_{7,9} = 42{,}265$. The difference is significant and respectively the standardized residual is $d_7 = 15{,}725$ and $d_9 = -15{,}755$. This provides us grounds to eliminate observations no.7 and no. 9 and to process the data again.

After their elimination the following regression model is obtained:

$$\begin{aligned}\hat{y} = {} & 9728x_1 + 6711x_2 + 43061x_3 + 297x_4 - 67802x_1x_2 - \\ & - 296703x_1x_3 - 13605x_1x_4 - 30688x_2x_3 - 8537x_2x_4 - \\ & - 47272x_3x_4 + 539390x_1x_2x_3 + 76168x_1x_2x_4 + \\ & + 320640x_1x_3x_4 - 81610x_2x_3x_4\end{aligned}$$

| | Sum of the squares | Degrees of freedom | Dispersion assessment |
|---|---|---|---|
| Regression | $Q_R = 1158{,}94$ | $v_R = 13$ | $s_R^2 = 89{,}149$ |
| Error | $Q_{rez} = 19{,}72$ | $v_{rez} = 29$ | $s_{rez}^2 = 0{,}680$ |
| Total | $Q_O = 1178{,}66$ | $v_O = 42$ | |

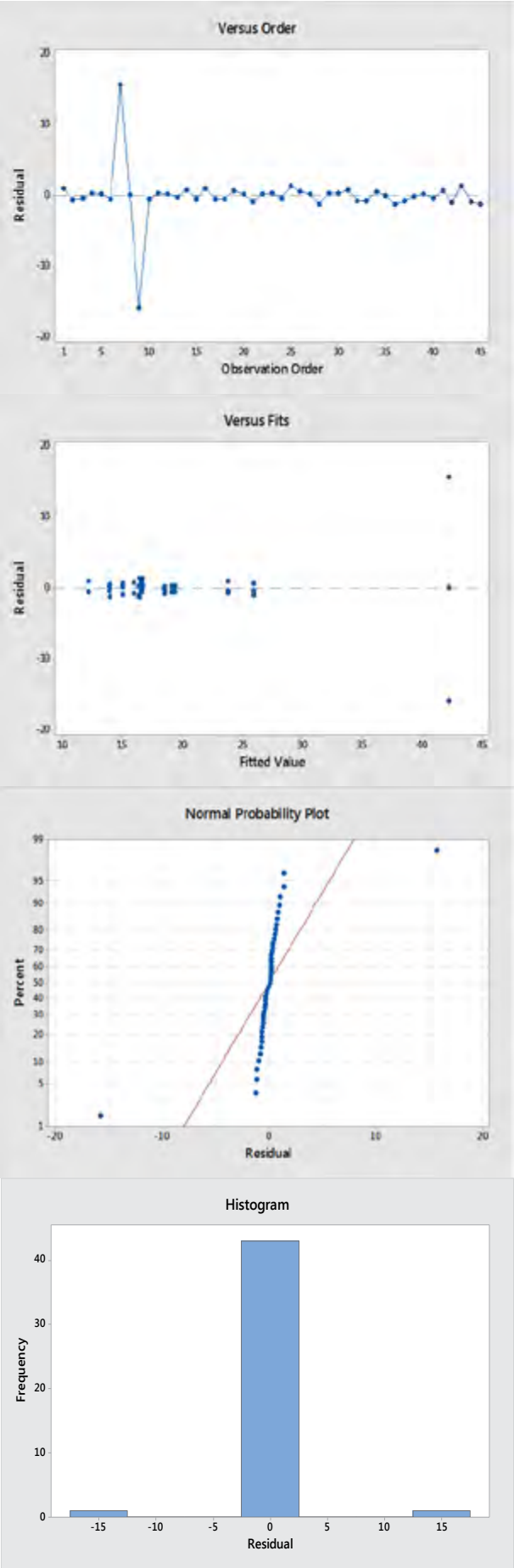



***Fig. 5.*** *Graphs residues*

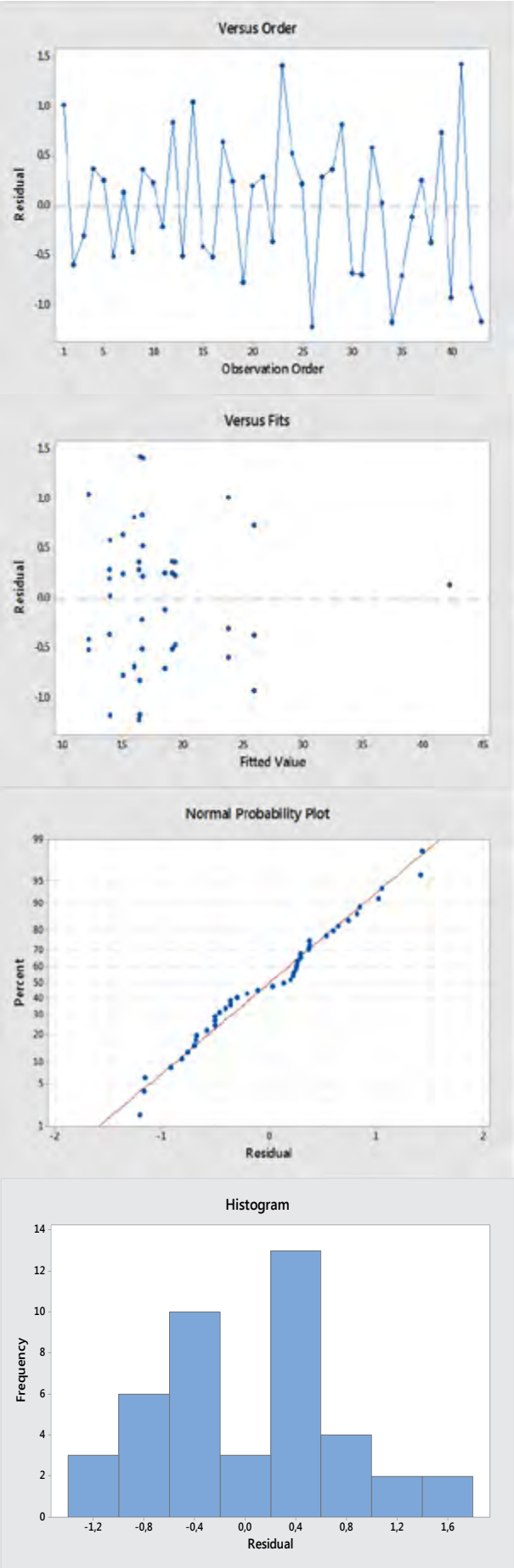



***Fig. 6.*** *Graphs residues*

***Model adequacy:***

The coefficient of determination is calculated $R^2 = 98,33\%$, while the corrected coefficient of determination has the following value $R^2_{adj} = 97,58\%$. In order to check the significance of $R^2$ a values was calculated having Fisher's distribution:

$$F = \frac{s_R^2}{s_{rez}^2} = \frac{89,149}{0,680} = 131,1 \qquad (11)$$

In Table [5] with Fisher's distribution $F_T$ was calculated with level of significance $\alpha = 0,05$ and degrees of freedom $v_R = 13;\ v_{rez} = 29$:

$$F_T = F(0,05;13;29) = 2,04 \qquad (12)$$

As $F > F_T$ $(131,1 > 2,04)$ a conclusion can be made that $R^2$ is significant.

In order the coefficient to be significant, the following should be true $|t_i| \geq t_T\ (\alpha; v_{rez})$. In [6] with Student's distribution, at level of significance $\alpha = 0,05$, $t_T = (0,05;29) = 1,699$ was calculated. On the basis of the comparison of $t_T$ with the values in Table 3, the conclusion can be made that all coefficients are significant, therefore the model is adequate and preserves itself as it is.

***Table 3*** *Quote from the report*

| Term | Коеф. | SE Coef | T | P | VIF |
|---|---|---|---|---|---|
| C2 | 9728 | 1425,3 | * | * | 2585076 |
| C3 | 6711 | 2092,7 | * | * | 3428745 |
| C4 | 43061 | 5232,1 | * | * | 1207901 |
| C5 | 297 | 73,5 | * | * | 182452 |
| C2*C3 | -67802 | 15827,6 | -4,28 | 0,000 | 3975959 |
| C2*C4 | -296703 | 41316,6 | -7,18 | 0,000 | 1498033 |
| C2*C5 | -13605 | 2164,0 | -6,29 | 0,000 | 3146107 |
| C3*C4 | -30688 | 16170,8 | -1,90 | 0,068 | 147091 |
| C3*C5 | -8537 | 3133,7 | -2,72 | 0,011 | 3973054 |
| C4*C5 | -47272 | 6357,1 | -7,44 | 0,000 | 910835 |
| C2*C3*C4 | 539390 | 40690,5 | 13,26 | 0,000 | 18526 |
| C2*C3*C5 | 76168 | 21834,0 | 3,49 | 0,002 | 3870952 |
| C2*C4*C5 | 320640 | 51851,2 | 6,18 | 0,000 | 1191430 |
| C3*C4*C5 | -81610 | 21834,0 | -3,74 | 0,001 | 132672 |

The analysis of the residuals is made by means of the charts of the standardized residuals, Fig.5.

The analysis of the residuals does not show disruption of the prerequisites for the regression analysis. On Fig. 5 it can be seen that all residuals are within the range $\pm 2$. Therefore a conclusion can be made that there are no gross errors.

## 6. Conclusion

**The results from the current study can be summarized as follows:**

- Experimentally, the quantitative values have been obtained of the modules of elasticity of 15 different polymer concrete composites.
- The opportunity for obtaining true information about the linear deformations of the viscous-elastic materials of the type of polymer concrete composite, with this set of measurement equipment is feasible and adequate.
- A table was designed and produced for determining the module of elasticity through bending tests of the samples.

## REFERENCES


1. ASTM-D-790. *Standard Test Methods for Flexural Properties of Unreinforced and Reinforced Plastics and Electrical Insulating Materials.*
2. Козловский А.Э., В.В. Бойцова. (2007). *Механические свойства материалов. Методы испытаний*. ГОУ ВПО «ИГХТУ» . Иваново.
3. Фудзий, Т., М. Дзако. (1982) *Механика разрушения композитных материалов*. Перев. с японского. М., "Мир".
4. ASTM C580 - 02(2008) - *Standard Test Method for Flexural Strength and Modulus of Elasticity of Chemical-Resistant Mortars, Grouts, Monolithic Surfacings, and Polymer Concretes*
5. *http://www.socr.ucla.edu/applets.dir/f_table.html#FTable0.05*
6. *http://www.sjsu.edu/faculty/gerstman/StatPrimer/t-table.pdf.*


The publication is related to work on a research project № 152PD0048-24/2015 on "Research and optimization of range polymer concrete composites in terms of their physical constants."

Contact:
Technical University of Sofia, branch Plovdiv
E-mail: ilgepo@abv.bg
E-mail: piyordanov@tu-plovdiv.bg
E-mail: sabi_sabev@abv.bg

© International Scientific Conference on Engineering, Technologies and Systems
TECHSYS 2016, Technical University – Sofia, Plovdiv branch
26 – 28 May 2016, Plovdiv, Bulgaria

# КОМБИНИРАНЕ НА ОСНОВНИ ФОРМИ В ДИЗАЙНА

ТРАЯН СТАМОВ

**Резюме:** *В тази работа се дискутират възможностите за комбиниране на основни форми, които се използват в дизайна. Знанието за възможните комбинации на форми и тяхното използване са от особено значение за креативния процес на дизайн и предоставя необходими инструменти за реален креативен дизайн и възможности не само в дизайна и традиционната дизайн култура, но също така и в нови области на познанието, където решаването на проблемите на външния вид на продуктите, се превръща в реална перспектива.*

**Ключови думи:** *формообразуване, основни формени категории в дизайна, комбиниране на форми*

# COMBINING OF BASIC SHAPES IN DESIGN

TRAYAN STAMOV

**Abstract:** *in this paper, the opportunities and applications of different combinations of basic shapes in design are discussed. The knowledge about the possible main combinations of shapes and their applications provides the necessary tools for real creative design process and opportunities not only in design and traditional design culture, but also in new areas of knowledge where solving problems of the appearance of products becomes a real prospect.*

**Key words:** *form-formation, main shapes applied in design, combining of shapes*

## 1. Увод

Основните постулати във формообразуването в контекста на съвременния дизайн са изучавани от редица български и чуждестранни автори. Проведено е широкообхватно проучване, систематизиране и класифициране на изграждащи форми, които се използват в дизайна. За по-пълна информация ще насочим читателя към литературни източници [1-8] и цитираната в тях литература. Ще отбележим обаче, че начините на образуване на формени категории са докладвани в много малък брой литературни източници [3, 7, 8].

Основните проблеми на една визуална организация съществуват във всеки дизайн, но те не могат еднакво да се разпознаят от всеки, защото се препокриват и с друга проблематика. Един дизайн никога не означава само един единствен проблем, една единствена задача и никога не представя само едно просто събиране на отделните проблеми. Всеки дизайн е съвкупност от по-малко, или по-голямо разнообразие от проблеми, които взаимно проникват един в друг и образуват едно цяло. С цел общите условия на даден дизайн да достигнат до съзнанието е нужен анализ на това цяло, както и систематизиране на изследването, за да се превърнат тези условия в разпознаваем проблем в тяхната взаимовръзка.

Комбинирането на формени категории е основа на творческия процес в дейността на дизайнера. Композициите от форми, които се използват при дизайн на продукти могат да предизвикват разнообразни емоционални реакции. Познанието на възможностите за комбиниране позволява разкриване на същността, характера и приоритетността на основни принципи, аспекти и критерии на формообразуването и композиционното формоизграждане.

В тази работа са дискутирани най-основните постулати, свързани с възможностите

Copyright © 2016 by Technical University of Sofia, Plovdiv branch, Bulgaria ISSN Online: 2535-0048

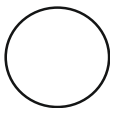
за комбиниране на основни формени категории, използвани в дизайна.

## 2. Постановка на проблема

Съществуват оскъдни източници, посветени на начините на образуване и изобразяване на базови формени категории, както и на начините на преминаване от една формена категория в друга. В тази секция ще направим кратък обзор на основните формени категории, които се използват в дизайна на продукти. Селектираните категории са разглеждани в [3, 7, 8]. Направеното в цитираните източници изследване на начините на повърхностно и пластично изобразяване на основни формени категории позволява неговото по-нататъшно разширяване и разглеждане на възможностите за комбинации на тези базисни формени категории.

### 2.1. Първа основна формена категория "Безпосочност"

Следвайки закона за развитието на движението от простото към разнообразното, като отправна точка при селектиране на формени категории се поставя въпросът за най-простия визуален характер, който трябва да се противопостави на най-елементарната визуална даденост. Формата, от която произлизат всички останали се определя като „*безпосочност*" [1, 3, 6, 7, 8]. В равнината основни елементи, които се използват при работа с тази формена категория са точка, кръгово петно или окръжност (Фиг. 1). В пространството за изобразяване на тази форма се използва сферата.



***Фиг. 1.*** *Една от основните фигури при първа основна формена категория*

Основното при характеризирането на такова кръгло петно, като най-простата възможна форма, която може да се забележи върху произволна повърхност, или може да се онагледи върху нея, е не големината му и не средството, чрез което то е изобразено, а е неговото приблизително равномерно закръгляне, неговата „безпосочност".

### 2.2. Втора основна формена категория „Направление"

При развитие на безпосочната форма чрез задаване на едно единствено направление се достига до нов обект, наречен „насочено петно". Този нов обект е обозначен, като нова основна възможност на формата, или категория на формата „*направление*" [8].

В равнината на тази форма съответства права линия, а в пространството, съответстват всички цилиндрични издължени форми (Фиг. 2).

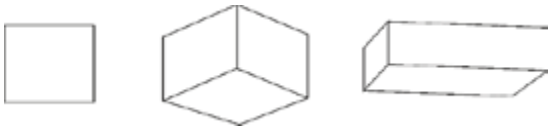


***Фиг. 2.*** *Втора основна форма, използвана в дизайна*

Тази форма се използва предимно при дизайн на продукти с характерна по-голяма дължина спрямо общата форма.

### 2.3. Трета основна формена категория "Противоположни направления"

Основният елемент, който се използва за повърхностно изобразяване при третата основна формена категория е квадрат [1, 3, 6, 7, 8], а в пространството куб или паралелепипед (Фиг. 3).



***Фиг. 3.*** *Основни елементи, които се използват при трета базисна формена категория*

Това са и основните форми, които се използват при геометрични преобразувания на мрежи, разгледани от Р. Райчев [2]. В пособието на Зицман и Шулц [8] тази форма е наречена „*противоположни направления*", тъй като е разглеждана като форма, получена след разширяване на правата линия (основен елемент при втората категория) в противоположно направление до получаването на лента. Рязка промяна на категорията на формата се получава тогава, когато височината на лентата стане равна на нейната дължина.

### 2.4. Четвърта основна формена категория „Разграничаване на направленията"

За постигане на промяна в направлението при елементи от третата формена категория се използва леко накланяне на едната страна на квадрат. Така се достига до нова, коренно различна категория с разграничени направления. Основна фигура, която се използва при повърхностно изобразяване на четвъртата

основна формена категория е триъгълник (Фиг. 4).



***Фиг. 4.*** *Базисна фигура при четвърта формена категория*

При 3-D дизайн с работа с тази формена категория се използват пирамидални елементи [2, 3, 6, 8]. В пособието на Зицман и Шулц [8] тази формена категория е наречена „*разграничаване на направленията*“.

### 2.5. Пета основна формена категория „Насочено движение“

Основните характеристики на петата базисна формена категория, наречена „*насочено движение*“ [7, 8] се изразяват в огънатите, закръглени и заоблени фигури, които я репрезентират, както в повърхнината, така и в пространството (Фиг. 5).



***Фиг. 5.*** *Развитие на форма при „насочено движение“*

От всички категории коментирани досега, насоченото движение предоставя най-съвършенна възможност, да се слеят повече форми в пълно единство, защото тази категория форми може да създаде по нов начин едно цяло, чрез безгранично вливане на отделните части една в друга, при което частите загубват своята самостоятелност така, че често те много трудно се разпознават, като отделни компоненти.

### 2.6. Неопределености на формите

При диференциране на произволна насочена форма е възможно да се постигне все по-голямо разделяне на движението и формата, докато накрая основната характеристика на движението и характеристиката на ясно определената форма се загубват и възниква една визуална даденост на проявление със съвсем други качества.

Тази последна категория на формообразуването е наречена „неопределена”, защото тук не може да се разпознае никакво определящо качество на формата (Фиг. 6).



***Фиг. 6.*** *Дизайн на обекти от формена категория “неопределеност“*

Целта на настоящата работа е да се изследват някои възможни комбинации на основни формени категории и тяхното приложение в дизайна.

## 3. Комбиниране на основни форми в дизайна

Въпросите на визуалния дизайн не се изчерпват с определяне на основните формени категории, техните възможности за контраст и подреждане и основните начини за визуално изобразяване. Всички основни формени категории, които разгледахме в Секция 2, се наблюдават в обкръжаващата ни среда в преобладаващия брой случаи не поотделно и ясно разделени, а смесени една с друга, съвпадащи и комбинирани. Това не означава само огромно разширяване на възможности за изобразяване при дизайн на продукти, изобилие от нови контрасти, това означава и значително по-големи трудности при свързването на тези контрасти и различия в едно изобразително цяло.

Предимството на дизайна в рамките на една ясна категория се състои в това, че самите формени категории са винаги много единни, поради наличието на истинско сродство на формите. Същественият въпрос, на който е посветена тази работа е как да се постигне единство на изображението при използване на повече от една, или на всички формени категории заедно.

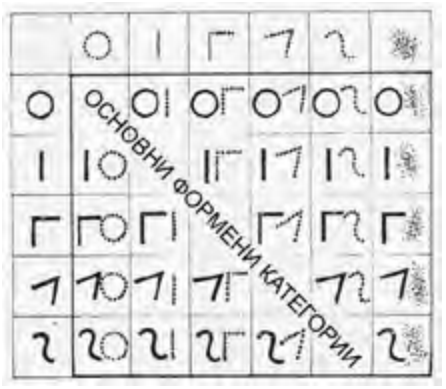
За да се избегне несвързаното подреждане на форми от различни формени категории една до друга, е важно да се намерят възможности за връзка и за уеднаквяване на цялото послание на дизайна. Съществуват разнообразни възможности за външно и вътрешно свързване на форми от различен вид. Съществено при това обаче е винаги връзката на тези форми с една трета величина, с нещо извън границите на формите, но което е общо за всичките.

Една външна връзка възниква например чрез единство на дадено качество: чрез единен цвят, чрез единните качества на повърхността, чрез еднаквата осветеност и т.н. Други образуващи фактори се състоят в единния ритъм или в общо отношение на контраст с трета величина. Освен това при изобразяването си формите естествено винаги са свързани и чрез своята обща връзка с предмета, който те нагледно изобразяват. Най-здравата вътрешна връзка на различните характеристики на формите от различен вид е налице тогава, когато те образуват подредена структура, която съответства като цяло на една от петте категории за онагледяване или е неопределена. При това тази категория, разглеждана като форма, не е необходимо да е в рамките на едно изображение. Тя трябва само да определя вида на връзките на частите към цялото или вида на взаимовръзката с цялото. Така например форми от формена категория „направление“ с една определена посока и форми от формена категория „разграничаване на направленията“ с диференцирани посоки могат да са в една напълно противоположна по посоки връзка, и то точно така, както е възможно при безпосочни форми и форми от „насочено движение“. Формите с насочени движения също могат да имат безпосочно подреждане. Същото важи по смисъл и за всички други форми и връзки от форми.

Трябва да отбележим, обаче, че и видовете изобразявания като подреждане, метрика, картинни изобразявания, могат да се комбинират помежду си. Освен това възниква рязката промяна в качеството само при комбиниране на по-голям брой форми, поради въздействията на отделните части към цялото.

От съществено значение при обясняване на възможностите за връзка на петте основни категории и неопределеностите на формите са два основни момента: структурата на подреждане, според която се подреждат отделните елементи и представените стойности на формата, или неопределеностите на формите. При основните категории структурата на подреждане и представените формени елементи са идентични: безпосочни форми са подредени безпосочно; насочените стойности на формата са подредени по една посока; форми с противоположни посоки имат структура на подреждане с противоположни посоки и т.н. При търсене на възможности за дизайн с комбинирано използване на базисните формени категории Таблица 1 [8] може да ни даде най-добре преглед на многото възможности за комбиниране, които се получават, ако ние свържем само две от категориите на формата една с друга.

***Таблица 1.*** *Връзки между двойки основни формени категории*




В дадената таблица не е посочено какъв е дялът на формите от двете основни формени категории. Дялът на формата на една, или друга основна категория форми може да преобладава, дори и структурата на подреждане да остава една и съща.

Диагоналът на таблицата диференцира основните категории. Основната форма и структурата на подреждане са съвпадащи.

Първият ред обяснява изображенията, които имат безпосочна структура на подреждане. В първата клетка от таблицата съвпадат структурата на подреждане и формата (това е категорията „безпосочност”). В следващата клетка структурата на подреждане отново е безпосочна. Представящите форми са или насочени (от категория „направление“), или комбинация от безпосочни и насочени, или безпосочни форми и насочени форми. Следващата клетка обединява изображенията, които са подредени безпосочно и представените форми показват или противоположност на направленията, или са комбинирани форми от безпосочни форми, форми с противоположни направления и безпосочни форми и форми с противоположни направления. Структурата на подреждане остава и в следващите клетки безпосочни. За формите с определена посока, и за формите с насочено движение е валидно същото, те могат да са представящи форми. Те могат да бъдат комбинирани и с безпосочна форма като в дизайна да доминира една от двете форми. Формите от „насочено движение“ също могат да са съединени с безпосочни форми при тяхното изобразяване. Структурата на подреждане тук е безпосочна. Така те могат да бъдат подредени безпосочно към формите с насочено движение.

Последната е демонстрирана в последната клетка на първия ред на Таблица 1. Такава комбинация се използва при изображения, които използват безпосочни форми и неопределеност на формата.

Цялата област на комбиниране на дадена формена категория с „неопределеност" се разглежда в последната колона на тази таблица.

Във вторият хоризонтален ред се повтарят посочените възможности, само че всички изображения имат насочена структура на подреждане (следват дадено направление).

В третият ред са дадени изображенията, които са подредени с протовоположни посоки.

Четвъртият ред символизира всички възможности за изобразяване при комбиниране с разграничаване на направленията.

Петият ред изяснява изображенията, които са с насочено движение.

Въпреки, че Таблица 1 показва голямо разнообразие от възможности за изобразяване, в нея са показани само комбинации по двойки на формени категории. Съществуват, естествено, възможности за комбиниране на три, и повече категории на формата. Но в основата на всички тези възможности е залегнало изискването различните форми да са организирани по една единна структура на подреждане. Това включва и факта, че има изображения, които са изобразени според една структура на подреждането (едно направление, противоположни направления и т.н.), но не чрез форми от тази категория. Например: Една композиция, която е подредена с противоположни посоки, но видимите формени елементи са безпосочни, с определена посока и с насочени движения. Структурата на подреждане и представени форми не са вече идентични, както това е в основните формени категории. Структурата на подреждане е разположена невидимо под стойностите на формата и определя нейното подреждане.

Възможностите на изобразяване с различни или комбинирани характеристики на формата върху повърхността могат сравнително лесно да бъдат пренесени и разглеждани за 2-D и 3-D дизайна. В таблица 2 са дадени 2-D композиции, получени при комбиниране на двойки формени категории. При 3-мерно изобразяване е необходимо да се определи дали да се подсили излъчването, посланието, стойността на отделни форми, или да се подчинят на главната форма. Освен това е важно да се прецени дали ще се изобразява равнинно, или с други думи акцентиращо на линията по нейния най-прост начин на изобразяване, или с линейни средства ще се създават пространствени стойности на изобразяване.

***Таблица 2.*** *2-D композиции от комбинации между двойки основни формени категории*




**4. Заключение**

В настоящата работа са дискутирани възможности за комбиниране на основни формени категории, използвани в 2-D и 3-D дизайна. Познанието за структурите при комбиниране е важно при обучение на бъдещи дизайнери, както и в реалната дизайнерска практика.

**ЛИТЕРАТУРА**

1. Желева-Мартинс, Д. (2000). *Тектониката като теория на формата и формообразуването*, Академично издателство "Проф. Марин Дринов", София.
2. Райчев, Р. (2002). *Структурна комбинаторика*, Анубис, София.
3. Стамов, Т. (2013). Дизайн и емоции. Основни форми, използвани в дизайна на съвременни транспортни средства, *Машиностроене и Машинознание*, Издателство на Технически университет-Варна, 19, 84-89.
4. Burrell, G. (2013). *Styles of Organizing. The Will to Form*, Oxford University Press, New

York.
5. Ching, F.D.K. (2007). *Architecture, Form, Space, and Order.* (Third Edition). John Wiley & Sons, New Jersey.
6. Itten, J. (1964). *Design and form. The Basic course at the Bauhaus and Later*, Reinhold Publishing Corporation, New York.
7. Stamov, T., (2015). Shapes applicable in design of contemporary vehicles: Differences in emotional impact and applications, *International Journal of Emerging Science and Engineering*, 3(8), 38-42.
8. Zitzmann, L., and Schulz, B. (1990). *Dokumente zur visuell-gestalterischen Grundlagenaus bildung*, Halle Burg Giebichenstein.

Контакти:
Траян Стамов, д-р., инж. диз., гл.ас.
Адрес: ТУ-София, Катедра МЕНК
Бул. „Кл. Охридски“ 8
1756 София
E-mail: tstamov@tu-sofia.bg

© International Scientific Conference on Engineering, Technologies and Systems
TECHSYS 2016, Technical University – Sofia, Plovdiv branch
26 – 28 May 2016, Plovdiv, Bulgaria

# ПОДОБРЯВАНЕ НА ЕКСПЛОАТАЦИОННИТЕ ПОКАЗАТЕЛИ НА ЗАДВИЖВАЩА ШАЙБА ЗА ВИСЯЩА ВЪЖЕНА ЛИНИЯ

ЖИВКО ИЛИЕВ, ГЕОРГИ ДИНЕВ

**Резюме:** *Извършен е преглед и анализ на проблемите свързани с експлоатацията на висящи въжени линии задвижвани с външна цилиндрична зъбна предавка. Направено е компютърно изследване, чрез което е получена картината на напреженията и деформациите в областите на най - голямо натоварване на зъбната двойка "задвижващо зъбно колело – задвижвано зъбно колело". Анализирани са възможните причини за възникване на неблагоприятни резонансни процеси посредством направен компютърен модален анализ. В заключителната част са направени изводи относно възможностите за оптимизиране на изследваните детайли.*

**Ключови думи:** *рудничен транспорт, задвижваща шайба, висяща въжена линия*

# IMPROVING THE MAINTANCE OF DRIVE SHEAVE OF HANGING ROPEWAY

ZHIVKO ILIEV, GEORGI DINEV

**Abstract:** *We conducted a review of the issues related to exploitation of pending ropeways with a spur gear transmission. A computer-aided research has been performed as it depicts stresses and deformations within the areas of most intensive loading of the gear couple i.e. the areas of 'the driving gear' and the areas of 'the driven gear'. The causes for unsound resonance processes have been investigated by the use of a computer-aided modal analysis. The final part offers conclusions which refer to the options for optimization of the investigated details.*

**Key words:** ***mine transport,*** *drive sheave, hanging ropeway, hanging*

## 1. Основни положения

Приложението на висящите въжени линии се определя най-вече от предимствата, който те притежават в сравнение с останалите видове рудничен транспорт. Най-често те се използват за транспортиране от мястото на добиване на полезното изкопаемо до мястото на преработка в обогатителните фабрики. Те са най-удобни при планински или силно пресечен релеф на местността, където за проправянето на автомобилни пътища или железопътни линии се изискват големи капитални вложения.

Понякога се оказва целесъобразно използването на висящи въжени линии и при равнинен релеф на местността, когато пътищата трябва да се прокарват с големи заобикаляния. Друго приложение на висящите въжени линии е за образуване на минни насипища. По техния принцип на действие те се разделят на три основни вида: -едновъжени; -двувъжени и многовъжени.

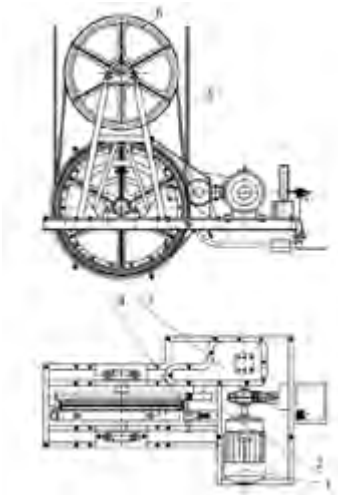
Когато вагонетката навлезе в товарната станция тя се откача от носещото въже и продължава да се движи върху висящия релсов път теглена от теглителното въже. Като след това продължава на самоход, спира на бункера за натоварване и се прибутва чрез прибутвачи до мястото за пускане в товарния клон. Като наближи изхода на станцията вагонетката вече се движи самоходно по наклонен участък, за да

Copyright © 2016 by Technical University of Sofia, Plovdiv branch, Bulgaria ISSN Online: 2535-0048

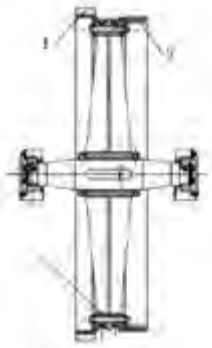
може скоростта й да стане равна на тази на теглителното въже.

Като обект на изследване и подобряване на експлоатационните показатели е силовата външна зъбна предавка на задвижващата станция за висяща въжена линия.

Общият вид на задвижваща станция за с вертикална шайба е дадена на ***фигура 1***. Нейните основни елементи са показани както следва: 1 – електрически двигател с мощност $N_{дв}$ = 75 kW и обороти n = 1030 об./min [1]; 2 – външна зъбна предавка; 3 – цилиндричен редуктор; 4 – лентова спирачка; 5 – теглещо въже и 6 – обръщателна шайба.



***Фиг. 1*** *Задвижваща станция за висяща въжена линия*



***Фиг. 2*** *Вертикална задвижваща шайба*

На ***фигура 2*** е изобразена вертикална задвижваща шайба със следните съставни детайли: - 1 задвижвано зъбно колело; 2 – спирачен барабан за лентовата спирачка и 3 – триеща шайба за въжето.

В ***таблица 1*** са дадени основните технически показатели на външната зъбна предавка. Параметрите за задвижващото и задвижваното зъбно колело са както следва: брой зъби - 19 и 106; въртящ момент 11 082 Nm и 58 279 Nm; честота на въртене 64 и 11 $min^{-1}$; маса на колелата – 563 и 639(само венеца) kg

***Таблица 1.*** *Параметри на външната зъбна предавка*

| ПАРАМЕТЪР | ЗАДВИЖВАЩО КОЛЕЛО | ЗАДВИЖВАНО КОЛЕЛО |
|---|---|---|
| БРОЙ ЗЪБИ, Z, БРОЯ | 19 | 106 |
| ЪГЪЛ НА НАКЛОН НА ЗЪБИТЕ,° | 0° | 0° |
| ДЕЛИТЕНЕН ДИАМЕТЪР,mm | 380 | 2120 |
| ЧЕСТОТА НА ВЪРТЕНЕ,[Hz] | 1,06 | 0,18 |
| Нормална сила в предавката [kN] | 111 | |
| МОДУЛ | 20 | |

## 2. Подход за подобряване на експлоатационните показатели

За подобряване на експлоатационните показатели в процеса на проектирането на технически транспортни съоражения може да се използват възможностите на съвременните софтуерни продукти. В конкретния случай при проектирането на едностъпална зъбна предавка от задвижващата шайба за висяща въжена линия оптимизация може да се търси чрез основните характеристики: междуосово разстояние - $a_w$, минимален инерционен момент - J , габаритен размер на зъбната предавка - L и маса на зъбните колела – M. За целта трябва да се реши оптимизационна задача като се използва алгоритъм за минимизиране на целева функция с дефинирани параметрични и функционални ограничения [5].

Друга възможност за конструкторът да търси творчески решения се базират на хипотезата на Нюъл и Саймън [8], като средство за универсални интелигентни действия и алгоритми от експертните системи [6]. В експертните системи се използват продукционни правила от тип „условие-действие“, което може да се илюстрира със следния алгоритъм за проверка за концентрация на напрежения чрез метода на крайните елементи [7].

Ако: 1) радиусът на закръгление е 1 mm.
2) напрежението е > ……MPa.
Тогава: Да се промени радиусът ……
Ако: напрежението е > ……MPa.
Тогава: Да се избере марка стомана …
Ако: напрежението е < ……MPa.
Тогава: Липсва концентрация на напрежения.

От гледна точка на изготвянето на комплект конструкторска документация като последен етап от процеса на проектиране на изделието отговарящо на изискванията регламентирани в европейската директива

дадена в [3] трябва да се разработва релевантна техническа документация. Тази документация обхваща проектирането, производството и функционирането на техническия обект за оценяване на съответствието със съществените изисквания за безопасност и опазване на здравето.

Един от съществените документи в процеса на проектирането представлява конструктивното досие което съдържа следните документи:

- сборен чертеж на цялата машина, както и чертежи на управляващите вериги;
- подробни и пълни чертежи, придружавани от изчислителни записки, резултати от изпитвания и сертификати;
- документи необходими за проверяване съответствието с приложените съществени изисквания за безопасност и опазване на здравето;
- документация относно оценката на рисковете, описваща прилаганата процедура, включително копие от инструкцията за монтаж.

Това характеризира жизнения цикъл на техническия обект и прогнозиране на неговата надеждност на етап проектиране и изпитване чрез използване на количествени показатели.

За осигуряване на качеството на продуктите все по-често се прилага метода FMEA (Failure Mode and Effects Analysis) като средство за намаляване на грешките при системния анализ с оглед откриване на причините които ги пораждат. Оценяването на риска за възникването на дефекти в зъбни предавки вкл. и зъбни колела чрез FMEA се потвърждава от публикуваните до сега разработки[2,4].

Контактът на зъбите в предавката се характеризира от комплексния показател моментно контактно петно. Изискването за добър контакт на зъбите в предавката има съществено значение за нейните експлоатационни показатели, тъй като при недостатъчно петно на допиране контактните напрежения се разпределят неравномерно. Критичното напрежение по повърхността на зъба се получава в резултат на вътрешно налягане. Това зависи от материала, натоварването и радиусът на кривина според Hohn [9] тъй като с радиусът на кривина се променя линията на контакт.

### 2.1. Методика на изследване

От техническите параметри на зъбните колела дадени в таблица 1 се вижда, че зъбната двойка е бавнооборотна и представлява високонатоварен предавателен механизъм. Поради тези причини, най – срещаните повреди са напукванията и счупванията на зъбите, както и тяхното износване до степен, при която е невъзможна нормалната и безопасна работа [13] на въжената линия.

Първият етап от провеждането на изследването е създаването 3D CAD модел на изследваната зъбна предавка. Случаят се отнася до показаната на фиг.3 конструкция на задвижваща шайба. Моделирането е осъществено в среда на Auto Desk Inventor с най-голямата възможна детайлизация за изходните параметри.

#### 2.1.1. Уточняване на видовете и броя на симулационните изследвания, както следва:

• линеен структурен анализ на зъбната предавка с цел определянето на големината и разпределението на еквивалентните напрежения;

• модален анализ за определянето на собствените честоти и форми с оглед на тълкуването на опасността за възникване на резонансни явления. [10, 11, 12]

За използван основен материал на зъбната двойка се приема стомана S 235 J2G3 БДС EN 10025, при която допустимите напрежения са от порядъка $[\sigma_{AL}] = 160MPa$ .

Разпределената сила *Fn*, която действа на контактната повърхност на зъбите определя натоварването на зъбите [14].

### 2.2. Резулатати от проведения линеен структурен анализ

В процеса на работа ще бъдат използвани само някои от възможностите на програмния продукт за изследване по МКЕ, а именно:

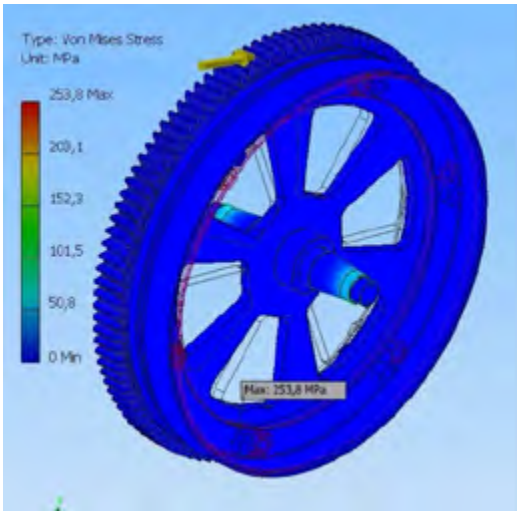
- Еквивалентно напрежение според теорията на von Mises [12];
- Коефициент на сигурност по теорията на Mises-Henky
- статични деформации (абсолютни и еквивалентни)

Според теорията на von Mises-Henky границата на провличането се определя от отношението между големината на еквивалентното напрежение по von Mises $\sigma_{VON}$ и тази на допустимото напрежение $[\sigma_{AL}]$ [12]

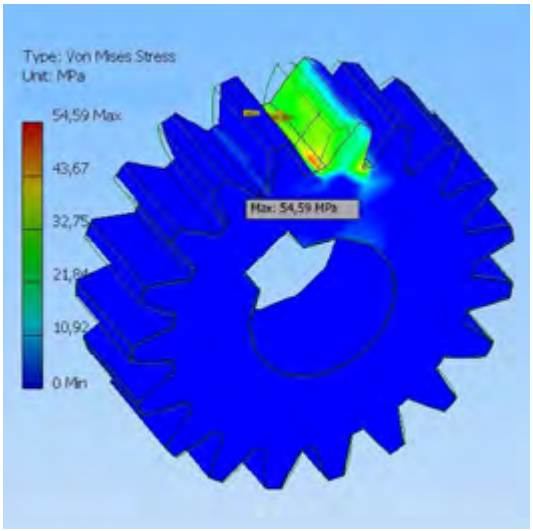
$$\sigma_{VON} \geq [\sigma_{AL}]$$

Напреженията по von Mises могат да се изразят чрез трите главни напрежения, съгласно зависимостта (1)

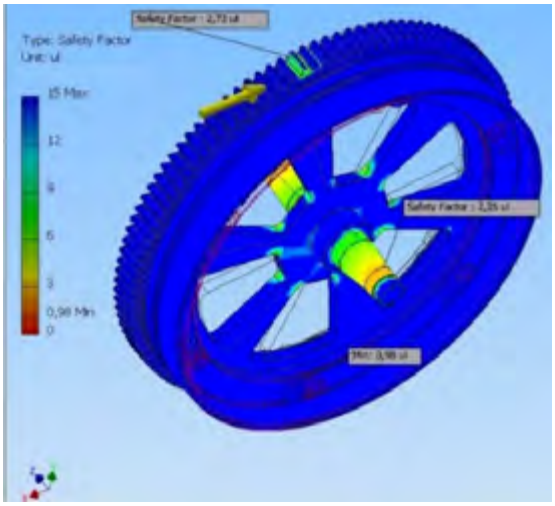
$$\sigma_{VON} = \sqrt{\frac{(\sigma_1 - \sigma_2)^2 + (\sigma_2 - \sigma_3)^2 + (\sigma_1 - \sigma_3)^2}{2}} \quad (1)$$



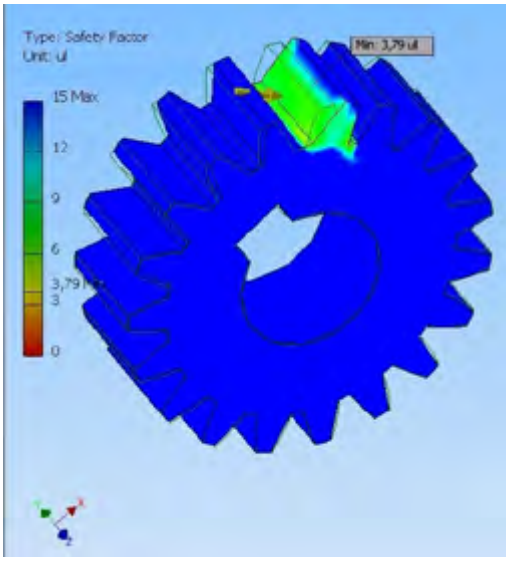

***Фиг. 3*** *Разпределение на еквивалентните напрежения в задвижваното колело*



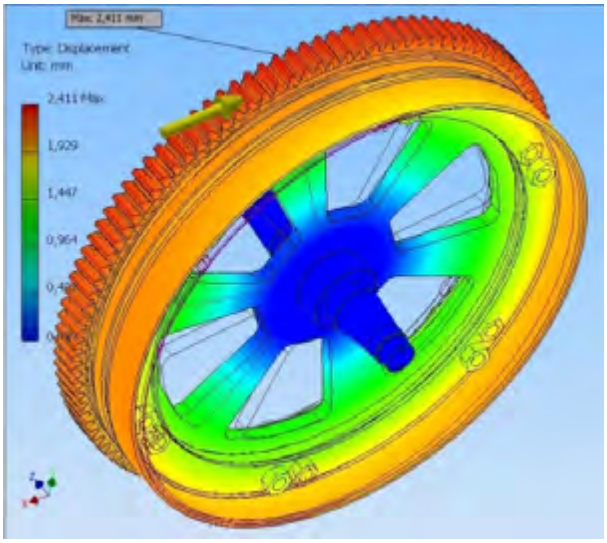

***Фиг. 6*** *Разпределение на еквивалентните напрежения в задвижващото колело*



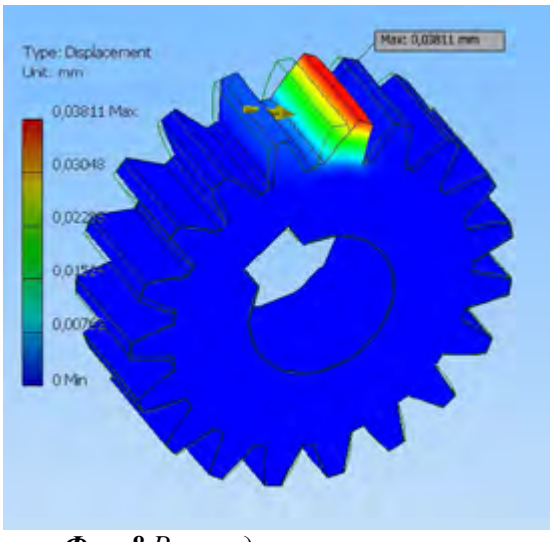

***Фиг. 4*** *Разпределение на фактора на сигурност (FOS) в задвижваното колело*



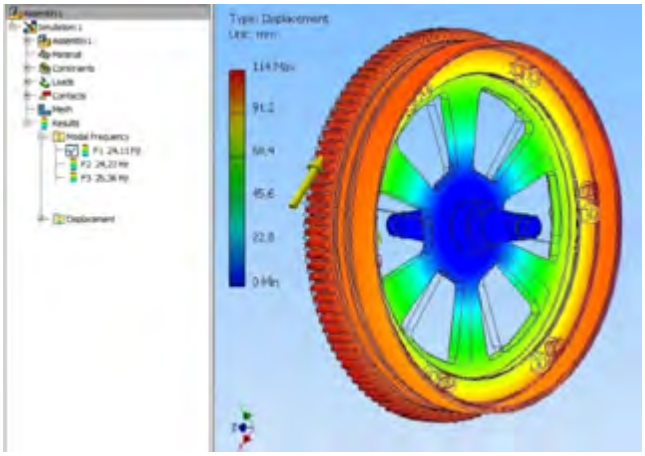

***Фиг.*** *7 Разпределение на фактора на сигурност (FOS) в задвижващото колело*



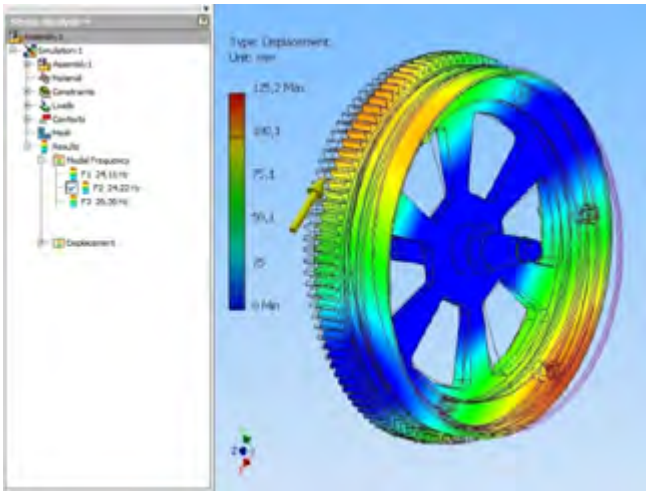

***Фиг. 5*** *Разпределение на еквивалентните премествaня в задвижваното колело*



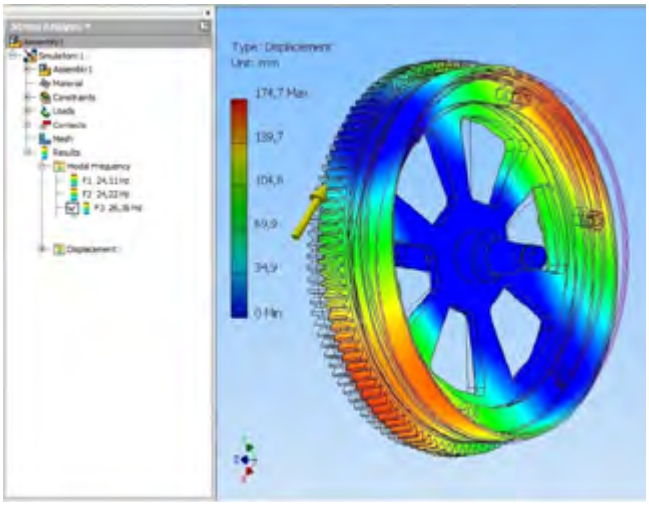

***Фиг. 8*** *Разпределение на еквивалентните премествaня в задвижващото колело*



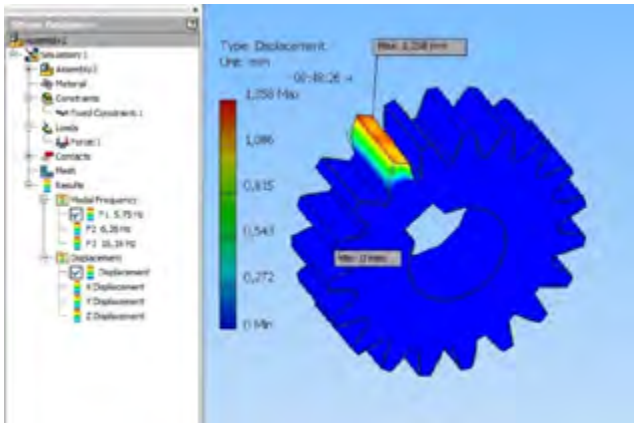
***Фиг. 9*** *Първа собствена форма на задвижваното колело при* ***24,11[Hz]***



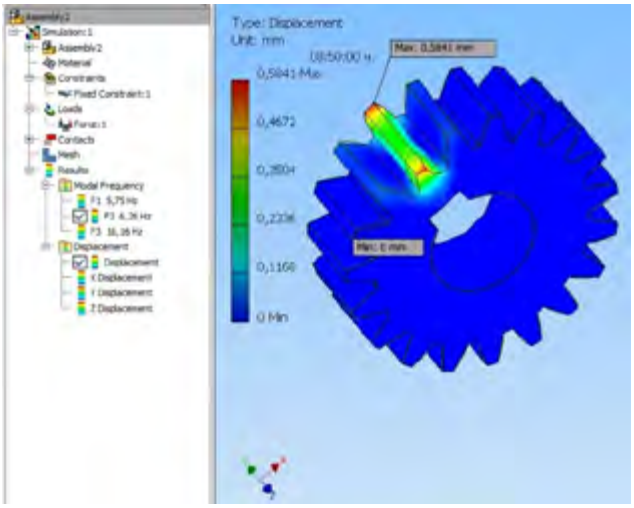
***Фиг. 10*** *Втора собствена форма на задвижваното колело при* ***24,22[Hz]***



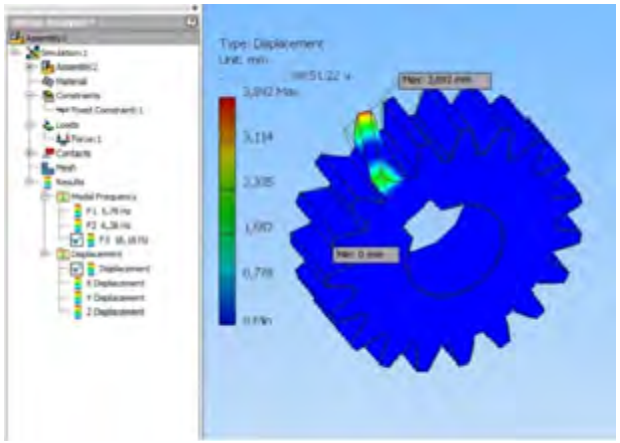
***Фиг. 11*** *Трета собствена форма на задвижваното колело при* ***26,36[Hz]***



***Фиг. 12*** *Първа собствена форма на задвижващото колело при* ***5,75[Hz]***



***Фиг. 13*** *Втора собствена форма на задвижващото колело при* ***6,26[Hz]***



***Фиг. 14*** *Трета собствена форма на задвижващото колело при* ***16,16[Hz]***

### 3. Анализ на получените резултати

От ***фигура 3*** се вижда, че максималните напрежения по Von Mises в задвижваното колело са 253,8 MPa. Те са концентрирани в

болтовите съединения. При разглеждане на ***фигура 4*** се забелязва, че точно в тези съединения се наблюдава и минималния фактор на сигурност FOS = 0,98( ≈ 1). Но максималните еквивалентни премествания се проявяват в зъбите на колелото със стойност 2,41 mm ***(фиг.5)***, което се обяснява с еластичната деформация на същите. Може да се направи заключението, че би могло да се увеличи фактора на сигурност чрез конструктивни изменения. Такива промени ще са приемливи, ако се увеличи например диаметъра на болтовите съединения.

При задвижващото зъбно колело максималните стойности за напрежението са около 54,6 MPa ***(фиг. 6)***. Възникналият фактор на сигурност за същото колело ***(фиг. 7)*** е 3,79 единици. Еквивалентните премествания ***(фиг.8)*** имат пикови стойности достигащи 0,038 mm. Получените резултати за малкото колело са очаквани и са в реални граници.

Резултатите от честотния анализ на задвижваното зъбно колело са визуализирани на ***фиг.9, фиг. 10 и фиг. 11***. Представените първа, втора и трета хармонични честоти на фигурите 9,10 и 11 са $f_1$ = 24,11Hz, $f_2$ = 24,22 Hz и $f_3$ = 26,36 Hz и представляват честоти на огъване на колелото Получените честоти за задвижващото колело са илюстрирани на фигурите ***фиг. 12, фиг. 13 и фиг. 14.*** Те имат следните стойности. $f_1$ = 5, 75 Hz, $f_2$ = 6,26 Hz и $f_3$ = 16,16 Hz.

Имайки в предвид, че честота на въртене на задвижващото колело е 1,06 [Hz], а за задвижваното е 0,18 Hz може да се счита, че няма застрашени от опасност за резонанс по отношение на системата „задвижващо зъбно колело – задвижвано зъбно колело“ елементи. Следователно установените по – горе собствени форми на трептене са от значение при поява на други смущаващи вибрации с честоти близки или равни на собствените.

## ЛИТЕРАТУРА


1. Дивизиев, В., Донев, К.П. (1975), *Въжени линии и кабелни кранове*, Техника, София.
2. Брагин В. Ф. Чобан (1997) *Оценка риска и последствий отказов комплексной системы, конструкций процесоов-Рынок и качество*, Ярославль, кн.1...
3. *Директива 2006/42/ ЕО на Европейския парламент и на съвета, Официален вестник на Европейския съюз*, 17.05.2006.
4. Динев Г. (2004) *Повреди в зъбните колела от колооснi редуктори на електрически локомотиви,* СОФТРЕЙД.
5. Динев Г.(2004.) *Основи на конструкторското документиране на зъбни предавки с цилиндрични зъбни колела*, СОФТРЕЙД.
6. Dimitrov K.( 2012) *Fault Diagnosis in Industrial systems*, PROPELIERS.
7. Tashev M., P. Jordanov(2012) *Engineering analysis with Finine Elements Method, EKS PRS*, Gabrovo.
8. Джаксън П., (1993) *Увод в експертните системи,* Софтех, София.
9. Höhn B., R. (2002) *Modern Gear Calculation*, VDI-International Conference on Gears, March.
10. Радлов К, Ж. Илиев (2011) *Възможности за използването на метода на крайните елементи при проектирането на дисков захранвач за минни и строителни материали*, UNITEH, Gabrovo.
11. Радлов К, Ж. Илиев (2012) *Изследване на напрегнато – деформационно състояние на стрелата на багер „Драглайн“ от лек тип*, „Технологии и практики при подземен добив и минно строителство“, гр.Девин.
12. Lawrence, K.,(2005) *ANSYS Workbench Tutorial, SDC Publications*, Texas
13. Hutov I., Al. Krilchev, Bl. Vladkova, R. Ganev (2014) *Einsatz der Hydrosprengung bei der Zerstorung von Bodenmassen und Schachtenaufbau,* I –st Internationalen Friberger Schachtkolloquium, Freiberg, Germany.
14. Шейретов, Х. (2003) *Ръководство за курсово проектиране на рудничнu транспортни машини*, София



Faculty of Mining Electromechanics
University of Mining and Geology”St.Ivan Rilski”, Sofia
Prof. Boyan Kamenov St.
1700 Sofia
Technical University of Sofia, Kliment Ohridski N8 Boul.
1700 Sofia
BULGARIA
E-mail: halkopirit@mail.bg
E-mail: gdinev@tu-sofia.bg

© International Scientific Conference on Engineering, Technologies and Systems
TECHSYS 2016, Technical University – Sofia, Plovdiv branch
26 – 28 May 2016, Plovdiv, Bulgaria

# АНАЛИЗ НА НАДЛЪЖНИ ПУКНАТИНИ В МНОГОСЛОЙНИ ГРЕДИ НАТОВАРЕНИ НА УСУКВАНЕ

ВИКТОР РИЗОВ

**Резюме:** *Представени са резултати от анализ на надлъжни пукнатини в многослойни греди с кръгло напречно сечение натоварени на усукване. Анализът е основан на линейно-еластичната теория на разрушението. Скоростта на освободената потенциална енергия на деформацията е определена във функция на усукващите моменти в сеченията пред и зад фронта на пукнатината. Полученото решение се отнася за греда с произволен брой слоеве. Дебелината на слоевете може да е различна.Всеки слой може да има различен модул на ъгловите деформации. Освен това, местоположението на пукнатината е произволно. Полученото общо аналитично решение е приложено за изследване на надлъжна пукнатина в двуслойна конзолна греда натоварена на чисто усукване. Резултатите са сравнени с едно известно решение.*

**Ключови думи:** *надлъжна пукнатина, многослойна греда, скорост на освободената потенциална енергия на деформацията, усукване*

# LONGITUDINAL FRACTURE ANALYSIS OF MULTILAYERED BEAMS LOADED IN TORSION

VICTOR RIZOV

**Abstract:** *Results are reported of longitudinal fracture analysis of circular beams loaded in torsion. Linear-elastic fracture mechanics is applied. The strain energy release rate is determined in a function of the torsion moments in beam cross-sections ahead and behind the crack front. The beams considered may have arbitrary number of layers. Each layer may have different thickness and shear modulus. Besides, the longitudinal crack may be located arbitrarily. The common analytical solution derived is applied to investigate a longitudinal crack in a bi-layer cantilever beam loaded in torsion. The results obtained are compared with a known solution.*

**Key words:** *longitudinal crack, multilayered beam, strain energy release rate, torsion*

## 1. Въведение

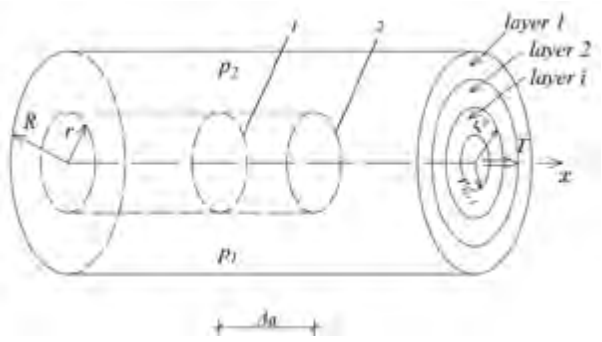
Многослойните гредови конструкции имат редица предимства в сравнение с гредите, изпълнени от традиционни конструктивни материали. Например, многослойните греди имат по-високо отношение якост – собствено тегло. Многослойните гредови конфигурации разкриват възможности за пълноценно използване на якостта на материала, като за целта в по-напрегнатите зони се поставят материали с по-висока якост. Гредовите конструкции от стоманобетон и стомана, усилени с ленти от полимерен композит също предсавляват многослойни системи. Многослойните конструкции се прилагат също за работа в агресивна среда (температурни разлики, химически агенти и др.), като от към страната на агресивното въздействие се прилагат слоеве от материали с подходящи свойства. Сандвич панелите, които благодарение на отличните си топлоизолационни свойства допринасят съществено за подобяване на енергийната ефективност на сградите, също представляват многослойни системи. Всичко това е предпоставка за широкото използване на

Copyright © 2016 by Technical University of Sofia, Plovdiv branch, Bulgaria ISSN Online: 2535-0048

многослойните материали в съвременната инженерната практика [1], [2]. Една от слабостите на многослойните конструкции е появата и нарастването на надлъжни пукнатини между слоевете. Тези пукнатини редуцират значително носимоспособността на конструкциите и могат да предизвикат катастрофално разрушение. В литературата са разгледани предимно надлъжни пукнатини в многослойни греди с правоъгълно напречно сечение, натоварени на специално огъване. Ето защо в настоящата разработка се анализира надлъжна пукнатина в многослойна греда с кръгло напречно сечение, натоварена на усукване (настоящата разработка е мотивирана също от факта, че конструктивни елементи, натоварени на усукване се срещат често в инженерната практика).

## 2. Анализ на скоростта на освободената потенциална енергия на деформацията

Обект на анализ в настоящата теоретична разработка е многослойна греда с кръгло напречно сечение натоварена на чисто усукване. Гредата е изпълнена от произволен брой концентрични слоеве, здраво свързани помежду си (залепени).




***Фиг. 1.*** *Участък от многослойната греда с фронта на пукнтината (1 – положение на фронта преди нарастване на пукнатината, 2 - положение на фронта след нарастване на пукнатината). Пукнатината е цилиндрична повърхнина с радиус r.*

Слоевете могат да имат различна дебелина и да са изпълнени от различни материали, т.е. да имат различни модули на ъгловите деформации. Между слоевете на произволно място има една начална надлъжна пукнатина, която представлява цилиндрична повърхнина (фронтът на пукнатината е окръжност с радиус *r*). Вътрешното рамо на пукнатината има кръгло напречно сечение с радиус *r*. Външното рамо на пукнатината има пръстеновидно напречно сечение с вътрешен радиус *r* и външен радиус *R*. Натоварването на гредата се състои от съсредоточени и/или разпределени усукващи моменти. Вътрешното рамо на пукнатината също може да е натоварено (например със съсредоточен усукващ момент, приложен върху крайното напречно сечение на вътрешното рамо). На фиг. 1 е показан малък участък от гредата с фронта на пукнатината. Основната цел на настоящата разработка е да се определи скоростта на освободената потенциална енергия на деформацията *G*, която се дефинира като

$$G = -\frac{\Delta U}{\Delta A_a}, \tag{1}$$

където

$$\Delta U = U_b - U_a \tag{2}$$

е изменението на потенциалната енергия на деформацията при нарастване на лицето на пукнатината с

$$\Delta A_a = 2\pi r \Delta a\,. \tag{3}$$

Тук $\Delta a$ е нарастването на дължината на пукнатината (фиг. 1). Анализът извършваме по линейно-еластичната теория на разрушението, т.е. приемаме, че гредата има линейно-еластично поведение (връзката между напреженията и деформациите се изразява със закона на Хук). Потенциалната енергия преди нарастване на пукнатината е

$$U_b = 2\pi\Delta a \sum_{i=1}^{i=n} \int_{r_{li+1}}^{r_{li}} \frac{1}{2}\tau_i \gamma r_1 dr_1\,, \tag{4}$$

където $n$ е броят на слоевете в гредата, $r_1$ е текущият радиус $(0 \le r_1 \le R)$, $\tau_i$ е разпределението на тангенциалните напрежения от усукването в разглеждания слой, γ е разпределението на ъгловите деформации, а радиусите $r_{li}$ и $r_{li+1}$ са показани на фиг. 1. Потенциалната енергия във вътрешното рамо след нарастване на пукнатината се дава с формулата

$$U_{a_1} = 2\pi\Delta a \sum_{i=1}^{i=n_1} \int_{r_{li+1}}^{r_{li}} \frac{1}{2}\tau_i \gamma r_1 dr_1\,, \tag{5}$$

където $n_1$ е броят на слоевете във вътрешното рамо на пукнатината. За външното рамо формулата е подобна, т.е.

$$U_{a_2} = 2\pi\Delta a \sum_{i=1}^{i=n_2} \int_{r_{li+1}}^{r_{li}} \frac{1}{2}\tau_i \gamma r_1 dr_1 , \quad (6)$$

където $n_2$ е броят на слоевете във външното рамо. Потенциалната енергия в раменатa на пукнатината след нарастването е

$$U_a = U_{a_1} + U_{a_2} . \quad (7)$$

След заместване на (2), (3), (4), (5), (6) и (7) в (1) получаваме

$$G = \frac{1}{r}\Big( \sum_{i=1}^{i=n_1} \int_{r_{li+1}}^{r_{li}} \frac{1}{2}\tau_i \gamma r_1 dr_1 + \sum_{i=1}^{i=n_2} \int_{r_{li+1}}^{r_{li}} \frac{1}{2}\tau_i \gamma r_1 dr_1 - \sum_{i=1}^{i=n} \int_{r_{li+1}}^{r_{li}} \frac{1}{2}\tau_i \lambda r_1 dr_1 \Big). \quad (8)$$

Тангенциалните напрежения в слоевете в ненапуканата част на гредата, т.е. преди нарастването на пукнатината, които участват в (4) се намират по закона на Хук

$$\tau_i = G_i' \gamma = G_i' r_1 \frac{\gamma_c}{R}, \quad (9)$$

където $\gamma_c$ е ъгловата деформация по периферията на напречното сечение, $G_i'$ е модулът на ъгловите деформации в текущия слой. В (9) е взето предвид, че ъгловите деформации са разпределени линейно по радиуса на напречното сечение на гредата. За определяне на $\gamma_c$ се използва условието за равновесие на напречното сечение на гредата:

$$T = 2\pi \sum_{i=1}^{i=n} \int_{r_{li+1}}^{r_{li}} G_i' r_1 \frac{\gamma_c}{R} r_1^2 dr_1 , \quad (10)$$

където $T$ е усукващият момент в напречното сечение пред фронта на пукнатината (фиг. 1). Ъгловата деформация по периферията на външното рамо на пукнатината се определя от следното условие за равновесие:

$$T_2 = 2\pi \sum_{i=1}^{i=n_2} \int_{r_{li+1}}^{r_{li}} G_i' r_1 \frac{\gamma_c}{R} r_1^2 dr_1 , \quad (11)$$

където $T_2$ е усукващият момент в напречното сечение на външното рамо зад фронта на пукнатината, $n_2$ е броят на слоевете във външното рамо на пукнатината. Уравнение (10) се прилага и за определяне на ъгловата деформация по периферията на вътрешното рамо на пукнатината. За целта (10) се записва по следния начин:

$$T_1 = 2\pi \sum_{i=1}^{i=n_1} \int_{r_{li+1}}^{r_{li}} G_i' r_1 \frac{\gamma_c}{R} r_1^2 dr_1 , \quad (12)$$

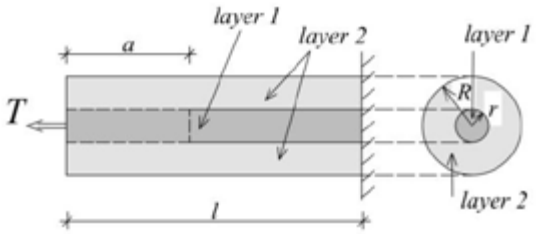
където $T_1$ е усукващият момент във вътрешното рамо зад фронта на пукнатината, $n_1$ е броят на слоевете във вътрешното рамо. Моментът $T_1$ се получава от равновесието на усукващите моменти в сеченията пред и зад фронта на пукнатината:

$$T_1 = T - T_2 . \quad (13)$$

Може да се обобщи, че формула (8) изразява търсеното общо решение на задачата за определяне на скоростта на освободената потенциална енергия на деформацията за надлъжна пукнатина в многослойна линейно-еластична греда с кръгло напречно сечение натоварена на чисто усукване. Скоростта на освободената потенциална енергия на деформацията фактически е изразена във функция на усукващите моменти в напречните сечения пред и зад фронта на пукнатината. Това значително улеснява практическото приложение на полученото в настоящата разработка общо решение.

За проверка на полученото решение е извършен анализ на скоростта на освободената потенциална енергия на деформацията за надлъжна пукнатина в двуслойна конзолна греда и е направено сравнение с известно решение [3]. Гредата е запъната в десния си край. Натоварването представлява съсредоточен момент $T$ приложен върху крайното ляво сечение на вътрешното рамо на пукнатината. Схема на гредата е показана на фиг. 2. Гредата е изпълнена от два здраво свързани (залепени) концентрични слоя. Вътрешният слой *1* има кръгло напречно сечение с радиус *r*. Външният слой *2* има пръстеновидно напречно сечение.

Между двата слоя има надлъжна пукнатина с дължина *a*. Външното рамо на пукнатината е ненатоварено. За гредата показана на фиг. 2 имаме $n_1 = 1$, $n_2 = 1$, $n = 2$, $T_1 = T$, $T_2 = 0$. Модулите на ъгловите деформации са съответно $G_1^{'}$ и $G_2^{'}$ във вътрешния и външния слой на гредата.




***Фиг. 2.*** *Двуслойна конзолна греда с надлъжна пукнатина между двата слоя (пукнатината е цилиндрична повърхнина с радиус r и дължина a)*

За определяне на скоростта на освободената потенциална енергия на деформацията прилагаме общото решение формула (8). След извършване на необходимите преобразования получаваме следния окончателен резултат:

$$G = \frac{T}{2\pi^2 r^5} \frac{G_2^{'}\left(R^4 - r^4\right)}{G_1^{'}\left(G_1^{'} - G_2^{'}\right)r^4 + G_1^{'}G_2^{'}R^4}. \quad (14)$$

Фактът, че формула (14) съвпада с решението за скоростта на освободената потенциална енергия на деформацията, получено в [3] представлява провека на анализа, разработен в настоящия доклад.

### 3. Заключение

В настоящата разработка е получено общо аналитично решение в затворена форма на задачата за определяне на скоростта на освободената потенциална енергия на деформацията за надлъжна пукнатина в многослойна греда с кръгло напречно сечение, натоварена на чисто усукване. Гредата е изпълнена от произволен брой здраво свързани концентрични слоеве, които имат различна дебелина и модули на ъгловите деформации, т.е. слоевете са от различни материали. Надлъжната пукнатина представлява цилиндрична повърхнина (фронтът на пукнатината е окръжност) разположена между два произволни слоя. Анализът е извършен по линейно-еластичната теория на разрушението, която се основава на предпоставката за линейно-еластично поведение на материала. Скоростта на освободената потенциална енергия на деформацията е получена във функция на усукващите моменти в напречните сечения на гредата пред и зад фронта на пукнатината, което значително улеснява практическото приложение на полученото аналитично решение (за да определим скоростта на освободената потенциална енергия на деформацията е достатъчно да познаваме броя, дебелината и модулите на ъгловите деформации на слоевете, местоположението на пукнатината, а също и усукващите моменти). За проверка на полученото решение е направено сравнение с известни резултати, публикувани в специализираната литература. Разгледана е надлъжна пукнатина в двуслойна конзолна греда натоварена с усукващ момент, приложен в крайното сечение на вътрешното рамо. Пълното съответствие между двете решения представлява проверка на полученото в настоящата разработка общо решение.

### ЛИТЕРАТУРА

1. Марков, И., Динев, Д. (2005-2006). Анализ на краевата зона на греда, усилена със залепена лента от фибро-армирани полимери, *Годишник на УАСГ*, том XLII, св. VI.
2. Ivanov, Ya. and Stoyanov, V. (2012) High Technologies and New Construction Materials in Civil Engineering, In: Education, Science, Innovations (*Proc. Ist Int. Conf. of the European Polytechnical University, June 9-10, 2011, Pernik, Bulgaria*), European Polytechnical University, pp. 161-169.
3. Rizov, V., Mladensky, A. (2012) Crack investigation in bilayered composite beam of circular cross-section. *Journal of Materials Science and Technology*, 20(1), 72-83.

**Благодарности:** Настоящата разработка е финансирана от ЦНИП при УАСГ-София (договор БН-189/16).

Адрес: Кат. Техническа механика, Университет по Архитектура, Строителство и Геодезия, 1 Хр. Смирненски бул., 1046-София, E-mail: V_RIZOV_FHE@UACG.BG

© International Scientific Conference on Engineering, Technologies and Systems
TECHSYS 2016, Technical University – Sofia, Plovdiv branch
26 – 28 May 2016, Plovdiv, Bulgaria

# ИЗСЛЕДВАНЕ НА НАДЛЪЖНА ПУКНАТИНА В МНОГОСЛОЙНА ГРЕДА ПРИ НЕЛИНЕЙНО ПОВЕДЕНИЕ НА МАТЕРИАЛА

ВИКТОР РИЗОВ

**Резюме:** *Извършен е теоретичен анализ на надлъжна пукнатина в многослойна греда с отчитане на нелинейното поведение на материала. Гредата има правоъгълно напречно сечение и е натоварена на огъване. Механичното поведение на гредата се описва със степенна конститутивна зависимост между напреженията и деформациите. Гредата е изпълнена от здраво свързани надлъжни хоризонтални слоеве с различна дебелина и материални константи. Надлъжната пукнатина е разположена произволно по височината на гредата. За изследване на пукнатината е приложен интегралът J. Въз основа на класическата гредова теория е получено аналитично решение на интеграла J. Резултатите от проведеното изследване могат да се прилагат за оптимизиране на структурата на многослойната греда с огледа осигуряване срещу поява на надлъжни пукнатини.*

**Ключови думи:** *надлъжна пукнатина, нелинейно поведение на материала, многослойна греда*

# LONGITUDINAL FRACTURE ANALYSIS OF A MULTILAYERED BEAM WITH NON-LINEAR MATERIAL BEHAVIOR

VICTOR RIZOV

**Abstract:** *A theoretical analysis of a longitudinal crack in a multilayered beam with taking into account the non-linear material behavior is performed. The beam has a rectangular cross-section and is loaded in bending. The beam mechanical behavior is described with a power-law constitutive stress-strain relation. The beam has horizontal layers with different thickness and material constants. The longitudinal crack is located arbitrarily along the beam height. The fracture analysis is carried-out by applying the J-integral approach. By using the classical beam theory, an analytical solution of the J-integral is derived. The results obtained can be applied for optimization of the multilayered beam structure with respect to the fracture performance.*

**Key words:** *longitudinal crack, non-linear material behavior, multilayered beam*

## 1. Въведение

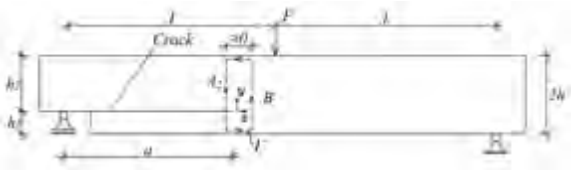
Една от перспективните насоки за развитие на инженерните конструкции и съоръжения е прилагането на многослойни гредови системи [1, 2, 3]. Използването на слоеве от различни материали разкрива много добри възможности за оптимизация с оглед намаляване на собственото тегло на конструкциите. Един от факторите, възпрепятстващи по-широкото навлизане на многослойните системи в съвременната инженерна практика е високият риск от поява и нарастване на надлъжни пукнатини между слоевете. Тези пукнатини рязко влошават поведението на конструкциите и могат в някои случаи да предизвикат катастрофално разрушение. В специализираната литература са изследвани надлъжни пукнатини в многослойни греди предимно въз основа на линейно-еластичната теория на разрушението, която предполага валидност на закона на Хук [1]. В действителност обаче материалите в много

Copyright © 2016 by Technical University of Sofia, Plovdiv branch, Bulgaria ISSN Online: 2535-0048

случаи имат нелинейно механично поведение. Ето защо основната цел на настоящата разработка е да се извърши изследване на надлъжна пукнатина в многослойна греда с отчитане на физическата нелинейност.

## 2. Нелинеен анализ с интеграла *J*

Гредата, показана на фиг. 1, е изпълнена от здраво свързани надлъжни хоризонтални слоеве, които имат различна дебелина.




***Фиг. 1.*** *Геометрия и натоварване на многослойна греда с надлъжна пукнатина*

Натоварването се състои от една съсредоточена вертикална сила *F*, приложена в средата на отвора. Гредата има правоъгълно напречно сечение с основа *b* и височина 2*h*. В гредата има надлъжна пукнатина с дължина *a*. Дебелината на долното и горното рамо на пукнатината е съответно $h_1$ и $h_2$. Механичното поведение на гредата се описва със следния степенен закон:

$$\sigma_i = H_{1i}\varepsilon_i^{n_{1i}}, \quad i = 1, 2, ..., n, \tag{1}$$

където $\sigma_i$ и $\varepsilon_i$ са разпределенията на напреженията и деформациите в поредния слой на гредата, $H_{1i}$ и $n_{1i}$ са материални константи, $n$ е броят на слоевете.

За изследване на пукнатината прилагаме интеграла *J* [4]:

$$J = \int_{\Gamma}\left[u_0\cos\alpha - \left(p_x\frac{\partial u}{\partial x} + p_y\frac{\partial v}{\partial x}\right)\right]ds, \tag{2}$$

където $u_0$ е интензивността на потенциалната енергия на деформацията, $\alpha$ е ъгълът между външната нормала към контура на интегриране и оста $x$, $p_x$ и $p_y$ са компонентите на напреженията по контура на интегриране $\Gamma$, $u$ и $v$ са компонентите на преместванията по оси $x$ и $y$, а $ds$ е диференциален елемент от контура $\Gamma$. Необходимо е да се уточни, че настоящият анализ е валиден за нелинейно-еластично поведение на материала, но може да се прилага и за еласто-пластично поведение при монотонно натоварване, т.е. когато компонентите на външното натоварване нарастват пропорционално на един параметър. Контурът на интегриране $\Gamma$ се състои от напречните сечения на гредата непосредствено пред и зад върха на пукнатината (фиг. 1). Долното рамо на пукнатината е ненапрегнато, следователно стойността на интеграла там е нула. Първо извършваме интегриране в участък $A_2$, който съвпада с напречното сечение на горното рамо на пукнатината. Компонентите на интеграла в поредния слой на горното записваме по следния начин:

$$p_{xi} = -\sigma_i = -H_{1i}\varepsilon^{n_{1i}},\ p_{yi} = 0,\ ds = dz_2,\ \cos\alpha = -1, \tag{3}$$

където ос $z_2$ започва от центъра на напречното сечение и е насочена надолу. Интеграла *J* в участък $A_2$ записваме като

$$J_{A_2} = \sum_{i=1}^{n_U}\int_{z_{2i}}^{z_{2i+1}}\left[u_{0i}\cos\alpha - \left(p_{xi}\frac{\partial u}{\partial x} + p_{yi}\frac{\partial v}{\partial x}\right)\right]ds,$$

където $n_U$ е броят на слоевете в горното рамо на пукнатината, $z_{2i}$ и $z_{2i+1}$ са координатите на горния и долния ръб на поредния слой. Интензивността на потенциалната енергия на деформацията в поредния слой получаваме по формулата

$$u_{0i} = \int_0^{\varepsilon} H_{1i}\varepsilon^{n_{1i}}d\varepsilon, \tag{4}$$

където деформацията се записва по класическата гредова теория като

$$\varepsilon = \kappa_2\left(z_2 - z_{2n_2}\right). \tag{5}$$

Тук $\kappa_2$ и $z_{2n_2}$ са кривината и координатата на нулевата линия на напречното сечение на горното рамо на пукнатината. След заместване на (5) в (4) и интегриране, получаваме

$$u_{0i} = \frac{H_{1i}\kappa_2^{n_{1i}+1}\left(z_2 - z_{2n_2}\right)^{n_{1i}+1}}{n_{1i}+1}. \tag{6}$$

Частната производна $\partial u/\partial x$ в (2) записваме като

$$\frac{\partial u}{\partial x} = \varepsilon = \kappa_2\left(z_2 - z_{2n_2}\right). \tag{7}$$

Заместваме (3), (6) и (7) в $J_{A_2}$ и интегрираме:

$$J_{A_2}=\sum_{i=1}^{n_U}\frac{H_{1i}n_{1i}}{(n_{1i}+1)(n_{1i}+2)}\kappa_2^{n_{1i}+1}\cdot \\ \cdot\left[\left(z_{2i+1}-z_{2n_2}\right)^{n_{1i}+2}-\left(z_{2i}-z_{2n_2}\right)^{n_{1i}+2}\right] \quad (8)$$

За определяне на $\kappa_2$ и $z_{2n_2}$ тук се използват следните условия за равновесие на напречното сечение на горното рамо на пукнатината:

$$N=\sum_{i=1}^{n_U}\int_{z_{2i}}^{z_{2i+1}}\sigma_i b dz_2\ ,\ M=\sum_{i=1}^{n_U}\int_{z_{2i}}^{z_{2i+1}}\sigma_i b z_2 dz_2\ , \quad (9)$$

където $N=0$ и $M=Fa/2$ са съответно надлъжната сила и огъващият момент в сечение $A_2$ (фиг. 1). След заместване на (1) и (5) в (9), получаваме следните изрази за *N* и *M*:

$$N=b\sum_{i=1}^{n_U}\left\{\frac{H_{1i}\kappa_2^{n_{1i}}}{n_{1i}+1}\left[(z_{2i+1}-z_{2n_2})^{n_{1i}+1}-\left(z_{2i}-z_{2n_2}\right)^{n_{1i}+1}\right]\right\}$$

$$M=b\sum_{i=1}^{n_U}\left(\psi_i+\rho_i\right),$$

където

$$\psi_i=\frac{H_{1i}\kappa_2^{n_{1i}}}{n_{1i}+2}\left[\left(z_{2i+1}-z_{2n_2}\right)^{n_{1i}+2}-\left(z_{2i}-z_{2n_2}\right)^{n_{1i}+2}\right]$$

$$\rho_i=\frac{H_{1i}\kappa_2^{n_{1i}}z_{2n_2}}{n_{1i}+1}\left[\left(z_{2i+1}-z_{2n_2}\right)^{n_{1i}+1}-\left(z_{2i}-z_{2n_2}\right)^{n_{1i}+1}\right].$$

Така получените изрази за *N* и *M* образуват система от две нелинейни алгебрични уравнения с неизвестни $\kappa_2$ и $z_{2n_2}$. Тази система се решава с помощта на компютърната програма MatLab за конкретни размери на гредата, големина на натоварването, брой и дебелини на слоевете, стойности на материалните константи в конститутивната зависимост (1).

Следващата стъпка е да се извърши интегриране в участък *B* на контура (фиг. 1). Този участък съвпада с напречното сечение на гредата пред върха на пукнатината. Компонентите на интеграла *J* записваме по следния начин:

$$p_{xi}=\sigma_i=H_{1i}\varepsilon^{n_{1i}}\ ,\ p_{yi}=0\ , \\ ds=dz_3\ ,\cos\alpha=1\ , \quad (10)$$

където ос $z_3$ започва от центъра на сечние *B* и е насочена надолу. Частната производна $\partial u/\partial x$ определяме като

$$\frac{\partial u}{\partial x}=\varepsilon=\kappa_3\left(z_3-z_{3n_3}\right)\ , \quad (11)$$

където $\kappa_3$ и $z_{3n_3}$ са кривината и координатата на нулевата линия на напречно сечение *B* на гредата. Интензивността на потенциалната енергия на деформацията записваме като

$$u_{0i}=\frac{H_{1i}\kappa_3^{n_{1i}+1}\left(z_3-z_{3n_3}\right)^{n_{1i}+1}}{n_{1i}+1}\ . \quad (12)$$

За определяне на $\kappa_3$ и $z_{3n_3}$ се прилагат условията равновесние на напречно сечение *B* на гредата

$$N=\sum_{i=1}^{n}\int_{z_{3i}}^{z_{3i+1}}\sigma_i b dz_3\ , \quad (13)$$

$$M=\sum_{i=1}^{n}\int_{z_{3i}}^{z_{3i+1}}\sigma_i b z_3 dz_3\ . \quad (14)$$

След интегриране на (13) и (14), получените уравнения образуват нелинейна алгебрична система за намиране на $\kappa_3$ и $z_{3n_3}$. За решавне на тази система се прилага програмата MatLab при конкретни размери, натоварване и стойности на материалните константи в конститутивната зависимост.

Формули (10), (11) и (12) се заместват в интеграла и се извършва интегриране. Резултатът е

$$J_B=-\sum_{i=1}^{n}\frac{H_{1i}n_{1i}}{(n_{1i}+1)(n_{1i}+2)}\kappa_3^{n_{1i}+1}\cdot \\ \cdot\left[\left(z_{3i+1}-z_{3n_3}\right)^{n_{1i}+2}-\left(z_{3i}-z_{3n_3}\right)^{n_{1i}+2}\right] \quad (15)$$

Окончателното нелинейно решение на интеграла *J* получаваме чрез сумиране на (8) и (15), т.е.

$$J=\sum_{i=1}^{n_U}\frac{H_{1i}n_{1i}}{(n_{1i}+1)(n_{1i}+2)}\kappa_2^{n_{1i}+1}\cdot \\ \cdot\left[\left(z_{2i+1}-z_{2n_2}\right)^{n_{1i}+2}-\left(z_{2i}-z_{2n_2}\right)^{n_{1i}+2}\right]- \\ -\sum_{i=1}^{n}\frac{H_{1i}n_{1i}}{(n_{1i}+1)(n_{1i}+2)}\kappa_3^{n_{1i}+1}\cdot \\ \cdot\left[\left(z_{3i+1}-z_{3n_3}\right)^{n_{1i}+2}-\left(z_{3i}-z_{3n_3}\right)^{n_{1i}+2}\right] \quad (16)$$

Така полученото нелинейно решение е проверено по следния начин. Известно е, че при линейно-еластично поведение на материала стойността на интеграла *J* съвпада със скоростта на освободената потенциална енергия на деформацията. Именно това положение е използвано за проверка на (16). Ясно е, че при $n_{1i}=1$ нелинейният конститутивен закон (1) се трансформира в закона на Хук. Ето защо при полагане на $n_{1i}=1$ в нелинейното решение на интеграла *J* би трябвало да получим формулата за скоростта на освободената потенциална енергия на деформацията в разглежданата греда (фиг. 1). За да направим проверката заместваме $n_{1i}=1$, $h_1=h_2=h$ и $n_U=n=1$ в (15). В резултат на това получаваме

$$J=\frac{21F^2a^2}{16Eh^3b^2}, \qquad (17)$$

където *E* е модулът на еластичност. Фактът, че (17) съвпада с формулата за скоростта на освободената потенциална енергия на деформацията в линейно-еластична хомогенна греда, когато рамената на пукнатината имат еднаква височина [1] представлява една проверка на (17).

### 3. Заключение

Представени са резултати от теоретичен анализ на надлъжна пукнатина в многослойна греда с отчитане на нелинейното поведение на материала. Гредата е с правоъгълно напречно сечение и е натоварена на огъване с една съсредоточена вертикална сила, приложена в средата на отвора. Гредата е изпълнена от здраво свързани (залепени) хоризонтални надлъжни слоеве с различна дебелина. В гредата има надлъжна пукнатина, произволно разположена по височината на гредата, т.е. рамената на пукнатината имат различна дебелина. Механичното поведение на гредата се описва чрез степенна конститутивна зависимост между напреженията и деформациите. Материалните константи в конститутивната зависимост имат различни стойности във всеки слой на гредата. Пукнатината е изследвана с помощта на интеграла *J*. Получено е аналитично решение в затворена форма, което се отличава с висока степен на общност (решението е валидно за надлъжна пукнатина с произволно разположение, броят на слоевете на гредата също е произволен). За проверка е направено сравнение с известно решение, публикувано в специализираната литература. Полученото тук аналитично решение е много удобно за извършване на параметрични изследвания. Резултатите от тези изследвания могат да се използват за оптимизиране на структурата на многослойните греди с оглед осигуряване срещу поява на пукнатини при нелинейно поведение на материала. Също така, полученото решение може да се прилага при проверка за нарастване на съществуваща пукнатина в многослойна греда. За целта с помощта на решението трябва да се изчисли стойността на интеграла *J* за дадена големина на външното натоварване и да се сравни с граничната стойност за изследвния материал. Ако изчислената стойност е по-малка от граничната, многослойната конструкция е осигурена срещу нарастване на пукнатината. Настоящата разработка допринася също и за развитието на нелинейната механика на пукнатините в многослойни конструктивни системи.

### ЛИТЕРАТУРА


1. Hutchinson, W., Suo, Z. (1992). Mixed mode cracking in layered materials. *Advances in Applied Mechanic*, 64, 804–810.
2. Марков, И., Динев, Д. (2005-2006). Анализ на краевата зона на греда, усилена със залепена лента от фибро-армирани полимери, *Годишник на УАСГ*, том XLII, св. VI.
3. Ivanov, Ya. and Stoyanov, V. (2012). High Technologies and New Construction Materials in Civil Engineering, In: Education, Science, Innovations (*Proc. Ist Int. Conf. of the European Polytechnical University*, *June 9-10, 2011, Pernik, Bulgaria*), European Polytechnical University, 161-169.
4. Broek, D. (1986). *Elementary engineering fracture mechanics*, Springer.


**Благодарности:** Настоящата разработка е финансирана от ЦНИП при УАСГ-София (договор БН-189/16).

Адрес: Кат. Техническа механика,
Университет по Архитектура,
Строителство и Геодезия, 1 Хр.
Смирненски бул., 1046-София.
E-mail: V_RIZOV_FHE@UACG.BG

© International Scientific Conference on Engineering, Technologies and Systems
TECHSYS 2016, Technical University – Sofia, Plovdiv branch
26 – 28 May 2016, Plovdiv, Bulgaria

# КИНЕМАТИЧЕН АНАЛИЗ НА ЛОСТОВО-ЗЪБЕН ПРЕОБРАЗУВАТЕЛ НА ДВИЖЕНИЕ

ГЕОРГИ УЧКУНОВ, АСЕН ВЕРГОВ

**Резюме:** *В настоящата статия е представен кинематичен анализ на един вид лостово-зъбна предавка с успоредни геометрични оси на валовете. Под лостово-зъбна предавка в случая се разбира предавка в чиято структура влизат лостови и зъбни механизми. Кинематичният анализ е извършен аналитично. За целта са използвани елементи от аналитичната геометрия и известни зависимости от механиката. Резултатите от този анализ са зависимости и диаграми, описващи моментната стойност на изходящите кинематични параметри.*

**Ключови думи:** *аналитичната геометрия, лостови механизми, скорост, зъбен механизъм*

# KINEMATIC ANALYSIS OF LEVER-GEAR MOVEMENT CONVERTOR

GEORGI UCHKUNOV, ASEN VERGOV

**Abstract:** *This article describes kinematic analysis of a kind of lever-gear transmission with parallel geometric axes of the shafts. In this case lever-gear transmission means a transmission in which lever and gear mechanisms are included. Kinematic analysis has been made according to analytic methods. In order to do that, elements of the analytic geometry and known dependencies of the mechanics are used. The results of this analysis are represented as dependencies and diagrams describing the current values of the kinematic parameter outputs.*

**Key words:** *analytic geometry, linkages, speed, gear teeth*

## 1. Въведение

Механичните предавки са предназначени за предаване енергия на неголеми разстояния – [1]. Числените стойности на ъгловите скорости на намиращите приложение силови машини (двигатели) и работните органи на машините, като колела на транспортни машини, валци на прокатни станове, гребни винтове, винтове на летателни средства, водещи валове на конвейери и др., по правило не са равни. Необходимо е съгласуване между скоростта и въртящия момент на силовата и работната машина. За тази цел широко приложение са намерили различни видове механични предавки, от които най-разпространени са зъбните.

Предавка е устройство, предаващо енергия от двигател към работна машина, като обикновено се изменят скоростта, силата и въртящия момент или се променят характерът, законът и посоката на движението – [2].

Основни параметри за предавките са:

- предавана мощност;
- предавателно отношение (ъглова скорост на задвижващия (входящия) и задвижвания (изходящия) вал);
- коефициент на полезно действие.



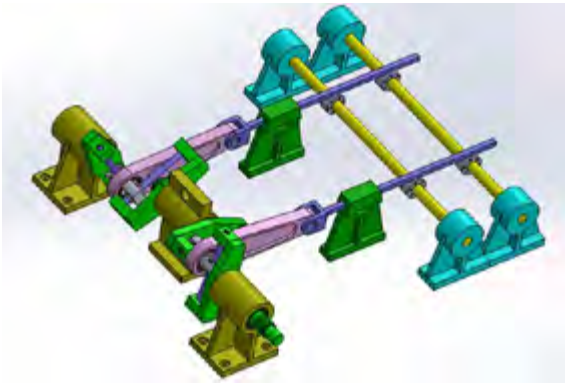

***Фиг. 1.*** *Видове предавки*

Copyright © 2016 by Technical University of Sofia, Plovdiv branch, Bulgaria ISSN Online: 2535-0048

В [1,2] според вида на използвания принцип предавките се разделят на: механични (триеща предавка, зъбна предавка, ремъчна предавка, верижна предавка, лостова предавка), хидравлични, пневматични, електрически и комбинирани – фиг. 1.

При преобразуване на въртеливо движение лостовите механични предавки са намерили ограничено приложение. Срещат се варианти на комбинирани лостово-зъбни и лостово гърбични предавки.

На фиг.2 е показан модел на една комбинирана лостово зъбна предавка с успоредни геометрични оси на входящия и изходящия валове.



***Фиг. 2.*** *Модел на лостово-зъбна предавка*

Определянето на положенията, скоростите и ускоренията на характерни точки от даден механизъм при известен закон на движение на водещото звено е често срещана инженерна задача.

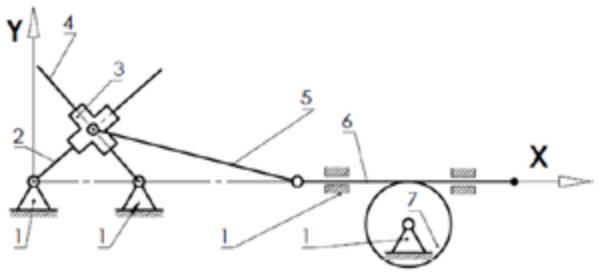
При различните зъбни и лостови механизми преместванията, скоростите, ускоренията и законите на тяхното изменение могат да бъдат определени с използване методите на аналитичната геометрия [3].

Целта на настоящата разработка е аналитично да се определи моментната стойност на изходящите кинематични параметри (скорост и ускорения).

## 2. Постановка на задачата

Апроксимацията (с възможност за приложение в среда на CAD/CAE система) на изследвания лостово-зъбен механизъм е показана на фиг. 3, която по своята същност е кинематична схема. Апроксимацията се заключава в намаляване броя на „секциите“ до една, като на фигурата елементите на предавката са със зададени конкретни размери.

На фиг.3 с 1 са обозначени стойките, с 2 и 4 съответно ляв и десен лост, с 3 кръстата кулиса, с 5 мотовилка, с 6 зъбна рейка, с 7 цилиндрично зъбно колело.




***Фиг. 3.*** *Кинематична схема*

За апроксимирания зъбно-лостов механизъм ще бъдат определени аналитично:

- моментната стойност на координатата X на точка B;
- моментната стойност на изходящата ъглова скорост;
- скоростта на звеното 6 по ос X .
- моментната стойност на предавателното отношение.

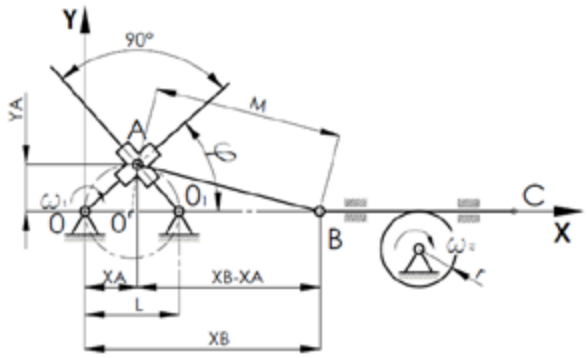
## 3. Аналитично решение на задачата

За решението на задачата ще използваме методите на аналитичната геометрия. За целта е направена помощна геометрична схема, показана на фиг.4, която е свързана с едно произволно положение на апроксимирания механизъм. За решението на задачата е използван алгоритъмът от [4] и [5], за решаване на аналогична задача.

В сила са следните зависимости:

$$YA = OA.\sin(\varphi) \qquad (1)$$

$$OA = L.\cos\varphi \qquad (2)$$




***Фиг. 4.*** *Помощна геометрична схема*

Звеното 6, показано на фиг.3, извършва транслационно движение. Следователно скоростите на точки B и C, като точки от звено 6 са еднакви. Ще се приведе един вариант за зависимости при определяне на кинематични параметри на точки от това звено.

В зависимост (1) се замества OA от израза (2) и се получава моментната стойност на YA във функция от ъгъл φ (зависимост (3)).

$$YA = L.\sin(\varphi).\cos(\varphi) = \frac{L.\sin(2\varphi)}{2} \qquad (3)$$

От друга страна е в сила зависимост (4).

$$XA = OA.\cos(\varphi) = L(\cos(\varphi))^2 \qquad (4)$$

От триъгълника определен с отсечките (YA), (XB-XA) и (M), който е правоъгълен, следва зависимост (5).

$$(XB - XA)^2 + YA^2 = M^2 \qquad (5)$$

От зависимост (5) се определя XB.

$$XB = \sqrt{M^2 - YA^2} + XA \qquad (6)$$

Заместват се в израз (6) отсечките XA и YA от изразите (3) и (4). Получава се зависимостта XB(φ) – зависимост (7).

$$XB(\varphi) = \sqrt{M^2 - \left(\frac{L\sin 2\varphi}{2}\right)^2} + L\cos^2\varphi \qquad (7)$$

Диференцираме зависимостта (7), спрямо променливата φ и получаваме зависимостта (8), която е аналог на скоростта на точка B.

$$VB(\varphi) = \frac{dXB(\varphi)}{d\varphi} = \\ = -\frac{L^2\sin 4\varphi}{4\sqrt{M^2 - \frac{L^2\sin^2 4\varphi}{4}}} - L\sin 2\varphi \qquad (8)$$

Едновременно умножаваме и разделяме лявата част на (8) с dt и получаваме израза (9).

$$\frac{dXB}{dt}.\frac{dt}{d\varphi} = VB(\varphi) \qquad (9)$$

След математическа обработка получаваме зависимост (10), която ни дава възможност да определим моментната скорост на звеното 6.

$$V_B = V_C = VB(\varphi).\omega_1 \qquad (10)$$

Ъгловата скорост на звеното 7 може да бъде определена с помощта на зависимост (11). Определяме и моментната стойност на предавателното отношение i(φ).

$$r.\omega_2 = V_B \qquad (11)$$

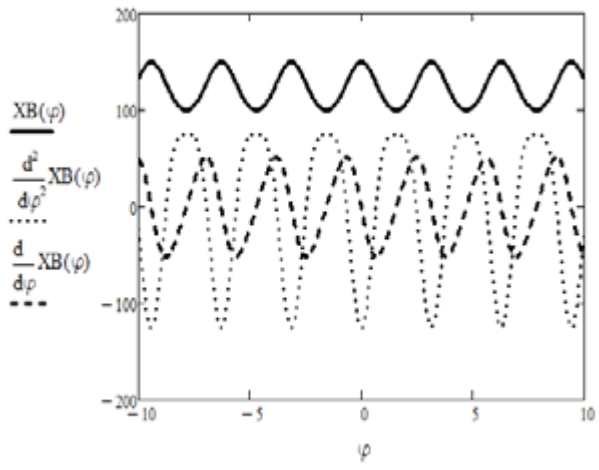
$$i(\varphi) = \frac{\omega_2}{\omega_1} \qquad (12)$$

Изведената зависимост (12) ни дава представа за изменението на предавателното отношение в зависимост от положението на водещото звено. Вижда се, че предавателното число е променлива величина.

По аналогичен начин е изведена зависимост за ъглово ускорение, която не е показана в настоящата работа.

В среда на Mathcad е изследван един вариант на разглежданата предавка. Зададени са следните стойности: r=20 mm; L=50 mm; M=100 mm; r=20 mm; ω1=3.14 rad.s-1 (30 RPM). По зададени зависимости софтуерът определя и визуализира в интервала на изменение на ъгъл φ, линейната скорост и ускорение на звено 6. На фиг.5 са показани получените графики за XB(φ), dXB/dφ и $d^2XB/d\varphi^2$, чрез които може да се придобие представа за изменението на преместването, скоростта и ускорението на звено 6. Генерирани са други диаграми, които не са показани в настоящата работа.

За същата предавка има възможност за изследване влиянието на промяната на параметъра L върху предавателното отношение.




***Фиг. 5.*** *Графична визуализация в среда на Mathcad*

**4. Резултати**

Разработен е геометричен модел на апроксимиран лостово-зъбен механизъм.

Получени са аналитични зависимости, позволяващи изследване на изходящата ъглова скорост, ъглово ускорение и предавателно отношение. Предавателното отношение е променлива величина.

Изменението на междуосовото разстояние L води до промяна на предавателното отношение.

Получените аналитични резултати са с графична визуализация и могат да бъдат сравнявани посредством симулация на една 3D апроксимация на пространствен зъбен механизъм в среда на CAD/CAE система.

Научните изследвания, резултатите от които са представени в настоящата публикация, са финансирани от Вътрешния конкурс на ТУ-София-2016 (Договор №162ПД0008-24). Авторите изказват своята благодарност на НИС при Технически университет – София.

**ЛИТЕРАТУРА**

1. Кудрявцев, В. Н., Державец, Ю. А., Глухарев Е. Г. (1971). *Конструкции и расчет зубчатых редукторов*. Справочное пособие под ред. В. Н. Кудрявцева. М.-Л., Машиностроение.
2. Арнаудов, К. Б., Димитров, И.П., Йорданов, П. В., Лефтеров, Л.С. (1980). *Машинни елементи*. София, Техника.
3. Артоболевский, И. И. (1981). *Механизмы в современной технике*, *том V – Кулачковые и фрикционные механизмы с гибкими звеньями*, Москва „Наука”.
4. Ташев, М. Д. (2013). Кинематичен анализ на зъбна предавка от водни съоръжения. *XXII МНТК „АДП-2013” Созопол.*
5. Ташев М. Д. (2014). Кинематичен анализ на зъбна предавка от водни съоръжения. *XXIII МНТК „АДП-2014” Созопол.*

Контакти
4000 Пловдив, ул. Ц. Дюстабанов №25
ТУ – София, филиал Пловдив
Катедра „Машиностроене и уредостроене”
E-mail: nablud47@abv.bg
E-mail: george_7@abv.bg

© International Scientific Conference on Engineering, Technologies and Systems
TECHSYS 2016, Technical University – Sofia, Plovdiv branch
26 – 28 May 2016, Plovdiv, Bulgaria

# ЕКСПЕРИМЕНТАЛНО ИЗСЛЕДВАНЕ НА ОБРАЗЦИ ОТ ХАРТИЯ ИЗПОЛЗВАНА ПРИ ПРОИЗВОДСТВОТО НА ВЪЛНООБРАЗЕН КАРТОН (НАВЪЛНЕН СЛОЙ)

ЙОРДАН КИРОВ, ГЕОРГИ УЧКУНОВ

**Резюме:** *Използването на вълнообразен картон се разширява непрекъснато за производство на голямо разнообразие от кутии и опаковки, предмети за рекламната индустрия, както и художествени творения. Броят на нововъведените екологични правила, определят изисквания за намаляване на използването на материали и прави продуктите по-леки. Направено е проучване за влиянието на използваното лепило, върху свойствата на хартията за навълнения слой.*

**Ключови думи:** *вълнообразен картон, хартия, анализи*

# EXPERIMENTAL STUDY OF PIECES OF PAPER USED IN PRODUCTION OF CORRUGATED CARDBOARD (CORRUGATED LAYER)

YORDAN KIROV, GEORGI UCHKUNOV

**Abstract:** *The use of corrugated paperboard is constantly expanding for producing of vast variety of boxes and packages, items for the advertising industry as well as artistic creations. Number of newly introduced regulations on the grounds of ecology have set requirements for lowering the use of material and making the products lighter. A survey was made of the influence of glue used on the properties of paper for corrugated layer.*

**Key words:** *corrugated paperboard, paper, analysis*

## 1. Въведение

Хартията се състои главно от растителни влакна, обработени и сплетени помежду си. Като основни влакнести полуфабрикати за получаване на хартията се използват влакната на дървото и сламата, дървесната и сламената целулоза.

Вълнообразният картон възниква като продукт от преработване на хартия и представлява един вълнообразен слой хартия или комбинация от няколко такива редуващи се с плоски слоеве. При производството на вълнообразен картон и опаковки от него, хартията за навълняване (флутинг) играе най-важната роля.

Флутингът е хартия, произведена от полуцелулоза (Semichemical fluting, SF). В основата си това е маса, получена по пътя на дълбока химическа обработка на хвойнова дървесина. Хартията за навълняване, която почти на 100% се състои от вторични изходни продукти (отпадъци), се нарича веленцоф (Wellenstoff, WS). Има и хартия за навълняване с високи якостни свойства, която със своя специален състав се използва за производството на вълнообразен картон, който е подходящ за хладилно съхранение и издържащ на влага, която се нарича аустрофлутинг (Austrofluting R).

Целта на настоящата работа е да се получат експериментални данни за влиянието на използваното лепило, върху свойствата на хартията за навълнения слой.

Copyright © 2016 by Technical University of Sofia, Plovdiv branch, Bulgaria ISSN Online: 2535-0048

За тази цел е необходимо да се модифицира стенд за тестване на съпротивление на плоско смачкване и с него да се проведат необходимите изпитвания. Да се подготви документация за изпитваните образци и тяхното изработване. Да се направи съответното изпитване и анализ на резултатите.

## 2. Описание на стенда и образците за изпитване.

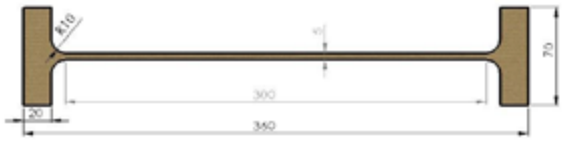
Изпитването се състои в определяне на якост на опън на материала. За целта се използва стенд, модел F18502 производство на фирма FRANK-PTI (фиг.1), който е модифициран за необходимите изследвания.



***Фиг. 1.*** *Стенд за изпитване на натиск на вълнообразен картон F18502 на FRANK-PTI*

Образеца се поставя в работната зона на стенда, която е между горната неподвижна плоча, която изпълнява ролята на опора и долна подвижна плоча. Закрепването в случая е модифицирано. Управлението на стенда се извършва посредством клавиатура извеждаща се на екрана. На него се показват и стойностите на измерваните величини, както и резултатите от изпитванията – механични показатели, определяни автоматично от приложния софтуер.

Изпитванията на опън се извършват върху ивица с широчина 5mm, като се използват образци, изрязани успоредно на нишките. Свободната дължина на ивицата (лентата) е 360 mm. Работната дължина на образците за всички видове материал е 300 mm. Схемата на типови образци е изобразена на (Фиг.2). В настоящото изследване е използвана серия от 11 образци за определяне якостта на даден тип хартия, като са изпитани с и без нанесен слой лепило. По изискванията на стандарта ISO1421-1998 минималния брой на образците, за определяне на средната якост на опън, е пет броя за всяко направление.



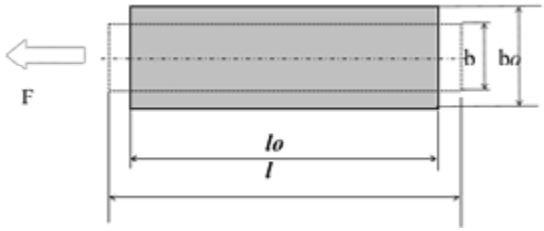

***Фиг. 2.*** *Схема на образец за изпитване*

## 3. Резултати от изследванията

Обикновено изследванията за якост на материала се провеждат като осови изпитвания на ивици. При тези изследвания се установява якостта успоредна на нишките. Изпитванията на едноосов опън се използват за определяне на характеристичната якост на материала и удължението при разкъсване и за определяне на модулите на еластичност и коефициента на Поасон. При опита на разкъсване за специално оформените образци, се търси максималната сила, при която образеца се разкъсва.

Необходимо е да бъдат направени изследвания, отчитащи влиянието върху якостта на проникналото в хартия свързващо средство – лепило.

Пробното тяло (фиг.3) има два края за захващане към изпитвателната машина и една работна зона, в която трябва да настъпи разрушаването.




*Фиг. 3. Схема на пробно тяло*

Тази зона е с начална дължина $l_o$, mm и начален напречен размер $b_o$, mm. На схемата се вижда състоянието на лентата, преди и след приключване на опита. При разпъване със сила F на прът с дължина $l_o$ и напречен размер $b_o$ се получават изменение на първоначалните му размери. Дължината се увеличава и става l, а напречният размер $b_o$ се намалява до b.

Данни от изследваните образци от AustroWelle 110 са показани в таблица 1, а от Austrofluting-R 112 са показани в таблица 2.

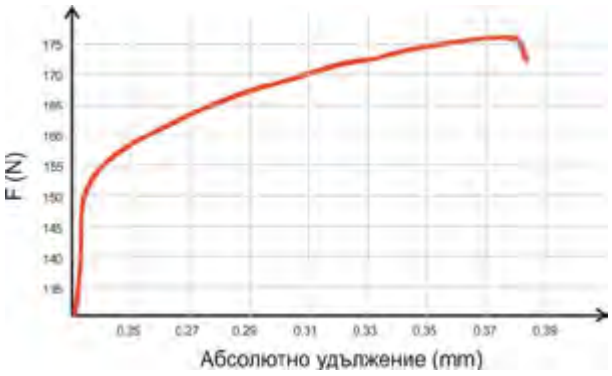
В резултат на теста се построява индикаторна диаграма на опън (фиг.4), с нейната координатна система и натоварваща сила F, N и абсолютно удължение ΔL, mm.

*Таблица 1*

| Austro Welle 110 | | | | |
|---|---|---|---|---|
| F (N) | Абсолютно удължение (mm) | С нанесен слой лепило | F (N) | Абсолютно удължение (mm) |
| 137 | 0.34 | | 155 | 0.28 |
| 140 | 0.38 | | 156 | 0.3 |
| 137.5 | 0.36 | | 156.5 | 0.31 |
| 138 | 0.35 | | 156 | 0.31 |
| 138.5 | 0.35 | | 156 | 0.29 |
| 138.5 | 0.37 | | 155.5 | 0.29 |
| 139.5 | 0.38 | | 157.5 | 0.33 |
| 138 | 0.34 | | 157 | 0.32 |
| 139 | 0.37 | | 156.5 | 0.31 |
| 139.5 | 0.38 | | 156 | 0.32 |
| 138 | 0.36 | | 155.5 | 0.29 |

*Таблица 2*

| Austro fluting R 112 | | | | |
|---|---|---|---|---|
| F (N) | Абсолютно удължение (mm) | С нанесен слой лепило | F (N) | Абсолютно удължение (mm) |
| 146 | 0.39 | | 176.5 | 0.36 |
| 145.5 | 0.34 | | 175.5 | 0.36 |
| 146 | 0.37 | | 177 | 0.39 |
| 146 | 0.36 | | 176.5 | 0.36 |
| 148 | 0.42 | | 177 | 0.38 |
| 145.5 | 0.35 | | 177.5 | 0.37 |
| 148 | 0.38 | | 176 | 0.33 |
| 147.5 | 0.37 | | 177.5 | 0.39 |
| 146 | 0.36 | | 176.5 | 0.34 |
| 147 | 0.37 | | 179 | 0.33 |
| 147 | 0.38 | | 176.5 | 0.34 |




*Фиг. 4. Индикаторна диаграма на опън*

От получените резултати от експеримента се определят абсолютно напречно свиване, надлъжна деформация, напречна деформация и коефициент на Поасон по известни зависимости от Съпротивление на материалите, дадени по-долу.

$$\Delta l = l - l_0 \qquad (1)$$

$$l_0.b_0 = l.b \qquad (2)$$

$$b = (l_0.b_0)/l \qquad (3)$$

След определяне на $b$ и известна стойност на $b_0$, определяме абсолютно напречно свиване $\Delta b$, като за целта се използва зависимост (4).

$$\Delta b = b - b_0 \qquad (4)$$

Надлъжната деформация се намира по формулата (5):

$$\varepsilon_x = \Delta l / l \qquad (5)$$

Напречната деформация се намира по формулата (6):

$$\bar{\varepsilon} = \Delta b / b \qquad (6)$$

От получените резултати за надлъжна и напречна деформация може да се изчисли и коефициента на Поасон μ

$$\mu = |\bar{\varepsilon}| / \varepsilon_x \qquad (7)$$

В таблица 3 са показани данните след изчисленията от резултатите на изследваните образци от AustroWelle 110, а от резултатите на изследваните образци от Austrofluting-R 112 са показани в таблица 4.

*Таблица 3*

| Austro Welle 110 | | | | | |
|---|---|---|---|---|---|
| l | b | Δb | εx | ε | μ |
| 300.34 | 4.99434 | -0.00566 | 0.001132 | -0.00113 | 1.001133 |
| 300.38 | 4.993675 | -0.00633 | 0.001265 | -0.00127 | 1.001267 |
| 300.36 | 4.994007 | -0.00599 | 0.001199 | -0.0012 | 1.0012 |
| 300.35 | 4.994173 | -0.00583 | 0.001165 | -0.00117 | 1.001167 |
| 300.35 | 4.994173 | -0.00583 | 0.001165 | -0.00117 | 1.001167 |
| 300.37 | 4.993841 | -0.00616 | 0.001232 | -0.00123 | 1.001233 |
| 300.38 | 4.993675 | -0.00633 | 0.001265 | -0.00127 | 1.001267 |
| 300.34 | 4.99434 | -0.00566 | 0.001132 | -0.00113 | 1.001133 |
| 300.37 | 4.993841 | -0.00616 | 0.001232 | -0.00123 | 1.001233 |
| 300.38 | 4.993675 | -0.00633 | 0.001265 | -0.00127 | 1.001267 |
| 300.36 | 4.994007 | -0.00599 | 0.001199 | -0.0012 | 1.0012 |
| **Austro Welle 110 с лепило** | | | | | |
| l | b | Δb | εx | ε | μ |
| 300.28 | 4.995338 | -0.00466 | 0.000932 | -0.00093 | 1.000933 |
| 300.3 | 4.995005 | -0.005 | 0.000999 | -0.001 | 1.001 |
| 300.31 | 4.994839 | -0.00516 | 0.001032 | -0.00103 | 1.001033 |
| 300.31 | 4.994839 | -0.00516 | 0.001032 | -0.00103 | 1.001033 |
| 300.29 | 4.995171 | -0.00483 | 0.000966 | -0.00097 | 1.000967 |
| 300.29 | 4.995171 | -0.00483 | 0.000966 | -0.00097 | 1.000967 |
| 300.33 | 4.994506 | -0.00549 | 0.001099 | -0.0011 | 1.0011 |
| 300.32 | 4.994672 | -0.00533 | 0.001066 | -0.00107 | 1.001067 |
| 300.31 | 4.994839 | -0.00516 | 0.001032 | -0.00103 | 1.001033 |
| 300.32 | 4.994672 | -0.00533 | 0.001066 | -0.00107 | 1.001067 |
| 300.29 | 4.995171 | -0.00483 | 0.000966 | -0.00097 | 1.000967 |

*Таблица 4*

| Austro fluting R 112 | | | | | |
|---|---|---|---|---|---|
| l | b | Δb | $\varepsilon_x$ | ε | μ |
| 300.39 | 4.993508 | -0.00649 | 0.001298 | -0.0013 | 1.0013 |
| 300.34 | 4.99434 | -0.00566 | 0.001132 | -0.00113 | 1.00113 |
| 300.37 | 4.993841 | -0.00616 | 0.001232 | -0.00123 | 1.00123 |
| 300.36 | 4.994007 | -0.00599 | 0.001199 | -0.0012 | 1.0012 |
| 300.42 | 4.99301 | -0.00699 | 0.001398 | -0.0014 | 1.0014 |
| 300.35 | 4.994173 | -0.00583 | 0.001165 | -0.00117 | 1.00117 |
| 300.38 | 4.993675 | -0.00633 | 0.001265 | -0.00127 | 1.00127 |
| 300.37 | 4.993841 | -0.00616 | 0.001232 | -0.00123 | 1.00123 |
| 300.36 | 4.994007 | -0.00599 | 0.001199 | -0.0012 | 1.0012 |
| 300.37 | 4.993841 | -0.00616 | 0.001232 | -0.00123 | 1.00123 |
| 300.38 | 4.993675 | -0.00633 | 0.001265 | -0.00127 | 1.00127 |
| **Austro fluting R 112 с лепило** | | | | | |
| l | b | Δb | $\varepsilon_x$ | ε | μ |
| 300.36 | 4.994007 | -0.00599 | 0.001199 | -0.0012 | 1.0012 |
| 300.36 | 4.994007 | -0.00599 | 0.001199 | -0.0012 | 1.0012 |
| 300.39 | 4.993508 | -0.00649 | 0.001298 | -0.0013 | 1.0013 |
| 300.36 | 4.994007 | -0.00599 | 0.001199 | -0.0012 | 1.0012 |
| 300.38 | 4.993675 | -0.00633 | 0.001265 | -0.00127 | 1.00127 |
| 300.37 | 4.993841 | -0.00616 | 0.001232 | -0.00123 | 1.00123 |
| 300.33 | 4.994506 | -0.00549 | 0.001099 | -0.0011 | 1.0011 |
| 300.39 | 4.993508 | -0.00649 | 0.001298 | -0.0013 | 1.0013 |
| 300.34 | 4.99434 | -0.00566 | 0.001132 | -0.00113 | 1.00113 |
| 300.33 | 4.994506 | -0.00549 | 0.001099 | -0.0011 | 1.0011 |
| 300.34 | 4.99434 | -0.00566 | 0.001132 | -0.00113 | 1.00113 |

### 4. Анализ на резултатите

За получените резултати при изпитване на образци без нанесен слой лепило (дадени в таблици 1, 2, 3 и 4), е налице относително добро съвпадение с данните от завода производител и получени по теоретичен път резултати, при двата различни типа хартии за навълняване.

И за двата типа материал якостта при образците със свързващите средства е по-висока. При направените експерименти не е отчетено влиянието на начина на захващане на образците към стенда (използването на двойно лепящи ленти). За избягване влиянието на този факт е необходимо да се извърши промяна на закрепването. Това евентуално ще бъде изпълнено на следващ етап.

### 5. Приложимост

Механичното взаимодействие между отделните слоеве представлява интерес, като изучаването му се налага с цел изясняване на възможностите за оптимизиране на този материал. Едно такова оптимизиране се налага поради редица новоприети нормативни документи чрез които институциите изискват от производителите на опаковки да се понижат масата на произвежданите от тях продукти и по този начин да се намали изразходвания количеството на изразходван материал. Това се налага предимно от екологични съображения.

Именно затова трябва да се отчитат особеностите на хартия за навълняване, при моделиране на натоварване на вълнообразен картон и опаковки от вълнообразен картон, оптимизация на технологичен процес и при анализиране процеса на рязане на вълнообразен картон и хартия.

Авторите изказват своята благодарност на НИС при Технически университет - София (проект №152ПД0043-24), с чиято финансова помощ са проведени настоящите изследванията.

### ЛИТЕРАТУРА

1. **Розалинов Д.**, Технология на опаковките от хартии и картони, София, 2005г
2. **Господинов Делян, Хаджийски Вилхелм, Стефанов Стефан** Моделиране на вълнообразен картон с използване на метода на крайните елементи, Научни трудове на Русевския университет - 2010, том 49, серия 9.
3. **HERBERT H. SCHUENEMAN, CP-P, MH.**, Paper and corrugated paperboard. 2009
4. **Шабиев Р.О., Смолин А.С., Парамонова Л.Л.** Изготовление и испытание лабораторных образцов бумаги и картона из вторичного сырья: учебно-методическое пособие / СПбГТУРП. - СПб., 2013. - 66 с.
5. *http://polygrafiamagazine.bg/*

Department of Mechanical Engineering
Technical University–Sofia,
Branch Plovdiv 25 Tsanko Diustabanov St.
4000 Plovdiv BULGARIA
E-mail: ykirov@abv.bg
E-mail: george_7@abv.bg

© International Scientific Conference on Engineering, Technologies and Systems
TECHSYS 2016, Technical University – Sofia, Plovdiv branch
26 – 28 May 2016, Plovdiv, Bulgaria

# МЕТОДИКИ ЗА СИНТЕЗ НА МЕХАНИЗМИТЕ НА ЕЛЕКТРОМЕХАНИЧНА ПРЕСА ЗА ПРОИЗВОДСТВО НА ПРОСЕЧЕНА МРЕЖА

ЗДРАВКО ВИТЛАРОВ

**Резюме:** *Разработени са три методики за синтез на механизмите от електромеханична преса за производството на метална просечена мрежа.Изведени са целевите функции и са определени допълнителни условия при синтеза.*

**Ключови думи:** *механизми, просечена мрежа, методики за синтез.*

# METHODS OF SYNTHESIS OF MECHANISMS OF ELECTRO MECHANICAL PRESS FOR EXPANDED METAL

ZDRAVKO VITLAROV

**Abstract:** *Developed are three methods for synthesis mechanisms of electro mechanical press for the production of expanded metal. Deduced are the target functions and are defined additional conditions for synthesis.*

**Key words:** *mechanisms, expanded metal, methods of synthesis*

## 1. Въведение

Металната просечена мрежа се изработва от листова въглеродна, поцинкована или неръждаема стомана, алуминиеви и медни сплави, никел сребро, титан и други метали. Тъй като се пройзвежда от плътни метални листове тя не се разплита, което я прави изключително пригодна за последваща технологична обработка. В зависимост от дебелината на изходния материал металната просечена мрежа се разделя на тежък, среден и лек тип с отвори предимно във формата на ромб, шестостен, овал и квадрат. Връзките на металните нишки във възлите добавят здравина и устойчивост. Образуваните отвори позволяват свободно преминаване на светлина, топлина, въздух, течности и звук но също така мрежата е недеждна преграда срещу различни нарушители. Металната просечена мрежа е изключително многостранен продукт с възможности за хиляди приловения.

Технологията за изработване на мрежата – просичане с последващо изтегляне обуславя безотпаднъчното и производство и я прави ценово атрактивна в сравнение с перфорираната ламарина.

## 2. Кинематична схема на електромеханична преса

След направеният литературен анализ на технологията и оборудването за реализирането и се стигна до кинематичната схема показана на фиг.1.

Задвижването на всички механизми се реализира от електродвигател 1. Посредством ремъчна предавка се задвижва коляновия вал на машината. От него получават движение всички механизми необходими за осъществяване на технологичнич процес:

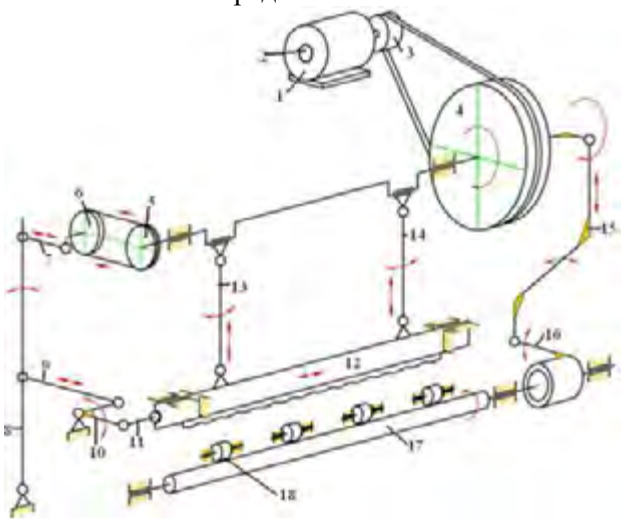
-механизъм за просичане и изтегляне– той се състои от звено 12 на който е закрепен режещият инструмент, мотовилки 13 и 14 и задвижващо звено във вертикално направление– коляновия вал;

-механизъм за структурно оформяне – с оглед изнасяне механизма извън зоната на

Copyright © 2016 by Technical University of Sofia, Plovdiv branch, Bulgaria ISSN Online: 2535-0048

рязане началното звено 6 се задвижва от коляновия вал посредством верижна предавка. Посредством лостова система (7, 8, 9, 10, и 11) се задвижва звено 12 в хоризонтално направление за реализиране на структурното оформяне;

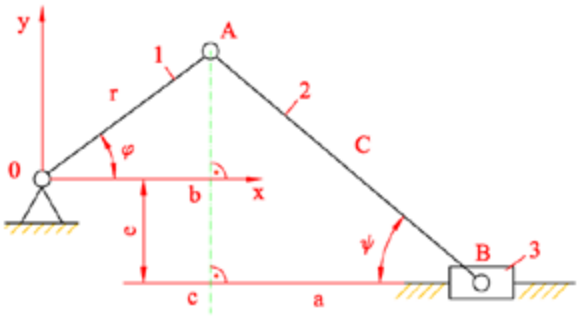
-механизъм за подаване на ламарината – еднопосочния съединител 16 се задвижва от коляновия вал посредством лоста 15.



***Фиг. 1.*** *Кинематична схема*

### 3. Методика за синтез на механизма за просичане и изтегляне

Механизмът реализиращ процеса просичане и изтегляне се апроксимира до коляно-мотовилков механизъм (фиг.2).




***Фиг.2*** *Механизъм за просичане*

Функцията на положението се изразява чрез [1]:

$$x_B = x_A + a = \\ = r\left[\cos\varphi + \sqrt{c_*^2 - \left(e_* + \sin\varphi\right)^2}\right] \qquad (1)$$

където:

$$x_A = r.\cos\varphi$$

$$y_A = r.\sin\varphi$$

$$a = \sqrt{c^2 - b^2} = \sqrt{c^2 - \left(e + r.\sin\varphi\right)^2}$$

$$C_* = \frac{c}{r}, e_* = \frac{e}{r};$$

$\varphi$ – ъгъл на завъртане на началното звено 1.

Уравненията дават положенията на звената 3 - $x_B$ и на 2 - $\psi$ в зависимост от завъртането на задвижващото звено 1 и размерите $r$, $c$ и $e$ на механизма.

Ходът на звено 3 се определя от:

$$h_3 = x_{Bmax} - x_{Bmin} = \\ = \sqrt[2]{(r+c)^2 - e^2} - \sqrt[2]{(r-c)^2 - e^2}, \qquad (2)$$

и скоростта на т.В:

$$v_B = w_1.\left[-y_A - \frac{x_A.e.(e+y_A)}{\sqrt[2]{c^2-(e+y_A)^2}}\right] \qquad (3)$$

Задачата на синтеза е сведена до определяне оптималните размери на звената ($r$, $c$, $e$) от механизма при зададена скорост ($v_B$) на рязане (определена от технологичния процес) и ход ($h_3$) на изпълнителното звено. Тогава целевата функция е зависимостта (3), зададена в неявен вид. Като допълнителни условия са поставени изискванията:

-условие за превъртане на началното звено - $e + r \le c$.

-кинематичните параметри ($v_B$, $a_B$) на звено 3 да са оптимални – плавно движение особенно по време на процеса рязане и изтегляне;

-предварително задаване на едното мъртво положение на изпълнителното звено;

-ъгълът на предаване на силата θ да не е по-голям от $\theta_{доп}$.

-осигуряване на необходимия ход на звено 3, съгласно изискванията на технологичния процес.

### 4. Методика за синтез на механизма за структурно оформяне

Механизмът реализиращ процеса на еластична деформация представлява лостов механизъм съставен от три асурови групи от втори клас (фиг.3).

Ходът на звено 7 се определя от:

$$h_7 = x_{Hmax} - x_{Hmin} \qquad (4)$$

където:

$$x_H = \\ = l_{FG}.cos(\propto_5 - \psi) + \\ + \sqrt[2]{l_{GH}^2 - [(y_H - y_F) + l_{FG}.sin(\alpha_5 - \psi)]^2}; \quad (5)$$

където:

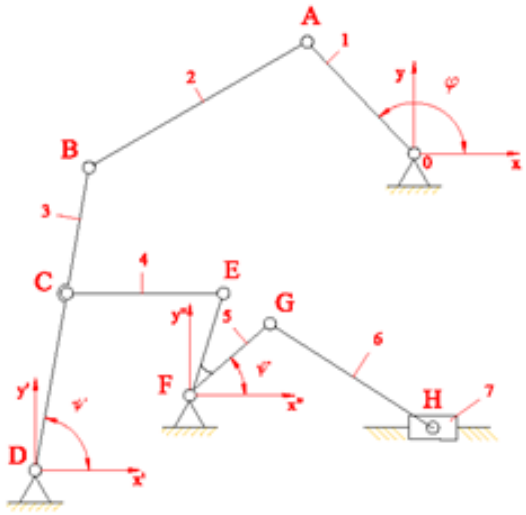
$$\alpha_5 = \pi - arcsin\frac{l_{DC}.sin\alpha_3}{\sqrt[2]{l_{DC}^2+x_F^2+y_F^2-A}} - \\ -arccos\frac{l_{FE}^2+l_{DC}^2+x_F^2+y_F^2-l_{CE}^2-A}{2.l_{FE}.\sqrt[2]{l_{DC}^2+x_F^2+y_F^2-A}}; \quad (6)$$

$$A = 2.l_{DC}.cos\alpha_3.\sqrt[2]{x_F^2+y_F^2};$$

$$\alpha_3 = \pi - arcsin\frac{l_{OA}.sin\varphi}{\sqrt[2]{l_{OA}^2+x_D^2+y_D^2-B}} - \\ -arccos\frac{l_{BD}^2+l_{OA}^2+x_D^2+y_D^2-l_{AB}^2-B}{2.l_{BD}.\sqrt[2]{l_{OA}^2+x_D^2+y_D^2-B}}; \quad (7)$$

$$B = 2.l_{OA}.cos\varphi.\sqrt[2]{x_D^2+y_D^2};$$

$\varphi$ – ъгъл на завъртане на началното звено 1.




***Фиг.3*** *Механизъм за структурно оформяне*

Зависимостта за изменение на скоростта на звено 7 се определя чрез диференциране на зависимост 5:

$$v_H = w_1.\left\{-l_{FG}.\dot{\alpha_5}.sin(\alpha_5 - \psi) + \right.$$

$$\left. + \frac{2.[(y_H-y_F)+l_{FG}.sin(\alpha_5-\psi)].l_{FG}.cos(\alpha_5-\psi).\dot{\alpha_5}.}{2.\sqrt[2]{l_{GH}^2-[(y_H-y_F)+l_{FG}.sin(\alpha_5-\psi)]^2}}\right\} \quad (8)$$

където: $\dot{\alpha_5}$.– производната на уравнение 6 спрямо $\alpha_3$ ;

$\dot{\alpha_3}$. - производната на уравнение 7 спрямо $\varphi$.

Задачата на синтеза е сведена до определяне оптималните размери на звената ($l_{OA}$, $l_{AB}$, $l_{BD}$, $l_{CD}$, $l_{CE}$, $l_{EF}$, $l_{FG}$, $l_{GH}$, $x_D$, $y_D$, $y_H$) от механизма при зададена скорост ($v_H$) на рязане при пластичната деформация (определена от технологичния процес) и ход ($h_7$) на изпълнителното звено. Тогава целевата функция е зависимостта (8), зададена в неявен вид. Като допълнителни условия са поставени изискванията:

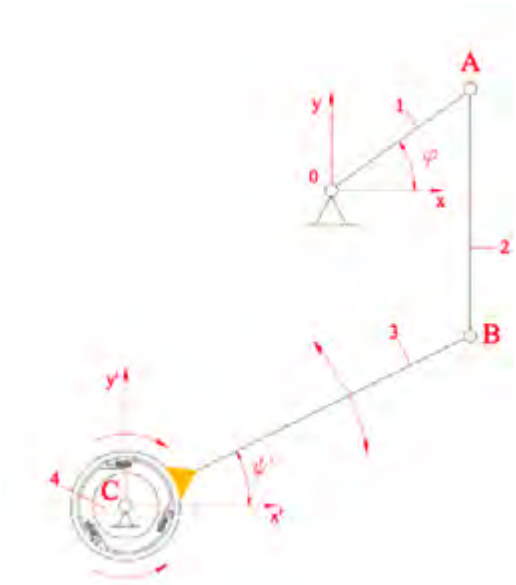
-условие за превъртане на началното звено - $l_{OA} + \sqrt{x_D^2 + y_D^2} \leq l_{AB} + l_{DB}$.

-кинематичните параметри ($v_H$, $a_H$) на звено 7 да са оптимални – плавно движение особенно по време на процеса пластична деформация при структурното оформяне;

-предварително задаване на едното мъртво положение на изпълнителното звено 7;

-ъгълът на предаване на силата $\theta$ да не е по-голям от $\theta_{доп}$.

-осигуряване на необходимия ход на звено 7, съгласно изискванията на технологичния процес.




***Фиг.4*** *Механизъм за подаване на ламарината*

## 5. Методика за синтез на механизма за подаване на ламарината

Кинематичната схема (фиг.4) на механизма реализиращ подаващото движение

на материала, представлява шарнирен четиризвенен механизъм.

Избираме две координатни системи *xOy* и $x'Cy'$. Преместването на материала се изразява чрез израза:

$$b = c.\propto_{3i}, \quad (9)$$

където:*c* – радиус на задвижващата ролка;

Функцията [1] на положението на изпълнителното звено 3 се изразява със следния израз:

$$\propto_{3i} = \pi - $$

$$-arcsin\frac{l_{OA}.sin\varphi_i}{\sqrt{l_{OA}^2 + x_C^2 + y_C^2 - 2.l_{OA}.A}} -$$

$$-\arccos\frac{l_{CB}^2+l_{OA}^2+x_C^2+y_C^2-l_{AB}^2-2.l_{OA}.A}{2.l_{CB}\sqrt{l_{OA}^2+x_C^2+y_C^2-2.l_{OA}.A}};$$

$\varphi_i = 0 \div 2.\pi$- ъгъл на завъртане на началното звено 1;

$$A = \sqrt{x_C^2 + y_C^2}.cos\varphi_i.$$

Ходът *b* на обработвания материал се определя от технологичния процес.

Задачата на синтеза е сведена до определяне оптималните размери на звената ($l_{OA}$, $l_{AB}$, $l_{CB}$, $x_C$, $y_C$) от механизма при зададен ход (*H*) на изпълнителното звено. Тогава целевата функция е зависимостта (9), зададена в неявен вид. Като допълнителни условия са поставени изискванията:

-условие за превъртане на началното звено - $l_{OA} + \sqrt{x_C^2 + y_C^2} \leq l_{AB} + l_{CB}$.

-кинематичните параметри ($\dot{\alpha}_3$, $\ddot{\alpha}_3$) на звено 3 да са оптимални – плавно движение особенно при работен ход;

-предварително задаване на едното мъртво положение на изпълнителното звено ($\alpha_{min}$);

-ъгълът на предаване на силата $\theta$ да не е по-голям от $\theta_{доп}$.

**6. Резултати**

Разработени са методики за синтез на механизмите необходими за реализиране на технологичен процес за производството на метална просечена мрежа.

Изведени са целевите функции за определяне на оптималните кинематични размери на отделните механизми необходими за реализиране на технологичен процес за изработване на метална просечена мрежа.

Определени са и допълнителни условия към целевите функции необходими за реализиране на оптимизационния процес за всеки един от механизмите.

Авторът изказва своята благодарност на НИС при Технически университет - София (проект №162ПД0018-24), с чиято финансова помощ са проведени настоящите изследванията.

**ЛИТЕРАТУРА**

1. Минчев Н., Живков В., Стоянов П., Алипиев О., Теория на механизмите и машините, СОФТТРЕЙД, С., 2011.

2. © 2010 Dexmet Corporation., Expanding technology.

Контакти
Адрес: 4000 Пловдив,
бул. Санкт Петербург № 61.
E-mail: z_vitlarov@tu-plovdiv.bg

© International Scientific Conference on Engineering, Technologies and Systems
TECHSYS 2016, Technical University – Sofia, Plovdiv branch
26 – 28 May 2016, Plovdiv, Bulgaria

# МАТЕМАТИЧЕН МОДЕЛ ЗА ВИБРОУДАРНО РЯЗАНЕ НА ОПТИЧНИ СТЪКЛА

АНГЕЛ ЛЕНГЕРОВ, ДЕЧКО РУСЧЕВ, СТИЛИЯНА ТАНЕВА,
ГЕОРГИ ЛЕВИЧАРОВ

**Резюме:** *В статията е изведен математичен модел описващ траекторията на движение на отрезна стрела от виброударна уредба за рязане на оптични стъкла. Това позволява изследване на кинематиката и динамиката на взаимодействието на елементите на колебателната система „заготовка – отрезен диск“.*

**Ключови думи:** *оптични стъкла, виброударно рязане, математичен модел*

# MATHEMATICAL MODEL OF OPTICAL GLASS CUTTING BY APPLYING VIBRATING IMPACT

ANGEL LENGEROV, DECHKO RUSCHEV, STILIYANA TANEVA,
GEORGY LEVICHAROV

**Abstract:** *This article provides the mathematical model describing the movement trajectory of the cutting arm of a vibrating impact machine intended for cutting optical glasses. This allows to study the kinematics and dynamics of the interaction of the elements in the oscillating system "detail – cutting disc".*

**Key words:** *optical glass, vibrating impact cutting, mathematical model*

## 1. Въведение

Теоретичното оценяване на степентта на влияние на създадените в условия на виброударно рязане принудени трептения при рязане на оптични стъкла може да бъде представено чрез математичен модел. Така се създава възможност за числено описание на траекторията и законите на движение на отрезна стрела с центробежен вибратор. Могат да бъдат определени и усилията на контактното взаимодействие между режещия инструмент и обработваната оптична заготовка при зададени големини на принудени трептения.

## 2. Изложение

При форматиране на докладите се използват параграфните стилове от шаблона.С двойно кликване върху файла на шаблона ще се отвори нов документ, в който трябва да поместите вашия материал.Стиловете към шаблона не трябва да се редактират. С цел опростяване пресмятанията при разработване на математичния модел, заменяме действието на центробежния вибратор 1 с движеща хармонична сила $F(t)$. Отрезната стрела 2, която я считаме за абсолютно твърда е закрепена от десния си край шарнирно. Уредбата сработва след включване на въртеливо движение на отрезния диамантен диск 5 и постъпателно (статично) виброударно преместване на заготовката 6 перпедикулярно на вектора на скоростта на диска. Докосването на опорния винт 3 до еластичната основа 4 (демпфера) става по-рано от това на отрезния диск 5 с оптичната заготовка 6. Равновесно състояние настъпва в момента на уравновесяване на силите на тежестта на системата и силите на взаимодействие между контактуващите елементи („отрезен диск – оптична заготовка" и „ винт – еластична опора"). За опростяване на пресмятането масите на стрелата, на вибратора и устройствата за създаване на статично натоварване на детайла се заменя с две съсредоточени маси (на фиг.1 - точки 1 и 2). За начало на координатната система се приема оста на завъртане на

Copyright © 2016 by Technical University of Sofia, Plovdiv branch, Bulgaria ISSN Online: 2535-0048

отрезната стрела. Означенията, използвани в математичния модел са следните:

$\alpha$ - ъгъл, определящ положението на стрелата;

$m$ - маса на ексцентрика;

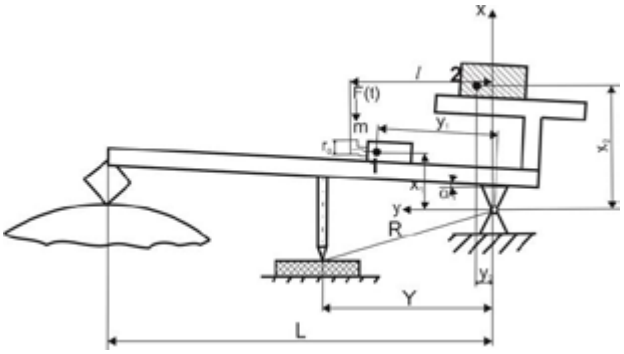
$m_1$ - маса на системата (без противотежестта);

$m_2$ - маса на противотежестта;

$k_1$ - еластична константа на демпфера;

$k_2$ - еластична константа на опората „детайл-отрезен диск“;

$\xi$ - ефективен демфиращ коефициент.




***Фиг.1.*** *Математичен модел на отрезната уредба*

Масовият инерционен момент $I$ на системата относно оста на въртене на диска, се изразява така [1, 2]

$$I = m_1\left(x_1^2 + y_1^2\right) + m_2\left(x_2^2 + y_2^2\right). \quad (1)$$

Ъгълът $\alpha_e$ между правата, минаваща през контактната точка на упора с демфера и оста на въртене и правата, минаваща през контактната точка на оптичния детайл с отрезния диск и оста на въртене се изчислява по формулата

$$\alpha_e = -\frac{\Delta h}{L},$$

където $\Delta h$ е разстоянието между оптичния детайл и отрезния диск в момента на контакт на упора с демфера.

Тогава уравнението за равновесие на системата, приема вида

$$\left(m_1 y_1 + m_2 y_2\right) g = \left(\alpha_0 + \frac{\Delta h}{L}\right) k_1 Y^2 + \alpha_0 k_2 L^2 , \quad (2)$$

където $\alpha_0$ е ъгъла на равновесното състояние.

Следователно

$$\alpha_0 = \frac{\left(m_1 y_1 + m_2 y_2\right) g - \dfrac{\Delta h k_1 Y^2}{L}}{k_1 Y^2 + k_2 L^2}. \quad (3)$$

Движещата хармонична сила и движещият момент се определят по зависимостите

$$F(t) = m r_0 \left(2\pi v\right)^2 \sin\left(2\pi v t\right) \quad (4)$$

$$Me(t, v) = m r_0 l \left(2\pi v\right)^2 \sin\left(2\pi v t\right) \quad (5)$$

Резултантният момент на действащите сили (тежестта и реакциите на опорите), в зависимост от ъгловото отклонение на положението на стрелата от равновесното положение ($\delta = \alpha - \alpha_0$), т.е. се определя от системата

$$\hat{M}(\delta) = \begin{cases} -\delta\left(k_1 y^2 + k_2 L^2\right) & при\ \delta^3 - \alpha_0 \\ \alpha_0 k_2 L^2 - \sigma k_1 y^2 & при\ \delta < -\alpha_0 \end{cases}. \quad (6)$$

Уравнението на движение на системата е

$$I\ddot{\delta} = \hat{M}(\delta) - \xi\dot{\delta} + Me(t, v). \quad (7)$$

и след заместване в (7) на променливите

$$Y_1 = \dot{\delta} \quad Y_0 = \delta \quad \dot{Y}_0 = Y_1 . \quad (8)$$

Получаваме

$$\dot{Y}_1 = \frac{I}{I}\left[\hat{M}\left(Y_0\right) - \xi Y_1 + Me(t, v)\right]. \quad (9)$$

Уравнение (9) при малки смущаващи сили (при малки маси $m$, такива че ъгъла на отклонение от равновесното положение не превишава $\alpha_0$) може да се реши аналитично.

Това дава възможност уравнение (7) да се запише във вида

$$I\ddot{\delta} + \xi\dot{\delta} + \left(k_1 Y^2 + k_2 L^2\right)\delta = Me(t, v), \quad (10)$$

представяйки

$$Me(t, v) = m r_0 l \left(2\pi v\right)^2 exp^{i2\pi v t}, \quad (11)$$

и замествайки го в уравнение (10), получаваме уравнението за устойчив режим на рязане

$$\delta(t) = A exp^{i2\pi\nu t} . \quad (12)$$

Заместваики (12) в (10) и при отчитане на (11), получаваме

$$-A(2\pi\nu)^2 I + i2\pi\nu\xi A + (k_1 Y^2 + k_2 L^2) A = \\ = mr_0 l (2\pi\nu)^2 . \quad (13)$$

Оттук получаваме, че

$$A = \frac{mr_0 l (2\pi\nu)^2}{(k_1 Y^2 + k_2 L^2 - (2\pi\nu)^2 I + 2\pi\nu\xi i)} . \quad (14)$$

От уравнение (14) определяме, че

$$|A| = \frac{mr_0 l (2\pi\nu)^2}{\sqrt{k_1 Y^2 + k_2 L^2 - ((2\pi\nu)^2 I)^2 + (2\pi\nu\xi)^2}} . \quad (15)$$

Откъдето за резонансната получаваме

$$\nu_0 = \frac{1}{2\pi}\sqrt{\frac{k_1 Y^2 + k_2 L^2}{I}} . \quad (16)$$

### 3. Заключение

Получен е математичен модел, описващ траекторията на движение на отрезна стрела от виброударна уредба за рязане на оптични стъкла. За различни амплитуди на колебателни движения на системата е възможно да се определят усилията на контактните взаимодействия между отрезния диск и обработваните заготовки. При реализиране на различни виброударни режими на рязане (когато ъгълът на отклонение на отрезната стрела спрямо равновесното си положение превишава $\alpha_0$) и наличие на големи смущаващи сили, математичният модел позволява определянето на степента на динамично въздействие между отрезния диск и разрязваните заготовки от оптични стъкла.

## ЛИТЕРАТУРА


1. Кумабэ Д. Вибрационное резание./ Пер. с яп. С. Л. Масленникова; Под ред. И. И. Портнова, В. В. Белова. М.: Машиностроение, 1985, с. 424.
2. Грефе Гюнтер и др. Фина оптика. Технология на оптичното производство, Техника, София, 1985.



Technical University of Sofia, Branch Plovdiv
25 Tsanko Dystabanov St.
4000 Plovdiv
BULGARIA
E-mail: anlen@tu-plovdiv.bg
E-mail: ruschev@tu-plovdiv.bg
E-mail: s.taneva@ tu-plovdiv.bg
E-mail: alplast@evrocom.net

© International Scientific Conference on Engineering, Technologies and Systems
TECHSYS 2016, Technical University – Sofia, Plovdiv branch
26 – 28 May 2016, Plovdiv, Bulgaria

# ИЗСЛЕДВАНЕ ВЛИЯНИЕТО НА ПРОЦЕСА SPHERICAL MOTION BURNISHING ВЪРХУ ЕНЕРГИЙНИЯ БАЛАНС НА СИСТЕМАТА „ИНСТРУМЕНТ-ЗАГОТОВКА“

ГЕОРГИ ЛЕВИЧАРОВ

**Резюме:** *В статията е изследван процеса на заглаждане на външни цилиндрични повърхнини, известен като "Spherical motion burnishing" (SMB) и е разгледан в енергиен аспект. Енергийнишят баланс на системата „инстррумент-заготовка“ е представен чрез първия закон на термодинамиката. Чрез теоретични зависимости е показано влиянието на различните параметри на процеса SMB върху компонентите на енергийния баланс. Направени са необходимите изводи за оптималните стойности на параметрите на процеса.*

**Ключови думи:** *spherical motion burnishing; пластична деформация, енергийни параметри, енергиен баланс*

# STUDY THE INFLUENCE OF SPHERICAL MOTION BURNISHING PROCESS ON THE ENERGY BALANCE OF THE SYSTEM „TOOL - WORK-PIECE“

GEORGY LEVICHAROV

**Abstract:** *In this article the burnishing process of external cylindrical surfaces called "Spherical motion burnishing" (SMB) has been analyzed in a power aspect. The energy balance in the system "work-piece - tool" has been studied in correspondence with the first thermodynamics law. The influence of different parameters of the SMB process on the components in the energy balance equation has been analyzed. The respective conclusions for rational values of the process parameters have been made.*

**Key words:** *spherical motion burnishing; plastic deformation, energy parameters, energy balance*

## 1. Въведение

В общото машиностроене преобладават елементите, подложени на променливи натоварвания и в частност на циклични натоварвания. Механизмът на уморно разрушение е типичен за ротационни детайли от типа на валовете и въртящите се оси, което определя умората на материала като лимитиращ фактор за тяхната работоспособност [1, 5, 9, 10]. От друга страна, работоспособността на някои елементи с работни външни цилиндрични повърхнини (например оси, втулки и ролки във верижните предавки) се лимитира от тяхната износоустойчивост. И в двата случая е в сила тезата за решаващото значение на състоянието на повърхностния слой.

Експлоатацията на елементите с работни външни цилиндрични повърхнини провокира зараждане на микропукнатини и износване на повърхностните им слоеве. Основният фактор, който определя с какви темпове и в какава степен тези негативни ефекти се развиват във времето, е технологичният процес на обработване и в частност довършващото обработване. Довършващото обработване има решаващо значение, тъй като от вида му зависи както микрогеометрията (грапавост, вълнообразност, резки и следи от обработката),

Copyright © 2016 by Technical University of Sofia, Plovdiv branch, Bulgaria ISSN Online: 2535-0048

така и физико-механичното състояние (остатъчните напрежения, микротвърдостта и структурата) на повърхностния слой.

Едни от най-разпространените методи за довършващо обработване чрез пластично деформиране на външни цилиндрични повърхнини са: заглаждане със сфери (ball burnishing) [4], заглаждане с ролки (roller burnishing) [3], дълбоко ролкуване (deep rolling) [5], елмазно заглаждане (diamond burnishing) и др. Същността им се състои в прилагане на повърхностно третиране с помощта на деформиращи инструменти - сфери или ролки, а при някои се разчита на допълнително въздействие с лазер или чрез генерирани вибрации. Преобладаващите работни схеми са: разположен в държач деформиращ елемент, като се разчита на деформираща сила, създадена от пружина (еластична система) или разположени в сепаратор деформиращи елементи.

Характерна особеност на тези методи е наличието на прекъснат контакт между обработваната заготовка и деформиращите инструменти в напречно сечение, което рефлектира в неравномерно качество на обработените повърхнини. Като контрапукт на този основен недостатък на съществуващите методи е синтезиран метода "Spherical motion burnishing" (SMB).

*Основна цел на настоящото изследване е да се анализира влиянието на различни параметри на процеса SMB по енергиен критерий.*

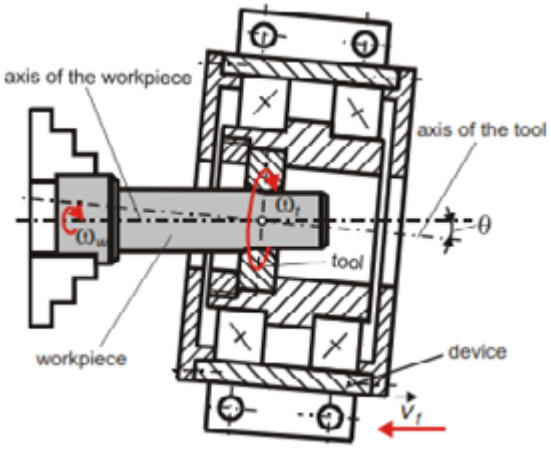
## 2. Изложение

### 2.1. Същност на метода SMB

Същността му се състои в преминаване на инструмент с вътрешна тороидална работна част при гарантирана стегнатост със заготовката в присъствието на мажещо вещество. Принципната схема на метода SMB съответства на формообразуване чрез обхождане при непрекъснат контакт в напречно сечение между тороидалната работна повърхнина на инструмента и заготовката в условията на триене при плъзгане.

Методът може да бъде класифициран като смесено заглаждане, тъй като съчетава предимствата на уякчаващо, размерно и уякчаващо заглаждане, съгласно класификацията, направена в [6].

Характерна особеност на метода SMB е специфичната му кинематика, подобна на метода “Сферично дорноване” - инструментът извършва *сложно движение* по отношение на неподвижната заготовка - *суперпозиция от сферично движение и праволинейна транслация*




***Фиг.1.*** *Схема на устройството и инструмента*

по направление на оста на заготовката. В резултат всяка точка от екватора на работната част на инструмента се движи по “удължена”, респ. “скъсена” сферична крива по отношение на координатна система, свързана със заготовката, което дава наименованието на метода.

На фиг. 1 са показани общ вид и принципна схема на устройство за реализиране на метода върху конвенционални стругови машини. Въртеливото движение от вретеното на струговата машина се предава на заготовката, която се върти около оста си с ъглова скорост $\dot{\omega}_w$ . Инструментът, чиято ос сключва малък ъгъл θ с оста на заготовката (фиг. 1) получава въртеливо движение около оста си с ъглова скорост $\dot{\omega}_t$, поради наличие на стегнатост между инструмента и заготовката. Инструментът се премества по оста на заготовката със скорост $v_f$, обезпечавайки обработване по цялата й дължина.

### 2.2. Анализ на процеса smb в енергиен

#### 2.2.1. Енергиен баланс в системата “инструмент - заготовка”

Предвид термомеханичната им природа, металообработващите процеси се характеризират със значителна част на дисипирала енергия и следователно, могат да се разглеждат като механични системи с дисипативнн процеси. Типичен представител на механичните системи с дисипативни процеси е термодинамичната система “инструмент-заготовка” на металообработващите процеси за пластично деформиране [8].

Съгласно първия закон на термодинамиката за енергийния баланс на системата инструмент-заготовка при процеса SMB съгласно [7] след пренебрегване на масовите сили може да се запише:

$$d\bar{A}^e = \left|dA_Q^e\right| + \left|dA_{el}^i\right| + \left|dA_{pl}^i\right| \quad (1)$$

$$d\bar{A}^e = \left(M_e\omega_e + P_a v_f\right)dt \quad (2)$$

е елементарна работа на външните активни сили на входа на системата:

$$\left|dA_Q^e\right| = dQ^e = \int_{F_0} p_{n,i} v_i^{a(t,w)} dF_0 dt \quad (3)$$

е елементарна работа на силите по контактното точково множество $F_0$ (КТМ), която дисипира в топлина; $v_i^{a(t,w)}$ е релативната скорост на съвпадащите точки на инструмента и заготовката по КТМ в неподвижната координатна система $Ox_i$;

$$\left|dA_{el}^i\right| = \sum_{r=1}^{r=2} \int_{V^{(r)}} \sigma_{ij}^{el(r)} \xi_i^{el(r)} dV^{(r)} dt \quad (4)$$

е елементарна работа на вътрешните повърхнинни сили за еластична деформация на заготовката и инструмента,

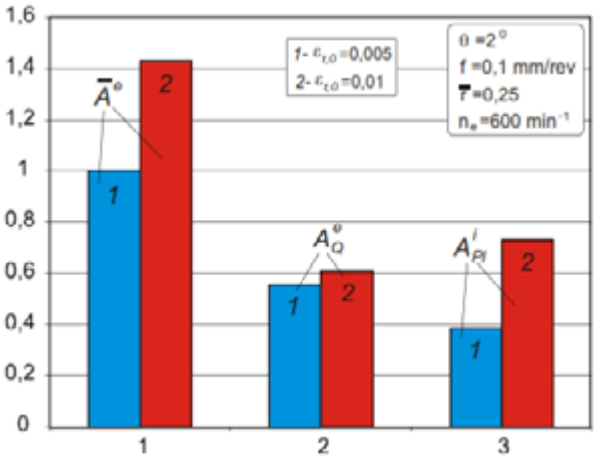
$$\left|dA_{pl}^i\right| = \sum_{r=1}^{r=2} \int_{V^{(r)}} \sigma_{ij}^{pl(r)} \xi_i^{pl(r)} dV^{(r)} dt \quad (5)$$

е елементарна работа на вътрешните повърхнинни сили за пластична деформация на заготовката; $\sigma_{ij}^{(r)} = \sigma_{ij}^{el(r)} + \sigma_{ij}^{pl(r)}$ е тензор на напреженията, $\xi_{ij}^{(r)} = \xi_{ij}^{el(r)} + \xi_{ij}^{pl(r)}$ е тензор на скоростите на деформацията.

2.2.2. Влияние на параметъра $\varepsilon_{t,0}$

Извършено е сравнение по енергиен критерий за две стойности на параметъра $\varepsilon_{t,0}$. Работата на външните активни сили $\bar{A}^e$ за обработване на цялата заготовка за случая с параметри $f = 0.10\ mm/rev$; $\bar{r} = 0.25$; $\varepsilon_{t,0} = 0.005$, избран за базов, е нормализирана към единица. Всички останали работи по-нататък са изразени като части от единицата.

На фиг. 2 е показано сравнение по енергийния критерий за двата случая на $\varepsilon_{t,0}$: съответно $\varepsilon_{t,0} = 0.005$ и $\varepsilon_{t,0} = 0.01$. Във втория

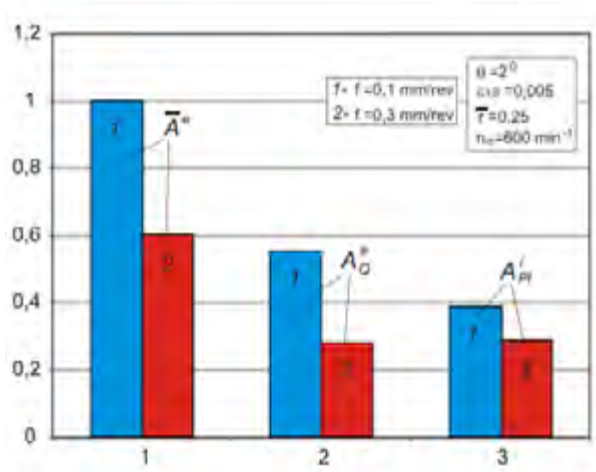



***Фиг. 2.*** *Сравнение по енергиен критерии за две стойности на параметъра* $\varepsilon_{t,0}$

случай работата $\bar{A}^e$ се увеличава с около 43%, като това увеличение е за сметка на компонентата $A_{pl}^i$, която се увеличава почти двойно. Независимо от двукратното увеличение на $\varepsilon_{t,0}$, работата от силите на триене $A_Q^e$ се увеличава незначително (около 5%).

2.2.3. Влияние на подаването $f$

На фиг. 3 е показано сравнение по енергийния критерий за две стойности на подаването $f$: $f = 0.10\ mm/rev$ и $f = 0.30\ mm/rev$.



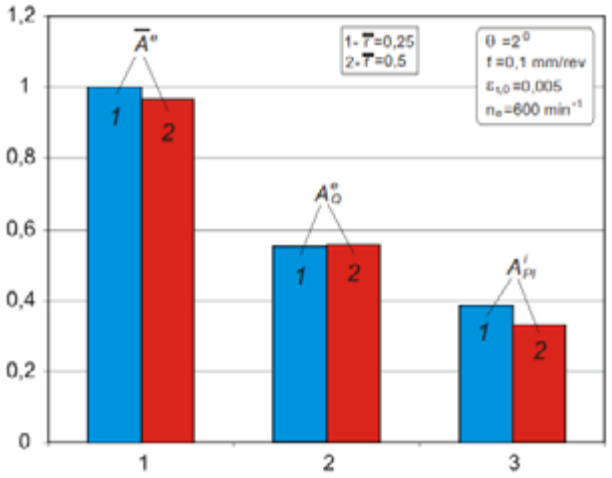

***Фиг. 3.*** *Сравнение по енергиен критерий за две стойности на параметъра* $f$

Работата на външните активни сили $\bar{A}^e$ за обработване на цялата заготовка значително намалява (с около 40%) при трикратно увеличение на подаването. Намаляването е основно за сметка на намалената работа от

силите на триене $A_Q^e$ (с почти 50%). Същевременно намалява и работата за пластична деформация $A_{pl}^i$ (с около 10%).

2.2.4. Влияние на безразмерния радиус $\bar{r}$

Анализирано е влиянието на безразмерния радиус на инструмента $\bar{r}$ върху компонентите в уравнение (2) за две негови стойности, съответно $\bar{r} = 0.25$ и $\bar{r} = 0.5$ (фиг. 4).

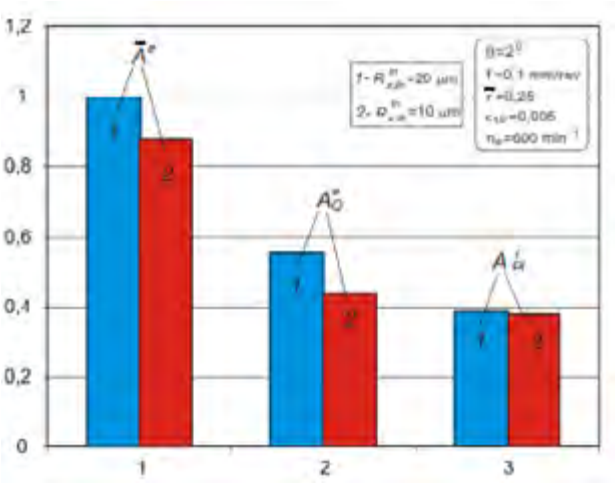



***Фиг. 4.*** *Сравнение по енергиен критерий за две стойности на параметъра* $\bar{r}$

Работата на външните активни сили $\bar{A}^e$ за обработване на цялата заготовка намалява с около 4% при двукратно увеличение на безразмерния радиус. Намаляването е основно за сметка на намалената работа за пластична деформация $A_{pl}^i$. Същевременно, макар и без практическо значение, се увеличава работата от силите на триене. Като цяло може да се заключи, че при равни други параметри, безразмерният радиус влияе слабо върху енергийните характеристики на процеса.

2.2.5. Влияние на началната грапавост

На фиг. 5 е показано сравнение по енергийния критерий за двата случая на начална граапавост $R_{z,th}^{in} = 20\ \mu m$ и $R_{z,th}^{in} = 10\ \mu m$. Двойно по-малката начална грапавост по критерий $R_z$ довежда до намаляване на входната работа $\bar{A}^e$ с около 12%. Това намаление е почти изцяло за сметка на намалената работа от силите на триене, докато работата за пластично деформиране се намалява незначително (с по-малко от 1%).




***Фиг. 5.*** *Сравнение по енергиен критерий за две стойности на началната грапавост*

## 3. Заключение

• На основата на първия закон на термодинамиката е изследвано влиянието на различни параметри върху енергийния баланс в системата “инструмент-заготовка”.

• Увеличаването на номиналната стегнатост на процеса SMB, респ. на параметъра $\varepsilon_{t,0}$ е почти пропорционално на нарастването на необходимата работа на външните активни сили $\bar{A}^e$. Основен относителен дял в това увеличение има работата за пластична деформация $A_{pl}^i$ за сметка на незначително нарастване на работата на силите от триене $A_Q^e$.

• При равни други условия, увеличаването на подаването води до значително намаляване на работата на външните активни сили $\bar{A}^e$. Това се дължи основно на намалената работа от силите от триене $A_Q^e$ и в по-малка степен на по-малко работа за пластична деформация $A_{pl}^i$. Намалената работа от силите от триене при по-голямо подаване е резултат от по-малкия брой пъти на смяна на знака на релативната скорост по токовата линия “инструмент-заготовка”, което е следствие от особената кинематика на процеса SMB. Същевременно, по-голямото подаване рефлектира в нарастване на необходимата за процеса осова сила, чиято работа като относителен дял в работата на външните активни сили е значително по-малка в сравнение с работата на въртящия момент, което е очевидно от фиг. 3. Изложените аргументи налагат решаване на задачата за избор на оптимална стойност на подаването при компромис от гледна точка на минимизиране на

необходимата за процеса мощност и сигурност на закрепващите механизми.

• В енергиен аспект е целесъобразно методът SMB да се прилага върху образци с по-малка предварителна грапавост. Същевременно, предварителната грапавост трябва да се оптимизира в аспект на необходими разходи за предшестващи операции и минимизиране на необходимата за процеса осова сила.

## ЛИТЕРАТУРА


1. Cai, C.Q., Shin, C.S., A normalized area-compliance method for monitoring surface crack development in a cylindrical rod. Int. J. Fatigue, 27 (7), 801-809, 2005.
2. El-Axir, M. H., A method of modeling residual stress distribution in turning for different materials, International Journal of Machine Tools and Manufacture, 42 (9) 1055-1063, 2002.
3. El-Tayeb N. S. M., K. O. Low, P. V. Brevern, Influence of roller burnishing contact width and burnishing orientation on surface quality and tribological behaviour of Aluminium 6061, Journal of Materials Processing Technology 186 (1-3) (2007) 272-278.
4. Hassan A. M., An investigation into the surface characteristics of burnished cast Al-Cu alloys, International Journal of Machine Tools and Manufacture 37 (6) (1997) 813-821.
5. Jujerm P., I. Altenberger, Fatigue performance enhancement of steel using mechanical surface treatment, Journal of Metals, Materials and Minerals 17(1) (2007) 59-65.
6. Korzynski, M., 2007. Modelling and experimental validation of the force-surface roughness relation for smoothing burnishing with a spherical tool. Int. J. Mach. Tools Manuf. 47 (12), 1956-1964.
7. Maximov JT, Duncheva GV. A new 3D finite element model of the spherical Mandrelling process. Finite Elements in Analysis and Design 44 (6-7) (2008) 372-382.
8. Maximov JT. Thermodynamic optimization of mechanical systems with dissipative processes. International Journal of Mechanical Sciences 48 (1) (2006) 62-74.
9. Сучков А. Г., Костадинов В. С, Кършаков М. К, Григоров В. И., Кънев И. Т., 1984. Довършващо обработване чрез повърхностно пластично деформиране. "Техника", София.
10. Яиенко В. К., Г. З. Зайиев, В. Ф. Притченко, Л. И. Ивщенко, 1985. Повишение несущей способности деталей машин алмазпим вьзглаживанием. М., Машиностроение.



Technical University of Sofia, Branch Plovdiv
25 Tsanko Dystabanov St.
4000 Plovdiv
BULGARIA
E-mail: alplast@evrocom.net

© International Scientific Conference on Engineering, Technologies and Systems
TECHSYS 2016, Technical University – Sofia, Plovdiv branch
26 – 28 May 2016, Plovdiv, Bulgaria

# ИЗСЛЕДВАНЕ НА ИМПУЛСНО ВИГ-ЗАВАРЯВАНЕ С ПОСТОЯННИ ЧЕСТОТА И СРЕДЕН ТОК

ТЕОФИЛ ЯМБОЛИЕВ

***Резюме:*** Съществуват режими за импулсно заваряване, при които чрез комбинации от стойности на импулсния, фоновия ток и продължителността на импулса средният ток и количеството внесена топлина от дъгата остават постоянни. Целта на изследването е да установи какъв режим да бъде предпочитан, ако честотата, средният ток и още един от посочените параметри са постоянни по големина, а другите два се променят.

Установено е, че при постоянни среден и фонов ток отлична геометрия, структура и твърдост на метала на шева и зоната на термично влияние се осигуряват от импулсен ток с минимална стойност. Увеличаване на импулсния ток води до провисване на шева. При постоянни среден и импулсен ток променливите фонов ток и продължителност на импулса не предизвикват съществени изменения в геометрията и структурата на съединението, а твърдостта му в различни зони се изменя в границите 185-279 HV0,1.

**Ключови думи:** *аустенитна стомана, ВИГ заваряване, импулсен ток, микроструктура, твърдост*

# STUDY OF PULSED TIG WELDING WITH CONSTANT FREQUENCY AND MEAN CURRENT

TEOFIL IAMBOLIEV

***Abstract:*** There are pulsed welding conditions outlined by constant mean current and heat input although the pulse and base current as well as the pulse duration may be varied. The goal of this study is to find appropriate welding conditions provided the mean current and one of the pulse current parameters are held constant while the two other parameters vary.

It was found that at constant mean and base current the minimum pulse current value resulted in excellent geometry, microstructure and hardness of the weld metal and the heat affected zone. An increase of the pulse current provoked a molten metal sink. At constant mean and pulse current as well as variable base current and pulse duration had no significant effect on the geometry and microstructure. The hardness of the weld varied within 185-279 HV0,1.

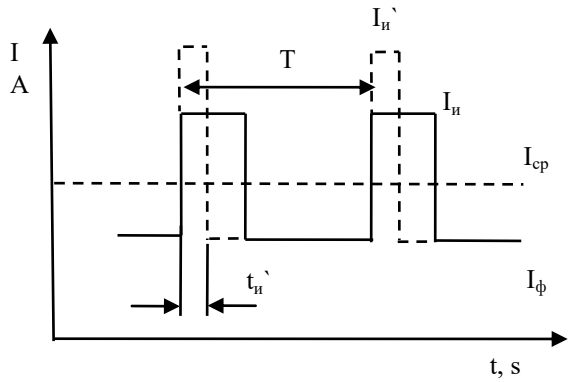
**Keywords:** *austenitic steel, TIG welding, pulse current, microstructure, hardness*

## 1. Въведение

Импулсното ВИГ заваряване (ИВИГ) се отличава от заваряването с постоянен ток с редица предимства - издребняване на зърната в метала на шева [1, 2], по-тясна зона на термично влияние (ЗТВ) [3], подобрени механични свойства [4, 5], понижени остатъчни напрежения и деформации на съединението и по-ниска енергоемкост при заваряване [1-5].

На фиг. 1 с плътна линия са показани параметрите на тока при импулсното заваряване. Средният ток се изчислява от зависимостта:

Copyright © 2016 by Technical University of Sofia, Plovdiv branch, Bulgaria ISSN Online: 2535-0048




*Фиг. 1 Параметри на тока при ИВИГ заваряване: основен режим (плътна линия) - $I_и$, - импулсен ток; $I_ф$ - фонов ток, $t_и/T$ - относителна продължителност на импулса; T – период; твърд режим, постоянен фонов ток (пунктир)*

$$I_{ср} = I_и \frac{t_и}{T} + I_ф\left(1 - \frac{t_и}{T}\right) \qquad (1)$$

От (1) следва, че съществуват комбинации от стойности на параметрите $I_и$, $I_ф$ и $t_и/T$, при които средният ток остава постоянен по големина. Стопяването на метала и образуването на ваната става по време на импулса, а втвърдяването й – пълно или частично, по време на паузата, в която тече слабият фонов ток. Затова интерес представлява въпросът какъв режим на заваряване да бъде предпочетен – „твърд" режим с краткотраен импулс и голям $I_и$ или „мек" режим, представен от продължителен импулс с малък $I_и$. При твърдия режим дъгата упражнява удар върху стопилката, а електродинамичните сили я привеждат в интензивно вълнообразно движение. Потоци от прегрята стопилка се движат от анодното петно към опашката на ваната по повърхността, а също и по напречното й сечение в дълбочина. Следователно е оправдано очакването, че при постоянна големина на средния ток видът на режима – твърд или мек, може да влияе върху геометрията и структурата на шева и зоната на термично влияние.

Литературното проучване показа, че липсват публикувани резултати от изследвания по поставения въпрос. Настоящата работа цели да изследва влиянието на режима на заваряване върху геометрията, структурата и микротвърдостта в характерни зони на заварените съединения.

## 2. Методика на работа

За ИВИГ заваряване са използвани планки с размери 200x140x2 mm от аустенитна стомана 1.4404 (X1CrNiMo 17 12 2, AISI 316L) по БДС EN 10088-2 с химически състав: 0,017% C, 0,54% Si, 1,76 % Mn, 0,002 % S, 0,034 % P, 16,91 % Cr, 10,1 % Ni 2,06 % Mo, 0,045 % N. Планките са обезмаслени с ацетон и прихванати без заваръчна междина. За осигуряване на равнинност и газова защита за корена на шева планките са установени в приспособление. Заварени са челни съединения без добавъчен метал и без подложка. За запалване и извеждане на дъгата са използвани технологични планки. Линейната енергия е определена по (2):

$$q_л = \frac{\eta I_{ср} U}{v} \qquad (2)$$

където: η=0,55 – ефективен топлинен коефициент на дъгата; U – напрежение на дъгата, V.

От (1) могат да бъдат изразени импулсният ток, фоновият ток и относителната продължителност на импулса:

$$I_и = \left[I_{ср} - I_ф\left(1 - \frac{t_и}{T}\right)\right]\frac{1}{\frac{t_и}{T}} \qquad 3)$$

$$I_ф = \left(I_{ср} - I_и \frac{t_и}{T}\right)\frac{1}{1 - \frac{t_и}{T}} \qquad (4)$$

$$\frac{t_и}{T} = \frac{I_{ср} - I_ф}{I_и - I_ф} \qquad (5)$$

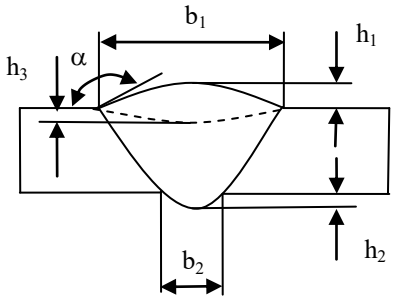
Използвани са токоизточник Kempi Mastertig 2300 MLS$^{TM}$ ACDC иториран W-електрод с диаметър 2,4 mm и ъгъл на заточване 30$^o$. Диаметърът на газовата дюза е 12 mm. В предишни изследвания е получен качествен шев на режим: $I_и$=164 A, $I_ф$=52 A, $t_и/T$=0,47, f=3 Hz, v=3,5 mm/s, дължина на дъгата L=2 mm, напрежение на дъгата 10 V, разход на защитен газ 6,5 l/min и 5,5 l/min, съответно за лицето и корена на шева. Този режим е приет за основен в изследването. Големината на средния ток, изчислена по (1), е $I_{ср}$=105 A, а линейната енергия на заваряване, изчислена по (2), е 173 J/mm.

По у-е (3) със среден ток $I_{ср}$=105 A, фонов ток $I_ф$=52 A и $t_и/T$=0,33-0,60, с отчитане

възможностите на заваръчния токоизточник, са изчислени границите на изменение на импулсния ток $I_и$.=120-210 А. От този интервал са избрани стойности, които осигуряват добре оформен шев с пълен провар и върху планка са стопени ивици.

Аналогично с $I_{ср}$=105 А при $I_и$.=164 А и $t_и/T$=0,42-0,54 за фоновия ток е изчислен възможен интервал на изменение $I_ф$=31-61 А. При $I_и$.=120-210 А и $t_и/T$=0,47 фоновият ток се изменя в интервала $I_ф$=11-91 А. За сравнение са изследвани режими, при които $I_и$.=170-210 А и $t_и/T$=0,40 – в този случай интервалът на изменение на фоновия ток е $I_ф$=34-61 А. Макар разликата между двете стойности на $t_и/T$ да е само 0,07, тя е съществена, тъй като е установено, че отклонение на $t_и/T$ с 0,02 от стойността му в оптимален режим на заваряване може да доведе до пробив на ваната или до непровар [6]. Избраните режими се съдържат в табл. 1 до табл. 3. Във всички опити честотата е 3 Hz.

Влиянието на параметрите на импулсния ток върху свойствата на заварените съединения е окачествено чрез геометрията на шева по фиг. 2, структурата и микротвърдостта на шева и ЗТВ.




*Фиг. 2 Размери на шева*

## 3. Резултати

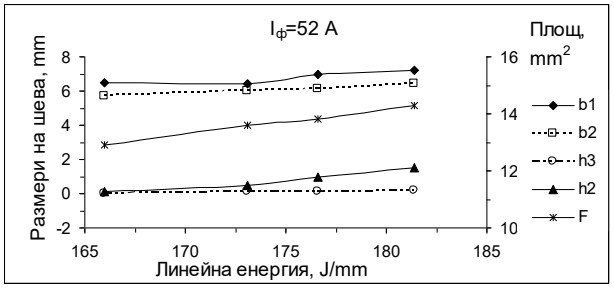
### 3.1 Заваряване с постоянни по големина среден и фонов ток

Импулсният ток и продължителността на импулса се изменят по пунктирната линия на фиг. 1. Данните за режима се съдържат в табл. 1. Геометрията на шева е представена на фиг. 9, а, б.

Качествен шев се получава при заваряване с ниски стойности на импулсния ток - режими 1 и 2 от табл. 1. Въпреки постоянната дължина на дъгата 2 mm, напрежението й нараства с импулсния ток. Това повишава линейната енергия до 10 % в зависимост от режима. С приблизително същата стойност нарастват ширината и площта на шева, фиг. 3. При импулсен ток 190-210 А се появява вдлъбване по лицевата страна и провисване на корена на шева, които удовлетворяват изискванията на ниво С, но са недопустими за ниво В на БДС ISO 5817 [7].

*Таблица 1 Режими на заваряване с постоянен фонов ток*

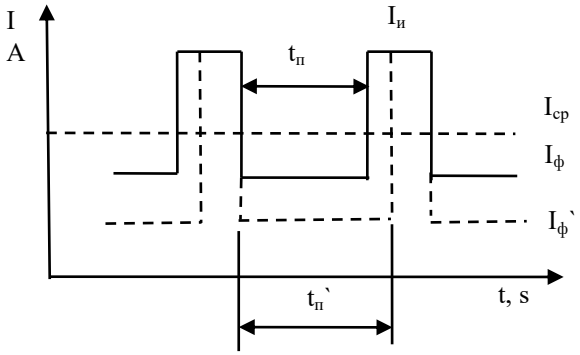
| Режим № | $I_и$ А | $I_ф$ А | $t_и/T$ | $I_{ср}$ А | U V | $q_л$ J/mm |
|---|---|---|---|---|---|---|
| 1 | 140 | 52 | 0,60 | 105 | 10 | 164 |
| 2 | 164 | | 0,47 | | 10,5 | 173 |
| 3 | 190 | | 0,38 | | 10,7 | 176 |
| 4 | 210 | | 0,33 | | 11 | 181 |




*Фиг. 3 Геометрия на шева при заваряване с постоянни среден и фонов ток; F – площ на напречното сечение на шева*

### 3.2 Заваряване с постоянни по големина среден и импулсен ток

Фоновият ток и продължителността на импулса се изменят според пунктирната линия на фиг. 4 и данните в табл. 2.




*Фиг. 4 Изменение на параметрите при заваряване с постоянни среден и импулсен ток*

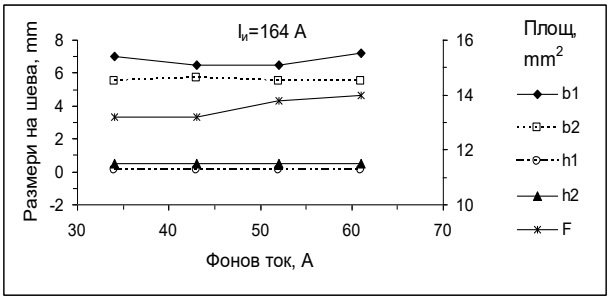
Напрежението на дъгата не се влияе от измененията на фоновия ток. Тъй като средният

© International Scientific Conference on Engineering, Technologies and Systems
TECHSYS 2016, Technical University – Sofia, Plovdiv branch
26 – 28 May 2016, Plovdiv, Bulgaria

*Таблица 2 Режими на заваряване с постоянен импулсен ток $I_и$*

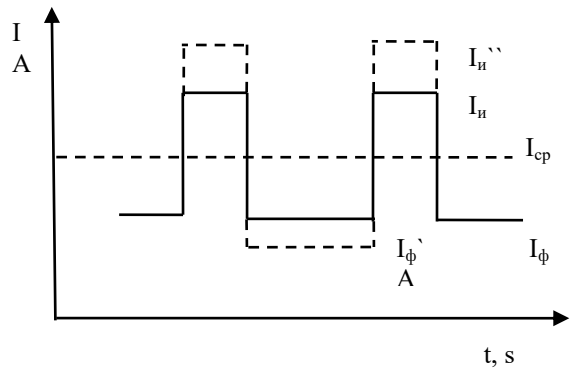
| Режим № | $I_и$ A | $I_ф$ A | $t_и/T$ | $I_{ср}$ A | U V | $q_л$ J/mm |
|---|---|---|---|---|---|---|
| 2 | 164 | 52 | 0,47 | 105 | 10,5 | 173 |
| 5 | | 61 | 0,42 | | 10,5 | 173 |
| 5a | | 43 | 0,51 | | 10,5 | 173 |
| 6 | | 34 | 0,54 | | 10,5 | 173 |

Изменението в геометрията на шева в зависимост от фоновия ток е показано на фиг. 5. Налице е промяна в размерите и площта на шева в границите на 1-3 %, която може да се счита за незначима. Геометрията на шева удовлетворява изискванията на ниво В на БДС ISO 5817.




*Фиг. 5 Геометрия на шева при заваряване с постоянни среден и импулсен ток; F – площ на напречното сечение на шева*

### 3.3 Заваряване с постоянни среден ток и продължителност на импулса

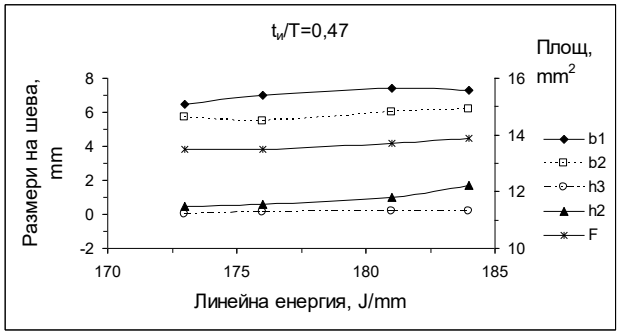



*Фиг. 6 Изменение на параметрите при заваряване с постоянни среден ток и продължителност на импулса*

Импулсният ток се повишава, а фоновият ток се понижава или обратно, без да се

*Таблица 3 Режими на заваряване с постоянна продължителност на импулса $t_и/T$*

| Режим № | $I_и$ A | $I_ф$ A | $t_и/T$ | $I_{ср}$ A | U V | $q_л$ J/mm |
|---|---|---|---|---|---|---|
| 2 | 164 | 52 | 0,47 | 105 | 10,5 | 173 |
| 7 | 180 | 38 | | | 10,7 | 176 |
| 8 | 200 | 20 | | | 11 | 181 |
| 8a | 210 | 11 | | | 11,1 | 182 |
| 9 | 170 | 61 | 0,40 | 105 | 10,6 | 174 |
| 10 | 190 | 48 | | | 10,9 | 179 |
| 11 | 210 | 34 | | | 11 | 181 |




*Фиг. 7 Геометрия на шева при заваряване с продължителност на импулса $t_и/T=0,47$; F – площ на напречното сечение на шева*

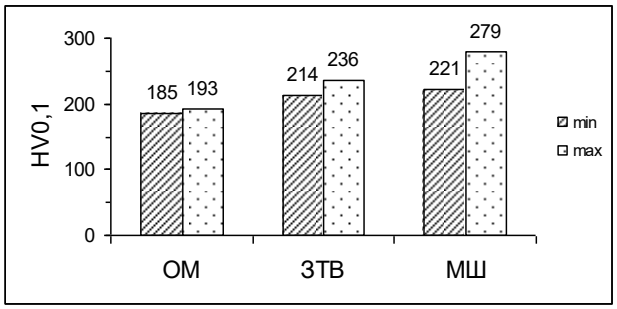
И тук, както в т. 4.3.1, при нарастване на импулсния ток напрежението на дъгата и линейната енергия се повишават с 4-5 %. Това повишение не влияе съществено върху геометрията на шева – ширината и площта му се изменят в границите 1-3 %. При заваряване с импулсен ток, по-голям от 180 А по лицевата страна на шева възниква вдлъбване 0,10-0,17 mm в зависимост от режима. В този случай геометрията на шева удовлетворява ниво С на БДС ISO 5817 [7].

От сравнението на резултатите, получени при заваряване с различна продължителност на импулса - $t_и/T=0,47$, фиг. 7, и $t_и/T=0,40$, следва, че не настъпва съществена промяна в геометрията на шева.

Copyright © 2016 by Technical University of Sofia, Plovdiv branch, Bulgaria ISSN Online: 2535-0048

### 3.4 Микротвърдост

Фиг. 8 показва минималните и максималните стойности на микротвърдостта, измерени в основния метал, ЗТВ и в метала на шева на съединения, получени от изследваните режими. Микротвърдостта се изменя в границите 185-279 HV0,1 и се влияе несъществено от избраните режими. Металът на шева има повишена микротвърдост, но максималната й стойност е достатъчно ниска и гарантира висока пластичност на съединението. Повишената твърдост в шева и ЗТВ се дължи вероятно на остатъчен ферит и на остатъчните заваръчни напрежения.




*Фиг. 8 Микротвърдост в различни зони на заварените съединения*

### 3.5 Металография

Формата и макроструктурата на шевове, заварени с постоянни стойности на различни параметри, са показани на фиг. 9. Всички шевове се отличават с плавен преход към основния метал. С минимално провисване и без надрези сред тях е шевът на фиг. 9, а, заварен с режим 1 от табл. 1. Шевовете, заварени с импулсен ток 210 А, провисват в корена или са леко вдлъбнати откъм лицевата страна, фиг. 9, б.



а

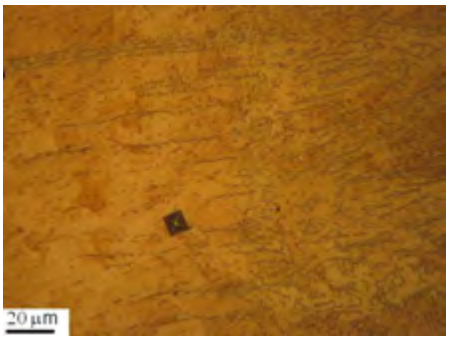



б

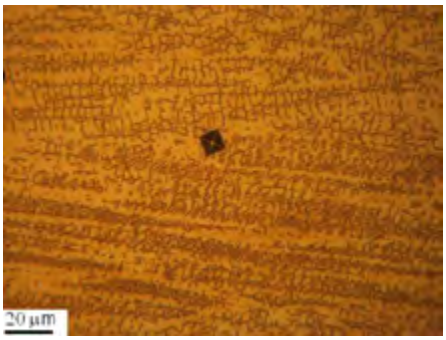
*Фиг. 9 Макроструктура на шевове, заварени с постоянен фонов ток: а) режим 1, табл. 1, F=12,8 mm$^2$; б) режим 4, табл. 1, F=14,3 mm$^2$*

Тези отклонения от оптималната форма на шева се дължат на повишената линейна енергия на заваряване и обуславят надрезно действие при наличие на променливо натоварване.

На фиг. 10 е представена микроструктурата на метала на шева, заварен с фонов ток 52 А на режими 1 и 2 от табл. 1. Шевът е плътен. Изграден е от аустенит и скелетообразен остатъчен ферит, който му придава необходимата технологична якост.




а




б

*Фиг. 10 Микроструктура на шевове, заварени с постоянен фонов ток 52 а, табл. 1: а) режим 1: I=164 А, I=52 А $t_u$/T=0,6, q=164 J/mm, линия на сплавяване; б) режим 2: I=164 А, I=52 А $t_u$/T=0,47, q=173 J/mm, метал на шева*

### 4. Изводи

1. При ИВИГ заваряване с постоянни по големина честота, среден и фонов ток и продължителност на импулса качествен шев се получава с минимален импулсен ток. Повишаване на импулсния ток в определените граници предизвиква нарастване на напрежението и на площта на шева до 10 %, съпътствано от провисване на корена.

2. ИВИГ заваряване с постоянни по големина честота, среден и импулсен ток и променливи фонов ток или продължителност на импулса не предизвиква съществени изменения

в линейната енергия. Получава се качествен шев.

3. В избраните интервали за вариране на параметрите на импулсния ток микротвърдостта на метала на шева, зоната на термично влияние и основния метал се изменя в границите 185-279 HV0,1.

## ЛИТЕРАТУРА

1. Becker, D., C. Adams, Jr. The role of pulsed GTA welding variables in solidification and grain refinement. Welding Journal, 1979, 5, 143-s – 152-s.

2. Balasubramaniana M.,V. Jayabalan, V. Balasubramanian Developing mathematical models to predict grain size and hardness of argon tungsten pulse current arc welded titanium alloy. Journal of Materials Processing Technology, 196, 2008, 222–229.

3. Goyal, V., P.K. Ghosh, J. Saini Process controlled microstructure and cast morphology of dendrite in pulsed current gas metal arc weld deposits of aluminium and Al-Mg alloy, Met. Mater. Trans., 38A, 8, 2007, 1794-1805.

4. Balasubramanian, V., V. Ravisankar, G. Madhusudhan Effect of pulsed current welding on mechanical properties of high strength aluminum alloy. Int J Adv Manuf Technol, 2008, 36, 254–262.

5. Lakshminarayanan, A., K., Shanmugam, V. Balasubramanian Effect of Autogenous Arc Welding Processes on Tensile and Impact Properties of Ferritic Stainless Steel Joints. Journal of Iron and Steel Research International. 2009, 16, 1, 62-68.

6. Ямболиев, Т., Иванов, Т. ВИГ Заваряване на аустенитна неръждаема стомана с обикновена и импулсна дъга. Journal of the Technical University Sofia, Branch Plovdiv, Fundamental Sciences and Applications", Techsys 2011, 16, 2011, 243-247.

7. БДС ISO 5817 - Заваряване. Нива за качество на несъвършенствата

Контакти
E-mail: tiamb@tu-plovdiv.bg

© International Scientific Conference on Engineering, Technologies and Systems
TECHSYS 2016, Technical University – Sofia, Plovdiv branch
26 – 28 May 2016, Plovdiv, Bulgaria

# SECTION 5 • СЕКЦИЯ 5

## TRANSPORT AND AVIATION ENGINEERING

## ТРАНСПОРТНА И АВИАЦИОННА ТЕХНИКА

© International Scientific Conference on Engineering, Technologies and Systems
TECHSYS 2016, Technical University – Sofia, Plovdiv branch
26 – 28 May 2016, Plovdiv, Bulgaria

# ACCIDENT MODELLING OF A QUADCOPTER

KONSTANTIN METODIEV

**Abstract:** *In the paper hereby, results obtained through a quadcopter flight simulation after a motor failure are presented. The approach towards solving the problem is deterministic. The system ODE describing the quadcopter motion are solved numerically for each degree of freedom. The study goal is determining a falling trajectory initial parameters so that the damaged quadcopter no longer threatens the people who happen to be beneath.*

**Key words:** *quadcopter, flight dynamics, accident*

## 1. Introduction

Wide usage of relatively new kind of unmanned aerial vehicle (UAV) called "Quadcopter" offers broad possibilities of taking aerial imagery and aerial observation at low cost. Because of that, it is affordable for mass user. Simultaneously, the matter of civil UAV flight safety is still under consideration in our country thanks to lack of statistics data and applicable regulations. Light as it is, the quadcopter gains significant momentum while falling from great height. Therefore, it appears to be a dangerous object for everyone who happens to be nearby on the ground. An eloquent example of similar accident is what happened in ski resort Madonna di Campiglio on 22nd of December, 2015. The shooting TV drone fell just next to contestant Marcel Hirscher who narrowly avoided severe injuries.

Reasons for accident happening could be bird collision, battery depletion, autopilot or engine failure, pilot's error, radio link loss, etc.

The problem being investigated in the paper hereby is working out approximately flight parameters prior to a failure so that aviation accident as defined in [1] to be avoided for sure. It is numerical simulation that is employed as a tool during computing the vehicle falling trajectory, not statistical approach. The results obtained could be useful to authorities to put together regulations of civil UAVs flight maintenance in the territory of Republic of Bulgaria. The results published in the paper however are not definitive, so any complement experiment should be carried out in addition. The author takes responsibility provided that the results obtained are approximate and tentative.

## 2. Flight dynamics

The investigation is carried out in two stages. First, the quadcopter motion is derived following engine failure until it crashes into the ground. A criterion of hitting ground based target is specified. During the second stage, a system ODE describing both translational and rotational motion is worked out numerically. Having had the initial conditions and real quadcopter data, the falling trajectory is simulated until the quadcopter crashes into the ground.

### 2.1. Quadcopter motion simulation as a point mass within vertical plane

A point mass moving within XY frame of reference is described by following system ODEs, [2]:

$$\begin{aligned} m\ddot{x} &= \sum_i F_{x,i} = 0 \\ m\ddot{y} &= \sum_i F_{y,i} = -mg \end{aligned} \tag{1}$$

In order to work out the point trajectory, the Reverse Rigid Body Dynamics problem must be solved. The initial conditions are velocity $V_0$, angle in relation to the horizon α, and flight height h. The system common integral is

$$\begin{aligned} x &= C_1 t + C_3 \\ y &= -\frac{1}{2} g t^2 + C_2 t + C_4 \end{aligned} \tag{2}$$

The integration constants, dependent of the initial conditions, are as follows:

Copyright © 2016 by Technical University of Sofia, Plovdiv branch, Bulgaria ISSN Online: 2535-0048

$$C_1 = V_0 \cos\alpha \quad C_2 = V_0 \sin\alpha$$
$$C_3 = 0 \qquad\quad C_4 = h \tag{3}$$

Then, the equations describing the point motion in terms of a parameter are following:

$$x = V_0 t \cos\alpha$$
$$y = -\frac{1}{2} g t^2 + V_0 t \sin\alpha + h \tag{4}$$

Finally, for the flight trajectory, it yields:

$$y = x.tg\alpha - \frac{g x^2}{2V_0^2}\left(1 + tg^2\alpha\right) + h \tag{5}$$

The last equation is quadratic in terms of the powers of tg$\alpha$. The solution curves family has an envelope which in turn could be found by working out following equations:

$$y - f(x, p) = 0$$
$$\frac{\partial y}{\partial p} = 0 \quad p = tg\alpha \tag{6}$$

After excluding the parameter p, for the envelope it yields:

$$y = \frac{-g}{2V_0^2} x^2 + \frac{V_0^2}{2g} + h \tag{7}$$

The derived curve is called “Safety Parabola” for the velocity $V_0$ set in advance. All ground based objects with coordinates below the parabola are potential targets.

### 2.2. Quadcopter motion simulation as a rigid body within 3D space

In order to derive the equations describing quadcopter motion in 3D space, the following symbols are adopted, fig. 1.



***Fig. 1.*** *Adopted project symbols.*

In the project, two Cartesian frames of reference are utilized. The ground based fixed frame is used to derive the mass center motion while the fixed frame of reference is suitable to obtain the rotational motion law. The body fixed frame axes are aligned with quadcopter arms. The yaw axis is complementary of the others so that the so-formed triad is right-handed. Each rotor rotates with angular velocity ωi, i = 1 ... 4. Also, the angles θ, ϕ, ψ are put down next to the fixed frame axes, so are the torques τθ, τϕ, τψ.

#### 2.2.1. Translation

In ground based fixed frame of reference, the quadcopter acceleration depends upon the thrust, the gravitational force, and the air drag. The system ODE describing mass center motion are, [3]:

$$m\ddot{\vec{x}} = \begin{Vmatrix} 0 \\ 0 \\ -mg \end{Vmatrix} + R\vec{T}_B + \vec{F}_D \tag{8}$$

where

$$R = \begin{Vmatrix} c_\phi c_\psi - c_\theta s_\phi s_\psi & -c_\psi s_\phi - c_\phi c_\theta s_\psi & s_\theta s_\psi \\ c_\theta c_\psi s_\phi + c_\phi s_\psi & c_\phi c_\theta c_\psi - s_\phi s_\psi & -c_\psi s_\theta \\ s_\phi s_\theta & c_\phi s_\theta & c_\theta \end{Vmatrix} \tag{9}$$

is a linear operator transforming a vector from ground based to body fixed frame and vice-versa. The symbols “c” and “s” denote respectively cosine and sine functions whilst the subscripts denote function argument. The vector

$$\vec{T}_B = \sum_{i=1}^{4} T_i = k \begin{Vmatrix} 0 \\ 0 \\ \sum_i \omega_{p,zi}^2 \end{Vmatrix}, \quad N \tag{10}$$

is the total thrust obtained from all on-board engines. It depends upon the rotor axis angular velocity ωp squared. The dimensional coefficient

$$k = \left( \frac{K_\upsilon K_\tau \sqrt{2\rho A}}{K_t} \right)^2, \quad kg.m \tag{11}$$

is dependent of the area A swept by the propeller, the air density ρ as well as three proportional coefficients reading the propeller blade configuration (Kτ), the counter electromagnetic force (Kυ), and the rotor current consumption (Kt). The vector

$$\vec{F}_D = -k_d \begin{Vmatrix} \dot{x} \\ \dot{y} \\ \dot{z} \end{Vmatrix}, \quad N \tag{12}$$

denotes the air drag force which is proportional to the quadcopter velocity times the dimensional coefficient kd, kg/s.

Details about obtaining the above equations could be found further in [3].

### 2.2.2. Rotation around a fixed point

Attitude of a rigid body which rotates around fixed point (three DOFs, i.e. rotations) could be derived by means of three Euler angles in fixed frame of reference, [4]. In this particular case, the body motion is described by following equations:

$$I\dot{\vec{\omega}} + \sum_{i=1}^{4} I_p \dot{\vec{\omega}}_{p,i} + \vec{\omega} \times \left[ I\vec{\omega} + \sum_{i=1}^{4} \left( \vec{\omega} + \vec{\omega}_p \right) \right] = \vec{\tau} \tag{13}$$

where subscript p denotes parameter relevant to the engine propeller. By means of the operator

$$\vec{\omega} = \begin{Vmatrix} \omega_x \\ \omega_y \\ \omega_z \end{Vmatrix} = \begin{Vmatrix} 1 & 0 & -s_\theta \\ 0 & c_\phi & c_\theta s_\phi \\ 0 & -s_\phi & c_\theta c_\phi \end{Vmatrix} \cdot \frac{d}{dt} \begin{Vmatrix} \phi \\ \theta \\ \psi \end{Vmatrix}, \quad s^{-1} \tag{14}$$

one could transform the angular velocity scalar components into the vector quantity **ω**. The matrix

$$I_{(p)} = \begin{Vmatrix} I_{x,(p)} & 0 & 0 \\ 0 & I_{y,(p)} & 0 \\ 0 & 0 & I_{z,(p)} \end{Vmatrix}, \quad kg.m^2 \tag{15}$$

is composed by mass moments of inertia. Both the propeller blade and the quadcopter have axes of symmetry which is why the products of inertia are zeroed. The vector

$$\vec{\tau} = \begin{Vmatrix} \tau_\phi \\ \tau_\theta \\ \tau_\psi \end{Vmatrix} = \begin{Vmatrix} Lk\left(\omega_{p,1}^2 - \omega_{p,3}^2\right) \\ Lk\left(\omega_{p,2}^2 - \omega_{p,4}^2\right) \\ b\sum_{i=1}^{4} (-1)^{i+1} \omega_{p,i}^2 \end{Vmatrix}, \quad N.m \tag{16}$$

denotes the torque affecting the quadcopter due to rotation of all available rotors in fixed frame of reference. The distance L is measured between the rotor axis and Z quadcopter axis, fig. 1. The dimensional coefficient

$$b = C_x \frac{1}{2} \rho A R_p^3, \quad kg.m^2 \tag{17}$$

takes into consideration the air drag force solely related to the propeller blade. It depends upon the air density ρ, the blade cross section contour area A, the propeller radii R, and the drag coefficient Cx. The system (13) gives the gyroscopic torque due to propeller angular acceleration. In the system equations the following transformation has been made:

$$I_p \dot{\vec{\omega}}_{i,p} = \vec{\tau}_{p,i} \tag{18}$$

which expresses an explicit relationship between angular momentum variation in time and torque. Besides, the following assumptions have been made in advance, [5], [6]:

$$I_x = I_y; \quad \omega_{x,p} = \omega_{y,p} = 0 \tag{19}$$

## 3. Numerical experiment

Both vehicle and propeller mass characteristics are obtained by means of Autodesk Inventor IDE v. 2016, [7]. A certain material has been assigned to each quadcopter part, i.e. PVC and Aluminum 6061. The quadcopter mass is 1094 gram whilst the inertia tensors are

$$I = \begin{Vmatrix} 23.84 & 0 & 0 \\ 0 & 23.84 & 0 \\ 0 & 0 & 47.14 \end{Vmatrix} E-03 \quad kg.m^2 \tag{20}$$

$$I_p = \begin{Vmatrix} 1.99 & 0 & 0 \\ 0 & 62.02 & 0 \\ 0 & 0 & 61.25 \end{Vmatrix} E-06 \quad kg.m^2 \tag{21}$$

Further details follow:

- Arm length L = 310E–03 m
- Coefficient k, formula (11), k = 10E–04 kg.m
- Coefficient kd, formula (12), kd = 0.25 kg/s
- Coefficient b, formula (17), b = 10E–07 kg.m$^2$
- Rotor angular velocity ωp, formula (16), $\omega_{p,i}$ = 1047 s$^{-1}$, i = 1 and 3; $\omega_{p,i}$ = –1047 s$^{-1}$, i = 2 and 4.

Having had these data and the initial conditions

$$\vec{x} = \begin{Vmatrix} 0 \\ 0 \\ 100 \end{Vmatrix} \quad \dot{\vec{x}} = \begin{Vmatrix} 27.78 \\ 0 \\ 0 \end{Vmatrix} \quad \vec{\theta} = \dot{\vec{\theta}} = \begin{Vmatrix} 0 \\ 0 \\ 0 \end{Vmatrix} \tag{22}$$

the equations (8) and (13) are worked out numerically following the explicit Euler method with constant time step of 5 msec. The utilized IDE is Matlab v.2015a. During integration, each time step consists of following stages which are to be performed in a row:

- The vector $d\boldsymbol{\theta}/dt$ is transformed in accordance with formula (14).
- The RHSs of equations (8) are computed by means of formulae (9) … (12).
- The linear acceleration at current time step is computed through equation (8).
- The additives taking part in system (13) are computed by formulae (14) … (18).
- The angular acceleration at current time step is computed by equation (13).
- The angular velocities vector $|\omega x\ \omega y\ \omega z|^T$ is integrated following the expression

$$\omega_{i+1} = \omega_i + \dot{\omega}_i dt \qquad (23)$$

- The angular velocity $d\theta/dt$ is computed by formula (14) and the results obtained by expression (23). The trigonometric functions periodic property must be taken into consideration so as to succeed inverting the matrix in (14). Otherwise, the matrix is singular.
- The vector $|\theta\ \phi\ \psi|^T$ is integrated numerically by means of formula

$$\theta_{i+1} = \theta_i + \dot{\theta}_i dt \qquad (24)$$

- The mass center velocities and coordinates are derived further having had the results after working out equations (8)

$$\begin{aligned} \dot{x}_{i+1} &= \dot{x}_i + \ddot{x}_i dt \\ x_{i+1} &= x_i + \dot{x}_i dt \end{aligned} \qquad (25)$$

## 4. Results

Having had the mentioned initial conditions (22), precisely flight height of 100 m and velocity of 100 km/h, a preliminary estimation of impact spot coordinates has been carried out by means of formulae (5) and (7).

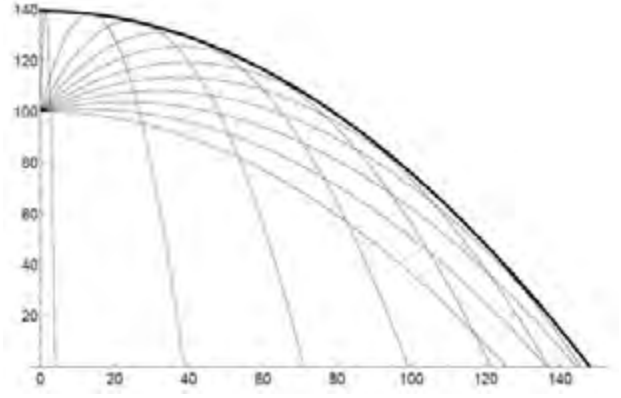



***Fig. 2.*** *Safety parabola at initial speed of 100 km/h*

In fig. 2, there are 10 possible fall trajectories shown which depend upon the angle in relation to the horizon. The trajectories envelope is also shown with thick line. It is obvious that the maximum range following a failure is approximately 150 meters.

Having preliminary estimated the falling spot, numerical simulation of the trajectory immediately after failure of all motors has been carried out following formulae (8) and (13). In the very moment of failure, the trajectory angle is 0 deg. The results are shown in fig. 3. Euler angles variation is not observable in this case. The distance covered by the quadcopter after failure is approximately 120 m.

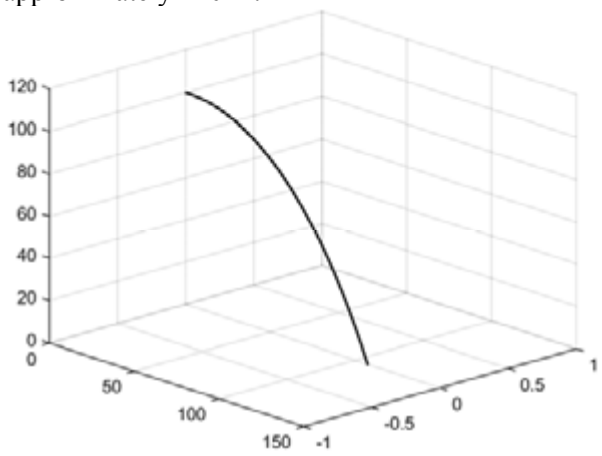



***Fig. 3.*** *Falling trajectory with no thrust.*

Another complementary study of the quadcopter falling trajectory with single engine failure has been carried out. The derived trajectory as well as the angles $\phi$, $\theta$ and $\psi$ variations are shown in fig. 4…7. The Euler angles values vary within $[0; 2\pi]$ rad on making at least one revolution along each body fixed axis. The distance covered by the quadcopter after failure is approximately 100 m. The simulation duration is 2000 steps at 5 msec, i.e. 10 sec in total.

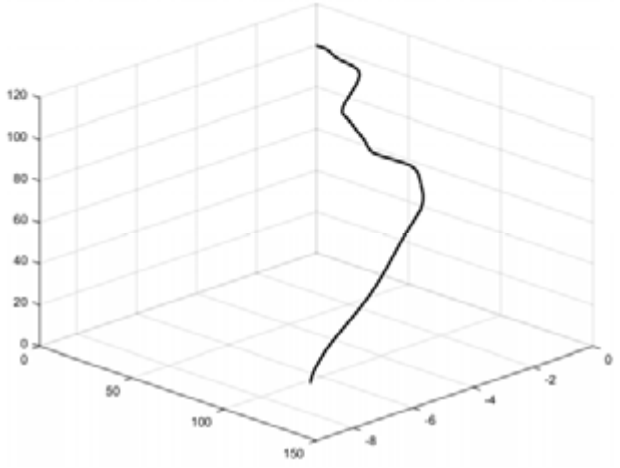



***Fig. 4.*** *Falling trajectory with all but one working motors.*

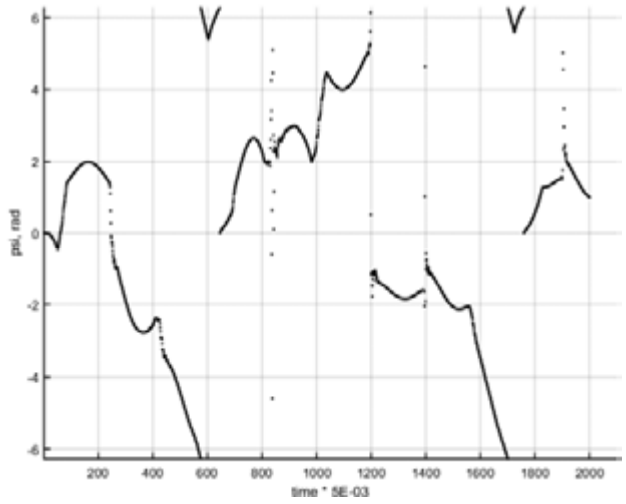



***Fig. 5.*** *Angle ϕ variation*

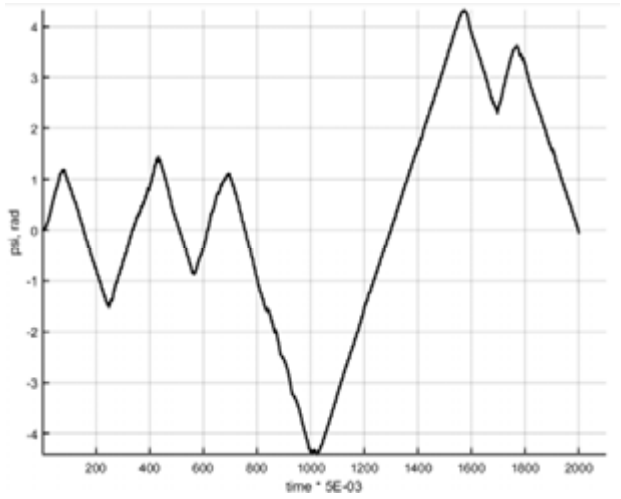



***Fig. 6.*** *Angle θ variation*

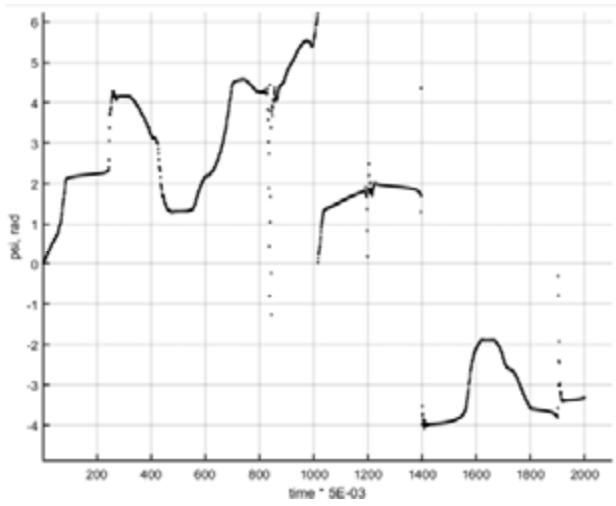



***Fig. 7.*** *Angle ψ variation*

## 5. Discussion

By means of preliminary analysis of falling trajectory (fig. 2) and assumed initial conditions, it is observable that people who are closer than 150 m to the failure point are in potential danger. The flight model in accordance with equation (5) however does not render an account of an important factor, i.e. the air drag. Having the three dimensional motion simulation made, it is found out that the large value of drag force (the friction drag prevails) could shorten the safety parabola significantly. However, it is not possible to envisage the wind speed at the time of failure. Besides, zero initial values of angles $\phi$, $\theta$ and $\psi$ are set in equation (22) which is one possibility among many. Nevertheless, a good correlation between the results obtained by 2D and 3D models and depicted in fig. 2 and fig. 3 is observable. The differences are explicable: the reason is the air drag taken in consideration in 3D motion model.

The dimensional coefficients in 3D model are derived under following assumptions, [8]:

- Power supply 12V DC
- Rotor angular velocity 10E+03 rpm
- Motor efficiency 50%
- Air density 1.225 kg/m$^3$

The exact values of coefficients determination are an elaborate problem which is off topic. Having the project precision in mind, it is solely required to keep the coefficients' order of magnitude correct. Further information about coefficients determination could be found in [5] and [9].

Conclusively, it should be noted that by means of the proposed model it is possible to work out a numerical solution under certain assumptions. The results obtained show that a quadcopter flight area must be limited to a certain distance to people being on the ground. This distance depends upon the mentioned parameters. People absence right below the quadcopter in the very moment of failure does not exclude accident from happening. This is the reason why a safe zone must be introduced. It is a malpractice to film mass activities from the air should the prescribed requirements are not met. The quadcopter itself is a complex apparatus with many electrical and mechanical onboard units. This circumstance increases the failure probability and justifies the current study.

The proposed mathematical model could be used further to study motion of a drone which has number of rotors different than four. For this purpose, it is necessary to modify equations (10) and (16). Another application could be determination of PID coefficients to stabilize and control quadcopter motion around the mass center. In this case the model might serve as an end unit

and replace the real machine, [3]. Another interesting problem is determining the minimum number of working motors so as to make up for failure of a single one. The model precision could be enhanced further if one takes into account the propeller blade flapping.

## REFERENCES


1. https://en.wikipedia.org/wiki/Aviation_accidents_and_incidents
2. Bachvarov, S., A. Djondjorov, B. Cheshankov, N. Malinov, *Manual of Solving Problems in Theoretical Mechanics, part II, Dynamics,* pages 32, 361, Publishing House Technics, Sofia, 1991, in Bulgarian
3. Gibiansky, A., *Quadcopter Dynamics, Simulation, and Control*, web, 2012
4. Mueller, M., R. D'Andrea, *Stability and Control of a Quadcopter despite the Complete Loss of One, Two or Three Propellers*, 2014 IEEE International Congress on Robotics and Automation, Hong Kong, China, 2014
5. Jirinec, T., *Stabilization and Control of Unmanned Quadcopter*, Master thesis, Czech Technical University in Prague, 2011
6. Stepaniak, M., *A Quadrotor Sensor Platform*, PhD thesis, Ohio University, 2008
7. https://grabcad.com/library/quadcopter-30
8. https://en.wikipedia.org/wiki/Motor_constants
9. Tayebi, A., S. McGilvray, "*Attitude stabilization of a four-rotor aerial robot,*" 43rd IEEE Conference on Decision and Control, vol. 2, pp. 1216–1221, 2004



Author's contacts:
Space Research and Technology Institute
Bulgarian Academy of Sciences
Acad. Georgy Bonchev str., block 1
Sofia, 1113
Bulgaria
Phone: +359 2 979 34 66
e-mail: komet@space.bas.bg

© International Scientific Conference on Engineering, Technologies and Systems
TECHSYS 2016, Technical University – Sofia, Plovdiv branch
26 – 28 May 2016, Plovdiv, Bulgaria

# AN EXPERIMENTAL STUDY OF THE INFLUENCE OF ADVANCE PROCESSOR ON SOME OPERATING PERFORMANCE INDICATORS OF SPARK IGNITION ENGINE WORKING WITH LPG

KRASIMIR AMBAREV

**Abstract:** *This article presents the results of experimental study of the effects of embedding of advance processor A.E.B. PUMA on some operating performance indicators of spark ignition engine Honda D15Z8 in his work with LPG. There are also analyzed data for acceleration time from 0 to 100 km / h with the engine working respectively with: gasoline, LPG with switched on advance processor and LPG with switched off advance processor. The times were compared with the acceleration time specified by the factory. There are also analyzed the results of measurements of power and torque of the driving wheels with the engine running on gasoline, LPG by working with switched on and working with switched off advance processor.*

**Key words:** *experimental study, SI engine performance, LPG, advance processor.*

## 1. Introduction

The depletion of the oil reserves globally and the increasingly strict requirements towards environmental pollution are a prerequisite for the use of gas fuels both in the newly manufactured, and for conversion of the existing motor vehicles in order to work with such fuels. The use of gas fuels in the internal combustion engines is related to a number of other advantages as well [1]. In the commonly integrated gas systems intended for the engine to work with gas fuel, the operational times of the gas injectors are defined through adjustment of the times of the gasoline injectors my means of correction coefficients for every operational mode of the engine. That is, an operating card for the alternative fuels is created, on the basis of the gasoline fuel card of the respective engine. In the commonly integrated LPG systems of fourth generation, belonging to the low or average price class, there is no option for correction of the angle of ignition timing, defined on the basis of the factory set card, in the instances when the engines work with LPG. Having in mind the fact that the speed of combustion of the fuel-air mixture is different when the engine works with gasoline and with LPG, an additional correction is required of the angle of ignition timing in the different operational modes. In the engine control systems of the automobiles without knock sensor, there is no option for correction of the angle of ignition timing when working with fuels with different properties. In such instances, in order to improve the performance and the cost effectiveness of the engine when working with LPG, it is recommended to install an external advance processor, correcting the angle of spark ignition timing in the different operational modes of the engine. Different types of advance processors exist. In some of them the angle of spark ignition timing is corrected depending on the rotation frequency, while in others there is a further correction due to the engine loading, which is detected by the signal of the MAP sensor or the flow meter.

There are different methods of measuring the engine power. In some of them the engine is fixed on a special stand with loading device, while in the others the power of the driving wheels is measured. In this instance the motor vehicle is positioned on a roll-stand. On the grounds of respective relationships the engine power is calculated on the basis of the driving wheels, i.e. in this instance it is measured indirectly. Other variant for indirect measuring of the engine power is by means of road tests related to the determination of the dynamic characteristics of the automobile. They include measuring the time necessary for the motor vehicle to reach the preliminary set speed, which is usually 100 km/h, measurement of the distance necessary to reach the set speed.

Copyright © 2016 by Technical University of Sofia, Plovdiv branch, Bulgaria ISSN Online: 2535-0048

It has been found out that the time for steady motion of the cars in urban traffic is just 15-25%, while the time for acceleration is 30-45% of the total time. Therefore an important dynamic characteristic of the automobiles is to accelerate fast, which impacts their average speed of movement and is in direct relation with the power performance of the engine.

The acceleration is achieved though consecutive transition from the slower to the faster gears, and it is characterized with the following major indicators: linear acceleration, time and distance for acceleration from the set initial to the end speed.

In the theoretical analysis of the acceleration the initial time is not taken into account, during which time in the case of starting from stationary position the angular velocity of the crankshaft of the engine and the primary shaft of the gear box are equaled by smooth switching on the clutch. This time is short and it does not influence significantly the total time for the acceleration. In addition to this, when pressing the clutch usually the accelerator pedal is pressed to its maximum, which corresponds to the engine operation as per external speed characteristic. Under these conditions the greatest accelerations are achieved.

The following equation is used for calculating the acceleration:

$$a = \frac{D - \psi}{\delta_a} g \,. \qquad (1)$$

Therefore the acceleration depends on the difference that expresses the reserve of dynamic factor after overcoming the driving resistance, and on the influence of the rotating masses, expressed by the coefficient $\delta_a$.

The acceleration time within a certain range is calculated analytically with the equation

$$t_y = \int_0^{t_y} dt = \int_{V_u}^{V_y} \frac{1}{a} dV \,. \,. \qquad (2)$$

The acceleration distance for the same speed rangeis calculated with the equation

$$S_y = \int_0^{S_y} dS = \int_0^{t_y} V dt \,. \qquad (3)$$

## 2. LPG operating system for Internal combustion engines

In a light passenger vehicle make Honda Civic Aerodeck, supplied with 16-valve, 4-stroke engine with spark ignition, with code D15Z8, which is with gasoline injection fuel system PGMFI, developed by Honda, an LPG system is installed, consisting of a computer supplied with electric installation AC STAG 300 ISA2 [2], a fuel injector for LPG – Alex Barracuda BR124P, reducer-evaporator [3] – Tomasetto AT09 Alaska, euro-gauge and gas container, homogenized according to standard ECE 67R-01 for operation with alternative fuels, as well as the necessary pipes.



***Fig. 1.*** *Front kit of LPG system*

The LPG/CNG injection rail Valtek $3\Omega$, included in the standard front kit offered on the market – Fig.1 is replaced with a gas injector by the company Alex, model Barracuda BR124 [4] – Fig. 2.



***Fig. 2*** *.Injection rail Alex Barracuda*

In addition, an advance processor is installed, produced by the Italian company A.E.B., model 515N Puma [5], shown on Fig. 3.

This type of advance processor is integrated in series in the electric chain between the electronic control unit of the engine and the commutator, which in this engine is positioned in the housing of the ignition distributor of the engine. The purpose of the advance processor is to dephase over time the electric impulse to the commutator generated by the electronic control unit of the engine. The introduced correction depends on the rotation frequency of the crankshaft according to a preliminary set algorithm

in its software. There is an option to switch off the advance processor in instances of idle running of the engine. For this purpose it is connected to the throttle position sensor.




***Fig. 3.*** *Reprogrammable timing advance processor A.E.B. Puma*

The advance processor is supplied with the software required for the respective engine – version 515N-07. A basic value is set of the angle of correction at 6 degrees, through the switches on the device PCB.

During the tests the motor vehicle is equipped with standard sized tires 185/60R14, product of the company Kleber Krisalp HP2, mounted on metal rims. The pneumatic tires are with pressure according to the instructions of the factory producer.

The measurements are made on a horizontal asphalt road, without wind.

For the measurements a board computer „Infoboard“ is used, „touch screen“ version [6]. „Infoboard“ is built on the basis of a 16 bits processor, supplied with colour sensor display. It has own operational system, powered by DC constant voltage by the diagnostics 5 pin connector of the car. It works with electronic control units of the engine compatible with the standard OBD2A, which is the original control unit of the engine with code D15Z8. For making the connection between „Infoboard“ and the electronic control unit of the car, a standard communication protocol ISO 9141-2 is used, where the connection is through the k-line through the diagnostics 5 pin connector of the car.

The board computer offers options such as: measuring the fuel consumption – in a certain moment and average for the given distance, average for the exploitation process of the vehicle, detailed data for each separate trip; provides an option related to the cost effective driving of the vehicle, reading and visualization of live data, clearing of errors, software for time and distance of acceleration, service intervals, expenditures related to the exploitation of the car, allowed speed assistant, option for recording the test results, and others.




***Fig. 4.*** *Board computer „Infoboard“, “touch screen” version*

A speed test was used for the measurements-“Speed Test” from the menu “Dyno”. The measurements include the time and distance of acceleration of the car from 0 to 100 km/h. The data for the rotation frequency and speed of motion are obtained from the respective sensors of the engine control system. The time is measured by the integrated timer.

It is necessary to start the test when the car is moving, before stopping at the start position. As a result of the measurement the relationship is visualized between the speed and time, as well as between the rotation frequency of the crankshaft and the time. The acceleration time and the acceleration distance are calculated necessary for reaching a certain speed.

The board computer allows also measurements of the power and the torque of the driving wheels, for first gear when the engine works with gasoline, with LPG with switched on or switched off advance processor. The programme “Dyno Run” from the menu “Dyno” is used. As a result of the measurements, the graphic relationship is obtained between the power and torque of the driving wheels and the rotation frequency. The display shows the maximum value of each of the two variables and the rotation frequency at which they are reached.

### 3. Experimental research

In order to determine the results of the operation of the advance processor on the engine performance, consecutive measurements were made of the acceleration time of the car from speed 0 to 100 km/h [7]. The measurements are done at initial angle of displacement of the correction curve – 6

degrees and the engine operating with: 1) gasoline; 2) LPG with switched on advance processor; 3)LPG with switched off advance processor. The plane of the correction coefficients for the gas injectors during the measurements is presented in Fig.5.

When the engine operating with LPG and the advance processor is switched on and switched off, the multiplier map is the same.

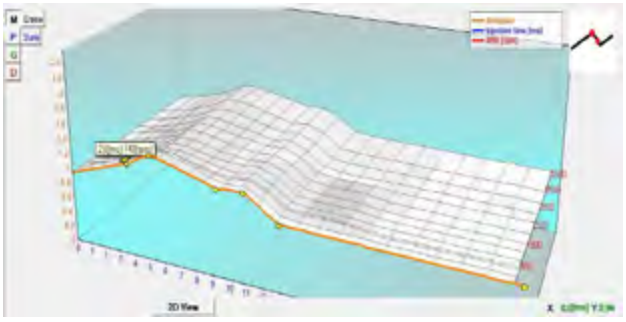


***Fig. 5.*** *3D multiplier map*

The results obtained from three consecutive measurements of each one of the three cases are average weighted and visualized on Fig. 6, 7 and 8.

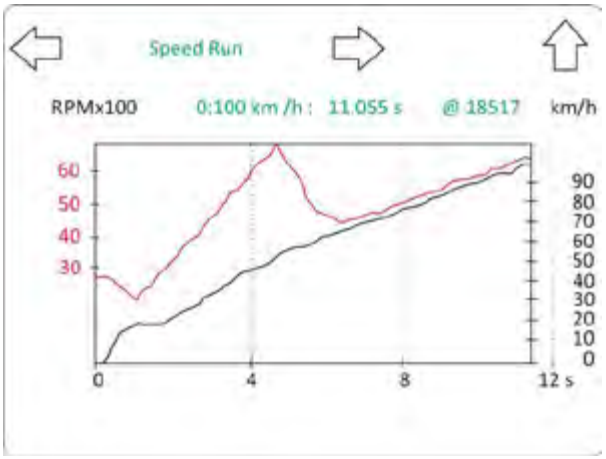



***Fig. 6.*** *Vehicle speed and engine speed with gasoline*




***Fig. 7.*** *Vehicle speed and engine speed with LPG and switched on advance processor.*

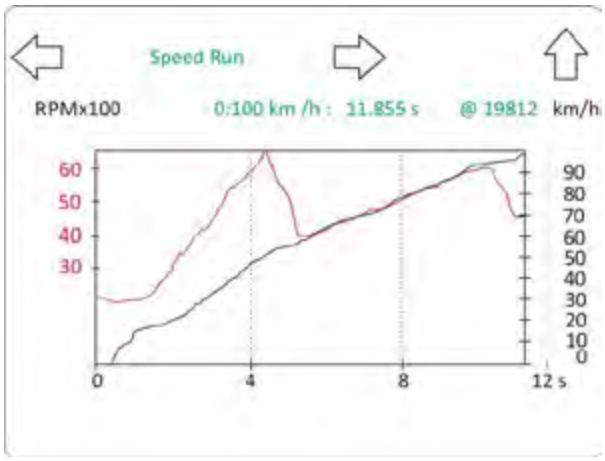



***Fig. 8.*** *Vehicle speed and engine speed with LPG and switched on advance processor.*

The results from the measurements are summarized in Table 1.

***Table 1.****Time and distance of acceleration from 0 to 100 km/h*

| Fuel | Time of acceleration, [s] | Distance of acceleration, [m] |
|---|---|---|
| Gasoline Petrol 96 Extra Force® | 11,055 | 185 |
| LPG and switched on advance processor | 11,452 | 188 |
| LPG and switched off advance processor | 11,855 | 198 |
| Gasoline [8] | 11,1 | - |

On the basis of the results obtained in the measurements, the following more significant conclusions can be made:

1) When the engine works with LPG and switched on advance processor, the acceleration time increases with 3,59% compared to the variant when the engine is working with gasoline, while the acceleration distance increases with 1.62%.

2) When the engine works with LPG and switched off advance processor, the acceleration time increases with 7.24% compared to the variant when the engine is working with gasoline, while the distance increases with 7.02%.

When measuring the power of the driving wheels and the torque, three measurements of the engine were made, while working with: 1) gasoline; 2) LPG with switched on advance processor; 3) LPG with switched off advance processor. The measurements were made on a horizontal, asphalt

road, without wind [9]. The results from the measurements are presented on Fig. 9, 10 and 11.

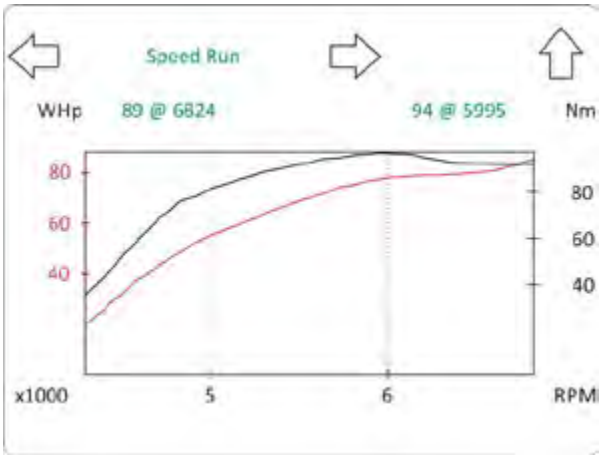



***Fig. 9.*** *Power and torque of the spark ignition engine operating with gasoline*

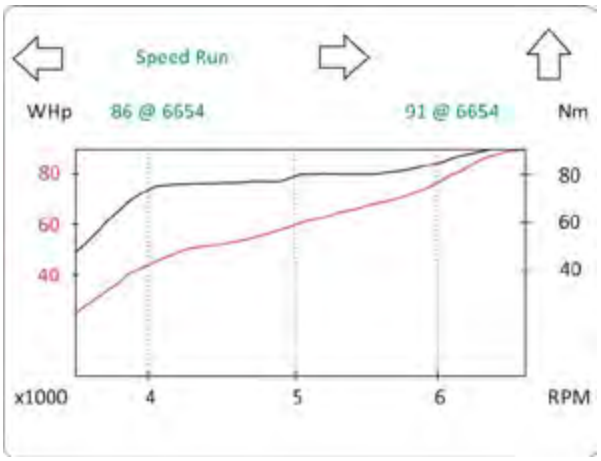



***Fig. 10.*** *Power and torque of the spark ignition engine operating with LPG and switched on advance processor.*




***Fig. 11.*** *Power and torque of the spark ignition engine operating with LPG and switched off advance processor.*

The results from the measurements are summarized and presented in Table 2.

***Table 2.****Power and torque at driving wheels*

| Fuel | Power, [WHP]/ [rpm] | Torque, [Nm]/ [rpm] |
|---|---|---|
| Gasoline Petrol 96 Extra Force® | 89/6824 | 94/5995 |
| LPG and switched on advance processor | 86/6654 | 91/6654 |
| LPG and switched off advance processor | 82/6793 | 87/5084 |
| Gasoline [8] | 114/6500* | 134/5400** |

* Engine power, [HP]
** Engine torque, [Nm]

The performed measurements show the following:

1) When the engine works with LPG and switched on advance processor, the measured power of the driving wheels is lower with 3,37%, the torque – with 3,19%, compared to operating the gasoline.

2) When the engine works with LPG and switched off advance processor the acceleration time increases with 7,87% compared to the engine operating with gasoline, while the distance is increased with 7,44%.

If we take that the transmission performance is 0,85, then the maximum measured power of the driving wheel corresponds to 105 HP power of the engine.

## 4. Conclusion

The use of advance processor in cars with spark ignition engines without the option for automatic correction of the angle of ignition timing improves the dynamic performance of the car, and in particular the power performance of the engine. The best results with regards to time and distance of acceleration from 0 to 100 km/h are achieved when the engine operates with gasoline. The highest power and torque of the internal combustion engine is observed when it is operating with gasoline. The performed measurements show that better results are achieved of the spark-ignition engine with LPG with switched on advance processor, compared to the variant of switched off advance processor. The relatively small differences in the measured results

gives us grounds to assume that the function of the advance processor does not influence significantly the exploitation performance of the engine with LPG systems of fourth generation subjected to testing.

## REFERENCES


1. Ivanov, Z. и Dimitrov, A. (2009), *LPG systems for cars*, Tehnika, Sofia.
2. http://www.ac.com.pl/en/produkt/362/stag-300-isa2
3. http://www.tomasetto.com/en/products/lpg-reducers/model-at09
4. http://www.autogaz-alex.pl/index.php?option=com_content&view=article&id=190:05-barracudaen
5. http://www.aeb.it/Products/Products/ProdID/24/CatID/8 &catid=21:injectors&Itemid=133&lang=en
6. http://www.infobordbg.com/
7. Meywerk M. (2015), *Vehicle dynamics*, Publisher, John Wiley & Sons Ltd.
8. http://www.automobile-catalog.com/auta_perf1.php
9. Neykov S., Yordanov P., Katsov D., Penchev S. (2006), *Handbook for laboratory works in "Automotive Engineering part I",* Publishing - Printing unit of the Technical University of Sofia, Branch Plovdiv, Plovdiv.



Technical University of Sofia,
Branch Plovdiv
25 Tsanko Diustabanov St,
4000 Plovdiv
Bulgaria
e-mail: kambarev@tu-plovdiv.bg

© International Scientific Conference on Engineering, Technologies and Systems
TECHSYS 2016, Technical University – Sofia, Plovdiv branch
26 – 28 May 2016, Plovdiv, Bulgaria

# ГАООБМЕНЕН ПРОЦЕС ПРИ БЕНЗИНОВИТЕ ДВИГАТЕЛИ С ГАЗОТУРБИННО ПЪЛНЕНЕ

РАДОСЛАВ КОСТОВ

**Резюме:** *В статията са анализирани, физичната основа на газообменните процеси и показателите, по които се осъществява усъвършенстването на газообменните процеси при бензиновите двигатели с вътрешно горене с газотурбинно пълнене.*

**Ключови думи:** *бензинов двигател, газообмен, газотурбинно пълнене*

# GAS EXCHANGE PROCESS IN PETROL ENGINE TURBOCHARGED

RADOSLAV KOSTOV

**Abstract:** *The article analyzes the main physical principles and indicator of gaseous exchange processes and leads to the improvement of the gas exchanges in the petrol engines turbocharged.*

***Key words**: petrol engines, gas exchange, turbocharged*

## 1. Основни положения

Във връзка със задълбочаването през последните години енергийна криза се появи необходимостта да се проведат по широки и задълбочени изследвания за повишаване на икономичността на сега работещите в експлоатация двигатели.

Сред успехите на бензиновите двигатели през последните двадесет и пет години най-важно е може би внедряването на турбокомпресора, задвижван от отработилите газове и използван за принудително пълнене на двигателя. Чрез принудителното пълнене се увеличава ефективната мощност на двигателя, повишава се горивната икономичност и се намалява отделянето на токсични компоненти в отработилите газове. В същото време няма съществено увеличаване на масата и габаритите на двигателя.

Решаващ фактор за повишаване на мощността и икономичните показатели на двигателя е и газообменът поради, което той винаги е бил обект на непрекъснати изследвания. За оценка на много основни фактори, определящи качеството на работния процес, топлинното и механичното натоварване на редица най-напрегнати детайли и възли на буталните двигатели са индикаторните диаграми на високите налягания в цилиндрите и диаграмите на помпените ходове (пълнене и изпускане). За оценка на КПД и протичането на характеристиките на турбокомпресора в действителните условия на работа съвместно с двигателя. Особено важно има значителното изменящите се във времето параметри на отработилите газове пред турбината. Определянето на параметрите на въздуха в пълнителния колектор е важно за оценката на условията на работа на компресора и за осъществяването на задълбочен анализ на напълването на цилиндрите с въздух.

В условията на принудително пълнене, характерно е значителното изменение на налягането в характерните точки на индикаторната диаграма и освен това диаграмата на помпените ходове е единствен източник за двигателите с принудително пълнене за определяне на помпените загуби, представляващи значителна част от сумарните механични загуби. Това определя интереса към индицирането на налягането в цилиндрите при газообмените процеси.

Copyright © 2016 by Technical University of Sofia, Plovdiv branch, Bulgaria ISSN Online: 2535-0048

## 2. Цел на анализа

Целта на настоящия анализ е да се представи състоянието на проблема с физическите основи на газообмените процеси и показателите по които се осъществява газообменния процес на бензиновите двигатели с газотурбинно пълнене.

## 3. Същност на проблема

По отношение на физическите основи на газообмения процес за двигател с газотурбинно пълнене може да спомена, че очистването на цилиндрите от отработили газове и напълването му с прясно работно вещество са основните процеси на газообмена. Тяхната продължителност се определя от фазите на газоразпределението, т.е. от момента на отваряне и затваряне на пълнителните и изпускателните клапани.

При четиритактовите двигатели продължителността на газообмена е по-голяма от продължителността на такта пълнене и изпускане. Изпускателните клапани се отварят на ъгъл $\alpha_1$ от завъртането на коляновия вал преди ДМП, а пълнителния клапан се затваря на ъгъл $\alpha_4$ след ДМП. Общата продължителност на газообмена съответства на 400º – 520º от завъртането на коляновия вал – фиг. 1.

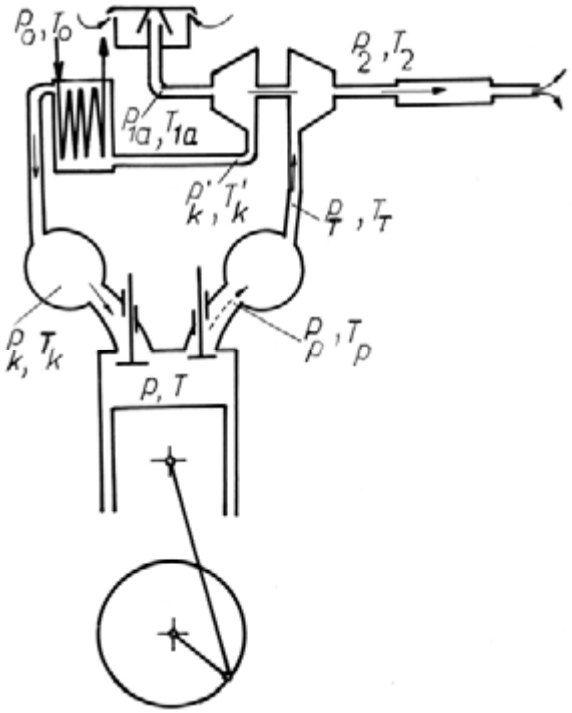



***Фиг. 1.*** *Фазова диаграма на газоразпределението*

Параметрите, характеризиращи газа при постъпването му в цилиндъра и при напускането ми от него, влияят съществено върху газообменния процес. На фиг. 2 е показана снема на пълнителния и изпускателния тракт на т. нар. комбинирани двигатели и са обозначени параметрите на газ в характерните му точки.

Газообменния процес се разделя на няколко периода (свободно изпускане, изпускане, пълнене и дозареждане) в зависимост от параметрите на газа във пълнителния и изпускателния тракт. Това разделение в значителна степен е условно, но то улеснява изучаването на физическата същност на явлението.

Същността на потичане на газообмена в четиритактов бензинов двигател с газотурбинно пълнене се състои в следното. В началото на отваряне на изпускателния клапан, налягането в цилиндъра на комбинирания двигател може да достигне до 0,6 – 0,8 MPa и повече в зависимост от налягането $p_к$ на пълнене.




***Фиг. 2.*** *Схема на газообмен при комбиниран двигател*

Скоростта на изтичане на газовете от цилиндъра при свободно изпускане зависят от разликата на налягането в цилиндъра p и в изпускателния колектор $p_p$. В началото на отварянето на изпускателния клапан, налагането $p_p$ е значително по-ниско от налягането p, а отношението им е по-малко от критичното:

$$\frac{p_p}{p^*} < \frac{p_{кр}}{p^*} = \left(\frac{2}{\kappa+1}\right)^{\frac{\kappa}{\kappa-1}}, \qquad (1)$$

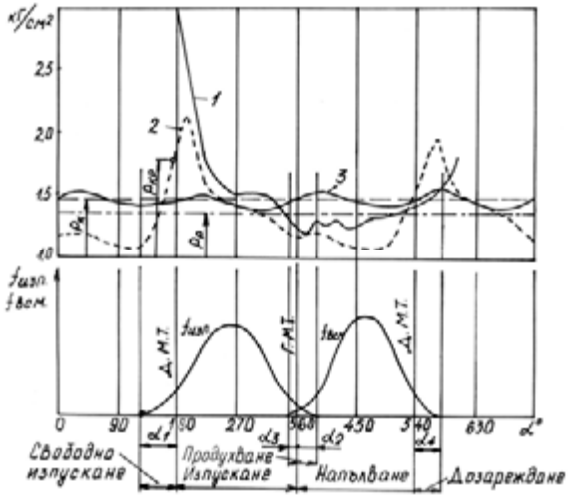
където: p* е налягането на заприщения поток в цилиндъра.

Приемайки за продуктите на горене к=1,3 получаваме $p_{кр} \big/ p^* = 0{,}546$. С достатъчно приближение, скоростта на изтичане на газа през клапаните в над критичната област

на изтичане, когато $\frac{p_p}{p} < \frac{p_{кр}}{p}$ може да се приеме равна на критичната скорост. Скоростта на газа в критично състояние е:

$$Q_{кр} = \sqrt{2.9{,}81.\frac{\kappa}{\kappa+1}RT^*}\,, \qquad (2)$$

където: $T^*$ е температурата на заприщения поток в цилиндъра.




***Фиг. 3.*** *Изменение на налягането в цилиндъра при пълненето и изпускането, в съответствие с фазите на газоразпределение и хода на клапана*

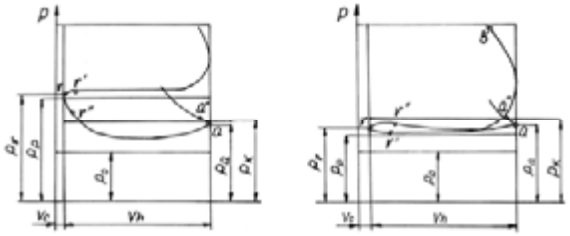
1 – налягане в цилиндъра; 2 – налягане в изпускателния тръбопровод;
3 – налягане в изпускателния тръбопровод

Интегралът $\int_{\alpha_1}^{\alpha_2} fd\alpha$ е еквивалентен на площта под кривата на изменението на проходното сечение на пълнителния или изпускателния клапан и се нарича ъгъл–сечение. Пропускателната способност на органите на газоразпределението се характеризира с тяхното време сечение

$$\int_{t_2}^{t_1} fdt = \frac{\int_{\alpha_1}^{\alpha_2} fd\alpha}{6n}. \qquad (3)$$

В началото на свободното изпускане налягането $p_{B'}$ (фиг. 4) и температурата на газа в цилиндъра бързо се повишават, тъй като количеството на газа се намалява, а обема на цилиндъра се увеличава. Вследствие на бързото изменение на налягането в изпускателния тръбопровод се образува вълна на налягането (крива 2 от фиг. 3). В резултат на падането на налягането в цилиндъра и увеличаването му в изпускателния тръбопровод, отношението $p_p / p$ бързо расте и при положение на буталото близо до ДМП достига критични стойности.

Критичната скорост на изтичане на газа в надкритичната област по време на свободното изпускане се намира в границите 500-700 m/s. При работа на двигателя на частични режими, преминаването на скоростта през критични стойности става по-рано по отношение на ДМП, тъй като налягането в цилиндъра в началото на изпускането е по-малко отколкото на номинален режим.



***Фиг. 4.*** *Изменението на налягането в цилиндъра на четиритактов двигател по време на газообмен*

а – комбиниран двигател при $p_к / p_p < 1$;

б – комбиниран двигател при $p_к / p_p > 1$

В подкритичната област при $\frac{p_p}{p} > \frac{p_{кр}}{p}$, скоростта на изтичане на газа от цилиндъра се намалява значително по-бързо отколкото в надкритичната област. През по-голямата част на процеса изпускане, отделянето на продуктите от горенето става вследствие на намаляване на обема на цилиндъра при движение на буталото към ГМП. При завъртането на коляновия вал на 15º–20º след ДМП, налягането в цилиндъра се установява близо до налягането в изпускателния колектор.

Скоростта на газа и изменението на налягането в изпускателния тръбопровод зависят от скоростта на движение на буталото и отношението на площта на проходното сечение към площта на буталото. Голямо влияние на скоростта и налягането оказват газодинамичните явление в изпускателния тръбопровод и в цилиндъра.

Температурата на газовете в цилиндъра по време на изпускането, когато налягането се изменя в малки граници, остава почти постоянно. Понижаването на температурата е възможно вследствие отдаване на топлина в стените на цилиндъра, но то е незначително и обикновено не се отчита. Средната скорост на газовете през изпускателните клапани на нормален режим на двигателя е 60-150 m/s.

По време на припокриването на клапаните, изменението на параметрите на газа

в цилиндрите зависи от отношението $p_к / p_p$. Ако средното налягане $p_к < p_p$, то в момента на отварянето на пълнителния клапан (точка r' от фиг. 4а) налягането в цилиндъра може да бъде по-голямо от това във пълнителния колектор. В този случай е възможно преминаването на продуктите от горенето от цилиндъра във пълнителния тръбопровод. При правилно подбран ъгъл на предварително отваряне на пълнителния клапа, количеството на отработилите газове, което преминава в изпускателния тръбопровод е незначително, тъй като площта $f_{пкл}$ – проходното сечение на пълнителния клапан, в началото на отварянето до ГМП има неголямо значение и може да отсъства обратно връщане на газове.

В резултата налягането и ускорението на газовата маса в изпускателният тръбопровод по време на припокриването на клапаните, зад изпускателните клапани може да се образува вълна на разреждане (фиг.3). Това е възможно в случай, че налягането в изпускателния колектор е по-ниско от налягането в цилиндъра и в пълнителния колектор. При такова съотношение на наляганията протича така нареченото продухване на цилиндъра, въпреки че средното налягане $p_к$ е по-малко от средното $p_p$. Използването на вълните на разреждането в случая $p_к / p_p < 1$ може да обезпечи продухването при работа на двигателя в тесен диапазон на режима на работа. За избягването на преминаването на отработили газове в пълнителния колектор при двигатели работещ на променлив режим, ъгъла на припокриване на клапаните при $p_к / p_p < 1$ се прави малък.

Налягането в цилиндъра p в края на изпускането в ГМП обикновено е по-голям от средното налягане $p_p$ в изпускателния колектор, затова известно време след ГМП изтичането през изпускателния клапан продължава. С намаляването на количеството газ в цилиндъра и увеличаването на обема му, налягането и температурата му бързо спада (фиг. 4а).

Ако отношението на налягането $p_к / p_p > 1$, то въздухът започва да навлиза в цилиндъра веднага след отварянето на пълнителния клапан. Едновременно с това до затварянето на изпускателния клапан (точка r'' фиг. 4б) продължава изтичането на газ от цилиндъра – протича продухване. В началото на продухването от цилиндъра изтичат само продуктите на горенето. Когато постъпващия в цилиндъра въздух достигне изпускателния клапан, започва изтичането на смес от прясно работно вещество и отработили газове. Количеството на прясното работно вещество, оставащо в цилиндъра след завършването на газообмена в този случай е по-малко от постъпващото, а коефициента на продухване $\varphi_n > 1$.

По време на продухвано, количеството на остатъчните газове се намалява и с увеличаването на коефициента на излишък на продухвания продукт $\varphi_к$ се стреми към нула.

Температурата $T_r$ на остатъчните газове зависи от степента на сгъстяване, натоварването и оборотите на двигателя. При изчисляването на работния цикъл, величината $T_r$ се оценява ориентировъчно, като се отчита, че тя е близка до температурата на отработилите газове, измерена в изпускателния колектор. Грешката за $T_r$ при малки стойности на коефициента на остатъчни газове $\gamma_r$, в крайните резултати се отразява незначително. За бензинов двигател с газотурбинно пълнене Tr = 900º – 1000º.

В резултат на смесването на постъпващото в цилиндъра прясно работно вещество с продуктите от горенето, температурата на газовете бързо пада и затова процеса на напълване остава приблизително постоянен.

При отношение $p_к / p_p > 1$, налягането в цилиндъра по време на продухването може да се увеличи или намали. Ако налягането $p_к$ е значително по голямо от $p_p$,то количеството на въздуха, постъпващо в цилиндъра след отварянето на пълнителния клапан е по-голямо от количеството на изтичащите газове. В резултат на това количеството на сместа от прясно работно вещество и продуктите от горенето нараства, а налягането се увеличава, нищо че обемът след ГМП също се увеличава.

На номинален режим в повечето комбинирани двигатели $p_к / p_p > 1$. На частични режими съотношението на налягането зависи от условията на съвместна работа на компресора, турбината и буталната група. Те се определят от техните характеристики и принципната схема на комбинирания двигател.

При работа на комбинирания двигател с газова връзка, по товарната характеристика на номинален режим, отношението $p_к / p$ с намаляване на натоварването се увеличава.

При продухването се подобрява очистването на цилиндъра от продуктите на горенето, понижава се температурата на нагретите детайли – бутало, изпускателни клапани, цилиндрова глава и с това се повишава надеждността и дълговечността на двигателя. От друга страна, голяма част от работата се губи за

сгъстяване на продухания въздух в компресора и ефективния КПД на двигателя при повишаване на интензивността на продухването се понижава. По опитен път е установено, че с увеличаването коефициента на продухване повече от 1,2, понижението на температурата на буталото на четиритактов двигател става много бавно, а ефективния КПД продължава да намалява. В съществувате комбинирани двигатели $\varphi_n = 1{,}0 - 1{,}25$.

Налягането в цилиндрите по време на напълването е по-малко от налагането в пълнителния колектор приблизително с големината на хидравличните загуби във пълнителния тръбопровод и пълнителите клапани. Тези загуби зависят главно от скоростта на движението на въздуха и конструктивните особености на пълнителния тракт. На скоростта на прясното работно вещество влияе скоростта на буталото, отношението на площта на буталото към площта на проходното сечение на клапана, а така също и характера на газодинамичните явления във пълнителния тръбопровод.

По време на дозареждането, прясното работно вещество продължава да постъпва в цилиндъра, тъй като налягането $p_a$ в цилиндъра при положение на буталото в ДМП е по-малко от налягането $p_к$ (фиг. 3 и фиг. 4) и сгъстяването в цилиндъра до момента на затварянето на пълнителния клапан протича с променливо количество работна смес. Продължителността на дозареждането зависи от налягането $p_a$ в цилиндъра при положение на буталото в ДМП и налягането $p_к$. Ако по време на дозареждането налягането в пълнителния колектор нарасне то дозареждането се увеличава и обратно. За повишаването на количеството работна смес, постъпваща по време на дозареждането, пълнителния клапан трябва да се затвори малко по-късно от момента , в който налягането в цилиндъра става равно на налягането в пълнителния колектор. Ако той се затвори по-късно, работната смес ще изтече обратно от цилиндъра и в резултат от това количеството прясно работно вещество може да се намали, нищо че в началото е имало дозареждане.

По отношение на показатели по които се оценява съвършенството на газообменния процес на двигател с газотурбинно пълнене, основните критерии за съвършенството на газообменния процеси са качеството на напълването и очистването на цилиндрите. Мощността на двигателя при равни други условия е токова по-голяма, колкото количеството на прясното работно вещество, намиращо се в цилиндъра след завършването на напълването е по-голямо. Очевидно количеството прясно работно вещество зависи от съвършенството на очистването на цилиндъра от продуктите на горенето. Част от обема на цилиндъра се заема от отработилите газове, който не са успели да се отделят (напуснат).

Съвършенството на очистването на цилиндъра се оцелява чрез коефициента на остатъчните газове – отношението на количеството киломолове остатъчни газове $M_r$ към количеството киломолове прясно работно вещество $M_1$

$$\gamma_r = \frac{M_r}{M_1}. \qquad (4)$$

Ако количеството на остатъчните газове прясно работно вещество се изразява в килограми то:

$$\gamma_r = \frac{G_r.m_1}{G_1.m_r}, \qquad (5)$$

където: $m_1$, $m_r$ са съответните молекулни маси.

Практическото количество прясно работно вещество, което постъпва в цилиндъра се отличава значително от теоретичното, защото налягането в края на пълненето при всички четиритактови двигатели е по-малко от налягането в пълнителните органи $p_к$, вследствие наличието на хидравлични загуби във пълнителния тракт, в това число и в пълнителните органи. Температурата на прясното работно вещество в цилиндъра в края на напълването обикновено е по-висока от $T_к$, тъй като по време на напълването се загрява от стените на цилиндъра, чиято температура е по-висока от $T_к$.

Степента на запълване на цилиндрите с прясно работно вещество се характеризира с коефициента на напълване – отношението на количеството прясно работно вещество,,кум теоретичното количество (това, което може да запълни работния обем на цилиндъра при налягане $p_к$ и температура $T_к$)

$$\eta_v = \frac{M_1}{M_t} = \frac{G_1}{G_t} = \frac{G_1}{\rho_k.V_h}, \qquad (6)$$

където: $G_t$ е теоретичната маса на прясното работно вещество;

$\rho_к$ - плътността на прясното работно вещество при налягане $p_к$ и температура $T_к$.

За бензинови двигатели с газотурбинно пълнене $\eta_v = 0{,}75 - 0{,}90$.

Количеството на прясното работно вещество, постъпващо в цилиндъра през пълнителите органи (клапани) по време на продухването не остава цялото в цилиндъра. Част от него изтича през изпускателните клапани в изпускателния тръбопровод и не участва в осъществяването на работния цикъл на буталния двигател.

Отношението на количеството въздух $G_k$ постъпващо по време на продухването и напълването, към количеството прясно работно вещество $G_1$, се нарича коефициент на продухване

$$\varphi = \frac{G_k}{G_1} = \frac{M_k}{M_1}. \qquad (7)$$

Реципрочната стойност на коефициента на продухване се нарича коефициент на използване на продухвания въздух

$$\eta_u = \frac{1}{\varphi} = \frac{G_1}{G_k}. \qquad (8)$$

Този коефициент определя частта въздух останала в цилиндъра от цялото количество постъпи в цилиндъра по време на газообмена.

Сумарен коефициент на въздушното отношение – отношението на разхода на въздух на двигателя към разхода на въздух, теоретично необходим за пълното изгаряне на горивото

$$\alpha_c = \frac{G_k}{l_0 . G_m}, \qquad (9)$$

където: $G_k$ е разход на въздух, kg/h;

$G_m$ - разход на гориво, kg/h;

$l_0$ - количеството въздух, теоретично необходимо за пълното изгаряне на 1 kg гориво.

След преработване на горната формула получаваме

$$\alpha_c = \frac{G_1}{l_0} . \frac{G_k}{G_k} = \alpha . \varphi . \qquad (10)$$

**4. Заключение**

В заключение може да кажем следното, че оценката на качеството на газообмена, направена само по качеството на очистването и напълването е недостатъчна. Протичането на газообмена е неразривно свързана и с други процеси, съставящи действителния цикъл на двигателите с газотурбинно пълнене.

Някой от коефициентите, характеризиращи газообмена са непосредствено свързани с температурните напрежения в такива детайли на двигателя като изпускателни клапани, бутала и др., изпитващи големи натоварвания. Затова при избора на параметрите и показателите за протичане на газообмена при бензиновите двигатели е необходимо да се отчитат и факторите на надеждност и дълговечност на двигателя.

**ЛИТЕРАТУРА**


1. Гуревич М.И. (1979). *Теория струй идеальной жидкости*. Москва.
2. Дьятченко Н.Х. и др. (1974). *Теория двигателей внутреннего сгорания. Ленинград*, Машиностроение.
3. Димитров П.И, (2000). *Двигатели с вътрешно горене*, ТУ-София.
4. Орлин А.С. и др. (1973). *Системы поршневых и комбинировонных двигателей*, Москва.
5. Цинер К., (1978). *Наддув двигателей внутренего сгорания*, Ленинград.



Контакти – стил „Contacts”
Адрес
E-mail: vasil_ivanov@abv.bg
E-mail: stanimira@abv.bg
E-mail: ivan_kirilov@abv.bg

© International Scientific Conference on Engineering, Technologies and Systems
TECHSYS 2016, Technical University – Sofia, Plovdiv branch
26 – 28 May 2016, Plovdiv, Bulgaria

# ТЕНДЕНЦИИ В РАЗВИТИЕТО НА МОРСКИТЕ ПРОТИВОМИННИ СИСТЕМИ

НИКОЛАЙ ГЕОРГИЕВ, АЛЕКСАНДЪР КОЛАРОВ

**Резюме:** *Съвременният противоминен комплекс представлява информационен комплекс, развърнат на много нива, в който най-високото ниво заема бреговия информационен център, а противоминните кораби са превърнати в негови резиденти, които развърнати в морето изпълняват неговите команди. Наблюдава се обрат в хидроакустичните технологии, използвани в борбата с морските мини, който се характеризира с преход от простото откриване на морската мина като локална хидроакустична цел към подробен мониторинг на подводната обстановка чрез обединението на двете технологии – традиционната хидролокация с пеленгуване на контрастна енергитична точка от отразен хидроакустичен сигнал, и сонарите със страничен обзор. Процедурата по преобразуване на наблюдаваното изображение на морското дъно на индикатора на сонара със страничен обзор в стандартна хидроакустична карта, която съдържа два информационни слоя, дава възможност да бъдат съпоставяни данни от различни сонари, получени при различни галсове и при различна дълбочина на антената и да бъде създавана база данни, използвана за класификация на целите.*

**Ключови думи:** *противоминни кораби, сонар със страничен обзор, хидроакустични карти, класификация, подводни самоходни автономни апарати, многолъчев ехолот, акустични видеокамери, морска мина.*

# TRENDS IN THE DEVELOPMENT OF NAVAL MINE COUNTERMEASURES SYSTEMS

NIKOLAY GUEORGUIEV, ALEKSANDAR KOLAROV

**Abstract:** *The modern complex to detect sea mines is a complex of informative type deployed on many levels, in which the highest occupied coastal information center and mine hunters ships were converted into its residents who deployed in the sea obeying his commands. There is a twist in sonar technology used in the fight against sea mines, which is characterized by transition from the simple opening of the maritime mine as local sonar target to detailed monitoring of the underwater environment through unification of the two technologies - traditional hydro location to determine the direction to contrast energetic point of reflected acoustic signal and a side scan sonar. The procedure for converting the observed image of the seabed indicator sonar with side survey in the standard sonar map that contains two information layers allows you to be compared data from different sonar obtained under different voice mail and at various depths of the antenna and be created database used for classification purposes.*

**Key words:** *classification, mine hunter, sea mine, AUVs, multipath echo sounder, side scan sonar, hydro acoustic map, hydro acoustic map.*

## 1. Въведение

Съвременните противоминни системи, предназначени за откриване и унищожаване на морски мини, използват най-новите постижения в областта на хидоакустиката в съчетание с оптически средства, магнитометри и информационни технологии. Съвременният противоминен комплекс представлява

Copyright © 2016 by Technical University of Sofia, Plovdiv branch, Bulgaria ISSN Online: 2535-0048

информационен комплекс, развърнат на много нива, най-високото от което заема бреговия информационен център, а противоминните кораби са превърнати в негови резиденти, които развърнати в морето изпълняват неговите команди. Това състояние е плод на еволюцията на противоминната практика, съгласно която до скоро противоминния кораб се разглеждаше като самостоятелна система, способна напълно да реши всички задачи по откриването и неутрализирането на морските мини [1].

В процеса на тази еволюция първоначално контактните и неконтактните тралове загубиха своята ефективност поради повишената трална устойчивост на морските мини. По-късно, когато на смяна на котвените мини дойдоха дънни мини с противохидроакустично покритие и средства за тяхната маскировка, все по-неефективни станаха и противоминните хидроакустични станции, които осигуряваха откриване на миите по енергийния контраст на отразената от целта хидроакустична енергия. Тези факти доведоха до обрат в хидроакустичните технологии, използвани в борбата с морските мини, които се характеризират с преход от простото откриване на морската мина като локална хидроакустична цел на обкръжаващия фон – морско пространство или дъно, към подробен мониторинг на подводната обстановка. Последният се извършва чрез съставяне на детайлна хидролокационна карта на участъците от морското дъно, представляващи оперативен и тактически интерес, обследване на всяка подозрителна цел и фиксация на всички локални изменения. При това, доколкото физическите размери на съвременните морски мини са от порядъка на 1 м, то разрешаващата способност и точността на привързване на хидроакустичната карта не трябва да превишава тази стойност. Именно тези изисквания са основната причина за стесняване на диаграмата на насоченост и повишаване на работната честота на хидролокаторите за секторен и кръгов обзор, а също и за включване на сонарите за страничен обзор в състава на хидроакустичното въоръжение на противоминните кораби. По този начин стана обединението на двете технологии – традиционната хидролокация с пеленгуване на контрастна енергитична точка от отразен хидроакустичен сигнал и сонарите със страничен обзор, които първоначално се използваха като профилографи на морското дъно [2].

## 2. Изложение

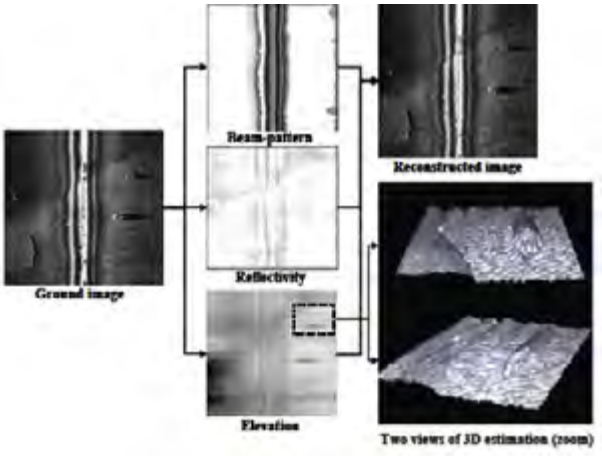
Използването на способа за класификация на дънните мини и възможността да се подобри различимостта на мината при малки ъгли на плъзгане на диаграмата на насоченост стимулираха появата на сонари за страничен обзор с антени с променлива дълбочина. Реализираната идея за съставяне на хидроакустични карти по пътя на групиране на данните от страничния обзор се оправдаха само в случаите, когато повърхността на морското дъно е относително равна и еднородна [3]. Изследванията показаха, че акустическите неоднородности и особено неравностите на морското дъно рязко намаляват качеството на хидроакустичната картина, която се променя в зависимост от ракурса и разстоянието до дъното. Поради това, без специални процедури е невъзможно да се съпоставят изображенията на един и същи участък от неравно морско дъно от екраните на различни хидролокатори, както и от екрана на един и същи хидролокатор, когато се е изменила геометрията на обзора.

Една от тези процедури е преобразуването на наблюдаваното изображение на морското дъно на индикатора на сонара със страничен обзор в стандартна хидроакустична карта, която съдържа два информационни слоя. Първия слой съдържа разпределението на локалните стойности на коефициента на обратното разсейване $S(0)$ , т.е. за ъгъл на падане перпендикулярен към повърхността. Локалните стойности на $S(0)$ се привързват към хоризонталните координати.

Вторият информационен слой съдържа подробни данни за релефа на дъното, на основата на които може да бъде определен наклонът на произволна локална площадка на повърхността на морското дъно[4].

Стойността на $S(0)$ се изчислява по стойността на сигнала от дънното разсейване в съответствие с ъгловата зависимост на коефициента на обратното разсейване по закона на Ламберт, което съответства на експерименталните данни. Това предположение е вярно когато обратното разсейване се формира или на границата твърд грунт-вода или при достатъчно тънък повърхностен слой върху твърдия грунт. За всички типове грунт това изисква отноително високи честоти,

докато за по-ниски честоти това предположение е оправдано за каменисто или пясъчно дъно. При ниски честоти и при тинесто дъно напр. обратното разсейване се формира не само на границата грунт-вода, но и във вътрешността на утаечните структури на дъното. Естсествено най-често тинестите дъна нямат големи и стръмни неравности, поради което то грешките при изчисляването на S(0) са приемливи в повечето слуаи.




***Фиг. 1*** *Преобразуване на сонарно изображение в хидроакустична карта*

От казаното по-горе следва, че стандартната хидролокационна карта съответства на вида на повърхността на морското дъно гледано вертикално от горе и на нея са отбелязани всички хидроакустични нееднородности, включително различни тела, които могат да бъдат и цели (дънни мини). Слабата честотна зависимост на обратното разсейване на звуковите вълни от морското дъно и разположените върху него цели в честотния диапазон на сонарите за странично обследване прави хидро-локационнаата карта универсален инструмент, който дава възможност да бъдат съпоставяни данни от различни сонари, получени при различни галсове и при различна дълбочина на антената [5]. По нея могат да бъдат задавани условичта на обзора и параметрите на сонара, да бъдат предварително изчислени зоните на акустическа сянка от обекти от релефа на дъното, да бъде определена априорната вероятност за откриване на дънна мина в зададена акватория при отчитане на конкретнитефонови характеристики, както и предложения за маневриране на противоминния кора при различните галсове.

В интерес на класификацията на целите е подходящо създаването на база с данни за съхраняване на хидроакустическите изображения при всички предшестващи галсове в определен район. Това дава възможност да се пристъпи към класификация на целите по тяхната хидроакустична сянка, а фиксацията на сянката при захождане към целта от различни ъгли позволява да се възстанови формата на обекта по формата на сянката. Важна информация дава оценката на еквивалентния радиус на целта.

Изпълнението на тези условия завършва съвременния етап на развитие на хидроакустичните технологии, използвани за борба с морското минно оръжие.

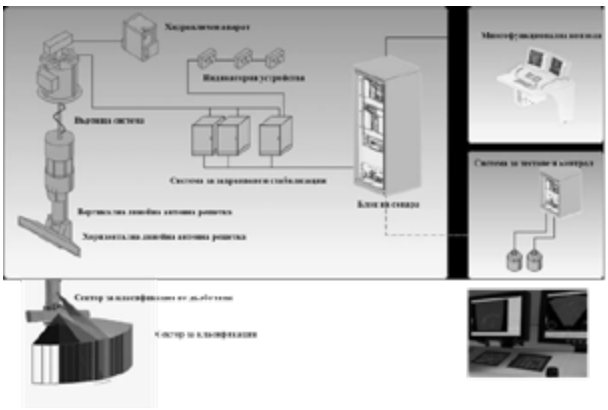
В зависимост от носителя и от конструктивното изпълнение на противоминните хидроакустични средства най-общо те могат да бъдат обособени в следните групи:

- корабни подкилни противоминни хидроакустични станции (сонари);
- буксируеми (спускаеми) противоминни сонари, които могат да бъдат използвани от надводен кораб или вертолет;
- потивоминни сонари, монтирани на подводници.

Противоминни комплекси, монтирани на борда на самоходни управляеми или автономни подводни апарати (AUV, Remote Minehunting System (RMS), autonomous Remote Multi-Mission Vehicle (ARMMV)). Функционалната схема на съвременен подкилен противоминен сонар е показана на Фиг.2.

Този тип сонари обикновенно функционират в пет различни режима:

1. Търсене на мини в сектор по курса на кораба;
2. Работа за противоминна безопасност на кораба - контрол за минната обстановка и сигнализиране при поява на миноподобна цел;
3. Търсене на мини в режим на страничен обзор (side scan);
4. Тестване на системата;
5. Симулация на минна обстановка за тренировка и обучение.



***Фиг. 2*** *Функционална схема на съвременен подкилен противоминен сонар*

Сонарът осигурява откриване и класифициране на мино подобни обекти с едновременно обработка по ниво на отразение хидроакустичен сигнал (ехо сигнал) формата и характеристиките на хидроакустичната сянка на фона на отраженията и шумовете. За целта обикновенно те са мултичестотни, като всяка честота е оптимизирана за конкретна задача, както следва:

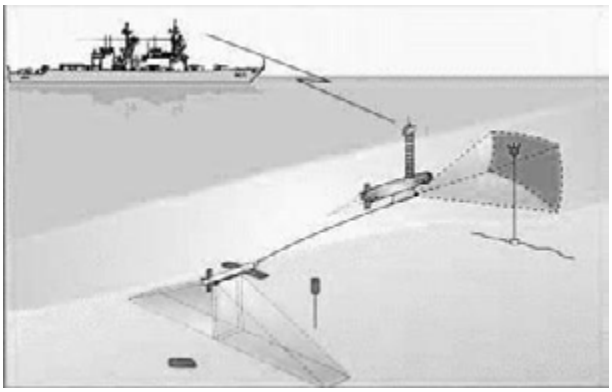
- ниска честота (Low Frequency) – от 75 ÷150 kHz – за работа в режим 1 и 2 за откриване на котвени и дънни мини на голяма дистанция в хоризонтален сектор 15° ÷ 90° по курса на кораба и вертикален сектор от 3° ÷ 30°. Сонарът осигурява 3D изобразяване на подводната обстановка и откриване на дънни мини на тинесто, пясъчливо и каменисто дъно;
- висока честота (High Frequency) - от 200 ÷300 kHz – за работа в режим 3 при всички дънни видове за откриване и класификация на дънни мини по ехо сигнал и хидроакустичната сянка;
- много висока честота (Very High Frequency) - от 400 ÷600 kHz – за работа в режим 3 за класификация при висока резолюция върху скалисто дъно със силна дънна реверберация.

Ширината на хоризонталния и вертикалния сектор на обследване (сканиране) при HF и VHF обикновенно са в границите съответно 10° ÷ 30° и 10° ÷ 20°. Излъчваният хидроакустичен импулс е с продължителност в границите 0.1 ÷ 0.5 ms с честотна модулация тип HFM / LFM / CW.

Предназначението на монтиран на подводница противоминен сонар е ранно откриване и предупреждение за котвени и дънни мини, включително и за навигационни препятствия, в широк сектор по курса на подводницата [8]. Основните типови тактико-технически характеристики са:

- работна честота - от 70 ÷100 kHz;
- тип на излъчвания импулс - HFM / LFM / CW;
- продължителност на импулса – 100 μs ÷ 2 ms;
- ширина на диаграмата на насоченост по хоризонтала/вертикала - 1º/2º;
- сектор на обследване по вертикала/хоризонтала - 120º/90º;
- формат на електронната карта - ENC, DNC, ARC.

Съвременните самоходни автономни или телеуправляеми подводни апарати (Фиг.2 - Remote Minehunting System) като правило се оборудват с многолъчеви хидролокатори за кръгов /секторен/ обзор с електронно сканиране на лъча, доплеров измерител на скоростта (доплеров лаг) в комплекс с инерциална навигационна система, многолъчев ехолот, профилометър, звуковизьор (акустическа видеокамера), фотосистема, хидролокатор за страничен о бзор с хидроакустични антени тип антенна решетка със синтезирана апритура, хидроакустическа система за навигация с дълга или ултракъса база и хидроакустични модеми за комуникация.

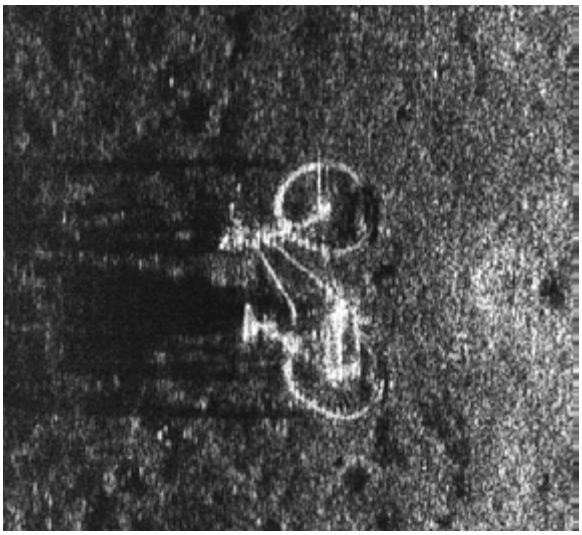


***Фиг. 3*** *Принцип на функциониране на съвременна самоходна автономна противоминна система*

За изпълнение на противоминни задачи основно се използват сонара за секторен обзор, за откриване на котвени мини, и комплекс, съставен от сонар за страничен обзор, многолъчев ехолот, профилометър и звуковизьор - за откриване на дънни мини.

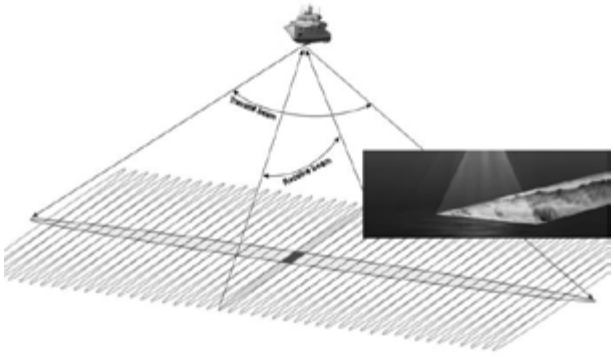
Акустичните видеокамери представляват миниатюрни многолъчеви хидролокатори, работещи на висока честота – от 450 kHz ÷ 1.2 MHz, със скорост на обновяване на

изображението до 25 кадъра в секунда и далечина на действие до 120 м.



***Фиг. 4*** *Хидроакустична снимка на велосипед на морското дъно, направена с помоща на звуковизьор*

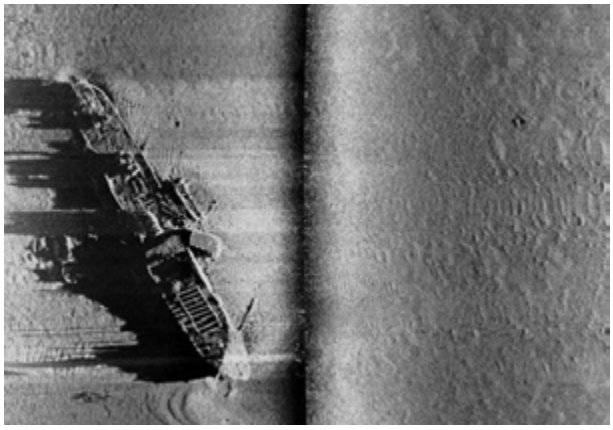
Многолъчевите ехолоти, които могат да се използват и качеството на секторни сонари по направление на движението – електронно сканиране в сектор от 10° до 160°, реализират до 256 фокусирани с ширина на диаграмата на насоченост 0.5° ÷ 1° лъчи, с честота от 200 ÷ 400 kHz. Някои от тях имат и режим на изобразяване на амплитудата на отразения сигнал във всеки от лъчите [9].



***Фиг. 5*** *Принцип на действие на многолъчев ехолот*

Хидролокаторите за страничен обзор със синтезирана апритура работят в широк честотен диапазон – от 200 kHz ÷ 1,25 MHZ и продължителност на честотно модулираните импулси от 50 μs до 1 ms.

Интерферометрическите сонари от този тип осигуряват висока резолюция от 25 x 25 mm по цялата полоса на обзора. Този тип сонари изпълняват модерна интерферометрична обработка на сигнала в съответствие с топографията на морското дъно, което позволява прецизно позициониране на целите на морското дъно.



***Фиг.6*** *Изображение на индикатора на сонар със страничен обзор*

### 3. Заключение

На базата на изложеното следва, че за повишаване на ефективността на процеса на търсене и класификация на дънни мини могат да се приложат следните подходи:

- в състава на противоминния хидроакустичен комплекс трябва да бъде включен блок за подробно измерване на релефа (профилограф), например многоканален или многолъчев ехолот;
- целесъобразно е всеки сонар за страничен обзор да изпълнява не само функциите за откриване на потенциални цели, а и да се използват като измервателен блок пригоден за съставяне на хидролокационна карта и за нейното ползване;
- противоминният кораб с неговото въоръжение да не бъде самостоятелно средство, а да стане резидент на бреговия (корабен) информационен център, където да се съсредоточи цялата обработка на информацията и да се извършва управлението на операцията по търсене и унищожаване на мини;
- цялата система трябва да бъде обединена със средства за телеметрия и свръзка, позволяваща да се извършва обмен и обработка на информацията в реално време;
- навигационното осигуряване трябва да позволява привързване към географските координати с точност не по-малка от 1 м;

- с навлизането на въоръжение на подводни дистанционно управляеми роботи и апарати, които разполага с необходимите хидроакустични комплекси, всеки противоминен кораб да се превърне в регионален или локален център на подобна противоминна система, която да оперира в ограничен периметър.

## ЛИТЕРАТУРА


1. Смирнов. С. А.(2014), *Гидроакустические технологии в борьбе с морскими минами* - ФГУП «ЦНИИ «Морфизприбор», Санкт-Петербург, УДК 681.883.22
2. RA. Neill, *Optimizing display parameters for side-scan sonar operators*, Proc. 9th Commonwealth Def. Sci. Org Conference, Auckland, NZ 2011 г.
3. S. Reed, Y. Petillot and J. Bell, (2004) *Mine detection and classification in side scan sonar*, Sea Technology, Nov 04, 35-39.
4. E. Coiras, P.-Y. Mignotte, Y. Petillot, J. Bell and K. Lebart, (2007) *Supervised target detection and classification by training on augmented reality data*, IETRadar, Sonar & Navigation 1 (No.1), 83-90.
5. E. Coiras, Y. Petillot and D.M. Lane, (2007) *Multiresolution 3-D reconstrudion from side-scan sonar images*, IEEE Trans. Image Processing 16 (No.2), 382-390.



Контакти:

1. Николай Георгиев

Адрес: София 1574, ул. "Шипченски проход" 67. Институт по металознание, съоръжения и технологии „Акад. Ангел Балевски“ с Център по хидро- и аеродинамика – БАН,
тел: (+359 2) 46-26-250
факс: (+359 2) 46-26-202
E-mail: niki0611@abv.bg

2. Александър Коларов

Адрес: 9003 Варна, кв. Аспарухово, ул. "Уилям Фруд" № 1, п.к. 58. Център по хидро-и аеродинамика.
тел.: + 359 52 370 512
факс: + 359 52 370 514
E-mail: aleksandar_kolarov@abv.bg

© International Scientific Conference on Engineering, Technologies and Systems
TECHSYS 2016, Technical University – Sofia, Plovdiv branch
26 – 28 May 2016, Plovdiv, Bulgaria

# МЕТОД ЗА ПОВИШАВАНЕ ПРОТИВОМИННАТА УСТОЙЧИВОСТ НА ДЪННИ МИНИ

НИКОЛАЙ ГЕОРГИЕВ, АЛЕКСАНДЪР КОЛАРОВ

**Резюме:** *Развитието на технологията за реализиране на морска роботизирана техника позволи създаването на автономни самоходни подводни апарати (autonomous underwater vehicle – AUV), с бордови сонари, даващи изображения на морската среда с висока резолюция, които са особено ефективни за откриване обекти на морското дъно. Най-общо, като се вземат в предвид новите тенденции в обработването на сигналите, филтрирането им по признак и алгоритмите, реализирани в приемните устройства на противоминните сонари, за намаляване на тяхната ефективност при откриване на мини по хидроакустическата им сянка и ниво на отразен сигнал, може да бъде направен извод, че дънните мини трябва да се правят ниски, със сложни и неправилни форми за намаляване на различаването им. Едно от решенията, което да доведе до намаляване на ефективността на противомините сонари, е създаването на източник на отговарящи имитиращи хаотични импулсни смущения с параметри, близки до тези на тези облъчващия сонар, и интензивност, съответстващи на тези на евентуални отражения от фиктивни дънни образования с ефективните отразяваща повърхност.*

**Ключови думи:** *класификация, идентификация, хидроакустична сянка, имитиращи/отговарящи смущения, реверберация, делта-маска.*

# METHOD OF ENHANCING ANTI-MINING RESISTANCE TO BOTTOM MINES

NIKOLAY GUEORGUIEV, ALEKSANDAR KOLAROV

***Abstract:*** *The development of technology for the realization of marine robotic techniques allow the creation of autonomous self-propelled underwater devices (autonomous underwater vehicle - AUV), with onboard sonars giving images of the marine environment in high resolution, which are particularly effective for detecting objects on the seabed. Broadly into account new trends in signal processing, filtering them on the ground and algorithms implemented in host devices sonar to search for mines, reducing their effectiveness in mine detection by Hydro-Acoustic their shade and level of reflected signal It can be concluded that bottom mines must be made low, with complex and irregular shapes to reduce distinguishing them. One solution to reduce the effectiveness of this type of sonar is creating a source of fulfilling imitating chaotic pulse interference with parameters similar to those of such exposures sonar and intensity corresponding to these potential impacts of fictitious bottom formations with effective reflective surface.*

**Key words:** *classification, identification, sonar shadow imitating / corresponding interference, reverb, delta-mask.*

## 1. Въведение

Съвременните противоминнн системи за откриване и унищожаване на дънни морски мини използват най-новите достижения в областа на хидроакустиката в съчетание с оптически средства, магнитометри и информационни технологии, което ги превръща в информационен комплекс, организиран на

Copyright © 2016 by Technical University of Sofia, Plovdiv branch, Bulgaria ISSN Online: 2535-0048

много нива. Простото откриване на мината като локална хидролокационна цел на фона на обкръжаващата среда все повече се преобразува в мониторинг на подводната обстановка и създаване на детайлна хидролокационна карта на участъци от морското дъно, с което се гарантира безопасността на корабоплаването в крайбрежните райони, с подробно обследване за фсяка подозрителна цел и фиксиране на всички локални изменения.

Развитието на технологията за реализиране на морска роботизирана техника позволи създаването на автономни самоходни подводни апарати (autonomous underwater vehicle – AUV), с бордови сонари, даващи изображения на морската среда с висока резолюция, които са особено ефективни за откриване обекти на морското дъно. Поради високата отговорност и срочния характер на подобни противоминни мисии е приоритетно вграждането на „интелигентност“ в AUVs така, че да може да реагира незабавно в съответствие с получената информация. За постигането на тази цел е необходимо да бъдат изпълнени две основни задачи – създаване на алгоритъм за откриване и класифициране на обектите в почти реално време и алгоритъм за оптимално адаптиране маршрута на AUV в съответствие с получената информация.

Когато анализираме процесите за усъвършенстване на методите и средствата за повишаване ефективността на противоминните действия, не трябва да се игнорира факта, че освен като заплаха за корабоплаването, морското минно оръжие представлява важен инструмент за защита на дейностите в прилежащите морски пространства срещу противниковите сили в случаи на война или въоръжени комфликти и има реален възпиращ ефект.

Най-общо, като се вземат в предвид новите тенденции в обработването на сигналите, филтрирането им по признак и алгоритмите, реализирани в приемните устройства на противоминните сонари, за намаляване на тяхната ефективност при откриване на мини по хидроакустическата им сянка и ниво на отразен сигнал, могат да бъдат направени следните изводи за това на какви условия трябва да отговаря съвременна дънна мина, а именно [1]:

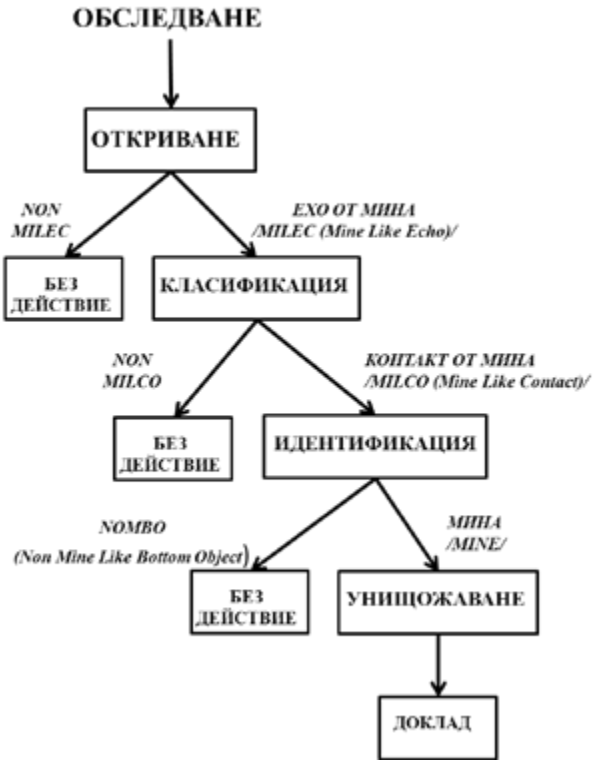
1. Нисък вертикален профил - за да прави по-малка хидроакустична сянка сянка;
2. Ниска отразяваща енергетична способност - оценява се по центъра на тежестта и ако една маса е с по голяма площ тя е по-ниско контрастна;
3. Голяма площ - маскира се сянката, а освен това филтрите за големина на целта (относно габарити на известни мини) не я класифицират като миноподобна цел;
4. Симетричност на формата - обикновенно се процедира двукратен поиск на перпендикулярни галсове и се оценяват (изваждат) сигналите от целите.

Анализът на тези условия показва, че първото и частично второто, могат да бъдат постигнати с помоща на конструктивни решения и използването на камуфлажни и материали с ниска отразяваща способност.

Останалите условия трябва да бъдат моделирани с помоща на активни средства за повишаване противоминната устойчивост на дънните мини.

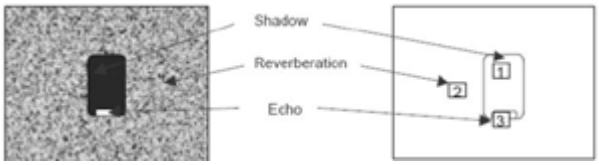
## 2. Изложение

Класическият противоминен процес се състои от три етапа: (1) откриване, (2) класификация и (3) идентификация (евентуално последвано от обезвреждане на мини), който може да бъде описан със схемата, показана на Фиг.1.




***Фиг. 1*** *Блок-схема на етапите, които се извършват при реализиране на противоминния процес*

Принципът на анализиране на сонарното изображения е с отчитането на дъната реверберация и появата на акустична сянка зад обекта [2]. Може да се приеме, че сонарното избражение съдържа три вида пиксела: реверберация, ехо и сянка - Фиг.2.




***Фиг. 2*** *Структура на сонарно изображение*

Всяка категория пиксели може да бъде описана със статистическа функция на разпределение или с еквивалентна функция на плътност на вероятностите. Тази функция описва статистически поведението на пиксела, което е приблизително равно на вероятността даден пиксел да взема своите цифрови стойности в рамките на определен интервал.

Ако приемем, че характеристиките на сонара и на обекта са известни, всеки пиксел може да принадлежи към един от следните статистически закони [3]:

- дънната реверберация P1(x);
- хидроакустичната сянка P2(x);
- ехо-сигнала P3(x);-
- неопределени P_(x).

Статистическата поведението на изображението може да бъде представено с 2D маска (или решетка). Всеки квадрат на решетката съответства на пикселите на изображението и включва броя на индекса от Закона за статистиката, свързан с този пиксел – (Фиг. 3 – 2D маска на изображението на Фиг. 2).

| | | | | | | | | | | |
|---|---|---|---|---|---|---|---|---|---|---|
| 2 | 2 | 2 | 2 | 2 | 2 | 2 | 2 | 2 | 2 | 2 |
| 2 | 2 | 2 | 2 | 2 | 2 | 2 | 2 | 2 | 2 | 2 |
| 2 | 2 | 2 | 2 | 1 | 1 | 1 | 2 | 2 | 2 | 2 |
| 2 | 2 | 2 | 2 | 1 | 1 | 1 | 2 | 2 | 2 | 2 |
| 2 | 2 | 2 | 2 | 1 | 1 | 1 | 2 | 2 | 2 | 2 |
| 2 | 2 | 2 | 2 | 1 | 1 | 1 | 2 | 2 | 2 | 2 |
| 2 | 2 | 2 | 2 | 3 | 3 | 3 | 2 | 2 | 2 | 2 |
| 2 | 2 | 2 | 2 | 2 | 2 | 2 | 2 | 2 | 2 | 2 |
| 2 | 2 | 2 | 2 | 2 | 2 | 2 | 2 | 2 | 2 | 2 |

***Фиг. 3*** *2D маска на сонарно изображение*

Използвайки теоретичната маска на известен обект в хипотеза $H_1$ (ако обектът е мина) или $H_0$ (ако съответства на откриване на фалшиви аларми) и се предполага, че пикселите са независими, функция на плътността на вероятностите на изображението може да се запише като продукт на функциите на плътността на вероятностите на нейните пиксели (Neyman-Pearson) [4]:

$$\prod_{i,j} \frac{p\left(\frac{x_{ij}}{H_0}\right) \geq 1}{p\left(\frac{x_{ij}}{H_1}\right) < 0} \text{ праг (Threshold)} \qquad (1)$$

където: Xij е стойността на пикселите на ред i и колона j.

За оптимизиране на процеса на обработка на сонарното изображение и сянката обикновенно се използва делта-маска, описвана с детерминирани статистически закони, например сенки на пръстен и квадрат (Фиг. 4).



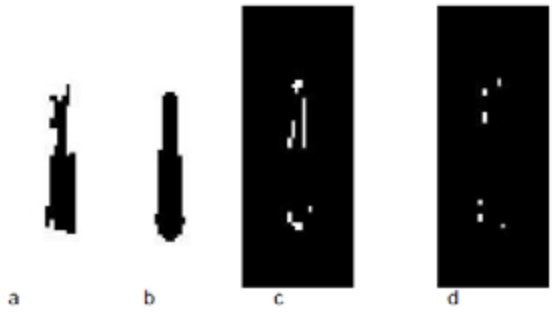
***Фиг. 4*** *Делта маска на сонарно изображение*

Определянето на типа на делта-маската е свързано преди всичко с центрирането на сянката по H0 и H1. Съществуват много варианти за определяне на центъра на делта-маската като съвпадащ с центъра на тежестта (или центъра на масата, медицентъра или геометричния център на изображението и др [5]. Оптималният вариант при избора на делта-маска е минимизирането на броя на нейните пилсели, което матиматически може да се изрази с формулата:

$$\prod_{i,j \in \Delta} \frac{p\left(\frac{x_{ij}}{H_0}\right) \geq 1}{p\left(\frac{x_{ij}}{H_1}\right) < 0} Threshold \qquad (2)$$

Ако изберем делта-маска, която е разделена на 6 подмаски - $\Delta^{12}$, $\Delta^{13}$, $\Delta^{21}$, $\Delta^{23}$, $\Delta^{31}$ и $\Delta^{32}$, суб-маските $\Delta^{11}$, $\Delta^{22}$ и $\Delta^{33}$ няма да представляват интерес, защото не

допринасят за статистическо решение. Примерните маски на NOMBO (камък) (Фиг. 5a) и за мина „Манта“ (Фиг. 5b), които съответстват на суб-маски $\Delta^{21}$ и $\Delta^{12}$, са показани съответно на Фиг.7c и 7d.




***Фиг.5*** *Примерни маски на реални цели*

По време на противоминна операция сонара може да се сблъска с голямо разнообразие от ситуации, определящи различни маски на формата на сянката на мина, зависещи основно от вариации на позицията на мината на морското дъно. Например, завъртането на мината около вертикалната и ос предизвиква разнообразие от маски, илюстрирани на Фиг. 6.



***Фиг.6*** *Вариации на маска на мина*

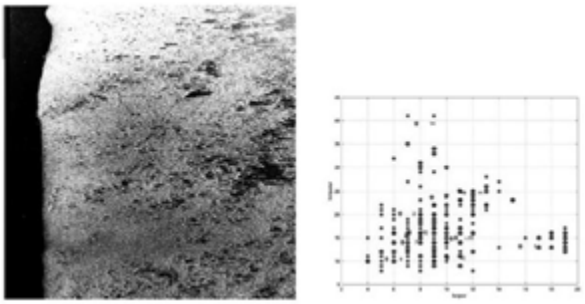
За дадени характеристики на сонара (честотен диапазон, резолюция, ъгъл, шум, реверберация и ехо), статистическата променлива, представляваща изображение на мината и статистическата променливата представляваща изображение на MAMBO (от дъното) трябва да се считат за статистически смеси. Сместа може да се представи с помощта на набор от делта-маски. Всяка делта-маска на наблюдаваната площадка съответства на сбор на конкретна маска на мина с конкретна маска от отражение от дъното. Всяка делта-маска в сместта се характеризира с тегловен коефицент $q_n$, който характеризира вероятността решението да бъде засегнато от преобладаващото влияние на дадена маска. Този процес може да се характеризира с формулата[6]:

$$\sum_{k,l\ k\neq l}^{3\ 3} (a_h^{k\ l_n} \cdot \chi_{2N^{kl_n}})\ \mathrm{Threshold}_n, q_n \qquad (3)$$

където:

- $N^{kl}$ е броя на пикселите на суб-маската $\Delta^{kl}$;
- $\chi_{2N^{kl_n}}$ е хи-квадрат вариации (chi-squarevariable) с $2N^{kl}$ градуса на свобода;
- $a_h^{k\ l}$ е съвкупност от реални коефициенти в зависимост от средното измерено съотношение на шум (сянка), реверберация и ехо.

На Фиг. 7 е показана маската на сонарно изображение на дъното, която трябва да бъде сравнявана с маската на вероятно поставена дънна мина.



***Фиг.7*** *Сонарно изображение на и съответната маскана маска*

Опитът от използването на сонари за страничен обзор показва, че сред най-значимите характеристики на хидроакустичната сянка от подводни обекти се явяват:

- средната яркост на сянката, което е мярка за тъмнина на сянката на обекта;
- средната яркост на осветяване, което е мярка за яркостта на осветяване на обекта;
- разсейването на сянката;
- разсейването от дъното;
- контраст между сянка и осветяване, което е абсолютната разлика от средната яркост на сянката и средната сила на осветяване;

- контрастът между сянка и фон, който е абсолютната разлика от средната яркост на сянката и средната сила на фона.

Ефективното противодействие на ефективността на описаната по-горе стандартна процедура на функциониране на противоминен сонар може да бъде постигнато когато маскирането на формата, сянката и отразяващата повърхност на мината бъдат моделирани с помоща на активни средства - източници на отговарящи имитиращи хаотични импулсни смущения с параметри: - честота на повторение на импулсите *T*; - продължителност на импулса τ; - честота на запълване на импулса $f$ и интензивност *I*, съответстващи на тези на евентуални отражения от фиктивни дънни образования с ефективните отразяваща повърхност σд, или на преизлъчване на приети хидроакустични импулси след време, разчетено за да бъде постигнат желания резултат.

В първия случай ще се постигне маскиране на мината чрез промяна на реализираната от алгоритмите на сонара делта-маска, а във втория – създаване на допълнителни елементи в делта-маската на грунта, което да затрудни анализа от сместа на маските от целта и грунта.

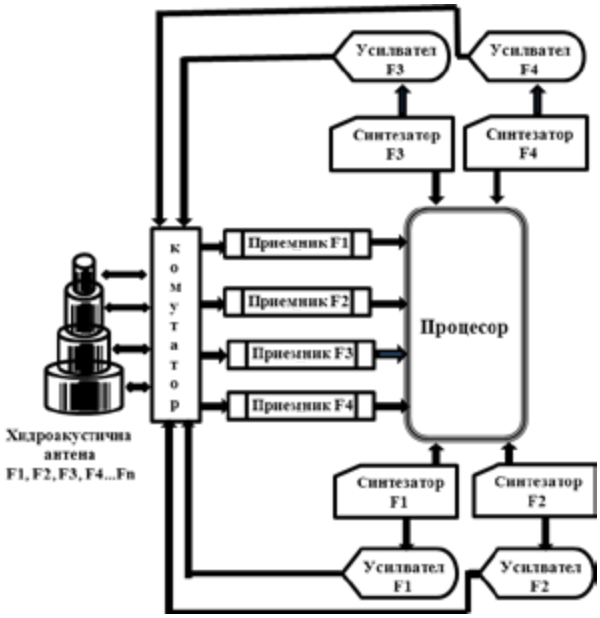
Източникът на тези имитиращи/отговарящи смущения може да бъде поместен в тялото на самата мина или около нея в зависимост от характера на грунта и тактическите особености на района на противоминните действия.

Активирането на този/тези елементи е целесъобразно да се извършва автоматично след облъчване с хидроакустически сигнал, който се класифицира като от противоминен сонар.

Функционалната схема на имитиращ/ отговарящ елемент е показана на Фиг. 8.

Хидроакустичната антена е мулти честотна и се състои от необходимия брой пиезокерамични преобразуватели, така че да се покрива целият диапазон на работа на противоминните сонари, а именно:

- много ниска честота (Very Low Frequency) – от 75 ÷ 120 kHz;
- ниска честота (Low Frequency) – от 120 ÷ 200 kHz;
- висока честота (High Frequency) - от 200 ÷ 400 kHz;
- много висока честота (Very High Frequency) - от 400 ÷ 800 kHz.




***Фиг.8*** *Функционална схема на имитиращ/ отговарящ елемент*

Синтезаторите трябва да могат да изработват всяка честота в зададения поддиапазон.

Процесорът трябва да генерира импулси с продължителност в границите 0.1 ÷ 1 ms с честотна модулация тип HFM / LFM / CW.

Работата на активното устройство за създаване на отговарящи имитиращи хаотични смущения протича по следния начин:

- излъчените от противоминния сонар импулси в направление към мината попадат на хидроакустичната антена;
- пиезокерамичният преобразувател, който притежава съответната честотна лента, го преобразува в електрически сигнал (импулс), а комутаторът го насочва към съответния приемник за обработване и усилване;
- в процесора се извършва класификация на зондиращия сигнал и при положителна оценка се активира работата на един от синтезаторите като едновременно започва да променя параметрите му;
- когато сигналът от избрания синтезатор стане еднакъв със запомнения по честота на повторение на импулсите, продължителност и

честота на запълване на импулса, той се градуира по интензивност и време на закъснение и след стандартно усилване се излъчва през комутатора от съответния преобразувател;
- процесорът можа да командва ново излъчане без да чака попадане на нов зондиращ импулс, съгласно заложената програма.

## 3. Заключение

Съвременните противоминнн системи за откриване и унищожаване на дънни морски мини използват най-новите достижения в областа на хидроакустиката като за целта се използват специални сонари, работещи на-често в импулсен режим. Процесът на откриване се извършва на базата на два допълващи се фактора:

- отразената енергия от мината на фона на отраженията от морските дънни образувания (на базата на сравняване на формата и интезивността на отраженията, дължащи се на ефективните отразяващи повърхности съответно на мината - σм и на дънните образувания - σд;
- наличието на хидроакустична сянка след местоположението на мината, която разкрива не само факта за наличие на цел, но и ориентировъчната и форма.

Усилията са дънните мини да се правят ниски, със сложни и неправилни форми за намаляване на различаването им. Това не-винаги е възможно, особено ако дъното е пясъчно или леко каменисто. Едно от решенията, което да доведе до намаляване на ефективността на противомините сонари, е създаването на източник на отговарящи имитиращи хаотични импулсни смущения с параметри (*T, τ, f*), близки до тези на облъчващата ултразвукова вълна, и интензивност, съответстващи на тези на евентуални отражения от фиктивни дънни образования с ефективните отразяваща повърхност σд. Разполагане на този източник може да се извършва в периметъра около позицията или на/в самата мина. Активирането може да се извършва дистанционно по команда от брега или автономно - при облъчване от противоминен сонар.

## ЛИТЕРАТУРА


1. J. A. Fawcett (2001) *Image-based classification of sidescan sonar detections*, Proceedings of CAD/CAC 2001, Halifax, Nov. 12-14,.
2. S.Reed, Y.Petillot, J.Bell (2004) *A model based approach to the detection and classification of mines in sidescan sonar*, Applied Optics, Vol. 43, Issue 2, p237-246.
3. G.J.Dobeck (2001) *Algorithm fusion for automated sea mine detection and classification*, Proc. MTS/IEEE Oceans Conf. and Exhibition, pp.130-134.
4. S.Reed, I.Tena Ruiz, C.Capus, Y.Petillot (2006). *The fusion of large scale classified side-scan sonar image mosaics*, Accepted for publication in IEEE Trans. Image Processing.
5. S. Williams, O. Pizarro, M. How, D. Mercer, G. Powell, J. Marshall, and R. Hanlon (2009), "*Surveying noctural cuttlefish camouflage behaviour using an AUV*," in Proceedings of the IEEE International Conference on Robotics and Automation, , pp. 214–219.
6. I. Quidu, J. Ph. Malkasse, G. Burel, and P. Vilbe (2010). "*Mine Classification based on raw sonar data: an approach combining Fourier descriptors, statistical models, end genetic algorithms"*, Providence, Proceedings of Oceans.



Контакти:

1. Николай Георгиев
Адрес: София 1574, ул. "Шипченски проход" 67. Институт по металознание, съоръжения и технологии „Акад. Ангел Балевски“ с Център по хидро- и аеродинамика – БАН,
тел: (+359 2) 46-26-250
факс: (+359 2) 46-26-202
E-mail: niki0611@abv.bg

2. Александър Коларов
Адрес: 9003 Варна, кв. Аспарухово, ул. "Уилям Фруд" № 1, п.к. 58. Център по хидро-и аеродинамика.
тел.: + 359 52 370 512
факс: + 359 52 370 514
E-mail: aleksandar_kolarov@abv.bg

© International Scientific Conference on Engineering, Technologies and Systems
TECHSYS 2016, Technical University – Sofia, Plovdiv branch
26 – 28 May 2016, Plovdiv, Bulgaria

# SECTION 6 • СЕКЦИЯ 6

## NATURAL SCIENCES

## ПРИРОДНИ НАУКИ

© International Scientific Conference on Engineering, Technologies and Systems
TECHSYS 2016, Technical University – Sofia, Plovdiv branch
26 – 28 May 2016, Plovdiv, Bulgaria

# $L_p(k)$ - SOLUTION OF NONLINEAR VOLTERRA-HAMMERSTEIN INTEGRAL EQUATIONS

ATANASKA GEORGIEVA, ALBENA PAVLOVA

**Abstract:** *In this paper we study the existence of $L_p(k)$ - solution over compact intervals of nonlinear Volterra-Hammerstein integral equations. The existence of such a solutions is based on well-known Schauder's fixed point theorem in Banach space. We give example which illustrates main result.*

**Key words:** *nonlinear Volterra-Hammerstein integral equations, Schauder's fixed point theorem, compact operator, $L_p(k)$ - solution*

## 1. Introduction

Integral equations play a very important role in nonlinear analysis and find numerous applications in engineering, mathematical physics, economics and so on (see [1], [4], [8]). For instance, the nonlinear Volterra-Hammerstein integral equations appear in nonlinear physical phenomena such as electro-magnetic fluid dynamics, reformulation of boundary value problems with a nonlinear boundary condition (see [4]).

The existence of solutions for nonlinear Volterra-Hammerstein integral equations has been considered in many paper and books [3], [4], [7]. In this paper we find sufficient conditions for the existence of $L_p(k)$ - solutions of nonlinear Volterra-Hammerstein integral equations. In [5] are found sufficient conditions for the existence of solutions in spaces $L_p(k)$ $(1 \le p < \infty)$ of linear nonhomogeneous impulsive differential equations with an unbounded linear operator.

## 2. Preliminaries

Let $X$ be a Banach spaces. By $C(X,X)$ we denote the space of all continuous operators acting in $X$. Let $\mathbb{R}_+ = [0,+\infty)$.

We consider the nonlinear Volterra-Hammerstein integral equation

$$x(t) = f(t) + \int_a^t V(t,s)\, g(s,x(s))\, ds \tag{1}$$

where the functions $f(\cdot) : [a,b] \to \mathbb{R}$, $g(\cdot,\cdot) : [a,b] \times \mathbb{R} \to \mathbb{R}$ and the kernel $V(\cdot,\cdot) : [a,b] \times [a,b] \to \mathbb{R}$.

We introduce the following conditions:

(H1) There exists a function $k(\cdot,\cdot) : [a,b] \times [a,b] \to \mathbb{R}_+$, positive constant $M_1$ such that $\sup_{t\in[a,b]} \int_a^t k(t,s)ds < M_1$, $\inf_{t\in[a,b]} k(t,s) \neq 0$ and $|V(t,s)| \le k(t,s)$, where $a \le s \le t \le b$.

(H2) There exist functions $k_1(\cdot)$, $k_2(\cdot) : [a,b] \to \mathbb{R}_+$ for all $s \in [a,b]$ and positive constants $M_2$, $M_3$ such that $\sup_{t\in[a,b]} k_1(t) < M_2$, $\sup_{t\in[a,b]} \int_a^t k_2(s)ds < M_3$ and $|V(t,s)| \le k_1(t)k_2(s)$, $a \le s \le t \le b$.

We introduce the following space

$$L_p(k) = \left\{ x(\cdot) : [a,b] \to \mathbb{R}; \sup_{t\in[a,b]} \int_a^t k(t,s)|x(s)|^p\, ds < \infty \right\} \text{ for } 1 \le p < \infty$$

with norm

Copyright © 2016 by Technical University of Sofia, Plovdiv branch, Bulgaria ISSN Online: 2535-0048

$$\|x\|_{L_p(k)} = \sup_{t\in[a,b]}\left(\int_a^t k(t,s)|x(s)|^p\,ds\right)^{\frac{1}{p}}.$$

**Definition.** *The solution* $x$ *of the nonlinear Volterra-Hammerstein integral equation* (1) *is said to be* $L_p(k)$*-solution if* $x \in L_p(k)$.

By using Schauder's fixed point theorem, we prove the existence of a $L_p(k)$-solution of nonlinear Volterra-Hammerstein integral equation (1).

**Theorem 1.** [6] *Let* $K$ *be a closed and convex subset of a Banach space* $X$. *The operator* $T \in C(K,K)$ *and compact. Then* $T$ *has a fixed point in* $K$.

### 3. Existence of $L_p(k)$-solution

**Theorem 2.** *Let the following conditions are fulfilled:*

***1.****The kernel* $V(t,s)$ *satisfies the following conditions:*

***1.1.*** *The condition (H1) hold.*

***1.2.*** $\lim\limits_{h\to 0}\sup\limits_{t\in[a,b]}\int\limits_a^t k(t,s)\left(\sup\limits_{\tau\in[a,b]}|V(s+h,\tau)-V(s,\tau)|^p\right)ds = 0$ *and* $\sup\limits_{\tau\in[a,b]}|V(s,\tau)| \in L_p(k)$.

***2.*** *The function* $g(s,x)$ *satisfies the following conditions:*

***2.1.*** *There exist the functions*

$G(\cdot):[a,b]\to\mathbb{R}_+$, $\Phi(\cdot):\mathbb{R}_+\to\mathbb{R}_+$ *such that* $|g(s,x)| \le G(s)\Phi(|x|)$ *for all* $s\in[a,b]$, $x\in\mathbb{R}$, *where* $G \in L_q(k)$, $\dfrac{G}{k_3} \in L_q(k)$, $k_3(s) = \dfrac{1}{\inf\limits_{t\in[a,b]} k(t,s)}$, $\Phi(|x|) \le L|x|$ *for all* $x\in\mathbb{R}$ *and some positive constant* $L$, $\dfrac{1}{p}+\dfrac{1}{q}=1$.

*Moreover, assume that the function* $G$ *satisfies the condition* $2^{\frac{1}{q}} L.M_1.\|G\|_{L_q(k)} < 1$.

***2.2.*** *There exists positive constant* $L_1$ *such that* $\left|\dfrac{\partial g}{\partial x}(s,x)\right| \le L_1$ *for each* $s\in[a,b], x\in\mathbb{R}$.

***3.*** *The function* $f \in L_p(k)$ *and* $\lim\limits_{h\to 0}\sup\limits_{t\in[a,b]}\int\limits_a^t k(t,s)|f(s+h)-f(s)|^p ds = 0$.

*Then the nonlinear Volterra-Hammerstein integral equation* (1) *has a* $L_p(k)$ *-solution.*

**Proof:** Let $r>0$ be a positive real number to be fixed later and define the closed ball $B_r$ of $L_p(k)$ by $B_r = \{x\in L_p(k) : \|x\|_{L_p(k)} \le r\}$. It is clear that $B_r$ is a closed and convex subset of $L_p(k)$.

Let $T$ be the operator defined on $L_p(k)$ by

$$Tx(t) = f(t) + \int_a^t V(t,s)g(s,x(s))\,ds,\quad t\in[a,b]. \tag{2}$$

First, we will prove that the operator $T: B_r \to B_r$ is continuous.

Let $x\in B_r$. Then from conditions 1.1, 2.1 and Hölder's inequality for the operator $T$ we have

$$|Tx(s)| \le |f(s)| + \int_a^s |V(s,\tau)||g(\tau,x(\tau))|d\tau \le |f(s)| + \int_a^s k(s,\tau)G(\tau)\Phi(|x(\tau)|)d\tau \le$$

$$\le |f(s)| + \left(\sup_{s\in[a,b]}\int_a^s k(s,\tau)|x(\tau)|^p d\tau\right)^{\frac{1}{p}}.\left(\sup_{s\in[a,b]}\int_a^s k(s,\tau)G^q(\tau)L^q d\tau\right)^{\frac{1}{q}} =$$

$$= |f(s)| + L.\|x\|_{L_p(k)}.\|G\|_{Lq(k)} \le |f(s)| + r.L.\|G\|_{Lq(k)}.$$

Hence

$$\|Tx\|_{L_p(k)} = \left( \sup_{t\in[a,b]} \int_a^t k(t,s)|Tx(s)|^p ds \right)^{\frac{1}{p}} \le \left( \sup_{t\in[a,b]} \int_a^t k(t,s)\left(|f(s)| + r.L.\|G\|_{L_q(k)}\right)^p ds \right)^{\frac{1}{p}} \le$$

$$\le 2^{\frac{p-1}{p}} \left( \left( \sup_{t\in[a,b]} \int_a^t k(t,s)|f(s)|^p ds \right)^{\frac{1}{p}} + \left( \sup_{t\in[a,b]} \int_a^t k(t,s) r^p.L^p.\|G\|^p_{L_p(k)} ds \right)^{\frac{1}{p}} \right) =$$

$$= 2^{\frac{1}{q}} \left( \|f\|_{L_p(k)} + r.L.\|G\|_{L_q(k)} \left( \sup_{t\in[a,b]} \int_a^t k(t,s) ds \right)^{\frac{1}{p}} \right) \le 2^{\frac{1}{q}} \left( \|f\|_{L_p(k)} + r.L.\|G\|_{L_q(k)}.M_1^{\frac{1}{p}} \right).$$

Consequently

$$\|Tx\|_{L_p(k)} \le 2^{\frac{1}{q}} \left( \|f\|_{L_p(k)} + r.L.M_1^{\frac{1}{p}}.\|G\|_{L_q(k)} \right). \tag{3}$$

Hence the condition $T(B_r) \subset B_r$ is satisfies for any positive real number $r$ satisfying $r \ge \dfrac{2^{\frac{1}{q}}\|f\|_{L_p(k)}}{1 - 2^{\frac{1}{q}} L.M_1^{\frac{1}{p}}.\|G\|_{L_q(k)}}$ .

Next we prove that the operator $T$ is continuous over $B_r$.

Let $\{x_n\}$ be a sequence of $B_r$ converting to $x$ in the norm $\|.\|_{L_p(k)}$. Since $(B_r, \|.\|_{L_p(k)})$ is complete, then $x \in B_r$.

From condition 2.2 and Hölder's inequality we have

$$|Tx_n(s) - Tx(s)| \le \int_a^s |V(s,\tau)||g(\tau, x_n(\tau)) - g(\tau, x(\tau))| d\tau \le$$

$$\le \int_a^s k(s,\tau) \left| \frac{\partial g}{\partial x}(s, \theta_s x_n(\tau) + (1-\theta_s)x(\tau)) \right| |x_n(\tau) - x(\tau)| d\tau \le$$

$$\le \int_a^t k(s,\tau) L_1 |x_n(\tau) - x(\tau)| d\tau \le \left( \sup_{s\in[a,b]} \int_a^s k(s,\tau)|x_n(\tau) - x(\tau)|^p d\tau \right)^{\frac{1}{p}} \left( \sup_{s\in[a,b]} \int_a^s k(s,\tau).L_1^q d\tau \right)^{\frac{1}{q}} =$$

$$= L_1.M_1^{\frac{1}{q}}.\|x_n - x\|_{L_p(k)}$$ , where $\theta_s \in (0,1)$.

Hence

$$\|Tx_n - Tx\|_{L_p(k)} = \left( \sup_{t\in[a,b]} \int_a^t k(t,s)|Tx_n(s) - Tx(s)|^p ds \right)^{\frac{1}{p}} \le \left( \sup_{t\in[a,b]} \int_a^t k(t,s) L_1^p.M_1^{\frac{p}{q}}.\|x_n - x\|^p_{L_p(k)} ds \right)^{\frac{1}{p}} =$$

$$= L_1.M_1^{\frac{1}{q}}.M_1^{\frac{1}{p}}.\|x_n - x\|_{L_p(k)} = L_1.M_1.\|x_n - x\|_{L_p(k)} .$$

Then $\lim_{n\to\infty} \|Tx_n - Tx\|_{L_p(k)} = 0$ and hence the operator $T$ is continuous over $B_r$.

We will prove that the operator $T$ is compact in $B_r$.

We denote the set $T(B_r) = \{Tx : x \in B_r\}$. We will prove that $T(B_r)$ is a compact subset in $B_r$.

By using compactness criterion in the spaces $L_p(k)$ from [2] the compactness of the set $T(B_r)$ is ensured:

1. There exists positive constant $C$, such that $\|Tx\|_{L_p(k)} \le C$, for all $x \in B_r$.

2. $\lim\limits_{h\to 0}\left(\sup\limits_{t\in[a,b]}\int\limits_a^t k(t,s)|Tx(s+h)-Tx(s)|^p ds\right)^{\frac{1}{p}}=0\,.$ (4)

From (3) we obtain that the constant $C=2^{\frac{1}{q}}\left(\|f\|_{L_p(k)}+r.L.M_1^{\frac{1}{p}}.\|G\|_{L_q(k)}\right)$.

Consequently $T(B_r)$ is uniformly bounded.

We will prove the condition (4).

Let $x\in B_r$. From condition 2.1 and Hölder's inequality we have

$$|Tx(s+h)-Tx(s)|^p\le$$

$$\le 2^{p-1}|f(s+h)-f(s)|^p+2^{2(p-1)}\left(\int\limits_a^s|V(s+h,\tau)-V(s,\tau)||g(\tau,x(\tau))|d\tau\right)^p+$$

$$+2^{2(p-1)}\left(\int\limits_s^{s+h}|V(s+h,\tau)||g(\tau,x(\tau))|d\tau\right)^p\le$$

$$\le 2^{p-1}|f(s+h)-f(s)|^p+2^{2(p-1)}\left(\int\limits_a^s\frac{k^{\frac{1}{p}+\frac{1}{q}}(s,\tau)}{k_3(\tau)}|V(s+h,\tau)-V(s,\tau)|G(\tau)L|x(\tau)|d\tau\right)^p+$$

$$+2^{2(p-1)}\left(\int\limits_s^{s+h}k(s+h,\tau)G(\tau)L|x(\tau)|d\tau\right)^p\le$$

$$\le 2^{p-1}|f(s+h)-f(s)|^p+$$

$$+2^{2(p-1)}\left(\int\limits_a^s k(s,\tau)|V(s+h,\tau)-V(s,\tau)|^q\frac{G^q(\tau)}{k_3^{\,q}(\tau)}L^q d\tau\right)^{\frac{p}{q}}.\left(\sup_{s\in[a,b]}\int\limits_a^s k(s,\tau)|x(\tau)|^p d\tau\right)^{\frac{1}{p}.p}+$$

$$+2^{2(p-1)}\left(\int\limits_s^{s+h}k(s+h,\tau)G^q(\tau)L^q d\tau\right)^{\frac{p}{q}}.\left(\int\limits_s^{s+h}k(s+h,\tau)|x(\tau)|^p d\tau\right)^{\frac{1}{p}.p}\le$$

$$\le 2^{p-1}|f(s+h)-f(s)|^p+$$

$$+2^{2(p-1)}L^p.\sup_{\tau\in[a,b]}|V(s+h,\tau)-V(s,\tau)|^p.\|x\|^p_{L_p(k)}.\left\|\frac{G}{k_3}\right\|^p_{L_q(k)}+$$

$$+2^{2(p-1)}L^p.\left(\int\limits_s^{s+h}k(s+h,\tau)G^q(\tau)d\tau\right)^{\frac{p}{q}}.\|x\|^p_{L_p(k)}\,.$$

Then

$$\left(\sup_{t\in[a,b]}\int\limits_a^t k(t,s)|Tx(s+h)-Tx(s)|^p ds\right)^{\frac{1}{p}}\le$$

$$\le\left(\sup_{t\in[a,b]}\int\limits_a^t k(t,s)\left[2^{p-1}|f(s+h)-f(s)|^p+2^{2(p-1)}L^p.\sup_{\tau\in[a,b]}|V(s+h,\tau)-V(s,\tau)|^p.\|x\|^p_{L_p(k)}.\left\|\frac{G}{k_3}\right\|^p_{L_q(k)}+\right.\right.$$

$$\left.\left.+2^{2(p-1)}L^p.\left(\int\limits_s^{s+h}k(s+h,\tau)G^q(\tau)d\tau\right)^{\frac{p}{q}}.\|x\|^p_{L_p(k)}\right]ds\right)^{\frac{1}{p}}\le$$

$$\le 2^{\frac{p-1}{p}}\left(\sup_{t\in[a,b]}\int\limits_a^t k(t,s)|f(s+h)-f(s)|^p\,ds\right)^{\frac{1}{p}}+$$

$$+2^{\frac{2}{q}} L.\|x\|_{L_p(k)} .\left\|\frac{G}{k_3}\right\|_{L_q(k)} \left( \sup_{t\in[a,b]} \int_a^t k(t,s) \sup_{\tau\in[a,b]} |V(s+h,\tau)-V(s,\tau)|^p \, ds \right)^{\frac{1}{p}} +$$

$$+2^{\frac{2}{q}} .L\|x\|_{L_p(k)} .\left( \sup_{t\in[a,b]} \int_a^t k(t,s) \left( \int_s^{s+h} k(s+h,\tau) G^q(\tau) d\tau \right)^{\frac{p}{q}} ds \right)^{\frac{1}{p}}.$$

From conditions 1.2, 3 and $G \in L_q(k)$ it follows

$$\lim_{h\to 0} \left( \sup_{t\in[a,b]} \int_a^t k(t,s)|Tx(s+h)-Tx(s)|^p ds \right)^{\frac{1}{p}} = 0 .$$

Hence the operator $T$ defined by (2) is compact in $B_r$.

From Shauder's fixed point theorem it follows the nonlinear Volterra-Hammerstein integral equation (1) has a $L_p(k)$-solution in $B_r$. □

**Theorem 3.** *Let the following conditions are fulfilled:*

***1.*** *The kernel* $V(t,s)$ *satisfies the following conditions:*

***1.1.*** *The condition (H2) holds.*

***1.2.*** $\lim_{h\to 0} \sup_{t\in[a,b]} \int_a^t k_2(s) \left( \sup_{\tau\in[a,b]} |V(s+h,\tau)-V(s,\tau)|^p \right) ds = 0$ *and* $\sup_{\tau\in[a,b]} |V(s,\tau)| \in L_p(k_2)$.

***2.*** *The function* $g(s,x)$ *satisfies the following conditions:*

***2.1.*** *There exist the functions*

$G(\cdot) : [a,b] \to \mathbb{R}_+$ , $\Phi(\cdot) : \mathbb{R}_+ \to \mathbb{R}_+$, *such that* $|g(s,x)| \le G(s)\Phi(|x|)$ *for all* ***Грешка! Невалиден вграден обект.****,* $x \in \mathbb{R}$, *where* $G \in L_q(k_2)$, $\frac{G}{k_2} \in L_q(k_2)$, $\Phi(|x|) \le L|x|$ *for all* $x \in \mathbb{R}$ *and some positive constant* $L$, $\frac{1}{p}+\frac{1}{q}=1$.

*Moreover, assume that the function* $G$ *satisfies the condition* $2^{\frac{1}{q}} L.M_2.M_3.\|G\|_{L_q(k_2)} < 1$.

***2.2.*** *There exists positive constant* $L_1$ *such that* $\left|\frac{\partial g}{\partial x}(s,x)\right| \le L_1$ *for all* $s \in [a,b], x \in \mathbb{R}$.

***3.*** *The function* $f \in L_p(k_2)$ *and* $\lim_{h\to 0} \sup_{t\in[a,b]} \int_a^t k_2(s)|f(s+h)-f(s)|^p ds = 0$.

*Then the nonlinear Volterra-Hammerstein integral equation* (1) *has a* $L_p(k_2)$*-solution.*

The Theorem 3 is proof analogously of Theorem 2.

## 4. Examples

We will give an example, which illustrate conditions of Theorem 2 and Theorem 3.

**Example 1.**

Consider the nonlinear Volterra-Hammerstein integral equation

$$x(t) = \frac{e^{-t}}{t+1} + \int_0^t \frac{\sin\frac{1}{8}(t+2s+1)}{(s^2+1)} e^{-s} \ln(sx(s)+1) ds \ , \ t \in [0,1].$$

In this case the functions $f(t) = \frac{e^{-t}}{t+1}$ , $t \in [0,1]$, kernel $V(t,s) = \frac{\sin\frac{1}{8}(t+2s+1)}{s^2+1}$ and $g(s,x) = e^{-s}\ln(sx+1)$.

For the functions $k(\cdot,\cdot)$, $G(\cdot)$ and $\Phi(\cdot)$ we obtain $k(t,s)=\frac{t}{8}+\frac{s}{4}+\frac{1}{8}$, $G(s)=e^{-s}$ and $\Phi(|x|)=|x|$.

For the constants $M_1$, $L$ and $L_1$ we obtain $M_1=\frac{3}{8}$, $L=1$ and $L_1=1$.

It is easily seen that the functions satisfy the conditions of Theorem 2.

**Example 2.**

Consider the nonlinear Volterra-Hammerstein integral equation

$$x(t)=t^2e^{-t}+\int_0^t\frac{(s+t)}{4}\ln(1+t)se^{-sx(s)}arctgx(s)ds\ ,\ t\in[0,1].$$

In this case the functions $f(t)=t^2e^{-t}$, kernel $V(t,s)=\frac{(s+t)}{4}\ln(1+t)$ and $g(s,x)=se^{-sx}arctgx$.

For the functions $k_1(\cdot)$, $k_2(\cdot)$, $G(\cdot)$ and $\Phi(\cdot)$ we obtain $k_1(t)=t$, $k_2(s)=\frac{s+1}{4}$, $G(s)=s$ and $\Phi(|x|)=|x|$.

For the constants $M_2$, $M_3$, $L$ and $L_1$ we obtain $M_2=1$, $M_3=\frac{1}{2}$, $L=1$ and $L_1=1+\frac{\pi}{2}$.

It is easily seen that the functions satisfy the conditions of Theorem 3.

## REFERENCES


1. Agarwal R.P., O'Regan D., Wong P.J. Y. (1999). *Positive solutions of differential, difference and integral equations*. Kluwer Academic, Dordrecht.
2. Antonevich A.B., Radyno Y.V., (1984). *Functional analysis and integral equations*. Minsk Higher School, 351 p.
3. Banas J., Darwish M. A., Olszowy L., Sadarangani K. (2015). *Existence and asymptotic behavour of solutions of differential and integral equations in some functional spaces*. Hindawi Publishing Corporation, Journal of Functional Spaces, ID 235043.
4. Burton T.A. (1983). *Volterra integral and differential equations*, Academic Press, New York.
5. Georgieva A., *Properties of $L_p(k)$-solutions of linear nonhomogeneous impulsive differential equations with unbounded linear operator*, Anniversary International Conference REMIA 2010, 129-135 p.
6. Karoni A. (2005). *On the existence of continuos solutions of nonlinear integral equations*. Applied Mathematics Letters (18) , 299-305 p.
7. Mateknejad K., Nouri K., Mollapourasi R. (2009). *Existence of solutions for some nonlinear integral equations*, Communications in nonlinear science an numerical simulations vol.14, issue 6, 2559-2564 p.
8. O'Regan D., Meehan M.(1998). *Existence theory for nonlinear integral and integro-differential equations*, Kluwer Academic, Dordrecht.



Department of
Mathematics, Physics and Chemistry
Technical University – Sofia,
Plovdiv Branch
25 Tsanko Dyustabanov Str.
4000 Plovdiv
BULGARIA
E-mail: akosseva@gmail.com

Faculty of Mathematics and Informatics
Plovdiv University
24 Tsar Asen Str.
4000 Plovdiv
BULGARIA
E-mail: atanaska@uni-plovdiv.bg

© International Scientific Conference on Engineering, Technologies and Systems
TECHSYS 2016, Technical University – Sofia, Plovdiv branch
26 – 28 May 2016, Plovdiv, Bulgaria

# ODD-DIMENSIONAL SPACES WITH SYMMETRIC AFFINE CONNECTION

IVAN BADEV, GEORGI ZLATANOV

**Abstract:** *Studies odd-dimensional spaces with symmetric affine connection equipped with additional structures. Riemann spaces are determined which contain such structures.*

**Key words:** *spaces with affine connection, coordinate net, Riemann spaces, composition.*

**Mathematics Subject Classification (2010): 53B05, 53B99.**

## 1. Introduction

Spaces with symmetric affine connection, Weyl space and Riemann spaces with additional structures are studied in [1, 3, 4, 5, 8]. In the studied of these spaces additional structures are define with tensors of type (1, 1). By help of $n$ independent vector fields in [10, 11] we introduce an apparatus for the study of spaces symmetric affine connection which contain special compositions or special nets.

This apparatus is used for learning triples of compositions [2] almost paracontact structures, almost complex structures [6] and structures defined with tensors of any kind [7].

In the present work, by means of the same apparatus we study special odd-dimensional spaces endowed with a symmetric affine connection and a covariantly constant affinor. This affinor is defined by $n+1$ independent vector fields and their reciprocal covectors. The obtained results are applied to $2n+1$ dimensional Riemann spaces.

## 2. Basic notions

Let $A_{2n+1}$ be a space endowed with a symmetric affine connection $\nabla$. The Christoffel symbols of $\nabla$ are denoted by $\Gamma^{\nu}_{\alpha\beta}$.

Let us introduce the following notations

$$\begin{aligned} &\alpha,\beta,\gamma,\sigma,\nu,\delta = 1,2,...,2n+1 \\ &i,j,s,k = 1,2,...,n \\ &\bar{i},\bar{j},\bar{s},\bar{k} = n+1,n+2,...,2n. \end{aligned} \tag{1}$$

Let $\underset{\alpha}{V}{}^{\beta}$ be independent vector fields. The net defined by $\underset{\alpha}{V}{}^{\beta}$ is denoted by $\{\underset{\alpha}{V}\}$. The reciprocal covector fields $\overset{\alpha}{V}{}_{\beta}$ of the vector fields $\underset{\alpha}{V}{}^{\beta}$ are determined by

$$\underset{\alpha}{V}{}^{\beta}\overset{\nu}{V}{}_{\beta} = \delta^{\nu}_{\alpha} \Leftrightarrow \underset{\beta}{V}{}^{\nu}\overset{\beta}{V}{}_{\alpha} = \delta^{\nu}_{\alpha}, \tag{2}$$

where $\delta^{\nu}_{\alpha}$ is the identity affinor.

Let $\{\underset{\alpha}{V}\}$ is the coordinate net. Then we have [10, 11]

$$\begin{aligned} &\underset{1}{V}{}^{\alpha}(1,0,0,...,0), \underset{2}{V}{}^{\alpha}(0,1,0,...,0),..., \underset{2n+1}{V}{}^{\alpha}(0,0,...,0,1), \\ &\underset{1}{V}{}_{\alpha}(1,0,0,...,0), \underset{2}{V}{}_{\alpha}(0,1,0,...,0),..., \underset{2n+1}{V}{}_{\alpha}(0,0,...,0,1). \end{aligned} \tag{3}$$

In addition to the usual coordinates $x^{\alpha}(\alpha = 1,2,...,n+1)$, in $A_{2n+1}$ we introduce coordinates with respect to the coordinate net $\{\underset{\alpha}{V}\}$ which will be denoted by $\overset{\alpha}{u}$.

The following derivative equations are known to be valid [9, 10]

$$\nabla_{\sigma}\underset{\alpha}{V}{}^{\beta} = \underset{\alpha}{\overset{\nu}{T}}{}_{\sigma}\underset{\nu}{V}{}^{\beta}, \nabla_{\sigma}\overset{\alpha}{V}{}_{\beta} = -\underset{\nu}{\overset{\alpha}{T}}{}_{\sigma}\overset{\nu}{V}{}_{\beta}. \tag{4}$$

In accordance to [10, 11], in the parameters of the coordinate net $\{\underset{\alpha}{V}\}$ we have

$$\underset{\alpha}{\overset{\beta}{T}}{}_{\sigma} = \Gamma^{\beta}_{\sigma\alpha}. \tag{5}$$

In the space $A_{2n+1}$, we consider a composition $X_p \times X_q$ of two basic manifolds $X_p$ and $X_q, (p+q = 2n+1)$, i.e. their topological product. Two positions (tangent spaces) denoted by $P(X_p)$ and $P(X_q)$ pass thought each point of the

Copyright © 2016 by Technical University of Sofia, Plovdiv branch, Bulgaria ISSN Online: 2535-0048

space $A_{2n+1}$ [3, 4]. According to [3] the coordinates $\overset{\alpha}{u}$ are adapted to the composition $X_p \times X_q$.

It is known that a composition is completely defined by the affinor field $a_\alpha^\beta$, satisfying the condition [3, 4]

$$a_\alpha^\beta a_\beta^\nu = \delta_\alpha^\nu. \tag{6}$$

The composition $X_p \times X_q$ is of the type (c, c), or of the type (c,-), or of the type (-,c) if the positions $P(X_p)$ and $P(X_q)$, or the positions $P(X_p)$, or the positions $P(X_q)$ are translated parallely along any line of the space $A_{2n+1}$ [4].

Let us consider the following affinors

$$\begin{aligned} a_\alpha^\beta &= \underset{i}{V}^\beta \overset{i}{V}_\alpha + \underset{\bar{i}}{V}^\beta \overset{\bar{i}}{V}_\alpha - \underset{2n+1}{V}^\beta \overset{2n+1}{V}_\alpha \\ b_\alpha^\beta &= \underset{i}{V}^\beta \overset{i}{V}_\alpha + \underset{2n+1}{V}^\beta \overset{2n+1}{V}_\alpha - \underset{\bar{i}}{V}^\beta \overset{\bar{i}}{V}_\alpha \\ c_\alpha^\beta &= \underset{\bar{i}}{V}^\beta \overset{\bar{i}}{V}_\alpha + \underset{2n+1}{V}^\beta \overset{2n+1}{V}_\alpha - \underset{i}{V}^\beta \overset{i}{V}_\alpha . \end{aligned} \tag{7}$$

From (2) and (7) follow the equations $a_\alpha^\beta a_\beta^\nu = b_\alpha^\beta b_\beta^\nu = c_\alpha^\beta c_\beta^\nu = \delta_\alpha^\nu$. Hence the affinors (7) are defined compositions in $A_{2n+1}$. Let the affinor $a_\alpha^\beta$ define the composition $X_{2n} \times X_1$ with positions $P(X_{2n})$ and $P(X_1)$. The projecting affinors of this composition are given by: ${}^1a_\alpha^\beta = \underset{i}{V}^\beta \overset{i}{V}_\alpha + \underset{\bar{i}}{V}^\beta \overset{\bar{i}}{V}_\alpha$ and ${}^2a_\alpha^\beta = \underset{2n+1}{V}^\beta \overset{2n+1}{V}_\alpha$. Let the affinor $b_\alpha^\beta$ define the composition $Y_{n+1} \times Y_n$ with positions $P(Y_{n+1})$ and $P(Y_n)$. The projecting affinors of this composition are given by: ${}^1b_\alpha^\beta = \underset{i}{V}^\beta \overset{i}{V}_\alpha + \underset{2n+1}{V}^\beta \overset{2n+1}{V}_\alpha$ and ${}^2b_\alpha^\beta = \underset{\bar{i}}{V}^\beta \overset{\bar{i}}{V}_\alpha$. And let the affinor $c_\alpha^\beta$ define the composition $Z_{n+1} \times Z_n$ with positions $P(Z_{n+1})$ and $P(Z_n)$. The projecting affinors of this composition are given by: ${}^1c_\alpha^\beta = \underset{\bar{i}}{V}^\beta \overset{\bar{i}}{V}_\alpha + \underset{2n+1}{V}^\beta \overset{2n+1}{V}_\alpha$ and ${}^2c_\alpha^\beta = \underset{i}{V}^\beta \overset{i}{V}_\alpha$.

Obviously;

$$\begin{aligned} &\underset{i}{V}^\alpha, \underset{\bar{i}}{V}^\alpha \in P(X_{2n}), \underset{2n+1}{V}^\alpha \in P(X_1), \\ &\underset{i}{V}^\alpha, \underset{2n+1}{V}^\alpha \in P(Y_{n+1}), \underset{\bar{i}}{V}^\alpha \in P(Y_n), \\ &\underset{\bar{i}}{V}^\alpha, \underset{2n+1}{V}^\alpha \in P(Z_{n+1}), \underset{i}{V}^\alpha \in P(Z_n). \end{aligned}$$

## 3. Space $A_{2n+1}$ with additional structures

Let $A_{2n+1}$ be a space endowed with a symmetric affine connection. Consider the following affinor field

$$J_\alpha^\beta = \underset{i}{V}^\beta \overset{i}{V}_\alpha - \underset{2n+1}{V}^\beta \overset{2n+1}{V}_\alpha . \tag{8}$$

**Theorem**. The equation

$$\nabla_\sigma J_\alpha^\beta = 0 \tag{9}$$

it fulfilled if and only if the coefficients of derivative equations (4) satisfy

$$\underset{\bar{s}}{\overset{i}{\Gamma}}_\sigma = \underset{s}{\overset{\bar{i}}{\Gamma}}_\sigma = 0, \ \underset{s}{\overset{2n+1}{\Gamma}}_\sigma = \underset{\bar{s}}{\overset{2n+1}{\Gamma}}_\sigma = 0, \ \underset{2n+1}{\overset{i}{\Gamma}}_\sigma = \underset{2n+1}{\overset{\bar{i}}{\Gamma}}_\sigma = 0. \tag{10}$$

**Proof**. According to (4) equality (9) take the form

$$\begin{aligned} &\underset{i}{\overset{\nu}{\Gamma}}_\sigma \underset{\nu}{V}^\beta \overset{i}{V}_\alpha - \underset{\nu}{\overset{i}{\Gamma}}_\sigma \underset{i}{V}^\beta \overset{\nu}{V}_\alpha - \underset{2n+1}{\overset{\nu}{\Gamma}}_\sigma \underset{\nu}{V}^\beta \overset{2n+1}{V}_\alpha + \\ &\underset{\nu}{\overset{2n+1}{\Gamma}}_\sigma \underset{2n+1}{V}^\beta \overset{\nu}{V}_\alpha = 0. \end{aligned} \tag{11}$$

After contacting of (11) with $\underset{s}{V}^\alpha, \underset{\bar{s}}{V}^\alpha$ and $\underset{2n+1}{V}^\alpha$ successively we obtain

$$\begin{aligned} &\underset{s}{\overset{\nu}{\Gamma}}_\sigma \underset{\nu}{V}^\beta - \underset{s}{\overset{i}{\Gamma}}_\sigma \underset{i}{V}^\beta + \underset{s}{\overset{2n+1}{\Gamma}}_\sigma \underset{2n+1}{V}^\beta = 0 \\ &- \underset{\bar{s}}{\overset{i}{\Gamma}}_\sigma \underset{i}{V}^\beta + \underset{\bar{s}}{\overset{2n+1}{\Gamma}}_\sigma \underset{2n+1}{V}^\beta = 0 \\ &- \underset{2n+1}{\overset{i}{\Gamma}}_\sigma \underset{i}{V}^\beta - \underset{2n+1}{\overset{\nu}{\Gamma}}_\sigma \underset{\nu}{V}^\beta + \underset{2n+1}{\overset{2n+1}{\Gamma}}_\sigma \underset{2n+1}{V}^\beta = 0. \end{aligned} \tag{12}$$

The last equations are equivalent of (11). Since the vector fields $\underset{\alpha}{V}^\beta$ are independent, equalities (12) are equivalent to conditions (10).

**Corollary 1**. The equation (9) it fulfilled if and only if in the parameters of the coordinate net $\{\underset{\alpha}{V}\}$ the Christoffel symbols satisfy

$$\begin{aligned} &\Gamma^i_{\sigma s} = \Gamma^{\bar{i}}_{\sigma s} = 0, \Gamma^{2n+1}_{\sigma s} = \Gamma^{2n+1}_{\sigma \bar{s}} = 0, \\ &\Gamma^i_{\sigma 2n+1} = \Gamma^{\bar{i}}_{\sigma 2n+1} = 0. \end{aligned} \tag{13}$$

**Proof.** In the parameters of the coordinate net $\{\underset{\alpha}{V}\}$ we have (5). Hence they (10) and (13) are equivalent.

**Corollary 2**. The space $A_{2n+1}$ is a space of $(c,c)$ composition $X_{2n} \times X_1$ and $(c,-)$ composition $Y_{n+1} \times Y_n$ and $(-,c)$ composition $Z_n \times Z_{n+1}$ if a is satisfied (9).

**Proof.** Follows from [3, 4] and (13).

**Definition.** The one-dimensional generalized composition $Y_{n+1} \times Z_{n+1}$ will be called of type

$(c,c)$ if the positions $P(Y_{n+1})$ and $P(Z_{n+1})$ are translated parallely along any line of space $A_{2n+1}$.

**Corollary 3.** The one-dimensional generalized composition $Y_{n+1} \times Z_{n+1}$ is of type $(c,c)$ if is fulfilled (9).

**Proof.** Followed of [3, 4] and (13).

## 4. Riemann space $V_{2n+1}$ with additional structures

Let $V_{2n+1}$ be a Riemann space with metric tensor $g_{\alpha\beta}$ and connection of Levi-Civita. The fundamental equation is $\nabla_\sigma g_{\alpha\beta} = 0$.

Let vector fields $\underset{\alpha}{V}^{\beta}$ satisfies the equations $g_{\alpha\beta} \underset{i}{V}^{\alpha} \underset{\bar{j}}{V}^{\beta} = 0$, $g_{\alpha\beta} \underset{i}{V}^{\alpha} \underset{2n+1}{V}^{\beta} = 0$ and $g_{\alpha\beta} \underset{\bar{i}}{V}^{\alpha} \underset{2n+1}{V}^{\beta} = 0$. In parameters of coordinate net $\{\underset{\alpha}{V}\}$, the matrix of tensor $g_{\alpha\beta}$ is

$$(g_{\alpha\beta}) = \begin{pmatrix} g_{ij} & 0 & 0 \\ 0 & g_{\bar{i}\bar{j}} & 0 \\ 0 & 0 & g_{2n+12n+1} \end{pmatrix}.$$

Let the affinor (8) satisfy the equation (9). The coefficients of connection of Levi-Civita, in parameters of coordinate net $\{\underset{\alpha}{V}\}$ satisfy (13). According to [3, 4] the compositions $Y_{n+1} \times Y_n$ and $Z_{n+1} \times Z_n$ will be of type $(c,c)$. From equalities $\nabla_{\bar{s}} g_{ij} = 0$, $\nabla_{2n+1} g_{ij} = 0$, $\nabla_s g_{\bar{i}\bar{j}} = 0$, $\nabla_{2n+1} g_{\bar{i}\bar{j}} = 0$, $\nabla_s g_{2n+12n+1} = 0$, $\nabla_{\bar{s}} g_{2n+12n+1} = 0$ and (13) we obtain, that the linear element of the Riemann space $V_{2n+1}$ in coordinate net $\{\underset{\alpha}{V}\}$ is

$$ds^2 = g_{ij}(u^s)du^i du^j + g_{\bar{i}\bar{j}}(u^{\bar{s}})du^{\bar{i}} du^{\bar{j}} + g_{2n+12n+1j}(u^{2n+1})(du^{2n+1})^2. \quad (15)$$

Therefore the Riemann space $V_{2n+1}$ is a space of $Y_n \times Z_n \times X_1$ compositions and the positions $P(Y_n)$, $P(Z_n)$ and $P(X_1)$ are mutually orthogonal. The positions $P(Y_n)$, $P(Z_n)$ and $P(X_1)$ are translated parallely along any line of $V_{2n+1}$, then $Y_n \times Z_n \times X_1$ is a Cartesian composition.

The Riemann space $V_{2n+1}$, which allows Cartesian compositions $Y_n \times Z_n \times X_1$ with mutually perpendicular positions $P(Y_n)$, $P(Z_n)$ and $P(X_1)$ is compatible enough. His linear element is the sum of the line elements that determine the internal geometries of these positions. Between parallely positions exist isometric accordance.

The projecting affinors of composition $Y_n \times Z_n \times X_1$ are given by: ${}^1d_\alpha^\beta = \underset{i}{V}^{\beta} \overset{i}{V}_\alpha$, ${}^2d_\alpha^\beta = \underset{\bar{i}}{V}^{\beta} \overset{\bar{i}}{V}_\alpha$ and ${}^3d_\alpha^\beta = \underset{2n+1}{V}^{\beta} \overset{2n+1}{V}_\alpha$.

Obviously $\underset{i}{V}^{\alpha} \in P(Y_n)$, $\underset{\bar{i}}{V}^{\alpha} \in P(Z_n)$ and $\underset{2n+1}{V}^{\alpha} \in P(X_1)$.

For arbitrary vector $V^\alpha$ we have

$$V^\alpha = {}^1d_\beta^\alpha V^\beta + {}^2d_\beta^\alpha V^\beta + {}^3d_\beta^\alpha V^\beta =$$

${}^1V^\alpha + {}^2V^\alpha + {}^3V^\alpha$, when ${}^1d_\beta^\alpha V^\beta = {}^1V^\alpha \in P(Y_n)$, ${}^2d_\beta^\alpha V^\beta = {}^2V^\alpha \in P(Z_n)$, ${}^3d_\beta^\alpha V^\beta = {}^3V^\alpha \in P(X_1)$.

## REFERENCES


1. Adati T., Miyaza T., (1977), On paracontact Riemann manifolds. *TRU Math.,*13(2), 27-39.
2. Ajeti M., Teofilova M., Zlatanov G., (2011), Triads of compositions in an even-dimensional space with a symmetric affine connection. *Tensor, N.S.,* 73(2), 171-187.
3. Norden A.,P.,(1963), Spaces of Cartesian compositions. *Izv. Vyssh. Uchebn. Zaved. Math.,* 4, 117-125 (in Russian).
4. . Norden A.,P., Timofeev G. N., (1972), Invariant criteria for special compositions of multidimensional space. *Izv. Vyssh. Uchebn. Zaved. Math.,* 8, 81-89 (in Russian).
5. Sasaki S., (1980), On paracontact Riemann manifolds *TRU Math.,*16(2), 75-86.
6. Teofilova M., Zlatanov G., (2013), Odd-dimensional Riemann spaces with almost contact and almost paracontact structures. *Adv. Math. Sci. J.* 2, 25-35.
7. Teofilova M., Zlatanov G., (2014), Special spaces with a symmetric affine connection. *Tensor, N.S.,* 75(2), 154-165.
8. Timofeev G. N., (1976), Invariant characteristics of special compositions in Weyl spaces. *Izv. Vyssh. Uchebn. Zaved. Math.,* 1, 87-95 (in Russian).
9. Tsareva B., Zlatanov G.,(1996), Geometry of the nets in equiaffine spaces. *J. Geom.,*55, 192-201.
10. Zlatanov G. (2002), Compositions generated by special nets in affinely connected spaces. *Serdica Math. J.* 1001-1012.
11. Zlatanov G. (2011), Special compositions in affinely connected spaces without a torsion. *Serdica Math. J.* 37,211-220.

Badev Ivan
Technical University-Sofia branch Plovdiv
25 Tsanko Djustabanov str
4000 Plovdiv Bulgaria
E-mail: ivanbadev@abv.bg

Zlatanov Georgi
Faculty of Mathematics and Informatics,
Plovdiv University,
236 Bulgaria Bvld., 4003 Plovdiv Bulgaria
E-mail: zlatanovg@gmail.com

© International Scientific Conference on Engineering, Technologies and Systems
TECHSYS 2016, Technical University – Sofia, Plovdiv branch
26 – 28 May 2016, Plovdiv, Bulgaria

# CARTESIAN GENERALIZED COMPOSITIONS IN SPACES WITH A SYMMETRIC AFFINE CONNECTION

IVAN BADEV, MARTA TEOFILOVA, GEORGI ZLATANOV

**Abstract:** *An approach for generalization of the term composition is introduced. Cartesian generalized compositions in spaces with a symmetric affine connection are studied. Special characteristics of the spaces containing such compositions are obtained. Riemannian spaces endowed with special Cartesian generalized compositions are examined.*

**MSC (2010):** 53B05, 53B99
**Key words:** *spaces with affine connections, Riemannian spaces, Cartesian compositions, generalized compositions*

## 1. Introduction

In [7, 8], an apparatus for the study of spaces with a symmetric affine connection containing special compositions or nets is introduced. This apparatus is constructed by help of independent vector fields. The same apparatus is applied to the study of triples of compositions in [1], four-dimensional manifolds with additional structures in [2], and other tensor structures in [5].

In this paper, we introduce a generalization of the term composition. By help of the apparatus given in [7, 8], we explore Cartesian generalized compositions in spaces with a symmetric affine connection. In the parameters of the special coordinate net we obtain the metric tensor of a Riemannian space endowed with special Cartesian generalized compositions.

## 2. Basic Notions

Let $A_N$ be a space with a symmetric affine connection. Consider $r$ differentiable manifolds $X_{n_a} \subset A_N$, where by $n_a$ we denote the dimension of the manifold $X_{n_a}$. Further, consider the manifolds $Y_{m_1} = X_{n_1} \cup X_{n_r}$, $Y_{m_2} = X_{n_2} \cup X_{n_r}$,..., $Y_{m_{r-1}} = X_{n_{r-1}} \cup X_{n_r}$, where $n_1 + n_2 + ... + n_r \le N$. We will say that the manifolds $Y_{m_1}$, $Y_{m_2}$,..., $Y_{m_{r-1}}$ define an $m_{r-1}$ dimensional generalized composition of order $n_r$ which will be denoted by $Y_{m_1} \cup Y_{m_2} \cup ... \cup Y_{m_{r-1}}$. If $n_r = 0$ the manifolds $Y_{m_1}$, $Y_{m_2}$, ..., $Y_{m_{r-1}}$ define a usual composition in $A_N$. By $P(Y_{m_1})$, $P(Y_{m_2})$,..., $P(Y_{m_{r-1}})$ we will denote the positions (tangent spaces) of the manifolds $Y_{m_1}, Y_{m_2}, ..., Y_{m_{r-1}}$, respectively.

**Definition 1**. The generalized composition $Y_{m_1} \cup Y_{m_2} \cup ... \cup Y_{m_{r-1}}$ will be called *Cartesian* if the positions $P(Y_{m_1})$, $P(Y_{m_2})$,..., $P(Y_{m_{r-1}})$ are translated parallelly along any line in the space $A_N$.

Further we will use the following notations:

$$\alpha, \beta, \gamma, \delta, \sigma, \nu = 1, 2, ..., N; \tag{1}$$

$$i, j, k, s = 1, 2, ..., m; \quad \bar{i}, \bar{j}, \bar{k}, \bar{s} = m+1, m+2, ..., m+n; \tag{2}$$

$$a, b, c, d = m+n+1, m+n+2, ..., \quad m+n+p = N. \tag{3}$$

Let $\underset{\sigma}{v}{}^{\alpha}$ $(\alpha, \sigma = 1, 2, ..., N)$ be independent vector fields. The reciprocal covector fields to $\underset{\sigma}{v}{}^{\alpha}$ are denoted by $\overset{\sigma}{v}_{\alpha}$ and are determined by the following equations

$$\underset{\sigma}{v}{}^{\alpha} \overset{\sigma}{v}_{\beta} = \delta^{\alpha}_{\beta} \quad \Leftrightarrow \quad \underset{\beta}{v}{}^{\sigma} \overset{\alpha}{v}_{\sigma} = \delta^{\alpha}_{\beta}, \tag{4}$$

Copyright © 2016 by Technical University of Sofia, Plovdiv branch, Bulgaria ISSN Online: 2535-0048

where $\delta^{\alpha}_{\beta}$ is the identity affinor. The independent vector fields $\underset{\sigma}{v}^{\alpha}$ determine one-parameter families of lines $\underset{\alpha}{v}$ which define a net $\{\underset{\alpha}{v}\}$ in $A_N$.

Let us choose the net $\{\underset{\alpha}{v}\}$ for the coordinate net. Then, according to [7, 8] and (4), we have

$$\begin{array}{l} \overset{1}{v}{}^{\alpha}(1,0,...,0), \overset{2}{v}{}^{\alpha}(0,1,...,0),..., \overset{N}{v}{}^{\alpha}(0,0,...,1); \\ \overset{1}{v}_{\alpha}(1,0,...,0), \overset{2}{v}_{\alpha}(0,1,...,0),..., \overset{N}{v}_{\alpha}(0,0,...,1). \end{array} \tag{5}$$

In addition to the arbitrary coordinate net $x^{\alpha}$ ($\alpha = 1, 2, ..., N$) in $A_N$ we introduce the coordinates $u^{\alpha}$ with respect to the net $\{\underset{\alpha}{v}\}$.

The coefficients of the affine connection in $A_N$ and its rule of covariant differentiation are denoted by $\Gamma^{\sigma}_{\alpha\beta}$ and $\nabla$, respectively. According to [6, 7, 8], the following derivative equations hold

$$\nabla_{\sigma} \underset{\alpha}{v}{}^{\beta} = \underset{\alpha}{\overset{\nu}{\mathrm{T}}}{}_{\sigma} \underset{\nu}{v}{}^{\beta}, \quad \nabla_{\sigma} \overset{\alpha}{v}_{\beta} = -\underset{\nu}{\overset{\alpha}{\mathrm{T}}}{}_{\sigma} \overset{\nu}{v}_{\beta}. \tag{6}$$

In the parameters of the coordinate net $\{\underset{\alpha}{v}\}$ we have [6, 7, 8]

$$\underset{\alpha}{\overset{\beta}{\mathrm{T}}}{}_{\sigma} = \Gamma^{\beta}_{\sigma\alpha}. \tag{7}$$

### 3. Two-dimensional Cartesian generalized compositions of order *p*

Let us consider the following affinors

$$\begin{array}{l} a^{\beta}_{\alpha} = \underset{i}{v}{}^{\beta} \overset{i}{v}_{\alpha} + \underset{a}{v}{}^{\beta} \overset{a}{v}_{\alpha} - \underset{\bar{i}}{v}{}^{\beta} \overset{\bar{i}}{v}_{\alpha}, \\ b^{\beta}_{\alpha} = \underset{\bar{i}}{v}{}^{\beta} \overset{\bar{i}}{v}_{\alpha} + \underset{a}{v}{}^{\beta} \overset{a}{v}_{\alpha} - \underset{i}{v}{}^{\beta} \overset{i}{v}_{\alpha}. \end{array} \tag{8}$$

Since $a^{\beta}_{\alpha} a^{\sigma}_{\beta} = \delta^{\sigma}_{\alpha}$, according to [3, 4], the affinor $a^{\beta}_{\alpha}$ defines the composition $X_{m+p} \times X_n$. Let $P(X_{m+p})$ and $P(X_n)$ be the positions of basic manifolds $X_{m+p}$ and $X_n$, respectively. According to [7, 8], the projecting affinors of the composition $X_{m+p} \times X_n$ are given by

$${}^{1}a^{\beta}_{\alpha} = \underset{i}{v}{}^{\beta} \overset{i}{v}_{\alpha} + \underset{a}{v}{}^{\beta} \overset{a}{v}_{\alpha}, \quad {}^{2}a^{\beta}_{\alpha} = \underset{\bar{i}}{v}{}^{\beta} \overset{\bar{i}}{v}_{\alpha}. \tag{9}$$

Obviously $\underset{i}{v}{}^{\alpha}, \underset{a}{v}{}^{\alpha} \in P(X_{m+p}), \underset{\bar{i}}{v}{}^{\alpha} \in P(X_n)$. If $v^{\alpha}$ is an arbitrary vector field then $v^{\alpha} = {}^{1}a^{\alpha}_{\beta} v^{\beta} + {}^{2}a^{\alpha}_{\beta} v^{\beta} = \overset{1}{V}{}^{\alpha} + \overset{2}{V}{}^{\alpha}$, where $\overset{1}{V}{}^{\alpha} = {}^{1}a^{\alpha}_{\beta} v^{\beta} \in P(X_{m+p})$ and $\overset{2}{V}{}^{\alpha} = {}^{2}a^{\alpha}_{\beta} v^{\beta} \in P(X_n)$. Analogously, the affinor $b^{\beta}_{\alpha}$ defines the composition $X_{n+p} \times X_m$ with positions $P(X_{n+p})$ and $P(X_m)$ and projecting affinors

$${}^{1}b^{\beta}_{\alpha} = \underset{\bar{i}}{v}{}^{\beta} \overset{\bar{i}}{v}_{\alpha} + \underset{a}{v}{}^{\beta} \overset{a}{v}_{\alpha}, \quad {}^{2}b^{\beta}_{\alpha} = \underset{i}{v}{}^{\beta} \overset{i}{v}_{\alpha}. \tag{10}$$

Obviously $\underset{\bar{i}}{v}{}^{\alpha}, \underset{a}{v}{}^{\alpha} \in P(X_{n+p}), \underset{i}{v}{}^{\alpha} \in P(X_m)$.

**Theorem 1**. *The two-dimensional generalized composition $X_{m+p} \cup X_{n+p}$ of order p is Cartesian if only if the coefficients of the derivative equations (6) satisfy the following conditions*

$$\underset{j}{\overset{\bar{i}}{\mathrm{T}}}{}_{\sigma} = \underset{a}{\overset{\bar{i}}{\mathrm{T}}}{}_{\sigma} = \underset{\bar{j}}{\overset{i}{T}}{}_{\sigma} = \underset{a}{\overset{i}{\mathrm{T}}}{}_{\sigma} = 0. \tag{11}$$

**Proof.** The generalized composition $X_{m+p} \cup X_{n+p}$ is Cartesian if only if the positions $P(X_{m+p})$ and $P(X_{n+p})$ are translated parallelly along any line in the space $A_N$. According to [3, 4, 7, 8], the last condition holds if only if the projecting affinors ${}^{1}a^{\beta}_{\alpha}$ and ${}^{1}b^{\beta}_{\alpha}$ satisfy the following equalities

$${}^{1}a^{\alpha}_{\delta} \nabla_{\sigma} {}^{1}a^{\beta}_{\alpha} = 0, \quad {}^{1}b^{\alpha}_{\delta} \nabla_{\sigma} {}^{1}b^{\beta}_{\alpha} = 0. \tag{12}$$

By (6) and (9), the first equality of (12) takes the form

$$\begin{array}{l} (\underset{j}{v}{}^{\alpha} \overset{j}{v}_{\delta} + \underset{b}{v}{}^{\alpha} \overset{b}{v}_{\delta})(\underset{i}{\overset{\nu}{\mathrm{T}}}{}_{\sigma} \underset{\nu}{v}{}^{\beta} \overset{i}{v}_{\alpha} - \underset{\nu}{\overset{i}{\mathrm{T}}}{}_{\sigma} \underset{i}{v}{}^{\beta} \overset{\nu}{v}_{\alpha} \\ + \underset{a}{\overset{\nu}{\mathrm{T}}}{}_{\sigma} \underset{\nu}{v}{}^{\beta} \overset{a}{v}_{\alpha} - \underset{\nu}{\overset{a}{\mathrm{T}}}{}_{\sigma} \underset{a}{v}{}^{\beta} \overset{\nu}{v}_{\alpha}) = 0. \end{array} \tag{13}$$

Hence, by considering (4), from (13) we get

$$\begin{array}{l} \underset{j}{\overset{\nu}{\mathrm{T}}}{}_{\sigma} \underset{\nu}{v}{}^{\beta} \overset{j}{v}_{\delta} - \underset{j}{\overset{i}{\mathrm{T}}}{}_{\sigma} \underset{i}{v}{}^{\beta} \overset{j}{v}_{\delta} - \underset{j}{\overset{a}{\mathrm{T}}}{}_{\sigma} \underset{a}{v}{}^{\beta} \overset{j}{v}_{\delta} \\ - \underset{b}{\overset{i}{\mathrm{T}}}{}_{\sigma} \underset{i}{v}{}^{\beta} \overset{b}{v}_{\delta} + \underset{b}{\overset{\nu}{\mathrm{T}}}{}_{\sigma} \underset{\nu}{v}{}^{\beta} \overset{b}{v}_{\delta} - \underset{b}{\overset{a}{\mathrm{T}}}{}_{\sigma} \underset{a}{v}{}^{\beta} \overset{b}{v}_{\delta} = 0. \end{array} \tag{14}$$

Since the covector fields $\overset{\alpha}{v}_{\beta}$ are independent (14) is equivalent to the equations:

$$\begin{aligned} &\overset{\nu}{T}_{j\sigma}\overset{\beta}{v}_{\nu}-\overset{i}{T}_{j\sigma}\overset{\beta}{v}_{i}-\overset{a}{T}_{j\sigma}\overset{\beta}{v}_{a}=0,\\ &\overset{i}{T}_{b\sigma}\overset{\beta}{v}_{i}-\overset{\nu}{T}_{b\sigma}\overset{\beta}{v}_{\nu}+\overset{a}{T}_{b\sigma}\overset{\beta}{v}_{a}=0. \end{aligned} \tag{15}$$

The vector fields $\overset{\beta}{v}_{\alpha}$ are independent too. Therefore, equalities (15) are equivalent to $\overset{\bar{i}}{T}_{j\sigma}=\overset{\bar{i}}{T}_{a\sigma}=0$.

Reasoning analogously, the second equation of (12) is equivalent to $\overset{i}{T}_{\bar{j}\sigma}=\overset{i}{T}_{a\sigma}=0$ which proves the statement. ■

From (7) and (11) we obtain

**Corollary 1.** *In the parameters of the coordinate net equations (11) take the form*

$$\Gamma^{\bar{i}}_{\sigma j}=\Gamma^{\bar{i}}_{\sigma a}=\Gamma^{i}_{\sigma\bar{j}}=\Gamma^{i}_{\sigma a}=0. \tag{16}$$

**Application 1.** Let us consider a Riemannian space $V_N$ with metric tensor $g_{\alpha\beta}$ and Levi-Civita connection $\nabla$. Let the generalized composition $X_{m+p}\cup X_{n+p}$ be Cartesian. The vector fields $\overset{\beta}{v}_{\alpha}$ are chosen so that $g_{\alpha\beta}\overset{\alpha}{v}_{i}\overset{\beta}{v}_{\bar{j}}=g_{\alpha\beta}\overset{\alpha}{v}_{i}\overset{\beta}{v}_{a}=$ $=g_{\alpha\beta}\overset{\alpha}{v}_{\bar{i}}\overset{\beta}{v}_{a}=0.$ In the parameters of the coordinate net $\{\overset{\alpha}{v}\}$ the matrix of the tensor $g_{\alpha\beta}$ is given by

$$(g_{\alpha\beta})=\begin{pmatrix} g_{ij} & 0 & 0\\ 0 & g_{\bar{i}\bar{j}} & 0\\ 0 & 0 & g_{ab}\end{pmatrix}. \tag{17}$$

By (16), (17) and the fundamental equation

$$\nabla_{\sigma}g_{\alpha\beta}=0 \tag{18}$$

in the parameters of the coordinate net $\{\overset{\alpha}{v}\}$ we obtain $g_{ij}=g_{ij}(u^{s})$, $g_{\bar{i}\bar{j}}=g_{\bar{i}\bar{j}}(u^{\bar{s}})$, $g_{ab}=g_{ab}(u^{\alpha})$.

Further, let us use the notations (1), (2) and

$$\begin{aligned} &a,b,c,d=m+n+1,m+n+2,...,\\ &m+n+p=N-1. \end{aligned} \tag{19}$$

Consider the affinors

$$\begin{aligned} c^{\beta}_{\alpha}&=\overset{\beta}{v}_{i}\overset{i}{v}_{\alpha}+\overset{\beta}{v}_{a}\overset{a}{v}_{\alpha}-\overset{\beta}{v}_{\bar{i}}\overset{\bar{i}}{v}_{\alpha}-\overset{\beta}{v}_{N}\overset{N}{v}_{\alpha},\\ d^{\beta}_{\alpha}&=\overset{\beta}{v}_{\bar{i}}\overset{\bar{i}}{v}_{\alpha}+\overset{\beta}{v}_{a}\overset{a}{v}_{\alpha}-\overset{\beta}{v}_{i}\overset{i}{v}_{\alpha}-\overset{\beta}{v}_{N}\overset{N}{v}_{\alpha}. \end{aligned} \tag{20}$$

As $c^{\beta}_{\alpha}c^{\sigma}_{\beta}=\delta^{\sigma}_{\alpha}$ the affinor $c^{\beta}_{\alpha}$ defines the composition $X_{m+p}\times X_{n+1}$ [3, 4]. Let $P(X_{m+p})$ and $P(X_{n+1})$ be the positions of the basic manifolds $X_{m+p}$ and $X_{n+1}$, respectively. According to [7, 8] and (9), the projecting affinors of the composition $X_{m+p}\times X_{n+1}$ are given by

$${}^{1}c^{\beta}_{\alpha}={}^{1}a^{\beta}_{\alpha},\quad {}^{2}c^{\beta}_{\alpha}={}^{2}a^{\beta}_{\alpha}+\overset{\beta}{v}_{N}\overset{N}{v}_{\alpha}. \tag{21}$$

Analogously, the affinor $d^{\beta}_{\alpha}$ defines the composition $X_{n+p}\times X_{m+1}$ with positions $P(X_{n+p})$ and $P(X_{m+1})$ and projecting affinors given by

$${}^{1}d^{\beta}_{\alpha}={}^{1}b^{\beta}_{\alpha},\quad {}^{2}d^{\beta}_{\alpha}={}^{2}b^{\beta}_{\alpha}+\overset{\beta}{v}_{N}\overset{N}{v}_{\alpha}. \tag{22}$$

Let us prove the following

**Theorem 2.** *The two-dimensional generalized composition $X_{m+p}\cup X_{n+p}$ of order p is Cartesian if only if the coefficients of the derivative equations (6) satisfy the following conditions*

$$\overset{\bar{i}}{T}_{j\sigma}=\overset{\bar{i}}{T}_{a\sigma}=\overset{i}{T}_{\bar{j}\sigma}=\overset{i}{T}_{a\sigma}=\overset{N}{T}_{j\sigma}=\overset{N}{T}_{\bar{j}\sigma}=\overset{N}{T}_{a\sigma}=0. \tag{23}$$

**Proof.** According to [3, 4, 7, 8], the positions $P(X_{m+p})$ and $P(X_{n+p})$ are translated parallelly along any line in the space $A_N$ if only if the projecting affinors ${}^{1}c^{\beta}_{\alpha}$ and ${}^{1}d^{\beta}_{\alpha}$ satisfy the conditions

$${}^{1}c^{\alpha}_{\delta}\nabla_{\sigma}{}^{1}c^{\beta}_{\alpha}=0,\quad {}^{1}d^{\alpha}_{\delta}\nabla_{\sigma}{}^{1}d^{\beta}_{\alpha}=0. \tag{24}$$

By (6), (9) and (21) the first equality of (24) takes the form (14). Since the covector fields $\overset{\alpha}{v}_{\beta}$ are independent, equation (14) is equivalent to equations (15). As the vector fields $\overset{\beta}{v}_{\alpha}$ are independent it follows that equalities (15) are equivalent to the following conditions $\overset{\bar{i}}{T}_{j\sigma}=\overset{\bar{i}}{T}_{a\sigma}=\overset{N}{T}_{j\sigma}=\overset{N}{T}_{a\sigma}=0.$ Reasoning analogously, the second equation of (24) is equivalent to the conditions $\overset{i}{T}_{\bar{j}\sigma}=\overset{i}{T}_{a\sigma}=\overset{N}{T}_{\bar{j}\sigma}=\overset{N}{T}_{a\sigma}=0$ which completes the proof of the statement. ■

By (7) and (23) we obtain the following

**Corollary 2.** *In the parameters of coordinate net* $\{\underset{\alpha}{v}\}$ *equations (23) take the form*

$$\begin{aligned}&\Gamma^{\bar{i}}_{\sigma j}=\Gamma^{\bar{i}}_{\sigma a}=\Gamma^{i}_{\sigma\bar{j}}=\Gamma^{i}_{\sigma a}=\Gamma^{N}_{\sigma j}\\&=\Gamma^{N}_{\sigma\bar{j}}=\Gamma^{N}_{\sigma a}=0.\end{aligned}\tag{25}$$

**Application 2.** We consider the Riemannian space $V_N(g_{\alpha\beta})$ and the Cartesian generalized composition $X_{m+p}\cup X_{n+p}$. The vector fields $\underset{\alpha}{v}^{\beta}$ are chosen so that

$$\begin{aligned}&g_{\alpha\beta}\,\underset{i}{v}^{\alpha}\,\underset{\bar{i}}{v}^{\beta}=g_{\alpha\beta}\,\underset{i}{v}^{\alpha}\,\underset{a}{v}^{\beta}=g_{\alpha\beta}\,\underset{\bar{i}}{v}^{\alpha}\,\underset{a}{v}^{\beta}\\&=g_{\alpha\beta}\,\underset{i}{v}^{\alpha}\,\underset{N}{v}^{\beta}=g_{\alpha\beta}\,\underset{\bar{i}}{v}^{\alpha}\,\underset{N}{v}^{\beta}=g_{\alpha\beta}\,\underset{a}{v}^{\alpha}\,\underset{N}{v}^{\beta}=0.\end{aligned}$$

In the parameters of the coordinate net $\{\underset{\alpha}{v}\}$ the matrix of the tensor $g_{\alpha\beta}$ is given by

$$(g_{\alpha\beta})=\begin{pmatrix}g_{ij}&0&0&0\\0&g_{\bar{i}\bar{j}}&0&0\\0&0&g_{ab}&0\\0&0&0&g_{NN}\end{pmatrix}.\tag{26}$$

Having in mind (18), (25) and (26), in the parameters of coordinate net $\{\underset{\alpha}{v}\}$ we obtain $g_{ij}=g_{ij}(u^s,u^N)$, $g_{\bar{i}\bar{j}}=g_{\bar{i}\bar{j}}(u^{\bar{s}},u^N)$, $g_{ab}=g_{ab}(u^{\alpha})$ and $g_{NN}=g_{NN}(u^N)$.

## 4. Four-dimensional Cartesian generalized compositions of first order

Let $A_{2n+1}$ be a space with a symmetric affine connection. Further we will use the notations

$$\begin{aligned}&i,j,s,k=1,2,...,m;\\&\bar{i},\bar{j},\bar{k},\bar{s}=m+1,m+2,...,m+n;\\&a,b,c=m+n+1,...,m+n+p;\\&\bar{a},\bar{b},\bar{c}=m+n+p+1,...,m+n+p+q=2n.\end{aligned}\tag{27}$$

Let us consider the affinors

$$\begin{aligned}{}_1J^{\beta}_{\alpha}&=\underset{i}{v}^{\beta}\,\underset{}{v}^{i}_{\alpha}+\underset{2n+1}{v}^{\beta}\,\underset{}{v}^{2n+1}_{\alpha}-\underset{\bar{i}}{v}^{\beta}\,\underset{}{v}^{\bar{i}}_{\alpha}-\underset{a}{v}^{\beta}\,\underset{}{v}^{a}_{\alpha}-\underset{\bar{a}}{v}^{\beta}\,\underset{}{v}^{\bar{a}}_{\alpha},\\{}_2J^{\beta}_{\alpha}&=\underset{\bar{i}}{v}^{\beta}\,\underset{}{v}^{\bar{i}}_{\alpha}+\underset{2n+1}{v}^{\beta}\,\underset{}{v}^{2n+1}_{\alpha}-\underset{i}{v}^{\beta}\,\underset{}{v}^{i}_{\alpha}-\underset{a}{v}^{\beta}\,\underset{}{v}^{a}_{\alpha}-\underset{\bar{a}}{v}^{\beta}\,\underset{}{v}^{\bar{a}}_{\alpha},\\{}_3J^{\beta}_{\alpha}&=\underset{a}{v}^{\beta}\,\underset{}{v}^{a}_{\alpha}+\underset{2n+1}{v}^{\beta}\,\underset{}{v}^{2n+1}_{\alpha}-\underset{i}{v}^{\beta}\,\underset{}{v}^{i}_{\alpha}-\underset{\bar{i}}{v}^{\beta}\,\underset{}{v}^{\bar{i}}_{\alpha}-\underset{\bar{a}}{v}^{\beta}\,\underset{}{v}^{\bar{a}}_{\alpha},\\{}_4J^{\beta}_{\alpha}&=\underset{\bar{a}}{v}^{\beta}\,\underset{}{v}^{\bar{a}}_{\alpha}+\underset{2n+1}{v}^{\beta}\,\underset{}{v}^{2n+1}_{\alpha}-\underset{i}{v}^{\beta}\,\underset{}{v}^{i}_{\alpha}-\underset{\bar{i}}{v}^{\beta}\,\underset{}{v}^{\bar{i}}_{\alpha}-\underset{a}{v}^{\beta}\,\underset{}{v}^{a}_{\alpha}.\end{aligned}\tag{28}$$

Since ${}_1J^{\beta}_{\alpha}\,{}_1J^{\sigma}_{\beta}=\delta^{\sigma}_{\alpha}$, according to [3, 4], the affinor ${}_1J^{\beta}_{\alpha}$ defines the composition $X_{m+1}\times X_{n+p+q}$. Let $P(X_{m+1})$ and $P(X_{n+p+q})$ be the positions of the basic manifolds $X_{m+1}$ and $X_{n+p+q}$, respectively. Obviously $\underset{i}{v}^{\alpha},\underset{2n+1}{v}^{\alpha}\in P(X_{m+1})$ and $\underset{\bar{i}}{v}^{\alpha},\underset{a}{v}^{\alpha},\underset{\bar{a}}{v}^{\alpha}\in P(X_{n+p+q})$. According to [7, 8], the projecting affinors have the form

$$\begin{aligned}{}^1_1J^{\beta}_{\alpha}&=\underset{i}{v}^{\beta}\,\underset{}{v}^{i}_{\alpha}+\underset{2n+1}{v}^{\beta}\,\underset{}{v}^{2n+1}_{\alpha},\\{}^2_1J^{\beta}_{\alpha}&=\underset{\bar{i}}{v}^{\beta}\,\underset{}{v}^{\bar{i}}_{\alpha}+\underset{a}{v}^{\beta}\,\underset{}{v}^{a}_{\alpha}+\underset{\bar{a}}{v}^{\beta}\,\underset{}{v}^{\bar{a}}_{\alpha}.\end{aligned}\tag{29}$$

Similarly, the affinors ${}_2J^{\beta}_{\alpha}$, ${}_3J^{\beta}_{\alpha}$, ${}_4J^{\beta}_{\alpha}$ define the compositions $X_{n+1}\times X_{m+p+q}$, $X_{p+1}\times X_{m+n+q}$, $X_{q+1}\times X_{m+n+p}$, respectively, with positions $P(X_{n+1}),P(X_{m+p+q});\ P(X_{p+1}),P(X_{m+n+q});\ P(X_{q+1}),P(X_{m+n+p})$ The projecting affinors of these compositions are given by

$$\begin{aligned}{}^1_2J^{\beta}_{\alpha}&=\underset{\bar{i}}{v}^{\beta}\,\underset{}{v}^{\bar{i}}_{\alpha}+\underset{2n+1}{v}^{\beta}\,\underset{}{v}^{2n+1}_{\alpha},\\{}^2_2J^{\beta}_{\alpha}&=\underset{i}{v}^{\beta}\,\underset{}{v}^{i}_{\alpha}+\underset{a}{v}^{\beta}\,\underset{}{v}^{a}_{\alpha}+\underset{\bar{a}}{v}^{\beta}\,\underset{}{v}^{\bar{a}}_{\alpha},\\{}^1_3J^{\beta}_{\alpha}&=\underset{a}{v}^{\beta}\,\underset{}{v}^{a}_{\alpha}+\underset{2n+1}{v}^{\beta}\,\underset{}{v}^{2n+1}_{\alpha},\\{}^2_3J^{\beta}_{\alpha}&=\underset{i}{v}^{\beta}\,\underset{}{v}^{i}_{\alpha}+\underset{\bar{i}}{v}^{\beta}\,\underset{}{v}^{\bar{i}}_{\alpha}+\underset{\bar{a}}{v}^{\beta}\,\underset{}{v}^{\bar{a}}_{\alpha},\\{}^1_4J^{\beta}_{\alpha}&=\underset{\bar{a}}{v}^{\beta}\,\underset{}{v}^{\bar{a}}_{\alpha}+\underset{2n+1}{v}^{\beta}\,\underset{}{v}^{2n+1}_{\alpha},\\{}^2_4J^{\beta}_{\alpha}&=\underset{i}{v}^{\beta}\,\underset{}{v}^{i}_{\alpha}+\underset{\bar{i}}{v}^{\beta}\,\underset{}{v}^{\bar{i}}_{\alpha}+\underset{a}{v}^{\beta}\,\underset{}{v}^{a}_{\alpha}.\end{aligned}\tag{30}$$

Let us consider the four-dimensional generalized composition of first order $X_{m+1}\cup X_{n+1}\cup X_{p+1}\cup X_{q+1}$ with positions $P(X_{m+1}),P(X_{n+1}),P(X_{p+1}),P(X_{q+1})$. We prove the following

**Theorem 3.** *The four-dimensional generalized composition* $X_{m+1}\cup X_{n+1}\cup X_{p+1}\cup X_{q+1}$ *is Cartesian if only if the coefficients of the derivative equations (6) satisfy the conditions*

$$\begin{aligned}
&\underset{j}{\overset{\bar{i}}{T}}\sigma=\underset{j}{\overset{a}{T}}\sigma=\underset{j}{\overset{\bar{a}}{T}}\sigma=0,\\
&\underset{\bar{j}}{\overset{i}{T}}\sigma=\underset{\bar{j}}{\overset{a}{T}}\sigma=\underset{\bar{j}}{\overset{\bar{a}}{T}}\sigma=0,\\
&\underset{a}{\overset{i}{T}}\sigma=\underset{a}{\overset{\bar{i}}{T}}\sigma=\underset{a}{\overset{\bar{a}}{T}}\sigma=0,\\
&\underset{\bar{a}}{\overset{i}{T}}\sigma=\underset{\bar{a}}{\overset{\bar{i}}{T}}\sigma=\underset{\bar{a}}{\overset{a}{T}}\sigma=0,\\
&\underset{2n+1}{\overset{i}{T}}\sigma=\underset{2n+1}{\overset{\bar{i}}{T}}\sigma=\underset{2n+1}{\overset{a}{T}}\sigma=\underset{2n+1}{\overset{\bar{a}}{T}}\sigma=0.
\end{aligned}\tag{31}$$

**Proof.** The generalized composition $X_{m+1}\cup X_{n+1}\cup X_{p+1}\cup X_{q+1}$ is Cartesian if only if the positions $P(X_{m+1})$, $P(X_{n+1})$, $P(X_{p+1})$ and $P(X_{q+1})$ are translated parallelly along any line in the space $A_{2n+1}$. According to [3, 4, 7, 8], the last condition holds if only if the projecting affinors ${}^1_1J^\beta_\alpha$, ${}^1_2J^\beta_\alpha$, ${}^1_3J^\beta_\alpha$ and ${}^1_4J^\beta_\alpha$ satisfy

$$\begin{aligned}
&{}^1_1J^\alpha_\delta\nabla_\sigma\,{}^1_1J^\beta_\alpha=0,\quad {}^1_2J^\alpha_\delta\nabla_\sigma\,{}^1_2J^\beta_\alpha=0,\\
&{}^1_3J^\alpha_\delta\nabla_\sigma\,{}^1_3J^\beta_\alpha=0,\quad {}^1_4J^\alpha_\delta\nabla_\sigma\,{}^1_4J^\beta_\alpha=0.
\end{aligned}\tag{32}$$

According to (6) and (29), the first equality of (32) takes the form

$$\begin{aligned}
&(v^\alpha_j v^j_\delta+v^\alpha_{2n+1}v^{2n+1}_\delta)(\underset{i}{\overset{\nu}{T}}\sigma v^\beta_\nu v^i_\alpha-\underset{\nu}{\overset{i}{T}}\sigma v^\beta_i v^\nu_\alpha\\
&+\underset{2n+1}{\overset{\nu}{T}}\sigma v^\beta_\nu v^{2n+1}_\alpha-\underset{\nu}{\overset{2n+1}{T}}\sigma v^\beta_{2n+1}v^\nu_\alpha)=0.
\end{aligned}\tag{33}$$

Since the covector fields $v^\alpha_\beta$ are independent (33) is equivalent to the equations

$$\begin{aligned}
&\underset{j}{\overset{\nu}{T}}\sigma v^\beta_\nu-\underset{j}{\overset{i}{T}}\sigma v^\beta_i-\underset{j}{\overset{2n+1}{T}}\sigma v^\beta_{2n+1}=0,\\
&\underset{2n+1}{\overset{i}{T}}\sigma v^\beta_i-\underset{2n+1}{\overset{\nu}{T}}\sigma v^\beta_\nu+\underset{2n+1}{\overset{2n+1}{T}}\sigma v^\beta_{2n+1}=0.
\end{aligned}\tag{34}$$

Since the vector fields $v^\beta_\alpha$ are independent it follows that equations (34) are equivalent to

$$\underset{j}{\overset{\bar{i}}{T}}\sigma=\underset{j}{\overset{a}{T}}\sigma=\underset{j}{\overset{\bar{a}}{T}}\sigma=0,\quad \underset{2n+1}{\overset{\bar{i}}{T}}\sigma=\underset{2n+1}{\overset{a}{T}}\sigma=\underset{2n+1}{\overset{\bar{a}}{T}}\sigma=0.$$

Analogously, one can prove that the rest of equations in (32) are equivalent to the rest of the equations (31).

**Corollary 3.** *In the parameters of the coordinate net* $\{v_\alpha\}$ *equalities (31) take the form*

$$\begin{aligned}
&\Gamma^{\bar{i}}_{\sigma j}=\Gamma^a_{\sigma j}=\Gamma^{\bar{a}}_{\sigma j}=0,\\
&\Gamma^i_{\sigma\bar{j}}=\Gamma^a_{\sigma\bar{j}}=\Gamma^{\bar{a}}_{\sigma\bar{j}}=0,\\
&\Gamma^i_{\sigma a}=\Gamma^{\bar{i}}_{\sigma a}=\Gamma^{\bar{a}}_{\sigma a}=0,\\
&\Gamma^i_{\sigma\bar{a}}=\Gamma^{\bar{i}}_{\sigma\bar{a}}=\Gamma^i_{\sigma\bar{a}}=0,\\
&\Gamma^i_{\sigma 2n+1}=\Gamma^{\bar{i}}_{\sigma 2n+1}=\Gamma^a_{\sigma 2n+1}=\Gamma^{\bar{a}}_{\sigma 2n+1}=0.
\end{aligned}\tag{35}$$

**Application 3.** Let $V_{2n+1}(g_{\alpha\beta})$ be a Riemannian space and the generalized composition $X_{m+1}\cup X_{n+1}\cup X_{p+1}\cup X_{q+1}$ be Cartesian. In the parameters of the coordinate net $\{v_\alpha\}$ the matrix of $g_{\alpha\beta}$ is given by

$$(g_{\alpha\beta})=\begin{pmatrix}
g_{ij} & 0 & 0 & 0 & 0\\
0 & g_{\bar{i}\bar{j}} & 0 & 0 & 0\\
0 & 0 & g_{ab} & 0 & 0\\
0 & 0 & 0 & g_{\bar{a}\bar{b}} & 0\\
0 & 0 & 0 & 0 & g_{2n+12n+1}
\end{pmatrix}.\tag{36}$$

By (18), (35) and (36) in the parameters of coordinate net $\{v_\alpha\}$ we obtain $g_{ij}=g_{ij}(u^s)$, $g_{\bar{i}\bar{j}}=g_{\bar{i}\bar{j}}(u^{\bar{s}})$, $g_{ab}=g_{ab}(u^c)$, $g_{\bar{a}\bar{b}}=g_{\bar{a}\bar{b}}(u^{\bar{c}})$ and $g_{2n+12n+1}=g_{2n+12n+1}(u^\alpha)$.

**Acknowledgement.** The second author would like to thank project NI15-FMI-004 of the Scientific Research Fund, Plovdiv University, Bulgaria.

## REFERENCES

1. Ajeti, M., Teofilova, M. and Zlatanov G. (2011). Triads of compositions in an even-dimensional space with a symmetric affine connection. *Tensor, N. S.,* 73(3), 171-187.
2. Ajeti, M. (2014). Four dimensional spaces with a symmetric affine connection and additional structures. *Tensor, N. S.,* 75(1), 145-153.
3. Norden, A.P. (1963). Spaces of Cartesian composition, *Izv. Vyssh. Uchebn. Zaved. Math.,* 4, 117-128 (in Russian).
4. Norden, A.P. and Timoffev, G.N. (1972). Invariant criteria for special compositions of multidimensional spaces, *Izv. Vyssh. Uchebn. Zaved. Math.,* 8, 81-89 (in Russian).

5. Teofilova, M. and Zlatanov, G. (2014). Special spaces with a symmetric affine connection, *Tensor, N. S.,* 75(2), 154-165.
6. Zlatanov, G. and Tsareva, B. (1996). Geometry of the nets in equaffine spaces, *J. Geom.,* 55, 192-201.
7. Zlatanov, G. (2002). Compositions generated by special nets in affinely connected spaces, *Serdica, Math., J.,* 28, 1001-1012.
8. Zlatanov, G. (2011). Special compositions in affinely connected spaces without a torsion, *Serdica, Math., J.,* 37, 211-220.

Ivan Badev
Technical University-Sofia, Plovdiv Branch,
25 Tsanko Diustabanov Str., 4000 Plovdiv.
E-mail: ivanbadev@tu-plovdiv.bg

Marta Teofilova, Georgi Zlatanov
Plovdiv University,
236 Bulgaria Blvd., 4003 Plovdiv
E-mail: marta@uni-plovdiv.bg
E-mail: zlatanovg@gmail.com

© International Scientific Conference on Engineering, Technologies and Systems
TECHSYS 2016, Technical University – Sofia, Plovdiv branch
26 – 28 May 2016, Plovdiv, Bulgaria

# AN ALGORITHM FOR DETERMINING AND COMPARING THE LEVELS OF ECONOMIC DEVELOPMENT IN THE DISTRICTS IN BULGARIA

DELYANA DIMOVA

**Abstract:** *This article presents an algorithm for determining and comparing the levels of economic development in the districts in Bulgaria. The necessary information is extracted from the created relational database. These data concerning gross domestic product, gross value added, employment rate and salaries are studied, compared and analysed for the relevant time interval. The developed algorithm can be also used in analyzing other economic and financial indicators.*

**Key words:** *algorithm, data processing, relational database, economic development*

## 1. Introduction

There is a huge quantity of text, audio, video, and other documents available on the Internet, on about any subject. Users need to be able to find relevant information to satisfy their particular information needs. There are two ways of searching for information: to use a search engines or to browse directories organized by categories. There is still a large part of the Internet that is not accessible (for example private databases and intranets) [1].

As the Web keeps expanding, it is increasingly difficult for the Information Retrieval (IR) systems to find relevant information which can satisfy users' needs based on simple search queries. The users express their need using queries [2]. The problem for search engines is not only to find topic relevant results, but results consistent with the user's information need [3, 4]. IR is different from data retrieval, which is about finding precise data in databases with a given structure [1]. The quality of information depends on the accuracy, integrity and consistency of the data in a database [5]. Ideally, this can be achieved if one item of data is stored only once. In reality this may not be possible as some duplication of data may be necessary in certain database architectures, e.g. relational databases make use of tables to store data and establish relationships between the tables by common fields [5].

Structured information in various guises is becoming ubiquitous on today's computers. This may include a user's contacts list, their calendar of events, other structured files such as spreadsheets or databases. In addition to this, unstructured textual content may refer or add information to entities from a user's structured information space [6].

The current paper considers some of these exposed problems. National Statistical Institute provides economic and financial information on its website [7]. These data on gross domestic product, gross value added, employment rate, salaries, employees and etc. are saved in separate files. The information from the files is structured and stored in a created relational database [8]. This database should be expanded. In this context three new relational schemes are designed. The built database contains the following eleven tables (fig. 1):

- Countries (id_country, name);
- Value income (id, year, value-avg-household, id_source, value-avg-person, structure);
- Income sources (id_source, sources, id_country);
-Provinces (id_pro, province, id_country);
- Expenditure groups (id-g, expenditure group, id-country);
- Employees (id3, number, year, id_pro, employment rate);
- Salaries (id2, salary, year, id_pro);
- Value groups (id-v, year, avg- household, avg-person, structure, id-g).
- Households expenditure (id, share-home, share-food, total expenditure per person, year, id_pro);
- Household income (id1, share-salary, share-pensions, share-other social transfers, total income per person, year, id_pro);

Copyright © 2016 by Technical University of Sofia, Plovdiv branch, Bulgaria ISSN Online: 2535-0048

- Gdp_Gva (id, years, Gva, Gdp, Gdp per capita, Id_pro)

The aim of this article is to present an algorithm for determining and comparing the levels of economic development in the districts in Bulgaria. The necessary information is extracted from the relational database. These data concerning gross domestic product, gross value added, employment rate and salaries are studied, compared and analysed for the relevant time interval.

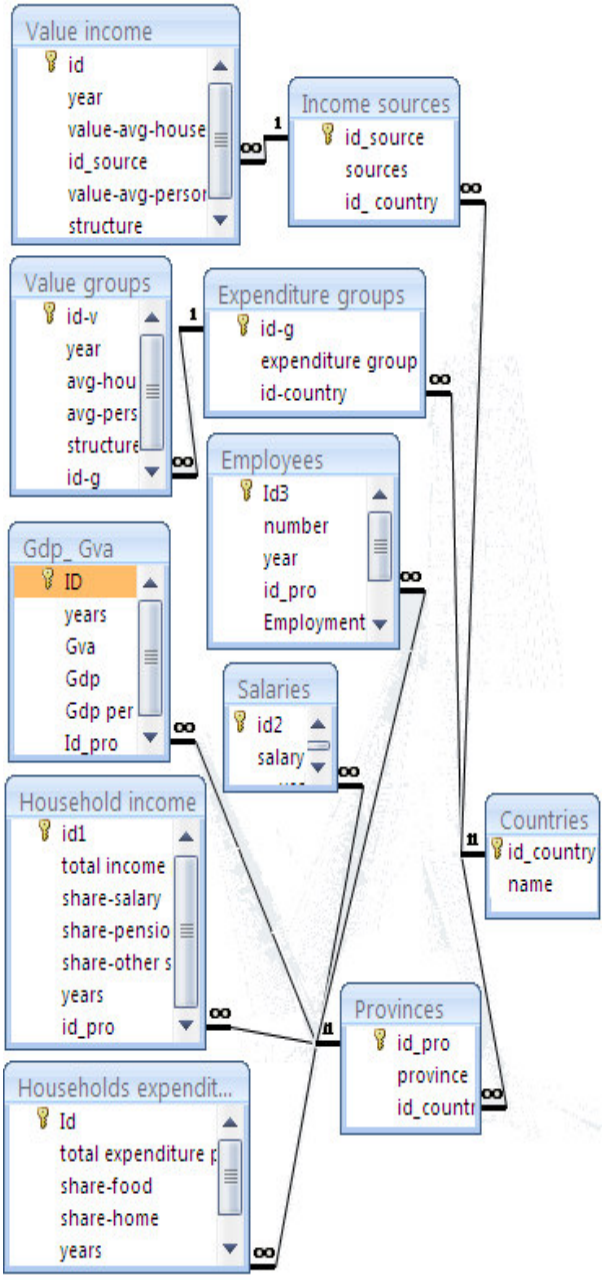



***Fig. 1.*** *General scheme of the relational database*

## 2. Description of the algorithm

The scheme of the developed algorithm is presented in fig. 2. The input data for the algorithm are stored in the relational database. The information concerning the studied indicators (gross domestic product, gross value added, employment rate and salaries) in the relevant districts is searched in several fields located in the following tables:

- Countries (id_country, name);
- Provinces (id_pro, province, id_country);
- Salaries (id2, salary, year, id_pro);
- Employees (id3, number, year, id_pro, employment rate);
- Gdp_Gva (id, years, Gva, Gdp, Gdp per capita, Id_pro).

Users could select the time interval. In this study, the research period covers generally 14 years from 2000 to 2013. The algorithm also allows the user to choose any smaller or larger period.

Practically, the choice of tables from the database depends on the choice of the relevant indicators. Data for the first two indicators (gross domestic product (Gdp), gross value added (Gva)) are extracted from the tables Countries, Provinces and Gdp_Gva. Information about the next two indicators (employment rate and salaries) respectively, is extracted from the tables Countries, Provinces, Employees and Countries, Provinces; Salaries. The obtained data from the database are also presented in tabular form. They should be compared and analysed. For this purpose it is necessary to find:

- The highest and the lowest value of the studied indicators for the given years;
- The intervals within which the values of the indicators change;
- The indicators that have insignificant change for the defined period;
- Percentage change of the salaries in the considered districts for the given years;
- The change of the employment rate for selected time interval;

These data for each of the indicators (gross domestic product, gross domestic product per capita, gross value added, employment rate and salaries by districts) also need to be arranged in ascending order of values for each year of the time interval. The obtained information could be summarized as a result of this sorting process. There are cases in which users could choose studying of data only for some of the listed indicators. It is also possible to include the data for all 28 districts in Bulgaria or part of them.

The levels of economic development in the relevant districts are determined on the basis of the performed comparisons and analysis. The results of data processing enable the user to present the obtained conclusions for given time period. The studied information about the listed indicators could be provided in graphical form. This allows to track much more quickly the dynamics of change of indicators for arbitrary selected interval. The developed algorithm can be also used in analyzing

other economic and financial indicators.

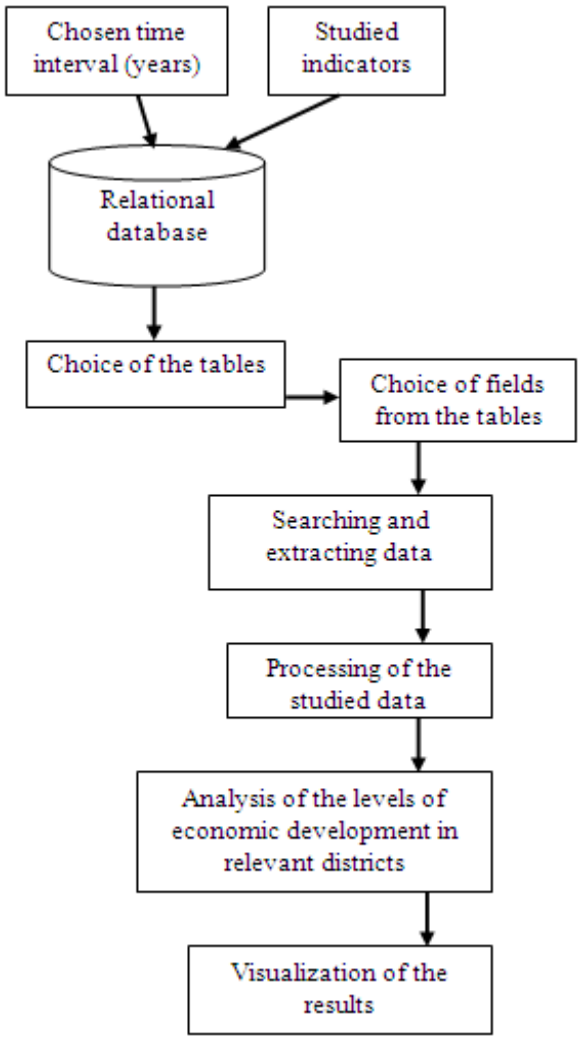



***Fig. 2.*** *Scheme of the algorithm*

### 3. Results and discussion

The choice of indicators determines these tables in the relational database from which the studied information could be searched. The developed software is used for finding and extracting the data concerning the above listed economic indicators for 14-years time interval. Subsequently, the obtained information is sorted by pre-defined criteria. As a result, for the selected 28 districts, the values of the gross domestic product for each year from the included period are arranged in ascending order. Invariably, the first five positions in the investigated time interval are occupied from the following districts:

- Sofia (capital);
- Plovdiv;
- Varna;
- Burgas;
- Stara Zagora.

In this case, as can be seen from table 1 the values of the gross domestic product in the district of Sofia (capital) are highest. The software calculates that their increase is more than 4,5 times for the period from 2000 to 2013. The second position is ranked from the district of Plovdiv. The other three districts change their positions (from third to fifth) within the examined 14 year period. It should be noted an interesting fact. Quite naturally, the values of the mentioned indicator are significantly higher in the district of Sofia (capital) in comparison with those in the other districts.

The analysis shows that the values of the gross domestic product for the years between 2000-2004 are the lowest in two districts:

- Vidin;
- Targovishte.

In the period 2005-2013 the values of the studied indicator are lowest in the following districts:

- Vidin;
- Silistra.

***Table 1.*** *Presentation of the sorted data for the investigated districts*

| Year | District | GDP (million BGN) | Year | District | GDP (million BGN) |
|---|---|---|---|---|---|
| 2000 | Stara Zagora | 1 187 | 2007 | Stara Zagora | 2 715 |
| 2000 | Varna | 1 742 | 2007 | Burgas | 3 351 |
| 2000 | Burgas | 1 829 | 2007 | Varna | 4 312 |
| 2000 | Plovdiv | 2 058 | 2007 | Plovdiv | 4 659 |
| 2000 | Sofia (capital) | 7 148 | 2007 | Sofia (capital) | 23 484 |
| 2001 | Burgas | 1 539 | 2008 | Stara Zagora | 3 224 |
| 2001 | Stara Zagora | 1 710 | 2008 | Burgas | 3 818 |
| 2001 | Varna | 1 928 | 2008 | Varna | 4 993 |
| 2001 | Plovdiv | 2 333 | 2008 | Plovdiv | 5 058 |
| 2001 | Sofia (capital) | 8 554 | 2008 | Sofia (capital) | 27 433 |
| 2002 | Burgas | 1 654 | 2009 | Stara Zagora | 3 421 |
| 2002 | Stara Zagora | 1 699 | 2009 | Burgas | 3 701 |
| 2002 | Varna | 2 111 | 2009 | Varna | 4 816 |
| 2002 | Plovdiv | 2 480 | 2009 | Plovdiv | 5 481 |
| 2002 | Sofia (capital) | 9 945 | 2009 | Sofia (capital) | 27 989 |
| 2003 | Burgas | 1 869 | 2010 | Stara Zagora | 3 322 |
| 2003 | Stara Zagora | 1 901 | 2010 | Burgas | 3 680 |
| 2003 | Varna | 2 280 | 2010 | Varna | 4 630 |
| 2003 | Plovdiv | 2 755 | 2010 | Plovdiv | 5 539 |
| 2003 | Sofia (capital) | 10 799 | 2010 | Sofia (capital) | 29 316 |
| 2004 | Stara Zagora | 2 103 | 2011 | Stara Zagora | 3 336 |
| 2004 | Burgas | 2 136 | 2011 | Burgas | 3 963 |
| 2004 | Varna | 2 616 | 2011 | Varna | 5 178 |
| 2004 | Plovdiv | 3 148 | 2011 | Plovdiv | 6 062 |
| 2004 | Sofia (capital) | 12 402 | 2011 | Sofia (capital) | 31 754 |
| 2005 | Stara Zagora | 2 367 | 2012 | Stara Zagora | 3 913 |
| 2005 | Burgas | 2 685 | 2012 | Burgas | 3 976 |
| 2005 | Varna | 2 958 | 2012 | Varna | 5 400 |
| 2005 | Plovdiv | 3 663 | 2012 | Plovdiv | 6 178 |
| 2005 | Sofia (capital) | 11 602 | 2012 | Sofia (capital) | 31 726 |
| 2006 | Stara Zagora | 2 476 | 2013 | Burgas | 4 063 |
| 2006 | Burgas | 2 949 | 2013 | Stara Zagora | 4 071 |
| 2006 | Varna | 3 573 | 2013 | Varna | 5 323 |
| 2006 | Plovdiv | 4 017 | 2013 | Plovdiv | 6 374 |
| 2006 | Sofia (capital) | 18 173 | 2013 | Sofia (capital) | 32 232 |

*Source: Based on data from National Statistical Institute*

Invariably, the district of Vidin ranks the last position in the 14 year time interval.
In addition, it should be noted that similar results are also obtained from data processing for the second studied indicator (gross value added).

A little different is the situation for the examined data concerning gross domestic product per capita. As can be expected, the values of this indicator are again the highest in the district of Sofia (capital) and they significantly exceed those in other districts. At the beginning of the period (about 4 years) the values of the gross domestic product per capita in the district of Burgas are lower in comparison with those in the districts of Vratsa, Kyustendil, Gabrovo. Another fact is of an interest. More than ten districts have higher value of the studied indicator than this one in the district of Plovdiv in the first three years of the time interval. In the next years, this indicator increase gradually. The district of Plovdiv already occupied the 6$^{th}$ position in the last year from the examined period.

Specially, the data on the employment rate of population aged 15 years and over are investigated in the interval between 2008-2013. The values of this indicator have varied in quite wide range (from approximately 33% to 62%) for the chosen period. The developed software displays two districts where the employment rate is highest. In this case, as can be seen from table 2 they are the following:

- Sofia (capital);
- Blagoevgrad.

They occupy relevant the first two positions in the selected 6 years interval.

The number of districts, in which the employment rate is less than 40%, constantly increases. It already is seven in 2013 compared with 2008, where the district is only one. Eight of the twenty eight districts have had employment rate above 50% at the beginning of the period. This number decreased to four in the next year. Subsequently, the number of districts is only two in the last 4 years of the examined interval. Generally more are the districts in which the employment rate varies in range between 40%-45,9% in the period 2008-2013. A small part are those ones (from five to eight) in which this indicator reaches values between 46%-50%, during three consecutive years from 2010 to 2012 (table 2). The change of the values of the employment rate is relatively small (about 3,6%) in the investigated period in the following districts:

- Pernik;
- Razgrad;
- Stara Zagora.

At the same time, the change of this indicator is quite large (over 10%) in the 6 year period in five districts:

- Kardzhali;
- Lovech;
- Pazardzhik;
- Smolyan;
- Varna.

It should be noted that the employment rate declined steadily, only in the district of Lovech in throughout the studied time interval. While in the other districts, periods are alternated in which the indicator decreases and then increases or vice versa. The values of the employment rate are the lowest in the district of Vidin in the years between 2008-2012. The situation is quite different in the last year of the examined time interval. The lowest values are observed in the following districts:

- Silistra;
- Lovech;
- Targovishte.

***Table 2.*** *Visualization of the results for the employment rate*

| employment rate -% | | |
|---|---|---|
| year | min | max |
| 2008 | 39,1 | 61,5 |
| 2009 | 36,4 | 60,7 |
| 2010 | 35 | 57,4 |
| 2011 | 33,6 | 55,7 |
| 2012 | 37 | 55,7 |
| 2013 | 37,1 | 56,1 |

| year | district | | district | |
|---|---|---|---|---|
| 2008 | Blagoevgrad | 57,20 | Vidin | 39,10 |
| 2008 | Sofia (capital) | 61,50 | | |
| 2009 | Blagoevgrad | 55,40 | Vidin | 36,40 |
| 2009 | Sofia (capital) | 60,70 | | |
| 2010 | Blagoevgrad | 53,60 | Vidin | 35,00 |
| 2010 | Sofia (capital) | 57,40 | | |
| 2011 | Blagoevgrad | 53,80 | Vidin | 33,60 |
| 2011 | Sofia (capital) | 55,70 | | |
| 2012 | Blagoevgrad | 53,10 | Vidin | 37,00 |
| 2012 | Sofia (capital) | 55,70 | | |
| 2013 | Blagoevgrad | 51,4 | | |
| 2013 | Sofia (capital) | 56,1 | | |

| | number of the districts | | | |
|---|---|---|---|---|
| year | under 40% | 40%-45,9% | 46%-50% | over 50% |
| 2008 | 1 | 8 | 11 | 8 |
| 2009 | 2 | 11 | 11 | 4 |
| 2010 | 7 | 11 | 8 | 2 |
| 2011 | 7 | 14 | 5 | 2 |
| 2012 | 5 | 13 | 8 | 2 |
| 2013 | 7 | 9 | 10 | 2 |

*Source: Own calculation on the basis of data from National Statistical Institute*

In this study the data on the average annual salary are also investigated. The analysis shows that the values of this indicator are the highest in the period from 2000 to 2013 in six districts:

- Sofia (capital);
- Stara Zagora;
- Vratsa;
- Sofia;
- Varna;
- Burgas.

The average annual salary grows at the fastest pace in the district of Sofia (capital), as is shown in table 3. The developed software calculates that the increase is about 4 times in 14-years interval. The calculations also show that the average annual salary in the listed five districts is about 1,3 times lower in comparison with this one in the district of Sofia (capital). Another interesting fact should be noted. The values of the indicator in the district of Vratsa are higher in 2002 than those in 2003. A similar situation is obtained for the examined indicator in the district of Smolyan in the period 2010-2011.

Invariably, the average annual salary in the district of Smolyan is the lowest in the first 6 years of the considered time interval. Its values increased gradually over the next five years. Then this indicator decreased again at the end of the period. The district of Vidin has ranked last by average annual salary in the years between 2008-2013. The rate of growth of this indicator is the slowest in the mentioned district. The values of the studied indicator are very similar in the second half of the period in the following districts:

- Blagoevgrad;
- Haskovo.

The percentage change of the average annual salary is calculated in 2013 compared to 2012. The software displays that it varies in wide range from 1,6% to 9,75% (table 3). It should be noted that the number of the districts in which the percentage increase is about 6,57% to 6,93% is the largest. In the case, these districts are:

- Gabrovo;
- Razgrad;
- Lovech;
- Kyustendil;
- Sofia (capital);
- Plovdiv.

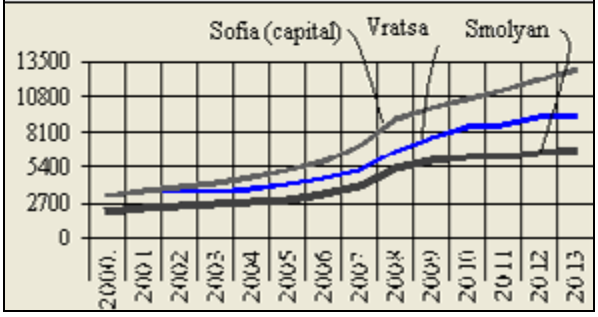
As a result of this research could be done the following conclusion: The level of economic development in the district of Sofia (capital) is significantly higher in the examined period. Then rank the districts of Varna, Burgas, Stara Zagora and Plovdiv. The level of economic development in the districts of Vidin, Silistra, Targovishte is lower in comparison with this one in the other districts in the considered years.

***Table 3.*** *Analysis of the data for average annual salary*

| year | districts | % | districts | % |
|---|---|---|---|---|
| 2 013 | Vidin | 5,81 | Burgas | 5,44 |
| | Vratsa | 1,65 | Sliven | 6,22 |
| | Lovech | 6,62 | Stara Zagora | 3,26 |
| | Montana | 6,44 | Yambol | 6,47 |
| | Pleven | 6,02 | Blagoevgrad | 4,7 |
| | Veliko Tarnovo | 7,71 | Kyustendil | 6,77 |
| | Gabrovo | 6,93 | Pernik | 5,12 |
| | Razgrad | 6,62 | Sofia | 3,65 |
| | Ruse | 6,07 | Sofia (capital) | 6,57 |
| | Silistra | 7,67 | Kardzhali | 9,19 |
| | Varna | 4,2 | Pazardzhik | 5,87 |
| | Dobrich | 6,32 | Plovdiv | 6,71 |
| | Targovishte | 9,75 | Smolyan | 4,36 |
| | Shumen | 4,77 | Haskovo | 5,01 |

| period | | districts | period | | districts |
|---|---|---|---|---|---|
| 2000 | 2014 | Sofia (capital) | 2000 | 2014 | Stara Zagora |
| 2000 | 2014 | Sofia | 2000 | 2014 | Burgas |
| 2000 | 2014 | Varna | 2000 | 2014 | Vratsa |

| increase | increase |
|---|---|
| 4 times | 1.3 times |




*Source: Own calculation on the basis of data from National Statistical Institute*

## 4. Conclusion

This article presents an algorithm for determining and comparing the levels of economic development in the districts in Bulgaria. The necessary information is extracted from a created relational database. These data concerning gross domestic product, gross value added, employment rate and salaries are studied, compared and analysed for the relevant time interval. The examined period includes the years from 2000 to 2013. The developed algorithm can be also used in analyzing other economic and financial indicators. The software has been developed for data processing. It significantly helps users - economists and financiers in decision making in their practice.

## REFERENCES


1. Inkpen, D. Information Retrieval on the Internet. Available at: http://www.site.uottawa.ca/~diana/csi4107/IR_draft.pdf, [2016-02-23]
2. Suma, D., Acharya, U. D., Geetha, M., Raviraja Holla, M. (2014). XML Information Retrieval: An overview. *International Global Journal for Engineering Research*, volume 10, issue 1, pp. 26-32
3. Mamoon, H., El-Bakry, H., Slamaa, A. (2014). Visualization for Information Retrieval in Regional Distributed Environment. *IJCSNS International Journal of Computer Science and Network Security*, vol.14, no.9, pp. 12-27
4. Mamoon, H., El-Bakry, H., Salama, A. (2013). Interactive Visualization of Retrieved Information. *International Journal of Knowledge Engineering and Research*, vol. 2, issue 4, pp. 217-231
5. Ram, S. (2008). Teaching Data Normalization: Traditional Classroom Methods versus Online Visual Methods – a Literature Review. *Proceedings of the 21st Annual Conference of the National Advisory Committee on Computing Qualifications (NACCQ)*, Auckland, New Zealand, pp. 327-330
6. Tablan, V., Damljanovic, D., Bontcheva, K. (2008). A Natural Language Query Interface to Structured Information. In: Bechhofer, S., Hauswirth, M., Hoffmann, J., Koubarakis, M. (eds.) ESWC 2008. *LNCS*, vol. 5021, pp. 361–375. Springer, Heidelberg
7. National Statistical Institute: http://www.nsi.bg
8. Dimova, D. (2013). Software for Extraction and Assessment of Data for Household Budget in Bulgaria. *Proceedings of the international scientific conference Unitech'13*, Gabrovo, Bulgaria, volume II, pp. II-245-II-248


Department „Mathematics, Informatics and Physics" Agricultural University,
12 Mendeleev blvd, Plovdiv, Bulgaria,
E-mail: delyanadimova@abv.bg

© International Scientific Conference on Engineering, Technologies and Systems
TECHSYS 2016, Technical University – Sofia, Plovdiv branch
26 – 28 May 2016, Plovdiv, Bulgaria

# PARAMETRIC REGRESSION MODELS FOR CUBR LASER

ILIYCHO ILIEV

**Abstract:** *A comparison of the developed polynomial regression models of first, second and third level of the output laser power of CuBr laser is presented. It is found that regression equations involving all 10 independent variables (predictors) show better statistical indicators and more faithfully describe the influence of the input laser characteristics on the output laser power.*

**Key words:** *Copper bromide vapor laser, laser output power, parametric model, polynomial model, regression analysis, regression model*

## 1. Introduction

The object of study in this paper is a low-temperature copper bromide vapor (CuBr) laser, with a wavelength of 510.6 nm and 578.2 nm. It is accepted that metal vapor and metal compound vapor lasers have been studied in great detail through experiments and in theory. During the last few years as a result of active experiment development, a significant increase (up to 120-150 W) of the output power was achieved. Copper bromide (CuBr) vapor lasers continue to be the most powerful laser source in the visible spectrum. This is the reason for its active application in medicine, physics, chemistry, ecology, technology, and scientific research. There are over 2000 scientific publications, papers, books, and monographs in renowned science journals in this field, as well as papers presented at prestigious science conferences. For this reason, they are subject to particular interest and rank among the 12 most commercialized lasers in the world. They are manufactured in many countries throughout the world - Russia, USA, China, England, Bulgaria, etc. The use of copper halides gives significant advantages to this type of lasers when compared to pure copper lasers. The first of these advantages is that the operating temperature of the active laser tube is reduced by around 1000 $^{o}$C as compared to pure copper lasers working at temperatures of about 1500 $^{o}$C. This allows the use of cheaper material for the manufacture of the laser tube - usually quartz. Another advantage is that CuBr vapor lasers are cooled by air and do not require additional water- or another type of cooling.

## 2. Subject of study

The subject of investigation is a copper bromide vapor laser which is an original Bulgarian design developed at the Laboratory of Metal Vapor Lasers at the Georgi Nadjakov Institute of Solid State Physics of the Bulgarian Academy of Sciences, Sofia. The first patent related to this laser is that of Sabotinov, N.V. et al., Bulg. patent No.:28674, 1975.

A conceptual schematic of the laser source is given in Fig. 1.

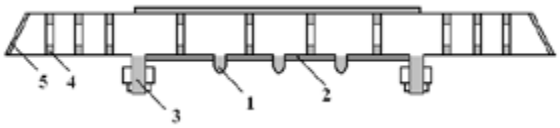



***Fig. 1.*** *Construction of CuBr laser tube: 1- reservoirs with copper bromide, 2- heat insulation of the active volume, 3- copper electrodes, 4- inner diaphragms, 5- tube windows*

Neon is used as a buffer gas. In order to improve efficiency, small quantities of hydrogen are added. Unlike the high-temperature pure copper vapor laser, the copper bromide vapor laser is a low-temperature one, with an active zone temperature of 500 °C. The laser tube is made out of quartz glass without high-temperature ceramics as a result of which it is significantly cheaper and easier to manufacture. The discharge is heated by electric current (self-heating). It produces light impulses tens of nanoseconds long. Its main advantages are: short initial heating period, stable laser generation, relatively long service life, high values of output power and laser efficiency.

On the base of a huge amount of experimental data different statistical regression

Copyright © 2016 by Technical University of Sofia, Plovdiv branch, Bulgaria ISSN Online: 2535-0048

models have be obtained in [1-3]. In this study the dependence of basic laser operational physical characteristics, such as the inner diameter of the laser tube, the length of the active laser zone, the input supplied electric power, pressure of the additional hydrogen gas and more on the output laser power is considered. The aim of the study is to summarize, compare and analyze the obtained linear and nonlinear models in order to identify the more reliable results, which describe the investigated dependency.

## 3. Data description

We use experimental data for copper bromide laser with wavelengths 510.6 nm and 578.2 nm, published in [1]. The initial data consist of more than 300 experiments including eleven laser parameters. The ten independent initial variable parameters (laser characteristics) are: D (mm) – inside diameter of the laser tube; *dr* (mm) – inside diameter of the rings; *L* (cm) – length of the active area (electrode separation); *Pin* (kW) – input electrical power; *PL* (kWm$^{-1}$) – input electrical power per unit length, *PH*2 (Torr) – hydrogen gas pressure, *Prf* (kHz) – pulse repetition rate; *PNe* (Torr) - neon gas pressure, *C* (pF) – equivalent capacity of the capacitor bank, *Tr* ($^{o}$C) – temperature of the CuBr reservoirs. The main dependant variable we observe here is the output laser power $P_{out}$ (W).

As it was previously established in [2], for our data, only the first six of these variables show statistically significant influence on the output laser power $P_{out}$. To this reason in this paper we use only the data about the first six variables, i.e. *D*, *dr*, *L*, *Pin*, *PL* and *PH*2. These six variables will be referred to as basic variables. While they correlate strongly each other, a direct construction of the regression models is not applicable [1]. So, we need to combine them mathematically in uncorrelated artificial group variables, called factors. This procedure is performed by the multivariate factor analysis. In our case we use three factors, which explain about 93-94% of any one of selected samples of examined data.

***Table 1.*** *Rotated component matrix with three factors*[(a)]

| Variables | Component (factor) | | |
|---|---|---|---|
| | F1 | F2 | F3 |
| Pin | 0.935 | | |
| Dr | 0.909 | | |
| L | 0.780 | | |
| D | 0.767 | | |
| PL | | -0.881 | |
| PH2 | | | 0.915 |

[(a)]Extraction Method: Principal Component Analysis. Rotation Method: Varimax with Kaiser Normalization. Rotation converged in 5 iterations.

There exist many different methods for extraction and rotation of factors. We use the more popular methods: principal component analysis for extraction of the selected number of factors and rotation by the Varimax method with Kaiser normalization [1]. For the initial data sample the obtained rotated matrix is shown in Table 1. For clarity, the factor loadings less than 0.5 are skipped.

## 4. Parametric regression models for CuBr laser

From the previously derived models we will present linear and non-linear parametric models for CuBr laser to analyze their statistical indicators. In these models the obtained factor variables are used as independent uncorrelated variables. This approach is also known as principal component regression [1].

### 4.1. General relationship between factors and laser output power for CuBr laser

Based on [2], in an exploratory manner, we will later on consider regression models using three groups of variables as predictors: first, second and third groups as follows:

$$F_1, F_2, F_3 \tag{1}$$

$$F_1,\ F_2,\ F_3,\ F_1^2,\ F_2^2,\ F_3^2,\ F_1.F_2,\ F_1.F_3,\ F_2.F_3 \tag{2}$$

$$\begin{aligned} &F_1,\ F_2,\ F_3,\ F_1^2,\ F_2^2,\ F_3^2,\ F_1.F_2,\ F_1.F_3,\\ &F_2.F_3,\ F_1^3,\ F_2^3,\ F_3^3,\ F_1^2.F_2,\ F_1^2.F_3,\\ &F_2^2.F_3,\ F_1.F_2^2,\ F_1.F_3^2,\ F_2.F_3^2,\ F_1F_2F_3 \end{aligned} \tag{3}$$

The corresponding models will be noted as 0, 1, and 2 order models, respectively.

The results from the modeling have been presented in this section. For parametric methods it is assumed that data and population distribution are nearly normal. All calculations and analyses have been carried out at level of significance 0.05. The comparison between models has been conducted via the commonly used indices, such as multiple correlation coefficient *R*, coefficient of multiple determination $R^2$ (RSquare), and adjusted $R^2$.

With the help of the three orthogonal PCA factors $F_1, F_2, F_3$ (first group of predictors (1)) and the stepwize or linear procedure we obtain the MLR (Multiple Linear Regression)-0th order models for estimation of the dependent variable $P_{out}$:

$$\hat{P}_{out} = 40.589 + 29.717F_1 + 4.155F_2 + 12.941F_3 \quad (4)$$

To note, that in fact, all coefficients as well as all subsequent estimates have been obtained at a lower significance level of 0.000 for model MLR-0th order, with no interactions.

Using the nine predictors (2) a more precise regression model was constructed, marked as MLR-1st order. The corresponding equation is:

$$\hat{P}_{out} = 38.283 + 28.090F_1 + 4.866F_2 + \\ + 11.992F_3 + 2.336F_1^2 \quad (5)$$

For the second-order model the obtained equations are, respectively:

$$\hat{P}_{out} = 38.270 + 39.511F_1 + 8.243F_3^2 + \\ 8.718F_3^3 - 2.294F_1^3 + 3.053F_2^2F_3 \\ - 0.976F_2^3 \quad (6)$$

This means that (2) and (3) describe 94.6% of the sample

The basic statistics of these models are given in Table 2. In this table we include the commonly used indices, such as coefficient of multiple determination $R^2$, adjusted $R^2$, and standard error of the estimate.

***Table 2.*** *Results from constructed parametric regression models for estimation of output laser power $P_{out}$ using MLR (Multiple Linear Regression)*

| Model | $R^2$ | $R^2$ Adj. | Std. Err. of the Estimate | Number of Predictors |
|---|---|---|---|---|
| (4) | 0.946 | 0.944 | 7.92540 | 3 |
| (5) | 0.950 | 0.948 | 7.63382 | 4 |
| (6) | 0.967 | 0.963 | 6.27075 | 7 |

### 4.2. General relationship between ten independent initial variable parameters and laser output power for CuBr laser

It must be noted, that some disadvantage of the obtained principle regression models (4)-(6) is that the actual physical variables are "hidden" behind the factor variables. Also the prediction of laser power requires the application of some specialized software and its skilled use. This makes the approach difficult for immediate use. For this reason, the issue of developing polynomial parametric models containing explicitly the 10 independent variables is topical.

The initial approach requires finding a linear regression relationship of the type:

$$\hat{P}_{out} = a_0 + a_1D + a_2dr + a_3L + a_4Pin + \\ + a_5PH2 + a_6PL + a_7PRF \\ + a_8PNe + a_9C + a_{10}Tr \quad (7)$$

where $a_i$, $i = 0,1,...,10$ are the regression coefficients (parameters) to be determined.

The factor and regression analysis performed showed that there is a high degree of correlation between the predictors and that an equation of type (7) is not statistically significant [1]. For this reason we will look polynomial models from the second, third and higher level. In [3] has developed a non-linear parametric model of the second degree, which is as follows:

$$\hat{P}_{out} = -18.308 + 0.686dr.Pin - 7.567Pin.C \\ + 27.569Pin - 4.362Pin^2 - 0.006L.PRF \\ + 0.274PRF.C - 0.612dr.C \\ + 0.259D.PH2 + 18.093C \quad (8)$$

Model equation (8) contains 8 of the 10 independent variables: *dr*, *D*, *L*, *Pin*, *PL*, *PRF*, PH2, and *C*. It does not include variables *PNe* and *Tr*.

Non-linear parametric model of the third degree [4] has the form:

$$\hat{P}_{out} = 10.243 + 64.453Pin - 0.143PL \\ + 0.023D.PRF + 0,303D.C \\ - 0.061dr.PL - 0.011L.PRF \\ - 0.419L.C - 2.009Pin.PL \\ + 0.437Pin.PRF + 2.341PL.PH2 \\ - 2.791PL.C - 0.579PRF.C \\ + 0.165C.Tr - 0.0121D^2 + 0,025.dr^2 \\ - 41.015PH2^2 - 11.333C^2 + 0.003PL^3 \\ - 2.1.10^{-5}PRF^3 + 1.613C^3 \quad (9)$$

It is observed that equation (9) contains only three third degree terms: $PL^3$, $PRF^3$ and $C^3$. Model equation (9) contains all 10 independent variables: *dr*, *D*, *L*, *Pin*, *PL*, *PRF*, PH2, *C*, *PNe* and *Tr*. The basic statistics of the models (8) and (9) are given in Table 3.

***Table 3.*** *Main statistical indicators of nonlinear models from second and third degree of the output laser power $P_{out}$ using MLR*

| Model | $R^2$ | $R^2$ Adj. | Std. Err. of the Estimate | Number of Predictors |
|---|---|---|---|---|
| (8) | 0.967 | 0.962 | 6.56416 | 10 |
| (9) | 0.976 | 0.972 | 5.67721 | 21 |

## 5. Discussion and conclusion

Comparing the basic statistical parameters in Tables 2 and 3 show that the non-linear patterns, included in equations (8) and (9) give higher statistical indices in terms of coefficients of determination $R^2$ and adjusted $R^2$ than those of type (5) and (6). This fact follows from statistical theory, i.e. models of higher degree give higher coefficient of determination. However, in our case we additionally obtained lower errors of estimates and better agreement of equations (8) and (9) with the known experimental data [1]. So, as a statistical inference we have to expect more accurate prediction of laser power when constructing new laser sources with high performance. The main reason in our opinion is that in equations (5) and (6) involved only 6 of all 10 independent physical parameters. Equation (8) contains 8 independent parameters, and equation (9) includes all the 10 variables.

From the previous analysis we can conclude that equation (9) has the best statistics. It describes more adequately the complex processes in the laser medium and can be accurately used in planning and creating new laser sources.

## ACKNOWLEDGMENTS

This work was supported in part by Paisii Hilendarski University of Plovdiv NPD under Grant NI15-FMI-004.

## REFERENCES

1. Gocheva-Ilieva, S.G. and Iliev, I.P. (2011). *Statistical models of characteristics of metal vapor lasers*. Nova Science Publ. Inc., New York.
2. Gocheva-Ilieva, S.G. and Iliev, I.P. (2010). Parametric and nonparametric empirical regression models: case study of copper bromide laser generation. *Mathematical Problems in Engineering*, volume 2010 (Article ID 697687), pp. 1-15.
3. Denev, N., Iliev, I. and Gocheva-Ilieva S. (2013). Second-degree polynomial model of laser generation for a GuBr laser. *WSEAS Transactions on Circuits and Systems*, volume 12(4), pp.129-139.
4. Iliev, I. and Denev, N. (2014). Parametric models of the third degree for output parameters of a CuBr laser. *International Journal of Scientific & Technology Research*, volume 3(11), pp. 28-32.

Department of Mathematics, Physics and Chemistry
Technical University–Sofia, Branch Plovdiv
25 Tsanko Diustabanov St.
4000 Plovdiv
BULGARIA
E-mail: iliev55@abv.bg

© International Scientific Conference on Engineering, Technologies and Systems
TECHSYS 2016, Technical University – Sofia, Plovdiv branch
26 – 28 May 2016, Plovdiv, Bulgaria

# RECTANGULAR PLATES IN SINGLE TRIGONOMETRC SERIES WITH SYMETRY

LILIYA B. PETROVA

***Abstract:*** *With a methode of trigonometric series is investigated a rectangular plate simply supported in two of their opposite ends, with symmetric support and with symmetric load. It is constructs automated the diagrams of normal displacement and a forces in a plate. It is made a verification and comparison of the results obtained.*

***Key words:*** *rectangular plates, single trigonometric series, symmetry*

## 1. A basic relationships of plates in cartesian coordinate system

*A differential equation for equilibrium for a plate with constant thickness*

$$\frac{\partial^4 w}{\partial x^4}+2\frac{\partial^4 w}{\partial x^2\partial y^2}+\frac{\partial^4 w}{\partial y^4}=\frac{q(x,y)}{D} \qquad (1)$$

where $q(x,y)$ is a function of the external load;

$w(x,y)$ - function of the normal displacements of the points of the middle surface of the plate;

$D=\frac{Et^3}{12(1-\nu^2)}$ is the cylindrical rigiditie of the plate;

$t$ - a thickness of the plate; $\nu$ - a Poisson's coefficient.

The expressions for forces in the plate and theirs positive directions are known.

*The boundaries conditions at the ends of the plate, according with its supported are known.*

The methode of single trigonometric series is applies at rectangular plates simply supported in two opposite ends and arbitrary supported in two other.

It is introduce a coordinate system $xOy$, according to the supported and to the loading of the plate.

*A function of the normal displacement of the points of the middle surface of the plate*

$$w(x,y)=\sum_m Y_m(y)\sin(\alpha_m x), \qquad \alpha_m=\frac{m\pi}{a}, \quad (m=1,2,...\infty) \qquad (2)$$

The choice of function of elastic surface of the plate satisfies the boundary conditions into simply supported ends of the plate in this case parallels of the axes $y$.

*Analytical expression for a function of external load*

$$q(x,y)=q\,f(x)\,f(y), \qquad (3)$$

where $q$ is an intesity of external load;

$f(x), f(y)$ are a functions of external load in directions of axis $x$ end $y$ at $q=1$;

*A development of external load in single trigonometric serie*

$$q(x,y)=\sum_m q_m(y)\sin(\alpha_m x),$$

where $q_m(y)=\frac{2}{a}\int_0^a q(x,y)\sin(\alpha_m x)dx \qquad (4)$

*A function $Y_m(y)$ from elastic surface of the plate*

It is determines from condition $Y_m(y)$ to satisfy the differential equation for equilibrium of the plate. It is follows homogeneous arbitrary differential equation about function $Y_m(y)$

$$Y_m^{IV}(y)-2\alpha_m^2 Y_m^{II}(y)+\alpha_m^4 Y_m(y)=B_m(y), \qquad (5)$$

where the right part has a kind $B_m(y)=\frac{q_m(y)}{D}$.

*General integral of arbitrary homogeneous differential equation about function $Y_m(y)$*

By a symmetry of the supported and of the loading in the functions $Y_m(y)$ fall axis symmetrical components

$$Y_m(y)=A_m ch\alpha_m y+D_m y sh\alpha_m y+\bar{Y}_m(y), \qquad (6)$$

*where*

Copyright © 2016 by Technical University of Sofia, Plovdiv branch, Bulgaria ISSN Online: 2535-0048

$\overline{Y}_m(y)$ is a partial integral of the unhomogeneous differential equation for function $Y_m(y)$ (it depends of the external loads).

$A_m$ и $D_m$ are an integration constants in an expressions for $Y_m(y)$.

The determination of the integration constants is make from the boundaries conditions into unspecified supported ends of the plate – in a case parallels of an axis $x$.

An expressions for forces in the plate, presented in the single trigonometric serie

The coefficients of the trigonometric serie for

bending, twisting moments and transverse forces

$$M_{x_m}(y)=\alpha_m^2 Y_m(y)+\nu Y_m^{II}(y)$$
$$M_{y_m}(y)=Y_m^{Ii}(y)-\nu\alpha_m^2 Y_m(y)$$
$$M_{xy_m}(y)=\alpha_m^2 Y_m^I(y)$$
$$Q_{x_m}(y)=\alpha_m^2\left(Y_m^{II}(y)-\alpha_m^2 Y_m(y)\right)$$
$$Q_{y_m}(y)=\left(Y_m^{III}(y)-\alpha_m^2 Y_m^2(y)\right) \qquad (7)$$
$$Q_{x_m}^*(y)=\alpha_m\left((2-\nu)Y_m^{II}(y)-\alpha_m^2 Y_m(y)\right)$$
$$Q_{y_m}^*(y)=\alpha_m\left(Y_m^{III}(y)-(2-\nu)\alpha_m^2 Y_m^I(y)\right)$$

reactions of the plate

$$r_{x_m}(y)_{\substack{x=0\\x=a}}=\mp\left[\alpha_m\left(-\alpha_m^2 Y_m(y)+(2-\nu)Y_m^{II}\right)\right]_{\substack{x=0\\x=a}}$$
$$r_{y_m}(y)_{\substack{y=0\\y=a}}=\mp\left[\alpha_m\left(-\alpha_m^2 Y_m(y)+(2-\nu)Y_m^{II}\right)\right]_{\substack{y=0\\y=a}}$$

A normal displacement, forces, reactions for a different values of a $m$

$$w_m(x,y)=Y_m(y)\sin(\alpha_m x)$$
$$M_{x_m}(x,y)=M_{x_m}(y)\sin(\alpha_m x)$$
$$M_{y_m}(x,y)=M_{y_m}(y)\sin(\alpha_m x)$$
$$M_{xy_m}(x,y)=M_{xy_m}(y)\cos(\alpha_m x)$$
$$Q_{x_m}(x,y)=Q_{x_m}(y)\sin(\alpha_m x) \qquad (8)$$
$$Q_{y_m}(x,y)=Q_{y_m}(y)\sin(\alpha_m x)$$
$$Q_{x_m}^*(x,y)=Q_{x_m}^*(y)\sin(\alpha_m x)$$
$$Q_{y_m}^*(x,y)=Q_{y_m}^*(y)\sin(\alpha_m x)$$
$$r_{x_m}(x,y)=r_{x_m}(y)\cos(\alpha_m x)$$
$$r_{y_m}(x,y)=r_{y_m}(y)\cos(\alpha_m x)$$

A summarize displacements, forces and reactions in the plate for a number $m$ keeping terms of the trigonometric serie in a point with coordinate $(x,y)$ are

$$w(x,y)=\sum_{m=1}^{\infty} w_m(x,y)$$

$$M_x(x,y)=\sum_{m=1}^{\infty} M_{x_m}(x,y) \quad M_y(x,y)=\sum_{m=1}^{\infty} M_{y_m}(x,y)$$
$$M_{xy}(x,y)=\sum_{m=1}^{\infty} M_{xy_m}(x,y) \qquad (9)$$
$$Q_x(x,y)=\sum_{m=1}^{\infty} Q_{x_m}(x,y) \quad Q_y(x,y)=\sum_{m=1}^{\infty} Q_{y_m}(x,y)$$
$$Q_x^*(x,y)=\sum_{m=1}^{\infty} Q_{x_m}^*(x,y) \quad Q_y^*(x,y)=\sum_{m=1}^{\infty} Q_{y_m}^*(x,y)$$
$$r_x(x,y)=\sum_{m=1}^{\infty} r_{x_m}(x,y) \quad r_y(x,y)=\sum_{m=1}^{\infty} r_{y_m}(x,y)$$

## 2. A solution of a plate

A rectangular plate has a geometry, supported and a loading shown in a fig. 1. To be construct the diagrams of the functions of the normal displacements and an internal forces in signed sections of plate.

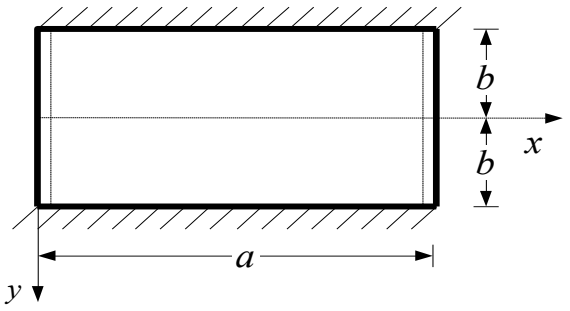



*Fig. 1*

*A characteristics of a plate*

A lengths of the side of the plate

$a=8\ m$; $b=2{,}5\ m$;

Module of elasticity $E=2.10^7\ \frac{kN}{m^2}$;

A Poisson's coefficient $\nu=0{,}17$

A coordinate system $xOy$.

A function of the external loads

$$q(x,y)=q=const$$

A function of the normal displacement of a point of the midle plane of the plate.

$$w(x,y)=\sum_m Y_m(y)\sin(\alpha_m x), \qquad \alpha_m=\frac{m\pi}{a},$$
$$(m=1,2,...\infty) \qquad (10)$$

The simply supported ends of the plate are parallels of an axes $y$.

*m - Fourier's coefficient in development of external load in serie at sin*

$$q_m(y)=\frac{2}{a}\int_0^a q(x,y)\sin(\alpha_m x)dx=\frac{2q}{m\pi}(1-\cos m\pi) \qquad (11)$$

*Arbitrary unhomogeneous differential equation about function* $Y_m(y)$

$$Y_m^{IV}(y)-2\alpha_m^2 Y_m^{II}(y)+\alpha_m^4 Y_m(y)=B_m(y). \qquad (12)$$

*General integral of arbitrary homogeneous differential equation about function* $Y_m(y)$

$$Y_m(y)=A_m ch\alpha_m y+D_m y sh\alpha_m y+\overline{Y}_m(y) \qquad (13)$$

*A derivates of the function* $Y_m(y)$

$$Y_m^{i}(y)=A_m\alpha_m sh\alpha_m y+D_m(sh\alpha_m y+\alpha_m y ch\alpha_m y)+\overline{Y}_m^{I}(y)$$

$$Y_m^{II}(y)=A_m\alpha_m^2 ch\alpha_m y+D_m\alpha_m(2ch\alpha_m y+\alpha_m y sh\alpha_m y)+\overline{Y}_m^{II}(y) \qquad (14)$$

$$Y_m^{III}(y)=A_m\alpha_m^3 sh\alpha_m y+D_m\alpha_m^2(3sh\alpha_m y+\alpha_m y ch\alpha_m y)+\overline{Y}_m^{III}(y)$$

*A partial integral* $\overline{Y}_m(y)$

At $q(x,y)=const$ the right part of homogeneous differential equation accepts a kind

$$B_m(y)=\frac{2q}{Dm\pi}(1-\cos m\pi)=\frac{4q}{Dm\pi}\left[1+(-1)^{m+1}\right]$$

or $$B_m(y)=\begin{vmatrix}\frac{4q}{Dm\pi} & (m=1,3,5,...)\\ 0 & (m=2,4,6,...)\end{vmatrix} \qquad (15)$$

The partial integral of unhomogeneous differential equation is searchs in kind of constant

$$\overline{Y}_m(y)=C=const \qquad (16)$$

Its determination to be made with a methode of undetermined coefficients. After a substituation in (12) be receive

$$0-2\alpha_m^2.0+\alpha_m^4.C=B_m(y)$$

$$C=\overline{Y}_m(y)=\frac{2qa^4}{Dm^5\pi^5}(1-\cos m\pi). \qquad (17)$$

*An integration constants* $A_m$, $D_m$.

A boundaries conditions at end $y=b$ - in this case fixed

$$w(x,b)=0 \qquad Y_m(b)=0$$

$$\frac{\partial w}{\partial y}(x,b)=0 \qquad Y_m^{I}(b)=0 \qquad (18)$$

A boundaries conditions at end $y=-b$ conduct to identical results.

It is introduces the signification $\theta_m=\alpha_m b$.

The equations for determination of integration constants accept a kind

$$A_m ch\alpha_m b+D_m b sh\alpha_m b+\overline{Y}_m(b)=0$$

$$A_m\alpha_m sh\alpha_m b+D_m(sh\alpha_m b+\alpha_m y ch\alpha_m b)+\overline{Y}_m^{I}(b)=0 \qquad (19)$$

After solution the received system equations for the integration constants is receives the following expressions

$$A_m=-\frac{sh\theta_m+\theta_m ch\theta_m}{ch\theta_m sh\theta_m+\theta_m}\overline{Y}_m\left(\frac{\theta_m}{\alpha_m}\right)+\frac{\frac{\theta_m}{\alpha_m}sh\theta_m}{ch\theta_m sh\theta_m+\theta_m}\overline{Y}_m^{I}\left(\frac{\theta_m}{\alpha_m}\right); \qquad (20)$$

$$D_m=\frac{\alpha_m sh\theta_m}{ch\theta_m sh\theta_m+\theta_m}\overline{Y}_m\left(\frac{\theta_m}{\alpha_m}\right)-\frac{ch\theta_m}{ch\theta_m sh\theta_m+\theta_m}\overline{Y}_m^{I}\left(\frac{\theta_m}{\alpha_m}\right)$$

It is follows the reverse going into solution of the methode of trigonometric series. It is determines the functions $Y_m(y)$, $M_{x_m}(y)$... $Q_{y_m}^*(y)$, $w(x,y)$, $M_x(x,y)$ ... $Q_y^*(x,y)$ and etc.

### 3. A numerical investigation

The solutions are made with a composed for a case computer's programm.

It is solve only half of a plate

A solutions are conduct with different keeping terms of the trigonometric's series.

A results obtained of the solutions for the displacements and forces are shown in a table 1-5.

Table 1.

| $m$ | $\alpha_m=\frac{m\pi}{a}$ | $\theta_m=\alpha_m b$ | $ch\theta_m$ | $sh\theta_m$ | $D\overline{Y}_m$ | $\overline{Y}_m^{I}$ | $\overline{Y}_m^{II}$ | $\overline{Y}_m^{III}$ | $DA_m$ | $DD_m$ |
|---|---|---|---|---|---|---|---|---|---|---|
| 1 | 0.3927 | 0.9817 | 1.5219 | 1.1472 | 2.1416e3 | 0 | 0 | 0 | -2.0738e3 | 353.7074 |
| 3 | 1.1781 | 2.9452 | 9.5339 | 9.4813 | 8.8130 | 0 | 0 | 0 | -3.5465 | 1.0547 |
| 5 | 1.9635 | 4.9087 | 67.7379 | 67.7305 | 0.6853 | 0 | 0 | 0 | -0.0597 | 0.0198 |
| 7 | 2.7489 | 6.8722 | 482.5516 | 482.5505 | 0.1274 | 0 | 0 | 0 | -2.0787e-3 | 7.2584e-4 |
| 9 | 3.5343 | 8.8357 | 3.4378e3 | 3.4378e3 | 0.0363 | 0 | 0 | 0 | -1.0376e-4 | 3.7286e-5 |
| 11 | 4.3197 | 10.7992 | 2.4491e4 | 2.4491e4 | 0.0133 | 0 | 0 | 0 | -6.4063e-6 | 2.3453e-6 |

Table 2.

| m | $Y_m(y)$, $Y_m^{I}(y)$, $Y_m^{II}(y)$, $Y_m^{III}(y)$ | | | | | | | | | | | |
|---|---|---|---|---|---|---|---|---|---|---|---|---|
| | $y=0$ | | | | $y=0,5b$ | | | | $y=b$ | | | |
| 1 | 67.8052 | 0 | -41.9981 | 0 | 38.7584 | -40.3471 | -12.3309 | 49.5051 | 0 | 0 | 92.5261 | 125.1540 |
| 3 | 5.2665 | 0 | -2.4372 | 0 | 3.3971 | -2.8876 | -1.8138 | 2.0395 | 0 | 0 | 11.4598 | 27.7569 |
| 5 | 0.6256 | 0 | -0.1523 | 0 | 0.4785 | -0.2772 | -0.3405 | -0.1849 | 0 | 0 | 2.6364 | 10.3631 |
| 7 | 0.1253 | 0 | -0.0117 | 0 | 0.1092 | -0.0386 | -0.0758 | -0.1216 | 0 | 0 | 0.9628 | 5.2933 |
| 9 | 0.0362 | 0 | -1.0326e-3 | 0 | 0.0339 | -6.8264e-3 | -0.0187 | -0.0467 | 0 | 0 | 0.4530 | 3.2022 |
| 11 | 0.0133 | 0 | -9.9277e-5 | 0 | 0.0129 | -1.4013e-3 | -4.9328e-3 | -0.0165 | 0 | 0 | 0.2481 | 2.1437 |

Table 3.

| m | $Dw(x,y)$ | | | | | | | | |
|---|---|---|---|---|---|---|---|---|---|
| | $x=0$ | | | $x=0{,}25a$ | | | $x=0{,}5a$ | | |
| | $y=0$ | $y=\frac{b}{2}$ | $y=b$ | $y=0$ | $y=\frac{b}{2}$ | $y=b$ | $y=0$ | $y=\frac{b}{2}$ | $y=b$ |
| 1 | 0 | 0 | 0 | 47.9455 | 27.4063 | 0 | 67.8052 | 38.7584 | 0 |
| 3 | 0 | 0 | 0 | 3.7240 | 2.4021 | 0 | -5.2665 | -3.3971 | 0 |
| 5 | 0 | 0 | 0 | -0.4424 | -0.3383 | 0 | 0.6256 | 0.4785 | 0 |
| 7 | 0 | 0 | 0 | -0.0886 | -0.0772 | 0 | -0.1253 | -0.1092 | 0 |
| 9 | 0 | 0 | 0 | 0.0256 | 0.0240 | 0 | 0.0362 | 0.0339 | 0 |
| 11 | 0 | 0 | 0 | 9.3982e-3 | 9.1308e-3 | 0 | -0.0133 | -0.0129 | 0 |
| $\sum_m$ | **0** | **0** | **0** | **51.1735** | **29.4260** | **0** | **63.0617** | **35.7516** | **0** |

Table 4.

| m | $M_x(x,y)$ | | | | | | | | |
|---|---|---|---|---|---|---|---|---|---|
| | $x=0$ | | | $x=0{,}25a$ | | | $x=0{,}5a$ | | |
| | $y=0$ | $y=\frac{b}{2}$ | $y=b$ | $y=0$ | $y=\frac{b}{2}$ | $y=b$ | $y=0$ | $y=\frac{b}{2}$ | $y=b$ |
| 1 | 0 | 0 | 0 | 12.4423 | 5.7087 | -11.1224 | 17.5961 | 8.0733 | -15.7294 |
| 3 | 0 | 0 | 0 | 5.4616 | 3.5520 | -1.3776 | -7.7238 | -5.0232 | 1.9482 |
| 5 | 0 | 0 | 0 | -1.7237 | -1.3453 | 0.3169 | 2.4377 | 1.9026 | -0.4482 |
| 7 | 0 | 0 | 0 | -0.6711 | -0.5925 | 0.1157 | -0.9491 | -0.8379 | 0.1637 |
| 9 | 0 | 0 | 0 | 0.3195 | 0.3016 | -0.0545 | 0.4519 | 0.4266 | -0.0770 |
| 11 | 0 | 0 | 0 | 0.1754 | 0.1710 | -0.0298 | -0.2480 | -0.2418 | 0.0422 |
| $\sum_m$ | **0** | **0** | **0** | **16.0040** | **7.7955** | **-12.1516** | **11.5647** | **4.2995** | **-14.1006** |

| m | $M_y(x,y)$ | | | | | | | | |
|---|---|---|---|---|---|---|---|---|---|
| | $x=0$ | | | $x=0{,}25a$ | | | $x=0{,}5a$ | | |
| | $y=0$ | $y=\frac{b}{2}$ | $y=b$ | $y=0$ | $y=\frac{b}{2}$ | $y=b$ | $y=0$ | $y=\frac{b}{2}$ | $y=b$ |
| 1 | 0 | 0 | 0 | 30.9541 | 9.4378 | -65.4258 | 43.7757 | 13.3470 | -92.5261 |
| 3 | 0 | 0 | 0 | 2.6020 | 1.8494 | -8.1033 | -3.6798 | -2.6154 | 11.4598 |
| 5 | 0 | 0 | 0 | -0.3976 | -0.4625 | 1.8642 | 0.5623 | 0.6541 | -2.6364 |
| 7 | 0 | 0 | 0 | -0.1221 | -0.1528 | 0.6808 | -0.1727 | -0.2160 | 0.9628 |
| 9 | 0 | 0 | 0 | 0.0550 | 0.0641 | -0.3203 | 0.0778 | 0.0907 | -0.4530 |
| 11 | 0 | 0 | 0 | 0.0299 | 0.0325 | -0.1755 | -0.0423 | -0.0459 | 0.2481 |
| $\sum_m$ | **0** | **0** | **0** | **33.1213** | **10.7684** | **-71.4799** | **40.5210** | **11.2145** | **-82.9449** |

| m | $M_{xy}(x,y)$ | | | | | | | | |
|---|---|---|---|---|---|---|---|---|---|
| | $x=0$ | | | $x=0{,}25a$ | | | $x=0{,}5a$ | | |
| | $y=0$ | $y=\frac{b}{2}$ | $y=b$ | $y=0$ | $y=\frac{b}{2}$ | $y=b$ | $y=0$ | $y=\frac{b}{2}$ | $y=b$ |
| 1 | 0 | 13.1507 | 0 | 0 | 9.2990 | 0 | 0 | 0 | 0 |
| 3 | 0 | 2.8236 | 0 | 0 | -1.9966 | 0 | 0 | 0 | 0 |
| 5 | 0 | 0.4518 | 0 | 0 | -0.3195 | 0 | 0 | 0 | 0 |
| 7 | 0 | 0.0881 | 0 | 0 | 0.0623 | 0 | 0 | 0 | 0 |
| 9 | 0 | 0.0200 | 0 | 0 | 0.0142 | 0 | 0 | 0 | 0 |
| 11 | 0 | 5.0242e-3 | 0 | 0 | -3.5526e-3 | 0 | 0 | 0 | 0 |
| $\sum_m$ | **0** | **16.5392** | **0** | **0** | **7.0559** | **0** | **0** | **0** | **0** |

| m | $Q_x(x,y)$ | | | | | | | | |
|---|---|---|---|---|---|---|---|---|---|
| | $x=0$ | | | $x=0{,}25a$ | | | $x=0{,}5a$ | | |
| | $y=0$ | $y=\frac{b}{2}$ | $y=b$ | $y=0$ | $y=\frac{b}{2}$ | $y=b$ | $y=0$ | $y=\frac{b}{2}$ | $y=b$ |
| 1 | 20.5988 | 7.1895 | -36.3349 | 14.5656 | 5.0838 | -25.6927 | 0 | 0 | 0 |
| 3 | 11.4826 | 7.6915 | -13.5007 | -8.1194 | -5.4387 | 9.5465 | 0 | 0 | 0 |
| 5 | 5.0346 | 4.2907 | -5.1766 | -3.5600 | -3.0340 | 3.6604 | 0 | 0 | 0 |
| 7 | 2.6358 | 2.4762 | -2.6466 | 1.8638 | 1.7509 | -1.8714 | 0 | 0 | 0 |
| 9 | 1.6002 | 1.5625 | -1.6011 | 1.1315 | 1.1049 | -1.1322 | 0 | 0 | 0 |
| 11 | 1.0717 | 1.0621 | -1.0718 | -0.7578 | -0.7510 | 0.7579 | 0 | 0 | 0 |

| $\sum_m$ | **42.4238** | **24.2725** | **-60.3318** | **5.1236** | **-1.2842** | **-14.7315** | **0** | **0** | **0** |
|---|---|---|---|---|---|---|---|---|---|

| | $Q_y(x,y)$ | | | | | | | | |
|---|---|---|---|---|---|---|---|---|---|
| | $x=0$ | | | $x=0{,}25a$ | | | $x=0{,}5a$ | | |
| | $y=0$ | $y=\frac{b}{2}$ | $y=b$ | $y=0$ | $y=\frac{b}{2}$ | $y=b$ | $y=0$ | $y=\frac{b}{2}$ | $y=b$ |
| 1 | 0 | 0 | 0 | -88.4972 | -39.4051 | -88.4972 | 0 | -55.7272 | -125.1540 |
| 3 | 0 | 0 | 0 | -19.6271 | -4.2761 | -19.6271 | 0 | 6.0473 | 27.7569 |
| 5 | 0 | 0 | 0 | 7.3278 | 0.6250 | 7.3278 | 0 | -0.8838 | -10.3631 |
| 7 | 0 | 0 | 0 | 3.7430 | 0.1204 | 3.7430 | 0 | 0.1702 | 5.2933 |
| 9 | 0 | 0 | 0 | -2.2643 | -0.0273 | -2.2643 | 0 | -0.0386 | -3.2022 |
| 11 | 0 | 0 | 0 | -1.5158 | -6.8487e-3 | -1.5158 | 0 | 9.6855e-3 | 2.1437 |
| $\sum_m$ | **0** | **0** | **0** | **0** | **-42.9700** | **-100.8337** | **0** | **-50.4224** | **-103.5254** |

| m | $Q_x^*(x,y)$ | | | | | | | | |
|---|---|---|---|---|---|---|---|---|---|
| | $x=0$ | | | $x=0{,}25a$ | | | $x=0{,}5a$ | | |
| | $y=0$ | $y=\frac{b}{2}$ | $y=b$ | $y=0$ | $y=\frac{b}{2}$ | $y=b$ | $y=0$ | $y=\frac{b}{2}$ | $y=b$ |
| 1 | 34.2877 | 11.2087 | -66.4929 | 24.2451 | 7.9257 | -47.0176 | 0 | 0 | 0 |
| 3 | 13.8658 | 9.4651 | -24.7063 | -9.8046 | -6.6928 | 17.4700 | 0 | 0 | 0 |
| 5 | 5.2829 | 4.8456 | -9.4731 | -3.7356 | -3.4264 | 6.6985 | 0 | 0 | 0 |
| 7 | 2.6625 | 2.6491 | -4.8433 | 1.8827 | 1.8732 | -3.4247 | 0 | 0 | 0 |
| 9 | 1.6032 | 1.6173 | -2.9301 | 1.1336 | 1.1436 | -2.0719 | 0 | 0 | 0 |
| 11 | 1.0721 | 1.0798 | -1.9614 | -0.7581 | -0.7636 | 1.3870 | 0 | 0 | 0 |
| $\sum_m$ | **58.7742** | **30.8657** | **-110.4071** | **12.9632** | **0.0598** | **-26.9587** | **0** | **0** | **0** |

| m | $Q_y^*(x,y)$ | | | | | | | | |
|---|---|---|---|---|---|---|---|---|---|
| | $x=0$ | | | $x=0{,}25a$ | | | $x=0{,}5a$ | | |
| | $y=0$ | $y=\frac{b}{2}$ | $y=b$ | $y=0$ | $y=\frac{b}{2}$ | $y=b$ | $y=0$ | $y=\frac{b}{2}$ | $y=b$ |
| 1 | 0 | 0 | 0 | 0 | -43.0568 | -88.4972 | 0 | -60.8914 | -125.1540 |
| 3 | 0 | 0 | 0 | 0 | -6.6282 | -19.6271 | 0 | 9.3737 | 27.7569 |
| 5 | 0 | 0 | 0 | 0 | 1.2522 | 7.3278 | 0 | -1.7709 | -10.3631 |
| 7 | 0 | 0 | 0 | 0 | 0.2916 | 3.7430 | 0 | 0.4124 | 5.2933 |
| 9 | 0 | 0 | 0 | 0 | -0.0773 | -2.2643 | 0 | -0.1094 | -3.2022 |
| 11 | 0 | 0 | 0 | 0 | -0.0222 | -1.5158 | 0 | 0.0314 | 2.1437 |
| $\sum_m$ | **0** | **0** | **0** | **0** | **-48.2407** | **-100.8337** | **0** | **-52.9542** | **-103.5254** |

Table 5.

| m | $r_x(x,y)$ | | | | | | $r_y(x,y)$ | | |
|---|---|---|---|---|---|---|---|---|---|
| | $x=0$ | | | $x=a$ | | | $x=0$ | $x=0{,}25a$ | $x=0{,}5a$ |
| | $y=0$ | $y=\frac{b}{2}$ | $y=b$ | $y=0$ | $y=\frac{b}{2}$ | $y=b$ | $y=b$ | $y=b$ | $y=b$ |
| 1 | 34.2877 | 11.2087 | -66.4929 | 34.2877 | 11.2087 | -66.4929 | 0 | 88.4972 | 125.1540 |
| 3 | 13.8658 | 9.4651 | -24.7063 | 13.8658 | 9.4651 | -24.7063 | 0 | 19.6271 | -27.7569 |
| 5 | 5.2829 | 4.8456 | -9.4731 | 5.2829 | 4.8456 | -9.4731 | 0 | -7.3278 | 10.3631 |
| 7 | 2.6625 | 2.6491 | -4.8433 | 2.6625 | 2.6491 | -4.8433 | 0 | -3.7430 | -5.2933 |
| 9 | 1.6032 | 1.6173 | -2.9301 | 1.6032 | 1.6173 | -2.9301 | 0 | 2.2643 | 3.2022 |
| 11 | 1.0721 | 1.0798 | -1.9614 | 1.0721 | 1.0798 | -1.9614 | 0 | 1.5158 | -2.1437 |
| $\sum_m$ | **110.4071** | **26.9587** | **0** | **-58.7742** | **-30.8657** | **110.4071** | **0** | **100.8337** | **103.5254** |

The partial integral, the integration constants and function of normal displacement in the solutions have a multiplier *D*.

The solutions continue while the difference between the first and the last unzerou value of displacement, force get a value sufficiently small.

For verification are written the equations for equilibrium for each term of the serie for half plate.

The results obltained are compared.

A cause of the symmetry oh the plate investigated, the results for the displacements and forces are written only for the square of plate.

**4. Conclusions**

The accuracy and the conjuance of the results for the displacements and forces are determine of the number of keeping terms in the trigonometric series and the dencity of the discretization set in the two directions of the –plate.

The method are applies an analogue with a different on distribution loads, symmetrical in relation of axis $x$ of the plate.

**REFERENCES**

[1]. Varbanov Chr., A. Tepavicharov, T. Ganev, Theory of elasticity and plasticity, *Thechnika*, Sofia, 1992.

[2]. Tc. Krustev, T. Karamanski and oth., Guidance for a solution of a problem of theory of elasticity, stability and dynamics of elastic's systems, *Thechnika*, Sofia, 1974.

[3]. Timoshenko S. P., S. Voinovski-Kriger, Plates and Shells, Moscow, 1966.

[4]. Szilard R, *Theory and Analysis of Plates*, *Classical and Numerical Method*, Prentice-Hall, New Jersry, 1976.

[5]. Vainberg D.B., E.D. Vainberg, A solution of a plates, Budivelnik, Kiev, 1970.

Liliya Petrova, Assoc. Prof. PhD Eng.-math.,
dep. "Mechanics", Univ. of Transport "T. Kableshkov",
158 Geo Milev Str., Sofia 1574, Bulgaria

E-mail: lbphr@abv.bg

© International Scientific Conference on Engineering, Technologies and Systems
TECHSYS 2016, Technical University – Sofia, Plovdiv branch
26 – 28 May 2016, Plovdiv, Bulgaria

# МАГНИТЕН МОМЕНТ И СКОРОСТИ НА СОБСТВЕНО ВЪРТЕНЕ В ТОРОИДЕН МОДЕЛ НА НЕУТРОНА

КИРИЛ КОЛИКОВ

**Резюме***: В настоящата статия моделираме неутрона във формално-евристичен смисъл като тор. Основание за това ни дава предишна наша работа. В нея намираме времето (периода) на собствено въртене на протона и модула на ъгловата му скорост. Доказваме за протона, че е изтеглен по екваториалната си окръжност. Ето защо не разглеждаме нуклоните като сфери, както ги представя стандартния модел.*

*Въз основа на тороидния модел на неутрона, ние извеждаме формула за магнитния му момент. Приемаме, че времето на собствено въртене и модулите на ъгловите скорости на неутрона и протона са равни. Оттук намираме възможните стойности за модула на линейната скорост на „екваториалните“ точки от повърхността на неутрона. Получаваме, че тя е близка до релативистичната скорост. Изчисляваме и огромни по модул стойности за пълното ускорение на тези точки за двата нуклона.*

**Ключови думи:** *неутрон, тороиден модел на неутрона, зарядова плътност на неутрона, магнитен момент на неутрона, собствено въртене на неутрона*

# MAGNETIC MOMENT AND VELOCITIES OF SELF-ROTATION IN TOROIDAL MODEL OF THE NEUTRON

KIRIL KOLIKOV

**Abstract:** *In the current paper the neutron is modeled in formal-heuristic sense as a torus. This paper is based on previous works of ours. In which we derive time (period) of self-rotation of the proton and its module of angular velocity. We prove the proton is stretched at its equatorial surface. This is the reason why we do not regard nucleons as spheres like the Standard model represents them.*

*We derive formula for its magnetic moment on the basis of a toroidal neutron model. We assume that the time of self-rotation and modules of angular velocities of the proton and neutron are equal. From here we find the possible values for module of linear velocity of equatorial points from the neutron's surface. We obtain that this velocity is close to relativistic. We calculate the enormous absolute values of full acceleration of these points for both nucleons.*

**Key words:** *neutron, toroidal model of the neutron, charge density of the neutron, magnetic moment of the neutron, self-rotation of the neutron*

## 1. Въведение

Стандартният модел на нуклоните ги представя като сфери [1, 2, 3]. Затова ние в [4] разглеждаме първо протона като въображаема сфера $S_p$, въртяща се с постоянна ъглова скорост около права $\xi$, минаваща през геометричния му център (центъра на масата) $O$ и перпендикулярна на равнината на собственото му въртене. Такова моделиране извършваме във формално-евристичния смисъл на Нилс Бор.

Copyright © 2016 by Technical University of Sofia, Plovdiv branch, Bulgaria ISSN Online: 2535-0048

Изчислявайки модула на линейната скорост $v_p = |\dot{v}_p|$ на екваториалните точки от повърхността на протона, в [4] получаваме, че $v_p$ е от порядъка на релативистичната скорост. А получената стойност на Лоренц-фактора за тези точки в сферичния модел показва, че протонът трябва да е изтеглен по екваториалната си окръжност. Именно това ни дава основание да моделираме нуклоните с тор и да изведем в [4] теоретично формула за магнитния момент на тор. В [5, 6, 7, 8] и по други съображения използваме тороиден модел на нуклоните. Този модел се използва и от други автори [9].

В настоящата статия моделираме неутрона с тор $T_n$, въртящ се с постоянна ъглова скорост $\dot{\omega}_n$ около права $\xi$, минаваща през геометричния му център и перпендикулярна на равнината на собственото му въртене. Съгласно [10] неутронът притежава положителен и отрицателен елементарни заряди, при което общият му заряд $n$ е равен на нула. Нека $R_+$ е усредненото разстояние от центъра на $T_n$ до слоя, разделящ положителната, а $R_-$ – разделящ отрицателната обемна зарядова плътност на неутрона. Тогава извеждаме теоретично формула за магнитния му момент $\mu_n$ чрез $e$, $R_+$, $R_-$ и времето (периода) $t_n$ на собственото му въртене.

Точно експериментално измерване на неутронния магнитен момент е извършено от Green и др. [11] през 1979г. Измерено е съотношението на магнитните моменти на неутрона и протона $\mu_n/\mu_p = -0.684979$ като се използва ядрено-магнитен резонанс (ЯМР). ЯМР е приложен за определяне на магнитния момент на неутрона още през 1947г. от Arnold и Roberts [12], но тогава не са получени точни резултати.

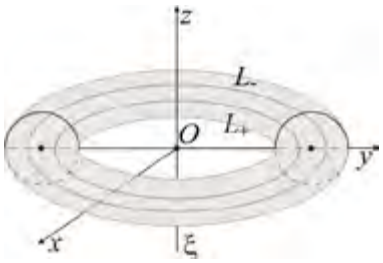
При структурирането на деутрона и тритона в [6], хелиона и $\alpha$–частицата в [7], ние приемаме, че модулите на ъгловите скорости на собственото въртене на неутрона $\omega_n = |\bar{\omega}_n|$ и на протона $\omega_p = |\dot{\omega}_p|$ са равни и следователно $t_n = t_p$. Въз основа на това тук намираме модула $v_n = |\dot{v}_n|$ на линейната скорост на „екваториалните“ точки от повърхността на неутрона, т.е. на точките, лежащи на окръжността $E_n$ на кръга, минаващ през центъра му и перпендикулярен на оста на собственото му въртене. Получаваме, че възможните стойности на $v_n$ са близки до релативистичната скорост. Освен това намираме огромни по модул стойности за пълните ускорения $a_n$ и $a_p$ на „екваториалните“ точки съответно от неутрона и протона.

Чрез данните за положителния и отрицателния зарядови радиуси на неутрона от [10] намираме $R_+$ и $R_-$. Оттам уточняваме стойностите за $\omega_n$, $t_n$, $v_n$ и $a_n$. Получените данни за $\omega_n$ и $t_n$ потвърждава коректността на нашето допускане, че $\omega_n = \omega_p$ и $t_n = t_p$.

## 2. Теоретично определяне магнитния момент на неутрона

Да моделираме във формално-евристичен смисъл неутрона с тор $T_n$. Нека $T_n$ в дадена инерциална система $J$ се върти с постоянна ъглова скорост $\bar{\omega}_n$ около права $\xi$, минаваща през неподвижния му в $J$ геометричен център (център на масата) $O$. Да въведем неподвижно свързана с $T_n$ дясна ортогонална координатна система $Oxyz$, така че оста $Oz$ да съвпада с $\xi$.

Както в [10] приемаме, че положителния и отрицателния заряди са равни на единичния заряд $e$. Нека $R_+$ е усредненото разстояние от центъра $O$ на тора $T_n$ до слоя, разделящ положителната обемна зарядова плътност, а $R_-$ е успоредното разстояние до слоя, разделящ отрицателната му обемна зарядова плътност. Приемаме, че тези заряди са разпределени равномерно по окръжности $L_+$ и $L_-$ с общ център $O$ и с радиуси, съответно $R_+$ и $R_-$ (Фиг. 1).




***Фиг. 1.*** *Въртящ се около оста $Oz$ тор, с равни по модул разноименни заряди, разпределени равномерно по окръжности $L_+$ и $L_-$.*

Окръжностите $L_+$ и $L_-$ се въртят с една и съща постоянна ъглова скорост $\bar{\omega}_n$ около центъра си $O$. Тогава, съгласно [13], модулът на магнитния момент на неутрона е

$$\mu_n = -\frac{\pi e}{t_n}(R_-^2 - R_+^2) \qquad (1)$$

където $e = 1.6012176487 \times 10^{-19}$ C, а $t_n$ е времето (периода) на собствено въртене на неутрона.

Съгласно експрименталните данни магнитният момент на неутрона е $\mu_n = -0.96623641 \times 10^{-26}$ JT$^{-1}$ [14], а класическият му радиус е $r_n \approx 1.1$ fm [15].

### 3. Определяне величините, характеризиращи собственото въртене на неутрона

В [4] ние намираме, че слоят, разделящ обемната зарядова плътност на протона, е на разстояние $R \in (0.70318; 0.84184)$ fm от неговия център. Определяме и възможните стойности на времето $t_p \in (1.76437; 2.52879) \times 10^{-23}$ s и на модула на ъгловата скорост $\omega_p \in (2.48466; 3.56116) \times 10^{23}$ Hz на собствено въртене.

Чрез тороидния модел на нуклоните ние моделираме деутрона и тритона в [6], както и хелиона и $\alpha$–частицата в [7], като приемаме, че ъгловата скорост $\bar{\omega}_n$ на собствено въртене на неутрона е равна на ъгловата скорост $\bar{\omega}_p$ на протона.

Нека $E_n$ е „екваториалната“ окръжност на тора $T_n$, т.е. окръжността на кръга с център $O$, чиято равнина е перпендикулярна на правата $\xi$ (Фиг.1). Означаваме с $v_n = |\bar{v}_n|$ модулът на линейната скорост на собствено въртене на точките от $E_n$ на неутрона. Скоростта $v_n = r_n \omega_n$ и е по-малка от скоростта на светлината във вакуум, която е $c = 2.99792458 \times 10^8$ ms$^{-1}$ [14]. Тогава за $r_n = 1.1$ fm установяваме, че:

$$\begin{aligned} \omega_n = \omega_p &\in (2.48466; 2.72538) \times 10^{23} \text{ Hz} \\ v_n &\in (2.73313; 2.99792) \times 10^8 \text{ ms}^{-1}. \end{aligned} \qquad (2)$$

С този резултат редуцираме интервалите за възможните стойности на $\omega_p = 2\mu_p / pR^2$ и $R \in (0.80380; 0.84184)$ fm за протона.

От $\omega_n = \omega_p$ следва още, че времето $t_n$ на собствено въртене на неутрона съвпада с времето $t_p = R^2 \pi p / \mu_p$ на собствено въртене на протона. Така редуцираме и интервала за възможните стойности на $t_p$

$$t_n = t_p \in (2.30543; 2.52879) \times 10^{-23} \text{ s}. \qquad (3)$$

Тогава, въз основа на експерименталната стойност за $\mu_n$ и от формула (1), получаваме, че

$$R_-^2 - R_+^2 \in (0.44256; 0.48544) \text{ fm}^2. \qquad (4)$$

В [10] са дадени стойностите на радиусите за отрицателното и положителното зарядово разпределение, съответно $r_- = 0.800$ fm и $r_+ = 0.726$ fm. Освен това съгласно радиалното разпределение на зарядите представено на Фиг. 1 от [16] можем да приемем, че $R_- \approx r_- + r_+/2$, а $R_+ \approx r_+/2$, т.е. че $R_- = 0.763$ fm и $R_+ = 0.363$ fm. Следователно $R_-^2 - R_+^2 = 0.453 \in (0.44256; 0.48544)$ fm$^2$. Това потвърждава получения от нас резултат (4).

При $R_- = 0.763$ fm и $R_+ = 0.363$ fm изчисляваме, че:

$$\omega_n = 2.67796 \times 10^{23} \text{ Hz}, \; t_n = 2.34625 \times 10^{-23} \text{ s и}$$
$$v_n = 2.94576 \times 10^8 \text{ ms}^{-1}.$$

### 4. Дискусия

Поради релативистичното въртене на точките от екваториалната окръжност, на нуклоните, те в евристично-формален смисъл би трябвало да се разглеждат по-скоро като торове. Тороидният модел на нуклоните, който разглеждаме не само в настоящата статия, а и в [5, 6, 7, 8], като интерпретация е много по-близо до вълновия подход, отколкото до корпускулярния модел.

Тъй като тангенциалното ускорение на „екваториалните” точки на нуклоните е равно на нула, то модулът на пълното им ускорение съответно на протона $a_p = |\dot{a}_p|$ и на неутрона $a_n = |\bar{a}_n|$, относно инерциалната система $J$, е равен на модула на нормалното (центростремителното) им ускорение, т.е. $a_p = v_p^2 / r_p$ и $a_n = v_n^2 / r_n$. Следователно за

$$v_p \in (2.09168; 2.99792) \times 10^8 \text{ ms}^{-1}$$
$$\text{и } v_n \in (2.73313; 2.99792) \times 10^8 \text{ ms}^{-1}$$

стойността на пълното ускорение на тези точки за всеки нуклон е огромна:

$$a_p \in (5.19712; 10.6761) \times 10^{31} \text{ ms}^{-2}$$
$$\text{и } a_n \in (5.19712; 10.6761) \times 10^{31} \text{ ms}^{-2}.$$

При $R_- = 0.763$ fm и $R_+ = 0.363$ fm получаваме $a_n = 7.88864 \times 10^{31}$ ms$^{-2}$.

Както е известно от общата теория на относителността, гравитационното ускорение в

произволна точка от гравитационното поле се интерпретира като интензитет на това поле в точката. Това е елементарно следствие от слабия принцип за еквивалентност в тази теория, а именно от неоспоримия факт за равенство на тежката и инертната маси, известен даже в Нютоновата механика и проверен експериментално с много голяма точност. Разглеждайки масата като гравитационен заряд, стигаме до извода, че намереният модул на пълното ускорение е всъщност големината на интензитета на инерчното (гравитационно отстранимото) поле, относно собствената отправна система на неутрона, за всички точки от неговата екваториална окръжност.

**5. Заключение**

В настоящата статия ние моделираме неутрона във формално-евристичен смисъл като тор и извеждаме теоретично формула за магнитния момент на неутрона.

Допускаме, въз основа на предишни наши работи [6, 7], че ъгловите скорости, а оттам и времето на собствено въртене на неутрона и протона са равни. Тогава от експерименталните данни за магнитния момент и радиуса на неутрона изчисляваме, че модула на линейната скорост на собствено въртене на точките от „екваториалната“ окръжност на неутрона е близка до релативистичната.

Получаваме и една нова величина в теорията на ядрените сили, а именно огромния по стойност модул на пълното ускорение на „екваториалните“ точки на нуклоните, относно дадена инерциална система.

**ЛИТЕРАТУРА**


1. Allen, H. (1918). The Case for a Ring Electron, *Proc. Phys. Soc. London*, 31, 49-68. DOI: 10.1088/1478-7814/31/1/303
2. Compton, A. (1921). The magnetic electron, *J. Franklin I*, 192, 145-155. DOI: 10.1016/S0016-0032(21)90917-7
3. Tipler, P., Llewellyn, R. (2002). *Modern Physics*. W. H. Freeman.
4. Kolikov, K., Krastev, G., Epitropov, Y. (2016). Theoretical representation of the proton's magnetic moment and determination of its velocities of self-rotation (submitted).
5. Kolikov, K., Ivanov, D., Krastev, G. (2012). Electromagnetic nature of the nuclear forces and a toroid model of nucleons in atomic nuclei, *Natural Science*, 4, 47-56. http://www.scirp.org/journal/PaperInformation.aspx?paperID=16587
6. Kolikov, K., Ivanov, D., Krastev, G. (2012). Electromagnetic nature of the nuclear forces and toroid structure of the deuteron and triton, *Natural Science*, 4, 123-130. http://www.scirp.org/journal/PaperInformation.aspx?paperID=17328
7. Kolikov, K. (2012). Electromagnetic nature of nuclear forces and the toroid structure of the helion and the alpha particle, *Natural Science*, 4, 484-491. http://www.scirp.org/journal/PaperInformation.aspx?paperID=20783
8. Ivanov, D., Kolikov, K. (2013). Short-range action and long-range action of the electrostatic forces within atomic nuclei, *Natural Science*, 5, 508-513. http://www.scirp.org/journal/PaperInformation.aspx?PaperID=30256
9. Miller, G. (2008). Non-spherical shapes of the proton: existence, measurement, and computation, *Nuclear Physics News*, 18, 12-16.
10. Gentile, T. R., Crawford C. B. (2011). Neutron charge radius and the neutron electric form factor, *Phys. Rev. C*, 83, 055203.
11. Greene, G., Ramsey, N., Mampe, W., Pendlebury, J., Smith, K., Dress, W., Miller, P., Perrin, P. (1979). Measurement of the neutron magnetic moment, *Phys. Rev. D*, 20, 2139.
12. Arnold, W., Roberts, A. (1947). The Magnetic Moments of the Neutron and the Deuteron, *Phys. Rev.*, 71, 878. DOI: 10.1103/PhysRev.71.878
13. Yavorsky, B., Detlaf, A. (1985). *Handbook of physics*, Nauka, Moscow. (in Russian).
14. Mohr, P., Taylor, B., Newell, D. (2008). CODATA Recommended values of the fundamental physical constants: 2006, *Rev. Mod. Phys.*, 80, 633-730. DOI: 10.1103/RevModPhys.84.1527
15. Sardin, G., (1999). Fundamentals of the orbital conception of elementary particles and of their application to the neutron and nuclear structure, *Physics Essays*, 12, 204-220.
16. Haddad, S., Suleiman, S. (1999). Neutron charge distribution and charge density distributions in lead isotopes, *Acta Physica Polonica B*, 30, 119-126.



Контакти
Адрес
Факултет по математика и информатика, ПУ „П. Хилендарски“, ул. Цар Асен 24, 4000, Пловдив, България
E-mail: kolikov@uni-plovdiv.bg

© International Scientific Conference on Engineering, Technologies and Systems
TECHSYS 2016, Technical University – Sofia, Plovdiv branch
26 – 28 May 2016, Plovdiv, Bulgaria

# ФИЗИКА И ПРОИЗВОДСТВО

ИВАН СТОЯНОВ ВЪЛКОВ

**Резюме:** *Фундаменталната роля на физиката за развитието на науката, както и за изучаването на различните процеси (на микро и макро ниво) в природата е неоспорима. Физиката е задължителна дисциплина, която се изучава в техническите вузове. Програмата, по която се осъществява обучението, обхваща широк кръг от въпроси, касаещи различни производствени и технологични проблеми в машиностроителните предприятия, особено в тези с широк спектър на произвежданите изделия. Имайки предвид горе неописаното, основния въпрос, чийто отговор ще бъде потърсен в тази работа е: „Има ли място за професионална реализация за човек с висше образование с ОКС "Физик" в машиностроителните предприятия ?"*

**Ключови думи:** *физика, машиностроително предприятие, технологични и производствени процеси, реализация.*

# PHYSICS AND PRODUCTION

IVAN STOYANOV

**Abstract:** *The fundamental role of physics for scientific development, as well as for studying the various processes in nature (at a micro and macro level) is undeniable. Physics is a compulsory course, studied at technical universities. The curriculum, according to which the training is realized, covers a wide range of topics, concerning various production and technological problems in machine-building enterprises, especially in companies with a wide spectrum of products. Based on the aforementioned facts, the main question to be answered in this paper is: "Is there a place for professional development for a person with higher educational degree "Physicist" in machine building companies?"*

**Key words:** *physics, machine-building company, technological and production processes, professional realization*

## 1. Увод

В тази работа искам да споделя моя опит като физик с около 10 г. стаж в машиностроителен комбинат „Вазовски машиностроителни заводи". В едно производство (както гражданско, така и специално, т. е. разбирай военно) всеки висшист се сблъсква с най – различни проблеми (разбирай предизвикателства) и ако е настроен позитивно, (т. е. има хъс да се справи с проблемите) той има огромно поле за дейност и професионално развитие.

Когато се говори за обучението по физика като част от образователния процес на студентите, не трябва да се забравя следното: Освен Големия адронен колайдер (LHC) в Европейския център за ядрени изследвания (CERN) [1], космическите сонди и телескопи като „Хъбъл" (HST) [2], обсерваторията за наблюдение и регистрация на гравитационни вълни (LIGO), опитите за регистрация на осцилациите на неутриното (SK-ND и SNO) [3] физиката има и непосредствено отношение към стандартните и рутинни производствени процеси. Физикът трябва да има нестандартен поглед върху процесите, като едновременно с това владее чисто физическия подход към тях [4]. Той трябва да умее да „отсява" главните

Copyright © 2016 by Technical University of Sofia, Plovdiv branch, Bulgaria ISSN Online: 2535-0048

параметри, които играят основна роля в разглежданите (или използвани) процеси. Да оцени как тяхното изменение ще доведе до отклонение (естествено в положителна посока) в крайните резултати.

## 2. Изложение

Завършил съм „Физически факултет" на СУ „Климент Охридски" - гр. София, специалност „Атомна физика", производствен профил. Още като студент винаги съм се увличал от експериментални и приложни разработки. Във втори курс под ръководството на един от нашите преподаватели се занимавахме с разработката и изследването на кварцови резонатори за лазерни системи. В трети курс вниманието ни привлече "Ефект на Мьос Бауер" и приложението му за изследвания в областта на материалознанието и медицината. В трети курс вече се бяхме ориентирали за темите на дипломните работи и се стигна до темата "Анихилация на позитрони в метални образци". Същността на темата беше свързана с дейноста на Института по метали "А. Балевски" към БАН по изследване промяната на кристалната решетка в повърхностния слой на металите при висока степен на пластична деформация. Обстоятелствата се стекоха така, че вместо да се занимавам с атомна и ядрена физика, постъпих на работа в МК „ВМЗ", тъй като бях негов стипендиант (независимо от всичко по-късно със съдействието на ръководството на комбината сключих договор и бях едноличен изпълнител на тема „Проектиране и изработка на графитов колиматор за топлинни неутрони" внедрен в ИЯИЯЕ – БАН).Започнах работа като обикновен работник на длъжност „Монтьор-изпитател". Извършвахме изпитание на изделия на ударо- и виброустойчивост, електроизпитания в различни климатични условия (тропически, полярни, прахо- и капкоустойчивост). Техниката ни беше на отлично за времето си ниво. Разполагахме със стендове за изпитание на фирмата "Брюл и Кер", климатични камери на фирмата "ИЛКА" – Германия и много други. По – късно бях назначен на длъжност „Н-к ОТК" на голям цех за специално производство, в който имаше термичен, галваничен, механичен, сборъчен и хидравлични участъци. Това ми даде възможност да се запозная с различни технологични процеси и да разширя познанията си в много области – термообработка на детайли, галваника, хидронатоварвания, спектрален анализ на материали и др. След това пак по стечение на обстоятелствата започнах работа като началник на лаборатория по „Прецизни измервания" в лагерното производство. В онези години „ИТР" - инженерно-техническите работници бяха изпращани по за един месец на „помощ" в производството. По начало производствените процеси винаги са били интересни за мен. Прякото ми участие в тях доведе до генериране и внедряване на редица рационализации, някои от които със значителен икономически ефект, други – с промяна на самия процес, а трети – с внедряване на нова апаратура и приспособления за контрол на изделия. Накратко ще опиша някои от тях.

В галваниката имам три рационализации. Две от тях касаят процеса поцинковане. Същността на първата беше в електроизолиране на притискателните пружини, осъществяващи контакта на изделието с отрицателния полюс на електрозахранването (катода). Върху тези пружини се отлагаше много цинк, който по - късно се изхвърляше заедно с използваната за разцинковане солна киселина. С въвеждане на рационализацията се икономисваха стотици килограми цинк и хиляди литри солна киселина. Втората рационализация касаеше икономия на цинкови аноди. С нейното внедряване се спестяваха 50% от анодите, тъй като някои от тях с минимална обработка се използваха дву- и трикратно (но за различни изделия). Третата рационализация беше свързана с процеса „твърдо анодиране" – в технологичния процес беше въведена конструираната и изработена от мен противотокова двувитлова турбина с въздушно задвижване турбина за обезпечаване на отрицателни температури за анодирането. Икономическия ефект не беше ообено голям, но значително се подобриха условията за работа на оператора, като значително се съкрати неговото пребиваване в областта, наситена с изпарения на сярна киселина.

В областта на изпитания на проводниците конструирах и изработих специален съд за електроизпитание при условията на вакуум и високи налягания, какъвто до момента нямаше в ЦЗЛ – централната заводска лаборатория.

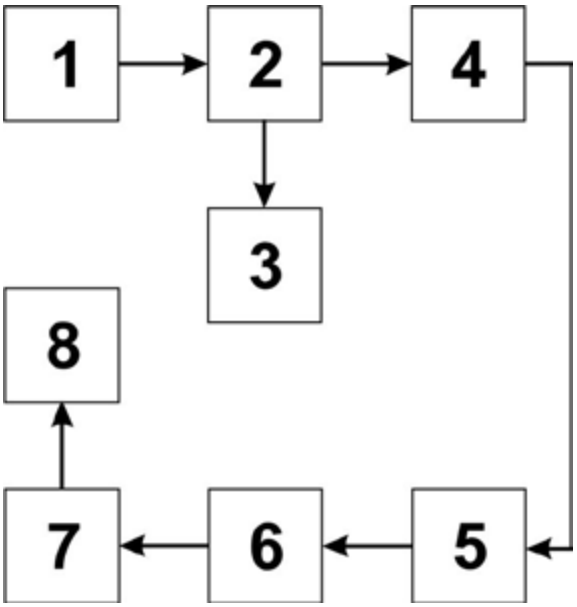
Докато завеждах лабораторията по „Прецизни измервания", внедрих две рационализации – едната беше свързана с ремонт и възстановяване на електросъпротивителни датчици за измерване на триещия момент на търкалящи лагери, а другата с конструиране и внедряване на приспособление към прибора „GRINDO SONIC" за измерване модула на Юнг и твърдостта на абразивни инструменти с форма на паралелепипед

(измерването се осъществява на база определяне и регистрация на собствените честоти на трептене, възникващи при възбуждане на телата чрез удар).

По същото време работехме по една тема, свързана с разработка на методи за разчет и анализ на размерните вериги на търкалящи лагери с отчитане на технологичните погрешности на размерите, геометричната форма и взаимното разположение на повърхностите на детайлите. Темата се базираше на метода "Фурие – анализ" на периодични функции, резултатите от който имаха пряко отношение за оценка състоянието на обработващите машини, използван инструмент и режими на обработка, отговорни за качеството на изделията.

Особено интересна беше рационализацията, при която беше внедрен пилотен хелий-неонов лазер, трасиращ остта на поток от инфрачервено излъчване, което трябваше да бъде регистрирано от определено изделие.

И накрая ще завърша с едно мое рационализаторско предложение, което беше с огромен икономически ефект, но така и не беше признато (според мен, по субективни причини и замесени икономически интереси). Предложението касаеше преработката и пласмента на отпадъчен алуминий главно под формата на стружки, който се използва в значителни количества в МК „ВМЗ". До заявяване на моето предложение алуминият се топеше с нафтова горелка, при която се изпаряваше (т. е. безвъзвратно се губеше) около 80% от материала за преработка. Температурата, развивана от нафтовата горелка беше около 800$^{o}$C,а температурата на топене на алуминия е малко по-ниска от 500$^{o}$C. В основата на предложението (фиг. 1) стоеше внедряване на технологична линия от: преса за обезмасляване и пакетиране на стружките, елеватор за транспорт към електроиндукционна пещ за претопяване с точност ±1$^{o}$C от желаната за постигане температура.




Фиг. 1. Технологичен процес и оборудване за преработка на отпадъчен алуминий: 1 – отпадъчен алуминий; 2 – преса за пакетиране и обезмасляване; 3 – съд за масло за вторично използване; 4 – елеватор; 5 – индукционна пещ; 6 – форми за отливане в блокчета; 7 – устройство за охлаждане; 8 – склад

При това положение загубите на материал се свеждаха практически до нула. По онова време претопеният алуминий се изнасяше по „второ направление" и приходите от него бяха в US долари. Ще оставя без коментар причините за отхвърляне на рационализационното предложение. Цялото предложено от мен оборудване беше българско производство (пресата беше плевенско производство, индукционната пещ беше на "Мехатроника" - Габрово), при което общата цена за капиталовложения беше около три пъти по-ниска в сравнение с вносното оборудване.

### 3. Заключение

Приключвайки тази статия, ще кажа следното: Физиката е интересна, макар и сложна и трудна дисциплина за изучаване. Независимо (а може би точно) поради това при добро усвояване на материала, тя дава необходимите предпоставки за добра професионална реализация на току – що завършилите образованието си студенти в различните предприятия. Не трябва да се забравя обаче, че наученото на студентската скамейка съвсем не е достатъчно за успешна кариера. Човек непрекъснато се развива и усъвършенства, като не само придобива нови знания, но и ги прилага в практика. Разбира се, всичко това е свързано с

индивидуалните възможности на човек, но трябва да се помни поговорката: „Едно е да знаеш, друго е да можеш, трето и четвърто – да го направиш”. Лично аз при решаване на даден проблем или при реализация на определена идея се придържам към принципа: „Наблюдение, експеримент, анализ на резултатите, вземане на решение”.

Всеизвестно е, че в момента разполагаме с мощни технически, технологични и компютърни системи, но винаги съм вярвал и съм поддържал идеята, че най – важният фактор във всяка една дейност и производство е човешкият. Физиката е многолика наука и ако човек внимателно се вглежда в заобикалящата го среда (и естествено има желание), винаги ще намери какво да създава, развива и усъвършенства.

**4. Литература**

1. home.cern/topics/large-hadron-collider
2. hubblesite.org/the_telescope/
3. www.ps.uci.edu/~superk/nuosc.html
4. Капица П. Л., “Експеримент, теория, практика”, изд. “Наука и изкуство”, София, 1977

**Контакти:**
Адрес: 4000, гр. Пловдив, ул. “Цанко Дюстабанов” № 25, ТУ-София, филиал Пловдив
e-mail: ivan_v52@yahoo.com

© International Scientific Conference on Engineering, Technologies and Systems
TECHSYS 2016, Technical University – Sofia, Plovdiv branch
26 – 28 May 2016, Plovdiv, Bulgaria

# SECTION 7 • СЕКЦИЯ 7

## INDUSTRIAL MANAGEMENT

## ИНДУСТРИАЛЕН МЕНИДЖМЪНТ

© International Scientific Conference on Engineering, Technologies and Systems
TECHSYS 2016, Technical University – Sofia, Plovdiv branch
26 – 28 May 2016, Plovdiv, Bulgaria

# PRINCIPLES AND INSTRUMENTS OF LEAN METHODOLOGY

TONI MIHOVA, VALENTINA NIKOLOVA - ALEXIEVA

**Abstract:***The report referred to the essence, principles and tools of LEAN methodology.Based on research conducted in fifty large Bulgarian enterprises gives the results on their willingness to make this management methodology in real practice.*

**Key words:***LEAN thinking Just in Time, 5S, TPL*

## 1. Introduction

Industrial globalization that has taken place in recent decades has forced manufacturers to produce high quality products in the most efficient manner.Striving to improve manufacturing operations has become a key issue for the industry.There was a need for Bulgarian producers to be flexible and competitive.Businesses put increasing pressure on production, companies seeking to improve their operational management through the implementation of new initiatives, methodologies and tools.One of them is LEAN methodology. Bulgarian companies have shown interest in it from the 70s.It is a set of tools and techniques developed by industrial giant "Toyota" from its suppliers, but also by its competitors in the automobile sector. Long since, the ideas that create left the borders of Japan and are widespread in the USA, Western Europe, China, India, Turkey and others.Adapted to Bulgarian reality, they are applicable and useful for the modern Bulgarian industry. Their logic, simplicity, precision and focus on continuous improvement help enterprises to deal with most of the production problems.

The aim of the report is revealing the essence of this management methodology, its principles and instruments, an indication of the results of the survey on attitudes to it and on this basis, formulate conclusions and recommendations for the use of LEAN philosophy.

## 2. Essence of the LEAN methodology

LEAN concept was born from the giants of thought Adam Smith, Frederick Taylor, Henry Ford and Edward Deming. It was put into practice by the creator of Toyota factories - Kiishiro Toyoda. Taiji Ono approach developed under the name TPS (Toyota Production System), subsequently became known as Lean.

### 2.1. Definitions

Will point out three definitions, we think most clearly reflect the essence of LEAN methodology. - LEAN is a management approach that directs and limits the cost of inputs only in achieving goals that create added value for the end customer. [1]

- Methodology that aims to build a production system reduces the time between order and delivery by eliminating surplus [2].

- Overall concept of corporate governance, including the knowledge and tools that organizations use to get rid of all activities and procedures to production processes, time-consuming, but not creating added value for the users of its products.The application of LEAN tools, especially in combination with this concept of Six Sigma, has a remarkable impact on the results of each organization adopted it as its philosophy. [3]

If we summarize, we could look LEAN methodology as an approach for effective business management and human resources.

### 2.2.Lean Principles

In their book “The Machine That Changed the World” Womack and Jones define 5 principles of Lean Manufacturing. These Lean Principles define the philosophy of LEAN.

These principles are:

1.Specify Value as perceived by the Customer 2.Identify the Value Stream

3.Make the Value Flow through the Value Stream. 4.Pull the Value from the Value Stream

5.Strive for Perfection.

These LEAN principles can be used to define the aim of any lean system which is to “Clearly specify value in order to line up all the activities for a specific product (family) along a value stream and

Copyright © 2016 by Technical University of Sofia, Plovdiv branch, Bulgaria ISSN Online: 2535-0048

make the value flow smoothly at the pull of the customer in pursuit of perfection" [4],[5]

### 2.2.1.The Principle of Value

The value changes over time and depends on the customer.In creating its operating and use resources that create value except "wasteful" - any activity that consumes resources but no added value.[5],[6].The customer is willing to pay for value, but not for "the wasteas".In the manufacture, as mentioned below most frequently observed kinds of surplus are known as 7 losses.Lean thinking allows us to find these losses and consequently reduce them.




***Fig.1.*** *LEAN Principles*

**Overproduction -** producing more than is possible to sell such products or for which there is no demand.In both cases we produce a product without being sure that there is a customer who wants it and will buy it.So we expend resources that are not redeemed. Overproduction is considered the largest of the seven losses.

**Movement -** unnecessary movement of materials, semi-finished products, people, tools, documents and more.Excess movement impedes the work, makes it more tiring, time consuming and so on.But the customer unwilling to pay for unnecessary movement.

**Transport-**cross-flows,imbricated or counterclaims flows in production, unnecessary transportation of products from one process to the next,unnecessary transportation to and from treatment, or something still not in place or notlocated near the site of its usage. The customer is unwilling to pay for unnecessary transportation.

**Downtimes -** big losses from freezing working capital in production due to staysand a periods of waiting - before and after processing operations between the departments and interoperational stocks,a man waiting to release the machine, machine waiting to be loaded by the operator, a station waits another stationto submit his work, workers wait for their boss to order what to do, production stays due to lack of materials or for repairing damaged machines. The customer does not want to pay for unnecessary downtime.[6]

**Inventory -** machines, tools and gadgets that rarely or never use, plus it positioned along the process that impede him and cluttering.The process can be clogged by the accumulation of the working areas of machinery and transport corridors waiting for treatment products, stopped batches unnecessary at present tools and devices or overcrowded wastage isolators.It does not bring value to the customer and he does not want to pay.[5]

**Overproduction -** in production may have excessive auxiliary, elaboration or corrective operations due to the thoughtlessness of the technology.Or the technology is not stabilized, leading to scrap and repeated operations.The customer does not want to pay that we have not yet learned to do things well from the first time.

**Wastage** – every product come out of production, which is of low quality and has remained unfit for use. Often wastage entails loss during processing and therefore reuse of materials.wastage is usually the result of the implementation of the remaining losses.

Production surpluses impede adaptability, increase permanent and direct costs, lower productivity and quality, create discomfort in the workplace. With more expensive and poor quality product can not achieve upward customer satisfaction. As a result, sharply worsened overall picture of production and commercial efficiency.

LEAN approach facilitates production and functional managers and professionals to focus on such decisions that lead to increased value added for the customer.

### 2.2.2.The Lean Principle of Value Stream

The value stream is the series of interrelated processes that produce the value; from raw material through to use. Just the steps that add the value, not those steps that add no value. Value adding and non-value adding steps make up every process. Within lean we are looking to remove or minimize those non-value adding steps.

We are looking at the value stream from the point of view of the product (or value), not looking at individual departments or even companies. This can be mapped using tools such as value stream mapping to create current and future state maps of the overall flow.

Think about the actual processes when you define the process stream; not in terms of your companies departments.[6]. Many lean implementations end up creating value streams where there are no "departments" as such but a pure flow through the company for the value itself.

**2.2.3.The Principle of Making Value Flow**

The ideal flow would be "one piece flow", however this is often not feasible due to machine setups and the need to flow multiple product streams through individual machines or cells. But what we are trying to achieve is the "flow" of products or value from one step to the next, each step being a value adding step. Never delay a value adding step by a non-value adding step, where possible have these done in parallel to the value adding one.This flow is achieved through a whole host of ideas and tools from Kanban, to small machines, through cell design and so on.




***Fig.2.*** *Wastes of Lean Manufacturing*

**2.2.4. Pull systems a Lean Principle**

One of the biggest wastes in any system is that of inventory; inventory hides all of the other problems in your system and causes so many other wastes. Inventory takes up space, it requires stacking, storing and transporting, it eats your capital!

The ideal system is one where the customer makes the order and you manufacture that product only when ordered. This is an ideal situation and many industries do not believe that they can achieve it. But lean is a never ending journey and with evolving technology and customer requirements it is possible to achieve it.

Consider a book; if you go into a book store there are shelves that are stacked high with thousands of books, some which will never be purchased and will either be sent to "bargain clearance outlets" or will be pulped. The reason being that the huge presses that produce these books have to be run for "economic" batch sizes. But with today's technology people no longer need the printed book, they can download the text to their kindle or laptop and read it on demand. For those that still want the feel of the printed word in their hands many bookstores now have machines which will print and bind your individual book while you wait! Single piece flow at the demand of the customer in an industry that would have laughed at you if you suggested it a few years ago!

Pull production rather than pushing production through a factory using scheduling can be achieved very simply in many cases. By using kanban systems and "supermarkets" it is possible to set up your production so that customer orders can be quickly satisfied when they are made and the parts either manufactured to order from standard components or drawn from a small buffer stock and then replenished in much the same way a super market will refill the shelves as customers buy product. In fact it is a super market that gave the idea for this method of production.

**2.2.4.Perfection**

If you achieve the first four steps you will have already prevented a huge amount of waste (seven wastes) from appearing within your processes. However; with the help and support of all of your employees you need to strive towards perfection; delivering exactly what the customer wants, when they want it at an acceptable (Minimum) price with zero waste.

Don't go out and benchmark your competitors and try to match them or beat them by a little; the aim is zero waste and the ability to deliver your customers value.

Involve every employee within your company in implementing lean tools such as Kaizen to drive continuous improvement of each and every aspect of your company. Lean is not just about improving a production cell; it also about improving every other process from order processing to invoicing and customer service.

**2.3. LEAN tools**

We will briefly examine some of the basic LEAN tools developed several decades by leading companies to achieve excellence in terms of efficiency, quality of organization.

**2.3.1.LEAN thinking**

LEAN thinking is a business methodology that aims to provide a new way to think about how to organize human activities to deliver more benefits to society and value to individuals while eliminating waste. The term lean thinking was coined by James P. Womack and Daniel T. Jonesto capture the essence of their in-depth study of Toyota's fabled Toyota Production System.

The aim of lean thinking is to create a lean enterprise, one that sustains growth by aligning customer satisfaction with employee satisfaction, and that offers innovative products or services profitably while minimizing unnecessary over-costs to customers, suppliers and the environment. The basic insight of lean thinking is that if you train every person to identify wasted time and effort in

their own job and to better work together to improve processes by eliminating such waste, the resulting enterprise will deliver more value at less expense while developing every employee's confidence, competence and ability to work with others.

**2.3.2.Just In Time**

"Just in time" is to produce only what is needed in the quantity you need and when the need of the customer. JIT is a symbol of: short production cycle; minimized stocks of materials and unfinished production; balancedproduction load; minimum transportation, higher labor productivity and timely delivery is simply the result of all this.Summarized JIT works to reduce most of the groups of "surplus" (identified through the creation of VSM).

So specify those goals can be achieved only if used well-established methodology. JIT methodology is based on several instruments here we mention some of them.

One of the main tools in the JIT is the creation of a suitable processing scheme (Layout).

**2.3.3. „5 S"**

In brief „5 S" is a system in which through various practical methods applied by a team effort, the people maintenance neat and clean workplaces, workstations and departments.

Good layout in the workshop itself is a prerequisite for efficient processes as it saves time for operators.On the other hand it is also a barometer of quality: in how workers relate to instruments used, how maintain the purity of their workplace can judge their attitude towards work itself and to quality.In summary "5 S" gives an overall assessment of the commitment of employees and management to the company and its condition.

Five steps are: "Sort" "Systematic arrangement"; "Shining purity; "Standardisation"; "Self-discipline".The steps in 5S are built logically and consistently.The proper study of the system leads to so desired goals - clean and stackedworkplaces, convenient and pleasant working environment.

**2.3.4. TPM**

TPM is a system created and developed in Japan for several decades.With an initial focus on the production and machines, it evolved into a program covering almost all activities in the organization.TPM aims to:

creating a corporate culture that maximizes the efficiency of the production system;

- practical organization of production to prevent losses before they emerged throughout the life cycle of the production system in order to achieve zero accidents, zero defects and zero failures;

-full involvement of all departments of the company including document production, maintenance, research and developed marketing, etc;

- engaging all employees from top management to machine operators;

- achieving zero losses through activities "overlapping small teams."

**2.3.5.Kaizen**

Kaizen – a Japanese word that literally translated means a change for the "better".The most common perception of the word is related to continuous improvement.Kaizen ensure that we continue to develop and improve.In most plant managers think that if you put a box in which employees put written proposals from them, it will begin to fill.Of course in business practice there are different situations and many companies tried this approach are not convinced that it works.When it undertake an effective system for generating Kaizen must first consider what causes people not to put proposals in the box, namely:

1. The level of the majority of employees in our factories is so low that they can not work up the guts to take pen and paper and write a proposal.

2. They are afraid lest someone scolded them for what they wrote or simply laughs onthem.

3. Even if there is anyone who dares to write something, the process of giving feedback is so long that one forgets what he wrote or it is no longer valid.

4. The senior and middle level management are not involved in the process.

How to eliminate causes and to create a working system?For this purpose it is necessary to build an entirely new structure of the organization in which production is divided into teams of about 10 people and each team is responsible unless his leader and his coach.All representatives of the administration become coaches and give their direct contribution to production.It is they who encourage and motivate operators to participate in the process of continuous improvement - Kaizen.In so created structure the language with the most Kaizen and his coach have a chance to be the best after a fair competition with clear criteria.Through this approach, we encourage the competitive spirit in people, but not greedy, pechelbarski sense, but as a desire to outdo the other [2].

**3. Results of the survey**

The study was conducted in 50 large companies in Bulgaria on knowledge of the methodology LEAN, attitudes about the use and effects of adopting some of LEAN techniques and instruments. The methods we used are questionnaires and interviews with managers of

enterprises. The survey was conducted between October 2015 - February 2016.

What are the concrete results concerning the examination of LEAN practices?

80% of participants indicated in questionnaires that are highly aware of the essence, principles and tools of LEAN methodology. The main sources of information mentioned by them are seminars, conferences and various forms of training.

15% of them know to a lesser extent managerial approach, 3% said they did not know and 2 percent did not respond.

In response to the second question related to attitudes about using some of the LEAN principles and tools, 70% think they are not adequately prepared.The reasons most often found answers: "Not applicable to us," "We do not have the necessary financial resources" "I will meet resistance from the workers," "Too radical change will be," "I do not think it is necessary at this stage."

And only 10% are reflected in polls that have implemented some of LEAN tools.

Interesting is the fact that they are companies with foreign participation.From interviews with them about the results of LEAN practices, we can systematize the following benefits:

1. After the implementation of Just in Time in four enterprisesis reported:
- a significant reduction in unnecessary movements and balance of work which leads to increased productivity;
- terminated a large number of cross back and forth movements of raw materials and blanks;
- reduced volume of work in progress blocking valuable financial resources;
-clarity of material flow in production.
2. Following the introduction of KANBAN system in 2 enterprises have improved significantly: - communication and coordination between the units "Planning" - "Logistics" - "Production";
- places for stocking of raw materials;
- operator efficiency - largely in order and vision of stocks overcome chronic chaos and scratching materials;
- machine downtime due to organizational problems with the materials.
3. Following the introduction of the “5S” in 4 companies:
- a system layout for all instruments;
- the working environment is visualized;
- remove unnecessary items.
The conclusions from the survey include:

1. The highest percentage of respondents are familiar with the essence of LEAN methodology, its tools and principles.
2. Attitudes of the majority of study participants were skeptical about turning LEAN approach in actual practice.
3. A relatively small part implemented some major LEAN tools,actually. The results have led to increased productivity and efficiency of the activities of these companies.

**4.Conclusion**

The report made a attempt to mark some important aspects of the LEAN philosophy for effective business management.The survey results show that there is still a small part of Bulgarian companies, which mainly those with foreign participation reap the benefits at issue management methodology.

Requirements for enhancing the competitiveness of Bulgarian enterprises make it necessary to increase the efficiency of their operations. In this connection it is necessary to use the opportunities offered by LEAN methodology.

**REFERENCES**


1. Lean THINKING, http://lean.bg/wcm/lean-thinking/
2. Principles and tools in the Lean methodology, teaching materials of "LEAN Bulgaria" Ltd, 2016
3. Jorgova, Julia A., Framework for applications of Lean tools for visualization and analysis in the services, Scientific University of Rousse - 2011, Volume 50, Series 5.1,Lean Thinking | Lean
4. Principles,http://leanmanufacturingtools.org/
5. Yordanova-Dinova, S. Georgieva, Study the economic profitability of milk processing companies in the country, ISSN 1314 -1880, (www.hst.bg/bulgaria/cnference.htm).
6. Yordanova-Dinova, P.,S. Georgieva, Analysis of the effectiveness inthe "milk processing" companies (analysis of turnover of current assets) Scientific papers, Series B " Volume XVII, Plovdiv, 2015, pp. 261-265.



**Author’s contacts:**
Assoc.prof. Toni Mihova, Ph.D.
Technical University – Sofia, branch of Plovdiv
E-mail: expert2009@abv.bg

Assoc.prof.Valentina Nikolova-Alexieva, Ph.D.
University of food technologies,
E-mail: valentina_nikolova@abv.bg

© International Scientific Conference on Engineering, Technologies and Systems
TECHSYS 2016, Technical University – Sofia, Plovdiv branch
26 – 28 May 2016, Plovdiv, Bulgaria

# MANAGEMENT OF THE MOTIVATION PROCESS IN ENTERPRISES

MINA ANGELOVA

**Abstract:** *The functioning of Bulgarian industry in crisis conditions has a negative influence over human resources 'state in enterprises. A subject of this article is the pre-conditions for achieving a development through ensuring a competitive advantage of human factor in order to manage the motivation process. The survey is based upon own questionnaire through the personnel in export enterprises located in Bulgaria, Plovdiv area. The results of the empirical research draw a general conclusion that the formation, ratification and development of the employees in enterprises ought to be a strategic factor for industrial growth.*

**Key words:** *motivation, demotivation, management, human resources, enterprise*

## 1. Introduction

The dynamic changing economic environment demands from the enterprises to provide more flexibility and ability to change according to the new conditions of outside environment. Together with the challenges by the variables influencing enterprise's activity (economic, political, scientific, technical, social etc.) the management must direct its attention to the employee's problems, the leading one of which is the motivation process.

The enterprises counter the everyday necessity to fight for surviving in rapidly changing and non-secure environment and this process becomes stronger in continuing economic crisis. The research of factors and reasons for a human resource demotivation in companies based in Bulgaria is a question of current interest because of the high level of insecurity of their employee which under certain conditions blocks the thinking, creates a feeling for helplessness. The enterprise's managers are faced with serious challenges in the context of competitive power which cause the necessity of unstoppable organizational changes, decreasing the possibility of life-long hire, individualizing the connection "employee-employer", etc.

The enterprises aim to optimize activities, decrease expenses and broaden markets which involve risky and undefined activities. As a result of the economic recession a serious reduction of the production along the last years is observed, typical for most of the enterprises. This worsens the production processes and their organization. Directly affected are the human resources in enterprises, leading to systematically decrease of their motivation. The high level of non-satisfied human needs in complicated crisis periods explains their increased tension. In practice the existing tension leads to demotivation in labor process.

*An object* of this article is the specialists in Machine building enterprises.

*A subject* of this paper is an investigation of motivation real condition of specialists and opportunities to overcome the existing demotivation process aiming to provide a positive change in the enterprises.

*The research thesis* in the article is that the investigating and overcoming specialists' demotivation is a basic condition for managing the motivation process and consequently providing an enterprises' competitiveness through the human factor.

## 2. Methodical conditions

In scientific aspect the currentness of the theme originates from observed and established serious problems in the society, business and public administration, which is proved by researches in the field of motivation problems. The researched literature and existing methods force the attention in the following statement. The motivation aspect of human resource management has a various theoretic and methodical development. The motivation management includes many principles, approaches and instruments. However they give just a partial and thus insufficient answer of a basic question for the motivation: what presents, how to recognize and how to overcome the demotivation condition in the enterprises. Based on the literature research there

Copyright © 2016 by Technical University of Sofia, Plovdiv branch, Bulgaria ISSN Online: 2535-0048

are arguments that the demotivation problems are marked but there is not enough scientific development which shows a "niche" for guidance of explorative efforts.

### 2.1. Preliminary considerations

The methodic for investigating and measuring the demotivation level is based on the following principles:

-Giving a priority of a new component in the labor environment which the author names a *demotivation model* with its specific characteristics, demotivation factors, operative processes.

-The demotivation (whatever is its condition and level in enterprises) has to do with the people in a concrete enterprise and in this context it is dependent on multiple characteristics of the enterprise, the industrial sector in which it is located, the politics and mechanisms orientated to managing the human resources (and more precisely establishing the gaps in them), its condition and functioning.

-Perceiving the motivation (resp. demotivation) problematic as a significantly important for the whole human resource management.

In the job process it is necessary to be marked the intersection between company's goals and interests and those of every specialist.

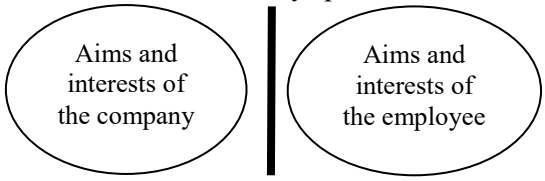



**Fig. 1.** *Goals of the company and the separate employee*

The section between both circles shows what extent the aims of one employee overlap with the company's aims. This section is dynamic in time and demands consequent work and investigation in the company. Both circles could not completely pass with each other but when they touch or separate themselves there is a demotivation problem.

### 2.2. Investigation methods

The investigation is based upon the process method. It's made a survey with own questionnaire which includes a demotivation profile of specialists and a demotivation model. The results are drawn with statistic software SPSS 19.0 v. It's used the method of expert evaluation made by the author and interviews with enterprise's managers.

## 3. Empirical research of demotivation

For the purposes of the research it is important the evaluation of mechanical engineering sector in Plovdiv area, Bulgaria. In these enterprises are observed new foreign and local investments, technical and material updates, reconstructions etc. which is an evidence for an existing potential for development in the sector. According to data of National statistical institute [6] the production of industrial enterprises in branch "Machine building and equipment with a general and specific purpose" for 2014 is 2 406 million levs and there is an increase of 4,2 million levs compared with 2013. The sector develops due to a number of incentives and the support by the Law for investment encouragement, the lowest expenses for acquisition of state and municipal lands in Bulgaria, an exemption from taxes for changing the land status, a financing from the European funds and a financial scheme for a grant up to 10 percent of the expenses of the investment project (50% for scientific researches and development).

On estimates of MIET the sector's development outlines a potential for production increasing and necessities of more employees in the engineering sector.



**Fig. 2.** *Index of localization of GDP by sectors (The Machine building for south central region is 1.23)*

In order to manage successfully an object it is necessary to know its characteristics [1]. This is valid as well as for the demotivation related research. In this aspect the practical study starts with expert's identification on their basic specifications.

In this research the employees belong only to the category "specialists". In the investigated enterprises there are 486 specialists, 219 of which participated in the survey. That is equal to 45.06% of all and meets the requirements for representativeness and reliability of the results.




**Fig. 3.** *Education of specialists*

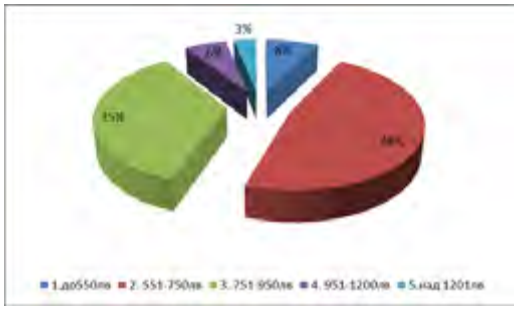


**Fig.4.** *Basic salary*

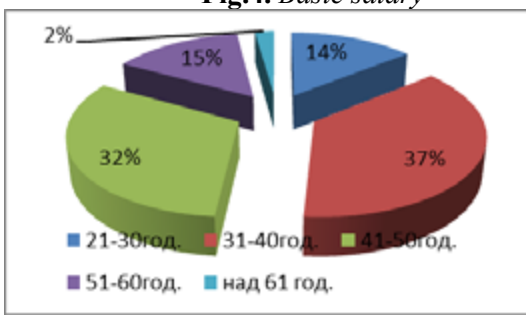



**Fig.5.** *Age of specialists*

Most specialists are with university education – a bachelor degree 58% and master degree 28%. The higher level of education is the more complex employee's necessities are. The managers must force various motivation stimuli according to the personal expectations of every worker. The basic salary of 48% of specialists in enterprises is less than the average in Bulgaria that is a strong demotivating factor when is not connected with an adequate bonus system. Most specialists are young people from 31 to 40 years old. They have more personal expenses than the older workers and more expectations in working environment. They are flexible and have the ability to change rapidly their working place. This is a factor which has to be highlighted by the owners and senior managers.

The demotivation analysis indicates that the specialists experience the demotivating influence significantly. The answers from the questionnaire prove non-optimized stabilizing factors in the enterprises and a missing coordinated influence from the managers through motivating factors.

### 3.1. Developing a demotivation model

The idea for developing a demotivation model is to create a new element in the working environment, which has to be taken into consideration by conducting of employee's surveys, attestations and analysis of the labor environment. The basic results of the survey are included in this model and it can be used in future analysis. On the next page in figure 6 is presented the demotivation model which is a result from the research. (See Fig. 6.)

## 4. Conclusion

Providing competitive advantages of enterprises through the human factor and its transformation into a "human capital" is connected with the development of policies and management of the motivation process. The human capital formation is based on a targeted investment in the employees, which involves a knowledge enrichment, improved abilities and competencies in combination with increasing or high level motivation. These activities seek to achieve a new and higher quality of the human resources, which leads to increasing the labor productivity. The presence of demotivation is a restrictive factor for the enterprises but its timely revealing and the direction of urgent measures for its overcoming, combined with remotivation, aiming to a high labor motivation, are useful turning points for future work. These are prerequisites for a competitive edge of the human resources and therefore for an industrial growth of the enterprises. A profound "observation" by the managers and the specialists in human resources department should be made so that the motivation policy is properly implemented.

## REFERENCES

1. Herzberg, F. (1968) *One more time: how do you motivate employees?* Harvard Business Review, 46 (1): pp. 53–62.
2. Iravani, M. *Demotivating factors influencing rubber production workers*, Management science letters available on www.growingscience.com/ms1
3. Kryukunenko, D. (2007) *Development of staff demotivation system as an element of motivation management at an enterprise*; Donetsk National Technical University, Ukraine, Volume 132, Issue 6, Pages 212-217
4. McCleland, D. (1978) *Managing motivation to expand human freedom*, American Psychologist, 33(3) pp.201-210
5. Smithers G., Walker, D. (2000) *The effect of the workplace on motivation and demotivation of construction professionals*, Construction Management & Economics, vol. 18, issue 7, pages 833-841
6. National statistical institute available on http://www.nsi.bg/en

Authors' contacts:
Address: 21 Port Artur str, Plovdiv, Bulgaria
Phone: +359 887 461 272
E-mail: mina.marinova@abv.bg

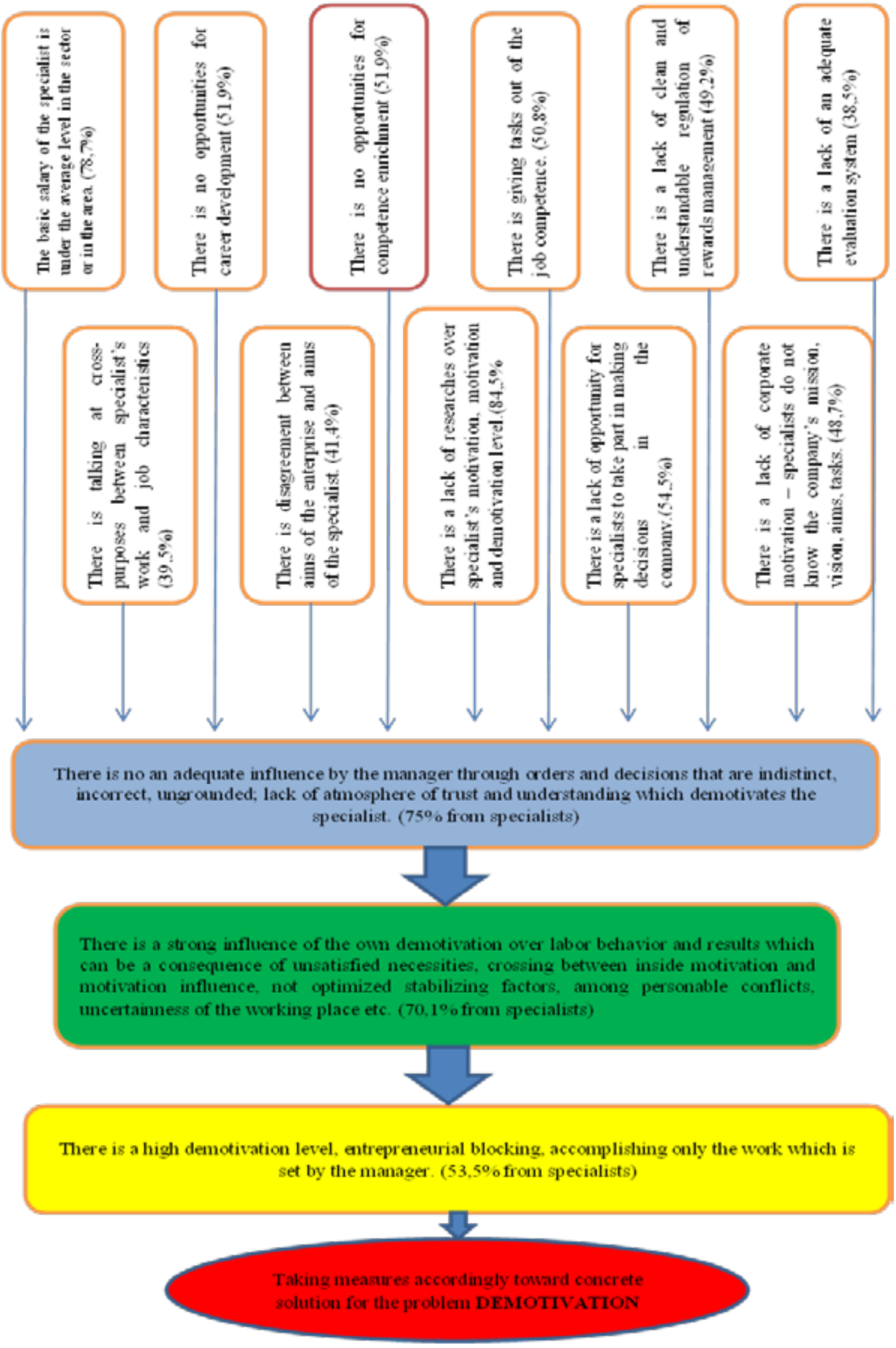



**Fig. 6**. *A demotivation model*

© International Scientific Conference on Engineering, Technologies and Systems
TECHSYS 2016, Technical University – Sofia, Plovdiv branch
26 – 28 May 2016, Plovdiv, Bulgaria

# CAUSES, PREVENTION AND CORRECTION OF PROJECT FAILURES AND BUDGET OVERRUNS

THOMAS-MICHAEL MOSER

**Abstract:** *Many large ICT projects do not complete in quality, time and budget or fail completely. The influence of greater efforts and diminishing results as economic rule is highlighted. The necessity of firm negotiation procedures between the contract parties is described. Project methodologies are discussed in their relevance and contribution to project success in large and complex environments. A pragmatic flexible portfolio of methods tailored to the specific project scenario seems advisable. It is shown why social communication and clear contractual commitments must be fully integrated into the engineering process.*

**Key words:** *Project management methodologies, Information Communication Technologies, Software engineering, Social interactions, Project failures, Risk management, Organizational turnarounds, Negotiation procedures and contracts, Portfolio management, Agile work, HERMES, V-model, SCRUM, Team work*

## 1. The Situation

The situation of the Information Communication Technology (ICT) markets is characterized by increased complexity and bigger capital requirements than ever before. The failure rate of ICT projects is high. A study of 5,400 large ICT projects shows:

17% percent fail to such an extent that they pose a risk to the entity to get out of business.

45% cost more than planned; 56% do not meet full specifications and are of lower value than projected. About 7% are not ready in time [1].

The causes may appear as resulting only from reasons of economics and management. But, the causes symbolize an underlying web of interdependencies reaching above the common scope of monetary and organizational considerations [2]. They link with social interaction issues, powers of groups and roles, and political factors.

## 2. Purpose of the contribution

This paper should provide a short insight into the causes of project failures, how to prevent them, and what corrective measures to apply. The methodology follows a scientific approach that arguments and conclusions must be consistent, repeatable and measurable. Out of scope are deep reaching explorations because of the summary exposition of the contribution.

## 3. Greater efforts and diminishing results

There seems to be a paradox that greater efforts do not result in the same expected amount of greater results. One can see that projects fail at a considerable rate even when supplied with more money or resources. This seems to be a contradiction.

The "laws" of microeconomics supply a possible answer. Economics and management do not represent a true science like physics and mathematics; hence, they must be evaluated by other means as by tests, controls and audits. Therefore, this "law" is being described by a socio-economic scientific approach. "Economics is the science which studies human behavior as a relationship between given ends and scarce means which have alternative uses"[3].

The "greater efforts and diminishing results" rule is according to Stigler "As equal increments of one input are added; the inputs of other productive services being held, constant, beyond a certain point the resulting increments of product will decrease, i.e., the marginal product will diminish" [4].

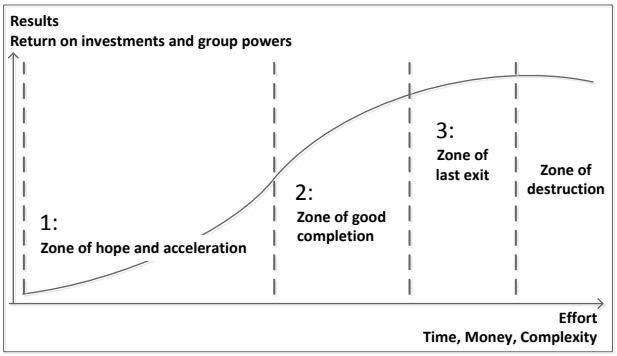



Fig. 1 Diminishing returns of results

The x-axis (right) shows the effort under the course of time, money (investments), and complexity of

Copyright © 2016 by Technical University of Sofia, Plovdiv branch, Bulgaria ISSN Online: 2535-0048

interrelated matters of the project. The y-axis (up) demonstrates the outcome as of project results. The results show four zones:

Zone 1 represents “hope and acceleration”. The project kick-off took place. The team is full of spirits. During short time frames results are being achieved by an accelerating pace. Administrative overhead is at a minimum or ignored to a large extent.

Zone 2 starts with the “turning point”. More and more efforts are required to get increasing results. It may present leads to the fulfillment of project results to a large extent and gives time for consideration to finish the project under a positive close. This demands that there is acceptance that project results may be fulfilled to only 80% or similar, but are working after deployment (fit for use).

Zone 3 is described as the opportunity of the “last exit”. It culminates to the saturation point of a complete project fulfillment. Compared to the preceding two zones, only small additional increments of results are achievable compared to the efforts of time and money by increasing complexity. Under managerial human jargon there is the talk of “better more 80% results than costly striving after the one 100% illusion”. The zone 3 represents the last chance of the exit out of the project before decline to retirement/death. The exit shows four principal choices:

If agreed by the sponsors and stakeholders of the project, a reduced set of features will conclude the project, working if not totally “100% perfect”, but being operational.

The project will be terminated to be migrated to a new kick-off with lessons learned to get things better and faster.

The project will be integrated/migrated to a similar environment of specifications and scope.

The project will be closed as not being successful. All effort commitments must be written off. The motto prevails: "Better an end with horror than a horror without end [5]".

Zone 4 is the area behind the optimum. All efforts are increasingly greater than the results being anticipated. This leads to retirement of the project by orderly closure or sudden death of activities and funding. The longer this phase lasts, the more results will be destroyed. Therefore, zone 4 can be described as “zone of destruction”.

### 4. Negotiation procedures to handle diminishing results and project failures

There exist inherent factors combined with efforts to achieve results which are persistent and must be considered.

The feeling and experience is widespread that commonly applied methods cannot find an answer how to better master failures and collapses of large and complex undertakings. There is the famous widespread quote by Albert Einstein: You can never solve a problem on the level on which it was created. “Probleme kann man niemals mit derselben Denkweise lösen, durch die sie entstanden sind“ [6].

Many project management engineering methods base on the classic opinion of the hierarchical organizational model. This was driven to perfection by the German constructional context of the “Aufbau- und Ablauforganisation”, meaning defining the structural set-up (Aufbau) and the process flows (Ablauf) between the units within the organization [7].

The organization followed a strict top-down methodology. This model worked quite well during war times and the progressive build of economies after destruction. Human resources had been considered as productive factors (human “capital”, de facto an investment opportunity), but not with their own personal factors as creativity and motivational participation [8].

We are in the evolution of the information age. Information technology and communication by the internet span the whole globe; reaching from rich to poor, from small to big. The classic central organizational formula of governing from the top to all dispersed units on a global scale does not find an economic and manageable answer to rising complexity and fragmentation by inflicting different systems and cultures.

A different methodology compared to classic organizational concepts must be considered to overcome project failures and budget overruns [9].

On the stipulation that new methods must be applied, this provokes the question how to go (Что делать?) [10]. It points to a decision on whether there should be an “elite” decision to implement new organizational structures and procedures; or should this better follow a spontaneous “open” organizational pattern [11].

The necessary change in methodology presents those two alternatives, as an elite driven project or an open society (community) approach.

It would be too easy to make a strict decision for the one way or another. Mostly, one does not have green fields to start entirely from scratch with activities.

Large complex project endeavors do rarely grow from the sudden. They are based in large systems environments with traits in corporate history, where culture and interest groups of sometimes diverging goals, strategies, and tactics exist. This can be resolved by a negotiating (bargaining) process between the interest groups and their stakeholders [12].

This process aims to define the methods to handle diminishing results and projects failures. It is characterized by the following five general phases:

Phase 1: Prenegotiation: This important first phase sets the conditional framework and prepares management about vision, mission, strategies, and the tactical operational measures necessary. The result is either to proceed with opening the project, or finish the preliminary undertakings as not being feasible for going into realization.

Phase 2: Negotiators: On approval that the project will be undertaken, the negotiators will be named. They will represent the major interest groups and might form the steering committee later. The negotiators typically come from sides of the general management or others as sponsors, technical bodies, the operations department, from finance, legal and others being involved. Normally, a team approach will be followed to arrive at constructive results.

Phase 3: Negotiations: After having named the negotiators and established the body for work, the negotiation process will start. Normally, the process opens with demands from the operations department bringing a comprehensive (wish) list of requirements on the desk. This list might be extreme in demands and constitutes the first negotiation topic to start with. This might be countered by the technical department, finance, legal and motions of the sponsor. The counter offer will be very low in order to reduce the requirements list and keep spending and risks at a minimum.

Both sides will prioritize their demands and reduce them to a level that an agreement will be possible. Once, they have arrived at an agreement, an informal preliminary contract will be made. If the parties cannot reach an agreement, the situation might be at deadlock, which is up for decision by management or goes into a new round for negotiations; possibly by an appointed conciliator and/or exchange of named negotiators. The negotiation can be put on hold or break down in case.

Phase 4: Contract: Once, the informal preliminary contract has been made, the written final binding contract will be worked out. It will be sent to management and sponsor for review, ratification, and approval. It contains the purpose of the project, vision, mission and project charter; the financing, quality management; functions and roles involved, risk management and controlling principles. Attached, there will be the operational project plan with work break-down structure, timeline, milestones and controlling/updating provisions and naming of the steering committee if necessary. After signature by management, the project goes live. One of the leading standards to follow is the "PMBOK® Guide & Standards" [13], giving a suitable project management body of knowledge.

Phase 5: Project Implementation: After ratification and approval, the project will be implemented as agreed in the project plan. If there are discrepancies during execution, they will be rated whether there are new features which will be handled by change management; or severe disputes which need handling by issue management.

Those five phases are mandatory for any project situation whether new, restart, migration or turnaround. Most project failures and budget overruns have their origins in missed or vague results of the negotiation process. The major roots and causes result from:

Poor or no prenegotiations have been executed. Lacking vision and managerial commitment provoke a failing project from the beginnings.

The panel of negotiators show no even representation of interests, or have important stakeholders missing. One sided contract parties may pressure decisions which carry high risks for implementation success.

The negotiations will not meet the purpose of mutual benefits. Either the operational side poses requirements which are unrealistic or vague. Or the technical side blocks changes in order not getting bothered. Finally, finance or legal might construct blocking factors without fully knowing neither technical requirements nor understanding necessities by operations.

The final contract has not been carefully worked out. Especially, the points of escalation management, risk management and sanctions must be clearly written down and agreed upon by all parties involved. Often, the project plan has not passed quality control in reference to standards and best practices incorporated. In order to "reduce" cost, the budget might be too low and does not secure enough risk coverage provisions. This is one of the major factors for budget overruns and delays or the complete project break down.

After substantial failures at the Department for Works and Pensions with huge losses of around £663m [14] and other deficiencies, the UK government has enforced a guidance which permits a valuable orientation on how to plan, evaluate and control spending [15].

## 5. Methods and feasibilities

The above framework of negotiations, phases and work results showed the foundation on which successful projects must be started, modified, repaired or finished.

After establishment of this framework foundation, the operational deployment of methods and metrics can be established. Often, methodology will be put in front of all activities instead of the fundamentals for adequate negotiations to enable the participating units to achieve project success [16]. Without a stable organizational framework - integrating

creative and motivated people - methodologies have got no suitable foundation.

First, an agreement (contract) must be made, and then the methodology can come into effect. Methodology is like a tool, enabling a set project situation to run most efficiently.

The methodology should secure that the work is conducted not ad-hoc driven; but planned, consistent and repeatable. Several methodologies serve this purpose.

It is not in the scope of this paper to discuss the pros and cons of several methodologies in detail; but to mention the importance on how to handle methodologies under operational deployment requirements. There is no "perfect" methodology as "one size fits all" under common jargon. Methods depend on the environment where they will have to be applied to. Economics and management can be explained from a social perspective; they represent a social science. Hence, methods in social environments are subordinated under the value judgments of parties involved, i.e. human evaluations, beliefs and trends in industry. Therefore, no "real" or "true" methodology will exist in this context.

One can only find a pragmatic answer from experience. There is the dilemma between choices and personal goals and values of decision makers, and demands by organizational bodies. When large and complex project situations are expected to suffer from severe failures or are in danger to break down, it may be best to implement a portfolio of methodologies.

The decision for only one - "the one" - methodology carries high risks of being wrong as the decision is based on personal judgments of a decision body. It seems advisable to run a portfolio approach. A portfolio is a collection of objects of a certain commonly defined type. Portfolio management has been successfully applied to the management of ICT project departments [17].

Hence, in many cases there cannot be a single-sided methodology seem appropriate. One should build a portfolio of methodologies to prevent or repair problematic project situation of failures and budget overruns.

The common project methodologies can be clustered into traditional, agile and impulse driven. The following summary list of clusters of methodologies has been derived from large project exposure over 25 years by the author. It does neither constitute a binding list nor complete overview, attributed to the requirements of an aggregated view in this paper. The focus applies to major methodologies used in software engineering methods.

Traditional: The beginnings are with the waterfall model, a methodology to have a top-down sequential flow with fall back options in case of failures. This may be regarded as old-fashioned today, but is still suitable for clearly defined projects over a longer timeline. Many variations exist as the spiral model among others [18].

The V-model [19], (V means "**V**orgehensmodell", translated to "procedural methodology") has its origin in large German public projects, designed after the successful economic build-up period, dating back to 1992. Like the analogy to a V-letter shape it combines requirements analysis (left V-letter side with tests against the right opposite V-letter horizontal side on user acceptance and similar below). Each development step is mirrored by symmetrical verification and validation. The V-model has got many variations which have been successfully transferred to industry, especially in the tools and machinery industry, also to the premium car manufacturers and suppliers. It became the reference model to leading German technology export oriented conglomerates. The latest version of the V-model has advanced to the "XT" suffix which means "eXtreme Tailoring."

The Swiss HERMES methodology [20] is developed and maintained by Swiss government authorities. It derives best practices as there are from the German V-model and CMMI® [21] and others with the focus on work flow perfection and extensive document management under strict auditing requirements. HERMES shows perfection to detail and seems applicable to complex projects as in e-government and big data environments.

Agile: The agile method is an answer to the common dilemma that undertakings seem to take too long and errors get detected too late. A solution was provided to cut ways short and get better results. The basics of agile are to leave the sequential process like in the classic waterfall methodology and intensify communication and coordination. Teams work closely together, ideally all people are in one large room. Developers and testers collaborate on the workplace together on the screen and in group meetings. Builds are done in short intervals and may contain many parallel development branches merged [22]. One method is Extreme Programming (XP) which puts teamwork and communication as top priority. The industry uses the methodology of Simultaneous Engineering [23] (or Concurrent Engineering in American English usage). The traditional separation of the construction process and the following phases of production planning is broken. Both phases are overlapping to shorten the cycles. Again, teamwork and communication are the core components in parallel and integrated workflows. It is frequently used in mechatronics which demand the integration of mechanics, electronics, electric works and software engineering.

Impulse driven: The end user (customer) is in the focus. The "end user" is understood internally as product owner as in production, marketing, sales, finance and others.

The "user stories" are in plain common language. They build with their requirements scenarios the foundation from which the development process starts. There will be short development cycles (Sprints) of only several weeks or months, or even shorter. Constant interactions between the end user and the development teams are monitored and coordinated so that the results can be better adapted to vague, changing and volatile requirements. Presently, the SCRUM framework [24] is used to a large extent under those circumstances.

## 6. Conclusions

The findings show that large and complex projects fail at a considerable rate. The financial losses can be very high and may endanger companies or institutions.

It seems that the causes are routed less in the wrong application of methodologies or tools. Social communication, a defined negotiation process and clear contracts are at least equally important.

One might conclude that a good team with committed management but having only average methodologies and tools might reach more than an inferior team with diverging stakeholder groups and uncommitted management even when supplied with best tools and latest methodologies.

Common practice still emphasizes the formal side of methodologies and show strong exposure to find the right tools and frameworks. Nevertheless, this attitude seems not to warrant the road to success as cases of large failed projects demonstrate.

Due to overall rapid changes in requirements, shorter time-to-market cycles and increasing process complexities, a pragmatic flexible portfolio of methods tailored to the specific situation seems advisable.

Social interactions and contractual firmness, with the full commitment of all parties involved, must be regarded as equal parts and have to be fully integrated with the formal engineering process.

## REFERENCES


1. Michael Bloch, Sven Blumberg, Jürgen Laartz (2012). *Delivering large-scale IT projects on time, on budget, and on value*. Research paper. McKinsey & Company. New York.
2. Natalie Disque (2016). *Project Management Collection: Failed IT Project Business Cases, A Career Guide to Lessons Learned: Boxset of Business Cases from IT, Government and Healthcare Industries*. CreateSpace. North Charleston.
3. Lionel Charles Robbins, Baron Robbins (1932). *An Essay on the Nature and Significance of Economic Science.* Macmillan. London.
4. George J. Stigler (1987). *The Theory of Price.* Macmillan. New York.
5. Ian Slater (1987). *Orwell: The road to airstrip one.* Second Edition. P. 216. McGill-Queen's University Press. Montreal & Kingston, London, Ithaca.
6. Albert Einstein commonly quoted; nevertheless represents an unsourced attribution.
7. Erich Gutenberg (2008). *Theorie der Unternehmung.* Gabler. Wiesbaden.
   Erich Gutenberg (2000). *Theory of the firm.* Springer. Berlin.
8. Alan G. Robinson, Dean M. Schroeder (2014). *The Idea-Driven Organization: Unlocking the Power in Bottom-Up.* Ideas Berrett-Koehler Publishers. Oakland.
9. Warren Parry (2015). *Big Change, Best Path: Successfully Managing Organizational Change with Wisdom, Analytics and Insight.* Kogan Page. London, Philadelphia.
10. Николай Гаврилович Чернышевский (1975). *Что делать?* Серия "Литературные памятники" Л. Наука. Moscow.
11. Karl R. Popper (author), Alan Ryan (introduction), E.H. Gombrich, contributor (2013*). The Open Society and Its Enemies.* Princeton University Press. Princeton.
12. Carrie J Menkel-Meadow, Andrea Kupfer Schneider, Lela Porter Love (2014). *Negotiation: Processes for Problem Solving (Aspen Casebook)* 2nd Edition. Aspen Publishers. New York.
13. Project Management Institute (2015). *A guide to the Project Management Body of Knowledge (PMBOK Guide)*. 5th edition. Project Management Institute (PMI). Newton Square, PA.
14. Charlotte Jee (2014). *HM Treasury admits to potential £663m of Universal Credit IT cost write-off.* COMPUTERWOLDUK. London.
15. HM Treasury (2015). *Guidance. Early financial cost estimates of infrastructure programmes and projects and the treatment of uncertainty and risk.* HM Treasury, Infra-structure UK. London.
16. Robert K. Wysocki (2013). *Effective Project Management: Traditional, Agile, Extreme (2013).* 7th edition. Wiley. New York.
17. F. Warren McFarlan (1981). *Portfolio Approach to Information Systems*. Harvard Business Review. Harvard Business Publishing. Watertown, Massachusetts.

18. Richard Hall Thayer (Author), Merlin Dorfman (Author), Steve Tockey (Foreword, Contributor), Friedrich L. Bauer (Foreword), Norma E Fenton (Contributor), & 3 more (2013). *SOFTWARE ENGINEERING ESSENTIALS, Volume III: The Engineering Fundamentals (Volume 3); 4th edition*. Software Management Training Press. Carmichael, California.
19. Der Beauftragte der Bundesregierung für Informationstechnik (BIT) 2016. *V-Modell XT®.* Bundesministerium des Innern (BMI). Berlin.
20. Schweizerische Eidgenossenschaft, Bundesverwaltung (2016). Informationssteuerungs-organ des Bundes ISB. *Projektmanagement-Methode HERMES.* Schweizerische Eid-genossenschaft. Bern.
21. CMMI® Institute (2016). *CMMI® for Development (CMMI-DEV), Version 1.3*. CMII Institute. Pittsburgh, PA, US.
22. Robert C. Martin (2013). *Agile Software Development, Principles, Patterns, and Practices*. Pearson Education Limited. Harlow, United Kingdom.
23. Gerhard Pahl, W. Beitz, Jörg Feldhusen, Karl-Heinrich Grote (2007). *Engineering Design: A Systematic Approach 3rd ed.* Springer. Heidelberg.
24. Kenneth S. Rubin (2012). *Essential Scrum: A Practical Guide to the Most Popular Agile Process*. Addison-Wesley. Boston.

Authors' contacts

Thomas-Michael Moser
ul. Hashovska Nr. 21
4000 Plovdiv
Bulgaria

E-mail: thomas.moser@bulcor.com

© International Scientific Conference on Engineering, Technologies and Systems
TECHSYS 2016, Technical University – Sofia, Plovdiv branch
26 – 28 May 2016, Plovdiv, Bulgaria

# WILL AGILE METHODS RESOLVE THE COMPLEXITY CRISIS IN SOFTWARE ENGINEERING?

THOMAS-MICHAEL MOSER

**Abstract:** *The accelerating growth of technologies exercises increasing pressure on people and system. This complexity crisis does not only cover software engineering but extends to products, markets, companies and users. Agile work seems to provide a solution. A case of classic versus agile realization is discussed. The culture of an organization and cross functional socio-economic relations seem to be more important than monetary funds and the application of state-of-the-art technologies. It is proposed to apply a portfolio mix of classic and agile methods to become faster at less cost with better quality.*

**Key words:** *Project management methodologies, Information Communication Technologies, Social interactions, Project failures, Risk management, Organizational turnarounds, Agile work, HERMES, V-model, SCRUM, Team learning, Cross-functional communication*

## 1. Present challenges for engineering

We live in a world where we experience accelerating pressure on people and systems. The business side of software engineering enforces shorter development cycles at less cost and with higher quality results. The global market economies favor those who are faster and better on features, tailor-made flexibility and price [1].

## 2. Purpose and scope of this paper

This paper describes what "agile" software engineering means and what it is good for, based on extensive project experience by the author. The scope of this contribution aims to show how to use the agile engineering methodology, and how to prevent and cure project failures. Out of scope is an in-depth evaluation of methodologies due to the summary character of this paper.

## 3. The roads to "agile"

The decline of the classic mainframe started with the arrival of the personal computer, the decline continued when distributed processing was established. We got a "complexity crisis" which covers not only the software engineering, but extends to products, markets, companies and users [2].

What does "agile" mean? Agile is the ability to move quickly and easily ahead. It comes from the Latin verb «agere» which means to do, to make, to act. This demands to cooperate, communicate and coordinate with others to achieve a joint objective.

"Complex systems are networks made of a number of component that interact with each other, typically in a nonlinear fashion. Complex systems may arise and evolve through self-organization, such that they are neither completely regular nor completely random, permitting the development of emergent behavior of macroscopic scales [3]".

Agile work seems to provide solutions for the situation that software engineering has to be done faster with better quality and at lower cost responding to global competitive requirements. This has been further elaborated by the <agilemanifesto.org> with the "Principles behind the Agile Manifesto" [4].

### 3.1. Case of classic versus agile realization

This paper will speak from a practical standpoint, trying to avoid to take a position for one or another methodology.

The comparison is a pragmatic summary list, not a theoretical essay. It serves as sketch and is not intended as proposition for doing projects in some exclusive way. The following case is fiction but based on real world work aggregated from numerous projects to present practical explanations in order to support insight and possible lessons learned.

### 3.2. Case scenario of development program

A large international company wants to replace the present line of a diagnostics machine. The application for this new machine must be developed as a mechatronics undertaking, i.e. for the mechanical parts by steering the sensors, actors, bus systems, embedded systems, step motors etc. The resulting data will be collected in a commercial database for which an application must be written to run the database as data warehouse with ETL-procedures.

Copyright © 2016 by Technical University of Sofia, Plovdiv branch, Bulgaria ISSN Online: 2535-0048

Organization of the program: One large room for 3 teams with a basic machine prototype. One team has technical engineers for the mechanical/electrical design. The other team takes care of the mechatronics and embedded systems. The third (team 3) develops the commercial application, i.e. database, warehouse, web application and the interface to internal commercial requirements.

It is assumed that one team has a headcount from 12 to 20 people. The program consists of one program director, one project manager for each one team with up to three team leads. Programmers and team leads must be hired as contractors. The same applies to the build and configuration manager.

In order to keep this short case simple, we further assume that all other factors stay the same (ceteris paribus clause). This means, we assume that supporting factors like the staff function of quality management, systems architect; back office of work package planning, program office etc. are set equal to both: the classic versus agile engineering work.

We only watch the team 3 for the commercial, web based application.

### 3.3. Development infrastructure

Let's start with the basic software development infrastructure by mentioning the major components only.

The classic case uses classic methodology and works in a Microsoft Windows environment, following the leading German software engineering methodology, the V-Model [5] and the Swiss HERMES methodology for large and complex environments [6]. The agile side works under Linux.

Technical environment of the classic case:

Windows Server 2012R2, Framework: Visual Studio 2015 Enterprise with Team Foundation Server (TFS), HP Quality Center for testing, SQL Server 2014. NoSQL will not be being considered as it does not fit into the one vendor industrial standard SQL family line. File hosting and general project management collaboration are possible on Azure.

General program and project management are executed with MS Project. Development tracking of work packages, builds and releases will be operated with TFS [7] and Visual studio.

Technical environment of the agile case:

LAMP development environment. MariaDB version 10. For web services horizontal scaling and sharding of vague data loads, NoSQL as MongoDB, Couchbase or similar may be considered. Framework deployed: Eclipse IDE platform [8]. Open to use the following frameworks: Zend Framework, Symfony, CodeIgniter, CakePHP, Smarty, Laravel and others. The LAMP stack will run in virtual machines. File hosting and team collaboration run on GitHub. General program and project management are conducted with Open Project.

### 3.4. Process flow of classic phases

#### 3.4.1. Preliminary project work to do

List of business requirements
Development cost estimate, risk provisions
Timeline estimate
Participants, stakeholders, contracts
Draft of project plan
Proposal of alternatives to management for decision: Make - rework - on hold, or cancel

**"Go" by management for the classic way**
**Program starts**

Program and project plans established
Monitoring, controlling and updating
Change and issue management active
Sourcing of manpower/contracting

Discussion and opinion:

MS Project gives good enterprise choice. Database and office suite in exchange with Active Directory work well. GANNT charts with resources are fully deployed.

There is easy to find certified manpower used to work in clearly defined organizational structures.

As requirements are vague in the beginnings, manpower might lack creativity and flexibility to adapt to uncertainty as development is still open and might experience early frustration by the unknown.

High costs exist for licensing frameworks and tools. Team Foundation Server and HP Quality Center are tough to handle; they show more of an "old school" forms' orientation. One cannot live creativity, but must follow quite predefined rigid structures and workflows. The systems do not adapt to people - but people must adapt to the system.

Visual Studio is not too much different to Eclipse on the agile side, but based on latest programming languages as C#. It is preconditioned to define a unified platform. This seems better than Open Source, fragmented by fluctuations among market players and possible lack of support.

#### 3.4.2. Concept of operations

Design of the operations of software engineering program and projects, laid down by leading project management standards as in the Project Management Body of Knowledge [9]. Technically, Visual Studio provides excellent control by unified build processes as with continuous integration [10]. Branching and merging during development are fully controllable and can be automated to a large extend.

### 3.4.3. Requirements and architecture

Solicitation of requirements are done with the business side. Modelling and coding of requirements with unique IDs are established. The Pflichtenheft (duty book) with requirements of business and formalized with UML use cases are compiled; which will be symmetrically mirrored by the Lastenheft (list of specifications) as programming instructions according to platform, architecture, languages and tools.

The top level design of the architecture of systems structure and flows, drawn by hardware, software, communication paths, will be worked out.

### 3.4.4. Detailed Design

The refinements of the architecture with the requirements will fully be signed-off by business and technical staff. The design is now ready for the programming phase.

### 3.4.5. IMPLEMENTATION

This covers the execution of the programming work according to the detailed design specifications and the final list of requirements being approved by all stakeholders.

### 3.4.6. Tests, integration, operation and maintenance

Integration, Test, Verification

Integration of modules programmed. Unit and module tests by programmers and test department. Verification that modules work under integration by quality management and quality assurance.

Tests are conducted to cases developed during the detailed design phase.

System verification and validation

Quality management and quality assurance check the working function of the complete system against the test cases derived from the requirements and architecture phase. Verification checks that the formal coding works in input, output, processing and communication. Validation confirms the systems usability whether graphical user interfaces, ergonomics of handling etc. match business requirements.

Operation and maintenance

This final phase covers end user testing against the concept operations from the side of business. It will be concluded by the sign-off by business and the management of the end user. The system goes live into production. Development and ICT hand the system over to maintenance; either in-house, at client site (on premise) or outsourced.

Discussion and opinion:

The classic way shows a clearly defined process. It can be easily monitored and controlled over all process phases. In contrast it requires a high level of disciplines by all participants among all phases. During quite early phases, requirements and designs must be defined with their according test cases. Our time is characterized by rapid changes in end-user needs, shortage of specialists and tight budgets under increasing time pressure.

The classic methodology seems to work best if there is a very structured environment allowing for extended development cycles to provide excellent quality just in time or better.

The classic way is less feasible if business cannot clearly define use cases under rapidly changing market demands and insecure outcome of endeavors in risky global markets' environments.

If business scales down in a hierarchical way under clearly defined scope of business, the classic methodology works best.

The classic way has a less successful position to answer unpredictable changes as there are demand spikes in horizontal markets as in the information industry and online business, where flexibility and sudden changes must be served instantly.

Next, there will be the agile methodology as case sketch, considering the phases under the requirements of the development infrastructure according to 3.3. mentioned above. This is oriented on SRUM [11] as one of the leading methodology.

## 3.5. Process flow of agile phases

### 3.5.1. Preliminary project work to do

This is similar to the classic way as in 3.4.1.

**"Go" by management for the agile way**
**The program starts**

Program and project plans established
Monitoring, controlling and updating
Change and issue management active
Sourcing of manpower/contracting

Discussion and opinion:

Open source project planning tools barely match industry standards. An own solution must be made. It is difficult to deploy GANNT charts with resources in large programs. There are third party offers available, but this works against the mandate of a unified software landscape.

Manpower seems to be abundant on a global scale, but to evaluate some kind of standardized certification, qualification and experience seems difficult if not impossible sometimes. High risk provision must be made for people not matching qualifications, detected by daily work after sourcing and being hired. High personnel role changes and fluctuation in the beginnings must be anticipated. New hires and training require additional funds and cause delays in meeting deadlines of projects.

There is a relatively small cost for the development infrastructure to start with - as Open Source has fairly low cost (but is not entirely free under commercial usage). Enterprise support requires budgets.

People in the open source community are used to work under stress; they share, are flexible and creative. They do not get frustrated on uncommon things and chaotic start-up environments and work conditions as under time and budget pressure.

Many open source tools are flexible and joyful to operate. One can live creativity. But, one needs deep practical knowledge to work efficiently with scripting by command lines during daily routines.

The Eclipse IDE framework is not too much different compared to Visual Studio. But it is heavyweight on JAVA, coming of age [12]. Nevertheless, Open Source provides many intelligent choices and flexibility in design and application.

### 3.5.2. Concept of operations

The concept of operations by the agile methodology is completely different compared to the classic one. There is the assumption that requirements in the beginnings will be vague and can only be resolved by communication and coordination between the stakeholder groups [13].

Agile is a role driven development model. Three main roles exist. First, there is the Product owner. He is the communicator who works with the stakeholders and the agile team. He can transmit requirements from the business side to the technical side of the team and vice versa.

Next is the Scrum master. He is responsible for getting the team to work efficiently by removing impediments. He takes care that the work packages are on track by coordinating and supervising the backlog. The Scrum master must not have to be considered as project lead or similar. He has got no management function. His role is better seen as team facilitator to enable smooth and efficient work.

The third role is represented by the Development team. They realize the engineering work in steps of certain short work phases, called Sprints, normally within cycles of four weeks, or even shorter or longer.

### 3.5.3. Work flow principles

The team is self-organizing. Meetings to coordinate are held daily, mostly done as 20 minutes' stand-ups late in the morning. Work packages are pasted with sticky notes on a large poster or wall as task board. They follow a swim lane principle as planned, under work, pending, done, or similar.

When the sprint finishes, two meetings will be held. One is the sprint review to show what has been done and what points require clarification or rework.

The other meeting at the end of a sprint is the sprint retrospective where participants and stakeholder discuss the status, lessons learned and improvements.

The work packages are tracked by the work backlog showing what is planned, under work, finished; pending or needing resolution. The backlog is graphically shown as "burn-down chart", depicting the "ideal curve" of projected time of deadline, and milestones, against the curve of the actual backlog with prognosis implied. This is frequently shown in real-time reporting on monitors in the development room to give immediate feedback. The feedback comes from TFS or other systems where the development engineering work is captured. There are two types of charts. One is the sprint burn-down chart, the other one constitutes the release burn-down chart.

Discussion and opinion:

The above mentions major topics of the SCRUM methodology as an agile way to demonstrate the completely different character compared with classic software engineering methods.

Requirements under agile are derived from "user stories". This enables the end-user (business side) to formulate their wishes, demands and stipulations in common language. The requirements are then transformed into work packages, being further analyzed, formalized, and discussed by the team under coordination of the product owner and facilitation of the scrum master.

Compared to classic ways, this agile procedure shows better ways when requirements are vague and there is time pressure. This is often the way, when business says: "Just make us, …, do this …" without further specifying what exactly to do when and how with what concrete results. This attitude is quite typical in large environments. Agile helps to refine this and produce results during the sprint period.

Therefore, agile allows for a fast head start and can produce tangible results quickly. It may resolve parts by the "complexity crisis" mentioned at the beginnings of this paper. Vague, unknown or "tricky" requirements, demands, and expectations can be divided and put into smaller pieces to work on, to resolve; and to present working solutions within a relatively short time frame.

On the other hand, "agile" might be misunderstood as "liberty", like free style programming. This is not appropriate. Agile requires a constant personal involvement of creative and motivated participation. This is tougher to follow than a common "ordered to execute" management scheme.

Normally, organizations are still bound to a hierarchical organization set-up. Agile on the contrary is cross functional, similar to a matrix organization. Agile trades speed against clearly defined

routes and outcome. The product owner and scrum master must coordinate and balance between diverging stakeholder and group interests, but have no real decision power. This leaves a lot of responsibility to the team members.

This is less of an engineering matter but shows that a cultural, socio-economic phenomenon exists. Agile teams must be "social" people, but also excellent in technically complex matters to resolve them quickly in a fast and creative way.

Most large complex projects are either outsourced or work in environments with many specialists from different cultures and nations. They first must find a common basis – the "team building" [14] has to take place. They must understand each other and being able to communicate freely in order to falsify work results, share findings; and have to change course quickly. It seems uncommon for some people to work self-directed in a team coordinated pattern, instead of executing clear and direct work orders. And others who will act freely, might be misguided to see "their" code results as something of their "own" not sharing with others easily.

Both the product owner and the scrum master must be personalities to guide the team by coordination and protection through the ups and downs of complex projects.

With the right mix of people and a flexible organizational environment, agile may beat classical project methodologies when complexity must be quickly broken up under time and budget pressure.

### 4. What is the outcome of the case?

Naturally, one must follow-up what happened to the outcome of the case sketch depicted in chapter 3.1. in this paper. Here is how it turned out.

Prior projects were done in the classic way, only. Later, management demanded shorter development cycles with less budgets over time. Inspired by the trend to agile work, two large project were switched to agile methodology completely.

The first project went for two years and got stuck by internal reasons. Insufficient funds or the lack of qualified specialists did not play a major role. They could afford an excellent technical development environment and hired the best specialists they could acquire. The team finding was difficult from the start and continued. The corporate environment remained conservative and did not open up to cross functional work. The agile teams started to retreat from open work to some kind of "splendid isolation". As there was no true cross functional support, many of the team members became frustrated, worked on their own. They participated in team communication in a formal way, and lost empathy for others.

The development process got out of control. Because "flexibility" existed as main agile principle, individual development branches grew to more than 200 during one sprint. To make a build and release, those more than 200 branches had to be merged, causing numerous errors and exceptions during the consolidation and merge process. The build manager grew his team to five assistants writing scripts and algorithms to handle the chaotic growth wave of merges during the build and release process at the end of each sprint. He "advanced" to some "authority" of sole power owner, and became the "single point of failure" in the process. The flood of errors and break-downs of builds grew from month to month.

The project had to be stopped. Nobody could detect all error causes and repair them under reasonable economic effort anymore. As consequence, the project was outsourced and redone later. A substantial write-off and time delay had to be accepted.

The second project started two years later. The organization had acquired deeper awareness of the roots and causes. In order to get things faster and better, the headcount was doubled. The rule of diminishing results was not obeyed. Applied to the situation it means that just doubling the specialist workers does not necessarily mean to get more work done faster. Similar deficiencies as in the prior project started to build up. Wasted funds began to accumulate, deadlines of sprints and major releases were delayed more than six months, the product quality dropped from sprint to sprint.

But, the project was turned around and saved. Other departments like systems integration were bound into the development process early, participating in Scrum meetings and sending testers from systems integration to the desk of the developers. Testing was jointly done on a day by day basis. The project finalized successfully. Still under more cost and later than projected, but it worked, and the diagnostics machinery could be completed. Again, the cross functional open workstyle was the success factor.

### 5. Lessons learned and conclusions

It seems to be too easy to conclude that agile work saves the engineering efforts from the complexity crisis and realizes things better, faster, and at less cost.

Agile is embedded into the environment of the organization where it has got the working area. If the environment is not matching agile organization culture and set-up; then, agile concepts cannot succeed as expected.

The prerequisite is that the organizational structure must be permissible for cross functional agile work based on open communication and cooperation. If the organization is not "mature" enough [15] to provide this capable environment of creative self-

organization; projects of agile nature may end in isolated spaces, doomed for failure.

As mentioned above, agile work is less a matter of funds and technically state-of-the art methodology. Agile will prosper when compatible cultural and socio-economic conditions exist.

Therefore, the pre-project organizational situation in a large environment must be analyzed carefully whether mature, capable prerequisites are given, before a commitment for or against agile projects can be made.

If this procedure is too difficult to decide, one might consider to follow a portfolio mix. This means to enrich the classic methodology with agile parts – as in the web technologies engineering sections for example – to better master vague requirements, hard to predict environments or challenges of horizontal big data scaling, just to mention a few scenarios.

On the other hand, during agile projects, "conservative" classic process flows can be implemented into certain cycles, mainly to include traditionally working departments in the agile work as there are mechanical engineering or systems integration to name some as an example. This gives support to narrow cultural and socio-economic distances and to bridge organizational maturity disparities.

## REFERENCES


1. Kate Gillespie, H. David Hennessey. (2016). *Global Marketing*. 4th Edition. Routledge. New York, NY.
2. John L Mariotti. (2008). *The Complexity Crisis: Why too many products, markets, and customers are crippling your company--and what to do about it*. Published by Adams Media, an F+W Publications Company. Avon, Massachusetts.
3. Hiroki Sayama. (2015). *Introduction to the Modeling and Analysis of Complex Systems*. Page: 3. Open SYNY Textbooks, Milne Library. State University of New York at Genesco. Genesco, New York.
4. Website on one of the leading agile initiatives: http://www.agilemanifesto.org/
5. Der Beauftragte der Bundesregierung für Informationstechnik (BIT) 2016. *V-Modell XT®*. Bundesministerium des Innern (BMI). Berlin.
6. Schweizerische Eidgenossenschaft, Bundesverwaltung (2016). *Informationssteuerungsorgan des Bundes ISB. Projektmanagement-Methode HERMES.* Schweizerische Eidgenossenschaft. Bern.
7. Gary Gauvin. (2015). *Essentials of Administering Team Foundation Server 2015: Using TFS 2015 to accelerate your software development*. 1st ed. 2015 Edition. Springer Science+Business Media. New York.
8. Ram Kulkarni. (2015). *Java EE Development with Eclipse*. 2nd Edition. Packt Publishing. Birmingham, United Kingdom.
9. Project Management Institute (2015). *A guide to the Project Management Body of Knowledge (PMBOK Guide)*. 5th edition. Project Management Institute (PMI). Newton Square, PA.
10. Jez Humble. David Farley. (2011). *Continuous Delivery: Reliable Software Releases through Build, Test, and Deployment Automation*. Pearson Education, Boston, MA.
11. Robert C. Martin. (2013). *Agile Software Development, Principles, Patterns, and Practices*. Pearson Education Limited. Harlow, United Kingdom.
12. Jaroslav Tulach. (2008). *Practical API Design: Confessions of a Java Framework Architect*. Springer-Verlag. New York, NY.
13. Dean Leffingwell. (2011). *Agile Software Requirements: Lean Requirements Practices for Teams, Programs, and the Enterprise (Agile Software Development Series)*. Addison-Wesley, Pearson Education, Inc. Boston, MA.
14. Paul Gustavson. Stewart Liff. (2014). *A Team of Leaders: Empowering Every Member to Take Ownership, Demonstrate Initiative, and Deliver Results*. American Management Association. New York, NY.
15. CMMI® Institute (2016). *CMMI® for Development (CMMI-DEV), Version 1.3*. CMII Institute. Pittsburgh, PA.



Authors' contacts

Thomas-Michael Moser
ul. Hashovska Nr. 21
4000 Plovdiv
Bulgaria

E-mail: thomas.moser@bulcor.com

© International Scientific Conference on Engineering, Technologies and Systems
TECHSYS 2016, Technical University – Sofia, Plovdiv branch
26 – 28 May 2016, Plovdiv, Bulgaria

# ИНТЕГРИРАНО ИЗПОЛЗВАНЕ НА СТАТИСТИЧЕСКИ ПОДХОДИ ЗА ОЦЕНЯВАНЕ НА БИЗНЕС СРЕДАТА НА ОСНОВАТА НА ДАННИ ОТ АНКЕТНИ ПРОУЧВАНИЯ

АНТОНИЯ ЛАЗАРОВА

**Резюме:** *Основната цел на този научен доклад е представянето на познати до момента статистически подходи за оценка на бизнес средата и пътищата за тяхното интегрирано използване в динамично променяща се бизнес обстановка.*

*Във връзка с така дефинираната основна цел могат да се поставят следните научни задача:*

1. *Представяне на познати до момента статистически подходи за оценка на бизнес средата.*
2. *Представяне на интегрирано използване на различни статистически подходи в динамично променяща се бизнес обстановка.*

**Ключови думи:** *бизнес среда, статистически подход, оценка на динамична бизнес среда, анкетни карти*

# INTEGRATED USE OF STATISTICAL APPROACHES FOR EVALUATION THE BUSINESS ENVIRONMENT BASED DATA QUESTIONNAIRE SURVEY

ANTONIA LAZAROVA

**Abstract:** *The main objective of this scientific report is the presentation of prior art statistical approaches for assessing business environment and means for their integrated use in a dynamically changing business environment.*

*In relation to the defined primary purpose can be placed following research task:*

*1. Presentation of prior art statistical approaches to assess the business environment.*

*2. Presentation of the integrated use of various statistical approaches to dynamically changing business environment.*

**Key words:** *business environment, statistical approach, assessing the dynamic business sphere inquiry cards*

## 1. Въведение

Обичайна практика при бизнес изследванията чрез анкетни карти е като резултат от проучването да се получава разпределение по относителни дялове на анкетираните по отделните въпроси., които характеризират отделните същностни страни на бизнес средата. Този подход е подходящ само тогава, когато се разглеждат два или три компонента от всички, но при многофакторен

Copyright © 2016 by Technical University of Sofia, Plovdiv branch, Bulgaria ISSN Online: 2535-0048

модел са възможни изкривявания на информацията, както и загуби от масива. Ето защо актуалността на този проблем следва да се разглежда като необходимост от интегриран цялостен подход към бизнес анализите чрез анкетни карти, а не като самостоен проблем в рамките на отделно изследване. Обикновено предмет на изследването е количествената характеристика на бизнес средата, като се наблюдава безогледно използване в анкетните проучвания на категорийни признаци, на които трудно могат да се поставят количествени оценки. Обикновено в учебниците се говори за вътрешна и външна бизнес среда на организациите или за основните подлежащи на статистическо изследване елементи на бизнес средата, но не се коментира избора на скали и статистически признаци в рамките на анкетното проучване.

## 2. Статистически подходи за оценка на бизнес средата. Статистически признаци и скали, използвани традиционно в анкетни проучвания.

Традиционно при анкетни проучвания на бизнес средата се направи разлика дали анализът се провежда вътре в рамките на организацията и се разглеждат вътрешноорганизационни фактори на средата или е анализ на външната за организацията среда. Това диференциране се извършва, обаче само в теоретичен порядък, на практика, от чисто статистическа гледна точка става дума за използване на еднаква скали, еднакви честотни разпределения, въпреки различните съдържателно критерий на изследване.

***Таблица 1.*** *Брой проучвания на бизнес средата в България в периода 2013 - 2015 година*

| Период | Вид на проучването | Възложител на проучването | Общ брой |
|---|---|---|---|
| 2013 - 2014 | Изследване на външната конкурентна среда на организацията | Стопански организации | 121 |
| | | Организации с нестопанска цел | 4 |
| | | Други | 3 |
| 2014 - 2015 | Изследване на външната конкурентна среда на организацията | Стопански организации | 130 |
| | | Организации с нестопанска цел | 2 |
| | | Други | 5 |
| | Изследване на вътрешната среда на организацията | Стопански организации | 16 |
| | | Други | 12 |

***Таблица 2.*** *Статистически признаци и скали, използвани традиционно в анкетни проучвания.*

| **2013 / 2014 Изследване на външната конкурентна среда на организацията** | | |
|---|---|---|
| **Стопански организации** | **Организации с нестопанска цел** | **Други** |
| Качествени (дихотонни) *Вариационни признаци* | Качествени (дихотонни) *Вариационни признаци* | Качествени (дихотонни) *Вариационни признаци Ликертови скали* |
| Неметрирани *Непрекъснати вариационни скали* | Неметрирани *Непрекъснати вариационни скали* | Неметрирани *Непрекъснати вариационни скали Многомерни честотни разпределения* |
| **2014/ 2015 Изследване на външната конкурентна среда на организацията** | | |
| **Стопански организации** | **Организации с нестопанска цел** | **Други** |
| Качествени (дихотонни) *Вариационни признаци Метрирани признаци* | Качествени (дихотонни) *Вариационни признаци* | Качествени (дихотонни) *Вариационни признаци* |
| Неметрирани *Непрекъснати вариационни признаци Прекъснати скали* | Неметрирани *Непрекъснати вариационни скали* | Ликертови скали *Непрекъснати вариационни скали* |
| **2014/ 2015 Изследване на вътрешната среда на организацията** | | |
| Стопански организации | Други | |
| Качествени (дихотонни) *Вариационни признаци Метрирани признаци* | Качествени (дихотонни) *Вариационни признаци* | |
| Неметрирани *Непрекъснати вариационни признаци Прекъснати скали* | Ликертови скали *Непрекъснати вариационни скали* | |

От таблица 1 и таблица 2 става ясно, че на практика независимо дали се изследва външната или вътрешната среда на организацията при бизнес анализите, които се правят в България в периода 2013 – 2015 година се използват едни и същи статистически скали и признаци, чрез което се ограничават не само възможностите за анализ, но и е възможно да има промяна и липса на съпоставимост при първичната информация. Ето защо възниква необходимостта да говорим за интегрирано

използване на различни статистически подходи в динамично променяща се бизнес обстановка.

## 3. Интегрирано използване на различни статистически подходи в динамично променяща се бизнес обстановка

### 3.1. Парадокс на Ръсел

Парадоксът на Ръсел може да бъде изразен така „Нека вземем множеството от множествата, които не принадлежат на себе си. Принадлежи ли то на себе си?“. Парадоксът показва, че при теория на множествата в смисъла на Кантор на практика става дума за една противоречива теория. Проблемът идва от там, че считаме, че можем да построим множество въз основата на всяко свойство. Така някои от тези свойства (и това именно е случаят в парадокса на Ръсел) генерират нестабилни самопрепращащи се цикли и съответно би трябвало те да бъдат изключени.

Ако $A = \{B | B \notin B\}$, то тогава $A \in A \Leftrightarrow A \notin A$. Първото решение е теорията на типовете на Ръсел, според която множествата са с йерархични типове. Дадено множество може да съдържа само обекти стриктно по-малки от него самото.[3]

При бизнес анализите най-често от възложителят зависи кое е по-голямото и по-малкото в бизнес средата, която се изследва, в следствие, на което с подбрани макар и правилно, традиционно използвани прости скали и съответните им статистически признаци, при статистическа обработка възниква парадокс на Ръсел.

### 3.2. ANOVA

Чрез ANOVA може да се борави с една, две или три променливи, чрез които доста по-точно може да се определи дали разликата между извадковите средни е достатъчна, за да приемем, че те не се различават случайно, а е налице реална разлика между представяните от тях популации. ANOVA позволява измерване на резултатите по количествена скала и позволява наблюдения на стойностите във времето. Създава и обективни условия по случаен признак да бъдат разделени участниците в изследването в рамките на три или повече експериментални условия.[4]

Ако еднофакторният ANOVA не даде статистически значими резултати, често е възможно да се направи мотивиран избор за комплексно сравнение, което компенсира този проблем. Много често в практиката при такава ситуация се използва MANOVA.

### 3.3. MANOVA

В статистиката, многовариантен анализ на вариациите MANOVA е процедура за сравняване на многомерни средства примерни. Като многовариантно процедура, тя се използва, когато има две или повече зависими променливи, и обикновено е последвано от тестовете за значимост, включващи индивидуални зависими променливи отделно. Той помага да се отговори на следните въпроси:

Независимата променлива има ли значително въздействие върху зависимите променливи?

Какви са отношенията между зависимите променливи?

Какви са отношенията между независимите променливи?

MANOVA е генерализирана форма на един статистически анализ на вариациите (ANOVA), въпреки че, за разлика от един статистически ANOVA, той използва вариация-ковариация между променливите при тестване на статистическата значимост на средните разлики. Усложнение при използването на MANOVA е, че разпределението на тези статистически данни в рамките на нулевата хипотеза не е лесно и може да се сближи само с изключение на няколко ниско измерни случаи.[1]

### 3.4. Определяне на цената като компонента: Жизнен цикъл на потребителя и жизнен цикъл на продукта. Определяне на прага на рентабилността на организациите.

През призмата на пазарната цена като компонента на анализ не само в рамките на изследване на конкуренцията в отрасъла, но и като вътрешно присъщ елемент на анализ в организацията , може да се направи вътрешно организационен анализ на жизнен цикъл на потребителя и жизнен цикъл на продукта. Чрез него ще се постигнат следните положителни ефекти:

- Жизненият цикъл на продукта касае не конкретна стокова единица, а в по-общ план продукта като разновидност на определена продуктова линия. Този окрупнен подход ще създаде обективна възможност за изследване не само в рамките на маркетинговия микс на организацията, но и за набавяне на сравнителни данни за цените на конкуренти сходни или еднакви продукти.
- Създава се възможност чрез правилно подбрани категорийни, неметрирани признаци и чрез Ликертови скали да се опише продължителността и

последователните изменения на пазарния живот на даден продукт.

– Създава се обективна възможност да се работи в по-дългосрочен период с резултатите от това изследване чрез ANOVA и MANOVA и то да се повтаря в определен период от време, тъй като продуктите имат сравнително ограничен живот.

Познаването на тези фази и способността да се оцени на какъв етап от развитието си се намира предприятието води до по-добро разбиране на съществуващите проблеми и до откриване на предизвикателства. От гледна точка на бизнес анализа можем да разграничим следните фази в жизнения цикъл на предприятието.

***Таблица 3.*** *Етапи/фази/ на жизнения цикъл на предприятието през призмата на на цената като компонента.*

| Етапи/фази/ на жизнения цикъл на предприятието | Основни характеристики на етапа | Възможности за статистически бизнес анализ в динамично променяща се среда |
|---|---|---|
| 1. Фаза на възникване | Избор на правна форма, седалище, предмет на дейност. Основни проблеми – недостатъчен брой клиенти, организиране и снабдяване на производството със суровини и материали, неизградена логистика и неясен маркетинг на продукта. | Изследване за наличие на парадокс на Ръсел. Външни изследвания на конкурентна среда на база на вторични данни чрез верижни индекси. |
| 2.Растеж/развитие/ | Разширяване на дейността, обновяване на техниката и модернизиране. Извършва се интензивен маркетинг. Изгражда се контролингът в предприятието. Търси се възвръщаемост на активите и вложения труд. | Финансово - счетоводен анализ. Анализ през призмата на жизнения цикъл на продукта. Теория на моментите за изследване на продажбите. |
| 3.Стабилизация (зрялост) | Необходимост от разширяване на продуктовата линия, оптимизация на разходите за производство, логистиката следва да се оптимизира. | ANOVA MANOVA Теория на моментите за изследване на продажбите. Финансово - счетоводен анализ. Външни изследвания на конкурентна среда на база на вторични данни чрез верижни индекси. |
| 4.Насищане (спад) | Под заплаха от несъстоятелност и ликвидация предприятието следва да въведе иновация, да диферсифицира портфейл и активи, да опита да въведе иновации. | Изследване за наличие на парадокс на Ръсел. ANOVA MANOVA Теория на моментите за изследване на продажбите. Финансово - счетоводен анализ. Външни изследвания на конкурентна среда на база на вторични данни чрез верижни индекси. Диаграма на Вороной |

От таблица 3 става ясно, че статистическият подход в динамична бизнес среда дава широки възможности както за оценка на външната за предприятието среда, така и за вътрешната. Самоцелното използване само на статистически методи за оценка на анкетни проучвания в бизнеса само по себе си е вредно, защото възниква обективната необходимост мениджмънта на предприятието да се съобрази със следните компоненти:

- Седалището и дейността на предприятието – Ако предприятието е локализирано в голям град, то неговите конкуренти обикновено са повече и по-разпознаваеми.
- Наличието на външни за дружеството маркетингов или счетоводен отдел – Голяма част от дружествата възлагат на счетоводни къщи или на индивидуални счетоводители изготвянето на първичната им счетоводна информация. След настъпилите промени в Закона за счетоводството през 2016 година, много прецизно трябва да се гледа на изработването на финансово – счетоводен анализ на конкретно дружество.

- Ако маркетинговият отдел също е външен за съответното предприятие изключително трудно извън сферата на рекламата и изготвянето на рекламни материали може ефективно да се проследи неговата дейност. Обикновено в България собствениците и управители на малки и средни предприятия считат, че щом са на лица продажби или ръст на продажбите маркетинговия отдел работи добре. Това, обаче не винаги е така.
- Наличието на система за контрол в предприятието още във фазата на растеж, когато се предполага, че продажбата на продуктите му нараства – При липса на такава система обикновено има проблеми в хода на производствения и технологичен процес, загуби от мащаба на производството, трудна възвръщаемост на вложените средства след етапа на растеж и всичко това неминуемо води до свиване на производството и продажбите. Разбира се, контролингът не означава непременно видео наблюдение на цеховете. Контролингът означава да се изработи цялостна система за оценка на качеството на произвежданата продукция, система за оценка на персонала, система за оценка на извършените маркетингови дейности, така че накрая чрез обща интеграция на всички системи да може да се изгради в мениджмънта цялостна представа как действа предприятието и как на практика е позиционирано то на пазара. В динамичната бизнес среда, такъв анализ следва да се извършва изключително бързо и статистиката разполага с инструментариум за това. Например в едно предприятие, чийто предмет на дейност е транспорта, освен цялостен анализ на външната среда, в това число и международните превози и още във фазата на растеж би следвало да използват Диаграмата на Вороной.
- Използване на метода на моментите в дългосрочен план за оценка на покупките на индивидуални потребители - Този статистически подход може да се използва, ако целта на дружеството е да скъси известните вече етапи, през които преминава индивидуални потребител при осъществяване на покупки. Прилагането на анкетни проучвания тук би донесло информация за стила на живот на групата потребители, които купуват стоките на организацията, както и отношението им към потреблението. Изключително важен акцент при използването на метода на моментите е, че се отчита етапа на стимул от страна на организацията, който да подбуди потребителя към покупка. Важно и неразривно условие е този стимул да бъде комерсиален. [2]

В рамките на едно анкетно проучване в динамична бизнес среда могат успешно да се използват интегрирано Коефициентът на Тейл и коефициент на Джини във фаза на растеж.

Във фазата на зрялост на предприятието е желателно да се разшири продуктовата линия, да се оптимизира логистичното обслужване на производството. Освен посочените в таблица 3 статистически методи в зависимост от отрасъла могат да се използват и :

- Сезонни модели за краткосрочно прогнозиране, когато в анкетната карта за използвани метрирани признаци. Този подход успешно може да се съчетае и с финансово – счетоводен анализ на предприятието.
- Мултипликативен трендов прогностичен модел, който може да се използва удачно с прекъснати и непрекъснати метрирани признаци. Чрез специално подбрани категорийни признаци в една и съща анкетна карта може да се използва и триангулация на Делони, ако отрасъла, в който е предприятието го позволява.
- Използване на ANOVA и MANOVA , чрез които да се изгради метода на експоненциалните плъзгащи се средни за краткосрочно прогнозиране.
- На база на верижни индекси от външна бизнес среда и данни от външни източници е възможно да се изгради цялостна прогноза на отрасъла и чрез съвместното използване на подходящо подбрани признаци в анкетните проучвания да се проследи динамиката на бизнес средата в определен бъдещ модел.

  Във фазата на спад предприятието следва да изследва жизнения цикъл на своите продукти и обикновено маркетолозите в такава ситуация използват PEST – анализ или Матрицата на Бостънската консултантска група. Тези подходи, макар и масово използвани не дават необходимата цифрова информация за ръст или спад при различните групи продукти. Поради

тази причина следва те да се използват със съответни статистически данни или най-добре едновременно да се интегрират във вид на въпроси в анкетна карта. Това от своя страна предполага използването на различни като структура анкетни карти в рамките на жизнения цикъл на предприятието, не само заради променените условия, при което то ще съществува, но и заради потребностите от анализ на вътрешната организационна среда.

Обикновено в етапа на спад малко маркетолози търсят взаимовръзката между жизнения цикъл на предприятието и жизнения цикъл на продукта през призмата на цената. Обикновеното и масово решение е диверсификация на продуктовата линия, но не включвайки анализ има ли реална нужда тя да се случва.

**4. Изводи**

Всичко казано до тук показва, че в зависимост от спецификата и особеностите на всичко предприятие избора на статистически методи в динамична бизнес среда при прилагането на анкетни проучвания следва да бъде различен.

**5. Заключение**

В заключение може да се каже, че е изпълнена основната цел на настоящия научен доклад, а именно - представянето на познати до момента статистически подходи за оценка на бизнес средата и пътищата за тяхното интегрирано използване в динамично променяща се бизнес обстановка.

**ЛИТЕРАТУРА**


1. Коен, Б., Лий, Р.Б. *Основи на статистиката за социални и поведенчески науки*, изд. Изток – Запад, с .193
2. Лазарова, А. *Метод на моментите при вземане на решение за покупка при индивидуални потребители, Европейско висше училище по икономика и мениджмънт*, Научни трудове, Годишник на ЕВУИМ, книга 15/ 2015, ISSN 1312 739X, с. 71.
3. Rang,B., Thomas,W., *Zermelo's discovery of the "Russell Paradox" , Historia Mathematica*, v. 8 n. 1, 1981, p. 15–22 .
4. Rosenbaum, Paul R.. *Observational Studies (2nd ed.)*. New York: Springer-Verlag, 2002, p.67.



д-р Антония Лазарова
Адрес: гр. Пловдив ул. „Задруга“ 18
Европейско висше училище по икономика и мениджмънт
E-mail: toni_23_bg@yahoo.com

© International Scientific Conference on Engineering, Technologies and Systems
TECHSYS 2016, Technical University – Sofia, Plovdiv branch
26 – 28 May 2016, Plovdiv, Bulgaria

# ФОРМИРАНЕ НА МОДЕРНА СИСТЕМА НА ДАНЪЧНО ОБЛАГАНЕ В РЕПУБЛИКА АЛБАНИЯ

НИКОЛАЙ ПАТОНОВ, АРДИАН ДУРМИШИ

**Резюме:** *Настоящият доклад има за цел да представи накратко еволюцията на системата на данъчно облагане в Република Албания. Изложението проследява основните етапи, през които е преминала данъчната система до достигането й до съвременното й състояние. На основата на направения анализ са изведени препоръки за по-нататъшното й развитие.*

**Ключови думи:** *данъчна система, частна собственост, данъчна администрация*

# FORMATION OF A MODERN TAX SYSTEM IN THE REPUBLIC OF ALBANIA

NIKOLAY PATONOV, ARDIAN DURMISHI

**Abstract:** *The paper is intended to make a short presentation of the evolution of the tax system of the Republic of Albania. The study follows main stages through which the system has passed to achieve its today's appearance. Recommendations for its further development have been made on the base of the analysis.*

**Key words:** *tax system, private ownership, tax administration*

Организираната данъчна система от съвременен тип в Република Албания започва да функционира през ранните години на миналия век. Но, като практика данъчното облагане има дълги исторически традиции по земите на днешната албанска държава. [1]

От историческа гледна точка началото на данъчното облагане се свързва с установяването на права върху частната собственост [5]. Ето защо, данъчното облагане на територията на днешна Албания може да се отнесе към времето на установяването на първите илирийски държавни формирувания. Включването на тези земи в пределите на големите империи – римска, византийска и османска, предполага и налагането на характерните за тях данъчни системи.

През османския период започва развитие на данъчна система, основана на принципа за документална обоснованост [5]. Това е и началото на модерно данъчно облагане, използващо данъчни документи от установяването до окончателното поласяване на данъчното задължение. Ето защо цел на настоящата разработка е да проследи еволюцията на системата на данъчно облагане в Република Албания, като започне от времето, в което са поставени основите на модерното данъчно облагане.

Обявявилото през 1928 г. независимост албанско кралство наследява османската данъчна система, която заапазва своето функциониране до края на Втората световна война. След края на войната развитието на данъчната система е белязано от дълъг период на функциониране в условията на командно-административна икономика. През тези години данъчната система придобива

Copyright © 2016 by Technical University of Sofia, Plovdiv branch, Bulgaria ISSN Online: 2535-0048

значение и роля на една силно централизирана структура за акумулиране на ресурс.

Демократичните промени и възстановяването на частната собственост в началото на деветдесетте години на миналия век поставят начало и на продължителни реформи за цялостно преустройство на албанската данъчната система. Така в нейното устройство и функциониране се въведоха съвременни принципи и практики [4].

В албанската историография е възприето времето от първите стъпки до изграждането на съвременна данъчна система с модерна данъчна администрация да се обособява в няколко етапа. [5]

**1. Първи етап - от началото на седемнадесети век до създаването на независима албанска държава**

От началото на седемнадесети век до края на двадесете години на двадесети век по албанските земи се прилага законово установената система на данъчно облагане в османската държава [5]. През този период на данъчно облагане подлежат ползваните земеделски земи, лични доходи, тютюневи изделия, алкохолни напитки, правото да се изповядва различна от доминиращата религия.

Облагането на дохода до 1907 г. има поголовен характер. Така всяко лице, което реализира доход, без значение от източника на този доход, дължи данък в размер на пет гроша месечно, за месеците, в които се придобива доходът. С развитието на занаятите и манифатурното производство османското данъчно законодателство установена своеобразна прогресия при облагането на различни по размер доходи, като въвежда диференциране на облагаемите доходи според източника.

След обособяването на автономна албанска облат в рамките на османската държава през 1912 г. започва въвеждането на изменения в наследеното османско данъчно облагане. Така тогавашното министерство на финансите изготвя първия закон за облагане на дохода, който е приет през 1927 г. Според него „всяка печалба, реализирана при упражняването на занаят, свободна професия, търговия, управление на селскостопански предприятия, горски стопанства и други дейности, както и заплатите на работниците в частния сектор, са обект на данък по този закон” [6].

**2. Вторият етап (1928 – 1944 г.)**

Този период започва със създаването на независимото албанско кралство и управлението на крал Ахмед Зог. През тези години фискалната система включва три групи приходоизточници, а именно преки данъци, данъци върху потребленито и мита, фискални монополи.

Основно това са данъци върху животни, сгради, данък върху печалбата, данък върху доходите и наследствата, данък върху горските производства, такса за добив на кариерни материали, както и данък на основата на здължението на населението за изграждане и поддръжка на пътищата.

Покупките на алкохол, кафе, тютюневи изделия и луксозни стоки също са облагани с данък. Това е първообраз на акцизно облагане в новосъздадената албанска държава.

**3. Трети етап (1944 – 1990 г.)**

Периодът, който обхваща този етап от развитието на албанското данъчно облагане, се подразделя на два подпериода, а именно период на отворена данъчна система и период на централизирана данъчна система.

В първите години след Втората световна война са положени основите на командно-административна икономика. През този период са установени специални данъци за т. нар. големи и малки търговски производители, които са направили богатството си по време на войната, които в сметка водят до тяхното разоряване. От 1944 г. до началото на 60-те години частната собственост все още съществува. Ето защо през този период данъчната система прилага дискриинационно облагане, което има за цел масовата колективизация на частна собственост и превръщането ѝ в социалистическа държавна собственост.

Вторият подпериод, който условно започва от началото на 60-те години на миналия век, обхваща развитието на данъчна система в условията на общонародна собственост, която по

същността си е една силно централизирана данъчна система. Понятието за данъчна система се използва условно, защото облагане на частната сообственост не е налице поради липса на такава. През този период изчезва облагането на печалбата в истинския му смисъл. Държавните предприятия и земеделските кооперации внасят в държавния бюджет дял от своята печалба. По същия начин са облагани и изплащаните от държавните предприятия доходи под формата на работна заплата.

**4. Четвърти етап (от началото на 90-те години на миналия век до наши дни)**

След промените в началото на деветдесетте години на миналия век е възстановена данъчната система в смисъла на институционализирана данъчна система. В този период се създаде нормативна регламентация на приложимите данъци и устройството на данъчната администрация [2].

В периода 1990-1991 г. са засилени преговорите за сътрудничество със международните финансови институции - Световна банка и Международен валутен фонд. С помощ от тези институции са подготвени и приети първите фискални пакети.

Паралелно с разработване на основните нормативни актове на новото данъчно облагане, са предприети мерки за реформиране и утвърждаване на структурата на данъчната администрация. Така отдел „Приходи" в Министерство на финансите е преобразуван в Дирекция „Данъчното облагане".

В края на 1991 г. и началото на 1992 г. е завършено началното законодателно регламентиране на основните данъци. Липсата на опит в изработването на данъчно законодателство, адекватно на новите пазарни условия, е основната причина приетите през този период нормативни актове да не са достатъчно ефективни.

В началото на 1993 г. са положени значителни усилия за разработване на цялостен пакет от фискални закони, които да очертаят контурите на съвременното албанско данъчно законодателство. През тази година е изработена нова регламентация на облагането с данък върху оборота, акцизното облагане, облагането на печалбата на малкия бизнес, както и облагането на личните доходи.

Важна стъпка в развитието на албанската данъчна система е цялостното реорганизиране на данъчната администрация, извършено през 1995 г. с техническата помощ на Международния валутен фонд. При тази реформа са обособени три основни функционални структури, а именно: 1. сектор „Данъчна регистрация", 2. сектор „Плащане на данъчни задължения", 3. сектор „Данъчен контрол и мерки за административна принуда".

Друга основополагаща стъпка с положителен характер е регламентирането на всички административни процедури с един нормативен акт през 1999 г. По този начин се създаде ясно обособяване на данъчно материално и данъчно процесуално право.

По пътя към модернизиране на данъчната администрация все повече се поставя акцент върху отношенията с данъчно задължените лица. Поставя се също акцент върху информираността на задължените лице за услугите, които предоставят органите на данъчната администрация [3]. Преследваната от данъчната администрация цел е да се повиши доверието в нея от страна на отделния данъкоплатец и широката общественост, като се убедят в ефективното функциониране на цялата административна структура.

Работата на данъчната администрация е един от факторите с определящо значение за събираемостта на данъчните приходи. Ето защо следва да се преследва повшаването на качеството на изпълнение на функцията обслужване на данъкоплатци. Тази дейност се състои в оказване на помощ на данъкоплатците във връзка с прилагането на законодателството за всички задължения и права, които данъкоплатците имат във връзка с данъчното облагане. Понастоящем тази задача се изпълнява от отдел „Обслужване данъкоплатци" към Главна дирекция „Данъчно облагане". Важно значение има и

създадената дирекция „Големи данъкоплатци”.

### 5. Заключение

На основата на изложеното можем да обобщим, че към настоящия етап от развитието на данъчната ситема на Република Албания следва да се предприемат действия за по-широкото въвеждане на информационните технологии в счетоводството, обмена на информация, контролната дейност във връзка с данъчното облагане на физическите и юридическите лица. Наред с това, модернизацията на данъчното законодателство и администрация следва да се движи в посока на постигане на съответствие със законодателството на страните от Европейската общност и възприемане на добрите административни практики на тези страни. Също следва да се изгради инфраструктура за ефективен обмен на информация със страните членки във връзка с облагането с данък върху добавената стойност, както и процедури за извършване на свързани действия за събиране на публични вземания от субекти, разположени на територията на съответната страна.

### ЛИТЕРАТУРА


1. Binaj, A., (2006), *Biznesi, politika fiskale dhe Shqipëria në tranzicion: përmbledhje artikujsh Studimorë*, Ekonomia, Tiranë.
2. Dhamo, S., (2005), Subjektivizmi i pushtetit te organeve fiskale, permiresimi i mekanzimave te transaparences dhe apelimit ne legjislacionin fiskal ne funksion te uljes se informalitetit, *Shtator*, pp.47-51.
3. Manoku, El., Kalia, M., 2013, Marketing in the Tax Administration in Albania, Scientific Annals of the "Alexandru Ioan Cuza" University of Iasi, Economic Sciences Section, Vol. 60/1, pp. 1-12.
4. Prenga, K., & Ciceri, B., (1998), *Roli i politikës fiskale në ekonominë e tregut*, Tiranë.
5. Zaho, L., & Duraj, B., (2013), *Tregjet dhe institucionet financiare*, Albpaper, Tiranë.
6. Law № 2575 от 11.31.1927 г.



Контакти
д-р Николай Патонов,
ЮЗУ „Н. Рилски” Благоевград
Адрес:, ул. „Крали Марко” 2
E-mail: patonec@mail.bg

д-р Ардиан Дурмиши
Университет „Александер Джувани”
Елбасан, Албания
E-mail: ardiandurmishi@yahoo.com

© International Scientific Conference on Engineering, Technologies and Systems
TECHSYS 2016, Technical University – Sofia, Plovdiv branch
26 – 28 May 2016, Plovdiv, Bulgaria

# ПОТЕНЦИАЛИ ЗА РАЗВИТИЕ НА ТРАНСПОРТНАТА ИНФРАСТРУКТУРА НА БЪЛГАРИЯ В КОНТЕКСТА НА УСТОЙЧИВОТО РАЗВИТИЕ

ИВАНКА БАНКОВА

**Резюме:** *Транспортната инфраструктура и транспорта имат основно значение за устойчивото развитие на обществото, тъй като осигуряват мобилност на населението и подпомагат промишлеността и търговията. Транспортът има пряко влияние и върху икономическото развитие, като играе ролята на свързващо звено между производителите, от една страна, и суровините, трудовия пазар и потребителите, от друга. С икономическия растеж обемът на товарните превози и броят на превозените пътници нарастват, а необходимостта от транспортиране на стоките и услугите стимулира икономическата активност. Поради това този отрасъл е от голямо значение за конкурентоспособността и заетостта в страната.*

*Главната социална функция на транспорта е да осигури достъп до основни услуги като здравеопазване, образование, търговия, туризъм, спорт и развлечения. Основните икономически и социални облаги от транспорта, които се балансират изключително трудно с високите социални разходи и разходите за околната среда, определят транспортния сектор като изключително важен за устойчивото развитие.*

**Ключови думи:** *транспорт, транспортна инфраструктура, устойчиво развитие*

# POTENTIALS FOR THE DEVELOPMENT OF TRANSPORT INFRASTRUCTURE OF BULGARIA IN THE CONTEXT OF SUSTAINABLE DEVELOPMENT

IVANKA BANKOVA

**Abstract:** *Transport infrastructure and transport are essential for the sustainable development of society, as they provide mobility of the population and support industry and trade. Transport has a direct impact on the economic development, it acts as a link between producers on the one hand, and raw materials, labor market and consumers, on the other. With the economic growth, the amount of cargo transportation and the number of passengers are increasing, and the need for transportation of goods and services stimulate the economic activity. Therefore, this sector is of great importance for the competitiveness and employment in the country.*

*The main social function of transport is to provide access to basic services such as health, education, trade, tourism, sport and entertainment. The fundamental economic and social benefits of the transport that balance extremely difficult with high social costs for environment, determine the transport sector as crucial for the sustainable development*

**Key words:** *transport, transport infrastructure, sustainable development*

Copyright © 2016 by Technical University of Sofia, Plovdiv branch, Bulgaria ISSN Online: 2535-0048

**Увод**

Независимо от факта, че Европейският съюз (ЕС) като цяло представлява просперираща икономическа общност, налице са различия в състоянието и развитието на 268-те региона в съюза. За да развива търговия, да създава работни места, да повишава икономическия си растеж и да съхрани околната среда, Европа се нуждае от добри транспортни връзки. Ето защо, в рамките на най-радикалната промяна на инфраструктурната политика на ЕС от нейното създаване през 80-те години на XX век, се създава основна транспортна мрежа, базирана на девет главни коридора: 2 коридора Север-Юг, 3 коридора Изток-Запад; и 4 диагонални коридора. Благодарение на тази мрежа предстои да се преобразуват връзките Изток-Запад, избягване на задръстванията, модернизиране на инфраструктурата и рационализиране на трансграничните транспортни операции в интерес на пътниците и предприятията в целия ЕС. [6] Основната транспортна мрежа трябва да бъде завършена до 2030 г. като целта е да подобри връзките между различните видове транспорт и да допринесе за постигането на целите на ЕС в областта на изменението на климата.

Една от целите на инфраструктурната политика на Република България, като част от политиката за устойчиво регионално развитие, е да подпомогне обновяването и развитието на републиканската и местна пътни мрежа, за да има по-добра пътна достъпност между различните региони, както и във вътрешността на градските зони. [8]

Обединяването на територията на страната чрез по-добра достъпност и мобилност се явява фактор от решаващо значение за подобряване достъпа до здравни грижи, образование и културни събития, повишаване на регионалната конкурентоспособност, развитието и създаването на работни места и др. Тази интеграция е силно зависима от няколко основни инфраструктури – магистрали, първокласни и второкласните пътища, телекомуникациите и газоразпределителната мрежа и др.

## 1. Специфични особености и предизвикателства пред устойчивото развитие

Под „устойчиво развитие” следва да се разбира такова общество, което в отговор на изменение на вътрешните и външните условия е способно да установи ново, съответстващо на тези изменения равновесие както вътре в себе си, така и в цялата среда на своето съществуване.

Устойчивото развитие е концепция, която се изгражда върху основата на устойчиви форми на развитие, осигуряващи по-висока степен на функциониране на системата. Този процес не се откъсва от динамиката на разумното потребление. Устойчивото развитие е обективна необходимост и следва да се предприемат ефективни действия за неговото осъществяване. [2] Устойчивото развитие не трябва да се разглежда като застинал процес, константна на производство и потребление. Предизвикателство е да се намери баланс между икономическите, социалните и екологичните съображения в процеса на формулиране и приемане на политическите решения.

Проблемът е световен и безпрецедентен по своите мащаби и форми на проявление. Той обаче е нерешим без регионални и национални цели и стратегии за неговото осъществяване. Това дава основание да се обобщи, че устойчивото развитие е една прагматична потребност на бъдещето развитие на човечеството, императив, който няма политически алтернативи. [4]

За да бъде осигурена устойчивост, отделните политики, приети в краткосрочен план, е необходимо да бъдат съобразени с дългосрочните цели на ЕС. В контекста на Лисабонската стратегия това предполага съгласуваност между краткосрочните и дългосрочните цели, с оглед да се постигне баланс между политиката за ускоряване на растежа и увеличаване на заетостта, от една страна и целите, свързани с опазването на околната среда, от друга. Необходимо е ЕС и държавите-членки да разработят инструменти за оценка на въздействието, с чиято помощ ще имат възможност да вземат информирани и компетентни решения. Тези инструменти трябва да отчитат всички разходи и предимства, както краткосрочни и дългосрочни, така и конкуренцията в глобален мащаб. [1] Това е една необходима мярка за запазване на водеща позиция на Европа в света, в областта на опазването на околната среда, без да пренебрегва ефекта на ангажимента свързан с растежа и заетостта.

Достойният живот и благосъстоянието са невъзможни без грижа за средата, в която живее човека. Необходимо условие за достигането на тези цел е опазването на екосферата, от която зависи живота на всеки. [2]

В Стратегията за устойчиво развитие на Р България [10] са заложени цели, планирани са действия и инструменти, които интегрират

икономически, социални и екологически аспекти и представляват единна рамка за създаване на общи правила, процедури и изисквания при разработването на стратегически, планови и програмни документи с въздействие върху устойчивото развитие. В този смисъл документът продължава да се развива според потребностите на времето, тъй като основната му роля е да предизвестява навреме потенциалните заплахи пред устойчивото развитие и да инициира превантивни действия/дейности. Този документ влияе върху разработването или актуализирането на документи, свързани със секторни политики и програми за действие. Като национален документ Стратегията е ориентирана към националното устойчиво развитие и изпълнението на всички договори и конвенции по които Р България е страна в тази област. Тя е документ за социално и икономическо партньорство при широко участие на гражданското общество.

Някои от предизвикателствата за устойчивото развитие, които стоят и пред България се изразяват в следното:[11]

- Изменението на климата;
- Повишаване цените на енергията и ограничените възможности за нови енергийни източници;
- Растящия социален и регионален дисбаланс;
- Ускорената регионална интеграция в условията на глобална икономическа конкуренция, нарастваща зависимост между страни и региони в световен мащаб;
- Въздействието на разширяването върху икономическата, социалната и териториалната кохезия;
- Влиянието на застаряването на населението и миграционните процеси върху пазара на труда;
- Увеличаването на транспортния трафик;
- Свръх експлоатацията на екологичните ресурси и загубата на биоразнообразие, по-специално разширяване на урбанизираните територии и депопулация на някои райони.

За постигане на устойчиво развитие безспорен приоритет на ЕС е политиката за териториално кооперирание и устойчиво градско развитие. Основните приоритети на градското развитие в контекста на регионалното сближаване и в съзвучие с основните ключови политики на ЕС – Лисабонската стратегия и Обновената Стратегия за устойчиво развитие, както и Лайпцигската харта за устойчиви европейски градове и Териториалния дневен ред на ЕС са [5]:

- Засилване на регионалната идентичност и териториалното многообразие: процес на сътрудничество между централните и местните власти, частния сектор, научните среди, неправителствените организации;
- Засилване на иновативното градско развитие в градските агломерации, градовете и регионалните центрове чрез създаване на иновативни клъстери за сътрудничество между бизнеса, научните среди и администрацията;
- Нови форми на партньорство и териториално управление между градските и селските райони чрез разработване на общи стратегии за регионално развитие с привличане на частния сектор;
- Насърчаване на транс-европейското управлението на риска по отношение промяна на климата, крайбрежните и планинските зони;
- Нов подход към запазване на екологичното и културното многообразие чрез насърчаване на проекти, насочени към опазване на ландшафта;
- Опазване на здравето на населението;
- Укрепване и разширяване на транс-европейските мрежи чрез интегрирано развитие на транспортните системи, достъп до информационни и комуникационни технологии във всички региони, развиване на възможности за възобновяеми енергийни източници.

## 2. Предизвикателства пред развитието на транспортна инфраструктура на Република България

Главната социална функция на транспорта е да осигури достъп до основни услуги като здравеопазване, образование, търговия, туризъм, спорт и развлечения. Основните икономически и социални облаги от транспорта, които се балансират изключително трудно с високите социални разходи и разходите за околната среда, определят транспортния сектор като изключително важен за устойчивото развитие. Транспортът има значително негативно въздействие върху околната среда. Той влияе пряко върху биологичното разнообразие. Емисиите на замърсители в транспорта се отразяват върху качеството на въздуха и могат да увредят растенията и животните и по този начин да въздействат върху човешкото здраве.[10]

Една от целите на устойчивото развитие е задоволяването на нуждите от транспортни услуги да става с намаляващо вредно въздействие от дейността на транспорта.

Насоките в бъдещото развитие на сектора са постигане на устойчиви нива на потребление на енергия в транспорта, редуциране на емисиите от парникови газове и пренасочване на транспортната дейност към по-ефективни и благоприятни за околната среда видове транспорт.[9]

Основните показатели при задоволяване на потребностите от транспортни услуги са:

- Модернизиране на транспортната инфраструктура като ключов показател;
- Енергийното потребление в транспорта по видове транспорт;
- Разпределението на товарните превози по видове транспорт;
- Делът на международните превози в железопътния транспорт;
- Дял на електротранспорта от обема на градските превози;
- Делът на новорегистрираните и регистрираните нови МПС;
- Лицата, загинали при пътнотранспортни произшествия.

Проблем, идентифициран във връзка с характеристиките и качествата на инфраструктурата, е липсата на непрекъснати, последователни и постоянни транспортни мрежи, които да осигуряват бързо и безопасно придвижване на по-дълги разстояния. [9] Пример за това е липсата на автомагистрални връзки между главните градове и граничните контролно-пропускателни пунктове. Определените транспортни проекти, които са в процес на строителство, няма да задоволят този дефицит, а растежът на транспортното търсене ще засили проблема и ще продължи да се отразява неблагоприятно върху икономическото развитие на страната. Ако настоящите тенденции продължат, състоянието на голяма част от активите на транспортната мрежа ще се влошат. Допълнителното търсене на транспортни услуги ще доведе до претоварване и амортизиране на инфраструктурата и намаляване качеството на предоставяните услуги за потребителите. Въпреки прогнозния спад за България за броя на населението и растежа, собствеността на леките автомобили и личните доходи, и ако не бъдат извършени съществени промени в железопътните услуги (бързина и качество), до 2020 г. се предвижда спад в търсенето на железопътните пътувания.[8] След присъединяването на страната ни към ЕС, въздушните пътнически пазари показват високи темпове на растеж, свързани с развитието на бизнеса и туристическата индустрия.

Предизвикателствата пред въздушния транспорт са по-малко, отколкото за другите видове транспорт и са по-лесно преодолими. Ефективният интермодален транспорт, подкрепен от нови и подобрени терминали, има възможност да предостави значителни предимства в три области [7]:

- Подобряване на цялостната транспортна ефективност, което ще намали разходите на операторите и потребителите и ще подкрепи икономическото развитие;
- Намаляване на процента на нарастване на автомобилния товарен трафик чрез предоставяне на допълнителни стимули за използване на железопътен и воден транспорт, посредством подобрени интермодални съоръжения;
- Стимулиране на устойчиво развитие на транспорта и екологична защита чрез пренасочване на пътническия и товарен трафик от автомобилния транспорт към по-екологосъобразните видове транспорт.

**3. Приоритети и потенциали за развитие на транспортна инфраструктура**

Транспортният сектор на България е призван да съдейства за икономическото и социално развитие на страната, като осигурява ефикасен транспорт; подпомага балансираното регионално развитие; отчитайки кръстопътното положение на България и нейния транзитен потенциал, съдейства за пълноценното интегриране на страната в Европейските структури.

Към 2020 г. България, в съответствие с плановите документи, трябва да притежава модерна, безопасна и сигурна транспортна система, която да удовлетворява потребностите за качествен транспорт и да предоставя много по-големи възможности за избор на населението и бизнеса.[10]

Модернизирането на транспортната система е съществена необходимост за повишаване качеството на живота, за високото икономическо развитие и подобряване състоянието на околната среда. Устойчивото развитие на обществения транспорт, като част от развитието на сектора като цяло, е предпоставка за повишаване мобилността на населението и намаляване на социалната изолация на определени групи.

Транспортната политика на Република България следва изпълнението на глобалната мисия на транспортния сектор, която намира своето по-конкретно измерение в специфични стратегически приоритети.[9]

За ефективното поддържане, модернизация и развитие на транспортната

инфраструктура и интегриране на българската транспортна система в европейската е необходимо фокусиране върху изграждането, модернизацията и поддържането на транспортна инфраструктура, която е част от европейските транспортни коридори. Подобряването и развитието на инфраструктурните връзки и постигането на оперативна съвместимост, както и привличане на международен трафик ще повиши конкурентоспособността на българските транспортни фирми. Това би спомогнало за повишаване на ефективността на пазарите на стоки, услуги и работна сила. Интелигентните транспортни системи дават възможност за подобряване на екологосъобразността, ефикасността и безопасността на транспорта. [9]

Областите на въздействие, свързани с реализацията на тези политики, се изразяват в:

- Поддържане, модернизация и развитие на железопътна инфраструктура – държавата ще подпомогне изграждането на модерни железопътни линии по основните направления от Трансевропейската транспортна мрежа; с приоритизиране на проектите в съответствие с тяхната европейска „добавена стойност"; изграждане на железопътни връзки към пристанищата и летищата на страната; развитие на железопътните възли в транспортни центрове. [8]
- Поддържане, модернизация и развитие на пътната инфраструктура – Република България е поела ангажимент да подпомогне изграждане на автомагистралите по основните трасета от TEN-T; довършване и реконструкция на съществуващата пътна мрежа. Инвестициите са фокусирани върху АМ „Струма"; Довършване изграждането на АМ „Хемус"; Изграждане на АМ/СП „Черно море"; Изграждане на СП „Рила"; Изграждане на АМ „София – Калотина"; Изграждане на АМ „Марица"; Изграждане на АМ „Тракия". Очакваните резултати от изпълнение на мерките са: подобрена пътна инфраструктура; увеличена скорост; намалено времетраене за пътуване; увеличен трафик и капацитет на транспортната инфраструктура; повишена безопасност. [8]
- Подобряване корабоплаването по река Дунав чрез удълбочаване, изграждане на буни, укрепване на бреговете и др.; модернизация и оптимизация на дейностите по поддръжка на плавателния път с цел постигане на целогодишна плавателност по реката и повишаване на трафика [9].
- Развитие на транспортната инфраструктура чрез публично-частно партньорство. Предстои приключване на стартиралите процедури за отдаване на концесия на обекти от транспортната инфраструктура на страната; ефективна подготовка и последващо предоставяне на концесии на други обекти от транспортната инфраструктура (пристанища или пристанищни терминали, летища, железопътни гари и др.); осъществяване на контрол и др.
- Участие във формирането на европейската политика в областта на транспорта и укрепване на международното сътрудничество чрез хармонизиране на българското с европейското законодателство и участие в международни прояви, свързани с формирането на транспортната политика.
- Постигане на висока степен на безопасност и сигурност на транспорта – целта е подобряване на безопасността и сигурността на различните видове транспорт и опазване живота и здравето на потребителите на транспортни услуги, от една страна и от друга – повишаване на доверието.
- Създаване на нова и актуализиране на действащата нормативна база, за да подпомогне въвеждането на международните и европейски стандарти за безопасност и сигурност в различните видове транспорт.
- Повишаване на административния капацитет по отношение на контрола върху безопасността на транспорта и разследването на транспортни произшествия.
- Подобряване на технологичната среда за функциониране на информационните системи за контрол на транспортните процеси.
- Ограничаване негативното въздействие на транспорта върху климата, околната среда и здравето на хората. Чрез насърчаване употребата на горива и енергии от алтернативни и възобновяеми енергийни източници, развитие и увеличаване на дела на екологосъобразните видове транспорт.

Добре би било държавата да съдейства за изграждане и въвеждане в експлоатация на интелигентни транспортни системи по републиканската пътна мрежа и вътрешноградския транспорт в големите градове; за увеличаване дела на биогоривата за автомобилния транспорт. Да се стимулира ползването на „хибриден" и електрически автомобилен транспорт.

Необходимо е да се създаде благоприятна среда и предпоставки за съществен ръст на превозите с интермодален транспорт и комбинираните превози. Като се насърчи използването на обществен транспорт за да се намалят пътуванията с лични моторни превозни средства.

Обновяването и модернизацията на транспортния парк, инсталациите и съоръженията може да се реализира с подкрепа на държавата чрез разработване на политика за симулиране обновяването на транспортния парк и модернизация на подвижния състав в железопътния сектор, както и на модернизация на транспортния парк в автомобилния сектор.

Устойчиво развитие на масовия обществен транспорт е възможно чрез подготовката на инвестиционни проекти за реконструкция и рехабилитация на разпределителните пътища (II клас) и пътища за достъп (III клас). Подобрението на транспортна инфраструктура подобрява свързаността на регионите и общините и осигуряването на по-добър достъп до всички национални обекти.

Строителството на модерна транспортна инфраструктура е изисква време, дългосрочен подход и осигуряване на стабилни финансови потоци, както и решителност и ангажираност на всички институции и организации, имащи отношение към този процес. От голямо значение е усвояването на средства от европейските фондове, за което е наложително да се подготвят жизнени инфраструктурни проекти и съфинансиране от държавата.

**Заключение**

В резултат на изследването може да се обобщи, че България разполага с достатъчна гъстота на транспортната инфраструктура. Основен проблем, идентифициран във връзка с характеристиките и качествата на инфраструктурата обаче е липсата на непрекъснати, последователни и постоянни транспортни мрежи, които да осигуряват бързо и безопасно придвижване на по-дълги разстояния, което се отразява негативно върху възможностите за устойчиво развитие. Пример за това е липсата на автомагистрални връзки между главните градове и граничните контролно-пропускателни пунктове.

Поради постоянния недостиг на средства, приблизително една трета от републиканската пътна мрежа е в лошо експлоатационно състояние и се нуждае от спешни мерки за привеждане към проектните параметри. Също така е необходима модернизация на съществуващите пътища и повишаване на товароносимостта им. [9] Транспортните проекти, които са в процес на строителство, няма да разрешат този въпрос, растежът на транспортното търсене предстои да засили проблема и да продължи да се отразява неблагоприятно върху икономическото и социално развитие на страната, както и на околната среда.

Преодоляването на дефицитите чрез успешно резлизиране на потенциалите за подобряване на транспортната инфраструктура в България, ще предостави равни възможности на гражданите за достъп до здравни услуги, качествено образование, възможности за подходяща работа, екологично чиста околна среда и осигуряване на благоприятна бизнес среда – задължително условие за постигане на устойчиво развитие.

## ЛИТЕРАТУРА


1. Андонова, К. Интегрирано регионално развитие. Теоретични и приложни аспекти. Варна, УИ на ВСУ „Ч. Храбър“, 2012.
2. Беев, И. Концепцията за Устойчиво развитие: конкурентен ред или нормативна регулация, УНСС. 2010.
3. Великова, М. Политики и практики в местното самоуправление. Варна, УИ на ВСУ „Ч. Храбър“, 2008.
4. Григоров, Н. Устойчивото развитие в Р.България , учебно пособие, Варна, 2000/2001
5. Крамер, Л., Европейско право на околната среда, София, 2009.
6. Насоки на ЕС за развитие на Трансевропейската транспортна мрежа за периода 2014-2020
7. Оперативна програма „Региони в растеж“ за периода 2014 – 2020 г.
8. Национална програма за развитие: България 2020.
9. Национална стратегия за устойчиво развитие на Република България за периода 2007-2013.
10. Стратегия за развитие на транспортната инфраструктура на Република България до 2015 г.
11. Официален сайт на МРРБ:



Контакти:
Д-р Иванка Банкова
Гр. Варна – 9007
К.к. „Чайка“
ВСУ „Черноризец Храбър“
Катедра „Администрация, управление и политически науки“
E-mail: bankova.v@gmail.com

© International Scientific Conference on Engineering, Technologies and Systems
TECHSYS 2016, Technical University – Sofia, Plovdiv branch
26 – 28 May 2016, Plovdiv, Bulgaria

# ОЦЕНЯВАНЕ НА РЕЗУЛТАТНОСТТА НА СЪТРУДНИЧЕСТВО В БИЗНЕС МРЕЖИ

СВЕТОСЛАВ ДИМКОВ[1], ОТМАН АХМЕД[2]

**Резюме:** *Понастоящем съществуват твърде малко теоретични разработки върху оценяване на сътрудничество в бизнес мрежи, като почти не съществуват разработки, в които сътрудничество да се оценява на база на комплексни индикатори. Настоящата работа прави опит за преодоляване на тази ситуация чрез предлагане на концептуален модел за оценяване на резултатността на сътрудничество в бизнес мрежи. С помощта на разработения модел се анализират последиците от сътрудничество. На база на обстоен литературен анализ са формулирани тестови индикатори, които могат да спомогнат за подобряване на резултатност на сътрудничество.*

**Ключови думи:** *колаборативни иновации, бизнес мрежи, динамични виртуални предприятия*

# ASSESSING THE EFFECTIVENESS OF COLLABORATION IN BUSINESS NETWORKS

SVETOSLAV DIMKOW[1], OTMAN AHMED[2]

**Abstract:** *There are currently too little theoretical work on the evaluation of collaboration in business networks, as there are hardly any studies in which collaboration can be estimated on the basis of complex indicators. This work attempts to overcome this situation by offering a conceptual model for assessing the effectiveness of collaboration in business networks. Using the developed model helps to analyze the effects of cooperation. Based on a detailed literary analysis are formulated test indicators that can help improve the effectiveness of cooperation..*

**Key words:** *collaborative innovations, business networks, dynamic virtual enterprises*

## 1. Въведение

В днешно време жизнения цикъл на продуктите все повече се съкращава като същевременно рязко нараства търсенето на персонализирани продукти. Това са два от факторите, които тласкат към сформирането на бизнес мрежи, при които създаването на компонентите на продуктите и асемблирането им е разделено между различни партньори. При повечето от съвременните продукти броят на доставчиците е значителен, разнообразието на компонентите е голямо, а производствените технологии при компонентите са твърде различни. Всичко това поражда твърде сложни взаимоотношения в бизнес мрежите и твърде сложни задачи при планиране, организиране и координиране. Участниците в бизнес мрежите са с необвързани интереси, така че постигането на сътрудничество с традиционни управленски методи е твърде трудно и рисковано. При изпълнение на клиентска поръчка ако един от участниците в мрежата закъснее с доставката, това силно застрашава завършването на поръчката и поражда риск от анулирането й. В крайна сметка всичко това подкопава конкурентоспособността на мрежата. Следователно, усъвършенстването на координирането на взаимодействията и синхронизирането на дейността на множество партньори силно ще повиши способността за реагиране на клиентски поръчки и значително ще повиши резултатност на бизнес мрежите.

Едно управленско средство със значителна мощ, с което може да се решат

Copyright © 2016 by Technical University of Sofia, Plovdiv branch, Bulgaria ISSN Online: 2535-0048

споменатите проблеми са динамичните виртуални предприятия. Те са ефективно и гъвкаво средство за реализиране на сътрудничество при изпълнение на клиентски поръчки. Но за ефективното функциониране на тези виртуални предприятия е необходимо разработването на система за ефективно оценяване на резултатност на сътрудничество и дефиниране на ефективни средства за непрекъснато усъвършенстване на сътрудничеството в дългосрочен план.

През последните години изучаването на резултатност на сътрудничество се взема все по-сериозно от теоретици и експерти. Но все още съществуват твърде оскъдни проучвания върху резултатност от сътрудничество, а още по-малко върху резултатност от сътрудничество при бизнес мрежи и динамични виртуални предприятия. Затова настоящата работа се фокусира върху разработването на система за оценяване на резултатност при сътрудничество, базиране на система от индикатори. Тази система можа да послужи за основа при оценяване на резултатност от сътрудничество при реализиране на конкретни динамични виртуални предприятия.

## 2. Сътрудничество при реализиране на иновации

През последните години три драстични промени (технологична, информационна, институционална) коренно променят бизнес средата, в която възникват бизнес стратегиите. Резултат от този рязък преход е възникването на т.нар. „Нова икономика". Взети заедно, тези промени имат за резултат ескалиране на конкуренцията, налагане на строги императиви за ориентирани към потребителите стратегии, чрез които да се постигне бърза реакция на променящото се потребителско търсене и на силно разширената продуктова диференциация, чрез която се удовлетворят потребителските изисквания. Всички тези фактори пораждат нови императиви, които могат да се формулират най-общо като „Иновации от изтеглящ тип" (pull innovation). Основна черта на тези иновации е сътрудничеството между бизнес организациите.

Намбисан [1] дефинира колаборативните иновации като колективен подход към създаване на иновации и разрешаване на проблеми, който се базира на впрягане на ресурси и креативност от външни мрежи и общности с цел усилване и усъвършенстване на иновационния процес и разширяване на мащаба и качеството на иновационните резултати. От тази гледна точка може да се определи и основната характеристика на колаборативните иновации - иновационен процес от отворен тип, при който на най-ранен стадий действащи лица от една организация, други организации и посредници са интегрирани в иновационния цикъл (генериране на идеи; избор; реализация; разпространение). Следователно, траекторията на развитие на иновациите трябва да се определя от наличността на иновационни активи, а не от формалните граници на една организация. Нещо повече, ролята на действащите лица в по-малка степен се определя от формални правила, а по-скоро от степента на съответствие между проблемите и наличните иновационни активи. Съобразно наличността на иновационни активи иновационният цикъл може да се разпредели между действащите лица или да се осъществи от една организация. В това отношение значима е ролята на информационните технологии. Те са основното средство за изграждане на бизнес мрежи и за осигуряване на непрекъснат поток от идеи и информация.

## 3. Влияние на колаборативните способности върху организационната резултатност

Според Хаймерикис [2], резултатността на бизнес мрежи се влияе от способностите им и от качествата на връзките им, които обхващат редица икономически и социални фактори. Конфигурирането на ресурсите, съвместимостта на партньорите и координацията са икономическите фактори, докато доверието, ангажираността и комуникативността са релационни фактори.

Релационните фактори (доверие, комуникативност и ангажираност) могат да имат и ключово значение на вътрешно (интра) организационно сътрудничество, когато неформалното сътрудничество се проявява като комуникиране и координация. Така може да се постигне нарастване на организационната резултатност чрез по-добра координация между организационните звена [3].

На ролята на сътрудничеството се набляга в ситуации на висока пазарна или технологична неопределеност или организационна комплицираност.

Ефектът на сътрудничеството върху организационната резултатност е по-силен при сложни продукти и услуги [4] или при неопределени и променящи се икономически условия. При такива условия способностите да се сътрудничи са от ключово значение в условията на т.нар. „Нова икономика", когато конкурентоспособността се базира на знания и на непрестанни иновации.

Тейлър [5] счита, че способността да се сътрудничи може да компенсира умерени и дори посредствени технологични умения, когато една организация преследва технологични иновации. Ако тези способности се считат за допълващи на технологичните способности, такова съчетание под формата на мета способности може да позволи непрекъснато развитие на динамични способности, които играят ключова роля за организационната резултатност и са източник на устойчиво конкурентно предимство [6].

## 4. Концепция за оценяване на резултатност при сътрудничество

За да се създаде концепция за оценяване на резултатност при сътрудничество при динамични виртуални предприятия най-напред трябва да се изяснят нейните основни елементи. Т.е., трябва да се изясни какво ще се оценява, как ще се оценява и как ще изглеждат резултатите от оценката. Предлаганата от авторите концепция обхваща седем компонента (фиг. 1): обект на оценката на резултатност; базов модел за оценяване на резултатност; система от показатели за оценяване на резултатност; добри практики (стандарти, бенчмарк) за оценяване на резултатност; методи за оценяване на резултатност; организиране на процеса за оценяване на резултатност; резолюция съобразно оценката за резултатност.




***Фиг. 1.*** *Концепция за оценяване на резултатност при сътрудничество*

**Обект на оценката на резултатност.** Обектът на оценката за резултатност са динамични индустриални предприятия от гледна точка на интересите на всички заинтересовани страни: клиенти подаващи поръчките; модератори на дейността във виртуално предприятие (контрактори); изпълнители на отделни дейности по изпълнението на поръчките (субконтрактори). Тъй като броят на участниците в бизнес мрежите е значителен, то оценяването на всички дейности по обработката на клиентските поръчки е твърде трудно. Затова е необходимо формулиране на система от цели на динамичното виртуално предприятие, която да отчита индивидуалните целите, роли и бизнес процеси на всеки от ангажираните за изпълнението на конкретна клиентска поръчка.

**Базов модел за оценяване на резултатност.** По същество базовият модел представлява референтен модел, който спомага за формирането на комплексни индикатори на резултатност. При оценяване на резултатност най-често се използват финансови показатели; ключови показатели за резултатност (Key Performance Indicators KPI); процесно ориентирани показатели (SCOR модел); стратегически ориентирани показатели (Balanced Scorecard - BSC). Архитектурата на предлагания базов модел се базира на процесно ориентирани показатели (SCOR модел) и е представена на фиг. 2.




***Фиг. 2.*** *Базов модел за оценяване на резултатност при сътрудничество*

**Система от показатели за оценяване на резултатност.** Системата от показатели за оценяване на резултатност обхваща ключови показатели за резултатност (Key Performance Indicators KPI), чрез които ще се извършва оценката. Системата използва комплексни индикатори, които се изчисляват на база на първични показатели. Оценката на резултатност се извършва чрез качествено и количествено определими индекси.

**Добри практики (стандарти, бенчмарки) за оценяване на резултатност.** Добрите практики за резултатност са критерии за преценка на получените резултати. Дефинирането на добри практики (стандарти) се основава предимно на очаквания и желани цели. Получаваните индекси за оценка на резултатност трябва да включват показатели,

които правят резултатите от оценяването сравними и съпоставими с целите (бенчмарки). На практика количествените индикатори (бенчмарки) се определят на база на предходни данни за резултатност на бизнес процеси и под процеси, на очаквания за целевите стойности в бъдеще, на данни за резултатност на конкуренти, на преценки на експерти и др. Качествено определимите индекси(бенчмарки) се определят на база на дискусии с експерти от проблемите области, Делфи метод и др.

**Методи за оценяване на резултатност.** Методът за оценяване на резултатност е специфично средство за определяне на крайните резултати чрез изчисляване на специфични стойности, които се сравняват с критерии за оценка. Чрез такива методи се гарантира, че се правят правилни изводи на база на научно обосновано оценяване. Тъй като в едно динамично виртуално предприятие са ангажирани множество заинтересовани субекти, всеки от които има свои необвързани интереси, оценяването е твърде сложно и многоцелево, включващо множество индекси. Крайната преценка се прави на база на многокритериална оценка на синергията от сътрудничество.

**Организиране на процеса на оценяване на резултатност.** Чрез организацията на процеса на оценяване се определят отговорностите на всеки от участниците в процеса и се подрежда във времето и пространството протичането на процеса. Системата за оценяване при реализиране на динамични виртуални предприятия включва множество индустриални предприятия, които са в отношения на кооперирание, което прави процеса на организиране твърде сложен, а реализирането му на практика още по-сложно. Също така е твърде сложно да се формира система от подходящи компенсации на усилията и наказателни мерки тъй като тези средства при сътрудничество са твърде различни от средствата вътре в предприятията. Но във всички случаи ядрото на системата за оценяване на резултатност при сътрудничество трябва е във водещо предприятие (примерно контрактор при определена клиентска поръчка). Това е основният изпълнител на поръчката, който възлага на субконтрактори отделни елементи на продуктите или отделни бизнес процеси. Контракторът е модератор на динамичното виртуално предприятие, чиято основна роля е посредничество между възложителя (потребителя) и останалите участници във виртуалното предприятие. Архитектурата на системата за оценяване се базира на общите цели на сформираното динамично индустриално предприятие и отчита интересите на всички участници в него, изразявани на база на консенсус между всички участници относно индикатори, стандарти и методи за оценка и др.

**Резолюция съобразно оценката за резултатност.** Резолюцията изразява постигнатите резултати от системата за оценяване на резултатност от сътрудничество. Това е окончателната преценка, базирана на стойностите на всички индикатори (индексите) и на всички събрани данни, резултати от статистическа обработка и анализи. Всичко това формира рамка за вземане на управленски решения, свързани със сътрудничество.

Разгледаните по-горе елементи са в тясно взаимодействие, функционират едновременно изглаждат цялостна система за оценяване на резултатност от сътрудничество.

## 5. Проектиране на система за оценяване на резултатност от сътрудничество

В настоящата работа сътрудничеството се дефинира като: Базирана на интегриране на ресурси делова дейност, чийто процеси се реализират чрез управленски методи и средства като: споделяне на информация; централизирано доставяне на елементи и компоненти за продукти; вертикално синхронизиране на взаимодействията с потребителите; хоризонтални взаимодействия между субконтракторите. Основната цел е: минимизиране на времето за реакция на клиентски заявки; минимизиране на разходите за запаси; максимизиране на резултатност на динамичните виртуални предприятия.

Съчетано с интегрираните бизнес процеси сътрудничеството при динамични виртуални предприятия включва следните елементи:

- **Синергия между модератора на виртуалното предприятие (контрактора) и заявителите на продукти.** Въз основа на изграденото с течение на времето доверие (съвместното участие в бизнес мрежата) следва да се формира дългосрочно базирано на сътрудничество партниране и съвместно планиране на деловата дейност. С това се цели подобряване на качеството на създаваните продукти и цялостната ефикасност на бъдещи динамични виртуални предприятия;
- **Синергия между модератора на виртуалното предприятие (контрактора) и субконтракторите.** Контракторът трябва да осигури безпроблемни взаимодействия с

всички субконтрактори за да може да планира реакцията си на постъпилите заявки за продукти. Управлението на търсенето от страна на контрактора успешно се реализира чрез обмен на информация и съвместно проектиране на бизнес процеси;

- **Сътрудничество между субконтракторите в дефинираното динамично виртуално предприятие.** Търсенето на определени елементи за създаваните продукти много тясно обвързва създаващите отделните елементи субконтрактори. Затова да се постигне максимална резултатност на сътрудничеството трябва да се осигури и тясно сътрудничество между всички субконтрактори. Интеграцията между контрактор и заявители и контрактор и субконтрактори може значително да се улесни чрез постигане на сътрудничество между субконтракторите;

  -Способности за реализиране на логистично обслужване. За постигане на максимална ефективност на сформираното динамично виртуално предприятие трябва да се формират способности за организиране на логистичното обслужване при изпълнение на клиентските заявки – постигане на желана степен на сътрудничество; навременност на доставките; качество и ефикасност на логистичното обслужване.
- **Поддържане на сътрудничеството от модератора на динамичното виртуално предприятие.** Става въпрос най-вече за планиране, организиране и контролиране на дейностите (бизнес процесите) за взаимодействията във виртуалното предприятие и непрекъснатото им усъвършенстване. Чрез поддържането на сътрудничеството от страна на модератора се постигат редица значими цели като: съкращаване на сроковете за изпълнение на клиентски поръчки; минимизиране на загубите; ловко управление на разходите; постигане на гъвкави реакции; интензивен обмен на информация и др.

## 6. Избор на йерархична система от индикатори

Основно изискване към системите показатели за оценяване на резултатност от сътрудничество е обосноваността на избора на първични показатели. Постигането на значително подобряване на обосноваността може да се постигне чрез обстойно литературното проучване и интервюиране на експерти от изследваните индустриални сектори [7]. За да гарантират обосноваността на избраните първични показатели за разработваната йерархична система от индикатори авторите на настоящата работа са извършили обстойно литературно проучване на взаимоотношения в различни бизнес мрежи и са провели серия от разговори с мениджъри на предприятия от българския мебелен клъстер. В резултат на всичко това е разработена система от 20 първични показателя, които са групирани в четири групи. На базата на четирите групи първични показатели са дефинирани четири специализирани индикатора, чрез които се характеризират взаимоотношенията между: заявител-контрактор; контрактор-субконтрактори; контрактор-контрактор; заявител-субконтрактори.

## 7. Заключение

В настоящата работа е представен методологичен подход за оценяване на резултатност при сътрудничество, който има потенциал да подпомогне бизнес организациите при оценяване и усъвършенстване на начинания за колаборативни иновации. Чрез литературното проучване са идентифицирани факторите, които имат положително и отрицателно въздействие върху процесите, свързани с реализация на колаборативни иновации.

Това е начална версия на модел за оценяване на резултатност при сътрудничество, която изисква по-нататъшно усъвършенстване и оценяване в практически условия.

Предвижда се валидирането на разработения модел да се възложи на експертна група от мениджъри от предприятията на български мебелен клъстер. На всички участници в групата ще се предостави пълна информация за структурата и характеристиките на модела, съпроводена с въпросник. Получената обратна връзка ще се анализира от авторите и ще се извършат усъвършенствания и корекции. Предвижда се с усъвършенствания модел да се извърши изследване на колаборативните иновации в предприятията от български мебелен клъстер на база на конкретни иновационни решения. Основна цел на замисленото изследване е да се тества валидността на модела и да се идентифицират областите, в който той проявява несъвършенства.

**ЛИТЕРАТУРА**


1. Nambisan, S., Agarwal, R., & Tanniru, M. (1999). Organizational mechanisms for enhancing user innovation in information technology. *MIS quarterly*, 365-395.
2. Heimeriks, K., & Schreiner, M. (2002). Alliance capability, collaboration quality, and alliance performance: An integrated framework. *Eindhoven Center for Innovation Studies,* Eindhoven, 31-49.
3. Schramm-Klein, H., & Morschett, D. (2006). The relationship between marketing performance, logistics performance and company performance for retail companies. *International Review of Retail, Distribution and Consumer Research,* 16(02), 277-296.
4. Kahn, K. B., & Mentzer, J. T. (1996). Logistics and interdepartmental integration. *International Journal of Physical Distribution & Logistics Managemen*t, 26(8), 6-14.
5. Tyler, B. B. (2001). The complementarity of cooperative and technological competencies: a resource-based perspective. *Journal of Engineering and technology management,* 18(1), 1-27.
6. Miles, R. E., Miles, G., & Snow, C. C. (2005). *Collaborative entrepreneurship: How communities of networked firms use continuous innovation to create economic wealth.* Stanford University Press.
7. Hensley, R. L. (1999). A review of operations management studies using scale development techniques. *Journal of Operations Management,* 17(3), 343-358.



Контакти
Адрес
Технически университет – София
Стопански факултет
Климент Охридски 8
1756 София
[1]E-mail: sdim@tu-sofia.bg
[2]E-mail: otman1980@yahoo.com

© International Scientific Conference on Engineering, Technologies and Systems
TECHSYS 2016, Technical University – Sofia, Plovdiv branch
26 – 28 May 2016, Plovdiv, Bulgaria

# РАЗВИТИЕ НА БИЗНЕС ОРГАНИЗАЦИИТЕ ЧРЕЗ КОЛАБОРАТИВНИ ИНОВАЦИИ

СВЕТОСЛАВ ДИМКОВ

**Резюме:** *В настоящата работа се изказва мнението, че съществува необходимост от нова форма на иновации в развитието на бизнес организациите поради факта, че традиционният (затворен) подход за извършване на иновации не допринася за решаване на възникващите в съвременната бизнес среда проблеми. Целта на настоящата работа е идентифициране, анализиране и систематизиране на характеристиките на колаборативните иновации и проучване на възможностите за приложението им в българската бизнес практика.*

**Ключови думи:** *колаборативни иновации,отворени иновации, иновационен процес*

# DEVELOPMENT OF BUSINESS ORGANIZATIONS THROUGH COLLABORATIVE INNOVATIONS

SVETOSLAV DIMKOW

**Abstract:** *This work expresses the opinion that there is a need for a new form of innovations in the development of business organizations because traditional (closed) approach for innovations does not contribute to solving emerging in today's business environment issues. The purpose of this work is to identify, analyze and systemize the characteristics of collaborative innovation and exploring the possibilities for their application in Bulgarian business practice.*

**Key words:** *collaborative innovations, open innovations. Innovation process*

## 1. Въведение

В работата се прави анализ на колаборативни иновации с доставчици и индивидуални и бизнес потребители. Под колаборативни иновации авторът разбира процес на ангажиране при създаване на нови продукти и услуги. Колаборативните иновации са една от формите на т.нар. „отворени иновации" [1], които могат да се определят като системно търсене, съхраняване и използване на знания в и извън границите на бизнес организациите при протичане на иновационния процес [2]. Концепцията по принцип включва съчетани процеси и потоци знания в и извън бизнес организациите [1,2]. Отворените иновации дават представа, доколко границите на организациите са пропускливи за потоци знания [3].

Колаборативните иновации са по-всеобхватни от отворените иновации, защото обхващат процеси в които бизнес организациите и потребителите се ангажират при създаване на съвместни иновации.

Целта на настоящата работа е идентифициране, анализиране и систематизиране на характеристиките на колаборативните иновации и проучване на възможностите за приложението им в българската бизнес практика.

## 2. Сътрудничество при реализиране на иновации от изтеглящ тип

През последните години три драстични промени (технологична, информационна, институционална) коренно променят бизнес средата. Резултат от този рязък преход е възникването на т.нар. „Нова икономика". Взети заедно, тези промени имат за резултат

Copyright © 2016 by Technical University of Sofia, Plovdiv branch, Bulgaria ISSN Online: 2535-0048

ескалиране на конкуренцията, налагане на строги императиви за реализирани ориентирани към потребителите стратегии, чрез които да се постигне скоростна реакция на променящото се потребителско търсене и силно изразена продуктова диференциация. Всички тези фактори пораждат нови условия, които могат да се формулират най-общо като „Иновации от изтеглящ тип" (pull innovation). Основна черта на тези иновации е сътрудничеството между бизнес организациите.

Възникването на новата ориентация на процесите има каталитичен ефект върху бизнес организациите да разширят концепциите си за процеси от изтеглящ тип и да увеличат потенциала на иновационните си процеси. Изтеглящите иновации разширяват иновационния фокус от вътрешно организационни вертикални (йерархични) процеси към изграждане на системи за създаване на стойност (познати още като стойностни мрежи - value network), които се разпростират вертикално и хоризонтално вътре в организациите и частично до външни бизнес организации, ангажирани с доставката на продуктите до потребителите.

Основна организационна промяна, свързана с изтеглящите иновации е сътрудничеството между бизнес организациите. Сътрудничеството отдавна е считано за ценно средство за подобряване на иновациите. Ползата произтича от споделянето на знания и последствията от това върху иновациите. В условията на т.нар. „Нова икономика" търсенето на сътрудничество за обмен на знания е естествен резултат от специализацията и заслужава особено внимание. Но съществува и втори мотивационен фактор за сътрудничество. Сътрудничеството е основно средство за реализиране на процес на проектиране на продукти, който се простира отвъд организационните граници и достига до потребителите.

Прилагането на колаборативни иновации за бизнес системи от изтеглящ тип при новата икономика се разраства, тъй като организациите стават все по-необвързани и по-специализирани. Третирането на знанията като организационни активи и ясното разграничаване на експлицитни (документирани) от имплицитни (скрити) знания налага схващането за разглеждане на знанията като ограничени ресурси. От тази гледна точка днес бизнес организациите са принудени да търсят достъп до външни източници на знания, вместо да създават знания вътрешно организационно. По този начин, знанията се превръщат в най-обменяния ресурс, който е и катализатор на сътрудничеството. Докато значителна част от експлицитните знания могат да се открият в готови продукти, имплицитните знания, които са от ключово значение за познаване на процесите, трябва да се придобият. Нуждата от придобиване на такива знания за разширяване на познавателните области на организациите пораждат усилия за колаборативни иновации.

## 3. Колаборативни иновации с потребители

Значението на сътрудничеството с потребителите при разработване на иновативни продукти и услуги се признава отдавна. В резултат на това, такова сътрудничество става основен компонент на усилията на много развиващи се организации.

Последствията от съвместни иновации с потребители са значителни тъй като се извършва промяна на бизнес парадигмата. Днес бизнес организациите натрупват знания от потребителите си, а съвременните технологии тласкат иновациите напред все по-бързо, възникват отворени форми на иновации [4,5,6,7].

Бизнес организациите оперират при все по-тясно сътрудничество с доставчици и потребители за получаване на нови идеи и знания от тези външни източници [8,9]. Намаляването на икономиите от мащаб от изследователската и развойна дейности пораждат такива сътрудничества [10,11]. Разрастването и разширяването на сътрудничеството между бизнес организациите трансформира естеството на конкурирането и кооперирането [6].

## 4. Оценяване на колаборативни иновации

Един от основните критерии за оценяване е, дали колаборативните иновации спомагат да се преодолеят рестриктивните аспекти на бизнес средата. Колаборативните иновации трябва да са способни да влияят върху социо-техническата среда на една организация.

Като реакция на ограниченията пред една бизнес организация колаборативните иновации трябва да спомагат за: отваряне на иновационния цикъл към вътрешно организационни и външни иновационни активи; улесняване на поемането на рискове; насърчаване на позитивната нагласа към извършването на иновации и поемането на риск в условията на съвременната бизнес среда.

Колаборативните иновации отварят иновационния цикъл за разнообразна група

действащи лица в рамките на организационната йерархия и извън границите на една организация [12,13,14]. Чрез отваряне на иновационния цикъл се позволява протичането на иновационни активи в границите на бизнес организациите и извън тях. Следователно, иновационният процес има потенциал да подобри елементите на иновационния цикъл по алтернативни начини.

Генерирането на идеи се опростява защото организациите използват широка гама от знания и експертизи в и извън границите си [15]. Реализирането и разпространението на идеи се улеснява поради подкрепата, която оказват действащите лица, участващи в генерирането и избора на идеи. Те са по-склонни да приемат иновациите и да поемат отговорности. Колаборативни иновации предоставят на организациите благоприятни възможности да насочат реализацията и разпространението на идеи към действащи лица, които са с най-значими способности и така да укрепят реализирането и елементите на разпространението на иновационния цикъл.

## 5. Ръководене и управление на колаборативни иновации

Пречките при колаборативни иновации могат да се отстранят или минимизират чрез упражняване на подходящо ръководене и управление [16,17]. При твърде сложните процеси на колаборативни иновации много неща могат да се объркат между намерения и изпълнение.

**На първо място** събирането на подходящи и ангажирани действащи лица в устойчиви взаимодействия може да се провали поради: липса на минал опит и традиции във взаимодействията; негативни възприятия от предишни взаимодействия; трудности за мотивиране на подходящи действащи лица да отделят време и да положат усилия за интерактивно участие [16].

**На второ място** когато действащите лица се съгласят да взаимодействат, често това е поради това че осъзнават нуждата да обменят и обединяват идеи и ресурси с цел да разрешат спешни или значими проблеми. Но взаимодействията не винаги стимулират сътрудничеството поради надделяване на конфликта на интереси. Освен това сътрудничеството маже да се провали поради надделяване на недоверие и опортюнистично поведение, наличие на процедурна неопределеност и наличие на несъвместими и деструктивни познавателни модели [16,18,19].

**На трето място** когато действащите лица се ангажират с процеса са сътрудничество те могат да не допринесат за създаване на иновации. Повтарящи се прояви на сътрудничество в затворени и устойчиви бизнес мрежи с едни и същи участници, които с течение на времето са развили сходни гледища за света, ще задушават творчеството, ще възпират създаването, прототипирането и реализирането и нови и смели идеи и ще снижават разпространението на иновациите [20].

В обобщение, съществува опасност различни препятствия да нарушат връзката между взаимодействие, сътрудничество и иновации. Добрите намерения за общуване с цел сътрудничество и изучаване и експлоатиране на нови идеи не са достатъчни за реализиране на колаборативни иновации. За да се постигне устойчивост на процеса на колаборативни иновации трябва да се приложат уместни методи за ръководство и управление.

**На първо място** с цел да се създаде добре функционираща интерактивна среда с активни и ангажирани действащи лица ръководителите и мениджърите трябва да оперират като организатори [21]. Организаторите имат за цел да мотивират, упълномощават и да обединяват действащите лица, да създават и формират интерактивна среда, да определят дневния ред на взаимодействията, да изясняват интерактивните процеси и да насърчават взаимното нагаждане на очакванията [16].

**На второ място**, ръководителите и мениджърите трябва да насърчават и улесняват сътрудничеството между заинтересованите субекти оперирайки като посредници. Посредниците имат за цел да формират или изясняват взаимно обвързаности, да управляват процеса на сътрудничество чрез декомпозирането му на различни етапи, да формират доверие и да разрешават спорове чрез съгласуване на интереси на базата на общи модели и да отстраняват препятствия пред сътрудничеството [18,22].

**На последно място** напредъкът на колаборативни иновации може да се подпомогне ако ръководителите и мениджърите изпълняват ролята на катализатори, които прилагат предприемачески подходи за ръководене и управление. Катализаторите спомагат за преформатиране на проблемите давайки нови знания и нови роли на действащите лица, извличат полза от съществуващите и възникващите ограничения и благоприятни възможности, управляват риска и насърчават трансформиращото натрупване на знания и нетрадиционно мислене [22].

## 6. Съвместно създаване на продукти с потребители

Бизнес организациите се сблъскват с различни източници на неопределеност, породени от техните технически и управленски способности и от целевите пазари. Томке [23] класифицира неопределеностите, свързани с иновационни проекти на: технически, производствени, потребностни и пазарни. За минимизиране на тези неопределености бизнес организациите трябва трансферират и да имат достъп до различни типове информация [24].

Днес общото разбиране за иновационен процес се основава на схващането, че бизнес организациите рядко извършват иновации сами, а иновационният процес се основава на интерактивни взаимоотношения между създатели на продукти, потребители и много други различни институции [25].

Отворените иновации се характеризират с кооперирание за извършване на иновации в рамките на мащабни хоризонтални и вертикални мрежи от университети, стартиращи бизнес организации, доставчици и конкуренти. Бизнес организациите трябва да използват както свои идеи от развойните си звена, така и идеи от външната среда и трябва да използват вътрешни и външни пътища за достъп до пазарите с цел да постигнат напредък на технологиите си.

Целта е да се получи достъп до външна информация, с което да се минимизират неопределеностите в иновационните проекти. Неформалните отношения дефинират иновативността на отворените иновации. Отворените иновации се простират извън обичайните договорни отношения за създаване на съвместна стойност. Те включват нови форми за създаване на стойност, които се базират на неформални, недоговорни, гъвкави и краткосрочни взаимоотношения.

Достъпът до потребителска информация е едно от основните изисквания за всяка иновация. Съществуват два традиционни подхода за придобиване на такава информация. Входящи данни от потребители могат да бъдат придобити или явно чрез допитване до потребителите относно нуждите и предпочитанията им посредством маркетингови проучвания и анкетиране на фокус групи, или чрез проучвания в сферата на потребителите (анализиране на данни за продажби, Интернет съдържание, анкетиране на сътрудници по продажбите).

Потребителите могат да имат различни роли в иновационния процес. Едни потребители могат да предоставят ключова информация за бъдещи тенденции и възможни технологични решения, а други да са по-подходящи за оценяване на иновативни концепции или за участие в прецизиране на прототипи. Всички тези роли гравитират около три начина за използване на генерираната от потребителите информация при разработване на нови продукти:

- проучване в средата на потребителите;
- допитване до потребителите;
- създаване на иновации с потребителите.

**Проучване в средата на потребителите.** При този подход продуктите се проектират от името на потребителите. Това е типичното схващане за т.нар. „Пазарна ориентация". Бизнес организациите използват съществуващата потребителска информация от различни източници като: обратна връзка от сътрудници по продажбите; анализиране на данни за продажби от предходни периоди; анализиране на Интернет съдържание; отчети от проучвания на трети страни и др. за определяне на потребителските нужди [26]. Друг значим източник при този подход са анализи на резултатност на съществуващи продукти (на самата организация и на конкурентите).

**Допитване до потребителите.** При този подход освен изучаване на данни за предпочитанията на потребителите се извършва явно допитване до тях за получаване на входни данни към иновационния процес. В ранните фази на иновационните проекти потребителските предпочитания или неудовлетворените нужди се идентифицират чрез проучвания, интервюта с количествени показатели или фокус групи. Един съвършен и доказан метод е т.нар. „управлявани от резултати иновации", който съчетава група методи за проучване и оценка в съгласуван модел [27]. В по-късните фази на иновационния процес на потребителите се представят различни решения или концепции, така че те да могат да реагират на представените им конструкции [26].

**Създаване на иновации с потребителите.** При предходните два подхода потребителите остават изолирани от бизнес организациите. При този трети алтернативен метод потребителите са активно ангажирани в проектирането или разработването на бъдещите продукти с помощта на средства, които се предоставят от организациите, създаващи продуктите. Тук става въпрос за активно интегриране на потребителите в иновационния процес [28], за изграждане на схващане за т.нар. „клиентоцентричност" [29,30]. Създателите на продукти упълномощават потребителите сами да проектират решения или прилагат

методологии за ефикасно трансфериране на иновативни решения от потребителите към бизнес организациите. Това са форми на отворени иновации с потребителите (customer co-creation). Съвместното създаване с потребители се определя като активен, креативен и социален процес, основан на сътрудничество между производители и потребители [31].

Основната полза от съвместно създаване на продукти с потребители е разширяване на базата данни за нуждите, приложенията и технологичните решения, които пребивават в сферата на потребителите на продукти или услуги. Това е ново разбиране за отворени иновации с потребителите [32,33,34].

Съществуват три характеристики, които влияят върху концептуалните димензии на методите за съвместно създаване с потребители [35]:

- **стадий на иновационния процес.** Стадият на иновационния процес характеризира момента, когато входящата информация от дейностите по съвместно създаване постъпва към процеса за разработване на нови продукти;
- **степен на сътрудничество.** Степента на сътрудничество характеризира структурата на лежащите в основата на отворените иновации отношения;
- **степен на свобода.** Степента на свобода характеризира естеството на задачите, които се възлагат на потребителите.

Ако се вземат под внимание тези три характеристики са възможни осем типа съвместно създаване с потребители.

## 7. Заключение

Настоящата работа накратко описва характеристиките на колаборативните иновации като средство за развитие на съвременните организации. Идентифицирани са основните характеристики та тези иновации и изискванията към тях за да се превърнат в средство за постигане на устойчива конкурентоспособност. Набелязани са основните елементи на бъдещ модел за оценяване на възможностите за прилагане на колаборативни иновации.

## 8. Литература


1. Gianiodis, P.T., Ellis, S.C and Secchi, E. (2010). Advancing a typology of open innovation. International Journal of Innovation Management, 14, pp. 1-42.
2. Lichtenthaler, U. (2011). Open innovation: past research, current debates, and future directions. Academy of Management Perspectives, 25, pp. 75-93.
3. Chesbrough, H. and Crowther, A.K. (2006). Beyond high tech: early adopters of open innovation in other industries. R&D Management, 36, pp. 229-236.
4. Chesbrough, H. W. (2003). Open Innovation: The New Imperative for Creating and Profiting from Technology. Boston, MA: Harvard Business School Press.
5. Chesbrough, H.W. and Appleyard, M.M. (2007). Open innovation and strategy. California Management Review, 50, pp. 57-76.
6. Lichtenthaler, U. (2008). Open innovation in practice: an analysis of strategic approaches to technology transactions. IEEE Transactions of Engineering Management, 55, pp. 148-157.
7. Prandelli, E., Sawhney, M. and Verona, G. (2008). Collaborating with Customers to Innovate: Conceiving and Marketing Products in the Networking Age. Cheltenham: Edward Elgar.
8. Prahalad, C.K. and Ramaswamy, V (2000). Co-opting customer competence. Harvard Business Review, 78, pp. 79-87.
9. Skaggs, B.C. and Youndt, M. (2004). Strategic positioning, human capital, and performance in service organizations: a customer interaction approach. Strategic Management Journal, 25, pp. 85-99.
10. Chesbrough, H.W. (2006). Open Business Models: How to Thrive in the New Innovation Landscape. Boston, MA: Harvard Business School Press.
11. van der Meer, H. (2007). Open innovation - the Dutch treat: challenges in thinking in business models. Creativity and Innovation Management, 16, pp. 192-202.
12. Nambisan, Satish. 2008. Transforming Government Through Collaborative Innovation. IBM Center for the Business of Government.
14. Harris, M., & Albury, D. (2009). The innovation imperative. NESTA, London.
15. Fung, H. G., Gao, G. Y., Lu, J., & Mano, H. (2008). Impact of Competitive Position on Export Propensity and Intensity: An Empirical Study of Manufacturing Firms in China. Chinese economy, 41(5), 51-67.
16. Ansell, Christopher and Alison Gash. (2008). Collaborative Governance in Theory and Practice'. Journal of Public Administration Research and Theory, 18(4): 543-571.
17. Sorensen, Eva. (2012). Governance and Innovation in the Public Sector. In David Levi-

Faur (ed.) Oxford Handbook of Governance. Oxford: Oxford University Press.
18. Straus, David. (2002). How to Make Collaboration Work. San Francisco, CA: Berrett Koehler.
19. Koppenjan, Joop, and Erik-Hans Klijn. (2004). Managing Uncertainties in Networks: Public Private Controversies. London: Routledge.
20. Skilton, Paul F., and Kevin J. Dooley. (2010). The effects of repeat collaboration on creative abrasion. Academy of Management Review. 35(1): 118-134.
21. Newman, Janet. (2011). Public Leadership as Public-making. Public Money and Management. 31(5): 315-321.
22. Crosby, Barbara and John Bryson. (2010). Integrative Leadership and the Creation and Maintenance of Cross-sector Collaboration. Leadership Quarterly. 21(2): 211-230.
23. Thomke, S. (2003). Experimentation matters: Unlocking the potential of new technologies for innovation. Boston, MA: Harvard Business School Press.
24. Cassiman, B. and Veugelers, R. (2006). "In search of complementarity in innovation strategy: internal R&D and external knowledge acquisition." In: Management Science, 52(1), 68-82.
25. Laursen, K. and Salter, A. (2006). "Open for innovation: The role of openness in explaining innovation performance among UK manufacturing firms." In: Strategic Management Journal, 2 7(2), 131-150.
26. Dalian, E. and Hauser, J. R. (2002). "The virtual customer." In: Journal of Product Innovation Management, 19(5), 332-353.
27. Ulwick, A.W. (2002). "Turn customer input into innovation." In: Harvard Business Review, 80(1), 91-97.
28. von Hippel, E. (2005). Democratizing Innovation. Cambridge, MA: MIT Press.
29. Piller, F.T. (2004). Innovation and Value Co-Creation. Habilitationsschrift an der Fakultat fur Wirtschaftswissenschaften der Technischen Universitat Miinchen.
30. Tseng, M. M., Kjellberg, T. and Lu, S. C. Y. (2003). "Design in the new e-commerce era." In: CIRP Annals -Manufacturing Technology, 52(2), 509-519.
31. Piller, F.T. and Ihl, C. (2009). "Open Innovation with Customers — Foundations, Competences and International Trends." In: Expert Study commissioned by the European Union, The German Federal Ministry of Research, and Europaischer Sozialfond ESF. Published as part of the project "International Monitoring". Aachen: RWTH ZLW-IMA 2009.
32. Reichwald, R. and Piller, F.T. (2009). Interaktive Wertschbpfung: Open Innovation, Individualisierung und neue Formen der Arbeitsteilung. 2nd. Edition, Wiesbaden: Gabler.
33. Tapscott, D. and Williams, A. D. (2006). Wikinomics: How Mass Collaboration Changes Everything. New York, NY: Portfolio.
34. Seybold, P. (2006). Outside Innovation. Crown Business: New York.
35. Diener, K. and Piller, F. (2010). The Market for Open Innovation. Raleigh, NC: Lulu 2010.

Gianiodis, P.T., Ellis, S.C and Secchi, E. (2010). Advancing a typology of open innovation. International Journal of Innovation Management, 14, pp. 1-42.

Контакти
Адрес:
Технически университет – София
Стопански факултет
Климент Охридски 8
1756 София
[1]E-mail: sdim@tu-sofia.bg

© International Scientific Conference on Engineering, Technologies and Systems
TECHSYS 2016, Technical University – Sofia, Plovdiv branch
26 – 28 May 2016, Plovdiv, Bulgaria

# ВЪЗМОЖНОСТИ И ПРОБЛЕМИ ПРИ ОЦЕНЯВАНЕ НА ТРУДОВИТЕ ПОСТИЖЕНИЯ

СВЕТЛАНА БОРИСОВА

**Резюме:** *Оценяването на трудовите постижения е специфичен инструмент за получаване на широко-обхватна информация за оценяваните лица. Тази дейност има важно значение, както за хората, така и за организациите и не бива да се прилага самоцелно. Резултатите от качествено извършената оценка на трудовите постижения, могат да се използват като основа за осигуряване на възможности за индивидуално развитие и повишаване на организационните резултати. В практиката обаче, освен ползи от оценяването се открояват и някои проблеми, които чрез подходящ управленски подход могат да се трансформират в добри възможности за оптимизиране на работата.*

**Ключови думи:** *оценяване, трудови постижения, възможности, проблеми.*

# OPPORTUNITIES AND PROBLEMS IN THE ASSESSMENT OF LABOUR ACHIEVEMENTS

SVETLANA BORISOVA

**Abstract:** *Evaluation of labor achievements is a specific tool to obtain wide-ranging information-rated entities. This activity is important both for people and organizations and should not apply sake. The results of the qualitative assessment carried out of the labor achievements, can be used as a basis for providing opportunities for personal development and improving organizational performance. In practice, however, unless benefits of the evaluation also highlights some problems through proper management approach can translate into better opportunities to optimize work.*

**Key words:** *evaluation, labor achievements, opportunities, problems.*

## 1. Въведение

Оценяването на трудовите постижения осигурява важна информация за степента и качеството на изпълнение на трудовите задачи и постигнатите от хората цели в съответствие с конкретните им задължения и отговорности, за определен времеви период. Оценяването дава възможност да се постигне съответствие между конкретната длъжност и лицето, което я заема и в случаите когато се получи разминаване – да се търсят възможности за решаване на констатираните проблеми.

## 2. Резултати и възможности за подобряване

Оценяването се провежда чрез попълване на специфичен формуляр, в който максимално систематизирано се записват от оценяваните лица конкретните резултати.

В България, съгласно действащата нормативно-законова уредба, оценяването може да се извърши от оценяващ ръководител, на когото работещият е пряко подчинен, от комисия или от самия оценяван. Писмената форма значително улеснява аналитичната работа и изготвянето на окончателното становище на ръководителя или комисията. В организации с по-специфичен характер на дейността оценяването може да се извърши от клиенти, доставчици и др., каквато е например практиката в големите търговски вериги.

Честотата на оценяване е различна, което също е в пряка зависимост от типа на организацията и спецификата на дейността. Периодичността варира от един до няколко пъти

Copyright © 2016 by Technical University of Sofia, Plovdiv branch, Bulgaria ISSN Online: 2535-0048

през определен интервал от време. В държавната администрация, например, трудовото представяне на служителите традиционно се осъществява един път в годината, в съответствие със Закона за държавния служител [1] и Наредбата за условията и реда за оценяване изпълнението на служителите в държавната администрация [2], докато в частния сектор положението е различно. Процесът по оценяване приключва с оформяне на крайно становище от ръководителя, в което окончателната оценка е показател за степента на постигнатите цели на организацията или изпълнението на индивидуалните трудови задачи (преките задължения), т.е. дали постиженията на конкретния служител са в съответствие с естеството на извършената работа. Взима се под внимание и в каква степен изпълнената работа отговаря на притежаваните професионално-квалификационни способности. Резултатите от качествено извършената оценка на трудовото представяне, могат да се използват като основа за осигуряване на възможности за индивидуално развитие и повишаване на организационните резултати.

Оценяването на трудовите постижения има важно значение, както за хората, така и за организациите и не бива да се подценява. Върху него трябва да се постави акцент като на специфичен инструмент за получаване на широко-обхватна информация. В случаите, когато то е неформално, се осъществява от непосредствения ръководител в хода на работата. В най-общата ситуация този вид оценяване се основава на взаимоотношенията между ръководителите и изпълнителите.

В зависимост от целите и значението на управлението на трудовите постижения е препоръчително да се използва по-рационален и обективен подход чрез провеждане на формално оценяване. Целите могат да бъдат различни, но задължително трябва да са ясно дефинирани и постижими, защото самоцелното оценяване би довело до редица проблеми, които да рефлектират отрицателно върху оценяваните.

За усъвършенстване на управлението на трудовите постижения е препоръчително да се търсят възможности за съчетаване на индивидуалните с организационните цели. Както пише авторът Б. Колчагова [3]) „На практика това става чрез последователно диференциране на организационните, колективните и индивидуалните цели и след изпълнението им по обратен път достигането им, чрез което в крайна сметка се подобрява организационната ефективност“. Предвид това, целите на самото оценяване биха могли да се диференцират като:

- *Установяване нивото на професионално-квалификационните способности на оценяваните*, които трябва да бъдат в пряка взаимовръзка със заеманата длъжност. В един от своите значими трудове, авторът Д. Шопов [4] посочва, че „…установяването на степента, в която подготовката, специалните знания, професионалните умения, трудовите навици и нагласите на заетите лица отговарят на изискванията на длъжността, служи за определяне на потребностите от образование и квалификация; оценяване и усъвършенстване на системата за повишаване на квалификацията и за преквалификация; разработване на програми за повишаване на квалификацията, за преквалификация и кариерно развитие; оценяване и усъвършенстване на мотивационната система в предприятието; подпомагане на работниците и служителите по-добре да изпълняват своите трудови задачи и задължения; набиране на информация за определяне на потребностите от човешки ресурси и др.” Когато чрез писмената форма за оценка на трудовите постижения се определя нивото на професионалната квалификация е необходимо да се отчита и съответствието с изискванията в длъжностните характеристики.

- *Оптимизиране работата на персонала.* Постига се чрез ефективно управление на постигнатите цели, изпълнението на задълженията и развитието на личната компетентност. Чрез получените резултати могат да се разкрият възможностите за подобряване на работата с насоченост към бъдещо развитие на организацията и нейните служители.

- *Справедливо определяне на трудовите възнаграждения спрямо постиженията.* Това означава, че при определяне на възнаграждението трябва да се отчитат способностите и приноса на служителите в постигане на организационните цели. Когато е изградена и функционира точна, ясна и справедлива система за оценка на трудовите постижения, възнаграждението на труда се възприема като един от основните фактори за стимулиране. Освен основните критерии при определяне на размера на работната заплата (времетраене на работата или изработеното) добре би било добре да се вземат предвид способностите и личния принос на хората към крайните резултати и постигнатите организационни цели [5]. Справедливото възнаграждение би трябвало да бъде свързано с

установяване на схеми, базирани на премии, бонуси или участие в печалбата, както и други форми за насърчаване на хората, които да бъдат основа заложени като основни в критериите за оценка. Необходимо е ръководителите да имат ясна представа относно резултатите, които трябва да бъдат постигнати. Добре обоснованите и регламентирани възнаграждения предварително отстраняват предпоставките за конфликт на интереси, неравностойност или дискриминация в организациите.

• *Определяне на потребностите от обучение и повишаване на професионалната компетентност.* В тази връзка, необходимостта от обучение и повишаване на професионалната компетентност на оценяваните много точно се установява чрез периодична оценката на трудовите постижения. От друга страна, да се определи реално необходимостта от обучение, например, на ръководния състав, е твърде сложно, поради което трябва да се отчита и развитието на организацията.

Въз основа на резултатите от оценяването, може реално да се прецени необходимостта от подобряване на отделни качества на оценявания, включително и неговата професионална квалификация. Например, могат да се разработят програми за повишаване на квалификацията и преквалификацията на оценяваните според установената необходимост от определен вид обучение. Добре известен е факта, че инвестицията в обучение си заслужава, въпреки необходимостта от значителни финансови средства. Като начало е препоръчително да се разработят програми, съдържащи информация относно контингента на обучаваните, техният брой, видът на обучението, график и по възможност финансова стойност на обучението. В тази връзка, ръководителите никога не бива да изпускат възможността да проведат предварителен разговор с оценяваните, при които е констатирана нуждата от обучение. Това ще помогне да се доизясни видът и конкретната форма на обучение. Подобен разговор помага да се проучи действителното желание или нежелание от страна на оценяваните за включването им в обучението. В практиката се установява, че твърде често хората не са обективни при вземането на решение за включване в конкретен вид обучение и причините за това са твърде много.

• *Определяне на нуждите от кариерно развитие на всеки служител.* Тази цел най-лесно се постига след като ръководството се запознае с отразената информация във формулярите за оценка. Бъдещият потенциал за развитие на оценяваните не би следвало да се подценява, а да се използва стратегически. Хората с потенциални възможности за развитие следва да бъдат повишени в длъжност, както това е възприето, например, в държавната администрация. Процесът може да се улесни чрез въвеждането на прозрачни процедури за професионално и кариерно развитие [6].

• *Формиране на резерв от кадри.* Повишаването в по-висока длъжност е обвързано с оценката от изпълнението на длъжностните задължения, с обучението и кариерното развитие на персонала. Формирането на резерв от кадри ще бъде необходим при преминаване на по-висока длъжност, евентуално напускане, пенсиониране и т.н.

• *Подобряване на трудовите взаимоотношения, в т. ч. между ръководители и подчинени.* Това може да се постигне на база различните показатели за компетентност, в т.ч. релевантна за ситуациите комуникативна компетентност, лидерска, управленска, стратегическа и др. компетентност. Във връзка с комуникативната компетентност, Маринов [7] посочва: „Комуникативната компетентност на практика означава, че комуникиращите помежду си системи и индивиди са в състояние да разберат и вникнат в същността на различните за събитията гледни точки и проумеят съответните им референтни рамки. Респективно взаимното разбиране между хората, ако изобщо това е възможно, изисква известна съотнесеност на психологичните актове, осъществявани от двете взаимодействащи си страни, което не означава идентичност на мисленето".

• *Мотивиране на оценяваните лица.* Информацията, получена в резултат от оценката на трудовите постижения успешно може да се използва за създаване на условия за стимулиране на хората, с цел повишаване качеството на изпълнение на произтичащите от длъжността функции и задачи, както и приобщаване към целите и мисията на организацията. Ръководителите могат да потърсят възможности за допълнителни форми за стимулиране, когато получените резултати превишават очакваните. Препоръчително е да се търси баланс между напредъка в работата, преизпълнението на предварително заложените цели и финансовото или друг вид стимулиране.

• *Разкриване на нови щатни длъжности или съкращаване.* Оценката на трудовите постижения е ефективна, когато трябва да се вземат решения относно качеството и числеността на персонала. Съществуват

организации, особено държавни, в които щатните длъжности значително превишават реално необходимият брой, който е достатъчен за тяхното нормално функциониране. Препоръчително е да се направи реална преценка за работата на служителите и е допустимо да се направи списък с тези, които биха могли да бъдат съкратени. При евентуални съкращения следва да се запазят тези служители, които имат по-висока квалификация и работят по-добре. Пристъпвайки към тази мярка, работодателите имат задължение да установят дали конкретният оценяван не се ползва със защита при уволнение, съгласно Кодекса на труда [8]. Трябва да се отбележи, че когато в организацията започнат вълнения и слухове за съкращения най-добрите сътрудници започват да си търсят нови работни места, а тези които не са достатъчно уверени в себе си и може би не са необходими на никого настояват да останат на своето работно място. В крайна сметка, съкратените ще си потърсят нови възможности за работа, докато ръководителите ще останат с тези, които нямат къде да отидат. Поради тази причина, преди съкращаването на определени служители, ръководителите е необходимо да направят обективна (реална) оценка на трудовите постижения на персонала.

### 3. Инструментариум на оценяването

Проучванията сочат, че в практиката повечето от организациите използват, едновременно два критерия за оценка на трудовите постижения, а именно: критерии, ориентирани към индивидуалните качества (личностни и професионални) и такива, ориентирани към оценяване на получените резултати. Много често тези два критерия се използват паралелно [9], и при попълване на картата „оценка на работата" прекият ръководител дава и своето становище за потенциала на работника за евентуалното му развитие и повишение. След това в рамките на вътрешните процедури за подбор на персонал се прави един по-общ сравнителен анализ на потенциала на всички служители и работници".

Изборът на метод за оценка на персонала (количествен или качествен) е от важно практическо значение. В тази връзка, е необходимо да се отчитат: спецификата на категорията персонал, длъжностите и с каква цел ще се използват получените резултати.

### 4. Ползи и проблеми при оценяването

Потенциала на даден служител е трудно да се оцени, поради което в световната практика, широко се прилага оценяване от прекия ръководител, комисия или се съчетава със самооценяване. Авторът Б. Колчагова [10] посочва, че „у нас все още в много организации то се извършва от атестационна комисия, но същевременно се прави оценяване от прекия ръководител и самооценяване. В някои случаи оценяването се извършва от колективен орган въз основа на предварително направените и предложени оценки на ръководителя. Тази практика на оценяване има доста формален характер и не може да изпълни ролята, която му се възлага."

В процеса на оценяване ръководителите и оценяваните срещат редица трудности, въпреки безспорните ползи от него. Основните положителни моменти конкретно се свеждат до следното:

- При формалното оценяване, работодателите получават точна и изчерпателната информация за степента на изпълнение на трудовите задължения и квалификацията на работещите в организацията, за справяне с възложените задачи в трудовата дейност, както и изпълнението на други функции и роли на атестирания служител;
- Оценяването помага в търсенето на нови форми за мотивиране;
- Благодарение на оценката на трудовите постижения, ръководителите могат да увеличат производителността, тъй като персоналните оценки въздействат психологически върху оценяваните лица и са своеобразен стимул за изпълнение на по-голям обем от работа, в съответствие с поставените цели;
- Други ползи, произтичащи от резултатите по оценяването, са свързани с възможностите за ротация на работните места, необходимостта от посещение на допълнителни квалификационни курсове, създаване на условия за израстване на служителите и т.н., чието усъвършенстване се налага като обективна необходимост в резултат от оценката на трудовото представяне, формиране на резерв от кадри при очертаващо се повишение, напускане или пенсиониране;

В своята цялост, информацията, която се събира чрез формата за оценяване е достоверна и непредубедена и може да бъде предпоставка за подобряване на комуникациите и предприемане на конкретни управленски решения, подходящи за повишаване на трудовите резултати в организацията.

Освен ползи, от оценяването на трудовите постижения, в практиката се срещат и някои проблеми. Така например:

- Въвеждането на оценяване на трудовите постижения, без да се разбира неговият смисъл и цели, ангажира ценно време и средства на ръководителите, което може да се счита като основен недостатък. Оценяване, осъществявано по примера на други организации, може да окаже негативно влияние върху организационната култура, организационния климат и взаимоотношенията между членовете в колектива;
- Твърде често оценяването се възприема единствено като метод за констатация относно равнището на постижения на хората, а не като подход чрез който те трябва да се мотивират, за да разкрият по-пълно възможностите си и да израстват в кариерата.
- Постоянното пряко наблюдение на служителите в колектива, не винаги позволява на ръководителите да направят обективна оценка на реалните резултати, получени чрез формуляра за оценяване. В някои случаи, в резултат на създалите се приятелски взаимоотношения между оценявания и оценяващия, заключителната оценка на оценяващия ръководител може да бъде една и съща за някои от оценяваните. Проблемът идва от там, че в повечето случаи оценяваните получават еднаква заключителна словесна оценка (например: „Много добър“), въпреки че резултатите от попълнените формуляри могат да съдържат различни данни. Крайните оценки за някои конкретни оценявани лица, понякога са предварително ясни. Върху тази основа се изграждат съмненията относно субективността на получаваната оценка за работата и приноса на оценяваните в стремежа им към постигане на поставените организационни цели. По отношение на този проблем, Г. Гергинова [11] отбелязва, че „когато точките на някои от оценяваните са по-малко, това по-скоро изглежда субективно, а не логически неизбежно, в следствие от описания с думи анализ на работата на оценявания служител. В редки случаи, в които може да бъде открита някоя критична бележка, тя е формална и не се отразява на крайния резултат“. По принцип, формалното оценяване създава впечатление, че е рационално и обективно като подход, който се основава на целите, но крайните оценки, понякога се считат за недостатъчно достоверни.

Ако оценката не отразява конкретно приноса на служителя, авторите Лейзиър и Гибс [12] посочват, че „…това може да предизвика няколко отрицателни последици. Възможно е служителят да открие, че връзката между изпълнение и заплащане е несигурна и да изисква компенсация на риска, повишавайки по този начин разходите. В рамките на оценяването е необходимо да бъде изградена добра система за поощряване. Важно е организациите да се стремят към ефективни методи и процедури за оценяване на изпълнението.” В тази връзка, когато в оценъчния формуляр приоритетно значение се отдаде на критериите свързани с личностните и професионалните качества на хората могат да се очакват известни затруднения свързани с измерването на степента на изявяване на тези качества. Друго затруднение може да възникне от трудната доказуемост на валидността на някои критерии, например, до колко решаващи за успеха са усърдието и съзнанието за разходите или не може да се избегне субективността в преценката на ръководителя.

Значително по-малко срещани са случаите, в които служителите считат, че не е необходимо да се оценяват трудовите им постижения и незначителен е броят на становищата, в които оценяваните са убедени, че оценяването на изпълнението е изключително необходим инструмент, даващ възможност да се решават много важни проблеми. Такива или подобни проблеми, могат да се преодолеят, например, с помощта на външни консултанти, с чието съдействие да се изгради подходяща система за оценка, която да бъде достатъчно ефективна. Алтернативен вариант, до колкото обстоятелствата позволяват това, е да бъде обособена централизирана система за оценяване, което може да осигури еднакво прилагане на критериите за оценяване спрямо всички оценявани в зависимост от спецификата на длъжността [13].

В различни по своята дейност организации, се срещнат различни становища по отношение на ползите и проблемите свързани с оценяването на трудовото представяне. Практиката показва, че оценяваните не разбират достатъчно смисъла на тази дейност, поради това, че не са достатъчно информирани. На повечето хора, очакванията им са свързани с ползите за тях, произтичащи от оценяването, което трябва да бъде в логическа взаимовръзка с получените индивидуални резултати. Някои дори считат, че оценката може, в някаква степен дори да им навреди, отколкото да им помогне за бъдещото им кариерно развитие. Тук е мястото да отбележим, че резултатите от индивидуално представяне, особено когато надвишават очакваните, би трябвало да бъдат обвързани с предоставянето на различни допълнителни ползи за оценяваните, като например: по-високо заплащане (под формата на стимули), предложение (от страна на ръководителя) за

кариерно развитие, допълнително обучение и др.

### 5. Заключение

Оценяването на персонала е специфична форма на контрол и важен компонент от системата за управление на персонала, но целите и ползите не винаги са достатъчно ясни за оценяваните. Индивидуалните цели биха могли да се обвържат с приоритетите и целите на организацията, като се засили вниманието и ангажираността на персонала към най-важните от тях. [14,15,16].

Използването на подходящи методи за оценяване, могат да бъдат гаранция за обективност, въпреки непрекъснато съпътстващите в практиката проблемни ситуации. В тази връзка е възможно да се очаква подобряване на резултатите и качеството на трудовите отношения, ако оценяването е коректно за всички оценявани, заемащи еднаква длъжностна позиция и индивидуалните резултати се обвържат със специфична система за награждаване, квалификационни курсове или преместване на по-подходяща позиция.

В заключение може да се отбележи, че когато оценяването се осъществява като непрекъснат процес, може това ще подпомогне дейностите допринасящи за повишаване на организационните резултати, а качеството на трудовите отношения непрекъснато да се усъвършенства, като се сведат до минимум рисковите ситуации.

### ЛИТЕРАТУРА


1. Zakon za darzhavniya sluzhitel. Obn. DV. br. 67 ot 27 yuli 1999. V sila ot 27.08.1999, posl. izm. i dop. DV. br. 68 ot 02.08.2013.
2. Naredba za usloviyata i reda za otsenyavane izp"lneniyeto na sluzhitelite v d"rzhavnata administratsiya. Obn. DV. br. 49 ot 29.06.2012, priyeta s PMS № 129 ot 26.06.2012.
3. Kolchagova, B., (2015). *Menidzhmant na choveshkite resursi*, str. 107, Softtreid, Sofia.
4. Shopov, D. i dr., (2013) *Kak da upravlyavame choveshkite resursi v predpriyatiyeto* , str. 327-328, IK Trud i pravo, Sofia.
5. Kolchagova, B., (2009). *Menidzhmant na choveshkite resursi*, str. 94, King, Sofia.
6. Lyubomirova, A. (2014). Otkritata komunikatsiya – yedna predpostavka za yefektivno prilagane na sistemata za otsenka na izpalneniyeto na darzhavnite sluzhiteli u nas. Retorika i komunikatsii. YElektronno nauchno spisaniye.
7. Marinov, R., (2002). Komunikatsionna kultura i komunikativna kompetentnost, Mrezha@, 1, str. 13, <http://www.euro2001.net/
8. Kodeks na truda. Obn. DV. br. 26 ot 01.04.1986. i br. 27 ot 04.04.1986. V sila ot 13.04.1990, posl. izm. i dop. DV. br. 61 ot 25.07.2014. <http://www.noi.bg/images/bg/legislation/Codes/KT.pdf>
9. Zlateva, Ts. (2009). Savremenni metodi za otsenyavane na personala. Mezhdunarodna nauchna konferentsiya *„Menidzhmant i inzhenering”*, TU-Sofia, str. 139 Sozopol.
10. Kolchagova, B., (2009). *Menidzhmant na choveshkite resursi*, str. 96, King, Sofia.
11. Gerginova (2013). Byurokratichen konveyyer za „opakovaneto” na magistratite kato profesionalisti, Statiya: Sadebni reportazhi, http://judicialreports.bg/
12. Leyziar, P. YE. i Gibs, Dzh., M., S., (2009). *Ikonomika na personala*. Str. 306, Klasika i stil, Sofia.
13. Gerginova (2013). Byurokratichen konveyyer za „opakovaneto” na magistratite kato profesionalisti, Statiya: Sadebni reportazhi, http://judicialreports.bg/
14. Malinovskiy, P., Metody otsenki personala. 2002.http://www.cfin.ru/management/people/malinovsky.shtml>
15. Donald Kirkpatrick’s evaluation model; review, remaining material, design and code Alan Chapman 1995-2005, www.businessballs.com
16. Hendry, C., (1995). Human Resource Management, Oxford, Butterworth-Heinemann Ltd.



Контакти –
ТУ-София
Стопански факултет
Катедра „ИИИМ”
Бул. „Климент Охридски” 8
E-mail: sborisova@tu-sofia.bg


MILARA
INTERNATIONAL


televic
Providers of reliable interaction


SMC


Sensata
Technologies


steca
Elektronik


ZOBELE
GROUP


LIEBHERR


SOCIETE GENERALE
ЕКСПРЕСБАНК


PROX 2
we make metal work


ASIC
DEPOT

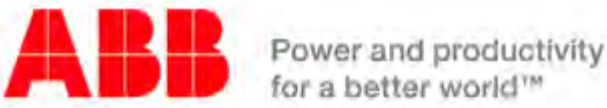

EVN
bulgaria


Schneider
Electric


Lufthansa Technik
Sofia
More mobility for the world


SKF


vis|comp
we develop the web


ABB
Power and productivity
for a better world™


NEOCHİM PLC
FERTILIZERS, ORGANIC AND INORGANIC CHEMICALS


Autodesk
Silver Partner
Manufacturing


Visteon